

E-ISSN: 2709-9369
P-ISSN: 2709-9350
www.multisubjectjournal.com
IJMT 2019; 1(1): 118-121
Received: 25-02-2019
Accepted: 29-04-2019

Riptika Pal
Librarian, Achhruram
Memorial College Jhalda,
Purulia, West Bengal, India

How technology supports library in providing services effectively

Riptika Pal

Abstract

This paper discussed the role of technology in library by establishing a relationship between 'library' and 'technology'. Over the years, libraries had supported education through information and reference services. It provides programs to meet the needs of the people in search for educational skill. Library resources are distributed to the institution, including prisoners, hospitals, rehabilitation programs as well as disabled and elderly people's homes. Now library acquires technology to provide services to the remote users. Libraries are using the Information Technology in general and to automate a wide range of administrative and technical process, build databases, networks and provide better services to their users. The use of IT has become imperative for the efficient management of modern libraries. Library Automation is one of the major applications of IT in libraries. It is helped to change the libraries In-house activities (Acquisition, Cataloguing, Indexing, Serial control, Circulation etc.) from manual system to automation (Venkataraman, 1998). The current study highlights the areas where ICT can be applied. Basically, the paper explains different technologies and their use in the library operation.

Keywords: Information technology, library automation, ICT, digital library, software

1. Introduction

Technology makes our life easier than ever. It gives a digital platform for today's generation and has become part of our lives. There are so many devices available in the market from which anyone can acquire knowledge and enhance skills by reading them. Also library has been considered as a great source of information rather we can say it's a most authentic source of information. Few years back library had seemed to be neglected due to the lack of updated information. But the scenario has become different now. Librarians play the major role in supporting library with the help of technology. Today libraries continue to serve as points for the public's first exposure to new technologies. The very nature of a librarian's service role within the academic sector and community, helping students learn in any and all subjects, and using the best tools for the job, makes them the perfect person to ask about what tools are the most efficient, as they can provide training and guidance. This not only helps students, but could help administrators and planners in the process of acquiring new technology, and in selecting the best software.

2. How library helps in teaching and learning

Libraries are considered to be one of the more efficient teaching components. A good library is a must for the intellectual, moral and spiritual progress and growth of a community's peoples. People acquire education through institution like schools, colleges, agencies and organizations and library is the most outstanding of such institution. A library is fundamentally an organized set of resources, which include human services as well as the entire spectrum of media (e.g., text, video, hypermedia). However, to realize fully the benefits of technology in our education system and provide authentic learning experiences, educators need to use technology effectively in their practice. Libraries serve social and intellectual roles in bringing together people and ideas also.

Libraries also played an important role in any nation. If the nation is to build up and attain an assess potential of growth per capita income, the large percentage should be educated. Libraries can also inspire education to every individual of all ages. They teach skills and strategies individuals need to learn and achieve. Libraries is like a storehouse of knowledge as most of the topics including history, geography, economics, politics and science related topics are all available. Without a library, any educational institution will not be complete. These types of libraries are present in many colleges and universities. Libraries played an important role in the modern society for education and research.

Corresponding Author:
Riptika Pal
Librarian, Achhruram
Memorial College Jhalda,
Purulia, West Bengal, India

In other words, it is an important tool for the development of the society by enhancing the cause of education and academic research. The library provides information to thousands of peoples who need them. With the development in Science and Technology, there is an explosion in information. In order to meet the growing needs of users, many steps are taken to upgrade the existing ones and building of new ones. Information is power as well as access to data is essential for the development of individuals and companies.

3. Impact of technologies in library services

The growth of information and the dependency on it have paved the way for the information society and subsequently the knowledge society. Information has always been prime factor for the development of society and is often regarded as a vital national resource. Information services try to meet this objective. Information has become important part of our lives and should be available when needed. Information services are generated using new tools and techniques to facilitate the right users to the right information (Khodeh and Dhar, 2002) [4]. The implementation of information technology in the libraries has demanded new forms of library services to get more user satisfaction. Digital library service has evolved after the implementation of IT in the library and information centers. Information technology has had a significant impact and has successfully changed the characteristics of information services being generated in libraries. The past two decades have seen great changes in library due to information technology. The technological advancement has made significant impact on the growth of knowledge and unlocking of human potential. In library, the impact is clearly visible on information resources, services, and people (Manjunatha, 2007) [7].

Another impact is remote access of variety of commercial and noncommercial information sources i.e. online full text databases, e-journals, e-books, library catalogue (OPAC) etc. The present-day information seekers can access the worldwide information through internet on their desktop without any time limitation.

4. Benefits of technologies in library

ICT has changed the nature of Libraries. A variety of terms such as hybrid, digital and virtual library are used to refer to the academic library. A digital library can be defined as a "Managed collection of information with associated services where the information is stored in digital format and accessible over a network". The virtual library has been defined as "Remote access to the content and services of libraries and other information resources, combining an on-site collection of current heavily used materials both print and in electronic form with an electronic network which provides access to and delivers from the external worldwide library and commercial information and knowledge sources. Hybrid libraries are libraries that provide access to both electronic resources and paper-based resources". From the definitions, it is clear that most of today's Libraries fall in the hybrid category. The internet has made information access and retrieval both simple and complex. Information retrieval systems are being designed to suit the need of end users and therefore try to simplify the process.

5. ICT based services available in library

The emergence of the information revolution as championed

by information and communication technology (ICT) has enabled libraries to devise viable strategies for improved service delivery (Igwe, 2010) [3]. Library uses various technologies to provide information to its users. Followings are the some of the ICT tools which are basically used for different communication purposes. Libraries are also providing various ICT-based services to their users, including the following.

5.1 RFID Technology

New technology has changed the way of library transaction (check-in and check-out). Libraries are providing ICT-based library services to increase the possible ways of fast and user-friendly services. One of the best invention of technology for library is the 'Radio Frequency Identification' (RFID). Nowadays, libraries are adopting RFID technology to provide enriched and efficient library services. This technology achieves the fourth law of library science, (i.e. 'save the time of the users') by providing quick and effective services (Ranganathan, 1931) [9].

5.2 Closed-Circuit Television (CCTV)

CCTV stands for Closed Circuit Television and also known as video surveillance (Kumar & Svensson, 2015) [6]. This technology plays an important role in the library management. Through the help of CCTV librarian can supervise the whole activities of libraries. It helps to look after the staffs as well as the users.

5.3 Social Media

Social media like Facebook, Twitter, Blogs, etc. have become the central focus for quickest information dissemination. Most of the libraries are using these social media for the promotion or marketing of their e-resources. Basically, Blogs are used to disseminate short communication of library, whereas Facebook has become most useful ICT tool for every kind of information dissemination. Now, Facebook live plays a very significant role for telecast the current ongoing programme.

5.4 Resource Sharing

ICT can be used for resource sharing among libraries and information centers. It provides a great prospect for sharing both the human and material resources of a library with others library. The role of technology is very much significant for cooperative acquisition, cooperative processing (cataloguing and classification), exchange of information materials (e-resources), joint publication, networking, joint training of personnel, interchange of staff for seminars, and workshops (Igwe, 2010) [3].

5.5 Use of Library Automation Software

Library automation is the excellent way of reducing the human involvement for library services. The aims of the current automation technology is to provide maximum services in minimum time and lowest cost. Library automation is the application of ICTs to library operations and services. Many library automation software's are available for library operation such as Libsys, Koha, SLIM21, etc.

5.6 Web-based Online Public Access Catalogues (Web-OPAC): It is the computer form of library catalogue to access information materials in the library. It is an online

database of materials held by a library or group of libraries. It is a computerized library catalogue made available to the public. Most OPACs are accessible over the internet to users all over the world (Mishra and Mishra, 2014) ^[8].

5.7 Digital Library Service

Digital library provides a variety of digital information sources. It reduces the physical space; the user can access to information remotely and it also provides access to distributed information resources. Its advantage is that it has the ability to handle multilingual content.

5.8 Electronic Document Delivery Service

The libraries are implementing ICT-based Inter-Library Lending (ILL) using networks to deliver copies of journal articles and other documents in digital format like PDF (Portable Document Format) to the users' desktops. It helps the users to access information which is not available in their respective libraries.

5.9 Institutional Repository Service

Institutional Repository (IR) is a set of services that a university offers to the members of its community for the management and distribution of digital materials by the institution and its community members.

Librarians bring skills and standards required to manage digital information resources and work towards continued preservation of and access to digital resources.

5.10 Current Awareness Service- CAS

Current Awareness Services has been an important means for keeping the users up to date in their areas of interest. A current awareness service may be as simple as a copy of the table of contents or a bulletin containing bibliographic records, of articles selected from the current issues of journals and other material, and usually organized by subjects.

5.11 Audio-Visual Services

Many libraries particularly media libraries and large academic and public libraries hold audiovisual material such as music, films, pictures, and photographs etc. The new multimedia of an audio CD, Video CD (VCD), and Digital Video Disks (DVD) have the advantage of higher storage capacity, random access and longer life than audio and video tapes and cassettes. Many libraries allow their members to borrow these. Multimedia documents can now be played on standard PCs, stand-alone or networked.

5.12 Electronic theses and dissertations (ETDs)

Related to institutional repositories, especially in university libraries, is the provision of access to full-text copies of Electronic Theses and Dissertations (ETD). Without ICTs it has been impossible to access full-text copies of theses and dissertations from a remote location.

5.13 Electronic Books Service

Electronic books (e-Books) are one way to enhance the digital library with global 24X7 accesses to authoritative information, and they enable users to quickly retrieve and access specific research material easily, quickly, and effectively.

5.14 Electronic Journals: Many publishers who offer

subscriptions to print journals, sometimes also offer a subscription to the electronic version of the journal free of charge. Some of the publishers who are providing e-journals include Emerald, Elsevier, Sage, Springer, EBSCO, J-Gate, John Wiley, etc.

5.15 Electronic Mail (E-mail) Service

This is the most widely used resource of the internet. It is used for sending and receiving of messages otherwise known as mails. The messages are communicated through electronic device. E-mail enables faster and cheaper organizational communication.

5.16 Internet Service

This ICT resources is a means to speedy flow of information. It is a network of computers, communicating with others, often via telephone line. The internet provides a worldwide platform for information sharing among individuals, institutions and organizations. The use of internet enables the provision of current and useful information to enhance productivity and good governance.

5.17 Document Scanning Services

Scanner is important equipment in the modernization of library. It is useful for scanning text, image and content pages of books and providing great help for establishing a digital and virtual library.

5.18 Reprographic Service

Reprographic technology is used for the reproduction of the documents. Using technology, the photocopy and the reproduction of the documents has become very easy and accessible. In this technology, printed documents are converted into digital form, then photocopy is prepared. For the same, computer scanner and software is required. This service is provided to library users for photocopy of some pages of books, journal articles or other materials.

5.19 Library Network Service

The important function of the network is to interconnect computers and other communication devices so that data can be transferred from one location to another instantly. Networks allow many users to share a common pathway and communicate with each other.

6. Conclusion

The internet has thus integrated nearly all aspects of the library activities, the librarians can now use the Internet for exploiting the catalogue of the other institutions, ordering books and journals online, participate in ILL, use e-mail, and discuss through list serves, support reference service through remote databases. Effective application of information technology in library transmits users' satisfaction. The present scenario demands the updated technology for the faster and approachable library services. Gradually, new technologies are developed, consequently there is the need to develop our skills and capacity to provide enhanced library services. Library resources must be used at a large amount. The successfulness of a library and the library professional always depends on the quality of the service. The government has also launched support programs to improve the quality and standards of higher education in India. The technology that enables library services has improved the teaching-learning scenario in an

efficient way to reach the target users.

7. References

1. Gannie SA. A Glimpse of Information Technology Enable Library Services. *Int J Digit Libra Serv.* 2013;3(1):78-82.
2. Hensley CB. Selective Dissemination of Information (SDI): State of the Art. In: *Spring Joint Computer Conference*; c1963. p. 257-262. Available from: <https://www.computer.org/csdl/proceedings/afips/1963/5062/00/50620257.pdf>
3. Igwe KN. Resource Sharing in the ICT Era: The Case of Nigerian University Libraries. *J Interlibr Loan Doc Deliv Electron Reserve.* 2010;20(3):173-187. <https://doi.org/10.1080/1072303X.2010.491016>
4. Kjode S, Dhar U. Library services and functions in changing environment - An overview. *Indian J Inf Libr Soc.* 2002;15(1&2):24-29.
5. KMP. Use of ICT resources and services at state university libraries in Gujarat: a study; c2018. Available from: <http://hdl.handle.net/10603/247168>
6. Kumar V, Svensson J (Eds.). *Promoting Social Change and Democracy through Information Technology.* IGI Global; c2015.
7. Manjinatha K, Pai RD, Mathew SK. *Impact of Technology on quality of services in technical and management libraries in Karnataka.* Manipal, T.A. Pai Management Institute; c2007.
8. Mishra L, Mishra J. ICT resources and services in university libraries. *Int J Digit Libra Serv.* 2014;4(3):243-250.
9. Ranganathan SR. *The Five Laws of Library Science.* Madras Library Association (Madras, India) and Edward Goldston (London, UK). Available from: <http://arizona.openrepository.com/arizona/handle/10150/105454>
10. Spector JM. *Foundations of Educational Technology: Integrative Approaches and Interdisciplinary Perspectives.* Routledge; c2015.
11. Venkataraman P, Rao C. Impact of information technology on library operations and services. In: Satyanarayana B (Eds.). *Information Technology: Issues and Trends.* New Delhi: Cosmo Publication. 1998;1:184-193.

International Journal of Yogic, Human Movement and Sports Sciences

(ISSN: 2456-4419)

Volume- 3

Issue- 2

Jul – Dec

2018

Publisher By

AkiNik Publications

169, C-11, Sector-3, Rohini, Delhi-110085

Toll Free No: 18001234070

Mob: +91-9711224068



*The Largest E-Journal
Database & Gateway*



ISSN: 2456-4419

Impact Factor: (RII) 3.18

Volume 2018, 3(2): 351-356

© 2018 Yoga

www.ijyogajournal.com

Received: 22-05-2018

Accepted: 23-06-2018

SK Hilaluddin

Working As A Guest Lecturer,
Mandham Institute of Education
And Social Science, Dalmi-
Nadika, Purulia, West Bengal,
India

Sajal Maji

Working As A Guest Lecturer,
Mandham Institute of Education
And Social Science, Dalmi-
Nadika, Purulia, West Bengal,
India

Personality correlates of health related physical fitness awareness of elite track & field athletes

SK Hilaluddin and Sajal Maji

Abstract

The purpose of the study was, "Personality correlates of health related physical fitness awareness of elite track & field athletes". The Researcher selected the three sports clubs viz. Pune Athletic Club (Sarabhaug), Sarabhaug Sports Club and Balewadi Sports Club (Balewadi) for data collection considering purposive sampling technique. Further, total thirty (n= 30) elite male track and field athletes, age 18-24 yrs, representing three different sports clubs from Pune city were selected considering random sampling technique i.e., 10 athletes from each of the three clubs for research purpose. After that researcher collects the data, from those athletes with the help of Personality and HRPF awareness questionnaire. After the data collection the researcher analysis the data with the help of descriptive statistics (Pearson's product moment correlation method). To the personality correlate and awareness of track & field athletes.

Keywords: Personality, physical fitness awareness, track & field athletes

Introduction

Track and field is a sport which includes athletic contests established on the skills of running, jumping, and throwing. The name is derived from the sport's typical venue: a stadium with an oval running track enclosing a grass field where the throwing and jumping events take place. Track and field is categorized under the umbrella sport of athletics, which also includes road running, cross country running, and race walking.

The foot racing events, which include sprints, middle- and long-distance events, race walking and hurdling, are won by the athlete with the fastest time. The jumping and throwing events are won by the athlete who achieves the greatest distance or height. Regular jumping events include long jump, triple jump, high jump and pole vault, while the most common throwing events are shot put, javelin, discus and hammer. There are also "combined events" or "multi events", such as the pentathlon consisting of five events, heptathlon consisting of seven events, and decathlon consisting of ten events. In these, athletes participate in a combination of track and field events. Most track and field events are individual sports with a single victor; the most prominent team events are relay races, which typically feature teams of four. Events are almost exclusively divided by gender, although both the men's and women's competitions are usually held at the same venue. It is one of the oldest sports. In ancient times, it was an event held in conjunction with festivals and sports meets such as the Ancient Olympic Games in Greece. In modern times, the two most prestigious international track and field competitions are athletics competition at the Olympic Games and the IAAF World Championships in Athletics. The International Association of Athletics Federations is the international governing body^[1].

The sport of track and field has its roots in human prehistory. Track and field-style events are among the oldest of all sporting competitions, as running, jumping and throwing are natural and universal forms of human physical expression. The first recorded examples of organized track and field events at a sports festival are the Ancient Olympic Games. At the first Games in 776 BC in Olympia, Greece, only one event was contested: the stadion footrace. The scope of the Games expanded in later years to include further running competitions, but the

Correspondence

Sajal Maji

Working As A Guest Lecturer,
Mandham Institute of Education
And Social Science, Dalmi-
Nadika, Purulia, West Bengal,
India

¹ Mike Rosenbaum, "Introduction to track and field events", (New York: IBC publisher), 2014, p. 45.

introduction of the Ancient Olympic pentathlon marked a step towards track and field as it is recognized today-it comprised a five-event competition of the long jump, javelin throw, discus throw, stadion footrace¹², and wrestling¹³.

Track and field events were also present at the Panhellenic Games in Greece around this period, and they spread to Rome in Italy around 200 BC. After the period of Classical antiquity (in which the sport was largely Greco-Roman influenced) new track and field events began developing in parts of Northern Europe in the middle Ages. The stone put and weight throw competitions popular among Celtic societies in Ireland and Scotland were precursors to the modern shot put and hammer throw events. One of the last track and field events to develop was the pole vault, which stemmed from competitions such as the Fiedjeppen contest in the Northern European Lowlands in the 18th century¹⁴.

That same year, the International Amateur Athletic Federation (IAAF) was established, becoming the international governing body for track and field, and it enshrined amateurism as one of its founding principles for the sport. The National Collegiate Athletic Association held their first Men's Outdoor Track and Field Championship in 1921, making it one of the most prestigious competitions for students, and this was soon followed by the introduction of track and field at the inaugural World Student Games in 1923. The first continental track and field competition was the 1919 South American Championships, which was followed by the European Athletics Championships in 1934¹⁵.

For most people, personality is "what makes one individual different from another". The statement like "Mahatma Gandhi was a great personality", "our history teacher does not possess and impressive personality", and Shyam has no personality at all" are generally heard which speak volumes about individual differences which exist among people. Based on these descriptions, personality seems to refer to an 'attribute that people possess in large or small quantities, nor is it a concrete thing that one is - a sum total of all his traits and attributes which go to make him a unique individual like anyone else'¹⁶.

Methodology

This chapter contains the method of research design, population, sample, tools used for research apparatus or instrument employed statistical tools and procedures systematically. The study was conducted to establish the relation between personality and health related physical fitness awareness of track and field athletes belonging to Pune city. Standard procedure was followed to conduct this study. The data were collected with the help of standard questionnaires viz., HRPF (health related physical fitness) awareness and 16 PF. The methodology in details is given below.

Research design

This is a correlation study under the descriptive research. In this research, the investigator established the relationship between personality and health related physical fitness

awareness of athletes of Pune city. The two variables were assessed by two separate questionnaire.

Selection of the subject

Sample

Out of the population, the researcher selected only three sports clubs viz. Pune Athletic Club (Sarasbaug), Sarasbaug Sports Club and Balewadi Sports Club (Balewadi) for data collection considering purposive sampling technique. Further, total thirty (n= 30) elite male track and field athletes, age 18-24 yrs, representing three different sports clubs from Pune city were selected considering random sampling technique i.e., 10 athletes from each of the three clubs.

Variables

There were two dependent variables as follows:-

- Personality.
- Physical fitness awareness.

Tools used

The researcher has gone through the available literature in the library, reports of previous research studies and webs. Further, after a thorough discussion with the research guide, following questionnaires for survey have been chosen, which is easy to conduct in the field situation and requires minimum assistants, less money and less time.

The standard questionnaires administered in this study are given below.

Criterion measures	Author	Questionnaire	Sl. No
Points	T. K. Bera (2005)	HRPF awareness	1
Points	Raymond B Cattell (1943)	16 PF (Personality factors)	2

- The standard 16 PF questionnaire constructed by Raymond B Cattell with accepted level of reliability (0.92) and Validity (0.82) was the tool for the present study. There were 187 test items which were assessed with three points scale.
- Another standard questionnaire was health related physical fitness awareness, which was developed by T. K. Bera with the accepted level of reliability (0.74) and Validity (0.82). There were 25 test items which were assessed with three points scale.

Data collection

The researcher carried an authorization letter from the Principal of Bharati Vidyapeeth University's College of Physical Education, Pune and met the coaches / Heads of the other sports clubs situated in Pune city. After receiving permission from the Heads of the respective institutes/clubs, the researcher finalized the schedules (i.e., date and time) for data collection. However, prior to data collection, the researcher discussed with the subjects about the purpose of this research project and the steps for data collection. The students' doubts, if any, were clarified.

The athletes were asked to fill up HRPF and 16 PF questionnaires. Now the scores were preserved for data analysis.

Statistical Design

Descriptive statistics have been employed to process the data.

¹² Instone, Stephen, "The Olympics: Ancient versus Modern". (London, BBC publisher), 2010, p. 56.

¹³ Waldo E. Sweet, Erich "Segal, Sport and recreation in ancient Greece". (London: Oxford University Press), 2009, p. 37.

¹⁴ Jean-Paul Thuillier, "Le sport dans la Rome antique (French)", Paris, Errance, 1996, pp. 115-116.

¹⁵ South American Championships. (GBR Athletics), 2010, p. 157.

¹⁶ D. Lavallec, et al, "Sports Psychology: Contemporary Themes", (New York: Palgrave Macmillan Publishers), 2004, p. 143.

Further, to establish relationship between the scores of personality and physical fitness awareness, Pearson's product moment correlation method was employed.

Data analysis

To find out the relationship of personality and physical fitness awareness of elite track and field athletes, Pearson product moment correlation method was applied. The mean and

standard deviation of both the groups for the above mentioned items were calculated. The scores of personality and physical fitness awareness were computed for determination of correlation of coefficients.

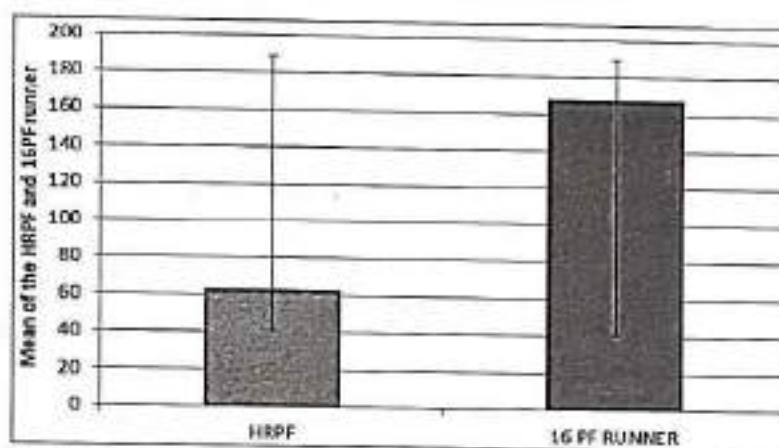
In order to determine the significance of relationship between scores of HRPF awareness and 16 PF, the level of significance was set at 0.05.

Descriptive statistics of HRPF awareness and 16 PF of runners

Correlation	SD	Mean	No. of Runners	Variable	Sl. No
0.166	6.16	62.62	13	HRPF awareness (Points)	1
	11.47	167.54	13	16 PF (Personality) (Points)	2

Represents the relationship of two variables (HRPF awareness and 16 PF) of the athletes participated in running event. Total number of such athletes was thirteen (n1=13). However, for the athlete of running event, the mean value of HRPF awareness was 62.62 (points) and the SD value was 6.16, whereas for the 16 PF the mean and SD values of these athletes were 167.54 and 11.47 respectively. Further, the

coefficient of relationship between the personality and physical fitness awareness as obtained was 0.160 which was not statistically significant even at the 0.05 level ($r=0.160$, $p>0.05$), because the calculated value ($r=0.160$) is less than the tabulated value ($r=0.514$). These findings in turn suggest that the runners personality has no relation with the physical fitness awareness.



Graphical representation of mean values of HRPF awareness and 16 PF of runners
Level of significance 0.05 tabulated value 0.514

The result as presented in Fig.4.1 also indicates similar findings, although there were differences in the mean values of the physical fitness awareness and the personality of the

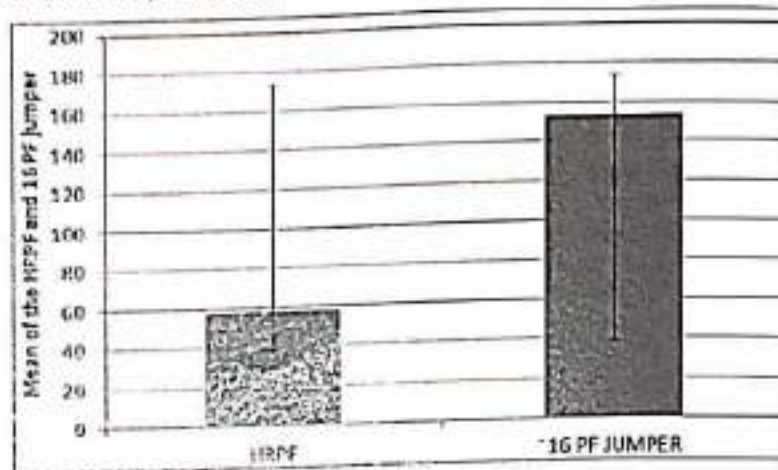
runners. This, in turn, suggests that there was no relationship between the scores of physical fitness awareness and the personality.

Descriptive statistics of HRPF awareness and 16 PF of Jumpers

Correlation	SD	Mean	Number of Jumper	Variables	Sl. No
0.227473	5.33	57.92	11	HRPF awareness (Points)	1
	12.35	153.25	11	16 PF (Personality) (Points)	2

Represents the relationship of two variables (HRPF awareness and 16 PF) of the athletes participated in jumping event. Total number of such athletes was eleven (n1=11). However, for the athlete of jumping event, the mean value of HRPF awareness was 57.92 (points) and the SD value was 5.33, whereas for the 16 PF the mean and SD values of these athletes were 153.25 and 12.35 respectively. Further, the

coefficient of relationship between the personality and physical fitness awareness as obtained was 0.227 which was not statistically significant even at the 0.05 level ($r=0.227$, $p>0.05$), because the calculated value ($r=0.227$) is less than the tabulated value ($r=0.553$). These findings in turn suggest that the jumpers' personality has no relation with the physical fitness awareness.



Graphical representation that mean values of HRPF and 16 PF of jumpers. Level of significance 0.05 tabulated value 0.553

The result as presented in Fig.4.2 also indicates similar findings, although there were differences in the mean values of the physical fitness awareness and the personality of the

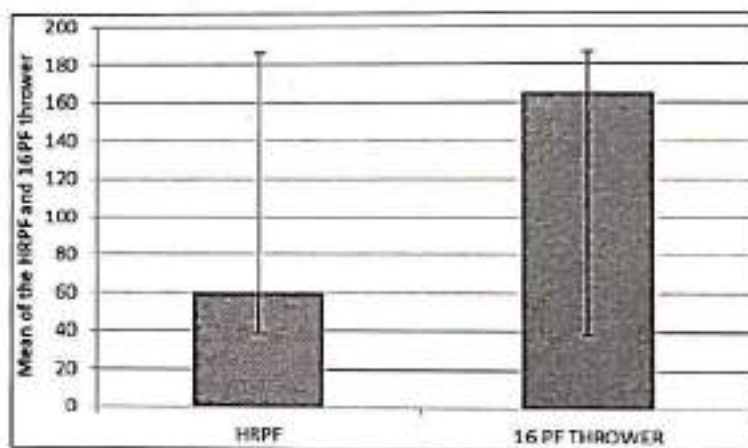
jumper. This, in turn, suggests that there was no relationship between the scores of physical fitness awareness and the personality.

Descriptive statistics of HRPF awareness and 16 PF of throwers

Correlation	SD	Mean	Number of Thrower	Variables	Sl. No
0.807	3.61	60.33	6	HRPF awareness (Points)	1
	13.16	164.83	6	16 PF (Personality) (Points)	2

Represents the relationship of two variables (HRPF awareness and 16 PF) of the athletes participated in throwing event. Total number of such athletes was six (n1=6). However, for the athlete of throwing event, the mean value of HRPF awareness was 60.33 (points) and the SD value was 3.61, whereas for the 16 PF the mean and SD values of these athletes were 164.83 and 13.16 respectively. Further, the

coefficient of relationship between the personality and physical fitness awareness as obtained was 0.807 which was statistically significant even at the 0.05 level ($r=0.807$, $p>0.05$), because the calculated value ($r=0.807$) is more than the tabulated value ($r=0.707$). These findings in turn suggest that the jumpers personality has relation with the physical fitness awareness.



Graphical representation that mean values of HRPF and 16 PF of throwers. Level of significance 0.05 tabulated value 0.707

The result as presented in Fig.4.3 also indicates similar findings, although there were differences in the mean values of the physical fitness awareness and the personality of the

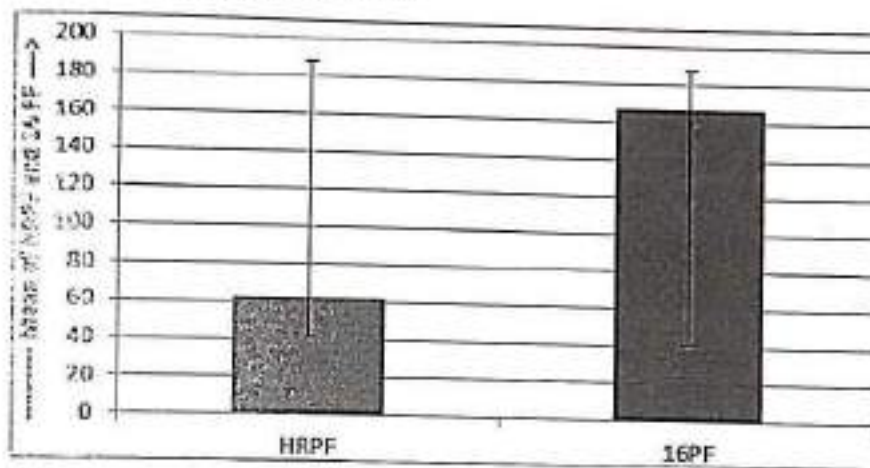
throwers. This, in turn, suggests that there has relationship between the scores of physical fitness awareness and the personality.

Descriptive statistics of HRPF awareness and personality of running, jumping and throwers

Correlation	SD	Mean	Number of athletes	Variables	Sl. No
0.267	5.37	62.37	30	HRPF awareness (Points)	1
	11.74	166.87	30	16 PF (Personality)(Points)	2

Represents the relationship of two variables (HRPF awareness and 16 PF) of the athletes participated in running, jumping and throwing event. Total number of such athletes was thirty ($n=30$). However, for the athlete of running, jumping and throwing event, the mean value of HRPF awareness was 62.37 (points) and the SD value was 5.37, whereas for the 16 PF the mean and SD values of these athletes were 166.87 and 11.74 respectively. Further, the coefficient of relationship

between the personality and physical fitness awareness as obtained was 0.267 which was not statistically significant even at the 0.05 level ($r=0.267$, $p>0.05$), because the calculated value ($r=0.267$) is less than the tabulated value ($r=0.349$). These findings in turn suggest that the runners, jumpers and throwers personality has no relation with the physical fitness awareness.



Graphical representation that mean values of HRPF and 16 PF.
Level of significance 0.05 tabulated value 0.349

The result as presented in also indicates similar findings, although there were differences in the mean values of the physical fitness awareness and the personality of the runners, jumpers and throwers. This, in turn, suggests that there were no relationship between the scores of physical fitness awareness and the personality.

Discussion of Findings

Keeping in mind the importance of the test taken for relation between personality and physical fitness awareness, the researcher has conducted this piece of research. There were 30 athletes from different sports coaching clubs of Pune city. Relationship between personality and physical fitness awareness has been measured by using two separate questionnaires and the score were recorded in marks.

Personality of athletes consists of different types of traits and physical fitness awareness depends upon different types of factors which makes every individual athlete differ from each other. It was, therefore, thought to determine the relationship of these two important aspects of human beings. In fact, logically both these variables must be related with each other. However, the result revealed that there is no relationship between personality and physical fitness awareness, because the calculated value (0.267) is less than the tabulated value (0.349).

The results further confirmed that no statistically significant relationship was seen between the scores of overall personality and overall physical fitness awareness exclusively for runners, because the calculated value (0.160) is less than the tabulated value (0.514).

Similar result was evident in the case of athletes of jumping event, where there was no relationship between personality and physical fitness awareness, because the calculated value (0.227) is less than the tabulated value (0.553).

It was thought that there must be a significant relationship between personality and physical fitness awareness of the athletes of throwing event, but amazingly the calculated value

(0.807) is more than the tabulated value (0.707) and hence there was no significant relationship between the variables of throwers.

Discussion of hypothesis

HO₁:- In case of runners, jumpers and throwers since calculated value of 'r' is less than tabulated value (0.349) the null hypothesis has been refuted at 0.05 level of significance.

HO₂:- In case of runners, since calculated value of 'r' is less than tabulated value (0.514) the null hypothesis has been refuted at 0.05 level of significance.

HO₃:- In case of jumpers, since calculated value of 'r' is less than tabulated value (0.553) the null hypothesis has been discarded at 0.05 level of significance.

HO₄:- In case of throwers, since calculated value of 'r' is more than tabulated value (0.707) the null hypothesis may be accepted at 0.05 level of significance.

Summary

In this chapter the contents of the entire previous chapters has been illustrated.

The purpose of the study has been to assess relation between personality and physical fitness awareness of track & field athletes in Pune city. For this purpose, 30 male subjects were selected as a sample. The age group of subjects was ranged in between 18-24 years. Considering the steps of correlation study, the data have been collected by the researcher and analyzed through Mean, Standard Deviation and correlation methods. The level of significance has been set at 0.05 level of confidence.

The 16 PF oriental questionnaire developed by Raymond B Cattell was collected from national psychological corporation, Agra, test was selected for the collection of data because it was found to be most reliable and have been very often used in research in profession physical education and sports.

The HRPF awareness questionnaire developed by T K Bera was selected for the collection of data because it was found to

be most reliable and have been very often used in research in profession physical education and sports.

Conclusion

This study, within the limitations, draws the following conclusions -

- There was no relationship between personality and physical fitness awareness of runners.
- There was no relationship between personality and physical fitness awareness of jumpers.
- Interestingly, there was a relationship between personality and physical fitness awareness among the throwers.
- Overall, health related physical fitness awareness has no statistically significant relationship with the personality level of track and field athletes.

Contribution to the knowledge

Literature revealed that personality may have a favourable impact with one's awareness of physical fitness and same results were expected in this study. However, the quality of personality seems to improved according to the increment of physical fitness awareness. However, this study did not agree with this. This study contributed an evidence of physical fitness awareness cannot be explained in terms of the scores in personality exclusively among the elite track and field athletes. This study, therefore, made a special contribution to the knowledge also in the field of individual games.

References

1. Mike Rosenbaum, Introductions to track and field events. (New York: BBC publisher), 2014, 45.
2. Instone Stephen. The Olympics: Ancient versus Modern. (London, BBC publisher), 2010, 56.
3. Waldo Sweet E. Erich Segal, Sport and recreation in ancient Greece. (London: Oxford University Press), 2009, 37.
4. Jean-Paul Thuillier. Le sport dans la Rome antique (French). Paris, Errance, 1996, 115-116.
5. South American Championships. (GBR Athletics), 2010, 157.
6. Lavallec D *et al.* Sports Psychology: Contemporary Themes, (New York: Palgeave Macmillan Publishers), 2004, 143.

PISSN: 2394-1885
Printed Journal

E-ISSN: 2394-1893
Indexed Journal

CODEN: IJPEJB
Refereed Journal

Impact Factor (RJIF): 5.38
Peer Reviewed Journal

Index Copernicus ICV 2016: 75.07

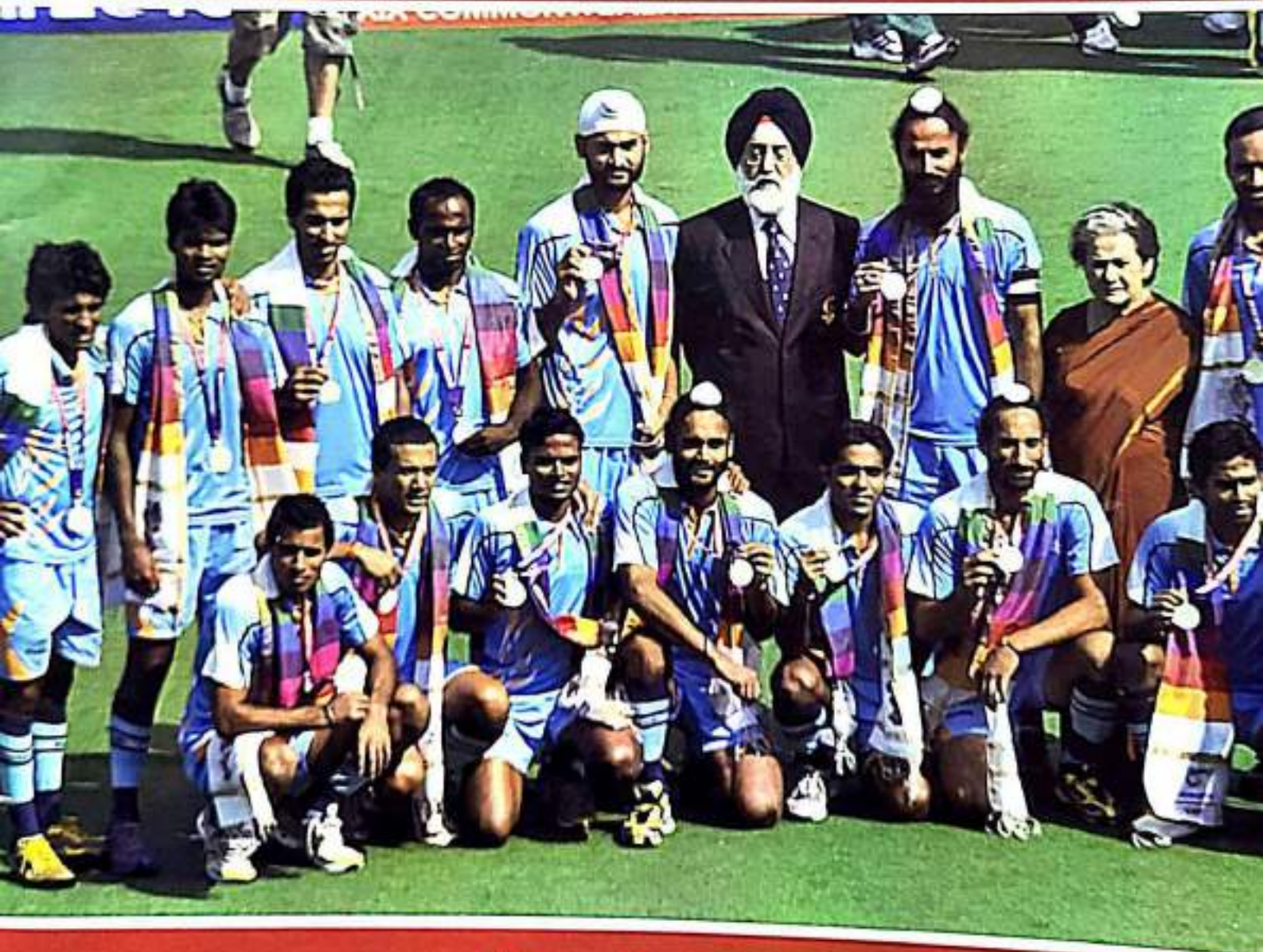
INTERNATIONAL JOURNAL OF PHYSICAL EDUCATION, SPORTS AND HEALTH

VOLUME 5

ISSUE 4

JUL-AUG

2018



PUBLISHED BY
TIRUPATI JOURNAL SOLUTIONS
NEW DELHI (INDIA)

International Journal of Physical Education, Sports and Health

P-ISSN: 2794-1422
E-ISSN: 2794-1470
Volume 5 Issue (4) July 2018
ISSN (Print) 2794-1422
ISSN (Online) 2794-1470
www.ijpesh.in
Volume 5, Issue 4, July 2018
Copyright © 2018, IJPEHS

Rajal Maji
Guest Lecturer, Madhya
Pradesh Institute of Education and Social
Science, Indore, Madhya Pradesh,
West Bengal, India

Development of norms for testing breath holding capacity of collegiate students of average health in Pune city

Sajal Maji

Abstract

The purpose of the study was "Development of Norms for Testing Breath Holding Capacity of Collegiate Students of Average Health in Pune City". The Researcher selected the Chandrasekhar Agarde college, Thane, Maharashtra College of physical education, S. P. Pune University Department of physical education for research purpose. 100 male collegiate students are selected for the data collection as per simple random sampling technique. After that researcher collects the data, from those collegiate students with the help of After Inhalation and After Exhalation.

After the data collection, the researcher analysis the data with the help of descriptive statistics (percentile norms and norms). To development of norms of collegiate students.

Keywords: After inhalation breathe holding, after exhalation breath holding capacity, collegiate students

Introduction

Norms are cultural products (including values, customs, and traditions) which represents individuals' basic knowledge of what others do and what others think that they should do (Cialdini, 2003) [1]. Sociologists describe norms as informal understandings that govern individuals' behavior in society. On the other hand, social psychology has adopted a more general definition, recognizing smaller group units, such as a team or an office, may also enforce norms separate or in addition to cultural or societal expectations. In other words, norms are regarded to exist as collective representations of acceptable group conduct as well as individual perceptions of particular group conduct (Lapinski, 2005) [2].

Norms running counter to the behaviors of the overarching society or culture may be transmitted and maintained within small subgroups of society. For example, noted that certain groups (e.g., cheerleading squads, dance troupes, sports teams, and sororities) have a rate of bulimia, a publicly recognized life-threatening disease that is much higher than society as a whole. Social norms have a way of maintaining order and organizing groups.

Although not considered to be formal laws within society, norms still work to promote a great deal of social control. Social norms can be enforced formally (e.g., through sanctions) or informally (e.g., through body language and non-verbal communication cues.) Because individuals often derive physical or psychological resources from group membership, groups are said to control discretionary stimuli; groups can withhold or give out more resources in response to members' adherence to group norms, effectively controlling member behavior through rewards and operant conditioning (Hackman, 1992) [3]. Social psychology research has found the more an individual values group-controlled resources or the more an individual sees group membership as central to his definition of self, the more likely he is to conform. Social norms also allow an individual to assess what behaviors the group deems important to its existence or survival, since they represent a codification of belief; groups generally do not

Correspondence

Rajal Maji
Guest Lecturer, Madhya
Pradesh Institute of Education and Social
Science, Indore, Madhya Pradesh,
West Bengal, India

¹ R. D. Cialdini, "Creating normative messages to protect the environment" (Current Directions in Psychological Science) 2002, pp 105-109

² M. K. Lapinski and R. N. Rimal, "An explication of social norms" (Communication Theory), 2005, pp 127-147.

³ J. R. Hackman, "Group influences on individuals in organizations" (Handbook of industrial and organizational psychology, Palo Alto: Consulting Psychologists Press), 1992, pp 214-245

punish members or create norms over actions which they care little about (Feldman, 1999)^[1]. Norms in every culture create conformity that allows for people to become socialized to the culture in which they live.

Life is absolutely dependent upon the act of breathing. Breathing is considered the most important of all the functions of the body as all other functions depend upon it. Breath-holding time (BHT) may be considered as one of indicators of efficiency of breathing function. BHT is defined as the time taken by the subject to hold his breath as long as he can. Normal voluntary breath-holding time is 45-55 seconds. Respiration can be voluntarily inhibited for some time, but eventually, the voluntary control is overridden. During voluntary breath-holding, tissues continue to use oxygen and produce carbon dioxide. Therefore, during breath-holding, arterial PO₂ falls and PCO₂ rises, resulting in a state of asphyxia. Since both these factors are powerful respiratory stimulants, a point is reached where the respiratory drive becomes so strong that the person cannot hold the breath any longer. The point at which breathing can no longer be voluntarily inhibited is called the breaking point. Thus, BHT is the time duration from the time of inhibition of breathing till the breaking point (Bijlani, 2004)^[2]. The maximal breath-holding time (BHT) has been used in respiratory physiology as a measure of ventilator response (Nunn, 1997)^[6], (Godfrey, 1969)^[7] (Godfrey, 1968)^[8]. The unpleasant bursting sensation in the lower chest and abdomen and the onset of irregular inspiratory muscle activity have been well documented at the breakpoint of the breath-holding manoeuvre (Fowler, 1954)^[9].

Respiratory efficiency can be increased by training. Respiratory efficiency tests facilitate the increase in the strength of the respiratory muscles. Age and sex also affect the breath-holding time (Kesavachandran, 2001)^[10].

The properties of breath-holding in humans and its possible cause the breath at breakpoint. The simplest objective measure of breath-holding is its duration, but even this is highly variable. Breath-holding is a voluntary act, but normal subjects appear unable to breath-hold to unconsciousness. A powerful involuntary mechanism normally overrides voluntary breath-holding and causes the breath that defines the breakpoint. The occurrence of the breakpoint breath does not appear to be caused solely by a mechanism involving lung or chest shrinkage, partial pressures of blood gases or the carotid arterial chemoreceptor. This is despite the well-known properties of breath-hold duration being prolonged by large lung inflations, hyperoxia and hypocapnia and being shortened by the converse manoeuvres and by increased metabolic rate.

Breath-holding has, however, two much less well-known but important properties. First, the central respiratory rhythm

appears to continue throughout breath-holding. Humans cannot therefore stop their central respiratory rhythm voluntarily. Instead, they merely suppress expression of their central respiratory rhythm and voluntarily 'hold' the chest at a chosen volume, possibly assisted by some tonic diaphragm activity. Second, breath-hold duration is prolonged by bilateral paralysis of the phrenic or vagus nerves. Possibly the contribution to the breakpoint from stimulation of diaphragm muscle chemoreceptors is greater than has previously been considered. At present there is no simple explanation for the breakpoint that encompasses all these properties (Parke, 2006)^[11].

Reviews of related literature

The investigator studied a lot of reviews on research from different related literature available so far in the Libraries and webs. Although the literature on breath holding capacity is very limited, the researcher collected some of the research abstracts that have been summarized below.

Singh *et al.*, (2014)^[12] assessed the effects of selected Pranayams on Breath-Holding Capacity, Cardio-Vascular Endurance & Reaction Time of high school students in Punjab. Two hundred boy's age group of 13 to 16 years from Govt High School, Kerala, Punjab and S.B.W.S.M.P. School, Barur, Punjab were selected as the research subjects. The Pranayams Training duration was of 10-weeks. The subjects were divided into two groups as experimental (Group A) and control (Group B). The experimental group underwent Pranayams Training for 10-weeks and control group did not receive the Pranayams Training. The 't' test was used to compare pre and post-training values. After 10-weeks Pranayams Training there was a significant ($P < 0.001$) difference between pre and post-testing of experimental group for the breath-holding capacity (pre=35.89±1.55, post=36.92±1.57), cardio-vascular endurance (pre=1710.27±50.73, post=1785.51±78.24) and reaction time (pre=24.81±0.40, post=23.55±0.43) as well as control group for the breath-holding capacity (pre=34.28±1.01, post=34.27±1.02), cardio-vascular endurance (pre=1580.94±13.62, post=1498.17±62.78) and reaction time (pre=25.90±0.50, post=25.83±0.52). The experimental group had a significant improvement on Breath-Holding Capacity, Cardio-Vascular Endurance & Reaction Time than the control group.

Rai (2014)^[13] determined the effect of 8 weeks yoga practices (Pranayama) on Breath holding capacity of school going children of Mahilpur. Methods - The method of this study was experimental research and sample were 30 students of senior secondary school of Mahilpur (12-15 Aged). Thirty subjects were randomized into two groups experimental group accomplished yoga practice (Pranayama) for eight weeks. Statistical Technique - Paired sample 't' test was used to analyse the data of the study in use of SPSS software. Result-it showed that eight weeks pranayama significantly increased the breath holding time of school children. Recommendation-it is also recommended other parameters of respiratory system need to investigate for further information of Mahilpur.

¹ D. C. Feldman, "The development and enforcement of group norms". *Academy of Management Review*, 9, 1, 1999, pp.47-55.

² R. L. Bijlani, "Understanding Medical Physiology, 3rd ed". (New Delhi-India: Jaypee Brothers Medical Publishers), 2004, p. 307.

³ JF Nunn, "Chapter 2: Control of breathing: breath holding. In: Applied respiratory physiology, 2nd ed." (London, England: Butterworth); 1977, p.95.

⁴ S. Godfrey and EJ Campbell, "Mechanical and chemical control of breath holding". *Quarterly Journal of Experimental Physiology Cognitive Medical Science*, 54, 1969, pp.117-128.

⁵ S. Godfrey and EJ Campbell, "The control of breath holding". (*Respiratory Physiology*), 1968, pp. 385-400.

⁶ W. Fowler, "Breakpoint of breath holding". *Journal of Applied Physiology*, 6, 1954, pp.539-545.

⁷ C. Kesavachandran, HR Nair and S Shaahi Dhár, "Lung volumes in swimmers performing different styles of swimming". *Indian J Medical Science*, 26, 2001, pp.669-676.

¹¹ M. J. Parke, "Breath-holding and its breakpoint". *Experimental Physiology*, 91, 1, 2006, p.1.

¹² Singh Bhupinder and Singh Ghuman Kuldip, "Effects of Selected Pranayams on Breath-Holding Capacity, Cardio-Vascular Endurance & Reaction" *IOSR Journal of Sports and Physical Education (IOSR-JSPE)*, 1, 3, Jan. 2014, pp.40-44.

¹³ Rai Vaibhav "Effect of Pranayama on Breath Holding Time of School Going Children of Mahilpur" *Journal of educational and practice*, 5, 26, 2014, pp. 13-18.

Singh (1975)^[10] prepared physical fitness norms for high and higher secondary school boys of Jammu and Kashmir State. Data was collected on 4200 male students belongs to six to seventh classes of age 13 to 19 years subjects randomly selected and they were administered the AAHPER Youth Fitness Test. Age wise norms were prepared in terms of Percentile scale, Hull Scale and T- Scale. (1991) conducted a study on computation of norms for 12 minute run/walk among school boys. Data was collected on 1000 school boys belongs to sixth to tenth classes of age 13 to 15 years subjects were randomly selected and they were administered the Cooper's 12 minute Run/Walk test. Age wise norms were prepared in terms of Hull scale.

Box (1973)^[11] conducted percentile norm tables for selected measures of strength, power, agility, flexibility, body composition, cardiorespiratory and muscular endurance from data which is collected at five schools of the Unity Christian School System of Hudsonville.

Coutts (1971)^[12] conducted a study to establish norms for the cooper's 12-minute run/walk test applicable to young males; eighty boys, eleven to fourteen years of age, served as the subjects. The difference between the two groups was statistically significant (P.01). The correlation coefficient between aerobic capacity and run/walk performance was 0.65, while the correlation was statistically significant (P.01); caution was advised in attempting to predict aerobic capacity from run/walk performance with young urban subjects.

Tiwari (2003)^[13] developed anthropometric norms for school children age ranging from 9-10 years. Total 200 male students were randomly selected from deferent schools of South Delhi. The anthropometric measurements were: weight, height, Sitting-height, skin fold measurement (biceps, triceps, supriliac and sub scapula) were tested t-scale, 6-sigma, 7sigma, (hull scale) norms were prepared.

Kumar (2003)^[14] developed the norms for two hand-eye co-ordinance. The study was conducted to test the reliability of two hand co-ordinance, to observe the effect of number of trails, to test the repeated reliability and to develop the norms for age and sex of physical education students of university of Delhi. The total of 200 (100 male and 100 female) subjects was randomly selected. The subjects were tested in different climatic conditions for four times.

Methodology

The purpose of this study is to construct the breath holding capacity norms for college level students in Pune city. Standard procedure has been followed to conduct the study. The methodology in details is given below.

Selection of the subject

Out of 400 a total of 300 male collegiate students with the mean age of 22 (± 2.15) years were selected as sample for this

study. The simple random sampling technique has been used for making the sample for this study. Three colleges have been selected purposively from Pune city to have the true representation of the population. The colleges which have been selected with the number of students were given below:

Variables

Due to paucity of time period and limitations on other feasibility, the researcher has selected two types of breath holding capacity as variables for the study as follows:

Breath holding Capacity -

- After inhalation, and
- After exhalation.

Tools used

Once the variable has been decided, the researcher has gone through the available literature in the library, reports of previous research studies and webs. Further, after a heavy brainstorming session with the research guide, following test has been chosen, which is easy to conduct in the field situation and requires minimum assistants and less time.

Variables	Tests	Unit
Breath Holding Capacity	Manually conducted with a simple stop watch	Maximum time for holding the breath (Secs.)

Data collection

The students were asked to sit in padmasana or in any comfortable sitting position. The stop-watch is kept ready. The subjects were then asked to inhale deeply and hold their breath by closing two nostrils and mouth till they can do. The time of holding the breath is measured by the stop watch in Secs. They were given 5 minutes rest till their pulse rate reaches the normal resting level. They were then asked to repeat the same trial once again. Out of these two trials, the highest breath-holding time (after inhalation) was the final score (secs.). Further, two similar trials were given to the students to record their breath-holding time (after exhalation) in secs. Now both the scores (i.e., breath-holding after inhalation and after exhalation) were preserved for data analysis.

Statistical Design

For establishing the norms on breath holding capacity immediately after inhalation and after exhalation the proper statistical technique (i.e., percentile norms) was employed. However, to compare the breath holding capacity after inhalation and exhalation, t-test was further employed.

Analysis of data

The data on selected breath holding variables collected from 300 male collegiate students of physical education in Pune city has been analyzed statistically and the results have been presented in this chapter in the form of tables and graphs.

Data analysis

This chapter deals with the results of descriptive statistical analysis of the data on the breath holding capacity variable i.e. 1) after inhalation and 2) after exhalation.

The mean and SD of data on breath holding capacity were calculated (Table 1) and then established the separate norms exclusively for - 1) breath holding capacity after inhalation and 2) breath holding capacity after exhalation (Table 2).

¹⁰ Singh, "the study on physical fitness norms of Punjab state high school boys", (retrieved on 18 august from http://shudhganga.inflibnet.ac.in/bitstream/10603/9607/10/10_chapter%202p.dflime), 1985, p-22.

¹¹ D. L. Box, "Physical Ability Testing of Male students in Grade four through twelve", (Completed Research in Health Physical education and Recreation), 1967, p.77.

¹² K. D. Coutts, "Application of Cooper's 12 Minute Run/Walk Test to Young Males", (Research Quarterly), 1971, p.54.

¹³ Tiwari Anil, "development of Anthropometric Norms, Among the Age Group 9-10 years of school Children", (Friends Publications, India, Delhi-09), 2003, pp.175-176.

¹⁴ Kumar Anil, "Development of norms for the two hand-eye co-ordinance test", (Friends publications (India), Delhi-09), 2003, pp.150-151.

Findings on norms

The result presented in revealed that –

- Mean and SD values of breath holding capacity after inhalation of the data on 300 males were 48.57 and 16.18

respectively.

- Mean and SD values of breath holding capacity after exhalation of the data on 300 males were 40.06 and 15.30 respectively.

Table 1: Descriptive statistics on breath holding capacity (n = 300)

Sl. No.	Variables	Mean	SD
1	After Inhalation (breath holding)	48.57	16.18
2	After Exhalation (breath holding)	40.065	15.305

The results on percentile norms have been presented in the results indicates that.

- In case of breath holding (after inhalation), the raw score of P₁₀ and P₉₀ were 28.70 Secs and 92.47 Secs respectively, whereas the score of P₅₀ was 46.81 Secs.
- In case of breath holding (after exhalation), the raw score of P₁₀ and P₉₀ were 23.27 Secs and 92.11 Secs respectively, whereas the score of P₅₀ was 37.08 Secs.

Table 2: Percentile grading of breathe holding capacity after inhalation

Raw Score	Percentile	Grading
71.59 – 92.47	P91 – P99	Excellent
60.89 – 69.56	P76 – P90	Good
36.08 – 60.43	P26 – P75	Average
29 – 35.56	P11 – P25	Fair
<28.7	Below P10	Poor

Shown that the percentile grading <28.7 is poor, 29-35.56 is fair, 36.08-60.43 is average, 60.89-69.56 is good, and 71.59-92.47 is excellent.

Table 3: Percentile grading of breathe holding capacity after exhalation

Raw Score	Percentile	Grading
62.74 – 92.11	P91 – P99	Excellent
47.92 – 60.26	P76 – P90	Good
29.69 – 47.55	P26 – P75	Average
23.72 – 29.57	P11 – P25	Fair
<23.27	Below P10	Poor

Similarly, Table indicates that percentile grading <23.27 is poor, 23.72-29.57 is fair, 29.69-47.55 is average, 47.92-60.26 is good, and 62.74-92.11 is excellent.

Findings on Breathe holding time (after inhalation Vs after exhalation)

The result of normative study, as presented above, infers that the norms of breathe holding capacity (after inhalation and after exhalation) are applicable and gradable. However, the raw score of 50th percentile (i.e., P₅₀) of breathe holding capacity after inhalation was 46.81 (secs) and after exhalation was 37.08. This indicates that the mean values viz., 46.81 (after inhalation) and 37.08 (after exhalation) are different. Therefore, the significant difference, if any, was determined by using 't' test and the level of significance was set at 0.05 level.

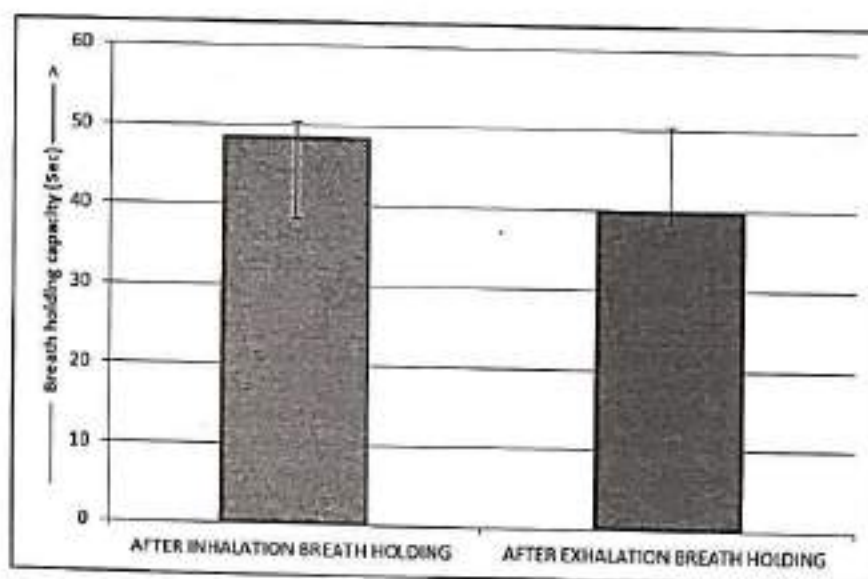
Table 4: Comparison on breath holding capacity after inhalation Vs after exhalation (n = 300)

Sl. No.	Variables	P ₅₀ values (Mean)	MD	SEM	t-value
1	After Inhalation	48.57	8.505	0.91	-6.6
2	After Exhalation	40.065			

*p<0.05, **p<0.01

The result of 't' test revealed that mean values of Breathe holding capacity after inhalation and after exhalation were different (t = -6.6, p<0.05). This result indicates that breathe

holding time after inhalation was greater than the breath holding time after exhalation.



Mean percentile values after inhalation and after exhalation (Breath Holding capacity)

Discussion of Findings

By keeping in mind the importance of the test taken for the breath holding capacity, the researcher has conducted this piece of research. There were 300 male students from different Physical Education institutes of Pune city. Breath holding capacity has been measured by using a stop watch and the time was recorded in Secs.

In fact, breathe holding capacity determines the better functioning of the respiratory system in human. There are two ways by which breathe holding capacity can be measured – 1) after inhalation and 2) after exhalation.

The result of the present investigation revealed that percentile norms of breath holding capacity (either after inhalation or after exhalation) are applicable to predict the respiratory function ability of the collegiate youths.

Further, the comparative result indicates that generally, the breathe holding time after inhalation was found greater than the breathe holding time after exhalation. As per traditional yoga, breathe holding capacity after inhalation is called antar kumbhaka and breathe holding capacity after exhalation is called bahya kumbhaka. Although both these kumbhakas are useful in pranayama, the most important factor is maintenance time of each kumbhaka. The result of the present study infers that the maintenance time of breath holding after inhalation was better than the maintenance time of breath holding after exhalation. The norms as obtained in this investigation would benefit the aspirants who intend to evaluate his/ her functional ability of respiratory system.

Discussion of Hypothesis

The result of normative study indicates that the norms of breath holding capacity (after inhalation and after exhalation) provide a quantitative measure to evaluate the breath holding time of the collegiate youths and the norms are also found gradable. Thus, the hypothesis – “H₁ –The normative scale would provide a quantity standard to measure the performance of collegiate students on breath holding capacity after inhalation and after exhalation” has been sustained. Therefore, the normative scale could provide a quantity of standard to measure the breath holding capacity of collegiate students.

Further, the result inferential statistics indicates that there was statistically significant difference in breath holding capacity of collegiate students after inhalation and after exhalation ($t=2.13, p<0.05$). This result in turn suggests that the null hypothesis- “H₀ –There would be no difference in breath holding capacity after inhalation and breath holding capacity after exhalation” has been refuted.

Summary

The purpose of the study has been to assess the Breath holding capacity of the collegiate students of physical education in Pune city, whether the norms of breath holding capacity can be established and whether the breath holding capacity is more or less before exhalation and after exhalation. For this purpose, 300 subjects were selected as a sample. The age group of subjects has been ranged in between 22+ years. Considering the steps of normative study, the data have been collected by the researcher and analyzed through Mean, Standard Deviation, Percentile, and ‘t’ test methods. The level of significance has been set at 0.05 level of confidence.

The finding of this study showed that the norms of breath holding capacity before-inhalation and after-exhalation can be applied to find the position of a breath holding related

performance score in different sport events. Moreover, percentile norms (P₉₅, P₇₅, P₅₀, P₂₅, and P₁₀ scores on breath holding capacity after inhalation were 92.47, 60.43, 46.81, 35.56 and 28.70, whereas the scores on breath holding capacity after exhalation were 92.11, 47.55, 37.08, 29.57 and 23.27 respectively) graded as per Likert’s five point scale may be treated as indicator to one’s anaerobic capacity related to sports performance and associated functional ability of circulo-respiratory system. However, accumulating evidence suggest that breath holding may be a useful method to help increase overall fitness abilities.

The result on comparative difference in breath holding time ($t=-6.6, p<0.05$) indicates that breath holding after inhalation was greater than after exhalation. This in turn suggests that retention of breath can initially be practiced after inhalation and after mastery over such practice breath-retention after exhalation may be practiced to enhance anaerobic capacity maximally, which in fact improves sports performance.

Although this study does not claim about its cure but firmly believes that progressive part of breath holding intervention may obviously increase capacity of collegiate students. However, other researchers being engaged with this field has also been benefited by the result of the present study.

Conclusion

Based on the findings of the study and within the limitations, the following conclusions were drawn-

- The norms of breathing holding capacity (after inhalation and after exhalation) are applicable to grade the collegiate students on their rich functional ability of circular-respiratory system which is useful for every sports person.
- Breath holding time after inhalation is higher than the breath holding time after exhalation.

Contribution to the knowledge

Literature revealed that several trails have been made so far on breath holding capacity along with moderate health of collegiate students. However, the quality of performance has been increased according to the increment of trail. This study contributed an evidence of trails on finding out the norms of breath holding capacity and the results have been found amazingly favourable among the collegiate students. This study, therefore, made a special contribution to the knowledge in the field of yoga and physical education in India.

References

1. Cialdini RD. Crafting normative messages to protect the environment. (Current Directions in Psychological Science), 2003, 105-109.
2. Lapinski MK, Rimal RN. An explication of social norms. (Communication Theory), 2005, 127-147.
3. Hackman JR. Group influences on individuals in organizations. (Handbook of industrial and organizational psychology, Palo Alto: Consulting Psychologists Press). 1992, 234-245.
4. Feldman DC. The development and enforcement of group norms. Academy of Management Review, 1999; 9(1):47-55.
5. Bijlani RL. Understanding Medical Physiology. 3rd ed. (New Delhi-India: Jaypee Brothers Medical Publishers). 2004, 307.
6. Nunn JF. Chapter 2: Control of breathing: breath holding. In: Applied respiratory physiology. 2nd ed. (London, England: Butterworth), 1977, 95.

7. Godfrey S, Campbell EJ. Mechanical and chemical control of breath holding. Quarterly Journal of Experimental Physiology Cognitive Medical Science. 1969; 54:117-128.
8. Godfrey S, Campbell EJ. The control of breath holding. (Respiratory Physiology). 1968, 385-400.
9. Fowler W, Breakpoint of breath holding. Journal of Applied Physiology. 1954; 6:539-545.
10. Kesavachandran C, Nair HR, Shashi Dhàr S. Lung volumes in swimmers performing different styles of swimming. Indian J Medical Science. 2001; 26:669-676.
11. Parkes MJ. Breath-holding and its breakpoint, Experimental Physiology. 2006; 91(1):1.
12. Singh Bhupinder, Singh Ghuman Kuldip. Effects of Selected Pranayams on Breath-Holding Capacity, Cardio-Vascular Endurance & Reaction. IOSR Journal of Sports and Physical Education (IOSR-JSPE). 2014; 1(3):40-44.
13. Rai Vaibhav. Effect of Pranayama on Breath Holding Time of School Going Children of mahilpur. Journal of educational and practice. 2014; 5(26):13-18.
14. Singh. The study on physical fitness norms of Punjab state high school boys (Retrieved on 18 august from http://shudhganga.inflibnet.ac.in/bitstream/10603/9607/1/0/10_chapter%202.pdf), 1986, 22.
15. Box DL. Physical Ability Testing of Male students in Grade four through twelve, (Completed Research in Health Physical education and Recreation), 1967, 77.
16. Coutts KD. Application of Cooper's 12 Minute Run/Walk Test to Young Males, (Research Quarterly), 1971, 54.
17. Tiwari Anil. development of Anthropometric Norms, Among the Age Group 9-10 years of school Children, (Friends Publications, India, Delhi-09), 2003, 175-176.
18. Kumar Anil. Development of norms for the two hand-eye co-ordination test, (Friends publications, India, Delhi. 2003; 09:150-151.

WWW.IJRAR.ORG

UGC and ISSN Approved, 5.75 Impact Factor

editor@ijrar.org

UGC and ISSN Approved

An International Open Access Journal
UGC and ISSN Approved | E-ISSN 2348-1269,
P- ISSN 2349-5138

INTERNATIONAL
JOURNAL OF RESEARCH
AND ANALYTICAL REVIEWS

IJRAR.ORG

INTERNATIONAL JOURNAL OF RESEARCH
AND ANALYTICAL REVIEWS (IJRAR)

*International Peer Reviewed, Open Access
Journal*

E-ISSN 2348-1269, P- ISSN 2349-5138 | Impact factor: 5.75 | ESTD Year: 2014

UGC and ISSN Approved and added in the UGC Approved List of Journals .

Website: www.ijrar.org



Website: www.ijrar.org

IJRAR

BEHAVIOR PROFILE OF ELITE TRACK AND FIELD ATHLETES

SAJAL MAJI*

*Guest lecturer, Achhruram Memorial College, Jhalda, Purulia-723202.

ABSTRACT:

The purpose of the study was, "Behavior profile of elite track and field athletes." The Researcher selected on the different sports clubs in Pune city for research purpose. Total 30 subjects for the study in which (N=30) and with the range of age is 18-24 years was selected for the data collection as per simple random technique method. After that researcher collects the data, from those athletes with the help of Behavior questionnaire.

After the data collection the researcher analyses the data with the help of descriptive statistics (Mean, SD, Hotelling t^2 -test).

KEYWORD: Behavior, Track & field, Athletes.

INTRODUCTION

Behavior is the range of actions and mannerisms made by individuals, organisms, systems, or artificial entities in conjunction with themselves or their environment, which includes the other systems or organisms around as well as the (inanimate) physical environment. It is the response of the system or organism to various stimuli or inputs, whether internal or external, conscious or subconscious, overt or covert, and voluntary or involuntary. Taking a behavior informatics perspective, a behavior consists of behavior actor, operation, interactions, and their properties. A behavior can be represented as a behavior vector. The behavior of humans (and other organisms or even mechanisms) falls within a range with some behavior being common, some unusual, some acceptable, and some beyond acceptable limits. In sociology, behavior in general includes actions having no meaning, being not directed at other people, and thus all basic human actions. Behavior in this general sense should not be mistaken with social behavior, which is a more advanced social action, specifically directed at other people. The acceptability of behavior depends heavily upon social norms and is

regulated by various means of social control. Human behavior is studied by the specialized academic disciplines of psychiatry, psychology, social work, sociology, economics, and anthropology.¹

Human behavior can either be premeditated by an individual or happen as a result of pressure, coercion and nudges. For example, teenagers and youth are influenced to act, dress, speak and think in certain ways by their role models. In addition, their mentors and peers can positively or negatively affect their behavior. These actions are also dependent on the capabilities and limitations of a person. For example, a person who is physically disabled may not have the predisposition to engage in competitive sports like able-bodied people.²

Human behavior refers to the array of every physical action and observable emotion associated with individuals, as well as the human race as a whole. While specific traits of one's personality and temperament may be more consistent, other behaviors will change as one moves from birth through adulthood. In addition to being dictated by age and genetics, behavior, driven in part by thoughts and feelings, is an insight into individual psyche, revealing among other things attitudes and values. Social behavior, a subset of human behavior, study the considerable influence of social interaction and culture. Additional influences include ethics, encircling, authority, rapport, hypnosis, persuasion and coercion.

Human behavior is experienced throughout an individual's entire lifetime. It includes the way they act based on different factors such as genetics, social norms, core faith, and attitude. Behavior is impacted by certain traits each individual has. The traits vary from person to person and can produce different actions or behavior from each person. Social norms also impact behavior. Due to the inherently conformist nature of human society in general, humans are pressured into following certain rules and displaying certain behaviors in society, which conditions the way people behave. Different behaviors are deemed to be either acceptable or unacceptable in different societies and cultures. Core faith can be perceived through the religion and philosophy of that individual. It shapes the way a person thinks and this in turn results in different human behaviors. Attitude can be defined as "the degree to which the person has a favorable or unfavorable evaluation of the behavior in question." One's attitude is essentially a reflection of the behavior he or she will portray in specific situations. Thus, human behavior is greatly influenced by the attitudes we use on a daily basis.³

Factors that affect human behavior include attitude, perception, genetics, culture, social norms and ethics of a society, religious inclination, coercion and influence by authority. Human behavior is defined as the range of actions and behaviors exhibited by humans at certain stages of development.

¹A. Minton Elizabeth and R. Khale Lynn, "Belief systems, religion, and behavioral economics." (New York: Business Expert Press, 2014), LLC. ISBN 978-1-60649-704-3.

²Longbing Cao, "In-depth Behavior Understanding and Use: the Behavior Informatics Approach". *Journal Information Science*, 180;(17), 2010, pp. 3067-3085.

³I. Ajzen and M. Fishbein, "Theory of reasoned action/Theory of planned behavior." (University of South Florida. Worth Publishers, 1999). ISBN 978-1-4292-4215-8.

Track and Field athletes

Track and field is a sport which includes athletic contests established on the skills of running, jumping, and throwing. The name is derived from the sport's typical venue: a stadium with an oval running track enclosing a grass field where the throwing and jumping events take place. Track and field is categorized under the umbrella sport of athletics, which also includes road running, cross country running, and race walking.

The foot racing events, which include sprints, middle- and long-distance events, race walking and hurdling, are won by the athlete with the fastest time. The jumping and throwing events are won by the athlete who achieves the greatest distance or height. Regular jumping events include long jump, triple jump, high jump and pole vault, while the most common throwing events are shot put, javelin, discus and hammer. There are also "combined events" or "multi events", such as the pentathlon consisting of five events, heptathlon consisting of seven events, and decathlon consisting of ten events. In these, athletes participate in a combination of track and field events. Most track and field events are individual sports with a single victor; the most prominent team events are relay races, which typically feature teams of four. Events are almost exclusively divided by gender, although both the men's and women's competitions are usually held at the same venue.

It is one of the oldest sports. In ancient times, it was an event held in conjunction with festivals and sports meets such as the Ancient Olympic Games in Greece. In modern times, the two most prestigious international track and field competitions are athletics competition at the Olympic Games and the IAAF World Championships in Athletics. The International Association of Athletics Federations is the international governing body.

METHODOLOGY

This is a survey type of study under the descriptive research. The study evaluated the behavior profile of track and field athletes belonging to Pune city. Standard Procedure was followed to conduct this study. This chapter contains the method of research design, population, sample, tools used for research, apparatus or instrument employed, statistical tools, procedures etc that have been presented systematically. The data were collected with the help of standard questionnaire viz., BOS (Behaviour Orientation Scale). The methodology in details is given below.

Selection of the subject

Population

All the elite track and field male athletes (N= 300 approximately), age 18-24 yrs, representing different sports clubs in Pune city were considered as the population of this study.

The Sample

Out of the population, the researcher selected only three sports clubs viz. Pune Athletic Club (Sarasbaug), Sarasbaug Sports Club and Balewadi Sports Club (Balewadi) for data collection considering purposive sampling technique. Further, total thirty (n= 30) elite male track and field athletes, age 18-24 yrs, representing three different sports clubs from Pune city were selected considering random sampling technique i.e., 10 athletes from each of the three clubs. The clubs which have been selected with the number of athletes were given below (Table 3.1).

Variables

There was only one variable "Behaviour profile" chosen for track and field athletes.

Tools used

The researcher has gone through the available literature in the library, reports of previous research studies and webs. Further, after a thorough discussion with the research guide, following questionnaire for survey have been chosen, which is easy to conduct in the field situation and requires minimum assistants, less money and less time.

The standard questionnaire administered in this study is given below

Sl. No	Questionnaire	Author	Purpose of the test
1.	Behavior Oriental Questionnaire (Machiavellianism Scale) in 2005	Dr. Prveen Kumar Jha	To measure the behavior profile of track and field athletes

The standard *BOS* questionnaire constructed by Dr. Praveen Kumar Jha has accepted level of reliability (0.39) and Validity (0.262).. There were 41 test items which were assessed with five points scale. The scores were expressed in points.

Statistical Design

- Descriptive statistics have been employed to process the data. Further, for profile analysis of behavior, *Hottelling²-test* was employed.

ANALYSIS OF DATA

The data on survey of behavior profiles variables collected from 30 male elite athletes in Pune city has been analyzed statistically by employing *Hottelling T²-test* and the results have been presented in this chapter in the form of tables and graphs.

Results of *Hottelling's T² test* on overall analysis of behaviour profiles of Track and Field athletes

The values of mean and SD on behavior profiles of the athletes were calculated and presented in Table 4.1.

Further, the related results on behavior profiles (analyzed by employing *Hottelling T²-test*) of the track and field athletes are presented in Table 4.2.

Table 4.1

Descriptive statistics of overall Behavior profiles of the track and field athletes

Sl. No	Dimensions	Mean	SD
1	Tactics	55.2	4.03
2.	Views	72	5.28
3.	Morality	17.76	2.67
4.	Behavior profile	144.96	8.79

Table 4.1 shows that the Mean and SD values of behaviour profiles on 30 male track and field athletes. The behavioural dimensions included in this study were *Tactics, Views and Morality*. The mean achievement values of *Tactics, Views and Morality* were 55.2 (SD=4.03), 72 (SD=5.28), and 17.76 (SD=2.67) respectively. The result indicates that the *Views-dimension of the athletes had highest score in behavior aspect, than the abilities of Tactics and Morality*. The mean achievement on overall behavior profile of the selected athletes was 144.67 (SD= 8.79).

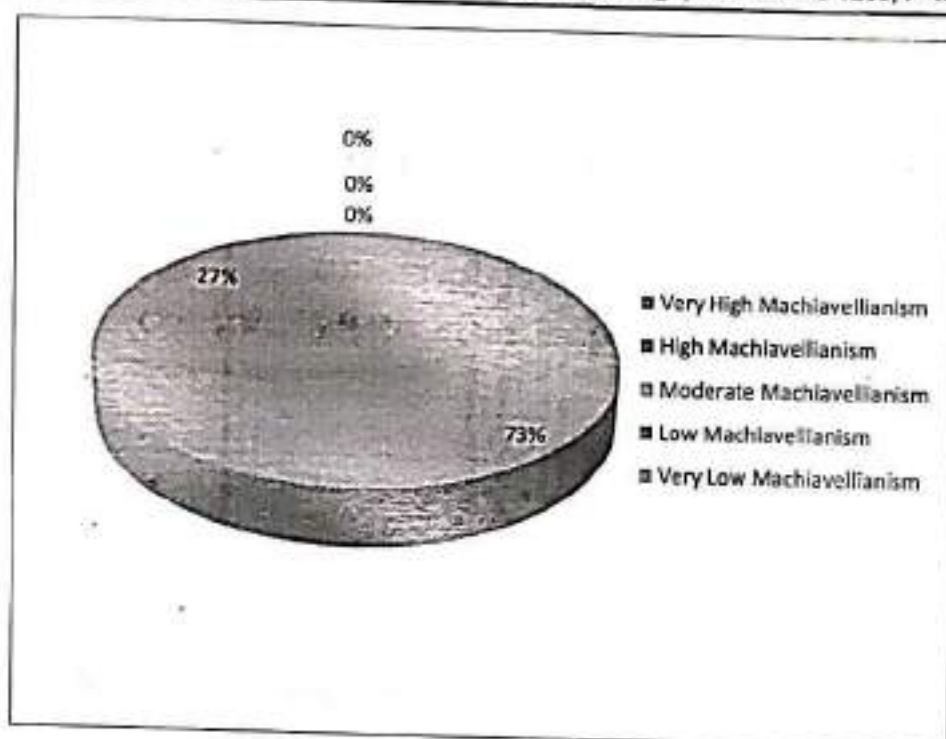


Fig 4.1 Overall norms observed in behavior profiles of athletes

The diagram (Fig. 4.1) revealed that the norms on behavior profile of the athletes are found Very high Machiavellianism 73%, High Machiavellianism 27%, Moderate Machiavellianism 0%, Low Machiavellianism 0% and Very low Machiavellianism 0%. This helps to interpret that the selected athletes possessed a range between moderate to very high Machiavellianism.

Table 4.2

Results on Hottelling T^2 test on Behavior profile of runners, jumpers and throwers

Sl. No	Dimensions	Hotteling t^2 test
1.	Runners	0.1
2.	Jumpers	0.06
3.	Throwers	0.07

Table 4.2 shows that the results of Hottelling T^2 test, where profiles on Runners, Jumpers and throwers were different. In fact, Runners profile ($T^2=0.1$) showed higher value than the values of Jumpers profile ($T^2=0.06$) and Throwers profile ($T^2=0.07$) respectively. This, in turn, helps to interpret that the Jumpers profile could achieve a low status as compared to the Runners profile and Throwers profile. This ensures that the selected athletes are more confined to Jumpers profile rather than other two profiles possessed further lower

value ($T^2=0.06$) that seems to reasonably good. Finally, the behavior profile of the selected events is found favorable.

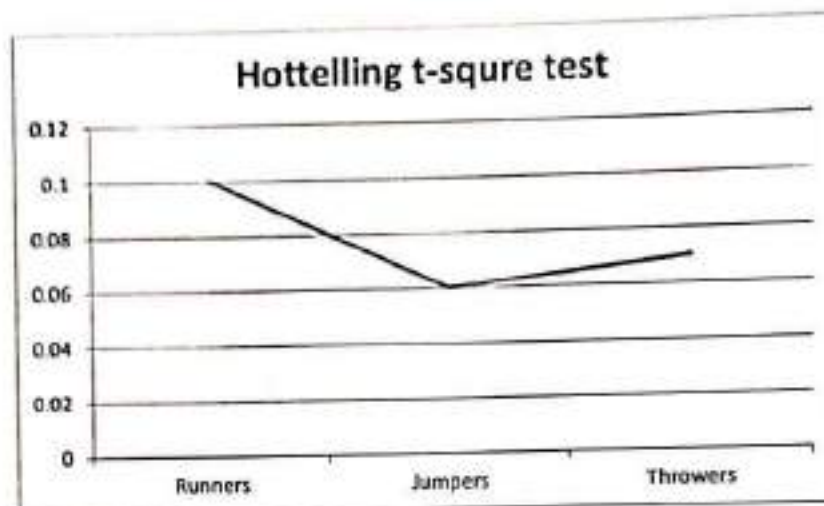


Fig 4.2 Track and Field events observed in profiles analysis of athletes

The diagram (Fig. 4.2) revealed that the behavior profile of the Runners, Jumpers and Throwers are different. This, in turn, helps to interpret that the Jumpers profile of the athletes could achieve a low status as compared to the Runners profile and Throwers profile.

Level of Significance: 0.01.

Tabulated value: 2.58

Table 4.3

Results on Hottelling T^2 test on Behavior profile and its dimensions of the athletes

Sl. No	Dimensions	Hottelling t^2 test
1.	Tactics	0.9
2.	Views	0.53
3.	Morality	2.04
4.	Behavior Profile	0.19

Table 4.3 shows that the results of Hottelling T^2 test, where profiles on Tactics, Views and Morality were different. In fact, Morality profile ($T^2=2.04$) showed higher value than the values of Tactics profile ($T^2=0.90$) and Views profile ($T^2=0.53$) respectively. This, in turn, helps to interpret that the Views profile of the athletes could achieve a low status as compared to the Tactics profile and Morality profile. This ensures that the selected athletes are more confined to Views profile rather than other two profiles and the overall behavior

profile possessed further lower value ($1^2 = 0.19$) that seems to reasonably good. Finally, the behavior profile of the selected athletes is found favourable.

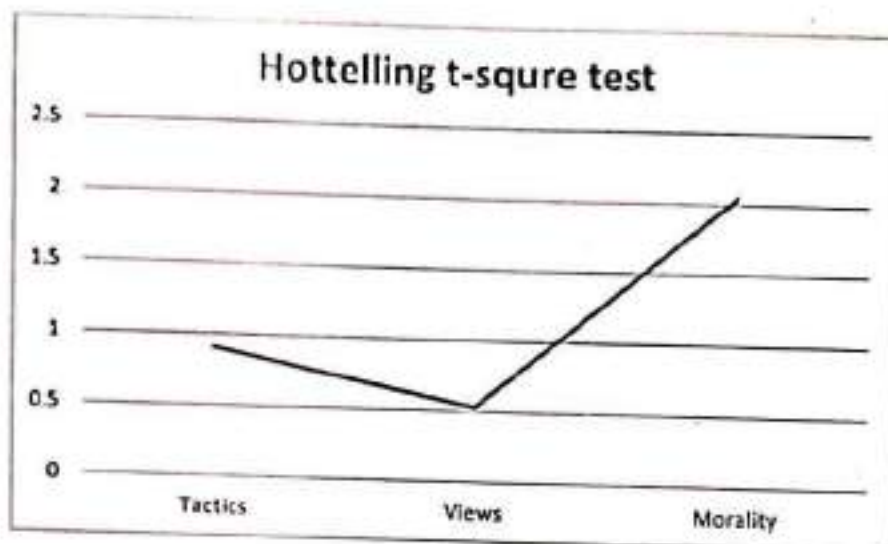


Fig 4.3 Overall factors observed in profiles analysis of athletes

The diagram (Fig. 4.3) revealed that Tactics, Views and Morality on behavior profile of the athletes are found different level of profile analysis. This, in turn, helps to interpret that the Views profile of the athletes could achieve a low status as compared to the Tactics profile and Morality profile.

Level of Significance: 0.01.

Tabulated value: 2.58

Discussion of Findings

By keeping in mind the importance of the test taken for the behavior profiles, the researcher has conducted this piece of research. There were 30 athletes from different institutes/clubs of Pune city. Behavior profiles have been measured by using questionnaires was recorded in marks.

Human behavior consists of different types of thought and behaviour layers which make every individual differ from each other. Hence, to understand human behavior profile the impact of psychology comes into existence. Psychology plays a role to connect between application of behavior profile, educational and theoretical science in every field including in the area of track and field athletics. It is the study of behaviour, performance and the mental operations of people. Thus, measuring and analyzing behavioural profiles may predict the usage and application of skill, knowledge and understanding various activities undertaken by humans and how they are used through daily activities, whether that is within events, talking to people, education and employment, relationships, treating mental health issues and even in the field of sports.

The research studies conducted on different human or people from different occupation revealed that one's behavior profile is very much influenced by the surrounding where he / she works or lives. This is, in fact, equally true in the case of track and field athletes.

This study was an endeavor in similar way to find out and compare the behavior profile among track and field athletes. In this aspect, the researcher had selected 30 athletes and the result revealed that -

- Behaviour profiles of the athletes represent three major profiles viz., Tactics, Views and Morality and they need to be inculcated to achieve better performance.
- There was significant difference between tactics profile, views profile and with the profile of morality of the selected athletes.
- There was significant difference in behaviour profiles between Runners, Jumpers and Throwers in track and field athletics.

Discussion of Hypothesis

The discussion presented above indicates that there exists statistically significant difference in behavior profiles of the runners, jumpers and throwers of track and field athletics. Appearance of such result infers that the hypothesis "*H₁-Behavior profiles of the runner, thrower and jumper may be different*" formulated in this investigation has been sustained. This, in turn, indicates that behavior profiles of the selected athletes of running, throwing and jumping events are not same and therefore they should be trained considering different strategies.

Summary

In this chapter the summary of the entire previous chapters has been illustrated.

The purpose of the study has been to assess behavior profile of track and field athletes in Pune city. For this purpose, 30 male athletes were selected as a sample. The age group of subjects has been ranged in between 18-24 years. Considering the steps of a descriptive study, the data have been collected by the researcher and analyzed through Mean, Standard Deviation. Further Profile analysis of athletes' behavior was done employing 'Hotelling t^2 -test' method. The level of significance has been set at 0.01 level of significance.

The BOS (Behaviour Oriental questionnaire) from national psychological corporation, Agra, developed by Dr. Prveen Kumar Jha was administered on specific groups track and field athletes exclusively on runners, jumpers and throwers. The collected data seems to be reliable and valid because the test administered is reliable and valid.

In order to determine and compare the Behavior profile of track and field athletes, the result of Hotelling t^2 -test was set with the tabulated value 2.58. The findings of Hotelling indicate that the behavioural

profiles on Tactics, Views and Morality were different among different types of athletes (runners, throwers and jumpers). In fact, Morality profile ($T^2=2.04$) showed higher value than the values of Tactics profile ($T^2=0.90$) and Views profile ($T^2=0.53$) respectively. This, in turn, helps to interpret that the Views profile of the athletes could achieve a low status as compared to the Tactics profile and Morality profile. This ensures that the selected athletes are more confined to Views profile rather than other two profiles and the overall behavior profile possessed further lower value ($T^2=0.19$) that seems to reasonably good. Finally, the behavior profile of the selected athletes is found although favourable, but is different according to the nature of sports events.

Conclusion

Based on the findings of the study and within the limitations, the following conclusions were drawn-

- Out of three components of behaviour profile, the views profile was found dominant among the track and field athletes.
- There was significant difference between behaviour profiles of Runners, Jumpers and Throwers in track and field athletics.

REFERENCES

- A. Minton Elizabeth and R. Khale Lynn, "Belief systems, religion, and behavioral economics." (New York: Business Expert Press, 2014), LLC. ISBN 978-1-60649-704-3.
- Longbing Cao, "In-depth Behavior Understanding and Use: the Behavior Informatics Approach". *Journal Information Science*, 180:(17), 2010, pp. 3067-3085.
- I. Ajzen and M. Fishbein, "Theory of reasoned action/Theory of planned behavior." (University of South Florida. Worth Publishers, 1999), ISBN 978-1-4292-4215-8.

Ethnobotanicals used for the Treatment of Skin Diseases with Special Emphasis on Carbuncle Disease from Purulia District of West Bengal in India

Ghanashyam Mahato¹, Bangamoti Hansda², Nilanjana Banerjee^{3,*}

Ghanashyam Mahato¹,
Bangamoti Hansda²,
Nilanjana Banerjee^{3,*}

¹Assistant Professor, Department of Botany, A.M. College, Jhalda, Purulia, West Bengal-723202, INDIA.

²Research Scholar, Department of Botany and Forestry, Vidyasagar University, Midnapore, West Bengal-721102, INDIA.

³Assistant Professor, Department of Botany, Vidyasagar University, Paschim Medinipur, West Bengal-721102, INDIA.

Correspondence

Nilanjana Banerjee

Assistant Professor, Department of Botany, Vidyasagar University, Paschim Medinipur, West Bengal-721102, INDIA.

Phone no: 919836960317;

E-mail: nilanjanab1@yahoo.com

History

- Submission Date: 13-10-2018;
- Review completed: 06-04-2019;
- Accepted Date: 21-04-2019.

DOI : 10.5530/pj.2019.11.118

Article Available online

<http://www.phcogj.com/v11/i4>

Copyright

© 2019 Phcogj.Com. This is an open-access article distributed under the terms of the Creative Commons Attribution 4.0 International license.

ABSTRACT

Background: From time immemorial ethnic people of Purulia district of West Bengal are well acquainted with different plant resources for the treatment of various skin diseases including 'carbuncle' and others skin diseases. Carbuncle, caused by the methicillin resistant *Staphylococcus aureus* is of major concern in this part of India, mostly dominated by tribes like Majhi, Munda, Santal, Birhor, Ho and Rajwar etc. Hot climate, overcrowded households, improper sanitation, very poor economic background and frequent burn accidents are of major issues for spreading of these bacterial infections. **Objective:** Present authors are trying to summarize these ethno-medicinal knowledge of the local, conservative traditional healers by using structured questionnaires given to them and are trying to analyze these information from scientific perspective. **Materials and Methods:** Plant samples were collected from March 2014 to May 2016, mostly during their flowering stage and a total of 62 people, both male (84%) and female (16%) were interviewed. Informant consensus factor, fidelity level and use value were calculated. **Results:** Fifty-nine herbal plants belongs to 35 families were recorded for the cure of various skin diseases, among which 10 plants are used individually during medication whereas 9 polyherbal formulations were used in various combinations during treatment. Five species of the families Moraceae and Asteraceae was found to be the most common medicinal plants, among which 44.89% are herbaceous in habit. Leaves (55.55%) are the most common plant part for their use. **Conclusion:** Therefore, the present paper has been written to document this rapidly vanishing huge knowledge of folklore which should be digitally conserved for futuristic approach on medicinal plants in India.

Key words: Ethnobotany, Carbuncle, Purulia, Use value, Informant consensus factor, Fidelity level.

INTRODUCTION

In ancient India plants were widely used for the treatment of skin disorders. In many countries till today, medicinal plants contribute significantly in the primary health care system of the rural population.¹⁻⁴ One of the most important skin ailments, mostly found in the tribal population of Purulia is **carbuncle** disease which is caused by the bacteria *Staphylococcus aureus*. However, the presence of carbuncle is actually the sign of active system to resist other skin infections.⁵ The infection is contagious and may spread to other areas of the body. Each year, around 500,000 patients in hospitals of the United States are attacked by Staphylococcal infection, chiefly by *S. aureus*.⁶ Since discovery *S. aureus* is experimentally resistant to a lot of antibiotics for example penicillin group (methicillin, oxacillin and cloxacillin),^{7,8} amino glycosides, macrolides, tetracycline, chloramphenicol and lincosamides. Vancomycin-resistant *S. aureus* (VRSA) is a strain of *S. aureus* that usually resistant to the glycopeptides. The first case of vancomycin-intermediate *S. aureus* (VISA) was reported in Japan in 1996.⁹

Since last two decades development of drug resistance as well as the appearance of undesirable

side effects of certain antibiotics lead us to search for new chemical structures having antimicrobial property from plant extracts.¹⁰ Although the people of Purulia traditionally used various herbal plants for preparing drugs and medicines to treat carbuncle and some skin diseases no such detail documentation has been done earlier. Hence, the primary objective of the present study is to investigate the folkloric wisdom practiced by the aboriginals residing in the Purulia district, one of the poorest district in India, against skin diseases with special emphasis on carbuncle.

MATERIALS AND METHODS

Study area

The study area is located in the western most part of West Bengal, India (Figure 1). This area is situated between 22°6' to 23°5' N latitude and 85°7' to 86°6' E longitude and has an area of 6259 km². Purulia district covers subtropical ecology with deciduous forest mainly with luxurious population of Sal, Palash, Piyal, Mohul etc. having high diurnal temperature during summer (upto 52°C) and with average rainfall 1300 mm. It is situated under Chotonagpur plateau having undulated topography and lateritic soil.

Cite this article: Mahato G, Hansda B, Banerjee N. Ethnobotanicals used for the Treatment of Skin Diseases with Special Emphasis on Carbuncle Disease from Purulia District of West Bengal in India. Pharmacogn J. 2019;11(4):745-53.

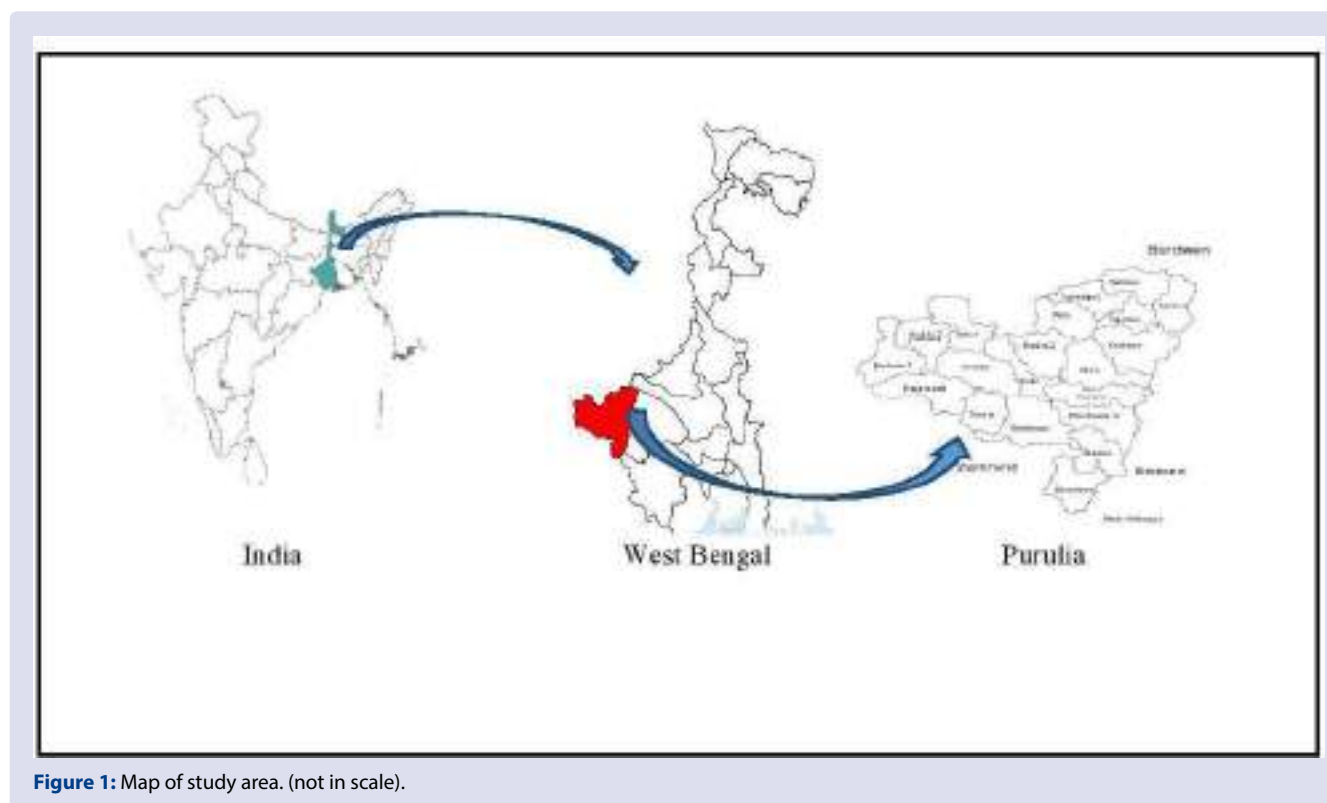


Figure 1: Map of study area. (not in scale).

Ethnobiological data collection and analyses

The survey was carried out from 20 field sessions based on ethnobiological explorations from 2014 to 2016. Main emphasis was given to the Maoist hot parts of the district. As GM, first author, knows some of the native languages of the tribes, semi structured questionnaires were placed to the informants following a standard ethnobotanical method in local vernacular or in Bengali.^{11,12} Herbarium specimens of these medicinal plants mostly in their flowering stage were collected for future references. The medicinal plant specimens were identified with the help of authentic herbarium specimens of Botanical Survey of India, books, floras and revisions¹³⁻¹⁶ and preserved, recorded and documented in the herbarium of Department of Botany, A. M. College, Jhalda.

Descriptive statistics were applied to compute the number and percentage of species, genera and families of ethnomedicinal plants, proportions of plant parts harvested, plant percentage from various sources, plant distribution among different families, life forms, nature of habitat and plant percentage in curing various ailments. Key informants are mostly more than fifty years old and are respectable persons of that locality (Figure 3). The collected data was analyzed with three quantitative tools viz. the informant consensus factor (F_{ic}), fidelity level (FL) and use value (UV). To test the level of homogeneity of information provided by different informants, Informants' Consensus Factor (F_{ic}) was calculated.¹⁷ $F_{ic} = \text{Nur} - \text{Nt} / (\text{Nur} - 1)$ (where Nur = number of use reports in each disease category; Nt = number of times species used). The value ranges from 0 to 1. High F_{ic} value (close to 1) means there is well-defined selection for the species on account of a specific disease category whereas low F_{ic} values (close to 0) indicate there is lack of consensus amongst the informants related to the medicinal uses of the species. Fidelity level (FL) index¹⁸ was used to determine the relative healing potential of each reported medicinal plant used against various ailments. Fidelity level (FL%) = $(N_p / N \times 100)$ (where N_p = the number of informants who independently indicated the use of a species for treating a particular disease and N = total number of informants who reported the plant for any given disease). The use value (UV)¹⁹ was

also calculated using the formula: $UV = (\Sigma U/n)$, where UV is the use value of species, 'U' is the total number of use reports per species and 'n' represents the total number of informants interviewed for a given plant. Values range from near 1 to 0. High UV means there are many use reports for a specific plant and that plant is marked important for treatment.

RESULTS

Ethnomedicinal plant diversity and uses reported by the informants

Medicinal plants were enlisted with scientific name and author citation, followed by local name, family, habit, plant part(s) used and ailment(s) against each disease (Table 1). A total number of 10 monoherbal formulations (MF) were recorded which were used singly for medication during treatment and 9 polyherbal formulations (PF) were used in combination by different ethnic groups of this area (Table 2). The highest number of medicinal plants were recorded in four families viz. Moraceae (5 species), Asteraceae (5 species), Amaranthaceae (4 species), Euphorbiaceae (3 species), Fabaceae (3 species) and Malvaceae (3 species), followed by families Amaryllidaceae, Asclepiadaceae, Solanaceae and Myrtaceae. Each of these families comprises two species.

The distribution of plant habit types, plant part(s) used and method of preparations are illustrated in Figures 2-4 respectively. Out of 59 species 44.89% herbaceous plants are mostly used for medication followed by 36.73% trees, 14.28% shrubs and 2.04% climbers (Figure 2). Leaves (55.55%) were found to be the most favored plant parts followed by roots (11.11%), whole plant (5.55%) and barks (5.55%) (Figure 3). Quantitative ethnobotanical analyses revealed high UV for *Curculigo orchioides* Gaertn. (0.81), *Hibiscus rosa-sinensis* L. (0.79), *Urginea indica* (Roxb.) Kunth (0.77), *Glossocardia bidens* (Retz) Veldkamp (0.88), *Smilax zeylanica* L. (0.82), *Elephantopus scaber* L. (0.72) etc. Highest F_{ic} value was represented by chicken pox (1), carbuncle (0.91) and ulcer (0.87) whereas lowest F_{ic} value was exhibited mouth ulcer (0) and nail

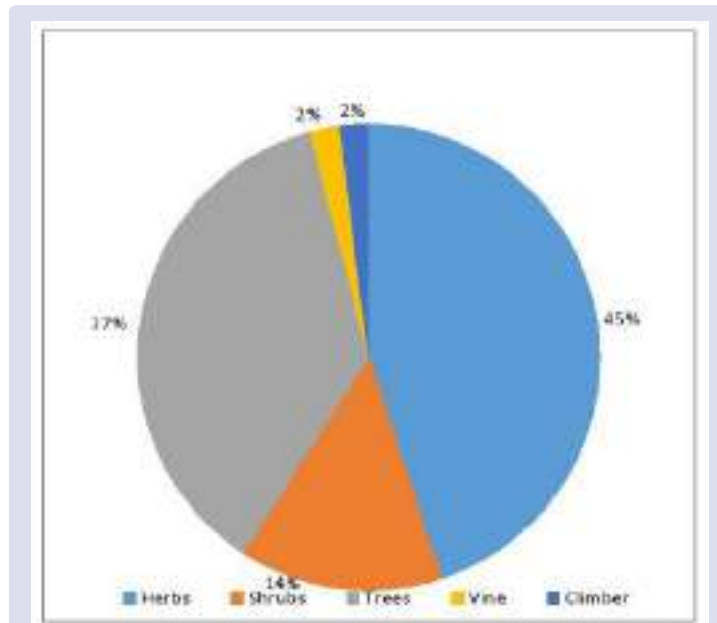


Figure 2: Percentage of habit types of the total studied plant specimens used for the treatment of carbuncle.

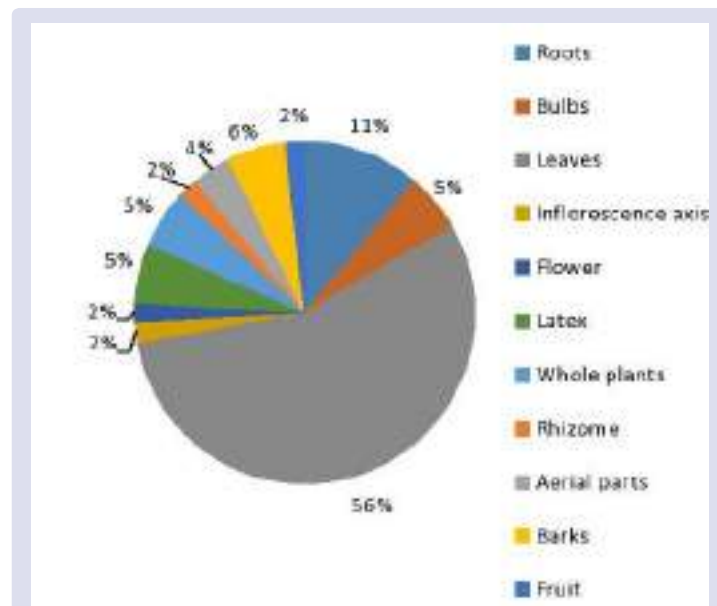


Figure 3: Percentage of plant parts used for medication.

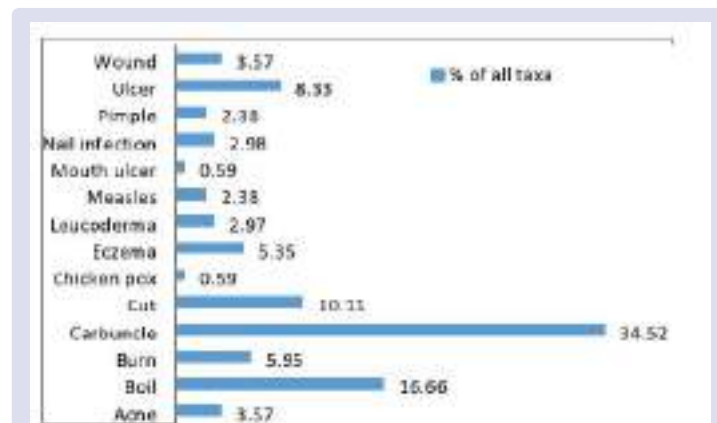


Figure 4: Percentage of species used for the treatment of a particular disease.

Table 1: Ethnobotanics used for carbuncle and some other skin diseases treatment.

Sl. No.	Latin name	Local Name	Family	Plant parts used	Ailments other than Carbuncle	UV value	Habit
1	<i>Achyranthes aspera</i> L.	Chitchiti	Amaranthaceae	Roots	Boi and Ulc	0.4	Herb
2	<i>Achyranthes bidentata</i> Blume	Chitni	Amaranthaceae	Roots	Mea	0.24	Herb
3	<i>Aerva sanguinolenta</i> (L.) Blume	Chaldhuya	Amaranthaceae	Aerial parts	Mea and Cut	0.42	Herb
4	<i>Ageratum conyzoides</i> L.	Bhabri	Asteraceae	Leaves	Cut,Boi	0.24	Herb
5	<i>Allium sativum</i> L.	Piyaj	Amaryllidaceae	Bulbs	Boi and Ulc	0.33	Herb
6	<i>Aloe vera</i> L.	Ghritakumari	Xanthorrhoeaceae	Leaves	Ulc,Cut,Acne and nail infection	0.54	Herb
7	<i>Amaranthus spinosus</i> L.	kata nate	Amaranthaceae	Leaves	Boi,Acne	0.22	Herb
8	<i>Andrographis paniculata</i> (Burm.f.) Wal. ex. Nes.	Kalmegh	Acanthaceae	Leaves	Ulc	0.43	Herb
9	<i>Annona squamosa</i> L.	Atapata	Annonaceae	Leaves	Boi and Pim	0.29	Tree
10	<i>Argemone mexicana</i> Linn	Siyalkata	Papaveraceae	Roots	Cut	0.21	Herb
11	<i>Artocarpus heterophyllus</i> Lam.	Kathal	Moraceae	Inflorescence axis(IA)	Boi and Leo	0.39	Tree
12	<i>Averrhoa carambola</i> L.	Kamranga	Oxalidaceae	Roots	Ulc	0.19	Tree
13	<i>Azadirachta indica</i> A. Juss.	Nim	Meliaceae	Leaves	Mea, Chick pox, Ulc and Boi	0.75	Tree
14	<i>Barleria lupulina</i> Lindl.	Bialyakaran	Acanthaceae	Leaves	Bur	0.26	Shrub
15	<i>Bauhinia purpurea</i> L.	kanchan	Leguminosae	Leaves	Boi and Bur	0.22	Shrub
16	<i>Boerhavia diffusa</i> L.	Kathasak	Nyctaginaceae	Leaves	Cut	0.39	Herb
17	<i>Bombax ceiba</i> L.	Bakul	Bombacaceae	Leaves	Mouulc	0.21	Tree
18	<i>Bryophyllum pinnatum</i> (Lam)Oken	Patharkuchi	Crassulaceae	Leaves	Boi	0.26	Herb
19	<i>Calotropis gigantea</i> (Linn.) R. Br.ex.Ait.	Akuni	Asclepidaceae	Leaves and Latex	Bur	0.37	Shrub
20	<i>Calotropis Procera</i> (Aiton) R. Br.	Akanda	Asclepidaceae	Leaves	Bur	0.26	Shrub
21	<i>Cannabis sativa</i> L.	Ganja	Cannabaceae	Leaves	Cut	0.12	Shrub
22	<i>Cotula anthemoides</i> L.	Tar dingla	Asteraceae	Whole plant	Ulc,Boi,Acne,Leo and Pim	0.88	Herb
23	<i>Crinum asiaticum</i> Linn.	Baniyaj	Amaryllidaceae	Bulbs	Boi	0.48	Herb
24	<i>Curculigo orchioides</i> Gaertn.	Talmuli	Hypoxidaceae	Roots	Boi,Bur,Leo and cut	0.81	Herb
25	<i>Curcuma longa</i> L.	Halud	Zingiberaceae	Rhizomes	Ulc ,Cut and Acne	0.52	Herb
26	<i>Cuscuta reflexa</i> Roxb.	Sarnalata	Convolvulaceae	Whole plant	Boi	0.47	Climber
27	<i>Cyperus rotundus</i> L.	Mutha	Cyperaceae	Whole plant	Ulc	0.47	Herb
28	<i>Datura metel</i> L.	Dhutra	Solanaceae	Leaves	Nail inf	0.15	Shrub
29	<i>Datura stramonium</i> L.,	Dhutrajhuri	Solanaceae	Leaves	Nail inf	0.09	Shrub
30	<i>Elephantopus scaber</i> L.	Mayurjhuti	Asteraceae	Roots	Boi,Bur and Ulc	0.42	Herb
31	<i>Euphorbia hirta</i> L.,	Lalpata	Euphorbiaceae	Aerial parts	Mea and Cut	0.42	Herb
32	<i>Euphorbia milii var. longifolia</i> D. Moul.	Latjhakha	Euphorbiaceae	Leaves	Bur	0.16	Herb
33	<i>Ficus benghalensis</i> L.	Asasta	Moraceae	Leaves and Bark	Pim	0.1	Tree
34	<i>Ficus hispida</i> L. f.	Dumur	Moraceae	Leaves and Latex	Boi and Bur	0.27	Tree
35	<i>Ficus racemosa</i> L.	Pagadumur	Moraceae	Leaves and Latex	Boi and Bur	0.39	Tree
36	<i>Ficus religiosa</i> L.	Jar	Moraceae	Leaves	Nail inf	0.03	Tree
37	<i>Gloriosa superba</i> Linn.	Barphuli	Colchicaceae	Leaves	Leo	0.22	Herb
38	<i>Glossocardia bidens</i> (Retz) Veldkamp	Pisainandi	Asteraceae	Whole plant	Ulc,Boi,Acne,Leo and Pim	0.88	Herb
39	<i>Gmelina arborea</i> Roxb. ex Sm.	Gamer	Lamiaceae	Barks	Wou and cut	0.24	Tree
40	<i>Hemidesmus indicus</i> (L.) R.Br.	Anantamuli	Apocynaceae	Aerial parts	Ecz and Ulc	0.47	Herb
41	<i>Hibiscus rosa-sinensis</i> L.	Jaba	Malvaceae	Leaves	Boi and Acne	0.79	Shrub
42	<i>Lawsonia inermis</i> L.	Natur	Lythraceae	Leaves	Cut	0.21	Shrub
43	<i>Lippia alba</i> (Mill.)N.E.Br.ex Britton and P.Wilson	laltia	Verbenaceae	Aerial parts	Ecz	0.47	Herb
44	<i>Madhuca longifolia</i> (Konig) J.F.Macbr.	Mahua	Sapotaceae	Flower	Boi, Ulc and Bur	0.58	Tree
45	<i>Magnifera indica</i> L.	Aam	Anacardiaceae	Leaves	Ecz and wou	0.4	Tree
46	<i>Piper betle</i> L.	Pan	Piperaceae	Leaves	Boi	0.5	Vine
47	<i>Polygala crotalaroides</i> Buch.-Ham. ex Dc.	Nilkantha	Polygalaceae	Root	Boi	0.45	Herb
48	<i>Psidium guajava</i> L.	Peyara	Myrtaceae	Leaves	Ecz and Nail inf	0.19	Tree
49	<i>Pterocarpus santalinus</i> L.f.	Set chandan	Fabaceae	Barks	Boi,Ecz and Wou	0.64	Tree
50	<i>Ricinus communis</i> L.	Jara	Euphorbiaceae	Leaves	Boi and cut	0.4	Tree
51	<i>Shorea robusta</i> Gaertn.	Sal	Dipterocarpaceae	Leaves	Boi,Ecz and Wou	0.42	Tree

Sl. No.	Latin name	Local Name	Family	Plant parts used	Ailments other than Carbuncle	UV value	Habit
52	<i>Sidacordata</i> (Burm. f.) Borss. Waalk.	Laltoa	Malvaceae	Leaves	Ecz	0.32	Herb
53	<i>Sida cordifolia</i> L.	Chalpata	Malvaceae	Leaves	Boi and cut	0.48	Herb
54	<i>Smilax zeylanica</i> L.	Ramdatun	Smilacaceae	Roots	Boi,Ecz and Wou	0.42	Shrub
55	<i>Syzygium cumini</i> (L) Skeels	Jam	Myrtaceae	Leaves	Wou and cut	0.63	Tree
56	<i>Tagetes patula</i> L.	Gandha	Asteraceae	Leaves	Cut and Ecz	0.6	Herb
57	<i>Tamarindus indica</i> L.	Tetul	Leguminosae	Leaves and Fruits	Boi and Ulc	0.73	Tree
58	<i>Urginea indica</i> (Roxb.)Kunth	Banpiyaj	Liliaceae	Bulbs	Boi,Leo, Cut and Ulc	0.77	Herb
59	<i>Vitex negundo</i> L.	Buyan	Verbenaceae	Leaves	Cut and Boi	0.61	Shrub

Wou = wound; Boi = Boil; Cut = Cut; Ulc = Ulcer; Leo = Leukoderma; Ecz = Eczema; Nail inf = Nail infection; Pim = Pimple; Mea = measles; Moulc = Mouth ulcer; Chick pox = Chicken pox; Bur = Burn; Acn = Acne;Car = Carbuncle.

Table 2: Details of formulations for medication.

Formulations	Plant species used singly / combinations	Parts used	Additives	Method of preparation	Mode of administration
MF1	<i>A vera</i>	L	Water	Paste	Apply on Carbuncle
MF2	<i>A indica</i>	L	Water	Form small pea sized pills	Once a day before breakfast
MF3	<i>C gigantea</i>	L + LA	NR	Burn to form ash	Apply on mouth of Carbuncle
MF4	<i>D metel</i>	L	NR	Burn to form ash	Apply on mouth of Carbuncle
MF5	<i>D stramonium</i>	L	Milk; Rhizome of kanchahalud/turmaric	Paste	Apply on Carbuncle
MF6	<i>V negundo</i>	L	Jira/Cumin seeds	Paste	Apply at starting time
MF7	<i>C anthemoides</i>	WH	Honey	Form small sized pills	Three times in a day before meal
MF8	<i>C viviparum</i>	BU	Milk from sheep	paste	Apply on mouth for seven days
MF9	<i>C orchioides</i>	RH	Water	Form small pea sized pills	Two times before to take meal
MF 10	<i>G bidens</i>	WH	Water	Paste	Applied on the affected parts twice a day for five days
PF1	<i>A aspera</i> + <i>A sativum</i> + <i>A paniculta</i> + <i>A squamosa</i> + <i>A heterophyllus</i> + <i>A indica</i> + <i>C viviparum</i> + <i>G bidens</i> + <i>A sanguinolenta</i> <i>A carambola</i> + <i>C Procera</i> + <i>C longa</i> + <i>E scaber</i> + <i>R communis</i> + <i>A vera</i> + <i>C anthemoides</i> + <i>A indica</i> + <i>L alba</i> <i>F recemosa</i> + <i>H rosa-sinsnsis</i> + <i>P guajava</i> + <i>S cordata</i> + <i>S cumini</i> + <i>C anthemoides</i> + <i>S zeylanica</i> + <i>A conyzoides</i>	R+BU+L+L+IA +L+BU+A+A	Talmichri made from palm tree; Honey	Grinding all the items, small pea-sized pills are made from a paste	Once in a day for five days
PF2		R+L+Rh +R +L +L+WH+L+L	Kalajira; Mirchi	After grinding all the ingredients pills are prepared from a paste	Thrice a day
PF3		L+L+L+L +L +WH+RT+L	Clarified butter(Ghee) of Cow milk;honey	Alltheingredientsaregrindedtoforma paste whichismixed well with Ghee.	One teaspoonful of mixture is taken before breakfast for 4 to 5 days.

Formulations	Plant species used singly / combinations	Parts used	Additives	Method of preparation	Mode of administration
PF4	<i>A bidentata</i> + <i>A Mexicana</i> + <i>B diffusa</i> + <i>B ceiba</i> + <i>B pinnatum</i> + <i>C viviparum</i> + <i>C orchiooides</i> + <i>B lupulina</i> <i>C anthemoides</i> + <i>C reflexa</i> + <i>E scaber</i> + <i>F hispida</i> + <i>G arborea</i> + <i>A spinosus</i>	R+R+L +L +L+BU+RH+L	Kalajira (Seeds of <i>Nigella sativa</i> L.; Ranunculaceae); Rabing (Fruit of <i>Piper nigrum</i> L.; Piperaceae); Michri (Sugar candy)	Paste	Apply on the affected part
PF5	<i>M longifolia</i> + <i>P santalinus</i> + <i>S cordifolia</i> + <i>U indica</i> + <i>C anthemoides</i> + <i>A indica</i> + <i>C orchiooides</i> + <i>G bidens</i> + <i>B purpurea</i>	FR+B+L+BU +WH+L+Rh+ WH+L	Blackpepper/Rabing (Fruit of <i>Piper nigrum</i> L.; Piperaceae); Cummin/Jira (Seeds of <i>Cuminum cyminum</i> L.; Apiaceae); Milk	A decoction is prepared in boiled water	Consumed with ginger.
PF6	<i>C viviparum</i> + <i>C orchiooides</i> + <i>C rotundus</i> + <i>E hirta</i> + <i>A paniculata</i> + <i>S zeylanica</i> + <i>P crotalaroides</i> <i>H indicus</i> + <i>C viviparum</i> + <i>F bengalensis</i> + <i>G superba</i> + <i>L inermis</i> + <i>C orchiooides</i> <i>M indica</i> + <i>P betle</i> + <i>S robusta</i> + <i>T patula</i> + <i>T indica</i> + <i>C anthemoides</i>	BU +R+ WH+A +L+RT+RT	Ada/Ginger (Rhizome of <i>Zingiber officinale</i> Roscoe; Zingiberaceae); adequate amount; Honey, equal to the amount of Ginger; Rice washed water	All the materials are mixed together to make a dough. Cakes/ pies are prepared from the dough	Cakes/pies are consumed in hot or warm condition
PF7	<i>C viviparum</i> + <i>C orchiooides</i> + <i>C rotundus</i> + <i>E hirta</i> + <i>A paniculata</i> + <i>S zeylanica</i> + <i>P crotalaroides</i> <i>H indicus</i> + <i>C viviparum</i> + <i>F bengalensis</i> + <i>G superba</i> + <i>L inermis</i> + <i>C orchiooides</i> <i>M indica</i> + <i>P betle</i> + <i>S robusta</i> + <i>T patula</i> + <i>T indica</i> + <i>C anthemoides</i>	A+BU+L+L+L+RH	Bark of mango/Aamtree (<i>Mangifera indica</i> L.; Anacardiaceae); Chun	All ingredients are grinded to a paste with the help of a mortar and pestle. Peas-like pills are made from this paste	Two pills are taken each day in empty stomach for 21 days
PF8	<i>C viviparum</i> + <i>C orchiooides</i> + <i>C rotundus</i> + <i>E hirta</i> + <i>A paniculata</i> + <i>S zeylanica</i> + <i>P crotalaroides</i> <i>H indicus</i> + <i>C viviparum</i> + <i>F bengalensis</i> + <i>G superba</i> + <i>L inermis</i> + <i>C orchiooides</i> <i>M indica</i> + <i>P betle</i> + <i>S robusta</i> + <i>T patula</i> + <i>T indica</i> + <i>C anthemoides</i>	L+L+L+L+FR+ RH	Cow urine	Mixed all to form paste	Apply on the affected part

L = Leaves; BU = Bulb; FR = Flower; RH = Rhizome; A = Aerial part; WH = Whole plant; B = Bark; R = Root; IA = Inflorescence axis; LA = Latex; NR = Not required.

infection (0.6) (Table 3). High FL designates a plant's ethno-medicinal usage agreed upon by a number of informants.

FL of the plants

Plants were classified according to specific disease concern and FL value.

Boil÷

Achyranthes aspera L. (24%), *Allium sativum* L. (28.57%), *Annona squamosa* L. (33.33%), *Artocarpus heterophyllus* Lam. (25%), *Azadirachta indica* A. Juss. (34.04%), *Bryophyllum pinnatum* (18.75%), *Cotula anthemoides* L. (27.77%), *Crinum latifolium* Linn. (46.66%), *Curculigo orchiooides* Gaertn. (12%), *Cuscuta reflexa* Roxb. (48.27%), *Elephantopus scaber* L. (23.07%), *Ficus hispida* L.f. (23.52%), *Ficus racemosa* L. (16.66%), *Hibiscus rosa-sinsis* L. (28.57%), *Madhuca longifolia* (Konig) J.F.Macbr. (16.66%), *Piper betle* L. (51.61%), *Pterocarpus santalinus* L.f. (15%), *Ricinus communis* L., (24%), *Shorea robusta* Gaertn., (23.07%), *Sida cordifolia* L. (33.33%), *Tamarindus indica* L., (40%), *Urginea indica* (Roxb.) Kunth (29.16%), *Vitex negundo* L. (36.84%).

Ulcer÷

Achyranthes aspera L. (28%), *Allium sativum* L. (14.28%), *Andrographis paniculata* (Burm.f.) Wal.ex. Nes. (59.25%), *Averrhoa carambola* L. (33.33%), *Azadirachta indica* A. Juss. (19.14%), *Cotula anthemoides* L. (25.92%), *Curcuma longa* L. (18.75%), *Cyperus rotundus* L. (55.17%), *Elephantopus scaber* L. (15.38), *Hemidesmus indicus* (L.) R.Br. (20.68%), *Madhuca longifolia* (Konig) J.F.Macbr. (13.88%), *Urginea indica* (Roxb.) Kunth (18.75%), *Aloe vera* L. (17.64).

Measles÷

Achyranthes bidentata Blume (26.66%), *Azadirachta indica* A. Juss. (6.38%), *Euphorbia hirta* L. (23.07%).

Cut

Aloe vera L. (8.8%), *Argemone mexicana* Linn (38.46%), *Boerhavia diffusa* L. (45.83%), *Curculigo orchiooides* Gaertn. (18%), *Curcuma longa* L. (15.62%), *Euphorbia hirta* L. (19.23%), *Hemidesmus indicus* (L.) R.Br. (6.66%), *Lawsonia inermis* L. (15.38%), *Ricinus communis* L. (28%), *Sida cordifolia* L. (20%), *Syzygium cumini* (L) Skeels (33.33), *Tagetes patula* L.

Table 3: Data analyses for Informants' consensus factor for specific disease category.

Category of ailments	Number of taxa	% of all taxa	Number of use reports	% all use reports	Informants' consensus factor (Fic)
Acne	6	3.57	32	2.56	0.84
Boil	28	16.66	214	17.12	0.87
Burn	10	5.95	53	4.24	0.83
Carbuncle	58	34.52	597	47.76	0.91
Cut	17	10.11	113	9.04	0.86
Chicken pox	1	0.59	5	0.4	1
Eczema	9	5.35	44	3.52	0.81
Leukoderma	5	2.97	19	1.52	0.77
Measles	4	2.38	13	1.04	0.75
Mouth ulcer	1	0.59	1	0.08	0
Nail infection	5	2.98	11	0.88	0.6
Pimple	4	2.38	12	0.96	0.73
Ulcer	14	8.33	104	8.32	0.87
Wound	6	3.57	32	2.56	0.84

(45.94%), *Tamarindus indica* L. (28.88%), *Urginea indica* (Roxb.) Kunth (12.5%), *Vitex negundo* L. (26.31%).

Acne÷

Aloe vera L. (11.76%), *Cotula anthemoides* L. (11.11%), *Curcuma longa* L. (21.87%), *Hibiscus rosa-sinsnsis* L. (30.61%).

Nail infection÷

Aloe vera L. (5.8%), *Datura metel* L. (23.33), *Datura stramonium* L. (66.66%), *Ficus religiosa* L. (50%), *Psidium guajava* L. (8.33%).

Pimple÷

Annona squamosa L. (16.66%), *Cotula anthemoides* L. (9.2%), *Ficus benghalensis* L. (66.66).

Chicken pox÷

Azadirachta indica A. Juss. (10.63%)

Mouth ulcer÷

Bombax ceiba L. (7.6%)

Burn÷

Calotropis gigantea (Linn.) R. Br.ex. Ait. (47.82%), *Calotropis procera* (Aiton) R. Br. (25%), *Curculigo orchiooides* Gaertn. (16%), *Elephantopus scaber* L. (19.23%), *Euphorbia milii* var. *longifolia* D. Moul. (40%), *Ficus hispida* L.f. (11.76%), *Ficus racemosa* L. (37.5%), *Madhucalongoifolia* (Konig) J.F.Macbr. (27.77).

Leukoderma

Artocarpus heterophyllus Lam. (25%), *Curculigo orchiooides* Gaertn. (14%), *Gloriosa superba* Linn. (7.1%), *Urginea indica* (Roxb.) Kunth (10.41%).

Wound÷

Gmelina arborea Roxb. Ex Sm. (13.33%), *Mangifera indica* L. (20%), *Pterocarpus santalinus* L.f. (15%), *Shorea robusta* Gaertn. (19.23%), *Syzygium cumini* (L) Skeels (35.89%).

Eczema÷

Hemidesmus indicus (L.) R.Br. (37.93%), *Mangifera indica* L. (24%), *Pterocarpus santalinus* L.f. (15%), *Shorea robusta* Gaertn. (19.23%), *Syzygium cumini* (L) Skeels (35.89%), *Tagetes patula* L. (16.21%), *Sida cordata* (Burm. f.) Borss. Waalk. (30%).

Carbuncle÷

Achyranthes aspera L. (48%), *Achyranthes bidentata* Blume (73.33%), *Allium sativum* L. (66.66%), *Aloe vera* L. (55.88%), *Andrographis paniculata* (Burm.f.) Wal.ex.Nes. (40.74%), *Annona squamosa* L. (50%), *Argemone mexicana* Linn (61.53%), *Artocarpus heterophyllus* Lam. (50%), *Averrhoa carambola* L. (66.66%), *Azadirachta indica* A. Juss. (29.78%), *Boerhavia diffusa* L. (54.16%), *Bombax ceiba* L. (92.30%), *Bryophyllum pinnatum* (Lam) Oken (81.25%), *Calotropis gigantea* (Linn.) R.Br.ex.Ait. (52.17%), *Calotropis procera* (Aiton) R. Br. (75%), *Cotula anthemoides* L. (25.92%), *Crinum viviparum* (Lam) R. Ansari & V.J. Nair, *Curculigo orchiooides* Gaertn. (40%), *Curcuma longa* L. (43.75%), *Cuscuta reflexa* Roxb. (51.72%), *Cyperus rotundus* L. (44.82%), *Datura metel* L. (66.66%), *Datura stramonium* L. (33.33), *Elephantopus scaber* L. (42.30), *Euphorbia hirta* L. (61.53%), *Euphorbia milii* var. *longifolia* D. Moul. (60%), *Ficus benghalensis* L. (33.33%), *Ficus hispida* L.f. (64.70%), *Ficus racemosa* L. (45.83%), *Ficus religiosa* L. (50%), *Gloriosa superba* Linn. (92.85%), *Gmelina arborea* Roxb. ex Sm. (80%), *Hemidesmus indicus* (L.) R.Br. (41.37%), *Hibiscusrosa-sinsnsis* L. (40.81%), *Lawsonia nermis* L. (84.61%), *Madhucalongoifolia* (Konig) J.F.Macbr. (41.66%), *Mangifera indica* L. (56%), *Piper betle* L. (48.38%), *Psidium guajava* L. (58.33%), *Pterocarpus santalinus* L.f. (52.5%), *Ricinus communis* L. (48%), *Shorea robusta* Gaertn. (42.30%), *Sida cordata* (Burm. f.) Borss. Waalk. (70%), *Sida cordifolia* L. (46.66%), *Syzygium cumini* (L) Skeels (30.76%), *Tagetes patula* L. (37.83%), *Tamarindus indica* L. (31.11%), *Urginea indica* (Roxb.) Kunth (29.16%), *Vitex negundo* L. (36.84%).

DISCUSSION AND CONCLUSION

We report a total of 59 plant species belonging to 35 different families which are used directly or with some additives (Table 2) for the treatment of carbuncle. Herbal formulations are usually made with dry dehydrated form rather than fresh form of plant parts. Dried plant parts are stored at homes throughout the year so that these can be used for treatment during off-season, especially in winter when leafy species become scarce. Usually, healers follow their own traditional knowledge for drug formulation and do not want to disclose it to the patients. In most of the cases they prefer leafy parts of different herbs. UV represents the relative importance of plants in that locality for drug formulation (Table 1). High Fic designates the use of a particular species reported by a large fraction of the interviewed informants for a particular disease and low Fic denotes the disparity amongst the informants in using a specific species against a specific disease. In many cases, medication was preferred in a composite mixtures from different plants/plant parts with the understanding that synergistic effect of phytochemicals of

different plants species may improve the rate of healing.²⁰ This classical knowledge, inherited by these local tribal healers from their ancestors is rapidly vanishing due to degradation of forest covers, uprooting of tribal population due to fast urbanization and industrialization and above all indifferent attitude of younger generation, although still maintaining the skeletal structure of primary healthcare system of Purulia district. Therefore, the present documentation is a preliminary attempt to pave the path for developing digitized database in future. A proper planning and management is the need of the age for their sustainable exploitation and conservation.

ACKNOWLEDGEMENT

The authors gratefully acknowledge the U.G.C. for financial support from U.G.C. minor research project no. F.PSW-204/15-16(ERO). We are indebted to the tribal people of Purulia who helped us a lot to give the manuscript a full shape. Their immense help inspire us to project their traditional knowledge globally through publication. GM, first author is grateful to the Principal, A.M. College, Purulia for giving permission for field work.

CONFLICTS OF INTEREST

None.

ABBREVIATIONS

FL: Fidelity Level; Fic: Informants' Consensus Factor; UV: Use Value; MF: Monoherbal Formulation; PF: Polyherbal Formulation.

REFERENCES

- Abbasi AM, Khan MA, Ahmad M, Zafar M, Jahan S, Sultana S. Ethno pharmacological application of medicinal plants to cure skin diseases and in folk cosmetics among the tribal communities of North-West Frontier Province, Pakistan. *J Ethnopharmacol.* 2010;128(2):322-35.
- Quave CL, Pieroni A, Bennett BC. Dermatological remedies in the traditional pharmacopoeia of Vulture-Alto Bradano, inland southern Italy. *J Ethnobiol Ethnomed.* 2008;4(1):5.
- Adetutu A, Witson AM, Corcoran O. Ethnopharmacological survey and *in vitro* evaluation of wound healing plants used in South-western Nigeria. *J Ethnopharmacol.* 2011;137(1):50-6.
- Saikia AP, Ryakala VK, Sharma P, Goswami P, Bora U. Ethnobotany of medicinal plants used by Assamese people for various skin ailments and cosmetics. *J Ethnopharmacol.* 2006;106(2):149-57.
- World Heritage Encyclopedia, http://www.worldbooklibrary.org/articles/Carbuncle;World_e-bookLibrary_ID-WHEBN000712333;Carbuncle-Pubmed,2011.
- Bowersox J. Experimental staph vaccine broadly protective in animal studies. NIH. 1999. Archived from the original on 5 May 2007. Retrieved 28 July 2007.
- Jevons MP. Celbenin-resistant staphylococci. *BMJ.* 1961;1(5219):124-5.
- Chambers HF. The changing epidemiology of *Staphylococcus aureus*? *Emerg Infect Dis.* 2001;7(2):178-82.
- Hiramatsu K, Hanaki H, Ino T, Yabuta K, Oguri T, Tenover FC. Methicillin-resistant *Staphylococcus aureus* clinical strain with reduced vancomycin susceptibility (PDF). *J Antimicrob Chemother.* 1997;40(1):135-6.
- Okemo PO, Bais HP, Vivanco JM. *In vitro* activities of *Maesa lanceolata* extracts against fungal plant pathogens. *Fitoterapia.* 2003;74(3):312-6.
- Paksoy MY, Selvi S, Savran A. Ethnopharmacological survey of medicinal plants in Ulukisla. *J Herbal medicine.* 2016;1-7.
- Modak BK, Gorai P, Dhan R, Mukherjee A, Dey A. Tradition in treating taboo: folkloric medicinal wisdom of the aboriginals of Purulia district, West Bengal, India against sexual gynaecological and related disorders. *J Ethnopharmacol.* 2015;169:370-86.
- Bentham G, Hooker JD. *Genera Planterum.* London: Lovell Reeve and Co. 1862-83;1-3.
- Prain D. *Bengal plants.* Dehra Dun: Bishen Singh Mahendra Pal Singh. 1903;1-2.
- Pal DC, Jain SK. *Tribal medicine.* Kolkata: Naya Prakash. 1998.
- Paria ND, Chattopadhyay SP. Flora of Hazaribagh district, Bihar. *Bot Survey of India.* 2005;2:1299.
- Trotter RT, Logan MH. Informant census: A new approach for identifying potentially effective medicinal plants. In: Etkin, L.N. (Ed.), *Plants in indigenous medicine and diet.* Redgrave, Bedford Hill, New York. 1986;91-112.
- Friedmen J, Yaniv Z, Dafni A, Palewitch D. A preliminary classification of the healing potential of medicinal plants, based on a rational analysis of an ethno pharmacological field survey among Bedouins in the Negev desert, Israel. *J Ethnopharmacol.* 1986;16(2-3):275-87.
- Phillips O, Gentry AH, Reynel C, Wilkin P, Galvez-Durand BC. Quantitative ethno botany and amazonian conservation. *Conserv Biol.* 1994;8(1):225-48.
- Gertsch J. Botanical drugs, synergy and network pharmacology: Forth and back to intelligent mixtures. *Planta Med.* 2011;77(11):1086-98.

GRAPHICAL ABSTRACT



ABOUT AUTHORS



Ghanashyam Mahato: Assistant Professor, Department of Botany, A.M. College, Jhalda, Purulia, West Bengal-723202, India.

SUMMARY

Fifty-nine herbal plants belongs to 35 families were used in various combinations during treatment. Most of the species belongs to Moraceae and Asteraceae families in comparison to other families. Herbaceous plants are most commonly used and leaves are the most common part for preparing formulations.



Bangamoti Hansda: Research Scholar, Department of Botany and Forestry, Vidyasagar University, Midnapore, West Bengal-721102, India.



Nilanjana Banerjee: Assistant Professor, Department of Botany, Vidyasagar University, Paschim Medinipur, West Bengal-721102, India.

Cite this article: Mahato G, Hansda B, Banerjee N. Ethnobotanics used for the Treatment of Skin Diseases with Special Emphasis on Carbuncle Disease from Purulia District of West Bengal in India. *Pharmacog J.* 2019;11(4):745-53.



Received on 03 September 2018; received in revised form, 13 November 2018; accepted, 16 November 2018; published 01 May 2019

BIOCHEMICAL STUDY OF AN ENDANGERED ETHNOMEDICINAL PLANT *CURCULIGO ORCHIOIDES* GAERTN. OCCURRING IN PURULIA DISTRICT OF WEST BENGAL, INDIA

G. Mahato¹ and N. Banerjee^{*2}

Department of Botany¹, A. M. College, Jhalda, Purulia - 723202, West Bengal, India.

Department of Botany², Vidyasagar University, Paschim Medinipur - 721102, West Bengal, India.

Keywords:

Ethnomedicinal, *Curculigo orchioides*, Antioxidant, Antibacterial

Correspondence to Author:

Dr. Nilanjana Banerjee

Assistant Professor,
Department of Botany,
Vidyasagar University, Paschim
Medinipur - 721102, West Bengal,
India.

E-mail: nilanjanab1@yahoo.com

ABSTRACT: Ethnic peoples from Purulia district of West Bengal in India use a lot of plants for their primary health care without studying phytochemical analysis and biological activities in detail. Main objectives of the present study are to evaluate the antibacterial and antioxidant activities of the whole plant extract of *Curculigo orchioides* using polar and nonpolar solvents. Total phenol content (TPC) was determined by Folin-Ciocalteu assay using Gallic acid (GA) as standard and total flavonoid content (TFC) by AlCl₃ method using quercetin as standard. The antibacterial screening was carried out by agar well diffusion method. Methanol extracts exhibit higher phenol (82.93 ± 2.74 mg of GA E/gm of the sample), flavonoid (48.41 ± 1.94 mg of QE/gm of the sample) and alkaloid (5.56 ± 1.56%) content in comparison to other solvents. Similarly, methanol extracts show higher free radicals scavenging property and there was a positive correlation between IC₅₀ values with total phenol and flavonoid content. A positive correlation exists in total phenol and flavonoid with antioxidant activities. The plant contains high phenolic and flavonoid content and exhibits antibacterial and antioxidant activities support the ethnomedicinal value of the plant.

INTRODUCTION: Plants have been used medicinally since prehistoric times. Although, after the discovery of the synthetic drug, the use of natural medicines has decreased drastically. However, synthetic drugs have some side effects¹, allergic reactions². So, humans seek some alternative source of medicine. Tribals from a rural area of Purulia district are mainly dependent on medicinal plants for their primary health care. One such traditionally used plant is *Curculigo orchioides* Gaertn. (Hypoxidaceae) commonly known as kalimusli, known in Purulia it as talmuli, is an important endangered medicinal plant used by the tribal people from all over the district for the treatment of carbuncle and cancer.

The plant is a small annual herb characterized by the yellowish flower, blackish tuberous primary root with dense lateral roots, aerial part possessing numerous linear leaves arranged in rosettes. According to WHO 80% world population relies on traditional medicines for the treatment of common illness³. At present, phytochemicals are more in demand in comparison to synthetic drugs due to its fewer side effects, lesser immuno-suppressive activity and wide use for the treatment of several diseases⁴. The rhizome of *C. orchioides* possesses immune stimulant potential⁵, hepatoprotective⁶, antioxidant⁷, and platelet regeneration effect⁸. The present study emphasizes on antibacterial activity against three strains of bacteria, antioxidant activity, total phenol and flavonoid content of the whole plant of *Curculigo orchioides*.

MATERIALS AND METHODS:

Plant Materials: Plant **Fig. 1** is obtained from the forest area of Bandwan in Purulia district, West Bengal, India and is identified with the help of

	QUICK RESPONSE CODE DOI: 10.13040/IJPSR.0975-8232.10(5).2417-22
	The article can be accessed online on www.ijpsr.com
DOI link: http://dx.doi.org/10.13040/IJPSR.0975-8232.10(5).2417-22	

books and literature, authenticated by Dr. Basanta Kumar Sing, Botanical Survey of India, Kolkata. A voucher specimen (AMC123) was documented in the herbarium of A.M. College, Jhalda.



FIG. 1: *CURCULIGO ORCHIOIDES*

Extract Preparation for Total Phenol, Flavonoid, Alkaloid, Antioxidant and Antibacterial Activities: Freshly collected whole plant of *Curculigo orchioides* (1800 grams) was washed with running tap water and then shade dried for eleven days. Dried plants crushed to form a powder (780 grams) and extracted successively with soxhlet extractor at 60 °C by using methanol, ethyl acetate, n-hexane and water for 24 h. After that solvent extracts are removed, filtered and concentrated by using a rotary evaporator at 60 °C under reduced pressure and 14 gm, 9 gm, 5 gm and 10 gm of the extract obtained respectively which were kept in a refrigerator at 4 °C for further study.

Determination of Total Phenol Content: Total phenol content was determined using Gallic acid as standard. Plant powder obtained from respective solvent extracts taken for Folin-ciocalteu assay with a slight modification of standard method⁹. The total phenol content was expressed as Gallic acid equivalents (mg of GAE/g sample) through the calibration curve of Gallic acid. Linearity in calibration curve was 10 to 100 µg/ml (r = 0.99).

Determination of Total Flavonoid Content: Total flavonoid content was determined by AlCl₃ method using quercetin as standard¹⁰. A mixture of 10% of 100 µl of AlCl₃, 100 µl NaNO₃(5%), 670 µl of 1 mM NaOH and 100 µl of the sample was vortexed and incubated in the dark at room temperature for 25 min. The O.D. value was measured at 510 nm. The experiment was repeated thrice.

Estimation of Alkaloid Content: Alkaloid content was determined by using a suitable method with slight modification¹¹. Five grams of the powdered methanol and aqueous plant extracts dissolved in 20 ml of 20% acetic acid prepared in methanol (v/v), then filtered after four hours. The filtrates were kept in a water bath for 30 min at boiling temperature. Ammonium hydroxide was poured into the extract, dropwise and produced some precipitation (ppt). The collected ppt was washed with dilute ammonium hydroxide and filtered. The residues obtained in the filter paper, dried and weighed.

$$\% \text{ of alkaloid} = \frac{\text{Weight of residues}}{\text{Weight of sample}} \times 100 \%$$

Antioxidant Activities:

DPPH Antioxidant Activity: DPPH antioxidant activity was carried out by procedure Zhu *et al.*,¹² with slight modification. By using respective solvents prepare a stock solution, from the stock solution make various concentrations (50-400 µg/ml). DPPH mixed with different concentrations, after 30 min incubation O.D. value at 517 nm taken by jasco V-630, USA. Ascorbic acid was measured in the same procedure. Antioxidant scavenging capacity was estimated by calculating IC₅₀ values.

ABTS⁺ Antioxidant Activity: For ABTS⁺ antioxidant assay, the method of Re *et al.*,¹³ was followed with slight modification. The ABTS⁺ radical cation was prepared by mixing an equal volume of 7 mM of ABTS⁺ stock solution with 2.45 mM of potassium persulfate and incubated in dark condition for 12-16 h at room temperature. Before experimental processing, the ABTS⁺ radical reaction mixture was diluted with ethanol to an absorbance of 0.700 ± 0.05 at 734 nm. The requisite amount of plant extract (50-400 µg/ml) was mixed with 2 ml of ABTS⁺ radical reaction mixture and incubated in the dark for 6 min. After that absorbance at 734 was recorded by UV-Vis spectrophotometer and percent free radical scavenging activity was determined by the following formula

$$\% \text{ free radical scavenging activity} = \frac{A_{\text{blank}} - A_{\text{sample}}}{A_{\text{sample}}} \times 100$$

Where A_{sample} and A_{blanks} are the respective absorbance's of tested samples and ABTS⁺ reaction mixture.

Hydrogen Peroxide Scavenging Activity:

Hydrogen peroxide scavenging activity was determined by using a method of Harborne¹⁴ with modifications. Aliquots of 0.1 ml from different concentrations of extracts were taken into the test tubes and make the volume up to 0.4 ml by adding with 50 mM phosphate buffer (pH 7.4) then add 0.6 ml of hydrogen peroxide solution, vortexes the mixtures and absorbance measured at 230 nm after 10 min, against a blank. Hydrogen peroxide scavenging abilities were calculated using the following equation:

$$\text{Hydrogen peroxide scavenging activity} = (1 - \text{absorbance of sample} / \text{absorbance of the mixture}) \times 100$$
In-vitro Antibacterial Assay:**Bacterial Strain and Culture Conditions:**

Authentic, pure cultures of pathogenic bacteria like *Escherichia coli* (*E. coli* MTCC 443), *Staphylococcus aureus* (*S. aureus* MTCC 3160) were provided by the microbiological laboratory and clinical detection center Paschim Medinipur and *Bacillus subtilis* from Vidyasagar University Microbiology Department Paschim Medinipur, India. They were cultured in tryptone soy broth or agar (TSB or TSA) in aerobic condition at 37 °C.

Well Diffusion Method: The good diffusion method was used to study the antibacterial activity as described by Bauer *et al.*¹⁵ Lawn bacterial cultures were spread on the Muller Hinton agar using a spreader. The wells were cut on the agar plates using a cork borer; plant extracts were poured into the well using sterile micropipette¹⁶. The plates were incubated at 37 °C for 24 h. After incubation, the diameter of the zone of inhibition was measured by using a scale.

Statistical Analysis: Statistical analysis was performed using Microsoft Excel-2010 software. Data are expressed as mean \pm SD from three replicates. EC₅₀ values were calculated by regression analysis. A probability of P<0.05 was considered significant.

RESULTS:

Total Phenol Content: Due to the presence of hydroxyl groups phenolic compounds are very important in plants as they can scavenge free radicals. TPC of *C. orchoides* was solvent dependent and expressed as milligrams of GA

equivalent. **Fig. 2** summarize the TPC and ranging from 35.7 ± 3.32 to 82.93 ± 2.74 . The methanol extract exhibited the highest total phenol content in comparison to other solvent extracts.

Total Flavonoid Content: Total flavonoid content also depend upon the solvent types as shown in **Fig. 2** varied from 12.46 ± 2.08 to 48.47 ± 1.94 mg of quercetin equivalent/gm of extract. The methanol extract showed the highest amount of flavonoid content **Fig. 2** followed by aqueous, ethyl acetate and n-hexane.

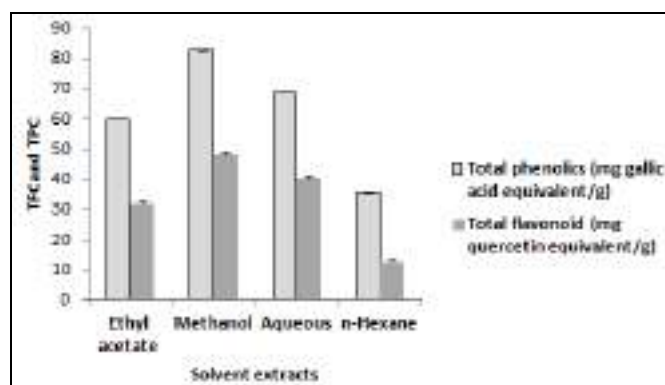


FIG. 2: TOTAL FLAVONOID CONTENT (TFC) AND TOTAL PHENOL CONTENT (TPC) IN VARIOUS SOLVENT EXTRACTS. Each value is represented as the mean \pm standard deviation (n=3)

Estimation of Alkaloid Content: Alkaloid content shows higher in methanol extract ($5.56 \pm 1.56\%$) in compare with water extract ($2.25 \pm 1.4\%$) **Fig. 3.**

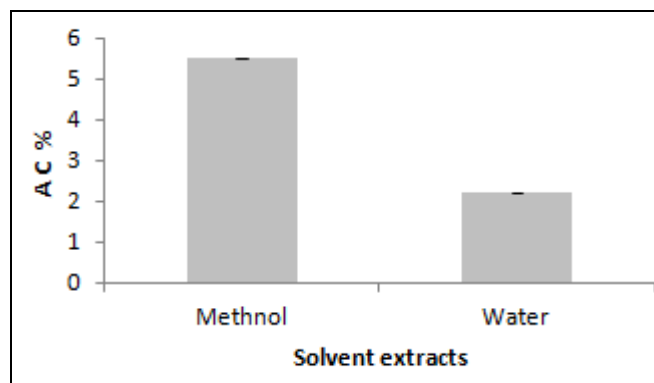


FIG. 3: ALKALOID CONTENT (AC) IN METHANOL AND AQUEOUS EXTRACT

In-vitro Antioxidant Activities:

DPPH Radical Scavenging Activity: Antioxidants present in the plant extracts decrease the absorbance of DPPH radical at 517 nm because of the reaction between antioxidants and radicals. It is noticeable by seeing the color changes from purple to yellow.

The scavenging effects of various solvent extract on DPPH radical **Fig. 4** shown in the following order: methanol > aqueous > ethyl acetate > n-hexane. The IC₅₀ value was shown in **Table 1**. Though the capability of scavenging the free radicals is very low in comparison with vit - C but plants have the potentiality to scavenge the free radicals and may be used as natural antioxidants.

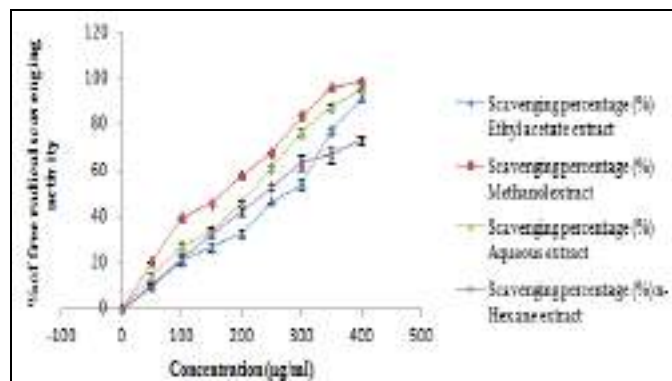


FIG. 4: DPPH ANTIOXIDANT ACTIVITY OF FOUR SOLVENT EXTRACTS. Each value is represented as the mean ± standard deviation (n=3)

ABTS Radical Scavenging Activity: **Fig. 5** shows the antioxidant capacity of various solvent extracts decrease in this order, methanol > aqueous > ethyl acetate > n-hexane. The IC₅₀ value of methanol extract was most pronounced in compare with other solvent extracts **Table 1**.

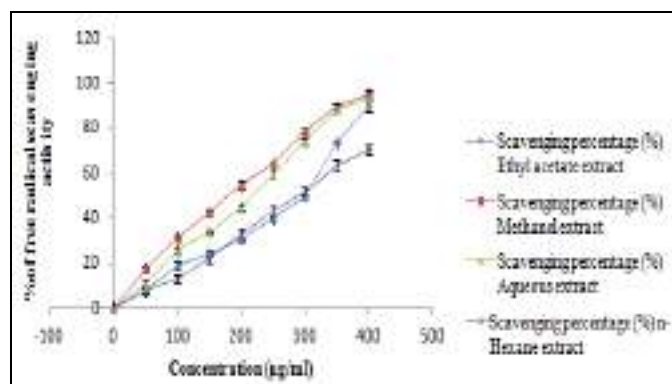


FIG. 5: ABTS^{•+} ANTIOXIDANT ACTIVITY OF FOUR SOLVENT EXTRACTS. Each value is represented as the mean ± standard deviation (n=3)

Hydrogen Peroxide Radical Scavenging Activity: The effect of different solvent extracts on hydrogen peroxide radical was concentration dependent (50-500 µg/ml) as shown in **Fig. 6**. In this study, results showed that various solvent extracts had strong potential in eradicating hydrogen peroxide at all concentrations. The IC₅₀ value of different solvent extracts shows in **Table 1**.

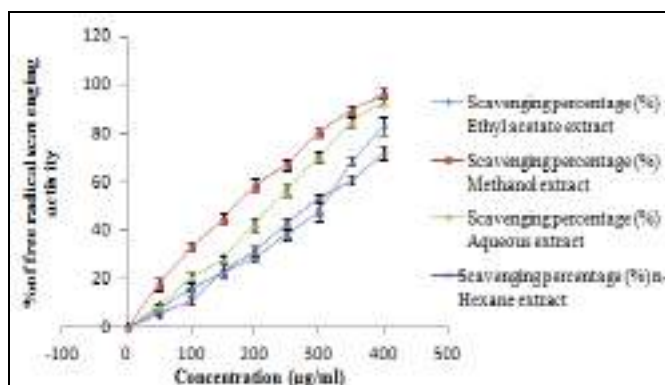


FIG. 6: HYDROGEN PEROXIDE RADICAL SCAVENGING ACTIVITY OF FOUR SOLVENT EXTRACTS. Each value is represented as the mean ± standard deviation (n=3)

IC₅₀ Value: Inhibitory concentration (IC₅₀) parameter was used for the interpretation of the results of antioxidant activities. The discoloration of the sample was plotted against sample concentration to determine the IC₅₀ value. Its value in four solvents extracts shown in **Table 1** by using three different assay techniques.

TABLE 1: IC₅₀ VALUES (µg/ml) FOR RADICAL SCAVENGING

Solvent extracts	DPPH radical	Hydrogen peroxide	ABTS radical
Ethyl acetate	247.321	277.43	260.98
Methanol	173.761	182.74	190.17
Aqueous	204.264	220.83	208.06
n-Hexane	252.22	289.58	289.14

Correlation (R) Between IC₅₀ Values of Antioxidant Activities with Total Phenol and Flavonoid Contents: There was a positive correlation (R) between IC₅₀ values of antioxidant activities with total phenol and flavonoid contents as shown in **Table 2**. R values from total phenolic with IC₅₀ vary from 0.737 to 0.795 and in case of flavonoids are 0.823 to 0.844.

TABLE 2: CORRELATION BETWEEN IC₅₀ VALUES WITH TOTAL PHENOL AND FLAVONOID CONTENT

IC ₅₀	Total phenolics	Total flavonoid
DPPH	0.785	0.823
H ₂ O ₂	0.795	0.844
ABTS	0.737	0.839

Antibacterial Activity: Methanol extract shown highest inhibition zone **Table 3** in comparison with other solvent extracts. Activity index measured to show the suitable solvents chosen to increase the biological activity.

TABLE 3: ANTIBACTERIAL ACTIVITY (ZONE OF INHIBITION, mm) OF VARIOUS SOLVENT EXTRACTS OF *C. ORCHIOIDES*

Bacteria		Methanol	Ethyl acetate	Aqueous	n-Hexane	Standard
<i>S. aureus</i>	IZ	13.12 ± 0.12	9.28 ± 0.42	11.32 ± 0.46	7.14 ± 0.32	25.56
	AI	0.51	0.36	0.44	0.27	
<i>E. coli</i>	IZ	18.32 ± 0.16	8.62 ± 0.26	13.67 ± 0.76	7.54 ± 0.21	24.89
	AI	0.73	0.34	0.54	0.30	
<i>B. subtilis</i>	IZ	14.54 ± 0.14	8.75 ± 0.24	12.46 ± 0.48	7.32 ± 0.12	21.52
	AI	0.67	0.40	0.57	0.34	

IZ = inhibition zone (mm) includes the diameter of disc (6 mm); AI = activity index = IZ of test sample/ IZ of standard; Standard: Ampicillin (1 mg/disc). Values are mean of triplicate replicates (mean ± S.D.)

DISCUSSION: Studies have revealed that medicinal plants are very good sources of antioxidant and play a significant role in the treatment of several diseases globally¹⁷. The plant *C. orchoides* contains a higher amount of phenolic compounds in the methanolic extract in comparison to other solvent extracts. Due to the presence of phenolic compounds plant exhibit antioxidant properties and methanolic extract shows more potential on free radical scavenging properties¹⁸. There was a positive correlation between phenolic compounds and IC₅₀ values; this study corroborates the findings of previous authors^{19,20}. The phenolics and polyphenols are the largest groups of secondary metabolites to have antimicrobial and antioxidant properties^{21,22}.

Naturally occurring plant flavonoids possess antimicrobial activities^{23, 24}. The variation in the antibacterial activity of flavonoids and phenolics is due to the number and positions of methoxy and phenolic groups within their structures^{25, 26}. The alkaloid extracts obtained from medicinal plant species have a multiplicity of host-mediated biological activities, including antimalarial, antimicrobial, antihyperglycemic, anti-inflammatory, and pharmacological effects^{27, 28}. With respect to different liver marker enzymes, such as aspartate aminotransferase (AST), alanine aminotransferase (ALT) and alkaline phosphatase (ALP) methanol extract of *C. orchoides* exhibit hepatoprotective properties. Nagesh and Shanthamme²⁹ reported the antibacterial property of rhizome extract against pathogenic bacteria. Mehta *et al.*,³⁰ identified some fatty acid from the root of *C. orchoides*. Anticancer phenolic compound curculigoside identified by Kubo *et al.*,³¹ from the rhizome of the plant. Whole plant extract and uses of different solvents vary the biological activities as reported by previous authors.

Further study on phytochemical analysis and isolation of bioactive components urgently needed for the development of natural medicine.

CONCLUSION: Due to the presence of secondary metabolites (Phenolic and flavonoid compounds) the studied plant exhibits antioxidant and antibacterial properties. Out of the four solvents used methanol has the more potential to extract the bioactive components from plant powder. This study supports the ethnomedicinal uses of the plant in Purulia district. Further research on phytochemical analysis and isolation of bioactive components urgently needed for the development of natural medicine.

ACKNOWLEDGEMENT: UGC, Government of India is acknowledged for financial assistance (Project no. F.PSW-204/15-16/ERO). We are indebted to the tribal people of Purulia who helped us a lot to give the manuscript a full shape. GM, the first author is grateful to the Principal, A. M. College, Purulia for giving permission for fieldwork.

CONFLICT OF INTEREST: No conflicts of interest.

REFERENCES:

1. Stanković N, Mihajilov-Krstev T, Zlatković B, Stankov-Jovanović V, Mitić V, Jović J, Čomić L, Kocić B and Bernstein N: Antibacterial and Antioxidant Activity of Traditional Medicinal Plants from the Balkan Peninsula. NJAS - Wageningen Journal of Life Sciences 2016; 78: 21-28.
2. Karahan F, Avsar C, Ozyigit II and Berber I: Antimicrobial and antioxidant activities of medicinal plant *Glycyrrhiza glabra* var. *glandulifera* from different habitats, Biotechnology & amp; Biotechnological Equipment 2016; 30(4): 797-04.
3. World Health Organization, 2002. WHO Traditional medicine strategy 2002-2005.
4. Lopez A, Hudson JB and Towers GHN: Antiviral and antimicrobial activities of Colombian medicinal plants. Journal of Ethnopharmacology 2001; 77: 189-96.

5. Lakshmi V, Pandey K, Anju Puri, Saxena RP and Saxena KC: Immuno stimulant principles from *Curculigo orchiooides*. Jou of Ethnopharmacology 2003; 89: 181-84.
6. Venukumar MR and Latha MS: Hepatoprotective effect of the methanolic extract of *Curculigo orchiooides*in CCl₄-treated male rats. Indian J. Pharmacol 2002; 34: 269-275.
7. Venukumar MR and Latha MS: Antioxidant activity of *Curculigo orchiooides*in Carbon tetrachloride induced hepatopathy in rats. Indian J. Clinical Biochem 2002; 17(2): 80-87.
8. Sarabjeet SS, Sunitha JK and Ramawat G: Platelet regeneration and bulbil formation *in-vitro* from leaf and stem explants of *Curculigo orchiooides*, an endangered medicinal plant. Scientia Horticulturae 1999; 79: 127-34.
9. Singleton VL, Orthofer R and Lamuela-raventos RM: Methods Enzymol 1999; 299: 152-78.
10. Zhishen J, Mengcheng T and Jianming W: The determination of flavonoid contents in mulberry and their scavenging effects on superoxide radicals. Food Chemistry 1999; 64: 555-59.
11. Tackie AN, Schiff PL and Cryptospirolepine JNR: A Unique Spiro-Noncyclic Alkaloid Isolated from *Cryptolepis Sanguinolenta*. J Nat Prod 1993; 56: 653-55.
12. Zhu K, Zhou H and Qian H: Antioxidant and free radical-scavenging activities of wheat germ protein hydrolysates (WGPH) prepared with alcalase. Process Biochemistry. 2006; 41(6): 1296-02. doi: 10.1016/j.procbio.2005.12. 029.
13. Re R, Pellegrini N, Proteggente A, Pannala A, Yang M and Rice-Evans C: Antioxidant activity applying an improved ABTS radical cation decolorization assay. Free Radical Biology and Medicine 1999; 26(9-10): 1231-37. doi: 10.1016/S0891-5849(98)00315-3.
14. Harborne JB: Phytochemical Methods. London: Chapman and Hall, Ltd.1973; 49-188.
15. Bauer AW, Kirby E, Sherris EM and Turk M: Antibiotic by standardized single disk method. Am J Clin Path 1966; 45: 493-6.
16. Tenover FC: Encyclopedia of Microbiology (Third Edition) 2009.
17. Fouche G, Afolayan AJ, Wintola OA and Khorombi TE: Senabe J. Effect of the aqueous extract of the aerial parts of *Monsonia angustifolia* E. Mey. Ex A. Rich., on the sexual behaviour of male Wistar rats. BMC Complement Altern Med 2015; 15: 343-8.
18. Algabri SO, Doro BM, Abadi AM, Shiba MA and Salem AH: Bay Leaves have Antimicrobial and antioxidant activities. J Pathogen Res 2018; 1: 1-3.
19. Jayathilake C, Rizliya V and Liyanage R: Antioxidant and free radical scavenging capacity of extensively used medicinal plants in Sri Lanka. Procedia Food Science 2016; 6: 123-26.
20. Akter K: Phytochemical profile and antibacterial and antioxidant activities of medicinal plants used by aboriginal people of New South Wales, Australia. Evid Based Complement Altern Med 2016; eCAM 2016: 4683059.
21. Stefanović O, Radojević I, Čomic L and Vasić S: Antibacterial activity of naturally occurring compounds from selected plants in antimicrobial agents, In Tech, Rijeka, Croatia, 2012. View at Google Scholar
22. Amić D, Davidović-Amić, Bešlo D and Trinajstić N: Structure-radical scavenging activity relationships of flavonoids. Croatica Chemica Acta 2003; 76(1): 55-61.
23. Cushnie TPT and Lamb AJ: Antimicrobial activity of flavonoids. Inter J Antimi Agents 2005; 26(5): 343-56.
24. Havsteen B: Flavonoids, a class of natural products of high pharmacological potency. Biochemical Pharmacology 1983; 32(7): 1141-48.
25. Wu T, He M and Zang X: A structure-activity relationship study of flavonoids as inhibitors of *E. coli* by membrane interaction effect. Biochimica et Biophysica Acta (BBA) – Biomembranes 2013; 1828(11): 2751-56.
26. Alcaraz LE, Blanco SE, Puig ON, Tomas F and Ferretti FH: Antibacterial activity of flavonoids against methicillin-resistant *Staphylococcus aureus* strains. Journal of Theoretical Biology 2000; 205(2): 231-40.
27. Boakye-Yiadom K: Antimicrobial properties of cryptolepis. J. Pharm. Science 1979; 68: 435-447.
28. Uday B, Dipak D and Ranajit B: Reactive oxygen species: oxidative damage and pathogenesis. Curr Sci 1999; 77(5): 658-65.
29. Nagesh KS and Shanthamma C: Antibacterial activity of *Curculigo orchiooides* rhizome extract on pathogenic bacteria. Afr J Microbio Res 2009; 3(1): 05-09.
30. Mehta BK, Bokadia MM and Mehta SC: Study of root oil compound fatty acids of *Curculigo orchiooides* roots. Indian Drugs, 1980; 18(3): 109-110.
31. Kubo M, Namba K, Nagamoto N, Nagao T, Nakanishi J, Uno H and Nishimura HA: New phenolic glucoside, curculigoside from the rhizome of *Curculigo orchiooides*. Planta Med 1983; 47(1): 52-55.

How to cite this article:


Mahato G and Banerjee N: Biochemical study of an endangered ethnomedicinal plant *Curculigo orchiooides* Gaertn. occurring in Purulia district of West Bengal, India. Int J Pharm Sci & Res 2019; 10(5): 2417-22. doi: 10.13040/IJPSR.0975-8232.10(5).2417-22.

All © 2013 are reserved by International Journal of Pharmaceutical Sciences and Research. This Journal licensed under a Creative Commons Attribution-NonCommercial-ShareAlike 3.0 Unported License.

This article can be downloaded to **Android OS** based mobile. Scan QR Code using Code/Bar Scanner from your mobile. (Scanners are available on Google Play store)

ORIGINAL ARTICLE

Effects of flask configuration on biofilm growth and metabolites of intertidal Cyanobacteria isolated from a mangrove forest

M. Veerabhadran¹ , S. Chakraborty¹, S. Mitra¹, S. Karmakar² and J. Mukherjee¹¹ School of Environmental Studies, Jadavpur University, Kolkata, India² Department of Pharmaceutical Technology, Jadavpur University, Kolkata, India**Keywords**

antimicrobial, conico-cylindrical flask, Cyanobacteria, hydrophobicity, planktonic, polymethyl methacrylate.

Correspondence

Maruthanayagam Veerabhadran, School of Environmental Studies, Jadavpur University, Kolkata 700032, India.

E-mail: vvmaruth@gmail.com

2017/2521: received 22 December 2017, revised 19 February 2018 and accepted 12 March 2018

doi:10.1111/jam.13761

Abstract

Aims: A novel approach was employed to study the growth of three cyanobacterial strains namely *Oscillatoria* sp. (AP17), *Leptolyngbya* sp. (AP3b) and *Chroococcus* sp. (AP3U). Furthermore, their broad metabolite profile, production of pigments, exopolysaccharide (EPS) and antimicrobial activity were evaluated in response to contrasting cultivation modes: biofilm or planktonic.

Methods and Results: The biofilm culture mode was carried out in the patented conico-cylindrical flask (CCF) and the planktonic culture mode was carried out in an Erlenmeyer flask (EF). The amount of polysaccharide that was released and that remained capsular/bound was higher in CCF compared to EF cultivation. Amount of chlorophyll *a* produced by *Oscillatoria* (AP17) was higher in the CCF compared to the EF cultivation. Highest antimicrobial activities were exhibited by *Leptolyngbya* (AP3b) biofilm than other biofilms as well as planktonic biomass. Metabolite profiles of Cyanobacteria were revealed by various chromatographic techniques and showed clear differences among the two contrasting modes of cultivation.

Conclusions: The results showed clear differences in the mode of growth for achieving maximum chlorophyll *a*, EPS and bioactive metabolite production of the Cyanobacteria.

Significance and Impact of the Study: The present study augmented the information which can enhance wider exploration of the biofilm mode of cultivation of Cyanobacteria.

Introduction

Cyanobacteria (blue-green algae) possess unique structural and functional features and are commonly perceived as a prolific renewable resource for the production of an array of biologically potent secondary metabolites (Raja *et al.* 2016). In nature, allelopathy (inhibition or stimulation of growth) or metabolite production is critical and governs some of the pivotal ecological functions of an organism such as survivability and defence against predators or grazers. Production of defensive chemicals is inherent to Cyanobacteria and those produced metabolites display strong resistance against grazers including

urchins, amphipods and herbivorous crabs (Mohamed 2013; Mazard *et al.* 2016). The information pertaining to biofilm-forming Cyanobacteria of the intertidal zone is limited and more research is desired. In this unique habitat, organisms are adapted to a wide range of climatic fluctuations (temperature, salinity, desiccation and wave action) as well as to the herbivorous grazers leading to the elevated stress in the epilithic biofilms (Dugan *et al.* 2013). Thus, biofilm-forming Cyanobacteria in particular could be harnessed for exploiting novel low volume yet high value specialized chemicals of immense industrial applications especially pharmaceuticals, nutraceutical and cosmeceuticals. Pramanik *et al.* (2011) reported the

antimicrobial activity of the extracts of Cyanobacteria isolated from the intertidal soil of Sundarbans mangrove forest, which showed positive results against *Bacillus subtilis* and multiple drug-resistant clinical isolates. Cyanobacterial strains isolated from microbial mats developed on the soil surface and mangrove pneumatophores were reported to produce toxins (microcystins and saxitoxins) and exhibited toxicity to brine shrimp (Mohamed and Al-Shehri 2015). The biofilm-forming Cyanobacteria are global primary producers in intertidal waters having high nutritional profile, which could be utilized in emerging functional food market as well (Nagarkar *et al.* 2004).

Benthos of estuarine Cyanobacteria growing in the transitional ecosystems has been identified as one of the most potential groups of organisms for biotechnological applications. Some of these are cyanobacterial metabolites with allelopathic and stimulating or inhibiting growth of planktonic microalgae (Lopes and Vasconcelos 2011). For the production of the pigments such as chlorophyll *a*, carotenoids and phycocyanins, *Nostoc* spp. were allowed to form biofilms in stones with different nutrient conditions and light intensity in batch cultivation method (Sanmartín *et al.* 2010). Artificially, biofilm growth of *Acaryochloris marina* induced in alginate beads (mimics the natural condition) demonstrated maximal cell-specific growth rates and population doubling times under both visible and near-infrared radiation irradiance (Behrendt *et al.* 2012). Gismondi *et al.* (2016) demonstrated that heterocytous Cyanobacteria of *Anabaena augstumalis* VRUC163, *Calothrix* sp. VRUC166 and *Nostoc* sp. VRUC167 strains efficiently removed phosphorus from the wastewater through a biofilm-based growth approach. Exopolymeric substances (EPSs) produced by cyanobacterial biofilm under natural conditions play important ecological roles such as structurally stable, hydrated microenvironment, chemical/physical protection against biotic and abiotic stress. Matrix of hydrated EPSs favours the formation of cyanobacterial biofilm on desert soils, lithic and exposed substrates (Rossi and De Philippis 2015).

Cyanobacterial culture conditions play a vital role for inducing the production of cell mass, primary metabolites (merocyclophane C and tolytoxin) and maximum chemical diversity (Crnkovic *et al.* 2018). Lipopeptide clusters were frequently found in biofilms of Cyanobacteria exhibiting antimicrobial, antifungal bioactivities, haemolytic activity and cytotoxic effects on human cells (Galica *et al.* 2017). The production of second messenger cyclic dimeric GMP (cyclic di-GMP or c-di-GMP) and biofilm formation were induced in *Synechocystis* and *Fremyella diplosiphon* through increasing the expression of diguanylate cyclase and phosphodiesterase genes (Agostoni *et al.* 2016). However, studies on biofilm-based cultivation

methods for Cyanobacteria remain limited. No studies have been done to establish differences in metabolite profiles of Cyanobacteria growing in planktonic and biofilm modes of growth. Previously, Mitra *et al.* (2012, 2015) applied the patented (US 8,945,917 B2, Sarkar *et al.* 2015) enhanced surface area conico-cylindrical flask (ES-CCF) which provides an additional surface area for biofilm mode of growth of intertidal micro-organisms and compared the production of cellulase by *Chaetomium crispatum*, xylanase by *Gliocladium viride*, melanin by *Shewanella colwelliana*, riboflavin by *Candida famata* in the planktonic and biofilm modes of growth. The application of the ES-CCF was extended in the present study to compare the metabolite profiles of three intertidal Cyanobacteria grown in the planktonic state in the common 500-ml Erlenmeyer flask and the biofilm mode in the ES-CCF. The analysis of the metabolites has been carried out using three levels of analytical techniques from the basic TLC to advanced HPLC followed by LC-MS. Next, the difference in the EPS production, pigments accumulation and growth has also been analysed, followed by measuring the antimicrobial activities of the three Cyanobacteria cultivated in the two contrasting modes of growth. To the best of our knowledge this is the first detailed analysis which could provide basis for enhancing the scope for developing eco-designs for large-scale productions of value added compounds from Cyanobacteria.

Materials and methods

Cultivation of Cyanobacteria

Out of eight cyanobacterial strains isolated from the Sundarbans (India) by Pramanik *et al.* (2011), three morphologically distinct strains belonging to different orders were selected during the present investigation. These strains were deposited in National Facility for Marine Cyanobacteria, Tiruchirappalli, Tamil Nadu, India. Accession numbers are BDU D004, BDU D005 and BDU D006 for *Oscillatoria* sp. (AP17), *Leptolyngbya* sp. (AP3b) and *Chroococcus* sp. (AP3U) respectively. The three cyanobacterial strains *Leptolyngbya* sp. (AP3b), *Oscillatoria* sp. (AP17) and *Chroococcus* sp. (AP3U) were isolated from Lothian Island (21°39'1"N 88°19'37"E), taxonomically characterized using the available literature and maintained in ASN-III medium at 27±2°C with a light intensity of 36.45 μmol photons m⁻² s⁻¹ in a light/dark (14/10 h) cycle and routinely subcultured at every 15-day interval. The late log-phase cells were harvested by centrifugation at 10 000 g (Eppendorf model 5810R, rotor F-34-6-38) for 10 min, blotted using the sterile filter paper for removing the excess water content and used as the mother inoculum for further experiments.

Hydrophobicity test in the biphasic system

The cyanobacterial cultures were taken in the early stationary phase (after 7–10 days of growth) and washed with ASN-III medium twice. Three millilitres of cyanobacterial suspension was taken and an equal volume of *n*-hexadecane was added. The mixture was vigorously shaken manually for 1 min, allowed to stand for 5 min, and then gently vortexed for 10 s. The tubes were again allowed to stand for 5 min to allow complete separation of the phases. The cyanobacterial cell surface property was measured by adherence to the biphasic (aqueous-hydrocarbon) system following Fattom and Shilo (1984).

Flask configurations, operating and culture conditions

The conico-cylindrical flask (CCF) (500 ml) was made up of hydrophobic polymethyl methacrylate (PMMA). Moreover, PMMA has the advantage of possessing a high level of clarity (92% light transmission), thereby almost comparable optical properties with glass. For sterilization, disassembled CCF components were immersed in 50% (v/v) benzalkonium chloride for 5 h, washed thoroughly in sterile water and dried at 60°C. After that, all the components of the CCF were surface-sterilized under UV light (TUV15W/G15T8, Philips, The Netherlands) in a laminar airflow bench for 30 min. To each Erlenmeyer flask or PMMA-CCF, 150 ml of ASN-III medium was added along with equal inoculum (0.18 mg ml⁻¹ dry weight).

Measurement of planktonic and biofilm biomass

Late log-phase culture (planktonic biomass) was harvested by centrifugation at 10 000 g for 10 min. The biofilms were scrapped off from the surface of the slides by sharp scalpel at the end of the experiment. Biomass were washed thrice with sterile distilled water for removing the salts and further dried at 50°C. Finally, the constant dry weight of biomass was determined on an analytical balance (Sartorius AG, Germany model GD103).

Extraction and analysis of EPS

In order to obtain capsular/bound polysaccharides (CPS), dried cyanobacterial pellet was incubated with 0.1 mol l⁻¹ sulphuric acid at 95°C for 1 h. After the incubation, samples were centrifuged (4000 g, 5 min; Eppendorf model 5810R, rotor F-34-6-38) and the resulting supernatant was separated from the pellet. Similarly, released polysaccharide (RPS) was extracted from the cell-free culture liquids (Gacheva *et al.* 2013). Both supernatants were precipitated with ethanol in a ratio 1 : 3 (v/v) (supernatant: 99% ethanol) and polysaccharides

were pelletized at 10 000 g for 10 min. The pellets were washed thrice with 65% ethanol to remove any contaminants if left and dried at 37°C (Di Pippo *et al.* 2013). Total carbohydrate in the RPS and CPS were determined by the Anthrone method (Schneegurt *et al.* 1994).

Determination of chlorophyll *a* and phycobiliprotein concentration

The cyanobacterial pellet was treated with a 90% methanol for complete extraction of chlorophyll *a*. After centrifugation at 10,000 g for 10 min at 4°C, chlorophyll *a* (C) was spectrophotometrically quantified at 665 nm. Phycobiliproteins (PBP) were extracted from the freshly harvested biomass by the method of freeze thawing in 0.05 mol l⁻¹ phosphate buffer (pH 6.8). The biomass was frozen at -20°C for 48 h and then thawed at 5°C by adding phosphate buffer. It was followed by centrifugation at 10 000 g for 10 min at 4°C. The amounts of phycoerythrin (PE), phycocyanin (PC) and allophycocyanin (APC) in the supernatant fraction were calculated by measuring the optical densities at 565, 620 and 650 nm (Tandau de Marsac and Houmard 1988). Pigment concentration was calculated based on the following equations

$$C(\mu\text{g g}^{-1}) = (\text{OD}_{665\text{ nm}} \times 13.9), \text{PC}(\text{mg g}^{-1}) \\ = (\text{OD}_{620\text{ nm}} - 0.7 \times \text{OD}_{650\text{ nm}}) / 7.38$$

$$\text{APC}(\text{mg g}^{-1}) = (\text{OD}_{650\text{ nm}} - 0.19 \times \text{OD}_{620\text{ nm}}) / 5.65$$

$$\text{PE}(\text{mg g}^{-1}) = (\text{OD}_{565\text{ nm}} - 2.8[\text{PC}] - 1.34[\text{APC}]) / 12.7$$

Preparation of extracts

Cyanobacterial extracts (CBE) were obtained by homogenization of 1 g of dry biomass with 10 ml of 1 : 1 chloroform (CHCl₃) : methanol (MeOH). Furthermore, the homogenate was filtered using Whatman no. 1 filter paper. The filtrate was evaporated to dryness and stored at -20°C.

Analysis of metabolite profiles

Thin layer chromatography

Each crude extract (25 mg ml⁻¹) was dissolved in CHCl₃-MeOH (1 : 1, v/v) and applied (10 μl) to form a single spot in a corner of an aluminium-backed silica gel TLC sheet. The TLC sheets were developed in acetonitrile : heptane : chloroform (1 : 4.5 : 4.5 v/v/v), dried and sprayed by anisaldehyde sulphuric acid reagent. The plates were heated at 105°C and the spots were visualized to detect lichen constituents (depside—acid residues linked by ester group, depsidones—additional ether bond

between aromatic rings) (violet) (Roullier *et al.* 2011), phenols (blue), terpenes (red), sugars (grey) and steroids (green). Finally, the r_f (distance travelled by solute/distance travelled by solvent) value was measured.

High performance liquid chromatography

Twenty microlitres of CBE ($25 \mu\text{g } \mu\text{l}^{-1}$) was subjected to analytical high performance liquid chromatography (HPLC) for metabolite profile analyses. HPLC (Model: Shimadzu, SPD-M20A, Japan) was performed using a reverse phase column (Merck, Lichrospher-100, RP-18, end-capped, 250×4.6 mm, particle size $5 \mu\text{m}$) and operated at 25°C . The solvent was degassed for at least 30 min before use. The isocratic chromatographic separation parameters were—detection: PDA 254 nm; mobile phase: mixture of acetonitrile 60%, water 40%, flow rate of 1 ml min^{-1} . The total run time was 45 min (Challouf *et al.* 2011; Afreen *et al.* 2017).

Liquid chromatography–electrospray ionization-MS

Crude organic extract of Cyanobacteria amounting to 100 ng ml^{-1} was dissolved in 1 : 1 acetonitrile : water. Chromatographic separation was achieved using Phenomenex Kinetex $5 \mu\text{C}18$ 100A 50×3 mm column. The mobile phase (0.1% formic acid in Milli Q water and mixed with 10 mmol l^{-1} ammonium acetate and 0.1% formic acid in acetonitrile) was used at the rate of 0.2 ml min^{-1} . Triple Quadrupole LC-MS Mass Spectrometer (API 2000, AB Sciex Instruments, Applied Biosystems, MDS Sciex, Toronto, Canada) within built LC-20AD pump and PDA coupled with triple quadrupole tandem mass spectrometer was used. ESI-MS conditions and parameters were operated by Analyst 1.5 software (Applied Biosystems, MDS Sciex, Toronto, Canada). The high-intensity m/z peaks were picked by using the software (seeMS, ProteoWizard 3.0.10827). The molecular structure was predicted for high-intensity m/z by using the Mass Database (<http://www.massbank.jp/en/database.html>). Finally, from the literature, the possible biological activities were assigned for the molecular structure (Hastings *et al.* 2013; Download Free Scientific Publications, <http://freefullpdf.com/#gsc.tab=0>).

Antimicrobial assay

Antimicrobial properties of marine Cyanobacteria extracts were tested against the bacterial strains *Staphylococcus aureus* MTCC 2940, *B. subtilis* MTCC 441 and fungus *Candida albicans* MTCC 227. The bacterial and fungal cultures were cultivated in Muller–Hinton Broth (MHB) and incubated overnight at 37°C . After 12–18 h, the microbial cultures were harvested and the turbidity adjusted to 10^6 CFU per ml. CBE were initially solubilized

in 10% methanol (MeOH) at 10 mg ml^{-1} (Jerez-Martel *et al.* 2017). Aliquots of $50 \mu\text{l}$ of CBE or solvent (negative control) and $30 \mu\text{l}$ of $3.3 \times$ strength MH broth were added to the appropriate microtitre wells. Finally, $10 \mu\text{l}$ of microbial suspension was added to each well to achieve a concentration of 5×10^5 CFU per ml. After incubation (37°C for 18–24 h), $10 \mu\text{l}$ of resazurin was added and kept for 4 h in the incubator shaker. The colour change was then assessed by using ELISA plate reader at excitation 560 and emission 590 nm (Sarker *et al.* 2007). Percentage of inhibition calculated by applying the formula

$$\% \text{ of inhibition} = (\text{Control} - \text{Test}) / \text{Control} \times 100$$

Results

Hydrophobicity test

After mixing with *n*-hexadecane, the *Oscillatoria* (AP17) filaments remained in the aqueous lower phase, indicating their hydrophilicity, whereas *Leptolyngbya* (AP3b) filaments transferred to the hydrocarbon upper phase (hydrophobicity) and *Chroococcus* (AP3U) dispersed in the aqueous and hydrocarbon phase (intermediate; Fig. 1).

Effect of flask configuration and surface property on growth, biofilm formation, EPS production and pigment accumulation

The initial inoculum of the three strains settled and grew at the bottom of EF and CCF. After 7 days, in CCF, the culture started to attach and grow to form biofilms on the rectangular strips of the inner arrangement of the CCF cultivation (Fig. 2a–d). Biofilm formation (as recorded by average dry weights) was found to be high in *Oscillatoria* (AP17) (0.0665 ± 0.02 g) than *Leptolyngbya* (AP3b) (0.030 ± 0.007 g) and *Chroococcus* (AP3U) (0.0286 ± 0.008 g), whereas no biofilm was observed in the EF setup. Biofilms formed by *Oscillatoria* (AP17), *Leptolyngbya* (AP3b) and *Chroococcus* (AP3U) contained much higher proportion of CPS (70 ± 0.28 ; 66.304 ± 5.6 and $8.2 \pm 0.07 \text{ mg g dw}^{-1}$ respectively) than the planktonic biomass of EF (58.7 ± 4.6 ; 59.2 ± 9.4 and $1.6 \pm 0.2 \text{ mg g dw}^{-1}$ respectively). Cell suspension RPS-polysaccharides was found to be higher (22 ± 1.3 ; 49.7 ± 2.8 and $29.15 \pm 4 \text{ mg l}^{-1}$ respectively) in the PMMA-CCF cultivation of *Oscillatoria* (AP17), *Leptolyngbya* (AP3b) and *Chroococcus* (AP3U) against the EF setup (10.42 ± 0.7 ; 43.4 ± 4.4 and $10.16 \pm 0.2 \text{ mg l}^{-1}$ respectively). Planktonic cell growth was always higher in the EF compared to the CCF.

Among the two configurations tested for three cyanobacterial cultivation, *Oscillatoria* (AP17) and *Chroococcus* (AP3U) accumulated highest amount of

chlorophyll *a* in biofilms (1378 ± 211 and $183.18 \pm 5.7 \mu\text{g g}^{-1}$) than in planktonic (657 ± 140 and $65.72 \pm 1.9 \mu\text{g g}^{-1}$) growth. However, this was reversed for *Leptolyngbya* (AP3b): biofilm ($548.3 \pm 3.8 \mu\text{g g}^{-1}$)



Figure 1 Adherence of Cyanobacteria to hydrocarbon or partitioning of Cyanobacteria in the biphasic system. Test tubes containing *Leptolyngbya* sp. AP3b (left), *Chroococcus* sp. AP3U (middle) and *Oscillatoria* sp. AP17 (right). [Colour figure can be viewed at wileyonlinelibrary.com]

and planktonic ($849.7 \pm 2.8 \mu\text{g g}^{-1}$). PC and APC concentrations of *Leptolyngbya* (AP3b) were higher in the planktonic (9.6 ± 0.3 and $25.4 \pm 0.5 \text{ mg g}^{-1}$ respectively) compared to the biofilm (4.3 ± 0.3 and $16.8 \pm 0.4 \text{ mg g}^{-1}$), while PC, APC and PE concentrations of AP17 and AP3U did not vary significantly in planktonic (PC: $1.3 \pm 1.2 - 7.8 \pm 1.8$; APC: $2.6 \pm 1.9 - 3.7 \pm 1.4$; PE: $1.2 \pm 0.1 - 3.9 \pm 0.5 \text{ mg g}^{-1}$) and biofilm (PC: $2.0 \pm 1.3 - 7.7 \pm 0.2$; APC: $3.9 \pm 1.8 - 4.4 \pm 0.1$; PE: $1.6 \pm 0.1 - 3.6 \pm 0.7 \text{ mg g}^{-1}$) growth.

Effect of flask configuration and surface property on metabolite profile by TLC, HPLC and LC-MS

A descriptive (qualitative) analysis of the class of components (steroids: green arrows; phenols: blue arrows; sugars: orange arrows; lichen constituents: violet arrows; identical spots: black arrows; unique spots: yellow arrows) that were clearly visible in the material used in the exposures (Fig. 3). TLC of the crude extract of *Oscillatoria* (AP17) biofilm (CCF) depicted 10 spots, whereas EF cultivation of planktonic extracts displayed eight spots. The R_f values $\{(0.18, 0.38, 0.47, 0.53, 0.58, 0.67, 0.92, 0.98)\}$ (3–10) indicated eight spots were identical in the both extracts. Two unique spots with the R_f values $\{(0.07, 0.13)\}$ (1–2) detected in the biofilm (CCF) extracts were not found in the planktonic (EF) biomass (Fig. 3a). TLC of the crude extract of *Leptolyngbya* (AP3b) cultivated in CCF exhibited eight spots, whereas EF-cultivated extracts showed 10 spots. Seven spots with different R_f values $\{(0.04, 0.51, 0.54, 0.55, 0.62, 0.87, 0.91)\}$ (1, 3–6, 10–11) were identical in both extracts (CCF and EF). Unique spots with the R_f values of 0.09, 0.70, 0.75 (2, 8–9) was

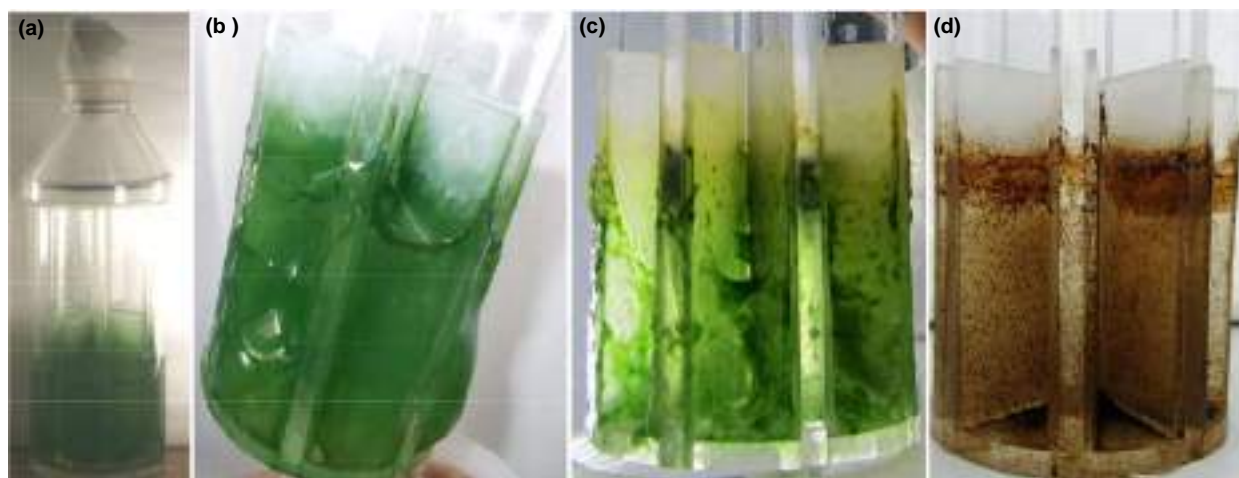


Figure 2 Biofilm growth of Cyanobacteria. (a) Biofilm cultivation of *Oscillatoria* sp. AP17 in PMMA-CCF setup, (b) Biofilm formation of *Oscillatoria* sp. AP17, (c) *Leptolyngbya* sp. AP3b and (d) *Chroococcus* sp. AP3U on inner arrangement of the CCF cultivation. [Colour figure can be viewed at wileyonlinelibrary.com]

observed in EF. Nevertheless, CCF setup displayed a single unique spot $\{(0.63) (7)\}$ (Fig. 3b). TLC of the crude extract of *Chroococcus* (AP3U) cultivated in CCF showed 11 spots, whereas EF cultivation extracts exhibited 16 spots. The R_f values showed nine spots $\{(0.21, 0.47, 0.52, 0.55, 0.57, 0.65, 0.80, 0.88, 0.98) (2, 7-10, 12, 15, 17, 19)\}$ identical in both extracts. Unique spots with R_f values of $\{(0.18, 0.29, 0.40, 0.62, 0.70, 0.72, 0.96) (1, 3, 5, 11, 13-14, 18)\}$ and $\{(0.26, 0.37, 0.83) (4, 6, 16)\}$ were detected EF and CCF-cultivated extracts only (Fig. 3c).

There were several peaks with retention time (min) of 0.421, 1.226, 1.648, 2.243, 4.821, 13.645, 15.994, 18.614, 22.964 and 35.422 observed in the HPLC profiles of all biofilms. Growth of Cyanobacteria in different configuration (CCF and EF) resulted in dissimilar metabolite profiles. There were several different major peaks and relative percentage of the peak area in the HPLC profiles of CBE as evident (Fig. S1a-f, Table S1a-c).

In the present investigation, the LC-MS analysis of biofilm and planktonic crude extracts showed a different metabolite profile. The identification and quantification of metabolites was out of the purview of this study and therefore not attempted. The main objective was to demonstrate differences in metabolite profile arising due to varied cultivation techniques. The high mass intensity peak was picked-up in biofilm and planktonic set up (Fig. S2, Table 1). It was possible to assign the biological activity observed for the high-intensity mass peaks from the

literature (Table 1). While *Oscillatoria* (AP17) biofilm and planktonic extract gave rise to 13 and 20 intensive mass peaks (Table 1a, Fig. S2a,b). The biofilm and planktonic extract of *Leptolyngbya* (AP3b) possessed 21 and 24 intensive mass peaks (Table 1b, Fig. S2c,d). However, the biofilm and planktonic extract of *Chroococcus* (AP3U) displayed 21 and 22 intensive mass peaks (Table 1c, Fig. S2e,f).

Effect of flask configuration and surface property on antimicrobial activity

Cyanobacterial extracts exhibited different antimicrobial activity when cultured under different configurations. The PMMA-CCF-cultivated *Leptolyngbya* (AP3b) and *Chroococcus* (AP3U) extracts had higher antibacterial activity (72 ± 6 and $52 \pm 4\%$ respectively) against *B. subtilis* than EF (59 ± 4 and 0% respectively). The EF- and CCF-cultivated *Oscillatoria* (AP17) extracts did not show activity against tested microbes ($7 \pm 0.4 - 20 \pm 0.8\%$). No significant activity was detected when all the extracts were checked against *S. aureus* ($7 \pm 0.3 - 14 \pm 9\%$) and *C. albicans* ($7 \pm 0 - 21 \pm 9\%$).

Discussion

The conventional mass propagation strategies for cultivating different cyanobacterial strains are being used since long for commercial exploitation. However, the

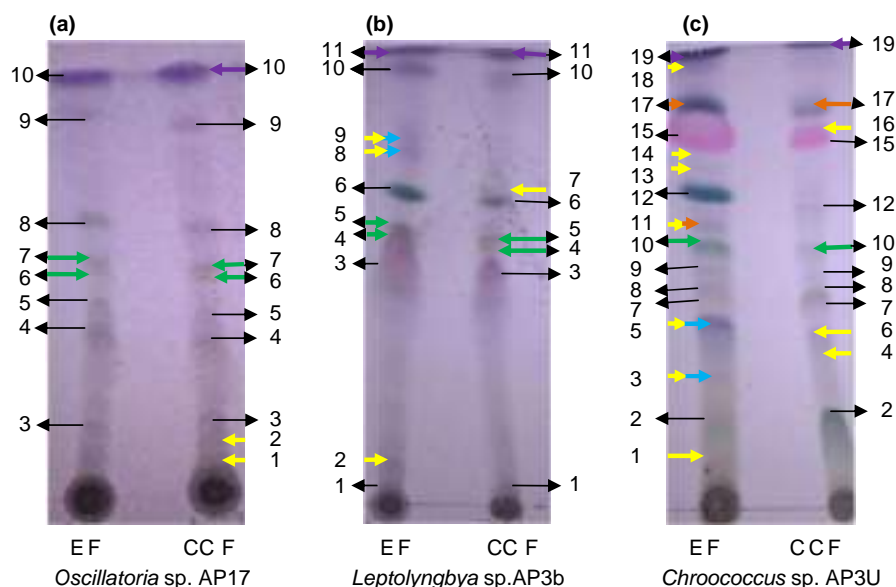


Figure 3 Qualitative identification of compound classes in the cyanobacterial extracts cultivated in EF and CCF. Extract was loaded on silica gel plates and developed with acetonitrile : heptane : chloroform (1 : 4.5 : 4.5 v/v/v) solvent mixture. After development, the plate was sprayed with anisaldehyde sulphuric acid reagent. Violet, orange blue and green arrows indicate the presence of lichen constituents, sugars, phenols and steroids respectively. Black and yellow arrows indicate the presence of identical and unique spots. EF, Erlenmeyer flask; CCF, conico cylindrical flask. [Colour figure can be viewed at wileyonlinelibrary.com]

Table 1 High-intensity peak found in cyanobacterial crude extracts were analysed by LC-MS. High-intensity peak detected in the molecular range of EF and CCF cultivation of cyanobacterial extracts that show significant changes in profiles and biological activity between planktonic and biofilm. The high-intensity *m/z* peaks were picked by using the software. The molecular structure was predicted for high-intensity *m/z* by using the mass database. Finally, from the literature, the possible biological activities were assigned for the molecular structure

<i>m/z</i> range	EF	Biological functions	CCF	Biological functions
(a) <i>Oscillatoria</i> sp. AP17				
100–200	162.6	Anti-inflammatory (Zhao <i>et al.</i> 2013)	158.7	Fungicide (Thurman <i>et al.</i> 2005)
	187.4	Antimicrobial (Zhao <i>et al.</i> 2014)		
200–300	212.8	Macrophage-stimulating activity (Perry <i>et al.</i> 2015)	203.9	–
300–400	389.1	–	–	–
400–500	411.6	Antimycobacterial (Bose <i>et al.</i> 2015)	401	–
	437	–	430.4	Inhibitory effects on superoxide anion generation and elastase release (Sung <i>et al.</i> 2009)
	462.8	Anticancerous food (Abu-Reidah <i>et al.</i> 2015a)		
	488.8	–		
500–600	516.3	Antimicrobial (Mallocci <i>et al.</i> 2015)	502.7	–
	542	–	556.8	–
	578.5	Antidepressant effect (Wu <i>et al.</i> 2015)	582.4	–
600–700	613	–	608.8	Antioxidant (Shi <i>et al.</i> 2012)
700–1000	717.5	–	729.2	–
	743.3	–	807.5	–
	800.6	–	953.6	–
	826.3	–	980.2	–
	906.3	–		
	932.2	–		
	959.2	–		
	984.7	–		
(b) <i>Leptolyngbya</i> sp. AP3b				
100–200	135.8	–	–	–
	162.9	–	–	–
200–300	287	Antimicrobial activity (Shaaban <i>et al.</i> 2012)	268.6	Antifungal (Hastings <i>et al.</i> 2013)
300–400	315.1	c-Src kinase inhibitory activity (Chand <i>et al.</i> 2014)	296.7	Antimicrobial activity (Elleuch <i>et al.</i> 2010)
	341.1	Neuroprotective effect (Jiang <i>et al.</i> 2013)	324.8	Oligoglycerol Derivative (Singh <i>et al.</i> 2016)
	367.6	–	359.6	Antitumor activity (Cao <i>et al.</i> 2016)
	394.7	Nutraceutical (Abu-Reidah <i>et al.</i> 2015b)	384.8	Antioxidant activity (Xu <i>et al.</i> 2016)
400–500	421	–	415.2	Radical scavenging activity (Li <i>et al.</i> 2009)
	446.9	Protective effects on cardiocytes (Li <i>et al.</i> 2015)	441.3	Acetylcholinesterase inhibitory activity (Xiaoming <i>et al.</i> 2013)
	460.5	–	466.7	–
	476.9	Antibacterial (Voukeng <i>et al.</i> 2017)	482.9	Bacteriotoxic and fungitoxic (Chen <i>et al.</i> 2017)
500–600	502.9	–	508.8	Polyphenolic compound (Flamini <i>et al.</i> 2015)
	585.2	–		
600–700	610.5	Antiradical potential (Petrica <i>et al.</i> 2014)	605.9	–
	686.8	Mutagenic activity (Zanutto <i>et al.</i> 2012)	692.7	–
700–1000	766.3	–	778.2	–
	794	–	806.2	–
	824.6	–	832.7	–
	850.7	–	858.1	–
	877.2	–	883.5	–
	902.4	–	910.2	–
	928	–	938.1	–
	954.4	–	965.3	–
	980	–	990.5	–
	(c) <i>Chroococcus</i> sp. AP3U			
200–300	207	–	276.5	Neuroprotective activity (Entrena <i>et al.</i> 2005)
	268.9	Antifungal (Hastings <i>et al.</i> 2013)		
	295	Antimicrobial (Nagia <i>et al.</i> 2012)		

(Continued)

Table 1 (Continued)

<i>m/z</i> range	EF	Biological functions	CCF	Biological functions
300–400	322.7	Antimicrobial (Hsiao <i>et al.</i> 2015)	316.7	–
	351.2	Volatile compounds (Richters <i>et al.</i> 2016)	342.5	Antibacterial activity (Song <i>et al.</i> 2014)
			372.8	–
400–500	383.1	–	397.7	Antispasmodic (Mao <i>et al.</i> 2016)
	453	Inhibition of alpha–glucosidase (Ali <i>et al.</i> 2015)	449.5	Immune booster and Antidiarrhoeal (Lai <i>et al.</i> 2013)
	492.4	–	474.5	Cytotoxicity (Nguyen <i>et al.</i> 2015)
			499.9	–
500–600	518.4	–	526.4	Protein kinase activity (Jiménez-Sánchez <i>et al.</i> 2017)
	544.4			
	569.5			
	595.8	UV–protective (Hermánková–Vavříková <i>et al.</i> 2017)	551.3	Antibacterial (Widsten <i>et al.</i> 2014)
600–700			576.2	–
	628.4	Cytotoxic (Liu <i>et al.</i> 2012)	604.7	–
	658.3	–	635.1	–
	684.6	–	66.3	–
			691.5	–
700–1000	711.6	–	717.1	–
	847.8	–	863.4	–
	874	–	893.1	–
	899.4	–	921.3	–
	924.5	–	947.4	–
	950.4	–	972.4	–
	976	–	997	–

nonconventional or innovative approaches are seldom attempted, the present investigation is one such effort wherein applicability of the CCF for cyanobacterial biofilm cultivation was proposed in place of commonly used laboratory Erlenmeyer flask. This was done to achieve enhanced biofilm growth, improved pigment, EPS and antimicrobial metabolite production. Such an approach to produce biofilm was executed in the past to study the biomass and lipid production of biofilm-forming Cyanobacteria in designed batch systems and in a semi-continuous flow incubator cultivation system (Bruno *et al.* 2012).

Based on the surface property obtained from the hydrophobicity test of the mentioned strains, it appeared that *Oscillatoria* (AP17) was hydrophilic while *Leptolyngbya* (AP3b) was hydrophobic in nature but the hydrophobicity of *Chroococcus* (AP3U) was found to be intermediate in nature. In our study, biofilm as well as planktonic growth of the cyanobacterial strains were not corroborated with cell surface hydrophobicity. All the three strains preferably grew more at a faster rate as suspended in the bottom of EF compared to CCF, yielding higher planktonic biomass in EF. Gradually, the organisms started to attach and form biofilm on the PMMA strips within a stipulated time, but failed to attach to the conventional flask due to lack of enhanced surface area, thereby forming no biofilm in EF. This might be the

reason of getting some biofilm growth in the PMMA vessels, although not higher than the planktonic growth of EF. Considering, both the vessels, CCF and EF showed comparable productivity in terms of total biomass (planktonic + biofilm) growth. In CCF, the growth was distributed in planktonic as well as biofilm formation due to having increased surface area, whereas the EF showed only planktonic growth.

The biofilm was highest in *Oscillatoria* (AP17), followed by *Leptolyngbya* (AP3b) and *Chroococcus* (AP3U). The density of the biofilm (attached biomass) varied among the three organisms. The development of *Stigeoclonium* sp. biofilms on polypropylene bundle was higher than other surface materials (nylon mesh, polyethylene mesh, polycarbonate plate and viscose rayon) used for cultivation by Kim *et al.* (2015). Mixed culture of seven algae produced high biofilm growth on cellulose than silicone rubber, polystyrene, polycarbonate, glass and acrylic. These data showed the surface materials could play an important role for the production of biofilm, an important assumption when considering the possibility of using cyanobacterial cultures for mass cultivation aimed at industrial application (Genin *et al.* 2014).

EPS from cyanobacterial biofilm acts as an organic reservoir for the entire microbial community (Stuart *et al.* 2016). Intertidal environments are characterized by fluctuations in environmental parameters, thereby

considered as 'oligotrophic or poikilotrophic' which often experience a nutrient-limiting condition (Richert *et al.* 2005). Cyanobacteria of the intertidal zone are constantly exposed to fluctuations in temperature, UV radiation, desiccation and salinity and to combat these effects of extreme ecological fluctuations, overproduction of EPS takes place (Olsson-Francis *et al.* 2013). Previous studies by Rougeaux *et al.* (2001) have demonstrated that Polynesian microbial mats produce large amounts of exopolysaccharides associated with Cyanobacteria as the predominating species. The results in the present study highlighted the comparative account of the biofilm formation in terms of EPS production between enhanced surface area CCF vessel and the EF, which shows that CCF vessel promotes the biofilm formation in the PMMA strips at the solid-liquid interface, probably behaving as a new oligotrophic or poikilotrophic environment, thereby producing significantly higher amounts of EPS than in the EF. Although the planktonic biomass was much higher in EF than the in biofilm of CCF, the EPS formation was not dependent on the biomass-biovolume effect, rather the production was aimed to develop more nutrient as well as water channels to withstand the new environment by the strains *Oscillatoria* (AP17) and *Chroococcus* (AP3U). On the contrary, the strain *Leptolyngbya* (AP3b) produced comparable amounts of EPS, when cultivated as planktonic mode in EF and biofilm mode in CCF.

The results showed that biofilm mode of growth on surface material PMMA could potentially promote chlorophyll *a* accumulation in *Oscillatoria* (AP17) and *Chroococcus* (AP3U) than planktonic biomass, it was reversed in *Leptolyngbya* (AP3b). In previous studies, the chlorophyll content was decreased in the cell suspension, while the remaining chlorophyll resided in biofilm-forming cells attached to the surface (Parnasa *et al.* 2016). Earlier studies with benthic diatoms and microphytobenthos from intertidal mudflat, reported the positive relationship between extracellular carbohydrates and chlorophyll, suggesting that EPS production was coupled with photosynthesis (Cyr and Morton 2006). This observation supports our study, where enhanced rate of photosynthesis in the biofilm of *Oscillatoria* (AP17) and *Chroococcus* (AP3U) might have resulted in greater RPS and CPS formation in CCF mode of cultivation. Meanwhile, lesser chlorophyll formation in *Leptolyngbya* (AP3b) biofilm grown under CCF indicated decreased rate of photosynthesis followed by insignificant EPS synthesis.

Measurement of the concentration of the accessory pigments (PC, APC and PE) in case of strains *Oscillatoria* (AP17) and *Chroococcus* sp. AP3U did not vary significantly along with the change in their surface properties. This observation shows a general trend that the major pigment like chlorophyll *a* content was influenced much

more by the change in surface material than that of the accessory pigments. However, the increase in the overall APC and PC content for *Leptolyngbya* (AP3b) in comparison to the other strains can probably be explained due to its growth pattern. *Oscillatoria* (AP17) and *Chroococcus* (AP3U) were able to attach to the surface uniformly, whereas *Leptolyngbya* (AP3b) exhibited some clumping (Fig. 2c). Agusti and Phlips (1992) observed that to achieve maximum light absorption for photosynthesis, the accessory pigment contents increased to attain a comparatively less uniform growth pattern. Authors also reported that Cyanobacteria colonies avoided self-shading with increasing size by reducing internal pigment concentration as colony size increased. The ability of many Cyanobacteria species to develop colonies may increase the efficiency of light absorption than single celled Cyanobacteria.

In this study, metabolite profiles were studied and compared by preliminary (TLC) and advanced technique (HPLC and LC-MS). TLC profile of the CCF and EF cultivation revealed that all the spots identified in case of EF and CCF were almost identical for *Oscillatoria* (AP17) and *Leptolyngbya* (AP3b), while for *Chroococcus* (AP3U), visible spots showed a clear difference between CCF and EF. Furthermore, HPLC investigation of the metabolite profile showed a remarkable difference between both the area and the retention time for the metabolites studied in the crude extracts. The study demonstrated the direct relation between mode of growth and the metabolite profile. Previous report persuasively confirmed that the profiles of cyanobacterial secondary metabolite production varied under different light and phosphate levels (Repka *et al.* 2004). The LC-MS mass intensity profiles divulged significant differences in biofilm and planktonic extracts. However, the high intensity of the mass did not always match with the planktonic CBEs (Table 1). The mass found with high intensity in Cyanobacteria exhibited wide range of biological activities such as antioxidant, anti-inflammatory, immunomodulatory, anticancerous, antidiabetic, antimicrobial, antidepressant, antifouling, enzyme inhibitors, toxicity (cytotoxicity, bacteriotoxic and fungitoxic), protective effect and quorum sensing (Table 1). These results indicated that the change in metabolite profile among different biomasses might be attributed to different amounts of the major high-intensity compounds produced by the Cyanobacteria. It might be also because that the sensitivity of TLC, HPLC and LC-MS was enough to detect some difference in chemical profile (not for identification and quantification) and this difference may be attributed to the different modes of cultivation. Thus, it is certain that there is a difference in terms of the metabolites produced.

In conclusion, the purpose of this study was to utilize a suitable device, with the enhanced surface area, an

alternative to the commonly used laboratory Erlenmeyer flasks, which would enable researchers to verify if surface attachment and biofilm formation of benthic Cyanobacteria would enhance the production of RPS, CPS, pigments and metabolites of Cyanobacteria on a small scale. The biofilm mode of growth and flask configuration affects the overall RPS production; Cyanobacteria grown on PMMA and CCF cultivation had the highest production of RPS among the Cyanobacteria tested, this aspect could be successfully utilized in applications having direct role in pharmaceutical, nutraceutical and cosmeceutical industry. Differences in the biofilm formation between Cyanobacteria grown on PMMA were largely attributed to the biofilm growth rate which was independent of an organism. In future, the isolation of planktonic cyanobacterial species and their behavioural studies under EF and CCF will be evaluated. This study needs more detailed analysis and future research focusing on analysing the monosaccharide compositions of both RPS, CPS and elucidating the structure of the bioactive molecules. Efforts to scale-up the process are urgently needed.

Acknowledgements

The authors thank the funding agencies University Grants Commission [F.42/2006 (BSR)/BL/1415/0332 dated 01/07/2015] and Ministry of Earth Science [18/07/2013 MoES-2/DS/6/2007 PCIV] for their financial assistance.

Conflict of interest

No potential conflict of interest was reported by the authors.

References

- Download Free Scientific Publications. 2017. (May 20, 2017). <http://freefullpdf.com/#gsc.tab=0>
- Mass Database. Mass Spectral Database. 2006-2012. Japan: Nara Institute of Science and Technology (May 20, 2017). <http://www.massbank.jp/en/database.html>
- Abu-Reidah, I.M., Ali-Shtayeha, M.S., Jamous, R.M., Arráz-Román, D. and Segura-Carretero, A. (2015a) Comprehensive metabolite profiling of *Arum palaestinum* (Araceae) leaves by using liquid chromatography-tandem mass spectrometry. *Food Res Int* **70**, 74–86.
- Abu-Reidah, I.M., Ali-Shtayeh, M.S., Jamous, R.M., Arráz-Román, D. and Segura-Carretero, A. (2015b) HPLC-DAD-ESI-MS/MS screening of bioactive components from *Rhus coriaria* L. (Sumac) fruits. *Food Chem* **166**, 179–191.
- Afreen, S., Shamsi, T.N., Baig, M.A., Ahmad, N., Fatima, S., Qureshi, M.I., Hassan, MdI, and Fatma, T.A. (2017) A novel multicopper oxidase (laccase) from cyanobacteria: purification, characterization with potential in the decolorization of anthraquinonic dye. *PLoS ONE* **6**, e0175144.
- Agostoni, M., Waters, C.M. and Montgomery, B.L. (2016) Regulation of biofilm formation and cellular buoyancy through modulating intracellular cyclic di-GMP levels in engineered cyanobacteria. *Biotechnol Bioeng* **113**, 311–319.
- Agusti, S. and Philips, E.J. (1992) Light absorption by cyanobacteria: implications of the colonial growth form. *Limnol Oceanogr* **37**, 434–441.
- Ali, L., Khan, A.L., Al-Kharusi, L., Hussain, J. and Al-Harrasi, A. (2015) New α -glucosidase inhibitory triterpenic acid from marine macro green alga *Codium dwarkense*. *Boergs Mar Drugs* **13**, 4344–4356.
- Behrendt, L., Schrameyer, V., Qvortrup, K., Lundin, L., Sørensen, S.J., Larkum, A.W. and Kühl, M. (2012) Biofilm growth and near-infrared radiation-driven photosynthesis of the chlorophyll d-containing cyanobacterium *Acaryochloris marina*. *Appl Environ Microbiol* **78**, 3896–3904.
- Bose, U., Hewavitharana, A.K., Ng, Y.K., Shaw, P.N., Fuerst, J.A. and Hodson, M.P. (2015) LC-MS based metabolomics study of marine bacterial secondary metabolite and antibiotic production in *Salinispora arenicola*. *Mar Drugs* **13**, 249–266.
- Bruno, L., Di Pippo, F., Antonaroli, S., Gismondi, A., Valentini, C. and Albertano, P. (2012) Characterization of biofilm-forming cyanobacteria for biomass and lipid production. *J Appl Microbiol* **113**, 1052–1064.
- Cao, G., Yang, K., Li, Y., Huang, L. and Teng, D. (2016) Synthetic strategy and anti-tumor activities of macrocyclic scaffolds based on 4-hydroxyproline. *Molecules* **21**, 212.
- Challouf, R., Trabelsi, L., Dhieb, R.B., Abed, O.E., Yahia, A., Ghazzi, K., Ammar, J.B., Omran, H. et al. (2011) Evaluation of cytotoxicity and biological activities in extracellular polysaccharides released by Cyanobacterium *Arthrospira platensis*. *Braz Arch Biol Technol* **54**, 831–838.
- Chand, K., Prasad, S., Tiwari, R.K., Shirazi, A.N., Kumar, S., Parang, K. and Sharma, S.K. (2014) Synthesis and evaluation of c-Src kinase inhibitory activity of pyridin-2 (1H)-one derivatives. *Bioorg Chem* **53**, 75–82.
- Chen, Y., Lu, H., Chen, Y., Yu, W., Dai, H. and Pan, X. (2017) Improved synthesis of 1-O-Acyl- β -D-glucopyranose tetraacetates. *Molecules* **22**, 662.
- Crnkovic, C.M., May, D.S. and Orjala, J. (2018) The impact of culture conditions on growth and metabolomic profiles of freshwater cyanobacteria. *J Appl Phycol* **30**, 375–384. <https://doi.org/10.1007/s10811-017-1275-3>
- Cyr, H. and Morton, K.E. (2006) Distribution of biofilm exopolymeric substances in littoral sediments of Canadian Shield lakes: the effects of light and substrate. *Can J Fish Aquat Sci* **63**, 1763–1776.
- Di Pippo, F., Ellwood, N.T.W., Gismondi, A., Bruno, L., Rossi, F., Magni, P. and De Philippis, R. (2013) Characterization of exopolysaccharides produced by seven biofilm-forming

- cyanobacterial strains for biotechnological applications. *J Appl Phycol* **25**, 1697–1708.
- Dugan, J.E., Hubbard, D.M. and Quigley, B.J. (2013) Beyond beach width: steps toward identifying and integrating ecological envelopes with geomorphic features and datums for sandy beach ecosystems. *Geomorphology* **199**, 95–105.
- Elleuch, L., Shaaban, M., Smaoui, S., Mellouli, L., Karray-Rebai, I., Fguira, L.F., Shaaban, K.A. and Laatsch, H. (2010) Bioactive secondary metabolites from a new terrestrial *Streptomyces* sp. TN262. *Appl Biochem Biotechnol* **162**, 579–593.
- Entrena, A., Camacho, M.E., Carrion, M.D., Lopez-Cara, L.C., Velasco, G., Leon, J., Escames, G., Acuna-Castroviejo, D. et al. (2005) Kynurenamines as neural nitric oxide synthase inhibitors. *J Med Chem* **48**, 8174–8181.
- Fattom, A. and Shilo, M. (1984) Hydrophobicity as an adhesion mechanism of benthic cyanobacteria. *Appl Environ Microbiol* **47**, 135–143.
- Flamini, R., De Rosso, M. and Bavaresco, L. (2015) Study of grape polyphenols by liquid chromatography-high-resolution mass spectrometry (UHPLC/QTOF) and suspect screening analysis. *J Anal Methods Chem* **2015**, 350259.
- Gacheva, G., Gigova, L., Ivanova, N., Iliev, I., Toshkova, R., Gardeva, E., Kussovski, V. and Najdenski, H. (2013) Suboptimal growth temperatures enhance the biological activity of cultured cyanobacterium *Gloeocapsa* sp. *J Appl Phycol* **25**, 183–194.
- Galica, T., Hrouzek, P. and Mareš, J. (2017) Genome mining reveals high incidence of putative lipopeptide biosynthesis NRPS/PKS clusters containing fatty acyl-AMP ligase genes in biofilm-forming cyanobacteria. *J Phycol* **53**, 985–998.
- Genin, S.N., Aitchison, J.S. and Allen, D.G. (2014) Design of algal film photobioreactors: material surface energy effects on algal film productivity, colonization and lipid content. *Bioresour Technol* **155**, 136–143.
- Gismondi, A., Pippo, F.D., Bruno, L., Antonaroli, S. and Congestri, R. (2016) Phosphorus removal coupled to bioenergy production by three cyanobacterial isolates in a biofilm dynamic growth system. *Int J Phytoremediation* **18**, 869–876.
- Hastings, J., deMatos, P., Dekker, A., Ennis, M., Harsha, B., Kale, N., Muthukrishnan, V., Owen, G. et al. (2013) The ChEBI reference database and ontology for biologically relevant chemistry: enhancements for 2013. *Nucleic Acids Res*, **41** (Database issue), D456–D463.
- Hermánková-Vavříková, E., Krenková, A., Petrásková, L., Chambers, C.S., Zápál, J., Kuzma, M., Valentová, K. and Kren, V. (2017) Synthesis and antiradical activity of isoquercitrin esters with aromatic acids and their homologues. *Int J Mol Sci* **18**, 1074.
- Hsiao, T.H., Sung, C.S., Lan, Y.H., Wang, Y.C., Lu, M.C., Wen, Z.H., Wu, Y.C. and Sung, P.J. (2015) New anti-inflammatory cembranes from the cultured soft coral *Nephthea columnaris*. *Mar Drugs* **13**, 3443–3453.
- Jerez-Martel, I., García-Poza, S., Rodríguez-Martel, G., Rico, M., Afonso-Olivares, C. and Gómez-Pinchetti, J.L. (2017) Phenolic profile and antioxidant activity of crude extracts from microalgae and cyanobacteria strains. *Hindawi J Food Qual* **2017**, 1–8.
- Jiang, R., Du, X., Zhang, X., Wang, X., Hu, D., Meng, T., Chen, Y., Geng, M. et al. (2013) Synthesis and bioassay of β -(1,4)-D-mannans as potential agents against Alzheimer's disease. *Acta Pharmacol Sin* **34**, 1585–1591.
- Jiménez-Sánchez, C., Olivares-Vicente, M., Rodríguez-Pérez, C., Herranz-López, M., Lozano-Sánchez, J., Segura-Carretero, A., Fernández-Gutiérrez, A., Encinar, J.A. et al. (2017) AMPK modulatory activity of olive-tree leaves phenolic compounds: bioassay-guided isolation on adipocyte model and in silico approach. *PLoS ONE* **12**, e0173074.
- Kim, B., Kim, D., Choi, J., Kang, Z., Cho, D., Kim, J., Oh, H. and Kim, H. (2015) Polypropylene bundle attached multilayered *Stigeoclonium* Biofilms cultivated in untreated sewage generate high biomass and lipid productivity. *J Microbiol Biotechnol* **25**, 1547–1554.
- Lai, T.N.H., Herent, M., Quetin-Leclercq, J., Nguyen, T.B.T., Rogez, H., Larondelle, Y. and André, C.M. (2013) Piceatannol, a potent bioactive stilbene, as major phenolic component in *Rhodomyrtus tomentosa*. *Food Chem* **138**, 1421–1430.
- Li, D.L., Li, X.M. and Wang, B.G. (2009) Natural anthraquinone derivatives from a marine mangrove plant derived endophytic fungus *Eurotium rubrum*: structural elucidation and DPPH radical scavenging activity. *J Microbiol Biotechnol* **19**, 675–680.
- Li, M., Wang, X., Zheng, X., Wang, J., Zhao, W., Song, K., Zhao, X., Zhang, Y. et al. (2015) A new ionone glycoside and three new rhemaneolignans from the roots of *Rehmannia glutinosa*. *Molecules* **20**, 15192–15201.
- Liu, H., Zhang, H., Yu, J., Xu, C., Ding, J. and Yue, J. (2012) Cytotoxic Diterpenoids from *Sapium insigne*. *J Nat Prod* **75**, 722–727.
- Lopes, V.R. and Vasconcelos, V.M. (2011) Bioactivity of benthic and picoplanktonic estuarine cyanobacteria on growth of photoautotrophs: inhibition versus stimulation. *Mar Drugs* **9**, 790–802.
- Mallocci, G., Vargiu, A.V., Serra, G., Bosin, A., Ruggerone, P. and Ceccarelli, M. (2015) A database of force-field parameters, dynamics, and properties of antimicrobial compounds. *Molecules* **20**, 13997–14021.
- Mao, F., Ni, W., Xu, X., Wang, H., Wang, J., Ji, M. and Li, J. (2016) Chemical structure-related drug-like criteria of global approved drugs. *Molecules* **21**, 75.
- Mazard, S., Penesyan, A., Ostrowski, M., Paulsen, I.T. and Egan, S. (2016) Tiny microbes with a big impact: the role of cyanobacteria and their metabolites in shaping our future. *Mar Drugs* **14**, 97.
- Mitra, S., Thawrani, D., Banerjee, P., Gachhui, R. and Mukherjee, J. (2012) Induced biofilm cultivation enhances

- riboflavin production by an intertidally derived *Candida famata*. *Appl Biochem Biotechnol* **166**, 1991–2006.
- Mitra, S., Gachhui, R. and Mukherjee, J. (2015) Enhanced biofilm formation and melanin synthesis by the oyster settlement-promoting *Shewanella colwelliana* is related to hydrophobic surface and simulated intertidal environment. *Biofouling* **31**, 283–296.
- Mohamed, Z.A. (2013) Allelopathic activity of the norharmane-producing cyanobacterium *Synechocystis aquatilis* against cyanobacteria and microalgae. *Oceanol Hydrobiol Stud* **42**, 1–7.
- Mohamed, Z. and Al-Shehri, A. (2015) Biodiversity and toxin production of cyanobacteria in mangrove swamps in the Red Sea off the southern coast of Saudi Arabia. *Bot Mar* **58**, 23–34.
- Nagarkar, S., Williams, G.A., Subramanian, G. and Saha, S.K. (2004) Cyanobacteria- dominated biofilms: a high quality food resource for intertidal grazers. *Hydrobiologia* **512**, 89–95.
- Nagia, M.M.S., El-Metwally, M.M., Shaaban, M., El-Zalabani, S.M. and Hanna, A.G. (2012) Four butyrolactones and diverse bioactive secondary metabolites from terrestrial *Aspergillus flavipes* MM2: isolation and structure determination. *Org Med Chem Lett* **2**, 9.
- Nguyen, T.T., Parat, M.O., Hodson, M.P., Pan, J., Shaw, P.N. and Hewavitharana, A.K. (2015) Chemical characterization and in vitro cytotoxicity on squamous cell carcinoma cells of *Carica papaya* leaf extracts. *Toxins (Basel)* **8**, E7.
- Olsson-Francis, K., Watson, J.S. and Cockell, C.S. (2013) Cyanobacteria isolated from the high-intertidal zone: a model for studying the physiological prerequisites for survival in low Earth orbit. *Int J Astrobiology* **12**, 292–303.
- Parnasa, R., Nagar, E., Sendersky, E., Reich, Z., Simkovsky, R., Golden, S. and Schwarz, R. (2016) Small secreted proteins enable biofilm development in the cyanobacterium *Synechococcus elongates*. *Sci Rep* **6**, 32209.
- Perry, J.A., Koteva, K., Verschoor, C.P., Wang, W., Bowdish, D.M. and Wright, G.D. (2015) A macrophage-stimulating compound from a screen of microbial natural products. *J Antibiot (Tokyo)* **68**, 40–46.
- Petrica, E.E.A., Sinhorin, A.P., Sinhorin, V.D.G. and Júnior, G.M.V. (2014) First phytochemical studies of japecanga (*Smilax fluminensis*) leaves: flavonoids analysis. *Rev Bras Farmacogn* **24**, 443–445.
- Pramanik, A., Sundararaman, M., Das, S., Ghosh, U. and Mukherjee, J. (2011) Isolation and characterization of cyanobacteria possessing antimicrobial activity from the sundarbans, the world's largest tidal mangrove forest. *J Phycol* **47**, 731–743.
- Raja, R., Hemaiswarya, S., Ganesan, V. and Carvalho, I.S. (2016) Recent developments in therapeutic applications of Cyanobacteria. *Crit Rev Microbiol* **42**, 394–405.
- Repka, S., Koivula, M., Harjunpa, V., Rouhiainen, L. and Sivonen, K. (2004) Effects of phosphate and light on growth of and bioactive peptide production by the Cyanobacterium *Anabaena* Strain 90 and its anabaenopeptilide mutant. *Appl Environ Microbiol* **70**, 4551–4560.
- Richert, L., Golubic, S., Guedes, R.L., Ratiskol, J., Payri, C. and Guezennec, J. (2005) Characterization of exopolysaccharides produced by cyanobacteria isolated from Polynesian microbial mats. *Curr Microbiol* **51**, 379–384.
- Richters, S., Herrmann, H. and Berndt, T. (2016) Different pathways of the formation of highly oxidized multifunctional organic compounds (HOMs) from the gas-phase ozonolysis of caryophyllene. *Atmos Chem Phys* **16**, 9831–9845.
- Rossi, F. and De Philippis, R. (2015) Role of cyanobacterial exopolysaccharides in phototrophic biofilms and in complex microbial mats. *Life* **5**, 1218–1238.
- Rougeaux, H., Guezennec, M., Mao, C.L., Payri, C., Deslandes, E. and Guezennec, J. (2001) Microbial communities and exopolysaccharides from Polynesian mats. *Mar Biotechnol* **3**, 181–187.
- Roullier, C., Chollet-Krugler, M., Pferschy-Wenzig, E., Maillard, A., Rechberger, G.N., Legouin-Gargadenec, B., Bauer, R. and Boustie, J. (2011) Characterization and identification of mycosporines-like compounds in cyanolichens. Isolation of mycosporine hydroxyglutamyl from *Nephroma laevigatum* Ach. *Phytochemistry* **72**, 1348–1357.
- Sanmartín, P., Aira, N., Devesa-Rey, R., Silva, B. and Prieto, B. (2010) Relationship between color and pigment production in two stone biofilm-forming cyanobacteria (*Nostoc* sp. PCC 9104 and *Nostoc* sp. PCC 9025). *Biofouling* **26**, 499–509.
- Sarkar, S., Roy, D. and Mukherjee, J. (2015) Council of Scientific and Industrial Research and School of Environmental Studies, New Delhi (IN). 2011/05/19. Enhanced surface area conico- cylindrical flask (es-ccf) for biofilm cultivation. US 8,945,917 B2.
- Sarker, S.D., Nahar, L. and Kumarasamy, Y. (2007) Microtitre plate-based antibacterial assay incorporating resazurin as an indicator of cell growth, and its application in the *in vitro* antibacterial screening of phytochemicals. *Methods* **42**, 321–324.
- Schneegurt, M.A., Sherman, D.M., Nayar, S. and Sherman, L.A. (1994) Oscillating behavior of carbohydrate granule formation and dinitrogen fixation in the cyanobacterium *Cyanothece* sp. strain ATCC 51142. *J Bacteriol* **176**, 1586–1597.
- Shaaban, M., Shaaban, K.A. and Abdel-Aziz, M.S. (2012) Seven naphtho-g-pyrones from the marine-derived fungus *Alternaria alternata*: structure elucidation and biological properties. *Org Med Chem Lett* **2**, 6.
- Shi, S., Ma, Y.Y., Zhang, Y., Liu, L., Liu, Q., Peng, M. and Xiong, X. (2012) Systematic separation and purification of 18 antioxidants from *Pueraria lobata* flower using HSCCC target-guided by DPPH-HPLC experiment. *Sep Purif Technol* **89**, 225–233.

- Singh, A.K., Nguyen, R., Galy, N., Haag, R., Sharma, S.K. and Len, C. (2016) Chemo-enzymatic synthesis of oligoglycerol derivatives. *Molecules* **21**, 1038.
- Song, F., Ren, B., Chen, C., Yu, K., Liu, X., Zhang, Y., Yang, N., He, H. et al. (2014) Three new sterigmatocystin analogues from marine-derived fungus *Aspergillus versicolor* MF359. *Appl Microbiol Biotechnol* **98**, 3753–3758.
- Stuart, R.K., Mayali, X., Lee, J.Z., Everroad, R.C., Hwang, M., Bebout, B.M., Weber, P.K., Pett-Ridge, J. et al. (2016) Cyanobacterial reuse of extracellular organic carbon in microbial mats. *ISME J* **10**, 1240–1251.
- Sung, P., Su, Y., Li, G., Chiang, M.Y., Lin, M., Huang, I., Li, J., Fang, L. et al. (2009) Excavatoids A–D, new polyoxygenated briaranes from the octocoral *Briareum excavatum*. *Tetrahedron* **65**, 6918–6924.
- Tandeau de Marsac, N. and Houmard, J. (1988) Complementary chromatic adaptation: physiological conditions and action spectra. *Methods Enzymol* **167**, 318–328.
- Thurman, E.M., Ferrer, I., Zweigenbaum, J.A., Garcia-Reyes, J.F., Woodman, M. and Fernandez-Alba, A.R. (2005) Discovering metabolites of post-harvest fungicides in citrus with liquid chromatography/time-of-flight mass spectrometry and ion trap tandem mass spectrometry. *J Chromatogr A* **1082**, 71–80.
- Voukeng, I.K., Nganou, B.K., Louis, P., Sandjo, L.P., Celik, I., Beng, V.P., Tane, P. and Kuete, V. (2017) Antibacterial activities of the methanol extract, fractions and compounds from *Elaeophorbia drupifera* (Thonn.) Stapf. (Euphorbiaceae). *BMC Complement Altern Med* **17**, 28.
- Widsten, P., Cruz, C.D., Fletcher, G.C., Pajak, M.A. and McGhie, T.K. (2014) Tannins and extracts of fruit byproducts: antibacterial activity against foodborne bacteria and antioxidant capacity. *J Agric Food Chem* **62**, 11146–11156.
- Wu, M., Zhang, H., Zhou, C., Jia, H., Ma, Z. and Zou, Z. (2015) Identification of the chemical constituents in aqueous extract of Zhi-Qiao and evaluation of its antidepressant effect. *Molecules* **20**, 6925–6940.
- Xiaoming, Q., Wen, Y., Zhipei, S. and Yong, D. (2013) Synthesis and biological evaluation of genistein carbamate derivatives. *Chin J Org Chem* **33**, 621–629.
- Xu, X., Yue, Y., Jiang, H., Sun, J., Tang, F., Guo, X. and Wang, J. (2016) Chemical constituents and antioxidant properties of *Phyllostachys prominens* Gramineae (W Y Xiong) leaf extracts. *Trop J Pharm Res* **15**, 569–575.
- Zanutto, F.V., Boldrin, P.K., Varanda, E.A., Fernandes de Souza, S., Sano, P.T., Vilegas, W. and Campaner dos Santos, L. (2012) Characterization of flavonoids and naphthopyranones in methanol extracts of *Paepalanthus chiquitensis* Herzog by HPLC-ESI-IT-MSn and their mutagenic activity. *Molecules* **18**, 244–262.
- Zhao, H.Q., Wang, X., Li, H.M., Yang, B., Yang, H.J. and Huang, L. (2013) Characterization of nucleosides and nucleobases in natural Cordyceps by HILIC-ESI/TOF/MS and HILIC-ESI/MS. *Molecules* **18**, 9755–9769.
- Zhao, J., Li, X., Gloer, J.B. and Wang, B. (2014) First total syntheses and antimicrobial evaluation of penicimonoterpene, a marine-derived monoterpene, and its various derivatives. *Mar Drugs* **12**, 3352–3370.

Supporting Information

Additional Supporting Information may be found in the online version of this article:

Figure S1 HPLC chromatograms of cyanobacterial extracts. *Oscillatoria* sp. (AP17) cultivated in EF (a) and PMMA-CCF (b). *Leptolyngbya* sp. (AP3b) cultivated in EF (c) and PMMA-CCF (d). *Chroococcus* sp. (AP3U) cultivated in EF (e) and PMMA-CCF (f).

Figure S2 Liquid chromatography mass spectra profile of cyanobacterial extracts. *Oscillatoria* sp. (AP17) cultivated in EF (a) and PMMA-CCF (b). *Leptolyngbya* sp. (AP3b) cultivated in EF (c) and PMMA-CCF (d). *Chroococcus* sp. (AP3U) cultivated in EF (e) and PMMA-CCF (f).

Table S1 Peak table of cyanobacterial extracts from EF and CCF cultivation analysed by HPLC. Red blocks indicate the values with area % similar (less than 1%) between EF and CCF while different retention time as well as the values with retention time similar (less than 1 min) between EF and CCF but different area %.



<https://doi.org/10.11646/phytotaxa.374.1.2>

***Oxynema aestuarii* sp. nov. (Microcoleaceae) isolated from an Indian mangrove forest**

SANDEEP CHAKRABORTY¹, VEERABADHRAN MARUTHANAYAGAM¹, ANUSHREE ACHARI², RIDDHI MAHANSARIA¹, ARNAB PRAMANIK³, PARASURAMAN JAISANKAR² & JOYDEEP MUKHERJEE^{1*}

¹*School of Environmental Studies, Jadavpur University, Kolkata 700 032, India*

²*Indian Institute of Chemical Biology, Jadavpur, Kolkata 700 032, India*

³*Department of Biochemistry, University of Calcutta, 35, Ballygunge Circular Road, Kolkata 700 019, India*

*Corresponding author: Tel. 0091 33 2414 6147; Fax 0091 33 2414 6414;

E mail: joydeep.mukherjee@jadavpuruniversity.in

Abstract

Taxonomic characterization by a polyphasic approach was carried out on two cyanobacteria, AP17 and AP24 isolated from soil biofilms of two separate islands, Lothian and Sagar respectively, of the Indian *Sundarbans*. The strains were studied morphologically by light microscopy, scanning and transmission electron microscopy. Growth responses to various salinities were recorded. Molecular data included sequencing and phylogenetic study of the 16S rRNA gene as well as analysis of the 14 regions of the 16S-23S ITS regions. Morphologically the strains were found to be non-heterocytous, having attenuated trichomes with a narrow, bent terminal cell without any crosswalls. Strains under investigation shared 99–100% 16S rRNA gene sequence similarity with *Oxynema thaianum* CCALA960, the type species of the novel *Oxynema* genus, recently separated from the *Phormidium*-Group I genus. However, cross walls in the apical portion of AP17 and AP24 were totally absent while the same was present in CCALA960. Additionally, optimal growth of AP17 and AP24 was recorded in 5–8% salinity and salinity above 14% inhibited growth of both strains, which were isolated from an intertidal environment; whereas *O. thaianum* CCALA960 which was found in a hypersaline environment could grow at 40% salinity. Insertion of 9 nucleotides in the D2 with spacer region, insertion of 2 nucleotides in the pre Box B spacer region, deletion of 2 nucleotides in the post Box B spacer region, deletion of 8 nucleotides in the D4 region, deletion of 8 nucleotides in V3 region and insertion of 2 nucleotides in the D5 region of the ITS sequences of AP17 and AP24 were observed in comparison to the analogous regions of CCALA960. Structural details of Box B helices of AP17 and AP24 revealed that although their lengths were identical with the reference, their sequences were completely different from CCALA960. Four nucleotide substitutions were observed in different positions in the Box B helix of *O. thaianum* CCALA960. Secondary structures of the V3 regions of AP17 and AP24 (containing 51 nucleotides) showed a small terminal bulge and a bigger bilateral bulge while the analogous structure of *O. thaianum* CCALA 960 (comprising of 59 nucleotides) showed one additional bilateral bulge in comparison to AP17 and AP24. Therefore, based on morphological, ecological and molecular differences in comparison to *O. thaianum* CCALA960, isolates AP17 and AP24 should be considered as a second novel species in the *Oxynema* genus, for which the name *Oxynema aestuarii* sp. nov. is proposed.

Key words: Cyanobacteria, morphology, *Oxynema*, salinity, *Sundarbans*, 16S-23S ITS

Introduction

The phenotypic plasticity of cyanobacteria arising out of their genetic diversity has enabled them to occupy diverse habitats all over the world. Mangroves are located in the ecotones of land-sea-estuary and provide a heterogeneous habitat along with high productivity (Chen *et al.* 2016). Cyanobacteria inhabiting the mangroves may undergo morpho-ecological changes for their survival which can promote species diversity (Debnath *et al.* 2017). Mangrove forests are distributed worldwide in the tropical and sub-tropical regions which includes about 118 countries (Giri *et al.* 2011). However, reports on mangrove cyanobacterial diversity are restricted to a few countries. As an example, diversity studies based on morphology as well as molecular identifiers was carried out in temperate estuaries of Portugal (Lopes *et al.* 2012) which revealed that morphological characters were occasionally not in the agreement with the phylogenetic

relationship and tended to change in response to the prevailing environmental conditions. Taxonomic investigation of two mangrove ecosystems near Sao Paulo (Brazil) using the polyphasic approach (Silva *et al.* 2014) showed the presence of some newly described genera like *Nodosilinea* and *Oxynema* along with various morphotypes of *Nostoc* and *Leptolyngbya*.

The landmass of the largest tidal mangrove forest in the world, the *Sundarbans* is shared between Bangladesh (62%) and India (38%) (Mondal & Debnath 2017). The ecology of this estuary is characterized by continuous tidal forcing and mixing of water columns that allows cyanobacterial species to thrive and thus producing immense genetic diversity (Neogi *et al.* 2016). The first report on the presence of algal communities in the Indian *Sundarbans* was published by Sen & Naskar (2002). Pramanik *et al.* (2011) assigned six cyanobacteria of the Indian *Sundarbans* to the *Lyngbya-Phormidium-Plectonema* (LPP) Group B and one each to *Oscillatoria* and *Synechocystis* genera based on morphological characteristics. Although the study of Pramanik *et al.* (2011) was not concentrated on the description of novel taxa, it was the opinion of Alvarenga *et al.* (2015) that the results obtained by Pramanik *et al.* (2011) may sustain the definition of novel cyanobacteria. Recently, Debnath *et al.* (2017) described a novel morphotype, *Leptolyngbya indica* isolated from the Lower Gangetic Plains in India which included the Sagar island of the *Sundarbans*.

Traditional taxonomy of cyanobacteria based on their phenotypic characters did not fully support the results of phylogenetic analysis (Rippka *et al.* 1979, Boone & Castenholz 2001, Gugger & Hoffmann 2004). Traditional practice caused the assemblage of many unrelated taxa into polyphyletic groups (Komarek *et al.* 2014). Numerous revisions of their systematics were undertaken to resolve the placement of taxa, which included the concept of the polyphasic approach (Komarek 2006): elucidating the total features of taxa including morphology, ecology as well as phylogeny. Recent trend in cyanobacterial taxonomy reveals application of the polyphasic approach for resolving taxonomic positions through a combination of morphological, ultrastructural, ecological as well as molecular data (Johansen & Casamatta 2005, Hoffmann *et al.* 2005, Komarek 2006). Nomenclature and classification of a taxon should be in a manner so as to reflect the evolutionary relationships among its similar groups. Although in the polyphasic approach concurrence of diacritical characters with molecular data resolved various generic entities, the delineation in species level involving continuous speciation forming morpho-species has not yet been ascertained (Hoffmann *et al.* 2005). Within this realm of cyanobacterial taxonomy, the study of the members belonging to the Oscillatoriales group always remained problematic due to lack of conspicuous characters (Anagnostidis & Komarek 1988, Komarek & Anagnostidis 2005). Rippka *et al.* (1979) classified these members under “LPP (*Lyngbya-Phormidium-Plectonema*) Group B” without any further generic resolution (Lamprinou *et al.* 2013). Komarek & Anagnostidis (2005) revised the concept of classification by including criteria like morphology of the sheath, cellular dimensions, cross walls, terminal cell, ultrastructural features such as thylakoidal arrangements, presence or absence of gas vacuoles, reproductive features and eco-physiological features including their niche habitat. Further, Komarek *et al.* (2014) proposed a revised classification based on morphological, ecological as well as molecular data where the members of LPP group showing polyphyly were transferred to family Microcoleaceae and Oscillatoriaceae. Many new genera like *Oxynema*, *Kamptomena* were derived from the *Phormidium* genus to reduce the polyphyly.

The *Oxynema* genus with the type species *Oxynema thaianum* (Chatchawan *et al.* 2012) has been recently separated from the most misidentified classical genus *Phormidium* (Dadheech *et al.* 2013), mainly based on the differences in trichome morphology, terminal cell shape, salinity preference along with the molecular data. In context to the present work, two (AP17 and AP24) of the eight cyanobacteria previously isolated by our workgroup (Pramanik *et al.* 2011) were assigned to the LPP Group B following Rippka *et al.* (1979). Pursuing the polyphasic approach, we now provide convincing evidence established on morphological, ecological and molecular differences from their nearest relative to prove that these two strains should be recognized as the second novel species of the *Oxynema* genus.

Materials and methods

2.1 Collection and maintenance of isolated strains The two strains (AP17 and AP24) used in this study were collected from soil surface biofilms of two separate islands (Fig. 1) of the Indian *Sundarbans* (Pramanik *et al.* 2011). AP17 was collected from the Lothian island while AP24 was obtained from the Sagar island (salinities of both sites ranged from 1.7 to 1.8%). The physical characteristics of the sampling sites are detailed in Pramanik *et al.* (2011). The cultures were maintained aseptically in Petri dishes as solid cultures as well as in liquid cultures in Erlenmeyer flasks in ASN III medium (Rippka *et al.* 1979). The cyanobacteria were grown in culture rooms having fluorescent irradiance (50 $\mu\text{mol photons. m}^{-2}. \text{s}^{-1}$) in 12:12hrs light : dark cycle at 25 ± 1 °C. All cultures were periodically checked for purity,

morphological and biochemical properties. No changes were observed during storage. Isolate AP17 was deposited in the Microbial Culture Collection (MCC), India and its duplicate was deposited in the National Facility for Marine Cyanobacteria (NFMC), India having accession numbers MCC 3874 and *Oscillatoria* sp. BDU D004 respectively. Isolate AP24 was also deposited in the MCC bearing accession number MCC 3873. Both the strains were authenticated by 16S rRNA gene sequencing and cryopreserved.

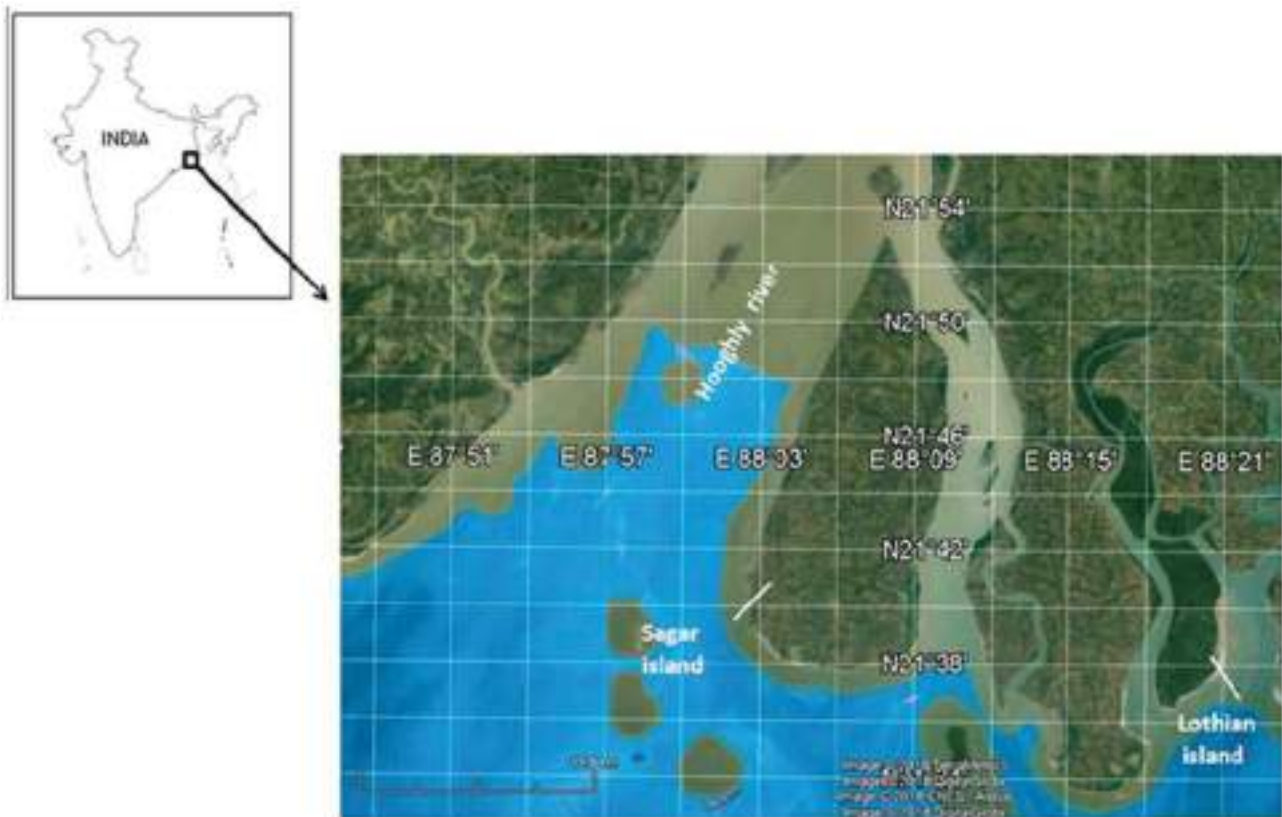


FIGURE 1. Map showing the studied area. Samples collected from the southern coast of Sagar island and entire coast of Lothian island (Image source: Google Earth).

2.2 Light microscopy Morphological identification was done by observing fresh filaments from the 10-day old cultures of AP17 and AP24 in a light microscope (Model DM750; Leica Microsystems, Buffalo Grove, USA) under 400–1000 magnification. Cellular dimensions were recorded with the associated software (LAS EZ, Leica Microsystems) in the microscope.

2.3 Scanning electron microscopy Fresh filaments of the strains under investigation were collected after centrifugation of 1 ml suspension at 8000 rpm (Eppendorf 5810R, rotor F-34-6-38, Hamburg, Germany). The cells were fixed in 3% glutaraldehyde for 2 hrs followed by washing in distilled water. Cells were dehydrated using increasing concentrations of ethanol from 30% for 15 min to 100% for 60 min. The samples were finally dried at the critical point and the grids were taken for observation under a scanning electron microscope (Jeol JSM-6700F, Jeol, Tokyo, Japan).

2.4 Transmission electron microscopy About 1 ml suspension of fresh cells from 8–10 day old cultures of AP17 and AP24 were taken and centrifuged at 8000 rpm (Eppendorf 5810R, rotor F-34-6-38, Hamburg, Germany). The pellet was washed thoroughly in distilled water followed by prefixing in 2.5% glutaraldehyde and 2% paraformaldehyde in 0.1 M phosphate buffer (pH 7.8) for 5–6 hrs at 4 °C. The samples were rinsed in 0.1 M phosphate buffer and excess fixative was washed off with the buffer. The cells were post fixed with osmium tetroxide (1% solution) for 60 min. Post-fixation was followed by dehydration of the cells by passing through increasing concentrations of ethanol. Samples were infiltrated and embedded in Araldite CY 212 for section cutting. The resin block was polymerized by heat treatment first at 50 °C overnight and then at 60 °C for 2 days followed by cutting of thin sections using an ultramicrotome. The sections were contrasted with uranyl acetate and lead citrate and finally observed under a TECNAI G20 transmission electron microscope (FEI, Eindhoven, Netherlands).

2.5 Growth response to salinity Reference strain *Oxytnema thaianum* CCALA960 was obtained from Culture Collection of Autotrophic Organisms (CCALA), Institute of Botany, CAS, Czech Republic. The dependence of growth

of the two isolated strains on NaCl was verified by cultivating AP17, AP24 and *O. thaianum* CCALA960 in BG11 medium having varying concentrations (w/v) of NaCl (0%, 2%, 3%, 5%, 8%, 10%, 12% and 14%). A suspension of trichomes was inoculated and cultivation was carried out at 30 °C and light intensity of 32–35 $\mu\text{mol photons m}^{-2} \text{s}^{-1}$ following the conditions described in Chatchawan *et al.* (2012) to ensure proper comparison of the growth response of our isolated cultures with the reference culture. The cultures were grown for 10 days and the optical density was measured at 750 nm each day.

2.6 DNA extraction, PCR amplification and sequencing Cells from the exponential phase of the axenic cultures (AP17, AP24 and CCLA960) were harvested and the total genomic DNA was extracted using Gene JET™ Genomic DNA Purification Kit (Cat. No. K0721, Thermo Scientific, Waltham, USA) following the manufacturer's protocol. Purity of the DNA was checked by gel electrophoresis in 1.5% agarose gel. PCR amplification of the 16S rRNA gene and the 16S-23S rRNA internal transcribed spacer (ITS) region was carried out in Mastercycler Nexus Gradient PCR machine (Eppendorf, Hamburg, Germany). For amplification of 16S rRNA gene, cyanobacterial specific forward primers CYA106F (5'CGGACGGGTGAGTAACGCGTGA3') (Nübel *et al.* 1997) and universal reverse primer 1492R (5'-ACCTTGTTACGACTT-3') (Lane 1991) were used while 16S-23S ITS regions were amplified by using forward primer 16SF (5'TGTACACACCGGCCCGTC3') and reverse primer 23SR (5'-CTCTGTGCCTAGGTATCC-3') (Iteman *et al.* 2000). The reaction conditions used for amplification of the 16S rRNA gene were: initial denaturation at 94 °C for 5 min followed by 30 cycles of 94 °C for 1 min; 50 °C for 1 min and 72 °C for 2 min and final extension at 72 °C for 10 min. The reaction conditions applied for amplification of the 16S-23S ITS region were: initial denaturation at 95 °C for 5 min followed by 30 cycles at 95 °C for 30 sec; 58 °C for 15 sec; 72 °C for 40 sec and final elongation step at 72 °C for 5 min. The PCR products were analyzed on a 1.5% agarose gel stained with ethidium bromide and PCR fragments of appropriate size were purified with Gene JET™ PCR Purification kit (Cat. No. K0701, Thermo Scientific, Waltham, USA). Construction of clone libraries from the purified PCR products of these samples was performed using InsTAclone™ PCR cloning kit (Cat no. K1213 and K1214, Thermo Scientific). The purified DNA fragments were inserted into the commercial cloning vector pCR 2.1 (Life Technologies, Invitrogen, USA). The vectors with inserted DNA were then transformed into *E. coli* DH5a cells. Screening of white and blue colonies were done and plasmids were isolated from the positive transformants with Thermo Scientific GeneJET Plasmid Miniprep Kit (Cat no. K0502 and K0503, Thermo Scientific). Plasmids were screened by digestion with restriction enzymes Eco RI and Hind III and the representative clones were selected for sequencing. The sets of primers used for the sequencing of the clones of 16S rRNA and 16S-23S ITS gene sequences were similar to the set used earlier for PCR amplification. Sequencing was carried out using an automated DNA sequencer (Genetic Analyzer 3500xL, Applied Biosystems, Waltham, USA). The resulting sequences of the 16S rRNA gene and 16S-23S ITS regions of the two isolates (AP17 and AP24) and the 16S-23S ITS region of the reference strain (CCALA960) were submitted to GenBank and their accession numbers are provided in Table 1.

TABLE 1. List of gene sequences of the cyanobacterial strains submitted in NCBI with their accession numbers.

	<i>Oxynema aestuarii</i>	<i>Oxynema aestuarii</i>	<i>Oxynema thaianum</i>
Strain	AP17	AP24	CCALA960
Gene Bank Accession no. for 16S rDNA	MG694263	MG694265	-
Gene Bank Accession no. for 16S-23S ITS rDNA	MG694266	MG694268	MG825656
Length of 16S rDNA (bp)	1387	1369	-
Length of 16S-23S ITS (bp)	543	541	547

2.7 Analysis of the 16S rRNA gene sequence and phylogenetic tree construction The sequences of the 16SrRNA genes of the two strains AP17 and AP24 and the reference strain were searched in Basic Local Alignment Search Tool (BLAST) within the robust database of National Center of Biotechnology Information (NCBI) and pairwise similarity was determined with the other members available in the database. Based on the similarity results, a consensus phylogenetic tree was constructed by choosing the partial sequences of 16S rRNA genes (length >1100 bp) of the closest relatives of the strains (AP17 and AP24) along with the sequences of the representative members (reference strains) of each cyanobacterial group from the NCBI database to establish a justified evolutionary relationship with the isolated strains. The 16S rRNA gene sequence of the reference strain was experimentally determined within this study. The sequences of the taxa having uncertain affiliation were excluded. The sequences were aligned in CLUSTAL W program (Larkin *et al.* 2007). The tree was constructed following the Maximum Likelihood (ML) analysis of the Phylogenetic Analysis Using Parsimony (PAUP*) version 4b10 (Swofford 2002) and the majority rule was selected. The multiple aligned sequences were examined for DNA substitution using the likelihood ratio statistic test implemented in the program

jModel Test version 0.1.1 (Posada 2008) to determine the best-fit model of our data. The (TPM2uf+I+G) models of substitution were found to be the best fit for the data. Gaps were excluded in the phylogenetic analysis. Confidence values of the branches of the phylogenetic tree were calculated by bootstrapping of 1000 replications. *Gloeobacter violaceus* was selected as an outgroup taxon. The phylogenetic tree obtained was visualized using TreeGraph 2 (Stover & Muller 2010). Another phylogenetic tree was constructed with the same multiple aligned sequences by using Neighbor Joining (NJ) method and the common branches which were highly supported in both ML and NJ methods were indicated by asterisks.

2.8 Analysis of 16S-23S ITS secondary structures The ITS secondary structures of the two cultures (AP17, AP24) under investigation and the reference strain CCALA960 were generated using the M-fold web server (version 2.3) (Zuker 2003) and redrawn in Adobe Illustrator CS5.1. The secondary structures were generated under ideal conditions of untangled loop fix and the temperature set to default (37 °C). Comparisons of the sequence lengths and secondary structures (wherever appropriate) of the different regions of the ITS sequences (14 regions in total) of AP17 and AP24 with the reference strain (CCALA960) were carried out following Johansen *et al.* (2011).

Results

3.1 Morphological characterization Strains AP17 and AP24 grew as blue-green mats attached to the surface of the flasks used for cultivation. The two cultures were morphologically similar and in context to Chatchawan *et al.* (2012) they may be affiliated to the *Oxynema* genus which was recently separated from the *Phormidium* -Group I on the basis of morphological features like attenuated trichomes, thylakoidal morphology and growth patterns. Light microscopy revealed that the strains consisted of straight, long, trichomes having simple, unbranched filaments. Akinetes, heterocytes or gas vacuoles were not observed in any trichome. Trichomes exhibited gliding movement. Cells were shorter in contrast to width (cell length: 1.5–2.5 µm; cell width: 2.03–2.45 µm); although cell length and width ratio were also found to be 1:1 (isodiametric) occasionally. The apical end of the trichome was consistently narrowed, pointed and slightly curved and regularly without calyptra (Fig. 2). The overall morphometric analysis of the two strains (AP17 and AP24) and their similarities/dissimilarities with the reference strain *Oxynema thaianum* CCALA960 are presented in Table 2. Scanning electron microscopy (Fig. 3) confirmed the presence of well-defined mucilaginous sheath around the filaments which were clearly observable where the trichomes broke apart. Constrictions in the cross walls were not prominent due to presence of sheath but were conspicuous only when the sheath was removed during SEM preparations. The length and the width ratio of the cells also depended on their positions: it was observed that the intercalary cells tended to be shorter than wide to isodiametric; whereas the cells in the apical portion of the filaments were longer than their width (Fig. 3b). Thylakoids were situated along the whole cell volume in the longitudinal axis of the cell. Apart from the overall arrangement, the thylakoid membranes were separated from each other by the presence of double row of phycobilisomes, the light harvesting antenna complex (Mullineaux 1999). TEM ultrastructural data of the strains under investigation also showed a prominent cell wall and cellular inclusions such as cyanophycin granules and carboxysomes were present. Gas vacuoles were completely absent (Fig. 4).

TABLE 2. Morphometric comparison of *Oxynema aestuarii* AP17 and AP24 with *Oxynema thaianum* CCALA960. Values of cell length and width are represented along with the confidence interval with confidence level at 95%.

Feature	<i>Oxynema aestuarii</i>	<i>Oxynema thaianum</i>
Filament	Solitary, filaments straight slightly curved ends	Solitary, filaments straight slightly curved ends
Sheath	Sheath well-defined, firmly attached, observed under electron microscope	Facultative, diffluent, rarely observed under electron microscope
Cell width (µm)	2.2 ± 0.09	7.9 ± 0.08
Cell length(µm)	1.56 ± 0.093	2.6 ± 0.09
Cell shape	Tends to be isodiametric. Sometimes cells shorter than wide	Rarely isodiametric, mostly shorter than wide
Apical cell type	Elongated, pointed, without any cross wall in the apical cell, without calyptra	Elongated, pointed, with cross walls present in the apical cell, without calyptra
Constrictions at cross wall	Slightly constricted at the cross wall	Slightly constricted at the cross wall
Motility	Exhibit gliding movement	Exhibit gliding movement
Habitat	Intertidal area (estuarine) with salinity ranging from 1.7–1.8‰	Hypersaline environment

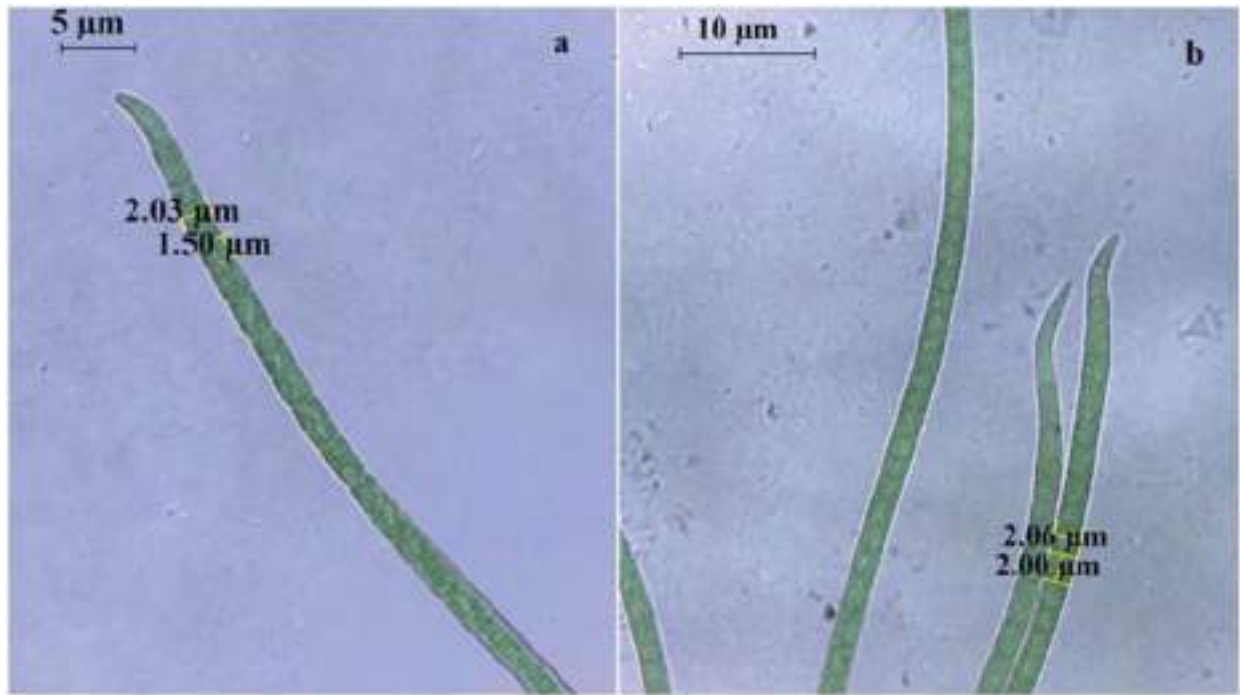


FIGURE 2. Light microscopy of *Oxyinema aestuarii*. **a.** Microphotograph showing the filaments of strain AP24 with cellular dimensions. **b.** Microphotograph of strain AP17 showing filaments with cellular dimensions.

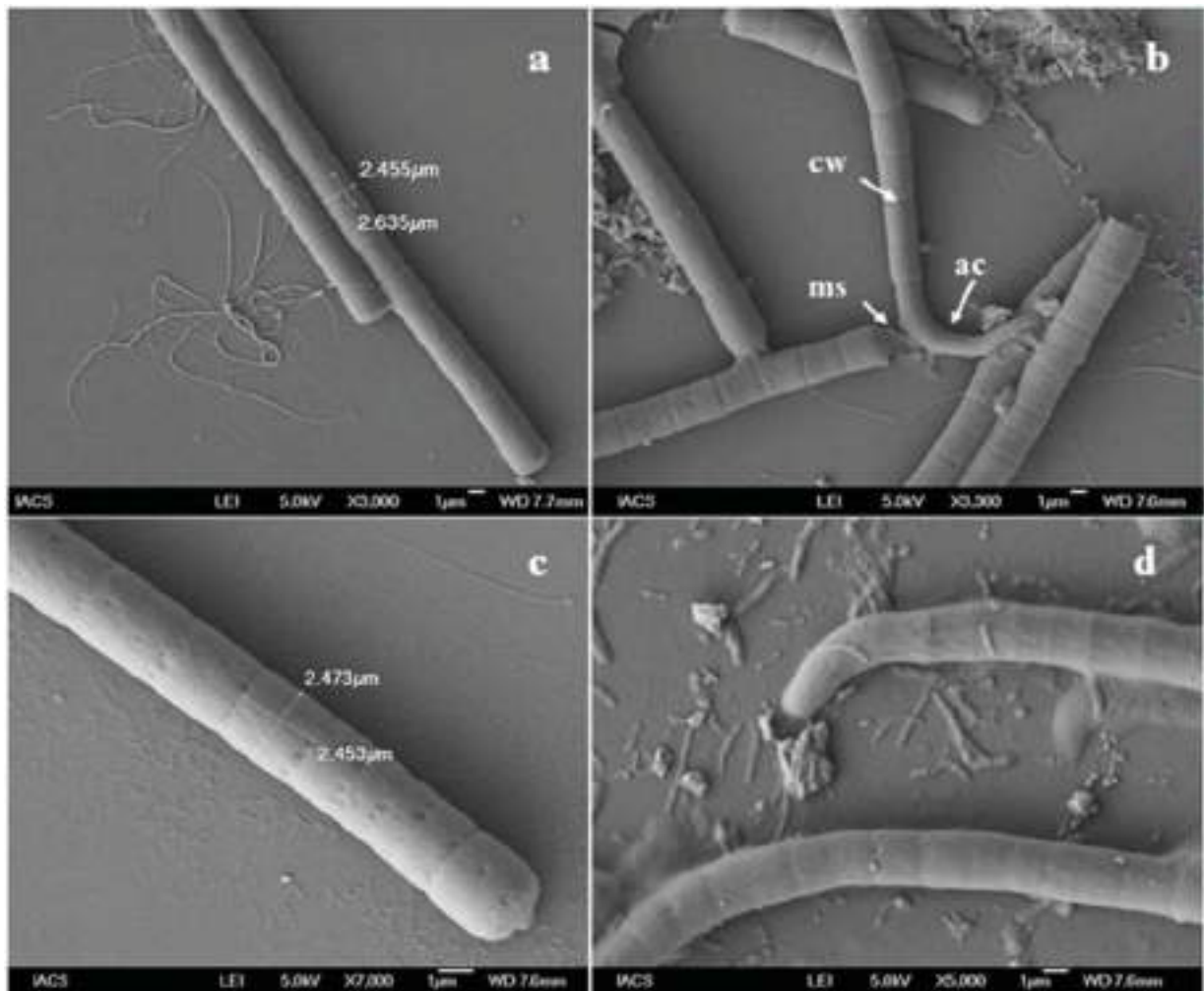


FIGURE 3. Scanning electron microscopy of *Oxyinema aestuarii* (non-axenic culture) **a.** and **b.** Part of filament of AP17 showing cellular dimensions along with apical cell morphology and mucilage sheath. **c.** and **d.** Part of filament of strain AP24 showing cellular dimensions. ac= apical cell, cw= cross wall, ms= mucilaginous sheath.

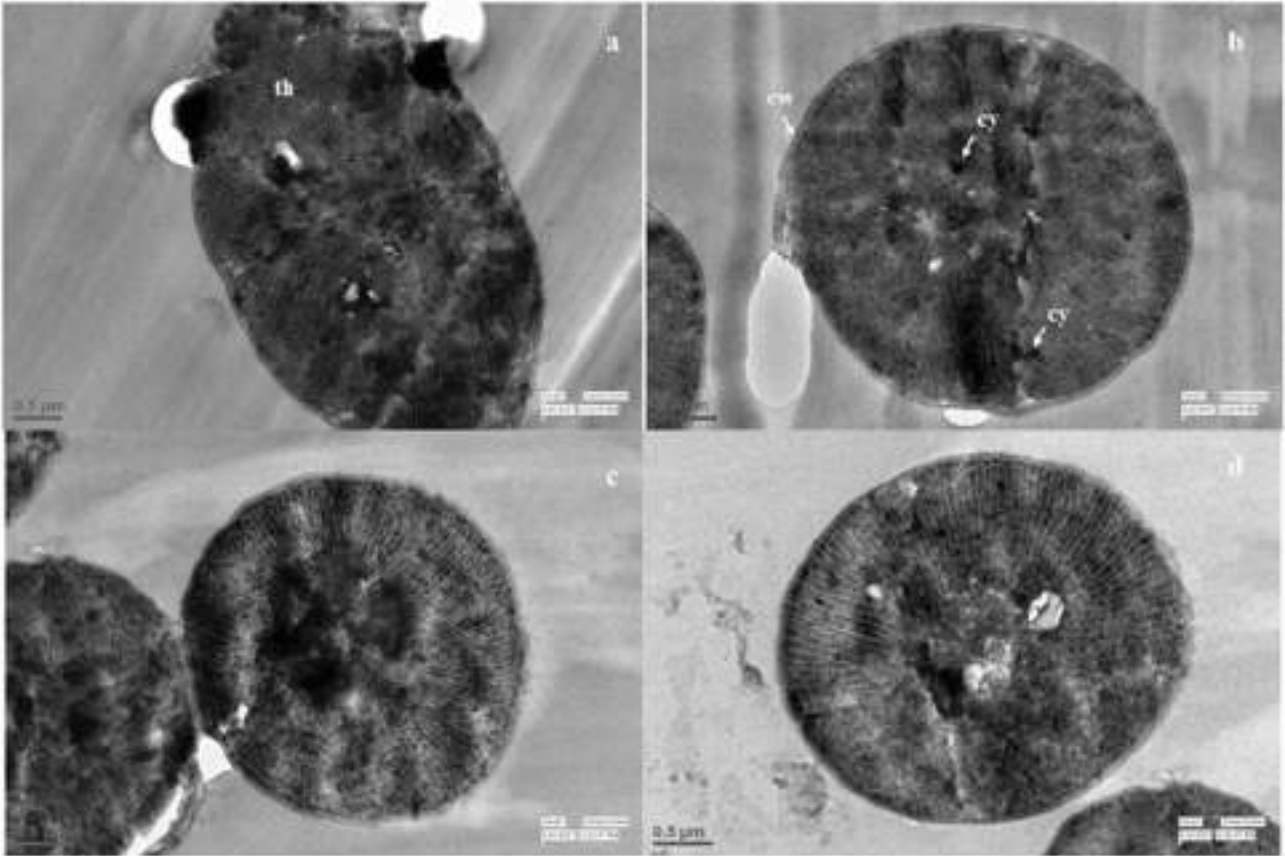


FIGURE 4. Transmission electron microscopy of *Oxyinema aestuarii*. **a** and **b**. Cross sections of the filaments of strain AP17. **c** and **d**. Cross sections of the filament of strain AP24. Characteristics show prominent radial arrangement of thylakoids and presence of few cynophycin granules. cw= cell wall, cy= cynophycin, th= thylakoids.

3.2 Response to salinity Results (Fig. 5a and 5b) indicate that the preferable range of salinity for the growth of AP17 and AP24 was 5–8% NaCl. Salinity above 14% inhibited the growth of both strains. The reference strain CCALA960 was described as a typical halophilic species with an optimum growth between 10–20% salt concentration (Chatchawan *et al.* 2012). The reference strain demonstrated growth above 20% salinity while the growth of AP17 and AP24 declined within 15% salinity.

3.3 Analysis of the 16S rRNA gene sequences and construction of the phylogenetic tree The phylogenetic analysis of our strains: AP17 (1387 bp) and AP24 (1369 bp) showed 99–100% sequence similarity with the closest species *Oxyinema thaianum* CCALA960 (JF729323.1) displaying query coverage of 81%. Chatchawan *et al.* (2012) included two more species under the genus *Oxyinema*, *O. acuminatum* and *O. lloydianum* which were earlier known to be *Phormidium acuminatum* (syn.= *Oscillatoria acuminata*) and *Phormidium lloydianum* (syn.= *Oscillatoria lloydiana*) respectively. The species were shifted from the *Phormidium* genus to the *Oxyinema* genus based on their morphological similarity. However, the comparison of 16S rRNA gene sequence of our isolates (AP17 and AP24) with the *Oxyinema acuminatum* sequence (available in NCBI database as *Oscillatoria acuminata* PCC6304, accession no. NR_102463.1) shows 91% sequence similarity with a query coverage of 100%. The low genetic similarity along with occurrence of them in separate clusters of the phylogenetic tree (Fig. 6) suggest that they are distantly related to each other which implies that *Oxyinema aestuarii* and *O. acuminatum* (syn.= *Oscillatoria acuminata*) are not the same species. So the comparison in the present study was restricted to *Oxyinema thaianum* CCALA960. The sequence similarity of AP17 and AP24 with any other genera was below 95%. The phylogenetic tree (Fig. 6) showed that the two strains represented a separate clade which was separated from the nearest clade by less than 95% similarity along with the closest-related taxa, *Oxyinema thaianum* CCALA960 as a sister taxon. The clade showing the relationship between the AP17, AP24 and the reference strain *Oxyinema thaianum* CCALA960 was supported by high bootstrap values.

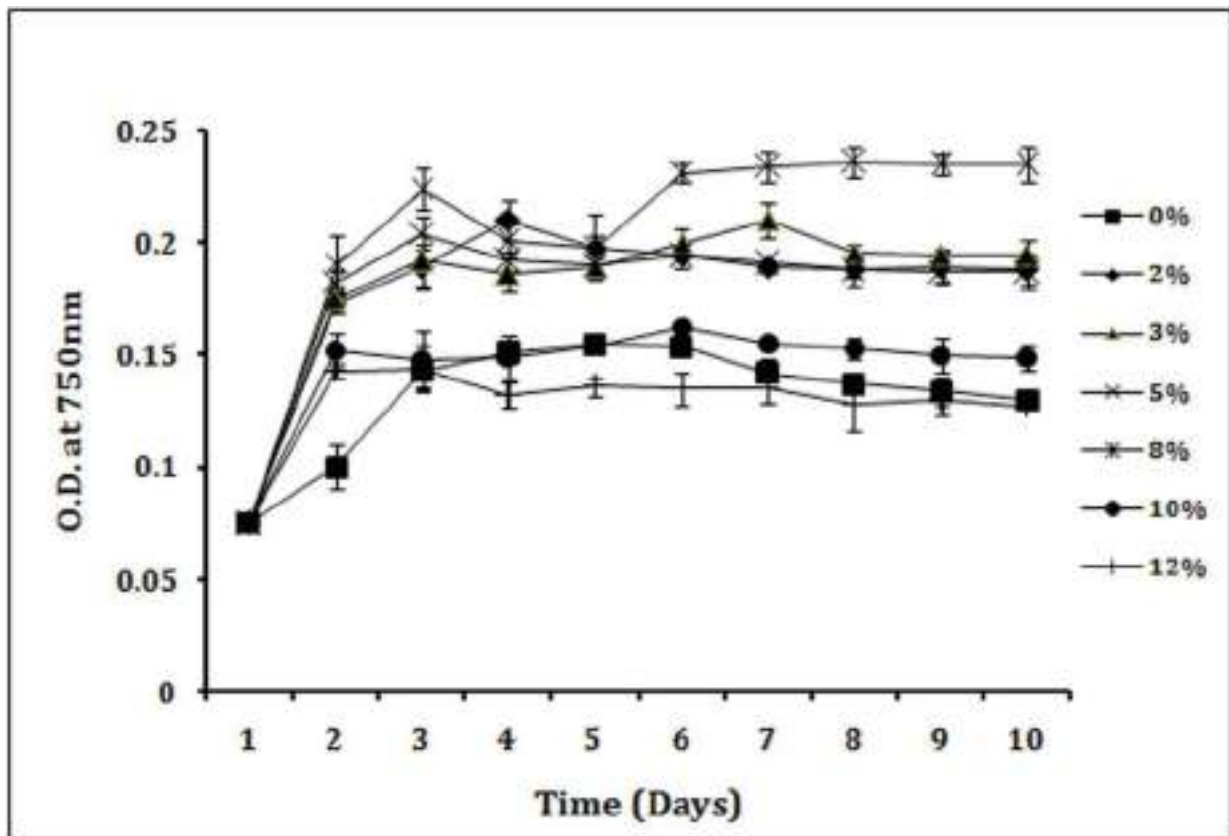


FIGURE 5a. Growth responses of AP17 to varying NaCl concentrations in BG11 medium. Data from triplicate experiments; error bars indicate mean \pm SD, n=3.

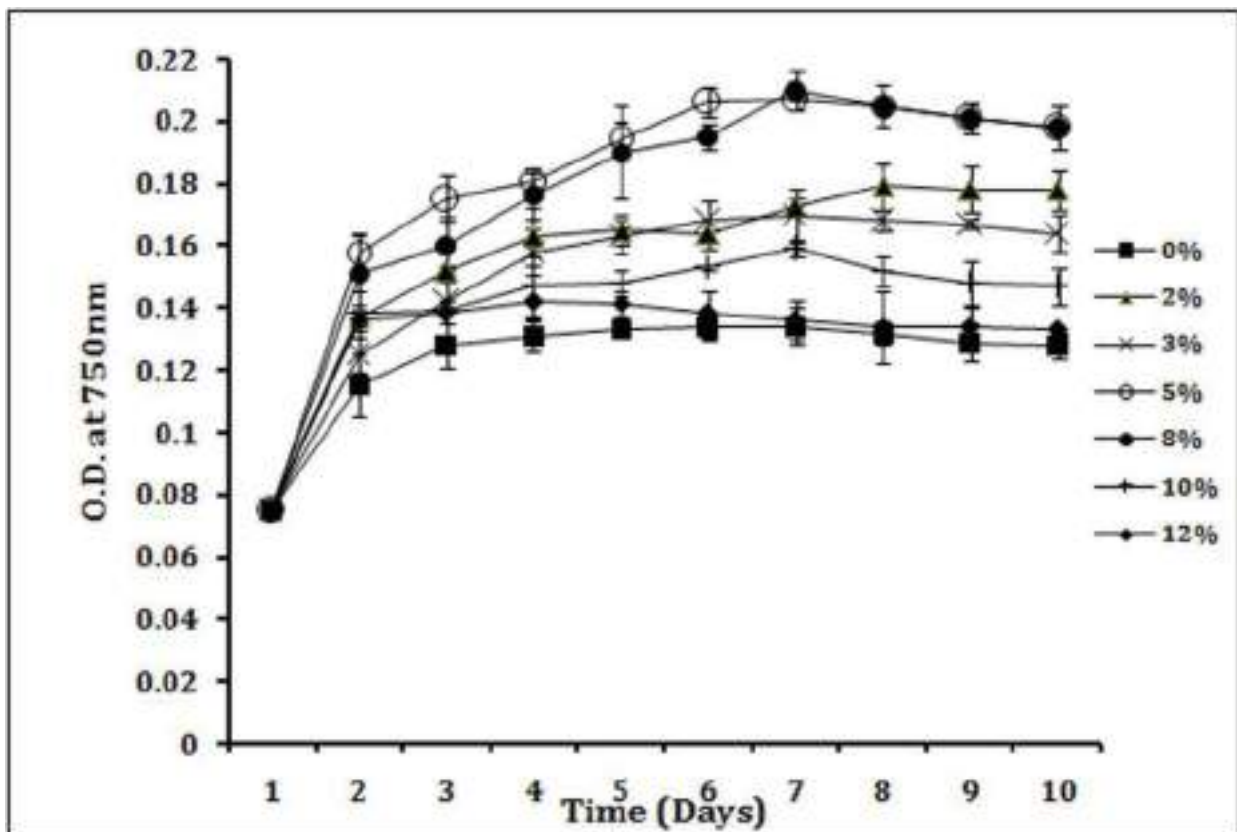


FIGURE 5b. Growth responses of AP24 to varying NaCl concentrations in BG11 medium. Data from triplicate experiments; error bars indicate mean \pm SD, n=3.

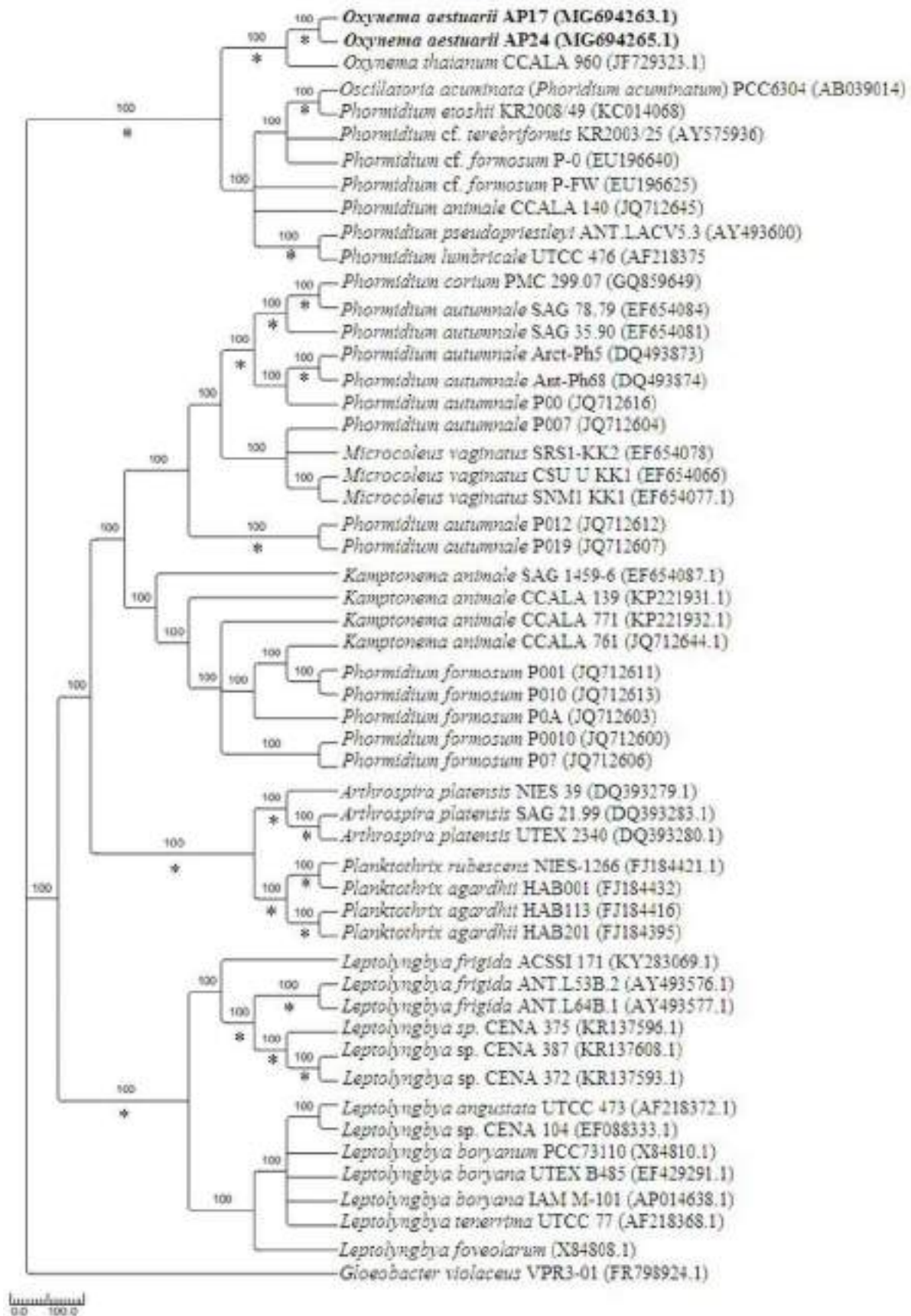


FIGURE 6. Unrooted Phylogenetic tree based on partial 16S rRNA gene sequences obtained by Maximum Likelihood (ML) analysis using PAUP* version 4b10 showing the relative position of *Oxynema aestuarii* strains AP17 and AP24 along with their phylogenetic relatives. Numbers at nodes indicate levels of bootstrap support (%) based on 1000 resampled datasets. Asterisks indicate branches that were also recovered using Neighbor-Joining (NJ) algorithm. GeneBank accession numbers are given in the parenthesis.

3.4 Analysis of the 16S-23S ITS gene sequences According to Johansen *et al.* (2011) the ITS comprising of the two tRNA genes can be apportioned into 14 regions: (i) leader (ii) D1-D1' helix (iii) D2 helix and spacer (iv) D3 spacer (v) tRNA^{Ile} gene (vi) spacer between tRNA genes, often including the V2 helix (vii) tRNA^{Ala} gene (viii) spacer preceding Box B (ix) Box B helix (x) spacer following Box B (xi) Box A (xii) D4 (xiii) V3 and (xiv) D5. Among them, the leader, two tRNA genes and Box A are of equal length, while the other 10 regions are highly variable in length, having an evolutionary history of multiple-base insertions and deletions and single-base substitutions. Table 3 shows insertion of 9 nucleotides in the D2 with spacer region, insertion of 2 nucleotides in the pre Box B spacer region, deletion of 2 nucleotides in the post Box B spacer region, deletion of 8 nucleotides in the D4 region, deletion of 8 nucleotides in V3 region and insertion of 2 nucleotides in the D5 region of the ITS sequences of AP17 and AP24 in comparison to the analogous regions of the reference strain CCALA960. D1-D1' helices consisted of 62 nucleotides and shared similar structures among the three strains which included a terminal loop and three bilateral bulges. The basal helix sequence near 5' end for D1-D1' helix which is highly conserved in all cyanobacterial genera and found to be 5'-GACCU (Iteman *et al.* 2000) was determined as 5'-GACCC in the strains under investigation as well as in the reference strain *Oxynema thaianum* CCALA960 (Fig. 7). Box B helix was 55 nucleotides long in three strains AP17, AP24 and CCALA960. However, four substitutions of nucleotides were observed in varying positions of the Box B helix of *O. thaianum* CCALA960 which has been indicated in Fig. 8. The overall structure of the Box B helix in the strains AP17 and AP24 is entirely different from the reference strain. The connection of the sub-terminal bilateral bulge to its lower bilateral bulge consisted of four nucleotide pairs in AP17 and AP24 while the same comprised of five nucleotide pairs in CCALA960. Such difference may arise due to the variable base present in the reference favoring a different configuration in the minimum free energy level. Furthermore, secondary structures of the V3 regions of AP17 and AP24 were compared with the similar structure of CCALA960. The secondary structures of our isolates (containing 51 nucleotides) showed a small terminal bulge and a bigger bilateral bulge while the analogous structure of the reference strain *O. thaianum* CCALA960 (comprising of 59 nucleotides) showed one additional bilateral bulge in comparison to AP17 and AP24 (Fig. 9).

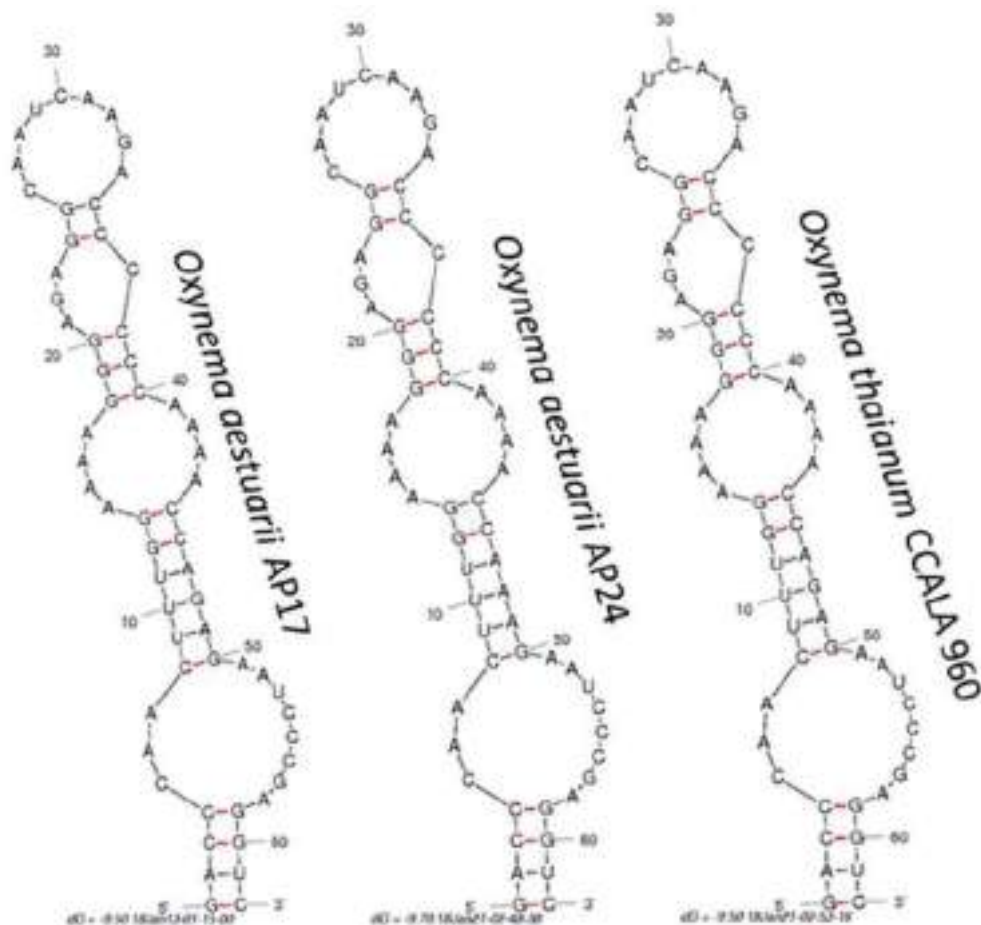


FIGURE 7. Comparative analysis of D1-D1' helices of the 16S-23S ITS regions of isolates (*Oxynema aestuarii* AP17 and AP24) and their closest phylogenetic relative *Oxynema thaianum* CCALA960. Secondary structures generated from M-fold web server (version 2.3), temperature: 37 °C default; structure: untangled loop fix

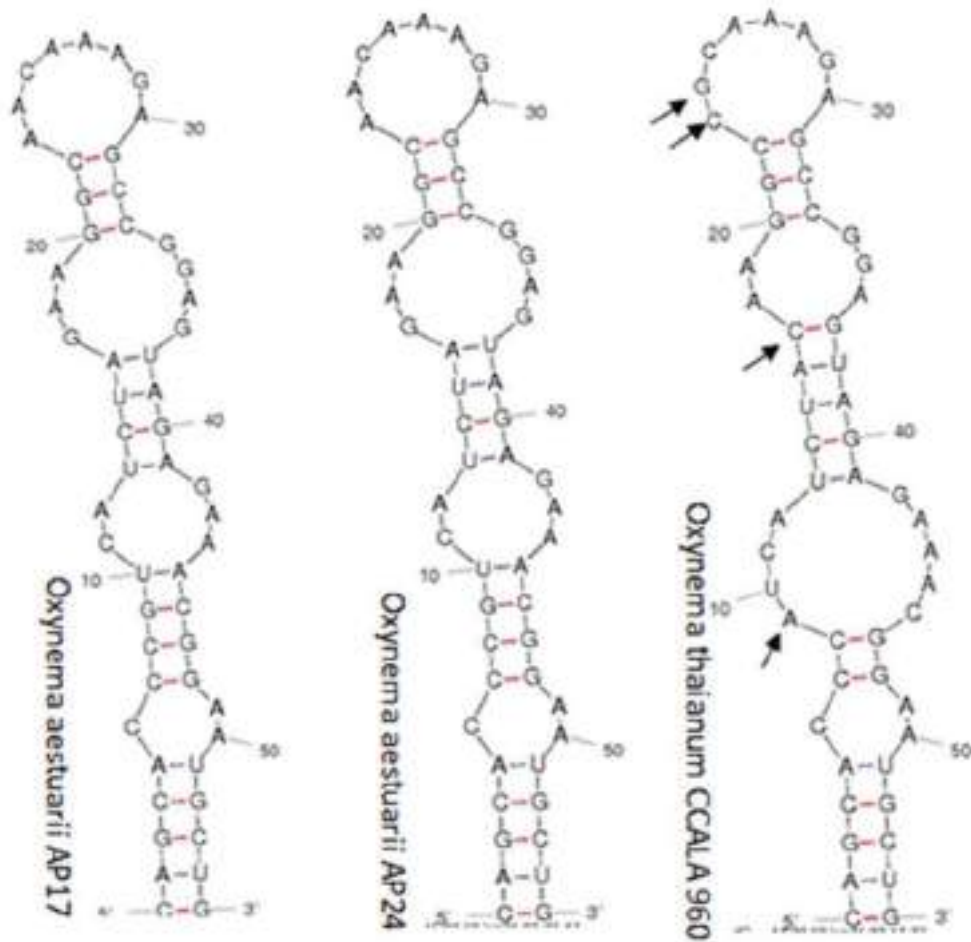


FIGURE 8. Comparative analysis of the Box B helices of the 16S-23S ITS regions of isolates (*Oxyneema aestuarii* AP17 and AP24) and their closest phylogenetic relative *Oxyneema thaianum* CCALA960. Secondary structures generated from M-fold web server (version 2.3), temperature: 37°C default; structure: untangled loop fix. Arrow heads in the reference strain *O. thaianum* indicate the variable nucleotides in contrast to the strain AP17 and AP24.

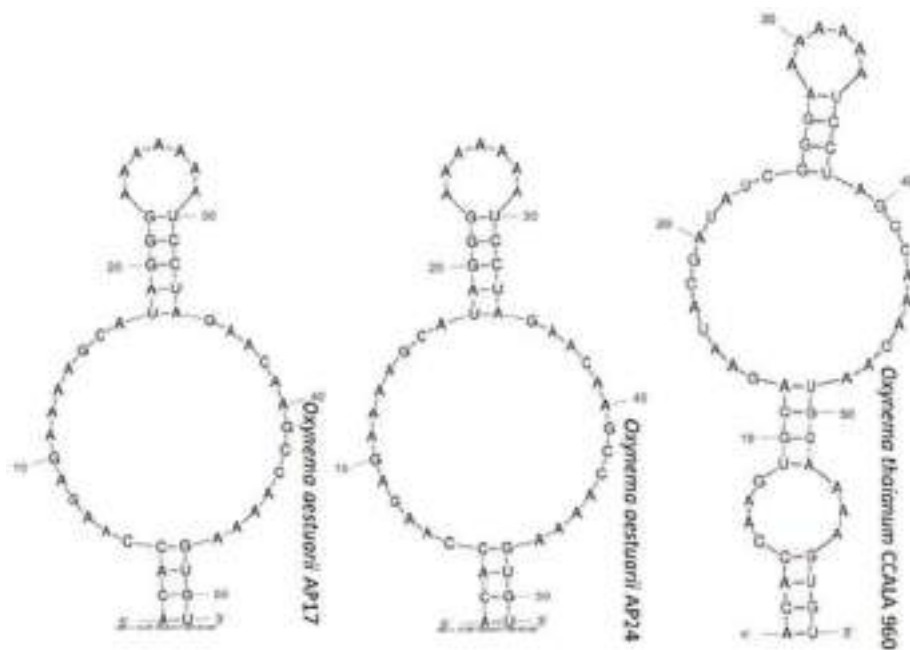


FIGURE 9. Comparative analysis of the V3 helices of the 16S-23S ITS regions of isolates (*Oxyneema aestuarii* AP17 and AP24) and their closest phylogenetic relative *Oxyneema thaianum* CCALA960. Secondary structures generated from M-fold web server (version 2.3), temperature: 37°C default; structure: untangled loop fix.

TABLE 3. Comparison of the nucleotides length of the ITS regions of *Oxynema aestuarii* AP17, *O. aestuarii* AP24 and *O. thaianum* CCALA 960. Differences are shown in bold.

Strains under investigation (AP17 and AP24) and reference strain	Leader	D1-D1' helix	D2 with spacer	D3 with spacer	tRNA ^{trp} gene	V2 spacer	tRNA ^{ala} gene	Pre Box B spacer	Box B	Post Box B spacer	Box A	D4	V3	D5
<i>Oxynema aestuarii</i> AP17	14	62	46	18	73	12	73	47	55	17	12	7	51	42
<i>Oxynema aestuarii</i> AP24	14	62	46	18	73	12	73	47	55	17	12	7	51	42
<i>Oxynema thaianum</i> CCALA 960	14	62	37	18	73	12	73	45	55	19	12	15	59	40

Discussion

This study describes a polyphasic approach to taxonomically identify two cyanobacteria isolated from the intertidal area of Indian *Sundarbans*. We provide morphological, ecological and molecular evidence in support of the claim for the novel species (*Oxynema aestuarii*) in the *Oxynema* genus which has been recently separated from the *Phormidium* genus (Chatchawan *et al.* 2012) and is so named (*O. aestuarii*) on the prevailing estuarine conditions of its habitat. The position of the *Phormidium* genus among the members of LPP group B sensu (Rippka *et al.* 1979) always remained debatable. Based on the molecular data as well as the autapomorphic features, *Oxynema thaianum* CCALA960 was separated from the *Phormidium* polyphyletic group (Chatchawan *et al.* 2012). Among the various morphological features, some of the characteristics should be given special importance in the taxonomy of this genus (*Oxynema*), namely cross walls in the pointed apical ends of the trichome, constrictions in the cross wall and the extent of mucilage sheath present around the trichome. These crucial characteristics along with the molecular phylogeny were the basis on which *Oxynema* was strongly claimed to be separated as a new genus from the other genera like *Oscillatoria*, *Geitlerinema* and *Phormidium* (Chatchawan *et al.* 2012). Terminal cell morphology which was one of the principal criteria for traditional classification (Komarek & Anagnostidis 2005) showed variations when our isolates were compared with the reference strain. As a major deviation from the reference strain, cross walls in the narrowed, pointed-rounded apical portion of the examined strains AP17 and AP24 were totally absent while the above feature was present in CCALA960 (Fig. 2). Cell size differed significantly: the cell width to length ratio of CCALA960 (Chatchawan *et al.* 2012) was found to be almost two times the ratio observed for AP17 and AP24 (Table 2). Appearance of the mucilaginous sheath in AP17 and AP24 in contrast to CCALA960 was different: strains AP17 and AP24 showed a firm sheath visible around the filament while facultative sheath (Fig. 3b), very rarely visible in the cultures, was noted in strain CCALA960 (Chatchawan *et al.* 2012). The cross sections of the filament in transmission electron microscopy (Fig. 4) showed a distinct pattern of thylakoids arranged radially within the cell but parallel to each other which is a characteristic feature of family Phormidiaceae (Komarek & Kastovsky 2003, Marquardt & Palinska 2007). Comparative study of our strains and the reference indicated that the overall pattern of thylakoidal arrangement was similar, although the inter-thylakoidal space of AP17 and AP24 remained much more appressed in comparison to CCALA960 which may be explained by the difference in the overall size of the phycobilisomes between the two strains (Westerman *et al.* 1994, Olive *et al.* 1997).

The two strains AP17 and AP24 were isolated from the intertidal regions of the *Sundarbans*, India (Pramanik *et al.* 2011) which is considered to be a brackish environment in terms of NaCl concentration (Naeimi & Zehtabian 2011) and characterized by typical estuarine conditions. The strains (AP17 and AP24) may be considered to be distinct from the reference strain CCALA960, which could grow up to 40% salinity (Chatchawan *et al.* 2012). This author considered ecology to be an important criterion for cyanobacterial species differentiation and it is also known that *Phormidium* species acquire some characters influenced by their environment (Casamatta *et al.* 2005). The strains AP17 and AP24 were isolated from the intertidal regions of two separate islands of Indian *Sundarbans* where the habitat is characterized by variable salinity (Pramanik *et al.* 2011). On the other hand, *Oxynema thaianum* CCALA960 was obtained from the salt works in the Petchaburi province of Thailand (Chatchawan *et al.* 2012) typified by a hypersaline environment. Chatchawan *et al.* (2012) ascertained that salinity played a pivotal ecological role in the growth and occurrence of *Oxynema* species.

A new species of *Phormidium*, namely *Phormidium etoshii* which shared close similarity with the other species was distinguished as a new taxa based on the morphological and ecological features (Dadheech *et al.* 2013). Likewise, *Arthronema gygaxiana* resolved with two strains of *Limnothrix* sp. based on 16S rRNA sequencing, although the taxon was determined to be *Arthronema* based on ecological and morphological features. Similarly, *Pseudoanabaena tremula*, in spite of having strong bootstrap support with *Leptolyngbya* in 16S rRNA-based phylogeny, this strain was assigned under *Pseudoanabaena* based on morphological characters (Casamatta *et al.* 2005). In yet another example, a novel species, *Tapinothrix clintonii* was found to be closest to *Leptolyngbya sensu stricto* based on 16S rRNA sequencing, but was separated from *Leptolyngbya* based on morphology and 16S-23S ITS secondary structures and was established as *Tapinothrix* (Bohunicka *et al.* 2011). It may be noted that the establishment of the new genus *Oxynema* was based on a single strain of the type species (*O. thaianum* CCALA960) (Chatchawan *et al.* 2012) whereas we propose the novel species *O. aestuarii* on the basis of two strains isolated from two different islands of the *Sundarbans* which are 24 kms apart and are separated by land mass (Fig 1), an occurrence corroborative to the views of Christensen *et al.* (2001) who recommended that novel species descriptions should be based on more than one isolate.

The degree of variability of the 16S rRNA sequences of AP17 and AP24 in relation to CCALA960 was lower (99–100%) in comparison to the variability in their ITS regions (91%) of the isolated and reference cultures. Fox *et al.* (1992) demonstrated that 16S rRNA sequence analysis is not sufficient for the species delineation of prokaryotes. Additionally, phylogenetic analysis based on 16S rRNA lacks sensitivity for those strains where evolutionary changes occur in the ecological perspective (Choudoir *et al.* 2012, Becraft *et al.* 2015). The impairment of the 16S rRNA analysis was also evidenced by the report of Engene *et al.* (2011) who showed that variable gene copies in the same genome limits species delineation by 16S rRNA analysis. The primary sequence and secondary structure of the 16S–23S ITS molecule has been especially helpful in defining genera and species of cyanobacteria as well as cryptic species (Rehakova *et al.* 2014, Johansen *et al.* 2017). Analysis of 16S-23S ITS regions were considered to provide better resolution in the taxonomical evaluation at species level (Flechtner *et al.* 2002, Segiesmund *et al.* 2008, Perkerson *et al.* 2011, Hasler *et al.* 2012, Osorio-Santos *et al.* 2014).

Detailed analysis of the ITS sequences of our isolated strains and *Oxynema thaianum* CCALA960 revealed significant differences. Variations in nucleotide lengths of six regions of the ITS sequences (Table 3) in addition to the four substitutions of nucleotides in varying positions in the Box B helix of *O. thaianum* CCALA 960 (Fig. 8) as well as the dissimilar secondary structures of V3 region of AP17 and AP24 in contrast to CCALA 960 (Fig. 9) were ample evidence to justify *Oxynema aestuarii* as a new species. Given the equal length of the Box B helix, the structural folding patterns of the ITS regions of AP17 and AP 24 in contrast to CCALA960 was substantially dissimilar. Similar observation was reported by Boyer *et al.* (2001) where analysis of ITS regions of *Scytonema hyalinum* demonstrated variable configuration although sequence length was equal. The variation of the ITS regions between our strains and the reference strain was well supported by the fact that changes in ITS structures occurs in between species (Iteman *et al.* 2000). Variations of ITS structure is a factor for discrimination among closely related species collected from diverse ecological niches (Janse *et al.* 2003) as observed in this investigation where AP17 and AP24 was obtained from an intertidal estuarine habitat and CCLA960 was isolated from a hypersaline environment. Frequent events of insertion and deletion in the segments of DNA of the 14 regions of the ITS sequence characterize its evolution (Johansen *et al.* 2011). These authors proved that *Leptolyngbya corticola* could be differentiated from *L. boryana*, *L. tenerrima*, *L. foveolarum* and an unnamed *Leptolyngbya* species principally in the spacer between the tRNA gene and Box B. Sequence and secondary structure of the helices of the 16S-23S ITS region may be considered as autapomorphic features (Johansen *et al.* 2011).

Conclusion

This investigation should be broadly recognized as an exploration of the largely uncharacterized cyanobacterial biodiversity of the world's mangroves. We performed this study in the *Sundarbans*, which is the world's largest tidal mangrove forest. This investigation was undertaken to decipher the taxonomical relationship between the type species (*Oxynema thaianum* CCALA960) of a novel genus (*Oxynema*) recently established after separation of this type species as a separate generic entity from the *Phormidium* genus (Chatchawan *et al.* 2012) and two close morphotypes of *O. thaianum* CCALA960 (strains AP17 and AP24 of this study). We provide evidence supporting another new species of *Oxynema* genus, *Oxynema aestuarii*, the novelty of which was proved by several biotopic characteristics such as molecular data (similarity of the 16S rRNA gene sequence with CCALA960 but major differences in the ITS regions);

morphologically (terminal cell morphology, cell width/cell length ratio, firm sheath as compared to CCALA960) as well as ecologically (different habitat and salinity preference in comparison to CCALA 960). The convincing difference in cell size between our isolates and the reference strain, presence of comparatively longer terminal cell in our isolated cultures compared to the reference, diverse salinity preferences and variations in the length and secondary structure of the ITS sequences compared to the reference were the distinctive features of *Oxynema aestuarii* which differed from *Oxynema thaianum* CCALA 960 and should be considered as the autapomorphic traits of this novel species. Recognition of *O. aestuarii* as another novel species of the newly-created *Oxynema* genus, confirmed the justification of the separation of *Oxynema* from the *Phormidium* genus. Our claim is further substantiated by the isolation of two strains (AP17 and AP24) from two different islands of Indian *Sundarbans*, which shared most of the features that altogether established them to be new species, namely *Oxynema aestuarii*. Identification of ecotypes on genetic basis is essential for hydrobiological studies in future.

Species description

Order: Oscillatoriales

Family: Microcoleaceae

Genus: *Oxynema*

Oxynema aestuarii Chakraborty & Mukherjee sp. nov.

Description: Trichomes attenuated, solitary, unbranched, blue-green (appeared as mats), cells 1.5–2.5µm long and 2.03–2.45µm in width, slight constrictions in the crosswalls, apical cells sharply pointed, always without any crosswalls and without calyptra, facultative and firm mucilaginous sheath, motile (gliding movement). Reproduction occurs vegetatively by the disintegration of hormogonia (short filaments). Akinetes, gas vacuoles, heterocytes absent, thylakoids radially arranged.

Habitat: Soil samples of brackish water (salinity 1.5%).

Type locality: Lothian island of the Indian *Sundarbans*.

Holotype: Holotype (AP17) deposited and cryopreserved in Microbial Culture Collection (MCC), India and a duplicate culture strain deposited in the National Facility for Marine Cyanobacteria (NFMC), India having accession numbers MCC 3874 and *Oscillatoria* sp. BDU D004 respectively.

Etymology: The specific epithet (*aestuarii*) reflects the occurrence of the species in the estuarine environment of intertidal areas of the Indian *Sundarbans*.

Acknowledgements

Authors thank Ministry of Earth Sciences Government of India for financial assistance through the project “Drugs from Sea” sub-project “Identification of eight obligately halophilic cyanobacteria of the *Sundarbans* and molecular characterization of antimicrobial compounds therefrom” (File No. MoES/09-DS/10/2013 PC-IV)

References

- Alvarenga, D.O., Rigonato, J., Branco, L.H.Z. & Fiore, M.F. (2015) Cyanobacteria in mangrove ecosystems. *Biodiversity Conservation* 24: 799–817.
<https://doi.org/10.1007/s10531-015-0871-2>
- Anagnostidis, K. & Komárek, J. (1988) Modern approach to the classification system of cyanophytes, 3-Oscillatoriales. *Algological Studies/Archiv für Hydrobiologie* 53: 327–472.
- Becraft, E.D., Wood, J.M., Rusch, D.B., Kuhl, M., Jensen, S.I., Bryant, D.A., Roberts, D.W., Cohan, F.M. & Ward, D.M. (2015) The molecular dimension of microbial species: 1. ecological distinctions among, and homogeneity within, putative ecotypes of *Synechococcus* inhabiting the cyanobacterial mat of Mushroom Spring, Yellowstone National Park. *Frontiers of Microbiology* 6: 590.
<https://doi.org/10.3389/fmicb.2015.00590>

- Bohunicka, M., Johansen, J.R. & Fucikova, K. (2011) *Tapinothrix clintonii* sp. nov. (Pseudanabaenaceae, Cyanobacteria), a new species at the nexus of five genera. *Fottea* 11: 127–140.
<https://doi.org/10.5507/fot.2011.013>
- Boone, D.R. & Castenholz, R.W. (2001) The Archaea and the Deeply Branching and Phototrophic Bacteria. In: Garrity, G., Boone, D.R. & Castenholz, R.W. (Eds.) *Bergey's Manual of Systematic Bacteriology*. Vol. 1. 2nd Edn. NY: Springer-Verlag, New York, pp. 473–487.
- Boyer, S.L., Flechtner, V.R. & Johansen, J.R. (2001) Is the 16S–23S rRNA Internal Transcribed Spacer region a good tool for use in molecular systematics and population genetics? A case study in cyanobacteria. *Molecular Biology and Evolution* 18: 1057–1069.
<https://doi.org/10.1093/oxfordjournals.molbev.a003877>
- Casamatta, D.A., Johansen, J.R., Vis, M.L. & Broadwater, S.T. (2005) Molecular and morphological characterization of ten polar and near-polar strains within the Oscillatoriales (cyanobacteria). *Journal of Phycology* 41: 421–438.
<https://doi.org/10.1111/j.1529-8817.2005.04062.x>
- Chatchawan, T., Komarek, J., Strunecky, O., Smarda, J. & Peerapornpisal, Y. (2012) *Oxyinema*, a new genus separated from the genus *Phormidium* (Cyanophyta). *Cryptogamie Algologie* 33: 41–59.
<https://doi.org/10.7872/crya.v33.iss1.2011.041>
- Chen, Q., Zhao, Q., Li, J., Jiang, S. & Ren, H. (2016) Mangrove succession enriches the sediment microbial community in South China. *Scientific Reports* 6: 27468.
<https://doi.org/10.1038/srep27468>
- Choudoir, M.L., Campbell, A.N. & Buckley, D.H. (2012) Grappling with Proteus: population-level approaches to understanding microbial diversity. *Frontiers of Microbiology* 3: 336.
<https://doi.org/10.3389/fmicb.2012.00336>
- Christensen, H., Bisgaard, M., Frederiksen, W., Mutters, R., Kuhnert, P. & Olsen, J.E. (2001) Is characterization of a single isolate sufficient for valid publication of a new genus or species? Proposal to modify Recommendation 30b of the Bacteriological Code (1990 Revision). *International Journal of Systematic and Evolutionary Microbiology* 51: 2221–2225.
<https://doi.org/10.1099/00207713-51-6-2221>
- Dadheech, P.K., Casamatta, D.A., Casper, P. & Krienitz, L. (2013) *Phormidium etoshii* sp. nov. (Oscillatoriales, Cyanobacteria) described from the Etosha Pan, Namibia, based on morphological, molecular and ecological features. *Fottea Olomouc* 13: 235–244.
<https://doi.org/10.5507/fot.2013.019>
- Debnath, M., Singh, T. & Bhadury, P. (2017) New records of Cyanobacterial morphotypes with *Leptolyngbya indica* sp. nov. from terrestrial biofilms of the Lower Gangetic Plain, India. *Phytotaxa* 316: 101–120.
<https://doi.org/10.11646/phytotaxa.316.2.1>
- Engene, N. & Gerwick, W.H. (2011) Intra-genomic 16S rRNA gene heterogeneity in cyanobacterial genomes. *Fottea* 1: 17–24.
<https://doi.org/10.5507/fot.2011.003>
- Flechtner, V.R., Boyer, S.L., Johansen, J.R. & DeNoble, M.L. (2002) *Spirirestis rafaelsensis* gen. et sp. nov. (Cyanophyceae), a new cyanobacterial genus from arid soils. *Nova Hedwigia* 74: 1–24.
<https://doi.org/10.1127/0029-5035/2002/0074-0001>
- Fox, G. E., Wisotzkey, J.D. & Jurtshuk Jr., P. (1992) How close is close: 16s rRNA sequence identity may not be sufficient to guarantee species identity. *International Journal of Systematic Bacteriology* 42: 166–170.
<https://doi.org/10.1099/00207713-42-1-166>
- Giri, C., Ochieng, E., Tieszen, L.L., Zhu, Z., Singh, A., Loveland, T., Masek, J. & Duke, N. (2011) Status and distribution of mangrove forests of the world using earth observation satellite data. *Global Ecology and Biogeography* 20: 154–159.
<https://doi.org/10.1111/j.1466-8238.2010.00584.x>
- Gugger, M.F. & Hoffmann, L. (2004) Polyphyly of true branching cyanobacteria (Stigonematales). *International Journal of Systematic and Evolutionary Microbiology* 54: 349–357.
<https://doi.org/10.1099/ijs.0.02744-0>
- Hašler, P., Dvořák, P., Johansen, J.R., Kitner, M., Ondřej, V. & Poulíčková, A. (2012) Morphological and molecular study of epipellic filamentous genera *Phormidium*, *Microcoleus* and *Geitlerinema* (Oscillatoriales, Cyanophyta/Cyanobacteria). *Fottea* 12: 341–356.
<https://doi.org/10.5507/fot.2012.024>
- Hoffmann, L., Komarek, J. & Kastovsky, J. (2005) System of cyanoprokaryotes (cyanobacteria)—state in 2004. *Archives of Hydrobiology Supplementary Algological Studies* 117: 95–115.
<https://doi.org/10.1127/1864-1318/2005/0117-0095>
- Iteman, I., Rippka, R., de Marsac, N.T. & Herdman, M. (2000) Comparison of conserved structural and regulatory domains within divergent 16S rRNA–23S rRNA spacer sequences of cyanobacteria. *Microbiology* 146: 1275–1286.
<https://doi.org/10.1099/00221287-146-6-1275>

- Janse, I., Meima, M., Kardinaal, W.E.A. & Zwart, G. (2003) High-resolution differentiation of cyanobacteria by using rRNA-Internal Transcribed Spacer Denaturing Gradient Gel Electrophoresis. *Applied and Environmental Microbiology* 69: 6634–6643.
<https://doi.org/10.1128/AEM.69.11.6634-6643.2003>
- Johansen, J.R., Maresi, J., Pietrasiak, N., Bohunicka, A.M., Zima Jr., J., Štenclová, L. & Hauer, T. (2017) Highly divergent 16S rRNA sequences in ribosomal operons of *Scytonema hyalinum* (Cyanobacteria). *PLoS ONE* 12: e0186393.
<https://doi.org/10.1371/journal.pone.0186393>
- Johansen, J.R., Kovacik, L., Casamatta, D.A., Fučíková, K., & Kaštovský, J. (2011) Utility of 16S-23S ITS sequence and secondary structure for recognition of intrageneric and intergeneric limits within cyanobacterial taxa: *Leptolyngbya corticola* sp. nov. (Pseudanabaenaceae, Cyanobacteria). *Nova Hedwigia* 92: 283–302.
<https://doi.org/10.1127/0029-5035/2011/0092-0283>
- Johansen, J. & Casamatta, D.A. (2005) Recognizing cyanobacterial diversity through adoption of a new species paradigm. *Algological Studies* 117: 71–93.
<https://doi.org/10.1127/1864-1318/2005/0117-0071>
- Komárek, J. & Anagnostidis, K. (2005) Oscillatoriales. In: Büdel, B., Gärdner, G., Krienitz, L. & Schagerl, M. (Eds.) *Süßwasserflora von Mitteleuropa, Bd. 19/2: Cyanoprokaryota*. Elsevier, München, 759 pp.
- Komarek, J. & Kastovsky, J. (2003) Coincidences of structural and molecular characters in evolutionary lines of cyanobacteria. *Algological Studies* 109: 305–325.
<https://doi.org/10.1127/1864-1318/2003/0109-0305>
- Komarek, J. (2006) Cyanobacterial Taxonomy: Current problems and prospects for the integration of traditional and molecular approaches. *Algae* 21: 349–375.
<https://doi.org/10.4490/ALGAE.2006.21.4.349>
- Komarek, J., Kastovsky, J., Mares, J. & Johansen, J.R. (2014) Taxonomic classification of cyanoprokaryotes (cyanobacterial genera) using a polyphasic approach. *Preslia* 86: 295–335.
- Lamprinou, V., Skaraki, K., Kotoulas, G., Anagnostidis, K., Economou-Amilli, A. & Pantazidou, A. (2013) A new species of *Phormidium* (Cyanobacteria, Oscillatoriales) from three Greek Caves: morphological and molecular analysis. *Fundamental and Applied Limnology* 182: 109–116.
<https://doi.org/10.1127/1863-9135/2013/0323>
- Lane, D.J. (1991) 16S/23S rRNA sequencing. In: Stackebrandt, E. & Goodfellow, M. (Eds.) *Nucleic acid techniques in bacterial systematics*. John Wiley and Sons, United Kingdom, pp. 115–175.
- Larkin, M.A., Blackshields, G., Brown, N.P., Chenna, R., McGettigan, P.A., McWilliam, H., Valentin, F., Wallace, I.M., Wilm, A., Lopez, R., Thompson, J.D., Gibson, T.J. & Higgins, D.G. (2007) Clustal W and Clustal X version 2.0. *Bioinformatics* 23: 2947–2948.
<https://doi.org/10.1093/bioinformatics/btm404>
- Lopes, V.R., Ramos, V., Martins, A., Sousa, M., Welker, M., Antunes, A. & Vasconcelos, V.M. (2012) Phylogenetic, chemical and morphological diversity of cyanobacteria from Portuguese temperate estuaries. *Marine Environmental Research* 73: 7–16.
<https://doi.org/10.1016/j.marenvres.2011.10.005>
- Marquardt, J. & Palinska, K. (2007) Genotypic and phenotypic diversity of cyanobacteria assigned to the genus *Phormidium* (Oscillatoriales) from different habitats and geographical sites. *Archives of Microbiology* 187: 397–413.
<https://doi.org/10.1007/s00203-006-0204-7>
- Mondal, S.H. & Debnath, P. (2017) Spatial and temporal changes of Sundarbans reserve forest in Bangladesh. *Environment and Natural Resources Journal* 15: 51–61.
- Mullineaux, C.W. (1999) The thylakoid membranes of cyanobacteria: structure, dynamics and function. *Australian Journal of Plant Physiology* 26: 671–677.
<https://doi.org/10.1071/PP99027>
- Naeimi, M. & Zehabian, G. (2011) The review of saline water in desert management. *International Journal of Environmental Science and Development* 2: 474–478.
<https://doi.org/10.7763/IJESD.2011.V2.172>
- Neogi, S.B., Dey, M., Kabir, S.M.L., Masum, S.J.H., Kopprio, G., Yamasaki, S. & Lara, R. (2016) Sundarban mangroves: diversity, ecosystem services and climate change impacts. *Asian Journal of Medical and Biological Research* 2: 488–507.
<https://doi.org/10.3329/ajmbr.v2i4.30988>
- Nübel, U., Garcia-Pichel, F. & Muyzer, G. (1997) PCR primers to amplify 16S rRNA genes from cyanobacteria. *Applied and Environmental Microbiology* 63: 3327–3332.
- Olive, J., Ajlani, G., Astier, C., Recouvreur, M. & Vernotte, C. (1997) Ultrastructure and light adaptation of phycobilisome mutants of *Synechocystis* PCC 6803. *Biochimica et Biophysica Acta* 1319: 275–282.
[https://doi.org/10.1016/S0005-2728\(96\)00168-5](https://doi.org/10.1016/S0005-2728(96)00168-5)

- Osorio-Santos, K., Pietrasiak, N., Bohunická, M., Miscoe, L.H., Kovacik, L., Martin, M.P. & Johansen, J.R. (2014) Seven new species of *Oculatella* (Pseudanabaenales, Cyanobacteria) *European Journal of Phycology* 49: 450–470.
<https://doi.org/10.1080/09670262.2014.976843>
- Perkerson III, R.B., Johansen, J.R., Kovacik, L., Brand, J., Kastovsky, J. & Casamatta, D.A. (2011) A unique Pseudanabaenalean (cyanobacteria) genus *Nodosilinea* gen. nov. based on morphological and molecular data. *Journal of Phycology* 47: 1397–1412.
<https://doi.org/10.1111/j.1529-8817.2011.01077.x>
- Posada, D. (2008) jModelTest: phylogenetic model averaging. *Molecular Biology and Evolution* 25: 1253–1256.
<https://doi.org/10.1093/molbev/msn083>
- Pramanik, A., Sundararaman, M., Das, S., Ghosh, U. & Mukherjee, J. (2011) Isolation and characterization of cyanobacteria possessing antimicrobial activity from the *Sundarbans*, the world's largest tidal mangrove forest. *Journal of Phycology* 47: 731–743.
<https://doi.org/10.1111/j.1529-8817.2011.01017.x>
- Řeháková, K., Johansen, J.R., Bowen, M.B., Martin, M.P. & Sheil, C.A. (2014) Variation in secondary structure of the 16S rRNA molecule in cyanobacteria with implications for phylogenetic analysis. *Fottea Olomouc* 14: 161–178.
<https://doi.org/10.5507/fot.2014.013>
- Rippka, R., Deruelles, J., Waterbury, J.B., Herdman, M. & Stanier, R.Y. (1979) Generic assignments, strain histories and properties of pure cultures of cyanobacteria. *Journal of General Microbiology* 111: 1–61.
- Segiesmund, M.A., Johansen, J.R., Karsten, U. & Friedl, T. (2008) *Coleofasciculus* gen.nov. (Cyanobacteria): morphological and molecular criteria for revision of the genus *Microcoleus* Gomont. *Journal of Phycology* 44: 1572–1585.
<https://doi.org/10.1111/j.1529-8817.2008.00604.x>
- Sen, N. & Naskar, K. (2002) Algal communities in the intertidal mangrove niches of Sundarbans. *Journal of Interacad* 6: 420–433.
- Silva, C.S.P., Genuário, D.B., Vaz, M.G.M.V. & Fiore, M.F. (2014) Phylogeny of culturable cyanobacteria from Brazilian mangroves. *Systemic and Applied Microbiology* 37: 100–112.
<https://doi.org/10.1016/j.syapm.2013.12.003>
- Stöver, B.C. & Müller, K.F. (2010) TreeGraph 2: combining and visualizing evidence from different phylogenetic analyses. *BMC Bioinformatics* 11: 7.
<https://doi.org/10.1186/1471-2105-11-7>
- Swofford, D.L. (2002) *PAUP*: Phylogenetic analysis using parsimony (and other methods), version 4b10*. Sinauer Associates, Sunderland.
- Westerman, M., Ernst, A., Brass, S., Boger, P. & Wehrmeyer, W. (1994) Ultrastructure of cell wall and photosynthetic apparatus of the phycobilisome-less *Synechocystis* sp. strain BO 8402 and phycobilisome-containing derivative strain BO 9201. *Archives of Microbiology* 162: 222–232.
<https://doi.org/10.1007/BF00301842>
- Zuker, M. (2003) Mfold web server for nucleic acid folding and hybridization prediction. *Nucleic Acid Research* 31: 3406–3415.
<https://doi.org/10.1093/nar/gkg595>



GENESIS AND SIGNIFICANCE OF COOPERATIVE TRANSPORT IN ANTS

Khokan Naskar^{1,*}, Srimanta Kumar Raut²¹Department of Zoology, Achhruram Memorial College, Jhalda, Purulia-723202, West Bengal, India²Ecology and Ethology Laboratory, Department of Zoology, University of Calcutta, 35, Ballygunge Circular Road, Kolkata - 700019, India

*Corresponding author email: khokan24@gmail.com

ABSTRACT

Food particles of different sizes and weight were offered to the ants in their natural foraging area at Garia, Kolkata, West Bengal, India to note the strategy being applied by the ants to carry the food to the nest and possible significance of such behavioural act. It is revealed that the ants did not bother for assistance of other members if the said food particle is manageable for transport individually, by keeping the food high at the head level following mandibular biting. But little heavier food particle induced the ant individual to apply either pushing or pulling or both the acts to carry a food particle. However, with the increase size and/or weight of the food particle the ants were seen to develop the cooperative transport system with a view to ensure procurement of the targeted food matter to the nest. To make the cooperative transport effective the ants apply any and all kinds of options viz. pulling and pushing by changing their position at frequent intervals on way of carrying act, perhaps to meet the requirement of quality food at the first instance though quantitative need could not be ruled out.

KEY WORDS: Ants, cooperative transport, genesis, significance.**INTRODUCTION**

The act of simultaneously moving an item by two or more individuals is defined as cooperative transport (Czaczkes & Ratnieks, 2013). Except humans this sort of behaviour is almost confined to ants. It is also stated that the ants follow the cooperative transport mechanism to carry a food item which is unmanageable individually (McCreery & Breed, 2014). Though cooperative transport in ants have drawn the attention of various workers (Hölldobler & Wilson, 1990 ; Moffett, 1992 ; Czaczkes & Ratnieks, 2013) the genesis of the said behaviour is still unknown. However, according to McCreery & Breed (2014) cooperative transport of food is a proximate behavioural mechanism that increases the size range of food available to a colony. It is also stated that the ant species who have developed the art of cooperative transportation are able to increase the amount of food accessible to them (Berman et al, 2011; Czaczkes & Ratnieks, 2013). Keeping these findings in mind we designed some experiments in view of our earlier findings (Naskar & Raut, 2014a, b, c, 2015a, b, c, d, e, f, g, 2016a, b, c, 2018) by offering food of different sizes to the ants occurring in their natural habitats at Garia (Kolkata), West Bengal, India to determine the genesis behind the manifestation of such behavioural act.

MATERIALS & METHODS

We offered different types of foods viz. biscuit fragments, sugar cubes, nut fragments, papad fragments, dead mosquito, fish fragments (both fresh and dry) and fragmented parts of animal's body like cockroach and other insects larvae of certain insects of different sizes to the ants on the ground floor of a house locating adjacent to a garden at Garia, Kolkata to note the collection strategy being applied by the ants irrespective of species. The experimental trials were made both in day and night hours

during post-winter and summer months (February-June). Due attention was paid to note the strategy the ants applied to carry the offered food materials to their nest. Also, due attention was paid to observe and record the behaviour of the ants to ensure transportation of the food matter from the offered sites to the nest.

RESULTS

The ants *Pheidole roberti*, *Paratrechina longicornis*, *Anoplolepis gracilipes*, *Monomorium pharaonis* were seen to come in contact of the food materials offered on way of their foraging movement. Except *M. pharaonis* an ant individual was seen to examine the food matters and applied the following strategies to carry the food matters concerned. *M. pharaonis* preferred to cut the food matter into small pieces to apply individual carrying strategy though rarely, they exhibited the cooperative food carrying behaviour.

Pushing strategy: When one ant came across of a piece of food matter which was manageable by her individually then she applied the pushing strategy to carry the same (Fig.1a). Here, the ant lifted the food matter by holding the same with her mandibles and started moving forward keeping the food materials high at the level of head (Fig.1b).

Pulling strategy:

This strategy is applied when the food material is little bit heavier than the food material selected for procurement by an ant through the application of pushing strategy. In this case the ant is unable to lift the food matter from the ground individually but she is able to carry the same on way of dragging i.e. through the application of pulling strategy (Fig.1c).

Pushing-Pulling strategy

In many instances an individual ant was seen to carry a piece of food material by pushing-pulling strategy. The ant is unable to lift the food material up from the ground by the help of biting with the mandibles but was able to push forward the food material by biting-pushing act. But, she was seen to change her position. From behind the food material she moved to front side to pull the food through

the biting by the mandibles. The said act was changed after few minutes to follow the pushing strategy (Fig. 1d). But, when the food matter was unmanageable for an ant individual she was seen to look for the assistance of other individuals of the said species to ensure transportation of the same. The behaviours exhibited by 2, 3, 4, 5 and 6 ant individuals involved in transporting a piece of food material were as follows.

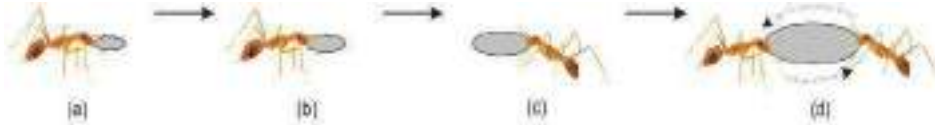


FIGURE 1: Strategies applied (a-d) by an ant individual to carry a food particle which was manageable herself, to the nest

By 2 ant individuals

Here, in some cases, one ant was seen to act as pusher (marked by 1) and the other (marked by 2) as puller (Fig.2a) while in some other cases both the ants were seen to act as either pusher (Fig. 2b) or puller (Fig. 2c) jointly.

But, in case of one pusher and one puller food-carrying strategy, at certain intervals puller was seen to change the place to act as pusher while the puller was seen to move to the opposite end of the food element to take the position of a pusher (Fig. 2d).

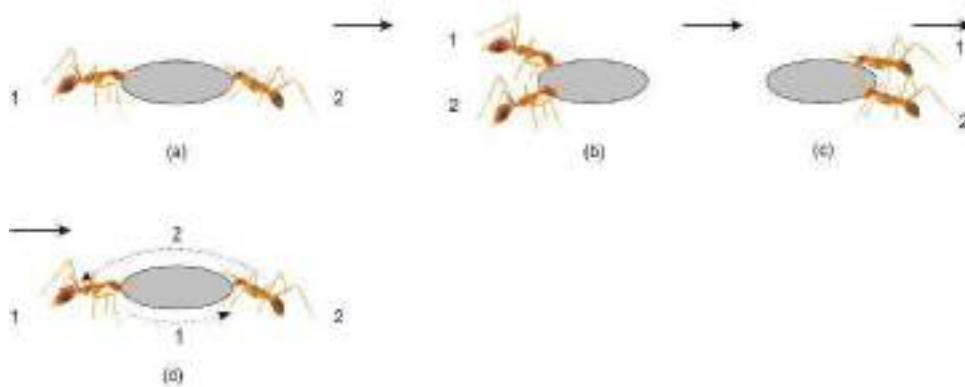


FIGURE 2: Strategies applied (a-d) by two ant individuals when a food particle was manageable by them, to carry the same to the destination.

By 3 ant individuals

Transportation of a food element while effected by the joint efforts of 3 ant individuals sometimes 1 was seen to act as pusher and 2 as puller (Fig.3a) or reverse i.e. 2 as pusher and 1 as puller (Fig.3b). But, depending upon the

distance to be travelled and the hurdles to overcome to reach at the destination the ants were seen to change their position (Fig.3c-f) to act as pusher or puller as per need to ensure transportation of the food matter.

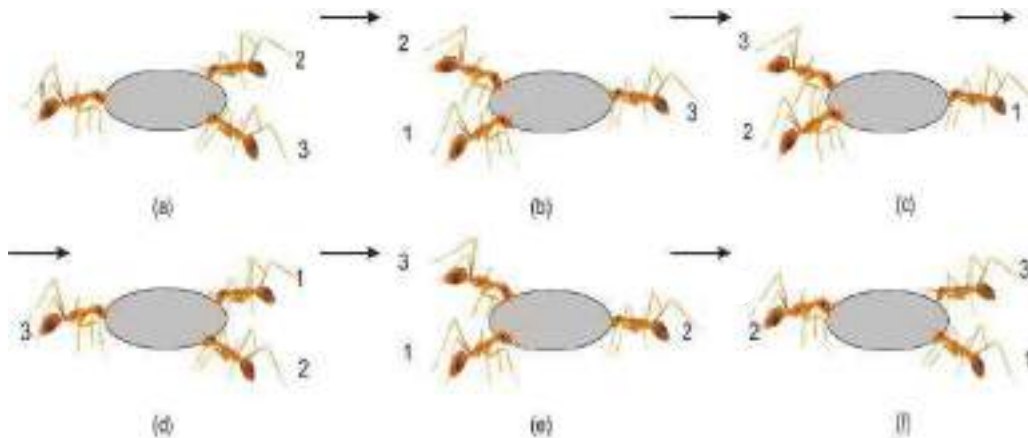


FIGURE 3: Strategies applied (a-f) by the three ant individuals when a food particle was manageable by them, to carry the same to the destination.

By 4 ant individuals

Usually, of the 4 ants 2 were seen to push the food material from the posterior end while other 2 were engaged in pulling the said material (Fig. 4a, b). But, in some cases 3 were seen either pushing or pulling the food element and the remaining one was either in pulling or pushing i.e. opposite act at the opposite end (Fig.4c-k). They were seen to change their position at frequent

intervals. Moreover, in some cases one ant was seen pushing the food matter from posterior end of the same while the other one was engaged in pulling the food matter being positioned at the anterior end. Each of the remaining two ants was seen to push the food matter being positioned at the lateral side of the food element (Fig.4k). They were seen to change their position at frequent intervals.

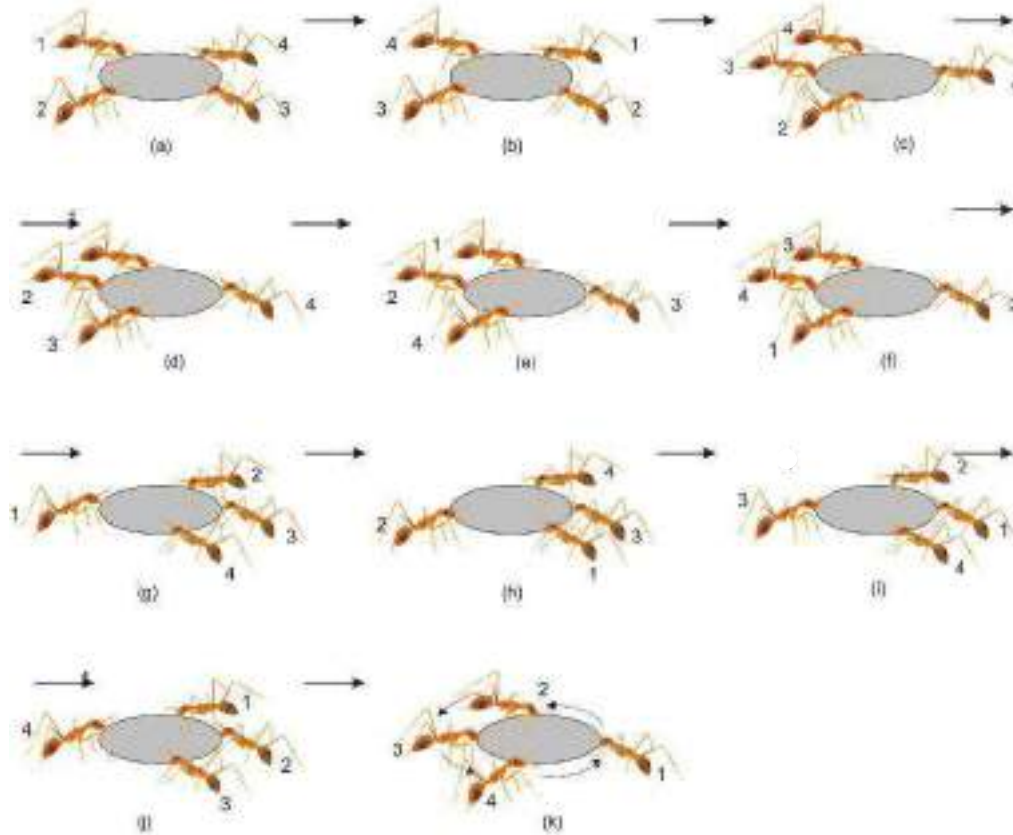


FIGURE 4: Strategies applied (a-k) by the four ant individuals when a food particle was manageable by them, to carry the same to the destination.

By 5 ant individuals

Of the 5 ants sometimes 2 or 3 were seen either in pushing or in pulling act at the posterior or anterior side respectively (Fig.5a, b). Also, in some other instances one ant was seen in pushing act at the posterior end of the food while another one was pulling the food being positioned at

the anterior end. The remaining 3 ants were also seen in pushing act, sometimes 2 of them positioned themselves at the lateral side either at the right side or at the left side of the food element and the other one at the other lateral side (Fig.5c). They were seen to change their position at frequent intervals.

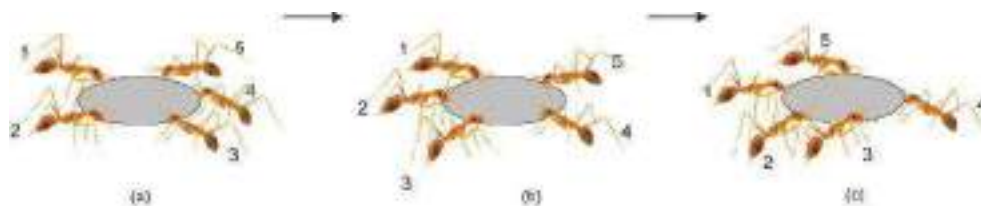


FIGURE 5. Strategies applied (a-c) by the five ant individuals when a food particle was manageable by them, to carry the same to the destination.

By 6 ant individuals

The ants were seen to take their position at different sides of the food element: sometimes one was seen in pushing act at the posterior end and the other one in pulling act at

the anterior end; of the remaining 4 ants 2 were seen in pushing act at the right marginal side while the other 2 were seen at the left marginal side in the pushing act (Fig.6a). Also, in some instances 2 ants were seen in

pushing and the other 2 ants were in pulling act while the remaining 2 ants were also seen in pushing act positioning one at the right lateral margin and the other one at the left lateral margin of the food material involved in carrying act (Fig. 6b). However, involvement of 3 ants as pusher at the

posterior end and the other 3 individual's involvement as puller at the anterior end of the food element was not uncommon (Fig.6c). They were seen to change their position at frequent intervals (indicated by arrows).

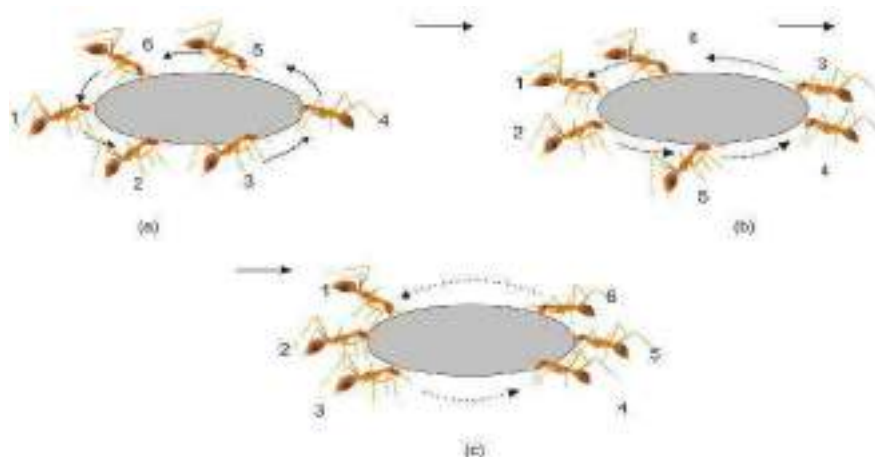


FIGURE 6. Strategies applied (a-c) by the six ant individuals when a food particle was manageable by them, to carry the same to the destination.

By more than 6 ant individuals

The food materials which were not manageable by 6 ant individuals were transported by active participation of many ant individuals where ants were seen to change their position at frequent intervals from pulling to pushing or vice versa activities. In cases of transport of a heavier food element where space for the required number of ants was not available a few ants were seen to move from the front side to the back or lateral sides to act as pusher. As there were no room for their position it was seen that each one of such workers tried effectively to find the space to bite the food matter with a view to push the same forward. Besides, it was also seen that the ants never failed to accommodate themselves at the definite location or site of the food element so as to ensure the movement of the said element which was snagged for the time being.

DISCUSSION

It appears that, ants left no option to transport the food material to the destination site. Depending upon the size/weight of the food to be procured the strategy applied varied to a great extent. As regards to a manageable food particle to be transported by a single ant the lifting option is unique. There exists no dispute regarding safe transportation of the said food particle. The immediate second option i.e. the pulling strategy emerged for transportation of a food particle slightly heavier than that one considered to be transported through lifting strategy. This stimulated us to think over the problem that the ant being a tiny creature at the bottom of the ladder of evolution is able to exercise its intelligence not only to estimate the weight of the food particle but also to select a second device i.e. pulling to enable her to carry the same. The climax of ant's intelligence in transporting food material perhaps, attained in developing the art of application of both the strategies i.e. pushing and pulling alternatively by the same ant individual. This indicates that the ant have developed the art of applying pulling and

pushing strategy alternately perhaps to overcome the impact of hurdle to carry the same alone. Therefore, she applied both the strategies to dislodge the snagged item. It is really cumbersome and stressful for an ant to carry a food item in such a way. But, even such being the case no consideration was taken into account for the help from other ant individual. That is, perhaps, up to such weight (or size) it is the task of an individual ant to manage the food item to carry the same to the nest as the energy to be spent by another ant in transporting the said item is not permissible so far cost benefit effect is concerned.

However, such behavioural adaptation is equally befitting in case of cooperative transport. Because, in cases of transporting a food item by two ant individuals the puller and pusher are also habituated to change their position to act as puller and pusher from time to time in course of carrying act. It is most likely that the ants have developed a communication system in respect to behavioural change from pusher to puller among themselves. Though frequent deadlock with no forward movement are the characteristic features of uncoordinated transport (Sudd 1965; Moffett 1986, 1992, Pratt 1989) random changes in the composition, orientation or behaviour of the group members are proved effective to resolve the deadlocks (Sudd 1965). But, in the present study it is noted that the change of place by the members of the cooperative transport group is not random at all, rather judicious. Because, involvement of 4, 5 or 6 ants in transporting a food item revealed the placement of individuals at various points to dislodge the snagged matter. This indicates that the ants are able to realize the hurdle induced problem in respect to barrier inhibiting the movement of the food item. This could be well judged from the fact of attempts of the ants to accommodate themselves almost forcibly because of lack of space, at particular sites of the food material which is being transported to the nest.

Thus, it appears that cooperative transport is a reflection of self learning behaviour of individual ant, of course, in a

coordinated way to ensure supply of food to the colony members both qualitatively and quantitatively. Though it is possible to meet the food demand of the colony members qualitatively on way of food collection by the ants individually there exists no possibility to provide food to the colony members from qualitative view, for certain ant species. To ensure the same cooperative transport is inevitable and thus was evolved.

ACKNOWLEDGEMENT

The authors are thankful to the Head of the Department of Zoology, University of Calcutta and to the Principal, Achhruram Memorial College, Purulia, West Bengal for the facilities provided. The ants specimens were identified by the Zoological Survey of India, Kolkata, India.

REFERENCES

Czaczkes, T.J. and Ratnieks, F.L.W. (2013) Cooperative transport in ants (Hymenoptera: Formicidae) and elsewhere. *Myrmeco. News*, **18**, 1-11.

Hölldobler, B. and Wilson, E.O. (1990) *The ants*. pp. 732, Harvard University Press, Cambridge, MA.

Moffett, M.W. (1986) Notes on the behaviour of the dimorphic ant *Oligomyrmex overbecki* (Hymenoptera: Formicidae). *Psyche A J. Entomo.* **93**, 107-116.

Moffett, M.W. (1992) Ant foraging. *Nati. geo Res. and Explo.* **8**, 220-231.

Naskar, K. and Raut, S. K. (2014a) Food searching and collection by the ants *Pheidole roberti* Forel. *Discov.* **32**, 6-11.

Naskar, K. and Raut, S. K. (2014b) Judicious foraging by the ants *Pheidole roberti* Forel. *Proc. Zool. Soc., Kolkata.* **68**, 131-138.

Naskar, K. and Raut, S.K. (2014c) Ants forage haphazardly : a case study with *Pheidole roberti* Forel. *Int. J. Sci. and Nat.* **5**, 719-722.

Naskar, K. and Raut, S.K. (2015a) Ants' foraging, a mystery. *Int. J. Inno. Sci. and Res.* **4** (2), 064-067.

Naskar, K. and Raut, S.K. (2015b) Foraging interactions between the Reddish brown ants *Pheidole roberti* and the

Black ants *Paratrechina longicornis* *Int. J. Res. Stud. in Biosci.* **3** (3), 183-189.

Naskar, K. and Raut, S.K. (2015c) Available food and ant's response. *Int. J. Eng. Sci. and Res. Tech.*, **4** (4), 368-372.

Naskar, K. and Raut, S.K. (2015d) Food-carrying strategy of the ants *Pheidole roberti*. *Int. J. Tech. Res. and Appl.* **3** (3), 55-58.

Naskar, K. and Raut, S.K. (2015e) Foraging behaviour following food contact in the ants *Pheidole roberti*. *Glo. J. Bio. Agri. and Health Sci.* **4** (2), 21- 24.

Naskar, K. and Raut, S.K. (2015f) Cue for ant's trail development. *Int. J. Res. in Eng. and App. Sci.* **5** (5), 182-192.

Naskar, K. and Raut, S. K. (2015g). Mysterious foraging of Pharaoh ant *Monomorium pharaonis*. *Int. J. Res. in Eng. and App. Sci.*, **5** (7), 67-71.

Naskar, K. and Raut, S.K. (2016a) Ants' food examination. *Proc. Zool. Soc., Kolkata.* **70** (2), 119-131.

Naskar, K. and Raut, S.K. (2016b) Winter quarter-induced foraging in ants. *Glo. J. Bio-Sci. and Biotech.* **5** (3), 318-323.

Naskar, K. and Raut, S.K. (2016c) Does colour of the food attract ants ? *Proc. Zool. Soc., Kolkata.* **71**(1), 25-29.

Naskar, K. and Raut, S.K. (2018) Food-induced food-transporting strategies of the ants *Pheidole roberti* and *Paratrechina longicornis* ; in *Entomology : Current Status and Future Strategies*. Ganguly, A. and K. Naskar (eds), pp. 125-133, Daya Publishing House, (Astral Int. Pvt. Ltd.), New Delhi.

Pratt, S.C. (1989) Recruitment and other communication behaviour in the ponerine ant *Ectatomma ruidum*. *Ethology.* **81**, 313-331.

Sudd, J.H. (1965) Transport of prey by ants. *Behav.* **15**, 234-271.



E-ISSN: 2320-7078

P-ISSN: 2349-6800

JEZS 2018; 6(1): 686-690

© 2018 JEZS

Received: 02-11-2017

Accepted: 03-12-2017

Arijit Ganguly

1) Fishery and Aquatic Ecology Laboratory, Department of Zoology, Rajiv Gandhi University, Rono Hills, Doimukh, Arunachal Pradesh, India

2) Department of Zoology, Achhruram Memorial College, Jhalda-723202, Purulia, West Bengal, India

Achom Darshan

Centre with Potential for Excellence in Biodiversity (CPEB II), Rajiv Gandhi University, Rono Hills, Doimukh, Arunachal Pradesh, India.

Ram Kumar

Fishery and Aquatic Ecology Laboratory, Department of Zoology, Rajiv Gandhi University, Rono Hills, Doimukh, Arunachal Pradesh, India

Santosh Kumar Abujam

Fishery and Aquatic Ecology Laboratory, Department of Zoology, Rajiv Gandhi University, Rono Hills, Doimukh, Arunachal Pradesh, India

Debangshu Narayan Das

Fishery and Aquatic Ecology Laboratory, Department of Zoology, Rajiv Gandhi University, Rono Hills, Doimukh, Arunachal Pradesh, India

Correspondence

Arijit Ganguly

1) Fishery and Aquatic Ecology Laboratory, Department of Zoology, Rajiv Gandhi University, Rono Hills, Doimukh, Arunachal Pradesh, India

2) Department of Zoology, Achhruram Memorial College, Jhalda-723202, Purulia, West Bengal, India

Relative assessment of diversity of wild ornamental fishes sampled from two river basins of Arunachal Pradesh, India

Arijit Ganguly, Achom Darshan, Ram Kumar, Santosh Kumar Abujam, Debangshu Narayan Das

Abstract

The present paper attempts to document the potential ornamental fishes (POFs) and assess their diversity in two river basins of Arunachal Pradesh that are still unexplored in such a way. Several diversity indices are computed river-wise and statistically compared. From Dikrong and Ranganadi river basin a total of 52 and 29 POF species are documented respectively. The species compositions are quite different in the two river basins may be because of their altitudinal differences. The computed diversity indices are a little confusing because one river is more diverse while the other has more species richness. Hence, diversity profiles are constructed using Renyi index. The intersecting profiles reveal the two river basins are non-comparable in terms of ornamental fish diversity. The paper concludes with the note that compilation of such information would be of immense value practically to generate a river-wise list of POF of the state to design fish conservation strategies in future.

Keywords: Biodiversity, Dikrong, ornamental fish (OF), potential ornamental fish (POF), Ranganadi

Introduction

North-Eastern region of India is one of the hot spots of freshwater fish biodiversity ^[1] which possesses great potential to support both food fish (FF) and ornamental fish (OF) industries of the country ^[2]. Arunachal Pradesh (26° 28'-29° 30' N and 90° 30'-97° 30' E) is the largest frontier state of North-East India having an area of 83,743 sq. Km that covers almost 60.93% of the Eastern Himalayan hotspot ^[3]. Being bordered with Bhutan, China, Bangladesh and Myanmar, the state of Arunachal Pradesh uniquely shares their flora and fauna ^[3]. Topographically the state is comprised of altitudinal zones forming three distinct ecological belts ^[4]. The northern part is characterized by mountain and sub-mountain terrains, and the southernmost part is gradually slopping towards the plains of the state of Assam, while the part in between constitutes the mid-altitudinal regions which have the greatest diversity ^[4]. Further this mountainous state is engorged with eleven river basins ^[5] and numerous streams that harbour enormously rich and diversified piscatorial forms, many of which have ornamental potential but not yet established as OF; these are the potential ornamental fishes (POF) of this state. Thus Arunachal Pradesh is highly promising to be the OF hub of India, only waiting for proper effort.

At present nearly 95% of the total OF supplied from this region is wild fishes that are caught directly from their natural habitat in order to be sold into the aquatics trade ^[6]. This practice is extremely harmful as it causes over-exploitation and ultimately results dwindling of this immense fish resource. In addition, the introduction of exotic species, pollution, global climate change, indiscriminate fishing for food etc. is making the situation even more critical ^[7-8]. According to a report of IUCN many of the fish species of Arunachal Pradesh have already become endangered or critically endangered ^[9], and the list is getting bigger with time. So, there is an urgent need to document the fishes of this state and assess the current status of their diversity so that necessary steps could be taken for their conservation. But such types of studies are lacking except some scattered information in the literature ^[10-11]. Under this backdrop, the present paper deals with documentation and assessment of the diversity of fishes with ornamental value (*i.e.* OF and POF) in Ranganadi and Dikrong river basins of Arunachal Pradesh, to ascertain the present status of their diversity in this region.

2. Material and methods

2.1 Sampling site

The two selected river basins are divided into four accessible sites on the basis of increasing altitude (Fig. 1). For Dikrong river basin, fishes are sampled from Doimukh (27°08'19" N 93°44'51" E, 120mt asl), Itanagar (27°06'30" N 93°36'27" E, 300mt asl), Sagalee (27°41'38" N 93°29'37" E, 932mt asl), and Dev (27°12'30" N 93°30'24" E, 1083mt asl), while for Ranganadi river basin sampling is done from Kimin (27°21'01" N 93°57'11" E, 193mt asl), Yazali (27°23'04" N 93°45'28" E, 611mt asl), Yachuli (27°25'53" N 93°45'42" E, 797mt asl), and Ziro (27°30'20" N 93°50'00" E, 1617mt asl).

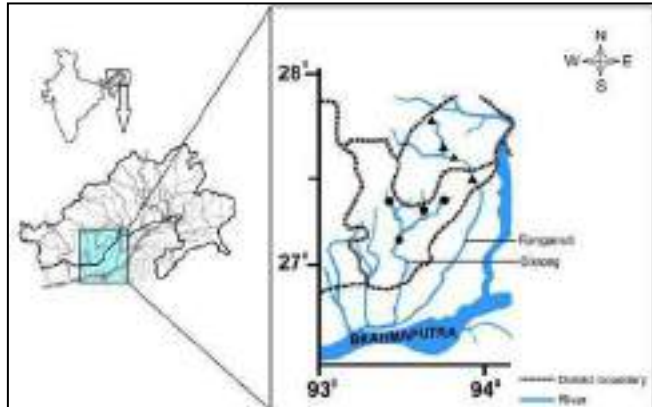


Fig 1: Map showing sampling sites in Dikrong (round black) and Ranganadi (triangle black) river basins of Arunachal Pradesh (map not in scale).

2.2 Field sampling

The fishes are randomly sampled for a period of three years using caste net, electrofisher and other indigenous traps from the rivers and their tributaries starting from July, 2012 till June, 2015. Collected specimens are identified up to species level and their counts are recorded on site, while the unidentified species are kept in 10% formalin and taken to the Rajiv Gandhi University Fisheries Museum (RGU-MF), where identification of the specimens is completed. Valid names of the documented fishes are obtained using the information of Vishwanath et al. and Eschmeyer [12-13]. The lists of the fishes with ornamental potential are then prepared separately for each of the river basins. Later, % relative abundance was calculated using the following formula:

$$\% \text{ Relative abundance} = \frac{\text{Number of individuals of a particular species}}{\text{Total number of individuals}} \times 100$$

2.3 Statistical analyses

Our hypothesis that species compositions within one river basin should be more similar than those from the other basin is tested by one-factorial permutational analysis of variance (PERMANOVA) based on presence/absence data and Bray-Curtis dissimilarities with 9999 permutations, followed by Bonferroni corrected pair-wise permutation test. Assessment of diversity and all the statistical analyses are carried out with the help of PAST software, version 3.02 (University of Oslo, Norway, <http://folk.uio.no/ohammer/past>).

2.4 Estimation of diversity

From the plethora of diversity indices the following three have been selected for the purpose:

$$\text{Shannon - Wiener index} = H' = - \sum_i \frac{n_i}{n} \ln \frac{n_i}{n}$$

[Where, n_i = number of individuals of taxon i , n = Total number of individuals]

$$\text{Simpson's diversity index} = D = 1 - \left(\frac{\sum n(n-1)}{N(N-1)} \right)$$

[Where, n = total number of organisms of a particular species, N = total number of organisms of all species]

$$\text{Berger - Parker index} = D = \frac{N_{\max}}{N}$$

[Where, N_{\max} is the number of individuals in the most abundant species, and N is the total number of individuals in the sample]

Evenness has been measured by the Buzas-Gibson evenness index using the following equation:

$$\text{Buzas - Gibson evenness index} = \frac{eH'}{S}$$

[Where eH' = Shannon-Wiener index, calculated using natural logarithms, S = Number of species]

Species richness has been estimated using Margalef and Menhinick indices by the following equations:

$$\text{Margalef index} = D_{mg} = \frac{S-1}{\ln N}$$

[Where S = Number of species, N = Total number of individuals in the sample]

$$\text{Menhinick index} = D_{mn} = \frac{S}{\sqrt{N}}$$

[Where S = Number of species, N = Total number of individuals in the sample]

For comparative assessment of the estimated alpha diversity of the two river basins, the diversity indices are subjected to permutation tests. To obtain a complete profile of the OF diversity of the selected river basins, the exponential of Renyi index is used taking different alpha values. The equation is:

$$\text{Renyi index} = H_\alpha = \left(\frac{1}{1-\alpha} \ln \sum_{i=1}^S p_i^\alpha \right)$$

[Where S = number of species, p_i = relative abundance of the i^{th} species, α = a scale parameter. According to Hammer, 2014 for $\alpha=0$, this equation gives the total species number, $\alpha=1$ gives an index proportional to the Shannon-Wiener index, and $\alpha=2$ gives the value of Simpson index.]

3. Results and discussion

Central Inland Fisheries Research Institute (CIFRI), Barrackpore, India, has recently made an attempt to collect data from selected sites of the rivers Ganga, Brahmaputra, Narmada, Tapti, Godavari and Krishna. The study reveals all these rivers to be pretty rich in fish fauna where Ganga already harbours the maximum number of species followed by Brahmaputra [14]. This finding is highly significant in the context of the rivers of Arunachal Pradesh being the tributaries of the great river Brahmaputra. Hence it is quite obvious that all the rivers of the state bear high species richness. The present assessment also supports this view as because Dikrong river basin possesses the total of 52 species under 38 genera and 18 families having ornamental value

(Table 1, along with relative abundance and IUCN status). From Ranganadi river basin total of 29 ornamental species are recorded that fall under 22 genera and 14 families (Table 2, along with relative abundance and IUCN status). Members of Cyprinidae family are found to be the most dominant group in both the rivers as reported earlier by many authors from different other parts of Himalayan water bodies ^[15-16].

Table 1: The list of ornamental and potential ornamental fishes documented from Dikrong River, Arunachal Pradesh, during study period (2012-2015) along with relative abundance (RA) and IUCN status ^[22].

Family	Species	% RA	IUCN Status
Cyprinidae	<i>Cabdio Jaya</i>	0.28	LC
	<i>Barilius bendelisis</i>	24.44	LC
	<i>Barilius vagra</i>	1.11	LC
	<i>Devario assamensis</i>	0.28	VU
	<i>Tor putitora</i>	0.28	EN
	<i>Puntius sophore</i>	5.00	LC
	<i>Cyprinion semiplotum</i>	1.11	VU
	<i>Cirrhinus reba</i>	0.28	LC
	<i>Labeo pangusia</i>	0.83	NT
	<i>Bangana dero</i>	0.55	LC
	<i>Schizothorax richardsonii</i>	3.33	VU
	<i>Crossochilus latius</i>	1.11	LC
	<i>Garra gotyla</i>	10.00	LC
<i>Garra sp. 1</i>	0.55	NA	
<i>Garra sp. 2</i>	0.83	NA	
Psilorhynchidae	<i>Psilorhynchus homaloptera</i>	1.66	LC
	<i>Psilorhynchus arunachalensis</i>	0.55	DD
Nemacheilidae	<i>Paracanthocobitis botia</i>	5.00	LC
	<i>Schistura sp</i>	0.28	NA
	<i>Physoschistura dikrongensis</i>	0.28	NE
Cobitidae	<i>Aborichthys kempfi</i>	1.11	NT
	<i>Aborichthys elongates</i>	5.00	LC
	<i>Botia dario</i>	1.39	LC
	<i>Botia rostrata</i>	1.39	VU
	<i>Lepidocephalichthys guntea</i>	5.28	LC
	<i>Canthophrys gongota</i>	0.28	LC
	Bagridae	<i>Mystus cavasius</i>	1.67
<i>Mystus tengara</i>		0.28	LC
<i>Mystus bleekeri</i>		0.83	LC
<i>Mystus sp</i>		1.94	NA
	<i>Mystus dibrugarensis</i>	0.28	LC
Olyridae	<i>Olyra longicaudata</i>	8.05	LC
Siluridae	<i>Pterocryptis gangelica</i>	1.67	DD
Amblycipitidae	<i>Amblyceps sp</i>	0.28	NA
Sisoridae	<i>Gogangra viridescens</i>	0.55	LC
	<i>Nangra assamensis</i>	0.55	LC
	<i>Gagata cenia</i>	1.11	LC
Erethistidae	<i>Erethistes pussilus</i>	0.28	LC
	<i>Hara jerdoni</i>	0.28	LC
	<i>Hara hara</i>	0.83	LC
	<i>Hara sp</i>	0.28	NA
Chacidae	<i>Chaca Chaca</i>	0.28	LC
Mastacembelidae	<i>Mastacembelus armatus</i>	0.55	LC
	<i>Macroganathus aral</i>	0.28	LC
Badidae	<i>Badis sp1</i>	0.83	NA
	<i>Badis sp2</i>	0.55	NA
	<i>Badis sp3</i>	0.28	NA
Nandidae	<i>Nandus nandus</i>	0.28	LC
Cichlidae	<i>Oreochromis mossambicus</i>	2.50	NT
Anabantidae	<i>Anabas testudineus</i>	0.28	DD
Osphronemidae	<i>Trichogaster fasciata</i>	2.22	LC
Tetraodontidae	<i>Leiodon cutcutia</i>	0.83	LC

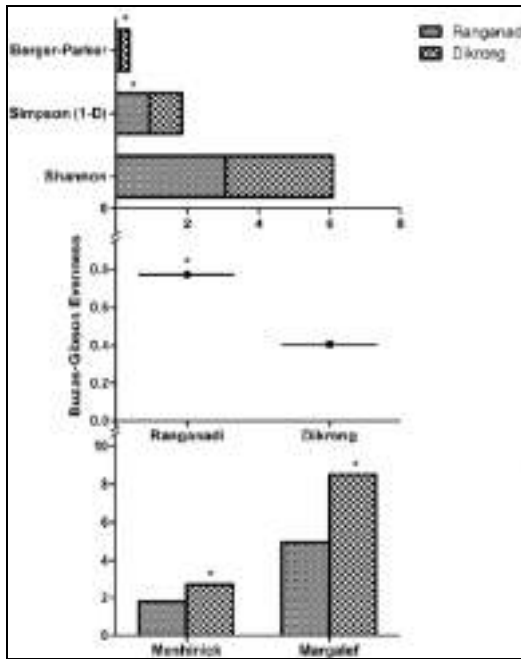
Note: NT= Nearly Threatened, LC= Least Concerned, VU= Vulnerable, NA= Not Applicable, DD= Data Deficient, EN= Endangered

Table 2. The list of ornamental and potential ornamental fishes documented from Ranganadi River, Arunachal Pradesh, during study period (2012-2015) along with relative abundance (RA) and IUCN status ^[22].

Family	Species	%RA	IUCN Status
Cyprinidae	<i>Barilius bendelisis</i>	4.45	LC
	<i>Neolessochilus hexagenolepis</i>	0.41	NT
	<i>Oreochthys sp</i>	11.74	NA
	<i>Pethia chola</i>	6.48	LC
	<i>Labeo gonius</i>	4.45	LC
	<i>Labeo calbasu</i>	1.62	LC
	<i>Schizothorax sp</i>	2.02	NA
	<i>Crossochilus latius</i>	4.86	LC
	<i>Garra annandalei</i>	0.81	LC
	<i>Garra gotyla</i>	6.88	LC
	<i>Garra sp1</i>	1.62	NA
	<i>Garra sp2</i>	5.67	NA
	Psilorhynchidae	<i>Psilorhynchus homaloptera</i>	4.05
Nemacheilidae	<i>Aborichthys kempfi</i>	0.41	NT
Cobitidae	<i>Botia rostrata</i>	5.67	VU
Siluridae	<i>Ompok bimaculatus</i>	0.81	NT
Schilbeidae	<i>Ailia coila</i>	2.43	NT
Amblycipitidae	<i>Amblyceps apangi</i>	0.41	NT
Erethistidae	<i>Pseudolaguvia sp</i>	1.21	NA
Belonidae	<i>Xenentodon cancilla</i>	1.62	LC
Mastacembelidae	<i>Macroganathus aral</i>	1.62	LC
	<i>Macroganathus pancalus</i>	2.83	LC
	<i>Mastacembelus armatus</i>	1.62	LC
Gobiidae	<i>Glossogobius giuris</i>	3.64	LC
Chandidae	<i>Chanda nama</i>	4.86	LC
	<i>Pseudambassis ranga</i>	2.43	LC
	<i>Parambassis sp</i>	4.45	NA
Osphronemidae	<i>Trichogaster chuna</i>	5.67	LC
Channidae	<i>Channa gachua</i>	5.26	LC

Note: NT= Nearly Threatened, LC= Least Concerned, VU= Vulnerable, NA= Not Applicable

Most interestingly it is notable that the species compositions are fairly different in the two river basins. When compared, only ten species (*Barilius bendelisis*, *Garra gotyla*, *Garra sp.1*, *Garra sp.2*, *Psilorhynchus homaloptera*, *Aborichthys kempfi*, *Botia rostrata*, *Crossochilus latius*, *Mastacembelus armatus*, *Macroganathus aral*) are found to be common in the samples of both river basins. The fact may be explained from the topographic point of view that the Ranganadi river basin is situated at a relatively higher altitude than the Dikrong basin. The differences in altitudes, physiographic factors, and climatic variables like temperature and rainfall being the determinants of distribution and species richness might have caused variation in the composition of fish species in the two river basins ^[17-19]. Our hypothesis that the species composition between the two river basins should be dissimilar is proved by statistical analyses ($p < 0.0001$, one way PERMANOVA, Bonferroni corrected pair-wise permutation test). Assessment of diversity reveals that Simpson and Berger-Parker indices are significantly higher in Ranganadi (Fig. 2). The third diversity index, *i.e.* Shannon-Wiener index does not show any significant variation between the two data sets, though the mean value is higher in Ranganadi (Fig. 2) confirming Ranganadi to be more diverse than the Dikrong basin.



Note: Asterisk (*) indicates significant difference.

Fig. 2: Measured diversity indices for the fishes sampled from the Dikrong and Ranganadi river basins of Arunachal Pradesh (2012-2015).

On the contrary, Buzas-Gibson evenness index proves that there is more chance to get individuals of same species in two subsequent samplings in Ranganadi (Fig. 2) indicating the possibility of more species richness in the Dikrong river. Menhinick and Margalef indices prove the above inference that Dikrong basin is more species rich (Fig. 2). However, the findings are confusing because one river basin is more diverse, while the other one has more species richness. In a similar situation Kindt and others suggest that studies attempting to compare different communities should not rely on only a single diversity index, or a combination of several indices; but should use techniques that are developed for diversity ordering, such as the Renyi diversity profile which is one of the most useful tools for comparing diversity [20]. Accordingly, the exponential of Renyi index has been used with various alpha values to construct OF diversity profiles of the river basins under this study. The finding shows that the profiles intersect each other, instead of one being constantly higher (Fig. 3). As stated by Hammer and colleagues where the profiles cross each other at any point, they are non-comparable in terms of diversity [21]. Hence it is ultimately concluded that the estimated OF diversity of the two river basins is non-comparable. In other words, both the communities are diverse in terms of OF in their own ways.

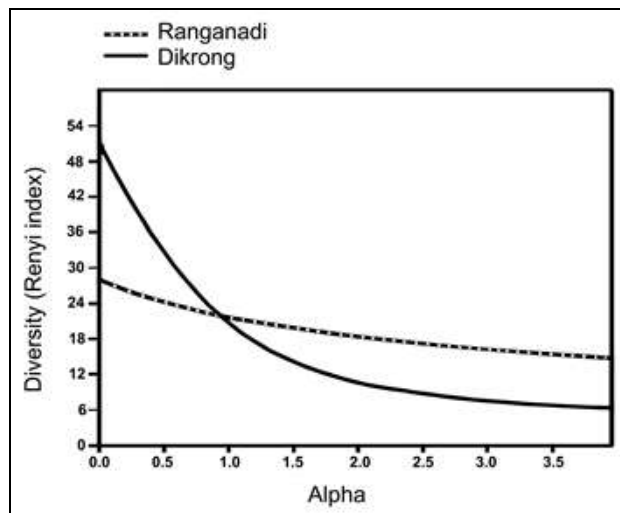


Fig 3: The diversity profile of the fishes sampled from Dikrong and Ranganadi river basins of Arunachal Pradesh (2012-2015).

4. Conclusion

The present study carried out in Dikrong and Ranganadi river basins of Arunachal Pradesh reveals the status of piscatorial diversity in a comparative manner. Similarly, other river basins of this state should also be explored in future. The compilation of such information would be of immense value practically to generate river-wise list of POF of the state. The indigenous people should also be made aware of the prospect of Of business and particularly the importance of fish conservation at least through the practice of fish culture and artificial propagation. The applicability of the finding as a whole being a fundamental ecological knowledge will cater the sustainable R & D activities as well as policy decisions for the highly sensitive mountain ecosystems and human welfare.

5. Acknowledgements

The authors are thankful to Department of Biotechnology (DBT), Govt. of India, for providing financial support under the project F. No. BT/382/NE/TBP/2012. Dr. Kenjum Bagra is specially acknowledged for his extensive field studies in the

Dikrong and Ranganadi river basins, and for generating raw data used for the present work.

6. References

1. Khomdram B, Dhar B, Ghosh SK. Jiribam, the Ornamental Fishes' Hot Spot Zone Of Manipur, India. *Journal of Agriculture and Veterinary Science*. 2014; 7(1):85-91.
2. Acharjee BK, Das M, Borah P, Purkayastha J. Ichthyofaunal Diversity of Dhansiri River, Dimapur, Nagaland, India. *Check List*. 2012; 8(6):1163-1165.
3. Tesia C, Bordoloi S. Ichthyofaunal Diversity of Charju River, Tirap District, Arunachal Pradesh, India. *Asian Journal of Experimental Biological Sciences*. 2012; 3(1):82-86.
4. Sharma N, Shukla SP. *Geography and Development of Hill Areas: A Case Study of Arunachal Pradesh*. Edn 1, Mittal Publications, New Delhi. 1992, 1-154.
5. Das DN, Laskar BA, Sarma D, Tyagi BC. Scope for mountain fishery based eco-tourism in Arunachal

- Pradesh: Potential and recommendations. In: Mahanta PC, Sarma D (Eds) Coldwater fisheries management. Edn 1, ICAR, Bimtal. 2010, 285-296.
6. Paul B, Chanda A. Indigenous Ornamental Fish Faunal Diversity in PaschimMedinipur, West Bengal, India. International Research Journal of Biological Sciences. 2014; 3(6):94-100.
 7. Alexandar R, Sankar SR. Diversity of Fish Fauna and Their Threats in Ousteri Lake, Puducherry, India. World Journal of Zoology. 2013; 8(2):154-158.
 8. Raj JP, Bleher H, Syed T, Gore S. Conservation status and threats of the ichthyofauna in the North region of the Western Ghats. International Journal of Fisheries and Aquatic Studies. 2014; 1(3):189-193.
 9. Jha KK, Chetri K, Ghosh TK, Jha VC. Distribution of an endangered fish species, *Chaca chaca* (Ham.-Buch.), in Arunachal Pradesh, India: A biodiversity hot spot. International Journal of Biology and Biological Sciences. 2014; 3(3):23-30.
 10. Mishra C, Dutta A. A new bird species from Eastern Himalayan Arunachal Pradesh—India's Biological Frontier. Current Science. 2007; 92(9):1205-1206.
 11. Bagra K, Das DN. Fish Diversity of River Siyom of Arunachal Pradesh, India: A case study. Our Nature. 2010; 8(X):164-169.
 12. Vishwanath W, Lakra WS, Sarkar UK. Fishes of North East India. Edn 1, NBFGR, Lucknow. 2007, 1-264.
 13. Catalog of fishes: Genera, species, references, 2015. <http://research.calacademy.org/research/ichthyology/catalog/fishcatmain.asp>
 14. Vijayasree TS, Radhakrishnan MV. Fish Diversity of Kuttanad River, Kerala State. International Journal of Fisheries and Aquatic Studies. 2014; 1(6):55-58.
 15. Atkore VM, Sivakumar K, Johnsingh AJT. Patterns of diversity and conservation status of freshwater fishes in the tributaries of River Ramganga in the Shiwaliks of the Western Himalaya. Current Science. 2011; 100(5):731-736.
 16. Saxena P, Saxena KK. Fish-diversity in relation to physico-chemical characteristics of river Devaha, District Pilibhit (U.P.) India. G- Journal of Environmental Science and Technology. 2014; 1(6):134-138.
 17. Ellu G, Obua J. Tree condition and natural regeneration in disturbed sites of Bwindi Impenetrable forest national park, South-western Uganda. Tropical Ecology. 2005; 46(1):99-111.
 18. Kharkwal G, Mehrotra P, Rawat YS, Pangtey YPS. Phytodiversity and growth form in relation to altitudinal gradient in the Central Himalayan (Kumaun) region of India. Current Science. 2005; 89(5):873-878.
 19. Sharma CM, Suyal S, Gairola S, Ghildiyal SK. Species richness and diversity along an altitudinal gradient in moist temperate forest of Garhwal Himalaya. Journal of American Science. 2009; 5(5):119-128.
 20. Kindt R, Dammev P, Simons AJ. Tree diversity in western Kenya: using profiles to characterise richness and evenness. Biodiversity and Conservation. 2006; 15(4):1253-1270.
 21. Hammer Ø, Harper DAT, Ryan PD. PAST: Paleontological Statistics Software Package for Education and Data Analysis. Palaeontologia Electronica. 2001; 4(1):1-9.
 22. The IUCN Red List of Threatened Species, 2016. Version 2015-4. <http://www.iucnredlist.org>

UGC Approved Journal No – 40957

(IIJIF) Impact Factor- 4.172

Regd. No. : 1687-2006-2007

ISSN 0974 - 7648

JIGYASA

AN INTERDISCIPLINARY PEER REVIEWED
REFEREED RESEARCH JOURNAL

Chief Editor : *Indukant Dixit*

Executive Editor : *Shashi Bhushan Poddar*

Editor
Reeta Yadav

Volume 11

September 2018

No. IX

Published by

PODDAR FOUNDATION

Taranagar Colony

Chhittupur, BHU, Varanasi

www.jigyasabhu.blogspot.com

E-mail : jigyasabhu@gmail.com

Mob. 9415390515, 0542 2366370

- **Modeling Financial Assets Returns Using Arma And Garch Tpyes Models In India** 569-591
Nehkholen Haokip, Assistant Professor, Department of Economics, Shyamal College (Eve.), University of Delhi
Anil Kumar Singh, Assistant Professor, Department of Economics, Shyamal College (Eve.), University of Delhi
- **Role of Social Support in Mental Health among Female Teachers** 592-606
Dr. Avantika Singh, Post-Doctoral Fellow, Ramveer Rananjay P.G. College, Amethi, Uttar Pradesh
Dr. Angad Singh, Associate Professor, Ramveer Rananjay P.G. College, Amethi, Uttar Pradesh
- **The Fitzgerald Enquiry and the Queensland Parliament** 607-617
Suman Mishra, Associate Professor, Department of Political Science, NSN PG College, Lucknow
- **A Study on Government Programmes for Safe Drinking Water in India** 618-621
Dr. Farida Ahmed, Assistant Professor, Department of Home Science, Faculty of Science, University of Allahabad, Allahabad, U.P.
Dr. Mohd. Zafarullah, Guest Faculty, Mahatma Gandhi Kashi Vidhyapith, Varanasi, U.P.
- **Agricultural Land Use Patterns in Jaunpur District: A Geographical Analysis** 622-638
Jyoti Kumar & A. R. Siddiqui
- **Kierkegaard's Subjective Truth** 639-643
Prasit Ranjan Ghosh, Associate Professor (Philosophy), Achhruram Memorial College, Jhalda, Purulia, West Bengal, A P.H.D. Research Scholar, Ranchi University, Ranchi

Kierkegaard's Subjective Truth

Prasit Ranjan Ghosh*

"Existentialism" is a Franco-German philosophy of the present century. It emphasizes the importance of human reality and its freedom in the scheme of things. The subjective human reality is completely free and is not even self-determined. The non-human objective is determined. Freedom of man implies that initially man is 'nothing' and he is to become what he is to be in future. Man is continuously projected in future and gathers 'essences' at will. With free being therefore "existence precedes essence" Objects of the nonhuman world cannot rise above their essences' and essence precedes existence" in their ease. Man realizes his freedom in anguish- the dreaded anxiety for shouldering the responsibility of his choice. He cannot rely upon anything external like society, state or god, and in free choice of values, an individual is alone. The existentialists are anti-intellectualists, emotional and great humanistic thinkers.

There are three theist existentialists named Kierkegaard, Jaspers and Marcel, Existentialism" is a recently developed Franco-German philosophical doctrine which emphasises subjective, human consciousness and its total freedom as central in the whole scheme of things. The origin of this philosophy is said to lie in the thoughts of a Danish philosopher of the 19th Century, Soren Kierkegaard. Jean Paul Sartre and Gabriel Marcel of France and Martin Heidegger and Karl Jaspers of Germany are important contemporary representatives of existentialism, though these thinkers have little in common, Sartre and Heidegger are atheistic Marcel and Jaspers are theistic existentialists. Heidegger even refuses to be called an Existentialist' of these J.P. Sartre is the most outstanding although he never develops existentialism as a systematic philosophy and the doctrine is already showing signs of disintegration. The Anglo-American philosopher of the present century, with their anti-metaphysical outlook, avoid existentialism as poison, existentialists, on the other hand, remains wholly indifferent to British Philosophical and there is

* Associate Professor (Philosophy), Achharam Memorial College, Jhalda, Purulia, West Bengal. A P.H.D Research Scholar, Ranchi University, Ranchi

no cordial communication between philosophers on the two sides of the English Channel.

S. Kierkegaard declared that "Truth is subjective". Philosophical truths relate to the subjective, human consciousness and to the world as it appears to that personal consciousness.

Natural sciences distinguished from philosophy, establish impersonal, objective truths and laws that govern facts which are independent of human mind.

Kierkegaard coming after Hegel, totally rejects theory of Absolute or Objective Idealism

Such idealism conceives human spirit as an incomplete manifestation of the objective, absolute spirit, infinite. Human spirit here is conceived as utterly dependent on the objective spirit which is impersonal. Man loses his freedom and independence and is only a shadow of the Absolute, according to Hegel. Kierkegaard rejects such dependence of finite or infinite and declares the freedom of human consciousness.

Natural Sciences do not take any account of personal human consciousness and its total freedom in knowledge and action. They rather ignore 'the subjective'. Freedom in choice of ends and ideals to the pursued in life is conspicuous in human existence. Though this is absent in impersonal nature, Existence or being in general is therefore divided by Sartre into two distinct groups (a) *Pour soi* or being-for-itself i.e. personal, human, subjective existence of consciousness which is essentially self-conscious; and (b) *En soi* or being-in-itself i.e. the being of non-human world. Sciences including psychology give us a knowledge of this *en soi* or of impersonal nature, which knowledge is abstract and universal.

Philosophy cannot add anything new to this abstract knowledge; but philosophy in showing the limits of scientific knowledge goes beyond. Jaspers calls this the "transcendence of Consciousness."

The *pour soi*, on which philosophy concentrates, is free and though this truth has been emphasised by other faith, but is hortative in asking us to realize our freedom. 'Philosophy' is the study of consciousness and self-consciousness of man which is synonymous with freedom of choice. Natural Sciences study the animal and the material world in so far as these are causally determined. Thus the contemporary existentialists follow their 'father' Soren Kierkegaard, in holding that philosophical truth is 'subjective'.

One of the salient features of 'existentialism' is the doctrine that human consciousness or being-for-itself is completely free in selecting his own, personal, mode of life. This individual consciousness of man is called 'Dasein' by Heidegger. 'Dasein' is particular mode of being and is not conceived as an example of the universal 'Humanity'. Individual man is completely alone in selecting future possibilities and is hemmed-in by 'nothingness' on all sides. He can rely upon nothing for his choices and is, perhaps, like a solitary 'window-less monad' of Leibniz. Man is therefore, oppressed by a sense of Himalayan responsibility for his choices.

This anguish or dread forces him to shift his own responsibility on others or on objective moral or political laws; as if we followed the moral or social imperatives in our will and as if we were not to be blamed for our choices. This is done, in insecurity and helplessness, for the sake of getting relief from anxiety. A free act implies some uncertainty or future eventualities, which is beyond logical comprehension.

Freedom knows no law and it cannot be made an object of scientific research.

The other salient feature of 'existentialism' is the doctrine of existence. Particularly being for itself (*pour-soi*), precedes essence. It is wrong, according to this theory, to take personal consciousness as an instance of some universal idea or concept i.e. of some 'essence'. In this sense existentialism is wholly opposed to Platonism. Plato thought that the particular objects of experience of a certain class have only a secondary being as instances of some universal 'essence' or other. 'Humanity', for example, is the essence or defining character of all men, without which a thing cannot be called a 'man'. Similarly, 'horseness' is the essence of all horses, 'treeness' of all trees. Each essence is indestructible and eternal whereas the particular exemplifications are non-eternal. An individual man is born and perishes in time, but the character 'Humanity' goes on forever.

The particular instances are appearances of the eternal essences, which latter, being permanent, are eternally real. Intellect or reason alone can comprehend the eternal universal or essences and the objects of sense-perception are mere appearances. Essences, being eternal, precede the origination of particulars or existence according to Plato or idealists in general.

Existentialism totally rejects the above view and holds that "Existence precedes essence". If the defining character is to be real it can be so by characterizing some particular existent.

This is clearly shown by Sartre with reference to being-for-itself. Human consciousness as a pure possibility is originally 'nothing', i.e. has no character or essence. It is thrown on the road of time and perpetually projects itself in future in order to realize its possibilities. The existence of particular consciousness cannot be denied without self-contradiction (of Descartes *cogito ergo sum*). This existence is originally pure, without any character- a 'that' without any 'what'. It is like Locke's *tabula-rasa* a blank sheet. Sartre says, 'Man first is and only afterwards he is this or that- man must create for himself his own essence'. In respect of personal consciousness, therefore, existence precedes essence, I perpetually create and recreate myself freely, now as a student, now as a grocer, now as a dancer, now as an advocate, now as a novelist and so on, 'Being a grocer', 'being a dancer' are characters or essences which I realize in order to be something.

Yet no essence is permanently branded in me and I am always free to realise my alternative possibilities. A man who has practiced robbery for a long time can suddenly turn a new life and become a saint. The thug Ratnakara becomes the sage Valmiki. For Sartre, as well as for Heidegger, human consciousness is a being with un-realised potential-a possibility. Such is 'For-itself' or *Pour Soi*. 'En soi' or 'In-itself' is solid, a massive, and is entirely actual. The future of a solid material thing is entirely determined by its essence. An ink-well is ink-well always and does not become anything else. There is no becoming for tables and chairs. But human beings perpetually create themselves in whatever way they choose. Man has no invariant essence that limits his freedom. Because I have no permanent character, I am basically 'nothing'. It is concluded that Kierkegaard's firmed beliefs, Strong emotion of pure subjectivity or reality or truth discovers existence of God in real existence of life. This realization of infinite God is real existence according to him. Kierkegaard feels deeply inwardness of individual's concrete consciousness. No objectivity is found in that individual's inwardness. Here the subjectivity is revealed.

To reveal subjectivity, a deep passion is raised at the background for presenting deep inwardness. Thus, he realized completely at this situation, the subjectivity is truth. This truth

reaches him to God through the individual's Journey of concrete consciousness.

Thus Kierkegaard grasped the existence of God through religious faith.

References :

1. Soren Kierkegaard, *Concluding Unscientific Postscript*, trns. D.F. Strawson, Princeton, University press 1941.
2. Soren Kierkegaard, translation, by Walter Lowrie, *The Concept of Dread*, University press, 1944
3. Jean paul Sartre, tr, by Hazel Barnes, *Being and Nothingness : An Essay on Phenomenological Ontology*, New Year, philosophical Library, 1956
4. Jean paul Sartre, tr, by Philip Mairet, *Existentialism and Humanism*, Methuen and Co.Ltd, London, 1957
5. J. Macquiritie, *Existentialism*, Penguin Books, 1972.
6. Mary Warnock, *Existentialism* Oxford University, 1979.
7. Karl Jaspers, *The Perennial scope of Philosophy*- Archon Book 1949.
8. Gabriel Marcel, *On the Ontological Mystery*.
9. Martin Heidegger, trs. By J. Macquiritie & F.S. Robinson, *Being and Times*- New York, Harper and Row, 1962.

UGC Approved Journal No – 40957

(IJIF) Impact Factor- 4.172

Regd. No. : 1687-2006-2007

ISSN 0974 - 7648

JIGYASA

AN INTERDISCIPLINARY PEER REVIEWED
REFEREED RESEARCH JOURNAL

Chief Editor : *Indukant Dixit*

Executive Editor : *Shashi Bhushan Poddar*

Editor
Reeta Yadav

Volume 13

June 2019

No. VI

Published by

PODDAR FOUNDATION

Taranagar Colony

Chhittupur, BHU, Varanasi

www.jigyasabhu.blogspot.com

www.jigyasabhu.com

E-mail : jigyasabhu@gmail.com

Mob. 9415390515, 0542 2366370

- **Impact of Pollution on Natural Water Resource
(The case of Sultanpur city)** 233-237
Dr. Nasreen, Associate professor, Ganpath Sahai P.G.
College Sultanpur U.P.
- **Role of Nutrition in Degenerative Diseases** 238-245
Akriti Mishra, Assistant Professor, Shri Agrasen
Kanya P.G. College, Varanasi
- **Differential Thermal Analysis (DTA) Technique
for Determination of Various Physical and
Chemical Changes Occurring In The Material
sample** 246-248
Jyotsna Srivastava, Department of Physics, R.S.K.D.
P.G. College, Jaunpur
Tushar Kant Srivastava, Department of Physics,
Udai Pratap (Autonomous) College, Varanasi
- **The Most Neglected Right : Rights of Street
Children** 249-256
Dr. Akash, Assistant Professor, Department of
Political Science, Sri Agrasen Kanya PG College,
Varanasi (U.P.)
- **Habitual life of house Sparrow** 257-261
Dr. Pushpa choudhary, Asst. Professor, Zoology
department, A.N.D.N.N.M.M.V Kanpur
- **An appraisal of Wall painting of Kushi
(Varanasi)** 262-269
Ravindra Kumar, Associate Professor (Officiating),
Delhi Institute of Heritage Research and Management,
New Delhi-110067
- **Doctrine of Consciousness in Advaita Vadanta
and Existentialism** 270-273
Prasit Ranjan Ghosh, Associate Professor, H.O.D
and Department of Philosophy, Achharam, Memorial
College, Jhalda, Purulia, West Bengal

Doctrine of Consciousness in Advaita Vedanta and Existentialism

Prasit Ranjan Ghosh*

Advaita Vedanta describes the absolute reality of the richest metaphysics and the absolute knowledge of Brahman. Brahman is the pure consciousness. In this context the theistic existentialism studies about self-consciousness of an individual man as existence only. So, both philosophies with their epistemology and metaphysics discuss about consciousness as well as self-consciousness. This paper shows that its comparative studies critically. Kierkegaard, the founder of existentialism admitted subjective truth only. Not only that, he objects to Hegel's objective truth and he admitted existence of God in his experience through religious believes as experience. He defined that truth is subjective truth. That is why he refused Hegel's objective truth which is the basis of his philosophy. He realized that God is the subject. Samkara's Advaita Philosophy showed that the subject of an individual self individual's self is consciousness as self-consciousness too. Samkara's Advaita philosophy deals with consciousness including to self-consciousness. He formulated that, Jiva = Consciousness = Brahma = Ultimate reality = Ultimate Existence. So, Samkara's Advaita philosophy and Existentialism discovered that existence is self-consciousness which is consciousness innature.

Key words : Consciousness, Self-Consciousness, Intentionality, Subjectivity, Freedom, Choice, Existence, Self and Individual man

This paper discusses comparative studies between Samkara's Advaita Vedanta and Theistic Existentialism in such a way that consciousness is the prime subject matter of both philosophies of Samkara's Advaita Vedanta and Theistic Existentialism. At present consciousness is the important interdisciplinary subject. Mahabakya of Aitareya Upanishad in the Rig-Veda is 'Prajnanam Brahma.'

This is the universal philosophy as the complete description of all. It can be said that the law of everything is Brahman. We cannot think of prajnanam as the Absolute knowledge which is without the existence of an Individual Self. And it is clear that an

* Associate Professor, H.O.D and Department of Philosophy, Achhruram, Memorial College, Jhalda, Purulia, West Bengal

Individual self implies an Individual man. So an equation can be formed from the Mahabakya of Prajnaram Brahma is as follows.

Prajna = The Absolute Consciousness = An Individual Jiva = An Individual Self = An Individual Man.

So the description of a man, an Individual self is essentially Brahman. 'Brahma Veda Brahmaiva bhavati' (Mundaka Upanishad: 3/2/9). When an aspirant as an Individual man who intends eagerly to practice Brahavidya through Shrabana, Manan and Nididhyasan of Vedanta by Brahma Vicar and finally an Individual becomes Brahman, the absolute manifestation of a man.

The man as the omniscient or Brahman is the historic discovery forever. In Advaita Vedanta, Jiva, An Individual Self and Brahma as The Absolute Reality or Absolute Being. Jiva = An Individual Self = Brahman = The Absolute Reality = Akhandam (infinite) = Saccidanandam. According to Samkara, an Individual Self and Brahman are identical. Brahman is Saccidanandam which is the identical terms of sat (The Absolute Existence). Cit (The Absolute Consciousness) and the Ananda (The Absolute peace). So, we draw a law of everything from the Vedanta which is as follows. Sat = Cit = Ananda = Saccidananda = The Absolute Existence = The Absolute Consciousness = The Absolute Peace.

The above law which Vedanta states is the Blueprint of everything, the total description of all universes as whole.

So, it is clear that Vedanta declares the complete description of all. Everything is essentially consciousness. So, only and one thing is constant in the universe that is the pure consciousness. Samkara stated that all Vedas, Upanishads, The Gita as the essence of 'Kevala Advaita Vedanta' what he expressed all in a half sloka (half sentence) only. This follows as;

"Brahman Satya, Jagat Mithya, Jiva Brahmaiva napara". Brahman is the Truth, Jagat (Universe) is false and Jiva and Brahma (Individual man and The Absolute Consciousness are identical).

This means that Brahman (the Absolute Consciousness) is truth. Truth is eternal being. Jagat (Universe) is false. False means what is transient (Anitya) and the pure consciousness or the Absolute Consciousness as Brahman and Jiva (the Individual Self) are not different.

Truth is the eternal Being. The unchanged Universal Being forever. The Universal Being is the Absolute Reality, the pure consciousness. All names and forms are universes as the world. All changes are also included in names and forms.

All changes = All forms = The whole universe = Jagat = False. But essence of all or the fundamental base of all things for eternal is the unchanged eternal the absolute consciousness or Brahma. Prajna is the Absolute Knowledge which stands for Brahman. Here epistemology and Metaphysics are identical to each other.

Knowledge is consciousness. Experience is a form of consciousness. This is the unique description as well as law in Vedanta which describes the all universe vividly. Everything of the whole universe is described and defined with only and one eternal thing consciousness, Brahman. This is also concluded here that only one thing in universe as consciousness is the absolute free. So, Freedom = Consciousness, only Brahman, the pure consciousness is one and only controller of the universe. Consciousness or Brahman controls everything. Only and unique theory is absolutely free and this is essentially consciousness only. Advaita Vedanta discovers it in world. Brahman is Saccidananda or existence, consciousness as well as the absolute peace. So, freedom is identical to consciousness. The Being as Brahman or consciousness is free. Existence as Brahman is free. Brahman Exist freely forever. Vedanta proclaims that existence is consciousness. Existence is free.

According to Advaita Vedanta, Existence or Consciousness or The absolute peace or Brahman is free who controls all.

In Existentialism, Existence an essence is their main discursion. They discuss about Consciousness, Freedom, Individual man, Self-regulation. Actually those terms of existentialism are not new concepts. It is clear that self-contradiction is really false forever. Advaita Vedanta shows that Brahman as Existence or Consciousness or Peace is completely free from self-contradictory. So, it is clear that existence precedes essence follows self-contradictory is existentialism.

Vedanta shows that, Existence = Consciousness = Brahman = Essence. So, Existence precedes consciousness was self contradictory. Here existence is not consciousness is found is existentialism. But in Advaita Vedanta, Existence is Consciousness. Sat = Cit = Ananda = Saccidananda = Brahman.

So, Existence and consciousness are identical, they are not absolutely different but the same thing. Human being is consciousness. His goal is to become Brahman.

All Individual man as consciousness or self-consciousness (because self-consciousness is a form of the pure consciousness) are becoming to be Brahman.

This is a really man making process which Advaita Vedanta can be stated as process of attaining Brahma (Brahma Veda, Brahmaiva Bhavati) Pre-reflective consciousness and reflective consciousness are consciousness in nature. They are identical and non-dual. It is clear to state that consciousness is the Being and prior to all. That is why being is non-dual pure consciousness. The pure Consciousness is free from all.

So, Consciousness and Freedom are the same. Freedom means consciousness or self-consciousness. It can be concluded that consciousness is the Absolute Being - Freedom - Non dual - The Akhanda or The infinite Consciousness.

The logic is that only Ultimate thing as non-dual. Pervading all having eternal existence is consciousness. So, consciousness controls everything including all individual man. Only one thing exists as consciousness is free from all pluralities and differences.

References :

1. Swami Vireswarananda, Brahma Sutras, Advaita Ashrama
2. Samkaracarya, Panceikaranam, Udbodhan, Kolkata
3. Sri Sri Sadananda Yogindra, Vedantasar, B.K. Pal, Sanskrit Pustak Bhandar, Kolkata.
4. Aitareyo Upanishad
5. A critical study of Sartre's ontology of Consciousness, Burdwan University, Burdwan, 1978.
6. Soren Kierkegaard, Concluding unscientific postscript, Tran, D.Swenson, Princeton University Press, 1941.
7. Jean - Paul Sartre, Being and Nothingness, T.R. Hazel & E. Berne.

A critical study in the theory of Atomism of The Naya - Vaisesika philosophy

Prasit Ranjan Ghosh
Assistant Professor in Philosophy
Achhruram Memorial College, Jhalda,
District - Purulia
Pin - 723 202
W.B., India

ABSTRACT

The Naya - Vaisesika Philosophy proclaims that Paramanus are material cause of the world. Paramanus as atoms are the tiniest things of the world. Atoms or Paramanus are not divisible. They are absolutely undivided partless matter. They are non-conscious things. Though all paramanus are minutest but they are different both in quality and quantity. Each paramanu is compact. No empty space is found in a paramanu or in an atom. Atoms are eternal. They are indestructible. All paramanus are real things. The paramanus or atoms of the Naya-Vaisesika Philosophy are inactive and motionless. Only GOD produces motion in them and then they are combined in motion in creation. Existence of GOD is important in this system for the creation of the world with atoms. This paper shows that a critical study in the theory of Atomism of The Naya-Vaisesika Philosophy. Lastly a conclusion will be derived.

Keywords: Atom, Paramanu, motion, adrista, GOD, matter, energy, substance, guna, knowledge, omnipotent, omniscient, space, time and consciousness.

The Naya-Vaisesika Philosophy describes the world with pluralistic views. They admit that cause and effect are not same kind. Always effects are new kind. In creation of the world, GOD is the efficient cause but paramanus are material cause. GOD produces motion in all inactive atoms or paramanus. Paramanus or atoms are determined and controlled by GOD. Some Naiyayikas and Vaisesikas admit that - adrista are unseen cause which gives motion to motionless paramanus at the beginning of the world. But Adrista is a unconscious thing. An unconscious thing has no power to give motion in all eternally motionless atoms. This very function of the creation of the world is GOD's own activity. He has volition. He is omnipotent and hence only GOD giving motion in all paramanus. That is why all atoms are non-conscious thing but creation of the world is fully spiritual. GOD controls all paramanus in creation.

In Naya-Vaisesika philosophy, Akash, Drk (space), Kal (time), selves and individual minds are eternal and infinite. Out of nine Dravyas (substances), five are eternal, four are infinite and one mind is eternally tiny thing (anupariman). All paramanus of earth, water, fire and air are infinite and eternal. Four substance as Prithivi (earth), Apa (water), Tejas (fire) and Vayu (Air) are four bhutas as composite things. They are transient. Eternally indivisible paramanus of four kinds (earth, water, fire and vayu) unite by GOD's exerting motion. By the combination of atoms, all types of composite things are formed. All such compound things are made of eternally motionless paramanus of earth, water, fire and air.

Thus the Naya-Vaisesika system explain the whole universe with very nine substances (dravyas).

“The dravyas are nine in number, (i) ‘earth’ (prithivi), (ii) ‘Water’ (apa). (3) ‘fire’ (Tejas). (iv) ‘air’ (vayu), (v) akas. (vi) time (kala), (vii) space (dik), (viii) self (atman) and (ix) Manas (man) and they together with their various properties and relation explain the whole universe”¹.

The Naya-Vaisesika philosophy holds that all compound things have their parts according to the causality theory of the system, cause and effect are two new things. Effect is not inherent in its cause.

“Earth, water, fire and air are eternal as atoms and non-eternal as composite products. There are atoms of earth, water, fire and air. They are minutes and indivisible units of physical substances”²

Here it is clear that all things as living and non living things are really composite things are really composite things. To create such living things and non-living things as physical composite things are new things as effects. All effects are produced through theory of causality named Asatkaryavada by GOD as efficient cause and material cause of such four kinds paramanus or atoms.

All living things are produced by GOD with selves, minds, akas, space (dik), Time (kala) and four kinds atoms.

Before creation, GOD, selves, Akas, space (dik), Time (kal), four kinds of eternal paramanus and minds are present at the rest. No motion exists in the universe. The whole universe is at the rest with such nine substances at the beginning of the creation according to the Naya-Vaisesika philosophy.

“The vaisesika maintains that a dyad (dvyanuka) is produced by conjunction of two atoms, which are active or moving. The motion of the atoms is produced by GOD”³.

GOD controls the physical world with his moral order. So mechanical law of atoms are always under control and direction of GOD himself. He governs the universe.

Earlier Vaisesikas introduces the concept of ADRISTA as the “unknown cause” or ‘Unexplained Nature”.

“Adrasta (lit. unseen) stands for “unknown cause” or “unexplained nature” in the earlier Vaisesika writers”⁴

Later Vaisesik writers admit that adrasta is the unconscious agent. So they admit that GOD as the pure consciousness be the efficient cause of the nature.

Udayana admit that GOD is the source of motion as unmoved eternal reality. “GOD is the creator of motion which is the cause of conjunction of the atoms into dyads. A dyad is produced by two atoms, the material cause, their conjunction, the non-inherent cause and the agency of GOD, the efficient cause”⁵.

GOD controls the Adrasta as the unseen cause. Adrasta is also unconscious. Though all atoms are unconscious as material things. But they do not themselves more and unite themselves in bigger magnitude in the creation of the world.

So the omniscient and omnipotent GOD controls all such atoms and Adrasta too. “He is guided by the law of Karma representing the unseen power of merits and demerits. The unseen power is unintelligent and needs GOD as the supervisor and the controller”⁶.

A system for the conjunction of atoms are found in the Naya-Vaisesika. Two unconscious and eternal atoms are joined with the help of GOD. GOD exerts motion in atoms. In this stage, only two paramanus are joined and called as Dvyanuk. Dvyanuk is unperceived. After creating of Dvyanuk, three moving dvyanuks (dyad) are combined and a triad named tryanuk is formed. Tryanuk is perceptible. Caturanuka (a quartad) is formed when four triads (tryanuks) are together combined.

“A quartrad (caturanuk) is produced by the conjunction of four triads, which are active. The quartrads are combined into larger and larger composite substances. The qualities of the composite products are produced by those of component atoms, which are their inheritent cause.”⁷

When matter is divided, its measurement is reduced. The process of division of things ends to paramonus which have parts but not nothingness. So the process of division ends at the atoms, otherwise infinite regress is found. To avoid infinite regress, the Naya-Vaisesika admit that every material things are composed of minutest things which are eternally partless and we call them paramanus. Thus Naiyayikas and Vaisesikas admits the existance of paramanus. They show that all paramanus of a mustard seed is less than the all paramanus of mountain. It is possible due to the existence of partless atoms which are present in them. A master seed is a part of a living plant. It is a body of the living plant. So all bodies of living things are also composed of atom according to the Naya-Vaisesika philosophy. “If all substances were endlessly divisible into an infinite number of parts, the there would be no difference in the magnitude of things. And a mountain and a mustard seed would be of equal dimension. So we must admit that atoms are the minutest parts of composite substances which are partless and indivisible.”⁸

The system holds that all composite things have their parts according to the causality theory of the Naya-Vaisesika philosophy. All compound are made of eternally partless atoms. The features of all compound things are production and destruction. All galaxies, stars planets, living things, non-living things and all components of environment are composed of atoms or paramanus.

The Naya-Vaisesika does not admit completely materialism. The system of Indian philosophy admits spiritualism as the prime guiding principle by which atomism is fully controlled. The Naya-Vaisesika's GOD is the pure consciousness as the absolute knowledge. So GOD is the omniscient. The Naya-Vaisesika's GOD does not create eternal space, eternal time, infinite dik (space), minds selves and all four kinds of paramanus. GOD operates paramanus and produces motion in paramanus to move for the construction of all composite things.

“The Vaisesika Atomism is not materialistic because the vaisesika school admits the reality of the spiritual substances - souls and GOD - and also admits the Law of Karma.”⁹

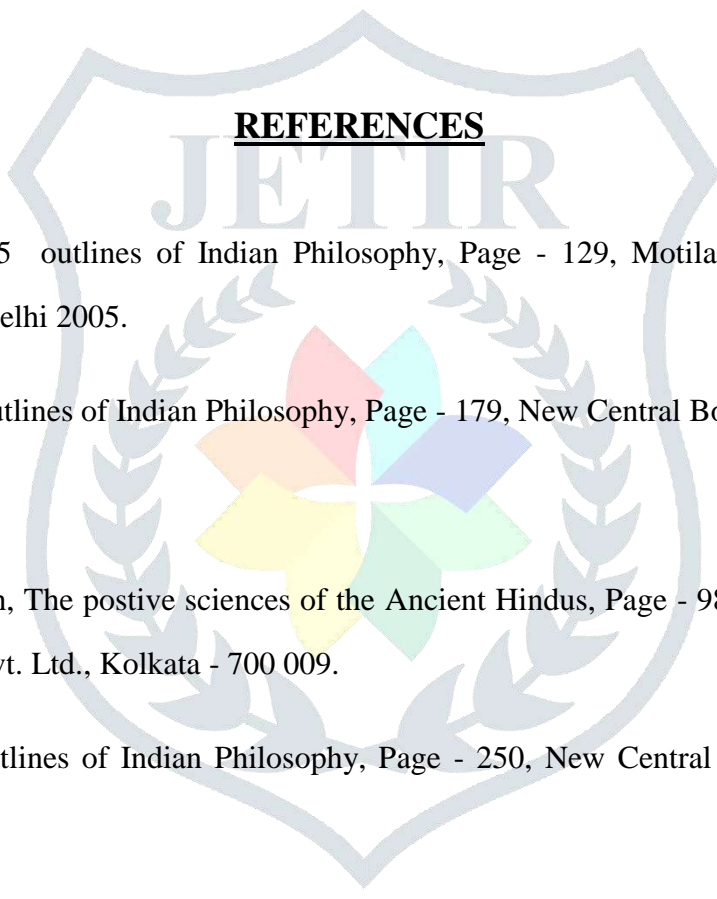
Vaisesika atomism agrees with Greek atomism of Leucippus and Democritus about atoms having indivisible, partless, imperceptible, material and eternal. They admit that atom are material too. But Greek philosophers admit only quantitative or numerical differences in atoms. But the Naya-Vaisesika hold both quantitative and qualitative differences in atoms. The atoms of earth, water, fire and air possesses different qualities or gunas. The Greek atomists admit that motion is inherent in atoms. But the Naya-Vaisesika admits that no motion is present in atoms. Motion is spiritual according the Naya-Vaisesika system, but Greek atomists and all scientists including physicists admit that motion is material as well as mechanical and physical.

But old Indian philosophy urges that all universe is at rest at the beginning of universe. No motion implies the completely absence of Force, energy, attraction, repulsion and conjunction. In a word, no motion, no creation.

But the Naya-Vaisesika shows that consciousness produces motion for creation. Only consciousness produces motion in atoms.

Now I conclude in the research paper that the efficient cause, GOD is the omnipotent and omniscient. Only GOD's knowledge unite two atoms as dvyanuka or dyad at the beginning creation. GOD also produce motion in motionless atoms to combine dvyanuk which is also unperceived to us. So GOD as the only omnipotent and omniscient gives motion in atoms to combine atoms and He has knowledge only to unite atoms. The omniscient and the omnipotent GOD implies the pure consciousness. The pure consciousness as GOD exerts motion and gives his knowledge to combine atoms. Then the creation begins. To begin the creation of the world, GOD's exerting motion and His knowledge is necessary. Otherwise eternally motionless atoms remains forever without creation. This is logical and unique model of the universe by the Naya-Vaisesika system.

REFERENCES

- 
- The logo for JETIR (Journal of Emerging Technologies and Innovative Research) is a shield-shaped emblem. It features a central five-petaled flower with petals in red, cyan, purple, yellow, and green. The flower is surrounded by a laurel wreath. The word 'JETIR' is written in large, light blue, serif capital letters across the top of the shield.
- [1.] Hiriyanna, M.2005 outlines of Indian Philosophy, Page - 129, Motilal Banarasidass Publishers Private Limited, Delhi 2005.
- [2.] Sinha Jadunath, outlines of Indian Philosophy, Page - 179, New Central Book Agency, Cal-9, 1992.
- [3.] Ibial, Page - 179
- [4.] Seal Brajendranath, The postive sciences of the Ancient Hindus, Page - 98, Debajyoti Datta, Shishu Sahitya Samsad Pvt. Ltd., Kolkata - 700 009.
- [5.] Sinha,Jadunath outlines of Indian Philosophy, Page - 250, New Central Book Agency, Calcutta - 700009, 1992.
- [6.] Sharma,Chandradhar A critical survey of Indian Philosophy, Page - 185, Motilal Banarasidass Publishers Private Limited, Delhi 2009.
- [7.] Sinha Jadunath Sinha, outlines of Indian Philosophy, Page - 179, New Central Book Agency, Cal-9, 1992.
- [8.] Idib, 180
- [9.] Sharma Chandradhar, A critical survey of Indian Philosophy, Page - 185, Motilal Banarasidass Publishers Private Limited, Delhi 2009.

Groundwater Contamination in Singur Block, West Bengal

Dr. Sharmistha Mukherjee

Assistant Professor

Achhruram Memorial College, Jhalda, Purulia

And

Rittika Ghosh

Abstract

Being an idiosyncratic element water support all forms of life. So, we need to be concerned about this precious natural resource as it can be remaining same as it was before. Water has a unique chemical property due to its polarity and hydrogen bonds which means it is able to absorb or suspended many different compounds (WHO,2007), thus, in nature, water is not pure as it acquires contaminants from its surrounding and those arising from humans and animals as well as other biological activities. Contamination of groundwater, either from anthropogenic or natural sources with several social impacts, has now turned to be a major environmental concern in different countries of the world. Millions of people are hanging on groundwater containing elevated level of various contaminants for drinking water purpose. Nine districts of West Bengal are under the virulent effect of this heavy metal. Several lithological and stratigraphic studies revealed the stratigraphic position and the possibility of arsenic contamination in the lower gangetic delta region (Mondal. V. & Adhikari. R., 2017). This talks about the various harmful contaminants that their impacts. A number of different thematic maps have been created to show the status of groundwater contamination by various contaminants in Singur block. The paper also tries to find out the locational distribution and pattern of groundwater contamination through landuse analysis and many groundwater features in Singur Block of West Bengal.

Keywords

Groundwater, Bacteriological, Escherichia-coli, pneumoconiosis, choroiditis, siderosis

Introduction

Groundwater contamination occurs when man-made products such as chemicals get into the groundwater and cause it to become unsafe and unfit for human use. Materials from the land's surface can move through the soil and end up in the groundwater. For example, pesticides and fertilizers can find their way into groundwater supplies over time. Road salt, toxic substances from mining sites, and used motor oil also may seep into groundwater. In addition, it is possible for untreated waste from septic tanks and toxic chemicals from underground storage tanks and leaky landfills to contaminate groundwater. Natural groundwater contamination by various contaminant and the sufferings of people as a result, has become crucial water quality problem in many parts of the world. It has been recognized that as contaminated ground water used for irrigation may pose an equally serious health hazard to people eating food from the irrigated crops and that as accumulating in irrigated soil poses a serious threat to sustainable agriculture in affected areas. Groundwater plays an important role as a source of drinking water for many rural and urban families. Though groundwater is less susceptible rather than surface water bodies still it is contaminated while rainwater infiltrates through soil strata. Drinking water derived from the contaminated sources cause serious health issues to humans and also to the animals. Iron is an important part of hemoglobin but absorption of excess iron in drinking water may cause conjunctivitis, retinitis if it contacts and remain in the tissue. If we take excess arsenic in drinking water it can create serious health issues such as gastrointestinal, cardiovascular problem, hematological effects, dermal effects, carcinogenic effects etc. Chemical and bacteriological contamination leads to skin problems, nausea, vomiting, diarrhea etc. The present study reviews the status and the impacts of various groundwater contaminants such as iron, arsenic and others. This report reviews on

the status of contamination of Singur block based on National rural drinking water programme report data. Sample data has been also collected from the affected areas to analyze its impact. So, further study is very much essential.

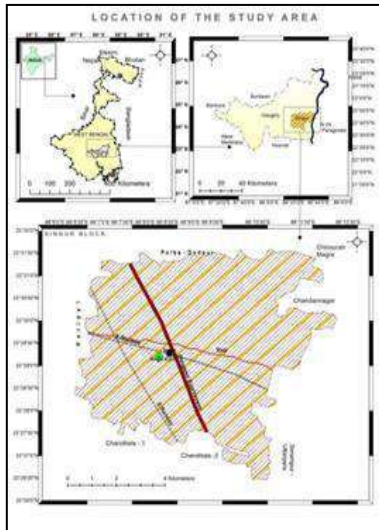
Literature review

Groundwater occurrence studies shows that the pathogenic viruses and bacteria can occur in groundwater sources and that people may become ill due to exposure to contaminated ground water. Pathogens found in groundwater sources may include enteric viruses and enteric bacterial pathogens such as Escherichia-coli (E-coli), salmonella etc. (www.epa.gov/safewater, july2007). Underground water in many regions of the world is contaminated with various harmful contaminants. Therefore, review of the available literature focuses on adverse effects of various contaminants. The effect of drinking contaminated water can be much more serious, however in India, “37.7% million Indians are affected by waterborne diseases annually” and 1.5 million children are estimated to die of diarrhea alone”. These staggering statistics are particularly caused by the lack of hygienic condition. According to them, “approximately 88% of India’s total disease load is due to lack of clean water and sanitation and improper management of solid and liquid waste [US EPA, 1999 a, b]. Children, transient and the elderly are such populations because of potentially high risk of dehydration from diarrhea that may be caused by high levels of sulfate in drinking water [www.epa.gov/safewater, July 2007]. Groundwater occurrence studies and outbreak data show that pathogenic viruses and bacteria can occur in groundwater sources and that people may become ill due to exposure to contaminated ground water. Pathogens found in groundwater sources may include enteric viruses and enteric bacterial pathogens such as Escherichia Coli, Salmonella etc. Groundwater is vulnerable to contamination by anthropological activities. Chongming and Jingjie,2001 indicated in their paper that groundwater overexploitation has induced serious environmental problems such as land subsidence and groundwater quality degradation. M. C. Kundu et al. (2007), stated that The NO₃-N content in groundwater also varied significantly in different blocks of the Hooghly district, the magnitude being 0.01 to 4.56 $\mu\text{g mL}^{-1}$ with mean value 0.67 $\mu\text{g mL}^{-1}$. The concentration of NO₃-N decreased with increasing depth of the wells. Singur have comparatively high concentration of NO₃ in their groundwater in this district. Kundu & Mandal, (2008), showed that the average Fluoride in the groundwater varied little in different blocks of the Hooghly district, it ranged from 0.01 to 1.18 $\mu\text{g mL}^{-1}$ with a mean value of 0.36 $\mu\text{g mL}^{-1}$, showing that water had Fluoride concentration above the permissible limit of 1.5 $\mu\text{g mL}^{-1}$ prescribed by the WHO (1997). The concentration of Fluoride in groundwater in this district from different sources ranged from 0.13 to 0.51, 0.01 to 1.18, 0.03 to 1.12, 0.07 to 0.70 and 0.05 to 1.00 $\mu\text{g mL}^{-1}$ for open well, TW, STW, MDTW and DTW respectively. Kuroda,2008 explained that groundwater in urban areas is sometimes contaminated with multiple contaminants at higher concentrations than in rural areas. Researcher has used water balance analysis, mass balance analysis, solute balance analysis. Groundwater contaminants in urban areas include inorganic, organic and microbial contaminants. Momodu and Anyakora,2010 studied that High concentration of these heavy metals and in some cases the levels were above WHO specified Maximum Contaminant level. A significant risk to this population given the toxicity of these metals and the fact that for many. Ghazavi and Ebrahimi,2015 showed in their paper how to estimate aquifer vulnerability by applying the DRASTIC and GOD models. The model also used interactive geodatabase, compile the geospatial data. Patra S. et al. (2015), stated that in the case of Singur, the pre-monsoon readings of SGWL in 2007 is 15.65 mbgl. In 2013 it was fallen down 18.55 mbgl. The rate of falling is 2.9 mbgl. The post monsoon readings of SGWL in 2007 is 11.490 mbgl and in 2013 is 12.2 mbgl resulting to the falling rate 0.71mbgl. gradual decline in pre-monsoon groundwater level also suggests that a high rate of groundwater withdrawal for domestic and agricultural and industrial purposes. Singur blocks have been categorized as Semi-critical Based on the stage of groundwater development and long term pre and post monsoon water level trend. Mitra, B. Lohochoudhury, (2019), stated that Human induced environmental pollution causes a lot of damage to our environment because humans pollute the surface environment and this pollution affects the groundwater, for example, the use of chemical pesticides, polluted running water, and industrial effluent. In Hooghly district there are government negligence and lack of sustainable policies to support pro environmental human activities which may cause groundwater

pollution. Ghosh, Pal and Santra, 2019 revealed in their research paper through empirical methodology and interpolation approach how spatial mapping of seasonal and annual groundwater arsenic contamination can be done. Arsenic concentration value seasonally fluctuates irrespective of depth of tube well. They said that major cause is that during post-monsoon season the part of rain water percolates through soil grains. Average groundwater arsenic concentration is gradually increasing with the passage of time.

Location and Area

Singur is a census town in Ganga-Brahmaputra delta belt which contains arsenic metal in its soil strata, 34 km far away from Howrah city with the growing urbanization and increased use of groundwater. Rising and climbing withdrawal of groundwater is also positive here. To fulfill the needs and demands of the population



huge quantity of water withdraws for agriculture and other purposes. 16 blocks of Hugli district contain arsenic contaminated ground water above WHO guideline value ($10 \mu\text{g/L}$) and 11 blocks above standard value for arsenic in drinking water ($50 \mu\text{g/L}$) and Singur block is also in that list (School of Environmental Studies, JU). Iron in water is also another problem. The presence of iron in drinking water is objectionable for a number of reasons unrelated to health. Under pH conditions existing in drinking water supplies, ferrous salts are unstable and precipitate as insoluble ferric hydroxide, which settles out as rusty silt, such water tastes unpalatable, promotes the growth of iron bacteria and the silt gradually reduces the flow of water in the piping. It is located at $22^{\circ}81'N$, $88^{\circ}23'E$. It had an average elevation of 14 meters and is situated on the Ganges delta. The total area of Singur Community Development block is 155.99 Sq.km.

Fig 1: Location of the study area

Objectives

The main target of this study is to emphasize on various contaminants which are responsible for contaminating groundwater in Singur block. To fulfill this, target my objectives are as follows:

- 🔔 Providing land use pattern map
- 🔔 Providing an outlook of population status and its density and the trend of population growth
- 🔔 Gram Panchayat-wise analysis of various contaminants that are responsible for groundwater contamination in Singur block
- 🔔 The status of contamination through the thematic maps
- 🔔 Analysis of the shortcomings of risk to human health

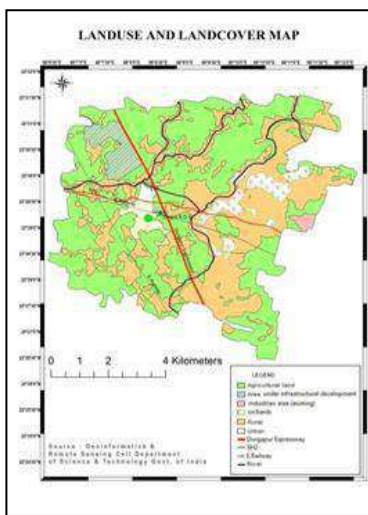
Database and Methodology

Population statics of Singur block have been represented using census data. The map of Singur block has been collected from the website of land reforms and that map has been prepared by Geoinformatics & Remote Sensing Cell Department of Science and Technology Gov. of West Bengal, Kolkata. After geo-referencing this map all the thematic representations have been prepared. The statistics to present the status of contamination have been collected from the website of National Rural Drinking Water Programme and the arsenic data has been collected from the website of School of Environmental Studies, Jadavpur University. To check the reality and impacts of the contaminated groundwater primary samples are also collected. Census data, secondary data related to the major problems, maps and various literatures related to this topic are collected in the pre-field session. Then obtained information is integrated using special database system (GIS) and with the help of GIS software ArcGIS.10 all the thematic representation is done.

Problems

In most developing countries the primary risk to human health is due to bacteriologically contaminated drinking water which leads to flulike symptoms. The effect of drinking contaminated drinking water can be much more serious, however in India, 37.7 million Indians are affected by waterborne diseases annually and 1.5 million children are estimated to die of diarrhea alone. This is caused because of lack of hygienic condition (Ministry of Rural Development). Rapid growth of settlement to provide shelter to the population leads to unhygienic circumstances and improper sanitation and waste management leads to such above mentioned problems. The major problems are described below:

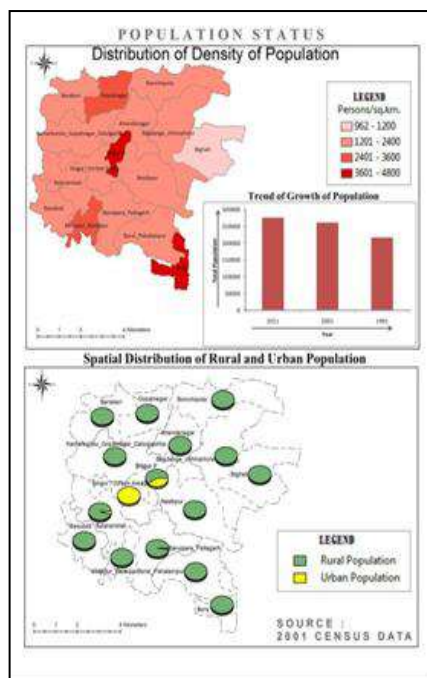
1. Landuse Pattern



In the fig 2 we can see the maximum portion of the land is agricultural land. Percentage of multicrop land is greater than the single crop land. In the middle section of the map we can see Saraswati River flowing north to south while in the west section of the map we can see Kana River which is a canal of Damodar is flowing west to north east. This canal, water bodies and also groundwater through hand pumps are used for irrigation in those fields. As in the maximum lands multi crops agricultural activities occur throughout the year. So, use of pesticide, herbicide, and insecticide is much more. This chemical infiltrate into groundwater or because of eating vegetables growing in those fields heavy metals are also transported in our body.

Fig 2: Landuse pattern in Singur Block, West Bengal

2. Population Status



As per the 2011 Census of India, Singur CD Block had a total population of 276,413, of which 223,951 were rural and 52,462 were urban. There were 140,334 (51%) males and 136,079 (50%) females. Population below 6 years was 24,276. Scheduled Castes numbered 47,037 (17.02%) and Scheduled Tribes numbered 4,069 (1.47%). As per the 2001 census, Singur block had a total population of 260,729, out of which 131,286 were males and 129,443 were females. Decadal growth in West Bengal was 17.84 per cent. Singur block registered a population growth of 1.65% during the 1991- 2001 decade. Decadal growth for Hooghly district was 15.72%. Thereafter, Singur experienced an accelerating growth rate. As the area is a plain land the distribution of population is also even. 21382 persons (as per 2011 census) are distributed over an area of 155.99sq km. with an average density 2008 persons per Sq km. Population density map has been prepared Gram Panchayat wise by mean standard deviation method. Another thematic map has been prepared to show spatial distribution of rural urban population (Fig. 3).

Fig 3: Population status in Singur Block, West Bengal

3. Groundwater Contamination

a) Iron in Drinking Water

Iron is believed to be the tenth most abundant element in the universe. Iron is a harmless, though sometimes annoying element present in public and private water supplies. Iron can be found in meat, whole meal products and vegetables. The human body absorbs iron in animal products faster than iron in plant products. Iron is an essential part of hemoglobin; the red coloring agent of the blood that transports oxygen through our bodies. Iron may cause conjunctivitis, choroditis and retinitis if it contacts and remain in the tissues. Chronic inhalation of excessive concentration of iron oxides fumes or dusts may result in development of benign pneumoconiosis called siderosis, which is observable in x-ray change. Inhalation of excessive concentration of iron oxide may enhance the risk of lung cancer development in workers exposed to pulmonary carcinogens. Fig no 4 shows the concentration of iron in inside and outside habitations in each gram Panchayat of Singur block. Fig 4 shows the actual picture.

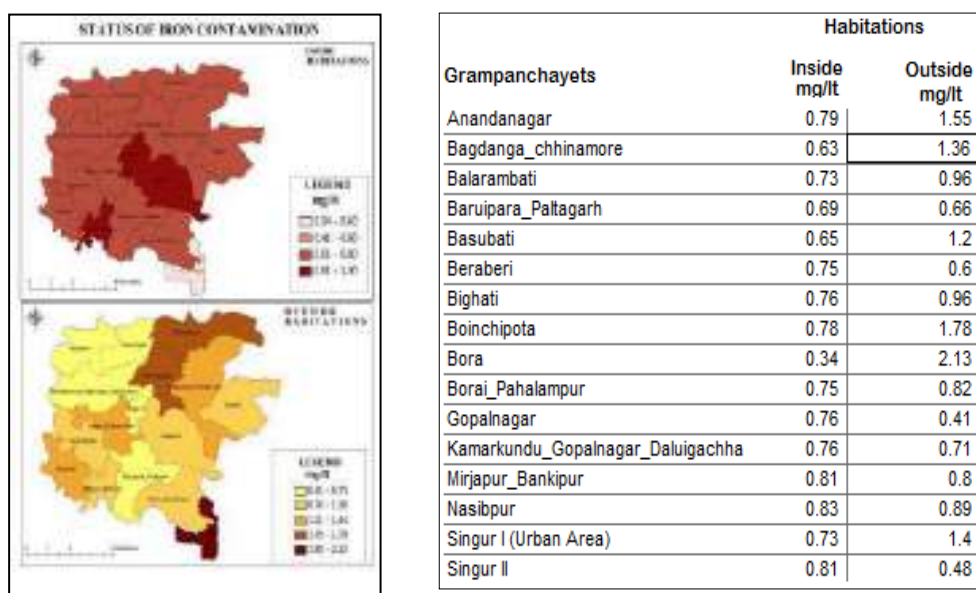
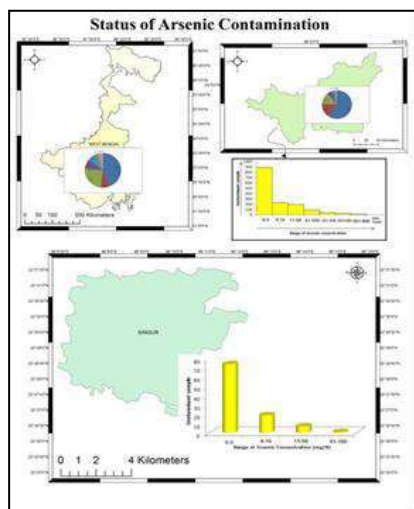


Fig 4: Iron status in Singur Block, West Bengal

b) Arsenic in Drinking Water



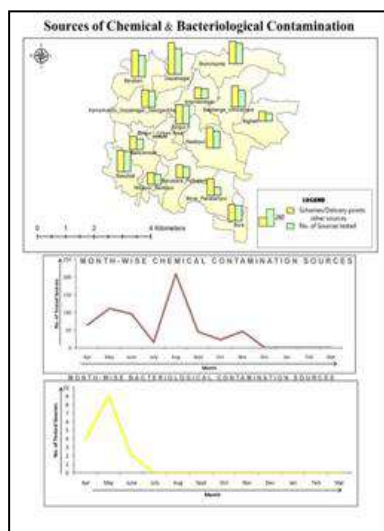
Arsenic is a metalloid element, having properties of both metals and nonmetals. Arsenic concentration in soil and in sedimentary rocks are generally higher than average in the earth's crust due to movement and accumulation of arsenic through weathering processes.



Source: School of Environmental studies, JU.

Intake of drinking water having arsenic concentration beyond the permissible limit of 0.05 mg/lit has deleterious effect on human health i.e. cardiovascular (heart failure) problem; gastrointestinal (burning lips, painful swallowing, thirst, nausea and severe abdominal colic); hematological effects (anemia and leucopenia); hepatic effects; neurological effects (headache, mental confusion, coma); dermal effects (skin disorder); carcinogenic effects (lung cancer) etc. Representative study has been shown in the fig (4) to show the status of arsenic in Singur block respect to Hooghly district and the state West Bengal.

Fig: 5 Arsenic status in Singur Block, West Bengal

c) Chemical and Bacteriological Contamination

Harmful chemicals can get into our body if you breathe, eat or drink them or if they are absorbed through your skin. Uses of fertilizers are also responsible for chemical (like nitrate which effects cardiovascular system) concentration in water. Bacteriologically contaminated drinking water leads to flu like symptoms such as nausea, vomiting and diarrhea. Children who suffer from frequent diarrhea are more vulnerable to malnutrition and opportunistic infections such as pneumonia. Fig. 6 show no. of sources and tested sources and also month-wise no of contaminated sources. Fig. 7 shows the status of chemical & bacteriological contamination

Fig 6: Source of chemical & bacteriological contamination

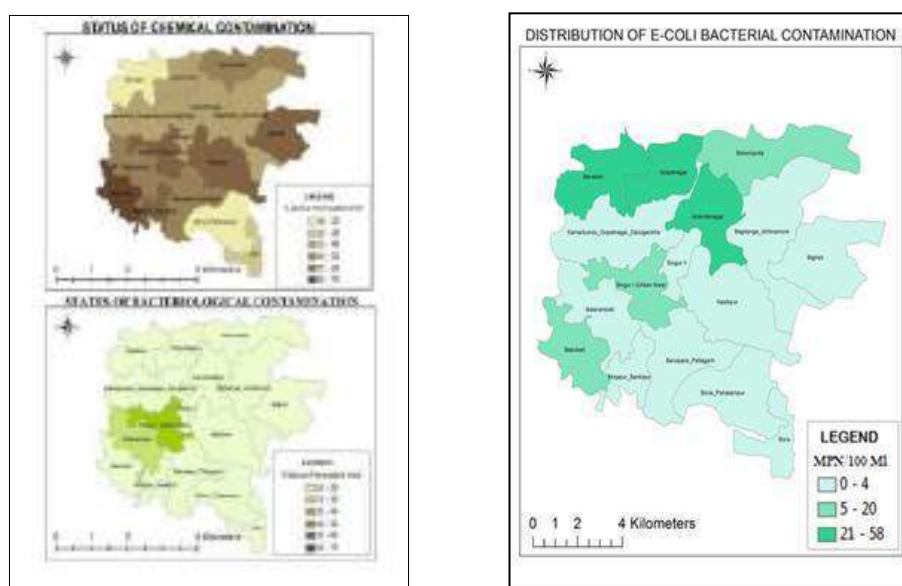


Fig 7: Status of chemical & bacteriological contamination Fig. 8 Status of E. coli in groundwater

d) E. coli contamination

Escherichia coli (commonly abbreviated E. coli) is a gram – negative, rod shaped bacterium of the genus Escherichia that is commonly found in the lower intestine of warm-blooded organisms (endotherms). The presence of E. coli in water is a strong indication of recent sewage or animal waste contamination. E. coli comes from human and animal wastes. During rainfall, snow melts or other precipitation, E. coli may be washed into streams, rivers, lakes or groundwater. When this water is used as source of drinking water and the water is not treated or inadequately treated, E. coli may end up in drinking water. Due to this bacterial infection often causes severe bloody diarrhea and abdominal cramps; sometimes the infection causes non-bloody diarrhea (Fig. 8).

Result

So, from the diagram we can clearly understand the status of contaminants in Singur block. Iron contamination is so high especially in outside habitations of all gram Panchayet. Percentages of samples with arsenic $>10\mu\text{g/l}$ in Singur is 7.9 and %of samples with arsenic $>50\mu\text{g/l}$ is 1.0. Though arsenic concentration is not that much huge in Singur still positive acceleration is not needed. Chemical, bacteriological and E. coli contamination is also high in some gram Panchayet of Singur block. As this block is turning to a town, urban population is also increasing. As rural population is maximum in this block, improper urinal facility, clumsy house condition is responsible for mixing of various contaminants in groundwater that comes from human waste. The usage of fertilizers and pesticides also responsible for groundwater contamination. Another reason of contamination is industrial waste and household waste. Primary survey has been done to show the availability of urinal facility, cleanliness of houses and also on the diseases (Fig. 9).

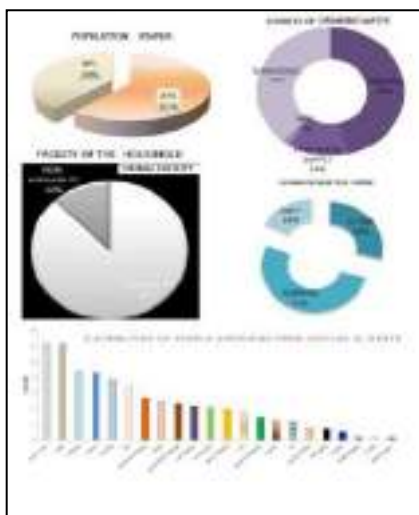


Fig 9: primary sample survey analysis

Conclusion

By drinking contaminated groundwater can causes serious health issues. An old Indian custom recommends that water should be drunk after it has been allowed to stand overnight and then filtered through a piece of fine cloth. But this procedure will not work where the contamination level is too high with various contaminants. From the above analysis of secondary data and primary sample survey it is clear that various blocks are contaminated even the urban areas. So, we should concern about such hazardous condition. There are various filters are available in the market for water purifying. Every family should use those filters. In now a day Reverse Osmosis is the best method of purifying contaminated water. And proper land use planning is also important as Singur is becoming a city. As water is similar to life we cannot ignore contaminated sources so extra study in it needed.

BIBLIOGRAPHY

Alex Colter, R. L. Mahler, Iron in drinking water, PNW589.

Armstrong, C.W., Stroube, R.B., Rubio, T., 1984. Outbreak of fatal arsenic poisoning caused by contaminated drinking water. Arch. Environ. Health 39: 276-279.

Adriano, D.C., 2001. Trace Elements in Terrestrial Environments: Biogeochemistry, Bioavailability and Risks of Metals, 2nd ed., Springer, New York.

Annual action plan on disaster management of Singur Community Development block (2014-15)

Bhattacharya, P., Frisbie, S.H., Smith, E., Naidu, R., Jacks, G., Sarkar, B., 2002. Arsenic in the environment: a global perspective. In: Sarkar B, editor. Handbook of heavy metals in the environment. New York: Marcell Dekker, 147-215.

Chatterjee, D., Islam, F.S., Gault, A.G., Boothman, C., Polya, D.A., Charnock, J.M., 2004. Role of metal-reducing bacteria in arsenic release from Bengal delta sediments. Nature 430: 68-71.

Chowdhury, T.R., Basu, G.K., Mandal, B.K., Biswas, B.K., Samanta, G., Chowdhury, U.K., 1999. Arsenic poisoning in the Ganges Delta. Nature 401: 545-6.

- Das, B., Rahman, M.M., Nayak, B., Pal, A., Chowdhury, U.K., Mukherjee, S.C., Saha, K.C., Pati, S., Quamruzzaman, Q., Chakraborti, D., 2009. Groundwater Arsenic Contamination, Its Health Effects and Approach for Mitigation in West Bengal, India and Bangladesh; *Water Qual. Expo. Health* 1: 5-21.
- D. Chakraborti, B. das, M. M. Rahman, U. k Chowdhury, B. Biwas, A.B Goswami, B. Nayak, A. Pal, M. K. Sengupta, S. Ahamed, A. Hossain, G. Basu, T. Roychow dhury, D. Das, 20 years study report on arsenic contamination in W.B, *Mol. Nutr. Food Res.* 2009,53, pp - 542-551
- Das, D., Samanta, G., Mondal, B.K., Chanda, C.R., Chowdhury, P.P., 1996. Arsenic in groundwater in six districts of West Bengal, India. *Environ. Geochem. Health* 18:5-15.
- Garai, R., Chakraborty, A.K., Dey, S.B., Saha, K.C., 1984. Chronic arsenic poisoning from tubewell water. *J. Ind. Med. Assoc.* 82: 34-35.
- Guha Mazumder, D.N., 2008. Chronic arsenic toxicity & human health. Review Article, *Indian J. Med. Res.* 128, October 2008, pp. 436-447.
- Hindmarsh, J.T. and McCurdy, R.F., 1986. Clinical and environmental aspects of arsenic toxicity. *CRC Crit. Rev. Clin. Lab. Sci.* (1986) 23: 315-347.
- Jain, C.K. and Ali, I., 2000. Arsenic: occurrence, toxicity and speciation techniques. *Water Res.* 34(17): 4304-4312.
- Kapaj, S., Peterson, H., Liber, K. and Bhattacharya, P., 2006. Human Health Effects From Chronic Arsenic Poisoning– A Review, *J. Environ. Sci. Health A*, 41: 2399-2428.
- Mazumder, D. N. G., Chakraborty, A. K., Ghose, A., Gupta, J. D., Chakraborty, D. P., Dey, S. B., and Chattopadhyay, N., 1988. Chronic arsenic toxicity from drinking tubewell water in rural West Bengal. *Bull. World Health Organ.* 66: 499-506.
- Saha, A.K., Chakraborti, C. and De, S., 1997. Studies of genesis of arsenic in groundwater in parts of West Bengal. *Indian Soc Earth Sci.* 24: 1-5.
- Saha, K. C., 2003. Review of arsenicosis in West Bengal, India: A clinical perspective. *Crit. Rev. Environ. Sci. Technol.* 33: 127-163.
- Smedley, P.L. and Kinniburgh, D.G., 2002. A review of the source, behaviour and distribution of arsenic in natural waters. *Appl. Geochem.* 17: 517-68.
- Statistical handbook of Hugli
- Various articles available on website
- Website of National Rural Drinking Water Programme (Indiawater.gov.in)
- Website of School of Environmental Studies, Jadavpur University
- www.epa.gov/safewater/afacto.html



Impact of Landform on Agricultural Land Use Pattern: A Case Study of Salda River Basin in Purulia District, West Bengal

Manoj Kumar Mahato^{1*} and N. C. Jana¹

¹*Department of Geography, The University of Burdwan, Burdwan,
West Bengal, India.*

Authors' contributions

This work was carried out in collaboration between both authors. Both authors read and approved the final manuscript.

Article Information

DOI: 10.9734/JGEESI/2019/v21i330125

Editor(s):

(1) Dr. Anthony R. Lupo, Professor, Department of Soil, Environmental, and Atmospheric Science, University of Missouri, Columbia, USA.

Reviewers:

(1) K. Adonia Kamukasa Bintoora, Nkumba University, Uganda.

(2) Riad Hosein, University of the West Indies, Trinidad.

(3) Wilfred Ochieng Omollo, Kisii University, Kenya.

Complete Peer review History: <http://www.sdiarticle3.com/review-history/49255>

Received 14 March 2019

Accepted 29 May 2019

Published 01 June 2019

Original Research Article

ABSTRACT

The present study is concerned with the analysis of landform characteristics of Salda River basin and its impact on agriculture land use pattern. The Salda basin is one of the sub-basins of Subarnarekha River, with diversified landscape pattern in the western part of Purulia district in West Bengal. This basin is constituted by plateaus, plains with terraces, scarps, inselbergs, which is evolved under polycyclic evolution. The development of polycyclic geomorphic processes in this basin is typified by diverse morphology and drainage, which largely influence the land use pattern in this area. These diverse landscape patterns indicate the interaction of litho-tectonic-structural and various geomorphic processes with recent human intervention.

The main objectives of the present study are to analyse the landforms characteristics, correlate them with land use and identify problems as well as prospects of agricultural land utilization. The entire study is based on both primary and secondary data. Extensive field survey has been conducted to collect primary information regarding terrain characteristics, micro relief, slope characteristics, hydrological attributes, soil character, natural vegetation, environmental hazards.

*Corresponding author: E-mail: mahatomanojkumar16@gmail.com;

The Survey of India topographical sheets, meteorological data, agricultural production data, land use and land cover data have been collected for the analysis of geomorphological characteristics, land classification, and agricultural land use pattern.

This study reflects the typical land characteristics of the fringe area of Chhotanagpur plateau, where some typical geomorphic attributes control the productivity of the land and also controls the socio-economic conditions of the local people. The present authors have tried to examine the typical geomorphic attributes and their effects on present productivity of the land in a micro level study, where agriculture is the main source of income.

Keywords: Landform; land use; agriculture; river; geomorphic; landscape pattern.

1. INTRODUCTION

A landform is a natural feature of the solid surface of the Earth or other planetary body. Landforms together make up a given terrain, and their arrangement in the landscape is known as topography. Land is a product of nature and three dimensional dynamic bodies. Actually the advent of civilization and their further development are intimately linked with the land [1]. It is well-known that the rational and sustainable use of land is one of the most important Indicators of economic growth [2]. Land use suitability analysis is the process of determining the suitability of a given land area for agricultural use [3]. Agricultural land use of any area is primarily dependent on the geomorphological characteristic [4]. Due to poor-socio-economic status, the land of the area under study is not being properly utilized.

The Salda basin is one of the sub-basins of Subarnarekha drainage basin, with diversified landscape pattern in the western part of Purulia district of west Bengal. Salda River and its tributaries drain a part of eastern fringe of Chhotanagpur plateau. The basin covers an area of about 94 sq. km or 23287 acres comprising portion of Jhalda-I Community Development Blocks of Purulia district in West Bengal. The Salda basin is constituted by plateaus, plains with terraces, scarps, inselbergs, which is evolved under polycyclic evolution. The development of polycyclic geomorphic processes in this basin typified by diverse morphology and drainage which are largely influenced the land use pattern in this area. Those diverse landscape patterns indicate the interaction of litho-tectonic-structural and various geomorphic processes with recent human intervention in the evolution. The present study is concerned with the analysis of landform characteristics of Salda River basin and their impacts on agricultural pattern in this area.

1.1 Objectives of the Study

The main objectives of the present study are:

1. To analyze the landform characteristics of the study area.
2. To make correlation between landform characteristics and agriculture.
3. To analyze the problems and prospects of agricultural land use.

2. METHODS AND MATERIALS

2.1 Area and Location

The Salda River basin is bounded by latitudes of 23°18'00" N to 23°22'30" N and longitudes of 85°53'30" E to 86°02'36" E. The basin includes a small tract of 48 mouzas of Jhalda-I Community Development Block of Purulia district. The basin with its great diversity both in the polycyclic landscape and the land use pattern extends through the undulating Archean plateau being delineated by 73 I/ 3, 73 E/15, numbers Survey of India maps.

It is a small tributary of Subarnarekha River. It originates from a dome-shaped hill (618 Metres above sea level), known as Pokhriya Pahar. It drains the undulating highland of Jhalda-I C. D. Block and flows westwards ultimately joins with Subarnarekha River near Magha mouza. The height of the confluence is 238 m.a.s.l. The geographical area of this basin is 94 sq. km or 23227.9 acres.

2.2 Methodological Flow Chart

To gain insight into the cropping pattern in Salda basin, the spatial distribution pattern of crops and their problems and prospects, crop diversification pattern are also analyzed. Such an exercise helps to identify the most important crops of the

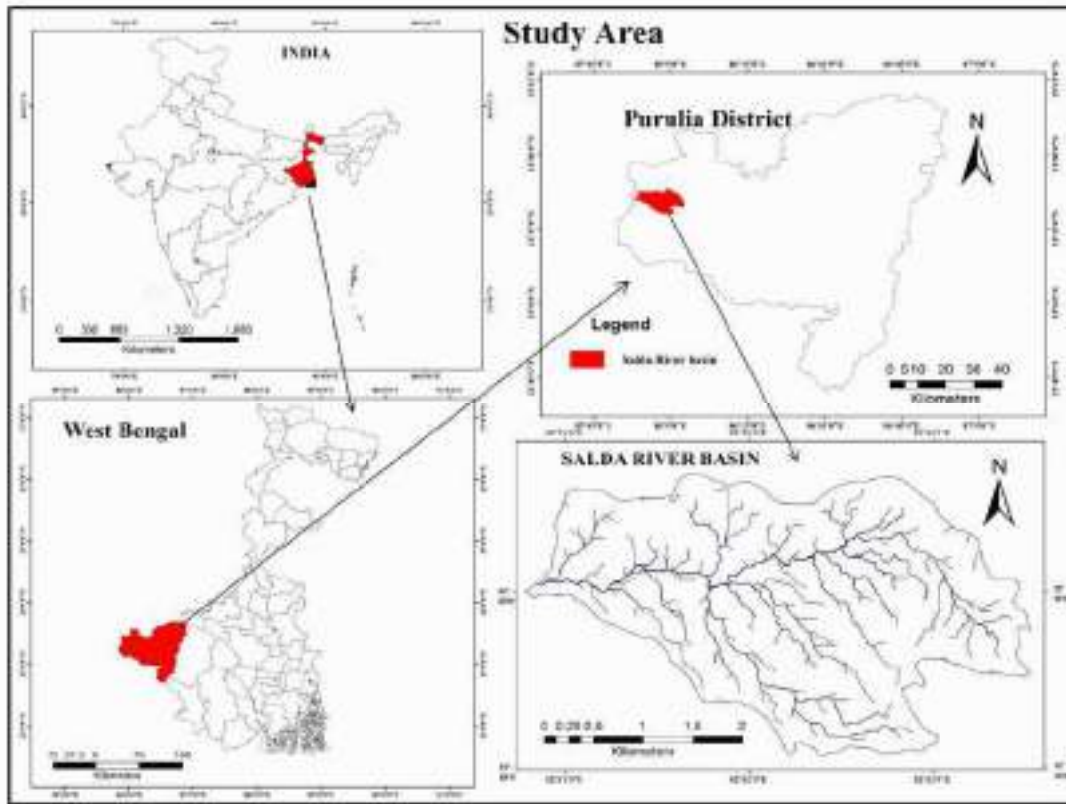


Fig. 1. Location of the study area

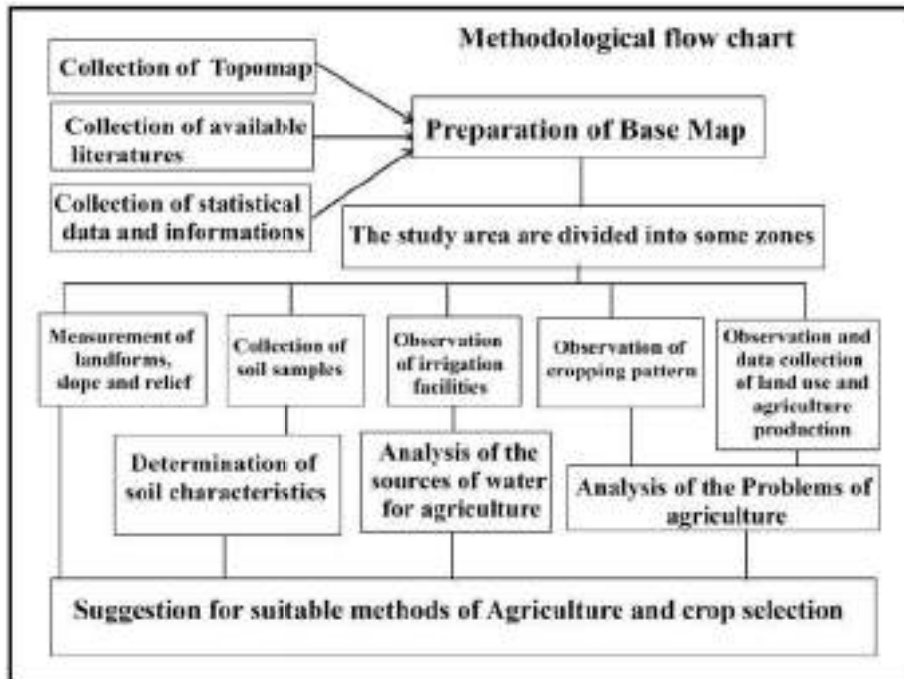


Chart 1. Methodological flow chart

region and their areal differentiation in the diversified agricultural economy of the basin.

The authors have converted all the production's units through "Google unit converter" for better understanding of the actual scenario regarding the status of production.

The variables have been calculated by using these following formulas-

* *Percentage of total area under crops = (particular crop coverage area / net cropped area) x 100*

** *Per Acre production = total particular cropped production of surveyed area / bearing cropped area.*

2.3 Data Collection

The entire study is based on both primary and secondary data, the detail are:

- Extensive field work was conducted to collect primary information regarding terrain characteristics, micro relief, slope characteristics, hydrological attributes, soil character, natural vegetation, environmental hazards etc.
- The Survey of India topographical sheets have provided an excellent base to understand the realistic geographical situation through the entire study.
- Meteorological Data have been collected from The Indian Meteorological Department, Kolkata.
- Land use and Land cover data have been collected directly from Cadastral maps and secondary data from Block Land Records Office, Jhalda-I and District Census Handbook Puruliya", Directorate of Census Operations West Bengal (Retrieved 6 December 2016).
- Agricultural production data were collected directly from household survey and District Statistical Handbook, Purulia 2013, 2014 and 2015.

2.4 Tectonic History

The study area is a part of the ancient (Pre-Cambrian) landmass of the Peninsular India, which have been stable and unaffected by any recent geological movement. The only structural disturbance in this part was vertical downward or upward movement. These structural upliftments are mainly due to tectonic disturbances [5].

Tectonically the study area is an old land surfaces with inselbergs prevail of eastern part of Ranchi penplain [6]. This old land surface suffered from tectonic disturbances due to drifting of Gondwana landmass during Permo-Carboniferous to Jurassic period. More recent evidences shows Tertiary upliftments occur in younger landscape. These Tertiary uplifts of this study area have acted for the side effects of the Himalayan orogeny. It seems possible that the epeirogenic uplift during the Tertiary period has been responsible for initiating successive cycles [7].

2.5 Geological Structure

The western part of Purulia is well marked by its varied geological formations. The study area is constituted by various stratigraphic units, ranging from the oldest Archaeans (Pre-cambrian) to the younger Tertiary - Quaternary formations [7]. To study the regional geological accounts of this areal units distribution of various rock groups, tectono-structural history is essential for the analysis of the terrain pattern. The role of these rock formations, including the structural and tectonic characteristics in the development of present multi-cyclic landscape patterns as well as the land use pattern is significant. The unequal uplifts or tilts in the different parts of the study area have also caused the development of striking differences in the topographic expressions in the different terrain units within the region.

The major part of the present area is occupied by various types of granitic rocks. Maximum area covered by Granite-gneiss and migmatite. Northern, north-eastern and south-eastern portion of the basin are dominated by Pre-Cambrian Intrusive Granite, basically Manbhumi Granite Intrusive body. Beside small tract of Dolerite is found in the central portion of area. The stratigraphic succession of various geological formations found in the Salda River basin is given in Fig. 2.

2.5.1 Granite gneiss and migmatite

These are the main rock types of the Salda River basin, which are well exposed in hilly terrains, where dome shaped hill, steep and smooth slopes formed. Mainly these areas have no vegetation cover, except the hill tops are covered by little vegetation. The flat ground of these rocky terrains is covered by laterite soil and alluvial outcrops. Alluvial outcrops of these rocks are found in the side of river and Jore.

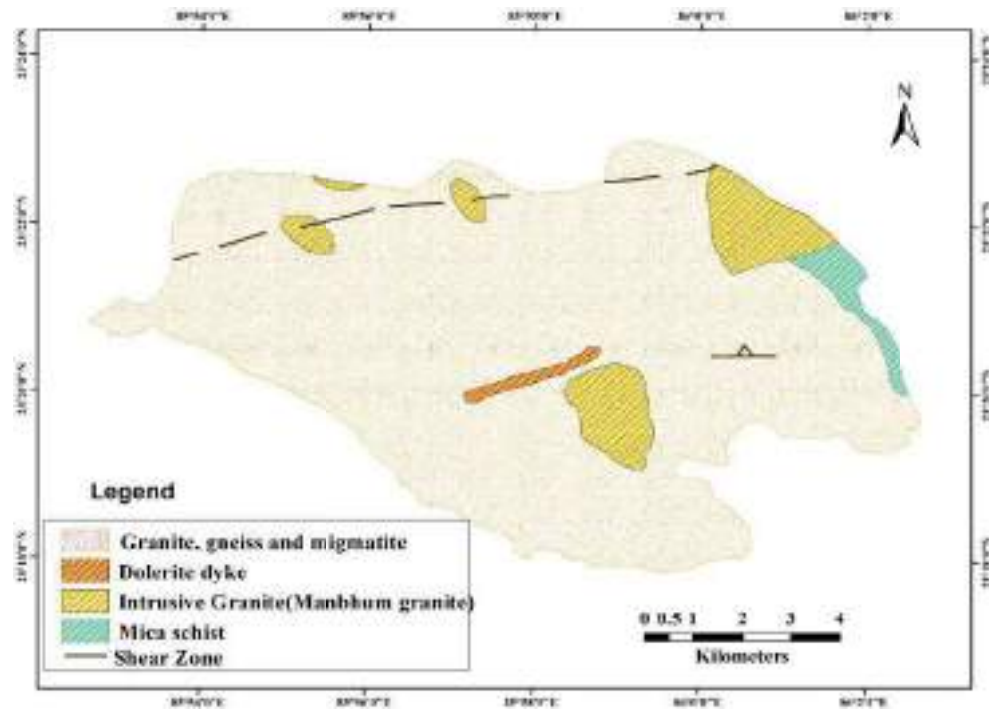


Fig. 2. Geological structure of Salda River basin
Source: Geological Map, published by Geological Survey of India, 2001

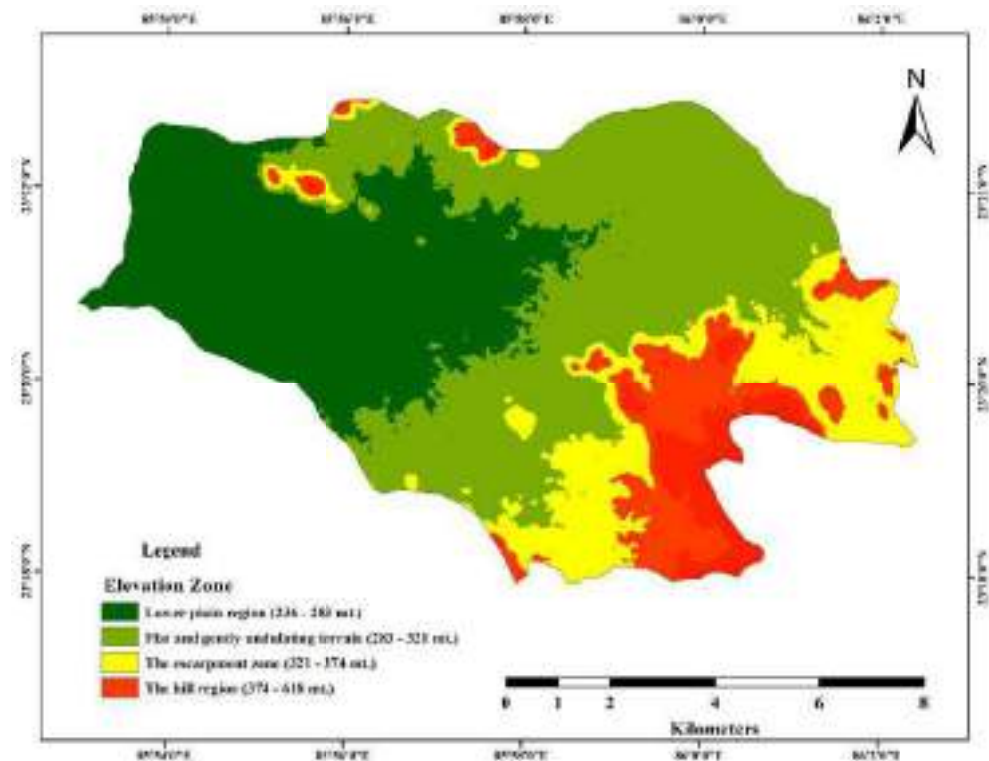


Fig. 3. Physiographic division of Salda River basin
Source: SRTM DEM, LISS-III



Plate no. 1. Dome shaped inselberge terrain at Pokhariya pahar

Source: Field survey on September, 2018



Plate no. 2. Flat and gently undulating Mahuldih mouza

Source: Field survey, September 2018

Table 1. Monthly average rainfall of study area during 1960 to 2010

Months	Jan.	Feb.	Mar.	Apr.	May.	Jun.	Jul.	Aug.	Sep.	Oct.	Nov.	Dec.	Annual
Rainfall In Mm	19.1	32.8	25.1	23.4	65	217.2	324.6	315.8	213.9	89.96	15	3.8	1353.46

Source: District Gazetteer, Purulia (1985) and Indian Meteorological Department, Kolkata

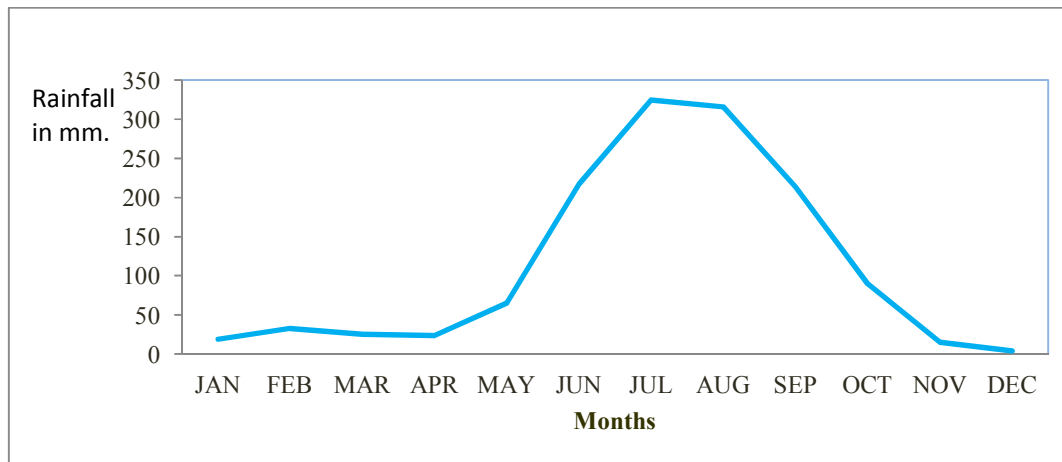


Fig. 4. Monthly average rainfall 1960 to 2010

Source: District Gazetteer, Purulia (1985) and Indian Meteorological Department, Kolkata

Most of these rocks are greatly heterogenetic in structure, texture and mineral composition. The granite-gneiss with good gneissose structure lying all over the area, but is abundant in the south. The gneissose structure is defined by alternate granulose and schistose bands of quartz and feldspars, and biotite and muscovite.

2.5.2 Intrusive granite

Granite intrusive body is very much common in the study area, which are collectively termed as

Manbhumi granite intrusion. Presently these are exposed by poly-cyclic erosional work. All of these intrusion bodies presently formed as a dome-shaped hill. Granite intrusions have sitting among the granite, gneiss and migmatite. It occupies in the hill area of south-eastern, eastern and north-western part, nearly Lagam-Iphurhatu Pahar (23°21'00" N, 86°1'30" E); Narahara Pahar under Mahakudar mouza (23°20'00" N; 85°59'30" E); Sikra Pahar under Mosina mouza(23°22'30" N; 85°57'26" E) and Bansa Pahar(23°22'00" N; 85°55'30" E).

Among them Bansa Pahar is completely barren and open rock masses are exposed as a hard rock body. It is located in the lower part of the basin, so its surrounding area is covered by laterite and alluvial soil. Although Lagam and Narahara Pahar are having vegetation cover but the slope of the hills are demarcated as a Manbhumi Igneous Intrusion. In present geological period Sikra Pahar shown as a form of batholith, where exfoliation is active as a weathering agent.

near Narahara Pahar Gotilwa to Tarhad. At Gotilwa to Tarhad the dolerite body runs almost E-W direction. Its length is approximately 2.8 km. The rock have medium grained and shows subophitic texture with lathes of plagioclase. Quartz and iron oxides are small proportions in this rock body under interstices portion.

Table 2. Range of rainfall (1960-2010)

Range in mm	No. of years
801- 900	1
901- 1000	0
1001- 1100	2
1101- 1200	10
1201- 1300	11
1301 – 1400	8
1401 – 1500	3
1501- 1600	7
1601- 1700	5
1701- 1800	1
1801-1900	2

Source: Indian Meteorological Department, Kolkata

2.6 Topographical Characteristics

Topographically this area is very much diversified with dome-shaped inselbergs, spurs, escarpments, undulating upland and erosional plain. Salda River Basin has different areas of elevations ranging from 238 meter to 618 meters. We can see the south-eastern part of the basin having an elevation 618 meter whereas the eastern part having an elevation 220 meter.

As a part of the Chhotanagpur Granite-gneiss tract, the Salda Basin did not experience any severe diastrophic disturbance in its long geological history, but it could not escape the impact of orogenic forces. The Salda Basin occupies the eastern part of the Pre-Cambrian Granite-gneiss tract. These tracts are very little disturbed and there are very few signs of structural disturbances throughout the basin.

2.5.3 Dolerite

Small intrusion of dolerite within the Granite gneiss are observed horizontally along the 23°20' N latitude extending 85°57'28" E to 85°59'00" E,

The physiographic divisions of the Salda River basin are: (i) The hill region, (ii) The escarpment zone, (iii) Flat and gently undulating terrain, (iv) Lower plain region.

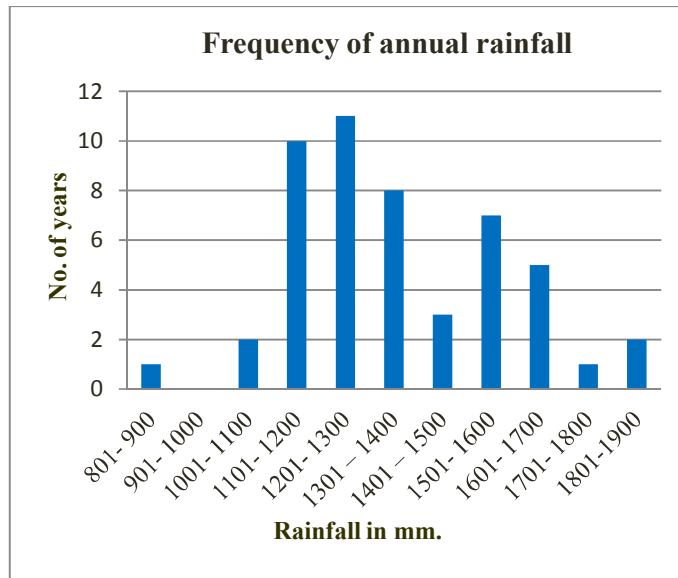


Fig. 5. Frequency of annual rainfall

Source: District Gazetteer, Purulia (1985) and Indian Meteorological Department, Kolkata

Table 3. Areas under different land classes (in 2007-2008)

Land classes	Area in acre	In percentage
Tikro	1240.59	5.34
Tarn	4258.56	18.32
Baidh	8926.85	30.05
Kanali	2759.94	11.87
Bahal	1345.90	5.79
Others	4755.16	28.61
Total area	23287.00	100.00

Source: Block Land Records Office, Jhalda-I

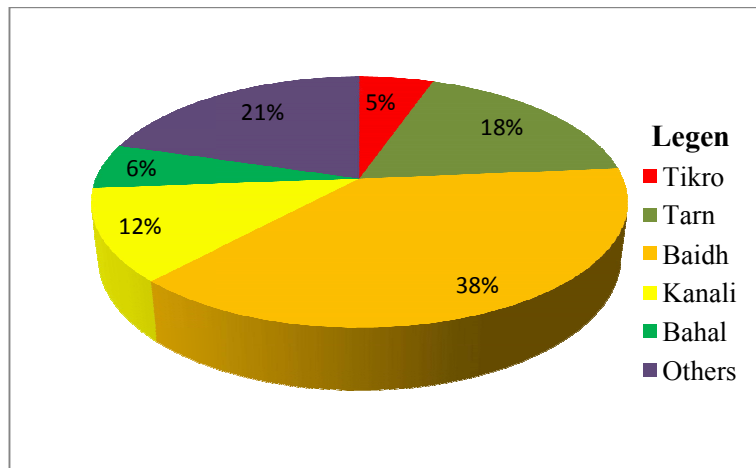


Fig. 6. Land classes of Salda River basin (In this pie chart others refers to pahar, pahar with forest, only forest, settlement and water body)

Source: Block Land Records Office, Jhalda-I

2.6.1 The hill region (375 meters and above sea level)

The hill region with an elevation of more than 375 meter above sea level is highest surface in the basin area. This portion lies in the eastern and south-eastern portion of the basin. Besides in the north and north-western portion Sikra Pahar with 491 meter, Pat - Jhalda Pahar with 483 meter and Bansa Pahar with 544 meter elevation from sea-level is small segment of this hill region. The significant geomorphic feature in this region is dome-shaped inselberges. There are number of dome-shaped inselberge, among of them Pokhariya Pahar (618 m), Baghbinda Pahar (543 m), Mahakudar Pahar (502 m), Narahara Pahar (446 m), Iphuratu Pahar (475 m), Metalya Pahar (544 m), Bansa Pahar (540 m), Sikra Pahar (491 m) etc. are significant. Among them Pokhariya Pahar, Baghbinda Pahar, Mahakudar Pahar are covered by little vegetation, whereas Bansa Pahar, Sikra Pahar is completely devoid of vegetation. There are several theories on the formation dome-shaped inselberges, but

Exhumation hypothesis is most applicable towards such of formation within the Salda basin.

2.6.2 The escarpment zone (320 meter to 374 meter form sea level)

The escarpment zone of eastern and south-eastern part of the basin and adjoining upland is also a geomorphological division sculptured mainly in Granite and Granite-gneiss by the parallel retreat of scarps and headword erosion of Salda River. Here land use pattern is more selective, depending upon morphology and slope of the terrain. The scrape face and tops are thickly forested while the adjoining level of flat and undulating terrain are cultivated.

2.6.3 Flat and gently undulating terrain (283 meter to 320 meter above the sea level)

Below the escarpment zone, a gently undulating Granite-gneiss terrain towards west is found having an elevation of below 320 meter. This is the largest part of the basin, which are gradually

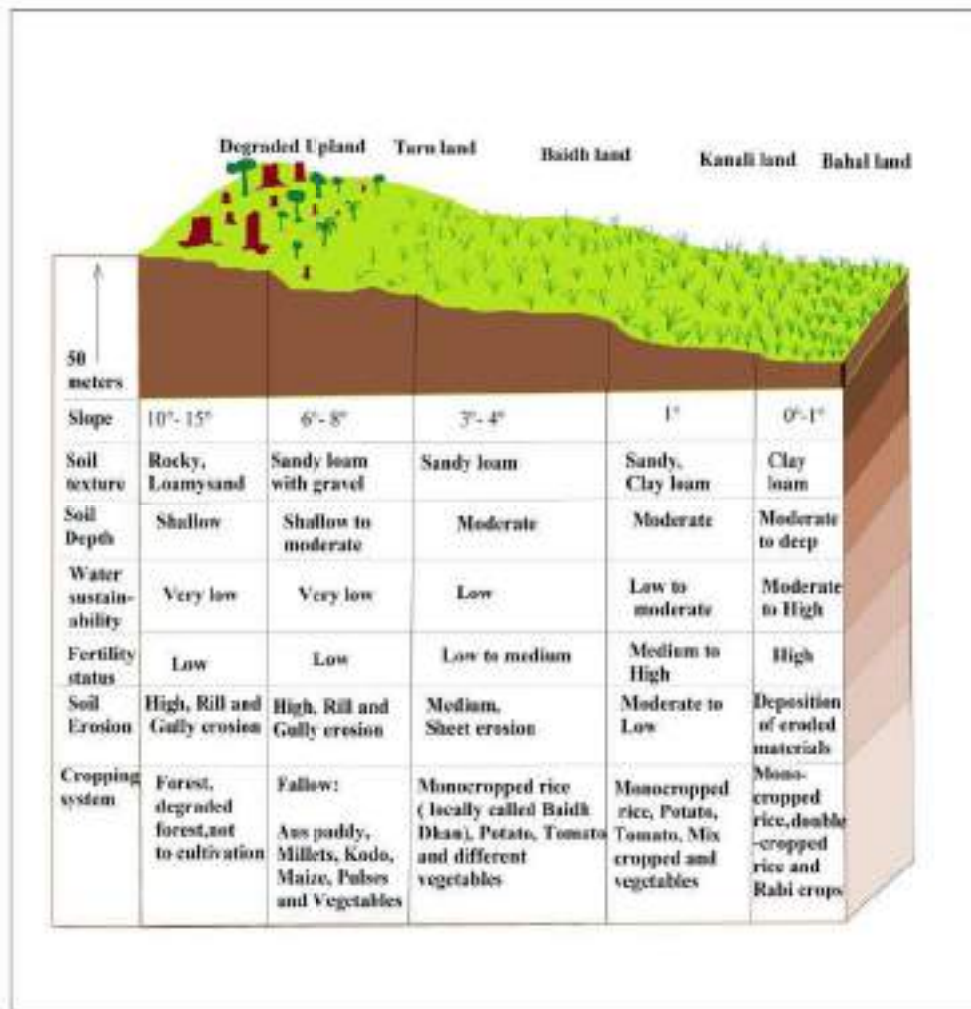


Fig. 7. Land classification and their characteristic features

Source: Field Survey

slopes down towards south-east of study area. This area is characterized by flat and gently undulating terrain with numerous gneiss domes and wide valley with Multi-channel River, large terraces, conspicuous gullied surface and small and large rocky exposures. Agricultural landscape is predominating but their main resistances are hard laterite soil, gullied surface, stony wastes and barren gravelly upland.

2.6.4 Lower plain region (280 meter to 238 meter above from sea level)

The lower Salda Plain is located in central to western, north-western and south-western portion of the basin. This part is slowly and gently sloping towards west and south-west with 238

meter to 280 meter elevation. Economically this portion is better than other area of the basin, because existence of suitable agricultural land. Lower plain is intensively cultivated due to plain surface, fertile land and sufficient supply of surface and ground water.

2.7 Climatic Characteristics

The climate of the Salda basin is a very significant factor both in the formation of variegated landscape and diversified land use in the area. Tropic of Cancer helps in the receipt of greater amount of insolation for the region in summer, which makes temperature condition high. Even during winter the temperature hardly drops below 7°C. Beside, altitude acts as one of

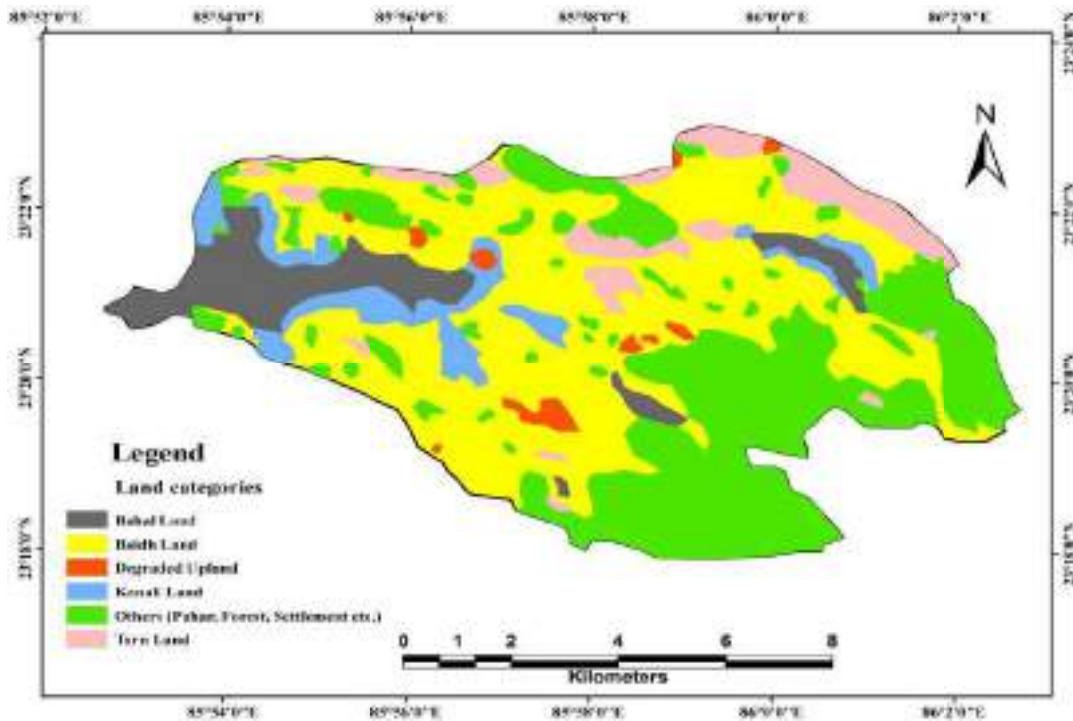


Fig. 8. Different types of land classes of Salda river basin

Source: SOI Topographical Map, 2010 and field survey



Plate no. 3. Tikro land at Mahakudar mouza

Source: Field Survey, September 2018

Plate no. 4. Bahal land at Baruakocha mouza

Source: Field Survey, September 2018

Table 4. Different types land utilization in the basin area, 2001-2011

Types of land use	2001-02		2010-11	
	Area (acres)	Percentage (%)	Area (acres)	Percentage (%)
Total area of basin	23287.00	100.00	23287.00	100.00
Area under forest	5842.71	25.09	5458.56	23.44
Area not available for cultivation	5321.08	22.85	4967.68	21.33
current fallow	1766.62	7.58	1684.5	7.23
Net shown area	10356.59	44.47	11076.26	47.56
Area shown more than once	2415.13	10.37	2821.4	12.12
Total cropped area	12771.72	54.84	13897.66	59.67

Source: Census of India 2001 and 2011, PART XII-A

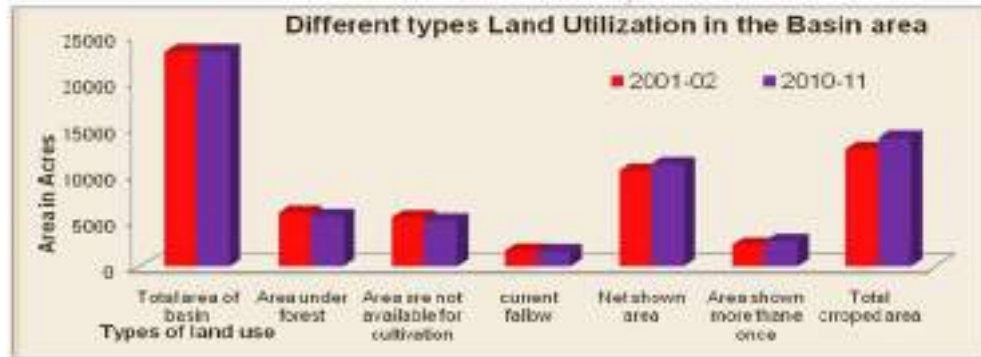


Fig. 9. Different types of land utilization in Salda basin

Source: Census of India 2001 and 2011, PART XII-A

Table 5. Crop-wise coverage area, percentage under net shown area, per acre production and total production under Salda River basin in 2017-2018

Name of crops	Cropping area (in acres)	Percentage of total area under crops	Per Acre production (in Kg.)	Total production (in Tons)
Aman paddy	6682.94	52.22	1072.84	7164.11
Aus paddy	26.87	0.20	734.11	19.72
Boro paddy	502.64	3.92	972.48	488.80
Wheat	297.06	2.32	781.46	232.14
Maize	551.42	4.30	974.09	537.13
Groundnut	337.88	2.64	673	227.39
Mustard	1139.86	8.90	331.04	377.34
Til	36.09	0.28	129.09	4.65
Arhar	201.44	1.57	435.85	87.79
Masoor	351.76	2.74	219.34	77.15
Chickpea	281.11	2.19	381.22	107.16
Linseeds(Tisi)	65.26	0.50	118.57	7.73
Peas	95.7	0.74	495.34	56.87
Potato	266.19	2.079	8885.06	2365.11
Vegetables	1972.89	15.41		
Total	12797.66	100.00		

Source: Field survey on September, 2018

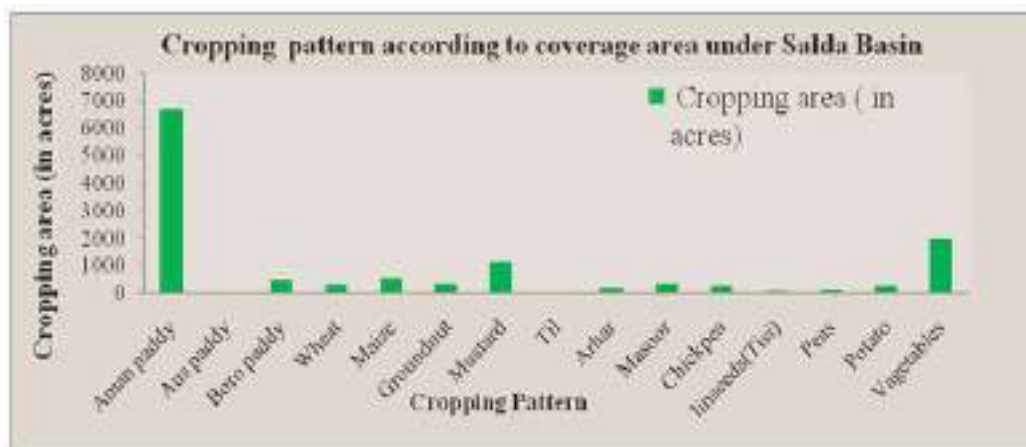


Fig. 10. Cropping pattern according to area under Salda basin

Source: Field survey on September, 2018

the important modifying agents of climate inside the basin. Geomorphologically, the basin is an area of varying levels, e.g., Upper basin of 618 m elevation, and lower plain of 238 m elevation. So the landforms are affected differently by their climatic elements.

The Salda Basin being located in the fringe areas of the eastern Chhotanagpur is characterized by tropical Monsoon type of climate. This can be well studied in the occurrences of seasonality of temperature and rainfall along with several local storms like Nor'wester and other associated features both in temporal and spatial dimensions. The mean annual rainfall of the basin varies from 1000 to 1400 mm. and means annual temperature varies from 30°C to 34°C.

2.7.1 Temperature

Mean annual temperature varies from 30.22°C to 33.77°C in different years of the basin. Temperature rises rapidly from the beginning of March. May is the hottest month with mean daily maximum temperature of 40.3°C and means daily minimum temperature of 27.2° C. On some days of May and June, the day temperature is sometimes pushed up above 45°C to 48°C by the dry land winds (Loo). January is the coldest month with the mean daily maximum temperature at 25.5°C and mean daily minimum at 12.8°C. In cold season sometimes minimum temperature is below 5°C due to the Western disturbances.

2.7.2 Rainfall

The average annual rainfall in basin area is 1363.10 mm. The rainfall during June to

September constitutes about 80% of annual rainfall, July being the rainiest month of the year (Tables 1 and 2).

2.7.3 Humidity

Relative Humidity is high during the monsoon season, being generally between 70% to 85%. After the withdrawal of south-west monsoon relative humidity decreases gradually, the driest part of the year is the hot season, when the relative humidity is 30% to 45%.

3. RESULTS AND DISCUSSION

3.1 Influence of Climate on Landform Development

The present study shows the landscape system, time lag in the response of evolutionary process, pedogenic processes with the respect of climatic element, which is present on polycyclic landscape including some traces of residual soils on soil profiles. The inherent landforms as well as the land use patterns of the polygenetic Salda basin are largely controlled by different climatic elements.

It has been observed that the landform of Salda basin exhibits many features. Advanced erosion generally exists with steep slopes viz. Pokhriya Pahar (618 m), Bighbinhdya Pahar (543 m) Iphuratu Pahar (475 m). Valleys broaden into wide depressions with flat and slightly undulating floors. The width of such lowlands often reaches in several kilometers in the lower part of the basin. Asymmetric, and cuesta-like ridges are common (Pokhriya Pahar). The stream beds are

Table 6. Various types of vegetables grown around the year in Salda Basin area

Month	Vegetables
January	Brinjal, Tomato, Cabbage, Cauliflower, Peas, Sem, Carrot, Beet,
February	Bitter Ground, Cabbage, Cauliflower, Peas, Carrot, Beet
March	Cucumber, Bitter Ground
April	Capsicum, Bottle Ground, Onion
May	Onion, Brinjal, Pepper, Bottle Ground, Watermelon
June	Bottle Ground, Okra, Pumpkin, Cucumber, Spinach, Bitter Ground
July	Same to June
August	Radish, Pumpkin, Spinach
September	Okra, Spinach, Brinjal
October	Tomato, Pepper
November	Brinjal, Tomato, Cabbage, Cauliflower,
December	Same to November

Source: Field survey in September, 2018

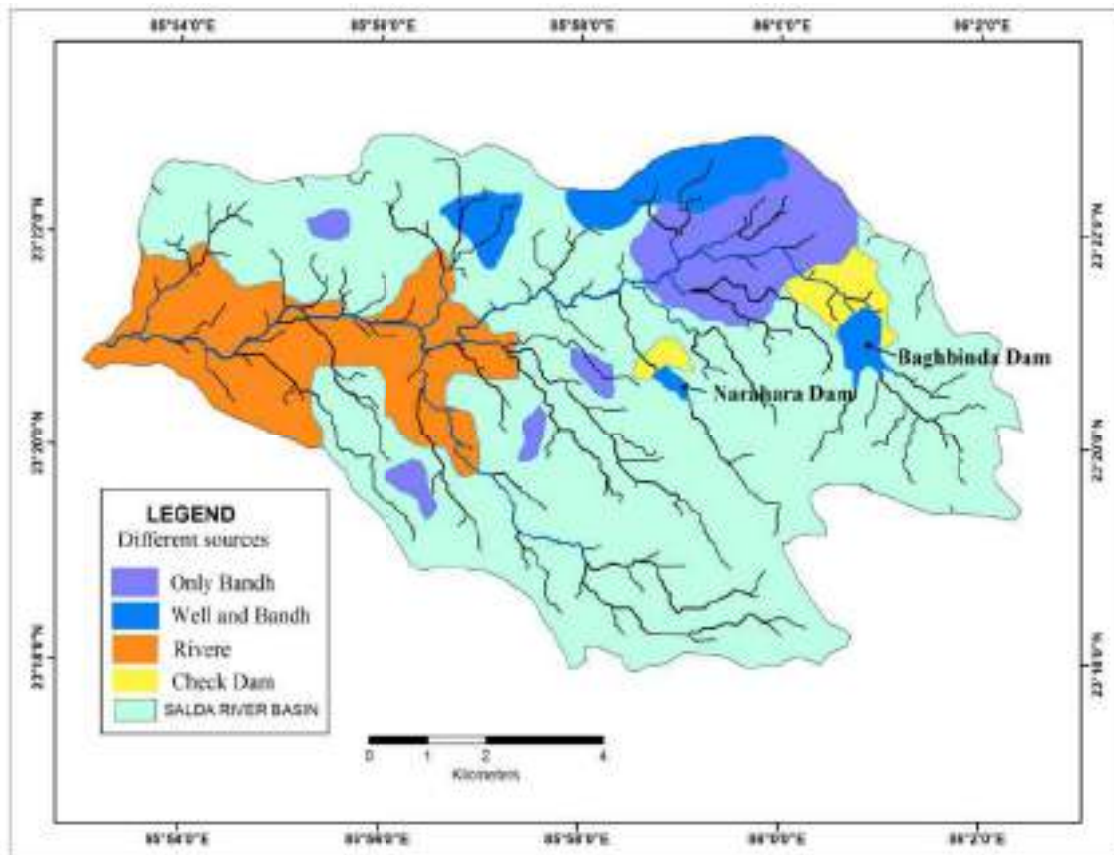


Fig. 11. Different sources of irrigation facilities in Salda River basin

Source: Field survey on September, 2018

far from having regular profiles even if the stream flows on a level or slightly undulating surface, which will justify the name of planation surface with inselbergs.

Mention should be made of inselbergs (residual hills), stone lines, gullied-surfaces, laterite capping or duri-crusts, scarpfalls, wide level plains at different altitudes in erosion surfaces, pediment like slope, terraces, floodplain deposits and planation surface, which constitute the polycyclic landscape of Salda basin. These topographic forms appear to affirm the change of climatic conditions which have played an important role.

The Salda is also a small river basin, so it is difficult to identify the influence of past climatic regime within this small latitudinal and longitudinal extension. However, indications of the effects of climatic change are mainly obtained from the inselberge dominated land surfaces on the lower reaches of the valley.

3.2 Influence of Climate on Agricultural Land Use

Each of the climatic elements has its own way of influencing land use. During June to September, the total rainfall is 1071.5 mm. of the basin. Rainfall is negligible in the rest of the year. Besides being concentrated in four months, it might delay in coming, it might stay longer or it might occur at longer intervals. All these peculiarities affect rice cultivation, which is the main crop of the basin. Yet the relatively high average rain makes rice predominant crop. The rains which are torrential are very damaging also to the surface of the lower basin because it creates inundation. Damages occur in the form of several types of soil erosion such as sheet erosion, rill erosion, gully erosion on the upper basin etc.

Temperature can affect land use adversely if it touches extremes. However, none of the months except mid-April to mid-June is injurious to plants

in the basin. The temperature in the basin for major part of the year remains constantly high and aid evaporation. Only during winter temperature is lower. On an average, the climate of the basin can be said to not congenial for successful land use in the basin, provided precaution against some of the adverse elements are taken.

3.3 Land Classification

The total land of the study area is 23287 acres. As the Salda River Basin is a part of the eastern fringe of Chhotanagpur plateau, so the general slope of the land is from west to east. But the actual slope of the Salda basin is opposite to regional slope direction from east to west. The land of the study area is also characterized by degradation surface which experiences accelerated soil erosion, mainly caused by gully and rill erosion, leaching and human interference through deforestation.

The land of the area under study is classified into five categories: (1) Tikro land / Degraded upland, (2) Tanr Land / Barhi, (3) Baidh Land, (4) Kanali Land, (5) Bahal Land / Low land / Garha (Table 3).

3.3.1 Tikro land

This area is situated in the upper part of the land classes. It is covered by rocky surface, boulder and gravels. It is totally unproductive and fallow land. Vegetation cover is also very low in this category. Somewhere this area is fully covered by opened Pre-Cambrian granite and gneiss rocks. Main soil texture is rocky and gravelly loamy sand, which are infertile and unproductive. This land spreads all over the study area, but upper and middle portion of the basin cover maximum portion. Mainly on the lower basin this rock masses are open on the surface by long geological erosional activities. The soil erosion is very rapid in this part due to absence of vegetation cover and wind action during long summer season.

3.3.2 Tanr land

Tanr is the lower portion of the Tikro Land. Laterite and Red-gravelly soils are present here, which represent low fertility and or soil capability. This area is characteristics by gentle slope towards flat upland. So water holding capacity is very low. As a result agricultural productivity is also very low. In the study area this land is mainly used for short duration Kharif crops, grazing and forestry.

3.3.3 Baidh land

The next category is Baidh, which is better than Tarn land for land utilization. The soil types in this land are laterite with sand, sandy loam, and sometimes fine sandy soil is also found. Percolation rate is also high, so it is less fertile land. The depth of soil horizon in this region is only 2 to 5 feet. Below 5 feet the parent materials are found. This land covers the largest area (8926.85 Acre) of the basin, which are maximum belong to north-eastern and central portion of the basin. Jhalda-Darda, Iloo-Jargo, and Khamar Panchyet cover largest amount of Baidh Land.

3.3.4 Kanali land

Kanali is that type of land which is relatively better than the Tarn and Baidh. Kanali land is generally situated between Baidh and Bahal. The water availability is good to moderate in monsoon season, so it is suitable for paddy cultivation. The soil in this land is alluvial and fine silt to clay. This type of land covers only 11.87% of total land of the study area. Eroded materials of upper lands are deposited in this land. So, if people ignore to prevent deposition then this land also becomes sandy and gravelly. Because main deposited materials are sand, gravel, pebble, bolder, stone. Besides, little amount of clay and silt is also deposited.

3.3.5 Bahal land

Bahal is the lowest most land surface of the study area and is the most valuable land for agricultural use. The soil in this category is fertile alluvial soil and clay-loamy in texture. Water table is very near to the ground and infiltration rate is very low so the water holding capacity is very high in this portion. This land is existing near the river bank and below the water body, which are mainly found in the lower basin area.

3.4 Land Utilization in Salda River Basin

This Basin area is located in the plateau fringe, so land utilization here is very much diverse type. Most of land are forest and unavailable for cultivation, which lying over the upper basin area. On the other hand, eastern, south-eastern, and northern part of the basin is mostly covered by forest and non-cultivated land. More than 51% area belongs to these categories. Only 43.37% area is used for agricultural purpose, of which 70% is found in the lower basin. In summer season, Rabi crops are practiced in the lower

basin area, which is mentioned as Area shown more than once. Land utilization of the study area is gradually changing in slower rate. Areas under forest, area are not available for cultivation and current fellow land are decreasing and net shown area and total cropped area are increasing in recent decade. Table 4 shows the diverse land utilization in basin area:

3.5 Cropping Patterns

The Cropping pattern in the Salda basin in relation to the importance of different crops has grown, especially in terms of their spatial and temporal context, represents the hierarchical order and in association with different crops at a point of time in the particular areal unit within the basin.

In the study area agriculture is the main occupation of the people, so the study of crop cultivation and its planning is of great importance.

The diversity of crop farming is the result of diversity in topographic, socio-economic and technological conditions of the basin. The main crops, crops coverage and production of the study area are mentioned in Table 5.

Table 5 shows different types of crops of the total Basin area, the total area is 23287.00 acres of 48 Mouza, where 10076.26 acres having net sown area and Gross cropped area is 12797.66 acre. Gross cropped area refers as cropping area. The Table 5 has shown the variables such as crop coverage areas, crops production, and diversified cropping practice regarding the land classes. The data has been collected in the form of local units that are commonly used by the local stakeholders, *Bigha, Mon* but this information are converted into traditional units like, *Acres, Kg.* and *Tons* etc.

3.5.1 Paddy

Paddy is the most important food grains in the Salda basin area. It has covered the largest portion (56.34%) of the total net cropped area and the production (7672.63 tons) of this crop is also highest compared to rest of the crops during the period 2017-2018. Due to lack of irrigation facilities this crop is being totally dependent upon the monsoon rainfall. This crop has been cultivated by using two methods, such as (i) transplantation method in low lands and (ii) broadcasting method in the uplands. The spatial

distribution of paddy cultivation indicates its close relation with soil, water and topography. In the study area paddy are mainly of three types: *Aus, Aman and Boro*. *Aman* has been largely cultivated all over the region during monsoon season, which is sown in June and reaped in mid-October. *Aman* has covered the largest portion the total cropped sown area in comparison to other crops. The cropped area is 6682.94 acres, which is 52.22% of total sown area. Whereas, *Aus* and *Boro* paddy was cultivated in small scale i.e. 26.87 acres and 502.64 acres respectively. In this basin area, *Aus* and *Boro* have been cultivated during the period of mid-June to September-December to March respectively.

3.5.2 Pluses

Pulses are the second important cereal in the Salda Basin. It is cultivated as dry crops, because *Tarn* land is mainly used for pulses cultivation in the monsoon season. The cereals like Tur (Arhar), Moong, Chickpea and Gram are cultivated for domestic consumption. Masoor is another pulse which is cultivated (351.76 acre in 2017-18) in *Kanali* land in winter season. Pulses are important because it is cultivated in less moisture with moderate fertile soil and also in the low rainfall conditions and prolonged dry spells. These pulses are used both for human consumption and cattle feed. Agricultural operation such as preparation of land for these type of pulses cultivation is very easy rather than the other crops. Pulses are grown well on a variety of soil; however, it is generally grown in the poorer soil.

3.5.3 Pea

Pea is grown as Rabi crop. The local people consider Pea as vegetable rather than pulse. Total peas cultivated area is 108.82 acres and total production is 53.81 tons.

The cultivation of the total pulses has spread over only in 9.94% of the total cultivated area in 2017-18.

3.5.4 Oil seeds

Various types of oilseeds are cultivated all over the basin area such as Kharif and Rabi in both the seasons. *Oil seeds like Til, Line seed (Tisi), Groundnut, Khasla* except *Mustard* are practiced during the Kharif season. Til, Line seed (Tisi), Groundnut, Khasla and Khasari are cultivated in

red, sandy loam soil of Tarn land. All of those oil seeds are cultivated during the onset of monsoon. Sub-tropical monsoon weather and well drained light sandy loam, red soils are well suited for this type of cultivation.

Mustard cultivation has been very much suitable for sub-tropical dry and cool winter climate. So it is practiced in largest area rather than others oilseeds. Mustard has covered 1139.86 acres area that is 8.90% of total net sown area and the amount of total production is 377.34 tons in 2017-18. It is cultivated on winter season in Baidh and Kanali land.

3.5.5 Potato

Potato is the important food crops of Salda River basin. It is grown in the subtropical condition in winter season on sandy-loam to loamy soil with 5.5 to 6.5 pH value. It is also known as 'friend of poor men', so most of the people select this crop after paddy cultivation in Kanali land. However, due to lack of water it is practiced in short duration providing 3 to 4 times irrigation. Therefore, total area coverage for potato is only 266.19 acre and total production is 2365.11 tons in 2017-2018.

3.5.6 Wheat

The percentage of wheat cultivation is only 3.19 % of net cultivated area of the basin. It is a Rabi crop, which requires low temperature, available irrigation and well drained fertile loamy-clay soil. This nature is rare in this area. So it is cultivated only in 297.06 acres and total production is 232.14 tons in 2017-18.

3.5.7 Maize

Maize is one of the most versatile emerging crops having wider adaptability under the basin area. It has the highest genetic yield potential among all the cereals. In the study area Maize cultivation mainly starts before the onset of monsoon, so it is a Kharif crop. Maize cultivation has been successfully done in Tarn and Baidh land, where soil is sandy-loam to loamy and pH value is 5.5 to 7.0. It is also cultivated under rainfed conditions on poorer soil.

3.5.8 Vegetables

Vegetables are most revenue earning crop in this area. In both Kharif and Rabi season this area produces different types of vegetables. Table 6 shows the different types of vegetables with growing season in Salda Basin.

3.5.9 Zaid crop

These crops are grown during the period from March to June. The zaid crops like Bitter Gourd, Sponge Gourd, Bottle Gourd, Watermelon, and Pumpkin are cultivated in the Basin area.

3.6 Irrigation Facilities

Owing to the peculiar topography the basin area has little irrigation facilities. Soil erosion is the main problem of upper basin for irrigation, where erratic and scanty rainfall is another problem of irrigation in whole basin area. Irrigation in the area is mainly facilitated from wells, bandh, and check dams, which is accumulated from run-off water. As the availability of water depends on rainfall, it is not assured for irrigation always. During summer months most of the Wells and Bandh get dried-up and hence irrigation is not possible. Two check-dams: Narahara Dam and Baghbinda Dam are small scale irrigation project; these are also dried-up in summer. Only lower basin has potentialities for irrigation in summer season from river. In addition to Salda River, people used to get irrigation water from the Rupai and Subarnarekha River. Therefore, lower basin has potentialities of irrigation in summer and hence this portion has huge capability of agriculture.

3.7 Land Classification and Its Impacts on Crop Selection

In this basin area land has been classified into five categories, such as Tikro, Tarn / Barhi, Baidh, Kanali and Bahal. The regional soil texture, soil fertility, water holding capacity, surface and ground water potentiality, irrigation facilities etc. are depended on those land categories. So, agricultural system and cropping patterns are fully influenced by the characteristics of land categories.

Tikro and Tarn land are not suitable for crop production. These lands are infertile and have high infiltration capacity. Due to undulating and sloppy character Tarn is suitable for pulses, maize and vegetable cultivation in monsoon season. Baidh land is also not suitable for agricultural practice like paddy cultivation. The cultivation in this type of land has increased with the growing demand of food grains with the passage of time. This type of land is used for paddy, oilseeds, and pulses cultivation with the help of irrigation facility.

Table 7. Cultivated crops, their problems and essential crop selection according to land classes

Land classes	Cultivated crops		Problems	Suitable crops		Remarks
	Kharif	Rabi		Kharif	Rabi	
1.Tikro	Not Cultivated	Not Cultivated	Drought, infertile, rapid soil erosion, rocky surface	Til	None	For the preventing soil erosion plantations measures are required.
2.Tarn Or Bari (near to settlement)	Aus Paddy, Maize, Groundnut, Til, Tur, Tisi, Pepper, Okra, Spinach, Radish, Brinjal, Sponge Gourd.	(near to settlement) Onion, Cucumber, Spinach, Cauliflower, Cabbage, Tomato, Coriander.	Water scarcity, Low fertility, Shallow soil depth, Soil erosion	Maize, Tur, Spinach, Tomato, and other remunerative vegetables	Spinach, Cauliflower, Cabbage, Tomato, and other remunerative vegetables	This land covers large area. So people want to cultivate selective remunerative vegetables. The crops having market demand need to be cultivated.
3.Baidh	Medium duration traditional paddy, locally called Baidh Dhan	Potato, Tomato, Mustard, Peas, Cauliflower, Cabbage, Chick Pea.	Water scarcity, need irrigation for suitable high yielding medium duration varieties. Low fertility.	Tomato, Radish, Pepper and other crops with market demand.	Same as practiced crops.	As this land has low fertility, sandy-loam soil and water holding capacity is very low, so, it needs short to medium duration crops.
4.Kanali	Medium to long duration Aman Paddy	Onion, Wheat, Chick Pea, Bitter Gourd, Pumpkin,	Lack of water. Unavailability of HYVs. Lack of irrigation facilities.	Same as practiced crops.	Same as practiced crops.	Need rigorous attention for cultivation, crop rotation. Emphasis on irrigation facilities.
5.Bahal	Long duration Aman Paddy	Short duration Boro Paddy	Excess water, Lack of proper nutrient management	Same as practiced crops	Same as practiced crops	Emphasis on well drainage.

Source: Field survey on September, 2018

Kanali and Bahal are most appropriate for cultivation. These types of land are suitable for both Kharif and Rabi crops with the help of irrigation facilities. Bahal land is basically used for paddy cultivation in monsoon season and Rabi season also. In the basin area main constraint for agriculture is lack of water, but Bahal is that type of land where water is available for both season. It is not suitable for potato, pulses, nut and oil seeds production (Table 7).

4. CONCLUSION

The present study has analyzed the landform characteristics, impact of landform and climatic elements on agricultural land use pattern of Salda River Basin. This area has unique characteristics of a complex and composite land unit. It has been classified into four geomorphological regions and five land classes, which have been considered as an important influential factors and one of the important determining elements upon the agricultural land use pattern. The characteristics of soil depth, soil texture, fertility, surface and ground water availability, irrigation facilities etc. are very much dependent upon the land categories.

The Salda River basin is a micro-basin of the Subarnarekha Drainage system, but it reflects the typical land characteristics of the fringe area of Chhotanagpur plateau, where some typical geomorphic attributes control the productivity of the land and also controls the socio-economic conditions of the local people. The present authors have tried to examine the typical geomorphic attributes and their effects on present productivity of the land in a micro level study, where they studied the land surface characteristics on the basis of Cadastral maps and extensive field works.

It is clear that the economy and livelihood of this area is very much dependent on the agricultural production which is influenced by unfavorable terrain conditions and unreliable monsoon rainfall. The western and central part of the basin is comparatively better in terms of the agricultural activities. The eastern and south-eastern parts are suffering from acute problems due to the existence of large tracts of barren land and forests. Each geomorphic division with its particular geomorphic processes is responsible for the development of distinct land use patterns within the Salda basin.

ACKNOWLEDGEMENTS

We are thankful to the Department of Geography, The University of Burdwan for providing necessary facilities. We are thankful to The Indian Meteorological Department, Kolkata for providing the Meteorological Data regarding this work. We are thankful to Block Land Records Office, Jhalda-I for providing Land use and Land cover data-sets. We are also thankful to Mr. Ranjit Mahato, Dept. of Geography, Nalanda Open University, during the field survey. The authors are very much thankful to Dr. Soumitra Sen (Associate Professor of A. M. College, Jhalda, under Sidho Kanho Birsha University, Purulia) for providing the valuable positive suggestions for the improvement of this paper.

COMPETING INTERESTS

Authors have declared that no competing interests exist.

REFERENCES

1. De NK, Jana NC. The land: Multifaceted Appraisal and Management, Sri Bhumi publishing co., Calcutta; 1997.
2. Feizizadeh B, Blaschke T. Land suitability analysis for Tabriz County, Iran: A multi-criteria evaluation approach using GIS. *Journal of Environmental Planning and Management*. 2012;1–23. Available: <https://www.tandfonline.com/doi/abs/10.1080/09640568.2011.646964>
3. Al-Shalabi MA, Mansor SB, Ahmed NB, Shiriff R. GIS based multicriteria approaches to housing site suitability assessment. In: XXIII FIG Congress, Germany. 2006;8–13. Available: http://fphid1076751.testsidr.dk/resources/proceedings/fig_proceedings/fig2006/papers/ts72/ts72_05_alshalabi_etal%20_0702.pdf
4. Hironi K. Land use planning and geomorphology - A study of Sawai Madhopur, Concept Pub. Co., New Delhi; 1991.
5. Ghosh S. Geomorphic land evaluation for sustainable use of land resources in Puruliya District, West Bengal. *Journal of Landscape Systems and Ecological Studies*. 2012;35(1):263-274. Kolkata. Available: <https://www.ceeol.com/search/article-detail?id=29113>
6. Bhattacharya BK, Ray P, Chakraborty BR, Sengupta S, Sen NN, Sengupta KS, Mukherji S, Maity T. West Bengal District

- Gazetteers, Purulia; Government of West Bengal. Published by Narendra Nath Sen, State Editor, West Bengal District Gazetteers, and Calcutta; 1985.
7. Dunn JA, Dey AK. The geology and petrology of eastern Singhbhum and surrounding areas, Mem. Geol. Surv. Ind. Vol. LXIX, pt. 2; 1942.

© 2019 Mahato and Jana; This is an Open Access article distributed under the terms of the Creative Commons Attribution License (<http://creativecommons.org/licenses/by/4.0>), which permits unrestricted use, distribution, and reproduction in any medium, provided the original work is properly cited.

*Peer-review history:
The peer review history for this paper can be accessed here:
<http://www.sdiarticle3.com/review-history/49255>*

ISSN 2278 - 1811
IC Value (2017) = 86.45
NAAS Score = 2.77
Indexed in Indian Citation Index (ICI)

₹ 300/-

ARTHSHAstra INDIAN JOURNAL OF ECONOMICS & RESEARCH

VOLUME : 8

ISSUE NUMBER : 4
(BI - MONTHLY)

JULY - AUGUST 2019

In This Issue

**How Does Economic Growth React
to Fiscal Deficit and Inflation? An
ARDL Analysis of China and India**

**Amba Agarwal
Amritkant Mishra
Mohini Gupta**

**A Curious Neglect of Cicero as the First
Predecessor of Asymmetric Information
by the Five Nobel Laureate Economists**

Arup Kanti Konar

**Is Fat Tax the Panacea for Fast
Food Consumption and Related
Health Issues in Urban India?**

**Arunima Singh
Parvati Pyarelal
Vineeth Mohandas**

**A Preliminary Survey of the
Theoretical and Practical Aspects
of UBI and Assessing its Feasibility
in the Context of the Indian Economy**

**Ketan K. Shah
Dhruvi G. Jani**

A Curious Neglect of Cicero as the First Predecessor of Asymmetric Information by the Five Nobel Laureate Economists

* Arup Kanti Konar

Abstract

In 1996, two economists, and in 2001, three economists, were jointly awarded the Nobel Prize in Economics by the Royal Academy of Sciences of Sweden for their revolutionary contributions to asymmetric information. The contribution of the first predecessor of asymmetric information was neither cited/quoted nor acknowledged by at least one of the five Nobel laureate economists in their works. This is a curious neglect of Cicero as the first predecessor of the concept of asymmetric information by the five Nobel laureate economists. Hence, Stigler's Law of Eponymy: "No scientific discovery is named after its original discoverer" (Stigler, 1980, p. 147) is also applicable to Cicero. The objectives of this article were four-fold: (a) to disclose the name of the earliest predecessor of the concept of asymmetric information: Marcus Tullius Cicero (106 - 43 BC), who was an ancient Roman Stoic philosopher, (b) to disclose how Cicero described the informational asymmetry between the sellers and buyers of the markets in terms of the different examples of economic exchange or transaction by "few words, with gentleness and efficiency," (c) how Cicero has elevated the discussion of asymmetric information from positive to normative or moral perspective, which can be found in his treatise, entitled, *De Officiis* (44 BC), whose English translation is *On Duties* and (d) to indicate that the concept of adverse selection, which is one of the problems of asymmetric information, was first coined by the Chicago university economist Carlos C. Closson in the article "Social selection" in 1896.

Keywords : data, information, knowledge, normative, understanding, wisdom

JEL Classification : B31, D82, D83

Paper Submission Date : March 5, 2019 ; Paper sent back for Revision : July 20, 2019; Paper Acceptance Date : August 1, 2019

"We must first know what we ought to do, and then live according to that knowledge" (Hazlitt & Hazlitt, 1984, p. 40).

The discussion of asymmetric information or informational asymmetry is included as a separate chapter in the microeconomic textbooks for the undergraduate and post graduate students. In better words, asymmetric information has become a staple in microeconomic education at the lower and higher levels. But surprisingly and unfortunately, no microeconomic textbook or article has disclosed the name and contribution of the "first predecessor of asymmetric information." However, only few lines about Cicero's example(s) of asymmetric information have been rewritten in the literatures like Editors (2007), Baloglou (2012), Faccarello and Kurz (2016), and Jeadan (n.d.).

The Nobel Prize in economics was awarded by the Royal Academy of Sciences of Sweden jointly (a) in 1996 to the two economists : James Mirrlees (UK) and William Spencer Vickrey (USA) for their fundamental

* Principal & Associate Professor of Economics, Achhruram Memorial College, Jhalka, Purulia, West Bengal - 723 202. (E-mail : akkonar@gmail.com)

DOI : 10.17010/ajer/2019/v8i4/148069

contributions to the economic theory of incentives under "asymmetric information," and (b) in 2001 to the three economists: George Arthur Akerlof (USA), Andrew Michael Spence (USA), and Joseph Eugene Stiglitz (USA) for their analysis of markets with "asymmetric information."

At least one (e.g. Joseph Eugene Stiglitz) of the foregoing five Nobel laureates mentioned the names of the "early and earlier predecessors" (not the earliest predecessor) of asymmetric information. Analogously, in the discussion about the history of the idea of asymmetric information, James Madison University economist, Jr. J. Barkley Rosser (2003), followed suit. But none of the six economists (five Nobel laureates and one non-Nobel laureate) did mention, cite, quote, or acknowledge the name of the "first predecessor" of the concept of "asymmetric information." Unfortunately, this is a curious neglect of Marcus Tullius Cicero (106-43 BC) as the real inventor of the concept of asymmetric information by the five Nobel laureate economists.

The contributions of the foregoing five Nobel laureate economists constitute the foundation of the "economics of information," which was formally introduced by another American Nobel laureate (1982) economist, George Joseph Stigler (1961), who was the father of Stephen Mack Stigler. Stigler's Law of Eponymy, which states that "no scientific discovery is named after its original discoverer" (Stigler, 1980, p. 147) is named after Stephen Mack Stigler.

Asymmetric information, which has been explicated with sophistication by George A. Akerlof (1970), is the sub-set of the "economics of information." The Nobel Committee described Akerlof's (1970) article as "the single most important study in the literature on economics of information." The researches of the foregoing five Nobel laureate economists are associated with the informational asymmetries between the sellers and buyers of the markets by which the market-mechanism is vitiated, and in consequence, the markets cannot function as the best or efficient allocators of resources for their imperfection. Hence, owing to the malfunctioning of the markets caused by the asymmetry of information between the sellers and buyers of the markets, governmental intervention may be required in the capitalist systems for reducing or ruling out the market imperfections.

The only cause of such a "curious neglect of Cicero as the first contributor to asymmetric information" lies in the asymmetry of information, knowledge, and/or wisdom by which the foregoing five economists were awarded the Nobel Prize in Economics in 1996 and 2001. By any criterion, originators of new ideas should be rewarded and recalled, irrespective of time and number of ardent readers. All wisdoms are knowledge, but the converse is not true. In better words, wisdom is the subset of knowledge. Surprisingly, none of the five Nobel Laureate economists as well as the Nobel Committee demonstrated the acknowledgement or gratefulness to the first predecessor of asymmetric information consciously or unconsciously. Hence, the foregoing five Nobel laureates were absolutely devoid of "wisdom" and not "knowledge" (because a researcher's optimal or super-optimal amount of knowledge is the precondition of realizing the Nobel Prize), if such acknowledgement had not been shown deliberately and consciously. Absolute ignorance or unawareness of the five Nobel laureates about Cicero's work may be the cause of their non-citation or non-acknowledgement.

A stone is broken by the last stroke of a hammer. This does not mean that the first stroke is useless. The last stroke should not neglect the first stroke and should be grateful to the first stroke for its first effective contribution to break a stone. Thus, the moral values of humans should not be reducible.

Hence, the objectives of this article are four - fold :

- (i) To discover the name of the earliest predecessor of the concept of asymmetric information : Marcus Tullius Cicero (106- 43 BC), who was an ancient Roman Stoic philosopher,
- (ii) To disclose how Cicero has described the informational asymmetry between the sellers and buyers of the markets in terms of the different examples of economic exchange or transaction by "few words, with gentleness and efficiency,"

(iii) How Cicero has elevated the discussion of asymmetric information from positive to normative or moral perspective, which can be found in his treatise, entitled, *De Officiis* (44 BC), whose English translation is *On Duties*, and

(iv) To indicate that the concept of adverse selection, which is one of the problems of asymmetric information, was first coined by the Chicago University economist, Carlos C. Closson in the article "Social selection" in 1896. Though there are English translations of Cicero's *De Officiis* by only several authors (e.g. Cockman, 1833, 1839; Griffin & Atkins, 1991; Peabody, 1887; Miller, 1913), the translation by Walter Miller (1913), who was a professor of Latin in the University of Missouri, is preferred as the sole source of reference for discussing Cicero's views about asymmetry of information in economic exchange or transaction in this paper.

Incomplete or imperfect knowledge can be indicated by asymmetry of knowledge. Like knowledge, information is also asymmetric. Asymmetry means heterogeneity, differentiability, or inequality. However, symmetry means homogeneity, uniformity, or equality. Asymmetric knowledge has two forms: (a) absolute asymmetry, which says that no one individual knows all things in the universe. It means that intra-personal knowledge about all things in the universe is absolutely limited or bounded, and (b) relative asymmetry, which tells that one individual has more or less knowledge about a particular thing in the universe than the other individual. It means that inter-personal knowledge about a particular thing in the universe is unequal.

Relative asymmetry, which is a matter of degree, is of two types: (a) Strong relative asymmetry, which indicates that inter-personal knowledge about a particular thing in the universe is extremely or unprecedentedly unequal. For example, one individual has 100%, while the other individual has 0% knowledge about a particular thing in the universe, and (b) weak relative asymmetry, which suggests that inter-personal knowledge about a particular thing in the universe is moderately or mildly unequal. For example, one individual has 60%, while the other individual has 40% knowledge about a particular thing in the universe.

Information, Knowledge, and Wisdom

Wisdom, knowledge, understanding, information, and data cannot be interchangeably used. It means that they are not synonymous. From the Chorus of T. S. Eliot's (1934) *The Rock*, we find the following relationship among information, knowledge, and wisdom:

Where is the wisdom we have lost in knowledge?
Where is the knowledge we have lost in information?

Further, the following remark of Neil D. Fleming (1996) is also relevant to recall (cited in Erickson, 2009, p. 13):

A collection of data is not information.
A collection of information is not knowledge.
A collection of knowledge is not wisdom.
A collection of wisdom is not truth.

Moreover, the following lines are reminded us by R. L. Ackoff (1999):

An ounce of information is worth a pound of data.
An ounce of knowledge is worth a pound of information.
An ounce of understanding is worth a pound of knowledge.

Data means symbols. Information implies data, which are processed to be useful and which provides answers to "who," "what," "where," and "when" questions. Knowledge is the application of data and information and it provides answers to "how" question. Understanding refers to the appreciation of "why" question. Wisdom is the evaluated understanding (Ackoff, 1989).

Information relates to description, definition, or perspective (what, who, when, where). Knowledge comprises of strategy, practice, method, or approach (how). Wisdom embodies principle, insight, moral, or archetype (why) (Erickson, 2009, p. 15).

In better words, data represents a fact or statement of event without relation to other things. Information embodies the understanding of a relationship of some sort, possibly cause and effect. Knowledge represents a pattern, which connects and generally provides a high level of predictability as to what is described or what will happen next. Wisdom embodies more of an understanding of fundamental principles embodied within the knowledge, which are essentially the basis for the knowledge being what it is. Wisdom is essentially systemic (Bellinger, Castro, & Mills, n.d.).

Wisdom is a right understanding, a faculty of discerning good from evil; what is to be chosen and what rejected; a judgment grounded upon the value of things, and not the common opinion of them; an equality of force, and a strength of resolution. To be wise is the use of wisdom, as seeing is the use of eyes, and well-speaking the use of eloquence. No man is born wise; but wisdom and virtue require a tutor, though we can easily learn to be vicious without a master. However, we have only words of wisdom without the works (Hazlitt & Hazlitt, 1984).

According to Lombardo (2012), wisdom is the highest expression of self-development and future consciousness. It is the continually evolving understanding of and fascination with the big picture of life, of what is important, ethical, and meaningful, and the desire and creative capacity to apply this understanding to enhance the well-being of life, both for oneself and others. Wisdom synthesizes cognitive capacities, such as expansive and informed thinking and creative and practical knowledge, with emotional sensitivity and depth and ethical consciousness. Wisdom unites mind, heart, action, and ethical values. Wisdom is identified as the highest expression of future consciousness. Wisdom, in fact, can be seen as cosmically expansive and ethically informed thinking tied to action. Why search for wisdom and enlightenment? The pursuit of wisdom and enlightenment is critically important to living the good life - to realize what is best in us, to giving meaning and purpose to our existence. Wisdom and enlightenment bring quality to life. Wisdom answers the question of how to live; enlightenment answers the question of what to live for. Knowledge and wisdom are journeys rather than destinations; there is no absolute enlightenment.

A Brief Sketch of Asymmetric Information

Capitalism is a global system. The future will tell whether capitalism will be sustainable or unsustainable. However, in reality, capitalism sustains, and anti-capitalism (e.g. socialism or communism) has been reduced or ruled out from the world. The sustainability (or unsustainability) of capitalism depends on the success (or failure) of the markets. The participants of the markets are the sellers and buyers, while the variables of the market are the demand, supply, price, quality, and quantity of the commodity sold and bought in the market. The market participants are the rational decision-making units. The success of market is indicated by the realization of the socially optimal or efficient allocation of scarce resources by the market mechanism. One of the criteria of market efficiency is that market participants possess or acquire perfect or complete information (or symmetric information) about the characteristics of the commodity bought and sold in the market. In reality, market participants cannot always acquire perfect or complete information because the search for or acquisition of information inflicts cost to the market participants, which is called the "cost of information." This means that market participants undertake "rationally decisionized action" under uncertain conditions. However, the failure of the market depends on the diverse determinants. One of the crucial determinants of market failure is that the

market participants are equipped with imperfect or incomplete information, which may be renamed as asymmetric information or informational asymmetry (Maddala & Miller, 1989).

Asymmetric information exists in the market if the market participants (sellers and buyers) are not equipped with an equal amount of information about the (hidden or unobservable) characteristics of the commodity (e.g. quality) bought and sold in the market. In better words, if one market participant possesses or acquires more or less information than the other market participant about the (hidden or unobservable) features of the commodity bought and sold in the market, then asymmetry of information is existent in the market. In the market, the participant who is equipped with more, better, or stronger information about the characteristics of the commodity bought and sold in the market has a "comparative advantage" about the information, while the other participant possessing less, worse, or weaker information has a "comparative disadvantage" about the information. If "more (or over) informed market participants" confront with the "less (or under) informed market participants" in the market, then asymmetric information exists in the market.

The eventual and inevitable problems of asymmetric information in the markets are the (a) problems of adverse selection or unfavorable selection (which is renamed as hidden information) and (b) problems of moral hazard (which is renamed as hidden action) (Maddala & Miller, 1989). It is needful to note that the concept of adverse selection or unfavorable selection was first coined by Chicago University economist Carlos C. Closson in the article "*Social selection*" in 1896 (Closson, 1896, p. 462).

(1) Problems of Adverse Selection or Hidden Information : Adverse selection indicates that the commodities with adverse features will be substituted for the commodities with favorable features in the market with asymmetric information by the price mechanism, and eventually, no market will exist at all. This means that the commodities with adverse features will drive out the commodities with favorable features from the market with asymmetric information by the price mechanism leading to the eventual non-existence of the market. For example, in the second-hand car market, the sellers possess more information about the real quality of the cars, and they do not want to disclose the true quality of the cars to the less informed buyers, since the sellers have an intrinsic propensity to exploit (or to gain more advantage from) the less informed buyers. In consequence, the less informed buyers are compelled to buy the commodities with adverse features through the price mechanism, and eventually, such price mechanism rules out the existence of the second-hand car market. This is called the adverse selection in the second-hand car market. From the example of the second-hand car market, it can be pointed out that adverse selection is such a market phenomenon by which the less informed buyers are affected by three sorts of adversity: (a) the buyer is adversely informed by the better informed seller, (b) the adversely informed buyer is compelled to buy the commodity with adverse (or undesired) features, and (c) the adversely informed buyer, buying the commodity with adverse (or undesired) features, enjoys adverse (or less-favorable) gain from market exchange compared to the seller's gain, since the seller enjoys the dual gain: profit from sale and extra-profit from his "dishonesty" (indicated by the non-disclosure of the hidden characteristics of the commodity bought and sold). All the foregoing three sorts of adversities enjoyed by the adversely informed buyer constitute the "cost of buyer's (partial or perfect) ignorance."

(2) Problems of Moral Hazard or Hidden Action : On the contrary, moral hazard is a market phenomenon, where one market participant (say, A) fails to observe, discover, or identify the decisionized action/activity of the other market participant (say, B) in the post-purchased position or period (or after the commodity is bought) owing to asymmetry of information, and in consequence, one market participant (say, B) passes the cost of his/her altered decisionized action/activity on to the other market participant (say, A) after the commodity is bought. For example, the individuals, who have purchased insurance for cars, confront the problem of moral hazard in the insurance market for cars with asymmetric information. In the insurance market for cars, the insurance companies are the sellers, while the car-owners are the buyers of the insurance for cars. In such a market, the

sellers (insurance companies) are less informed than the buyers (car-owners) about the nature of car-driving (careful or careless car-driving) and the condition (good or bad condition) of the car insured after the car is bought. A person, who has purchased insurance for a car, may drive the car carelessly, since if any accident occurs for his/her carelessness, he/she knows that the cost of such an accident will be borne by the insurance company, not by himself/herself. In consequence, the careless car owners will purchase more insurance for cars, while the careful car owners will be compelled to purchase less insurance for cars, and eventually, the size of the insurance market for cars will be reduced or ruled out through the price mechanism of the insurance market for cars. In better words, the careless car owners will be substituted for the careful car owners in the insurance market for cars, and eventually, the existence of such a market will be ruled out by the market mechanism.

(3) Consequences of Asymmetric Information : The consequences of asymmetric information can be summarized by the following points :

- (i) The market for the commodity with adverse features is substituted by the market for the commodity with favorable features.
- (ii) The market cannot function efficiently or achieve social optimality. It is needful to note that all efficient things are effective, but the converse is not true.
- (iii) The size of the market is reduced or ruled out.
- (iv) In the market with asymmetric information, the exploitation of the "weaker information holder" by the "stronger information holder" is inevitable.
- (v) "Dishonest dealings" tend to drive "honest dealings" out of the market. The "cost of dishonesty" lies not only in the amount by which the purchaser is cheated. The cost also must include the loss incurred from driving legitimate businesses out of existence. Dishonesty in business is a serious problem in underdeveloped countries (Akerlof, 1970).
- (vi) The "high cost of ignorance" will be borne by the weaker informed market participants.
- (vii) In economic exchange or transaction, in which asymmetric information is congealed, the stronger informed participant has the ability to gain more advantage from the exchange, while the weaker informed participant gains less advantage.
- (viii) By analogy of Akerlof (1970), it can be emphasized that asymmetric information may create "illegal markets" (Becker & Wehinger, 2013). Markets are illegal if the product itself or the exchange of it violates legal stipulation. Illegality deprives actors of the legal protection of property rights provided by the state for legal market transactions and limits their access to business strategies and organizational forms. In the absence of a stable legal framework and credible enforcement of contracts, long-term productive investment becomes impossible. "Illegal markets" should not be confused with the "informal economy." Illegal enterprises involve the production and commercialization of goods, which are defined in a particular place and time as illicit, while informal enterprises deal, for the most part, with licit goods. Problems of asymmetric information show up in illegal markets much more forcefully than in legal markets because goods are not subject to administered quality regulations – such as safety regulations and quality standards. The buyer of a counterfeit medication, for instance, has no reliable information on the effective substances in the product. At the same time, suppliers are excluded

from offering the "signals of reputation" used in legal markets. There are no legally enforceable warranties or damage compensation (Beckert & Wehinger, 2013).

(ix) Uncertainty regarding product quality may be accepted by the customer out of either desperation or "deliberate ignorance," which can emerge from a lack of an alternative legal market for the product (e.g. organ transplantation) or a lack of the financial means to buy the licit product (e.g. fake medication). Deliberate ignorance can be expected if the value of the product emerges primarily from symbolic qualities, which are visible to the customer (Beckert & Wehinger, 2013).

(x) Cheating and fraudulent practices undermine the efficiency of the markets.

(4) Remedies for Asymmetric Information - Government vs Market : In order to reduce or rule out the consequences of asymmetric information, a rethinking of the relationship between markets and governments is inevitable. Hence, the crucial question is - what is the role of governments in reducing or ruling out asymmetric information in the markets ?

In a more globalized and complex economy, governments have fewer levers to pull, and these levers are less potent than before. Neither "market fundamentalism" nor "central planning" has worked. Yet, one thing is certain: the choice is not between big government and small government, it is about creating an effective government. What matters is what governments do, not how big they are. The size of governments may well have to shrink. But the responsibilities of governments may well have to expand - to enable, regulate, stabilize, and legitimize markets so they can work better (Menon, 2012).

Cicero's Examples of Asymmetric Information by Walter Miller (1913)

Example 1 : Trade of Grain

In his *On Duties (De Officiis)*, published in 44 BC, Marcus Tullius Cicero (106 - 43 BC) wrote the following passages:

(1) Expediency vs. Moral Rectitude in Business Relations : As I said above, cases often arise in which expediency may seem to clash with moral rectitude, and so, we should examine carefully and see whether their conflict is inevitable or whether they may be reconciled. The following are problems of this sort :

Suppose, for example, it is a time of dearth and famine at Rhodes, with provisions at fabulous prices; and suppose that an honest man has imported a large cargo of grain from Alexandria and that to his certain knowledge also several other importers have set sail from Alexandria, and that on the voyage, he has sighted their vessels laden with grain and bound for Rhodes; is he to report the fact to the Rhodians or is he to keep his own counsel and sell his own stock at the highest market price ? I am assuming the case of a virtuous, upright man, and I am raising the question how a man would think and reason who would not conceal the facts from the Rhodians if he thought that it was immoral to do so, but who might be in doubt whether such silence would really be immoral. (Miller, 1913, p. 319)

(2) Diogenes vs. Antipater : In deciding cases of this kind, Diogenes of Babylonia, a great and highly esteemed Stoic, consistently holds one view; his pupil Antipater, a most profound scholar, holds another. According to

Antipater, all the facts should be disclosed, that the buyer may not be uninformed of any detail that the seller knows ; according to Diogenes, the seller should declare any defects in his wares, in so far as such a course is prescribed by the common law of the land ; but for the rest, since he has goods to sell, he may try to sell them to the best possible advantage, provided he is guilty of no misrepresentation.

"I have imported my stock," Diogenes's merchant will say, "I have offered it for sale ; I sell at a price no higher than my competitors – perhaps even lower, when the market is overstocked. Who is wronged?" (Miller, 1913, pp. 319-321).

(3) Is Concealment of Truth Immoral ? The following extracts have been taken from Miller (1913, pp. 321 - 323):

"What say you?" comes Antipater's argument on the other side :

It is your duty to consider the interests of your fellow-men and to serve society ; you were brought into the world under these conditions and have these inborn principles which you are in duty bound to obey and follow, that your interest shall be the interest of the community and conversely that the interest of the community shall be your interest as well ; will you, in view of all these facts, conceal from your fellow-men what relief in plenteous supplies is close at hand for them ?

"It is one thing to conceal," Diogenes will perhaps reply :

Not to reveal is quite a different thing. At this present moment, I am not concealing from you, even if I am not revealing to you, the nature of the gods or the highest good; and to know these secrets would be of more advantage to you than to know that the price of wheat was down. But I am under no obligation to tell you everything that it may be to your interest to be told.

"Yes," Antipater will say, "but you are, as you must admit, if you will only bethink you of the bonds of fellowship forged by nature and existing between man and man."

"I do not forget them," the other will reply, "but do you mean to say that those bonds of fellowship are such that there is no such thing as private property? If that is the case, we should not sell anything at all, but freely give everything away."

In this whole discussion, you see, no one says, "However wrong morally this or that may be, still, since it is expedient, I will do it." However, the one side asserts that a given act is expedient, without being morally wrong, while the other insists that the act should not be done, because it is morally wrong. (Miller, 1913, pp. 321 - 323)

Example 2 : Sale of House

The following extracts have been taken from Miller (1913, pp. 323 - 325):

(1) A Vendor's Duty :

Suppose again that an honest man is offering a house for sale on account of certain

undesirable features of which he himself is aware but which nobody else knows ; suppose it is unsanitary, but has the reputation of being healthful ; suppose it is not generally known that vermin are to be found in all the bedrooms ; suppose, finally, that it is built of unsound timber and likely to collapse, but that no one knows about it except the owner ; if the vendor does not tell the purchaser these facts but sells him the house for far more than he could reasonably have expected to get for it, I ask whether his transaction is unjust or dishonourable.

"Yes," says Antipater. It is ; for to allow a purchaser to be hasty in closing a deal and through mistaken judgment to incur a very serious loss, if this is not refusing 'to set a man right when he has lost his way' (a crime which at Athens is prohibited on pain of public execration), what is ? It is even worse than refusing to set a man on his way : it is deliberately leading a man astray.

Can you say, answers Diogenes, that he compelled you to purchase, when he did not even advise it ? He advertised for sale what he did not like ; you bought what you did like. If people are not considered guilty of swindling when they place upon their placards FOR SALE : A FINE VILLA, WELL BUILT, even when it is neither good nor properly built, still less guilty are they who say nothing in praise of their house. For where the purchaser may exercise his own judgment, what fraud can there be on the part of the vendor ? But if, again, not all that is expressly stated has to be made good, do you think a man is bound to make good what has not been said ? What, pray, would be more stupid than for a vendor to recount all the faults in the article he is offering for sale ? And what would be so absurd as for an auctioneer to cry, at the owner's bidding, 'Here is an unsanitary house for sale ?'

(2) Cicero's Decision in this Case : The following extract has been taken from Miller (1913, pp. 325 - 327) :

In this way, then, in certain doubtful cases, moral rectitude is defended on the one side, while on the other side, the case of expediency is so presented as to make it appear not only morally right to do what seems expedient, but even morally wrong not to do it. This is the contradiction that seems often to arise between the expedient and the morally right. But I must give my decision in these two cases ; for I did not propound them merely to raise the questions, but to offer a solution. I think, then, that it was the duty of that grain-dealer not to keep back the facts from the Rhodians, and of this vendor of the house to deal in the same way with his purchaser. The fact is that merely holding one's peace about a thing does not constitute concealment, but concealment consists in trying for your own profit to keep others from finding out something that you know, when it is for their interest to know it. And who fails to discern what manner of concealment that is and what sort of person would be guilty of it ? At all events he would be no candid or sincere or straightforward or upright or honest man, but rather one who is shifty, sly, artful, shrewd, underhand, cunning, one grown old in fraud and subtlety. Is it not inexpedient to subject oneself to all these terms of reproach and many more besides ?

(3) Concealment of Truth vs. Misrepresentation and Falsehood : The following extracts have been taken from Miller (1913, pp.327 -329):

If, then, they are to be blamed who suppress the truth, what are we to think of those who actually state what is false? Gaius Canius, a Roman knight, a man of considerable wit and literary culture, once went to Syracuse for a vacation, as he himself used to say, and not for business. He gave out that he had a mind to purchase a little countryseat, where he could invite his friends and enjoy himself, uninterrupted by troublesome visitors. When this fact was spread abroad, one Pythius, a banker of Syracuse, informed him that he had such an estate ; that it was not for sale, however, but Canius might make himself at home there, if he pleased ; and at the same time, he invited him to the estate to dinner next day. Canius accepted. Then Pythius, who, as might be expected of a money-lender, could command favours of all classes, called the fishermen together and asked them to do their fishing the next day out in front of his villa, and told them what he wished them to do. Canius came to dinner at the appointed hour; Pythius had a sumptuous banquet prepared; there was a whole fleet of boats before their eyes; each fisherman brought in turn the catch that he had made; and the fishes were deposited at the feet of Pythius.

"Pray, Pythius," said Canius thereupon, "what does this mean? – all these fish? – all these boats?"

"No wonder," answered Pythius; "this is where all the fish in Syracuse are ; here is where the fresh water comes from ; the fishermen cannot get along without this estate."

Inflamed with desire for it, Canius insisted upon Pythius's selling it to him. At first, he demurred. To make a long story short, Canius gained his point. The man was rich, and, in his desire to own the countryseat, he paid for it all that Pythius asked, and he bought the entire equipment, too. Pythius entered the amount upon his ledger and completed the transfer. The next day, Canius invited his friends ; he came early himself. Not so much as a thole-pin was in sight. He asked his next-door neighbor whether it was a fisherman's holiday, for not a sign of them did he see.

"Not so far as I know," said he, "but none are in the habit of fishing here. And so I could not make out what was the matter yesterday."

(4) Criminal Fraud : The following extract has been taken from Miller (1913, pp. 329 - 331):

Canius was furious; but what could he do ? For not yet had my colleague and friend, Gaius Aquilius, introduced the established forms to apply to criminal fraud. When asked what he meant by "criminal fraud," as specified in these forms, he would reply: "Pretending one thing and practicing another" – a very felicitous definition, as one might expect from an expert in making them. Pythius, therefore, and all others who do one thing while they pretend another are faithless, dishonest, and

unprincipled scoundrels. No act of theirs can be expedient, when what they do is tainted with so many vices.

Then an honest man will not be guilty of either pretence or concealment in order to buy or to sell to better advantage..... We must, therefore, keep misrepresentation entirely out of business transactions : the seller will not engage a bogus bidder to run prices up nor the buyer one to bid low against himself to keep them down ; and each, if they come to naming a price, will state once for all what he will give or take. (Miller, 1913, p.331)

"To conclude, then, it is never expedient to do wrong, because wrong is always immoral; and it is always expedient to be good, because goodness is always moral" (Miller, 1913, p.335).

With this verdict, he established the principle that it was essential to good faith that any defect known to the vendor must be made known to the purchaser. If his decision was right, our grain dealer and the vendor of the unsanitary house did not do right to suppress the facts in those cases. (Miller, 1913, p. 337)

Now reason demands that nothing be done with unfairness, with false pretence, or with misrepresentation. Is it not deception, then, to set snares, even if one does not mean to start the game or to drive it into them ? I find, is neither by custom accounted morally wrong nor forbidden either by statute or by civil law ; nevertheless, it is forbidden by moral law. For there is a bond of fellowship. (Miller, 1913, p. 339)

"It is not in accord with nature that anyone should take advantage of his neighbour's ignorance. And no greater curse in life can be found than knavery that wears the mask of wisdom" (Miller, 1913, p. 343).

If a man knowingly offers for sale wine that is spoiling, ought he tell his customers? Diogenes thinks that it is not required; Antipater holds that an honest man would do so. These are like so many points of the law disputed among the Stoics.

In selling a slave, should his faults be declared – not those only which the seller is bound by the civil law to declare or have the slave returned to him, but also the fact that he is untruthful, or disposed to gamble, or steal, or get drunk ? (Miller, 1913, p. 367)

The one thinks such facts should be declared, the other does not. "If a man thinks that he is selling brass, when he is actually selling gold, should an upright man inform him that his stuff is gold, or go on buying for one shilling what is worth a thousand?" (Miller, 1913, p. 367).

Concluding Comments

Cicero's description of "asymmetric information" is based on the "morality of market," which has been demonstrated by Prasad (1999), and in this sense, Cicero can be credited with the originator of the "Economics of Morality" (Gorga, 2015). Besides, asymmetry of information has been elevated by Cicero from positive to

normative or moral perspective. On the contrary, the five Nobel laureate economists have confined their analysis of asymmetric information within the orbit of positive economics. They also have failed to realize the role of wisdom in the market mechanism. If all the individuals, including the market participants in the world, are equipped with "true wisdom," then asymmetry of information or knowledge will be wiped out from the markets in the capitalist systems. As a result, the existing or persistent market inefficiency will also be wiped out, and then, global capitalism will be sustainable because, "wisdom does not teach our fingers, but our minds" (Hazlitt & Hazlitt, 1984, p. 15). This means that information and/or knowledge may be asymmetric, but wisdom is symmetric or unique. While knowledge has the ability to discover the "causes, consequences and cures" of asymmetry of information in the markets, wisdom demands the "moral justification" of asymmetric information in the markets, since the "morality of market" is backed up by wisdom. Hence, "Cicero's invention of Asymmetric Information in 44 BC" should be included in *An Eponymous Dictionary of Economics: A Guide to Laws and Theorems Named After Economists* by Julio Segura and Carlos Rodriguez Braun (2004).

The complementary relationship among teaching, learning, and research will question or challenge the "established knowledge or ideas," which will induce the research-intensive teachers to invent "new knowledge or ideas" by their research activities. The new knowledge or ideas realized from the research activity will encourage the teachers to substitute "new curricula" for "established curricula" in the economic education. Thus, the contribution of Cicero as the first predecessor of asymmetric information should be included in the microeconomic textbooks.

The interaction among teaching, learning, and research activities in the future will determine whether *The End of Asymmetric Information* (2001), written by the California University economist James C. Robinson, is inevitable or not (Robinson, 2001).

The Nobel Prize may be treated as the reward for optimal or super-optimal knowledge, but not the reward for optimal or super-optimal wisdom of the researchers.

In the instantaneously electronic communicative society, information and knowledge are increasing at an increasing rate, while wisdom is either decreasing or increasing at a decreasing rate. In such a situation, the prospective researchers should engage themselves to examine the impact of wisdom on market vis-à-vis the impact of market on wisdom in order to reduce or rule out market inefficiency.

An impression persists that market erodes morality. However, San Jose State University economist Fred E. Foldvary (2013) claimed that the market is a system of voluntary exchange, and voluntariness implies morality. Hence, the market is inherently moral.

The limitations of this article are as follows: (a) though it has disclosed the first predecessor of asymmetric information as well as adverse selection, it fails to discover the first predecessor of moral hazard, and (b) it fails to examine the impact of market on wisdom and the impact of wisdom on the market.

By any criterion, the foregoing five Nobel laureate economists were absolutely unaware or ignorant of the contribution of Cicero as the first predecessor of asymmetric information. However, their unawareness or ignorance does not establish the newness of truth.

"Ignorance is the first requisite of the historian – ignorance, which simplifies and clarifies, which selects and omits, with a placid perfection unattainable by the highest art."

....Giles Lytton Strachey (1880-1932), British writer and critic

References

Ackoff, R. L. (1989). From data to wisdom. *Journal of Applied Systems Analysis*, 16(January), 3-9.

- Ackoff, R. L. (1999). *Ackoff's best*. New York : John Wiley & Sons.
- Akerlof, G. A. (1970). The market for "lemons": Quality uncertainty and the market mechanism. *Quarterly Journal of Economics*, 84(3), 488 - 500.
- Baloglou, C. P. (2012). The tradition of economic thought in the Mediterranean world from the ancient classical times through the Hellenistic times until the Byzantine times and Arab-Islamic world. In J. G. Backhaus (ed.), *Handbook of the history of economic thought* (pp. 7 - 91). New York : Springer.
- Beckert, J., & Wehinger, F. (2013). In the shadow: Illegal markets and economic sociology. *Socio-Economic Review*, 11(1), 5 - 30.
- Bellinger, G., Castro, D., & Mills, A. (n.d.). *Data, information, knowledge, and wisdom*. Retrieved from <http://www.systems-thinking.org/dikw/dikw.htm>
- Closson, C. C. (1896). Social selection. *Journal of Political Economy*, 4(4), 449 - 466.
- Cockman, T. (1833). *Cicero's The offices*. New York : J. & J. Harper.
- Cockman, T. (1839). *Cicero's The offices*. New York : Harer & Brothers.
- Editors. (2007). Cicero on the ethics of information asymmetry. *Journal of Political Economy*, 115(4), p 1. DOI : <https://doi.org/10.1086/523904>
- Eliot, T. S. (1934). *The rock*. London: Faber & Faber.
- Erickson, T. (2009). *Knowledge management*. New Delhi: Global Vision Publishing House.
- Faccarello, G., & Kurz, H. D. (Ed.). (2016). *Handbook on the history of economic analysis* (Vol. II). Cheltenham, UK and Northampton, MA, USA: Edward Elgar.
- Fleming, N. D. (1996). *Coping with a revolution : Will the internet change earning ?* (Occasional Paper for Faculty). Lincoln University, Canterbury, New Zealand. Retrieved from http://www.vark-learn.com/documents/Information_and_knowledge.pdf
- Foldvary, F. E. (2013, June 17). *Do markets promote immoral behavior?* Fee. Retrieved from <https://fec.org/articles/how-markets-promote-moral-behavior/>
- Gorga, C. (2015). Economics of morality: Economics of Moses, economics of Jesus. *Mother Pelican: A Journal of Solidarity and Sustainability*, 11(4). Retrieved from pelicanweb.org/solisustv11n04page3.html
- Griffin, M. T., & Atkins, E. M. (eds.) (1991). *Cicero On duties*. Cambridge: Cambridge University Press.
- Hazlitt, F., & Hazlitt, H. (1984). *The wisdom of the stoics : Selections from Seneca, Epictetus and Marcus Aurelius*. London : University Press of America.
- Jeadan, C. (n.d.). *The pitfalls of following nature: Stoic appeals to nature as a normative guideline*. Retrieved from <http://ecpr.eu/Filestore/PaperProposal/5dbf>
- Lombardo, T. (2012). Wisdom, consciousness and the future. *Mother Pelican: A Journal of Solidarity and Sustainability*, 8(1). Retrieved from <http://www.pelicanweb.org/solisustv08n01page6.html>
- Maddala, G. S., & Miller, E. M. (1989). *Microeconomics: Theory and applications*. New York and New Delhi: McGraw - Hill Book Company.

- Menon, R. (2012, June 13). Markets and governments: A historical perspective. *The Globalist*. Retrieved from <https://www.theglobalist.com/markets-and-governments-a-historical-perspective/>
- Miller, W. (1913). *Cicero De officiis*. London : William Heinemann Ltd. and New York: G. P. Putnam's Sons.
- Peabody, A. P. (1887). *Ethical writings of Cicero: De officiis; De senectute; De amicitia, and Scipio's dream*. Boston : Little, Brown & Co.
- Prasad, M. (1999). The morality of market exchange: Love, money, and contractual justice. *Sociological Perspectives*, 42(2), 181 - 213.
- Robinson, J. C. (2001). The end of asymmetric information. *Journal of Health Politics, Policy and Law*, 26(5), 1045 - 1053.
- Rosser, Jr. J. B. (2003). A Nobel Prize for asymmetric information: The economic contributions of George Akerlof, Michael Spence, and Joseph Stiglitz. *Review of Political Economy*, 15(1), 3 - 21.
- Segura, J., & Braun, C. R. (eds.) (2004). *An eponymous dictionary of economics: A guide to laws and theorems named after economists*. Cheltenham, UK and Northampton, USA: Edward Elgar.
- Stigler, G. J. (1961). The economics of information. *Journal of Political Economy*, 69(3), 213 - 225.
- Stigler, S. M. (1980). Stigler's law of eponymy. *Transaction of the New York Academy of Sciences*, 39(1), 147 - 157.

About the Author

Arup Kanti Konar has acquired his Ph.D degree from IGNOU, New Delhi. His research interest and publications are not confined to economics discipline only. He is the member of the editorial board of more than seven national and international journals.

Published on the 5th and 6th Day of Every Two Months
Registered with the Registrar of Newspapers under Regd. No. DELENG/2012/43957

Printed and Published by Satya Gilani on behalf of Associated Management Consultants (P) Ltd. Y-21, Hauz Khas, New Delhi-110016 and Printed at M. S. Printers, C-108/1 Back side, Naraina Industrial Area, Phase - 1, New Delhi - 110028 and Published at Y-21, Hauz Khas, New Delhi-110016. Editor : Satya Gilani.

ISSN 2278 - 1811

IC Value (2018) = 83.44

NAAS Score = 2.77

Indexed in Indian Citation Index (ICI)

₹ 300/-

ARTHSHAstra INDIAN JOURNAL OF ECONOMICS & RESEARCH

VOLUME : 8

ISSUE NUMBER : 6
(BI - MONTHLY)

NOVEMBER - DECEMBER 2019

In This Issue

**How Interdisciplinary is Interdisciplinary
Economics?**

Arup Kanti Konar

**Debating Investment Led Demand
and Demand Led Investment**

Rajiv Khosla

**Impact of Agglomeration Economies
on Productivity of Pharmaceutical
Firms of Himachal Pradesh**

Himanshu

Dilasha Anand

**Grey Relational Analysis of the
Determinants of Direct Sales
of Food Crops in India**

Kishor Chandra Sahu

M. V. Ramana Murthy

B. Sasidhar

How Interdisciplinary is Interdisciplinary Economics?

Arup Kanti Konar¹

Abstract

Interdisciplinarity of economics still proliferates. Interdisciplinary colonization can be substituted for simply interdisciplinarity. Interdisciplinarity of economics can be translated or mapped into the fact that economics is colonizing (or imperialising) and being colonised by non-economics disciplines in the name of interdisciplinary economics. Evidence indicates that colonization of economics by non-economics discipline(s) is more powerful than colonization of non-economics discipline(s) by economics.

Keywords: economics, discipline, interdisciplinarity, colonisation, imperialism

JEL Classification: A12, A19, Y80, Z1

Paper Submission Date : November 1, 2019 ; Paper sent back for Revision : November 13, 2019 ; Paper Acceptance Date : December 1, 2019

"All the human sciences interlock and can always be used to interpret one another : their frontiers become blurred, intermediary and composite disciplines multiply endlessly, and in the end, their proper object may even disappear altogether" (Foucault, 1970, p. 357).

Only the title of the *Journal of Interdisciplinary Economics*, which is being published by SAGE since 1985, has induced me to write this article. Further, the title of an article by Mark Blaug (2001), "No History of Ideas, Please, We're Economists" encouraged me to shorten this article. Blaug (2001) clearly warned against too excessive emphasis upon history of ideas and against too little regard for the discussion about the core ideas in the article. Perhaps, John Kenneth Galbraith once said: Economists are most economical with ideas. The shortest article ever published in an economics journal was written by Cook (1972): A "one line" proof of the Slutsky equation, which had about 350 words including four equations.

This short article has been written to disclose that economics as an academic discipline is colonising (or imperialising) and is being colonised by non-economics academic disciplines in the name of interdisciplinary economics.

By any criterion, economics has acquired the status of interdisciplinarity. Secondly, economics has multitude of interdisciplinarity, which can be classified into two sets: (a) Set of X economics, where the prefix X stands for disciplinary adjective or noun (e.g. geographical economics or family economics) and (b) Set of economic Z, where the suffix Z stands for disciplinary noun (e.g. economic sociology). Thirdly, interdisciplinarity of economics still proliferates.

The relevant examples of the Set of X economics are alphabetically as follows: A : agricultural economics, anthropological economics, architectural economics, astronomical economics, aviation economics ; B : behavioural economics, biological economics, biomass economics, bioenergy economics, biophysical economics, business economics ; C : caring economics, civilian economics, climatological economics, complexity economics, communicative economics, communist economics, computational economics, conflict

¹ Principal & Associate Professor of Economics, Achhraram Memorial College, Jhalda, Purulia - 723 202, West Bengal. E-mail : akkonar@gmail.com

DOI : 10.17010/ajjer/2019/v8i6/150839

economics, consumer economics, cosmological economics (cosmoeconomics), criminological economics, cultural economics ; D : dairy economics, defence economics, degrowth economics, demographical economics, development economics ; E : ecological economics, econometrics, education economics, energy economics, engineering economics, entrepreneurial economics, entomological economics, environmental economics, ergodicity economics, ergonomic economics, ethical economics, evolutionary economics ; F : family economics, financial economics, feminist economics, forensic economics, forestry economics ; G : genoconomics, geoeconomics, geographical economics, geological economics, growth economics, green economics, gender economics ; H : happiness economics, health economics, hermeneutical economics, humanistic economics, human resource economics ; I : ideological economics, industrial economics, information economics, infrastructural economics, innovation economics, institutional economics ; L : labour economics, land economics, law economics, library economics, local economics ; M : mathematical economics, managerial economics, medical economics, mental health economics, metaphysical economics, military economics, mineral economics, monetary economics, moral economics, mythological economics ; N : neurological economics, neurophysiological economics, neuropsychological economics ; O : oceanographic economics ; P : pathological economics, participatory economics, peace economics, philosophical economics, physical economics (or physioeconomics), physiological economics, poor economics, psychophysiological economics, political economics, psychological economics, public economics ; R : regional economics, regulatory economics, religious economics, resource economics, rural economics ; S : semiotic economics, sexual economics, social economics, social ecological economics, sociological economics, spiritual economics, sports economics, strategic economics, sustainability economics, systems economics ; T : theological economics, thermoeconomics, transport economics, telecommunication economics ; U : underdevelopment economics, urban economics, underclass economics ; W : warfare economics, welfare economics ; and Z : zoological economics.

On the other hand, the relevant examples of the Set of economic Z are as follows : economic agriculture, economic anthropology, economic archaeology, economic architecture, economic astronomy ; economic biology, economic botany ; economic cosmology ; economic development, economic demography ; econophysics, economic environment, economic ergonomics, economic entomology, economic ethics, economic epidemiology, economic ethnography, economic ethnomusicology ; economic feminism ; economic geography, economic geology, economic growth ; economic happiness, economic health, economic hermeneutics ; economic institution, economic infrastructure ; economic management, economic mythology, economic morality ; economic neurology ; economic oceanography, economic ornithology ; economic politics, economic philosophy, economic psychology ; economic resource, economic religion ; economic sociology, economic sustainability ; economic theology, economic thermodynamics ; economic welfare, economic warfare, and economic zoology.

Now, let us differentiate between X economics (where X stands for disciplinary adjective or noun) and economic Z (where Z stands for disciplinary noun). We are aware of the difference between mathematical philosophy and philosophical mathematics : Mathematical philosophy is the result of mathematisation of philosophy and it emerges from philosophy, while philosophical mathematics is the result of philosophisation of mathematics and it arises from mathematics. Let us, for example, assume that X economics is geographical economics and economic Z is economic geography. In truth, geographical economics, which is the result of geographisation of economics, emerges from economics, but economic geography, which is the result of economisation of geography, arises from geography. Analogously, sociological economics, which is the result of sociologisation of economics, arises from economics, but economic sociology, which is the result of economisation of sociology, emerges from sociology. Thus, X economics, which is the result of Xisation of economics, comes from economics, while economic Z, which is the result of economisation of Z, comes from Z. In better words, X economics (e.g. mathematical economics) or Xisation of economics (e.g. mathematisation of

economics) means colonisation of economics by non-economics discipline(s), while economic Z (e.g. economic biology) or economisation of Z (e.g. economisation of biology) implies colonisation of non-economics academic discipline(s) by economics. From the foregoing examples of Set of X economics and Set of economic Z, it is amply clear that colonisation of economics by non-economics discipline(s) is more powerful than colonisation of non-economics discipline(s) by economics.

Hence, following Balkin (1996), it can be emphasized that interdisciplinarity means colonisation of one (or more) academic discipline(s) by another (or other) academic discipline(s). Let us see what Balkin (1996) actually argued about interdisciplinarity :

"Interdisciplinarity results when different disciplines try to colonise each other. If the takeover is successful, work is no longer seen as interdisciplinary ; rather, it is seen as wholly internal to the discipline as newly constituted" (p. 952).

"Interdisciplinarity is an attempt by disciplines to expand their empires, to colonise and to take over other disciplines by extending their sphere of influence over them" (p. 960).

If this colonisation is sufficiently successful, it will not be understood as colonisation. It will simply be seen as part of the general methodology of the colonised discipline. The old discipline continues to exist, but with a new methodology, a new set of questions for study, or new criteria of Kuhnian normal science. Alternatively, the colonised discipline will simply seem to disappear, absorbed into the conquering discipline or reconceptualised as a subspecialty (pp. 960–961).

"There is no reason why a discipline could not be colonising while it is being colonised" (p. 963).

"Moreover, economics has itself been successfully colonised by other disciplines, particularly mathematics and statistics" (p. 963).

"Disciplines colonise primarily not through invaders but through turncoats – that is, through persons trained primarily in the host discipline" (pp. 968–969).

Economic(s) imperialism was first coined by Kenneth Ewart Boulding (1969). But Gray Stanley Becker was the first economic imperialist in the world of economics. Many literatures reveal that economics is imperialising non - economics disciplines. The examples of such literatures can chronologically be given by : (a) Stillman (1955), (b) Brenner (1980), (c) Stigler (1984), (d) Hirshleifer (1985), (e) Radnitzky and Bernholz (1987), (f) Rothbard (1989), (g) Siegers (1992), (h) Udehn (1992), (i) Buckley and Casson (1993), (j) Zaratiegui (1999), (k) Fine (2000), (l) Lazear (2000), (m) Maki (2002), (n) Rubinstein (2006), (o) Fine (2009), (p) Fine and Milonakis (2009), (q) Maki (2009), (r) Kuorikoski and Lehtinen (2010), (s) Brock (2012), (t) Klonschinski (2014), (u) Bogenhold (2016), (v) Pinto (2016), (w) Marchionatti and Cedripi (2017) and (x) Falgueras - Sorrauren (2018).

Further, the imperialism of economics over non - economics disciplines will be evident from the remarks about economics of the following authors :

- (i) Jacob Viner : Economics is what economists do (Boulding, 1941, p.1).
- (ii) Frank Knight : Economists are those who do economics (Bogenhold, 2016, p. 2).
- (iii) H. Geoffrey Brennan : Economics is what economists attempt (Nevile, 1998, p. 132).
- (iv) Robert W. Clower : Economics is a social astronomy (Clower, 1994, p. 807).
- (v) Ariel Rubinstein : Economics is a culture and not a science (Rubinstein, 2008, p. 493).
- (vi) Jack Amariglio, Stephen Resnick, and Richard Wolff : No discipline of economics exists. Or, rather, no unified discipline exists (Amariglio, Resnick, & Wolff, 1990, p. 109).

(vii) Philip Mirowski : Economics is social physics and physics is nature's economics (Mirowski, 1989).

Moreover, the article, "The Superiority of Economists" by Fourcade, Ollion, and Algan (2015) is an ample indication of the imperialism of economics over non-economics disciplines.

However, I am also aware of inverted economic(s) imperialism that is why Duhs (2005) wrote: "Inverting Economic Imperialism..." while Michie, Oughton, and Wilkinson (2002) wrote: "Against the New Economic Imperialism..."

If we are ardent to know the problem of interdisciplinarity of economics or any other discipline, the following literatures may be relevant : Fish's (1989), "Being Interdisciplinary is so Very Hard to do," Balkin's (1996), "Interdisciplinarity as Colonisation," Lynch's (2006) "It's not Easy Being Interdisciplinary," and Graff's (2016), "The Problem of Interdisciplinarity in Theory, Practice and History."

It can be concluded that economics as an academic discipline is colonising and being colonised by non-economics academic disciplines in the name of interdisciplinary economics.

References

- Amariglio, J., Resnick, S., & Wolff, R. (1990). Division and difference in the discipline of economics. *Critical Inquiry*, 17(1), 108–137.
- Balkin, J. M. (1996). Interdisciplinarity as colonization. *Washington and Lee Law Review*, 53(3), 949–970.
- Blaug, M. (2001). No history of ideas, please, we're economists. *Journal of Economic Perspectives*, 15(1), 145–164.
- Bogenhold, D. (2016). *Economics with social sciences : On the 'imperialism of economics' debate and its scientific roots*. In 16th International Conference of the Charles Gide Association for the Study of Economic Thought, 14–16 April 2016, Strasbourg.
- Boulding, K. E. (1941). *The skills of the economist*. Cleveland, OH: Howard Allen Inc Publishers.
- Boulding, K. E. (1969). Economics as a moral science. *American Economic Review*, 59(1), 1–12.
- Brenner, R. (1980). Economics, an imperialist science. *Journal of Legal Studies*, 9(1), 179–188.
- Brock, H. W. (2012, August 12). Larry Summers and the imperialism of economics. *The Globalist*. Retrieved from <https://www.theglobalist.com/larry-summers-and-the-imperialism-of-economics/>
- Buckley, P., & Casson, M. (1993). Economics as an imperialist social science. *Human Relations*, 46(9), 1035–1052.
- Clower, R. W. (1994). Economics as an inductive science. *Southern Economic Journal*, 60(4), 805–814.
- Cook, P. J. (1972). A "one line" proof the Slutsky equation. *American Economic Review*, 62(1/2), 139.
- Duhs, A. (2005). Inverting economic imperialism: The philosophical roots of ethical controversies in economics. *Journal of Interdisciplinary Economics*, 16(3), 323–339.
- Falgueras - Sorrauren, I. (2018). The convoluted influence of Robbins's thinking on the emergence of economics imperialism. *Cambridge Journal of Economics*, 42(5), 1473–1494.
- Fine, B. (2000). Economics imperialism and intellectual progress : The present as history of economic thought. *History of Economic Review*, 32(1), 10–35.

- Fine, B. (2009). A question of economics: Is it colonising the social sciences? *Economy & Society*, 28(3), 403–425.
- Fine, B., & Milonakis, D. (2009). *From economics imperialism to freakonomics: The shifting boundaries between economics and other social sciences*. London: Routledge.
- Fish, S. E. (1989). Being interdisciplinary is so very hard to do. *Profession*, 89, 15–22.
- Foucault, M. (1970). *The order of things: An archaeology of the human sciences*. New York: Random House.
- Fourcade, M., Ollion, E., & Algan, Y. (2015). The superiority of economists. *Journal of Economic Perspectives*, 29(1), 89–114.
- Graff, H. J. (2016). The problem of interdisciplinarity in theory, practice and history. *Social Science History*, 40(4), 775–803.
- Hirshleifer, J. (1985). The expanding domain of economics. *American Economic Review*, 75(6), 53–68.
- Klonschinski, A. (2014). Economic imperialism in health care resource allocation. *Journal of Economic Methodology*, 21(2), 158–174.
- Kuorikoski, J., & Lehtinen, A. (2010). Economics imperialism and solution concepts in political science. *Philosophy of the Social Sciences*, 40(3), 347–374.
- Lazeur, E. P. (2000). Economic imperialism. *Quarter Journal of Economics*, 115(1), 99–146.
- Lynch, J. (2006). It's not easy being interdisciplinary. *International Journal of Epidemiology*, 35(5), 1119–1122.
- Maki, U. (2002). Explanatory ecumenism and economics imperialism. *Economics and Philosophy*, 18(2), 235–257.
- Maki, U. (2009). Economics imperialism: Concepts and constraints. *Philosophy of the Social Sciences*, 39(3), 351–380.
- Marchionatti, R., & Cedrini, M. (2017). *Economics as social science: Economics imperialism and the challenge of interdisciplinarity*. New York & Abingdon, Oxon: Routledge.
- Michie, J., Oughton, C., & Wilkinson, F. (2002). Against the new economic imperialism: Some reflections. *American Journal of Economics & Sociology*, 61(1), 351–365.
- Mirowski, P. (1989). *More heat than light: Economics as social physics: Physics as nature's economics*. Cambridge: Cambridge University Press.
- Nevile, J. (1998). Is value-free economics possible? *History of Economics Review*, 28(Summer), 129–133.
- Pinto, M. F. (2016). Economics imperialism in social epistemology: A critical assessment. *Philosophy of the Social Sciences*, 46(5), 443–472.
- Radnitzky, G., & Bernholz, P. (eds.) (1987). *Economic imperialism: The economic method applied outside the field of economics*. New York: Paragon House Publishers.
- Rothbard, M. (1989). The hermeneutical invasion of philosophy and economics. *Review of Austrian Economics*, 3(1), 45–59.
- Rubinstein, A. (2006). Freak-freakonomics. *Economists' Voice*, December, 1–6. Retrieved from <http://arielrubinstein.tau.ac.il/papers/freak.pdf>

- Rubinstein, A. (2008). Comments on neuroeconomics. *Economics and Philosophy*, 24 (3), 485 – 494.
- Siegers, J. J. (1992). Interdisciplinary economics. *De Economist*, 140(4), 531 – 547.
- Stigler, G. J. (1984). Economics: The imperial science? *Scandinavian Journal of Economics*, 86(3), 301 – 313.
- Stillman, C. W. (1955). Academic imperialism and its resolution: The case of economics and anthropology. *American Scientist*, 43(1), 77 – 88.
- Udehn, L. (1992). The limits of economic imperialism. In, U. Himmelfarb (ed.), *Interfaces in economic and social analysis*. London: Routledge.
- Zaratiegui, J. M. (1999). The imperialism of economics over ethics. *Journal of Markets & Morality*, 2(2), 208 – 219.

About the Author

Dr. Arup Kanti Konar acquired Ph.D. degree from IGNOU, New Delhi. His research interests and publications are not confined to economics discipline only. He is the member of the editorial board of more than seven national and international journals.

Published on the 5th and 6th Day of Every Two Months
Registered with the Registrar of Newspapers under Regd. No. DELENG/2012/43957

Printed and Published by Satya Gilani on behalf of Associated Management Consultants (P) Ltd. Y-21, Hauz Khas, New Delhi-110 016 and Printed at M. S. Printers, C-108/1 Back side, Naraina Industrial Area, Phase - 1, New Delhi - 110028 and Published at Y-21, Hauz Khas, New Delhi-110 016. Editor: Satya Gilani.

শ্রী বিশ্ববিদ্যালয়
মহাকোত্তর বাংলা বিভাগীয়
পত্রিকা



Snatakottar Bangla Bibhagiyo Patrika
Research Journal, Vol-XXI, January, 2020
University Department of Bengali
Ranchi University, Ranchi, 834008
Jharkhand, India

Edited and Published by
Dr. Nivedita Sen
Head, University Department of Bengali
Ranchi University, Ranchi - 834008
Jharkhand, India

Cover
Sohrai, a vibrant Mural art form of
Tribals of Jharkhand

প্রকাশকাল

জানুয়ারি, ২০২০

মুদ্রক

অরুণ চট্টোপাধ্যায়

শ্রীভারতী প্রেস

৮১/৩এ, রাজা এস.সি.মল্লিক রোড,

কলকাতা - ৭০০ ০৪৭

ISSN : 2454-3977

সৃষ্টি

প্রাণীজগৎ ও রবীন্দ্রনাথ কেতকী সর্বাধিকারী ৭
দলিত সাহিত্যের মাইল স্টোন : তিতাস একটি নদীর নাম

সুব্রত কুমার পাল ২০

নির্বাচিত সাহিত্যিকদের দৃষ্টিতে অবিভক্ত বিহার কাকলি সর্বাধিকারী ৩৬

শরৎচন্দ্রের গল্প উপন্যাসে পারিবারিক বিষয় ড. প্রিয়রঞ্জন লাহা ৪৬

রামায়ণ ও আর্ষেতর সমাজ ড. বৈদ্যনাথ কুমার ৫০

মহাশ্বেতা দেবীর ছোটগল্পে আদিবাসী জীবন দীপক পরামণিক ৫৫

ভ্রমণসাহিত্যের বিশিষ্ট শিল্পী বিভূতিভূষণ কঙ্কণ সহিস ৬১

‘সুবর্ণরেণু সুবর্ণরেখা— বিচিত্র মানুষের পদধ্বনি সুশান্ত বেরা ৭২

সুনীল ও নীললোহিতের উপন্যাসে ওপার বাংলার প্রসঙ্গ ও প্রভাব

রিয়া চ্যাটার্জী ৮০

‘বউ ঠাকুরানীর হাট’ এর পারিবারিক সম্পর্কের চিত্র

অসীম কুমার মুখার্জী ৯২

পঞ্চাশের মনস্তর ও নাট্যচর্চায় বিজন ড: তপন মণ্ডল ১০৭

শঙ্করীপ্রসাদ বসুর জীবন ও সাহিত্যকর্ম ড: শেখর রায় ১১৭

ঢাকা জেলার প্রবাদ : প্রসঙ্গ নারী ড. ইয়াসমীন আরা লেখা ১৪১

বরিশাল অঞ্চলের লোকবিশ্বাস-লোকসংস্কার ও বনার বচন

ড. নূর মোহাম্মদ মল্লিক ১৫৮

হাস্যরসের স্বাতন্ত্র্যে প্রভাতকুমার ও পরশুরাম

ড: পীতম ভট্টাচার্য ১৭০

প্রাবন্ধিক প্রমথ চৌধুরী ড. জয়ন্তী ভট্টাচার্য ১৭৬

বহুমাত্রিক সূচিত্রা ভট্টাচার্য ড. সুমিতা মণ্ডল ১৮২

লোকসমাজে ডাইনি-সমস্যা ড. রাজশ্রী মাহাতো ২০২

রবীন্দ্রকাব্যে শিক্ষা-শিক্ষক-শিক্ষার্থী ড. যশোদা বেরা ২১৭

বিভূতিভূষণ বন্দ্যোপাধ্যায়ের নির্বাচিত উপন্যাসে ‘প্রকৃতি’

সংহিতা গাঙ্গুলী ২২৭

নীলদর্পণ একটি সমীক্ষা রূপালী দাস ২৩৫

✓ রবীন্দ্রনাথের ‘মানসী’ কাব্যে নদীর প্রসঙ্গ শুভাশিস গোস্বামী ২৪১

রবীন্দ্রনাথের 'মানসী' কাব্যে নদীর প্রসঙ্গ শুভাশিস গোস্বামী

রবীন্দ্র-কাব্য-প্রবাহে 'মানসী' বিশেষ স্থান অধিকার করে আছে। 'কড়ি ও কোমল' (১২৯৩ বঙ্গাব্দ)-এর বছর চারেক পর প্রকাশিত 'মানসী' (১২৯৭ বঙ্গাব্দ) সমস্ত দিক দিয়েই এক অভিনব কাব্য প্রেরণার ফসল। গতানুগতিকতার পাশ থেকে মুক্ত হয়ে এখানে রবীন্দ্র-কবিপ্রতিভা স্বমহিমায় প্রতিষ্ঠিত হয়েছে। 'সঞ্চয়িতা'-র ভূমিকায় স্বয়ং কবি লিখেছেন, "... আমার আদর্শ অনুসারে ওরা প্রবেশিকা অতিক্রম করে কবিতার শ্রেণিতে উত্তীর্ণ হয়েছে।" ১৯৪০ খ্রিস্টাব্দে লিখিত 'মানসী' কাব্যের 'সূচনা' অংশেও কবি একই মত পোষণ করে লিখেছেন, "কবির সঙ্গে যেন একজন শিল্পী এসে যোগ দিল।" 'মানসী'-তেই রবীন্দ্রনাথের কবিকর্ম প্রকৃত শিল্পমর্যাদা লাভ করেছে, কবি আত্মশক্তিতে দৃঢ় প্রতিষ্ঠিত হয়েছেন। রবীন্দ্র-বিশেষজ্ঞ উপেন্দ্রনাথ ভট্টাচার্যও মনে করেন, "মানসী রবীন্দ্রনাথের প্রথম সার্থক কাব্যসৃষ্টি।" নানা দিক দিয়েই 'মানসী'-তে এসেছে নতুনত্বের স্পর্শ-ভাবনা তথা কল্পনার দিক থেকে, অলংকার রচনায় ও রূপচিত্রণে, ভাষা ও শব্দশক্তির দিক থেকেও। কবির বিকশিত কল্পনার স্পর্শে প্রতিটি সূক্ষ্ম অনুভব ও আবেগ 'মানসী'-তে মূর্ত ও জীবন্ত রূপ পরিগ্রহ করেছে এতে কোনো সন্দেহ নেই। তাই রবীন্দ্রকাব্যধারায় 'মানসী'র বিশিষ্ট স্থান।

'মানসী'র কবিতাগুলি বৈশাখ ১২৯৪ বঙ্গাব্দ থেকে কার্তিক ১২৯৭ বঙ্গাব্দের মধ্যে রচিত। কবিতাগুলি রচনার সময়েও কবি নানা স্থানে ছিলেন; ড. সুকুমার সেনের ভাষায়, "স্বদেশ-বিদেশে, জলে-স্থলে।"

একই ধরনের গতানুগতিক জীবনযাত্রা ও পরিবেশ কবি রবীন্দ্রনাথের কাছে বরাবরই স্বাভাবিক স্ফূর্তির অন্তরায় বলে মনে হয়েছে। জীবনে বহুবার বহুদেশ ভ্রমণ করেছেন, এমনকি বাসাবদলও করেছেন অজস্রবার।

রবীন্দ্রনাথের কাব্যভুবনে বারবার এসেছে বহু নদীর কথা। ব্যক্তিজীবনেও দেখি যে, নিজের শৈশব-কৈশোর বা প্রাক্ক্যৌবনে গঙ্গা বা জাহ্নবীর নিবিড় সান্নিধ্যে এসেছেন

১২
০৪
‘এবং মহুয়া’ - বিশ্ববিদ্যালয় মঞ্জুরী আয়োগ (UGC-CARE)

অনুমোদিত তালিকার অন্তর্ভুক্ত।

পত্রিকা ক্রমিক নং-৯৬ (ভারতীয় ভাষার ১১৪টির মধ্যে),

বাংলা, কলা বিভাগের পত্রিকা ক্রমিক নং-৩২।

এবং মহুয়া

(বাংলা ভাষা, সাহিত্য ও গবেষণার্থী মাসিক পত্রিকা)

২২ তম বর্ষ, ১১৬ (বিশেষ) সংখ্যা

জানুয়ারী, ২০২০

সম্পাদক

ড. মদনমোহন বেরা

সহসম্পাদক

অভীক প্রধান

যোগাযোগ :

ড. মদনমোহন বেরা, সম্পাদক।

পোলকুয়াচক, পোষ্ট-মেদিনীপুর, ৭২১১০১, জেলা-প.মেদিনীপুর, প.বঙ্গ।

মো.-৯১৫০১৭৭৬৫০

কে.কে. প্রকাশন

পোলকুয়াচক, মেদিনীপুর, পশ্চিমবঙ্গ।

১. এই চরিত্রের অধ্যয়নের :: সঞ্জিতা ঘোষ..... ২২৩

২. সত্যজিৎ রায়ের 'সত্যজিৎ রায়ের চরিত্র' :: শীলমাণী সান্নাধ্যায়..... ২২৬

৩. 'নৃত্যের অঙ্গন চরিত্র' :: শত মোকবিলার কাণ্ডারী..... ২৩২

৪. 'অন্তিম শীট'..... ২৪২

৫. 'উপন্যাসের পাঠ্যসংকলন' :: প্রমোদ রায়..... ২৪৬

৬. 'অমিতা' :: এক বিদ্রোহী নারী চরিত্র :: অনিমেষ সরকার..... ২৪৬

৭. 'সুখের ও অমিতা' :: এক জাহেই জম্মাভূতের গল্প..... ২৫৩

৮. 'সুখের ও অমিতা' :: এক জাহেই জম্মাভূতের গল্প..... ২৫৩

৯. 'অমিতা কুমার বানার্জী'..... ২৬২

১০. 'জান্নেত অরব' এর আলোকে রাজা ওইনিপোস-এক ট্রাজিক চরিত্র..... ২৬৯

১১. 'শূন্যের মুহূর্ত' প্রকরণে পাত্র-পাত্রীদের নামনির্বাচনের সার্থকতা..... ২৭০

১২. 'কনকলের কলমে আফসোসজনী 'তান': চরিত্রমূলক..... ২৮২

১৩. 'নেকাশী' :: হস্তির এক অনবদ্য সৃষ্টি..... ২৮৬

১৪. 'চলবে' :: ঐতিহ্যের অনুসরণে বিনির্ভিত চাঁদ চরিত্র..... ২৯০

১৫. 'বাল্য কবিতার 'বাবা' যখন চরিত্র..... ২৯৯

১৬. 'রবীন্দ্র জীবন ও সাহিত্যে ঠাকুরবাড়ির নারী..... ৩০৪

১৭. 'অশপূর্ণের 'সত্যবতী' :: মুক্তি চেতনা প্রতিবাদের নারী-জিহ্বা..... ৩১০

১৮. 'রামকুমার মুখোপাধ্যায়ের 'দুখে কেণ্ডা' উপন্যাস ::..... ৩১৬

১৯. 'অশপূর্ণের 'সত্যবতী' :: মুক্তি চেতনা প্রতিবাদের নারী-জিহ্বা..... ৩২৭

২০. 'অশপূর্ণের 'সত্যবতী' :: মুক্তি চেতনা প্রতিবাদের নারী-জিহ্বা..... ৩৩০

'আরণ্যক'-এর 'সরলা বন্য মেয়ে' : মঞ্চী ড. শান্তনু ভট্টাচার্য

বিভূতিভূষণের জনপ্রিয় উপন্যাসগুলির মধ্যে 'আরণ্যক' একটি। 'আরণ্যক' গ্রন্থাকারে প্রকাশের পূর্বে 'প্রবাসী' পত্রিকায় কার্তিক (১৩৩৪ বঙ্গাব্দ) সংখ্যায় প্রথম প্রকাশিত হয় এবং শেষ হয় ফাঘুন (১৩৪৫ বঙ্গাব্দ) সংখ্যায়। পরে গ্রন্থাকারে প্রকাশিত হয় ১৯৩৯ খ্রিস্টাব্দে। পরবর্তীকালে ভারতের প্রায় প্রত্যেকটি আঞ্চলিক ভাষায় এই গ্রন্থের অনুবাদ হয়— যা গ্রন্থটির সর্বজনগ্রাহ্যতা ও জনপ্রিয়তার পরিচায়ক। 'আরণ্যক' উপন্যাসের একটা বাস্তব প্রেক্ষাপট আছে। দিনপঞ্জি 'স্মৃতির রেখা' (১৯৪১ খ্রিঃ)-র বিভূতিভূষণ লিখেছেন— "এই জঙ্গলের জীবন নিয়ে একটা কিছু লিখবো— একটা কঠিন শৌর্যপূর্ণ, গতিশীল, ব্রাত্যজীবনের ছবি। এই বন, নির্জনতা, ঘোড়ায় চড়া, পথ হারানো— অন্ধকার— এই নির্জনে জঙ্গলের মধ্যে খুপরি বেঁধে থাকা। মাঝে মাঝে, যেমন আজ গভীর বনের নির্জনতা ভেদ করে যে ঠুঁড়ি পথটা ভিটে-টোলার বাথানের দিকে চলে গিয়েচে দেখা গেল, ঐ রকম ঠুঁড়ি পথ এক বাথান থেকে আর এক বাথানে যাচ্ছে— পথ হারানো, রাতের অন্ধকারে জঙ্গলের মধ্যে ঘোড়ায় করে ঘোরা, এদেশের লোকের দারিদ্র্য, সরলতা, এই *virile, active life*, এই সক্র্যার অন্ধকারে ভরা গভীর বন, ঝড়বনের ছবি— এই সব।" (১২.০২.১৯২৮)— তাই বলা ভালো, বাস্তব অভিজ্ঞতাকে উপজীব্য করে প্রকৃতি ও মানুষের ঐকতানে এক বিচিত্র এবং বিস্ময়কর সৃষ্টি বিভূতিভূষণের 'আরণ্যক'। বিশিষ্ট সমালোচকের মতে, "প্রকৃতির যে সূক্ষ্ম কবিত্বপূর্ণ অনুভূতি বিভূতিভূষণের উপন্যাসের গৌরব তাহা এই উপন্যাসে চরম উৎকর্ষ লাভ করিয়াছে। প্রকৃতি এখানে মুখ্য, মানুষ গৌণ। সীমাহীন অরণ্য প্রকৃতি লেখকের মন ও কল্পনাকে পূর্ণভাবে অধিকার করিয়াছে। ইহার প্রতি ঋতুতে, দিবা-রাত্রির প্রহরে প্রহরে, জ্যোৎস্না-অন্ধকারের বিভিন্ন পটভূমিকায়, পরিবর্তনশীল রূপ ও সূক্ষ্ম আবেদন আশ্চর্যরূপ বস্তুনিষ্ঠা ও কাব্যব্যঞ্জনার সহিত বর্ণিত হইয়াছে। সর্বোপরি ইহার সমস্ত পরিবর্তনশীলতার মধ্যে এক সুগভীর, অপরিমেয় রহস্যবোধ অবিচল কেন্দ্রবিন্দুর ন্যায় স্থির হইয়া আছে। প্রকৃতির এই ইন্দ্রজাল লেখক কত নিবিড় ও বিচিত্রভাবে অনুভব করিয়াছেন তাহা ভাবিলে বিস্মিত হইতে হয়।" বিভূতিভূষণের মতে, 'আরণ্যক' কোনো কল্পিত বিষয় নয়, লেখকের নিজের অভিজ্ঞতারই কথা এবং সেই অভিজ্ঞতাকেই সত্যচরণের মধ্য দিয়ে গল্পের ছলে বর্ণনা করা। সত্যচরণ উপন্যাসটির বন্ধন সূত্র রূপে নানা চরিত্র ও নানা উপখ্যানকে একত্রে বেঁধেছে। 'আরণ্যক' এক অর্থে চরিত্রের জাদুঘর। নানা চরিত্র তাদের নানা মাত্রা নিয়ে উপস্থিত হয়েছে। কত বিচিত্র তাদের

'এবং মত্হয়া' -বিশ্ববিদ্যালয় মঞ্জুরী আয়োগ (UGC-CARE)

অনুমোদিত তালিকার অন্তর্ভুক্ত।

পত্রিকা ক্রমিক নং-৯৬ (ভারতীয় ভাষার ১১৪টির মধ্যে),

বাংলা, কলা বিভাগের পত্রিকা ক্রমিক নং-৩২।

এবং মত্হয়া

(বাংলা ভাষা, সাহিত্য ও গবেষণামূলী মাসিক পত্রিকা)

২২ তম বর্ষ, ১২১ সংখ্যা

মে, ২০২০

সম্পাদক

ড. মদনমোহন বেরা

যোগাযোগ :

ড. মদনমোহন বেরা, সম্পাদক।

গোলকুঁয়াচক, পোষ্ট-মেদিনীপুর, ৭২১১০১, জেলা-প.মেদিনীপুর, প.বঙ্গ।

মো.-৯১৫৩১৭৭৬৫৩

কে.কে. প্রকাশন

গোলকুঁয়াচক, মেদিনীপুর, পশ্চিমবঙ্গ।

৪৩ আধুনিক রাজনৈতিক ও সামাজিক সভ্যতার বিকাশে বুদ্ধদেব ও রবীন্দ্রনাথ : একটি দার্শনিক পর্যালোচনা	৩৩৪
:: ড. গৌতম কুমার ঘোষ.....	
৪৪ ম্যাজিক রিয়ালিজমের প্রেক্ষিত	৩৪১
:: ড. নির্মল কুমার বর্মণ.....	
৪৫ মহাশ্বেতা দেবীর ছোটগল্পে প্রান্তিক জনজীবন চিত্র	৩৪৫
:: ড. মনমোহন গুরু.....	
৪৬ আদিবাসী সমাজে বিপন্ন শৈশব	৩৫৮
:: ড. মঙ্গল কুমার নায়ক.....	
৪৭ বাঁকুড়া জেলার আদিবাসী সমাজ ও সংস্কৃতি	৩৭০
:: ড. সুমন্ত মণ্ডল.....	
৪৮ নীরেন্দ্রনাথ চক্রবর্তীর কবিতায়সময়, সমাজ ও মানুষ	৩৮২
:: ড. শর্মিষ্ঠা আচার্য.....	
৪৯ কবি মনোহর দাসের 'অনুরাগবল্লী'	৩৮২
:: ড. শান্তনু ভট্টাচার্য.....	
৫০ নজরুলের ছোটগল্পে নারী পরিসর	৩৯৭
:: ড. সারদাব্রত লাহা.....	
৫১ রঙ্গলালের স্বদেশীয় সাহিত্যানুরাগ : প্রসঙ্গ বাঙ্গালা কবিতা প্রবন্ধ	৪০৪
:: ড. নরেন্দ্র নাথ রায়.....	
৫২ কবি গণেশ বসু আজও দশপ্রহরণ হাতে হাতে তুলে দেয়	৪১০
:: ড. জয়গোপাল মন্ডল.....	
০০লেখক পরিচিতি.....	৪১৮
০০০UGC--CARE list.....	৪২১-৪২২

কবি মনোহর দাসের 'অনুরাগবল্লী'

ড. শান্তনু ভট্টাচার্য

শ্রীচৈতন্যের তিরোধানের পর বিভিন্ন বৈষ্ণব আশ্রম এবং সেই সকল আশ্রমের প্রধান তথা মহাপ্রভদের কেন্দ্র করে বিচিত্র ধারায় বৈষ্ণব-আন্দোলন গতি পেতে থাকে। এইসব বৈষ্ণব কেন্দ্রিক স্ফুটন কোন ইতিহাস চৈতন্যসমকালে লেখা হয়নি। পরবর্তীকালে মহাপ্রভু গণের প্রবল প্রতিপত্তি এবং ধর্ম নিপুণের তাঁদের গুরুত্বপূর্ণ ভূমিকার কথা সম্ভবত জনসাধারণে প্রচারের জন্যে মহাপ্রভু-চরিতের আবির্ভাব। এই মহাপ্রভু-চরিতগুলিতে পাওয়া যায় নির্দিষ্ট এক বা একাধিক গোত্রমণী বা গোত্রমণীসমূহের জীবনকথা, কর্মধারা এবং সংঘের ওপর প্রভাব প্রতিপত্তির কথা। বৈষ্ণব মহাপ্রভু-কেন্দ্রিক চরিতসাহিত্যগুলির নিজস্ব কিছু বৈশিষ্ট্যও লক্ষ্য করা যায়। যথা-কোন একজন মহাপ্রভুর পূর্ণাঙ্গ জীবনী রচনার তুলনায় বিভিন্ন মহাপ্রভুর জীবনের যত যত ঘটনার বর্ণনা প্রদান, গুরু-শিষ্য পরম্পরা বা শাখা বর্ণনা করা, মহাপ্রভদের মাহাত্ম্য প্রতিষ্ঠার উদ্দেশ্যে প্রচুর অলৌকিক ঘটনার সন্নিবেশ ঘটানো এবং বৈষ্ণব সমাজের অগ্রগতিমূলক নানা তথ্য বিপিবদ্ধ করার প্রবণতা। আলোচ্য মনোহর দাসের 'অনুরাগবল্লী' গ্রন্থটি মহাপ্রভু-চরিত সাহিত্যের একটি উৎকৃষ্ট উদাহরণ।

মনোহর দাসের ব্যক্তি পরিচয় সম্পর্কে সাহিত্যের ইতিহাসে খুবই সংক্ষিপ্ত তথ্য পাওয়া যায়। বৈষ্ণবোচিত বিনয়ে কবি হমতো নিজ পরিচয় প্রদানে কাণ্ডার্য করেছেন। তাঁর রচিত 'অনুরাগবল্লী'র অষ্টম মঞ্জরীতে খুব সংক্ষিপ্তভাবে তাঁর আত্মপরিচয় কবি দিয়েছেন। শ্রীনিবাস আচার্যের এক শিষ্য রামচরণ চক্রবর্তী এবং তাঁর শিষ্য রামশরণ চট্টরাজ কবির গুরু ছিলেন। রামশরণ চট্টরাজের পিতা ছিলেন কৃষ্ণদাস চট্টরাজ, ইনি শ্রীনিবাস আচার্যের শিষ্য ছিলেন। কাটোয়ার নিকট বেগুনকোলা গ্রামে গুরু বাড়িতে মনোহর দাস থাকতেন। মনোহর দাস নামটি তাঁর গুরুর দেওয়া বলে কবি উল্লেখ করলেও তাঁর পূর্ব নাম কি ছিল সে বিষয়ে তিনি নীরব থেকেছেন। পরে গুরুর আদেশে কবি বৃন্দাবন চলে যান। বৃন্দাবনে অবস্থান কালেই গুরুর তিরোধান সংবাদ পান কবি। এর অতিরিক্ত আর কোনো তথ্য কবির ব্যক্তি জীবন সম্পর্কে পাওয়া যায় না।

মনোহর দাসের গ্রন্থ পাঠে সহজেই বোঝা যায় যে তিনি শিক্ষাপ্রাপ্তা ছিলেন। বৈষ্ণবশাস্ত্র এবং সাহিত্য সম্পর্কেও তাঁর স্পষ্ট ধারণা ছিল। 'অনুরাগবল্লী'তে সংকলিত নানা সংস্কৃত শ্লোক তাঁর সংস্কৃত জ্ঞানের পরিচয় বহন করে। 'অনুরাগবল্লী'র রচনাকাল বিষয়ক তথ্য কবি কাব্যের অস্ত্রমে দিয়েছেন।

বসুভদ্র কথায়ুক্ত শাকে চৈত্র সিতেমহলে।

বৃন্দাবনে দশমাস্ত্রে পূর্ণানুরাগবল্লিকা। (৮ অষ্টম মঞ্জরী)

৩৮৯ ।। এবং মহায়া-মে, ২০২০

বাঁচি বিশ্ববিদ্যালয়
স্নাতকোত্তর বাংলা বিভাগীয়
পত্রিকা



Snatakottar Bangla Bibhagiyo Patrika
Research Journal, Vol-XXI, January, 2020
University Department of Bengali
Ranchi University, Ranchi, 834008
Jharkhand, India

Edited and Published by
Dr. Nivedita Sen
Head, University Department of Bengali
Ranchi University, Ranchi - 834008
Jharkhand, India

Cover
Sohrai, a vibrant Mural art form of
Tribals of Jharkhand

প্রকাশকাল
জানুয়ারি, ২০২০

মুদ্রক
অরুণ চট্টোপাধ্যায়
শ্রীভারতী প্রেস
৮১/৩এ, রাজা এস.সি.মল্লিক রোড,
কলকাতা - ৭০০ ০৪৭

ISSN : 2454-3977

সূচি

- প্রাণীজগৎ ও রবীন্দ্রনাথ কেতকী সর্বাধিকারী ৭
দলিত সাহিত্যের মাইল স্টোন : তিতাস একটি নদীর নাম
সুব্রত কুমার পাল ২০
নির্বাচিত সাহিত্যিকদের দৃষ্টিতে অবিভক্ত বিহার কাকলি সর্বাধিকারী ৩৬
শরৎচন্দ্রের গল্প উপন্যাসে পারিবারিক বিঘটন ড. প্রিয়রঞ্জন লাহা ৪৬
রামায়ণ ও আর্যেতর সমাজ ড. বৈদ্যনাথ কুমার ৫০
মহাশ্বেতা দেবীর ছোটগল্পে আদিবাসী জীবন দীপক পরামণিক ৫৫
ভ্রমণসাহিত্যের বিশিষ্ট শিল্পী বিভূতিভূষণ কঙ্কণু সহিস ৬১
'সুবর্ণরেণু সুবর্ণরেখা— বিচিত্র মানুষের পদধ্বনি সুশান্ত বেরা ৭২
সুনীল ও নীললোহিতের উপন্যাসে ওপার বাংলার প্রসঙ্গ ও প্রভাব
রিয়া চ্যাটার্জী ৮০
✓ 'বউ ঠাকুরানীর হাট' এর পারিবারিক সম্পর্কের চিত্র
অসীম কুমার মুখার্জী ৯২
পঞ্চাশের মন্বন্তর ও নাট্যচর্চায় বিজন ড: তপন মণ্ডল ১০৭
শঙ্করীপ্রসাদ বসুর জীবন ও সাহিত্যকর্ম ড: শেখর রায় ১১৭
ঢাকা জেলার প্রবাদ : প্রসঙ্গ নারী ড. ইয়াসমীন আরা লেখা ১৪১
বরিশাল অঞ্চলের লোকবিশ্বাস-লোকসংস্কার ও খনার বচন
ড. নূর মোহাম্মদ মল্লিক ১৫৮
হাস্যরসের স্বাতন্ত্র্যে প্রভাতকুমার ও পরশুরাম
ড: পীতম ভট্টাচার্য ১৭০
প্রাবন্ধিক প্রমথ চৌধুরী ড. জয়ন্তী ভট্টাচার্য ১৭৬
বহুমাত্রিক সূচিত্রা ভট্টাচার্য ড. সুমিতা মণ্ডল ১৮২
লোকসমাজে ডাইনি-সমস্যা ড. রাজশ্রী মাহাতো ২০২
রবীন্দ্রকাব্যে শিক্ষা-শিক্ষক-শিক্ষার্থী ড. যশোদা বেরা ২১৭
বিভূতিভূষণ বন্দ্যোপাধ্যায়ের নির্বাচিত উপন্যাসে 'প্রকৃতি'
সংহিতা গাঙ্গুলী ২২৭
নীলদর্পণ একটি সমীক্ষা রূপালী দাস ২৩৫
✓ রবীন্দ্রনাথের 'মানসী' কাব্যে নদীর প্রসঙ্গ শুভাশিস গোস্বামী ২৪১

‘বউ ঠাকুরানীর হাট’ এর পারিবারিক সম্পর্কের চিত্র অসীম কুমার মুখার্জী

ঐতিহাসিক উপাদানে সমৃদ্ধ ‘বউ ঠাকুরানীর হাট’ উপন্যাসটি ইতিহাস থেকে উপাদান গ্রহণ করে রবীন্দ্রনাথ ঠাকুর রচনা করেন। বঙ্কিমচন্দ্র চট্টোপাধ্যায় যখন বাংলা সাহিত্যাকাশে উজ্জ্বল নক্ষত্রের মতো দীপ্যমান তখন রবীন্দ্রনাথ ঠাকুর গোধুলির স্নান অন্তাচলগামী সূর্যের আভার মতো রশ্মি নিয়ে আবির্ভূত হন বাংলা উপন্যাস সাহিত্যের জগতে। বঙ্কিমচন্দ্র উপন্যাসের শ্রেণি বিন্যাসের ধারায় সফল ঐতিহাসিক উপন্যাসকার। তবে শুধু ঐতিহাসিক নয়, সামাজিক গোত্রের প্রণেতাও। তখন ইতিহাস অবলম্বনে গ্রন্থ রচনা প্রায় একটি রীতি হয়ে দাঁড়িয়েছিল। তাই তৎকালীন সকল সাহিত্যকার এই ইতিহাস অবলম্বনে গ্রন্থ রচনা করেছিলেন। রবীন্দ্রনাথ ঠাকুরও এই রীতির বাইরে যেতে পারেননি। সফল উপন্যাসকার হিসেবে বঙ্কিমের প্রতিষ্ঠাকালে ঔপন্যাসিক রবীন্দ্রনাথের আবির্ভাব। বঙ্কিম-যুগে আবির্ভূত হয়েও তিনি ঐতিহাসিক উপন্যাস রচনার মতো সাহসী পদক্ষেপ গ্রহণ করেছিলেন। ‘বউ ঠাকুরানীর হাট’ তার নিদর্শন।

‘বউ ঠাকুরানীর হাট’ গ্রন্থটি ঐতিহাসিক গোত্রের হলেও পারিবারিক সম্পর্কের মধ্যেই আবদ্ধ সমস্ত চরিত্রগুলি। ইতিহাসের উপাদান-সমৃদ্ধ হলেও গ্রন্থটিতে মূলত স্থান পেয়েছে প্রতাপাদিত্যের পরিবার ও পিতৃব্য বসন্তরায় ও জামাতা রামচন্দ্রের কাহিনি। হনু সঙ্কুল ঘটনার টানা পোড়েনে প্রতাপাদিত্যের পরিবারের অন্তরমহলের ছবি এই উপন্যাসে উদ্ভাসিত। তাই উপন্যাসটি ইতিহাসাশ্রিত হলেও পারিবারিক সম্পর্কের উর্ধে নয়। প্রতাপাদিত্যের পিতা বিক্রমাদিত্যের মৃত্যু হলে বসন্ত রায় ছোট বালক প্রতাপাদিত্যকে মানুষ করেন। বার্ষিক্যে উপনীত হয়ে মোঘলের সঙ্গে সখ্য স্থাপন করে রাজ্যে শান্তি প্রতিষ্ঠা করেন। সৈন্যরা তলোয়ার ছেড়ে লাঙল ধরে চাষবাস করতে থাকে। গান বাজনা নিয়ে বসন্ত রায় চারিদিক আনন্দ হিল্লোলে পরিপূর্ণ করে রাখতেন। লেখকের পরিকল্পনায় ইতিহাসের সঙ্গে আরও অনেক উপাদান মিশে ‘বউ ঠাকুরানীর হাট’ উপন্যাসের বসন্ত রায় চরিত্রটির সৃষ্টি হয়েছে। ‘জীবন স্মৃতি’-তে শ্রীকণ্ঠ সিংহের বর্ণনা প্রসঙ্গে রবীন্দ্রনাথ লিখেছেন —

शोध, समीक्षण, सृजन एवं संचार का

मुक्तांचल

त्रैमासिक

वर्ष-6, अंक- 24, अक्तूबर-दिसम्बर 2019

संपादक : डॉ. पीरा सिन्हा
अतिथि संपादक : डॉ. शुभा उपाध्याय
प्रकाशक : आनंद कुमार सिन्हा
कला संपादक : शुभागता श्रीवास्तव
संपादकीय सहयोग : सुलेखा कुमारी एवं परमजीत पंडित
आकल्पक : सोनू प्रजापति

व्यवस्थापन एवं प्रबंधन :

विनोता लाल, सुशील कुमार पाण्डे, विनोद यादव, पार्वती शां.,
शुभा उपाध्याय, गुडिया राय, विद्या रजक एवं नगीना लाल दास।

परामर्श एवं विशेष सहयोग :

प्रो. शशि मुदीराजः प्राक्तन अध्यक्ष, हिंदी विभाग,
सेन्ट्रल यूनिवर्सिटी, हैदराबाद

प्रो. अरुण होताः अध्यक्ष, हिंदी विभाग, स्टेट यूनिवर्सिटी, बारासात

प्रो. मुक्तेश्वर नाथ तिवारीः विश्व भारती, शांति निकेतन

प्रो. दामोदर मिश्रः अध्यक्ष, हिंदी विभाग, विद्यासागर विश्वविद्यालय

प्रो. मनीषा झाः अध्यक्ष, हिंदी विभाग, उत्तर-बंग विश्वविद्यालय

डॉ. पंकज साहाः खड़गपुर कॉलेज, पश्चिम बंगाल

रणजीत सिन्हाः मिदनापुर कॉलेज (ऑटोनोमस), मिदनापुर

निशांतः काजी नजरूल विश्वविद्यालय, आसनसोल

रामप्रवेश रजकः हिंदी विभाग, कलकत्ता विश्वविद्यालय

संपर्क एवं प्रसारः

चौदनी सिन्हा (बर्मिंघम, यू.के.) : +447411412229

मनीष कुमार सिन्हा (दिल्ली) : 9716927587

मधु सिंह (कोलकाता) : 9883613002

संपादकीय कार्यालय :

आधुनिक अपार्टमेंट, 6/2/1 आशुतोष मुखर्जी लेन

सलकिया, हावड़ा-711 106, पश्चिम बंगाल

संपर्कः 0332675 1686, 09831497320

ई-मेलः muktanchalquarterly2014@gmail.com

sinhameera48@gmail.com

लेखकों से अनुरोध किया जाता है कि मुक्तांचल में प्रकाशन
हेतु सामग्री यूनिकोड वर्ड (Unicode Word) या
(Kurtidev010) में भेजें।

मुक्तांचलः A/c- 50200014076551, HDFC BANK
BURRABAZAR, KOLKATA- 700007,
IFSC CODE- HDFC0000219

पत्रिका में व्यक्त विचारों से संपादक को सहमति अनिवार्य नहीं
'मुक्तांचल' से संबंधित सारे विवादों के लिए न्याय-क्षेत्र
कलकत्ता उच्च न्यायालय होगा।

मुद्रकः शिक्षण, 50 सौताराम घोष स्ट्रीट, कोलकाता-700009

'हिंदी कहानी का समकाल' पर केंद्रित

पत्रिका का मूल्य

एक अंक- 50 रुपये

सदस्यता शुल्क : वार्षिक- 200 रुपये, आजीवन-2000 रुपये

संस्थाओं के लिए: वार्षिक- 250 रुपये, आजीवन-2500 रुपये

डाकखर्च (प्रत्येक अंक के लिए) अतिरिक्त 30 रुपये देय होगा।

'केंद्रीय हिंदी संस्थान, आगरा से सहयोग प्राप्त'

हिंदी कहानी में पार्वत्य जीवन का संदर्भ

गीतम सिंह राणा

हिंदी कहानियों में उक्त चर्चित समयतः पार्वत्य समाज कश्मीर, हिमाचल, कुमाऊँ, गढ़वाल व उत्तर-पूर्व के कतिपय उपविभक्ति हिंदी कहानियों में दर्ज है। कश्मीर की पृष्ठभूमि पर लिखने वाले मुख्य कहानीकारों में कृष्णचंद्र, उपेन्द्रनाथ अशक, चन्द्रकांता आदि हैं। हिमाचल की पृष्ठभूमि पर लिखने वाले कहानीकारों में चंद्रधर शर्मा गुलेरी, यशपाल, सुंदर लोहिया, श्रीनिवास श्रीकांत, योगेश्वर शर्मा, कुमार कृष्ण, सुदर्शन बरिष्ठ, मुरारी शर्मा, केशव, एस आर हरनोट आदि का नाम प्रमुखता से लिया जाता है। पार्वत्य जीवन से संबंधित हिंदी में सर्वाधिक कहानियाँ कुमाऊँ तथा गढ़वाल की पृष्ठभूमि पर लिखी गई हैं। इस पृष्ठभूमि पर विपुलता व वैविध्यता के साथ लिखने वाले कहानीकारों में इलाचन्द्र जोशी, यशपाल, रमा प्रसाद धिल्लियाल 'पहाड़ी', शिवानी, शैलेश मटियानी, शेखर जोशी, विद्यासागर नौटियाल, हिमांशु जोशी, रमेशचंद्र शाह, बल्लभ डोभाल, पानू खोलिया, मृणाल पाण्डेय, गंगाप्रसाद विमल, सुभाष पंत, बटरोही, पंकज विष्ट, रणोराम गढ़वाली आदि का नाम प्रमुखता से लिया जाता है। पूर्वोत्तर की पृष्ठभूमि पर लिखने वाले एकमात्र हिंदी कहानीकार अज्ञेय जी रहे हैं।

हिंदी में पार्वत्य जीवन से संबंधित लिखी गई कहानियाँ दो तरह की हैं। पहली तरह की कहानियों में पहाड़ के प्रति रोमानी दृष्टिकोण देखने को मिलता है। इस तरह के कहानीकारों में निर्मल वर्मा प्रमुख हैं। दूसरी तरह की कहानियों में पहाड़ की मनमोहक वादियों के आवरण तले मौजूद खुरदुरे यथार्थ का चित्रण मिलता है। कहने का तात्पर्य है कि वास्तव में यदि हमें पर्वत पर रहने वाले लोगों की संवेदनाओं-समस्याओं से रूबरू होना है तो हमें दूसरी तरह की कहानियों का सम्यक अनुशीलन करना होगा। चूँकि आज कहानी ने अपने आप को छोटे कलेवर के बावजूद मानवीय संदर्भों के साथ जुड़ने का सबसे सशक्त विधा के रूप में स्थापित कर लिया है अतः 'हिंदी कहानी में पार्वत्य जीवन का संदर्भ' की चर्चा के क्रम में दूसरी तरह की कहानियों का अनुशीलन ही समीचीन है।

कश्मीर के पार्वत्य समाज की पृष्ठभूमि पर हिंदी में कम ही कहानियाँ लिखी मिलती हैं और जो उपलब्ध हैं उनमें भी समय के प्रवाह के अनुरूप निरंतरता का अभाव मिलता है। कृष्णचंद्र कृत 'कश्मीर की कहानियाँ' का प्रकाशन वर्ष १९५४ है, जिसमें आजादी से कुछ पहले से लेकर कुछ वर्ष बाद तक के अशांत कश्मीरी समाज के यथार्थ का चित्रण रोमानियत के साथ मिलता है। इस सग्रह में कुल ग्यारह कहानियाँ संकलित हैं, जिसकी भूमिका में कहानीकार लिखते हैं- 'मैंने कश्मीर के सम्बन्ध में बहुत सारी कहानियाँ लिखी हैं। उसके हुस्न के सम्बन्ध में, उसके अदसूरती के सम्बन्ध में, उसके जागीरदाराना माहौल और लूट-खसोट के सम्बन्ध में। ये कहानियाँ मैं बराबर लिखता आया हूँ और आज भी, जब कश्मीर एक अजीब दर्दनाक सूरत-हालत से दो-चार है, मैं कश्मीर से सैकड़ों मील दूर रहकर भी उसके

सम्बन्ध में लिखने पर बजबुर हो गया हूँ। अगली पिछली कहानियों पर नजर डालते हुए मैंने यह महसूस किया है कि एक ऐसे सभ्य को सखा जकरत है जिसमें कश्मीर सम्बन्धी उन तमाम कहानियों को जमा करूँ जो कश्मीर के समाजी जीवन के विभिन्न पहलुओं को चित्रकारी करते हुए आज की परिस्थितियों के प्रतिशोत पहलुओं को उजागर करने में सहायक हो सके। यह सभ्य उम्मी जकरत का नतीजा है। इस सभ्य में मैंने कश्मीर सम्बन्धी कहानियों को इसी ढंग पर रक्खा है। 'शुक्राचर के कहानी सभ्य के बाद कश्मीर को पृष्ठभूमि पर लिखित एक महत्वपूर्ण सभ्य उपेन्द्रनाथ अरक कृत 'कहानी लेखिका और झेलम के सात पुल (१९५७)' है, जिसमें १९५६-५७ तक के समय का चित्रण मिलता है। इन दोनों सभ्य के प्रकाशन के एक अच्छे अंतराल के बाद इस विषय पर चन्द्रकाता कहानियाँ लिखती है। सन् १९७४ में इनके पहले कहानी-सभ्य 'सलाखों के पीछे' का प्रकाशन होता है। १९७४ से लेकर अब तक इनके कुल १३ कहानी-सभ्य आ चुके हैं। कश्मीर की ही आबोहवा में पली बड़ी चन्द्रकाता की कहानियों में वहाँ की सभ्यता और संस्कृति के साथ समसामयिक संदर्भों का बड़ा जीवंत चित्रण मिलता है।

हिमाचली पार्वत्य-पृष्ठभूमि पर पहले पहल कहानी लिखने का श्रेय गुलेरी जो एब यशपाल को जाता है। गुलेरी कृत 'होरे का होरा' में लहना सिंह की काँगड़ा के गाँव में अपने परिवार के पास वापसी दिखाई गई है। इसी प्रकार यशपाल कृत 'तेरह हजार की दुलंदी' की पृष्ठभूमि भी हिमाचल का पार्वत्य प्रदेश है। इन दोनों के बाद इस पृष्ठभूमि पर लिखने वाले महत्वपूर्ण कहानीकार सुंदर लोहिया हैं। इस संदर्भ में उनके द्वारा लिखित 'कालतार' काही चर्चित कहानी-सभ्य रहा है। सुंदर लोहिया के बाद के महत्वपूर्ण कथाकार मूलतः समकालीन कहानीकारों की श्रेणी में आते हैं। इनमें सुदर्शन वशिष्ठ एवं मुरारी शर्मा का नाम मुख्य रूप से आता है। सुदर्शन वशिष्ठ पिछले चार दशकों से हिमाचल केन्द्रित कहानी लेखन का कार्य कर रहे हैं। इनके अब तक १० कहानी-सभ्य प्रकाशित हो चुके हैं। 'सेमल के फूल', 'माणस गंध', 'ऋण का श्वा', 'घोड़ा पुराण', 'दादा का प्रेत', 'कोट',

'बिरादरी बाहर' आदि इनके द्वारा लिखित चर्चित कहानियाँ हैं। इनकी कहानियों की विशेषता है कि ये पार्वत्य पार्वतीय परिवेश से आरंभ होकर कच्चाई, छोटे शहरों की नब्ब टटोलते हुए राजनीति और दफ्तरी जीवन पर भी करारी चोट करती है। मुरारी शर्मा इसी क्रम में आने वाले अग्रणी महत्वपूर्ण समकालीन कहानीकार हैं। इनके अब तक दो कहानी सभ्य प्रकाशित हो चुके हैं - 'बाणपुत्र' और 'पहाड़ पर धूप'। इनकी कहानियों में हिमाचली गहरी लोकधर्मी संवेदनाओं का तानाबाना मिलता है। इनमें हिमाचली समाज में रहने वाले बजतरियों और दलितों के साथ पशुओं जैसा बर्ताव अंधविश्वासों, झूआड़ूत, तथा आर्थिक असमानता की व्यवस्था पर तोखे प्रहार के साथ-साथ बाजारी शक्ति के मजबूत होने के बरक्स पर्वतीय प्रदेश में उत्पन्न पर्यावरणीय संकट की चिंता भी देखने को मिलती है।

हिमाचली पार्वत्य-पृष्ठभूमि पर विपुलता एवं वैविध्यता के साथ लिखने वाले समकालीन कहानीकारों में एस. आर. हरनोट मुख्य हैं। इनकी कहानियों से गुजरते हुए हम अनायास ही बदलते समय के साथ पिछले चार दशकों की हिमाचली घड़कनों को महसूस कर सकते हैं। साथ ही समय के विकास के तदंतर हिमाचली पार्वत्य समाज में बढ़ती मूल्यबोध होना को भी इनकी कहानियों के कैववास पर बड़ी स्पष्टता के साथ चित्रित देख सकते हैं। बीसवीं सदी के नवें दशक से निरंतर सृजनरत इस कथाकार के अब तक कुल आठ कहानी सभ्य - 'पंजा', 'आकाशबेल', 'पीठ पर पहाड़', 'दारोश तथा अन्य कहानियाँ', 'जीनकाठी तथा अन्य कहानियाँ', 'मिट्टी के लोग', 'लिटन ब्लोक गिर रहा है' तथा 'कीलें' प्रकाशित हो चुके हैं। हिमाचल प्रदेश के पार्वत्य क्षेत्र के चनावन गाँव (जिला-शिमला) में जन्मे इस कथाकार ने हिंदी-पाठकों के मन को अपनी कहानियों के मार्फत सबसे ज्यादा आंदोलित किया है क्योंकि बचपन से लेकर अपनी समझदारी की उम्र तक इन्होंने जिस नैसर्गिक-सौन्दर्य-सपन्न पहाड़ी जीवन को जिया और साथ ही उसके खुरदुरे यथार्थ को अनुभूत किया, उसे इन्होंने जस का तस बड़ी कोमलता के साथ अपनी कहानियों में रख दिया है। इस बात को नकारा नहीं जा

शोधार्थी की कलम से

सकता है कि पार्वत्य प्रदेश पर मशीनी सभ्यता के पहुँचने के कारण वहाँ मानवीय संवेदना तथा प्राकृतिक मूल्यबोध को ध्वस्त किया है। वहाँ अमानवीयता, सत्ता को निरंकुशता, साम्प्रदायिकता, बाजारवादी, क्रूर, हिंसक, मनुष्य विरोधी तथा सबसे अधिक प्रकृति को विनष्ट करने वाली ताकतों ने अपने पैठ बना ली है, जिससे पूरे पहाड़ का आसित्व संकट में आ गया है। चूँकि हरनोट अपने समय के सजग प्रहरी है, अतः वे चौकन्ने होकर इन सभी शक्तियों से लड़ने के लिए अपनी कहानियों को बुनावट करते हैं। मशीनी सभ्यता के बढ़ते कदम के बरक्स पहाड़ में आई दरकनों तथा उसके दोहों की शक्तियों को शिनाखा करते हैं और उन्हें अपनी कहानों के मार्फत पेश करते हैं ताकि पहाड़, पहाड़ीपन और उसके नैसर्गिक प्राकृतिक सौंदर्य की रक्षा के लिए विनष्टकारी शक्तियों के विरुद्ध पहाड़ को जनता एक प्रबल प्रतिपक्ष के रूप में खड़ा हो सके। उनको कहानियों की इस विशेषता और उनको सजगता के सन्दर्भ में प्रो. सुरज शालीवाल का कहना है- "हरनोट की कहानियों में पहाड़ केवल पहाड़ के रूप में नहीं अपने पूरे परिवेश के साथ उपस्थित होता है। समय के विकास के साथ भूमंडलोल्लर पहाड़ी जीवन में आये बदलावों, टूटते रिरणों, सांस्कृतिक परिवर्तनों, और स्त्री पुरुष संबंधों के साथ रूढ़ियों की टूटती जड़ों जिस झनझनाहट के साथ हरनोट की कहानियों में आती हैं वे विस्मय उत्पन्न नहीं करती बल्कि यह सोचने को विवश करती है कि हरनोट अपने परिवेश के प्रति कितने सजग है।" २

हिंदी में पार्वत्य जीवन से संबंधित सर्वाधिक कहानियाँ उत्तराखण्ड की पृष्ठभूमि पर लिखी मिलती हैं। इसका मूल कारण हिंदी के विकास काल से ही इस क्षेत्र का संबंध हिंदी पट्टी से रहना है। कुमाउँ जनश्रुतिपरक लोकगीत के बोल "शहर मुरादाबाद, जो हाँ, घूम के आयो व्यापारी।" इस बात को प्रमाणित करता है कि इस क्षेत्र का संबंध व्यापार के मार्फत मुरादाबाद जैसे हिंदी प्रदेश से प्राचीन काल से रहा है। साथ ही उत्तराखण्ड में स्वतंत्रता पूर्व से ही प्रचलित 'काशी-अध्वपन-यात्रा' का प्रसंग भी इस बात को गवाही देता है कि भारत में संस्कृत काल से ही उत्तराखण्ड के अध्वेता ज्ञानार्जन

के उद्देश्य से काशी वास करते थे। इसके अतिरिक्त भौगोलिक दृष्टि से भी यह प्रदेश हिंदी-पट्टी से काफ़ी निकट होने के कारण भी यहाँ हिंदी साहित्य का प्रचार-प्रसार अन्य पार्वत्य प्रदेशों की तुलना में अधिक हुआ है।

उत्तराखण्ड के पार्वत्य जीवन से संबंधित कहानीकार एवं कहानियों को भाषा व सांस्कृतिक भूगोल की दृष्टि से दो वर्गों में बाँटकर देखना सही होगा। पहले वर्ग के अन्तर्गत उत्तराखण्ड का पश्चिमी हिस्सा गढ़वाल क्षेत्र से संबंधित कहानीकार एवं उनको कहानियों को देखा जा सकता है। इसके अन्तर्गत आने वाले महत्वपूर्ण कहानीकारों में रमा प्रसाद पिल्लियाल 'पहाड़ी', बल्लभ डोभाल, गंगा प्रसाद विमल, सुभाष पंत, विद्यासागर चौटियाल का नाम आता है। इस पृष्ठभूमि पर गंधेराता के साथ लिखने वाले प्रथम महत्वपूर्ण कहानीकार 'पहाड़ी' जी हैं। इनके गढ़वाली पार्वत्य समाज में निहित गरीबी, दलित शोषण, स्त्री शोषण आदि विषयों पर केंद्रित कुल पंद्रह कहानी संग्रह हैं। इनकी कहानियों में निहित इन संदर्भों के महत्व पर बात करते हुए गंगा प्रसाद विमल ने कहा है- 'विश्व के सर्वाधिक अंधेरे कोने, गढ़वाल में जन्मे, साधनहीन, वातावरण ने सृजेता के मनोलोक में विपन्नता के चित्रों ने अमिट प्रभाव छोड़ा। उन्हीं के समकालीन चन्द्र कुंवर वर्तवाल ने स्वयं अपने प्रामाणिक अनुबोध द्वारा दरिद्रता, दासता, और सांस्कृतिक औदास्य को परिव्याप्ति वाले क्षेत्र में निपट पिछड़ेपन का जो त्रासदायक अनुभव अपने काव्य सृजन में व्यक्त किया वह रमा प्रसाद पिल्लियाल 'पहाड़ी' को पर्वतीय होने के कारण सहज ही सृजनात्मक पीठिका के रूप में उपलब्ध था और उन्होंने उसी सूत्र के सहारे दरिद्र, दलित और स्त्री या अबला जैसे पक्षों को अपने सृजनात्मक कर्म के प्रमुख चुने जो इक्कीसवीं शताब्दी के आरंभ में साहित्यिक विमर्श के परिपक्व व केंद्रीय विषय बने और एक तरह से प्रवृत्ति सूचक सूत्रों के रूप में याद किए जाते हैं।' ३ 'पहाड़ी' जी के बाद इस पृष्ठभूमि पर बड़ी सजीदगी से लिखने वाले समकालीन कहानीकार सुभाष पंत हैं। इनके अब तक कुल सात कहानी-संग्रह प्रकाशित हो चुके हैं- 'तपती हुई जमीन (१९७७)', 'चौक के बाप की मौत (१९८०)',

शोधार्थी की कलम से

इसकी कहानियाँ (१९९७)', 'जिव और अन्य कहानियाँ (२००२)', 'मुंबोबाई की धारणा' (२००२), 'एक का पहाड़' (२००९) और 'छोटा होता हुआ आदमी' (२०१०)। इनकी कहानियों के केन्द्र में व्यवस्था को चक्को में पिघला पर्वतीय आप आदमी है। इस संदर्भ पर सुधास पंत के अलावे लिखने वाले कहानीकारों में विद्यासागर नैटिवाल का नाम आता है। इनके अब तक दो कहानी-संग्रह प्रकाशित हो चुके हैं- 'टिहरी की कहानियाँ' (१९८५) एवं 'मुच्चो होर' (२००५)। इन्होंने अपनी कहानियों में गढ़वाले पार्वत्य जीवन के संघर्ष को, उसकी अटप्ट जिजीविषा को, तमाम प्रवर्तित मिथकों, किंवदंतियों, रुद्रियों, अर्धावस्थाओं को एक नई कथा-शैली एवं प्रविधि के साथ बड़ी जीवन्ता व मार्मिकता के साथ उठाया है।

उत्तराखण्ड के पार्वत्य जीवन से संबंधित दूसरे वर्ग के कहानीकारों का संबंध इसके परिवर्तित हिस्से कुमाउँ प्रदेश के साथ है। इस वर्ग के अनर्गत आने वाले महत्वपूर्ण कहानीकारों में शिवानी, शैलेश मटियानी, शेखर जोशी, बटरोही, पंकज विष्ट, रणोराम गढ़वाली आदि का नाम प्रमुखता से लिया जाता है। कुमाउँ के पार्वत्य के संदर्भ में स्त्री अस्मिता के संकट का चित्रण शिवानी की कहानियाँ विशेष महत्वपूर्ण हैं। इसी प्रकार यहाँ के टॉल्लि प्रसंगों के चित्रण में शैलेश मटियानी की कहानियों का चित्रण महत्व है। शेखर जोशी की कहानियों में इस प्रदेश के सीधे-सरल, ठगे जाने की अधिशाल, छल-छन्दहीन रहन वारियों के करुण जीवन कथा का चित्रण मिलता है। बटरोही, पंकज विष्ट एवं रणोराम गढ़वाली इस पृष्ठभूमि पर गभीरता के साथ लिखने वाले महत्वपूर्ण समकालीन कहानीकार हैं।

उत्तर-पूर्व के पार्वत्य प्रदेश को उसके निष्क रूप में प्रस्तुत करने वाले सबसे पहले कहानीकार अज्ञेय जी रहे हैं। अज्ञेय जी सन् १९४३ से १९४६ के बीच अंग्रेजी सेना की नौकरी से जुड़े थे क्योंकि वे दूसरे विश्वयुद्ध के दौरान फासीवादी शक्तियों का विरोध 'मनसा-वाचा-कर्मणा'

संदर्भ करना चाहते थे। इसी उद्देश्य से वे ब्रिटिश सेना में इनकार की नौकरी से जुड़े। नौकरी के दौरान उनका ज्यादा समय पूर्वोत्तर में ही बिता। इस दौरान उन्होंने इस प्रदेश को काफ़ी करीब से देखा। नौकरी करके वे इन प्रदेशों को देखने के क्रम में वे इस प्रदेश की संस्कृतियों से जुड़ने चले गये, यही कारण है कि आगे चलकर इनका प्रतिफलन उनकी कहानियों व यात्रा वृत्तान्तों में देखने को मिलता है। पूर्वोत्तर के लोगों के जीवन, समाज, संस्कृति, परंपरा और उनकी मानसिकताओं को चित्रित करने वाली रचनाओं में उनके द्वारा लिखित पाँच कहानियाँ- 'होलीबॉन की बतखें', 'मेजर चौधरी की वापसी', 'जयदोल', 'नगा पर्वत की एक घटना' व 'नीली हँसी' विशेष उल्लेखनीय हैं। इन कहानियों के माध्यम से अज्ञेय ने पूर्वोत्तर जीवन की अनेक बारीकियों से परिचय करवाया है। इन कहानियों की प्रमुख विशेषता इनमें निहित स्त्री विमर्श है। इन कहानियों में लोकल के चित्रण के साथ-साथ कहानीकार ने दूसरे विश्वयुद्ध के दौरान वहाँ की जनजातीय स्त्री-जीवन में आई अस्मिताई ह्रास और उससे उनमें उत्पन्न टॉस को भी स्थान दिया है। स्त्री विमर्श के साथ इनमें पूर्वोत्तर भारत की इस भूमि पर लड़े गये द्वितीय विश्वयुद्ध के कारण इसकी सभ्यता-संस्कृति तथा जीवन-सम्बन्धों में आई गिरावट भी दर्ज है।

सन्दर्भ:

१. कृष्णचंद्र, कश्मीर की कहानियाँ, राजपाल एण्ड संज, कश्मीरी गेट, देहली, संस्करण. १९५४, पृष्ठ सं-१ 'दो शब्द'।
२. हरनाोट एस. आर., कौलें (कहानी-संग्रह), वाणी प्रकाशन, दरियागंज (नई दिल्ली), प्रथम संस्करण : २०१९, 'फ्लैप'।
३. विमल, गंगाप्रसाद, रमा प्रसाद विल्डिवाल 'पहाड़ों' संकलित कहानियाँ, राष्ट्रीय पुस्तक व्यास, भारत, पहला संस्करण : २०१६, 'भूमिका'।

संपर्क: शोधार्थी, हिंदी विभाग, उत्तर बंग विश्वविद्यालय, सिलीगुड़ी, दार्जीलिंग (प.बं.)

INTERNATIONAL JOURNAL OF ADVANCED RESEARCH (IJAR).

ISSN 2320-5407

Volume:- 07

Issue:-07



Journal homepage: <http://www.journalijar.com>

Journal DOI: [10.21474/IJAR01](https://doi.org/10.21474/IJAR01)



ISSN NO. 2320-5407

Journal Homepage: -www.journalljar.com

INTERNATIONAL JOURNAL OF ADVANCED RESEARCH (IJAR)

Article DOI:10.21474/IJAR01/9340
DOI URL: <http://dx.doi.org/10.21474/IJAR01/9340>



RESEARCH ARTICLE

A STUDY OF BURNOUT SYNDROME OF PHYSICAL EDUCATION TEACHER IN PURULIA DISTRICT.

Sajal Maji¹ And Sk Hitaluddin².

1. Guest lecturer, Achhruram Memorial College, Jhalda, Purulia.
2. Guest lecturer, Sewnarayan Rameswar Fatepurin College, Beldanga, Murshidabad.

Manuscript Info

Manuscript History

Received: 04 May 2019

Final Accepted: 06 June 2019

Published: July 2019

Key words:-

Burnout syndroms, Physical education Teachers.

Abstract

The purpose of the study was, "A study of burnout syndrome of physical education teacher in purulia district." The Researcher selected on the Different schools in purulia district for research purpose. Total 40 subjects for the study in which (N=40) and with the range of age is 25-45 years was selected for the data collection as per simple random technique method. After that researcher collects the data, from those teachers with the help of Burnout Syndroms questionnaire. After the data collection the researcher analyses the data with the help of descriptive statistics (Mean, SD, Percentage).

Copy Right, IJAR, 2019., All rights reserved.

Introduction:-

Burnout happens when the circumstances of our life no longer work for us, when we are no longer able to cope with the stress of our situation We struggle on, missing or ignoring all the warning signs – working harder and harder, getting less and less done – until our physical and emotional systems begin to fail. We are constantly striving to get control or return to normal yet feel overwhelmed at the task.¹

In 'normal circumstances', we tend to be motivated, committed, caring, conscientious and highly valued; we have energy, enthusiasm and clarity. In burnout these qualities diminish leaving us confused, lethargic, exhausted, irritated and unable to cope. This is why people who are burned out often see themselves as failing.²

The concept was traditionally examined in the context of human services, such as health care, social work, psychotherapy and teaching. One of the most prominent definitions describes burnout as a syndrome of emotional exhaustion, depersonalization, and reduced personal accomplishment that can occur among individuals who work with people in some capacity.³

¹ Wikipedia: [https://jaramuzaretreas.com/stress-burnout/what-is-burnout/\(16/03/2016\)](https://jaramuzaretreas.com/stress-burnout/what-is-burnout/(16/03/2016)).

² Schaufeli, W. B., Leiter, M. P. & Maslach, C. (2009). Burnout: 35 years of research and practice. Career Development International, 14, 204-220.

³ Maslach, C. & Leiter, M. P. (1997). The truth about burnout. San Francisco: Jossey Bass. Maslach, C., Schaufeli, W. B. & Leiter, M. P. (2001). Job burnout. In S. T. Fiske, D. L. Schachter & C. Zahn-Waxer (Eds.), Annual Review of Psychology, 53, 397-422.

Corresponding Author:-Sajal Maji.

Address:- Guest lecturer, Achhruram Memorial College, Jhalda, Purulia.

Exhaustion occurs as a result of one's emotional demands. Depersonalization refers to a cynical, negative or detached response to care recipients / patients. The reduced personal accomplishment refers to a belief that one can no longer work effectively with clients / patients / care recipients.

In the late 1980s burnout was more and more noticed also outside the work with patients and care recipients. In a more general way burnout can be seen as "a state of exhaustion in which one is cynical about the value of one's occupation and doubtful of one's capacity to perform". Researchers agree that stressors leading to burnout in human services can also be found in other occupations. One of the most radical definitions representing the general nature of burnout is "Burnout is the index of the dislocation between what people are and what they have to do. It represents an erosion in value, dignity, spirit, and will – an erosion of the human soul. It is a malady that spreads gradually and continuously over time, putting people into a downward spiral from which it's hard to recover." In summary, burnout can be defined as feelings of exhaustion, a cynical attitude toward the job and people involved in the job and through a reduced personal accomplishment or work efficiency. In a radical meaning burnout takes away a person's spirit and will. Contrary to a popular understanding, burnout can be found also outside human service professions.⁴

However, burnout still may be a greater problem in occupations where employees are more in interaction with other people (clients, customers, etc.) rather than dealing with things and information. Researchers agree that burnout does not occur "overnight". It is rather a result of a prolonged and slow process that may last even for years. According to several authors the "triggers" are excessive job demands and the employee's inability to continuously invest energy when meeting the demands. The development of burnout usually begins at an early stage of emotional exhaustion. High levels of emotional exhaustion consequently lead to a withdrawal from the people / clients / patients / customers the employees work with and also from their job in general. Such a withdrawal results in depersonalized reactions to people / clients / patients / customers and in a cynical attitude towards the job.⁵

In other words, emotional exhaustion may lead to the depersonalization stage of burnout. However, several authors claim that exhaustion and depersonalization develop rather parallel and have different antecedents. The development of burnout follows two processes." The first process is related to job demands which lead to frequent overtaxing and consequently to exhaustion. A lack of job resources (e.g., lack of social support), on the other hand, represents a second process which in the end leads to disengagement from work. If resources are not functional in meeting job demands, withdrawal behavior from work will occur. Withdrawal behavior consequently leads to disengagement which refers to "distancing oneself from one's work, and experiencing negative attitudes toward the work object, work content, and one's work in general". The third component of burnout, reduced personal accomplishment, is rather incidental in that process and is not seen as a core dimension of burnout.

Review Of Related Literatures

Freddi M et al., (2003)⁶ Emotional exhaustion, depersonalisation and personal achievement represent the main dimensions of the "burn-out syndrome" (B.O.). The risk of B.O. is especially elevated among people working in helping professions. These professionals work in settings that are characterized by a very strong emotional involvement. The representative sample of this study consisted of 100 subjects of whom a part of them worked in a psychiatric setting and others who didn't. All of them have been assessed through the M.B.I. and the E.P.Q. The purpose of the present study was especially: 1) to explore the existence of B.O. and its level, and 2) to verify the existence of some personality characteristics of employees which could be considered as possible predictors of B.O. syndrome. The statistical analysis showed that the three B.O. dimensions and therefore the B.O. syndrome were within the group of persons working in helping professions. The outcomes of this study encouraged an intervention focused on three parts: job organisation, self-management of psychological well-being and teamwork effectiveness.

⁴ Lee, R. T. & Ashforth, B. E. (1993). A further examination of managerial burnout: Toward an integrated model. *Journal of Organizational Behavior*, 14, 3-20.

⁵ Schaufeli, W. B. & Schreurs, P. J. G. (2005). Are there causal relationships between the dimensions of the Maslach Burnout Inventory? A review and two longitudinal tests. *Work & Stress*, 19, 238 – 255.

⁶Freddi M, Corradi A. Stress, job satisfaction, and quality of life in the health professions: the role of burn-out and personality features. *Recenti Prog Med*. 2003, 94(12):545-8.

Bauer J et al., (2003)⁷ this paper reviews the scientific concepts and the clinical aspects of the burn-out syndrome. According to recent studies, up to 25 % of the German working population appear to suffer from what the American physician and psychoanalyst, Herbert Freudenberger, has designated in 1974 as "burn-out syndrome". Characteristic features of this syndrome are emotional exhaustion, depersonalization and low personal accomplishment. People affected by the burn-out syndrome may suffer from depressive or anxious symptoms, from sleep disorders, chronic pain syndromes, or functional disorders of the cardiovascular or gastrointestinal system. Primary causes of the burnout syndrome include high demand combined with low influence, a high level of engagement without sufficient rewards or gratification, and a low level of social support. Preventive measures against burn-out include Balint-like supervision groups. In cases of a fully developed burn-out syndrome, affected persons should undergo either psychotherapy or a multimodal psychosomatic therapy.

Colasudro (1981)⁸ investigated the magnitude of burnout as measured by self-diagnosis and an established inventory in 215 public school teachers in San Diego. 16% were rated burned out by the inventory whereas 52% reported themselves burned out. Burnout was usually frequent at all ages but age group 30-39 was over-represented. The relationship of the variables of sex, grade assignment, ethnic status, marital status, number of children, educational qualification was not statistically significant to the measured burnout and self reported burnout.

Methodology:-

In this chapter, the selected of subjects, selections of variables and test, instrument reliability, administration of standard questionnaire and the statistical technique used to analysis the data have been discussed.

Selection of subjects

The researcher would take total 40 subjects for the study in which (N=40) and with the range of age is 25-45 years. The selected subjects would be from various schools of punalia district physical education teachers.

Sampling design

The researcher will take simple random sampling technique as appropriate tool for selecting the desire subjects of the study.

Variables of the Study

Variables for this study is Burnout syndrome

Tools to be used

Burnout syndromes standard questionnaire are used for this study. Reliability of Maslach Burnout Survey Iwanicki and Sachwab presented evidence substantiating the reliability of this test, when the adaptation was made for use the scale with teachers at least in the instance of the emotional exhaustion subscale for which internal consistency coefficient alpha estimates of reliability were .90 and .89 respectively for the frequency and intensity dimension. For depersonalization sub-scale .76 and .75 and for the personal accomplishment corresponding reliabilities of only .76 and .73 were obtained. Split-half method reliability for the Maslach Burnout Survey has been reported as .74 and .81

Validity of Maslach Burnout Survey Concurrent validity was determined in the following manner, first by correlating sub scales scores with independent behavioral ratings completed by subjects spouses and co-workers and second by correlating sub scale scores with scores on the job diagnostic survey, Hack man & Oldham; 1975, significant correlation for each of these methods range from .20 to .48 on the emotional exhaustion sub-scale, from .32 to .57 for the depersonalization measure and from .25 to .27 on the personal accomplishment sub scale.

Statistical design

Primarily the data was analyzed using Mean, SD and percentage scale.

⁷Bauer J, Häfner S, Kächele H, Wirsching M, Dahlbender RW. The burn-out syndrome and restoring mental health at the working place. *Psychother Psychosom Med Psychol*. 2003 May;53(5):213-22.

⁸Colasudro, M.M. (1981). A descriptive study of professional burnout among public school teachers in San Diego. *Dissertation Abstracts international*, 42(2), 470A

Data Analysis

The data collected from different school in Purulia district, Burnout syndrome was put in to statistical formula for analysis which has been present in this chapter. Analysis of Mean, SD and percentage has been employed to analyze the present data and the level of significance set at 0.05.

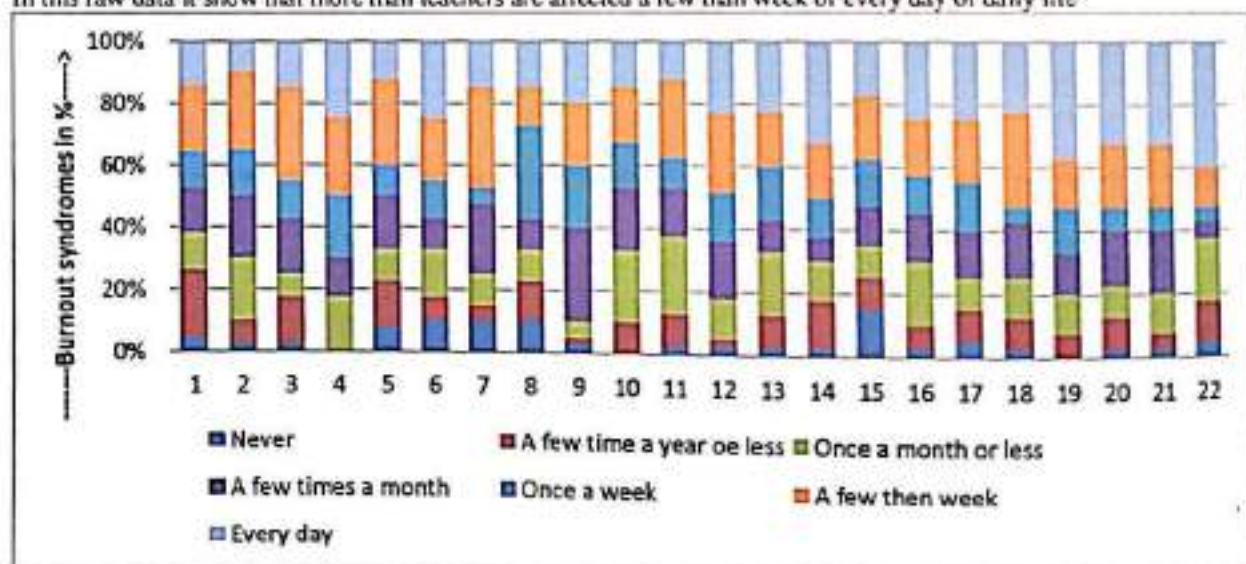
Findings

According to the survey of the variables under present study the analysis of percentage has been applied and the level of significance set at 0.05 levels. The statistical analysis has been presented through following tables-

Raw data and Percentage scale of burnout syndromes of all questions

Questions	Never	A few time a year or less	Once a month or less	A few times a month	Once a week	A few then week	Every day
1	2	9	5	6	5	9	6
2	1	3	8	8	6	10	4
3	1	6	3	7	5	12	6
4	0	0	7	5	8	10	10
5	3	6	4	7	4	11	5
6	4	3	6	4	5	8	10
7	4	2	4	9	2	13	6
8	4	5	4	4	12	5	6
9	1	1	2	12	8	8	8
10	0	4	9	8	6	7	6
11	1	4	10	6	4	10	5
12	1	1	5	7	6	10	9
13	1	4	8	4	7	7	9
14	1	6	5	3	5	7	13
15	6	4	4	5	6	8	7
16	1	3	8	6	5	7	10
17	2	4	4	6	6	8	10
18	1	4	5	7	2	12	9
19	0	3	5	5	6	6	15
20	1	4	4	7	3	8	13
21	1	2	5	8	3	8	13
22	2	5	8	2	2	5	16

In this raw data it show that more than teachers are affected a few than week or every day of daily life



Graphical representation of percentage scale of the burnout syndromes of physical education teachers

Discussion of findings:-

By keeping in mind the importance of the survey taken for the burnout syndromes, the researcher has selected an investigated entitled, "A study of burnout syndrome of physical education teacher in Purulia district". There are 40 teachers from different schools of Purulia district has been selected as subjects. To survey of Burnout syndromes standard questionnaire are used for this study. Reliability of Maslach Burnout Survey Iwanicki and Sachwab presented standard questionnaire has been taken. Undertaking research in the area of burnout syndromes of physical education teachers is needed and is important for our educational society.

So, to survey of burnout syndromes different schools of physical educations in Purulia district. Burnout syndromes could be given help to promote emotional, mental, physical exhaustion by excessive and prolonged stress of physical education teachers in their schools to betterment of teaching and skill practice situations of physical education schools. The statistical analysis of data collected on minimum 40 teachers in physical education schools of purulia district.

The result of the present investigation revealed that Burnout syndrome along with the modern era could help to improve upon teachers mental and physical exhaustion. It is a common problem of maximum worker of the society. The result of the present study has been supported by the earlier reports and established the progress of burnout syndromes.

Discussion of Hypothesis

The result of survey study indicates that the burnout syndromes provide a quantity to evaluate the burnout syndromes of physical education teachers are also found through percentage.

Further, the result inferential statistics indicates that there was statistically no significant difference in burnout syndromes of physical education teachers. This result in turn suggests that the null hypothesis- " H_0 -There is no significant difference in burnout syndromes of teacher's had found" has been accepted.

Summary

The purpose of this study was to find out a study of burn out syndrome from physical education teacher in Purulia district. In this study 40 physical education teachers were taken as a sample. Questionnaire are used for collection of data. Primarily the data was processed with descriptive statistics. For testing hypothesis the level of significance was set at 0.05. Finally, we found that:

1. The finding of this study showed that the survey of burnout syndrome can be applied to find out the situation of physical education teachers of school through questionnaires. Moreover, percentage scale of every question of the questionnaire is applied. However, accumulating evidence suggest that burnout syndromes may be a useful method to help physical education teachers of schools.
2. Although this study does not claim about its cure but firmly believes that progressive part of secondary schools intervention may obviously it helpful of physical education teachers. However, other researchers being engaged with this field has also been benefited by the result of the present study.
3. From, the variables studied as well as the overall evaluation of the syndrome, showed that as less teachers are never problems in burnout syndrome and above teachers face a burnout syndrome problems in every day life.

Conclusion:-

Following conclusions were given on the basis of the result-

1. Burnout is a societal problem that won't be solved by limiting work. The survey of burnout syndromes situations are less in physical education teachers. But, a few than week or every day burnout syndromes is high in physical education teachers.
2. It concluded that teachers presented evidence they have less teachers not affected by that syndromes, more than teachers are affected every day of his/her daily life by that syndromes of work load, physical exhaustion, fatigue and stress, although that can only be inferred by data.
3. We concluded that there is a need for teachers and administrators to have access to this kind of study in order to broaden information and allow greater knowledge of burnout syndrome.

References:-

1. Wikipedia: [https://jaramuzaretreats.com/stress-burnout/what-is-burnout/\(16/03/2016\)](https://jaramuzaretreats.com/stress-burnout/what-is-burnout/(16/03/2016)).
2. Schaufeli, W. B., Leiter, M. P. & Maslach, C. (2009). Burnout: 35 years of research and practice. *Career Development International*, 14, 204-220.
3. Maslach, C. & Leiter, M. P. (1997). The truth about burnout. San Francisco: Jossey Bass. Maslach, C., Schaufeli, W. B. & Leiter, M. P. (2001). Job burnout. In S. T. Fiske, D. L. Schachter & C. Zahn-Waxer (Eds.), *Annual Review of Psychology*, 53, 397-422.
4. Lee, R. T. & Ashforth, B. E. (1993). A further examination of managerial burnout: Toward an integrated model. *Journal of Organizational Behavior*, 14, 3-20.
5. Schaufeli, W. B. & Schreurs, P. J. G. (2005). Are there causal relationships between the dimensions of the Maslach Burnout Inventory? A review and two longitudinal tests. *Work & Stress*, 19, 238 – 255.
6. Freddi M, Corradi A. Stress, job satisfaction, and quality of life in the health professions: the role of burn-out and personality features. *Recent Prog Med*. 2003, 94(12):545-8.
7. Bauer J, Häfner S, Kächele H, Wirsching M, Dahlbender RW. The burn-out syndrome and restoring mental health at the working place. *Psychother Psychosom Med Psychol*. 2003 May;53(5):213-22.
8. Colasudro, M.M. (1981). A descriptive study of professional burnout among public school teachers in San Diego. *Dissertation Abstracts international*, 42(2), 470A.

VOLUME 6 , ISSUE 8

IJIRAS

INTERNATIONAL
JOURNAL
of

INNOVATIVE RESEARCH &
ADVANCED STUDIES

AUGUST 2019

An Analytical Study On Attitude Towards Information Technology Among Students And Physical Education Teachers Of Colleges In Western Districts Of West Bengal

Sajal Maji

Guest Lecturer, Achharam Memorial College, Jhalda, Purulia

Abstract: The purpose of this article is to share with the readers the findings of a study conducted to investigate the level of ICT use among teachers. Also, this study seeks to investigate the attitudes of teachers towards the use of ICT for educational purposes. Technology is now at the threshold of its maturity within all the sectors. An overview of the research in the value of using ICTs in teaching and learning process proved that the utilization of ICT has had a major influence on the teaching and learning process. Education is becoming an increasingly important tool to combat poverty and to establish a modern nation. Feature of modern society is the penetration of information technologies in all spheres of life, including schooling. In general, the new technologies have been recognized to play a valuable role in developing and improving the teaching and learning situations. The purpose of the study was, "An analytical study on attitude towards information technology among students and physical education teachers of colleges in western districts of West Bengal." The Researcher selected on the different colleges of western districts for research purpose. The researcher will take total 150 subjects for the study in which (N=75 students) and (N=75 teachers) with the range of age is above 21 years. The selected subjects will be colleges were selected for the data collection as per simple random technique method. After that researcher collects the data, from those teachers with the help of standard questionnaire.

After the data collection the researcher analyses the data with the help of descriptive statistics (Mean, SD, t-ratio).

Keywords: Attitude, information technology, students and teachers.

L. INTRODUCTION

This study determined the attitudes of students toward the course in Information Technology (IT) considering the following variables: the subject itself, the instructor, the instructional materials and the learning environment which are being utilized to provide learning experiences that would enhance the development of students' capabilities towards IT. Engineering students have high level of attitude towards the Introduction to Information Technology course, the instructors, the instructional materials and the learning environment. The computer units in the Computer Laboratory of Engineering must be arranged and maintained appropriately because some of the computer units were not functioning properly and infected of virus. Purchasing of updated computer and Information technology related books must be

prioritized by the library. Computer Journals and Magazines must be adequate enough for the research works of the students. **Keywords:** Attitude towards Computer, Engineering students, Information Technology, Instructional materials. The continuous development of computerization has far reaching effects on society and it is best that every learner be made conscious of the effects of computer on the different aspects of life. The computer is no longer lock up to the region of scientific, military, big business or academic circles. The computer came to be an everyday tool of the ordinary educated person. Information Technology (IT) in its broadest sense encompasses all aspects of computing technology; and as an academic discipline it is concerned with issues related to advocating for users and meeting their needs within an organizational and societal context through the selection,

creation, application, integration and administration of computing technologies.

The potentials of information and communication technology (ICT) to facilitate students' learning, improve teaching and enhance institutional administration had been established in literature. The use of information and communication technology as a tool for enhancing students' learning, teachers' instruction, and its catalyst for improving access to quality education in formal and non-formal settings has become a necessity. Recognizing the impact of new technologies on the workplace and everyday life, teacher education institutions try to restructure their education programmes and classroom facilities, in order to husband the potentials of ICT in improving the content of teacher education. Information and communication technology as tools within the school environment include use for school administration and management, teaching and learning of ICT related skills for enhancing the presentation of classroom work, teaching/learning repetitive tasks, teaching/learning intellectual, thinking and problem solving skills, stimulating creativity and imagination; for research by teachers and students, and as communication tool by teachers and student. Information and communications technologies are computer based tools used by people to work with information and communication processing needs of an organization. Its purview covers computer hardware and software, the network, and other digital devices like video, audio, camera, and so on, which convert information (text, sound, motion, etc.) into digital form. Successful integration of ICT in the school system depends largely on the competence and on the attitude of teachers towards the role of modern technologies in teaching and learning. Thus, experienced teachers, newly qualified, and student-teachers need to be confident in using ICT effectively in their teaching.

Simply having ICT in schools will not guarantee their effective use. Regardless of the quantity and quality of technology placed in classrooms, the key to how those tools are used is the teacher; therefore teachers must have the competence and the right attitude towards technology. Attitudes refer to one's positive or negative judgment about a concrete subject. Attitudes are determined by the analysis of the information regarding the result of an action and by the positive or negative evaluation of these results. There is a common saying that attitude determines altitude. Studies have established close links and affinities between teachers' attitude and their use of ICT. More positive attitudes towards the computer were associated with a higher level of computer experience. Students' confidence on ICT can be explained through the attitude and behaviors of their teachers. Teachers' behavior is a critical influence on students' confidence and attitude towards ICT as they provide important role model to their students. The literature suggests that lack of adequate training and experience is one of the main reasons why teachers do not use technology in their teaching. This also eventuates in teachers' negative attitude towards computer and technology. In addition, lack of confidence leads to reluctance to use computers by the teachers. Attitude of pre-service and in-service teachers towards computer and technology skills can be improved by integrating technology into teacher education. Findings have revealed that a significant

relationship exist between computer attitude and its use in institutions for pre-service teachers and also for serving teachers in the affective attitude, general usefulness, behavioral control, and pedagogical use. Attitude is a major predictor of future computer use. Study indicated the importance of appropriate responses to the trainee's feelings about using ICT as one of the factors critical to success. Thus, there is the need to take care of the emotional needs of student teachers as attitude is a major predictor of future ICT use. Student teachers have positive attitude and are highly enthusiastic about interactive whiteboards as an important feature of teaching and learning, and this motivated them to practice using the technology.

Technologies (ICTS) in the field of education. Theoretical and empirical studies have considered the importance of ICTs in the process of teaching and learning. This current paper investigates the level of ICT use for educational purposes by teachers in Jordanian rural secondary schools. The paper will contribute to the body of knowledge regarding the level of ICT use and also, concerning the importance of teachers' attitudes towards the use of ICT for educational purposes. The data for the study were collected through the use of quantitative data. In October 2008, a questionnaire was distributed to 650 teachers in Jordan, randomly selected. Four hundred sixty teachers responded to the questionnaire. The survey included questions concerning the level of ICT use as well as questions related to the attitudes of teachers towards the use of ICT. The findings of the study, which were obtained by analyzing the data collected from the teachers revealed that, teachers had a low level of ICT use for educational purpose, teachers hold positive attitudes towards the use of ICT, and a significant positive correlation between teachers' level of ICT use and their attitudes towards ICT was found. The findings suggest that ICTs use for educational purposes should be given greater consideration than it currently receives. In general, the results were consistent with those previously reported in studies related to the use of ICT in the educational settings. Students in terms of their attitude towards IT on one hand and the relationship with their low academic achievement on the other hand. All port pointed out that attitude involved particular responses like cognition, behavioral and affective responses having clear and specific associations with attitude object. Attitude in this study refers to three components, such as affection, behavior, and information technology.

The Teachers' Attitudes toward Information Technology (TAT) complements Teachers' Attitudes toward Computers Questionnaire to provide assessment in New Information Technologies. It is constructed primarily from semantic differential items using Teachers' Attitudes toward Information Technology statements such as Teachers' Attitudes toward Information Technology addresses the following areas: electronic mail, multimedia, the World-Wide Web, teacher productivity, and classroom productivity for students. Teachers' Attitudes toward Information Technology also includes subscales replicated from the Teachers' Attitudes toward Computers Questionnaire.

The purpose of this research study was to survey Internet users with psychiatric disabilities regarding issues related to their use of information technology (IT) and its connection to

self-determination in their lives. A Web-based survey was created and administered by the University of Illinois at Chicago (UIC) National Research and Training Center's (NRTC) Self-Determination and Technology Workgroup, comprised of mental health service consumers, advocates, and researchers interested in the application of IT to mental health issues. The study was designed to yield information that would be of use to those seeking to better understand how IT can enhance individual self-determination, to identify access gaps that exist and how to address them, and to appreciate the potential of IT applied to mental health advocacy efforts.

With technology advancing at an increasing rate, it is necessary to understand how it shapes or influences the learning process. As an ever present component in higher education pedagogy, more empirical evidence is needed to demonstrate the connections between students' references for learning and the use of this technology. This study contributes to a better understanding of technology usage, attitudes, and the academic achievement level among students at the universities in Iraq. Therefore, this study will be providing insights into the nature of the attitudes toward IT of the students and the relationship with their academic achievements which can explain their eventual success or failure. The confirmation of this relationship highlights the need for early intervention plans geared towards ensuring positive attitudes among the students and improving their level of academic achievement. Education is not only limited teaching the students according to prescribed syllabus at a specific school level. It has much broader objectives, goals and other concepts. Thus, education is becoming an increasingly important tool to combat poverty and to establish a modern nation. Feature of modern society is the penetration of information technologies in all spheres of life, including schooling. In general, the new technologies have been recognized to play a valuable role in developing and improving the teaching and learning situations.

II. REVIEWS OF RELATED LITERATURE

Tican (1996), Which sought to determine the attitude of students towards the IT Course itself, the instructor, the instructors' methods of teaching, instructional materials and the learning environment. Weighted mean, rank and Pearson - Product Moment Correlation Coefficient were the statistical tools used to analyze and interpret the data gathered. Results and Discussion the obtained weighted mean on the level of students' attitude towards the subject. The respondents were strongly agree that they find computer stimulating and challenging (WM = 4.77); they find lecture/hands-on as the most effective way to learn computer (WM = 4.69); they find computer relevant to their future career (WM = 4.65); Computer makes significant contribution to mankind (WM = 4.65); and they like computer because it requires critical and logical thinking and deep analysis which most of their classmates can follow (WM = 4.55). Students are being challenged by the activities of the course because they find its true essence and application to real life situation and they really appreciate its usefulness. Teaching and learning strategies in education have been radically revised with the

aim of providing better service to the learners through the intensive use of the ICT.

Plomp et al (2001), Identify three objectives which distinguished for the use of ICT in education such as, the use of ICT as object of study, the use of ICT as aspect of a discipline or profession; and the use of ICT as medium for teaching and learning. Peck and Doncott (1994) outlined ten reasons that technologies should be used in schools: (1) Technology enables teachers to individualize instruction, which allows students to learn and develop at their own pace in a non-threatening environment; (2) Students need to be proficient at accessing, evaluating and communicating, and information; (3) Technology can increase the quantity and quality of students' thinking and writing through the use of word processors; (4) Technology can develop students' critical thinking and allowing them to organize, analyze, interpret, develop, and evaluate their own work; (5) Technology can encourage students' artistic expression; (6) Technology enables students to access resources outside the school; (7) Technology can bring new and exciting learning experiences to students; (8) Students need to feel comfortable using computer, since they will become an increasingly important part of students' world; (9) Technology creates opportunities for students to do meaningful work, and; (10) Schools need to increase their productivity and efficiency. Thus, teachers are expected to make good use of modern teaching technology and develop effective teaching resources. Morgan (1997) claimed that when computers are used, there are many learning processes are engaged such as: (1) gather information; (2) teacher as facilitator; (3) involvement in experiential learning; (4) face-to-face communication; (5) expanded creativity, and (6) testing of new knowledge. For the purpose of answering question number one respondents were asked to respond to 13 Likert-scale items measuring their level of ICT use for educational purposes in rural secondary schools. The results of descriptive analysis (Means, Std. Deviations, and Percentages) were presented in Table 1. Examination of the Means, Std. Deviations and Percentages in Table 4.5, confirms that the highest Percentages of scores in the use of ICT tool for educational purposes by rural secondary school teachers were, "using Internet" (51.8% of the participants answered that they either use the internet "often" or "very often"), with Mean score (M=3.34), and Std. Deviation (SD=1.34), "using CD-Rom" (49.9% of the participants answered that they either use the CD-Rom "often" or "very often"), with Mean score (M=3.14), and Std. Deviation (SD=1.46), "using presentation" (47.3% of the participants answered that they either use the presentation "often" or "very often"), with Mean score (M=3.12), and Std. Deviation (SD=1.43), and "using word process" (26.4% of the participants answered that they either use the word process "often" or "very often"), with Mean score (M=2.55), and Std. Deviation (SD=1.25). The lowest Percentages of ICT use by rural secondary school teachers were scored: for the items "using simulations and games" (46.7% of the participants answered that they "never" simulations and games), with Mean score (M=2.03), and Std. Deviation (SD=0.87), "using Electronic mail" (40.0% of the participants answered that they "never" use Electronic mail), with Mean score (M=2.45), and Std. Deviation (SD=1.14), "using authoring" (39.1% of the participants answered that

they "never" use authoring), with Mean score (M=2.16), and Std. Deviation (SD=1.00), and "using spreadsheet program" (37.6% of the participants answered that they "never" use spreadsheet program) with Mean score (M=2.09), and Std. Deviation (SD=1.14). As shown in Table 1, the percentages of the level of ICT use show that rural secondary schools teachers highly use some ICT tools for educational purposes such as the Internet, CD-Rom, presentation and word processing. On the other hand, the findings show that rural secondary schools teachers have lowest levels of ICT tools such as, simulations and games, electronic mail, authoring, as well as spreadsheet applications. Results also indicated that the overall percentages of the use of ICT tools for educational purposes were reported as low levels. As for using ICTs for educational purposes, the participants' distribution was as follows 28.6% from the total sample reported that they never used the ICT tools for educational purposes, and 26.3% of the respondents reported that they rarely used ICT tools for educational purposes, while 25.1% from the total respondents reported that they often and very often used ICT for educational purposes. The overall average of the Mean scores of the use of ICT tools for educational purposes by rural secondary school teachers was (M=2.52) and the Std. Deviation (SD=1.19) confirming the results of the Percentages and indicated that the level of ICT use for educational purposes by rural secondary schools teachers found to be a low level.

III. METHODOLOGY

The purpose of this study is to construct "An analytical study on attitude towards information technology among students and physical education teachers of colleges in western districts of West Bengal" the health related physical fitness norms for school level boys and girls student of western districts. Standard procedure was followed to conduct this study.

SELECTION OF THE SUBJECT

The researcher will take total 150 subjects for the study in which (N=75 students) and (N=75 teachers) with the range of age is above 21 years. The selected subjects will be colleges.

SAMPLING TECHNIQUE

The researcher will take simple random sampling technique as an appropriate tool for selecting the desire subjects.

VARIABLES:

- Attitude towards information Technology
- Standard Questionnaire

TOOLS TO BE USED

For assessment of comparative study on attitude towards information Technology among students and of Physical Education Teachers of Colleges in western districts. Researcher is going to adopt following questioners:-

Sl No.	Variables	Test Item
1.	Attitude Information Technology	Questioners-Attitude Towards Information Technology For Students and Teachers ASTITT-NI Dr.(Mrs.) Nasrin Dr.(Mrs.) Fatima Islahi

Table 1

STATISTICAL DESIGN

The study is about to find out of the Selected an analytical study an attitude towards Variable within the information technology colleges in western district areas therefore, Pearson product movement will be applied as statistical tool for the study. The level of significant for this study is set at 0.05.

- ✓ Descriptive statistical technique was applied to find out the distribution of data on 't' ratio.
- ✓ Percentile scale was used to provide the grade to the obtain score on selected health related physical fitness variable.
- ✓ Cumulative frequency was done to find out the Frequency distribution on the score.
- ✓ Normative curve and normative scale was used with five different levels to provide the score on selected health related physical fitness.

IV. DATA ANALYSIS

The data collected from different colleges in western district of West Bengal, attitude information technology was put in to statistical formula for analysis which has been present in this chapter. Analysis of (Mean, SD and t-test) was employed to analyze the present data and level of significance was set at 0.05

FINDINGS

To comparison the attitude information technology variable under present study the analysis of (t-test) was applied and the level of significance was set at 0.05 levels. The statistical analysis is being presented through following tables.

Sl.No	Variables	Mean	SD	t-test
1.	Teachers attitudes	109.3867	15.82155	0.40844
2.	Students attitudes	108.76	13.01334	

Table 2: Comparison Attitude Information Technology toward Students and Teachers

Table shows the Teachers Attitudes Mean (109.3867) SD (15.82) and Students Attitudes Mean (108.76) SD (13.01334). It is also revealed by the table that calculated t-test (0.40844) is lesser than the tabulated. There for there is no significant difference 0.05.

- [4] Campbell, J. (1997). "The data needs of community-based peer support programs". St. MO: University of Missouri, Missouri Institute of Mental Health, February, 1997
- [5] Lust, B. M. et al. "Information Technology: Curriculum Guidelines for Undergraduate Degree Programs in Information Technology". Association for Computing Machinery (ACM), IEEE Computer Society, 2008 Ch. 1, p. 9.
- [6] Pelgrum, W. J. "Obstacles to the integration of ICT in education: results from a worldwide educational assessment." *Journal of Computers & Education*, 2001,37, 163-178.

IJIRAS

INDEXED JOURNAL

REFEREED JOURNAL

PEER REVIEWED JOURNAL

ISSN: 2456-0057

IMPACT FACTOR (RJIF): 5.48

INDEX COPERNICUS

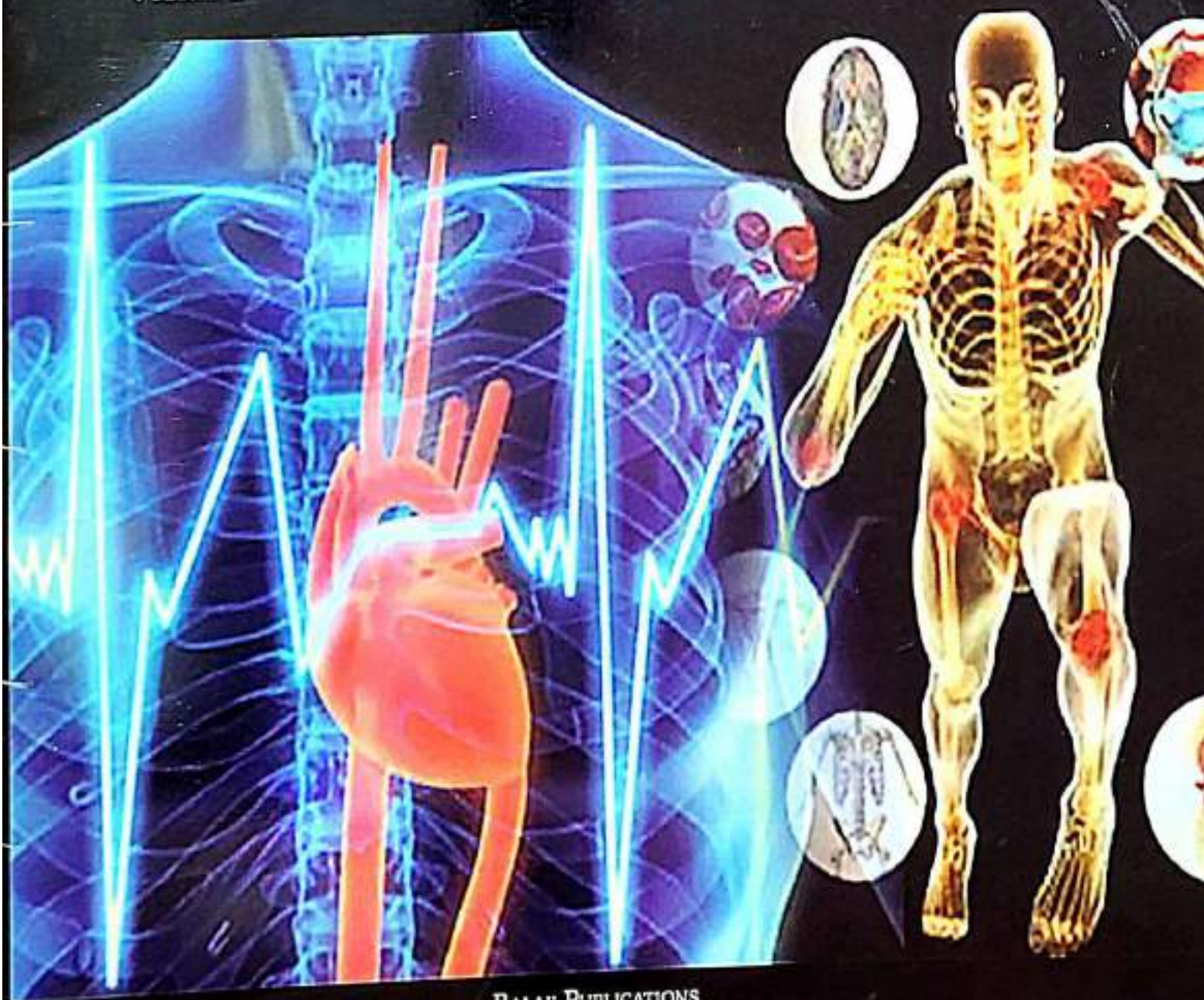
INTERNATIONAL JOURNAL OF PHYSIOLOGY, NUTRITION AND PHYSICAL EDUCATION

VOLUME 4

ISSUE 2

JUL - DEC

2019



BALAJI PUBLICATIONS
NEW DELHI, INDIA



ISSN: 2456-0057
IJPNPE 2019; 4(2): 261-265
© 2019 IJPNPE
www.journalofppns.com
Received: 21-05-2019
Accepted: 25-06-2019

Sajal Maji
Guest lecturer, Achharam
Memorial College, Jhalda,
Purulia, West Bengal, India

Comparison of neuromuscular coordination of handball and volleyball inter-collegiate players of Purulia district

Sajal Maji

Abstract

Neuro-muscular coordination in inter-collegiate players improves skill performance and decreases the risk of injuries during the activities. This coordination is primarily ascribed to the enhancement of eye-hand coordination. The purpose of the study was, "Comparison of Neuro-muscular Coordination of Handball and Volleyball inter-collegiate Players of Purulia district". The Researcher selected the various inter-collegiate players of Purulia district for research purpose. For comparing the neuromuscular researcher had selected total sixty subjects which were further divided into 30 handball and 30 volleyball players and age range from 18 to 21 years are selected for the data collection as per simple random sampling technique. After that researcher collects the data, from those players with the help of selected test.

After, the data collection the researcher analysis the data with the help of descriptive statistics (Mean, SD and 't'- test).

Keywords: Neuro-muscular coordination, handball and volleyball

Introduction

Movement analysts ranging from spectators and sportswriters, to teachers and coaches, to biomechanics and kinesiologists, to neuroscientists and robot cists believe that coordination is a desirable aspect of performance. Yet, there has been little coordination among movement analysts in the effort to understand and improve coordinated movement. Perhaps our disjointed activity is due in part to our diverse conceptions of coordination. If so, identifying and clarifying the various meanings of coordination may enable movement analysts to cooperate on the topic of coordination. Thus, the purpose of this paper is to ask and address a series of questions: What is meant by coordination. Are the meanings similar or different for professionals and non-professionals, for scholars and practitioners, Are the meanings complementary or contradictory for researchers in various fields, is there a common thread of meaning that could be used as both a basis of communication as well as a basis for research. Neuro-muscular coordination studies how to coordinate between the different parts of our body. They study individuals as well as group, observable the coordination's.

When the word coordination was first recorded in 1605, it meant "orderly combination" ⁽¹⁾. Though the basic meaning of coordination has not changed over the centuries, the contemporary meaning of coordination has become increasingly associated with harmonious and skillful movement; coordination is defined as the harmonious adjustment of action, as of muscles in producing complex movements.

Webster's connection between harmony and human movement has been accented in the physical education literature for teachers and coaches. For example, coordination has been defined as the "harmonious movement of independent body parts" ⁽²⁾, "the ability to integrate muscle movements into an efficient pattern of movement" ⁽³⁾ and "the use of muscles in such

Correspondence

Sajal Maji
Guest lecturer, Achharam
Memorial College, Jhalda,
Purulia, West Bengal, India

¹ Barnhart dictionary of etymology, (1988). New York: Wilson.

² Dictionary of the sport and exercise sciences, (1991), Champaign, IL: Human Kinetics.

³ Schurr, E. L. (1980). Movement experiences for children: A humanistic approach to elementary school physical education. Englewood Cliffs, NJ: Prentice-Hall.

a manner that they work together smoothly and effectively rather than hinder one another" [4]. Roget's association of coordination and skillful movement was echoed by Schurr: "Coordination makes the difference between good performance and poor performance." Also [5], related coordination to athletic exemplars: "Neuromuscular coordination reflects the ability of athletes to perform their sports activities or events with a smooth, balanced, and fluid motion." While many practitioners in physical education describe coordination in terms of harmony or skillfulness, some scholars in physical education are more apt to emphasize the pattern of movement. For instance, "coordinated actions of the human body are executed by the controlled application of muscular forces which produce distinctive patterns of segment motions" [6]. And coordination is "the relationship among movement variables that constrains them into a behavioral unit." Further, a coordination variable is a "factor that, when changed, necessitates a new pattern of coordination."

Neuromuscular training programs by evidence have shown a greater improvement in the performance and have become integrated into clinical practice in rehabilitation of an athlete. Information regarding joint movement and joint positions are provided by mechanoreceptors in the skin, muscles, tendons, ligaments, and joints combine with input from the vestibular and visual systems to maintain balance and perform specific activity. Injury can alter the normal physiological process of motor control, leading to insufficient neurologic input or improper processing at the spinal, brain stem, or cognitive centers leading to an inadequate response by the motor system. The neuromuscular co-ordination and activity is one of the key considerations in sports performance. The motor cortex does not specify motor unit activation rather the body attempts to achieve a specific movement by activating muscle and or muscle groups [7]. The movements and skilled activity always requires complicated neuromuscular co-ordination, this is learned over time through practice and experience. A trained athlete performance is based on the needs and it is modified according to the changes applied. The motor learning is one of the key principles of neuromuscular training. A trained athlete reaches advanced motor learning skills necessary to accomplish complex motor tasks.

A sportsperson can perform optimally only when he is in a perfect state of physical, physiological and psychological preparedness for a given competitive event or performance. She must, of course, be fully equipped technically and tactically. Such a performance cannot be expected overnight or all of a sudden. It can only be materialized through long and sustained efforts over the years following unflinching discipline and an unwavering commitment. In this process, the pattern, the physical educator and the coach or trainer, have to play a specific role at particular stages in the making of these men of great sporting acumen. Physical proficiency is an important area of motor performance. Ability refers to a more general trait of the individual which has been inferred from response consistencies on certain kinds of tasks.

Abilities are fairly enduring traits, which in adults, are more difficult to change. Many of these abilities are, of course, themselves a product of learning and develop at different stages, mainly during childhood and adolescence.

Introduction 5 Proficiency in any sport requires an ideal integration of numerous abilities developed into an ideal degree. However, performance measures of these abilities do vary from activity to activity. Fleishman identified the dimensions underlying the human performance into the physical proficiency (fitness) area and the psychomotor area. The factors of strength, power, stamina, flexibility, coordination and balance constituted proficiency whereas reaction-time, speed of movement, arm-hand steadiness, visual perception, manual dexterity and rate control were the abilities considered under psychomotor domain [8].

Team-handball is an Olympic sport ball game that is characterized by fast pace defensive and offensive action during the game with the objective of the game to score goals. To score goals, the offensive players (6 players and one goalie) attempt to establish an optimal position for the throwing player by fast movements over short distances performing powerful changes in direction (with and without the ball), one-on-one action against defensive players and passing the ball using different offensive tactics.

Review of related literature

Acsinte Alexandru *et al.* (2014) [9] was conducted to check the specialized sensory receptors in the muscles, joints and connective tissues enable the body to process information from a variety of stimuli, and turn that information into action. The key to creating what specialists refer to as movement intelligence involves individuals becoming consciously aware of their movements, and of the information their body is absorbing. To do this, stimuli are created to elicit a movement reaction through a variety of tasks or exercises. As skill improves, more stimuli are needed to continue improvement. So, the aim of this study was to prove the utility of complex and specific drills using additional materials in young handball players. The study has been developed on a sample of 10 young female handball players from CSS, Bacau, aged between 13-14 years. The evaluation of the subjects has been performed using the "T - Test", the "Slalom Test" and the "ZIGZAG Run Test", taken from the book "Functional Testing in Human Performance". The working protocol consisted in 8 coordinative and proprioceptive drills that were used during the training sessions and during warm-up, before official matches. An improvement in all values was recorded, as compared to the reference values.

Mette K Zebis *et al.* (2008) [10] the study was conducted with aimed to implement neuromuscular training during a full soccer and handball league season and to experimentally analyze the neuromuscular adaptation mechanisms elicited by this training during a standardized side cutting maneuver known to be associated with non-contact anterior cruciate

⁴ Hunter, M. D. (1966). A dictionary for physical educators, Doctoral dissertation, Indiana University, Bloomington

⁵ Wilmore, J. H. (1977). Athletic training and physical fitness: Physiological principles and practices of the conditioning process. Boston: Allyn and Bacon.

⁶ Putnam, C. A. "A segment interaction analysis of proximal-to-distal sequential segment motion patterns", *Medicine and Science in Sports and Exercise*, Vol. 23, (1991): pp. 130-144.

⁷ Black burn TA, McLeod WD, White D *et al.*, "EMG Analysis of Post rotator cuff exercises". *Athl. Train*, Vol. 25, (1990): pp. 40-45.

⁸ http://shodhganga.inflibnet.ac.in/bitstream/10603/95688/9/09_chapter%201.pdf (15/01/2017).

⁹ Acsinte Alexandru, Alexandru Elena, Hantau Cezar, Oscar Gutierrez Aquilar, Makoto Muramatsu, "Neuromuscular Coordination and Proprioceptive Training in Young Handball Players", *Procedia - Social and Behavioral Sciences*, Vol. 117, No. 19, (2014): pp. 451-456.

¹⁰ Mette K Zebis, Jesper Bencke, Lars L Andersen, Simon Dossing, Tine Alkjar, S Peter Magnusson, Michael Koer, Per Aagaard, "The Effect of Neuromuscular Training on Knee Joint Motor Control During Sidecutting in Female Elite Soccer and Handball Players", *Clin. J Sport Med*, Vol. 18, No. 3, (2008): pp. 329-337.

ligament (ACL) injury. Design: The players were tested before and after 1 season without implementation of the prophylactic training and subsequently before and after a full season with the implementation of prophylactic training. Participants: A total of 12 female elite soccer players and 8 female elite team handball players aged 26.63 years at the start of the study. Intervention: The subjects participated in a specific neuromuscular training program previously shown to reduce non-contact ACL injury. Methods: Neuromuscular activity at the knee joint, joint angles at the hip and knee, and ground reaction forces were recorded during a side cutting maneuver. Neuromuscular activity in the pre landing phase was obtained 10 and 50ms before foot strike on a force plate and at 10 and 50ms after foot strike on a force plate. Results: Neuromuscular training markedly increased pre landing activity and landing activity electromyography (EMG) of the semi-tenderness ($P, 0.05$), while quadriceps EMG activity remained unchanged. Conclusions: Neuromuscular training increased EMG activity for the medial hamstring muscles, thereby decreasing the risk of dynamic values. This observed neuromuscular adaptation during side cutting could potentially reduce the risk for non-contact ACL injury.

Tamara C Valovich McLeod *et al.* (2009) [11] was conducted to observe poor balance has been associated with increased injury risk among athletes. Neuromuscular-training programs have been advocated as a means of injury prevention, but little is known about the benefits of these programs on balance in high school athletes. Objective: To determine whether there is balance gains after participation in a neuromuscular-training program in high school athletes. Design: Nonrandomized controlled trial. Setting: All data were collected at each participating high school before and after a 6-wk intervention or control period. Participants: 62 female high school basketball players recruited from the local high school community and assigned to a training ($n = 37$) or control ($n = 25$) group. Intervention: Training-group subjects participated in a 6-wk neuromuscular-training program that included polymeric, functional-strengthening, balance, and stability-ball exercises. Main Outcome Measures: Data were collected for the Balance Error Scoring System (BESS) and Star Excursion Balance Test (SEBT) before and after the 6-wk intervention or control period. Results: The authors found a significant decrease in total BESS errors in the trained group at the posttest compared with their pretest and the control group ($P = .003$). Trained subjects also scored significantly fewer BESS errors on the single foam and tandem-foam conditions at the posttest than the control group and demonstrated improvements on the single-foam compared with their pretest ($P = .033$). The authors found improvements in reach in the lateral, antero-medial, medial, and posterior directions in the trained group at the posttest compared with the control group ($P < .05$) using the SEBT. Conclusion: The study demonstrates that a neuro-muscular training program can increase the balance and proprioceptive capabilities of female high school basketball players and that clinical balance measures are sensitive to detect these differences.

Bastiurea Eugen *et al.* (2014) [12] was evaluated the relationship between muscle strength and coordination

capacity was examined at 17 handball players aged between 16-18 years old ($M = 17.06$, $SD = 0.827$). Strength indices were calculated by reporting the measured values to body weight. "The muscle strain differentiation test of hands" was used for the neuromuscular coordination capacity and the "Pendulum-throw target" test for the throwing accuracy. The paper notes that muscle strength, being below the optimal values, does not significantly influence the coordination capacity ($CI = 95\%$). During this period, it is important to intensify the intramuscular coordination training, due to the qualitative aging of the SNC.

Methodology

This chapter describes the method of research design, population, sample, tools, used for research apparatus or instrument employed statistical tools and procedures systematically. This is a comparison type of study under the description research. The study was conducted on the handball and volleyball inter-collegiate players of Purulia district. Standard Procedure was followed to conduct this study. This was a comparative type of study under the Laboratory research. This comparison was conducted to find the "Comparison of Neuro-Muscular coordination between Handball and volleyball inter-collegiate players of Purulia district" of the data was collected with the help of standard test.

Selection of subject

For comparing the neuromuscular researcher had selected total sixty subjects which were further divided into 30 handball and 30 volleyball inter-collegiate players. All the subjects were students of colleges of Purulia district. The selection process for subjects was purely based on random sampling technique. The subject's age group was ranged from 18 to 21 years.

Sample

Simple random sampling method was employed for the selection of subject from colleges of Purulia district. The subjects were ($n=60$), 30 Handball and 30 volleyball players and age range from 18 to 21 years.

Selection of variables

Neuro-Muscular Coordination.

Table 1: Tools selected for the study

Sl. No.	Test	Purpose of the test
1.	Eye-Hand Coordination Test	To measure the Neuro-muscular coordination between handball and volleyball inter-collegiate players.

Statistical design

The collected data from selected subjects were treated on following statistical technique:-

The statistical analysis of Independent-'t' test was used for the present study and the level of significance is set at 0.05.

- Descriptive statistical technique was used to find out the scattering of the score.
- Independent "t" test was used to find out the significant difference between handball and volleyball players.

Analysis of data

The statistical analysis of data collected on 60 subjects (30 handball and 30 volleyball players) on Neuro-muscular coordination of inter-collegiate players of Purulia district has

[11] Tamara C Valovich McLeod, Travis Armstrong, Mathew Miller, Jamie L. Saucedo, "Balance Improvements in Female High School Basketball Players after a 6-Week Neuromuscular-Training Program", *Journal of Sport Rehabilitation*, Vol. 18, (2009): pp. 1-17.

[12] Bastiurea Eugenia, Stan Zenoviza, Rizescu Constantinb, Mihaila Ionc, Andronic Florinde, "The effect of muscle strength on the capacity of coordination in handball", *Procedia-Social and Behavioral Sciences*, Vol. 137, (2014) : pp. 3-10.

been presented in this chapter. The detailed statistical analysis are done systematically and presented in the form of tables and graphs. The depth analysis of the data presented in this chapter has been separated into two sections. The first section deals with descriptive statistical measures, of the Neuro-muscular coordination.

Table 2: Descriptive statistics on the neuro-muscular coordination of handball and volleyball inter-collegiate players

Group	N	Mean	MD	SD	SFM	DF	Cal. t.
Handball Players	30	33.56	4.19	4.83	0.88	58	0.077
Volleyball Players	30	37.77		4.07	0.74		

Significant at 0.05

Tabular-'t' Value (58) = 2.000

Table shows that, data collected on 30 handball players the mean was 33.56, standard deviation was 4.83 and standard Error of Mean was 0.88. For 30 volleyball players the mean was 37.77, standard deviation was 4.07 and standard Error of Mean was 0.74.

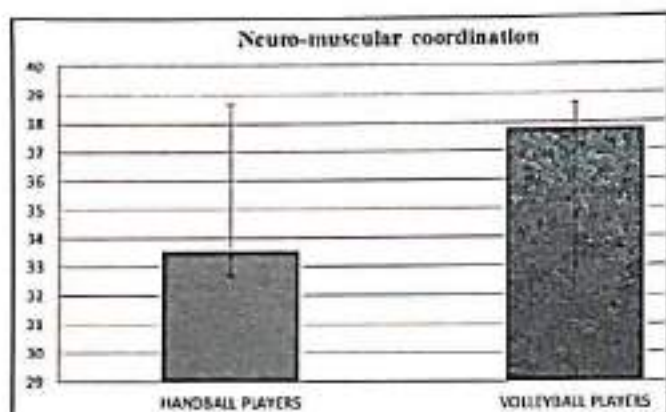


Fig 1: The graphical presentation of neuro-muscular coordination between the 30 handball and 30 volleyball inter-collegiate players has presented in the fig.

Discussion of findings

Human physiological is consists of different types of components of fitness which makes every individual humans differ from each other. Hence, when it comes to understand, Human Physiological traits the origin of physiological comes into exit. Physiological is the connection of applied to Neuro-muscular, educational and theoretical science. It is the study of coordination, performance and the mental operations of people. Physiological is also in reference to the usage and application of coordination and understanding various activities undertaken by humans and how they are used through daily activities, whether that is within events, talking to people, education and employment, relationships and coordination activities.

The research studies conducted on handball and volleyball players revealed that your coordination is very much influence from the different factors. In nut shell your Neuro-muscular coordination reflects the person coordination ability between muscle and neuron. The study was an Endeavour in similar way to find out and compare the diversity among the handball and volleyball inter-collegiate players in terms coordination. In this aspect the researcher had selected 30 handball and 30 volleyball players. The purpose was to assess the Neuro-muscular coordination of handball and volleyball inter-collegiate players of Purulia district.

In the light of the results of analysis researcher found that there were no significant difference was observed between the Neuro-muscular coordination of handball and volleyball inter-

Findings

This section deal with the descriptive statistical analysis applied on data collected from subjects on the Neuro-muscular coordination that are included in the study in the form of variables.

collegiate players of Purulia district. As studies shows that you're surrounding specially where you play having no influence on Neuro-muscular coordination. This dispersion because of demand of the sports and works which make you to react differs from situation to situation.

Here, also Neuro-muscular coordination of handball and volleyball players are regularly participating in sports activities and sports involvement bring changes in the performance in terms of coordination. Sports participation requires coordination between the neuron and muscular. Therefore, researcher felt these all above factors might be reasons to bring the no significant difference between handball and volleyball players Neuro-muscular coordination.

Discussion of hypothesis

On the basis of literature, discussion with experts and the research scholar's own understanding it was hypothesized that-

Ho: There would be no significant difference among handball and volleyball in relation with neuromuscular coordination. Hence, this above hypothesis is accepted.

Summary

The purpose of the study was to compare the Neuro-muscular coordination of handball and volleyball inter-collegiate players in Purulia district. The present study was conducted on the 30 handball and 30 volleyball players on the basis of evidence available in the literature and with personal experience as well as discussion with experts the following hypothesis was formulated what there may be significant difference in Neuro-muscular coordination of handball and volleyball players in Purulia district. The eye-hand coordination test was conducted for the collected, test was selected for the collection of data because it was found to be most reliable and have been very often used in research in profession physical education and sports.

In order to determine the Neuro-muscular coordination of handball and volleyball players independent 't'-test was employed and the level of significance was set (0.05) It is observe that, calculated value is 0.77 lower than the tabulated t- value 2.000, hence there is no significant difference was found between the Neuro-muscular coordination of handball and volleyball players.

Conclusion

On the basis of findings researcher able to draw following conclusion:-

- Researcher concluded the data collected on Neuro-muscular coordination from selected subject; handball and volleyball players has shown their coordination, but volleyball players had showed better responses in

comparison to handball players.

- Further, researcher able to conclude that there was no statistical significant difference was observed in between handball and volleyball players Neuro-muscular coordination.

References

1. Barnhart dictionary of etymology. New York: Wilson, 1988.
2. Dictionary of the sport and exercise sciences, Champaign, IL: Human Kinetics, 1991.
3. Schurr FL. Movement experiences for children: A humanistic approach to elementary school physical education. Englewood Cliffs, NJ: Prentice-Hall, 1980.
4. Hunter MD. A dictionary for physical educators. Doctoral dissertation. Indiana university, Bloomington, 1966.
5. Wilmore JH. Athletic training and physical fitness; Physiological principles and practices of the conditioning process. Boston: Allyn and Bacon, 1977.
6. Putnam CA. A segment interaction analysis of proximal-to-distal sequential segment motion patterns. *Medicine and science in sports and exercise*. 1977-1991; 23:130-144.
7. Black burn TA, McLeod WD, White B *et al*. EMG Analysis of Post rotator cuff exercises. *Athl. Train*. 1991-1990, 25:40-45.
8. http://shodhganga.inflibnet.ac.in/bitstream/10603/95688/9/09_chapter%201.pdf (15/01/2017).
9. Acinte Alexandra, Alexandru Eftene, Hantau Cezar, Oscar Gutierrez Aquilar, Makoto Muramatsu. Neuromuscular coordination and proprioceptive training in young handball players. *Procedia - social and behavioral sciences*. 2014; 117(19):451-456.
10. Mette K Zebis, Jesper Bencke, Lars L Andersen, Simon Dissing, Tine Alkjær, S Peter Magnusson, Michael Kaer, Per Aagaard. The effects of neuromuscular training on knee joint motor control during sidcutting in female elite soccer and handball players. *Clin. J sport med*. 2008; 18(3):329-337.
11. Tamariz C, Valovich McLeod, Travis Armstrong, Mathew Miller, Jamie L Sauer. Balance improvements in female high school basketball players after a 6-week neuromuscular-training program. *Journal of sport rehabilitation*. 2009; 18:1-17.
12. Bastiurea Eugena, Stan Zenoviaa, Rizescu Constantinb, Mihaela Ionec, Andronic Florinde. The effect of muscle strength on the capacity of coordination in handball. *Procedia-social and behavioral sciences*. 2014; 137:3-10.



<https://doi.org/10.11646/phytotaxa.422.1.4>

***Euryhalinema mangrovii* gen. nov., sp. nov. and *Leptoelongatus litoralis* gen. nov., sp. nov. (Leptolyngbyaceae) isolated from an Indian mangrove forest**

SANDEEP CHAKRABORTY¹, VEERABADHRAN MARUTHANAYAGAM¹, ANUSHREE ACHARI², ARNAB PRAMANIK³, PARASURAMAN JAISANKAR² & JOYDEEP MUKHERJEE^{1*}

¹ School of Environmental Studies, Jadavpur University, Kolkata 700 032, India

² Indian Institute of Chemical Biology, Jadavpur, Kolkata 700 032, India

³ Department of Biochemistry, University of Calcutta, 35, Ballygunge Circular Road, Kolkata 700 019, India

* Corresponding author

Tel. 0091 33 2414 6147

Fax 0091 33 2414 6414

E mail: joydeep.mukherjee@jadavpuruniversity.in

Abstract

Molecular data based revision of *Leptolyngbya*, the largest polyphyletic genus of the family Leptolyngbyaceae (Synechococcales) is imperative. Polyphasic approach to the taxonomic analysis of two (AP9F and AP25) cyanobacteria, tentatively designated positions in the “LPP-group” is described. Cell shapes of AP9F and AP25 were highly elongated whereas the cells of the reference strains (*Leptolyngbya boryana* and *Nodosilinea nodulosa*) were occasionally elongated to isodiametrical. Terminal cells of AP9F and AP25 appeared as flattened corners (not rounded), which was different from other Leptolyngbyaceae members. 16S rRNA gene sequences of AP9F (1366 bp) and AP25 (1408 bp) showed 95% and 92% similarities respectively with the non-redundant nucleotide sequences of their closest relatives of the *Leptolyngbya* genus. Test strains were located in the phylogenetic tree in a clade different from the ones containing the type species. A single operon having both tRNA^{ile} and tRNA^{ala} genes were present in the ITS regions of AP9F and AP25 compared to two operons in the ITS region of the genera *Leptolyngbya* and *Nodosilinea*: one having both tRNA^{ile} and tRNA^{ala} genes and another lacking both the genes. The secondary structures of the traditionally conservative D-stem region as well as the Box B helix and V3 regions of the ITS operons significantly varied between the test strains and also when compared with the corresponding sequences of *L. boryana* and *N. nodulosa*. Molecular phylogenetic and morphological data suggested AP9F and AP25 to be monophyletic taxa for which the names *Euryhalinema mangrovii* gen. nov., sp. nov. and *Leptoelongatus litoralis* gen. nov., sp. nov. are proposed respectively.

Keywords: Cyanobacteria, internal transcribed spacer region, *Leptolyngbya*, Sundarbans

Introduction

Correct taxonomical identity of any organism reflects the evolutionary foundation necessary to establish the relation between the organism’s genes and its behavior (Philippot *et al.* 2010). The Cyanoprokaryotes constitute a major share of the primary producers of the earth. Understandably, they require intense scientific attention to gain complete knowledge of their taxonomical identification, physiological characteristics and genetic composition. Cyanobacteria are ecologically important groups of organisms which are proven to be potential sources of commercially important secondary metabolites. This possibility has prompted the necessity of detailed investigations on the systematic positions of the Cyanoprokaryotes. The cyanobacterial biodiversity of the vast forestland of the Sundarbans, the world’s largest tidal mangrove forest is unexplored, only two species being validly described. Our group identified two strains (AP17 and AP24) as *Oxynema aestuarii* sp. nov. through a polyphasic approach (Chakraborty *et al.* 2018). *O. aestuarii* was the second novel species of the newly-formed genus *Oxynema*, which was separated from the *Phormidium*-Group I genus (Chatchawan *et al.* 2012). Debnath *et al.* (2017) also studied simple trichal non-heterocytous cyanobacteria in the alluvial arsenic-affected rice field soils and estuarine mangrove soil of the Indian Sundarbans and reported *Geitlerinema* cf. *calcuttense*, *Geitlerinema* cf. *jasorvense* and *Coleofasciculus* cf. *chthonoplastes* for the first time from India and described *Leptolyngbya indica* as a novel species. Debnath *et al.* (2017) also stressed the necessity for

upgradation of the cyanobacterial taxonomic literature of the Indian subcontinent. The possibility for identification of further novel species exists because it is known that cyanobacteria residing in the mangroves may undergo morpho-ecological changes for their survival which can stimulate speciation (Debnath *et al.* 2017). Additionally, the Sundarbans is typified by constant tidal forcing and mixing of water columns that permit cyanobacteria to flourish resulting in considerable genetic diversity (Neogi *et al.* 2016). Lopes *et al.* (2012) further noted that morphological characters of mangrove cyanobacteria were infrequently not in concurrence with phylogenetic relationships and had a tendency to change in response to the prevailing environmental conditions.

The overall alpha-level taxonomy to identify Cyanoprokaryotes is currently in a disordered state (Komarek 2006, Palinska & Surosz 2014). The general taxonomical approaches to classify cyanobacteria follow the principle of organizing these microorganisms as described by Komarek & Anagnostidis (2005) and Komarek *et al.* (2014) which has been subject to several revisions based on which around forty five new genera have been described between the years 2010 and 2015 (Bohunicka 2015). Out of eight cyanobacterial orders identified in the classification of Komarek *et al.* (2014), the order Synechococcales consists of many polyphyletic genera. Very recently a family-level revision was performed on the order Synechococcales and six new genera under the family Oculatellaceae (Synechococcales) were described (Mai *et al.* 2018). *Leptolyngbya* is the largest, heterogeneous and highly diversified genus which is polyphyletic in origin and has been suggested to be separated into several new genera (Casamatta *et al.* 2005, Komarek & Anagnostidis 2005, Johansen *et al.* 2008, Zammit *et al.* 2012, Komarek *et al.* 2014, Mai *et al.* 2018). Genus *Leptolyngbya* is believed to contain members which are morphologically alike but genetically very distant. Hence, a serious revision based on the molecular data of the *Leptolyngbya* genus is urgent to attain more resolved and reliable relationships among the member organisms of this genus. Accordingly, genus *Phormidesmis* (Komarek *et al.* 2009, Turichhia *et al.* 2009) and genus *Nodosilinea* (Perkerson *et al.* 2011) were separated from the *Leptolyngbya* genus and designated as novel genera. Furthermore, *Haloleptolyngbya* sp. (Dadheech *et al.* 2012), *Chroakolemma* sp. (Becerra-Absalon *et al.* 2018) and *Albertania* sp. (Zammit 2018) were distinguished from the *Leptolyngbya* genus through the polyphasic approach to taxonomy and established as novel generic entities.

The present study describes the polyphasic approach to taxonomic analysis of two (AP9F and AP25) out of eight cyanobacteria which were previously isolated from the Indian Sundarbans by our research group (Pramanik *et al.* 2011) and tentatively designated positions in the “LPP-group” following Rippka *et al.* (1979). Although this study was not designed to describe novel taxa, it was the view of Alvarenga *et al.* (2015) that the report of Pramanik *et al.* (2011) may support the definition of novel cyanobacteria. Against this background, we now propose that based on the polyphasic approach to taxonomic analyses encompassing molecular phylogenetic relationships of strains AP9F and AP25 with the other close members of the *Leptolyngbya* genus, the presence of morphological autapomorphic characteristics as well as ecological considerations, strains AP9F and AP25 be separated from the classical *Leptolyngbya* genus and be designated as two separate novel genera.

Materials and methods

2.1 Collection and maintenance of strains Cyanobacterial strains AP9F and AP25 were collected from the soil surface biofilms of the Lothian and Sagar islands respectively (Fig. 1) of the Indian Sundarbans. The details of the physical characteristics of the study site are mentioned in Pramanik *et al.* (2011). Pure cultures were aseptically maintained in ASN III liquid medium in Erlenmeyer flasks (Rippka *et al.* 1979) as well as in solid cultures in Petri dishes. The cultures were housed in a controlled environment having fluorescent irradiance ($50 \mu\text{mol photons m}^{-2} \text{s}^{-1}$) with 12:12 hrs light : dark photoperiod at 25 ± 1 °C (Chakraborty *et al.* 2018). Culture purity as well as other morphological and biochemical properties of the cultures were observed at regular intervals. No changes were noticed during storage. The isolates AP9F and AP25 having accession numbers MCC 3171 and MCC 3170 respectively were deposited in the Microbial Culture Collection (MCC), India where they are being cryopreserved.

2.2 Light microscopy Morphological examination was done by using a light microscope (Model DM750; Leica Microsystems, Buffalo Grove, USA) under 400–1000 magnification. Photomicrographs of fresh filaments from the 10-day old cultures of AP9F and AP25 were obtained by a camera (ICC50 HD) attached to the microscope (Chakraborty *et al.* 2018). Cellular dimensions were recorded by the help of the associated software (LAS-EZ, Leica Microsystems) provided with the microscope.

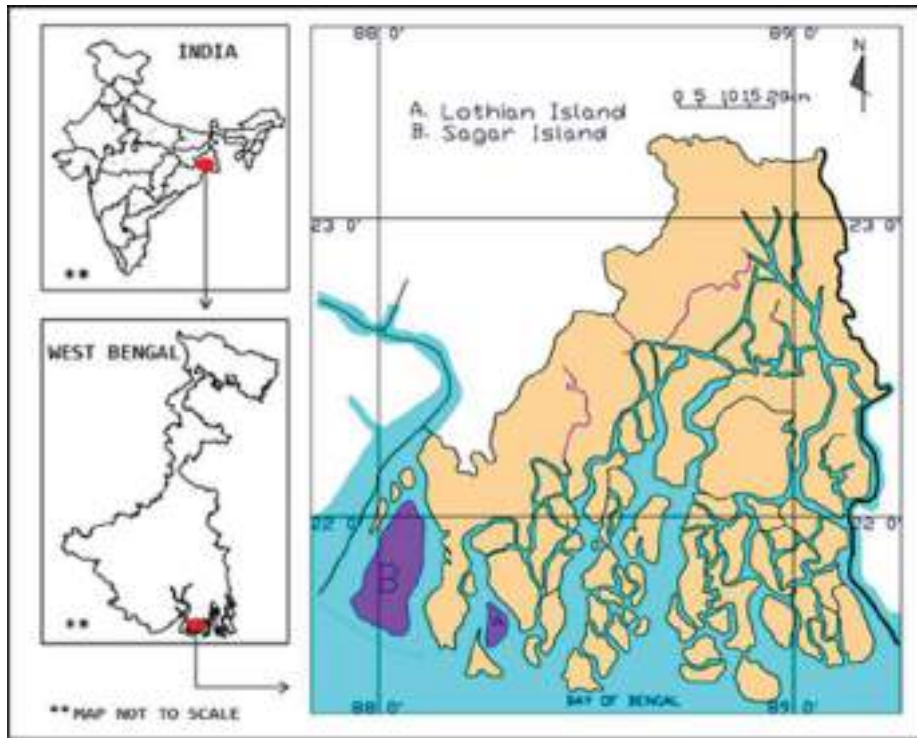


FIGURE 1. Map showing the location of sampling sites. Samples were collected from the Sagar and Lothian islands of Indian Sundarbans.

2.3 Scanning electron microscopy Fresh filaments of the test strains were obtained after centrifugation of 1 ml suspension at 8000 rpm (Eppendorf 5810R, rotor F-34-6-38, Hamburg, Germany). The cells were fixed in 3% glutaraldehyde for 2 hrs and subsequently washed in distilled water. Cells were dehydrated using increasing concentrations of ethanol from 30% for 15 min to 100% for 60 min. The samples were eventually dried at the critical point and the grids were observed under a scanning electron microscope (Jeol JSM-6700F, Jeol, Tokyo, Japan) following Chakraborty *et al.* (2018).

2.4 Transmission electron microscopy About 1 ml suspension of fresh cells from 8–10 day old cultures of AP9F and AP25 were centrifuged at 8000 rpm (Eppendorf 5810R, rotor F-34-6-38, Hamburg, Germany). The pellets were washed thoroughly in distilled water and subsequently pre-fixed in 2.5% glutaraldehyde and 2% paraformaldehyde in 0.1 M phosphate buffer (pH 7.8) for 5–6 hrs at 4 °C. The samples were rinsed in 0.1 M phosphate buffer and the leftover fixative was washed off with the buffer. The cells were post fixed with osmium tetroxide (1% solution) for 60 minutes. Thereafter, cells were dehydrated by passing through increasing concentrations of ethanol. Samples were then infiltrated and embedded in Araldite CY 212 (Agar Scientific, Stansted, UK) for cutting of sections. The resin block was polymerized by heat treatment at 50 °C overnight and subsequently a second treatment at 60 °C for 2 days was applied. Thin sections of the samples were cut by employing an ultramicrotome, thenceforth contrasted with uranyl acetate and lead citrate and observed under a TECNAI G20 transmission electron microscope (FEI, Eindhoven, Netherlands) following Chakraborty *et al.* (2018).

2.5 DNA extraction, PCR amplification and sequencing Cells from the exponential phase of the axenic cultures (AP9F and AP25) were harvested and the total genomic DNA was extracted using Gene JET™ Genomic DNA Purification Kit (Cat. No. K0721, Thermo Scientific, Waltham, USA) adhering to the manufacturer's protocol. Purity of the DNA was confirmed by gel electrophoresis in a 1.5% agarose gel. PCR amplification of the 16S rRNA gene and the 16S-23S rRNA internal transcribed spacer (ITS) regions were performed in a Mastercycler Nexus Gradient PCR machine (Eppendorf, Hamburg, Germany) as described in Chakraborty *et al.* (2018). Cyanobacterial specific forward primers CYA106F (5'CGGACGGGTGAGTAACGCGTGA3') (Nubel *et al.* 1997) and universal reverse primer 1492R (5'-ACCTTGTTACGACTT-3') (Lane 1991) were used for amplification of the 16S rRNA gene, while forward primer 16SF (5'TGTACACACCGGCCCGTC3') and reverse primer 23SR (5' CTCTGTGCCTAGGTATCC 3') as indicated in Itean *et al.* (2000) were applied for the amplification of the 16S-23S ITS regions. The reaction conditions employed for amplification of the 16S rRNA gene were: initial denaturation at 94 °C for 5 min thereafter 30 cycles at 94 °C for

1 min; 50 °C for 1 min and 72 °C for 2 min and ultimate extension at 72°C for 10 min. The reaction conditions used for amplification of the 16S-23S ITS region were: initial denaturation at 95 °C for 5 min thereafter 30 cycles at 95 °C for 30 sec; 58 °C for 15 sec; 72 °C for 40 sec and ultimate elongation step at 72 °C for 5 min (Chakraborty *et al.* 2018). The PCR products obtained after amplification were analyzed on a 1.5% agarose gel stained with ethidium bromide and PCR fragments of appropriate size were purified with Gene JET™ PCR Purification kit (Cat. No. K0701, Thermo Scientific, Waltham, USA). Construction of clone libraries from the purified PCR products was carried out using InsTAclone™ PCR cloning kit (Cat no. K1213, K1214, Thermo Scientific, Waltham, USA). The purified DNA fragments were inserted into the commercial cloning vector pCR 2.1 (Life Technologies, Invitrogen, USA) and the vectors with inserted DNA were then transformed into *E. coli* DH5 α cells. White and blue colonies were screened and plasmids were isolated from the positive transformants with Thermo Scientific GeneJET Plasmid Miniprep Kit (Cat no. K0502, K0503, Waltham, USA). Plasmids were digested with restriction enzymes Eco RI and Hind III and the representative clones were chosen for sequencing. The sets of primers used for sequencing of cloned products of the 16S rRNA gene and 16S-23S ITS regions were alike to the set applied earlier for PCR amplification. The sequencing was performed using an automated DNA sequencer (Genetic Analyzer 3500xL, Applied Biosystems, Waltham, USA) as described in Chakraborty *et al.* (2018). The ensuing sequences of 16S rRNA and 16S-23S ITS regions of the two test isolates (AP9F and AP25) were submitted to GenBank and their accession numbers are presented in Table 1.

TABLE 1. Gene sequences of the cyanobacterial test strains submitted in NCBI database with their accession numbers.

Gene sequences	Test strains	
	AP9F	AP25
GenBank Accession no. for 16S rDNA	MK402979	MK402980
GenBank Accession no. for 16S-23S ITS rDNA	MK402981	MK402982
Length of 16S rDNA (bp)	1366	1408
Length of 16S-23S ITS (bp)	459	506

2.6 Analysis of the 16S rRNA gene sequence and phylogenetic tree construction The sequences of the 16S rRNA genes of the strains under investigation (AP9F and AP25) were examined in the Basic Local Alignment Search Tool (BLAST) within the robust database of the National Center of Biotechnology Information (NCBI, <https://www.ncbi.nlm.nih.gov/genbank/>) and pairwise similarities were determined with the other members available in the database. A consensus phylogenetic tree was constructed based on the similarity results by selecting the partial sequences of 16S rRNA (length >1100 bp) of the closest relatives (based on BLAST hits) of the test strains (AP9F and AP25) as well as the sequences of the traditional cyanobacterial taxa from the NCBI database to establish a justified evolutionary relationship with the test strains (Chakraborty *et al.* 2018). The 16S rRNA gene sequences of the reference strains (*Leptolyngbya boryana* PCC6306 and *Nodosilinea nodulosa* UTEX2910) were obtained from the GenBank resources available in NCBI. The sequences of the taxa having ambiguous affiliation were excluded. The sequences were aligned in CLUSTAL W program (Larkin *et al.* 2007). Bayesian Inference (BI), Maximum Likelihood (ML) and Neighbor Joining (NJ) analysis were performed using these aligned sequences. BI analysis was conducted using MrBayes version 3.2.7a (Ronquist *et al.* 2012b), applying a GTR+G+I model of nucleotide substitutions. Two runs were conducted with four chains and each of the two runs was performed simultaneously for 10⁶ Markov Chain Monte Carlo (MCMC) generations. Temperature was empirically set to 0.2 and allowed the sampling of trees after every 100 generations. This analysis had an estimated sample size (ESS) exceeding 300 for all the parameters which is believed to be sufficient and accepted by the phylogeneticists (Drummond *et al.* 2006). The average standard deviation of split frequencies and the potential scale reduction factor (PSRF) value for all the parameters were below 0.01 and equaled to 1 respectively, indicating the statistical achievement of convergence of the MCMC chains (Gelman & Rubin 1992). The first 25% trees were discarded as a burn-in phase and a 50% majority rule consensus tree was calculated including posterior probabilities. The phylogenetic tree through ML analysis was constructed using the PAUP version 4b10 (Swofford 2002) where the majority rule was selected. Confidence values for the branches of the phylogenetic tree were determined by bootstrapping of 1000 replications. The multiple aligned sequences were analyzed for DNA substitution using the likelihood ratio statistical test implemented in the jModel Test version 0.1.1 program (Posada 2008) to ascertain the best-fit model of our data. The (GTR+I+G) model of substitution was retrieved as the best fit for the data for performing phylogenetic analysis using the Akaike Information Criterion. Gaps were not considered in the phylogenetic analysis. *Gloeobacter violaceus* was chosen as an outgroup taxon. The phylogenetic tree so generated was

visualized using TreeGraph 2 (Stover & Muller 2010). Another phylogenetic tree was constructed with the identical multiple aligned sequences by applying the Neighbor Joining (NJ) method. Finally, bootstrap values for both ML and NJ analyses were mapped on the BI analysis tree.

2.7 Analysis of 16S-23S ITS secondary structures While aligning the sequences of the operons among studied strains and reference strains, similar operons (i.e. operons having both tRNA genes for alanine and isoleucine respectively) were compared with each other and then folded to study the differences. The ITS secondary structures of the two strains under investigation (AP9F and AP25) as well as the reference strains *Leptolyngbya boryana* PCC6306 and *Nodosilinea nodulosa* UTEX2910 were generated using the M-fold web server, version 2.3 (Zuker 2003) and redrawn in Adobe Illustrator CS5.1. The secondary structures were obtained under ideal conditions of untangled loop fix and the temperature set to default at 37 °C. The structures of the D1-D1' helix and Box B helix regions of AP9F and AP25 were evaluated against equivalent structures of the reference strains. Comparisons of the sequence lengths and secondary structures (wherever appropriate) of the various regions of the ITS sequences (total 14 regions) of AP9F and AP25 with the reference strain were performed following Johansen *et al.* (2011) and described in Chakraborty *et al.* (2018).

Results

3.1 Morphological characterization Our studied strains (AP9F and AP25) were compared with each other as well as individually with the two reference strains (*Leptolyngbya boryana* and *Nodosilinea nodulosa*) following the polyphasic approach. Other members of family Leptolyngbyaceae were not morphologically congruent with the examined strains and displayed very contrasting features. Strains AP9F and AP25 showed moderate growth as bluish-green mat-like biofilm attached on the surface of Erlenmeyer flasks. Light microscopy (Fig. 2) revealed that both the strains possessed some common features like thin thallus, pale to bluish-green color and having filaments more or less densely entangled to form a floating mat-like biofilm or attached to the surface. Filaments were long, unbranched, straight or wavy with rounded ends. Cells were much longer than their width; length ranged from 1.25–2.6 µm and width 0.4–0.6 µm (AP9F) whereas dimensions of AP25 were 1.8–3.5 µm (length) and 0.4–0.5 µm (width). Mucilage sheath was absent in the filaments of AP9F. However, a very thin and inconspicuous sheath was facultatively visible in some cells of strain AP25 only under scanning electron microscope (Fig. 3 c, e). Presence/absence of sheath was not considered as a differentiating characteristic. Cells showed fine constrictions at their cross walls which was almost similar for both the strains. Trichomes of both the strains were non-heterocytous, without any akinetes or any aerotopes. Filaments were vegetatively propagated through hormogonia. A morphological comparison of the strains AP9F and AP25 with their close relatives is presented in Table 2. Cell length/width ratio of strain AP25 was significantly greater than that of strain AP9F (around 1.5 folds, see Table 2). Additionally, cell length/width ratios of the studied strains were conspicuously greater than the corresponding ratios of the reference strains: *Leptolyngbya boryana* (4.9 folds higher in AP9F and 7.5 folds higher in AP25) and *Nodosilinea nodulosa* (2.7 folds higher in AP9F and 4.2 folds higher in AP25). Cell shapes of AP9F and AP25 were observed to be highly elongated (Fig. 3) whereas the cells of the reference strains were occasionally elongated to isodiametrical. In the present study, the ends of the terminal cells of AP9F and AP25 appeared as flattened corners (not rounded, see Fig. 3b).

3.2 Ultrastructural studies The ultrastructural features of the two strains under examination were almost similar reflecting the overall characteristic of the family Leptolyngbyaceae (Fig. 4). Cellular features like constrictions in the cross walls, cell wall, sheath, which were difficult to be evaluated by light microscopy were clearly visible. Thylakoids were arranged in such a manner that the overall pattern may be said to be concentric but not well defined and were parallel to the cell wall. Inter-thylakoidal space was not appressed. Presence of a prominent cell wall, carboxysomes and cyanophycin were confirmed (Fig. 4a). In general, the thylakoids were arranged parietally which coincides with the evolutionary line in the Synechococcales. However, inter-thylakoidal spaces were found to be more distant in the strains AP9F and AP25 as compared to that in *Nodosilinea nodulosa* (Perkerson *et al.* 2011). This feature was also considered to be a diacritical marker for the differentiation among the taxa at the genus or species levels (Bruno *et al.* 2009).

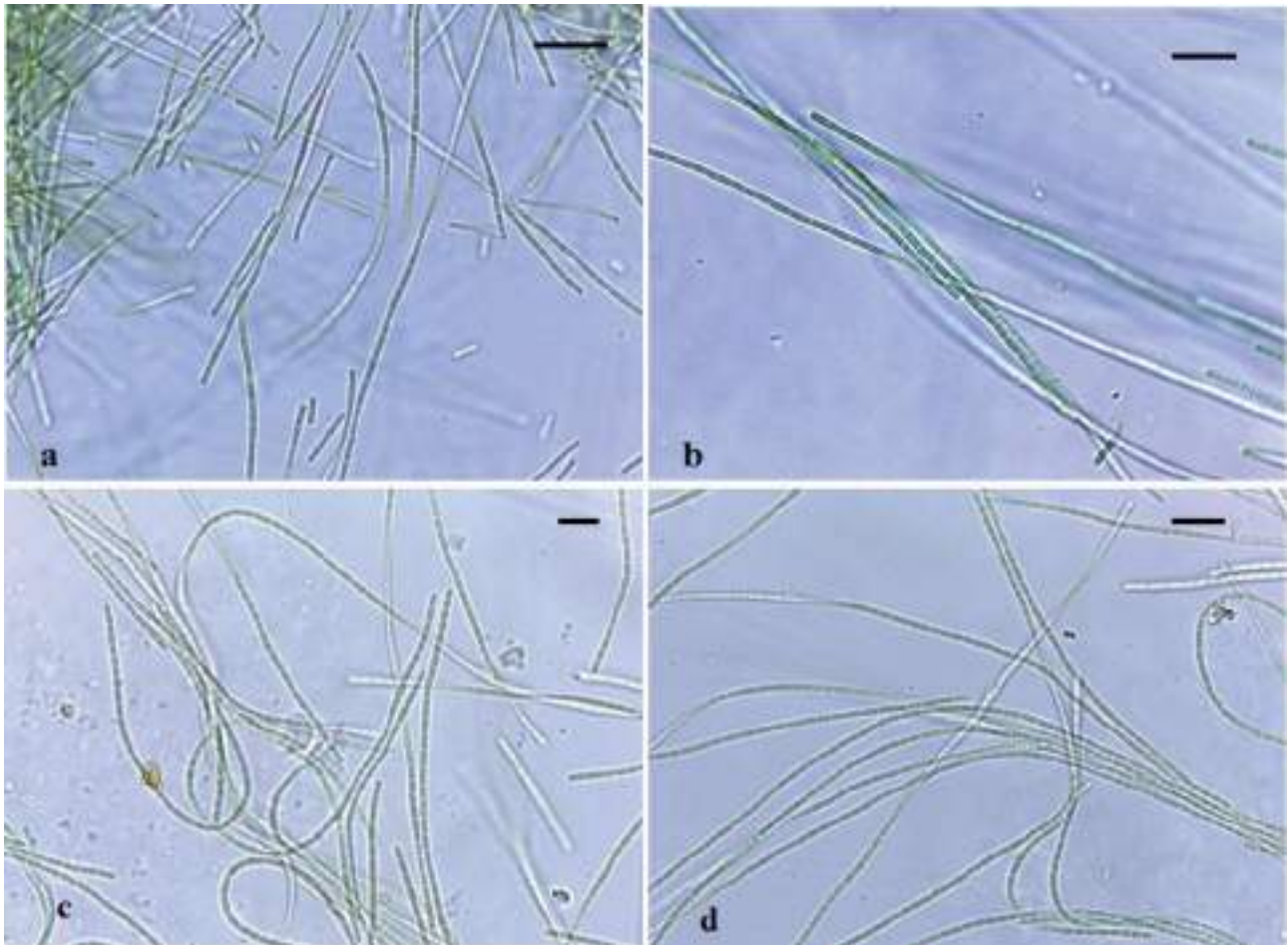


FIGURE 2. Light microscopy of AP9F and AP25. a-b. Microphotograph showing the filaments of strain AP9F. c-d. Microphotograph showing the filaments of strain AP25. Scale bars = 5 μ m

TABLE 2. Comparative analysis of morphology of test strains and reference strains *Leptolyngbya boryana* and *Nodosilinea nodulosa*. Characteristics of previously described genera were obtained from Johansen *et al.* (2001) and Perkeron *et al.* (2011). The values of the cell length/width ratio was calculated from the mean of cell length and width of 50 determinations (n=50).

Feature	AP9F	AP25	<i>Leptolyngbya boryana</i>	<i>Nodosilinea nodulosa</i>
Thallus	Pale bluish-green in color, fine mats	Pale bluish-green color mats	Blue-green colony	Greenish mats
Filaments	Thin, long, straight or wavy	Thin, long, straight or wavy	Thin, long, straight or wavy	Long, unbranched or rarely pseudobranched, forming nodules in low light
Mucilage sheath	Absent	Absent	Absent	Thin, colorless, occasionally become wide and diffuent
Constrictions at cross walls	Prominent constrictions	Prominent constrictions	Distinctly constricted	Distinctly constricted
End cells	Ends flattened like edges of a rectangle (not rounded)	Ends flattened like edges of a rectangle (not rounded)	Ends were rounded	Ends were rounded
Cell length/width ratio	3.85	5.88	0.78	1.38
False branching	Absent	Absent	Present	Occasionally
Cell shape	Elongated (much longer than the width)	Elongated (much longer than the width)	More or less isodiametric	Mostly isodiametric
Habitat	Intertidal area (estuarine) with salinity ranging from 1.7–1.8%	Intertidal area (estuarine) with salinity ranging from 1.7–1.8%	Metaphytic, lentic	Marine (planktonic tow) from depth 10m

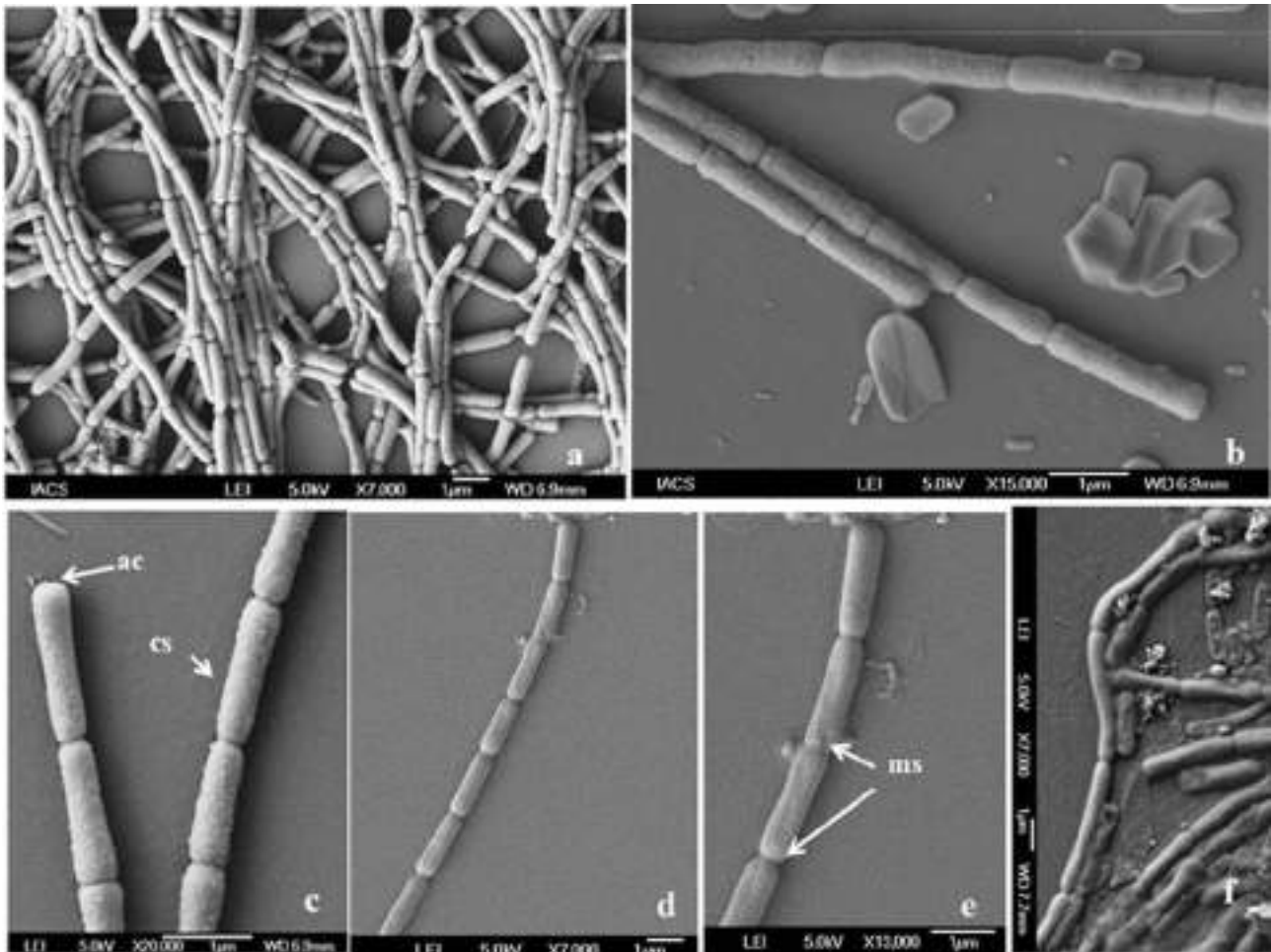


FIGURE 3. Scanning electron microscopy of AP9F and AP25. a-c. Part of the filament of AP9F showing cross wall constrictions and apical cell morphology. d-f. Part of the filament of strain AP25. ac= apical cell, cs= cell surface (rough), ms= facultative mucilaginous sheath

3.3 Analysis of the 16S rRNA gene sequences and construction of phylogenetic trees The PCR reactions described in section 2.5 generated partial 16S rRNA gene sequences of AP9F and AP25 having lengths 1366 bp and 1408 bp respectively. The phylogenetic analysis of the strains AP9F and AP25 revealed 95% and 92% similarities with the non-redundant nucleotide sequences of their closest relatives in NCBI respectively corresponding to the four top hits: accession numbers HM217066, KU569325, EU624415 and AB003168 for AP9F and accession numbers KT315912, JQ927355, EU249120 and KU569325 for AP25. The extent of similarity of the 16S rRNA sequences between AP9F and AP25 and members of genera such as *Chroakolemma* sp., *Albertania* sp., *Haloleptolyngbya* sp. were approximately less than 90%. Among the members of Leptolyngbyaceae, *Nodosilinea nodulosa* showed highest similarity of the 16S rRNA gene sequence (about 94%) with the strains under examination and was considered as reference strain. A type species of “true” group *Leptolyngbya sensu stricto* i.e., *Leptolyngbya boryana* was also selected as another reference strain. To establish the precise phylogenetic positions of the AP9F and AP25, a comprehensive phylogenetic analysis was conducted utilizing the 16S rRNA sequences of the different members of Leptolyngbyaceae along with the traditional taxa and other related family members available in GenBank. The resultant tree (Fig. 5) demonstrated that AP9F and AP25 are phylogenetically close to the species of the *Leptolyngbya* genus, however the two strains displayed separate lineages as evidenced by significant divergences from the closest relatives and supported by 100% bootstrap values in all the branches (Fig. 5). The clade consisting of AP9F and AP25 was sister to the clades of “true” *Leptolyngbya* (*Leptolyngbya sensu stricto*) and *Nodosilinea* respectively. The node containing strain AP9F also included a strain named “*Calothrix* sp. 96/26 LPP3” as a sister taxa which might represent a novel species under the proposed genera *Euryhalinema*. The clade of *Leptolyngbya sensu stricto*, *Chroakolemma* and *Albertania* (Fig. 5) were substantially supported by the bootstrap values of almost 100%.

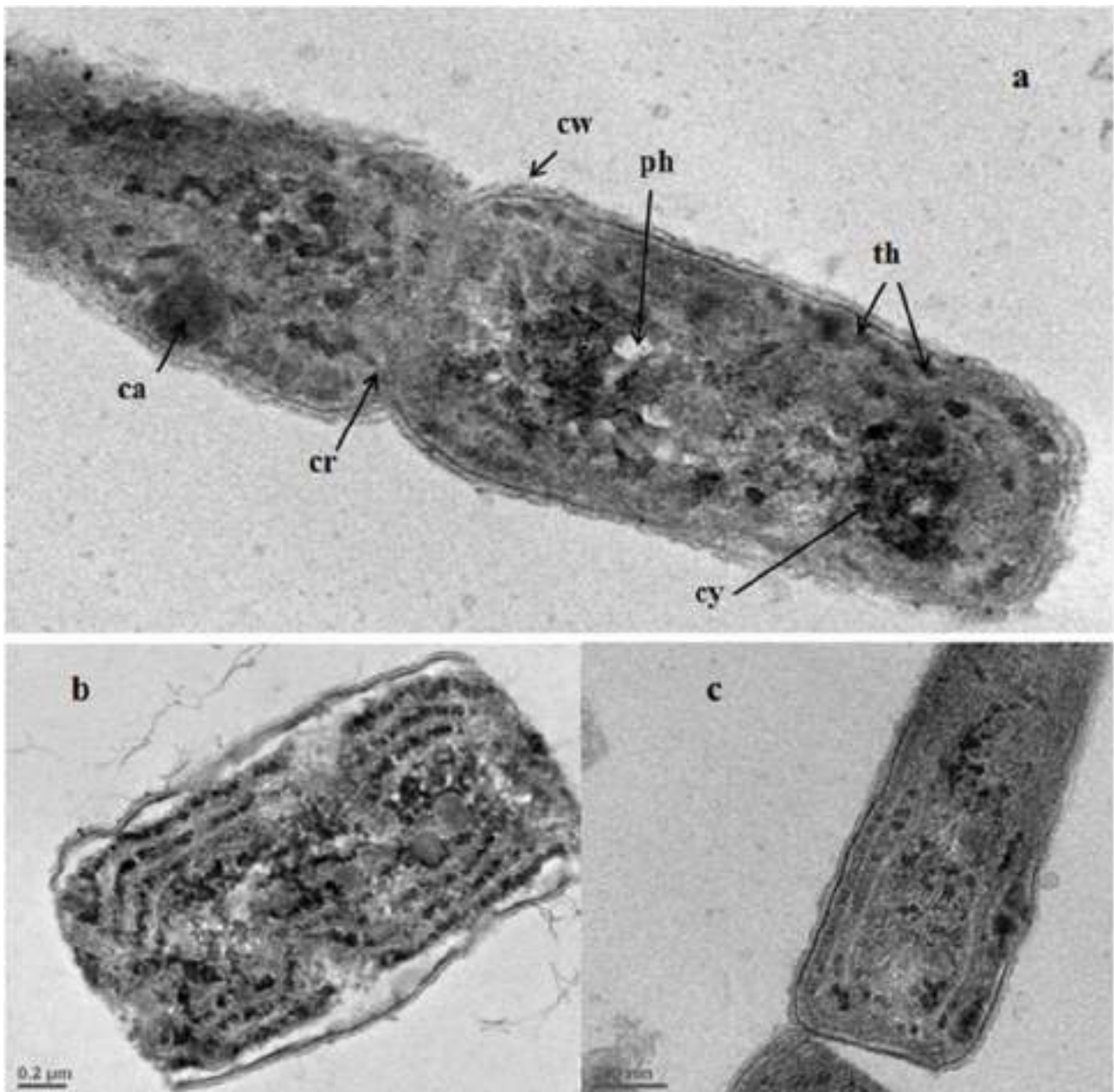


FIGURE 4. Transmission electron microscopy of AP9F and AP25. **a-b.** Cross sections of the filaments of strain AP9F. **c.** Cross sections of the filament of strain AP25. Characteristics show prominent concentric arrangement of thylakoids and presence of other features. cw= cell wall, cy= cynophycin, th= thylakoids, cr= cross walls, ca= carboxysomes, ph= phosphate body

3.4 Analysis of the 16S-23S ITS gene sequences PCR amplification of the ITS regions of AP9F and AP25 generated 459 bp and 539 bp long sequences respectively. The AP9F sequence was around 84% similar and the AP25 sequence was approximately 88% similar to the other equivalent sequences available in the NCBI database. The ITS regions of both the strains were characterized by the presence of a ribosomal operon having tRNA^{ile} and tRNA^{ala} genes. The structure of the D-stem region significantly varied between the strains under investigation and also when compared with the corresponding sequences of the type species of *Leptolyngbya* and *Nodosilinea* (Fig. 6). Additionally, the ITS operon consisted of other conserved and variable domains which are presented in Table 3. Secondary structures of D1-D1' helix, Box B helix and V3 regions of the ITS sequences determined for our strains were compared with similar sequences obtained from reference strains *Leptolyngbya boryana* and *Nodosilinea nodulosa* sharing morphological as well as molecular resemblances. The lengths of the D1-D1' helices of the ITS gene sequences of AP9F (67 nt) and AP25 (59 nt) were not only distinct from the two reference strains *Leptolyngbya boryana* (51 nt) (EF429290) and *Nodosilinea nodulosa* (62 nt) (KF307598) (Table 3) but also the structures varied in terms of the number of loops, sequences and the size of the terminus (Fig. 6). D1-D1' helix of the ITS gene sequence of AP9F consisted of

67 nucleotides having a small terminal loop of 3 nt, two bilateral and two small unilateral bulges (1 nt and 2 nt) in its secondary structure. D1-D1' helix of the ITS gene sequence of strain AP25 was constituted of 61 nucleotides and the secondary structure was significantly different when compared to the corresponding structure of AP9F. The D1-D1' helix of AP25 contained a large terminal loop of 11 nt, two small and a large unilateral bulge (6 nt) and the basal structure was dissimilar in comparison with the basal structure of the D1-D1' helix of AP9F (Fig. 6).

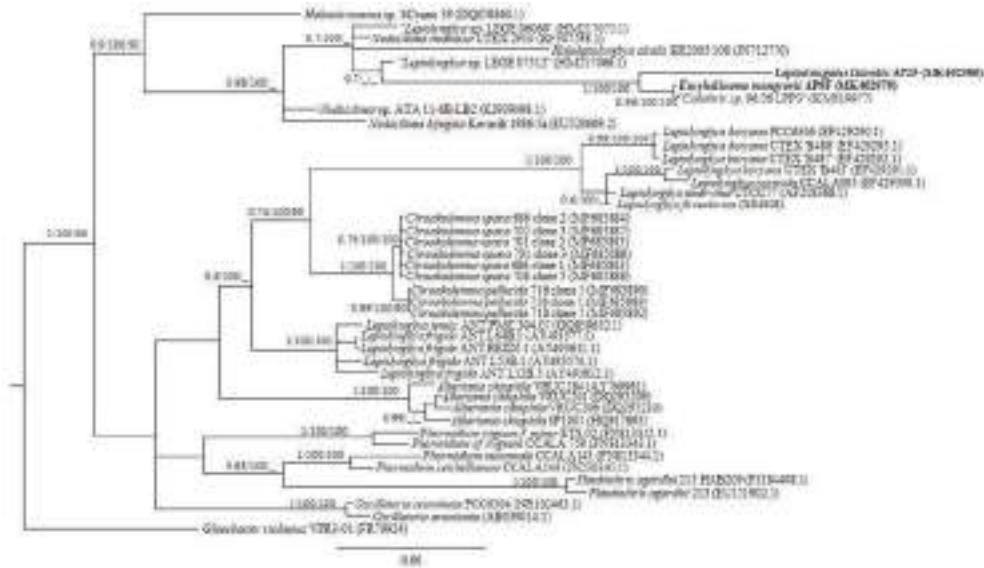


FIGURE 5. Bayesian Inference analysis with 43 OTUs belonging to Synechococcales and Oscillatoriales with *Gloeobacter violaceus* as outgroup. 1408 nucleotide of 16S rRNA gene sequences were aligned. Node support was indicated as BI posterior probability values/ ML bootstrap/NJ bootstrap; ‘_’ indicates less than 50% bootstrap support value. Taxa names in quotation marks eg. “*Calothrix*” were erroneously named or requires revision.

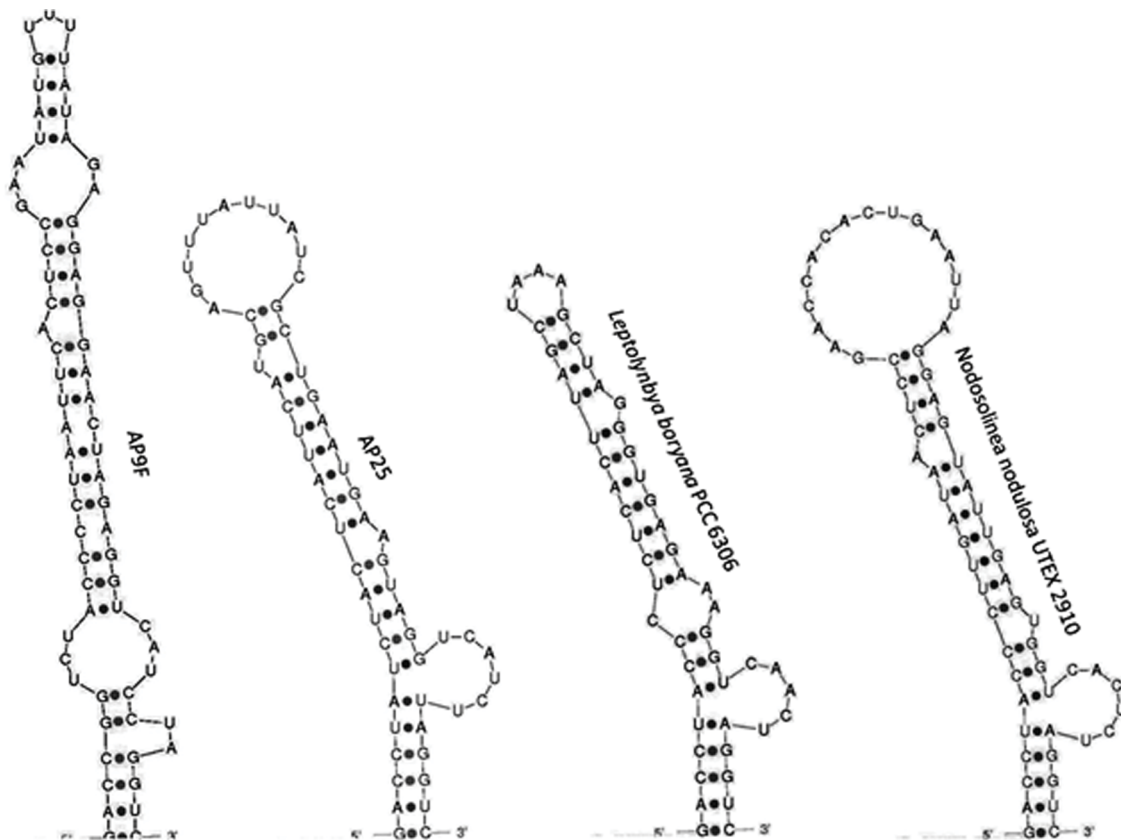


FIGURE 6. Comparative analysis of D1-D1' helices of the 16S-23S ITS regions of test strains (AP9F and AP25) and their closest phylogenetic relatives *Leptolyngbya boryana* and *Nodosilinea nodulosa*

TABLE 3. Comparison of the nucleotide lengths of the ITS regions of AP9F, AP25, *Leptolyngbya boryana* and *Nodosilinea nodulosa*. Significant differences are shown in bold. Only operons containing both tRNA genes are reported in this table for *Leptolyngbya boryana*, although operons containing no tRNA genes in the ITS were also recovered from this strain. Data of *Leptolyngbya boryana* and *Nodosilinea nodulosa* were obtained from Johansen *et al.* (2011) and Perkerson *et al.* (2011) respectively.

Strains under investigation (AP9F and AP25) and reference strain	Leader	D1-D1' helix	D2 with spacer	D3 with spacer	tRNA ^{ile} gene	V2 spacer	tRNA ^{ala} gene	Pre Box B spacer	Box B	Post Box B spacer	Box A	D4	V3	D5
AP9F	8	61	18	12	74	5	73	34	34	19	11	7	20	16
AP25	8	61	15	12	74	5	73	36	40	20	11	7	22	21
<i>Leptolyngbya boryana</i>	8	51	41	16	74	14	73	65	11	18	11	15	23	37
<i>Nodosilinea nodulosa</i>	8	62	20	19	71	8	73	24	40	18	12	7	27	12

The secondary structures of Box B helices of the ITS gene sequence of AP9F consisted of total 34 nt, the terminal loop being made up of 6 nt and a straight chain without any bulges. The Box B helix structure of the ITS gene sequence of AP25 contained total 40 nt having a terminal loop (4 nt), an unilateral loop (2 nt) and a bilateral bulge. The basal sequences of the ITS regions of both strains were identical (5' CAGC-GUCG 3'). The structural pattern of Box B helix of the ITS operon of AP25 (40 nt) differed from AP9F as well as from other two reference strains in having significantly smaller terminus (6 nt) along with a bilateral bulge and an unilateral bulge (4 nt), while the same structure in case of *Leptolyngbya boryana* (35 nt) possessed a comparatively larger terminus (7 nt) and a smaller unilateral bulge. The corresponding structure of *Nodosilinea nodulosa* (40 nt) consisted of a terminus (6 nt) and two single nucleotide unilateral bulges (Fig. 7). V3 helical regions of the ITS gene sequences of AP9F and AP25 comprised of 20 nt and 22 nt respectively. The overall structure of the V3 helix of the ITS operons of both strains showed a large terminal loop of 12 and 14 nt respectively and a common basal sequence: 5' AGUC-ACAG 3'. The folding pattern of the V3 helix of the ITS gene sequences also revealed noteworthy differences, not only between the two strains under investigation (AP9F and AP25), but also in comparison to the two reference strains. The length of the V3 helical region in case of AP25 was 2 nt longer when compared to the corresponding structure of AP9F. The difference in length was probably due to an insertion/deletion of two adenine nucleotides and substitution of 5'-ACG-3' to 5'-UAA-3' as evident from Fig. 8 (shown in orange color).

Discussion

The results of the taxonomic study using a polyphasic approach clearly demonstrated that strains AP9F and AP25 were diagnosable from the other members of Leptolyngbyaceae as evidenced from morphological, ultrastructural, ecological and molecular phylogenetic data. According to Martins *et al.* (2016), the morphological data for taxonomical assignments were not always informative and corroborative with the phylogenetic data. However, in the present investigation the proposal of assigning the two strains as novel genera as evidenced by morphological studies was supported by phylogenetic data.

AP9F and AP25 were taxonomically distinct based on certain morphological features that deserve special emphasis such as cellular dimensions, cell shape and shape of the terminal cell. Similar to our claim, two novel genera namely *Marileptolyngbya sina* and *Salileptolyngbya diazotrophicum* were separated from the closest genera *Leptolyngbya* and *Nodosilinea* considering difference in the cellular length as an apomorphic character (Zhou *et al.* 2018). Terminal cell morphology is also considered to be an important criterion (Komarek & Anagnostidis, 2005) for the separation of inter-generic entities (Chatchawan *et al.* 2012, Hasler *et al.* 2012, Martins *et al.* 2018). In the present study, the terminal cells of AP9F and AP25 were different from any other Leptolyngbyaceae members reported till date (Johansen *et al.* 2011). The variations in the distance of inter-thylakoidal space among the strains under investigation and the reference strains were observed. The distance between the appressed thylakoids depends on the distribution of phycobilisomes located in the thylakoids (Westerman *et al.* 1994, Olive *et al.* 1997) and their distribution depends directly on the ecological

habitats. The reach and distribution of sunlight on the thylakoidal surface and light availability is dissimilar in intertidal soil surface biofilms (AP9F and AP25) and the biofilms found in a lentic system, the habitat of the reference strains (Johansen *et al.* 2011).

The 16S rRNA gene sequence of strain AP9F showed 99% similarity and AP25 showed 94% similarity with an unpublished strain *Calothrix* sp. 96/26 LPP3 having GenBank Accession no. KM019977.1, which we believe is a wrongly submitted strain in the NCBI database. Strains AP9F and AP25 were found to be non-heterocytous strains in this study and actually displayed less than 85% similarity with the true *Calothrix* sp. which is known as a heterocytous species of cyanobacteria. Furthermore, some of the phylogenetic relatives identified on the basis of the 16S rRNA sequence data in the NCBI database lacked sufficient information such as availability in culture centers and publication records indicating requirement of future studies to assign proper positions in the phylogenetic tree. The phylogenetic relationship established in the present study demonstrated the taxa under investigation were located in a clade different from the one comprising the type species, which requires an urgent revision based on the polyphasic approach (Dadheech *et al.* 2012). The determined relationship raises the question: should the two strains AP9F and AP25 be assigned to new genera or be placed in the existing genera, i.e. *Leptolyngbya* and *Nodosilinea* respectively. The 16S rRNA gene sequences of both AP9F and AP25 showed less than 95% similarity with corresponding sequences of the other closely-related genera. Likewise, the identity of the 16S rRNA gene sequences between AP9F and AP25 was also less than 95%. Moreover, the branch length bearing *Leptolyngbya litoralis* (AP25) was much longer in terms of time scale than the branch length of *Euryhalinema mangrovii* (AP9F) which is a direct evidence of an evolutionary time difference or the difference in the rate of nucleotide substitutions per site between the two strains under investigation. This provides strong justification for assigning AP9F and AP25 in two separate novel genera and an assumption that the strain *Calothrix* sp. 96/26 LPP3 to be another species under the proposed genus *Euryhalinema mangrovii* (AP9F). Perkinson *et al.* (2010) described the polyphyletic nature of two genera *Geitlerinema* and *Limnothrix* which belonged to family Pseudanabaenaceae. Some of the strains were studied polyphasically and shifted from the *Geitlerinema* genus to the *Limnothrix* genus based on the differences in 16S rRNA gene sequence, although they were morphologically similar. Fiore *et al.* (2007) reported a novel genus *Brasilonema* on the basis of a well-supported clade (evident from 16S rRNA phylogeny) and was separated from the genus *Scytonema* which shared less than 95% 16S rRNA gene sequence similarity with *Brasilonema*.

The most striking differential feature of strains under investigation was the presence of a single operon having both tRNA^{ile} and tRNA^{ala} genes in the ITS regions of the AP9F and AP25 in comparison to the presence of two operons in the ITS region of typical species belonging to the genera *Leptolyngbya* as well as *Nodosilinea*: one having both tRNA^{ile} and tRNA^{ala} genes and another lacking both the genes (Iteman *et al.* 2000, Boyer *et al.* 2001, Boyer *et al.* 2002, Flechtner *et al.* 2002, Gugger *et al.* 2005, Řeháková *et al.* 2007, Finsinger *et al.* 2008). The comparison of the ITS regions between our isolated strains as well as between the closest comparable genera revealed that the folding patterns of AP9F and AP25 differed significantly not only from each other but also from the patterns of other closely-related genera. The variations in the structure of the D-stem regions is very interesting because traditionally the D-stem of the ITS regions are believed to be conservative; but in the present study sequences of the D-stem differed among the studied strains and the reference strains. This observation is supported by the results of Zammit *et al.* (2012) who noticed similar variations in the sequences of D-stem while establishing the novel genus *Oculatella subterranea*. Considerable variability in the structure of the Box B helices of the ITS gene sequences of the two strains under investigation were observed after drawing them with similar conserved basal sequences for all structures used for comparison. Such variability may be attributed to the rearrangement of bases that occurs in different genera and species leading to a stable secondary structure in the minimum free energy level (Chakraborty *et al.* 2018). The variable nucleotide sequences and the grossly different folding patterns of the D1-D1' helix, Box B helix and V3 helix regions of the ITS operons of the test strains in contrast to the reference strains was substantiated by the presence of separate evolutionary lineages of our strains distinct from the other Leptolyngbyaceae members, including *Leptolyngbya* and *Nodosilinea* as evidenced in the phylogenetic trees. The other regions of the ITS gene sequence were also highly variable among the strains under investigation and in comparison to the reference strains. Complete analysis of the secondary structures and the comparisons of length of different conserved and variable regions of ITS operons in our strains (AP9F and AP25) exhibited significant divergences from the type species of the morphologically and phylogenetically closest genera *Leptolyngbya boryana* and *Nodosilinea nodulosa*. These major deviations in the length, structure and sequences of the ITS operons of our strains in comparison to the equivalent regions of the type species was sufficient evidence to justify this characteristic as a vital apomorphic characteristic which may be applied to designate our strains as two separate novel genera. The secondary structure of the 16S-23S ITS region is an important standard for alpha-level taxonomy of cyanoprokaryotes (Boyer *et al.* 2001) and has frequently been applied for inter-generic differentiation (Johansen &

Casamatta 2005, Siegesmund *et al.* 2008, Johansen *et al.* 2011, Osorio-Santos *et al.* 2014, Martins *et al.* 2018, Zhou *et al.* 2018). Dadheech *et al.* (2012) also created a novel genus *Haloleptolyngbya* based on a polyphasic approach considering the differences of the ITS regions between the test strains and the type species as an apomorphy. AP9F was isolated from the Lothian island of the Indian Sundarbans while AP25 was collected from the Sagar island suggesting ecological separation to be a factor accountable for the morphological and molecular apomorphies that established AP9F and AP25 as two separate genera in the family Leptolyngbyaceae.

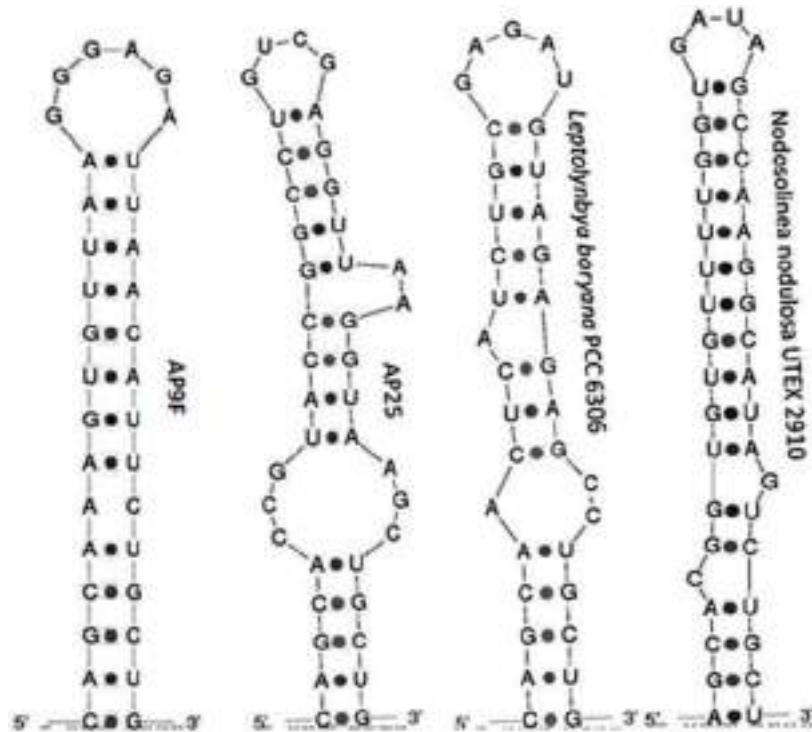


FIGURE 7. Comparative analysis of the Box B helices of the 16S-23S ITS regions of test strains (AP9F and AP25) and their closest phylogenetic relatives *Leptolyngbya boryana* and *Nodosilinea nodulosa*.

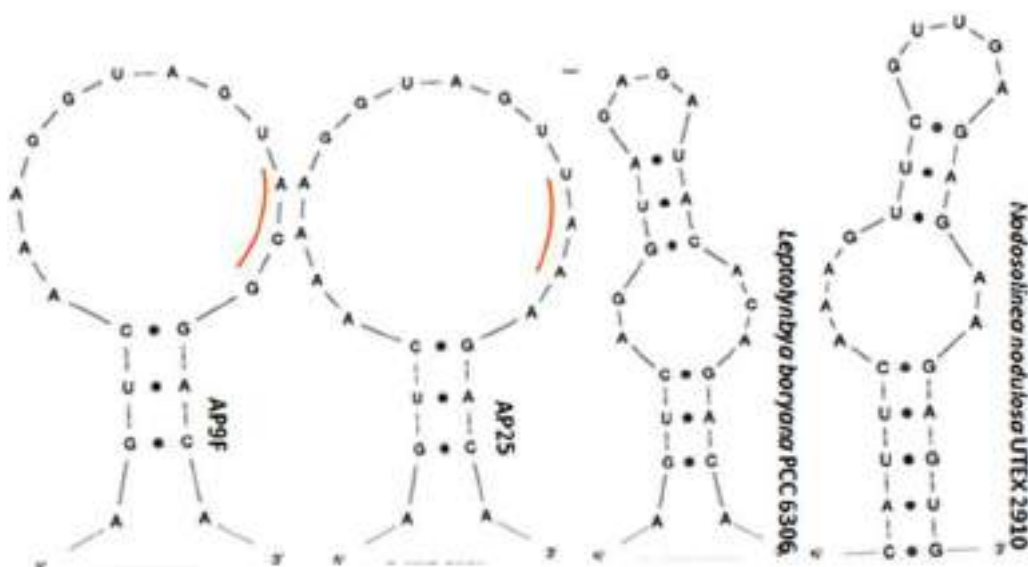


FIGURE 8. Comparative analysis of the V3 helices of the 16S-23S ITS regions of test strains (AP9F and AP25) and their closest phylogenetic relatives *Leptolyngbya boryana* and *Nodosilinea nodulosa*. Orange outline denotes the position of the occurrence of substitution of nucleotides in the test strains.

Conclusion

Strains AP9F and AP25 are monophyletic taxa and the putative genera to which the strains may be assigned should be distinct from the *Leptolyngbya* and *Nodosilinea* genera. The names *Euryhalinema mangrovii* gen. nov., sp. nov. and *Leptoelongatus litoralis* gen. nov., sp. nov. are proposed for AP9F and AP25 respectively. This work highlights the application of the polyphasic approach in cyanobacterial taxonomy to identify two novel genera by considering the total features of taxa: morphology, ecology and molecular data. The work is important as it contributes towards orderliness in the misidentified classical cyanobacterial genus, *Leptolyngbya*.

Descriptions

Order: Synechococcales

Family: Leptolyngbyaceae

Euryhalinema Chakraborty et Mukherjee, gen. nov.

Thallus blue-green. Filaments long, straight to slightly curved, trichome unbranched. Sheath absent. Cells much longer than wide, cylindrical, apical cells with flat ends, constrictions at the cross walls distinct.

Type species (designated here): *Euryhalinema mangrovii* Chakraborty et Mukherjee

Etymology: The generic epithet “*Euryhalinema*” is derived from *eurus* Greek for ‘wide’, *halinos* Greek for ‘of salt’ and *nema* Greek for ‘thread’.

Euryhalinema mangrovii sp. nov. Chakraborty et Mukherjee

Description: Filaments typically unbranched, straight, isopolar cyanobacterium attached to the soil surface (mainly sub-aerophytic) growing as an extensive mat-like biofilm. Cell shape appears to be having a slight broad apex and narrow base, much longer than wide, 1.25–2.6 µm long, 0.4–0.6 µm width, mucilaginous sheath completely absent, cell contents homogeneous, green without any granulated appearance, aerotopes absent, terminal cells consist of typical flattened ends. No heterocytes and akinetes. Cell division takes place by asymmetrical binary fission. Reproduction via the formation of hormogonia with the help of straight fragmentation of trichomes without producing any necridic cells.

Holotype (designated here): Holotype (AP9F) deposited and cryopreserved in the Microbial Culture Collection (MCC), India having accession number MCC 3171.

Type locality: Lothian island of the Indian Sundarbans.

Etymology: The specific epithet ‘*mangrovii*’ reflects the occurrence of this species in the soil of the mangrove region in the Indian Sundarbans.

Leptoelongatus Chakraborty et Mukherjee, gen. nov.

Thallus light greenish in color. Filaments long, straight, unbranched. Trichome covered with a thin diffuent mucilaginous sheath, cells much longer than wide, distinct constrictions at the cross wall.

Type species (designated here): *Leptoelongatus litoralis* Chakraborty et Mukherjee

Etymology: The generic epithet “*Leptoelongatus*” is derived from *leptos* Greek for ‘fine, thin’ and *elongatus* Latin for ‘elongated’ referring to the shape of the individual cells.

Leptoelongatus litoralis sp. nov. Chakraborty et Mukherjee

Description: Filaments typically unbranched, straight, isopolar cyanobacterium attached to the soil surface (mainly sub-aerophytic) growing as an extensive mat-like biofilm. Cell shape cylindrical, appears to be elongated, much longer than wide, 1.8–3.5 µm long, 0.8–1.8 µm width, facultative, mucilaginous sheath facultatively present, cell contents homogeneous, green without any granulated appearance, aerotopes absent, terminal cells consist of typical flattened

ends. No heterocytes and akinetes. Cell division takes place by asymmetrical binary fission. Reproduction via the formation of hormogonia with the help of straight fragmentation of trichomes without producing any necridic cells.

Holotype (designated here): Holotype (AP25) deposited and cryopreserved in the Microbial Culture Collection (MCC), India having accession number MCC 3170.

Type locality: Sagar island of Indian Sundarbans.

Etymology: The specific epithet '*litoralis*' in Latin meaning 'of the sea shore' which reflects the occurrence of this species in the intertidal area of the Indian Sundarbans.

Acknowledgements

Authors thank Ministry of Earth Sciences, Government of India for financial assistance through the sub-project "Identification of eight obligately halophilic cyanobacteria of the Sundarbans and molecular characterization of antimicrobial compounds therefrom" (File No. MoES/09-DS/10/2013 PC-IV) of the project "Drugs from Sea" and the Department of Science and Technology, Government of India for financial support through the DST PURSE Phase II project awarded to Jadavpur University.

References

- Alvarenga, D.O., Rigonato, J., Branco, L.H.Z. & Fiore, M.F. (2015) Cyanobacteria in mangrove ecosystems. *Biodiversity Conservation* 24: 799–817.
<https://doi.org/10.1007/s10531-015-0871-2>
- Becerra-Absalón, I., Johansen, J.R., Muñoz-Martín, M.A. & Montejano, G. (2018) *Chroakolemma* gen. nov. (Leptolyngbyaceae, Cyanobacteria) from soil biocrusts in the semi-desert Central Region of Mexico. *Phytotaxa* 367: 201–218.
<https://doi.org/10.11646/phytotaxa.367.3.1>
- Bohunicka, M. (2015) Towards a modern revision of the cyanobacteria, a critically important prokaryotic phylum. Phd. Thesis, University of South Bohemia, Faculty of Science, School of Doctoral Studies in Biological Sciences, České Budějovice, Czech Republic, 235 pp
- Boyer, S.L., Flechtner, V.R. & Johansen, J.R. (2001) Is the 16S–23S rRNA Internal Transcribed Spacer region a good tool for use in molecular systematics and population genetics? A case study in cyanobacteria. *Molecular Biology and Evolution* 18: 1057–1069.
<https://doi.org/10.1093/oxfordjournals.molbev.a003877>
- Boyer, S.L., Johansen, J.R. & Flechtner, V.R. (2002) Phylogeny and genetic variance in terrestrial *Microcoleus* (Cyanophyceae) species based on sequence analysis of the 16S rRNA gene and associated 16S–23S ITS region. *Journal of Phycology* 38: 1222–1235.
<https://doi.org/10.1046/j.1529-8817.2002.01168.x>
- Bruno, L., Billi, D., Bellezza, S. & Albertano, P. (2009) Cytomorphological and Genetic Characterization of Troglitic *Leptolyngbya* Strains isolated from Roman Hypogea. *Applied and Environmental Microbiology* 75: 608–617.
<https://doi.org/10.1128/AEM.01183-08>
- Casamatta, D.A., Johansen, J.R., Vis, M.L. & Broadwater, S.T. (2005) Molecular and morphological characterization of ten polar and near-polar strains within the Oscillatoriales (cyanobacteria). *Journal of Phycology* 41: 421–438.
<https://doi.org/10.1111/j.1529-8817.2005.04062.x>
- Chakraborty, S., Maruthanayagam V., Achari, A., Mahansaria, R., Pramanik, A., Jaisankar, P. & Mukherjee, J. (2018) *Oxynema aestuarii* sp. nov. (Microcoleaceae) isolated from an Indian mangrove forest. *Phytotaxa* 374: 24–40.
<https://doi.org/10.11646/phytotaxa.374.1.2>
- Chatchawan, T., Komarek, J., Strunecky, O., Smarda, J. & Peerapornpisal, Y. (2012) *Oxynema*, a new genus separated from the genus *Phormidium* (Cyanophyta). *Cryptogamie Algologie* 33: 41–59.
<https://doi.org/10.7872/crya.v33.iss1.2011.041>
- Dadheech, P.K., Mahmoud, H., Kotut, K. & Krienitz, L. (2012) *Haloleptolyngbya alcalis* gen. et sp. nov., a new filamentous cyanobacterium from the soda lake Nakuru, Kenya. *Hydrobiologia* 691: 269–283.
<https://doi.org/10.1007/s10750-012-1080-6>
- Debnath, M., Singh, T. & Bhadury, P. (2017) New records of Cyanobacterial morphotypes with *Leptolyngbya indica* sp. nov. from terrestrial biofilms of the Lower Gangetic Plain, India. *Phytotaxa* 316: 101–120.

<https://doi.org/10.11646/phytotaxa.316.2.1>

- Drummond, A.J., Ho, S.Y.W., Phillips, M.J. & Rambaut, A. (2006) Relaxed phylogenetics and dating with confidence. *PLoS Biology* 4: e88.
<https://doi.org/10.1371/journal.pbio.0040088>
- Finsinger K, Scholz, I., Serrano, A., Morales, S., Uribe-Lorio, L., Mora, M., Sittenfeld, A., Weckesser, J. & Hess, W.R. (2008) Characterization of true-branching cyanobacteria from geothermal sites and hot springs of Costa Rica. *Environmental Microbiology* 10: 460–473.
<https://doi.org/10.1111/j.1462-2920.2007.01467.x>
- Fiore, M.F., Sant'Anna, C.L., Azevedo, M.T.D., Komarek, J., Kastovsky, J., Sulek, J. & Lorenzi, A.S. (2007) The cyanobacterial genus *Brasilonema*, gen. nov., a molecular and phenotypic evaluation. *Journal of Phycology* 43: 789–798.
<https://doi.org/10.1111/j.1529-8817.2007.00376.x>
- Flechtner, V.R., Boyer, S.L., Johansen, J.R. & Denoble, M.L. (2002) *Spirirestis rafaensis* gen. et sp. nov. (Cyanophyceae) a new cyanobacterial genus from arid soils. *Nova Hedwigia* 74: 1–24.
<https://doi.org/10.1127/0029-5035/2002/0074-0001>
- Gelman, A. & Rubin, D.B. (1992) Inference from iterative simulation using multiple sequences. *Statistical Science* 7: 457–472.
<https://doi.org/10.1214/ss/1177011136>
- Gugger, M., Molica, R., Le Berre, B., Dufour, P., Bernard, C. & Humbert, J.F. (2005) Genetic diversity of *Cylindrospermopsis* strains (Cyanobacteria) isolated from four continents. *Environmental Microbiology* 71: 1097–1100.
<https://doi.org/10.1128/AEM.71.2.1097-1100.2005>
- Hašler, P., Dvořák, P., Johansen, J.R., Kitner, M., Ondřej, V. & Poulíčková, A. (2012) Morphological and molecular study of epipellic filamentous genera *Phormidium*, *Microcoleus* and *Geitlerinema* (Oscillatoriales, Cyanophyta/Cyanobacteria). *Fottea, Olomouc* 12: 341–356.
<https://doi.org/10.5507/fot.2012.024>
- Iteman, I., Rippka, R., de Marsac, N.T. & Herdman, M. (2000) Comparison of conserved structural and regulatory domains within divergent 16S rRNA–23S rRNA spacer sequences of cyanobacteria. *Microbiology* 146: 1275–1286.
<https://doi.org/10.1099/00221287-146-6-1275>
- Johansen, J. & Casamatta, D.A. (2005) Recognizing cyanobacterial diversity through adoption of a new species paradigm. *Algological Studies* 117: 71–93.
<https://doi.org/10.1127/1864-1318/2005/0117-0071>
- Johansen, J.R., Olsen, C.E., Lowe, R.L., Fucikova, K. & Casamatta, D.L. (2008) *Leptolyngbya* species from selected seep walls in the Great Smoky Mountains National Park. *Algological Studies* 126: 21–36.
<https://doi.org/10.1127/1864-1318/2008/0126-0021>
- Johansen, J.R., Kovacik, L., Casamatta, D.A., Fučíková K., & Kaštovský J. (2011) Utility of 16S-23S ITS sequence and secondary structure for recognition of intrageneric and intergeneric limits within cyanobacterial taxa: *Leptolyngbya corticola* sp. nov. (Pseudanabaenaceae, Cyanobacteria). *Nova Hedwigia* 92: 283–302.
<https://doi.org/10.1127/0029-5035/2011/0092-0283>
- Komarek, J. & Anagnostidis, K. (2005) *Cyanoprokaryota. 2. Teil: Oscillatoriales*. In: Büdel, B., Gärdner, G., Krienitz, L. & Schagerl, M. (Eds.) *Süßwasserflora von Mitteleuropa*. Elsevier, München 759 pp.
- Komarek, J. (2006) Cyanobacterial Taxonomy: Current problems and prospects for the integration of traditional and molecular approaches. *Algae* 21: 349–375.
<https://doi.org/10.4490/ALGAE.2006.21.4.349>
- Komarek, J., Kastovsky, J., Mares, J. & Johansen, J.R. (2014) Taxonomic classification of cyanoprokaryotes (cyanobacterial genera) using a polyphasic approach. *Preslia* 86: 295–335.
- Komarek, J., Kaštovský, J., Ventura, S., Turicchia, S. & Šmarda, J. (2009) The cyanobacterial genus *Phormidesmis*. *Algological Studies* 129: 41–59.
<https://doi.org/10.1127/1864-1318/2009/0129-0041>
- Lane, D.J. (1991) 16S/23S rRNA sequencing. In: Stackebrandt, E. & Goodfellow, M. (Eds.) *Nucleic acid techniques in bacterial systematics*. Chichester, United Kingdom: John Wiley and Sons, pp. 115–175.
- Larkin, M.A., Blackshields, G., Brown, N.P., Chenna, R., McGettigan, P.A., McWilliam, H., Valentin, F., Wallace, I.M., Wilm, A., Lopez, R., Thompson, J.D., Gibson, T.J. & Higgins, D.G. (2007) Clustal W and Clustal X version 2.0. *Bioinformatics* 23: 2947–2948.
<https://doi.org/10.1093/bioinformatics/btm404>
- Lopes, V.R., Ramos, V., Martins, A., Sousa, M., Welker, M., Antunes, A. & Vasconcelos, V.M. (2012) Phylogenetic, chemical and morphological diversity of cyanobacteria from Portuguese temperate estuaries. *Marine Environmental Research* 73: 7–16.
<https://doi.org/10.1016/j.marenvres.2011.10.005>

- Mai, T., Johansen, J.R., Pietrasiak, N., Bohunicka, M. & Martin, M.P. (2018) Revision of the *Synechococcales* (Cyanobacteria) through recognition of four families including *Oculatellaceae* *fam. nov.* and *Trichocoleaceae* *fam. nov.* and six new genera containing 14 species. *Phytotaxa* 365: 1–59.
<https://doi.org/10.11646/phytotaxa.365.1.1>
- Martins, M.D. & Branco, L.H.Z. (2016) *Potamolinea* *gen. nov.* (Oscillatoriales, Cyanobacteria): a phylogenetically and ecologically coherent cyanobacterial genus. *International Journal of Systematic and Evolutionary Microbiology* 66: 3632–3641.
<https://doi.org/10.1099/ijsem.0.001243>
- Martins, M.D., Machado-de-Lima, N.M. & Branco, L.H.Z. (2018) Polyphasic approach using multilocus analyses supports the establishment of the new aerophytic cyanobacterial genus *Pycnacronema* (Coleofasciculaceae, Oscillatoriales). *Journal of Phycology* 55: 146–159.
<https://doi.org/10.1111/jpy.12805>
- Neogi, S.B., Dey, M., Kabir, S.M.L., Masum, S.J.H., Kopprio, G., Yamasaki, S. & Lara, R. (2016) Sundarban mangroves: diversity, ecosystem services and climate change impacts. *Asian Journal of Medical and Biological Research* 2: 488–507.
<https://doi.org/10.3329/ajmbr.v2i4.30988>
- Nübel, U., Garcia-Pichel, F. & Muyzer, G. (1997) PCR primers to amplify 16S rRNA genes from cyanobacteria. *Applied Environmental Microbiology* 63: 3327–3332.
- Olive, J., Ajlani, G., Astier, C., Recouvreur, M. & Vernotte, C. (1997) Ultrastructure and light adaptation of phycobilisome mutants of *Synechocystis* PCC 6803. *Biochimica et Biophysica Acta* 1319: 275–82.
[https://doi.org/10.1016/S0005-2728\(96\)00168-5](https://doi.org/10.1016/S0005-2728(96)00168-5)
- Osorio-Santos, K., Pietrasiak, N., Bohunická, M., Miscoe, L.H., Kovacic, L., Martin, M.P. & Johansen, J.R. (2014) Seven new species of *Oculatella* (Pseudanabaenales, Cyanobacteria) *European Journal of Phycology* 49: 450–470.
<https://doi.org/10.1080/09670262.2014.976843>
- Palinska, K.A. & Surosz, W. (2014) Taxonomy of cyanobacteria: a contribution to consensus approach. *Hydrobiologia* 740: 1–11.
<https://doi.org/10.1007/s10750-014-1971-9>
- Perkerson III, R.B., Johansen, J.R., Kovacic, L., Brand, J., Kastovsky, J. & Casamatta, D.A. (2011) A unique Pseudanabaenalean (cyanobacteria) genus *Nodosilinea* *gen. nov.* based on morphological and molecular data. *Journal of Phycology* 47: 1397–1412.
<https://doi.org/10.1111/j.1529-8817.2011.01077.x>
- Perkerson III, R.B., Perkerson, E.A. & Casamatta, D.A. (2010) Phylogenetic examination of the cyanobacterial genera *Geitlerinema* and *Limnithrix* (Pseudanabaenaceae) using 16S rDNA gene sequence data. *Algological Studies* 134: 1–16.
<https://doi.org/10.1127/1864-1318/2010/0134-0001>
- Philippot, L., Andersson, S.G., Battin, T.J., Prosser, J.I., Schimel, J.P., Whitman, W.B. & Hallin, S. (2010) The ecological coherence of high bacterial taxonomic ranks. *Nature Reviews Microbiology* 8: 523–529.
<https://doi.org/10.1038/nrmicro2367>
- Posada, D. (2008) jModelTest: phylogenetic model averaging. *Molecular Biology and Evolution* 25: 1253–1256.
<https://doi.org/10.1093/molbev/msn083>
- Pramanik, A., Sundararaman, M., Das, S., Ghosh, U. & Mukherjee, J. (2011) Isolation and characterization of cyanobacteria possessing antimicrobial activity from the Sundarbans, the world's largest tidal mangrove forest. *Journal of Phycology* 47: 731–743.
<https://doi.org/10.1111/j.1529-8817.2011.01017.x>
- Řeháková, K., Johansen, J., Casamatta, D. A., Xuesong, L. & Vincent, J. (2007) Morphological and molecular characterization of selected desert soil cyanobacteria: three species new to science including *Mojavia pulchra* *gen. et sp. nov.* *Phycologia* 46: 481–502.
<https://doi.org/10.2216/06-92.1>
- Rippka, R., Deruelles, J., Waterbury, J.B., Herdman, M. & Stanier, R.Y. (1979) Generic assignments, strain histories and properties of pure cultures of cyanobacteria. *Journal of General Microbiology* 111: 1–61.
<https://doi.org/10.1099/00221287-111-1-1>
- Ronquist, F., Teslenko, M., van der Mark, P., Ayres, D., Darling, A., Höhna, S., Larget, B., Liu, L., Suchard, M.A. & Huelsenbeck, J.P. (2012b) MrBayes 3.2: efficient Bayesian phylogenetic inference and model choice across a large model space. *Systematic Biology* 61: 539–542.
<https://doi.org/10.1093/sysbio/sys029>
- Segiesmund, M.A., Johansen, J.R., Karsten, U. & Friedl, T. (2008) *Coleofasciculus* *gen.nov.* (Cyanobacteria): morphological and molecular criteria for revision of the genus *Microcoleus* Gomont. *Journal of Phycology* 44: 1572–1585.
<https://doi.org/10.1111/j.1529-8817.2008.00604.x>
- Stöver, B.C. & Müller, K.F. (2010) TreeGraph 2: combining and visualizing evidence from different phylogenetic analyses. *BMC Bioinformatics* 11: 7.
<https://doi.org/10.1186/1471-2105-11-7>

- Swofford, D.L. (2002) *PAUP*: Phylogenetic analysis using parsimony (and other methods), version 4b10*. Sinauer Associates, Sunderland.
- Turicchia, S., Ventura, S., Komárková, J. & Komárek, J. (2009) Taxonomic evaluation of cyanobacterial microflora from alkaline marshes of northern Belize. 2. Diversity of oscillatoriacean genera. *Nova Hedwigia* 89: 65–200.
<https://doi.org/10.1127/0029-5035/2009/0089-0165>
- Westerman, M., Ernst, A., Brass, S., Boger, P. & Wehrmeyer, W. (1994) Ultrastructure of cell wall and photosynthetic apparatus of the phycobilisome-less *Synechocystis* sp. strain BO 8402 and phycobilisome-containing derivative strain BO 9201. *Archives of Microbiology* 162: 222–232.
<https://doi.org/10.1007/BF00301842>
- Zammit, G. (2018) Systematics and biogeography of sciophilous cyanobacteria; an ecological and molecular description of *Albertania skiophila* (Leptolyngbyaceae) *gen. & sp. nov.* *Phycologia* 57: 481–491.
<https://doi.org/10.2216/17-125.1>
- Zammit, G., Billi, D. & Albertano, P. (2012) The subaerophytic cyanobacterium *Oculatella subterranea* (Oscillatoriales, Cyanophyceae) *gen. et sp. nov.*: a cytomorphological and molecular description. *European Journal of Phycology* 47: 341–354.
<https://doi.org/10.1080/09670262.2012.717106>
- Zhou, W., Ding, D., Ahmad, M., & Zhang, Y., Lin, X., Zhang, Y., Ling, J. & Dong, J. (2018) *Marileptolyngbya sina gen. nov., sp. nov.* and *Salileptolyngbya diazotrophicum gen. nov., sp. nov.* (Synechococcales, Cyanobacteria), species of cyanobacteria isolated from a marine ecosystem. *Phytotaxa* 383: 75–92.
<https://doi.org/10.11646/phytotaxa.383.1.4>
- Zuker, M. (2003) Mfold web server for nucleic acid folding and hybridization prediction. *Nucleic Acids Research* 31: 3406–3415.
<https://doi.org/10.1093/nar/gkg595>



ANTS' NECROPHAGY ON ANTS

*¹K. Naskar and ²S.K. Raut¹Department of Zoology, Achhruram Memorial College, Jhalda, Purulia-723202, West Bengal, India²Ecology and Ethology Laboratory, Department of Zoology, University of Calcutta, 35, Ballygunge Circular Road, Kolkata - 700019, India

*Corresponding author email: khokan24@gmail.com

ABSTRACT

Necrophagy in ants on the ant species *Camponotus compressus*, *Meranoplus bicolor*, *Pheidole roberti*, *Monomorium pharaonis*, *Crematogaster subnuda*, *Anoplolepis gracilipes*, *Tetraponera rufonigra*, *Paratrechina longicornis*, *Oecophylla smaragdina*, *Solenopsis geminata* occurring at Jhalda, Purulia, West Bengal, India was studied both in field conditions and in experimental trials under field environment. It is revealed that in their natural foraging area *A. gracilipes*, *Ca. compressus*, *Cr. subnuda*, *M. pharaonis*, *O. smaragdina*, *Pa. longicornis*, *Ph. roberti* and *T. rufonigra* are habituated to carry selective corpses either of their own species or of different species lying on the ground, to their nest. Also, in experimentally offered injured, freshly dead and semi-decomposed corpses of different ants, amongst the naturally dead ants corpses occurring in the field, were procured by the ant species, on priority basis, that is, injured, freshly dead individuals corpses to the nest. In all cases, depending on the size and weight of the corpses the ants applied either individual or cooperative transport mechanisms to carry the same.

KEYWORDS: Ants, foraging, necrophagy.**INTRODUCTION**

Ants have a wide range of food resources irrespective of plant and animal varieties (Abbott, 1978, Grover *et al.*, 2007, Cook *et al.*, 2011, Schultheiss. *et al.* 2013, Naskar and Raut, 2014a, b, c, 2015a, b, c, d, e, f, 2016a, b, c.). Even they are habituated to use the inorganic materials to ensure their survival (Kaspari, M., S.P. Yanoviak and R. Dudley, 2008, Naskar and Raut, 2016a). They may devour the organic food materials directly from the body of the living organisms or way of feeding the dead, semi-decomposed, or decomposed organisms (Wilson *et al.*, 1958, Howard *et al.* 1976, Banik *et al.*, 2010, López-Riquelme *et al.*, 2013). Depending on the type of food materials the ants may carry the same, either individually or cooperatively to the nest or engulf these at the source. Customarily, ants could be seen to feed on the corpse of other animals and also they are habituated to carry (Naskar and Raut, 2015, 2018a, 2018b, Czaczkes *et al.*, 2010, 2013) the same when possible, to the nest to feed the colony members. But, they are very much conscious to maintain the hygienic condition of the nests (Nonacs, 1990, Choe *et al.*, 2009, Czechowski *et al.*, 2009, Chapuisat, 2010, Heinze and Walter, 2010, Bos *et al.*, 2012, Diez *et al.*, 2012, 2013, Sun and Zhou, 2013). Because they have developed the habit to remove the left over parts of the food materials and corpse of their fellow members from the nest (Diez *et al.*, 2012, Lopez *et al.*, 2013). Moreover, moribund ants are seen to leave the nest to die in isolation (Heinze and Walter, 2010). Even, they are able to detect the presence of ectoparasite or of fungal spores on the nest-mate body and thus they ensure removal of the same by allogrooming (Lecklerc J.B. and Detrain C., 2016).

Keeping these findings in mind while we were investigating the causes of abundance of large number of dead ant individuals lying on the ground we came across the events of carrying some dead ants by some ant individuals from the said spot to their nest. We continued our observation for several months at frequent intervals and the phenomena of corpse carrying habit by different ant species, even corpse of the same ant species is being carried by the same ant species became clear to us, that the ants carry dead individuals to the nest. Moreover to ascertain, whether the ants select the freshly dead individuals or injured individuals or semi-decomposed individuals we carried out some experiments by offering injured, freshly killed or semi-decomposed ant individuals at the same site amidst the naturally occurring dead ant individuals on the ground. Our findings clearly indicate that, though necrophoresis in ants plays very important role to maintain the social prophylaxis (Leclerc and Detrain, 2016) it is also a very common habit in ants to carry corpses of ants into the nest, of course, definitely to meet up the need of the food of the colony members.

MATERIALS & METHODS

The western side of Achhruram Memorial College, Jhalda, Purulia (Latitude 23°36' North and Longitude 85°98' East), West Bengal, India where the entire ground remains under shade during noon and afternoon due to canopy configuration of the tall trees. Different kinds of ants could be seen roaming around on the ground almost throughout the day. On the ground, almost throughout the study area a large number of corpses of different species of ants *viz.*, *Camponotus compressus*, *Meranoplus bicolor*, *Pheidole roberti*, *Monomorium pharaonis*, *Crematogaster subnuda*, *Anoplolepis gracilipes*, *Tetraponera rufonigra*,

Paratrechina longicornis, *Oecophylla smaragnida*, *Solenopsis geminata* were seen lying here and there. The foraging ants of some of these species were also seen to carry some of these ant corpses, of course, after careful examinations to their destination. In some cases they were seen to consume the corpse at the spot. However, in many cases foragers were seen to examine a corpse several times prior to accept or reject the same. Even, in several occasions it is noted that the same corpse of ant species was examined by the foragers of different ant species, one after another, during our observation period and the corpse which was rejected by the first forager of an ant species was also rejected by the subsequent foragers of the said species. Sometimes, some foragers were seen to carry the part of an ant corpse to the targeted point. Such procurement processes were seen in the field irrespective of ant species.

To verify whether the ants have any preference for the corpse of a particular species and also for the corpse of freshly dead or semi-decomposed corpse or the live one available in injured state, we offered all these kinds of corpse of different ant species as well as the injured ones amongst the corpses of the ants belonging to different

species lying on the ground at the study site. Observations were carried out on different dates, at frequent intervals, on sunny days for a period of five hours at a stretch in daytime, in all cases. Due attention was paid to note the fate of experimentally offered ant materials continuously for the period of five hours after supplying the same on the ground.

RESULTS

Of the ten ant species noted at the study site species viz. *Anoplolepis gracilipes*, *Camponotus compressus*, *Monomorium pharaonis*, *Oecophylla smaragnida*, *Pheidole roberti*, *Paratrechina longicornis*, *Tetraponera rufonigra*, were seen (Fig.1A-D) to carry the corpses of different ant species either individually or cooperatively to their nest (Table 1). In experimental trials only six ant species exhibited such behavior during our study period (Table 2). In all trials the offered ant specimens were procured instantly by the foragers after coming in contact with the same if they belonged to injured or freshly dead ant specimens. In contrast rarely they had the choice for the semi-decomposed ones.

TABLE 1. Corpse of ant species consumed at the spot or carried to the nest by the ant species occurring in their natural habitats at Jhalda, Purulia, West Bengal, India.

Foraging ant species	Corpse of the ant species consumed at the site or carried to the nest
<i>Anoplolepis gracilipes</i>	<i>Anoplolepis gracilipes</i> , <i>Tetraponera rufonigra</i> ,
<i>Camponotus compressus</i>	<i>Camponotus compressus</i> , <i>Crematogaster subnuda</i> , <i>Meranoplus bicolor</i> , <i>Monomorium pharaonis</i> , <i>Oecophylla smaragnida</i> , <i>Pheidole roberti</i>
<i>Crematogaster subnuda</i>	<i>Crematogaster subnuda</i>
<i>Monomorium pharaonis</i>	<i>Crematogaster subnuda</i> (by splitting the corpse into small parts)
<i>Oecophylla smaragnida</i>	<i>Oecophylla smaragnida</i> , <i>Crematogaster subnuda</i>
<i>Paratrechina longicornis</i>	<i>Crematogaster subnuda</i> (Head portion)
<i>Pheidole roberti</i>	<i>Crematogaster subnuda</i>
<i>Tetraponera rufonigra</i>	<i>Tetraponera rufonigra</i>

TABLE 2. Results of experimental trials on the consumption of corpses of ants at the supplied site or carried to the nest by the ant species

Foraging ant species	Corpse of the ant species used as foods
<i>Camponotus compressus</i>	<i>Camponotus compressus</i> , <i>Crematogaster subnuda</i>
<i>Crematogaster subnuda</i>	<i>Crematogaster subnuda</i> , <i>Pheidole roberti</i>
<i>Meranoplus bicolor</i>	<i>Crematogaster subnuda</i>
<i>Monomorium pharaonis</i>	<i>Camponotus compressus</i> (by splitting the parts)
<i>Oecophylla smaragnida</i>	<i>Oecophylla smaragnida</i> , <i>Camponotus compressus</i>
<i>Pheidole roberti</i>	<i>Crematogaster subnuda</i>



FIGURE 1A *Paratrechina longicornis* carrying a corpse of *Camponotus compressus*



FIGURE 1B *Anoplolepis gracilipes* carrying a corpse of *Camponotus compressus*



FIGURE 1C *Oecophylla smaragdina* carrying a corpse of *Camponotus compressus*.



FIGURE 1D *Anoplolepis gracilipes* carrying a corpse of *Tetraoponera rufonigra*.

DISCUSSION

It is well evident that the ants, irrespective of species are habituated to use the corpse of their own species and/or other species as their food. This habit perhaps, developed in exigency of situation to fulfill the requirement of proteins, especially animal proteins of the colony members. Though the ants feed on different types of animal carcasses (Wilson *et al.*, 1958, Howard *et al.*, 1976, Banik *et al.*, 2010) to meet up their protein demands it is undoubtedly, a unique adaptation of the ants to enable them to compensate the need of protein, in absence of other proteinaceous, especially, animal food sources, to maintain the health of the colony members.

However, it seems that the ants are very much aware of the fact of hygienic condition of the colony perhaps to avoid any kind of infection. Most likely, for the said reason they have shown the preference for injured and freshly dead ant specimens over other kinds of specimens offered experimentally. Since, in field condition some corpses of ants belonging to different species were refused by all the visitors irrespective of species, it is granted that almost all kinds of ants are equally sensitive to detect such unacceptable corpses because of some particular reason. Thus, to save colony they are habituated to remove the corpse to a distant place from the colony (Diez *et al.*, 2012) or by disassociation of the sick ants from the colony (Boss *et al.*, 2011) or by introducing the habit of isolation of moribund ants from the society to die in isolation (Chapuisat, 2010, Heinze and Walter, 2010).

It is concluded that ants irrespective of species are habituated to feed on the corpses of their own species or of different species to ensure their survival. It is not known whether they would prefer their own corpses over other animal source food items is a matter of further research. Thus, though ants are necrophagous, this article provides first information on their necrophagy nature either on their own species or of different ant species.

ACKNOWLEDGEMENT

The authors are thankful to the Head of the Department of Zoology, University of Calcutta and to the Principal, Achhruram Memorial College, Purulia for the facilities provided. The ant's specimens were identified by the Zoological Survey of India, Kolkata, India.

REFERENCES

Abbott, A. (1978) Nutrients dynamics in ants. In M.V. Brian (ed.), pp 233-244. Production ecology of ants and termites. Cambridge University, London, United Kingdom.

Banik, S., Biswas, S., Karmakar, R., and Bhrahmachary, R. (2010) Necrophoresis in two Indian ant species, *Camponotus compressus* (Fabricius) and *Diacamma vagans* (Smith) (Insecta: Hymenoptera: Formicidae) Proc. Zool. Soc., **63**(2), 87-91.

Bos, N., Lefevre, T. Jensen, A.B. and D'Ettore, P. (2012) Sick ants become unsociable. J. Evol. Biol. **25**(2), 342-351.

Chapuisat, M. (2010) Social evolution; sick ants face death alone. Current Biology, **20**(3): R104-R105.

Choe, D.H., Millar, J.G. and Rust, M. K. (2009) Chemical signals associated with life inhibit necrophoresis in Argentine ants. PNAS. **106** (20), 8251-8255.

Cook, S.C., Eubank, M.D. Gold, RE and Behrner, S.T. (2011) Seasonality directs contrasting food collection behavior and nutrient regulation strategies in ants. PLoS One **6**(9), e25407 doi:10.1371/journal.pone.0025407.

Czaczkes, T.J., Nouvellet, P., and Ratnieks, F.L.W. (2010) Cooperative food transport in the Neotropical ant, *Pheidole oxyops* Insect. Soc. **58**, 153-161.

Czaczkes, T.J. and Ratnieks, F.L.W. (2013) Cooperative transport in ants (Hymenoptera:Formicidae) and elsewhere Myrmecological news **18**, pp. 1-11.

Czechowski, W., Marko, B. and Godzinska, E.J. (2009) Corpse carrying in ants (Hymenoptera:Formicidae): behavioural side effects of aggressive arousal or competitive signaling? *Polish Journal of Ecology*, **57**(20), 341-352.

Diez, L., Deneubourg, J. L. and Detrain, C. (2012) Social Prophylaxis Through distant corpse removal in ants. Naturwissenschaften. **99** (10), 833-842.

Diez, L., Moquet, L. and Detrain, C. (2013) Post mortem changes in chemical profile and their influence on corpse removal in ants. J. Chem. Ecol. **39** (11-12), 1424-1432.

Gro, R., and Dorigo, M. (2004) Cooperative transport of objects of different shapes and sizes. In: Dorigo *et al.* (Eds): Ants LNCS **3172**, 106-117. Springer Verlag, Berlin.

Grover, C.D., Kay, A.D., Monson, J.A., Marsh, T.C. and Holway D.A. (2007) Linking nutrition and behavioural dominance: carbohydrate scarcity limits aggression and activity in Argentine ants. Proc. R. Soc. Sec B Biol. Sci. **274**, 2951-2957.

Heinze, J and Walter, B (2010) Moribund ants leave their nests to die in social isolation. Current Biology, **20**(9), 249-252.

Howard, D.F. and Tschinkel, W.R. (1976) Aspects of necrophoric behaviour in the red imported fire ant, *Solenopsis invicta*. Behaviour, **56**, 158-180.

Kaspari, M., Yanoviak, S.P. and Dudley, R. (2008) On the biogeography of salt limitation: A study of ant communities. Proc. of the Nat. Acad. of Sci of the USA **105** (46), 17848-17851.

Kenne, M., Fotso Kuate, A., Hanna, R., Tindo, M., and Goergen, G. (2008) Foraging activity and diet of the ant, *Anoplolepis tenella* Santschi (Hymenoptera: Formicidae), in southern Cameroon African Entomology, **16**(1), 107-114.

- Leclerc, J.B. and Detrain, C. (2016). Ants detect but do not discriminate diseased workers within their nest. *The Science of Nature* 103:70.
- López-Riquelme, G.O. and Fanjul-Moles, M.L. (2013) "The Funeral Ways of Social Insects. Social Strategies for Corpse Disposal" *Trends in Entomology*, **9**, pp 71-129.
- McCreery, H.F. and Breed, M.D. (20140) Cooperative transport in ants; a review of proximate mechanisms. *Insect. Soc.* **61**, 99-110.
- Naskar, K. and Raut, S.K. (2014a) Food searching and collection by the ants *Pheidole roberti* Forel. *Discov.* **32**, 6-11.
- Naskar, K. and Raut, S. K. (2014b) Judicious foraging by the ants *Pheidole roberti* Forel. *Proc. of Zoo. Soc., Kolkata.* **68**, 131-138.
- Naskar, K. & Raut, S.K. (2014c) Ants forage haphazardly: a case study with *Pheidole roberti* Forel. *Int. J. Sci. and Nat.* **5**, 719-722.
- Naskar, K. and Raut, S.K. (2015a) Ants' foraging, a mystery. *Int. J. Inno. Sci. and Res.* **4** (2), 064-067.
- Naskar, K. and Raut, S.K. (2015b) Foraging interactions between the Reddish brown ants *Pheidole roberti* and the Black ants *Paratrechina longicornis* Int. J. Res. Stud. in Biosci. **3** (3), 183-189.
- Naskar, K. and Raut, S.K. (2015c) Available food and ant's response. *Int. J. Eng. Sci. and Res. Tech.,* **4** (4), 368-372.
- Naskar, K. and Raut, S.K. (2015d) Food-carrying strategy of the ants *Pheidole roberti*. *Int. J. Tech. Res. and Appl.* **3** (3), 55-58.
- Naskar, K. and Raut, S.K. (2015e) Foraging behavior following food contact in the ants *Pheidole roberti*. *Glo. J. Bio. Agri. and Health Sci.* **4** (2), 21- 24.
- Naskar, K. and Raut, S. K. (2015f) Mysterious foraging of Pharaoh ant *Monomorium pharaonis*. *Int. J. Res. in Eng. and App. Sci.,* **5** (7), 67-71.
- Naskar, K. & Raut, S.K. (2016a) Ants' food examination. *Proc. of Zoo. Soc., Kolkata.* **70** (2), 119-131.
- Naskar, K. & Raut, S. K. (2016b) Winter quarter-induced foraging in ants. *Glo. J. Bio-Sci. and Biotech.* **5** (3), 318-323.
- Naskar, K. and Raut, S.K. (2016c) Does colour of the food attract ants ? *Proc. of Zoo. Soc., Kolkata.* **71**(1), 25-29.
- Naskar, K. and Raut, S.K. (2018a) Food-induced food-transporting strategies of the ants *P. roberti* and *P. longicornis*; in *Entomology: Current Status and Future Strategies*. Ganguly, A. and K. Naskar (eds), pp. 125-133, Daya Publishing House, (Astral Int. Pvt. Ltd.), New Delhi.
- Naskar, K. and Raut, S.K. (2018b) Genesis and significance of cooperative transport in ants. *Global Journal of Bio-Science and Biotechnology* **7**(4), 633-637.
- Nonacs, P. and Lawrence, M.D. (1990). Mortality risk vs. food quality trade-offs in a common currency: ant patch preferences. *Ecological society of America.*
- Nondillo, A., Ferrari, L., Lerin, S., Bueno, O.C. and Botton., M. (2014) Foraging activity and seasonal food preference of *Linepithema micanas* (Hymenoptera: Formicidae), a species associated with the spread of *Eurhizococcus basiliensis* (Hemiptera: Margarodidae) *J. Econ. Entomol* **107**(4)1385-1391.
- Schultheiss. P. and Nooten., S. (2013) Foraging patterns and strategies in an Australian desert ant. *Austral Ecology.* **38**(8), 942-951.
- Sun Q and Zhou X (2013). Corpse management in social insects. *Int. J. Biol. Sci.* **9**(3), 313-321.
- Wilson, E.O., Durlach, N.I. and Roth, L.M. (1958) Chemical Releasers of Necrophoric Behavior in Ants. *Psyche* **65**, 108–114.

THE CONCEPT OF MOTION: THE VAISESIKA PHILOSOPHY AND MODERN SCIENCE.

PRASIT RANJAN GHOSH

Assistant Professor

HOD, Philosophy Department,

Achhruram Memorial College

Jhalda, Purulia, W.B., India.

ABSTRACT:

A great philosopher Kanad (300 BC), The founder of the Vaisesika Philosophy, described vividly about the whole cosmos. This philosophy treats as the metaphysics including physics in ancient time. Kanad wrote 'vaisesika sutra' in 300 BC. This philosophy deals with space, time, mass, motion and real things within the whole universe. All are logically described in this philosophy. All vaisesikas discuss fully the concept of motion (Karma) technically too. In the description of the universe, vaisesikas admit motion (Karma) as a padartha. 'Padartha' as a category is a technical term of the vaisesika philosophy. In physics, 'mass' 'energy', 'time' and 'motion' are technical terms. Such 'Padartha' is a technical term in the vaisesika philosophy. 'Padartha' means real things. Planets, stars and galaxies are real things. Vaisesika are realists and pluralists. They admit space, time, motion, minds, souls, material things and God. In evolution or creation of the cosmos in present, past and future, motion has an important role in the vaisesika system. Modern science with physics admit existence of motion as the basic reality. Here the concept of motion in vaisesika philosophy is discussed with modern science. Differences between them are shown.

Keywords : Padartha, Davya, Karma (Motion), Samyog (Conjunction), Dika (Space), Kala (Time) and Paramanu (Atom).

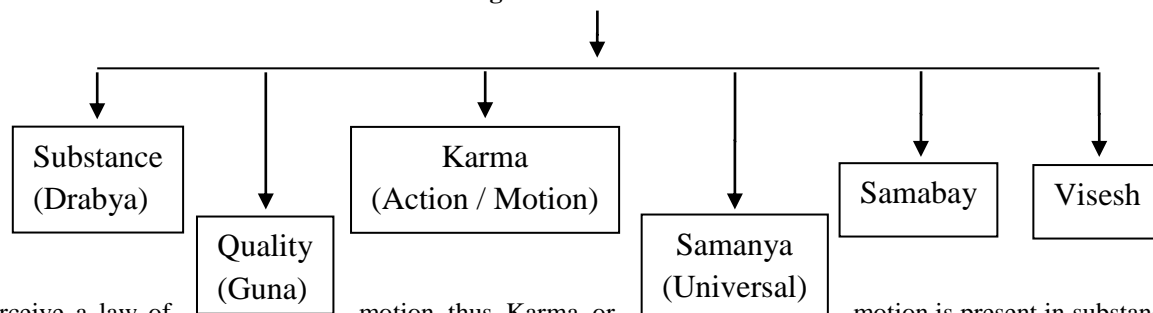
INTRODUCTION:

Kanad is one of the philosophers who proclaims that the 'Karma' as the action or motion is a basic thing in the world in 300 B.C. he admits that motion has an important role in the universe and he express that the motion exists in the physical objects.

"Water" is a word as a real thing water. Such word "Water" has a meaning of real thing named water. "Water" (a word) → water, an existing thing. Water is called padartha as the meaning of the word. According to Kanad, there is many things in the universe in the world. But though they are infinite in number, yet all such real things as meaning of the words are under six categories (Padharthas) only. They are all positive padarthas. They are dravya, guna (quality), karma (action / motion), samanya (universal), samavaya and visesh (particulars).

Motitions is one category or padartha in vaisesikha system according to Kanad. So motion is a real thing as an existent in the world. When science did not discover motion as an entity in the western countries, then Kanad discussed about motion in his vaisesika philosophy in 300 BC. We perceive many things in the world. But they are only six categories and dravya (substance), karma or motion and guna (quality) are the three of them. Meaning of the word as existing things

Categories of the Padartha



Kanad perceive a law of only.

motion thus Karma or

motion is present in substance or dravya

No dravya, No Karma or Motion. Karma or motion can't exist without dravya.

Kanad preached in his vaisesika philosophy in ancient time that there is no existence of the world if there is no motion in dravya.

(1)

Kanad explained theory of motion in such way that any kind of motion exists in substance only. Motion cannot exist without moving thing. But it is clear to say that all moving bodies are

finite. So, Kanad's theory of motion exists in finite substances and motion itself is non eternal things.

Therefore, whole space as Dika is always devoid of motion. Because the space (Dika) is infinite an eternal thing 'Motion resides in a corporeal substances of limited dimensions. It is non-eternal and resides in a non-eternal substance.'²

There are nine kinds of substances. They are Ksiti (earth), Apa (Water), Teja (fire, heat and light), Vayu (air), Akash (Sky or Ether), Dika (space), Kala (Time), Mana (Mind) and Atma (self).

Above all are real entities. But motion are not present in all mentioned things. Here it is clear that all entities of science including Biology and Physics are clearly mentioned in Vaisesika's nine substances.

'An incorporeal, ubiquitous substance, like ether, time, space or a soul, is incapable of motion'³.

Explanation with examples can be given. A moving fan is in motion. The motion is present in the fan. Here the fan is a substance and Karma (motion) is a category on Padartha which is present in another category of substance as a fan. An nonmoving fan is without motion. The fan can exist without motion, but motion cannot exist without substance (here the fan). 'The third category is Karma or Action. Like quality, it belongs to and is hers is a substance and cannot exist separately from it.'⁴

A fan as moving or un-moving consist of infinite atoms (Paramanu) in it. Larger substance are more atoms present in it.

(2)

The number of atoms in a mustard seed is less than that of number of atoms present in the Mountain Himalaya as a bigger substance. Such any galaxy is a greater number atoms than that of the number of atoms present in the Himalaya.

"Any number of motions or Vegas may be impressed on a particle, but so long as these are in a uniform direction the resultant motion or Vega is in a straight line, and may be conceived as one (Prasastapada,.....). It is only when we come to Gamana (curvilinear motion) and its causes that the question of composition assumes a real significance. In all such cases, each separate particle has only one Vega (impressed motion) in a definite direction at any given instant, but the composition of the successive motions and Vegas in the same particle produces the curvilinear motion, e.g. the rotation of each constituent particle of the potter's wheel. The motion of the body (e.g. the wheel) results from the combined motions of the particles. If pressure or impact produces motion in an opposite direction to the Vega already impressed on the body, the original direction would be changed, as is seen in the case of rebounding after striking the pestle is a typical instance of such change of direction in Vega or motion. The impressed fore, e.g. impact, produces a changed motion in a different direction. One view is that the original Vega (momentum) is destroyed before a new motion and a new Vega are produced by the impact".⁵

Vaisesika philosophy holds that any motion is caused by unconditional conjunction and disjunction. This is also a non-herent cause. It means that motion is not always present in a substance forever. It is a temporary thing. Though In physics, Motion is eternal. Motion is permanently present in atoms. But Kanad and other philosophers of the vaisesika system expressed that GOD or Advista as the unknown cause or the unexplained cause of the nature exerts motion to paramanu and then parmanu is in motion. And after that the creation starts in motion. All atoms are eternally present at the absolute rest before the creation of the universe.

God or Adrasta imposed motion on motionless atoms to activate motion in the universe. 'The later vaisesika maintain that GOD produces motion in the atoms, combines them into composite products.....'⁶.

Some qualities of the vaisesika philosophy are related with motion. Gravity, fluidity, Velocity and viscosity and elasticity are such qualities. Gravity is a quality of earth and water 'Earth' is a technical term in Indian Philosophy. It means that all solid states of matter having quality odour (gandha). If a liquid or gas or other substance has some kind of smell, then there is naturally present earth substance. Some solid particles having smell are present in liquid or in gas or in other substance. Kerosene, Petrol, Mustard Oil, Ghee, Bromine gas etc are examples of earth substance. According to vaisesika philosophy, any planet or a star or a galaxy is made of five physical substance of ksiti (earth), apa (air), Teja (fire, heat and light), Vayu (air) and Akash (ether or sky). Gravity is associated with motion of any planet or motion of a star or of a galaxy, a planet or a star or a galaxy is a falling body due very important role of gravity quality according to the vaisesika philosophy.

'Gravity is a quality of earth and water by virtue of which they tend to fall to the ground'⁷

Falling body falls due to gravity of the earth in physics. Gravitational force is associated with it. Einstein predicted graviton particle for the gravitational force.

(3)

This hypothetical quantum acts as contraction and expansion for the shape of the space and time or space -time. Kanad expressed it first that falling to the ground is due to gravity (vega). Vaisesika Fluidity is another quality of the Philosophy. Fluidity is the cause of flowing a type of motion. Fluidity quality is found in three substances. Fluidity has two kinds. They are natural and acquired. Natural fluidity is found in water substance.

But acquired fluidity exists in earth and fire. Natural fluidity is present in atoms (parmanus) of water. Natural fluidity is also found in non-eternal composite watery substances. Acquired fluidity of earth and fire is for conjunction with heat. Examples can be given as gold and butter become fluid third when it is contact with fire.

Viscosity is a quality known as oilness. It is a special property of water. Velocity is the cause of motion. A body is in motion with velocity. Velocity is present in earth, water, light, air and mass. Matter and its states of soiled liquid, gas and plasma and energy are really included in Kanad's theory of motion. So galaxy is also in motion. Stars, planets and all heavenly bodies are in motion according to Kanad.

Elasticity is a quality present in some tangible substances. "It is the quality of a substance, which makes it revert to its original state by virtue of its elasticity when an arrow discharged from it".⁸

(4)

Kanad introduced five kinds of motion (Karma) in his 'Vaisesika Sutra'. Those five kinds are

- (1) Utksepana (Upward motion), (2) avaksepana (downward motion), (3) Akunchana (contraction), (4) prasarana (expansion), and (5) Gaman (locomotion).

Kanad's kinds of motion satisfy all kinds of motion in modern physics as well as science.

"The third category is Karma or action..... Action is said to be of five kinds. (1) Upward movement (Utksepana) (2) downward movement (avaksepana) (3) Contraction (akanchara) (4) expansion (prasarana), and (5) Locomotion (gaman)".⁹

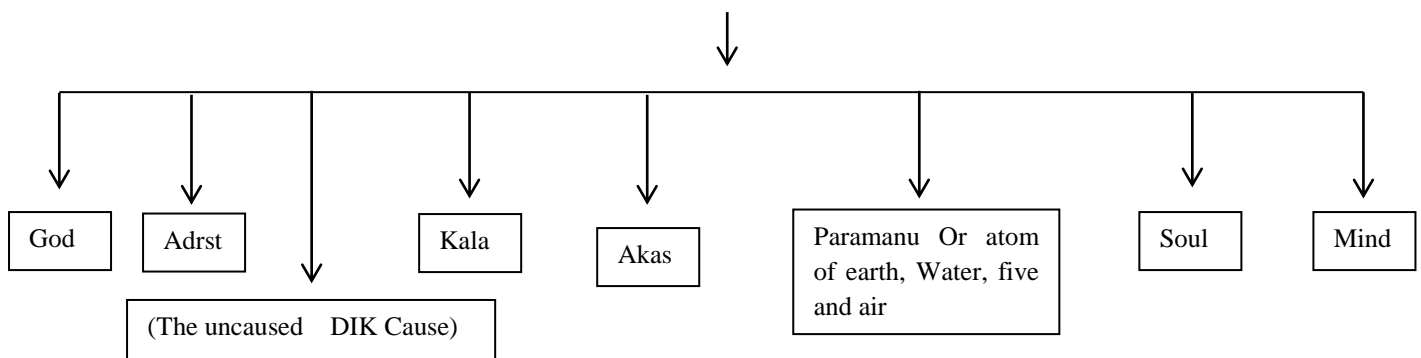
Ultimately all types of motion are derived from God. Firstly God imposes motion to motionless atom (Parmanu) to move. That is why paramanu (atom) is in motion and all moving bodies exist in motion. So atoms become mobile to form massive things. Thus motion is perceived in the world.

Conclusion:

Here it clear to say that the first thing called atom (Paramanu) is the basic fundamental thing. Paramanu is eternal and free at rest. But anything is made of such atoms with help of God's power of motion. Though God is at the also absolute rest, but God has only freedom to impose motion to atoms and all massive bodies to move, This doctrine of Kanad's motion states that atoms are finer things than that of electrons, protons as such sub atomic particles, high energy particles, all waves, strings etc. All physical Components of atoms (not Kanad's Paramanu), ions isotopes, molecules, electrons, protons, quarks, stings, matters and of energies are ultimately reduced to Kanad's Paramanu or Kanad's atom.

Kanad pointed out that Paramanu is motion is prior to all moving thigs. So all physical lowponents are is motion clue to the genesis of Kanad's parmau or atom according to Vaisesika Philosophy. So at the beginning of the universe Kanad's model shows that God as the only source of motion, the in finite time (Kala), Adrasta (unknown cause of unexplained nature), the whole space (Dik), Akash(sky), Souls (Atomas) mind.s (Manas) and all paramanu's of earth,

All eternal things at the creation of the world.



References

1. Radhakrishnan, S. 2009. Motilal Benarasi Dass Publishers Pvt. LTD Delhi, Indian philosophy, 179
2. Sinha, J.N. 1992. New central Book Agency Kolkata, Outlines of Indian Philosophy, 168

3. Ibid,168
4. Sharma, C. 2003. Motilal Benarasi Dass Publishers Pvt. LTD Delhi, A critical Survey of Indian Philosophy, 175 - 190
5. Seal, B. N. 2015 Shishu Sahitya Sansad Pvt Ltd,Kolkata -700009, The Positive Sciences of The Ancient Hindus, 105
5. Sinha, J. N. 1992, New central Book Agency Kolkata, Outlines of Indian Philosophy, 179
6. Ibid, 203,
7. Ibid, 204,
8. Sharma, C. 2003 Motilal Benarasi Dass Publishers Pvt. LTD Delhi, A critical Survey of Indian Philosophy,179



See discussions, stats, and author profiles for this publication at: <https://www.researchgate.net/publication/335842312>

In-beam spectroscopic study of ^{63}Zn

Article in *Physical Review C* · September 2019

DOI: 10.1103/PhysRevC.100.034314

CITATIONS

5

READS

266

13 authors, including:



Uday shankar Ghosh
Inter University Accelerator Centre

25 PUBLICATIONS 25 CITATIONS

[SEE PROFILE](#)



Siddarth Rai
Malda College

64 PUBLICATIONS 194 CITATIONS

[SEE PROFILE](#)



Buddhadev Mukherjee
Visva Bharati University

96 PUBLICATIONS 227 CITATIONS

[SEE PROFILE](#)




Arindam Biswas
Visva Bharati University

17 PUBLICATIONS 31 CITATIONS

[SEE PROFILE](#)

In-beam spectroscopic study of ^{63}Zn

U. S. Ghosh,¹ S. Rai,^{1,2} B. Mukherjee ,^{1,*} A. Biswas,¹ A. K. Mondal,¹ K. Mandal,¹ A. Chakraborty,¹ S. Chakraborty,³ G. Mukherjee,⁴ A. Sharma,⁵ I. Bala,⁶ S. Muralithar,⁶ and R. P. Singh⁶

¹Department of Physics, Siksha-Bhavana, Visva-Bharati, Santiniketan, Bolpur - 731235, India

²Department of Physics, Salesian College, Siliguri Campus, Siliguri - 734001, India

³Department of Physics, Institute of Science, Banaras Hindu University, Varanasi - 221005, India

⁴Variable Energy Cyclotron Centre, 1/AF Bidhannagar, Kolkata - 700064, India

⁵Department of Physics, Himachal Pradesh University, Shimla-171005, India

⁶Inter University Accelerator Centre, Aruna Asaf Ali Marg, New Delhi - 110067, India



(Received 15 March 2019; revised manuscript received 21 July 2019; published 16 September 2019)

Investigation on the excited states of ^{63}Zn was done through in-beam γ -ray spectroscopic techniques using the $^{52}\text{Cr}(^{18}\text{O}, \alpha 3n)$ fusion-evaporation reaction at a beam energy of 72.5 MeV. Detection of the emitted γ rays from the excited nuclei was performed in the coincidence mode using 14 Compton suppressed Ge clover detectors of the Indian National Gamma Array. Based on the γ - γ coincidence data, 13 new transitions have been placed in the level scheme following their coincidence relationship and intensity balance. Spin and parity assignments of the excited levels have been carried out by extracting the directional correlation from oriented states ratio and polarization asymmetry values of the emitted γ rays. Shell model calculations have been performed in the $f_{5/2}p_{g_{9/2}}$ model space with a ^{56}Ni core using the $jj44\text{bpn}$ interaction, to interpret the observed excited states of the nucleus. A reasonable agreement is found between the experimental findings and the shell-model calculations. In order to understand the evolution of a collective shape built on the $9/2^+$ (1704 keV) state, we have performed total Routhian surface calculations with a $1g_{9/2}$ quasineutron and found reasonable agreement.

DOI: [10.1103/PhysRevC.100.034314](https://doi.org/10.1103/PhysRevC.100.034314)

I. INTRODUCTION

Nuclear structure in $A \approx 60$ reveals both single particle and collective excitations with various competing shapes, namely, prolate, oblate, and triaxial. A striking interplay of single particles and collective degrees of freedom have been observed in many Ge [1–5] and Cu [6–10] isotopes in this region. Here, the active orbitals are $2p_{3/2}$, $1f_{5/2}$, $2p_{1/2}$ in the upper fp shell and the intruder $1g_{9/2}$ orbital. The lower excitations are due to the negative parity $2p_{3/2}$, $1f_{5/2}$, and $2p_{1/2}$ orbitals but most of the high spin states are mainly due to the presence of the high- j $1f_{7/2}$ and $1g_{9/2}$ orbitals. The coupling of the $1g_{9/2}$ orbital with $2p_{3/2}$ orbital gives rise to the onset of octupole correlation. Strutinsky-type potential energy calculations by Nazarewicz *et al.* predicted softness toward octupole correlations for nuclei with $N, Z \approx 34$ [11,12]. Presence of holes in $1f_{7/2}$ orbital and particles in $1g_{9/2}$ orbital leads to a transition from spherical toward deformed shapes and enhances the possibility of collective rotational excitations. A magic superdeformed band in $N = Z$ ^{60}Zn was first observed by Svensson *et al.* [13] and spin-parity, excitation energy of the superdeformed states in this band were measured first by identifying linking transitions connecting this band to the yrast line. Among $^{61,63,65}\text{Zn}$ isotopes, the structure of ^{61}Zn is very interesting as several normal and superdeformed bands have been observed in this nucleus at high spins [14–16].

Strongly coupled rotational band was first observed in ^{64}Zn [17,18] in this mass region and this band shows similar characteristics of those smoothly terminating rotational bands in the Sn-Sb nuclei of the $A \approx 110$ region [19]. The lowest collective band in ^{64}Zn was interpreted as based on the $\pi(f_{7/2})^{-1}(p_{3/2}f_{5/2})^2(g_{9/2})^1\nu(p_{3/2}f_{5/2})^4(g_{9/2})^2$ configuration. The structure of ^{62}Zn also draws attention as it was the first candidate in this mass region in which the superdeformed band was observed with a large deformation ($\beta_2 \approx 0.45$) [20]. Later, extended study on this isotope revealed two sets of strongly coupled rotational bands observed up to the terminating states of their respective configurations [21]. A milestone in more extensive study of the structure of ^{62}Zn was achieved by Gellanki *et al.* [22], which established ten new rotational bands along with two new superdeformed bands and extended the level scheme above 40 MeV in excitation energy. Similarly two highly deformed and one superdeformed bands in ^{65}Zn were established by Yu *et al.* [23]. A rotational band was also observed in ^{65}Zn , built on $1g_{9/2}$ neutron orbital which exhibits a band crossing at high rotational frequency [24]. In $^{60,61,62,64,65}\text{Zn}$, phenomena, like collective excitations including superdeformations, are reported to be due to a limited number of holes in the $1f_{7/2}$ subshell and excitation of one or more nucleons into $1g_{9/2}$ intruder orbitals above the ^{56}Ni core.

Previous investigations on medium and high spin states in ^{63}Zn were performed using proton, α , ^{12}C , ^{16}O , and deuteron beams [25–29]. The latest study with ^{16}O beam was done using 12 Compton suppressed HPGe detectors along with 14

*buddhadev.mukherjee@visva-bharati.ac.in

BGO detectors [28]. Singh *et al.* established a positive parity unfavored and a negative parity favored band in ^{63}Zn . The band head of the positive parity band is $9/2^+$ which couples with the excited vibrational core of ^{62}Zn producing higher excited positive parity states. The higher excited $13/2_1^+$, $17/2^+$, and $21/2^+$ states decay to the band head via the cascade of strong stretched electric quadrupole ($E2$) transitions. Here, we report on an experiment that was carried out with a comparatively efficient array to bring out more comprehensive knowledge on the high spin nuclear structure in ^{63}Zn .

II. EXPERIMENTAL DETAILS AND DATA ANALYSIS

In the fusion-evaporation reaction a beam of ^{18}O at 72.5 MeV was obtained from the 15-UD pelletron accelerator [30] at Inter University Accelerator Centre (IUAC), New Delhi. The beam was bombarded onto a ^{52}Cr (isotopic abundance $\approx 99\%$) target of thickness 1.0 mg/cm^2 backed by 8.0 mg/cm^2 ^{197}Au . The emitted γ rays were detected in coincidence mode with 14 Compton suppressed HPGe clover detectors of the Indian National Gamma Array (INGA) [31]. Out of the 14 clovers, four were kept at an angle of 123° and another four at 148° , while the remaining six were placed at an angle of 90° with respect to the beam direction. The detectors were kept at a distance of $\approx 25\text{ cm}$ from the target. Further details of the experiment can be found in Ref. [32,33]. Analysis of the data is performed with the help of the standard analysis packages viz. CANDLE [34], RADWARE [35], and INGASORT [36]. Angular correlation analysis is carried out using the method of directional correlation from oriented states (DCO) [37]. In the present INGA geometry, the DCO ratios (R_{DCO}) are obtained from the intensity ratios of the coincident events detected at the angles of 148° and 90° with respect to the beam direction. The DCO ratio is obtained from the formula

$$R_{\text{DCO}} = \frac{I_{\gamma_1} \text{ at } 148^\circ \text{ gated by } \gamma_2 \text{ at } 90^\circ}{I_{\gamma_1} \text{ at } 90^\circ \text{ gated by } \gamma_2 \text{ at } 148^\circ}, \quad (1)$$

where I_{γ_1} is the measured intensity of γ_1 when the gating transition is γ_2 . The expected R_{DCO} values for the stretched quadrupole and the dipole transitions are $\approx 1.0(2.0)$ and $\approx 0.5(1.0)$, for a pure quadrupole (dipole) gate. Here, in this work we measured DCO ratios from gates on 882 keV ($\frac{13}{2}^+ \rightarrow \frac{9}{2}^+$) and 1063 keV ($\frac{7}{2}^- \rightarrow \frac{3}{2}^-$) $E2$ and 640 keV ($\frac{9}{2}^+ \rightarrow \frac{7}{2}^-$) $E1$ transitions of ^{63}Zn . Measured DCO values of different transitions as obtained in this work are plotted in Fig. 1. The clover detector can be used as a Compton polarimeter [38–41] as it has closed geometry and using this facility the asymmetry in polarization of the Compton scattered photons was extracted to define electric or the magnetic nature of the γ -ray transitions from the coincidence data. Two asymmetric matrices were constructed from the coincidence data, with events corresponding to the single hits in any detector along one axis and the double-hit scattered events of the 90° detector on the other axis. The scattered events are either parallel or perpendicular, the asymmetry parameter is evaluated as

$$\Delta_{\text{asym}} = \frac{a(E_\gamma)N_\perp - N_\parallel}{a(E_\gamma)N_\perp + N_\parallel}, \quad (2)$$

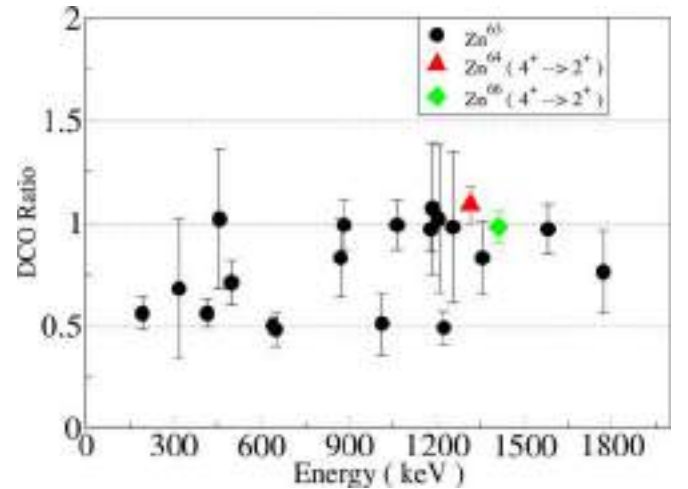


FIG. 1. DCO ratios of different transitions belonging to ^{63}Zn (gated by the $E2$ and $E1$ transitions, as mentioned in Table I). DCO ratios of the $4^+ \rightarrow 2^+$ transitions in $^{64,66}\text{Zn}$ gated by their respective $2^+ \rightarrow 0^+$ transitions, populated in the same reaction, are also presented for comparison. Please see Table I for details.

where $a(E_\gamma)$ is the asymmetry correction factor, representing the geometrical asymmetry of the present INGA setup and was determined from the ratio of the parallel (N_\parallel) and the perpendicular (N_\perp) scattered events obtained from an unpolarized source. It is defined as

$$a(E_\gamma) = \frac{N_\parallel(\text{unpolarized})}{N_\perp(\text{unpolarized})}. \quad (3)$$

The value of the asymmetry correction factor for the present detector setup is found to be $\approx 1.03(2)$ in the energy range ≈ 0.1 – 1.5 MeV using the standard ^{152}Eu radioactive source. Figure 2 shows the variation of the asymmetry correction factor within the γ -ray energy range ≈ 200 – 1500 keV for one

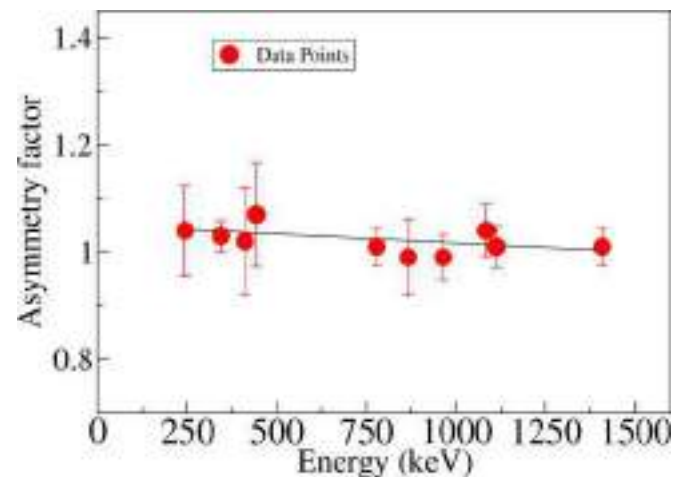


FIG. 2. Plot of asymmetry correction factor in the γ -ray energy range ≈ 200 – 1500 keV . Data points are fitted using the equation $a_0 E_\gamma + a_1$, where $a_1 = 1.044(17)$, $a_0 = -3.311 \times 10^{-5}$, and E_γ is the energy of the γ ray. This is measured using the radioactive ^{152}Eu source for one of the 90° clover detectors used in the present setup.

TABLE I. Values of the level energies (E_i) in keV, γ -ray energies (E_γ) in keV, initial (I_i^π) \rightarrow final (I_f^π) spin (in \hbar) parity, relative intensities (I_γ), branching ratio (B.R.), DCO ratio (R_{DCO}), and polarization asymmetry (Δ_{asym}) of the γ -ray transitions as obtained in this work for ^{63}Zn .

Level energy E_i (keV)	Gamma-ray energy ^a E_γ (keV)	Initial \rightarrow final spin-parity $I_i^\pi \rightarrow I_f^\pi$	Relative intensity ^f I_γ	Branching ratio ^g B.R.	DCO ratio R_{DCO}	Polarization asymmetry Δ_{asym}
192.94(8)	192.94	$5/2^- \rightarrow 3/2^-$	21.9(8)	100	0.56(8) ^d	
649.87(8)	456.93	$5/2^- \rightarrow 5/2^-$	1.91(6)	21.0(18)	1.02(34) ^e	
	649.87	$5/2^- \rightarrow 3/2^-$	16.5(7)	78.0(24)	0.48(8) ^d	0.03(11)
1063.20(7)	413.33	$7/2^- \rightarrow 5/2^-$	17.2(8)	19.0(6)	0.56(7) ^d	-0.02(8)
	870.26	$7/2^- \rightarrow 5/2^-$	13.78(72)	14.0(6)	0.83(19) ^d	-0.16(17)
	1063.20	$7/2^- \rightarrow 3/2^-$	100	66.8(12)	0.99(12) ^d	0.19(4)
1206.35(13)	1013.41	$7/2^- \rightarrow 5/2^-$	8.1(7)	50.2(23)	0.51(15) ^d	-0.25(22)
	1206.35	$7/2^- \rightarrow 3/2^-$	6.8(5)	49.8(24)	1.02(36) ^d	0.07(16)
1436.5(5)	1243.56 ^b	$9/2^- \rightarrow 5/2^-$		100		
1702.98(11)	266.48 ^b	$9/2^+ \rightarrow 9/2^-$	1.2(4)	1.2(4)		
	496.63	$9/2^+ \rightarrow 7/2^-$	13.2(7)	13.0(7)	0.71(11) ^d	-0.15(6)
	639.78	$9/2^+ \rightarrow 7/2^-$	109.3(23)	84.3(20)	0.50(4) ^d	0.01(5)
	1510.04 ^b	$9/2^+ \rightarrow 5/2^-$	1.7(4)	2.0(4)		
2050.39(12)	987.19	$9/2^- \rightarrow 7/2^-$	12(1)	92(10)	1.37(72) ^c	
	1857.45 ^b	$9/2^- \rightarrow 5/2^-$		8(3)		
2318.82(12)	1255.62	$11/2^- \rightarrow 7/2^-$	12.1(7)	100	0.98(37) ^c	
2585.23(15)	882.25	$13/2^+ \rightarrow 9/2^+$	78.8(24)	100	0.99(12) ^c	0.11(6)
2826.7(3)	1123.72	$11/2^{(+)} \rightarrow 9/2^+$	3.1(7)	100	1.67(67) ^e	
2934.6(6)	615.78 ^b	$13/2^- \rightarrow 11/2^-$				
	1498.1 ^b	$13/2^- \rightarrow 9/2^-$				
3357.5(6)	530.80 ^b		1.60(58)	100		
3480.7(4)	654	$(13/2^+) \rightarrow 11/2^{(+)}$				
	1777.72	$13/2^+ \rightarrow 9/2^+$	2.4(6)			
3527.7(3)	1208.88 ^b	$13/2^- \rightarrow 11/2^-$	2.2(6)	46(17)		
	1477.31 ^b	$13/2^- \rightarrow 9/2^-$	3.0(7)	54(18)		
3764.11(17)	1178.88	$17/2^+ \rightarrow 13/2^+$	66.6(20)	100	0.97(11) ^d	0.15(6)
3769.91(17)	943.21 ^b	$15/2^+ \rightarrow 11/2^{(+)}$	2.69(6)	35(9)		
	1184.68	$15/2^+ \rightarrow 13/2^+$	13.5(7)	65(16)	1.39(31) ^d	0.04(14)
4257.3(12)	899.80 ^b			100		
4355.0(3)	590.89 ^b	$(15/2^-) \rightarrow 17/2^+$	0.9(4)	8.0(36) ^h		
	874.30 ^b	$(15/2^-) \rightarrow (13/2^+)$	1.9(6)	46(13) ^h		
	1769.77	$(15/2^-) \rightarrow 13/2^+$	6.3(6)	46(6) ^h	0.76(20) ^d	
4365.5(6)	595.59 ^b		2.34(77)	100		
4684.2(8)	1326.70 ^b		2.81(64)	100		
4776.2(6)	421.20 ^b		1.79(70)	100		
5076.3(6)	721.30 ^b		1.91(58)	100		
5076.6(3)	1306.69	$(19/2^+) \rightarrow 15/2^+$	5.6(10)	31(12)	1.0(5) ^c	
	1312.49	$(19/2^+) \rightarrow 17/2^+$	1.0(4)	69(18)	1.01(60) ^c	
5334.7(11)	1570.59 ^b			100		
5346.06(20)	1581.95	$21/2^+ \rightarrow 17/2^+$	30.5(10)	100	0.97(12) ^d	0.16(5)
5406.5(4)	1878.80	$17/2^- \rightarrow 13/2^-$	1.3(5)		1.25(80) ^c	
	2471.90 ^b	$17/2^- \rightarrow 13/2^-$				
5424.5(4)	1660.39 ^b	$17/2^- \rightarrow 17/2^+$				
	1896.80 ^b	$17/2^- \rightarrow 13/2^-$				
	2489.90 ^b	$17/2^- \rightarrow 13/2^-$				
5916.1(3)	491.60 ^b	$19/2^- \rightarrow 17/2^-$				
	509.60 ^b	$19/2^- \rightarrow 17/2^-$	1.3(7)			
	570.04 ^b	$19/2^- \rightarrow 21/2^+$	0.8(5)			
	1561.10 ^b	$19/2^- \rightarrow 15/2^-$	1.8(4)			
6233.7(3)	317.60	$21/2^- \rightarrow 19/2^-$	1.8(5)	11.0(33)	0.68(34) ^c	
	809.20	$21/2^- \rightarrow 17/2^-$	7.6(7)	29.2(51)	1.78(1.25) ^c	
	827.20 ^b	$21/2^- \rightarrow 17/2^-$	3.7(5)	37.9(62)		
	887.64 ^b	$21/2^- \rightarrow 21/2^+$		15.8(42)		
	1157.17 ^b	$21/2^- \rightarrow (19/2^+)$	1.00(36)	5.9(39)		
6385.5(6)	1039.44 ^b		2.24(83)	100		

TABLE I. (*Continued.*)

Level energy E_i (keV)	Gamma-ray energy ^a E_γ (keV)	Initial \rightarrow final spin-parity $I_i^\pi \rightarrow I_f^\pi$	Relative intensity ^f I_γ	Branching ratio ^g B.R.	DCO ratio R_{DCO}	Polarization asymmetry Δ_{asym}
6487.3(11)	1410.75 ^b	(23/2 ⁺) \rightarrow (19/2 ⁺)		100		
6569.49(22)	335.79	23/2 ⁻ \rightarrow 21/2 ⁻	0.8(4)	8.8(17)	0.76(33) ^c	
	653.39	23/2 ⁻ \rightarrow 19/2 ⁻	2.84(47)	12.2(26)		
	1223.43	23/2 ⁻ \rightarrow 21/2 ⁺	27.3(9)	79.0(35)	0.49(8) ^d	0.15(13)
7524.5(8)	1139.00 ^b		2.23(43)	100		
7610.3(4)	1376.60 ^b	25/2 ⁻ \rightarrow 21/2 ⁻	3.9(8)	100		
7926.01(24)	1356.52	27/2 ⁽⁻⁾ \rightarrow 23/2 ⁻	11.0(21)	100	0.83(18) ^d	
9095.8(8)	1485.50 ^b	(29/2 ⁻) \rightarrow 25/2 ⁻				
	1169.79 ^b	(29/2 ⁻) \rightarrow 27/2 ⁽⁻⁾				
9773.3(11)	1847.29 ^b	(31/2 ⁻) \rightarrow 27/2 ⁽⁻⁾		100		
11048.3(9)	1952.50 ^b		0.76(28)	100		

^aThe uncertainties lie between 0.1 and 0.5 keV depending upon the intensities.

^bEstimation of R_{DCO} and Δ_{asym} was not possible due to the low intensities of the γ -ray transitions.

^cGate on $E2$, 1064 keV.

^dGate on $E2$, 882 keV.

^eGate on $E1$, 640 keV.

^fThe quoted error includes the fitting error plus a systematic error of 3% due to the uncertainties in efficiency and background subtraction.

^gBranching ratios are derived by gating from above and measuring the intensities of depopulating transitions unless otherwise mentioned.

^hBranching ratios are derived by gating from below and measuring the intensities of depopulating transitions.

of the 90° clover detectors used in the present experiment. It should be noted that a positive polarization asymmetry (Δ_{asym}) value implies the electric nature while a negative one implies the magnetic nature of the transition and a near zero value of Δ_{asym} indicates that there is a strong admixture. The validity of this method is well verified by the known nature of the transitions in ^{63}Zn and the neighboring $^{64,66}\text{Zn}$ isotopes which were also populated in the fusion evaporation reaction. The polarization asymmetry values for the different γ -ray transitions of ^{63}Zn , as obtained in this work, are tabulated in Table I and plotted in Fig. 3.

III. RESULTS AND DISCUSSION

Based on the coincidence relationship, relative intensity, angular correlation, and polarization measurements we have

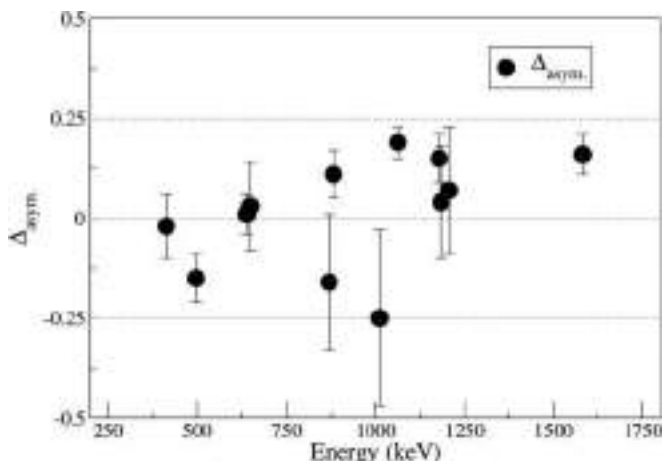


FIG. 3. Plot of polarization asymmetry values (Δ_{asym}) for different γ rays belonging to ^{63}Zn as obtained in this work.

proposed a new level scheme of ^{63}Zn . Here, almost all the previously reported transitions have been observed. New transitions observed in the present experiment are marked by asterisks in the level scheme (Fig. 4).

A total of 13 new transitions have been observed and placed properly in the level scheme. Some of the previously known and new transitions are shown in the gated spectra (Figs. 5, 6, and 7). Ground state spin-parity of ^{63}Zn , as reported earlier, is 3/2⁻ which is fed by 1063 keV strong (B.R. \approx 67%) γ ray from the 1063 keV, 7/2⁻ state. The measured DCO ratio and polarization asymmetry of this γ ray suggest that it is a stretched $E2$ type transition. The 1063 keV level also decays to 193 keV and 650 keV levels via emission of two strong (B.R. \approx 14%) 870 keV and (B.R. \approx 19%) 413 keV γ rays. The level at 193 keV, assigned with a spin-parity 5/2⁻, directly decays to the ground state via 193 keV transition with 100% branching. The measured DCO ratios and polarization asymmetries of 413 keV, 650 keV, and 1063 keV transitions suggest 5/2⁻ spin-parity value for the 650 keV state. The energy level at 1703 keV decays to the 1063 keV, 1206 keV, and 1437 keV levels via emission of 640 keV, 497 keV, and 266 keV γ rays and measured values of the DCO ratio and polarization asymmetry suggest a spin-parity value of 9/2⁺ for this state. A weak (B.R. \approx 2%) 1510 keV γ -ray transition is observed between 1703 keV (9/2⁺) and 193 keV (5/2⁻) states and the spin-parity of these states suggest $M2$ nature of 1510 keV γ -ray transition. So it is very interesting to note that 1510 keV $M2$ transition is competing with two strong $E1$ transitions (640 keV and 497 keV). This transition was also observed by previous work [28]. Here, ^{65}Ge is another good example where a 1105 keV transition between 9/2⁺ and 5/2⁻ states was observed and angular distribution measurement confirmed its $M2$ character [5]. The level at 3770 keV decays to the 9/2⁺ level via the cascade of two

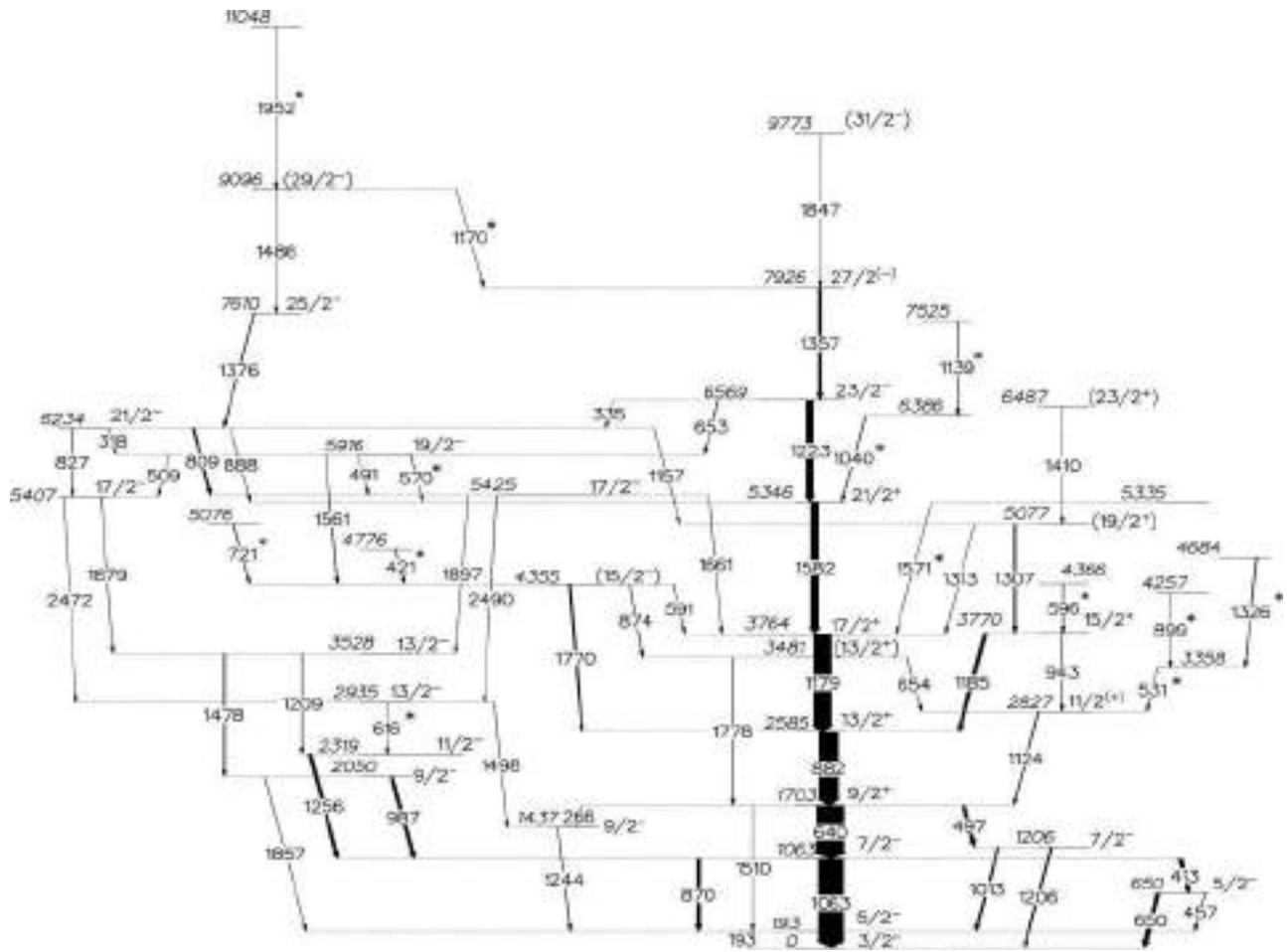


FIG. 4. Proposed level scheme of ^{63}Zn . Width of the arrows is proportional to the relative intensity of the respective transition observed in this experiment. The energies of the levels and γ rays are in keV.

strong (B.R. $\approx 65\%$) 1185 keV and (B.R. $\approx 100\%$) 882 keV γ rays. Measured values of the DCO ratio and polarization asymmetry suggest stretched electric quadrupole nature of

882 keV transition and mixed nature for 1185 keV. So, a spin-parity of $15/2^+$ is assigned for the 3770 keV state which

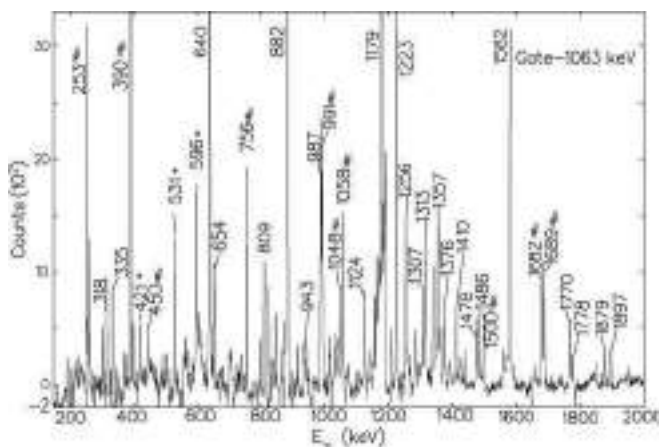


FIG. 5. Background subtracted γ - γ coincidence spectrum for ^{63}Zn gated on 1063 keV ($7/2^- \rightarrow 3/2^-$) transition. Here, y axis represents counts per 1.0 keV. New transitions are marked by asterisks (*) and contaminant peaks are identified with the # symbol.

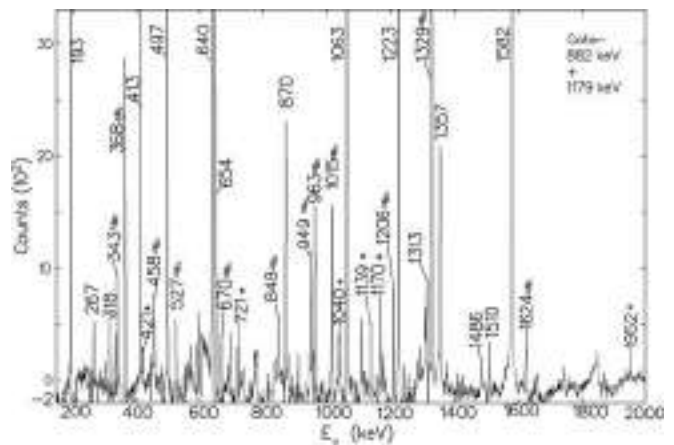


FIG. 6. Background subtracted γ - γ coincidence spectrum for ^{63}Zn in the sum gate of 882 keV ($13/2^+ \rightarrow 9/2^+$) + 1179 keV ($17/2^+ \rightarrow 13/2^+$) γ rays. Here, the y axis represents counts per 1.0 keV. New transitions are marked by asterisks (*) and contaminant peaks are identified with the # symbol.

was reported to be tentative in previous work. The measured values of DCO ratio and polarization asymmetry of 882 keV γ -ray transition confirm $13/2^+$ spin-parity value for the 2585 keV state, which is in disagreement with the assigned value of $3/2^-$ of a similar 2588 keV state reported by Leach *et al.* [29]. As Leach *et al.* used a deuteron beam of 22 MeV for the reaction, high spin states of ^{63}Zn could not be populated in their work—so most of the high spin states observed in the current heavy-ion induced experiment, could not be compared with them. However, a few states which are close in energy values are compared. The $15/2^+$ state decays to the $9/2^+$ state via the cascade of 943 and 1124 keV γ rays. Three new levels with energies 3358, 4257, and 4684 keV have been added just above the 2827 keV, $11/2^{(+)}$ state. The 4257 keV state decays through the cascade of 899 keV and 531 keV γ rays and the 4684 keV state through 1326 keV and 531 keV γ rays to the 2827 keV level. Another level with energy 4366 keV has been placed into the level scheme just above the 3770 keV level which decays to the 3770 keV state via the emission of the 596 keV γ ray. Spin-parity assignment could not be done for these new 3358, 4257, 4366, and 4684 keV levels for low intensity of the emitted γ rays. These new levels with energy 3358, 4257, and 4684 keV can be compared respectively with 3365 ($7/2^-$), 4260 ($9/2^+$), and 4689 keV ($5/2^-$) states observed by Leach *et al.* The 3764 keV level decays to the 2585 keV level via the emission of a strong (B.R. $\approx 100\%$) 1179 keV γ ray, the measured values of the DCO ratio and polarization asymmetry suggest a spin-parity of $17/2^+$ to this 3764 keV state. Previous work by Leach *et al.*, identified many low excited states which were not populated in the recent heavy ion induced reaction and a comparative study shows that assigned spin-parity of 193 and 650 keV states exactly match with our observations. Leach *et al.* were not able to determine spin-parity of 1703 keV state—they used National Nuclear Data Center reported values. The newly observed 5335 keV state decays to this $17/2^+$ state via 1571 keV γ ray. The 6569 keV level decays to the 3764 keV state via the cascade of strong (B.R. $\approx 79\%$) 1223 keV and (B.R. $\approx 100\%$) 1582 keV γ rays. The measured values of DCO ratio and polarization asymmetry predict stretched electric quadrupole nature of 1582 keV and stretched electric dipole nature of the 1223 keV transition. The 5346 keV level is fed by two new transitions 1040 keV and 1139 keV in cascade, as observed in this experiment and are placed according to their coincidence relationship and relative intensity.

The negative parity $9/2^-$ and $11/2^-$ states having energy 2050 keV and 2319 keV, respectively, feed the 1063 keV state by 987 keV and 1256 keV transitions and the measured DCO ratios predict mixed nature for these two γ rays. These two low excited states were also observed by Leach *et al.*, but without any information about spin-parity. One new transition of energy 616 keV connecting the $13/2^-$ (2935 keV) and $11/2^-$ (2319 keV) states has been found in this work. Two new levels at 5076 keV and 4776 keV are added to the level scheme and they feed the tentatively assigned $15/2^-$ spin-parity state via 721 keV and 421 keV γ rays, respectively, and the decay of this $15/2^-$ state is fragmented into three γ rays, 591 keV (B.R. $\approx 8\%$) to the $17/2^+$ state, 874 keV (B.R. $\approx 46\%$) to the tentatively assigned $13/2^+$ state, and

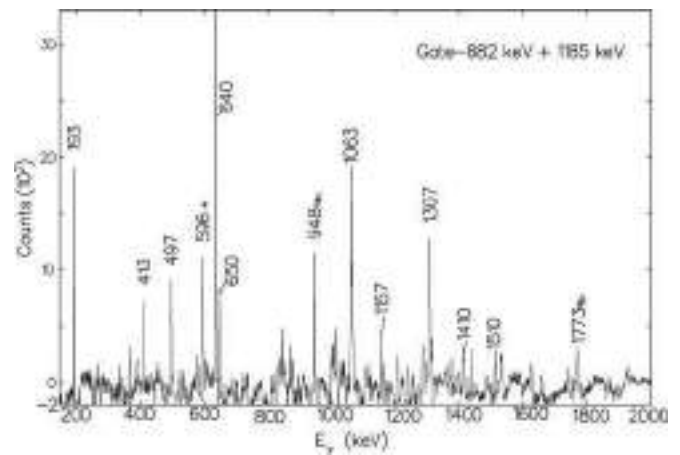


FIG. 7. Background subtracted γ - γ coincidence spectrum for ^{63}Zn in the sum gate of 882 keV ($13/2^+ \rightarrow 9/2^+$) + 1185 keV ($15/2^+ \rightarrow 13/2^+$) γ rays. Here, the y axis represents counts per 1.0 keV. New transitions are marked by asterisks (*) and contaminant peaks are identified with the # symbol.

1770 keV (B.R. $\approx 46\%$) to the $13/2_1^+$ state. The 5916 keV $19/2^-$ level decays to 5425 ($17/2^-$), 5346 ($21/2^+$), and 5407 keV ($17/2^-$) levels by 491, 570, and 509 keV γ rays, respectively. Here, the 570 keV γ ray is a new transition observed in this work. The 6234 keV level with spin-parity $21/2^-$ decays via 318 (B.R. $\approx 11\%$), 809 (B.R. $\approx 29\%$), 827 (B.R. $\approx 38\%$), 888 (B.R. $\approx 16\%$), and 1157 (B.R. $\approx 6\%$) keV transitions to both positive parity and negative parity states and is fed by the 1376 keV (100% branching) γ ray from 7610 keV state with spin-parity $25/2^-$. So, the energy level $21/2^-$ at 6234 keV decays mostly by fragmented γ rays. The fragmented decay pattern as observed in some of the negative parity states indicates that the corresponding wave functions are of highly complex nature. A new transition of 1952 keV has also been observed and is placed above the 9096 keV state which feeds the 7610 keV level via the 1486 keV γ ray. The 1170 keV transition is a new transition that connects the 9096 keV state having a tentative spin-parity $29/2^-$ to the 7926 keV $27/2^{(-)}$ state. The placement of the 1952 keV γ ray extends the level scheme up to 11 MeV. The energy states above $31/2^-$ are inaccessible in this experiment and this is probably due to the presence of long-lived isomers above this spin and excitation energy or may be due to the incomplete fusion caused by the loss of input angular momentum in this reaction. Also we cannot ignore the sharing of γ -ray yield because of the large density of states at such high excitation energy but a more obvious reason may be the limited sensitivity of the setup we used, which could not permit us to observe highly nonyrast states that were populated in the reaction. More access to higher spin ($>31/2\hbar$) states could have been gained by improving the sensitivity of the setup with the help of ancillary devices, such as the charged particle array along with the full INGA array consisting of 24 clover detectors.

A. Shell model calculations

Calculations on even- A Zn isotopes using anharmonic vibrator model [42,43] are able to explain many interesting

phenomena emerging out of lower excitations successfully. The structure of low lying levels in odd-mass isotopes of Zn is explained in terms of the coupling of the odd single particle to the vibrating core [44]. Quasiparticle-phonon coupling model was used by Weidinger [45] and by Throop [46] in order to understand the experimental decay scheme of ^{65}Zn and ^{67}Zn , respectively. Shell model calculations for $^{64,66,68}\text{Zn}$ with model space consisting of $p_{3/2}$, $f_{5/2}$, and $p_{1/2}$ orbitals outside the closed ^{56}Ni core, along with an effective Hamiltonian from Koops and Glaudemans, were done by Van Hienen *et al.* [47]. A comparison of quasiparticle-core coupling and shell model calculations with experiment exhibited very good agreement for low lying negative parity states for both ^{65}Zn and ^{67}Zn but a lack of similarity was observed for higher excited states. Similar situation arises for ^{63}Zn [27] with same model space and interaction.

In order to understand the observed nuclear structure in ^{63}Zn , shell model calculations have been performed in the present work using the interaction jj44bpn [48]. The shell-model code NUSHELLX [49] is used for this purpose. With the ^{56}Ni core, the valence space for the calculation consists of $2p_{3/2}$, $1f_{5/2}$, $2p_{1/2}$, and $1g_{9/2}$ proton and neutron orbitals. Here, the effective Hamiltonian jj44bpn, due to Brown and Lesitskiy [48], is a realistic interaction based on the Bonn-C potential, which has been obtained by fitting binding energies and excitation energies in the Ni, Cu, and Zn isotopes and nuclei close to $N = 50$. Previous calculations for $^{60,62,64,66}\text{Zn}$ [50] and ^{63}Cu [32] by Rai *et al.*, with the similar interaction and model space have produced very good agreements. The single particle energies for the $2p_{3/2}$, $1f_{5/2}$, $2p_{1/2}$, and $1g_{9/2}$ orbitals are taken to be 9.6566, 9.2859, 8.2695, and 5.8944 MeV, respectively. Reduced transition probabilities [$B(E2)$ values] have been calculated for the $21/2^+ \rightarrow 17/2^+$, $17/2^+ \rightarrow 13/2^+$, and $13/2^+ \rightarrow 9/2^+$ transitions using standard effective charges $e_p = 1.5e$ and $e_n = 0.5e$ and the calculated values are 11.81, 16.69, and 17.38 Weisskopf unit (W.u.), respectively. While taking the half-lives from Ref. [26] and using the experimental B.R. of the present work, we have obtained experimental $B(E2)$ values for $21/2^+ \rightarrow 17/2^+$, $17/2^+ \rightarrow 13/2^+$, and $13/2^+ \rightarrow 9/2^+$ transitions which are ($>$)14, 78 (23), and 20 (2) W.u., respectively. So shell model calculations for the transitions $21/2^+ \rightarrow 17/2^+$ and $13/2^+ \rightarrow 9/2^+$ produce near similar $B(E2)$ values as obtained from experiment but it is unable to reproduce the large collectivity [indicated by large $B(E2)$ value] for the transition $17/2^+ \rightarrow 13/2^+$. A comparison of the calculated energy levels with the experimental results shows overall good agreement for both parity states as shown in Fig. 8. All the energy states calculated by the shell model and labeled in Fig. 8 are of lowest energy values corresponding to the given spin-parity. The comparison is made here, only for the states having exactly measured or tentatively assigned spin-parity, therefore, experimentally observed levels, which do not have any assigned spin-parity, are not compared with the shell model calculation.

Spin and parity of ground state and first excited state are predicted correctly by jj44bpn interaction which are $3/2^-$ and $5/2^-$, respectively. While the energies of these two states are correctly predicted, that of second excited $5/2^-$ state is

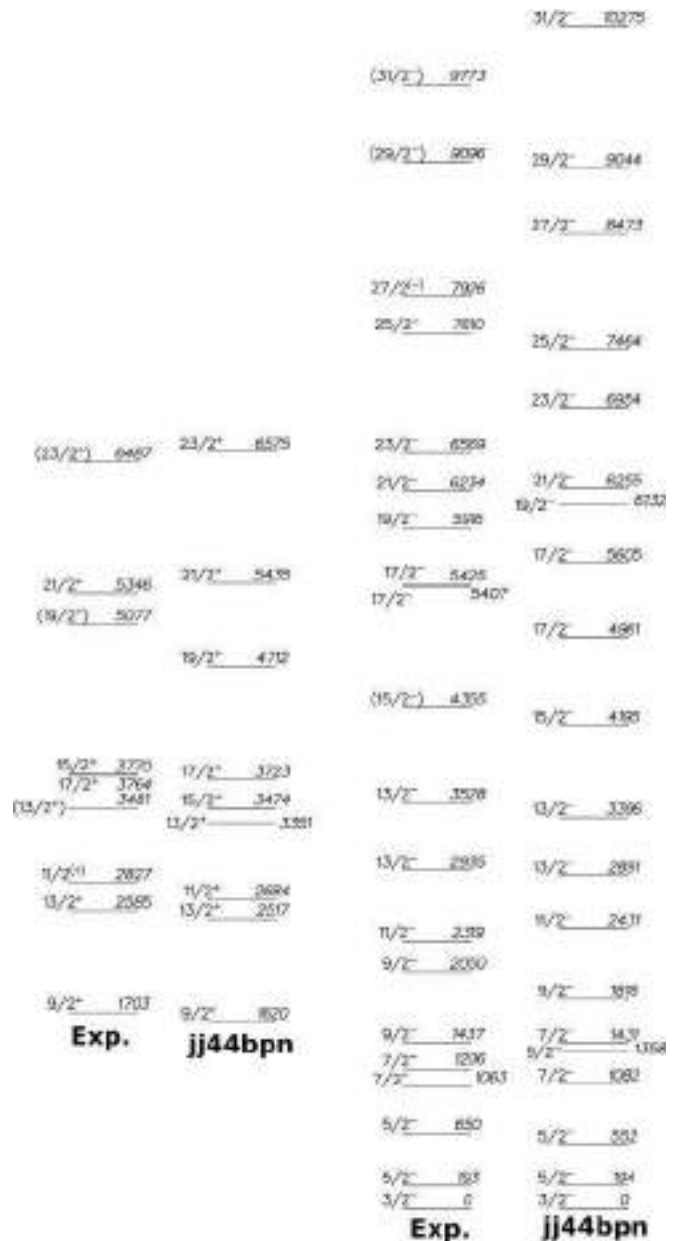


FIG. 8. Comparison of the shell model calculated level energies using the jj44bpn [48] interaction with the experimental values. The negative parity and the positive parity states are shown separately. The number on the left of the level represents the spin (in \hbar)-parity and that on the right represents the level energy in keV.

underpredicted by ≈ 100 keV. Very good matching between theory and experiment is observed for first $7/2^-$ and $9/2^-$ states, while that for the second excited $7/2^-$ state is over predicted and $9/2^-$ state is under predicted in the model. For the lower and moderate excitation energies a very good agreement between the calculated energies and experimental values is observed. For few high spin negative parity states lack of agreement is also observed. Similarly for all positive parity states from $9/2^+$ up to $23/2^+$, almost all the energy levels (with the exception of a little discrepancy for the $15/2^+$ and $19/2^+$ states) are reproduced well by the model

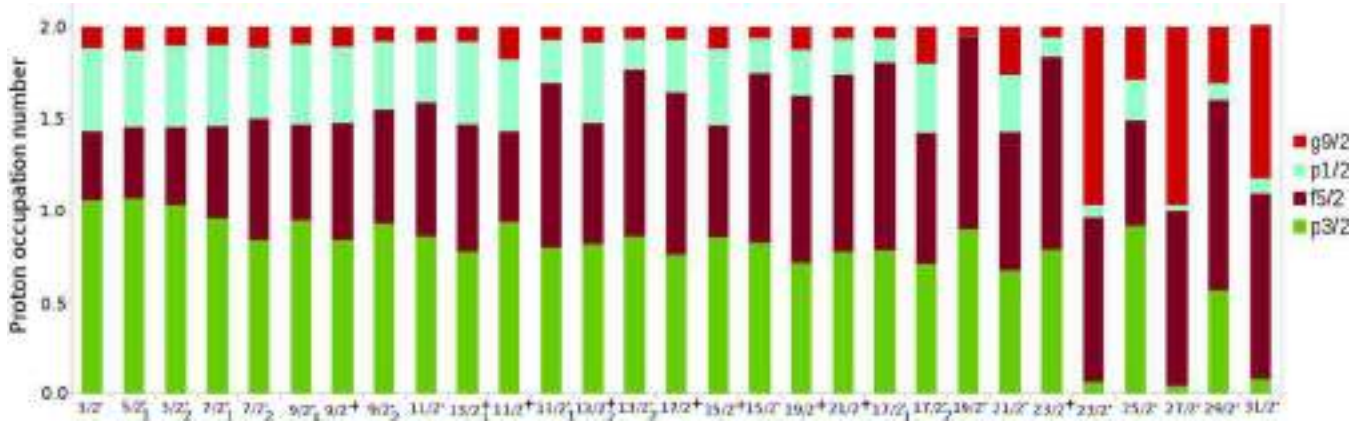


FIG. 9. Calculated occupation probabilities of the $p_{3/2}$, $f_{5/2}$, $p_{1/2}$, and $g_{9/2}$ orbitals for the proton in ^{63}Zn . The occupation probabilities are calculated from the shell model calculation using the jj44bpn interaction.

with the chosen interaction and model space. We have also calculated occupation probabilities for proton and neutron in the same model space and Hamiltonian. An occupation probability gives the strength of individual contribution of different orbitals ($2p_{3/2}$, $1f_{5/2}$, $2p_{1/2}$, and $1g_{9/2}$ in the case of present calculation) of both the proton and neutron in total wave function. So this calculation is important as it gives information regarding the structure of different levels. From the occupation number plots (Figs. 9 and 10), major contributions from the $p_{3/2}$ and $f_{5/2}$ orbitals to both kind of parity states are clearly evident. For $23/2^-$, $25/2^-$, and $27/2^-$ states, a large contribution in total wave function is coming from the intruder $1g_{9/2}$ orbital. Moreover, shell model calculations can not predict properly the energy values of $23/2^-$, $27/2^-$, and $31/2^-$ negative parity states. It indicates that origin of these states are different and may be due to the particle excitation from $f_{7/2}$ to $g_{9/2}$ orbital. The important role of $f_{7/2}$ holes in developing collective bands in neighboring Zn isotopes is well known. Most notable fact is that for all the positive parity states, the contribution of the $1g_{9/2}$ neutron in the total wave function is significant. Hence, a variety of structural effects are

expected due to this shape driving the $g_{9/2}$ orbital. So in order to investigate the possibility of collective nature and evolution of shapes we have done potential energy calculations for ^{63}Zn .

B. TRS calculation

The total Routhian surface (TRS) in a fixed quasiparticle configuration is defined as a sum of Strutinsky energy and the rotational energy. Here, Strutinsky energy contains liquid drop plus shell correction terms. Configuration is specified in terms of parity (π), signature (α), and excitation quantum numbers. We have performed TRS calculations for ^{63}Zn using the Hartree-Fock-Bogoliubov code of Nazarewicz *et al.* [51,52] for a single quasineutron in the $g_{9/2}$ orbital. Equilibrium shapes were calculated in the (β_2, γ) plane at each rotational frequency ($\hbar\omega$) minimizing with respect to β_4 . Here, β_2 , γ , and β_4 represent quadrupole deformation, triaxiality, and hexadecapole deformation parameters, respectively. As a residual interaction, the monopole pairing force has been taken with the strength from Ref. [52]. Here, the calculation

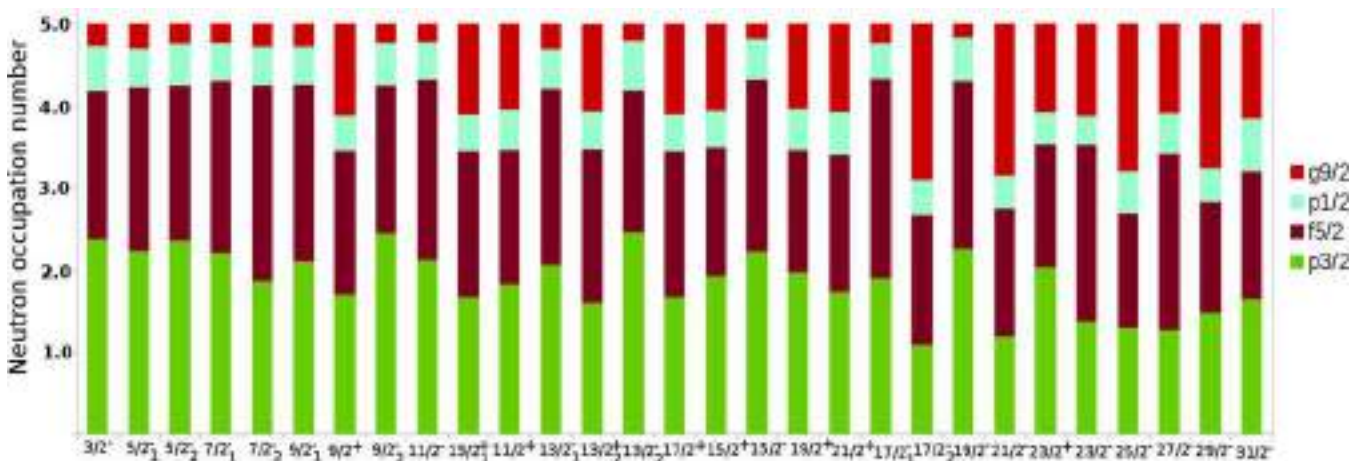


FIG. 10. Calculated occupation probabilities of the $p_{3/2}$, $f_{5/2}$, $p_{1/2}$, and $g_{9/2}$ orbitals for the neutron in ^{63}Zn . The occupation probabilities are calculated from the shell model calculation using the jj44bpn interaction.

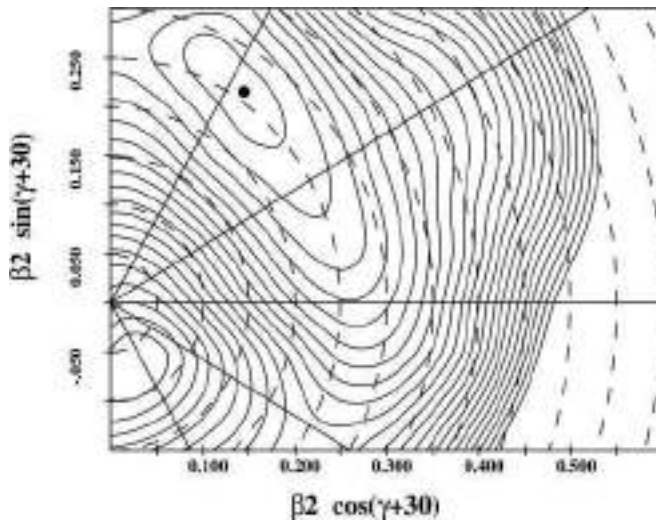


FIG. 11. TRS plot for ^{63}Zn for $(\pi, \alpha = +, +1/2)$ configuration at $\hbar\omega = 0.30$ MeV. Contours are 250 keV apart from each other. The shape corresponding to the energy minima is predicted to be triaxial ($\gamma \approx 23^\circ$) with $\beta_2 \approx 0.25$.

for positive parity and positive signature predicts collective triaxial shape with quadrupole deformation $\beta_2 \approx 0.25$ and triaxiality parameter $\gamma \approx 23^\circ$ for both $\hbar\omega$ values (i.e., at 0.30 MeV and 0.40 MeV) as shown in Figs. 11 and 12. Calculations at higher $\hbar\omega$ value (≈ 0.65 MeV) showed very near collective prolate shapes with $\gamma \approx 5^\circ$ and at a large value of quadrupole deformation $\beta_2 \approx 0.45$ (Fig. 13).

TRS calculations with a $g_{9/2}$ quasineutron predict the presence of collective triaxial deformed shape at low rotational frequency with moderate value of β_2 . It evolves to an enhanced collective prolate structure with the increase in rotational frequency. Though signs of such large deformation

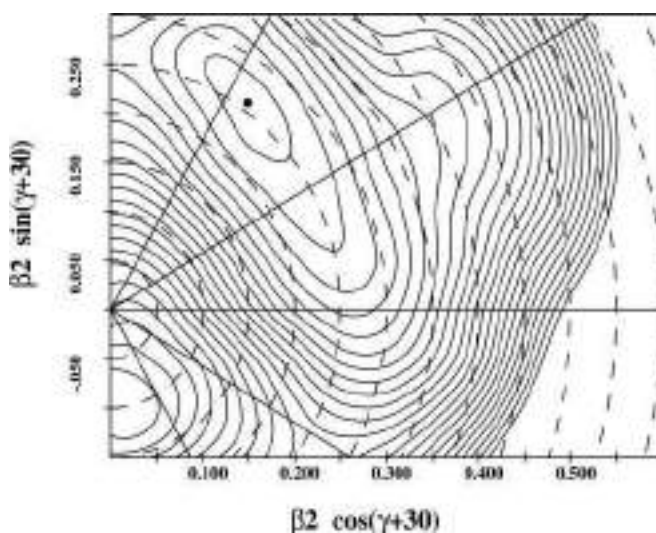


FIG. 12. Same as Fig. 11 at $\hbar\omega = 0.40$ MeV. The shape corresponding to the energy minima is predicted to be triaxial with almost similar values of the triaxiality and quadrupole deformation parameters as at 0.30 MeV.

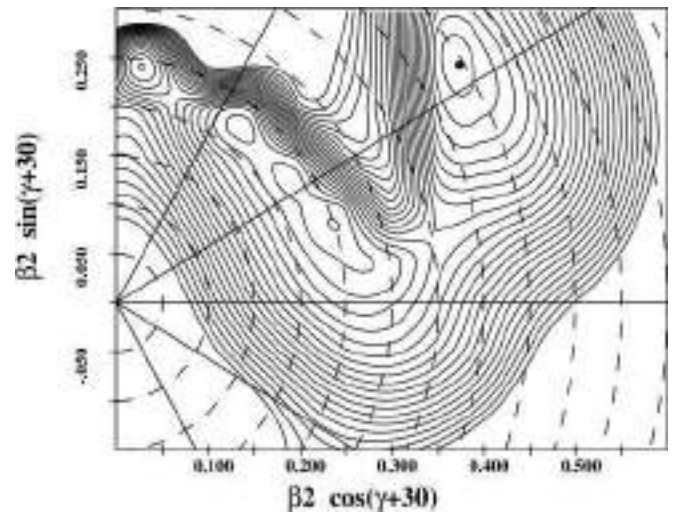


FIG. 13. Same as Fig. 11 at $\hbar\omega = 0.60$ MeV. The shape corresponding to the energy minima is predicted to be near prolate ($\gamma \approx 5^\circ$) with $\beta_2 \approx 0.45$.

($\beta_2 \approx 0.45$) as predicted by TRS could not be confirmed by the present experiment but further investigation is required in future to search for large collectivity at such large deformation.

IV. CONCLUSIONS

In the present work with an efficient array of clover detectors we have observed 13 new transitions and ten new levels in ^{63}Zn . The level scheme is extended up to an excitation energy of ≈ 11 MeV. Multipolarity of many transitions with their electric or magnetic nature has been established adequately by DCO and polarization measurement. Shell model calculations are performed in the $f_{5/2}pg_{9/2}$ model space with the ^{56}Ni core using the effective interaction $jj44\text{bpn}$ to interpret the obtained level structure of this nucleus. A reasonable agreement is found to exist between the observed level structure and the results from the shell model calculations. With an improved set of the two-body matrix elements and incorporating the full $fp_{g_{9/2}}$ model space, i.e., including the $1f_{7/2}$ orbital for calculations, a more accurate description may be obtained. Total Routhian surface calculations predict collective excitation with triaxial and prolate shape at moderate and large value of deformation parameter (β_2), respectively.

ACKNOWLEDGMENTS

We would like to acknowledge the support from the Pelletron staff of IUAC for providing an excellent beam and INGA collaborators for loan of detectors. Support from target laboratory and from D. Kanjilal, IUAC is highly acknowledged. We would like to thank S. Nandi (VECC), S. S. Bhattacharjee (IUAC), and R. Garg (IUAC) for their help during the experiment. We would also like to acknowledge the financial supports from SERB/DST (New Delhi) with File No. EMR/2015/000891 and IUAC (New Delhi) with

File No. UFR-49318. We are grateful to the Nuclear Data Review Group at NNDC, Brookhaven National Laboratory,

for the data consistency check on the manuscript and the least-squares fit calculation of the level energies.

-
- [1] P. J. Emnis *et al.*, *Nucl. Phys. A* **535**, 392 (1992).
[2] A. P. de Lima *et al.*, *Phys. Rev. C* **23**, 213 (1981).
[3] L. Chaturvedi *et al.*, *Phys. Rev. C* **43**, 2541 (1991).
[4] U. Hermkens *et al.*, *Z. Phys. A* **343**, 371 (1992).
[5] U. Hermkens *et al.*, *Phys. Rev. C* **52**, 1783 (1995).
[6] D. Rudolph *et al.*, *Phys. Rev. Lett.* **80**, 3018 (1998).
[7] C. Andreoiu *et al.*, *Phys. Rev. C* **62**, 051301(R) (2000).
[8] L. L. Anderson *et al.*, *Eur. Phys. J. A* **36**, 251 (2008).
[9] B. Mukherjee, S. Muralithar, R. P. Singh, R. Kumar, K. Rani, and R. K. Bhowmik, *Phys. Rev. C* **63**, 057302 (2001).
[10] C. Andreoiu *et al.*, *Eur. Phys. J. A* **14**, 317 (2002).
[11] W. Nazarewicz *et al.*, *Nucl. Phys. A* **429**, 269 (1984).
[12] W. Nazarewicz, *Nucl. Phys. A* **520**, 333c (1990).
[13] C. E. Svensson *et al.*, *Phys. Rev. Lett.* **82**, 3400 (1999).
[14] C.-H. Yu, C. Baktash, J. Dobaczewski, J. A. Cameron, C. Chitu, M. Devlin, J. Eberth, A. Galindo-Uribarri, D. S. Haslip, D. R. LaFosse, T. J. Lampman, I. Y. Lee, F. Lerma, A. O. Macchiavelli, S. D. Paul, D. C. Radford, D. Rudolph, D. G. Sarantites, C. E. Svensson, J. C. Waddington, and J. N. Wilson, *Phys. Rev. C* **60**, 031305(R) (1999).
[15] L.-L. Andersson *et al.*, *Eur. Phys. J. A* **30**, 381 (2006).
[16] L.-L. Andersson *et al.*, *Phys. Rev. C* **79**, 024312 (2009).
[17] A. Galindo-Uribarri *et al.*, *Phys. Lett. B* **422**, 45 (1998).
[18] D. Karlgren *et al.*, *Phys. Rev. C* **69**, 034330 (2004).
[19] A. V. Afanasjev, D. B. Fossan, G. J. Lane, and I. Ragnarsson, *Phys. Rep.* **322**, 1 (1999).
[20] C. E. Svensson *et al.*, *Phys. Rev. Lett.* **79**, 1233 (1997).
[21] C. E. Svensson *et al.*, *Phys. Rev. Lett.* **80**, 2558 (1998).
[22] J. Gellanki *et al.*, *Phys. Rev. C* **86**, 034304 (2012).
[23] C. H. Yu, C. Baktash, J. Dobaczewski, J. A. Cameron, M. Devlin, J. Eberth, A. Galindo-Uribarri, D. S. Haslip, D. R. LaFosse, T. J. Lampman, I. Y. Lee, F. Lerma, A. O. Macchiavelli, S. D. Paul, D. C. Radford, D. Rudolph, D. G. Sarantites, C. E. Svensson, J. C. Waddington, and J. N. Wilson, *Phys. Rev. C* **62**, 041301(R) (2000).
[24] B. Mukherjee, S. Muralithar, R. P. Singh, R. Kumar, K. Rani, R. K. Bhowmik, and S. C. Pancholi, *Phys. Rev. C* **64**, 024304 (2001).
[25] O. M. Mustaffa *et al.*, *J. Phys. G* **4**, 99 (1978).
[26] O. M. Mustaffa *et al.*, *J. Phys. G* **5**, 1283 (1979).
[27] P. A. S. Metford, T. Taylor, and A. Cameron, *Nucl. Phys. A* **308**, 210 (1978).
[28] A. K. Singh *et al.*, *Phys. Rev. C* **57**, 1617 (1998).
[29] K. G. Leach *et al.*, *Phys. Rev. C* **87**, 064306 (2013).
[30] G. K. Mehta *et al.*, *Nucl. Instrum. Methods Phys. Res. A* **268**, 334 (1988).
[31] S. Muralithar *et al.*, *Nucl. Instrum. Methods Phys. Res. A* **622**, 281 (2010).
[32] S. Rai *et al.*, *Eur. Phys. J. A* **54**, 84 (2018).
[33] U. S. Ghosh *et al.*, in *Proceedings of the DAE Symposium on Nuclear Physics 63* (Department of Atomic Energy, Government of India, 2018), p. 130.
[34] B. P. Ajith Kumar *et al.*, in *Proceedings of the 44th DAE-BRNS Symposium on Nuclear Physics* (Department of Atomic Energy, Government of India, 2001), p. 390.
[35] D. C. Radford, *Nucl. Instrum. Methods Phys. Res., Sect. A* **361**, 297 (1995).
[36] R. K. Bhowmik *et al.*, in [34], p. 422.
[37] K. S. Krane *et al.*, *Nucl. Data Tables* **11**, 351 (1973).
[38] G. Duchene *et al.*, *Nucl. Instrum. Methods Phys. Res. A* **432**, 90 (1999).
[39] K. Starosta *et al.*, *Nucl. Instrum. Methods Phys. Res. A* **423**, 16 (1999).
[40] S. Chakraborty *et al.*, *Braz. J. Phys.* **47**, 406 (2017).
[41] R. Palit *et al.*, *Pramana J. Phys.* **54**, 347 (2000).
[42] L. S. Kisslinger and K. Kumar, *Phys. Rev. Lett.* **19**, 1239 (1967).
[43] J. W. Lightbody, Jr., *Phys. Lett. B* **38**, 475 (1972).
[44] V. K. Thankappan and W. W. True, *Phys. Rev.* **137**, B793 (1965).
[45] A. Weidinger, E. Finckh, U. Jahnke, and B. Schreiber, *Nucl. Phys. A* **149**, 241 (1970).
[46] M. J. Throop, Y. T. Cheng, and D. K. McDaniels, *Nucl. Phys. A* **239**, 333 (1975).
[47] J. F. A. Van Hienen *et al.*, *Nucl. Phys. A* **269**, 159 (1976).
[48] A. F. Lisetskiy, B. A. Brown, M. Horoi, and H. Grawe, *Phys. Rev. C* **70**, 044314 (2004).
[49] A. Brown and W. D. M. Rae, *Nucl. Data Sheets* **120**, 115 (2014).
[50] S. Rai *et al.*, *Int. J. Mod. Phys. E* **25**, 11 (2016).
[51] W. Nazarewicz *et al.*, *Nucl. Phys. A* **512**, 61 (1990).
[52] W. Nazarewicz, J. Dudek, R. Bengtsson, T. Bengtsson, and I. Ragnarsson, *Nucl. Phys. A* **435**, 397 (1985).

PAPER

Magnetic and transport properties of the mixed $3d-5d-4f$ double perovskite $\text{Sm}_2\text{CoIrO}_6$

To cite this article: Suman Kalyan Pradhan *et al* 2021 *J. Phys.: Condens. Matter* **33** 335801

View the [article online](#) for updates and enhancements.

The banner features a background of overlapping, colorful book covers in shades of red, orange, and yellow. On the right side, the text is set against a light grey background.

IOP ebooks™

Bringing together innovative digital publishing with leading authors from the global scientific community.

Start exploring the collection—download the first chapter of every title for free.

Magnetic and transport properties of the mixed $3d-5d-4f$ double perovskite $\text{Sm}_2\text{CoIrO}_6$

Suman Kalyan Pradhan¹, Biswajit Dalal¹, Rafikul Ali Saha¹, Raktim Datta², Subham Majumdar²  and Subodh Kumar De^{1,*} 

¹ School of Materials Sciences, Indian Association for the Cultivation of Science, 2A & 2B Raja S.C. Mullick Road, Jadavpur, Kolkata 700032, India

² School of Physical Sciences, Indian Association for the Cultivation of Science, 2A & 2B Raja S.C. Mullick Road, Jadavpur, Kolkata 700032, India

E-mail: msskd@iacs.res.in

Received 25 February 2021, revised 12 May 2021

Accepted for publication 28 May 2021

Published 25 June 2021



CrossMark

Abstract

Iridium-based double perovskites having mixed $3d-5d-4f$ magnetic sub-lattices are expected to exhibit exotic magnetic phenomenon. In this paper, we report a study of structural, magnetic and transport properties of the mixed $3d-5d-4f$ double perovskite $\text{Sm}_2\text{CoIrO}_6$ (SMCO), which crystallizes in monoclinic structure with space group $P2_1/n$ and the crystal symmetry remains same throughout the measured temperature down to 15 K. High resolution synchrotron x-ray diffraction reveals an isostructural phase transition around 104 K. Magnetization measurements on polycrystalline samples indicate that SMCO orders ferrimagnetically at $T_{\text{FiM}} = 104$ K; while, a second transition is observed below 10 K due to the rare-earth (Sm^{3+}) ordering. The ferrimagnetic transition is well-understood by Néel's two-sublattice model, which is primarily ascribed to antiferromagnetic coupling between Co^{2+} and Ir^{4+} sub-lattices. Electronic transport measurement shows the insulating behaviour of SMCO, which follows Mott variable-range hopping conduction mechanism. However, dielectric measurements as a function of temperature rules out the presence of magneto dielectric coupling in this compound.

Keywords: double perovskite, ferrimagnetism, 3D Mott VRH

(Some figures may appear in colour only in the online journal)

1. Introduction

Double perovskite oxides $\text{A}_2\text{BB}'\text{O}_6$ containing alkaline or lanthanide ions at the A site and $3d-4d(5d)$ transition-metal (TM) ions at the B and B' sites offer a unique playground for exploring novel electronic and magnetic phenomena, due to their comparable energies of strong spin-orbit coupling (SOC), on-site Coulomb and crystal-field interactions [1]. Thus, from the perspective of new materials designing, double perovskites provide wide flexibility by virtue of choosing not only the TM

ions but also the alkaline and lanthanide ions. In addition, these double perovskites are found to exhibit a variety of interesting physical properties, such as half-metallic tunneling-type magnetoresistance, high-Curie-temperature ferrimagnetic (FiM) half-metals and insulators, multiferroicity, magnetocaloric, and exchange bias [2–12], enabling them to become a great prospect for spintronic applications. In general, the magnetic ground state and the temperature and magnetic field-dependent magnetization behavior for most of these materials are mainly determined by the TM ions at the B and B' sites through superexchange interaction [13–15]. However, the 12-coordinated alkaline ions do not take part directly in determining the magnetic properties of double perovskite, or otherwise influenc-

* Author to whom any correspondence should be addressed.

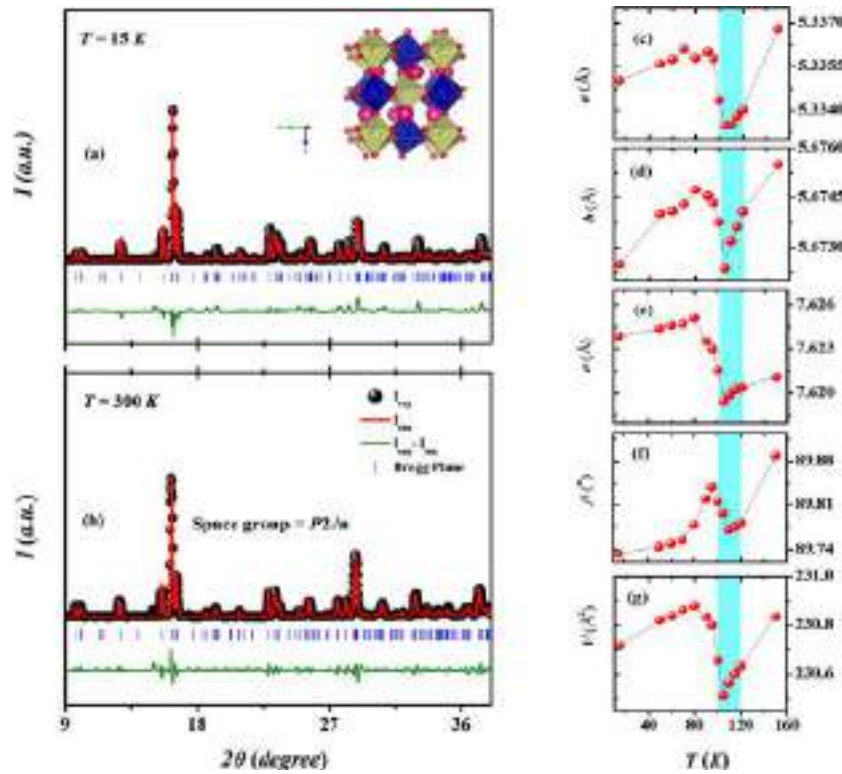


Figure 1. (a) and (b) show the synchrotron x-ray diffraction patterns of $\text{Sm}_2\text{CoIrO}_6$ measured at 15 and 300 K, respectively. Filled black circles represent the experimental data and the continuous red line represents the simulated pattern. The blue scattered lines are the Bragg peak. The green line represents the difference between the experimental and simulated pattern. The inset of (a) represents the refined crystal structure at 15 K. (c)–(g) Thermal variation of lattice parameters a , b , c , β and unit cell volume V .

ing indirectly through lattice distortion. On the other hand, lanthanide ions, in particular, rare-earth (RE) ions having unfilled $4f$ shell are especially interesting in magnetism due to their single-ion anisotropy effect (contribution from the large unquenched orbital angular momentum). Although, the d – f exchange interactions are weaker than d – d exchange interactions as the nature of $4f$ orbitals in RE atoms are strongly localized, these weak exchange interactions however can induce fascinating magnetic phenomenon in the double perovskites [16].

Iridates, more explicitly, iridium (Ir)-based double perovskites have gained a lot of attention in recent days and turned into a rapidly growing research topic in condensed matter physics as $5d$ Ir ions bring strong and unusual SOC, which results in diverse magnetic ground states. In case of $5d^4$ systems i.e., Ir^{5+} ions in an octahedral crystal field of A_2BIrO_6 (with A^{2+} and B^{3+} cations) compounds, it is expected that the strong SOC associated with the Ir ions drives the system into a ' $J_{\text{eff}} = 0$ ' nonmagnetic ground state. However, there are certain controversies in literature regarding the perfect ' $J_{\text{eff}} = 0$ ' ground state, and in most of the cases, it hasn't been achieved due to the presence of either electronic many-body effects or defects (chemical disorder and/or off-stoichiometry) [17–21]. In contrast, the systems having Ir^{4+} ions ($5d^5$, t_{2g}^5)

within octahedral oxygen cages lead to a ' $J_{\text{eff}} = 1/2$ ' Mott-insulating state, as the strong SOC splits t_{2g} level into a fully occupied $J_{\text{eff}} = 3/2$ quartet and a partially-filled $J_{\text{eff}} = 1/2$ doublet states [22]. Furthermore, the double perovskite iridates having strongly correlated $3d$ ions at the other B site are found to show exotic magnetic phenomenon along with the complex magnetic ground states. For instance, among the La_2BIrO_6 iridates, $\text{B} = \text{Mn}$ is found to show ferromagnetic (FM) ground state [23], the noncollinear antiferromagnetic (AFM) ground state (as well as a weak FM component) is reported for $\text{B} = \text{Ni}$, Fe , Co and Cu compounds [24–31], and the $\text{B} = \text{Mg}$ (Zn) exhibits AFM (canted) ground state [30, 32]. Recently, it is observed that the FM cluster glass and exchange bias behavior have emerged upon Cr-doping at the Cu site of $\text{La}_2\text{CuIrO}_6$ compound [31].

Although earlier studies have reported that $\text{La}_2\text{CoIrO}_6$ shows FM-like components at low temperature (from hysteresis loop measurements) [25, 27], more recent investigations have predicted a FiM ground state resembling to the AFM coupling between a weak FM moment of canted Co^{2+} spins and Ir^{4+} cations with a negative moment [28]. In contrast, a reentrant spin-glass magnetic state also has been found in this compound recently [33]. Since, the other members of this $\text{Ln}_2\text{CoIrO}_6$ family with Ln-site magnetic RE elements

Table 1. The Rietveld refined crystallographic parameters, such as fractional atomic coordinates (with Wyckoff positions), isotropic thermal parameters (B_{iso}) obtained from the $T = 15$ K, x-ray diffraction pattern of $\text{Sm}_2\text{CoIrO}_6$. Occ corresponds to site occupancies.

Space group: $P2_1/n$

$a = 5.3350 \text{ \AA}$, $b = 5.6724 \text{ \AA}$, $c = 7.6238 \text{ \AA}$, $\beta = 89.7325^\circ$

Unit-cell volume (V) = 230.7150 \AA^3

$R_p = 8.2$, $R_{wp} = 10$, $\chi^2 = 5$

Atom	x/a	y/b	z/c	B_{iso}	Occ
Sm ($4e$)	0.015 33	0.573 00	0.747 60	0.083	1.0
Co ($2b$)	0	0	0.5	0.715	0.85
Ir ($2b$)	0	0	0.5	0.715	0.15
Ir ($2a$)	0	0	0	0.715	0.85
Co ($2a$)	0	0	0	0.715	0.15
O1 ($4e$)	0.100 50	0.029 00	0.248 30	0.916	1.0
O2 ($4e$)	0.187 50	0.297 00	-0.05070	0.574	1.0
O3 ($4e$)	0.201 80	0.303 60	0.548 80	0.671	1.0

could bring a paramagnetism complexity in magnetism due to the interactions between three magnetic cations, researchers now focus on studying the physical properties of hetero-tri-spin $3d-5d-4f$ systems [34]. In this context, it is worthwhile to mention that $\text{Ln}_2\text{CoIrO}_6$ double perovskites with $\text{Ln} = \text{Eu}$, Tb and Ho show a high-temperature FiM transition and moderate magnetocaloric effects (MCEs); while, both $\text{Tb}_2\text{CoIrO}_6$ and $\text{Ho}_2\text{CoIrO}_6$ compounds exhibit a temperature-induced FiM-to-AFM phase transition and a field-induced spin-flop-like transition below AFM Néel temperature [35]. However, no reports have been found in literature till now to understand the complex magnetic and electrical behaviours of SMCO double perovskite having hetero-tri-spin configuration.

In this report, we have investigated the magnetic and transport behaviours of the polycrystalline double perovskite compound SMCO, synthesized by standard solid-state-reaction method. The powder diffraction pattern analysis confirms that SMCO crystallizes in the monoclinic structure with space group $P2_1/n$, alike other hetero-tri-spin systems in this $\text{Ln}_2\text{CoIrO}_6$ family [35]. Temperature and magnetic field-dependent magnetization measurements reveal that sample shows FiM transition at $T_{\text{FiM}} = 104$ K as well as the RE Sm^{3+} ions ordering at $T_{\text{R}}^{\text{Sm}} = 10$ K. However, the conventional Arrott plot rules out the validity of mean-field theory near paramagnetic-FiM phase transition. Temperature dependence of electrical resistivity measurement suggests that SMCO is an insulator, and shows Mott variable-range hopping (VRH) conduction behaviour. Dielectric measurements reveal the absence of magneto dielectric coupling in this as studied sample.

2. Experimental details

Polycrystalline sample of SMCO was prepared by the conventional solid-state-reaction method from stoichiometric amount of Sm_2O_3 (Sigma Aldrich, 99.99%), $\text{CoCO}_3 \cdot x\text{H}_2\text{O}$ (Sigma Aldrich, 99%) and IrO_2 (Sigma Aldrich, 99.99%). At first, these raw oxides and carbonate were mixed and ground thoroughly in an agate mortar, and heated at 873 K for 16 h in air. Then the mixture was reground and sintered at 1323 K

for 24 h in air, and subsequently furnace-cooled to room temperature. This process was repeated 3–5 times to get good quality homogeneous sample. The high resolution temperature dependent powder x-ray diffraction (XRD) measurements were performed using synchrotron facility ($\lambda = 0.77 \text{ \AA}$) at Photon Factory, National Laboratory for High Energy Physics (KEK) Japan, within temperature range 300 K to 15 K. Rietveld refinement [36] of the XRD data was performed using the FullProf software package [37] and the chemical unit cell has been drawn using the software VESTA [38]. The dc magnetization measurements were carried out on a Quantum Design superconducting quantum interference device magnetometer between 2 and 300 K, and applied magnetic field up to 70 kOe. The resistivity of the sample as a function of temperature was measured from 50 to 230 K using the standard four-probe method with dc current in a Physical Properties Measurement System (PPMS, Cryogenic Ltd., UK). The dielectric measurements were performed in the temperature range 5–270 K using low temperature facility (Cryogenics Ltd., UK) and frequency 1 kHz–1 MHz using LCR meter (KEYSIGHT E4980A).

3. Results and discussions

3.1. Crystal structure

The structural refinements of room temperature synchrotron XRD of SMCO has been carried out by considering monoclinic space group $P2_1/n$ (No. 14). Temperature dependent XRD patterns have been taken over a wide temperature range of 15–300 K. The Rietveld refinements of these XRD patterns have been performed using the same monoclinic space group $P2_1/n$ down to 15 K. The refined XRD patterns of both 15 K and room temperature (300 K) are presented in figures 1(a) and (b) respectively. The obtained lattice constants, unit cell volume, and the Wyckoff positions of individual atoms are summarized in table 1 for $T = 15$ K data. Thermal variations of refined lattice parameters, a , b , c , β and V are shown in figures 1(c)–(g). An anomaly at around 104 K is observed in the temperature dependent lattice parameters, signifying a structural phase transition happens in SMCO (shape variation of hkl plane (-112) and (200) are presented from 90–110 K temperature range in the appendix). Due to possible very small changes in the position coordinates across the phase transition, the present Rietveld refinements cannot conclusively determine the true symmetry of low temperature phase. Such kinds of difficulties are not unusual when the lattice distortions are weak [39, 40]. This probably originates from exchange striction results from the lattice degrees of freedom. Such a scenario causes the magnetically interacting atoms to change their relative distance so that the system gains the magnetic energy in lieu of the elastic energy [41]. A careful analysis of the XRD data at 15 K shows the presence of antisite disorder in the system. The best fit is obtained for a disorder of 15% in the system. The peak corresponding to ordering is $2\theta = 10^\circ$. However, the crystal structure consists of alternating octahedral of Co and Ir along three crystallographic directions, as shown in inset of

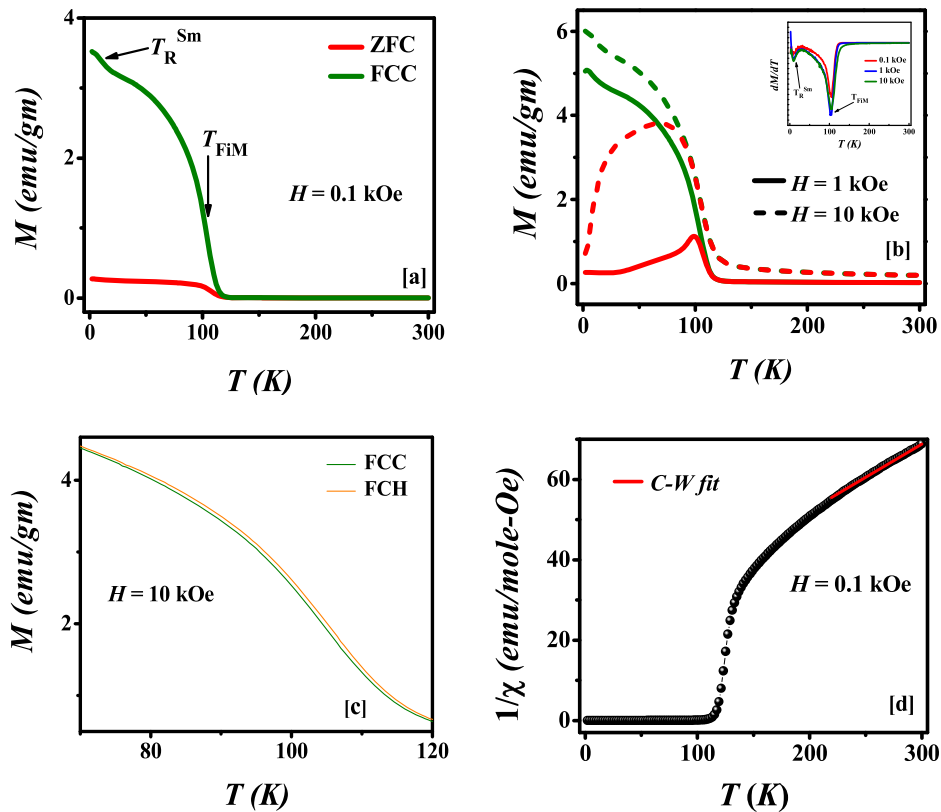


Figure 2. Temperature (T) dependent zero-field-cooled (ZFC: red) and field-cooled-cooling (FCC: green) magnetization (M) at various applied magnetic fields, $H =$ (a) 0.1 kOe (b) 1 kOe and 10 kOe (inset of (b) displays the first-order derivative spectra ($\frac{dM}{dT}$) of FCC $M(T)$ as a function of T for different H). (c) Variation of FCC and FCH data at $H = 10$ kOe in the temperature (T) interval 70–120 K. (d) The magnetic inverse susceptibility ($1/\chi$) as a function of temperature (T) under $H = 0.1$ kOe. Solid red line denotes Curie–Weiss (C–W) behavior at high temperature.

figure 1(a). The crystal structure also reveals that IrO_6 octahedra is connected with CoO_6 octahedra via corner sharing. These connectivities satisfy the Co–O–Ir bond angle $\sim 147.2^\circ$. In addition, we have also calculated the Goldschmidt tolerance factor (t) for this double perovskite compound, as it often gives an indication regarding the stability of crystalline phases. We obtain $t = 0.84$ for this double perovskite considering the ionic radius of $\text{Sm}^{3+} = 1.079 \text{ \AA}$, $\text{Co}^{2+} = 0.745 \text{ \AA}$, $\text{Ir}^{4+} = 0.625 \text{ \AA}$, and $\text{O}^{2-} = 1.40 \text{ \AA}$ [42]. It is well-known that the value $t \leq 0.96$ usually belongs to either orthorhombic or monoclinic structure [43], and the observed monoclinic structural model of SMCO is consistent with this t -value.

3.2. Magnetism

The thermal variations (2–300 K) of the dc magnetization (M) have been measured in the zero-field-cooled (ZFC), field-cool-cooling (FCC) and field-cool-heating (FCH) protocols under different applied magnetic fields. Figures 2(a) and (b) show the ZFC and FCC $M(T)$ data measured at external magnetic fields (H) = 0.1 kOe, 1 kOe, and 10 kOe. As the temperature decreases from room-temperature, both ZFC and FCC magnetizations increase slowly up to a particular temperature. A sudden jump in both ZFC and FCC magnetizations and a large contrast between them below this temperature

($T = 104$ K) indicate the onset of an FM-like ordering. Instead of T_C , we define this particular magnetic ordering temperature as T_{FiM} here, and the reason behind such preference is discussed later. With further decrease of temperature, FCC magnetization curve shows an extra anomaly around 10 K, which is attributed to the ordering (T_{R}^{Sm}) of RE Sm^{3+} spins. Both these magnetic transitions are clearly visible in the thermal variation of the first-order derivative of FCC magnetization ($\frac{dM}{dT}$) (see inset of figure 2(b)); however we observe very weak anomaly in the derivative spectra of ZFC magnetization at lower applied field due to ordering of RE ions, which is not shown here. In addition, we note that the shape of ZFC curve changes with increasing the external magnetic field. At lower applied field (say $H = 0.1$ kOe), no peak exists in the ZFC curve; while, a peak appears just below T_{FiM} for $H = 1$ kOe, which shifts to lower temperature and becomes broader with further increase of external magnetic field (in case of $H = 10$ kOe). This kind of characteristics of ZFC $M(T)$ peak is quite similar to that of the other double perovskite compound, such as $\text{Eu}_2\text{CoIrO}_6$ [35], in this series. Moreover, the bifurcation between ZFC and FCC magnetizations, along with a broad maximum in ZFC curve, signals the presence of large magnetocrystalline anisotropy in this compound.

A wide and thin hysteresis between the FCC and FCH data is observed around 104 K (110–120 K, slightly higher than

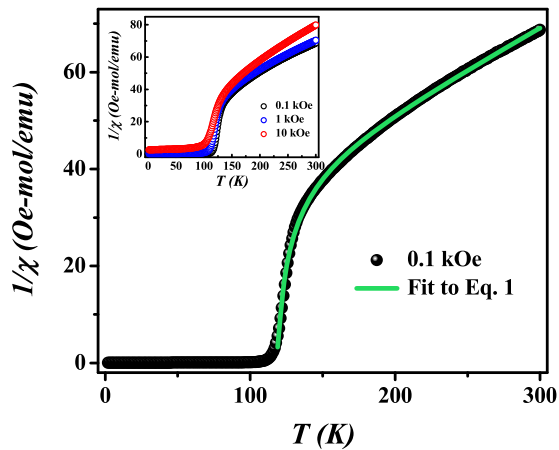


Figure 3. Green solid line suggests the agreement of the Néel's expression at high temperature. (Inset shows the inverse magnetic susceptibility $\{\chi^{-1}(T)\}$ as a function of temperature (T) for different applied magnetic field (H)).

the ordering temperature) (see figure 2(c)) for $H = 10$ kOe, which coincides with the anomaly of the temperature dependent refined lattice parameters (mentioned in section 3.1), signifying the phase transition. This similar kind of trend has been observed for $M(T)$ data measured at other external magnetic fields (H).

The effective magnetic moment of SMCO is calculated from the well-fitted $\chi^{-1}(T)$ data (using $H = 0.1$ kOe FCC data) by the Curie–Weiss (C–W) law, $\chi = C/(T - \theta)$ in the temperature range 230–300 K, where C is the Curie constant and θ is the C–W temperature (see figure 2(d)). The obtained effective magnetic moment (μ_{eff}) and C–W temperature (θ) from the fit are $6.95 \mu_{\text{B}}/\text{f.u.}$ and -117 K, respectively. The negative value of θ indicates the AFM interaction of the compound and is consistent with the Kanamori–Goodenough rule [15] as reflected by the Co–O–Ir bond angle (147.2° , as mentioned in the section 3.1). Since the theoretically calculated value ($\mu_{\text{Sm}}^{\text{theo}} = 0.84 \mu_{\text{B}}$, using $\mu_{\text{Sm}}^{\text{theo}} = g_{\text{Sm}} \sqrt{J_{\text{Sm}}(J_{\text{Sm}} + 1)}$ where g_{Sm} is the Landé g -factor) of effective moment of Sm^{3+} differs significantly from the experimentally observed value of $\mu_{\text{Sm}}^{\text{exp}} = 1.5 \mu_{\text{B}}$ [44], we consider $\mu_{\text{Sm}} = 1.5 \mu_{\text{B}}$, $\mu_{\text{Co}} = 4.8 \mu_{\text{B}}$ (for high-spin Co^{2+} in related double perovskites [35]), and $\mu_{\text{Ir}} = 1.4 \mu_{\text{B}}$ (taking the maximum value in these Ir-based double perovskites [35]) to calculate the expected effective moment of SMCO using the relation $\mu_{\text{eff}} = \sqrt{2\mu_{\text{Sm}}^2 + \mu_{\text{Co}}^2 + \mu_{\text{Ir}}^2}$. The calculated value of $5.43 \mu_{\text{B}}/\text{f.u.}$ is lower than the value obtained experimentally; though, the exact reason is unclear. However, we predict that the large difference between the experimental and theoretical effective moment values might be related to the canted AFM spin states associated with Dzyaloshinskii–Moriya interaction. We also believe that the C–W fitting to $\chi^{-1}(T)$ data for much higher magnetic field would provide better approximation of the theoretical μ_{eff} value.

To investigate the nature of magnetism in this double perovskite and its magnetic ground state, we plot the thermal variation of inverse dc susceptibility $\chi^{-1}(T)$ using $H = 0.1$ kOe FC magnetization data in figure 3. The $\chi^{-1}(T)$ exhibits true paramagnetic nature, and follows conventional C–W behaviour above 225 K. Below this temperature, $\chi^{-1}(T)$ significantly

deviates from C–W behaviour, and shows a sharp downturn (stair-like) before reaching the ordering temperature. This kind of stair-like feature in $\chi^{-1}(T)$, just above the ordering temperature, is often suggested the presence of Griffith's phase, and characterized by the short-range FM clustering due to competing magnetic interactions [45, 46]; however, almost field-independent behaviour of this stair-like feature (remains intact even at higher external applied field, see inset of figure 3) rules out the possibility of formation of Griffith's phase in the vicinity of magnetic ordering temperature. It is important to note that $\chi^{-1}(T)$ shows hyperbolic-kind of variation around the magnetic phase transition, which is in sharp contrast to the typical characteristic of FM materials. Nevertheless, the hyperbolic behaviour of $\chi^{-1}(T)$ above the onset of magnetic ordering is a distinctive of FiM materials, and can be analyzed by Néel's equation [47],

$$\chi^{-1}(T) = \frac{T - \Theta}{C} - \frac{\xi}{T - \Theta'}, \quad (1)$$

where the first term symbolizes simple C–W behaviour at high-temperature region, and last term is responsible for hyperbolic behaviour near FiM ordering [48, 49]. Here, Θ' and ξ are the fitting parameters, and their origins have been described in the two sub-lattice model of FiM [49]. The green solid line in figure 3 is the fitted curve to $\chi^{-1}(T)$ according to equation (1), and an exact fit thus establishes the FiM ordering around $T = 104$ K in this compound. The obtained parameters from this fitting are as follows, $C = 5.17 \text{ emu K mole}^{-1} \text{ Oe}^{-1}$, $\Theta = -137.55 \text{ K}$, $\Theta' = 109.84 \text{ K}$, and $\xi = 350.77 \text{ mole K emu}^{-1} \text{ Oe}^{-1}$. The FiM ordering in this compound mainly originates from the AFM coupling between the canted Co^{2+} and Ir^{4+} spins, as predicted for other compounds $\text{Ln}_2\text{CoIrO}_6$ ($\text{Ln} = \text{La}$, [28, 30] Eu , Tb , and Ho [35]) in this series. The ZFC isothermal magnetization $M(H)$ curves at various temperatures for SMCO are displayed in figure 4(a). The $M(H)$ curves at $T = 150$ K and 120 K do not show any hysteretic behaviour, and magnetization linearly increases with increasing field, implying the true paramagnetic state of the sample. With the decrease of temperature from 120 K to 110 K, the shape of the $M(H)$ curve slightly changes; while, the $M(H)$ curve at $T = 100$ K reveals thin hysteresis loop, and the magnetization starts to show linear field dependency from $H \geq 5$ kOe, thus indicating a typical FiM ground state. From figure 4(a), it is clear that the $M(H)$ curves show well-defined hysteresis loop as the temperature further decreases below 100 K, and the coercive field (H_C) and the remanent magnetization continuously increase with decreasing temperature. From the isothermal $M(H)$ curves measured at different temperatures, the estimated values of H_C are plotted as a function of temperature in figure 4(b), which clearly shows a sudden change in slope near the onset of FiM ordering, and H_C gradually increases with decreasing temperature below FiM ordering temperature and reaches the maximum value at $T = 2$ K. The strong linear field dependence of magnetization beyond the FiM hysteresis can be attributed to the gradual field alignment of the canted Co^{2+} and Ir^{4+} moments [35], and as a result, $M(H)$ curves do not show any sign of saturation at $H = 70$ kOe. It is worthwhile to mention that M does not saturate even up to 60 T

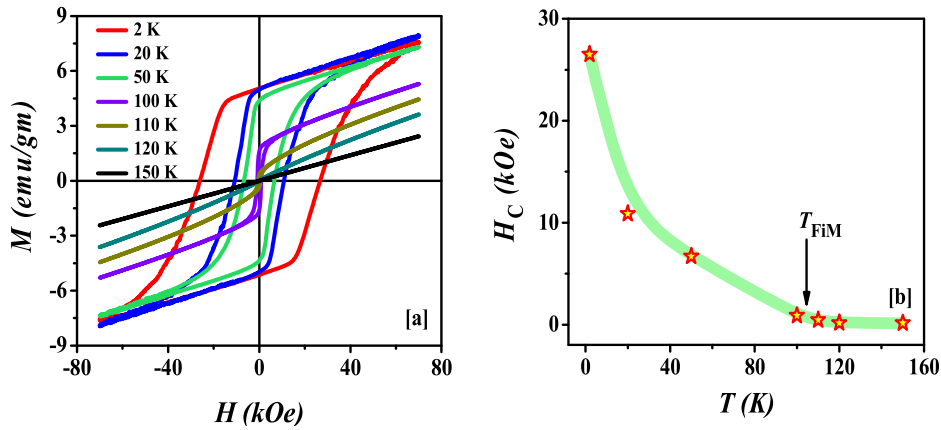


Figure 4. (a) Magnetization (M) vs Magnetic Field (H) loop ranging from -70 to 70 kOe at various temperatures, (b) temperature (T) dependence of obtained coercive field (H_C) from ZFC $M(H)$ loops.

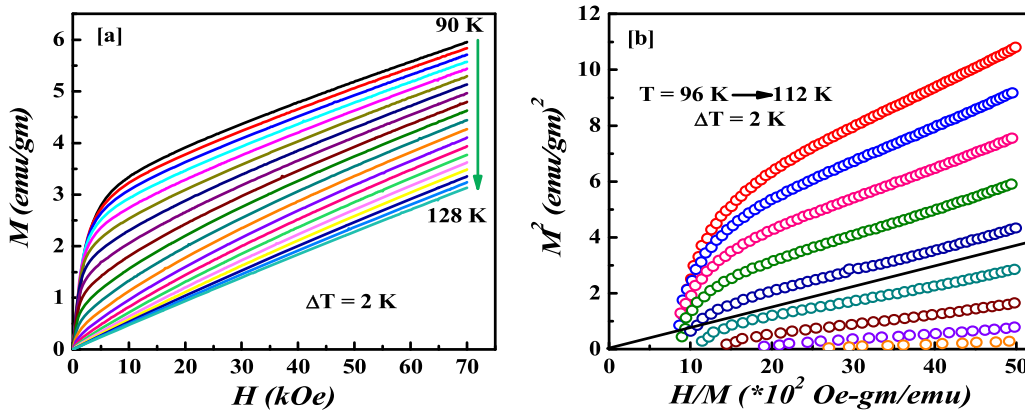


Figure 5. (a) M vs H isotherm (Virgin curve) around T_{FiM} , from temperature (T) between 90 and 128 K at the interval of 2 K. (b) Basic Arrott plots constructed from M - H data.

magnetic field (varies linearly with field) in similar Ir-based double perovskite materials [35].

To understand the nature of magnetic phase transition in-depth, we have carried out isothermal magnetization measurements in the vicinity of PM-FiM transition. Figure 5(a) shows a series of initial $M(H)$ isotherms (virgin legs) in between 90 – 128 K at an interval $\Delta T = 2$ K, showing a gradual change between PM and FiM states. However, it is advantageous to use the conventional Arrott plot (M^2 vs H/M) method [50] to determine the order of phase transition. Figure 5(b) displays the Arrott plot for this compound in between 96 – 112 K. The positive slope of M^2 vs H/M isotherms indicates that the PM-FiM phase transition in this compound is second order, which is in accordance with the Banerjee criteria [51]. Furthermore, according to the mean-field theory, M^2 vs H/M isotherms at different temperatures should manifest a set of parallel straight lines near the magnetic phase transition, and the line at $T = T_{\text{FiM}}$ must traverse the origin. In contrast, a non-linear variation of M^2 vs H/M curves has been found for SMCO, exhibiting a significant downward curvature at low-field region possibly due to the mutually misaligned magnetic domains [52]; while, the high-field linear portions show clear divergence. Hence, the mean-field theory fails to interpret the observed phase transi-

tion in SMCO, indicating the presence of critical fluctuations. Therefore modified Arrott plot method may be a good option to analyze the criticality [53].

The MCE has been investigated in order to understand the isothermal magnetic entropy change ΔS_M of the magnetic material when it is subjected to a changing external magnetic field, and to explore the possible applications in magnetic refrigeration technology. Besides the direct measurement through calorimetry method, it is well-established that ΔS_M can be calculated indirectly from magnetization measurements using Maxwell’s thermodynamic relation:

$$\Delta S_M = \int_0^H \left(\frac{\partial M(T, H)}{\partial T} \right) dH.$$

It is found that $-\Delta S_M$ reaches a maximum value around the magnetic ordering temperature, T_{FiM} at each field, where the value of $-\Delta S_M$ has been calculated from the isothermal $M(H)$ virgin curves of figure 5(a). The temperature and field dependence of $-\Delta S_M$ for SMCO is displayed in figure 6 through a three-dimensional surface plot. The magnitude of $-\Delta S_M$ increases with increasing field, and the maximum value of $-\Delta S_M$ is found to be $0.716 \text{ J kg}^{-1} \text{ K}^{-1}$ at $H = 70$ kOe, which

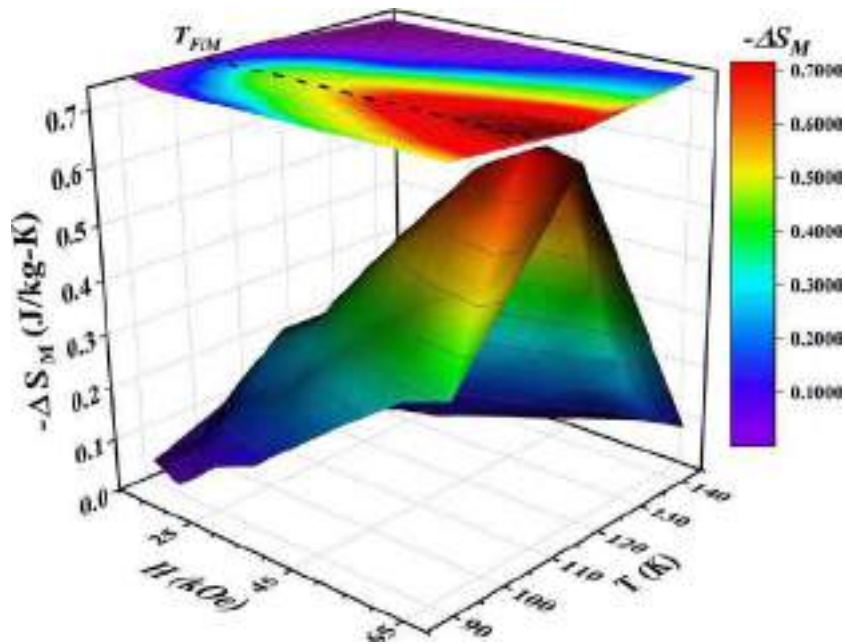


Figure 6. Thermal profile of field induced magnetic entropy change ($-\Delta S_M$) under the applied field changing from 10–70 kOe.

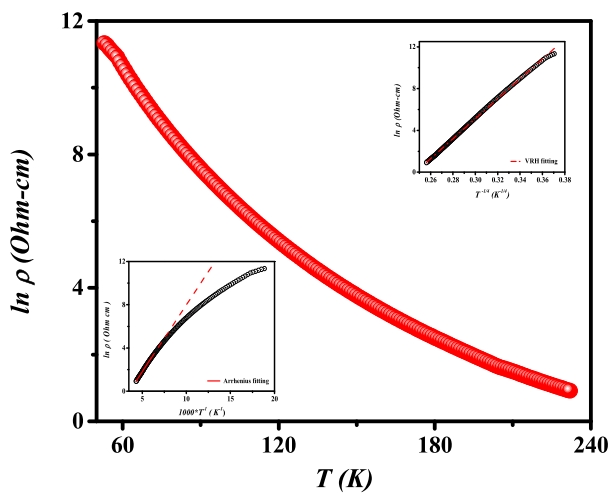


Figure 7. Temperature (T) dependence of resistivity (ρ) for SMCO. Upper and lower insets show the fitting results using VRH and Arrhenius model respectively.

is slightly higher than that of the value reported for $\text{Eu}_2\text{CoIrO}_6$ at $H = 8 \text{ T}$ [35]. A colour map of the $-\Delta S_M$ as a function of temperature, T , and magnetic field, H is also projected at the top of figure 6, where clear indications of the maximum value of $-\Delta S_M$ for all fields are found around at T_{FIM} .

In addition, the value of relative cooling power (RCP), which represents the refrigerant capacity of a magnetic material, can be evaluated for SMCO using the relation [54]:

$$\text{RCP} = -\Delta S_M^{\text{max}} \times \delta T_{\text{FWHM}},$$

where first and second terms denote the maximum value of magnetic entropy ($-\Delta S_M$) and the full-width at half-

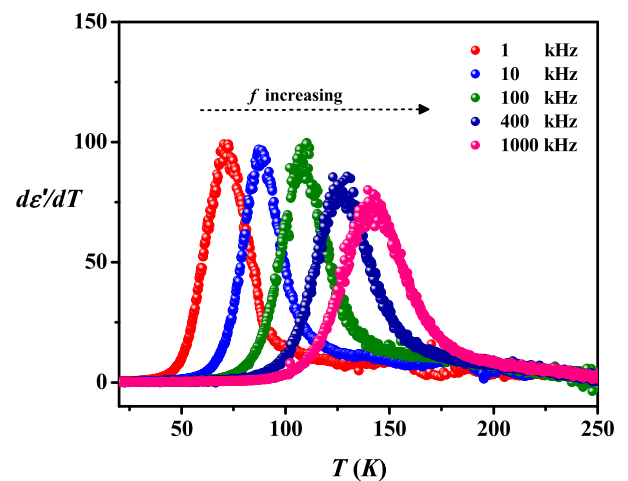


Figure 8. Thermal variation of first-order derivative of ϵ' with temperature (T) for different frequencies (f).

maximum of $-\Delta S_M$ peak at a particular magnetic field, respectively. RCP values are found to be 12.5 J kg^{-1} and 30 J kg^{-1} for $H = 10 \text{ kOe}$ and 70 kOe , respectively, showing a gradual increase with increasing external magnetic field.

3.3. Resistivity

The temperature dependent resistivity $\rho(T)$ measurement in the range 50–230 K (figure 7) shows that SMCO is an insulator, possibly due to large separation between the B-site cations, as also seen in nearly all double perovskites [55]. From Arrhenius fit (using the equation $\rho = \rho_0 \exp(E_a/k_B T)$) in the temperature interval 165–230 K, an activation energy of $E_a \sim 100 \text{ meV}$ is estimated from the slope of $\ln \rho$ ver-

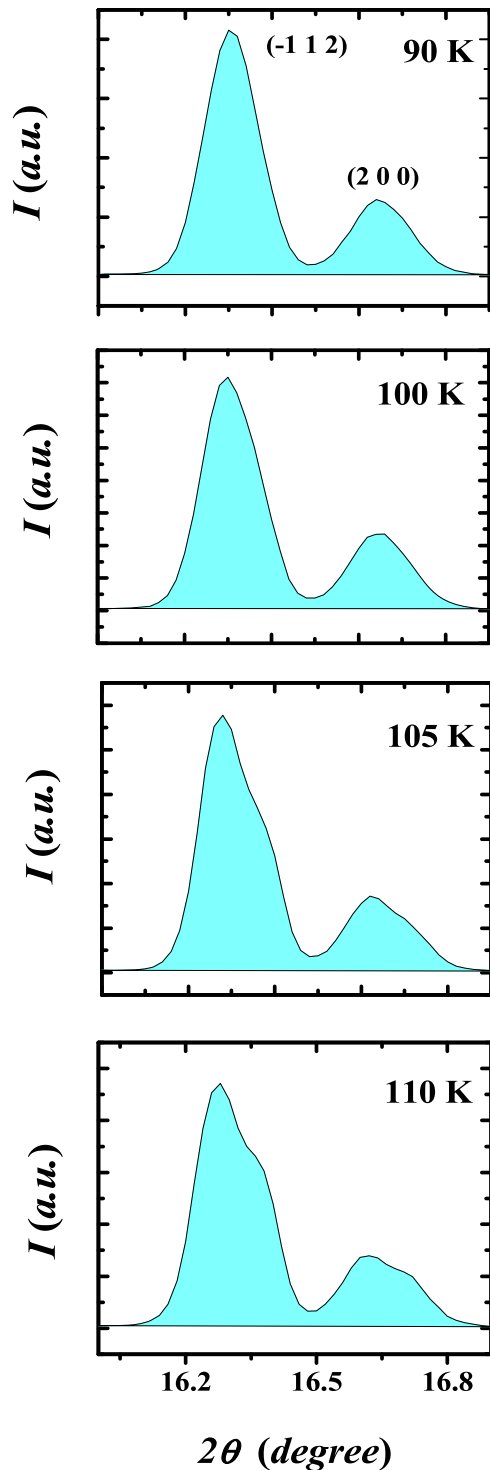


Figure 9. Plot of (-112) and (200) peak in the Intensity (I) vs 2θ plot from 90–110 K temperature range.

sus $(k_B T)^{-1}$ curve (lower inset of figure 7), which is worthy of comparison with other strongly insulating Ir-based oxides [56–58]. It is clear that linear fitting to the data in figure 7 deviates above 165 K, and hence, prompts us to understand the electrical conduction mechanism through other models. However, the linear dependence of $\ln \rho$ on $T^{-1/4}$ throughout the temperature range (50–230 K) indicates that Mott VRH

($\rho = \rho_0 \exp(T_0/T)^{1/4}$ in three-dimension) is the possible conduction mechanism in this compound (see upper inset of figure 7). Obtained parameters from VRH fitting are $\rho_0 \sim 6.22 \times 10^{-11} \Omega \text{ cm}$ and Mott characteristic temperature $T_0 \sim 83 \times 10^6 \text{ K}$.

3.4. Dielectric behaviour

Recently, our group has reported [59] the dielectric and impedance property of SMCO. No anomaly (or, peak) has been observed in ϵ' vs T spectra around the magnetic ordering temperature T_{FiM} , and ϵ' almost attains a constant value above 250 K. It is to be mentioned that the peak in thermal variation of first-order derivative of ϵ' with respect to temperature ($d\epsilon'/dT$) spectra for $f = 1 \text{ kHz}$ is centered around 70 K, which is well below the magnetic ordering temperature; whereas, this peak is positioned at 88 K (still below the T_{FiM}) for $f = 10 \text{ kHz}$ data (see in figure 8). Thus, the step-like features in ϵ' vs T spectra do not have any magnetic origin, implying the absence of significant magneto-dielectric coupling in this particular double perovskite.

4. Conclusions

In summary, we have successfully synthesized the mixed $3d-5d-4f$ double perovskite compound SMCO in polycrystalline form, and investigated the structural, magnetic and transport properties. SMCO crystallizes in the monoclinic structure with space group $P2_1/n$, and shows FiM order below $T_{\text{FiM}} = 104 \text{ K}$, likely arising from the AFM coupling between Co^{2+} and Ir^{4+} sub-lattices. A second magnetic transition is observed in $M(T)$ data around 10 K, which is associated with the ordering of RE Sm^{3+} spins. A moderate MCE is found around FiM transition, having maximum RCP value of 30 J kg^{-1} for $H = 70 \text{ kOe}$. Smaller magnetic moment of Sm^{3+} ion, $\mu(\text{Sm}) = 0.85 \mu_B$, directly gives negligible contribution to the overall magnetic coupling between $3d-5d-4f$ systems, in comparison with other compounds containing more f electrons. In general, crystalline anisotropy controls the spin configuration of $3d-5d$ sub-lattices at high temperature in case of oxide materials. However, the interaction of the d -sublattices and RE moments becomes significant at low temperature, which perhaps overcomes crystalline anisotropy forces and induces spin-reorientation, as observed in case of $\text{Ln}(\text{Tb, Ho})_2\text{CoIrO}_6$ double perovskites. In contrast, due to the presence of weak $f-d$ interaction between Co–Ir sublattices and Sm^{3+} moments (small moments) and large magneto-crystalline anisotropy, we probably have not seen any spin-reorientation phenomenon in this compound. So, eventually, Sm moments have significant role in determining the magnetic properties and behaviour of SMCO compound, although it has small moment. Electrical resistivity measurements suggest the insulating behaviour of the sample, in which Mott VRH conduction mechanism is detected. At the same time temperature dependent dielectric measurements of this as studied sample suggests it is not related to magnetic ordering. We hope our results will inspire more investigations of theoretical calculations, as well as experimental studies employing doping elements.

Acknowledgments

One of the authors, SKP, is thankful to Department of Science and Technology, Government of India for providing DST INSPIRE Fellowship (IF150147) and IACS during the tenure of work. RAS is thankful to CSIR, India and IACS for supporting fellowship. RD is thankful to SERB for providing fellowship during the tenure of the work. This work is funded by the Science and Engineering Research Board, Government of India, File No. EMR/2016/005437. Authors thank UGC-DAE Kolkata Centre for providing the dielectric measurement facility. Authors also thank the Department of Science and Technology, India for the financial support during the experiments at the Indian Beamline, PF, KEK, Japan, and Proposal No. 2018-IB-30.

Data availability statement

All data that support the findings of this study are included within the article (and any supplementary files).

Appendix

Figure 9 shows the modulation of (-112) and (200) hkl plane within temperature (T) range 90–110 K of SMCO. -112 plane is the most intense in the XRD data throughout the temperature scan. After 100 K; from the 105 K data the peak shapes are changed, justifies the structural phase transition happens in the as studied sample.

ORCID iDs

Subham Majumdar  <https://orcid.org/0000-0001-6136-1588>

Subodh Kumar De  <https://orcid.org/0000-0002-6385-3129>

References

- [1] Kim B J, Ohsumi H, Komesu T, Sakai S, Morita T, Takagi H and Arima T 2009 *Science* **323** 1329–32
- [2] Kobayashi K-I, Kimura T, Sawada H, Terakura K and Tokura Y 1998 *Nature* **395** 677–80
- [3] Kato H, Okuda T, Okimoto Y, Tomioka Y, Takenoya Y, Ohkubo A, Kawasaki M and Tokura Y 2002 *Appl. Phys. Lett.* **81** 328–30
- [4] Krockenberger Y *et al* 2007 *Phys. Rev. B* **75** 020404
- [5] Aréval-López A M, McNally G M and Attfield J P 2015 *Angew. Chem., Int. Ed.* **54** 12074–7
- [6] Feng H L *et al* 2016 *Phys. Rev. B* **94** 235158
- [7] Sakai M, Masuno A, Kan D, Hashisaka M, Takata K, Azuma M, Takano M and Shimakawa Y 2007 *Appl. Phys. Lett.* **90** 072903
- [8] Yáñez-Vilar S *et al* 2011 *Phys. Rev. B* **84** 134427
- [9] Moon J Y, Kim M K, Choi Y J and Lee N 2017 *Sci. Rep.* **7** 16099
- [10] Moon J Y, Kim M K, Oh D G, Kim J H, Shin H J, Choi Y J and Lee N 2018 *Phys. Rev. B* **98** 174424
- [11] Feng H L, Adler P, Reehuis M, Schnelle W, Pattison P, Hoser A, Felser C and Jansen M 2017 *Chem. Mater.* **29** 886–95
- [12] Feng H L, Reehuis M, Adler P, Hu Z, Nicklas M, Hoser A, Weng S-C, Felser C and Jansen M 2018 *Phys. Rev. B* **97** 184407
- [13] Anderson P W 1950 *Phys. Rev.* **79** 350–6
- [14] Goodenough J B 1955 *Phys. Rev.* **100** 564–73
- [15] Kanamori J 1959 *J. Phys. Chem. Solids* **10** 87–98
- [16] Campbell I A 1972 *J. Phys. F: Met. Phys.* **2** L47–50
- [17] Cao G, Qi T F, Li L, Terzic J, Yuan S J, DeLong L E, Murthy G and Kaul R K 2014 *Phys. Rev. Lett.* **112** 056402
- [18] Dey T *et al* 2016 *Phys. Rev. B* **93** 014434
- [19] Corredor L T *et al* 2017 *Phys. Rev. B* **95** 064418
- [20] Kayser P, Kennedy B J, Ranjbar B, Kimpton J A and Avdeev M 2017 *Inorg. Chem.* **56** 2204–9
- [21] Terzic J, Zheng H, Ye F, Zhao H D, Schlottmann P, DeLong L E, Yuan S J and Cao G 2017 *Phys. Rev. B* **96** 064436
- [22] Kim B J *et al* 2008 *Phys. Rev. Lett.* **101** 076402
- [23] Demazeau G, Siberchicot B, Matar S, Gayet C and Largeteau A 1994 *J. Appl. Phys.* **75** 4617–20
- [24] Powell A V, Gore J G and Battle P D 1993 *J. Alloys Compd.* **201** 73–84
- [25] Currie R C, Vente J F, Frikkee E and Ijdo D J W 1995 *J. Solid State Chem.* **116** 199–204
- [26] Uhl M, Matar S F and Siberchicot B 1998 *J. Magn. Magn. Mater.* **187** 201–9
- [27] Narayanan N, Mikhailova D, Senyshyn D, Trots D M, Laskowski R, Blaha P, Schwarz K, Fuess H and Ehrenberg H 2010 *Phys. Rev. B* **82** 024403
- [28] Kolchinskaya A *et al* 2012 *Phys. Rev. B* **85** 224422
- [29] Manna K *et al* 2016 *Phys. Rev. B* **94** 144437
- [30] Iakovleva M *et al* 2018 *Phys. Rev. B* **98** 174401
- [31] Pradhan S K, Dalal B, Kumar R, Majumdar S and De S K 2020 *J. Phys.: Condens. Matter* **32** 305803
- [32] Cao G *et al* 2013 *Phys. Rev. B* **87** 155136
- [33] Song J, Zhao B, Yin L, Qin Y, Zhou J, Wang D, Song W and Sun Y 2017 *Dalton Trans.* **46** 11691–7
- [34] Ferreira T, Morrison G, Yeon J and Zur Loye H-C 2016 *Cryst. Growth Des.* **16** 2795–803
- [35] Ding X, Gao B, Krenkel E, Dawson C, Eckert J C, Cheong S-W and Zapf V 2019 *Phys. Rev. B* **99** 014438
- [36] Rietveld H M 1969 *J. Appl. Crystallogr.* **2** 65–71
- [37] Rodríguez-Carvajal J 1993 *Physica B* **192** 55–69
- [38] Momma K and Izumi F 2011 *J. Appl. Crystallogr.* **44** 1272–6
- [39] Saha R A, Halder A, Saha-Dasgupta T, Fu D, Itoh M and Ray S 2020 *Phys. Rev. B* **101** 180406
- [40] Basu T *et al* 2014 *Sci. Rep.* **4** 5636
- [41] Strässle T, Juranyi F, Schneider M, Janssen S, Furrer A, Krämer K W and Güdel H U 2004 *Phys. Rev. Lett.* **92** 257202
- [42] Shannon R D 1976 *Acta Crystallogr. A* **32** 751
- [43] Philipp J B *et al* 2003 *Phys. Rev. B* **68** 144431
- [44] Kittel C 1976 *Introduction to Solid State Physics* (New York: Wiley)
- [45] Dalal B, Sarkar B and De S K 2016 *J. Alloys Compd.* **667** 248–54
- [46] Pathak A K, Paudyal D, Jayasekara W T, Calder S, Kreyssig A, Goldman A I, Gschneidner K A Jr and Pecharsky V K 2014 *Phys. Rev. B* **89** 224411
- [47] Néel M L 1948 *Ann. Phys., NY* **12** 137
- [48] Winkler E, Blanco Canosa S, Rivadulla F, López-Quintela M A, Rivas J, Caneiro A, Causa M T and Tovar M 2009 *Phys. Rev. B* **80** 104418
- [49] Dalal B, Sarkar B, Rayaprol S, Das M, Siruguri V, Mandal P and De S K 2020 *Phys. Rev. B* **101** 144418
- [50] Arrott A 1957 *Phys. Rev.* **108** 1394–6
- [51] Banerjee B K 1964 *Phys. Lett.* **12** 16–7
- [52] Aharoni A 1971 *Introduction to the Theory of Ferromagnetism* (New York: Oxford University Press)
- [53] Arrott A and Noakes J E 1967 *Phys. Rev. Lett.* **19** 786–9
- [54] Pecharsky V K, Gschneidner K A and Tsokol A O 2005 *Rep. Prog. Phys.* **68** 1479
- [55] Vasala S and Karppinen M 2015 *Prog. Solid State Chem.* **43** 1–36

- [56] Okabe H *et al* 2011 *Phys. Rev. B* **83** 155118
- [57] Singh Y, Manni S, Reuther J, Berlijn T, Thomale R, Ku W, Trebst S and Gegenwart P 2012 *Phys. Rev. Lett.* **108** 127203
- [58] Krajewska A, Takayama T, Dinnebier R, Yaresko A, Ishii K, Isobe M and Takagi H 2020 *Phys. Rev. B* **101** 121101
- [59] Datta R, Pradhan S K, Chatterjee S, Majumdar S and De S K 2021 *J. Alloys Compd.* **876** 160158

Cyanobacteria of the Indian Sundarbans: A Potential Source of Powerful Therapeutic Agents

Shayontani Basu¹, Veerabadhran Maruthanayagam¹, Sandeep Chakraborty¹, Arnab Pramanik², Anushree Achari³, Dr. Parasuraman Jaisankar³, Dr. Joydeep Mukherjee*¹

¹School of Environmental Studies, Jadavpur University, Kolkata 700032, India,

²Department of Biochemistry, University of Calcutta, 35, Ballygunge Circular Road, Kolkata 700 019,

³India Indian Institute of Chemical Biology, Kolkata- 700032, India

Abstract:

Mangrove forests occupy the estuarine ecotone and harbor a wide range of microorganisms along with a rich diversity of flora and fauna. Marine and estuarine organisms are known to produce unique molecules due to the aggressive, exigent, and competitive surroundings that are unlike those produced in the terrestrial environment. Marine cyanobacteria are a vast resource for new bioactive natural products useful in the development of therapeutics. The Sundarbans mangrove ecosystem harbours various unique microorganisms having different interesting properties. Discovery of a unique alkaline serine protease enzyme tolerant to bleach, detergent, high salt concentration and solvent, isolation and identification of obligately halophilic, euryhaline novel cyanobacteria from intertidal soil surface of the Sundarbans and identification of a pair of novel *Streptomyces* represent a few of the ongoing endeavors undertaken to explore the mostly untapped microbial diversity of the Sundarbans. This study focuses on two novel strains of cyanobacteria isolated from the intertidal soil surface biofilm of the Indian Sundarbans, which were cultivated on a large scale to yield a significant quantity of biomass for the extraction of secondary metabolites. The cyanobacterial biomass was extracted with a range of polar and non-polar solvents and the ethyl acetate fractions showed significant anti-angiogenic activity when tested against sunitinib (a protein kinase inhibitor). The extracts also showed significantly greater anti-inflammatory activity compared to dexamethasone, which has been shown to reduce the 28 day mortality rate of patients affected by COVID-19.

Keywords: Halophilic cyanobacteria, Indian Sundarbans, anti-inflammatory activity, anti-angiogenic activity.

Introduction

Modern day trends in drug discovery from natural sources stress the investigation of marine environment to yield numerous biologically active compounds many of which are antimicrobial in nature (Burja et al., 2001). The intertidal areas considered as interfaces of the ocean, atmosphere, and terrestrial environments harbour diverse microbial biofilm communities that are subjected to fluctuations in metal ion concentrations, temperature, desiccation, UV irradiation, and wave activities. The organisms in intertidal zones essentially spend part of their lives in extreme, arid conditions during emersion and half of their lives in stable, benign seawater. These conditions lead to the development of unique and specific characteristics of the inhabiting organisms (Zhang et al., 2013). These ecosystems experience tidal flooding, which causes environmental factors such as salinity and nutrient availability to be highly variable resulting in unique and specific characteristics of the inhabiting

organisms. The microbiome is one of the important communities of the mangrove ecosystem as the abundance of carbon and other nutrients sustains a large number of microbial communities which are adapted to the brackish and fluctuating environmental conditions (Pramanik et al., 2011). Marine cyanobacteria are a vast resource for new bioactive natural products useful in basic research, biomedical sciences, and the development of therapeutics (Gogineni et al., 2018).

Natural products of pharmacological importance derived from cyanobacteria

Cyanobacterial natural products are grouped according to their biosynthetic origins such as polyketides, cyanopeptides, alkaloids, isoprenoids and other metabolites. While major research has been towards investigating toxicity, many studies have shown cyanobacteria to produce compounds that are of pharmaceutical and biotechnological interest. Cyanobacterial compounds comprise 40% lipopeptides, 5.6% amino acids, 4.2% fatty acids, 4.2% macrolides and 9% amides. Most of the bioactivity shown by cyanobacteria tends to be from lipopeptides like cytotoxic (41%), antitumor (13%), antiviral (4%), antibiotics (12%) and the remaining 18% include anti-malarial, antimycotics, multi-drug resistance reversing agents, herbicides and immunosuppressive agents. A major part of cyanobacterial secondary metabolites are peptides or possess peptidic structures. Many important classes of cancer cell toxins with apoptotic properties have been characterized from marine cyanobacteria over the past years. Effects of cyclic peptides as anticancer agent with multitude targets have been reviewed. *Lyngbya majuscula* among other cyanobacterial genera collected from various coastal and deep-sea regions of the marine environment worldwide has proved to be one of the main sources for the production of natural products with anti-tumor and anti-cancer properties, regardless of their geographical distribution (Nagarajan et al., 2012). Many of the secondary metabolites secreted by cyanobacteria were found active against different mammalian cancer cell lines. Some important compounds isolated from cyanobacteria that target cancers are given as follows: colon cancers are targeted by minutissamides, microcystilide A, laxaphycins, cylindrocyclophanes and bauerines A-C while breast cancers are targeted by carbamidocyclophanes, dendroamide, hapalosin and tolyporphins; lung cancer is targeted by pahayokolide A; and prostate cancer by tychonamide. A few secondary metabolites isolated from cyanobacteria were shown to have profound activity against certain parasites causing deadly diseases. A compound isolated from freshwater cyanobacterium *Nostoc* displayed antiprotozoal activity against *Trypanosoma* and *Leishmania* and significant toxicity to malaria parasite. Pharmacologically important metabolites have been isolated from marine benthic and planktonic cyanobacteria that inhibit growth of severe bacterial, fungal and protozoal pathogens. Studying active concentration, active modules and mechanism of action of bioproducts on both prokaryotic and eukaryotic pathogens and/or parasites will help in their selection for clinical evaluation. A class of antifungal lipopeptides known as lobocyclamides were isolated from marine cyanobacterium *L. confervoides* collected from Cay Lobos, Bahamas (Nagarajan et al., 2012; Raja et al., 2016). Freshwater and terrestrial cyanobacteria are also proven to have the potential to produce compounds displaying cytotoxic, protease inhibiting and growth controlling properties on parasites, pathogens and harmful algae. Further studies on these metabolites may make synthesis of drugs containing the bioactive key components possible. Thus, a new vista may

open towards the treatment of life-threatening diseases (Nagarajan et al., 2012). Despite the wide range of natural products found in cyanobacteria, exploitation of these products is still not widespread.

Studies on the cyanobacteria of the Indian Sundarbans

The Sundarbans mangrove ecosystem harbours various unique cyanobacteria having pharmacologically important properties. Isolation and subsequent identification of obligately halophilic, euryhaline novel cyanobacteria from intertidal soil surface of the Sundarbans (Pramanik et al., 2011) represents one of the endeavors undertaken to explore the vastly unexplored microbial diversity of the Indian Sundarbans, under the guidance of Dr. J. Mukherjee (School of Environmental Studies, Jadavpur University). Based on morphological characteristics, six of the isolated cyanobacteria were assigned to the *Lyngbya-Phormidium-Plectonema* (LPP) group B, and one each was assigned to *Oscillatoria* and *Synechocystis* genera. A polyphasic approach-based taxonomic characterisation was performed for the cyanobacteria, which led to the discovery of four novel strains, out of which two are a novel species *O. aestuarii* belonging to the genus *Oxynema*. Cross walls in the apical portion of cells of the strains AP17 and AP24 were absent while the same were present in CCALA960. Additionally, optimal growth of AP17 and AP24 was recorded at 5–8% salinity and salinity above 14% inhibited growth of both strains, which were isolated from the intertidal soil surface; whereas *O. thaianum* CCALA960 which was found in a hypersaline environment could grow at 40% salinity. Differences between the internal transcribed spacer (ITS) sequences of the two strains isolated from the Indian Sundarbans and the reference strain included the insertion of 9 nucleotides in the D2 with spacer region, insertion of 2 nucleotides in the pre Box B spacer region, deletion of 2 nucleotides in the post Box B spacer region, deletion of 8 nucleotides in the D4 region, deletion of 8 nucleotides in V3 region and insertion of 2 nucleotides in the D5 region of the ITS sequences of AP17 and AP24, which were observed in comparison to the analogous regions of CCALA960. Structural details of Box B helices of AP17 and AP24 revealed that though their lengths were identical with that of the reference strain, their sequences were completely different from CCALA960. Four nucleotide substitutions were present in different positions in the Box B helix of *O. thaianum* CCALA960. Secondary structures of the V3 regions of both AP17 and AP24 (containing 51 nucleotides) showed a small terminal bulge and a bigger bilateral bulge while the analogous structure of *O. thaianum* CCALA 960 (comprising of 59 nucleotides) showed one additional bilateral bulge in comparison to AP17 and AP24. Therefore, based on morphological, ecological and molecular differences in comparison to *O. thaianum* CCALA960, isolates AP17 and AP24 were proposed to be members of a second novel species in the *Oxynema* genus, for which the name *Oxynema aestuarii* sp. nov. has been proposed (Chakraborty et al., 2018). The other two strains AP9F and AP25 are monophyletic taxa designated as *Euryhalinamamangrovii* and *Leptoelongatuslitoralis* (gen. nov., sp. nov.). The cells of AP9F and AP25 were highly elongated whereas the cells of the reference strains (*Leptolyngbya boryana* and *Nodosilinea nodulosa*) were occasionally elongated to isodiametrical. Terminal cells of AP9F and AP25 appeared as flattened corners (as opposed to rounded), which was different from the cell structure of other

Leptolyngbyaceae members. 16S rRNA gene sequences of AP9F (1366 bp) and AP25 (1408 bp) showed 95% and 92% similarities respectively with the non-redundant (nr) nucleotide sequences of their closest relatives of the *Leptolyngbya* genus. Test strains occupied a clade in the phylogenetic tree that was different from the ones containing the type species. A single operon containing both tRNA^{ile} and tRNA^{ala} genes were present in the ITS regions of AP9F and AP25 as compared to the presence of two operons in the ITS region of the reference genera *Leptolyngbya* and *Nodosilinea*: one in which both tRNA^{ile} and tRNA^{ala} genes are present and the other lacking both the genes. The secondary structures of the traditionally conservative D-stem region as well as the Box B helix and V3 regions of the ITS operons showed significant variation between the test strains and also when compared with the corresponding sequences of *L. boryana* and *N. nodulosa*. Molecular, phylogenetic and morphological data suggested AP9F and AP25 to be monophyletic taxa for which the names *Euryhalinemamangrovii* gen. nov., sp. nov. and *Leptoelongatuslitoralis* gen. nov., sp. nov. were proposed respectively (Chakraborty et al., 2019). Thus, the strains AP17, AP24, AP9F and AP25 isolated from the Sagar Island and Lothian Island of the Indian Sundarbans differed from the reference strains (*Oxynemathaiianum* CCALA960 for *Oxynemaestuariae*, *Leptolyngbyaboryana*, and *Nodosilineanodulosa* for *Euryhalinemamangrovii* and *Leptoelongatuslitoralis*) in terms of morphology, ecology and 16S- 23S ITS sequences (Chakraborty et al., 2018, Chakraborty et al., 2019). The aforementioned novel strains have been deposited and cryopreserved in the Microbial Culture Collection (MCC), India having accession numbers MCC 3874 (AP17), MCC 3873 (AP24), MCC 3171 (AP9F) and MCC 3170 (AP25).

Material and methods

Cyanobacterial isolates were established by aseptic collection of cyanobacterial soil surface biofilm, inoculation in artificial sea nutrient (ASN-III) medium, and subsequent incubation in fluorescent irradiance maintaining a 12-h:12-h light:dark cycle at 25±1°C, and plating the serially diluted homogenized biomass obtained after 40 days of growth. Individual colonies of filamentous cyanobacteria were isolated after 30 days on ASN-III plates, observed microscopically, and grown in liquid ASN-III medium supplemented cycloheximide and triple-antibiotic solution (containing penicillin G, chloramphenicol, and streptomycin sulfate) to prevent culture contamination. The cyanobacterial cell suspension so obtained was subsequently grown in antibiotic-free ASN-III medium for 30 days, and culture purity was confirmed by the absence of microbial growth in tryptone-yeast extract-glucose (TYG) broth (Pramanik et al., 2011; Chakraborty et al., 2018). Mass cultivation of the established cyanobacterial monoculture strains was done by growing them individually in 20 litre capacity plastic jars disinfected by washing with benzalkonium chloride followed by addition of 12 litres of sterile ASN III media and ~5 gm (wet mass) of cyanobacterial culture added to each of the jars as inoculum. Aeration was achieved with the use of pumps to ensure proper mixing of the media components, along with maintenance of the light and temperature conditions for growth (Pramanik et al., 2011). The cyanobacterial biomass of each of the two strains (one belonging to *Oscillatoria* sp. and the other being *Oxynemaestuariae*) thus obtained (~200g each) was dried at 50°C, divided into two parts and both parts extracted separately using ethyl acetate and n-butanol. The extracts were dried in vacuo and tested for anti-inflammatory activity and anti-angiogenic activity. The test for anti-inflammatory activity was performed using human

monocytic leukemia THP-1 cells that were pre-treated for 12h with standard compound Dexamethasone (1 μ M). Subsequently, pretreated cells were stimulated with LPS- 50 ng/ml for 4h. After treatments, cell supernatant was collected for TNF measurement using ELISA. (According to Clin Chem. 2005; 51(12):2252-6). Measurement of anti- angiogenic activity is based on the principle that the formation of capillary-like structures among endothelial cells plated at sub- confluent densities in matrigel matrix in the presence of the compound under investigation extrapolates to angiogenesis (Goodwin, 2007). The cell line used for this *in- vitro* assay is the EA.hy926 endothelial cell line obtained by the hybridization of human umbilical vein endothelial cells with the A549/8 human lung carcinoma cell line (Aranda et al., 2009).

Results and discussion

Secondary metabolites obtained from the cyanobacterial biomass extracts (with ethyl acetate) have shown promising anti- inflammatory activity and anti- angiogenic activity (the ability to prevent endothelial cells to form capillary-like structures) compared to the standards Dexamethasone and Sunitinib respectively (tested at CDRI, Lucknow) (unpublished report). Both the extracts from the cyanobacterial strains showed anti- angiogenic activity by reducing the capillary structures (>25% inhibition compared to standard compound, Sunitinib) at the initial 100 μ g/ml test dose (Table 1). Both extracts also showed \geq 75% inhibition of inflammatory activity compared to Dexamethasone at the initial 100 μ g/ml test dose (Table 2). Thus, the ethyl acetate extracts of these cyanobacterial strains can be further purified by column chromatography and HPLC for reduction of possible cytotoxicity.

Serial number	Extract Code	% Tubulogenesis inhibition
1	“Ethyl Acetate Extract” AP20	Active, lower dose to be tested
2	“Ethyl Acetate Extract” AP24	Active, lower dose to be tested
Standard	Sunitinib	~40

Table 1: Test results of ethyl acetate extracts of AP20 (*Oscillatoria* sp.) and AP24 (*Oxynema aestuarii*) for anti- angiogenic activity against Sunitinib (standard). Concentration of extract tested: 100 μ g/ml.

Source: Unpublished report, CDRI Lucknow.

Anti- inflammatory activity		
Serial number	Extract Code	% inhibition
1	“Ethyl Acetate Extract” AP20	\geq 85
2	“Ethyl Acetate Extract” AP24	\geq 85
Standard	Dexamethasone	~78

Table 2: Test results of ethyl acetate extracts of AP20 (*Oscillatoria* sp.) and AP24 (*Oxynema aestuarii*) for anti-inflammatory activity against Dexamethasone (standard). Concentration of extract tested: 100µg/ml.

Source: Unpublished report, CDRI Lucknow.

Conclusion

Despite the wide range of natural products of significant pharmacological value found in cyanobacteria, exploitation of these products is still not widespread. The growth of cyanobacterial biomass is quite slow, which is certainly one of the most important limiting factors due to which massproduction of bioactive compounds is limited. Further studies on the metabolites isolated from the cyanobacterial biomass may help in the synthesis of drugs containing the key components contributing to the bioactivity possible (Nagarajan et al., 2012). The study may prove to be a beneficial step in the discovery of several compounds of pharmacological interest from the largely unexplored mangrove microbiota of the Indian Sundarbans, opening a new vista towards the treatment of life-threatening diseases.

References

1. Aranda, E., and Owen, I. G. 2009. A semi-quantitative assay to screen for angiogenic compounds and compounds with angiogenic potential using the EA.hy926 endothelial cell line. *Biol Res* 42:377-389.
2. Burja, A.M., Banaigs, B., Abou- Mansour, E., Burgess, J.G., Wright, P.C. 2001. Marine Cyanobacteria- A prolific source of natural products. *Tetrahedron report no.* 590.
3. Chakraborty, S., Maruthanayagam, V., Achari, A., Mahansaria, R., Pramanik, A., Jaisankar, P., Mukherjee, J. 2018. *Oxynema aestuarii* sp. nov. (Microcoleaceae) isolated from an Indian Mangrove forest. *Phytotaxa* 374:24-40.
4. Chakraborty, S., Maruthanayagam, V., Achari, A., Pramanik, A., Jaisankar, P., Mukherjee, J. 2019. *Euryhalinamangrovii* gen. nov., sp. nov. and *Leptoelongatus litoralis* gen. nov., sp. nov. (Leptolyngbyaceae) isolated from an Indian mangrove forest. *Phytotaxa*, 422(1), 058-074.
5. Gogineni, V. and Hamann, M.T., 2018. Marine natural product peptides with therapeutic potential: Chemistry, biosynthesis, and pharmacology. *Biochimica et Biophysica Acta (BBA)-General Subjects*, 1862(1), pp.81-196.
6. Goodwin, A.M., 2007. In vitro assays of angiogenesis for assessment of angiogenic and anti-angiogenic agents. *Microvascular research*, 74(2-3), pp.172-183.
7. Nagarajan, M., Maruthanayagam, V., & Sundararaman, M. 2012. A review of pharmacological and toxicological potentials of marine cyanobacterial metabolites. *Journal of Applied Toxicology*, 32(3), 153-185.
8. Pramanik, A., Sundararaman, M., Das, S., Ghosh, U., & Mukherjee, J. 2011. Isolation and Characterization of Cyanobacteria Possessing Antimicrobial Activity from the Sundarbans, The world's Largest Tidal Mangrove Forest. *Journal of phycology*, 47(4), 731-743.
9. Raja, R., Hemaiswarya, S., Ganesan, V. and Carvalho, I.S., 2016. Recent developments in therapeutic applications of Cyanobacteria. *Critical reviews in microbiology*, 42(3), pp.394-405.
10. Zhang, W., Wang, Y., Lee, O.O., Tian, R., Cao, H., Gao, Z., Li, Y., Yu, L., Xu, Y. and Qian, P.Y., 2013. Adaptation of intertidal biofilm communities is driven by metal ion and oxidative stresses. *Scientific reports*, 3, p.3180.

খোয়াই

ISSN 2319 – 8389, Vol : 43, Issue : 43

KHOAI
UGC Care Listed Journal
Art and Humanities
Tri - Annual Journal



সংখ্যা ৪৩ : ২৫ বৈশাখ, ১৪২৮

শান্তিনিকেতন

সূচীপত্র

সম্পাদকীয়		
পারিবারিক সম্পর্কের বন্ধনে 'নৌকাডুবি'	-- অসীম কুমার মুখার্জী	৯
✓ রবীন্দ্রনাথের 'নদী': একটি অন্তরঙ্গ পাঠ	-- শুভাশিস গোস্বামী	১৪
রবীন্দ্রসঙ্গীতে বাস্তবতা, সমাজ নৈতিকতা ও বিশ্বমানবতার শিক্ষা	-- অসীম কুমার রায়	১৯
মুর্শিদাবাদের সংস্কারধর্মী প্রবাদ : সমীক্ষা ও মূল্যায়ন	-- নিবিড় কুমার ঘোষ	৩২
দারা শিকোর দার্শনিক ও আধ্যাত্মিক নিকটবর্তিতা	-- মহম্মদ ফায়েক, প্রহ্লাদ রায়, সিদ্দিকী ওয়াসিম রহমান	৩৬
সত্যজিৎ রায় পরিচালিত চলচ্চিত্রে প্রতিফলিত লোকসংস্কৃতি	-- পুলক গঙ্গুলী	৪১
রোসাঙ রাজসভার সাহিত্যে সূক্ষী সাধনার প্রভাব	-- তনুকা চৌধুরী	৪৮
বাংলা চলচ্চিত্রে ব্যবহৃত লোকসংগীত ও লোকনৃত্য	-- ইতি পাল	৫৫
মূল্যবোধ শিক্ষা : প্রসঙ্গ মধ্যযুগের ইংরেজি সাহিত্য	-- মৌসুমী পেড়িওয়াল	৬২
'রঘুবংশ' মহাকাব্যে বিজ্ঞানচেতনা	-- সঞ্জয় মণ্ডল	৬৯
'দিবে আর নিবে, মিলাবে মিলিবে': শিক্ষার প্রাঙ্গণে বিশ্বায়ন	-- নাফিসা সনম	৭২
সমুদ্রে জাতীয়তাবাদ : ঊনবিংশ ও বিংশ শতকে ভারত-		
-মহাসাগরীয় সমুদ্রবাণিজ্যে স্বদেশী প্রয়াস ও পরিণতি	-- সৌম্যজিৎ মুখার্জী	৭৮
অবনীন্দ্রনাথ ঠাকুরের 'বুড়ো আংলা' : বাংলার সমাজ ও সংস্কৃতি	-- শুভঙ্কর ঘোড়াই	৮৭
দ্বিজেন্দ্রলাল রায়ের খয়লাঙ্গ বাংলা গান	-- চন্দ্রানী দাস	৯৫
ভারতীয় রাগসঙ্গীত ও তাঁর উদ্দেশ্য	-- অরিন্দম সেন	১০৬
সূর্য-দীঘল বাড়ী : উপন্যাসে, চলচ্চিত্রে	-- তীর্থ দাস	১১২
বাংলা কথাসাহিত্যে ঝাড়খণ্ডের জনজীবন	-- অনিবার্ণ সাহু	১১৬
শিক্ষার আড়িনায় সর্ব লিঙ্গ সমন্বয় : লিঙ্গসমতার এক অধ্যায়	-- সুমেধা মুখার্জী ও উমাকান্ত প্রসাদ	১২৪
প্রগতি ও অগ্রগতি : ঊনিশ শতকে মেয়েদের জন্য বাংলা ভাষার পত্রিকা	-- সঞ্জিতা বসু	১৩৪
দূরস্থিত সংযোগ	-- ইন্দিরা দাশ	১৪৩
ইতিহাসের অন্তরালে ঊনিশ শতকের নিরিখে পট ও ব্রাত্য-		
-জনগোষ্ঠী পটুয়া শিল্পীদের যাপন আখ্যানের আলোচনা	-- রাকেশ কৈবর্ত	১৪৭

রবীন্দ্রনাথের 'নদী': একটি অন্তরঙ্গ পাঠ
শুভাশিস গোস্বামী

'চিত্রা' কাব্য প্রকাশিত হবার একমাস আগে (২২মাঘ, ১৩০২ বঙ্গাব্দ) রবীন্দ্রনাথের 'নদী' নামের ছন্দ কাব্যটি প্রকাশিত হয়। অতুপ্পূত্র বালেন্দ্রনাথের শুভ পরিণয়ের দিন এই কাব্যটি তাঁকে উপহার দেওয়া হয়। ১৯০৩ খ্রীষ্টাব্দে মোহিতচন্দ্র সেন যে কাব্যগ্রন্থ প্রকাশ করেন (২ আশ্বিন, ১৩১০ বঙ্গাব্দ) তার সপ্তমভাগে 'শিশু' পর্বে ময়ো স্থান পেয়েছিল 'নদী'। তখন থেকে সেখানেই আছে।

'বালাগ্রন্থাবলী'র অন্তর্গত এই কাব্যটির 'বিজ্ঞাপন' অংশে রবীন্দ্রনাথ লিখেছিলেন,—
“এই কাব্যগ্রন্থখানি বালক বালিকাদের পাঠের জন্য রচিত হইয়াছে। পরীক্ষার দ্বারা জানিয়াছি ইহার ছন্দ শিশু সহজেই আবৃত্তি করিতে পারে। বয়স্ক পাঠকদিগকে বলা বাহুল্য যে, প্রত্যেক ছন্দের আবেশের শব্দটির পরে কেতন ফাঁক দেওয়া হইয়াছে সেখানে স্বল্পকালমাত্র খামিতে হইবে।”

'নদী' কাব্যটির মূল আকর্ষণ হল রচনাভঙ্গির বিশিষ্টতা। রবীন্দ্রজীবনীকার গ্রন্থটি রচনার কিছু প্রেক্ষাপটে কথা জানিয়েছেন।^১ প্রথমত এই সময় তাঁর সন্তানদের শিক্ষাসহায়ক গ্রন্থের খুবই অভাব ছিল। বিশেষত যুজ্ঞান্বয়ী কবিতা খুবই কম। কন্যা রেশুকার পাঠ সহায়ক হিসাবেও এটি রচিত হয়ে থাকতে পারে।^২

দ্বিতীয়ত, এই সময়ে চলছিল 'সহজ পাঠ' এর খসড়া তৈরির কাজ। তাই শিশুদের বহনশক্তি উন্নত করা ও ছন্দ সৌন্দর্য উপভোগের জন্যে নতুন কাব্য সৃষ্টির প্রয়োজনও কবি উপলব্ধি করছিলেন।

রবীন্দ্রনাথের চেষ্টা ছিল সংযুক্ত ব্যঞ্জনবর্ণ যথাসাধ্য কম ব্যবহার করা। ৩০০ ছত্রের এই কবিতাটিতে যুজ্ঞান্বয় আছে মাত্র বারোটি।

ইন্দিরা দেবী 'নদী' কবিতাটির সঙ্গে ইংল্যান্ডের কবি রবার্ট সাদে রচিত 'Falls of Ladore' (কবিতার প্রকৃত নাম 'Cataract of Ladore', রচনাকাল ১৮২০ খ্রীষ্টাব্দ) কবিতাটির মিল খুঁজে পেয়েছিলেন।^৩ কবি সাদে কবিতাটি লিখেছিলেন তাঁর সন্তানদের জন্যে। বালকপুত্র প্রশ্ন করেছিলেন কবিকে, 'কীভাবে পাহাড়ের উপর থেকে নেমে আসে ঝর্ণাধারা ?'

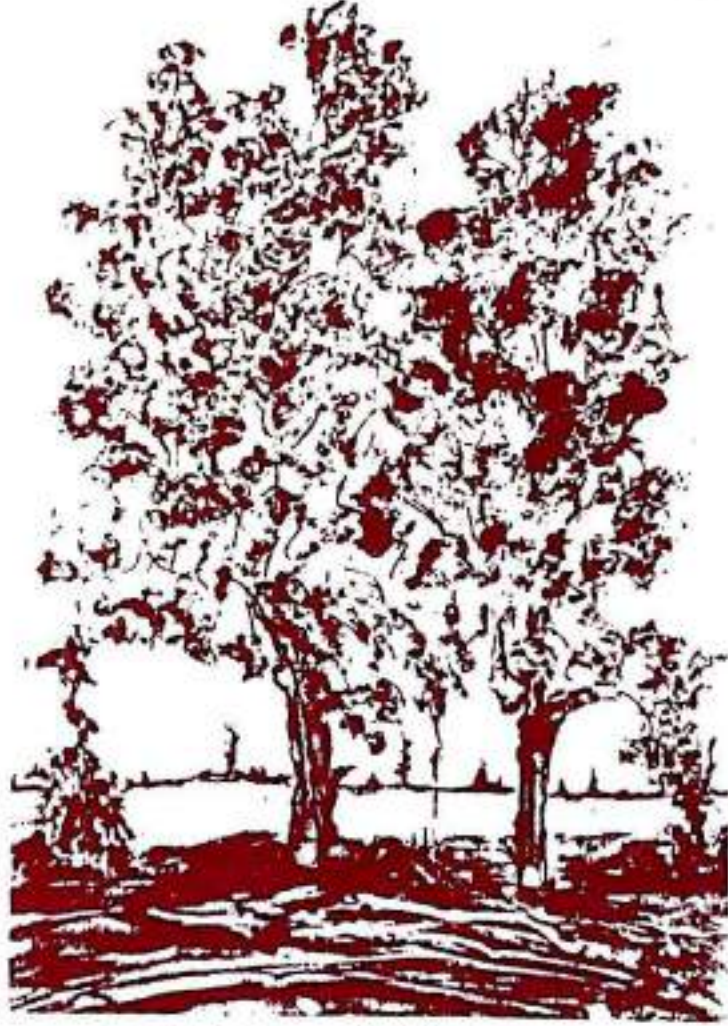
" How does the water
Come down at Ladore ?
My little boy asked me
Thus, once on a time ;
And moreover he tasked me
To tell him in rhyme."

কবি সাদে অনুপম শব্দ ও ধ্বনিমাধুর্যে পাহাড়ের উঁচু কোল থেকে হ্রদিত হিল্লোল দুলাকি চলে, নৃত্যরত ভঙ্গি ঝর্ণাধারার নেমে আসাকে বর্ণনা করেছেন। চার ছত্র উল্লেখ করছি —

খোয়াই

ISSN 2319 – 8389, Vol : 44, Issue : 44

KHOAI
UGC Care Listed Journal
Art and Humanities
Tri - Annual Journal



সংখ্যা ৪৪ : ২২ শ্রাবণ, ১৪২৮

শান্তিনিকেতন

Aesthetics of Raga- লোকবিশ্বাস ও লোকসংস্কার : মহাশেখতা দেবীর একটি উপন্যাস- নেল নভিংস এর শিক্ষাজীবনা- উনবিংশ শতাব্দীর দ্বিতীয়ার্ধে উত্তরবঙ্গের নগরায়ন ও নাগরিক পরিষেবা : প্রসঙ্গ মালদহ জেলা- ডিজিটাল ও অনলাইন দুনিয়ায় রবীন্দ্রগানের প্রচার ও প্রসার এবং করোনা আবহে তার ইতিবাচক ও নেতিবাচক প্রভাব - একটি সমীক্ষা ভিত্তিক মূল্যায়ন- Unselfishness is the essence of Morality according to Swami Vivekananda- রবীন্দ্রসঙ্গীতে ভারতীয় সংস্কৃতির নবজাগরণ- The Effectiveness of Virtual Field Trip on Academic Achievement of Students in Inclusive Classroom with respect to Teaching Forest Resources at Higher Secondary Level- 'ধুমিনালের দুই সঙ্গী' গল্পে সাম্প্রদায়িক দাঙ্গা ও সংকট উত্তরণের ছবি- ঔপনিবেশিক আমলে মালদা-র সাঁওতাল সমাজ- চেতন্য সংস্কৃতি ও বর্তমান সময়ে তার প্রাসঙ্গিকতা- "ইতিহাস ও ঐতিহ্যের সংস্কৃতি পৌষ সংক্রান্তি"- Teaching-Learning Strategies for Children with Disabilities in Inclusive Classrooms-	Shyamal Makhai শিশির সিং মন্দিরা সিংহ যতরত গোস্বামী শ্রী কৌশল কর্মকার Sabyasachi Mondal অনির্বাণ সায়ু Sanjoy Dutta & Dr. Mousumi Boral মৃদুল ঘোষ রাজেন হেমরম প্রবীর কুমার পাল অঞ্জন কন Dr.Gopal Singh Dr.Sharmila Yadav শুভাশিষ গোস্বামী শিরীণ মুস্তাফি অসীম কুমার মুখার্জী Sk Rashidul Haque রূপশ্রী ঘোষ সমীর প্রসাদ মুনায় কুমার মহাত্ত ড. চন্দ্রানী দাস Pritam Pyne & Dr. Umakant Prasad Dr. Prarthita Biwas & Dr. Shyamsundar Bairagya Ashok Barman DR. CHITRALEKHA MAITI & DR. ATREYA PAUL Dr. Atreya Paul DR . SURESH .J মীনাক্ষী ভট্টাচার্য্য সোমা দাস মণ্ডল অর্পিতা দাস Sajejev Singh. M. K	২০৬ ২১২ ২১৬ ২২৫ ২৪৬ ২৫৫ ২৫৯ ২৬৩ ২৬৯ ২৭৯ ২৮৬ ২৯৯ ৩০৪ ৩০৯ ৩১৬ ৩২২ ৩৩২ ৩৩৩ ৩৩৯ ৩৫১ ৩৬১ ৩৬৬ ৩৭১ ৩৭৬ ৩৮২ ৩৯১ ৪০১ ৪০৬ ৪১১ ৪২০ ৪২৬ ৪৩০ ৪৩৬ ৪৪১
রবীন্দ্রনাথের 'সন্ধ্যাসংগীত' কাব্যে নদীর স্থান- 'নভুন ইহুদি' : দেশভাগের জীবন্ত দলিল- পারিবারিক সম্পর্কের আলোকে 'চোখের বালি'- Population Education & Geography of Surul village: a Study- 'দেশ' পত্রিকার ছোটগল্পে গ্রামবাল্যের লোকসংস্কার- মহামারি করোনার করাল ছায়ায় : প্রসঙ্গ সাহিত্য প্রেম- বাংলা মঙ্গলকাব্যের পাঠক রবীন্দ্রনাথ- বিংশ শতাব্দীর কিংবদন্তী মহিলা সংগীতশিল্পী বেগম আখতার- Leadership Needs a Strategic Change to Prevent Child Labour : A Stage of Covid-19 Epidemic- Impact of Family Environment and Mobile Phone Addiction on the Academic Achievement of Undergraduate Students- Dhrupad Tradition of Vishnupur Gharana in West Bengal- উনবিংশ শতকের পটভূমিকায় বিশ্ববোধের উন্মেষ : বিশ্বশান্তির বাণী প্রচারে রামমোহন থেকে রবীন্দ্রনাথ- Evolution and Growth of Market System, Economy in Kolkata- Genesis and Development of Drainage and Sewerage System during Colonial period In Calcutta -1800-1948 A Historical Analysis of Ayacut settlement In Travancore in Southern India from 1883-1911- ভগবত গীতার আত্মতত্ত্ব: অদ্বৈত ও হৈতবাদের আলোকে পুনঃমূল্যায়ন- বাংলার নবজাগরণ ও জোড়াসাঁকো ঠাকুরবাড়ীর সঙ্গীত শিক্ষা- অর্থনৈতিক সংকটের প্রেক্ষাপটে দীপেন্দ্রনাথ বন্দ্যোপাধ্যায়ের জটামু : পুরাণের নবনির্মাণ- EARLY PANDYA INVASIONS IN SOUTH T		

রবীন্দ্রনাথের 'সন্ধ্যাসংগীত' কাব্য নদীর স্থান
শুভাশিষ গোস্বামী

রবীন্দ্রনাথ ঠাকুরের 'সন্ধ্যা সংগীত' কাব্যটির প্রকাশকাল নিয়ে সামান্য একটু বিতর্ক আছে। প্রথম ছাপা
১৯৮৮ খ্রিষ্টাব্দের ১২৮৮ বঙ্গাব্দের চৈত্র মাসে। কিন্তু বই হিসাবে প্রকাশিত হয় ১৯৮৯ বঙ্গাব্দের অসাদ মাসে,
১৯৮২ খ্রিষ্টাব্দের ৫ জুলাই। পুস্তকের পরিচয়পত্রে বই ছাপা আরম্ভের তারিখ ছাপা হয়েছিল।

প্রথম সংস্করণে কাব্যটিতে ছিল পঁচিশটি কবিতা, যার মধ্যে বারোটি কবিতা পূর্বে 'ভারতী' পত্রিকায় মুদ্রিত
কবিতা 'বিজ্ঞাপন' অংশে স্নায়ং গ্রন্থকার জানিয়েছিলেন --- "আমার রচিত কবিতার মধ্যে যেগুলি সন্ধ্যাসংগীত
শ্রেণীতে পড়ে, সেইগুলিই এই পুস্তকে প্রকাশিত হইল। ইহার অধিকাংশ কবিতাই গত দুই বৎসরের মধ্যে
রচিত হইয়াছে।" কাব্যটি সমকালে সাহিত্যসম্রাট বঙ্কিমচন্দ্র চট্টোপাধ্যায় কর্তৃক প্রশংসিত হয়েছিল।

রবীন্দ্রনাথের প্রাক 'সন্ধ্যাসংগীত' পর্বটি ছিল মূলত অনুকরণের পর্ব। বিশ্বরীন্দ্র চক্রবর্তী অন্নচন্দ্র
স্বামী প্রমুখের রচনার 'কপিবুক'। কবির নিজেরই স্বীকৃতি রয়েছে 'সূচনা' অংশে, --- "সেই কপিবুকের চৌকট
পর্বেই প্রথম দেখা দিল সন্ধ্যাসংগীত। _ সন্ধ্যাসংগীতেই আমার কাব্যের প্রথম পরিচয়।" জীবনস্মৃতি গ্রন্থের
'সন্ধ্যাসংগীত' নামক অধ্যায়েও রবীন্দ্রনাথ তাঁর কবি হয়ে ওঠার প্রাথমিক পর্বে রচিত এই কাব্যটি রচনাকালীন তাঁর
মনের প্রেক্ষাপটটি সবিস্তারেই তুলে ধরেছেন। স্মৃতিচারণা করতে গিয়ে লিখেছেন, --- "অব্য হিসাবে
সন্ধ্যাসংগীতের মূল্য বেশি না হতে পারে। উহার কবিতাগুলি যথেষ্ট কাঁচা। উহার ছন্দ ভাষা ভাব মূর্তি ধরিয়া
কিছুই হইয়া উঠিতে পারে নাই। _ সে লেখাটার মূল্য না থাকিতে পারে কিন্তু খুশিটার মূল্য আছে।"
সন্ধ্যাসংগীতকে রবীন্দ্রনাথ তাঁর 'প্রথম মুদ্রিত গ্রন্থ' বলেও স্বীকার করেছেন। এর পূর্বে রচিত সমস্ত কবিতাকেই
তিনি বদ দিয়েছিলেন তাঁর কাব্যগ্রন্থাবলী থেকে।

রবীন্দ্রনাথ তাঁর কবি হয়ে ওঠার পিছনে জ্যোতিন্দ্রনাথ (জ্যোতিরিন্দ্রনাথ ঠাকুর) ও নতুন বৌদানের (কাদম্বরী
দেবী) অনুপ্রেরণার কথা সপ্রসঙ্গ চিন্তে স্মরণ করেছেন আজীবন। বিশেষত স্নেহ-পরিচর্যায়-প্রীতিমধুরায় কাদম্বরী
দেবী রবীন্দ্রনাথের সাহিত্য প্রতিভার অফুরোদগমের সময় যথার্থই প্রেরণাদাত্রী হয়ে উঠেছিলেন। এই কাদম্বরী দেবী
১৯০১ বঙ্গাব্দের ৮ বৈশাখ স্নেহচায় আত্মহননের পথ বেছে নিয়েছিলেন। জীবনীকার জানিয়েছেন, কাদম্বরী দেবী
১৯০৬ একবার আত্মহত্যার চেষ্টা করেছিলেন। যার ফলস্বরূপ 'পারিবারিক বিশৃঙ্খলার প্রতিঘাত' রবীন্দ্রনাথের
জীবনের বিলাতযাত্রা স্বর্গিত হয়ে যায়। জ্যোতিরিন্দ্রনাথ পত্রীকে সুস্থ করবার জন্যে এবং জেডসাঁকোর পরিবেশ
থেকে সরে থাকবার জন্যে তৎকালীন বোম্বাই প্রদেশের কোনো পার্বত্য অঞ্চলে কিছুকাল অবস্থান করেছিলেন।
সম্রাট ১৯৮৭ বঙ্গাব্দের কার্তিক মাস নাগাদ। এই সময় জ্যোতিরিন্দ্রনাথ ও কাদম্বরী দেবী জেডসাঁকোর তেতলায়
কবির ঘরের যে অংশটায় থাকতেন সেটা সাময়িক রবীন্দ্রনাথের 'দখলে' আসে। সেই নির্জন দিনগুলিতে সেখানে
কবেই 'সন্ধ্যাসংগীত'--এর কবিতাগুলি লেখার সূত্রপাত। এই সময়পর্বেই কাব্যরচনায় পূর্বতন সংস্কারের আবেগ
থেকে তিনি মুক্ত হইলেন, ফিরে পাচ্ছিলেন নিজস্ব ছন্দও। 'জীবনস্মৃতি'--তে লিখেছেন, --- "নদী যেমন কাটা



হিজল

বঙ্গীয় সাহিত্য-সংস্কৃতি বিষয়ক গবেষণাধর্মী বাৎসরিক
(রেফারিড জার্নাল)

বর্ষ : ২৭, সংখ্যা : ২য়

ডিসেম্বর, ২০২০

সম্পাদক
সৌরভ রায়

সূচিপত্র

১

বাঙালির খাদ্য-সংস্কৃতি : সাহিত্যে ও ইতিহাসে (মধ্যযুগ থেকে উনিশ শতকের বাংলা)
বিকাশ রায় পৃ. - ৯

২

বাংলা নাটকে উত্তরবঙ্গ : একটি সীমাবদ্ধ আলোচনা
প্রণব কুমার ভট্টাচার্য পৃ. - ২৩

৩

স্বতন্ত্রতায় বিশিষ্টতায় সত্ত্বরের উপন্যাস
সেলিম বক্স মডল পৃ. - ৩২

৪

গদ্যকার রামকুমার মুখোপাধ্যায়ের দশটি ছোটগল্প : স্বতন্ত্র নির্মিতি
সাবলু বর্মণ পৃ. - ৩৭

৫

বাঙালি মহিলা ঔপন্যাসিকের উপন্যাসে দেশভাগ ও নারী স্বনির্ভরতা : অভিশাপ হয়েও আশীর্বাদ
কৃষ্টিশ্রী ভট্টাচার্য পৃ. - ৫৫

৬

যৌনতা : ধূসর পাণ্ডুলিপি
মনিরুল ইসলাম পৃ. - ৬১

৭

জমিদারির অবসানে গণতন্ত্রের সূচনা : প্রসঙ্গ 'মহিষকুড়ার উপকথা'
মৃদুল ঘোষ পৃ. - ৬৬

৮

রবীন্দ্রনাথের 'চৈতালি' কাব্যে নদীর স্থান
শুভাশিস গোস্বামী পৃ. - ৭৪

৯

কার্তিক লাহিড়ীর ছোটগল্পে রাবীন্দ্রিকভাবনা ও রবীন্দ্রসঙ্গীত
সুলতা হালদার পৃ. - ৮৪

১০

সুভাষ মুখোপাধ্যায় : রাজনৈতিক কর্মী ও কবি সত্ত্বার দ্বন্দ্ব
দেবাশিষ সরকার পৃ. - ৯১

১১

বিনতা রায়চৌধুরীর গল্প : নারীর মনস্তাত্ত্বিক জটিলতার স্বরূপ সন্ধান
মোসাঃ রাবেয়া বাসরি পৃ. - ৯৭

রবীন্দ্রনাথের 'চৈতালি' কাব্যে নদীর স্থান

শুভাশিস গোস্বামী

'চিত্রা'-র অব্যবহিত পরেই রচিত 'চৈতালি' কাব্যগ্রন্থে ১৩০২ বঙ্গাব্দের চৈত্রমাস থেকে ১৩০৩ বঙ্গাব্দের শ্রাবণ মাস পর্যন্ত রচিত কবিতা স্থান পেয়েছে। 'চিত্রা'-র শেষ কবিতা 'সিন্দুপারে' লেখা হয়েছিল ২০ ফাল্গুন ১৩০২ বঙ্গাব্দে। আর 'চৈতালি'র প্রথম কবিতা 'উৎসর্গ' রচিত হয়েছে ১৩০২ বঙ্গাব্দের ১৩ চৈত্র (অবশ্য এই কাব্যগ্রন্থে রচনাকালের দিক থেকে প্রথম কবিতা 'প্রভাত'। লেখা হয় ১১ চৈত্র)। কবিতাগুলির অধিকাংশই রচিত হয় পতিসরে, বাকি কয়েকটি সাজাদপুরে। যেহেতু সাজাদপুর রবীন্দ্রনাথদের জমিদারির ভাগে আর পড়ছে না, সুতরাং পদ্মা-তীরের এই অংশে বসবাসের পর্ব এবার শেষ হতে চলেছে। এইবারে তাঁর সঙ্গী হয়েছে পতিসর সংলগ্ন গ্রাম্য নদী নাগর। 'সূচনা' অংশে কবি লিখেছেন— "অল্প তার পরিসর, মত্বর তার স্রোত। তার একতীরে দরিদ্র লোকানয়, গোয়ালঘর, ধানের মরাই, বিচালির স্তূপ; অন্যতীরে বিস্তীর্ণ ফসল-কাটা শস্যক্ষেত ধূ ধূ করছে। কোনো এক গ্রীষ্মকাল এইখানে আমি বোট বেঁধে কাটিয়েছি।" মোহিতচন্দ্র সেন সম্পাদিত 'কাব্যগ্রন্থাবলী'র (আশ্বিন ১৩০৩ বঙ্গাব্দ) মধ্যে 'চৈতালি' প্রথম প্রকাশিত হয়। এর ভূমিকায় স্বয়ং কবি জানিয়েছিলেন— "চৈতালি শীর্ষক কবিতাগুলি লেখকের সব শেষের লেখা। তাহার অধিকাংশই চৈত্রমাসে লিখিত বলিয়া বৎসরের শেষ উৎপন্ন শস্যের নামে তাহার নামকরণ করিলাম।"

শ্রেণিগত দিক থেকে 'চৈতালি' 'সোনার তরী' বা 'চিত্রা' থেকে তেমন স্বতন্ত্র কিছু নয়। তবে বেশ বৃথতে পারা যায় যে, কবিমনের ভাবনা, কল্পনা ও অনুভূতি ধীরে ধীরে ভিন্নরূপ ধারণ করছে। আগের মত ভাবের অতিশয় আবেগ, কল্পনার মাধুর্য বা আসক্তির তীব্রতা অপেক্ষা এখানে যে সুরটি শোনা যাচ্ছে তা হল পূর্ণতার সুর, তৃপ্তির সুর। আগে যা ছিল 'সামান্য সত্য', এখন তা 'বিশিষ্ট' হয়ে উঠেছে।^১ একটি 'অখণ্ড নিসর্গানুভূতি' থেকেই এসেছে এই পূর্ণতা ও তৃপ্তির সুর।^২ 'চৈতালি'র ছোট ছোট কবিতাগুলিতেও দেখি যে, মানুষ ও প্রকৃতি মিলে একটি পূর্ণতার সুর সৃষ্টি করে কবিতাগুলিকে অপরূপ মাধুর্য দান করেছে।

'সোনার তরী'-'চিত্রা' যুগের তীব্র অনুভূতি 'চৈতালি'তে পরিণত হয়েছে গভীর উপলব্ধিতে। শান্ত সমাহিত চিন্তে কবি যেন সত্য দর্শন করেছেন আর ধীরে ধীরে তা ব্যক্ত করছেন। কবিতার আকারও অনেক সংক্ষিপ্ত হয়েছে এখানে। ভাষাতেও নেই অজস্র অলংকারের ঐশ্বর্য ও চমৎকারিত্ব। কবিতাগুলি যেন কবির উপলব্ধ সত্যের অনাড়ম্বর প্রকাশ। 'সূচনা' অংশে কবিই লিখেছেন সে কথা— "মনটা আছে ক্যামেরার চোখ নিয়ে, ছোটো ছোটো ছবির ছায়া ছাপ দিচ্ছে অন্তরে। অল্প পরিধির মধ্যে দেখছি বলেই এত স্পষ্ট করে দেখছি। সেই স্পষ্ট দেখার স্মৃতিকে ভরে রাখছিলুম নিরলংকৃত ভাষায়। অলংকার প্রয়োগের চেষ্টা জাগে মনে যখন প্রত্যক্ষবোধের স্পষ্টতা সম্বন্ধে সংশয় থাকে। যেটা দেখছি মন যখন বলে 'এটাই যথেষ্ট' তখন তার উপরে রঙ

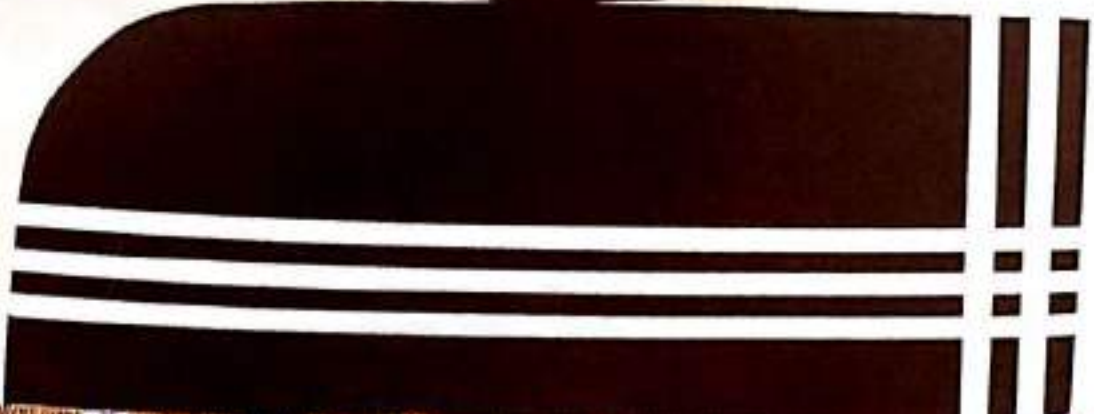
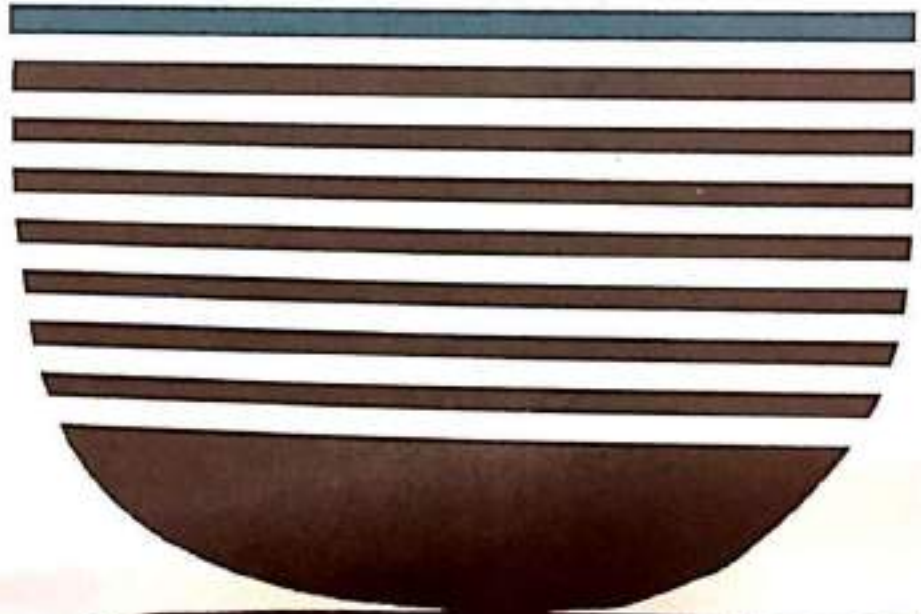
ISSN 2249-8133

নাব্যশ্রোত

ষান্মাসিক সমাজ ও সংস্কৃতি বিয়রক কাগজের জমি

পঞ্চদশ বর্ষ, প্রথম ও দ্বিতীয় সংখ্যা

অগাস্ট ২০২০ ও ফেব্রুয়ারি ২০২১



✓ প্রবন্ধগুচ্ছ- দুই

রবীন্দ্রনাথের 'চিত্রা' কাব্যে নদীর স্থান

শুভাশিস গোস্বামী ১০৯

গিরিশচন্দ্র ঘোষের নাটকের সংলাপ : একটি সংক্ষিপ্ত অবলোকন

কৌশিককুমার দত্ত ১২২

ভারত-নেপাল দ্বিপাক্ষিক সম্পর্কে চীনের প্রভাব :

একটি ঐতিহাসিক বিশ্লেষণ (১৯৫০-১৯৬০)

বাসুদেব দাস ১৩২

সার্থশতবর্ষে দেশবন্ধু চিত্তরঞ্জন : এক আপোষহীন মহাপ্রাণ

গার্গী সেনগুপ্ত ১৪৩

মহর্ষি পতঞ্জলির দৃষ্টিভঙ্গিতে ধ্যান ও সমাধি : একটি পর্যালোচনা

বিপ্লব বারিক ১৫৬

রমাপদ চৌধুরীর ছোটগল্পে সমাজ ও পরিবেশের প্রভাব

ড. অর্জুন দোগই ১৭০

প্রান্তজনের সংকট : নলিনী বেরার 'অপৌরুষেয়'

ও কাবেরী রায়চৌধুরীর 'শ্রীমান রজাবতী'

অসীম মণ্ডল ১৭৬

প্রবন্ধগুচ্ছ- তিন

আমার আখরগুলি

ড. সৈয়দ তানভীর নাসরীন ১৯৩

রবীন্দ্রনাথের 'চিত্রা' কাব্যে নদীর স্থান

শুভাশিস গোস্বামী

'সোনার তরী' ও 'চিত্রা' কাব্যের সময়ের ব্যবধান মাত্র একমাসের। 'সোনার তরী'-র শেষ কবিতা 'নিরুদ্দেশ যাত্রা' রচিত হয় ২৭ অগ্রহায়ণ ১৩০০ বঙ্গাব্দ। আর 'চিত্রা' কাব্যগ্রন্থের প্রথম কবিতা (রচনাকালের দিক থেকে) 'জ্যোৎস্নারাত্রে' (৬ মাঘ ১৩০০ বঙ্গাব্দ)। ৬ মাঘ ১৩০০ বঙ্গাব্দ থেকে ২০ ফাল্গুন ১৩০২ বঙ্গাব্দ পর্যন্ত 'চিত্রা' কাব্যগ্রন্থের কবিতাগুলির রচনার কাল।

'সোনার তরী' ও 'চিত্রা' দুই কাব্যগ্রন্থের কবিতাগুলি রচনাকালে কবির মানসিক পরিবেশ এবং লেখার পরিপ্রেক্ষিতেও মোটের উপর একইরকম। কবি তখনও বাস করছেন বোটে। তাঁর জীবনে মনে তখনও চলেছে 'নির্জন-সজনের নিত্য সংগম'। তাছাড়া কাব্যকল্পনা ও কাব্য প্রসাধনগত দিক থেকেও দুই কাব্যের মধ্যে পার্থক্য সামান্য। কবির objective দৃষ্টিভঙ্গি যেমন 'চিত্রা' পর্বে অনেকটা গভীর হয়েছে তেমনি 'সোনার তরী'-র সময়কার সৌন্দর্যধ্যানও আরও গভীরতর রূপ লাভ করেছে। কবির অতিশয় আত্মগত ও আত্মসচেতন ভাবকল্পনা থেকে জাত জীবনদেবতার ধ্যান— 'চিত্রা'য় আরও 'দৃঢ়তর ভিত্তির উপর প্রতিষ্ঠিত হয়েছে।'।^১ সর্বোপরি 'রিয়াল' ও 'আইডিয়াল'—এর দ্বন্দ্বও কিছুটা সমন্বয় লাভ করেছে এই পর্বে।

পদ্মা ও তার শাখানদীগুলির ঘনিষ্ঠ সান্নিধ্যে থাকার কারণে রবীন্দ্রনাথের 'চিত্রা' কাব্যগ্রন্থেরও বহু কবিতায় বিভিন্নভাবে উঠে এসেছে নদী প্রসঙ্গ। আমরা তেমন প্রাসঙ্গিক কবিতাগুলি আলোচনায় অগ্রসর হব।

'চিত্রা' কাব্যগ্রন্থ প্রকাশিত হয় ২৯ ফাল্গুন ১৩০২ বঙ্গাব্দ (ইং-১১ মার্চ ১৮৯৫ খ্রি.)। প্রথমত এই কবিতা সংকলনটিতে ছিল ৩৪টি কবিতা। পরে 'সোনার তরী' থেকে নিয়ে সুখ

শুভাশিস গোস্বামী : গবেষক, রাঁচী বিশ্ববিদ্যালয় (বাংলাভাষা ও সাহিত্য বিভাগ)। সহযোগী অধ্যাপক, অহরুরাম মেমোরিয়াল কলেজ, ঝালদা, পুরুলিয়া।

'এবং মহুয়া' - বিশ্ববিদ্যালয় মঞ্জুরী আয়োগ (UGC-CARE)

অনুমোদিত তালিকার অন্তর্ভুক্ত।

২০২০সালে প্রকাশিত ৮৬পৃ.তালিকার ৬০ পৃ.এবং ৮৪পৃ.উল্লেখিত।

এবং মহুয়া

(বাংলা ভাষা, সাহিত্য ও গবেষণামর্মী মাসিক পত্রিকা)

২২ তম বর্ষ, ১২৫ সংখ্যা

অক্টোবর, ২০২০

সম্পাদক

ড. মদনমোহন বেরা

সহসম্পাদক

পায়েল দাস বেরা

মৌমিতা দত্ত বেরা

যোগাযোগ :

ড. মদনমোহন বেরা, সম্পাদক।

খোলকুয়াচক, পোষ্ট-মেদিনীপুর, ৭২১১০১, জেলা-প.মেদিনীপুর, প.বঙ্গ।

মো.-৯১৫০১৭৭৬৫৩

কে.কে. প্রকাশন

খোলকুয়াচক, মেদিনীপুর, পশ্চিমবঙ্গ।

২৭. কুমুদরঞ্জন মল্লিকের প্রবন্ধে গ্রাম সমাজের রূপ ও রূপান্তর	
:: সখাটী কুমার পাল.....	২২৫
২৮. 'নন্দী কাঁথার মাঠ' এবং 'রূপসী বাংলা' : বঙ্গ প্রকৃতির রূপের বিচিত্র আলোচনা	
:: বাপি দত্ত.....	২৩০
২৯. কমল কুমার মুখোপাধ্যায়ের গল্প 'মতিলাল পাদরী' : ধর্ম বিশ্বাসের আড়ালে মানবিক চেতনা	
:: বেবী পাত্র (সামন্ত).....	২৩৫
৩০. সরলা দেবী চৌধুরাণী : উপনিবেশিক বঙ্গের বিপ্লবী আন্দোলনের অন্যতম উদ্যোগ	
:: চিত্ত সেন পরামানিক.....	২৪৫
৩১. 'কথা'র মধ্যে 'বাদ'-এর শ্রেষ্ঠত্ব বিচার	
:: প্রিয়ান্বিতা মাইতি (দাস).....	২৫৩
৩২. রবীন্দ্রসঙ্গীত : ব্যক্তিগত থেকে নৈব্যক্তিক অভিযাত্রা	
:: সুকান্ত চক্রবর্তী.....	২৬৭
৩৩. কাশীদাসী মহাভারতে রাজনৈতিক ও মনোস্তাত্ত্বিক দ্বন্দ্ব	
:: সৌমিতা মুখার্জী.....	২৭৪
৩৪. 'উদ্যোগ পর্ব' : এক বিশেষ সময়ের ইতিবৃত্তে গুঁরাও জীবন	
:: বৈশাখী কুণ্ড.....	২৮২
৩৫. রবীন্দ্র ছোটোগল্পে প্রতিবাদী নারী	
:: তাহমিজা খাতুন.....	২৮৭
৩৬. "দুঃখ তোমার ঘুচবে কবে?" রবীন্দ্রনাথ	
:: ড. অরুণ সরকার.....	২৯৪
৩৭. বাংলা মঙ্গলকাব্যে অস্তিত্বের সংকট	
:: ড. শান্তনু ভট্টাচার্য.....	৩০৩
৩৮. বাংলা থিয়েটারে নারী : উনিশ শতক	
:: ড. বিপুলকুমার মণ্ডল.....	৩১৪
৩৯. পাঠ্যপুস্তক রচয়িতা রবীন্দ্রনাথ	
:: ড. অর্চনা দত্তপাঠ.....	৩২৪
৪০. প্রকৃতি ও প্রকৃতির দ্বন্দ্ব অতীত বন্দ্যোপাধ্যায়ের উপন্যাস	
:: ড. সুব্রতকুমার দে.....	৩৩৩
৪১. এমন দিন কবে হবে তারা : প্রসঙ্গ 'বীরাসনা কাব্য'র তারা চরিত্র	
:: ড. শান্তনু চট্টোপাধ্যায়.....	৩৪৩

বাংলা মঙ্গলকাব্যে অস্তিত্বের সংকট

ড. শান্তনু ভট্টাচার্য

মঙ্গল কথাটির আভিধানিক অর্থ হল কল্যাণ। সাধারণভাবে যে কাল্যে দেবদেবীর তাকেই আমরা মঙ্গলকাব্য বলি। মঙ্গলকাব্যে আখ্যানমূলক কাব্য। পঞ্চদশ থেকে অষ্টাদশ শতাব্দী পর্যন্ত দীর্ঘ চারশত বছর ধরে বহু কবি এই কাব্যশাখায় একাধিক কাব্যলিখেছেন। ব্রিটিশ সমালোচকের মতে, 'বাংলাদেশে খ্রীষ্টীয় পঞ্চদশ শতাব্দীর শেষভাগ হইতে অষ্টাদশ শতাব্দীর শেষার্ধ পর্যন্ত পৌরাণিক, লৌকিক এবং পৌরাণিক-লৌকিক সংমিশ্রিত দেব-দেবীর লীলামহাত্ম্য, পূজা-প্রজার ও ভক্তকাহিনী অবলম্বনে যে-ধরনের সম্প্রদায়গত, প্রচারধর্মী ও আখ্যানমূলক কাব্য রচিত হইয়াছে, তাহাকে বাংলা সাহিত্যের ইতিহাসে মঙ্গলকাব্য বলা হয়।' মঙ্গলকাব্য সাধারণত চারটি অংশে বিভক্ত— বন্দনা অংশ, গ্রন্থোৎপত্তির কারণ অংশ, দেবখণ্ড, নরখণ্ড। মঙ্গলদেবদেবী চরিত্রে লোকভিত্তি, পৌরাণিক দেবতাদের সঙ্গে সংস্পর্শ, মানবিক স্বভাব প্রভৃতি বিশিষ্টতা লক্ষণীয়। মঙ্গলকাব্যগুলিতে মধ্যযুগের বাঙালিদের জীবনযাত্রার তথ্যনিষ্ঠ ছবি ধরা পড়েছে। নারীগণের পতিনিন্দা, বারমাস্যা, চৌতিশা, পুরাণ কথার উল্লেখ প্রভৃতি মঙ্গলকাব্যের রীতির অঙ্গগতি।

জীবনধারণে মানবসমাজ নানা সংকটের সম্মুখীন হয়। এই সংকট আবার কখনো কখনো অস্তিত্বের সঙ্গে যুক্ত হয়ে থাকে। সাহিত্যে জীবনের প্রতিচ্ছবি। তাই স্বাভাবিকভাবেই সাহিত্যেও অস্তিত্বের সংকটের প্রসঙ্গ ধরা পড়েছে নানাভাবে। মানব সমাজে অস্তিত্বের সংকট মূলত জীবন এবং জীবিকা কেন্দ্রিক। বাংলা মঙ্গলকাব্যের ধারায় দৃষ্টিপাত করলে আমরা এমন অনেক চরিত্র এবং প্রসঙ্গ পাব যাতে অস্তিত্বের সংকট নানাভাবে ফুটে উঠেছে। আলোচনার সুবিধার্থে বিশেষ কয়েকটি মঙ্গলকাব্যের বিশেষ কয়েকটি চরিত্র এবং প্রসঙ্গকে কেন্দ্র করে আমরা এগোবো যেখানে মানবসমাজের অস্তিত্বের সংকটগুলি বিশেষভাবে দৃষ্টি আকর্ষণ করে। বিজয়গুপ্তের মনসামঙ্গল, কবিকঙ্কণ মুকুন্দের চণ্ডীমঙ্গল এবং ভারতচন্দ্রের অন্নদামঙ্গল— এই কাব্যগুলিকে কেন্দ্র করে পরবর্তী অংশে আলোচনা বিষয়ে আলোকসম্পাত করা হবে।

বিজয়গুপ্তের মনসামঙ্গল কাব্যের দিকে দৃষ্টিপাত করলে প্রথমেই যে চরিত্রে অস্তিত্বের সংকট সর্বাপেক্ষা লক্ষিত হয় সে হল কেন্দ্রীয় চরিত্র মনসা। মনসা অযোনি সন্তান। জন্মলগ্ন থেকেই তিনি অবহেলিতা, লাঞ্ছিতা, অপমানিতা। তার খেদোক্তি—

“জন্মন দুঃখিনী আমি দুঃখে গেল কাল।

যেই ডাল ধরি আমি ভাগে সেই ডাল।।

‘এবং মহুয়া’ - বিশ্ববিদ্যালয় মঞ্জুরী আয়োগ UGC-CARE list-I 2021)
অনুমোদিত তালিকার অন্তর্ভুক্ত।

২০২১সালে প্রকাশিত ১৬শু তালিকার (৩১৯টির মধ্যে) ৩ শু ৩০নং উল্লেখিত।

এবং মহুয়া

(বাংলা ভাষা, সাহিত্য ও গবেষণামূলক মাসিক পত্রিকা)

২৩তম বর্ষ, ১৩৭ সংখ্যা

আগষ্ট, ২০২১

সম্পাদক

ড. মদনমোহন বেরা

সহসম্পাদক

শ্যামল মাস বেরা

বৌমিত্রা মাস বেরা

যোগাযোগ :

ড. মদনমোহন বেরা, সম্পাদক।

শোলকুঁয়াচক, পোষ্টি-মেদিনীপুর, ৭২১১০১, জেলা-প. মেদিনীপুর, প. বঙ্গ।

ফো. - ৯১৫০১৭৭৬৫০

ফে. ফে. প্রকাশন

শোলকুঁয়াচক, মেদিনীপুর, পশ্চিমবঙ্গ।

৫৩ আধুনিক ভারতে যোগচর্চা	
:: ড. বিজয় সরকার	৪১৫
৫৪ সংস্কৃত অলাংকারশাস্ত্রে শ্রীশ্রীচেতনা প্রবর্তিত ভক্তিরস	
:: ড. দিলীপ পণ্ডা	৪২৬
৫৫ ঊনবিংশ শতাব্দীতে নারী শিক্ষা ও উত্তরপাড়ার হিতকরী সভা :	
একটি পর্যালোচনা :: ড. মিলন কান্তি দাস	৪৩১
৫৬ ত্রিপুরার বাংলা কবিতাচর্চা :: ড. মৌসুমী পাল	৪৪০
৫৭ ধর্মশাস্ত্রে আলোচ্য স্বধর্ম :: ড. মুকুল মন্ডল	৪৪৭
৫৮ বিশুদ্ধ পাগলামির কারুশিল্প : অবনীন্দ্রনাথের যাত্রাপালা	
:: ড. প্রত্যাষ কুমার জনা	৪৫৪
৫৯ উত্তর-পূর্ব ভারতের রাজবংশী লোকদেবতা মাহান	
:: ড. কৃষ্ণকান্ত রায়	৪৬১
৬০ বরাক উপত্যকার সৃজন ভাবনার উদ্বোধন চেতনায় : প্রসঙ্গ	
কবি শক্তিপদ ব্রহ্মচারী ও অতীন দাসের কবিতা	
:: ড. কালীপদ দাস	৪৭২
৬১ মঙ্গলকাব্যের দেব-দেবী:আর্থ ও অনার্থ ধর্ম ও সংস্কৃতির মেলবন্ধন	
:: ড. শান্তনু ভট্টাচার্য	৪৮১
৬২ পঞ্চাশের কবি শক্তি চট্টোপাধ্যায় : ভাবনার নিজস্ব ভুবন	
:: ড. সুশান্তকুমার দোলই	৪৮৯
৬৩ নারীর ক্ষমতাশক্তি ও রাজা রামমোহন রায় : একটি পর্যালোচনা	
:: ড. স্বাগতা ভট্টাচার্য	৫০২
৬৪ ত্রিপুরার বাংলা ছোটগল্পে প্রান্তীয় মানুষ-জন	
:: ড. শংকরী দাস	৫১২
৬৫ সাহিত্যের বিয়র ও কয়েকটি সাহিত্যাত্মিক প্রসঙ্গ	
:: ড. সুমন ঘোষ	৫২১
৬৬ বাংলা গোয়েন্দা সাহিত্যের উদ্ভব	
:: ড. কৌষেয়ী ব্যানার্জি	৫২৬
৬৭ সংগীত প্রশিক্ষণে গুরুশিষ্য পরম্পরা এবং বৈজ্ঞানিক পদ্ধতিতে	
ব্যবধানিক শিক্ষা :: ড. লোপামুদ্রা চক্রবর্তী	৫৩০
৬৮ বিনয় মজুমদার : সৃষ্টিসুখে সমর্পিত	
এক কবির বিয়াদময় জীবন কথা :: ড. আশিস অধিকারী	৫৩৫
০০লেখক পরিচিতি	৫৫১
০০০UGC-CARE list	৫৫৫

संस्कृत भाषा में लिखित एक कविता का
संक्षिप्त परिचय
ए. ए. ए. ए.

संस्कृत भाषा में लिखित एक कविता का संक्षिप्त परिचय

संस्कृत भाषा में लिखित एक कविता का संक्षिप्त परिचय

संस्कृत भाषा में लिखित एक कविता का संक्षिप्त परिचय

संस्कृत भाषा में लिखित एक कविता का संक्षिप्त परिचय

संस्कृत भाषा में लिखित एक कविता का संक्षिप्त परिचय

'এবং মহুয়া' - বিশ্ববিদ্যালয় মঞ্জুরী আয়োগ (UGC-CARE)
অনুমোদিত তালিকার অন্তর্ভুক্ত।
২০২১সালে প্রকাশিত ৮৬পৃ.তালিকার ৬০ পৃ.এবং ৮৪পৃ.উল্লেখিত।

এবং মহুয়া

(বাংলা ভাষা, সাহিত্য ও গবেষণাধর্মী মাসিক পত্রিকা)

২৩তম বর্ষ, ১৩২ (ক) সংখ্যা

এপ্রিল, ২০২১

সম্পাদক

ড. মদনমোহন বেরা

সহসম্পাদক

পায়েল দাস বেরা

মৌমিতা দত্ত বেরা

যোগাযোগ :

ড. মদনমোহন বেরা, সম্পাদক।

গোলকুঁয়াচক, পোষ্ট-মেদিনীপুর, ৭২১১০১, জেলা-প.মেদিনীপুর, প.বঙ্গ।

মো.-৯১৫৩১৭৭৬৫৩

কে.কে. প্রকাশন

গোলকুঁয়াচক, মেদিনীপুর, পশ্চিমবঙ্গ।

U.G.C.- CARE List (2021) approved journal, Indian
Language-Arts and Humanities Group, out of 86 pages
placed in Page 60 & 84.

EBONG MAHUA

Bengali Language, Literature, Research and Referred with
Peer-Review Journal

23th Year, 132 (A) Volume

April, 2021

Published By

K. K. Prakashan

Golekuachawk, P.O.-Midnapur, 721101. W.B.

DTP and Printed By

K.K.Prakashan

Cover Designed By

Kohinoorkanti Bera

Communication :

Dr. Madanmohan Bera, Editor.

Golekuachawk, P.O.-Midnapur, 721101. W.B.

Mob.-9153177653

Email- madanmohanbera51@gmail.com /

kohinoor bera @ gmail.com

Rs 600

৫৭.মানবিক মূল্যবোধ গঠনে গান্ধীজীর সত্য ও অহিংসা নীতির প্রাসঙ্গিকতা :: সুমিত্রা মাহাত.....	৪৭২
৫৮.জাতি বৈষম্য নিরসনে সাংবিধানিক বিধিবিধান :: ড. তারক নাথ জাঁতুয়া.....	৪৮০
৫৯.ঋষিদে ধর্মনিরপেক্ষ চেতনা :: তপতী গায়ের.....	৪৮৭
৬০.সীওতালি ভাষা ও সাহিত্য বিকাশে পি.ও.বোডিং :: বাপি টুটু.....	৪৯২
৬১.সুনীতিকুমার চট্টোপাধ্যায়ের O.D.B.L. : বাংলা ভাষা চর্চার নানাদিক :: ড. স্বরূপ দে.....	৪৯৬
৬২.মহাভারতের নারী বিনির্মাণ : শীওলী মিত্রের 'কথা অমৃতসমান' :: সোনা মন্ডল.....	৫১০
৬৩.মহাশ্বেতা দেবীর উপন্যাসের আলোকে সীওতাল সম্প্রদায়ের ইতিবৃত্ত :: ড. অরুণাত মুখার্জী.....	৫২৩
৬৪.শিশু মনে স্বদেশ-ভক্তি ও স্বদেশ-প্ৰীতি জাগরণে বাংলা ছড়া :: ড. চিত্ত সেন পরামানিক.....	৫২৭
৬৫.বাংলাদেশের রাখাইন উপজাতির আর্থ-সামাজিক ও রাজনৈতিক জীবনধারা :: ড. রুমকি বোস (মজুমদার).....	৫৩২
৬৬.আন্তর্জাতিক রাজনীতির প্রেক্ষিতে বিশ্বায়ন ও উন্নয়ন :: মৃত্যুঞ্জয় পন্ডা.....	৫৪০
৬৭.লোকপাল ও লোকায়ুক্ত: তাত্ত্বিক পর্যালোচনা :: কৃষ্ণ কালি শঙ্কর সাউ.....	৫৪৬
৬৮.কথনসাহিত্যিক কণা বসু মিশ্রের উপন্যাসে নারী :: ড. শুক্লসম্ব বর্মণ.....	৫৫০
৬৯.অনিকেতভাবনা, নিপীড়ন এবং শোষণ: ভারতী মুখার্জীর Jasmine মিশ্র সাংস্কৃতিক পরিচয় সঙ্কটের উপন্যাস :: প্রদীপ কুমার বেরা.....	৫৫৮
৭০.সীওতালি ধারাবাহিক মৌখিক সাহিত্য :: ড. কিশন মুরমু.....	৫৬৫
৭১.আদিবাসী জীবন জীবিকা ও সংস্কৃতি : বিপন্নতার আলোকে :: রবীন্দ্রনাথ হাঁসদা.....	৫৭২
৭২.স্থানীয় রাজনীতির ক্ষেত্র বৃদ্ধি : প্রেক্ষিত আইন অমান্য আন্দোলন :: ড. সঞ্জয় ঢালী.....	৫৮২
৭৩.ইলেকট্রনিক বজ্য ও তার ব্যবস্থাপনা :: মধুসূদন গাঁড়াই.....	৫৯৪
০০লেখক পরিচিতি.....	৬০৪
০০০UGC-CARE list.....	৬০৮

মহাশ্বেতা দেবীর উপন্যাসের আলোকে সাঁওতাল সম্প্রদায়ের ইতিবৃত্ত

ড. অরুণাভ মুখার্জী

বাংলা সাহিত্য ধারায় মহাশ্বেতা দেবীর উপন্যাসের জগতে সাঁওতাল সম্প্রদায়ের জীবনলেখ্য একটি মাইলস্টোন হিসাবে ফুটে উঠেছে। সাঁওতাল সম্প্রদায়ের জীবন চর্চা, তথা জীবন ভাবনা উপন্যাসিক মহাশ্বেতা দেবী এতটা বহুবিস্ময়ভাবে চিত্রিত করেছেন যে, তা আর উপন্যাস থাকেনি - হয়ে উঠেছে জনজাতি উপজাতির জীবন্ত দলিল। আজও এই একবিংশ শতাব্দীর মুখে দাঁড়িয়ে যখন ভারতের মাটিতে অবমাননার নিয়ত নিবিড় উদ্ভাপ সঞ্চারিত করেছে জনৈতিক উন্নয়নের গাল ভরা প্রতিশ্রুতি, যখন ধাপে ধাপে, দফার পর দফা জনৈতিক কর্মসূচিকে রূপায়িত করার জন্য শীতাতপ নিয়ন্ত্রিত হোটেল গুলিতে আলোচনাচক্রের অনুষ্ঠান করতে করতে প্রশাসনিক আমলাদের রক্তচাপ ক্রমশ কমে পাচ্ছে, যখন ক্ষেতমজুরদের ন্যূনতম বেতন ধার্য করে তা কার্যকর করার জন্য জনপ্রিয় সরকারের মন্ত্রীদের চোখে ঘুম নেই - এমন এক কঠিন সময়েও সেই জনিতায় সংযুক্ত হয়নি দেশের লক্ষ লক্ষ আদিবাসী ও বিভিন্ন উপজাতি এবং বিভিন্ন প্রদেশের দুর্গম এলাকায় অবস্থিত হরিজনদের অস্তিত্ব। তাদের ভূমি নেই, ফল নেই, জল নেই, শরীরের পক্ষে ন্যূনতম প্রয়োজনীয় বস্তু লবণ নেই, নারীদের স্তন্যপান নেই, বেঁচে থাকার সার্থকতা নেই, সর্বোপরি নেই ভবিষ্যৎ। এদের বাঁচবার জন্য অবশ্য কিছু কিছু আইন আছে, ভালো ভালো প্রকল্প আছে, কিছু কিছু প্রতিশীল আমলাও আছেন। কিন্তু এই দুই মেরুর মধ্যবর্তী ভূগোলে দাঁড়িয়ে আছে এক দুর্জয় পাহাড় যা জোতদার - মহাজন - আমলাদের বহু শতাব্দী সঞ্চিত লোভ ও লালসার নির্মমতা ও হিংসার পাথর দিয়ে তৈরি। 'সুজলাং সুকলাং শীতলাং' ভারতবর্ষের এটিই আসল চেহারা; শিক্ষিত মধ্যবিত্তের লেখা কুলবা কলেজ পাঠ্য কবিতায়, গল্পে, গানে ও ইতিহাসে যা শেখানো হয়, এ তা নয়। প্রসিদ্ধ অর্থে এই ইতিহাসের প্রতি অনুরাগ আমাদের দেশের ডান ও বাম সব জনৈতিক দল নির্বিশেষে ঐকান্তিক অনুরাগ জন্মানোয় আছে, আগ্রহ আছে, কিন্তু বাস্তবায়িত আজও হয়নি। দেশের আসল ইতিহাস এত ভয়ংকর ভাবে নির্মম ও নিষ্ঠুর যে, তার মুখোমুখি হওয়ার সং সাহস দেখাতে কেউ সাহস পান না। তাই বহুতর আন্দোলনে আদিবাসী কৃষকের রক্ত ঝরলে আমরা অভিনন্দন জানাই,

ISSN 2319 – 8389, Vol : 43, Issue : 43

KHOAI
UGC Care Listed Journal
Art and Humanities
Tri - Annual Journal

KHOAI

A Collector on Literature and Culture

Chief Editor
Kishore Bhattacharya

VOLUME 43
9 May, 2021

SANTINIKETAN, BIRBHUM, PIN- 731235, W.B. INDIA

সূচীপত্র

সম্পাদকীয়

পারিবারিক সম্পর্কের বন্ধনে 'নৌকাডুবি'	-- অসীম কুমার মুখার্জী	৯
রবীন্দ্রনাথের 'নদী': একটি অন্তরঙ্গ পাঠ	-- শুভাশিস গোস্বামী	১৪
রবীন্দ্রসঙ্গীতে বাস্তবতা, সমাজ নৈতিকতা ও বিশ্বমানবতার শিক্ষা	-- অসীম কুমার রায়	১৯
মুর্শিদাবাদের সংস্কারময়ী প্রবাদ : সমীক্ষা ও মূল্যায়ন	-- নিবিড় কুমার ঘোষ	৩২
দারা শিকোর দার্শনিক ও আধ্যাত্মিক নিকটবর্তিতা	-- মহম্মদ ফায়েক, প্রদীপ রায়, দিগ্বিকী ওয়াসিম রহমান	৩৬
সত্যজিৎ রায় পরিচালিত চলচ্চিত্রে প্রতিফলিত লোকসংস্কৃতি	-- পুলক গঙ্গুলী	৪১
বোসাভ রাজসভার সাহিত্যে সূফী সাধনার প্রভাব	-- তনুকা চৌধুরী	৪৮
বাংলা চলচ্চিত্রে ব্যবহৃত লোকসংগীত ও লোকনৃত্য	-- ইতি পাল	৫৫
মূল্যবোধ শিক্ষা : প্রসঙ্গ মধ্যযুগের ইংরেজি সাহিত্য	-- বোসুমী পেড়িওয়াল	৬২
'বধুবংশম' মহাকাব্যে বিজ্ঞানচেতনা	-- সঞ্জয় মণ্ডল	৬৯
'দিবে আর নিবে, মিলাবে মিলিবে': শিক্ষার প্রাঙ্গণে বিশ্বায়ন	-- নারিসা সনম	৭২
সম্প্রদে জাতীয়তাবাদ : ঊনবিংশ ও বিংশ শতকে ভারত-		
মহাসাগরীর সমুদ্রবানিজ্যে স্বদেশী প্রয়াস ও পরিণতি	-- সৌমজিৎ মুখার্জী	৭৮
অবনীন্দ্রনাথ ঠাকুরের 'বুড়ো আংলা' : বাংলার সমাজ ও সংস্কৃতি	-- শুভঙ্কর ঘোড়ুই	৮৭
ছিলেক্তলান রায়ের খয়ালদা বাংলা গান	-- চন্দ্রানী দাস	৯৫
ভারতীয় রাগসঙ্গীত ও তাঁর উদ্দেশ্য	-- অরিন্দম সেন	১০৬
সূর্য-দীঘল বাড়ী : উপন্যাসে, চলচ্চিত্রে	-- জীর্ধ দাস	১১২
বাংলা কথাসাহিত্যে ঝাড়বণের জনজীবন	-- অনিবার্ণ সাহ	১১৬
শিক্ষার আভিনায় সর্ব লিঙ্গ সমন্বয় : লিঙ্গসমতার এক অধ্যায়	-- সূমেধা মুখার্জী ও উমাকান্ত প্রসাদ	১২৪
প্রগতি ও অগ্রগতি : ঊনিশ শতকে মেয়েদের জন্য বাংলা ভাষার পত্রিকা	-- সঞ্জিতা বসু	১৩৪
দূরস্থিত সংযোগ	-- ইন্দিরা দাশ	১৪৩
ইতিহাসের অন্তরালে ঊনিশ শতকের নিরিখে পট ও ব্রাত্য-		
জনগোষ্ঠী পটুয়া শিল্পীদের যাপন আখ্যানের আলোচনা	-- রাকেশ কৈবর্ত	১৪৭

পারিবারিক সম্পর্কের বন্ধনে 'নৌকাডুবি'

অসীম কুমার মুখার্জী

বঙ্গদ্রষ্ট প্রতিভার অমিত্যবী রথীন্দ্রনাথ ঠাকুর বাংলা সাহিত্যে এক সর্বজন বন্দিত নাম। দীর্ঘ আয়ুর বঙ্গদ্রষ্ট রথীন্দ্রনাথ বাংলা সাহিত্যে ভাষাবন্ধে করে গেছেন সমৃদ্ধ। ছেলেবেলা থেকে শুরু করে আমত্যা পর্যন্ত নিজের জীবনের কাহিনী-পরিবারের কাহিনী নানা রচনায় বাস্তব করেছেন। তিনি ছিলেন জোড়াসাঁকো ঠাকুর বাড়ির কর্মী সন্ন্যাসী। সকলের সঙ্গে ছিল তাঁর ঘনিষ্ঠ সম্পর্ক। ঠাকুরদা-ঠাকুরমা, দাদামশায়-দিদিমা, বাবা-মা, জ্যাঠা-জ্যাঠিমা, কাকা-কাকিমা, মাক-মাকি ভাই-ভাই, স্ত্রী-পুত্র-কন্যা ও সকল সম্পর্ক নিয়েই ছিল ঠাকুর বাড়ির অনন্দমহল। এই সম্পর্কের কথায় রথীন্দ্র উপন্যাস ও ছোট গল্পের কাহিনী নির্মাণের চয়নে ও বয়নে সাহায্য করেছে। অঙ্কন করেছেন এই পারিবারিক চিত্রে এক নির্মাণ শিল্প। যায় উৎকৃষ্ট প্রমাণ 'নৌকাডুবি' উপন্যাস। পারিবারিক সম্পর্কের বন্ধনে এই রচনার মূল প্রতিপত্তা বিষয়।

পিতা-পুত্র: ব্রজমোহন চৌধুরী ও রমেশ:-

'নৌকাডুবি' উপন্যাসের একটা গুরুত্বপূর্ণ চরিত্র ব্রজমোহন চৌধুরী। রমেশের বাবা। ব্রজমোহনের সক্রিয়তা উপন্যাসে নগ্ন। কিন্তু পিতা হিসেবে রমেশের জীবনের একমাত্র ভাগ্য বিধাতা। ভাগ্য নিয়ন্ত্রাণ্ড বলা যায়। রমেশের আইন পরীক্ষা সমাপ্ত করে বাড়ির উদ্দেশ্যে বণনা দেওয়ার কথা। কিন্তু তোরঙ্গ সাজাবার কোনো উৎসাহ তার দেখা যায়নি। একিঙ্কে বাড়ি আসার জন্য পিতা বরবার তাকে চিঠি লিখেছে। রমেশের উত্তর পরীক্ষার ফল বেবশেই বাড়ি ফিরবে। অস্বস্তিকর হলে বেসেভের বসায় জমজমট চায়ের আসরে বেহারা একখানি চিঠি রমেশের হাতে ধরিয়ে দিয়ে চলে গেল। চিঠি পড়ে শশবস্ত্র হয়ে পড়লে সকলেই রমেশকে জিজ্ঞাসা করলেন এত ব্যস্ততার কারণ কি। রমেশ বলল, "বরা দেশ হইতে আসিয়াছেন।" ব্রজমোহনবাবু পুত্রকে বললেন কালকেই দেশে যেতে হবে। কেন কোনো জরুরী কাজ আছে? পিতা বলিলেন, "এমন কিছু গুরুতর নহে।" পরের দিন ভোরের ট্রেনেই পিতা-পুত্র বাড়ির উদ্দেশ্যে যাত্রা করল।

বাড়ি পৌঁছে রমেশ বরব পেল তার বিবাহের পাট্রী এবং দিন দুটোই স্থির হয়ে গেছে। ব্রজমোহনের বলাবলু ঈশানের একমাত্র কন্যা রমেশের হবু স্ত্রী। কৃতজ্ঞতা বশত এই কন্যাকে পুত্রবধু করার অসীকার করেছেন ব্রজমোহন বাবু। কারণ যখন তার আর্থিক দুরবস্থা চলছিল তখন এই ঈশানের সাহায্যেই উত্তরণ। আজকে যে বাড়িবাস্ত্র তা-ও নাকি ঐ ঈশানের জ্ঞানই। তাই তার মৃত্যুর পর তার অসহায় স্ত্রী ও কন্যার প্রতি দায়বদ্ধতা থেকেই সম্বন্ধ সম্পর্কে প্রশ্ন তুললে ব্রজমোহনবাবু বলেন-- "ও সকল কথা আমি ভালো বুঝি না-- মানুষ তো ফুল কিংবা প্রজাপতি মত্রে নয় যে দেখার বিচারটাই সর্বাগ্রে তুলিতে হইবে। মেয়েটির মা যেমন সতী সাধী, মেয়েটিও যদি তেমনই হয়, তবে রমেশ যেন তাহাই ভাগ্য বলিয়া জ্ঞান করে"।

বিবাহের কথায় রমেশের মুখ শুকিয়ে গেল। মনে মনে সাহস জুগিয়ে একবার বিবাহের অসম্মতির কথা

वर्ष : 2020

अंक : 14

ISSN: 2231-0525

संवाद

PEER REVIEWED YEARLY RESEARCH JOURNAL



ENLIGHTENMENT TO PERFECTION

हिन्दी विभाग
उत्तर बंग विश्वविद्यालय
राजा राममोहनपुर
दार्जिलिंग - 734013

संवाद

PEER REVIEWED YEARLY RESEARCH JOURNAL

वर्ष : 2020 ISSN : 2231-0525 अंक : 14

: संपादक :

डॉ. सुनील कुमार द्विवेदी



ENLIGHTENMENT TO PERFECTION
Accredited by NAAC with Grade 'A'

हिन्दी विभाग
उत्तर बंग विश्वविद्यालय
दार्जिलिंग-734013

भूमंडलोत्तर हिमाचली जीवन और एस. आर. हरनोट की कहानियाँ

.गीतम सिंह राणा

समकालीन हिंदी कहानीकारों में एस. आर. हरनोट का नाम कोई परिचय का मोहताज नहीं है। ये हिमाचल प्रदेश की पार्वत्य-पृष्ठभूमि पर विपुलता के साथ लिखनेवाले एक ऐसे महत्वपूर्ण कहानीकार हैं, जिनकी कहानियों से गुजरते हुए आप अनायास ही बदलते समय के साथ पिछले चार दशकों की हिमाचली धड़कनों को महसूस कर सकते हैं। साथ ही समय के विकास के तदंतर हिमाचली पार्वत्य समाज में बढ़ती मूल्यहीनता को भी इनकी कहानियों के कैनवास पर बड़ी स्पष्टता के साथ चित्रित देख सकते हैं। बीसवीं सदी के नवें दशक से निरंतर सृजनरत इस कथाकार के अब तक कुल आठ कहानी संग्रह-‘पंजा’, ‘आकाशबेल’, ‘पीठ पर पहाड़’, ‘दारोश तथा अन्य कहानियाँ’, ‘जीनकाठी तथा अन्य कहानियाँ’, ‘मिट्टी के लोग’, ‘लिटन ब्लॉक गिर रहा है’ तथा ‘कीलें’ प्रकाशित हो चुकी हैं। आठ कहानी संग्रह के अतिरिक्त इनके द्वारा रचित एक उपन्यास ‘हिडिम्ब’ एवं हिमाचल की संस्कृति और जनजीवन पर पाँच महत्वपूर्ण पुस्तकों - ‘हिमाचल के मंदिर और उनसे जुड़ी लोक कथाएँ’, ‘यात्रा’, ‘हिमाचल से जान पहचान’, ‘हिमाचल एट ए ग्लास (संयुक्त कार्य) तथा ‘हिमाचल प्रदेश: मंदिर और लोकश्रुतियाँ’ का भी प्रकाशन हो चुका है। हिमाचल प्रदेश के पार्वत्य क्षेत्र के चनावग गाँव(जिला.शिमला) में जन्मे इस कथाकार ने हिंदी-पाठकों के मन को अपनी कहानियों के मार्फत सबसे ज्यादा आंदोलित किया है क्योंकि बचपन से लेकर अपनी समझदारी की उम्र तक इन्होंने जिस नैसर्गिक-सौन्दर्य-संपन्न पहाड़ी जीवन को जिया और साथ ही उसके खुरदुरे यथार्थ को अनुभूत किया, उसे इन्होंने जस का तस बड़ी कोमलता के साथ अपनी कहानियों में रख दिया है। यही कारण है कि इनकी कहानियों की पृष्ठभूमि के महत्व पर बात करते हुए ज्ञानरंजन कहते हैं -“एक जबर्दस्त पराजय और वियावान के बीच जहाँ साहित्य, संस्कृति विकास, व्यवस्था, सत्ता प्रशासन, सबकुछ लुप्त हो गया है और जहाँ मासूम बच्चे और असहाय वृद्ध ही बचे हैं, ऐसे भूखंडों में हरनोट ने अपनी रचना को केन्द्रित करने का प्रयास अपनी कहानियों के माध्यम से किया है।”

भारत के सन्दर्भ में जब भी पार्वत्य समाज की बात की जाती रही है, तभी हमारे जेहन में उसकी स्थानीय लोक संस्कृति पूरे वजन के साथ प्रस्तुत होती रही है और उस लोक संस्कृति की सबसे बड़ी खासियत उसका मानवीय व प्राकृतिक मूल्यबोध के साथ

काफी गहराई तक जुड़ा हुआ होना रहा है। रहा है कहने का तात्पर्य है कि मशीनी सभ्यता के विकास के बरक्स यह जुड़ाव कम हुआ है। कम क्या खात्मे की ओर ही अग्रसर है। इसका मूल कारण मशीनी सभ्यता के विकास की आड़ में पहाड़ तक पहुँची पूँजीवादी मानवीय मूल्यबोधहीन शक्तियों का पार्वत्य समाज को अपनी जकड़ में ले लेना व अधिकाधिक धन उगाहने के लालच में पूरे पहाड़ का अंधाधुंध दोहन करना है। इसके कारण पूरे पार्वत्य अंचल का समाज, संस्कृति व प्रकृति छतरे में पड़ चुकी है। हिमाचल का पार्वत्य अंचल इसका अपवाद नहीं है। मशीनी सभ्यता के बड़े कदम के बरक्स इसके समाज व संस्कृति में निहित मानवीय व सांस्कृतिक मूल्यबोध में दरकन स्पष्टतः देखी जा सकती है। इस सन्दर्भ में एस. आर. हरनोट की कहानियों का अनुशीलन बहुत ज़रूरी है।

पहाड़ पर पहुँची आधुनिकता व मशीनी सभ्यता का सबसे ज्यादा प्रभाव वहाँ की पारिवारिक संरचना की मजबूत बुनावट पर पड़ा है। इसने पारिवारिक बुनावट के तंतुओं को जार-जार कर देने का काम किया है, जिससे पारिवारिक संरचना के अंग छिन्न-भिन्न होकर अलग-थलग कराहते तज़र आ रहे हैं। आधुनिकता के सम्मोहन ने पड़े-लिखे पहाड़ी युवाओं को शहर की ओर उन्मुख कर दिया है। शहरी वातावरण में पढ़-लिखकर वे वहाँ की सुख सुविधाओं के जुगत की अंधी दौड़ में इस तरह शामिल हो गए हैं कि वे अपने पहाड़, पहाड़ीपन, पहाड़ी संस्कृति और साथ ही केवल उनके ही आसरे पहाड़ पर पड़े हुए वृद्ध अभिभावक तक से दूर हो गये हैं। इससे पहाड़ पर अपनी जिन्दगी बसर करनेवाले वृद्ध और शहर की आधुनिकता के फौस में फँसा युवा दोनों ही एक दूसरे से कटे छटपटाहट में जीवन व्यतीत कर रहे हैं। इस परिस्थिति का दंश पहाड़ से लगाव रखनेवाले वृद्धों को ज्यादा झेलना पड़ रहा है। इस सन्दर्भ में हरनोट की 'बिल्लियाँ बतियाती हैं', 'कागभाखा', 'मोबाईल', 'मिट्टी के लोग', 'जूजू' आदि कहानियाँ काफी महत्वपूर्ण हैं।

'बिल्लियाँ बतियाती हैं' हिमाचल की पार्वत्य पृष्ठभूमि पर लिखित एक ऐसी कहानी है, जिसमें कहानीकार ने पार्वत्य ग्रामीण परिवेश व शहरी परिवेश के मध्य मानवीय मूल्यबोध की दृष्टि से आये फर्क को बयां किया है। साथ ही आधुनिकता की दस्तक से पार्वत्य समाज की बुनावट-बुनावट में जो दरकने आई हैं, उनका भी चित्रण किया है। इस बात की सच्चाई से कोई भी मुकर नहीं सकता कि भोगवाद की बढ़ती लिप्सा और उसके तदंतर प्रायोजित सांप्रदायिकता, राजनैतिक प्रपंचों के कारण शहर हिंसा, दंगे-फसाद की गिरफ्त में आ चुके हैं। यह शहर में मानवीय मूल्यबोध के पतन को बयान करता है, जबकि इसकी तुलना में पार्वत्य गाँव में शांति-सद्भाव है। इसका मूल कारण पहाड़ों तक मशीनी सभ्यता का देर से पहुँचना है। इस सन्दर्भ में कहानी की मुख्य पात्र 'देवरू काकी' के

मनोभाव को व्यक्त करनेवाला कथन द्रष्टव्य है - शहर में कितनी बेचैनी बढ गई है। रोज कुछ-न-कुछ घटता ही है। दंगे-फसाद होते हैं, लाठियां-गोलियां चलती हैं। इन सभी के बीच उसके बेटे-बहू कैसे रहते होंगे। पोतू कैसे स्कूल जाता होगा। इसलिए अम्मा को अपना गाँव बड़ा भला लगता है। कहीं कुछ नहीं घटता। शांति है। चैन है। पर पहाड़ पर पहुँची मशीनी सभ्यता की मानवीय मूल्यबोधहीन मानसिकता ने वहाँ की शांति को नष्ट करना शुरू कर दिया है। पहाड़ पर रहनेवाला साधारण किसान खेती-मजदूरी करके, जरूरत पड़ने पर कर्ज लेकर, अपनी जमीन को रेहन पर रखकर भी अपने बच्चों को शहर में बड़ी-बड़ी डिग्रियों को दिलाने के लिए पढा तो रहा है, पर जब उन बच्चों को नौकरी मिल जा रही है तो वे शहर के ही तौर-तरीकों के मोहपाश में बंधे पहाड़ पर अपने वृद्ध अभिभावकों को छोड़ वहीं बस जा रहे हैं। इससे पहाड़ पर बसे ग्रामीण वृद्ध अभिभावकों की दशा बड़ी इतनीय होती जा रही है। इस सन्दर्भ में कहानी की पंक्तियाँ हैं - "उसके पिता की जिद रहती कि एक ही बेटा है, इसे अफसर नहीं बनाया तो हमारा कमाना व्यर्थ है। उसे खूब पढाया-लिखाया। हजारों कर्जा सर पर ले लिया। एक-दो खेत रेहन रख दिये। कॉलेज पूरा हुआ तो नौकरी भी लग गई। लेकिन उन बूढ़ों को यह भनक भी नहीं लगी कि शहर के तौर-तरीकों और चटक ने उसे उन दोनों से बहुत दूर कर दिया है।"

आधुनिकता और मशीनी सभ्यता की दस्तक ने सौहार्द-सम्पन्न पार्वत्य समाज में किस प्रकार विष घोलने का कार्य किया है, उसका मंजर हरनोट की 'कागभाखा' कहानी में देखने को मिलता है। इस कहानी की प्रमुख पात्र दादी आज के पक्षी-विज्ञानी सलीम अली की तरह कौवों की भाषा समझती है, जो पार्वत्य प्रदेश के मानव-मानवेतर संवेदनात्मक सम्बन्ध को दर्शाता है। कहने का तात्पर्य है कि मानवीय संवेदना की गहरी पैठ पार्वत्य ग्रामीण प्रदेशों की खासियत रही है। आधुनिकता के सम्मोहन में यह प्रदेश भी संवेदनहीन होता जा रहा है, जो इसके प्राकृतिक चरित्र के एकदम विपरीत है। जहाँ दादी जैसे लोगों का निवास है, जिसमें संवेदना इतनी घनी है कि वह मानवेतर तक के साथ भावनात्मक संबंध स्थापित कर पाती है, वहाँ भी यह ऋणात्मक परिवर्तन लक्षित हो रहा है। इस सन्दर्भ में दादी के मनोभाव को व्यक्त करनेवाली कहानी की ये पंक्तियाँ द्रष्टव्य हैं- "आज का समाज देखकर दादी भीतर ही भीतर कूडती है, जलती है, फूंकती है। जैसे गाँव ही बदल गया। पहले जैसे लोग नहीं रहे, दया, धर्म खत्म हो गया। ममता नहीं रही। एक-दूसरे के लिए अनजान बन गए। छोटी-छोटी बातों पर लड़ते-झगड़ते हैं। मारपीट करते हैं। भला-बुरा बोलते हैं।"

पहले कितना प्यार था। मिलजुल कर लोग आपस में रहते, एक-दूसरे के दुःख-सुख में आते-जाते, जैसे एक ही घर हो, एक ही परिवार हो।”

हिमाचल का पार्वत्य प्रदेश नैसर्गिक सौन्दर्य से सम्पन्न है, परंतु इस सौन्दर्यमय आवरण के तले निहित खुरदुरे यथार्थ को भी झुठलाया नहीं जा सकता है। देश में आजादी के बाद बनी सरकारों की नीतियों के कारण इन क्षेत्रों का समुचित विकास नहीं हो पाया है। आज भी पहाड़ के दूर-दराज के क्षेत्रों में गरीबी मुँह बाएँ खड़ी दिखती है। बतौर पेशा है। यहाँ के कुछ गरीबों को भिक्षावृत्ति ही चुनना पड़ता है। पूँजीवादी सोच के प्रतिनिधि के रूप में पहुँची मोबाईल कंपनियों के लोग यहाँ भी अपना पड़यंत्र रचने में सफल रहते हैं। अधिकाधिक मुनाफा कमाने की भूख ने उन्हें संवेदनहीन बना दिया है। वे इन क्षेत्रों में भी अपना उत्पाद बेचने और यहाँ की सीमित जनसंख्या को भी अपने गिरफ्त में लाने का काम करते हैं। इसके लिए वे गरीब भिखारी बच्चों तक के शरीर को अपने विज्ञापनों का वाहक बनाते हैं क्योंकि पहाड़ के इन दुर्गम प्रान्तों में यातायात की सुविधा के विकास के अभाव में उनका प्रचार महँगा पड़ जाता है, जबकि नन्हों का शरीर अपेक्षाकृत बहुत सस्ता पड़ता है। इसलिए वे संवेदनहीन होकर नन्हें बच्चों का भी अपने प्रचार माध्यम के रूप में बेझिझक उपयोग करने लगे हैं। अपने लुभावने प्रचार के मार्फत वे अपने उत्पाद रूपी अफीम का स्वाद पहाड़ की बेचारी भोली-भाली जनता को भी एक बार चखाना चाहते हैं, ताकि एक बार उनके चंगुल में फँसे ग्राहकों का आजीवन आर्थिक दोहन किया जा सके। इस मन्दर्भ को हरनोट की 'मोबाइल' कहानी प्रस्तुत करती है। इस तरह के प्रकरण को देखते हुए हरनोट अपनी इस कहानी में कहते हैं - "उस मोबाईल कम्पनी ने पहाड़ों के दूरदराज के इलाकों तक पहुँचने की जद्दोजेहद में अब भोले-भाले लोगों और उनके बच्चों का पुरजोर इस्तेमाल करना शुरू कर दिया था। लेकिन लोगों के पास यह सोचने का समय ही नहीं था कि यह घुसपैठ, बाजार को उनकी बहू-बेटियों के कमरों तक ले जा रही है।”

आधुनिक मशीनी सभ्यता के विकास ने मानव को अपार सुख सुविधायें प्रदान की हैं और साथ ही बढ़ती जनसंख्या के बरक्स जन्मी खाद्य संकट की समस्या का समाधान भी किया है; पर पहाड़ी ग्रामीण पारंपरिक मजदूरों के जीवन को बड़ा कष्टमय भी बना दिया है। हरनोट ने अपनी कहानी 'मिटटी के लोग' का विषय इसी को चुना है। हिमाचली पार्वत्य ग्रामीण प्रदेश में पहले से मौजूद सामंतवाद ने किसान-मजदूरों का शोषण तो किया ही था, पर बाद में वहाँ पहुँचे मशीनी विकासवाद के दैत्यों ने वहाँ के किसान-मजदूरों के जीवन को लीलना ही शुरू कर दिया है। उसके एक मंजर को बयान करते हुए कहानीकार अपनी कहानी के मुख्य पात्र मिटटी के घर बनाकर अपना पेट पालनेवाले 'बालदू' के बारे में

कहता है. "आज बालदू बेकार है। उसके हाथ में बेशक वही हुनर है। दक्षता है। महारत है। पर काम नहीं है। चंद सालों में क्या कुछ नहीं हो गया है। सब कुछ बदल गया है।" केवल पारंपरिक मजदूरी ही नहीं बल्कि पार्वत्य घरेलू उद्योगों पर भी मशीनी सभ्यता का नकारात्मक प्रभाव पड़ा है। हिमाचल के पार्वत्य ग्रामीण प्रदेश में बकरी-भेड़ों के बाल-ऊन से खारचे-पट्टू शाल बनाने के घरेलू उद्योग का प्रचलन हमेशा से रहा था। इन उद्योगों पर पहाड़ी जनसंख्या का कुछ भाग तो प्रत्यक्षतः निर्भर था और कुछ लोगों के लिए यह थोड़ा बहुत अतिरिक्त आमदनी का साधन हुआ करता था। पर आधुनिक मशीनी सभ्यता के आगमन ने, उसके मन लुभावन प्रचारों ने भोले-भाले पहाड़ी लोगों के स्वाद को बदलने और अपने उत्पादों को खपाने में सफलता हासिल की, जिसका परिणाम यह हुआ कि पहाड़ी घरेलू उद्योग के उत्पादों की माँग घटती गई और उससे जुड़े मजदूर बेकार होते गये। ऐसे ही एक प्रकरण का उल्लेख करते हुए हरनोट अपनी कहानी के पात्र 'रामेशरी चाची' की आर्थिक बदहाली के कारण को बताते हुए कहते हैं - "एक ज़माना था जब रामेशरी चाची बकरियों की बकराथा(बाल) निकाल कर उनके खारचे (गर्म दरियाँ) बना कर बेचा करती थी। भेड़ों की ऊन निकाल कर खुद पट्टू-शालों के लिए कातती भी थी और बेच भी दिया करती थी। दाम भी बहुत अच्छे मिल जाते थे। पर आज तो मशीनों से बनी चीजों का जमाना है। भेड़-बकरियों की ऊन और बालों की कद्र अब कहाँ रही।"

हिमाचली पार्वत्य ग्रामीण समाज में महिलाओं द्वारा अपने शिशुओं को लस्सी या मक्खन के बीच रत्तीभर अफीम चटा देने का प्रचलन था। वहाँ के लिए यह एक आम घटना थी क्योंकि ऐसा करने से शिशु पल भर में खेलते-खेलते ऊँघते और फिर पाँच-छः घंटों तक के लिए सो जाते थे, जिससे गृहणियों को घरेलू काम व पालतू मवेशियों को चारा-पानी देने का अवकाश मिल जाता था। सबसे बड़ी बात तो यह है कि इससे शिशु के शारीरिक व मानसिक स्वास्थ्य पर और साथ ही मातृत्व की घनी संवेदना पर इसका कोई प्रतिकूल प्रभाव नहीं पड़ता था। पर जबसे आधुनिकता ने पार्वत्य ग्रामों में दस्तक दी है, तब से इस संवेदना में क्षरण लक्षित होने लगा है। आधुनिकता के सम्मोहन में चटक दिखने व फिगर मेंटेनेंस की भावना के कारण मातृत्व की संवेदना का क्षरण होने लगा है। शिशुओं को बचपन से ही उनके पौष्टिक आहार मातृ-दुग्ध से दूर करने का काम शुरू हो गया है, जिससे शिशुओं के शारीरिक-मानसिक स्वास्थ्य पर बुरा प्रभाव पड़ रहा है। सबसे ज्यादा सोचनीय स्थिति तो यह है कि अब पार्वत्य समाज से जुड़े लोगों के घरों में भी अफीम का स्थान दूरदर्शन के कार्टूनो ने ले लिया है। अब गृहणियाँ फुर्सत के पल निकालने के लिए शिशुओं को अफीम चटाने के बजाय दूरदर्शन का रिमोट पकड़ा देती हैं, जिसका उनके शारीरिक व

मानसिक स्वास्थ्य पर बहुत ही बुरा प्रभाव पड़ रहा है। हरनोट ने अपनी 'जूजू' कहानी में इसी प्रसंग को विषय बनाया है। कहानीकार ने इसमें बुद्धू बक्से के कार्टून की लत लग चुके शिशुओं को मनोवैज्ञानिक रोगी के रूप में दर्शाया है, जिसके लक्षण घर पर दूरदर्शन के खराब हो जाने पर प्रकट होने लगते हैं। शिशु खाना-पीना छोड़कर रोने लगता है क्योंकि शिशु की मनोवैज्ञानिक जरूरतें पूरी नहीं हो पाती हैं, जो उस उम्र में उनके लिए सबसे अधिक आवश्यक है। कहानी में एक महीने से खराब तबियत वाले शिशु का इलाज करनेवाला डॉक्टर जब पर्ची में लिखकर देता है, "मैंने पर्ची पर दवाई नहीं लिखी है: शो हिम् जूजू एंड गेट योर चाइल्ड ओके।" तब आधुनिकता के सम्मोहन के कारण फैले इस रोग की भयानकता सामने प्रकट होती है।

पार्वत्य प्रदेश की लोक संस्कृति सदैव लोक-प्रकृति मैत्री का पर्याय रही है। यहाँ की संस्कृति के अंतर्गत आनेवाले रीति-रिवाज, व्रत-त्योहार, जीवन-पद्धति, रहन-सहन आदि विभिन्न अंग गहन प्रकृति मूल्यबोध से जुड़े रहे हैं। पर इस प्रदेश में मशीनी सभ्यता के कदम पड़ते ही लोक-प्रकृति के बीच का संतुलन गड़बड़ा गया है। मशीनी सभ्यता के 'टूल्स' ने पार्वत्य प्रदेश की प्रकृति पर इतने गहरे चोट किये हैं कि उसमें दरकनें आ गई हैं। ये दरकनें भविष्य में पुरे पहाड़ पर आनेवाले विनाशकारी संकट के संकेत हैं। पहाड़ का पूरा सौन्दर्य उसके प्राकृतिक संतुलन पर आश्रित है और इस संतुलन को बनाये रखने का श्रेय पहाड़ी संस्कृति को जाता रहा है। पर आधुनिक मशीनी आकर्षक सभ्यता के आवरण तले पहाड़ तक पहुँची पूँजीवादी मानसिकता ने उस संस्कृति में क्षरण ला दिया है, जिसका सबसे ज्यादा विनाशकारी प्रभाव पहाड़ के प्रकृति-पर्यावरण पर पड़ने लगा है। पहाड़ पर पहुँची पूँजीवादी शक्तियों ने अधिकाधिक धन कमाने के लोभ से ग्रसित होकर पहाड़ का अंधाधुंध दोहन शुरू कर दिया है। इन शक्तियों ने सत्ता से साँठ-गाँठ करके अपने काम को अंजाम देना शुरू कर दिया है। बेचारी पहाड़ की सीधी सरल जनता इनकी कारस्तानियों को समझ नहीं पा रही है और जो पढ़े लिखे समझदार लोग इस पड़यंत्र को समझ भी रहे हैं, वे इस साँठ-गाँठ की शक्ति के आगे निरीह बने हुए हैं। बीच-बीच में ये संगठित होकर इसका विरोध तो कर रहे हैं पर पूँजीवादी शक्तियाँ बड़ी चालाकी से इनसे निपटकर दोहन के नित-नवीन तरीके इजाद करने में सफल होती जा रही हैं, जिससे पूरा पहाड़ संकट के सम्मुखीन है। हिमाचल का पार्वत्य प्रदेश भी इस संकट से गुजर रहा है। हरनोट अपने समय और परिवेश के सजग प्रहरी हैं। उनकी सजग आँखें इन सभी घटनाओं पर ध्यान केन्द्रित किये हुए हैं। वे खतरे में आए पहाड़ और पहाड़ीपन को बचाने के निमित्त अपनी कहानियों के मार्फत मानवीय तथा प्राकृतिक मूल्यबोध को बचाये रखने की कवायद कर रहे हैं और

साथ ही साथ इसको विनष्ट करने वाले तत्वों तथा शक्तियों की पहचान लोगों को करवाते जा रहे हैं। इस सन्दर्भ में इनकी 'माफिया', 'बेजुबान दोस्त', 'नदी गायब है', 'आभी', लोग उल्लेखनीय हैं।

एस. आर. हरनोट कृत 'माफिया' कहानी हिमाचल के जंगलायत में तैनात सरकारी अफसरों, नेता तथा मंत्री के मिलीभगत से वन तथा वन्य पशुओं के गैरकानूनी ढंग से किये गये दोहन पर आधारित है। कहानी में यह दर्शाया गया है कि किस प्रकार नेता-मंत्रीगण पर्यावरण तथा वन्य जीव संरक्षण की खोखली डींगे हाँकते हैं, जबकि वास्तव में ये ही पार्वत्य प्रदेश के वन को काटकर तथा वन्य पशुओं को मारकर गैरकानूनी ढंग से इनकी खरीद-फरोख्त में लिस हैं और इसके लिए वे प्रशासन को अपनी पूंजी और चालाकी के दम पर ढाल के रूप में उपयोग करते हैं। कहानीकार इस गोरख-धंधे से जुड़े हर एक शख्स को माफिया ही घोषित करता है। इस माफियागिरी के धंधे की सबसे बड़ी खासियत है कि इसमें नेता, मंत्री तथा प्रशासन एक तंत्र के रूप में कार्य करते हैं। कहानी का सबसे महत्वपूर्ण स्थल वह है जहाँ मंत्री जी मोर-मोरनी के निवास स्थान मोरनी-धार को राष्ट्रीय उद्यान घोषित करने के उद्घाटन में आते हैं और उनकी आवभगत में उनके कारिंदे मोरनी को ही मारकर उसके मौस को अनूठे व्यंजन के रूप में पेश करते हैं; जिसकी खबर मंत्री सहित वहाँ मौजूद उसके तंत्र को है। कहानी का पात्र चुन्नी जो एक आठ वर्षीय बालक है, जब मोर की थाह लेने की कोशिश करता है तो उसे बताया जाता है कि मोरनी बीमार है। पर इसके बाद मंत्री और उनके कारिंदों की प्रतिक्रिया विस्मय में ढाल देनेवाली होती है। कहानीकार उनके दोहरे चरित्र का पर्दाफाश करते हुए कहता है - "चुन्नी ने आश्चर्य से उसकी तरफ देखा-वह हँस रहा था। उसका उत्तर कुछ दूसरे जंगलायत के कर्मचारियों ने भी सुन लिया था। उन्होंने एक ठहाका लगाया।" वास्तव में उनका यह सम्मिलित दर्प भरा ठहाका वन तथा वन्य पशुओं के गैरकानूनी दोहन के बरक्स उनका अपनी कारसाजी में सफल होकर समाज को ठेंगा दिखाने जैसा ही है।

पहाड़ी जंगल वाले ज़मीन अमूमन 'डोलोमाइट' तथा चूने पत्थर की पर्याप्त उपलब्धता वाली ज़मीन होती है। उस पर पूंजीपतियों का विशेष ध्यान रहता है क्योंकि वे क्षेत्र सीमेंट उद्योग की स्थापना के सबसे अनुकूल केंद्र होते हैं, जबकि ऐसे उद्योगों की स्थापना वहाँ की प्रकृति तथा पर्यावरण को बहुत अधिक क्षति पहुँचाने वाली होती है। बावजूद इसके पूंजीवादी शक्तियाँ मोटा धन खर्च कर सरकारी व्यवस्था तथा सत्ता को अपने षडयंत्र में शामिल करने में सफल हो जाती हैं। इसके लिए सरकार पहाड़ की भोली-

भाली जनता को विकास, रोजगार सृजन तथा आरामदेह जीवन देने का लालच देकर उनकी जमीनों को बहुत ही अदना-सा मूल्य देकर पूंजीपति-कम्पनियों को सौंप देती है। जो ज़मीन-खेती प्रेमी किसान अपनी ज़मीन देने से मुकरते हैं, वे भी सीमेंट उद्योग के शुरू होने पर उससे बड़ी मुसीबतों का सामना करने में अक्षम होकर जमीन देने के लिए बाध्य हो जाते हैं। हरनोट हिमाचली पार्वत्य पृष्ठभूमि में होनेवाली इस कारसाजी से लड़ने में अक्षम किसानों की मुसीबत को अपनी कहानी 'बेजुबान दोस्त' में बयां करते हुए कहते हैं - "जिन किसानों ने ज़मीनें नहीं दी थीं, उनकी मुसीबत भी कम नहीं थी। सीमेंट के लिए जिस पहाड़ी से पत्थर जाता, वहाँ दिन-रात ब्लास्ट होते रहते। उनसे कई मकानों में दरारें आ गई थीं। कुछ मकान तो गिर ही गए थे। मुआवज़े के नाम पर किसानों को आधी रकम भी नहीं मिल पाती थी।"¹⁰ पूंजीपति अधिकाधिक मुनाफ़ा कमाने के लोभ से ग्रसित होकर किस प्रकार पूरे पहाड़ के प्राकृतिक संतुलन को खत्म करने को आतुर हो चुके हैं और इसमें किस प्रकार पूरी व्यवस्था उनके षडयंत्र की भागीदार बनी हुई है; कहानीकार इस सच्चाई को इस कहानी में बयान करते हैं। साथ ही आनेवाले समय में पूरे पहाड़ के खतरे में आने का संकेत भी देते हैं। पहाड़ पर इस तरह का पर्यावरण संकट पैदा करनेवाली कम्पनियाँ किस प्रकार पर्यावरण प्रेमी होने का ढोंग रचती हैं, उसका चित्रण भी इस कहानी में मिलता है। उनके इस दोहरे चरित्र का पर्दाफ़ाश करते हुए कहानीकार कहता है - "पर्यावरण दिवस पर तो वे ज्यादा ही सक्रिय रहते। करोड़ों रुपये खर्च कर देते क्योंकि वे जानते थे कि फैक्ट्री लगाने से पहले पूरे प्रदेश में पर्यावरण प्रदूषित होने के डर से उनका विरोध होता रहा था।"¹¹ इसी प्रकरण पर केन्द्रित हरनोट की एक दूसरी कहानी 'लोग नहीं जानते थे उनके पहाड़ खतरे में हैं' भी है, जिसमें कहानीकार ने पूंजीवादी शक्ति और सत्ता के साथ पहाड़ों के शोषण में पूल की तरह काम करनेवाले स्थानीय सामंत, ठेकेदार, नेता के असल चरित्र का पर्दाफ़ाश किया है। सीमेंट कंपनियों के विकास के मार्फत पहाड़ी क्षेत्र के विकास के जो खोखले वादें सरकार और कम्पनी के लोग करते हैं, उसकी सच्चाई को बयान करते हुए कहानीकार कहानी के पात्र जीवन के माध्यम से कहता है - "उसे मालूम था कि जिन-जिन जगहों पर पहले इस तरह के कारखाने लगे हैं और प्राइवेट यूनिवर्सिटियाँ बनी हैं, उनकी वजह से पर्यावरण को भारी नुकसान पहुँच रहा है।.....ये लोग कंपनियों और सरकार के बीच पूल का काम किया करते, जिस पर उनके अपने स्वार्थ और सम्पन्नता की गाड़ियाँ बिना धुआँ उगले चुपचाप दौड़ती रहतीं।"¹²

पार्वत्य प्रदेश में बहनेवाली छोटी-बड़ी नदियाँ वहाँ निवास करनेवाले लोगों के लिए जीवन रेखा होती हैं। खासकर हिमाचल की नदियाँ तो 'ग्लेशियर' से पिघलकर प्राप्त

जल का महत्वपूर्ण स्रोत हैं। इन नदियों से ही वहाँ के लोगों को पेय जल की प्राप्ति होती है, मवेशियों को भी इसी जल के सहारे पाला जाता है और साथ ही इसी जल पर वहाँ का कृषि कार्य भी आश्रित है। इसके अतिरिक्त जल का यह बहाव पूरे पार्वत्य प्रदेश को एक संतुलन प्रदान किये हुए है। पर आधुनिक मशीनी सभ्यता के विकास ने इनका भी अंधाधुंध दोहन कर मुनाफ़ा कमाने का काम शुरू कर दिया है। पूंजीपति बड़ी चालाकी और अपनी धन की शक्ति से सारे पर्यावरणीय नियम-कानूनों को दरकिनार कर पहाड़ पर जल विद्युत उत्पादन केंद्र खोलने की अनुमति व्यवस्था से लेने लगे हैं। उनका ध्यान सिर्फ़ मुनाफ़ा कमाने पर आश्रित है। वे नदियों के जल को कृत्रिम जलाशय या सुरंग बनाकर उसमें एकत्रित करते हैं और उसका उपयोग जल विद्युत-उत्पादन के लिए करते हैं। इसके लिए ज़रूरत पड़ने पर वे पहाड़ के कुछ हिस्सों को 'डायनामाइट' से फोड़कर नदियों का रास्ता तक बदल दे रहे हैं, जिससे पहाड़ के लोगों का जीवन तो संकटापन्न हुआ ही है और साथ ही पूरे पहाड़ का प्राकृतिक संतुलन खतरे में पड़ता जा रहा है। यह आनेवाले समय में पूरे पहाड़ का उसके जनजीवन के साथ ख़त्म हो जाने का संकेत है और इस घोर अप्राकृतिक कुकृत्य में सत्ता तथा प्रशासन की मिलीभगत है। पहाड़ के संकटाभिमुख होने और उसमें पूंजीपति-व्यवस्था की मिलीभगत होने को केंद्र में रखकर हरनोट ने अपनी 'नदी गायब है' कहानी का ताना-बाना बुना है। वे पहाड़ी नदियों का पूंजीवादी शक्तियों के द्वारा दोहन के बरअक्स संकट की ओर अग्रसर पहाड़ और पहाड़ी जनजीवन का चित्रण अपनी इस कहानी में करते हैं - "नदी गायब होने के साथ उनके गाँव पर एक और संकट खड़ा हो गया था। उनका गाँव ऐसे पर्वतों की तलहटी में था, जहाँ ग्लेशियरों के गिरने का खतरा हमेशा बना रहता था। अब रोज़ डायनामाइट के धमाकों से टनों के हिसाब से उस नदी में चट्टानें गिरनी शुरू हो गई थी और नदी के किनारे जो घराट थे, वे पूरी तरह नष्ट हो गए थे।" हरनोट ने नदियों की आज़ादी को ख़त्म करके उन्हें जबरन सुला देने और जमकर उसका दोहन करने के भयंकर दुष्परिणाम को दर्शाते हुए अपनी कहानी 'भागादेवी का चायघर' में कहा है - "छोटी-बड़ी परियोजनाओं के भारी-भरकम बोझों से वे थकी-हारी घाटियों के बीच सोयी दिखती है। कभी जगती हैं तो उनका आक्रोश आसमान पर होता है। वे अपने प्रतिबंधों को भारी उफ़ान से तोड़ती चलती है और उनके रास्ते जो भी आये उसे लील लेती है।"¹⁴

हरनोट कृत 'आभी' हिमाचल प्रदेश के कुल्लू जिला के दुर्गम भानी क्षेत्र में 11500 फीट की ऊँचाई पर स्थित सरेउलसर झील और नदियों से उसे साफ़ रखनेवाली आभी प्रजाति की चिड़ियों की कहानी है। इस दुर्गम पहाड़ी झील क्षेत्र तक पहुँच चुकी मशीनी-

पूँजीवादी मानसिकता किस प्रकार इसे प्रदूषित करने में अपनी भूमिका निभा रही है, उसका जीवंत चित्र कहानीकार ने इसमें प्रस्तुत किया है। दूरिज्म उद्योग के विकास के कदम इस दुर्गम क्षेत्र पर पड़ चुके हैं, जिसके साथ इन झीलों की प्राकृतिक सुन्दरता को खत्म करनेवाले 'टूल्स' भी पहुँच चुके हैं। इन झीलों के अस्तित्व को सबसे ज्यादा खतरे में डालनेवाली प्लास्टिक पर्यटकों के मार्फत पहुँचने लगी है। प्लास्टिक से जल-मृदा प्रदूषण का खतरा तो है ही साथ ही साथ इस जल-मृदा पर आश्रित आभी तथा अन्य जीव समुदाय का भी अस्तित्व खतरे में पड़ने लगा है। इसके कारण पहाड़ की जैव-विविधता नष्ट हो रही है, जिसने पूरे पहाड़ के अस्तित्व को ही संकट के सम्मुखीन कर दिया है। इस परिस्थिति पर दूरिज्म उद्योग से जुड़े लोगों को अपने पहाड़ को बचाने की कवायद करते हुए कहानीकार कहता है - "वे नहीं जानते कि उनकी इन हरकतों से जंगल और पहाड़ बर्बाद हो रहे हैं। वे नहीं जानते कि उनकी गाड़ियों के शोर से जंगली जानवर के एकांत खत्म हो रहे हैं और वे दूर कहीं अपनी-अपनी खोहों में डर के मारे दुबके पड़े हैं।" सबसे दिलचस्प बात यह है कि मानव को इस पूँजीवादी मानसिकता ने इतना अंधा बना दिया है कि यह जानते हुए भी कि वह प्रकृति को क्षति पहुँचाकर स्वयं कभी बच नहीं सकता; इसके बावजूद वह प्रकृति के अंधाधुंध दोहन में लीन है। पहाड़ी जंगल के वृक्षों की गैरकानूनी कटाई व कटाई करनेवालों की लगामहीन विलासिता के कारण फेंके गये जलती बीड़ी-सिगरेट के टुकड़ों से पूरा का पूरा जंगल और जंगल में रहनेवाले जीव खत्म हो रहे हैं। इस परिस्थिति में मानवीय संवेदना भी छीज रही है क्योंकि वन में लगी आग से बचने के लिए प्रत्येक श्रमिक को दूसरे श्रमिक के आग में स्वाहा हो जाने का थोड़ा भी दुःख नहीं हो रहा है। वह केवल अपनी जान बचाने के लिए बेतहाशा दौड़ रहा है। दरअसल इस आग को कहानीकार ने सांकेतिक रूप से प्रकृति की भयानक प्रतिक्रिया के रूप में दर्शाया है, जिसमें सभी का जलकर खाक हो जाना तय है - "उस आदमी के साथी अभी भी दौड़ रहे हैं। उसे उस मरते साथी की परवाह नहीं है, अपनी जान की है। वे हर हालत में बचना चाहते हैं। जीना चाहते हैं। पर उन्हें लगता है कि आग की अनगिनत लपटें उनके पीछे भागती आ रही हैं, जिनसे बचना मुश्किल है।"

निष्कर्षतः यह कहना कोई अत्युक्ति नहीं होगी कि हिमाचल के पार्वत्य प्रदेश पर मशीनी सभ्यता के पहुँचने के कारण वहाँ मानवीय संवेदना तथा प्राकृतिक मूल्यबोध की भावना छीज रही है। वहाँ अमानवीयता, सत्ता की निरंकुशता, साम्प्रदायिकता, बाज़ारवादी, क्रूर, हिंसक, मनुष्य विरोधी तथा सबसे अधिक प्रकृति को विनष्ट करने वाली ताकतों ने अपनी पैठ बना ली है, जिससे पूरे पहाड़ का अस्तित्व संकट में आ गया है। चूँकि

हरनोट अपने समय के सजग प्रहरी हैं, अतः वे चौकसे होकर इन सभी शक्तियों से लड़ने के लिए अपनी कहानियों की बुनावट करते हैं। मशीनी सभ्यता के बढ़ते कदम के बरबक्स पहाड़ में आई दरकनों तथा उसके पीछे की शक्तियों की वे शिनाख्त करते हैं और उन्हें अपनी कहानियों के मार्फत पेश करते हैं ताकि पहाड़, पहाड़ीपन और उसके नैसर्गिक सौंदर्य की रक्षा के लिए विनष्टकारी शक्तियों के विरुद्ध पहाड़ की जनता एक प्रबल प्रतिपक्ष के रूप में खड़ा हो सके। उनकी कहानियों की इस विशेषता और उनकी सजगता के सन्दर्भ में प्रो. सूरज पालीवाल का कहना है . "हरनोट की कहानियों में पहाड़ केवल पहाड़ के रूप में नहीं अपने पूरे परिवेश के साथ उपस्थित होता है। समय के विकास के साथ भूमंडलोत्तर पहाड़ी जीवन में आये बदलावों, टूटते रिश्तों, सांस्कृतिक परिवर्तनों और स्त्री-पुरुष संबंधों के साथ रूढ़ियों की टूटती जंजीरों जिस झनझनाहट के साथ हरनोट की कहानियों में आती हैं, वे विस्मय उत्पन्न नहीं करती बल्कि यह सोचने को विवश करती है कि हरनोट अपने परिवेश के प्रति कितने सजग हैं।"¹⁷

सन्दर्भ सूची :

1. ज्ञानरंजन, दारोश तथा अन्य कहानियाँ (कहानी-संग्रह), आधार प्रकाशन, पंचकूला (हरियाणा), द्वितीय संस्करण: 2012, फ्लैप
2. हरनोट, एस. आर., बिल्लियाँ बतियाती हैं, दारोश तथा अन्य कहानियाँ (कहानी-संग्रह), आधार प्रकाशन, पंचकूला (हरियाणा), द्वितीय संस्करण: 2012, पृ.14
3. वही, पृ.12
4. वही, पृ.55
5. हरनोट, एस. आर., जीनकाठी तथा अन्य कहानियाँ (कहानी-संग्रह), आधार प्रकाशन, पंचकूला (हरियाणा), द्वितीय संस्करण: 2012, पृ.40
6. हरनोट, एस. आर., मिट्टी के लोग, मिट्टी के लोग (कहानी-संग्रह), आधार प्रकाशन, पंचकूला (हरियाणा), प्रथम संस्करण: 2010, पृ.28
7. वही, पृ.26
8. हरनोट, एस. आर., जूजू, लिटन ब्लाक गिर रहा है (कहानी-संग्रह), आधार प्रकाशन, पंचकूला (हरियाणा), प्रथम संस्करण: 2014, पृ.99

9. हरनोट, एस. आर., माफिया, दारोश तथा अन्य कहानियाँ (कहानी-संग्रह), आधार प्रकाशन, पंचकूला (हरियाणा), द्वितीय संस्करण: 2012, पृ.50
10. हरनोट, एस. आर., बेजुबान दोस्त, मिट्टी के लोग (कहानी-संग्रह), आधार प्रकाशन, पंचकूला (हरियाणा), प्रथम संस्करण: 2010, पृ.13
11. वही, पृ.14
12. हरनोट, एस. आर., लोग नहीं जानते उनके पहाड़ खतरे में हैं, लिटन ब्लाक गिर रहा है (कहानी-संग्रह), आधार प्रकाशन, पंचकूला (हरियाणा), प्रथम संस्करण: 2014, पृ.69
13. वही, पृष्ठ सं-79
14. हरनोट, एस. आर., कीलें, भागादेवी का चायघर (कहानी-संग्रह), वाणी प्रकाशन, दरियागंज (नई दिल्ली), प्रथम संस्करण: 2019, पृष्ठ सं-12
15. हरनोट, एस. आर., अभी, लिटन ब्लाक गिर रहा है (कहानी-संग्रह), आधार प्रकाशन, पंचकूला (हरियाणा), प्रथम संस्करण: 2014, पृष्ठ सं-12
16. वही, पृ.17
17. हरनोट, एस. आर., कीलें(कहानी-संग्रह), वाणी प्रकाशन, दरियागंज (नई दिल्ली), प्रथम संस्करण: 2019, फ्लैप



FOOD-SNATCHING BEHAVIOUR IN ANTS

¹KHOKAN NASKAR AND ²SRIMANTA KUMAR RAUT

¹Department of Zoology, Achhruram Memorial College, Jhalda,
Purulia-723202, West Bengal, India

²Ecology and Ethology Laboratory, Department of Zoology, University of Calcutta, 35,
Ballygunge Circular Road, Kolkata - 700019, India

¹. E-mail : khokan24@gmail.com | ². E-mail : srimantakraut@gmail.com

*Corresponding author

Received - 12.05.2020

Revised - 07.06.2020

Accepted - 02.07.2020

ABSTRACT

Foraging behaviour of the ants Anoplolepis gracilipes, Camponotus compressus, Crematogaster subnuda, Meranoplus bicolor, Monomorium pharaonis, Pheidole roberti and Tetraponera rufonigra was studied following supply of different food items in the open foraging ground with a view to note the interactions, if any. It is revealed that, in spite of available foods at the supplying sites Paratrechina longicornis, Pheidole roberti, Anoplolepis gracilipes and Tetraponera rufonigra are habituated to face the food-snatching operations initiated either by the foragers of the same species belonging to different colonies or by the other competing species who are very much involved in sharing the food resources from the same foraging area. Food-snatching event is associated with the abrupt and brutal attack by the snatcher ant on the ants carrying food to their nest. Thus, fighting in most cases was inevitable and many of the food-transporting ant individuals were seen injured severely. The food snatching behaviour exhibited by these ant species was not only to ensure the need of their food but also a strategy to treat the competing ant species psychologically by imposing fearful threat, as a dominant species, not to visit the said foraging ground again, in future.

Key words:- Ants, Foraging, Food-snatching, Tricks

INTRODUCTION

Ants forage at large here and there in their foraging area (Vowler 1955, Carroll and Janzen 1973, Traniello 1989, Sumpter and Beekman 2003, Wrege et al. 2005, Prabhakar et al. 2012, Li et al. 2014, Gathalkar and Sen 2018). Though there exists niche segregation it is very common to note the different ant species in foraging act side by side in certain spots (MacArthur and Levins 1967, Gordon 1995, Cerdá et al. 1998, Detrain et al. 2000, Albrecht and Gotelli 2001, Saar et al. 2018). As the availability of food resources, especially in view to the need of the colony members, varied to a great extent in respect to foraging area because of seasons competition both at the intra and interspecies levels is inevitable (Rust et al. 2000, Sanders and Gordan 2000, Bestelmeyer 2003, Grover et al. 2007, Cook et al. 2011, Pinto et al. 2018). Accordingly, ants have developed various devices like robbing and/or stealing by developing the dominating behavioural tricks over other neighbouring ant species (Lynch et al. 1980, Yamaguchi 1995, Breed et al. 2012, McGlynn et al. 2015, Paul and Annagiri 2018). Breed and coworkers (2012) discussed at length on the cleptobiosis in social insects in consideration with the phenomenon of theft of food among animals.

We are engaged in studying the different aspects of bioecology of the ants occurring in

NASKAR AND RAUT

the south-western region of the state West Bengal, India since 2010. And, in the meantime we did our best to report the food searching, food examination, food selection, food preference, foraging activities, food–transporting mechanisms, necrophagy as well as on some factors influencing foraging in *Camponotus compressus*, *Crematogaster subnuda*, *Pheidole roberti*, *Tetraponera rufonigra*, *Monomorium pharaonis*, *Anoplolepis gracilipes*, *Meranoplus bicolor* and *Paratrechina longicornis* ants (Naskar and Raut 2014a, b, c, 2015a, b, c, d, e, f, 2016a, b, c, 2018a, b, 2019).

However, in course of studies we paid due attention to note the food-snatching behaviour in a number of ant species in their common foraging area where we offered different types of food items experimentally, to note their foraging behaviour under such circumstances. Surprisingly, we had the opportunity to record a number of food-snatching events in the open foraging ground either on way of fighting or through the exercise of aggressive dominant power, one over other-be it member of the same species or different species, with a view to ensure their foraging success by hook or crook. As there exists, virtually no report on the said aspect of the ants we are describing the same in this article with a view to add further information on the tricky food collection behaviour in the foraging ground contrast to food robbing from the neighbouring nests or at the entry point of these nests by certain cunning ants.

MATERIALS & METHODS

For experimental studies on different aspects of food-selection, feeding, food transporting, and foraging activities in different ant species who are habituated to forage in the grounds in the south-western zone of West Bengal, India different types of food fragments viz. sugar cubes and fragments of sugarmade materials with different colouration, biscuit fragments, piece of nuts, dry fish, freshly dead mosquitoes, mustard seeds, coriander seeds, aniseeds, cumin seeds, chocolate fragments of different number and sizes as the cases applicable were offered at several locations in the foraging ground at different hours of the study of the study dates during the period of last 12 years at frequent intervals. Apart from other behavioural activities we paid due attention to note the ants who were victimized by other individuals of the same or different species at the time of food examination, food selection, food transportation because of aggression but abrupt attack with a view to snatch the food from the transporters on way of their movement towards the nest. Also, we noted the behaviours exhibited by the victimized ants and their food-snatcher ants in course of interactions, in respect to food-snatching events at per date and hours of the day concerned.

Photographs have been taken into account to visualize the facts the ants exhibited during their food-snatching operation. The experiments were carried out at Garia, Kolkata (South 24 parganas) as well as in and around the Achhruram Memorial College campus, Jhalda, Purulia, West Bengal, India.

RESULTS

During the study period of the total trials, 22 food-snatching events have been noted on different dates and hours of the study days (Table 1). The ant species involved in the food-snatching activities were *Pheidole roberti*, *Paratrechina longicornis*, *Anoplolepis gracilipes* and *Tetraponera rufonigra*.

DISCUSSION

Cleptobiosis is an well established behaviour in many animals including social insects (Breed et al. 2012). Also furtive behaviour in some foraging ants *Ectatomma ruidum* have also been noted by McGlynn and coworkers (2015). Moreover, interspecific competition through food robbing did not escape the sight of Yamaguchi (1995) in the harvester ant *Messor aciculatus*. All the above

mentioned behaviours have been developed in ants depending on the scarcity of food and/or to avoid trouble in searching and transporting the food materials to the colony. Undoubtedly, such types of behavioural adaptability is deviation from the normal nature of food searching, food selection and food transportation in ants. Such adaptabilities though have been triggered through the practice of aggressive foraging behaviour (Lynch et al. 1980, Yamaguchi 1995, Cerdá et al. 1998, Gathalkar and Sen 2018, Pinto et al. 2018). But, in this context the climax is attributed not only through the development of a distinct behavioural caste for robbing food from the conspecific nest and/or removing the food from the foragers at the entry point of their nest but also by developing the tricks for brood theft to get a good number of slaves to serve as foragers and colony maintainers (Paul and Annagiri 2018).

It is most likely that cleptobiosis in social insects is derived evolutionarily from established foraging behaviours (Breed et al. 2012) but the basic information in strengthening the said idea is being supplied through the present findings on the food-snatching behaviour in the ants *Ph. roberti*, *Pa. longicornis*, *A. gracilipes*, *T. rufonigra* during foraging in open ground. As the ants *Pa. longicornis* or *A. gracilipes* inhibited other ant species either to procure a food item or to carry the same to their nest at the spot where many more food items were available for their choice it is apparent that certain ant species, being members of the same foraging ground are motivated not to allow other species to share the resource. And, under any situation when these ants were finding the opportunity to transport the food to their nest these stranger ants, being in contact, did not care to snatch the food item either forcibly through a strong bite to the food item or abruptly attacking the ant or ants who are engaged in single or cooperative food-transporting mechanism (Czaczkes et al. 2010, Czaczkes and Ratnicks 2013, McCreery and Breed 2014, Naskar and Raut 2015, 2018a, b). Of course, dominant nature of a species influences habits of resource removal (Lynch et al. 1980, Yamaguchi 1995, Cerdá et al. 1998) from the other less dominant ant species it is well evident that, depending upon the physical ability of the food-transporter and the food-snatcher fighting is obvious as have been noted in course of food-snatching events between *Pa. longicornis*, *A. gracilipes* or between *Ph. roberti* and *Pa. longicornis*, or between *T. rufonigra* and *Pa. longicornis*. Mysteriously, in some interactions the snatchers were successful to drive away the food-carrying individuals or injured them heavily but did not procure the said food item. This indicates that the competitors attack these ants, not in all cases, to snatch the food item but to teach them a lesson of torture, brutal action and deprivation of food resources if they again visit the concerned foraging area. Simply, its an attempt to keep the competitors under psychological pressure.

In the present study it is also clear that food snatching though a common behavioural phenomenon in ants is not customarily an interspecific event. This sort of behaviour is also common between the members of the same species as could be revealed from the fact of food-snatching event exhibited by *A. gracilipes*. But, it is sure that these ants belong to different colonies. However, it is surprising that, being driven away by the snatcher ant the depriver ant, under certain instances, is tuned to return to the spot of interaction to collect the food item which she dropped on the ground during the attack, and was not taken away by the snatcher. This sort of behaviour the ants perhaps, admitted through their experience, as in some cases food item may not be procured by the snatcher ant. Though, according to Lynch and coworkers (1980) resource removal by a behaviourally subordinate species are reduced in the presence of a dominant species *Prenolepis imparis*, the present findings indicate that, under certain circumstances the weaker or less dominant species may have the opportunity to minimise the rate of reduction of loss of food

NASKAR AND RAUT

in course of foraging.

Thus, it is concluded that cleptobiosis in ants is originated from snatching habit and successively modified through thieving/stealing, robbing and brood-thieving to ensure easy success in obtaining food resources.

ACKNOWLEDGEMENT

The authors are thankful to the Head of the Department of Zoology, University of Calcutta and to the Principal, Achhruram Memorial College, Purulia for the facilities provided. The ant specimens were identified by the Zoological Survey of India, Kolkata, India.

Table 1. Food-snatching events in ants.

Date of observation	Timing of observation	Description of food snatching events
July 20, 2010	8.15 AM	A <i>Pheidole roberti</i> was carrying a piece of dry fish to her nest. On way a <i>Paratrechina longicornis</i> suddenly attacked her. <i>Ph. roberti</i> left the food piece and moved away. The <i>Pa. longicornis</i> , then picked up the said piece of dry fish and was moving towards her destination. But, the said <i>Ph. roberti</i> came back quickly to follow the <i>Pa. longicornis</i> . Soon she approached the said ant and attacked her ferociously. They fought for 2 minutes and finally <i>Pa. longicornis</i> moved away leaving the food item at the fighting spot. The said fish-food piece was then carried by <i>Ph. roberti</i> safely to her nest.
July 21, 2010	8.30 AM	An <i>Anoplolepis gracilipes</i> was on her way by pushing a piece of dry fish. On way a <i>Pa. longicornis</i> attacked her and tried to snatch the said fish piece from her. The fish piece was dropped on the ground because of tug of war for 95 seconds. But, in the meantime three more <i>Pa. longicornis</i> assembled there and took part in fighting with the <i>A. gracilipes</i> . Suddenly three more <i>A. gracilipes</i> joined in the interaction process and fighting was continued for another two minutes. But, finally all the four <i>A. gracilipes</i> left the fighting spot and the original snatcher <i>Pa. longicornis</i> carried the said dry fish piece successfully to her destination.
	8.43 AM	An <i>A. gracilipes</i> was on way to her nest pushing a piece of dry fish. Of on a sudden she was encircled by many <i>Pa. longicornis</i> individuals. Immediately one <i>Pa. longicornis</i> started pulling the fish piece from the <i>A. gracilipes</i> . But she was rigid to hold the said fish piece under her grip on way of biting the same strongly. Just after 35 seconds the other members of <i>Pa. longicornis</i> tried to attack her from all sides and then the food piece was out of the grip of <i>A. gracilipes</i> . The <i>Pa. longicornis</i> who was engaged in snatching the fish piece initially was able to move out of the battle field. The <i>A. gracilipes</i> being injured somehow escaped the dangerous situation and went away. Of the fighting <i>Pa. longicornis</i> three individuals quickly moved and joined with the fish-piece carrying <i>Pa. longicornis</i> to enable easy transportation of the same to their nest.
August 04, 2010	8.49 AM	An <i>A. gracilipes</i> was pulling a dry fish fragment to her nest. On the way she came across another <i>A. gracilipes</i> individual who tried to pull the said fish fragment in opposite direction (Fig 1.). The said event was continued for two minutes. Thereafter the original carrier ant stopped pulling activity and moved to the opposite end of the fish fragment where the rival <i>A. gracilipes</i> was trying to snatch the fish fragment. They started fighting. In the meantime, a <i>Pa. longicornis</i> took the opportunity to carry away the said fish fragments which was laid on the ground.
August 09, 2010	8.53 AM	There were some sugar cubes at the supplied site. Eight <i>Pa. longicornis</i> assembled there and were engaged in examining the sugar cubes. Mean while a big <i>A. gracilipes</i> appeared and started fighting with these <i>Pa. longicornis</i> . The <i>A. gracilipes</i> was compelled to leave the spot. Then each <i>Pa. longicornis</i> individual was seen to carry a sugar cube individually to their destination. But of on a sudden a large sized <i>A. gracilipes</i> was seen to attack these <i>Pa. longicornis</i> individuals. To save their life <i>Pa. longicornis</i> dropped the sugar cubes on the ground and moved hurriedly elsewhere. All the sugar cubes were procured by <i>A. gracilipes</i>
October 06, 2015	07.55 AM	<i>Ph. roberti</i> were assembled at the site of food supplied spot. They were just on way of carrying the sugar cubes. Suddenly five <i>Pa. longicornis</i> appeared there and attacked the <i>Ph. roberti</i> individuals who were carrying the sugar cubes. Consequently fighting started and <i>Ph. roberti</i> were dispersed. The sugar cubes were procured by <i>Pa. longicornis</i>

PROC. ZOOL. SOC. INDIA

October 27, 2015	09.58 AM	A <i>Tetraponera rufonigra</i> came in contact of the supplied sugar cubes. She checked five sugar cubes and then picked up one sugar cube with a view to carry the same to the nest. Just at that time a <i>Pa. longicornis</i> attacked her. The <i>T. rufonigra</i> dropped the sugar cube and started fighting with <i>Pa. longicornis</i> . After two minutes <i>T. rufonigra</i> was able to collect that sugar cube to carry the same to her nest. There were still six sugar cubes at the site and <i>Pa. longicornis</i> then, bite one of these sugar cubes to carry the same to her nest.
November 08, 2015	05.18 PM	An <i>A. gracilipes</i> drove away two <i>Pa. longicornis</i> while they were carrying a piece of pink sugar fragment on way of pulling and pushing system to their nest. The dropped sugar fragment was carried safely to the nest by the <i>A. gracilipes</i> .
November 09, 2015	09.26 AM	At the site a <i>Pa. longicornis</i> was eating a piece of murki (fragmented flat rice soaked with molasses) following examination of the supplied food items. In the meantime an <i>A. gracilipes</i> appeared there and forcibly drove away the <i>Pa. longicornis</i> (Fig 2.). Then <i>A. gracilipes</i> carried the said murki piece to her nest.
	09.28 AM	Two <i>Pa. longicornis</i> were carrying a piece of white sugar fragment to their nest. Suddenly an <i>A. gracilipes</i> gave a strong bite to the said sugar fragment and lifted the same while these two <i>Pa. longicornis</i> had no alternative but to leave the sugar fragment. Side by side, at a close distance another <i>A. gracilipes</i> was also seen to snatch a piece of yellow sugar fragment from two <i>Pa. longicornis</i> .
November 10, 2015	09.35 AM	Three <i>Pa. longicornis</i> were jointly transporting a piece of yellow sugar fragment. They were forcibly detached from the food fragment by an <i>A. gracilipes</i> who picked up the said sugar fragment and moved towards her nest.
	09.37 AM	An <i>A. gracilipes</i> attacked two <i>Pa. longicornis</i> who were on their way to the nest to deposit a sugar fragment. <i>Pa. longicornis</i> failed to resist the attack and thus the sugar particle was snatched by the <i>A. gracilipes</i> .
November 11, 2015	08.00 AM	A <i>Pa. longicornis</i> was carrying a salt grain from the supplied spot. On way she was attacked by an <i>A. gracilipes</i> . <i>Pa. longicornis</i> ran away dropping the salt grain. But <i>A. gracilipes</i> examined the said salt grain and left the place leaving the salt grain as such at the spot. <i>Pa. longicornis</i> came back to the said spot and picked up the salt grain for transporting the same to her nest.
	09.24 AM	A <i>Pa. longicornis</i> was on her way to nest with a piece of pink sugar fragment. Suddenly an <i>A. gracilipes</i> attacked her and snatched away the sugar fragment.
November 12, 2015	09.19 AM	An <i>A. gracilipes</i> chased a <i>Pa. longicornis</i> , who was carrying a piece of pink sugar fragment, suddenly and ferociously. The <i>Pa. longicornis</i> dropped the sugar fragment and quickly moved away. The snatcher transported the said sugar fragment to her destination.
	09.22 AM	A <i>Pa. longicornis</i> was pulling a biscuit fragment. But on way an <i>A. gracilipes</i> chased her. She left the biscuit fragment and moved away. But, the <i>A. gracilipes</i> did not collect the said biscuit fragment and left the place. The said <i>Pa. longicornis</i> came back to the spot and took the biscuit fragment to transport the same to her nest.
	09.23 AM	A <i>Pa. longicornis</i> was pulling a piece of white sugar fragment. She was attacked by an <i>A. gracilipes</i> on way of movement towards her nest. They fought for a while and the <i>Pa. longicornis</i> left the place leaving the sugar fragment. The said sugar fragment was carried by <i>A. gracilipes</i> to her nest.
	04.01 PM	A <i>Pa. longicornis</i> examined the offered food items at the site. She then, selected a piece of pink sugar fragment. She was pulling the same to her nest but on the way an <i>A. gracilipes</i> came in contact with the sugar fragment and started pulling the same in opposite direction. The interaction was continued for 80 seconds when another <i>A. gracilipes</i> joined in the tug of war. The sugar fragment was detached by <i>Pa. longicornis</i> and these two <i>A. gracilipes</i> carried the sugar fragment jointly to their nest.
	04.18 PM	A yellow sugar fragment was carrying by two <i>A. gracilipes</i> . One of them was pushing and the other one was pulling the said sugar fragment. Of on a sudden comparatively healthier <i>A. gracilipes</i> appeared and gave a strong bite to the sugar fragment at the lateral side. She then lifted the same and moved to her destination.

NASKAR AND RAUT

November 13, 2015	09.08 AM	One <i>Pa longicornis</i> was pulling a "batasa" (made of sugar) fragment from the offered site. She was attacked by an <i>A. gracilipes</i> on the way (Fig 3.). <i>A. gracilipes</i> very promptly snatched the batasa fragment and hurriedly moved towards her nest.
	09.16 AM	One <i>A. gracilipes</i> chased a <i>Pa. longicornis</i> , on the way, who was pushing a piece of white sugar fragment. <i>A. gracilipes</i> injured <i>Pa. longicornis</i> by damaging her legs through repeated biting. Consequently, <i>Pa. longicornis</i> failed to move forward and <i>A. gracilipes</i> snatched away the sugar fragment.
	09.21 AM	A piece of chocolate fragment was pulling by an <i>A. gracilipes</i> . A <i>Pa. longicornis</i> coming in contact with the chocolate fragment started to pull the same in opposite direction with a view to snatch the same (Fig 4.). But, <i>A. gracilipes</i> was able to manage her movement in a befitting manner to escape the chaser.

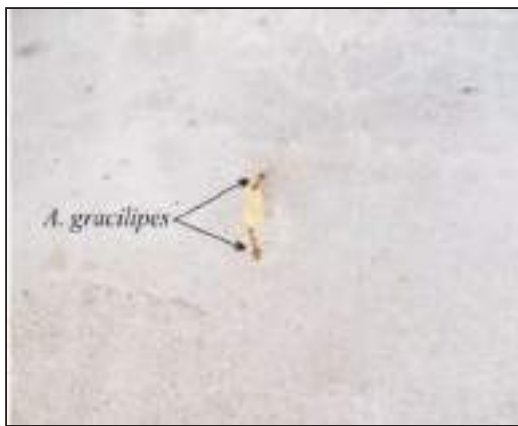


Fig. 1 Food-snatching act by an *A. gracilipes* from another *A. gracilipes*



Fig. 2 An *A. gracilipes* snatching a murki fragment from a *Pa. longicornis*.



Fig. 3 An *A. gracilipes* snatching a batasa fragment from a *Pa. longicornis*



Fig. 4 A *Pa. longicornis* snatching a chocolate fragment from a *A. gracilipes*

REFERENCES

- Albrecht, M and Gotelli, N. J. 2001:** Spatial and temporal niche partitioning in grassland ants. *Oecologia* 117:404-412.
- Bestelmeyer, B. T. and Wiens, J.A. 2003:** Scavenging ant foraging behavior and variation in the scale of nutrient redistribution among semi arid-grasslands. *J. Arid Environ* 2003, 53 (3): 373-386.
- Breed, M. D., Cook, C. and Krasnec, M. O. 2012:** Cleptobiosis in Social Insects. *Psyche* Article 1D484765, 7 pages doi:10.1155/2012/484765.
- Carroll, C. R. and Janzen, D. H. 1973:** Ecology of foraging by ants. *Annu. Rev. Ecol. Evol. Syst.* 1973, 4: 231-257.
- Cerdá, X., Retana, J., Manzaneda, A. 1998 :** The role of competition by dominants and temperature in the foraging of subordinate species in Mediterranean ant communities. *Oecologia* 1998, 117: 404-412.
- Cook, S. C., Eubank, M. D. Gold, R E and Behrner, S. T. 2011 :** Seasonality directs contrasting food collection behavior and nutrient regulation strategies in ants. *PLoS ONE* 2011, 6(9): e25407 doi:10.1371/journal.pone.0025407.
- Czaczkes, T. J., Nouvellet, P., Ratnieks, F. L. W. 2010 :** Cooperative food transport in the Neotropical ant, *Pheidole oxyops*. *Insectes Soc.* 2010, 58: 153-161.
- Czaczkes, T. J. and Ratnieks, F. L. W. 2010 :** Cooperative transport in ants (Hymenoptera: Formicidae) and elsewhere *Myrmecol. News* 2013, 18: 1-11.
- Detrain, C., Tasse, O., Versaen, N. and Pasteels, J. M. 2000. :** A field assessment of optimal foraging in ants: tail patterns and seed retrieval by the European harvester ant, *Messor barbarus*. *Insectes Soc.* 2000, 47: 56-62.
- Gathalkar, G and Sen. A. 2018 : Foraging and predatory activities of ants. *Intech Open*, 2018, DOI:10.5772/intechopen.78011.
- Gordon, D. M. 1995:** The development of an ant colony's foraging range. *Anim. Behav.* 1995, 49: 649-659.
- Grover, C. D., Kay, A. D., Monson, J. A., Marsh, T. C. and Holway D. A. 2007 :** Linking nutrition and behavioural dominance: carbohydrate scarcity limits aggression and activity in Argentine ants. *Proc. R. Soc. Sec B Biol. Sci.* 2007, 274:2951-2957.
- Li, L., Peng, H., Kurths, G., Yang, Y. and Hans, J. S. 2014 :** Chaos - order transition in foraging behaviour of ants. *Proc. Natl. Acad. Sci., USA* 2014, 111(23):8392-8397.
- Lynch, J. F., Balinsky, E. C., Vail, S. G. 1980 :** Foraging patterns in three sympatric forest ant species, *Prenolepis imparis*, *Paratrechina melanderi* and *Aphaenogaster rudis* (Hymenoptera: Formicidae). *Ecol. Entomol.* 1980, 5: 353-361.
- MacArthur, R. and Levins, R. 1967 :** The limiting similarity, convergence, and divergence of coexisting species. *Am. Nat.* 1967, 101: 377-385.
- McCreery, H. F., and Breed, M. D. 2014 :** Cooperative transport in ants; a review of proximate mechanisms. *Insectes Soc.* 2014, 61: 99-110.
- McGlynn, T. P., Graham, R., Wilson, J., Emerson, J., Jandt, J. M. and Jahren A. H. 2015 :** Distinct types of foragers in the ant *Ectatomma ruidum* typical foragers and furtive thieves.

NASKAR AND RAUT

- Anim. Behav.* 2015, 109: 243-247.
- Naskar, K. and Raut, S. K. 2014a** : Food searching and collection by the ants *Pheidole roberti* Forel. *Discovery*. 2014a, 32: 6-11.
- Naskar, K. and Raut, S. K. 2014b** :Judicious foraging by the ants *Pheidole roberti* Forel. *Proc. Zool. Soc.* 2014b, 68: 131-138.
- Naskar, K. and Raut, S. K. 2014c** :Ants forage haphazardly: a case study with *Pheidole roberti* Forel. *Int. J. Sci. Nat.* 2014c, 5: 719-722.
- Naskar, K. and Raut, S. K. 2016d** :Ants' foraging, a mystery. *Int. j. innov. Sci. Res.* 2015a, 4 (2): 064-067.
- Naskar, K. and Raut, S. K. 2015b** Foraging interactions between the Reddish brown ants *Pheidole roberti* and the Black ants *Paratrechina longicornis* *IJRBS*. 2015b, 3 (3): 183-189.
- Naskar, K. and Raut, S. K. 2015c** :Available food and ant's response. *IJESTR*, 2015c, 4 (4): 368-372.
- Naskar, K. and Raut, S. K. 2015d** :Food-carrying strategy of the ants *Pheidole roberti*. *Int. j. Tech. Res. and Appl.* 2015d, 3(3): 55-58.
- Naskar, K. and Raut, S. K. 2015c** :Foraging behaviour following food contact in the ants *Pheidole roberti*. *GJBAHS*, 2015e, 4 (2): 21-24.
- Naskar, K. and Raut, S. K. 2015f** :Mysterious foraging of Pharaoh ant *Monomorium pharaonis*. *Int. J. Appl Eng. Res.* 2015f, 5 (7): 67-71.
- Naskar, K. and Raut, S. K. 2016a** :Ants' food examination. *Proc. Zool. Soc.* 2016a, 70 (2): 119-131.
- Naskar, K. and Raut, S. K. 2016b** : Winter quarter-induced foraging in ants. *GJBB*. 2016b, 5 (3): 318-323.
- Naskar, K. and Raut, S. K. 2016c** : Does colour of the food attract ants? *Proc. Zool. Soc.* 2016c, 71(1): 25-29.
- Naskar, K. and Raut, S. K. 2018a** : Food-induced food-transporting strategies of the ants *Ph. roberti* and *Pa. longicornis* ; in *Entomology : Current Status and Future Strategies*. Ganguly, A. and K. Naskar (eds), 2018a, 125-133, Daya Publishing House, (Astral Int. Pvt. Ltd.), New Delhi.
- Naskar, K. and Raut, S. K. 2018b** : Genesis and significance of cooperative transport in ants. *GJBB*. 2018b, 7(4): 633-637.
- Naskar, K. and Raut, S. K. 2019** :Ant's necrophagy on ants. *GJBB*. 2019, 8(4): 335-339.
- Paul, B. and Annagiri, S. Tricks of the trade: Mechanism of brood theft in an ant. *PLoS One*. 2018, 13 (2): e0192144. Doi:10.1371/journal.pone0192144.
- Pinto, V., Reddy, M. S., Pratheepa, M. and Verghese, A. 2018** : Incidence of aggressive territoriality between two ant species: *Camponotus compressus* Fab and *Oecophylla smaragdina* Fab (Hymenoptera: Formicidae). *Curr. Sci.* 111(12): 2044-2046.
- Prabhakar, B., Dektar, K. N. and Gordon, D. M. 2012** :The regulation of ant colony foraging activity without spatial information. *PLoS Comput. Biol.* 8 (8) E1002670.doi : 10.1371/journal.pcbi.1002670

PROC. ZOOL. SOC. INDIA

- Rust, M. K., Reinson, D. A., Paine, E. and Blum, L. J. 2000:** Seasonal activity and bait preferences of Argentine ant (Hymenoptera: Formicidae). *J. Agri. Urban Entomol.* 17(4): 201-212.
- Saar, M., Subach, A., Reato, I, Liber, T., Pruitt, J. N. and Scharf, I. 2018:** Consistent differences in foraging behavior in 2 sympatric harvester ant species may facilitate coexistence. *Curr. Zool.* 64(5): 653-661.
- Sanders, N. J. and Gordan, D.M. 2000 :** The effects of inter-specific interaction on resource use and behaviour in a desert ant. *Oecologia.* 125(3): 436-443.
- Sumpter, D. J. T and Beekman, M. 2003 :** From nonlinearity to optimality: pheromone trail foraging by ants. *Anim. Behav.* 66: 273-280.
- Traniello, G. F. A. 1989 :** Foraging strategies of ants. *Ann. Rev. Entomol.* 1989, 34: 191-210.
- Vowler, D. M. 1995 :** The foraging of ants. *The British J. Anim. Behav.* 1955, 3(1): 1-13.
- Wrege, P. H., Wikelski, M., Mandal, J. T., 2005.** Rassweiler and Couzin, J. D. Antbirds parasitize foraging army ants. *Ecology.* 86 (3): 555-559.
- Yamaguchi, T. 1995 :** Interspecific competition through food robbing in the harvester ant, *Messor aciculatus* (Fr. Smith), and its consequences on colony survival. *Insectes Soci.* 1995, 42: 89-101.



A preliminary study on the juvenile stages of *Tenebrio molitor* Linnaeus, 1758 (Coleoptera: Tenebrionidae) and *Sphenarium purpurascens* Charpentier, 1842 (Orthoptera: Pyrgomorphidae) as exploitable nutraceutical resources

Arijit Ganguly¹ · Jose Manuel Pino Moreno²

Received: 31 May 2020 / Accepted: 10 February 2021
© African Association of Insect Scientists 2021

Abstract

Being rich in nutrients insects are potential nutraceutical resources. In the present study, we have selected the 8th instar larval stages of *Tenebrio molitor* and 5th instar nymphal stages of *Sphenarium purpurascens*, because these are the most sought after stages in the edible insect market in various states of the Mexican Republic. We have estimated their proximate composition and mineral contents and compared them with red meat and white meat. *S. purpurascens* has been found to be rich in protein and energy, whereas *T. molitor* contains maximum amount of fat and energy that are even better than that of red and white meat. Both of them also contain higher amount of minerals compared to red and white meat. It has been further observed that only 500g of insect flour can provide almost all the minerals in question, whereas the same amount of red and white meat can provide merely three of them. Thus, insects should be exploited as a source of nutraceuticals, more in depth study is necessary in this aspect though.

Keywords *T. molitor* · *S. purpurascens* · Nutraceuticals · Grub · Nymph

Introduction

The Indian Ayurveda and Hippocrates have reverberated the same opinion that our food should be our medicine (Wildman 2001; El-Sohaimy 2012), so it is necessary to practice a healthy feeding habit. Workers from around the world have developed an interest on the analyses of nutrient compositions of our common victuals and their possible influence on human health (Srividya et al. 2010). In this context a relatively new term “nutraceuticals” has been emerged, coined by Stephen De Felice from two different words “nutrient”, and “pharmaceuticals” (De Felice 1995; Biesalski 2001). Such products could be anything from dietary supplements, isolated nutrients, and herbal products to genetically engineered stuffs (Pandey et al. 2010). Later

on, various workers from different parts of the world have ushered information on the nutraceutical and medicinal compounds in various food materials. However, most of them are from plant related products; even though a few works on the animal products also have been reported (Barrera and Moreno 2018) the information is inadequate until now.

Very recently, insects have emerged as a potential food source for human and livestock (van Huis 2013). They definitely have a huge potential to be instated as a good nutraceutical resource that could be utilised as food additive for both human and in livestock industries. Nevertheless, the information is lagging far behind. Although authors like Ramos-Elorduy (2000), Costa Neto et al. (2006), Pino et al. (2009) have evaluated the medicinal and nutraceutical properties of insects such as grasshoppers, roaches, beetles, flies, bees and wasps, in China, Mexico, Brazil, Cuba etc. we need to get even more information in this aspect.

Keeping this idea in mind, in the present work we have selected the 8th instar larval stages of *Tenebrio molitor* Linnaeus, 1758 and 5th instar nymphal stages of *Sphenarium purpurascens* Charpentier, 1842, because these are the most

✉ Arijit Ganguly
arijitganguly87@yahoo.co.in

¹ Department of Zoology, Achhruram Memorial College, Jhalda, Purulia, India

² Department of Entomology, Institute of Zoology, National Autonomous University of Mexico, Mexico City, Mexico

sought after stages in the edible insect market in various states of the Mexican Republic, like the State of Mexico, Michoacán, Puebla, Oaxaca, Tlaxcala, etc. (van Huis et al. 2013). *T. molitor* is a coleopteran insect whose juvenile stage is known as “yellow meal worm”. This species is indigenous to Europe but now is distributed worldwide and considered as a serious pest of stored grains. In Mexico this insect is commonly used to feed companion animals owing to its nutritional value and ease of handling in captive conditions (van Huis 2013). Various authors have reported about their nutritional quality and they have found 43–65% crude protein, 7–32% fat, 20–27% carbohydrate and 213–247 Kcal/100g of energy, depending upon the developmental stage of the insects (Ravzanaadii et al. 2012; Heidari-Parsa et al. 2018). On the other hand, *S. purpurascens* is a short horn grasshopper species, which is also a serious pest of grain crop plants, and has been the most demanded edible insect resource for native Mexican people who consume them as “chapulines” since ancient times. In Mexico, chapulines are either toasted on a comal, and devoured along with “tortillas” and “pasilla chili sauce”, or just seasoned with salt and lemon (van Huis 2013). Authors like Ramos-Elorduy et al. (2012), Torruco-Uco et al. (2019), Celeste et al. (2020) have reported the nutritional contents of this insect species. They are reported to contain 60–64% crude protein, 11–15% fat, 20–25% carbohydrate and 384–403 Kcal/100g of energy depending on whether the experiments were carried out on nymphal or adult stage. Both the insect species are also reported to be rich in fatty acids, amino acids, vitamins and minerals (Virginia et al. 2015; Feng, 2018; Liu et al. 2020). In the present work, we have focused on the estimation of the proximate composition and mineral content of these two edible insects. Additionally we have made an attempt to compare our obtained results with that of red meat and white meat from the literature, and finally commented the consumption of how much of these insects can fulfill the demand of daily mineral consumption of an average healthy human being.

Materials and methods

Sampling of test insects

Collection of adult *S. purpurescens* was carried out in corn crop lands located in Tepotzotlán state of Mexico, which were then assembled, labeled and identified according to the key proposed by Márquez (1962). Then they were stocked in the insect rearing facility of our laboratory. When eggs hatched, nymphs were transferred to plastic boxes measuring 38cm × 30cm × 20cm and reared on a mixed diet of pesticide free fresh foliage of lettuce (*Lactuca sativa* L.), cabbage (*Brassica oleracea* L.), corn (*Zea maize* L.), and alfalfa (*Medicago sativa* L) in a set up following the

method described by Haldar et al. (1999). When the insects grew up to 5th instar nymphal stages, 600 individuals were separated for chemical analyses.

We have a population of rice bran fed *T. molitor* maintained since 1980s in the mass production insectaria of Entomology Laboratory, Department of Zoology, Institute of Biology of the Autonomous University of Mexico (UNAM). For chemical analyses 2,500 individuals of 8th instar larval stage were segregated.

Chemical analyses

The insects were oven dried at 70–80°C for about 48 hours until the weight became constant. Moisture free samples were then crushed into powder form using a mixer grinder, and 100g dry samples of each species were subjected to proximate composition, whereas 5g were used for mineral estimation following the procedure of AOAC (Helrich 1990). Crude protein was estimated by Kjeldahl (AOAC 988.05), fat was estimated using soxhlet apparatus (AOAC 920.39), crude fiber was estimated using acid-alkali digestion (AOAC 962.09), ash was estimated using a muffle furnace (AOAC 942.05), and nitrogen free extract was calculated by difference method. The energy was determined by an oxygen bomb calorimeter according to the method as mentioned in Anand et al. (2008). Determination of minerals (i.e. K, Mg, Zn, Fe, Cu and Na) was carried out using the AOAC method 968.08. For this purpose, 5 g of sample was weighed in a beaker, and 10 mL of concentrated nitric acid was added to it, heated for an hour until a translucent color was obtained. The solution was then cooled, recovered and filtered in a volumetric flask. De-ionized distilled water was added to this solution to make it 25 mL “stock solution”. Then the mineral contents were determined by atomic absorption spectrophotometry with the Perkin Elmer atomic absorption, model 2380. Calcium and phosphorus were determined using the hydride generation technique coupled to atomic absorption spectrophotometry. For calcium AOAC method 927.02, and for phosphorus AOAC method 965.17 was employed. All the chemical analyses were carried out in triplicate in the Laboratory of Animal Nutrition and Biochemistry of the Faculty of Veterinary Medicine and Zootechniques of UNAM.

Nutritional value of red and white meat

We have consulted various research articles (mentioned in Table 1, and Table 2) to obtain the nutritional values of different red meat and white meat resources. We have considered the mean values published in all the papers for each type of meat and tabulated the average data along with the nutrient quality of the selected insects.

Table 1 Proximate composition and energy content of the larval stages of *S. purpurascens* and *T. molitor* along with red meat and white meat

Sample	Crude Protein (%)	Ether Extract (%)	Ashes (%)	Raw Fiber (%)	Nitrogen-free Extract (%)	Gross energy Kcal/100g	Source
<i>Sphenarium purpurascens</i> nymph	67.8±0.076b	11.47±0.180b	4.87±0.043c	10.51±0.144c	4.65±0.076b	393.03±4.367b	Lab analysis
<i>Tenebrio molitor</i> grub	47.76±0.068a	38.29±0.122c	2.77±0.038b	6.91±0.162b	4.24±0.059b	552.37±6.082c	Lab analysis
Red meat	82.76±14.150b	12.37±4.073a	1.16±0.842a	0.079±0.007a	2.32±0.382a	127±5.611a	Adeniyi et al. (2011), Karakök et al. (2010), Bohrer (2017)
White meat	80.59±13.212b	10.92±3.567a	1.96±0.614a	0.082±0.004a	2.79±0.264a	121±6.203a	Adeniyi et al. (2011), Al-Yasiri et al. (2017), Karakök et al. (2010), Bohrer (2017)

Results are mean ± SD. Different letters within a column shows significant different values (One-way ANOVA, $P < 0.01$, Tukey's posthoc test)

Statistical analyses

The results were calculated as mean ± SD. For statistically comparing the obtained data between the two selected insect species and the conventional meat sources one-way analysis of variance (ANOVA) was carried out with the significance level of $P < 0.01$ followed by Tukey's posthoc test. All the calculations were carried out using Microsoft Excel 2007, and Past, version 3.26.

Results

The proximate composition of *S. purpurascens* and *T. molitor* along with red meat (i.e., beef, lamb, veal, pork etc.) and white meat (i.e. broiler chicken, quail, turkey etc.) are depicted in Table 1. It is not surprising to find out that red meat and white meat are having maximum amount of crude

protein (about 82% and 80% respectively). Nevertheless, *S. purpurascens* also has more than 67% protein content, while *T. molitor* is having the least amount (just above 47%) of the same. On the contrary, *T. molitor* contains more than 38% of crude fat which is significantly higher than that of *S. purpurascens* as well as the red and white meat. Crude fiber is present in the highest amount in *S. purpurascens* followed by *T. molitor* (more than 10% and 6% respectively), while both red and white meat have negligible amount of the same. This exact trend is evident in case of ashes too (more than 4% for *S. purpurascens*, more than 2% for *T. molitor*, more than 1% for red meat, and nearly 2% for white meat). NFE also is in greater amount in the insects (over 4% in both). *T. molitor* contains maximum gross energy followed by *S. purpurascens* (more than 552 Kcal/100g, and nearly 393 Kcal/100g respectively), while red meat and white meat are having just over 120 Kcal/100g of gross energy.

Table 2 Mineral content of the larval stages of *S. purpurascens* and *T. molitor* along with red meat and white meat

Sample	P (mg/Kg)	K (mg/Kg)	Ca (mg/Kg)	Mg (mg/Kg)	Zn (mg/Kg)	Fe (mg/Kg)	Cu (mg/Kg)	Na (mg/Kg)	Source
<i>Sphenarium purpurascens</i> nymphs	7562.8±312.1c	10824.3±441.5c	2120.7±103.8d	1107.1±10.7c	171.7±3.4d	113.6±3.1c	53.3±1.2d	447.5±8.2a	Lab analysis
<i>Tenebrio molitor</i> grubs	10118.9±214.2d	10318.1±352.6c	612.6±21.3c	3714.4±32.5d	132.2±2.8c	75.7±3.6b	22.4±0.8c	1706.2±11.4c	Lab analysis
Red Meat	2621.5±209.7b	4417.9±102.7b	74.2±15.9a	320.3±27.1b	38.1±11.8b	19.8±5.1a	1.3±0.3a	615.3±61.1b	Wyness et al. (2011), Williams (2007), Bohrer (2017)
White meat	1753.2±117.4a	2120.2±226.9a	132.3±16.1b	177.5±25.2a	17.1±7.6a	18.4±6.2a	2.9±0.8b	677.5±39.3b	Jokanović et al. (2014), Bohrer (2017)

Results are mean ± SD. Different letters within a column shows significant different values (One-way ANOVA, $P < 0.01$, Tukey's posthoc test)

Table 3 Daily mineral demand and amount of red meat, white meat and insect flour needed to attain that demand

Minerals	Daily demand(mg) According to FDA (2019) and FAO/WHO (2004) in adults	Supply			
		By red meat	By white meat	By <i>S. purpurascens</i>	By <i>T. Molitor</i>
P	600-800	About 300g	About 400g	About 100g	About 70g
K	4500-4700	About 1100g	About 2200g	About 400g	About 400g
Ca	1000-1200	About 20000g	About 12000g	About 500g	About 2000g
Mg	400-420	About 1400g	About 2200g	About 400g	About 150g
Zn	1.97-3.37	About 70g	About 140g	About 20g	About 20g
Fe	8-11	About 500g	About 500g	About 100g	About 150g
Cu	9-10	About 7500g	About 3500g	About 200g	About 500g
Na	1300-1500	About 2200g	About 2200g	About 3000g	About 800g

Table 2 shows a comparative representation of various minerals present in *S. purpurascens* and *T. molitor* along with pooled data of the same present in red meat and white meat. It is evident that the insects are a much better source of Zn, Fe, and Cu, compared to red meat and white meat, on the contrary in case of Na the least amount is present in *S. purpurascens* (slightly over 447 mg/Kg) even though *T. molitor* has the peak value of more than 1706 mg/Kg.

Table 3 shows the daily demand of the minerals in question by human, and the amount of dry mass of insects as well as red meat and white meat that can fulfill the daily need of the minerals. These values were obtained from the information already mentioned in Table 2, and presented as an approximation. According to Table 3, the daily demand of phosphorus (P) is 600-800 mg, and from Table 2 we get the content of P in *S. purpurescens* which is about 7562.8 mg/Kg. So, it is clear that 100g of *S. purpurescens* will provide about 756.28mg of the said mineral which is within the prescribed range. The approximate estimations for the other cases have

been derived in the same manner. It is evident from the table that 500g of both red and white meat can fulfill the need of P, Zn, and Fe. In contrast, 500g of dry biomass of *S. purpurescens* can fulfill the daily demand of almost all the minerals in question only leaving Na. The situation is almost similar in case of *T. molitor* also, where 500g could provide the daily demand of six of them only leaving Ca and Na. In Table 4, the deficiency maladies of the minerals in question are depicted. It is evident that these mineral deficiencies are mostly related to weak bone, debility, weak heart, and deprived immunity.

Discussion

Anand et al. (2008) have evaluated the proximate composition of four edible grasshoppers from India. In their study, it is found that these grasshoppers have protein content of around 63-65%. Our study follows the same pattern as *S. purpurascens* is having protein

Table 4 Deficiency maladies of the minerals selected for the present study

Minerals	Deficiency maladies	References
P	Rickets, Osteomalacia, Osteoporosis	FAO/WHO(2004); Kestenbaum and Tilman (2010)
K	Hypokalemia, leads to weakness	FAO/WHO 2004, Lanham-New et al. 2012
Ca	Osteoporosis, Memory loss, cramps, confusion	FAO/WHO (2004); Tulchinsky (2010), Kestenbaum and Tilman (2010)
Mg	Nausea, fatigue, irregular heart rhythm, poor memory, anxiety	FAO/WHO (2004); Kestenbaum and Tilman (2010)
Zn	Apetite loss, stunted growth, poor immune function, delayed sexual maturity, diarrhea, eye and skin lesions, hair loss, poor wound healing, weight loss	FAO/WHO (2004); Tulchinsky (2010)
Fe	Tiredness, pale skin, shortness of breath, head ache, palpitation, dry hair and skin, tongue and mouth soreness, restless legs, brittle fingernails, anemia	FAO/WHO (2004); Tulchinsky (2010)
Cu	Fatigue, weak and brittle bones, memory related problems, improper walking, cold sensitivity, pale skin, impaired vision, grey hair	Tsugutoshi (2004); Krupanidhi et al. (2008); Angelova et al. (2011)
Na	Nausea, Head ache, confusion, weakness	FAO/WHO 2004; Bellows and Moore 2013

slightly over 67%. However, energy content of those grasshoppers varies from 465–566 Kcal/100g, which is much higher than *S. purpurascens*. Sanchez-Muros et al. (2015) and Jajic et al. (2019) report protein percentage of *T. molitor* ranging from around 55–58% which is higher than our findings. Additionally, in their work the range of crude fat is in between 25 and 30%, which is lower than that of our findings. In any case, it is a proved fact that insects are not only a good source of protein, they are actually a better fat and energy source as well, compared to conventional meat resources (Kouřimská and Adámková, 2016).

Many edible insects have been found to be rich in iron content, and sometimes could have even more than in beef (Kinyuru et al. 2015). Our results also show this exact trend. According to van Huis (2013) the iron contents of mopane worms and *Locusta migratoria* range from 31 to 77 mg and 8 to 20 mg per 100 g of dry weight, respectively. Iron deficiency is one of the world's most widespread nutritional disorders; consequently, in developing countries anemia is extremely prominent in children and pregnant women (Mawani et al. 2016). Therefore, edible insects could be exploited to improve the status of iron deficiency (Kinyuru et al. 2015). Among conventional foods major source of Zn and Cu are oyster and beef, and the Zn content of oyster ranges in around 132mg/Kg (Kim et al. 2017). Our work supports this view as the content of Cu has been found to be much higher in the insects in comparison with red meat. Kim et al. (2017) evaluated five edible insects from Korea, but they have reported mealworm to have 11.4 mg/Kg of Cu, which is much less than our findings. The same authors have reported 27.2 mg/Kg of Cu in the grasshopper *Oxya chinensis*, but our chosen species of grasshopper *S. purpurescens* contains over 53 mg/Kg of Cu. Na and K are essential electrolytes that play important roles in physiology, such as nervous coordination. As reported by Ooninx et al. (2010), and Hyun et al. (2012), insects are a rich source of minerals such as sodium, potassium, calcium, phosphorus and magnesium. Our results are also in concert with this statement as it is evident here also that these minerals are in much higher amount in the selected insects compared to red meat and white meat. Ca, P, and Mg are essential elements of bone (Palacios 2006). The main conventional source of Ca is milk that contains 900–1300 mg/Kg of this element. It is evident that *T. molitor* is a slightly better source of Ca than meat, but *S. purpurascens* has an amount, which is almost double, compared to the amount of Ca in milk. However, Mg and P contents are found to be highest in *T. molitor*, whereas K content is almost similar in both the two insects where both the red meat and white meat contain a much lower amount of K.

Conclusion

Grasshopper and mealworm farming is a fast growing economy in various countries like China, Singapore, and Thailand. Recently US and UK based companies are also emerging. The prime goal of the insect farms is to provide protein rich food for human and livestock consumption. But from our findings, we could conclude that in addition to protein only a handful of insect flour is enough to provide ample amount of fat and energy, as well as they could act as a food additive that can supplement the minerals and keep the deficiency related maladies at bay. Thus, insects make a potential resource of nutraceuticals which demands further in depth research that will eventually encourage people to set up farms with different other insects, ultimately creating job opportunity.

Acknowledgements The authors thank the technical assistant of the Laboratory of Animal Nutrition and Biochemistry of the Faculty of Veterinary Medicine and Zootechniques of UNAM for extending kind helping hand regarding all the chemical analyses.

Authors' contributions AG and JMPM both have equal contribution for the preparation of this manuscript

Declarations

Consent for publication The authors confirm that both of them have consent for publication of this manuscript in its present form.

Conflicts of interest The authors state that there is no conflict/competing interest as far as their knowledge is concerned.

References

- Adeniyi OR, Ademosun AA, Alabi OM (2011) Proximate composition and economic values of four common sources of animal protein in South-western Nigeria. *Zootecnia Trop* 29:231–234
- Al-Yasiry ARM, Kiczorowska B, Samolińska W (2017) Nutritional value and content of mineral elements in the meat of broiler chickens fed *Boswellia serrata* supplemented diets. *J Elem* 22:1027–1037. <https://doi.org/10.5601/jelem.2017.22.1.1294>
- Anand H, Ganguly A, Haldar P (2008) Potential value of Acridids as high protein supplement for poultry feed. *Int J PoulSci* 7:722–725
- Angelova M, Asenova S, Nedkova V, Koleva-Kolarova R (2011) Copper in the human organism. *TJS* 9:88–98
- Barrera AIA, Moreno JMP (2018) Nutraceutical and Medicinal Insects: An Unexplored Research Field. In: Ganguly A, Naskar K (eds) *Entomology: Current Status and Future Strategies*, 1st edn. Daya Publishing House, Astral International, New Delhi, India, pp 137–168
- Bellows L and Moore R (2013) Sodium and the Diet. *Food and Nutrition Series, Health. Colorado state university extensión. Fact Sheet No. 9.354. pp 5.*

- Biesalski HK (2001) Nutraceuticals: the link between nutrition and medicine. In: Wildman REC (2001) Handbook of Nutraceuticals and Functional Foods, 1st edn. CRC press, Taylor and Francis, New York pp 1–9.
- Bohrer BM (2017) Review: Nutrient density and nutritional value of meat products and non-meat foods high in protein. Trends Food Sci Tech 65:103–112
- Celeste CIH, Acosta-Estrada B, Chuck-Hernández C, Serrano-Sandoval SN, Guardado-Félix D, Pérez-Carrillo E (2020) Nutritional content of edible grasshopper (*Sphenarium purpurascens*) fed on alfalfa (*Medicago sativa*) and maize (*Zea mays*). CyTA J Food 18:257–263. <https://doi.org/10.1080/19476337.2020.1746833>
- Costa Neto EM, Ramos-Elorduy J, Pino MJM (2006) Los insectos medicinales de Brasil: primeros resultados. Bol Soc & Ent Arag 38:395–414
- De Felice LS (1995) Thenutraceutical revolution, its impact on food industry. Trends Food Sci Tech 6:59–61
- El-Sohaimy SA (2012) Functional Foods and Nutraceuticals-Modern Approach to Food Science. World Appl Sci J 20:691–708. <https://doi.org/10.5829/idosi.wasj.2012.20.05.66119>
- FAO/WHO (2004) Vitamin and mineral requirements in human nutrition: report of a joint FAO/WHO expert consultation, Bangkok, Thailand, 21–30 September 1998. FAO/WHO, Rome
- FDA (2019) Interactive nutrition facts label. USFDA. https://www.accessdata.fda.gov/scripts/interactivenutritionfactslabel/factsheets/vitamin_and_mineral_chart.pdf. Accessed on 28 Dec 2019
- Feng S (2018) *Tenebrio molitor* L., entomophagy and processing into ready to use therapeutic ingredients: a review. J Nutr Health Food Eng 8:280–285
- Haldar P, Das A, Gupta RK (1999) A laboratory based study on farming of an Indian grasshopper *Oxya fuscovittata* (Marschall) (*Orthoptera: Acrididae*). J Orth Res 8:93–97. <https://doi.org/10.2307/3503431> <https://www.jstor.org/stable/3503431>
- Heidari-Parsa S, Imani S, Fathipour Y, Kheiri F, Chamani M (2018) Determination of yellow mealworm (*Tenebrio molitor*) nutritional value as an animal and human food supplementation. Arthropods 7:94–102
- Helrich K (1990) Official methods of analysis of the Association of Official Analytical Chemists. A.O.A.C, Philadelphia, USA
- Hyun SH, Kwon KH, Park KH, Jeong HC, Kwon O, Tindwa H, Han YS (2012) Evaluation of nutritional status of an edible grasshopper, *Oxya chinensis formosana*. Entomol Res 42:284–290
- Jajic I, Popovic A, Urosevic M, Krstovic S, Petrovic M, Guljas D (2019) Chemical composition of mealworm larvae (*Tenebrio molitor*) reared in Serbia. ContAgr 68:23–27. <https://doi.org/10.2478/contagri-2019-0005>
- Jokanović MR, Tomović VM, Jović MT, Škaljac SB, Šojić BV, Ikonić PM, Tasić TA (2014) Proximate and Mineral Composition of Chicken Giblets from Vojvodina (Northern Serbia). Int J Nutr Food Eng 8:986–989
- Karakök SG, Ozogul Y, Saler M, Ozogul F (2010) Proximate analysis. Fatty acid profiles and mineral contents of meats: a comparative study. J Muscle Foods 21:210–223
- Kestenbaum B, Tilman BD (2010) Disorders of Calcium, Phosphate, and Magnesium metabolism. In: Floege J, Johnson RJ, Feehally J (eds) Comprehensive clinical nephrology, 4th edn. Mosby, Elsevier, USA, pp 130–148
- Kim KS, Weaver CM, Choi MK (2017) Proximate composition and mineral content of five edible insects consumed in Korea. CyTA J Food 15:143–146. <https://doi.org/10.1080/19476337.2016.1223172>
- Kinyuru JN, Mogendi JB, Riwa CA, Ndung'u NW, (2015) Edible insects—a novel source of essential nutrients for human diet: Learning from traditional knowledge. Anim Front 5:14–19
- Kouřimská L, Adámková A (2016) Nutritional and sensory quality of edible insects. NFS J 4:22–26
- Krupanidhi S, Sreekumar A, Sanjeevi CB (2008) Copper & biological health. Indian J Med Res 128:448–461
- Lanham-New SA, Lambert H, Freassetto L (2012) Nutrient information: Potassium. Adv Nutr 3:820–821. <https://doi.org/10.3945/an.112.003012>
- Liu C, Masri J, Perez V, Maya C, Zhao J (2020) Growth performance and nutrient composition of mealworms (*Tenebrio molitor*) fed on fresh plant materials supplemented diets. Foods 9:1–10
- Márquez MC (1962) Estudio de las especies del género *Sphenarium* basado en su genitalia (*Acrididae: Orthoptera*), con la descripción de una especie nueva. An Inst Biol Univ Nac Auton Mex Ser Zoo 1–2:247–265
- Mawani M, Ali SA, Bano G, Ali SA (2016) Iron Deficiency Anemia among women of reproductive age, an Important Public Health Problem: Situation Analysis. Reprod Syst Sex Disord 5:1–6. <https://doi.org/10.4172/2161-038X.1000187>
- Ooninx DGAB, van Itterbeeck J, Heetkamp MJW, van den Brand H, van Loon JJA, van Huis A (2010) An exploration on greenhouse gas and ammonia production by insect species suitable for animal or human consumption. PLoS One 5:1–7
- Palacios C (2006) The role of nutrients in bone health, from A to Z. Crit Rev Food Sci Nutr 46:621–628
- Pandey M, Verma RK, Shubhini AS (2010) Nutraceuticals: new era of medicine and health. AJPCR 3:11–15
- Pino MJM, Ángeles CS, García A (2009) Substancias curativas encontradas en insectos nutraceuticos y medicinales. Entomol Mex 8:256–261
- Ramos-Elorduy J (2000) La etnoentomología actual en México en la alimentación humana, en la medicina tradicional y en el reciclaje y alimentación animal. Mem XXXV Cong Nac de Ent, pp 3–46.
- Ramos-Elorduy J, Moreno JMP, Camacho VHM (2012) Could Grasshoppers Be a Nutritive Meal? Food Nutr Sci 3:164–175
- Ravzanaadii N, Kim SH, Choi WH, Hong SJ, Kim NJ (2012) Nutritional value of mealworm, *Tenebrio molitor* as food source. Int J Indust Entomol 25:93–98
- Sanchez-Muros MJ, de Haro C, Sanz A, Trenzado CE, Villareces S, Barroso FG (2015) Nutritional evaluation of *Tenebrio molitor* meal as fish meal substitute for tilapia (*Oreochromis niloticus*) diet. Aquac Nutr 21:1–14
- Srividya AR, Nagasamy V, Vishnuvarthan VJ (2010) Nutraceutical as medicine. Pharmanest 1:132–145
- Torrucó-Uco JG, Hernández-Santos B, Herman-Lara Martínez-Sánchez CE, Juárez-Barrientos JM, Rodríguez-Miranda, (2019) Chemical, functional and thermal characterization, and fatty acid profile of the edible grasshopper (*Sphenarium purpurascens* Ch.). Eur Food Res Technol 245:285–292. <https://doi.org/10.1007/s00217-018-3160-y>
- Tsugutoshi A (2004) Copper deficiency and the clinical practice. Jpn Med Assoc J 47:365–370
- Tulchinsky TH (2010) Micronutrient deficiency conditions: Global Health Issues. Public Health Rev 32:243–255
- van Huis A (2013) Potential of insects as food and feed in assuring food security. Annu Rev Entomol 58:563–583. <https://doi.org/10.1146/annurev-ento-120811-153704>
- van Huis A, Itterbeeck JV, Harmke K, Mertens E, Halloran A, Muir G, Vantomme P (2013) Edible insects: future prospects for food and feed security. Food and Agriculture Organization of the United Nations, Rome, Italy
- Virginia MR, Quirino-Barreda T, García-Núñez M, Díaz-García R, Sánchez-Herrera K, Schettino-Bermudez B (2015) Grasshoppers *Sphenarium purpurascens* Ch. Source of proteins and essential amino acids. J Chem Chem Eng 9:472–476. <https://doi.org/10.17265/1934-7375/2015.07.008>

Wildman REC (2001) Handbook of Nutraceuticals and Functional Foods. CRC Press, Taylor and Francis, New York
Williams P (2007) Nutritional composition of red meat. *Nutr Diet* 64:S113–S119. <https://doi.org/10.1111/j.1747-0080.2007.00197.x>

Wyness L, Weichselbaum E, O'Connor A, Williams EB, Benelam B, Riley H, Stanner S (2011) Red meat in the diet: an update. *Nutr Bull* 36:34–77

*On the biomass production of
Spathosternum prasiniferum prasiniferum
(Walker, 1871) (Orthoptera: Acrididae) as
a potential insect to feed the livestock*

**Arijit Ganguly, Parimalendu Haldar &
Dipak Kr. Mandal**

**International Journal of Tropical
Insect Science**

e-ISSN 1742-7592

Int J Trop Insect Sci
DOI 10.1007/s42690-020-00328-z



Your article is protected by copyright and all rights are held exclusively by African Association of Insect Scientists. This e-offprint is for personal use only and shall not be self-archived in electronic repositories. If you wish to self-archive your article, please use the accepted manuscript version for posting on your own website. You may further deposit the accepted manuscript version in any repository, provided it is only made publicly available 12 months after official publication or later and provided acknowledgement is given to the original source of publication and a link is inserted to the published article on Springer's website. The link must be accompanied by the following text: "The final publication is available at link.springer.com".



On the biomass production of *Spathosternum prasiniferum prasiniferum* (Walker, 1871) (Orthoptera: Acrididae) as a potential insect to feed the livestock

Arijit Ganguly¹ · Parimalendu Haldar² · Dipak Kr. Mandal²Received: 22 June 2020 / Accepted: 9 October 2020
© African Association of Insect Scientists 2020

Abstract

In recent times short horn grasshoppers (i.e. acridids) have been emerged as a potential nutrient resource for livestock in India. But it is necessary to attempt their mass production for a sustainable supply which is also cost effective. In this context the present work aimed to evaluate the ability of annual production of *Spathosternum prasiniferum prasiniferum* (Walker, 1871). The insects were reared in captivity in natural condition without the aid of any environmental chamber that has been used in all the previous works. For estimation of biomass nymphal survival percentage, number of egg pods laid per female, number of eggs hatched per pod, sex ratio, energy content and dry body weight of adult individuals were taken into consideration. Then projected annual biomass was calculated from the obtained results. The findings were encouraging because we have estimated about 66,326 individuals, or 3.55 Kg of dry biomass i.e. 82,234.33 KJ of energy after one year starting from only one pair. Even though the probable annual biomass was found to be lower than the previous works, still it was a good amount, and heartening for mass scale production. Thus we have concluded the work with a notion that this might encourage small scale start up even by poor farmers who are unable to procure environmental chamber. However, other species should be explored in future that can produce a higher biomass.

Keywords Insect farming · Annual biomass · *Spathosternum prasiniferum prasiniferum*

Introduction

It is estimated that by the year 2050 there will more than nine billion people on earth and because of this global population boom and due to over-exploitation of food there will be a great scarcity of conventional protein sources (Kouřimská and Adámková 2016). In this context it is a must to look for alternatives (Madau et al. 2020). In recent times insects are emerging as an unconventional nutritionally rich food resource where anti-nutritional growth retardants are present in tolerance limit (Das and Mandal 2014). The ubiquitous presence made these marvel creatures a frequent ingredient in common

victuals from time immemorial throughout the world (Imathiu 2020). Nevertheless, only in recent days they are getting serious attention from the scientific community. Many workers established that insects are high in nutrients and energy, and many of them could be cultivated as mini-livestock (Zhou and Han 2006; Alexander et al. 2017). But accepting insects as food is not always very easy for any mature person having western influenced upbringing who consider these creatures as “poor man’s food”; and because of this social taboo we observe repugnance in consuming insects among the western and western influenced communities (Rodríguez-Miranda et al. 2019). In this context they could be used as an alternative nutrient supplement for the livestock industry.

Various workers have successfully used insects as alternative protein source for poultry, fish and pigs (Yen 2015). Among insects, the order Orthoptera (i.e. grasshoppers and crickets) has been found to contain about 43.9% to 77.1% protein with the highest quantity in *Melanoplus mexicanus* (Saussure, 1861) and 14.05 KJ to 21.88 KJ of energy where *Blaberus* sp. showed the best value (Ramos-Elorduy et al. 2012). Workers like Anand et al. (2008a) and Das and

✉ Arijit Ganguly
arijitganguly87@yahoo.co.in

¹ Department of Zoology, Achhruram Memorial College, Purulia, Jhalda, West Bengal 723202, India

² Department of Zoology, Visva Bharati University, Santiniketan, West Bengal 731235, India

Mandal (2013) effectively utilized the acridid grasshopper *Oxya* sp. as poultry feed. Likewise, Ganguly et al. (2014) proved acridid grasshoppers to be suitable to feed ornamental fishes, while Ghosh and Mandal (2019) reported lucrative results when these short-horn grasshoppers were used as a supplementary nutrient in table fish feed. However, any food resource needs to be produced in mass scale for sustenance. Therefore, acridid mass production is very much needed.

To address this issue Haldar and Nandy (1997) first attempted mass rearing of *Hieroglyphus banian* (Fabricius, 1798), *Acrida exaltata* (Walker, 1859), and *Oxya* sp. Later, Das et al. (2002) did a mass culture study on *Oxya fuscovittata* (Marschall, 1836). Anand et al. (2008b) compared the mass production abilities of *O. fuscovittata* and *S. pr. prasiniferum*. Das et al. (2012) successfully cultured *Oxya hyla hyla* (Surville, 1831). The results proved *O. hyla hyla*, *O. fuscovittata*, and *S. pr. prasiniferum* are the major candidate species for mass culture. According to them both the *Oxya* species have higher potential of mass production in comparison with *S. pr. prasiniferum*. It should be noted that all these studies utilized environmental chamber so that the insects could be reared in optimum temperature, photo period, and humidity. But, we should keep in mind that many poor farmers who are interested to start acridid farming would not be able to procure sufficient amount of environmental chambers. And those who could afford such apparatus will have huge start up cost.

Considering this scenario, the present work was designed to evaluate the mass production ability of the oligophagous short-horned grasshopper (i.e. acridid) *S. pr. prasiniferum* which is comparatively a less studied species. Das and Mandal (2013) opined that this insect species could be an alternative nutrient resource. Their study revealed that this grasshopper species contains more than 65% crude protein, 7% fat, and over 6% of carbohydrate on dry matter basis. The energy content was reported to be 2347 KJ/100 g. Additionally they were also found to be rich in fatty acids, amino acids, vitamins and minerals, where anti-nutritional factors like oxalate, tannin, and phytin were present in significantly low titer. Ganguly et al. (2013) reported that *S. pr. prasiniferum* is one of the most abundant tetravoltine (i.e. completing four generations in a year) acridid species in the state of West Bengal in India, where the present work was conducted. According to that report their gestation period is about four weeks, nymphal duration is about 40–50 days, and adult duration is about 30–40 days. They start copulating soon after reaching maturity, and start laying egg pods within 8–12 days of adulthood. Thus it is observed that *S. pr. prasiniferum* can complete four generations annually. This oligophagous insect may affect the entire winter crop (sown during June–August and harvested in November–January), and summer seedlings of sorghum and wheat (Sown during January–February and harvested in April–May) in the state of

West Bengal, India. As it was evident that these insects mainly target plants under Poaceae family, in our work also they were reared on four food plants of the same family, and nymphal survival and reproductive potential was estimated. Then their probable annual biomass was calculated from those data assuming a single pair as a starting point. The entire study had been conducted in natural condition during May, 2019 to August, 2019, and without the use of environmental chamber. The prime goal of this study was to get an idea whether there will be sufficient biomass even if environmental chambers are not used in acridid farms.

Material and methods

Stocking of *S. pr. prasiniferum*

Fifty adult males and fifty females of *S. pr. prasiniferum* were collected from the grasslands of Santiniketan, West Bengal, India. They were stocked in 5 plastic boxes measuring 38 cm × 30 cm × 20 cm with 10 males and 10 females in each. For rearing purpose leaves of *Cynodon dactylon* (L.) Pers. was offered to the insects in a set up as described by Haldar et al. (1999). Taxonomic identification up to sub-species level was confirmed with the help of the authentic guidebook of Bhowmik (1986), published by the Zoological Survey of India.

Food plants

Seeds of *Sorghum halepense* (L.) Pers., *Triticum aestivum* L., and *Oryza sativa* L. were bought from the local market and sowed in the “Entomology Experimental Plot” in the Department of Zoology campus of Visva Bharati University. No pesticides were administered to the food plants. When the seedlings emerged fresh leaves were clipped and offered to the insects in the experimental sets each day. The common “Durva grass” *C. dactylon* was abundant in the same pesticide free experimental plot and they were also clipped and offered to the sets afresh each day.

Experimental set up

The experiment was conducted in 12 plastic boxes as we have used one food plant per set and there were four food plants in triplicates. Rearing was done by the same Haldar et al. (1999) method. Each box measured 38 cm × 30 cm × 20 cm, and was fitted with nylon mesh of about 1 mm wide pore size for proper aeration. The bottoms of the boxes were covered with 5 cm deep sterilized sand that was previously boiled in water in 100 °C for ten minutes. Each day some water was sprinkled to keep the sand moist so that the humidity of the experimental boxes could be maintained. When eggs hatched out from the

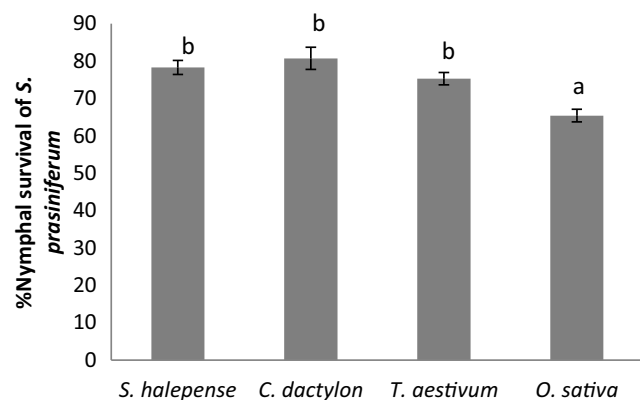


Fig. 1 % Nymphal survival of *S. prasiniferum* fed with different food plants. Values are means \pm SD. **Note:** Values with different letters are significantly different ($F = 30.41$, $P < 0.01$, one-way ANOVA, Tukey's pair-wise test)

stock sets, same day hatched 492 fledglings were randomly selected and placed in the experimental sets with 41 individuals in each.

Estimation of selected parameters

For the computation of annual biomass production, parameters like nymphal survival, number of egg pods laid per female, number of eggs hatched per pod, sex ratio, dry body weight, and energy content of adult individuals were taken into consideration. For the estimation of dry body mass 51 adult males and 51 adult females were separately collected from stock sets and freeze killed followed by oven drying at 60 °C until the weight became constant. Finally they were weighed individually and the mean values of their dry body masses were expressed in grams. After that the dry insect carcass was crushed in powder form by a mixer grinder and mixed with fixed proportion of benzoic acid as burning agent to make pellets weighing 1 g. Later, the mixed pellets were charged with digital oxygen bomb calorimeter (model EIE-220A, EIE Instruments Pvt. Ltd., Ahmedabad, India) and energy was expressed in terms of KJ/100 g. Sex ratio was estimated by random sampling of 1000 individuals from the grasslands of Santiniketan by sweeping technique and number of males and females were calculated separately. Other estimations were made in the experimental set up. Nymphal survival was expressed as percentage of nymphs reaching adulthood. When first copulating pair was observed in all the boxes, they were regularly checked for counting number of egg

pods along with the number of adult females in each. Thus average number of egg pods laid per female was estimated. Known amount of egg pods (usually 8–10) were kept inside sterilized moist sand in 80 ml plastic cups fitted with nylon net at the top. When hatching started, numbers of fledglings were calculated, recorded, and were transferred to the stock sets. When there were no hatching recorded for 30 days it was assumed no more eggs to be hatched; then average number of eggs hatched per pod was estimated.

Computation of projected annual biomass

For the computation of total biomass produced in a year we started with a single pair. Multiplying the total egg pods laid per female and eggs hatched per pod we got the probable number of fledglings hatched from one female. Then the mortality percentage was subtracted to obtain total number of insect attaining adulthood. Later, they were separated as male and female groups according to their sex ratio that we obtained from our field sampling data. Thus we have reached to total number of adult males and females in the first generation. We followed the same pattern to attain the total number of individuals in three subsequent generations owing to the tetra-voltinity of *S. pr. prasiniferum*. The total annual production of males and females were obtained by adding the numbers of all the four generations. Finally, the numbers were separately multiplied with individual dry body weight, and energy.

Statistical analyses

Data were presented as means \pm SD. Food plant specific difference between nymphal survivals, egg pods laid per female, and eggs hatched per pod were subjected to one way analysis of variance (ANOVA) taking food plants as independent variable. Mean separations were conducted by Tukey's pair-wise test where ANOVA showed significant difference. Disparity between mean dry weight of adult males and females were obtained by independent t test. All the analyses were performed at 95% confidence level (i.e. $\alpha = 0.05$) using Microsoft excel, and Past version 3.20.

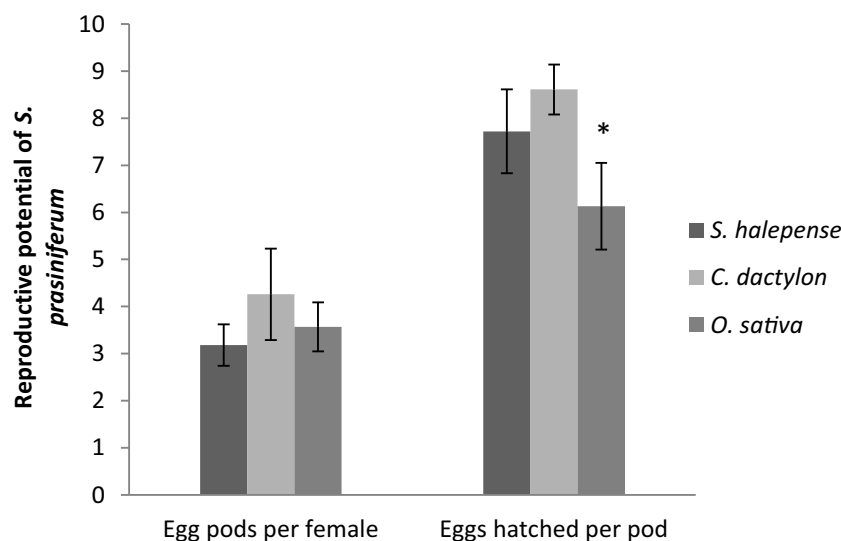
Results

Percentage of nymphal survival is summarized in Fig. 1. *C. dactylon* fed groups had the highest mean survival

Table 1 One way ANOVA table of nymphal survival

Source of Variation	SS	df	MS	F	P value	F crit
Between Groups	406.9347	3	135.6449	30.41212	0.000101	4.066181
Within Groups	35.6818	8	4.460225			
Total	442.6165	11				

Fig. 2 Reproductive potential of *S. prasiniferum* fed with different food plants. Values are means \pm SD. **Note:** Asterisk (*) shows significant lower value in *O. sativa* fed groups compared to *C. dactylon* fed ones ($F = 7.4$, $P < 0.05$, one-way ANOVA, Tukey's pair-wise test). Other values are insignificant



(80.73%), even though it did not vary significantly from the results of *S. halepense* and *T. aestivum* fed groups ($P > 0.05$, Tukey's pair-wise test). On the other hand *O. sativa* fed groups showed significant low survival (65.41%) compared to the other three plant fed groups ($F = 30.41$, $P < 0.01$, one-way ANOVA, Tukey's pair-wise test, Table 1). Reproductive potential of *S. pr. prasiniferum* is depicted in Fig. 2. Here it should be noted that *T. aestivum* fed groups did not lay any egg pod. Highest number of egg pods were observed in *C. dactylon* fed groups (i.e. 4.26) and the lowest value of 3.18 was recorded in the *S. halepense* fed sets. However, in this case statistical analysis did not show any significant difference ($F = 1.916$, $P = 0.227$, one-way ANOVA, Table 2). Nevertheless, the parameter of eggs hatched per pod showed statistically significant result in one way ANOVA ($F = 7.401$, $P < 0.05$, Table 3). Here, the highest mean value 8.61 was observed in *C. dactylon* fed groups. Mean separation by Tukey's pair-wise test revealed that the result of *S. halepense* and *C. dactylon* fed groups did not vary significantly ($P > 0.05$), however *O. sativa* fed groups showed the lowest mean value of 6.13 which was significantly lower than *C. dactylon* fed groups ($P < 0.05$). In this study *C. dactylon* fed groups almost always showed better survival and reproductive potential. Hence we have selected those results for the computation of projected annual biomass production. Figure 3 represents the mean dry weight of adult males and females that were 0.045 g and 0.065 g respectively. Independent t test revealed that females always had higher dry mass than that of

males ($P < 0.05$) owing to their robustness. Finally, the energy content was observed to be 2316.46 KJ per 100 g of dry biomass.

For the calculation of sex ratio 1000 individuals were randomly collected from the grasslands near the campus of Zoology department of Visva Bharati University, santiniketan. Among them 572 were recorded to be males and 428 were females. Thus we have calculated the ratio as $\text{♂}:\text{♀} = 572:428 = 5.7:4.3$.

In the present study we considered the tetravoltinity to calculate the probable annual biomass, which was computed for four generations starting with a single male and female pair (Fig. 4). It is already mentioned that we have selected the results of *C. dactylon* fed groups for this calculation. It is evident from Fig. 2 that average number of egg pods laid per female is 4.26, while eggs hatched per pod is 8.61. So from one female we can expect $4.26 \times 8.61 = 36.68$ fledglings. Then we considered the nymphal survival percentage to estimate the total number of individuals reaching adulthood. The nymphal survival percentage of *C. dactylon* fed groups was 80.73. So, it was assumed that 80.73% of 36.68 i.e., about 29.61 individuals will reach maturity. Then we divided this number according to sex ratio of $\text{♂}:\text{♀} = 5.7:4.3$ to obtain 16.88 males and 12.13 females, and thus completed the first cycle. The second cycle started with 12.13 females and we followed the same pattern up to fourth generation that we used to compute the first one. Lastly the total number of males and females were summed up and we obtained a total of about

Table 2 One way ANOVA table of egg pods laid per female

Source of Variation	SS	df	MS	F	P value	F crit
Between Groups	1.7946	2	0.8973	1.916079	0.227252	5.143253
Within Groups	2.8098	6	0.4683			
Total	4.6044	8				

Table 3 One way ANOVA table of eggs hatched per pod

Source of Variation	SS	df	MS	F	P value	F crit
Between Groups	9.4706	2	4.7353	7.401219	0.023994	5.143253
Within Groups	3.8388	6	0.6398			
Total	13.3094	8				

37,806 males and 28,520 females to be produced in one year. After multiplying these numbers with respective dry weights we obtained 1.7 Kg of male and 1.85 Kg of female dry biomass or 3.55 Kg of total annual dry biomass. Lastly, total annual biomass in terms of energy was estimated by multiplying the energy content (2316.46 KJ/100 g) with the total dry mass (3.55 Kg) and we obtained 82,234.33 KJ.

Discussion

Acridid biomass is directly proportional to nymphal survival, fecundity and fertility, which are well dependent on the food plants on which these insects feed. Hence, a suitable food plant ought to be found out for a sustainable farming of acridids as mini-livestock. In this context, Ganguly et al. (2010) first reported *S. halepense* to be a suitable food plant for the mass rearing of *O. fuscovittata*. Later, Das et al. (2012) evaluated the nutritional ecology of *O. hyla hyla* and *S. pr. prasiniferum* where three different grasses like *Dactyloctenium aegyptium* (L.) Willd., *C. dactylon*, and *Brachiaria mutica* (Forssk.) Stapf were fed to them. In their study the authors reported *B. mutica* to be the best food plant followed by *C. dactylon*. Ganguly et al. (2013) studied life history, growth rates, food consumption and utilization indices of *S. pr. prasiniferum* fed with different food plants. According to them *S. halepense* followed by *C. dactylon* gave the best results. In the present work we have estimated nymphal survival and reproductive potential of the same insect with the same food plants, and we obtained *C. dactylon* and *S. halepense* to be the best ones. Considering all the parameters we could easily conclude that these two plants are the best choice for mass rearing of this insect.

On the other hand, although acridids are considered to be paddy pest, *O. sativa* fed groups did not show good results. In a similar work Nzekwu and Akingbohunge (2002) reported that nymphal duration of *Oedalues nigeriensis* Uvarov, 1926 was very low when fed with *Seteria gracilipes* Hubbard and *Axonopus compressus* (Sw.) P. Breauv. Hence it is evident that food plants are an important prerequisite for the livelihood of acridid species (Riffat and Muhammad 2007; Riffat and Wagan 2007; Das et al. 2012). In the present study higher nymphal survival was obtained in *C. dactylon* followed by *S. halepense* and highest nymphal mortality was observed in

O. sativa fed groups. This occurred may be because of the interaction between the nutritional demand of the insect and nutrients present in the plants. While studying the nutritional ecology of *O. fuscovittata*, Ganguly et al. (2010) reported nutritional quality of *S. halepense*, *C. dactylon*, *T. aestivum* and *O. sativa*. According to their result, *S. halepense* contained maximum amount of crude protein, and fat (more than 15% and 3% of dry body weight respectively). *C. dactylon* fell next in terms of crude protein that was about 11.5%. *C. dactylon* and *T. aestivum* shared similar protein and fat contents, but the latter had higher carbohydrate (84.43%) and very low crude fiber (2.27%). On the other hand *O. sativa* contained the lowest amount of protein (just over 6%). The nutritional values were very much aligned with the results obtained in the present case. It is a well known fact that dietary nitrogen can impact survival and reproductive potential of acridids (Rode et al. 2017). In the present work we have obtained least nymphal survival percentage in *O. sativa* fed groups as the protein content was the lowest in this plant. Apart from survival, food plants also have significant effect on the fecundity and fertility. While describing the importance of choice of food plants Awmack and Leather (2002), and Branson (2006) mentioned that host plant quality can directly affect insect reproductive strategies like egg size, quality and allocation of resources to eggs; even choice of oviposition sites may be influenced by plant quality. In the present work *T. aestivum* fed groups were observed to be unable to produce any egg pod. Relatively higher amount of carbohydrate and significantly low fiber content might be a cause behind this. Egg pods laid per female did not vary significantly between

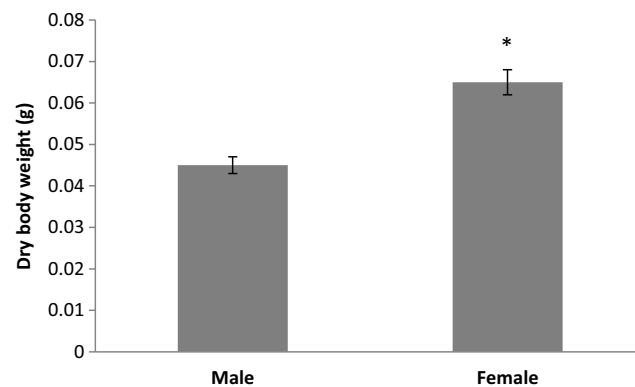
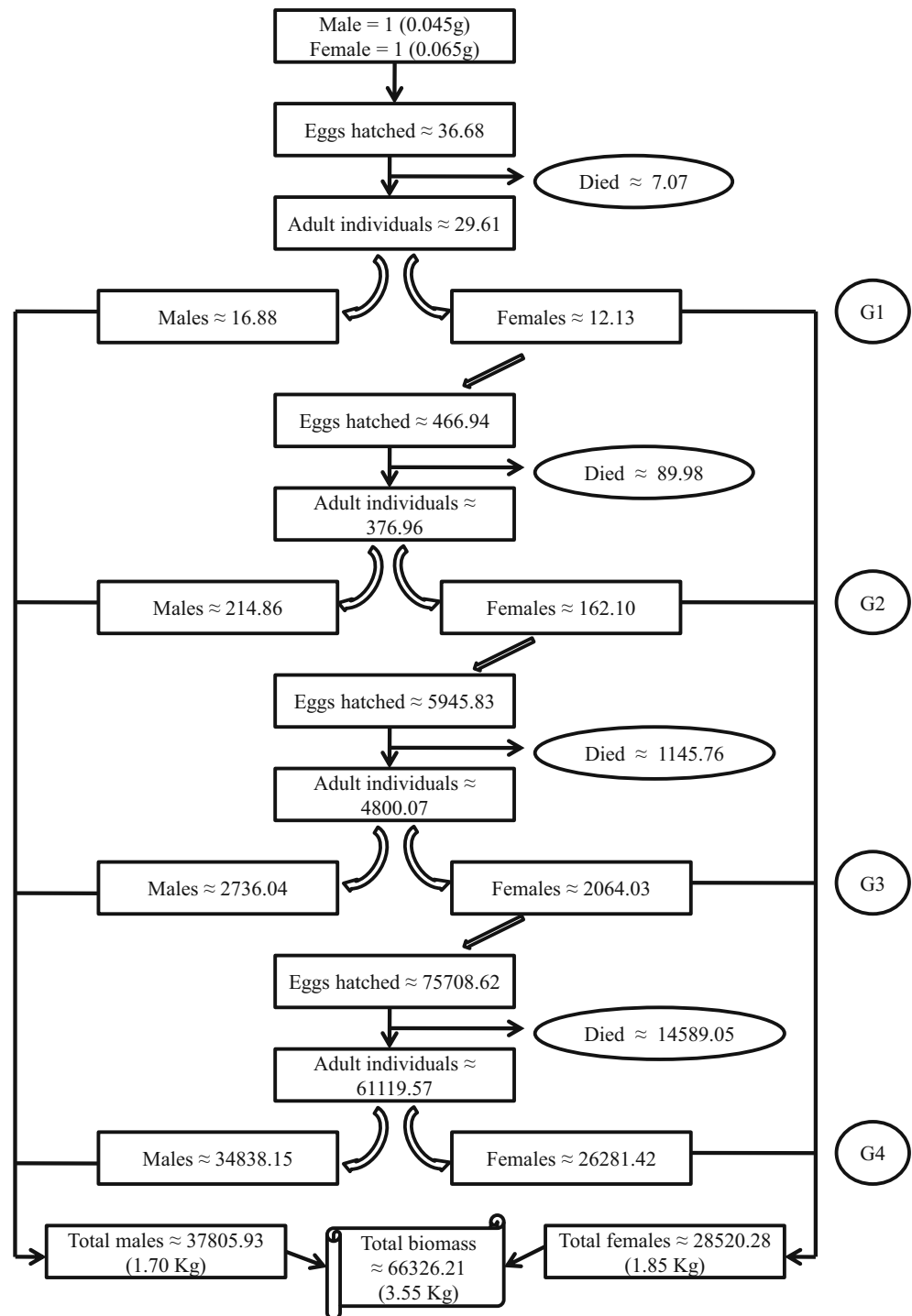


Fig. 3 Mean dry body weight (g) of adult males and females. Values are means \pm SD. **Note:** Asterisk (*) shows significant higher mean dry weight in female *S. pr. prasiniferum* ($P < 0.05$, independent t test)

the other three plant-fed groups, but the mean number of eggs hatched per pod was the lowest in *O. sativa* fed sets. These findings have also been supported by Abdel-Rahman (2001), and Das et al. (2002). The results of the present study clearly showed food plant specific variations in nymphal survival, fecundity and fertility that may directly affect mass production, and *C. dactylon* fed groups had the capacity to produce the highest biomass.

The mass production of *S. pr. prasiniferum* was attempted by Anand et al. (2008b) and Das et al. (2012). Both of these two works projected around 10 Kg of dry biomass annually assuming a single pair as a starting point which was fairly higher than our finding of 3.55 Kg. Here it should be noted that we did not use any environmental chamber for the present study. We should also mention that even this lower biomass is encouraging because if we could obtain more than three

Fig. 4 The conceptual model of projected annual biomass of *S. prasiniferum* starting with a single pair and fed with *C. dactylon*



kilograms of dry biomass only from one pair annually, we could produce hundreds of kilograms of *S. pr. prasiniferum* biomass in an insect mini-livestock farm with bigger area. We hope that our findings will hearten the farmers at the grassroots level to take up insect farming as a start-up since they will obtain a good biomass even without environmental chamber. However, other acridid species such as *Oxya* sp. should be given trial in future because of their ability to produce higher biomass and find out whether they can also provide better production without the aid of environmental chamber.

Lastly it should be noted that in the present study the rearing had been done for only one generation and the same trend was utilized for the calculation of the annual biomass. However, practically this could not be the case in nature. Insect production is very much dependant on temperature, photoperiod and humidity, that cannot be the same throughout the year (Ma et al. 2017). Thus, survival, growth, life span, and reproductive potential will have season wise variation that may lead to a quite different biomass with respect to the findings of the present study. Nevertheless, the present work mainly focused on whether mass production of *S. pr. prasiniferum* is possible without using any costly apparatus. The findings were much encouraging and demand future works on the assessment of the economical aspects of acridid farm building, maintenance and production cost which was out of the scope of this paper. We conclude with the hope that in near future realistic acridid grasshopper farms might be built where a tangible annual biomass will be attained to feed the livestock.

Acknowledgements The authors thank the Head, Department of Zoology, Visva Bharati University for providing laboratory facilities to conduct this study. The University Grants Commission, Govt. of India, is acknowledged for providing financial assistance.

Authors' contributions AG DKM and PH have equal contribution for the preparation of this manuscript.

Data availability Not applicable.

Compliance with ethical standards

Declaration of competing interest The authors declare that they have no known competing interests with respect to this paper.

Ethics approval Not applicable.

Consent to participate Not applicable.

Consent for publication All the three authors have consent for publication of this manuscript in its present form.

Code availability Not applicable.

References

- Abdel-Rahman KM (2001) Food consumption and utilization of the grasshopper *Chrotogonus lugubris* Blanchard (Orthoptera, Acridoidea, Pyrgomorphidae) and its effect on the egg deposition. *J Cent Eur Agric* 2:263–270
- Alexander P, Brown C, Arneth A, Dias C, Finnigan J, Moran D, Rounsevell MDA (2017) Could consumption of insects, cultured meat or imitation meat reduce global agricultural land use? *Glob Food Sec* 15:22–32. <https://doi.org/10.1016/j.gfs.2017.04.001>
- Anand H, Das S, Ganguly A, Haldar P (2008a) Biomass production of acridids as possible animal feed supplement. *J Environ Sociobiol* 5: 181–190
- Anand H, Ganguly A, Haldar P (2008b) Potential value of acridids as high protein supplement for poultry feed. *Int J Poult Sci* 7:722–725
- Awmack CS, Leather SR (2002) Host plant quality and fecundity in herbivorous insects. *Annu Rev Entomol* 47:817–844. <https://doi.org/10.1146/annurev.ento.47.091201.145300>
- Bhowmik HK (1986) Grasshopper fauna of West Bengal. Zoological Survey of India, Calcutta
- Branson DH (2006) Life history responses of *Ageneotettix deorum* (Scudder) (Orthoptera: Acrididae) to host availability and population density. *JK Entom Soc* 79:146–155. <https://doi.org/10.2317/0501.11.1>
- Das M, Mandal SK (2013) Assessment of nutritional quality and anti-nutrient composition of two edible grasshoppers (Orthoptera: Acrididae) - a search for new food alternative. *IJMPS* 3:31–48
- Das M, Mandal SK (2014) *Oxya hyla hyla* as an alternative protein source for Japanese quail. *Int Sch Res Notices* 2014:1–14. <https://doi.org/10.1155/2014/269810>
- Das A, Das S, Haldar P (2002) Effect of food plants on growth rate and survivality of *Hieroglyphus banian* (Fabricius) (Orthoptera: Acrididae), a major paddy pest in India. *Appl Entomol Zool* 37: 207–212. <https://doi.org/10.1303/aez.2002.207>
- Das M, Ganguly A, Haldar P (2012) Annual biomass production of two acridids (Orthoptera: Acrididae) as alternative food for poultry. *Span J Agric Res* 10:671–680. <https://doi.org/10.5424/sjar/2012103-222-11>
- Ganguly A, Chakravorty R, Sarkar A, Haldar P (2010) Johnson grass [*Sorghum halepense* (L.) Pers.] A potential food plant for attaining higher biomass in acridid farms. *Philipp Agric Scientist* 93:329–336
- Ganguly A, Chakravorty R, Haldar P (2013) Assessment of consumption utilization and growth of *Oedaleus abruptus* (Thunberg) and *Spathosternum prasiniferum prasiniferum* (Walker) (Orthoptera: Acrididae) fed with various food plants in laboratory conditions. *Ann Soc Entomol Fr* 49:160–171. <https://doi.org/10.1080/00379271.2013.810027>
- Ganguly A, Chakravorty R, Sarkar A, Mandal DK, Haldar P, Ramos-Elorduy J, Moreno JMP (2014) A preliminary study on *Oxya fuscovittata* (Marschall) as an alternative nutrient supplement in the diets of *Poecillia sphenops* (Valenciennes). *PLoS One* 9:1–7. e111848. <https://doi.org/10.1371/journal.pone.0111848>
- Ghosh S, Mandal DK (2019) Nutritional evaluation of a short-horned grasshopper, *Oxya hyla hyla* (Serville) meal as a substitute of fishmeal in the compound diets of rohu, *Labeo rohita* (Hamilton). *Jo BAZ* 80: 1–8. <https://doi.org/10.1186/s41936-019-0104-4>
- Haldar P, Nandy NC (1997) Feasibility of grasshopper farming in West Bengal—a review on laboratory based studies. *J Inter Des* 1:160–161
- Haldar P, Das A, Gupta RK (1999) A laboratory based study on farming of an Indian grasshopper *Oxya fuscovittata* (Marschall) (Orthoptera: Acrididae). *J Orth Res* 8:93–97. <https://doi.org/10.2307/3503431>
- Imathiu S (2020) Benefits and food safety concerns associated with consumption of edible insects. *NFS J* 18:1–11. <https://doi.org/10.1016/j.nfs.2019.11.002>

- Kouřimská L, Adámková A (2016) Nutritional and sensory quality of edible insects. *NFS J* 4:22–26
- Ma L, Wang X, Liu Y, Su MZ, Huang GH (2017) Temperature effects on development and fecundity of *Brachmia macroscopa* (Lepidoptera: Gelechiidae). *PLoS One* 12:1–12. <https://doi.org/10.1371/journal.pone.0173065>
- Madau A, Arru B, Furesi R, Pulina P (2020) Insect farming for feed and food production from a circular business model perspective. *Sustainability* 12:1–15. <https://doi.org/10.3390/su12135418>
- Nzekwu AN, Akingbohunge AE (2002) The effect of various host plants on nymphal development and egg production in *Oedaleus nigeriensis* Uvarov (Orthoptera: Acrididae). *J Orthop Res* 11:185–188. [https://doi.org/10.1665/1082-6467\(2002\)011\[0185:TEOVHP\]2.0.CO;2](https://doi.org/10.1665/1082-6467(2002)011[0185:TEOVHP]2.0.CO;2)
- Ramos-Elorduy J, Moreno JMP, Camacho VHM (2012) Could grasshoppers be a nutritive meal? *Food Nutr Sci* 3:1–12. <https://doi.org/10.4236/fns.2012.32025>
- Riffat S, Muhammad SW (2007) Some studies of growth, development and fecundity of grasshopper *Hieroglyphus oryzivorus* Carl, (Orthoptera: Acrididae) on food plants in Sindh. *Pak Entomol* 29:9–13
- Riffat S, Wagan MS (2007) The effect of food plants on the growth rate fecundity and survivality of grasshopper *Hieroglyphus nigrorepletus* I. Bolivar (Orthoptera: Acrididae) a major paddy pest in Pakistan. *J Biol Sci* 30:27–32. <https://doi.org/10.3923/jbs.2007.1282.1286>
- Rode M, Lemoine NP, Smith MD (2017) Prospective evidence for independent nitrogen and phosphorus limitation of grasshopper (*Chorthippus curtipennis*) growth in a tallgrass prairie. *PLoS One* 12. <https://doi.org/10.1371/journal.pone.0177754>
- Rodríguez-Miranda J, Alcántar-Vázquez JP, Zúñiga-Marroquín T, Juárez-Barrientos JM (2019) Insects as an alternative source of protein: a review of the potential use of grasshopper (*Sphenarium purpurascens* Ch.) as a food ingredient. *Eur Food Res Technol* 245:2613–2620. <https://doi.org/10.1007/s00217-019-03383-0>
- Yen AL (2015) Foreword: why a journal of insects as food and feed? *J Insects as Food Feed* 1:1–2. <https://doi.org/10.3920/JIFF2015.x001>
- Zhou J, Han D (2006) Proximate amino acid and mineral composition of pupae of the silkworm *Antheraea pernyi* in China. *J Food Compos Anal* 19:850–853. <https://doi.org/10.1016/j.jfca.2006.04.008>

Publisher's note Springer Nature remains neutral with regard to jurisdictional claims in published maps and institutional affiliations.



Special Issue on "Medicinal Chemistry"

J. Indian Chem. Soc.,
Vol. 97, August 2020, pp. 1287-1294

Zinc and copper homeostasis is crucial to maintain the cellular health and their role in viral diseases including COVID-19

Sneha Mondal^a, Sounik Manna^b, Tarun Kr. Barik^c and Santi M. Mandal^{*d}

^aDepartment of Chemistry, Visva-Bharati, Santiniketan-731 235, India

^bDepartment of Microbiology, Midnapore College (Autonomous), Paschim Medinipur-721 101, West Bengal, India

^cDepartment of Physics, Achhruram Memorial College, Jhalda, Purulia-723 202, West Bengal, India

^dCentral Research Facility, Indian Institute of Technology Kharagpur, Kharagpur-721 302, West Bengal, India

E-mail: mandalsm@gmail.com

Manuscript received online 02 July 2020, accepted 28 July 2020

Both, zinc and copper play important roles in human metabolic processes. In humans, zinc (Zn) is required directly for the chemical catalysis and/or maintaining the structure of nearly 10% of total body proteins. It plays a significant role not only in immune defence but also takes part in DNA and protein synthesis, growth and development throughout the life span as well as in tissue repair. On the other hand, copper (Cu) is crucial to strengthen the skin, epithelial tissue, connective tissue and blood vessels. Cu helps to increase the level of haemoglobin, melanin and myelin in our body. Both of these trace metals possess antioxidant like properties. However, it is necessary to balance the optimal concentration of Zn or Cu in blood serum to avoid the associated organ damage. Excess zinc intake increases the incidence of chronic kidney disease (CKD) which is harmful to normal renal function and thus elevated the risk of prostate cancer. Similarly, the one and only reason for heart, kidney and liver failure including Wilson disease is the excess amount of copper. Both of these trace metals are responsible to deal with brain diseases. Thus, there are many "faces" of Zn and Cu in the maintenance of cellular network including immunomodulatory regulation and infection prevention. Zinc appears to inhibit the enzymatic processes of viral protease and polymerase, as well as different physical processes for instance virus attachment, inflammation, and viral uncoating. Ideally, the clinicians should monitor zinc status of the individuals and advice for the supplements when necessary, otherwise deficiency of these micronutrients could lead to the onset of severe secondary diseases.

Keywords: Zinc, copper, immunomodulatory, signalling network, viral infection.

Introduction

It has been estimated that nearly two to four grams of zinc (Zn) is distributed throughout the human body¹. Even though copper (Cu) is considered as the third most abundant trace metal [next to iron and zinc], its total amount in the human body ranges only between 75–100 mg². Zinc and copper ions are involved with numerous aspects of cellular metabolism via electrochemical oxidation and reduction reactions. The proportion of copper to zinc is clinically more significant than the concentration of both of these trace metals³. Like oxidation and reduction reactions in electrochemical cell, copper and zinc metal ions play similar role in presence of human cell plasma, where the electron movement occurred in Zn and Cu through an electrically conducting

pathway as an electromagnetic wave – leading to a better model for the cellular neurotransmission process.

Zn has versatile functions in physical improvement, enzymatic catalysis and signal transduction of biological system. Under certain circumstances the attachment of zinc to membrane is followed by binding with redox-active metals (like iron and copper), not only but also zinc acts as an essential component of both intracellular and extracellular Cu/Zn superoxide dismutase (Cu/Zn-SOD). The behaviour of zinc like an antioxidant is controlled by means of various regulators such as NF- κ B, p53, AP-1, and some other enzymatic actions during cellular signal transduction at multiple cell levels. Several studies have shown that Zn supplement is helpful to improve the pathological conditions⁴.

Zn is a crucial metal indispensable for proper assembly and progress for functioning of nearly about 2800 macromolecules and more than 300 enzymes. Around 83% of zinc proteins carry out enzymatic catalysis in prokaryotic organisms⁵. Eukaryotic organisms also use Zn for various biological purposes such as the regulation of zinc-related proteins in catalytic reactions (47%), DNA transcription (44%), protein transport (5%), and signalling pathways (3%). Zn is essential in stabilization of the membrane construction mechanism, and it supports to maintain membrane integrity against damages due to changes in osmotic potential, platelet aggregation, and other progressions⁶. Subsequently, the extensive shortage of Zn is associated with several health consequences for example weaknesses, growth and development retardation while it is required for proper immune, reproductive, and neurosensory systems^{4,5}.

Importance of zinc in human biochemical reactions:

Zinc does not contribute to redox active reaction under physiological conditions in contrast to other transition metals. It is designated as the second most abundant trace metal, found in eukaryotes second only to iron. It operates as a Lewis acid to receive a pair of electrons. Zinc remains as a stable ion in an organic medium and it is reported to be a perfect metal cofactor for reactions like proteolysis and the hydration of carbon dioxide with the necessity of redox-stable ion. The crystallization of insulin with zinc was the first proof of Zn-proteins/peptides combination⁷, while the zinc finger motif was first identified within the transcription factor TFIIIA of *Xenopus*. Human genome encodes almost 10% of the zinc proteins, which remarkably points out the physiological importance of zinc in cellular biology. After the initial recognition of zinc from erythrocyte carbonic anhydrase, it has been reported to appear within all six classes of enzymes defined in the enzyme commission (EC). The functioning of several enzymes, transcriptional factors, and other proteins shows an essentiality towards zinc; there exists a possible interaction between these proteins and Zn through definite regions like zinc-finger, LIM, RING finger domains etc. In the interior part of protein structure, zinc is coordinated by nitrogen, oxygen, and sulfur atoms with distinct coordination numbers⁸. It is suggested from zinc proteome analysis that nearly 9% of proteins in eukaryotes are zinc proteins with the number significantly enhanced in higher organisms. The number of zinc-binding motifs in zinc proteomes is governed by the intramo-

lecular zinc binding sites although it is a difficult task to recognize them⁹.

Physiological role of zinc in immune homeostasis:

The essentiality of zinc was first predicted in the year of 1869 while studying the growth of *Aspergillus niger*. At length of time, consistent growth of plants, rats and birds was found to be regulated by an indispensable role of Zn. Subsequently, different hazardous problems like immune deficiency, diarrhoea, alopecia, brain dysfunctions, uncoordinated healing process of wound, loss of appetite, liver disease, chronic inflammation, certain neuropsychological abnormalities such as emotional instability, irritability, and depression etc. are triggered by zinc deficiency, although up to 1961, zinc was not considered as a vital micronutrient for human body. Maximum zinc deficit cases are identified from the elderly, vegans/vegetarians people or the individual with chronic diseases like lymphopenia, liver cirrhosis or inflammatory bowel disease, defective lymphocyte responses from the developing countries like Africa and Asia while its global approximation varies from 17% to 20%. Mainly, zinc tends to be accumulated in the skeletal muscles and bones¹⁰. So, for the maintenance of proper Zn-balance in our body, zinc intake is necessary in our diet on a daily basis keeping it in mind that excess may be harmful. Different health related aspects like eye lesion and wound in skin, disorder in taste, alopecia, impaired immune function, deceleration in growth may arise from zinc deficiency while the excessive Zn-intake shows toxicity such as nausea, vomiting, fever, headaches and chronic kidney disease (CKD). Zinc supplementation is potential enough to reduce the occurrence of pneumonia in children from developing countries, diarrhoea, infections and to improve immunity¹¹. It is also useful in boosting the growth of children and in reducing impaired vision as well as the muscle atrophy¹². Zn also successfully reduced the time scale of symptoms caused by rhinovirus. Herpes simplex virus (HSV) infection can be effectively treated with zinc sulfate¹³. Infection caused by rhinovirus can be successfully inhibited by binding of zinc to virion. Reproductive cycle of HIV-1 virus¹⁴, vaccinia virus¹⁵, and polioviruses can also be hindered with *in vitro* zinc treatment. It was evidenced that zinc at its lowest concentration (10 μ M), showed 800-fold reduction in RSV virus when studied *in vitro*. Zn transporters function as intracellular signal transducers and Zn also acts like a neuromodulator in synaptic transmission. Zn homeostasis is

Mondal *et al.*: Zinc and copper homeostasis is crucial to maintain the cellular health and their role in viral diseases *etc.*

maintained by a number of Zn transporters which signifies proper cellular functioning.

Zinc homeostasis in human body:

There are two different types of intracellular zinc pools (i) protein-bound zinc and (ii) loosely bound Zn^{2+} i.e. “free” zinc. Very small amount of zinc exists as free-zinc ions due to toxicity of zinc within cells and majority of zinc belongs to the first type. Mature human body possesses nearly 2–3 g zinc. Skeletal muscle cells can store upto 60% zinc, nearly 30% zinc is accumulated in case of bone cells, 5% in the cells of liver and skin while the rest 2–3% in other tissues. Less than 1% of the total body zinc is derived from blood serum. The albumin protein combines loosely with nearly 80% of serum zinc and the other 20% is tightly combined with α_2 -macroglobulin protein^{16,17}. Human body can adjust with a ten-fold increased Zn, consumed on a daily basis for the maintenance of homeostasis. Almost, nearly 0.1% of the whole Zn is added in regular diet (breast milk for children). The strict regulation of Zn absorption from food mainly occurs in the duodenum and jejunum; the absorption rises up to 90% when there is inadequate accessibility of dietary Zn. In case of excess Zn intake, it is released from the gastrointestinal tract and is also discarded through shedding off mucosal epithelial cells¹⁸ and renal excretion¹⁹. Generally, in mammals, over 30 proteins, together with ZnT and ZIP transporters, function properly to maintain systemic zinc homeostasis; however, humoral mediators have not been recognized in case of zinc mediated metabolism (Fig. 1).

Distribution of zinc within cell:

Nearly 50% zinc is distributed within cell cytoplasm, 30–

40% in nucleus and 10% in membrane²⁰. Total cellular zinc concentration varies between 10–100 μM range while the cytosolic concentration fluctuates between picomolar and low nanomolar range. In case of intracellular organelles, mitochondrial free zinc concentration have been quantified as 0.14 pM²¹, 0.2 pM concentration have been reported from mitochondrial matrix²², 0.9 pM from ER, and approximately 0.2 pM from the Golgi²³, although elevated level of zinc (~300 pM and 5 nM) concentrations have been reported from mitochondria and the ER²⁴. So, the zinc balance is maintained through a complex sequence of uptake, distribution, storage, and efflux along with a central role of ZnT and ZIP transporters at cellular and subcellular level. Both of these transporters cause movement of zinc between vesicles and organelles of cell cytosol, leads to buffer disorder, a condition which is termed as “buffering” and “muffling”²⁵.

Distribution of zinc within cellular vesicles/granules:

Excess amount of labile zinc is considered as chelating agent due to its accumulation within cells and tissues. Release of zinc from synaptic vesicles is predicted within the range of approximately 100 to 300 μM . Beside, soft tissues (200 nmol/g wt on average), zinc tends to be aggregated within the tissues of prostate gland at a 3- to 15-fold higher range than the range reported from other²⁶. However, a massive reduction of higher zinc level found in prostate cancer and carcinoma is an indication of its significance in metabolic activity of prostate gland. Accumulation of higher concentration of zinc within the β -cells of pancreas is mandatory for crystallization of insulin molecule. Correspondingly, higher zinc content is also reported from GH containing dense-core secretory granules of anterior pituitary cell line, epithelial and myoepithelial cells of submandibular salivary gland, sperm cells, exocrine cells of pancreas, pigment epithelial cells of retina, paneth cells of intestine and mast cells. Various processes occur within subcellular compartments due to zinc accumulation. At the time of meiotic maturation from prophase I to metaphase, higher amount of zinc is introduced and concentrated within the cortical granules of oocytes, necessary for growth detention following meiosis I. During egg activation, accumulated zinc is discarded from the oocyte to reduce zinc bioavailability immediately after intracellular calcium oscillations, termed as “zinc spark”²⁷. Zinc also tends to be aggregated within subcellular compartments during specific pathological situations.

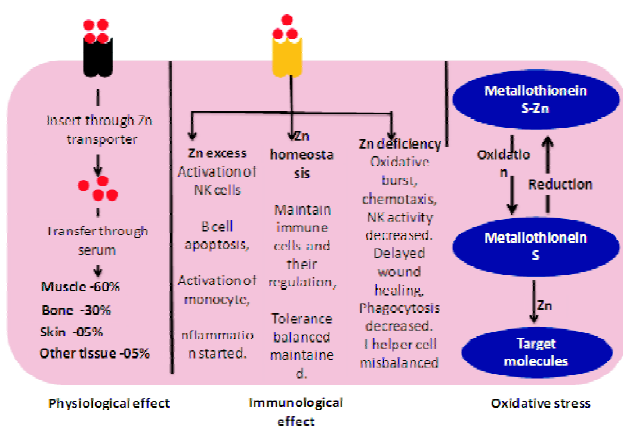


Fig. 1. Schematic representation of immuno-physiological effect of Zn homeostasis in cell.

Metallothionein and MTF-1 – storing house of zinc within cytosol:

61–68 amino acids together with 20–21 cysteines form MTs, which can combine up to 7 equivalents of zinc as well as another metal cations with a valence of two. 5–15% of zinc is tied up by MTs located in the cytosol. Approximately 12 MTs from humans and 4 MTs from mice are reported. In case of mammals, the MT molecule is divided into two zinc binding domains: α and β domains. MTs also serve as zinc acceptors and donors. In the promoter region of MTs excess zinc can tie up metal-response element-binding transcription factor-1 (MTF-1) and metal response element (MRE, 5'-TGCRcnCGGCC-3')²⁸ leading to a significant increase in MT-I and MT-II expression in mice. In vertebrates MT genes are induced in response to zinc by metal-responsive transcription factor-1 (MTF-1) comprising 6 C₂H₂ zinc finger motifs which show a significant contribution towards zinc sensing and metal responsive transcriptional activation. Zinc finger motif also acts as DNA-binding domains with increased level of cellular zinc. MTF-1 maintains zinc homeostasis to increase the transcription of host genes – MTs, *ZnT1*, and *ZnT2*^{28–30}, which are related with the reduction of zinc induced toxicity as well as additional suppression of a set of genes such as zinc transporter *ZIP10*. But in later situation, Pol II movement is physically spoiled. MTF-1 is indispensable for liver development of embryo.

Antiviral effect of zinc:

Several *in vitro* studies have suggested the antiviral nature of zinc where concentrations are necessary for the measurement of antiviral activity. Antiviral zinc concentrations can extend upto mM concentrations whereas human plasma zinc concentration ranges between 10–18 μ M. The antiviral potency of zinc depends on its availability although it is definitely virus-specific (Fig. 2). The details of antiviral effects of zinc are given below:

Herpesviridae: Restriction of the protein ubiquitination pathway can inhibit the herpes simplex virus reproduction and a reduction in NF- κ B activity accompanied by zinc ionophore pyrithione. Remarkably a decreased repetition as well as extent of disease outbreak was revealed from the performance of several relevant zinc application studies in humans^{31,32}. The effectiveness of recent implementation, along with *in vitro* studies indicates the coating of entire HSV virus particle by unbound zinc to prevent infection. Mechanisti-

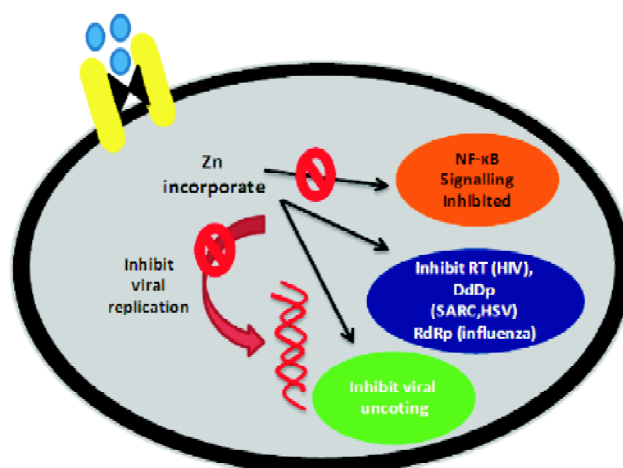


Fig. 2. Schematic representation of the mechanistic approach of Zn as antiviral agent.

cally, zinc ions retard Human alphaherpesvirus 3, usually referred to as the varicella-zoster virus by their *in vitro* inactivation. Both HSV and Varicella-Zoster virus, the members of *Alphaherpesvirinae* subfamily, are genetically related, and possess identical inhibition strategy.

Picornaviridae: Before 1980, it was revealed that zinc can inhibit picornavirus, encephalomyocarditis virus (EMCV), poliomyelitis causing virus – poliovirus, foot and mouth disease virus (FMDV). In case of coxsackievirus B3 which belongs to picornaviridae family, zinc hinders the autocatalysis to encode 3C protease from its precursor 3CD protease to inhibit viral polyprotein processing³³. Zinc seems to bind and alter the viral polyprotein tertiary structure of EMCV³³.

Flaviviridae: Flaviviruses are mainly transmitted by insects. Mosquito-borne diseases caused by dengue virus and West Nile virus, as well as the hepatotropic virus such as hepatitis C virus are grouped under flaviviridae family. *In vitro* studies confirmed the diminished level of HCV replication (mainly inhibition of HCV RdRp) (approximately 50% by 100 μ M ZnSO₄) by zinc salts; however, in case of *E. coli*, the IC₅₀ value is near about 60 μ M³⁴.

Togaviridae: Togaviruses mainly involve the viruses which are transmitted by arthropod vectors like mosquitoes in the Semliki forest, Western equine encephalomyelitis causing agent, and Chikungunya virus. Receptor-mediated endocytosis, with the subsequent virus and endosomal membrane fusion, as well as the release of new virion particle into the cytoplasm are the steps involved in viral replication.

Mondal *et al.*: Zinc and copper homeostasis is crucial to maintain the cellular health and their role in viral diseases *etc.*

Zinc has been revealed as an efficient inhibitor of Semliki forest virus and sindbis virus's membrane fusion using liposomal vesicle³⁵, RBCs³⁶, and BHK Strain 21. To inhibit membrane fusion step of viral replication process, at low endosomal pH, zinc ions form a complex with one (i.e. envelope glycoprotein 1) of the two enveloped glycoproteins of virus through specific histidine residue³⁷.

Retroviridae: Viruses belonging to retroviridae family are identified on the basis of their capability for the transcription of RNA into DNA utilizing reverse transcriptase (RT) and therefore permitting incorporation of new DNA into the host cell genome. The integrated genome of virus called provirus within host cell DNA thus becomes the major barrier to virus healing pathway specifically for HIV-1, with the production of specific infection within host deprived of any symptom i.e. remains dormant. It is well established that there is a correlation between the cellular concentration of Zn ion and CD4⁺ T cells count in HIV infection³⁷. The inhibition of the HIV-1 protease³⁸, and viral transcription was reported to be inhibited by zinc. However, stimulation of zinc influx into monocytes by HIV remains inconsistent.

Papillomaviridae: HPVs, the oncogenic viruses, can stimulate proliferation in basal epithelial cells, give rise to swelling. Although cutaneous swelling is limited as well as non-dangerous, genetic variants of HPV (HPV-16 and -18) are the main source of cancer that occurs in the cells of the cervix³⁹. E6 and E7 genes of HPV encode oncoproteins and both of them are important components for cell proliferation and apoptosis by reviving the degeneration of tumour suppressor's p53 and pRB, respectively⁴⁰. Although nuclear zinc appears to boost up HPV replication, treatment with exogenic zinc (CIZAR, zinc chloride and citric acid anhydrous) can successfully prevents construction of E6 and E7 genes and regain the role of tumour suppressor's p53 and pRB causing cell death of cervical malignant cells. Although down regulating mechanism of E6 as well as E7 expression by zinc is unknown, but zinc induction may lead up to a barrier in different part of viral life cycle.

Zn-Cu homeostasis in health:

It has been reported that a competition between copper and zinc absorption occurs in small intestine⁴¹. After binding with protein metallothionein, both of these elements are absorbed by the cells facing the small intestine. Over expression of metallothionein production in the enterocytes is due

to Excessive zinc ingestion. After tie up of zinc or copper with metallothionein, its movement through the enterocyte gets blocked. Zinc absorption is regulated by stimulating the synthesis of this protein. Copper possesses a higher affinity for metallothionein than zinc⁴² and so it displaces zinc from metallothionein and thus undergoes a preferential binding to the metallothionein, with leftover in the enterocytes; when the intestinal cells are discarded, they lost in faces. Thus, due to mucosal blockage zinc gives rise to a negative copper balance. Failure to mobilize adsorbed Cu from the intestinal cells forms the basis of Menkes syndrome. High doses of zinc given for a longer period in patients, causes an abnormality with Wilson disease which is decreased by the incorporation of Cu into ceruloplasmin by the reduction in biliary excretion of Cu⁴³. Myeloid hyperplasia has been shown in the bone marrow due to zinc-induced copper deficiency. Oral zinc ingestion causes suspiciously high toxicity comparative to copper – a process to influence copper deficiency. In case of humans, multiple antagonistic side effects involve a reduction in copper-dependent enzymes for instance superoxide dismutase, ceruloplasmin, and cytochrome c oxidase; fluctuations in immunological constraints, cholesterol, and its lipoprotein distribution.

Zinc and copper are the most important element which act as ion cofactor in receptors, proteins, different enzymatic reactions and hormones⁴⁴. This Zn-Cu duo can reduce the oxidative stress by stimulation of metallothionein synthesis to form structural ions of SOD⁴⁵⁻⁴⁷. This duo has the essential role in redox potential mechanism and their imbalanced ratio may be the main cause for an improved susceptibility to oxidative damage⁴⁸⁻⁵⁰, although acute Zn depletion causes a decrease in innate and adaptive immunity, chronic insufficiency with increased inflammation⁵¹. Contrarily, excess Cu may be related with an inflammatory response, though it is not clear whether copper has pro-oxidant or antioxidant like effects. Deactivation of unbound radical as well as prevention of associated damage promoted by the antioxidant properties of copper. In opposition to that, unbound radical induced cellular damage may be triggered by the pro-oxidant like behaviour of copper. This is because ceruloplasmin, as the key copper-containing protein, has been exposed to act both as an antioxidant and pro-oxidant in different situations⁵².

Maintenance of the dietary ratio of copper-zinc is very important as higher intake of Zn can affect Cu absorption

and the raised levels have been reported to introduce a negative impact on health status. Zinc acts as a signalling molecule to promote different types of cellular proliferation and growth. If the Zn level decreases with the increased level of Cu, intracellular and extracellular anti-oxidant defence mechanism will be highly affected. According to a research, metabolic and endocrine alterations with enhanced aging might be an indication of "survival" reactions to genotoxic stress that could stimulate tumorigenesis⁵³.

Physiochemical effect of Zn on COVID-19:

Since December 2019, there was a rapid outbreak of a virus named as severe acute respiratory syndrome coronavirus 2 (SARS-CoV-2), causing coronavirus disease-19 (COVID-19) to almost every country of the world. But until now there is no inhibition strategy to keep control of SARS-CoV-2 infection due to lack of approved vaccines or pharmaceutical therapies. Due to the role of zinc as immune modulator in infection as well as its nature like antiviral agents, it is regarded as one of the optional treatments for COVID-19. Inhibition of proteolytic processing of replicase polyproteins by Zn was reported previously. In fact, it was shown that zinc can inhibit the RNA dependent RNA polymerase (RdRp) activity of Hepatitis E virus. Moreover, it was also shown that zinc ionophores blocked coronavirus RdRp activity as well as coronavirus replication⁵⁴. Chloroquine (CQ) and hydroxychloroquine (HCQ), which are generally prescribed for the treatment of malaria and associated inflammatory conditions, might be an alternative tactic because both of these drugs behave like weak bases with an elevated pH level and tend to accumulate within endosomes, lysosomes, or golgi vesicles⁵⁵. In case of SARS-CoV-2, during the replication procedure within host cell, specifically the increased pH of lysosomes, could restrict the pH-dependent phases like membrane fusion and viral uncoating. This elevated pH within intracellular compartments seems to inhibit SARS-CoV-2 replication, because it requires acidification of endosomes for appropriate functioning. Therefore, it is assumed that an inhibiting effect of CQ and HCQ might be important for the treatment of SARS-CoV-2 infected patients. Earlier findings revealed that chloroquine as a zinc ionophore, increases Zn²⁺ flux into the cell⁵⁶. Treatment with zinc supplementation without chloroquine shows some positive effects in treatment⁵⁷. Theoretically, such effectiveness of Zn with substantial lower toxicity may also be detected by means of additional zinc

ionophore activity of quercetin and epigallocatechin-gallate⁵⁸. Targeting Zn ions in viral protein structure is another approach for modulation of COVID-19. Zn helps in protein destabilization of MERS-CoV and SARS-CoV⁵⁹. Zn-ejecting agents (e.g. antialcoholism drug disulfiram) may be used as potential antiviral agents for SARS-CoV-2 treatment by ejecting Zn²⁺ from the predicted target site to inhibit viral replication. SARS-CoV-2 utilizes angiotensin-converting enzyme 2 (ACE2) for entry into host cells. So, modification of ACE2 receptor was also thought as the potential therapeutic strategy in COVID-19. It is also reported the susceptibility of 100 μM zinc to reduce the activity of recombinant human ACE-2 in rat lungs. The consequence of zinc on SARS-CoV-2 and ACE2 interaction appeared to be only imaginary even though this concentration is close to the physiological values of total zinc⁶⁰. Impaired mucociliary clearance caused by HCoV 229E, induced ciliary dyskinesia although neither HCoV 229E nor HCoV-OC43 infection triggered a substantial reduction in ciliary beat frequency. Improvement of length of cilia from bronchial epithelium of Zn-deficient rats⁶¹, as well as increased ciliary beat frequency was boosted by Zn supplementation. We therefore postulate that zinc supplement will enhance nCoV-2019 induced dysfunction via mucociliary clearance.

Conclusion

There is a well-organized system within human body for proper management and regulation of vital trace metals. But once this system fails to operate accurately, anomalous levels of trace metals can be a significant threat to human health. Zinc as a vital trace element, performs many fundamental activities of cellular metabolism, significant to all forms of life. Generally, over 300 enzymes possess the essentiality of zinc for their proper functioning. This trace metal is also assisted with improved immune mechanism, faster wound curing, synthesis of DNA or protein and cell division. The antioxidant like properties of zinc may defend against faster aging. On the other hand, copper permits many critical enzymes to function properly and thus achieves an important place in metabolism. It basically maintains the firmness of skin, blood vessels, epithelial and connective tissue all over the body. It also takes part in the production of hemoglobin, myelin, melanin and collagen. Copper behaves both as an antioxidant and a pro-oxidant. Zinc acts like an intracellular signalling molecule with an important role in cell-mediated

Mondal *et al.*: Zinc and copper homeostasis is crucial to maintain the cellular health and their role in viral diseases *etc.*

immune response and oxidative stress. At the same time, zinc deficiency is the cause of many long-term illnesses which is needed to be altered to evade complications. Different types of diseases can be prevented with supplements, and at the same time certain types of medications cause disturbed Cu and Zn concentrations which may results in onset of other diseases. Therefore, it is very much necessary to keep a well-maintained balance between Zn and Cu than their individual concentration in blood serum.


References

1. M. Dardenne, J. M. Pleau, B. Nabama, P. Lefancier, N. Denien, J. Choay and J. F. Bach, *Proc. Natl. Acad. Sci. USA*, 1982, **370**, 5373.
2. M. S. Willis, S. A. Monaghan, M. L. Miller, R. W. McKenna and W. D. Perkins, *et al.*, *Am. J. Clin. Pathol.*, 2005, **123**, 125.
3. J. Osredkar and N. Sustar, *J. Clinic. Toxicol.*, 2019, **S3**, 001.
4. A. Hamnett and R. J. Mortimer, *J. Electroanal. Chem. Interfacial. Electrochem.*, 1987, **234**, 185.
5. J. Osredkar and N. Sustar, *J. Clinic. Toxicol.*, 2011, **S3**, 001.
6. S. R. Lee, *Oxid. Med. Cell. Longev.*, 2018, **2018**, 9156285.
7. D. A. Scott and A. M. Fisher, *J. Clin. Invest.*, 1938, **17**, 725.
8. T. Kochanczyk, A. Drozd and A. Krezel, *Metallomics.*, 2015, **7**, 244.
9. C. Andreini, I. Bertini and A. Rosato, *Acc. Chem. Res.*, 2009, **42**, 1471.
10. M. J. Jackson, "Physiology of Zinc: General Aspects", Springer Publishers, London, 1989, pp. 1-14.
11. Z. A. Bhutta, R. E. Black, K. H. Brown, J. M. Gardner, S. Gore,
12. A. Hidayat, F. Khatun, R. Martorell, N. X. Ninh, M. E. Penny, J. L. Rosado, S. K. Roy, M. Ruel, S. Sazawal and A. Shankar, *J. Pediatr.*, 1999, **135**, 689.
13. Age-Related Eye Disease Study Research Group, *Arch Ophthalmol.*, 2001, **119**, 1417.
14. A. Wahba, *Acta Dermatol. Venerol.*, 1980, **60**, 175.
15. Y. H. Haraguchi, S. Sakurai, B. M. Hussain and H. Hoshino, *Antivir. Res.*, 1999, **43**, 123.
16. E. Katz and E. Margalith, *Antimicrob. Agents. Chemother.*, 1981, **19**, 213.
17. M. J. Jackson, Springer, 1989, pp. 1-14.
18. J. P. Barnett, C. A. Blindauer, O. Kassar, S. Khazaipoul, E. M. Martin, P. J. Sadler and A. J. Stewart, *Biochim. Biophys. Acta*, 2013, **1830**, 5456.
19. C. M Taylor, J. R. Bacon, P. J. Aggett and I. Bremner, *Am. J. Clin. Nutr.*, 1991, **53**, 755.
20. M. Hambidge and N. F. Krebs, *Annu. Rev. Nutr.*, 2001, **21**, 429.
21. H. Rink, *Biofactors*, 2014, **40**, 27.
22. J. G. Park, Y. Qin, D. F. Galati and A. E. Palmer, *ACS Chem. Biol.*, 2012, **7**, 1636.
23. B. J. McCranor, R. A. Bozym, M. I. Vitolo, C. A. Fierke, L. Bambrick, B. M. Polster, G. Fiskum and R. B. Thompson, *J. Bioenerg. Biomembr.*, 2012, **44**, 253.
24. Y. Qin, P. J. Dittmer, J. G. Park, K. B. Jansen and A. E. Palmer, *Proc. Natl. Acad. Sci. USA.*, 2011, **108**, 7351.
25. P. Chabosseau, E. Tuncay, G. Meur, E. A. Bellomo, A. Hessels, S. Hughes, P. R. Johnson, M. Bugliani, P. Marchetti, B. Turan, A. R. Lyon, M. Merckx and G. A. Rutter, *ACS Chem. Biol.*, 2014, **9**, 2111.
26. R. A. Colvin, W. R. Holmes, C. P. Fontaine and W. Maret, *Metallomics.*, 2010, **2**, 306.
27. M. C. Franz, P. Anderle, M. Burzle, Y. Suzuki, M. R. Freeman, M. A. Hediger and G. Kovacs, *Mol. Aspects. Med.*, 2013, **34**, 735.
28. A. M. Kim, M. L. Bernhardt, B. Y. Kong, R. W. Ahn, S. Vogt, T. K. Woodruff and T. V. O'Halloran, *ACS Chem. Biol.*, 2011, **6**, 716.
29. G. W. Stuart, P. F. Searle and R. D. Palmiter, *Nature*, 1985, **317**, 828.
30. L. A. Lichten, M. S. Ryu, L. Guo, J. Embury and R. J. Cousins, *PLoS One.*, 2011, **6**, e21526.
31. H. R. Godfrey, N. J. Godfrey, J. C. Godfrey and D. Riley, *Altern. Ther. Health Med.*, 2001, **7**, 49.
32. B. B. Mahajan, M. Dhawan and R. Singh, *Indian J. Sex. Transm. Dis. AIDS*, 2013, **34**, 32.
33. S. Shishkov, T. Varadinova, P. Bontchev, C. Nachev and E. Michailova, *Met. Based Drugs*, 1996, **3**, 11.
34. S. A. Read, G. Parnell, D. Booth, M. W. Douglas, J. George and G. Ahlenstiel, *J. Viral Hepat.*, 2018, **25**, 491.
35. J. Corver, R. Bron, H. Snippe, C. Kraaijeveld and J. Wilschut, *Virology*, 1997, **238**, 14.
36. E. Zaitseva, A. Mittal, D. E. Griffin and L. V. Chernomordik, *J. Cell. Biol.*, 2005, **169**, 167.
37. C. Y. Liu and M. Kielian, *J. Virol.*, 2012, **86**, 3588.
38. E. Mocchegiani and M. Muzzioli, *J. Nutrition*, 2000, **130**, 1424S.
39. Y. Haraguchi, H. Sakurai, S. Hussain, B. M. Anner and H. Hoshino, *Antiviral Res.*, 1999, **43**, 123.
40. K. Hoppe-Seyler, F. Bossler, J. A. Braun, A. L. Herrmann and F. Hoppe-Seyler, *Trends. Microbiol.*, 2018, **26**, 158.
41. S. N. Bae, K. H. Lee, J. H. Kim, S. J. Lee and L. O. Park, *Biochem. Biophys. Res. Commun.*, 2017, **484**, 218.
42. E. R. Broun, A. Greist, G. Tricot and R. Hoffman, *JAMA*, 1990, **264**, 1441.
43. V. Yuzbasiyan-Gurkan, A. Grider, T. Nostrant, R. J. Cousins and G. J. Brewer, *J. Lab. Clin. Med.*, 1992, **120**, 380.
44. N. Kumar, "Fifty Neurological Cases from Mayo Clinic", Oxford University Press, Oxford, England, 2004, 131.
45. J. C. Fleet, "Biochemical and Physiological Aspects of Hu-

- man Nutrition", Philadelphia, PA, Saunders, 2000.
46. M. Fukuoka, E. Tokuda, K. Nakagome, Z. Wu, I. Nagano and Y. Furukawa, *J. Inorg. Biochem.*, 2017, **175**, 208.
 47. J. C. Rutherford and A. J. Bird, *Eukaryot Cell.*, 2004, **3**, 1.
 48. N. Saydam, T. K. Adams, F. Steiner, W. Schaffner and J. H. Freedman, *J. Biol. Chem.*, 2002, **277**, 20438.
 49. M. Soinio, J. Marniemi, M. Laakso, K. Pyörälä, S. Lehto and T. Rönnemaa, *Diabetes Care.*, 2007, **30**, 523.
 50. A. Ceriello, *Metabolism*, 2000, **49**, 27.
 51. L. O. Klotz, K. D. Kröncke, D. P. Buchczyk and H. Sies, *J. Nutr.*, 2003, **133**, 1448.
 52. P. Bonaventura, G. Benedetti, F. Albarède and P. Miossec, *Autoimmun. Rev.*, 2015, **14**, 277.
 53. S. Bo, M. Durazzo and R. Gambino, *et al.*, *J. Nutr.*, 2008, **138**, 305.
 54. B. Schumacher, G. A. Garinis and J. H. Hoeijmakers, *Trends Genet.*, 2008, **24**, 77.
 55. A. J. W. Velthuis, S. H. E. van denWorm, A. C. Sims, R. S. Baric, E. J. Snijder and M. J. van Hemert, *PLoS Pathog.*, 2010, **6**, e1001176.
 56. J. M. Rolain, P. Colson and D. Raoult, *Int. J. Antimicrob. Agents*, 2007, **30**, 297.
 57. J. Xue, A. Moyer, B. Peng, J. Wu, B. N. Hannafon and W. Q. Ding, *PLoS One*, 2014, **9**, e109180.
 58. M. Guastalegname and A. Vallone, *Clin. Infect. Dis.*, 2020.
 59. H. Dabbagh Bazarbachi, G. Clergeaud, I. M. Quesada, M. Ortiz, C. K. O'Sullivan and J. B. Fernandez Larrea, *J. Agric. Food Chem.*, 2014, **62**, 8085.
 60. M. H. Lin, D. C. Moses, C. H. Hsieh, S. C. Cheng, Y. H. Chen, C. Y. Sun and C. Y. Chou. *Antiviral Res.*, 2018, **150**, 155.
 61. R. Speth, E. Carrera, M. Jean-Baptiste, A. Joachim and A. Linares, *FASEB J.*, 2014, **28**, 1067.
 62. A. Darma, R. G. Ranuh, W. Merbawani, R. A. Setyoningrum, B. Hidajat, S. N. Hidayati, A. Andaryanto and S. M. Sudarmo, *Indones Biomed. J.*, 2020, **12**, 78.

REVIEW

Electrochemical communication in biofilm of bacterial community

Sounik Manna¹ | Chandan Ghanty² | Piyush Baidara³ | Tarun Kr. Barik⁴ |
Santi M. Mandal¹ 

¹Central Research Facility, Indian Institute of Technology Kharagpur, Kharagpur, West Bengal, India

²Department of Chemistry, School of Science, OP Jindal University, Raigarh, Chhattisgarh, India

³Department of Microbiology and Immunology, University of Arkansas for Medical Sciences, Little Rock, Arkansas

⁴Department of Physics, Acchuram Memorial College, Jhalda, West Bengal, India

Correspondence

Santi M. Mandal, Central Research Facility, Indian Institute of Technology Kharagpur, Kharagpur, West Bengal 721302, India.

Email: mandalsm@gmail.com

Abstract

Electrochemical communication during biofilm formation has recently been identified. Bacteria within biofilm-adopt different strategies for electrochemical communication such as direct contact via membrane-bound molecules, diffusive electron transfer via soluble redox-active molecules, and ion channel-mediated long-range electrochemical signaling. Long-range electrical signals are important to communicate with distant members within the biofilm, which function through spatially propagating waves of potassium ion (K^+) that depolarizes neighboring cells. During propagation, these waves coordinate between the metabolic states of interior and peripheral cells of the biofilm. The understanding of electrochemical communication within the biofilm may provide new strategies to control biofilm-mediated drug resistance. Here, we summarized the different mechanisms of electrochemical communication among bacterial populations and suggested its possible role in the development of high level of antibiotic resistance. Thus, electrochemical signaling opens a new avenue concerning the electrophysiology of bacterial biofilm and may help to control the biofilm-mediated infection by developing future antimicrobials.

KEYWORDS

antibiotic resistance, bacterial biofilm, electrochemical signaling, membrane potential

1 | INTRODUCTION

Bacteria are the unicellular organisms; they lack intracellular membrane compartmentalization, but they possess an outer cell envelope [1]. The extracellular membrane of the bacteria plays an important role in their overall physiology. The outer cell surface of bacteria mediates exchange processes and adhesive properties. Such processes involve different types of electrochemical and immunological interactions occurring on the cell

membrane. These different types of interactions help in cell growth, cell division, and biological communication. The bacterial outer surface is formed by different macromolecular components such as carboxylate, phosphate, and amino group that are ionized in different environmental conditions (e.g., pH) [2]. Such ionization processes are responsible for an electrostatic interaction on the cell periphery [1]. Bacteria are present in aqueous nutrient environments, and therefore they must be hydrated outside to transport nutrient and waste particles

Sounik Manna and Chandan Ghanty contributed equally to this study.

[3]. Physicochemical factors of bacterial surfaces, such as electrostatic charge, are important with respect to overall polarity, to maintain and protect the hydrophilicity of bacterial cell surface for essential functioning of the cell. The net surface charge of a bacterial cell can be measured on the basis of zeta potential [4]. Zeta potential is the electrical potential of the common boundary between the bacterial surface and the aqueous environment [5]. Zeta potential can be measured by calculating cellular electrophoretic movement in an electric field [1]. Recently, Czerwińska-Główka and Krukiewicz [6] have summarized the electrochemical methods to characterize the biofilm over conventional techniques for monitoring their growth and development.

When bacterial cells are cultured at different physiological conditions (with varying pH), the cell surface acquires a net negative electrostatic charge [1], as shown in Figure 1. Positive counterions first attach to the negatively charged surface, forming a rigid layer called the Stern layer. The surface continues to attract more positive ions, but now these counterions experience repulsion from other counterions in the vicinity and by the Stern layer itself. Again, there is a competition between counterion neutralization and molecular motion, and as a result of such competition, an interfacial electrical diffuse layer is formed. Stern layer and diffuse layer are together called a double layer [7]. In the inner region, the Stern layer contains the surface charge as well as electrostatically bound counterions. The outer region extends into the aqueous environment, which contains a more diffuse distribution of anions and cations. This condition

of the environment with varying pH contributes to electrostatic interactions between the cells and other charged surfaces [8]. Measurement of zeta potential can provide an approximate measure of the potential of the Stern layer in bacteria.

The bacterial outer cell envelope consists of different ionized phosphoryl and carboxylate molecules, which are the cause of bacterial net electronegativity as the surface charge. In Gram-positive bacteria, the cell wall is formed by peptidoglycan, which influences inner electronegativity, because there exist substituted phosphoryl groups, with teichoic and teichuronic acid residues as substituents, as well as unsubstituted carboxylate groups [9]. In contrast, Gram-negative bacterial peptidoglycan is encapsulated within the periplasmic space and the outer membrane. Therefore, these are not exposed to the extracellular environment. However, in Gram-negative bacteria, phosphoryl and 2-keto-3-deoxyoctonate carboxylate groups of lipopolysaccharide, present in the outer membrane, serve as the negative electrostatic surface charge, which is present in the outer region of the outer membrane [10]. In Gram-positive and -negative bacteria, although different surface layers are found in the exterior of the cell walls, they similarly affect cell surface charge properties at physiological pH. Extracellular polysaccharides are present in the bacteria, which are naturally acidic in nature and may be attached with the cell surface as relatively compact capsules. In contrast, diffuse slime layers, which are loosely associated with the cell surface, consist of symmetric paracrystalline arrays, which are visible only with the help of electron

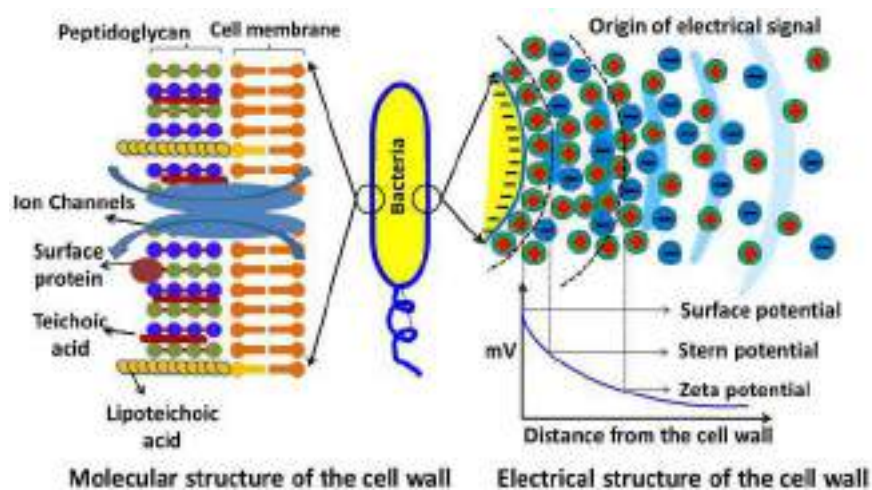


FIGURE 1 The molecular and electrical structure of the cell wall. The molecules present in the bacterial membrane play a role in the production of electric charge on the cell wall. A double-layer (Stern layer and diffuse layer) structure of a bacterial cell, which is cultured at different physiological conditions, is presented. Positive counterions first attach to the negatively charged surface and form a rigid layer called the Stern layer. The surface continues to draw more positive ions, but these counterions experience repulsion from other counterions in the surrounding area and by the Stern layer itself. So, there is a competition between counterion neutralization and molecular motion; such competition results in the formation of an interfacial electrical diffuse layer

microscopy [11]. They are formed by divalent cation-stabilized protein or glycoprotein subunits, which are associated noncovalently in a lateral way on the cell wall surface in an extensive diversity of bacteria. These charged components of the bacterial membrane have created the basis of electrochemical communication between the inner and outer surface [12].

Often some bacteria grow by adhering to each other, and they also adhere to a fixed surface to form bacterial biofilm. These adherent cells are submerged in a slime layer. Bacteria within biofilm can communicate their behavior through different forms of coordination [13–16]. Quorum sensing is a way for the cell-to-cell signaling process in bacteria [17]. Recently, it has been established that bacterial cell-to-cell communication mechanism is dependent on ion channel-mediated electrical signaling [18]. This electrical signaling has enabled cell-to-cell communication within a biofilm community [16,18]. It has been observed that *Bacillus subtilis* biofilm can energetically communicate extracellular potassium signals, which creates electrical waves that spread through the biofilm and organize metabolic states, thereby accumulating cooperative ability [16,18]. This K⁺ channel-mediated electrical signaling communication occurs between the interior and peripheral cells. The electrical signal is generated by different organisms, and its attraction seems to be a genetic mechanism that allows cross-species interactions.

On the other hand, the peptidoglycan layer is broader than Gram-negative bacteria, whereas the lipopolysaccharide layer in Gram-positive bacteria is just vice versa. Bacteria require proton motive force for their growth and sustainability. The proton motive force is produced in the bacterial cell membrane during energy generation. This proton motive force in the inner membrane produces bacterial electrochemical signaling and generates the potential charges in the membrane [19]. In the free-living planktonic state, bacteria have the ability to form the biofilm, and sessile cells adhere to the substrate and strengthen the biofilm [20].

However, electrical signals can control the direct bacterial motility by changing the membrane potential. Such long-range electrical signaling could deliver a generic mechanism for bacterial societies and control the motile behavior of unsociable cells.

2 | DIFFERENT PHYSIOLOGICAL PROCESSES OF BACTERIAL ELECTRICAL COMMUNICATION

To maintain the optimum cell function of a unicellular organism, it is important to control the interfacial

physiology of these organisms. Ionized phosphoryl and carboxylate substituents are present on the outer cell envelope of macromolecules, due to which bacterial cell surfaces have a net negative electrostatic charge. The major electrical signaling communication in biological systems is the action potential in neurons, which is communicated by ion channels [21]. Several years of research on ion channels have provided important insights into the structural basis of such neuronal signaling [22,23]. In particular, the prokaryotic K⁺ channels *kcsA* provided the first physical information on ion discernment and conductance [24]. Recently, it has been documented that bacteria have many significant classes of other ion channels such as chloride channel, sodium channels, ionotropic glutamate receptors, and calcium-gated potassium channels [25–28]. However, the inherent role of ion channels in bacteria has mostly remained unclear [29,30]. Different types of ion channels present in bacteria are not only responsible for cellular processes, but these ion channels are also responsible for electrochemical communication between their own environments. These ion-specific channels of bacteria also have unique functions like extreme acid-resistant response and osmoregulation [31]. It also remains indistinct that these ion channels can maintain other unique functions in prokaryotes. The study of the bacteria in their native background, the biofilm community, may reveal new signs about the function of ion channels in bacteria. Bioelectrochemistry is a very well-known phenomenon in human system, but in bacteria, bioelectric currents particularly exist in an agglomerated form in the biofilm. During biofilm formation, bacteria are able to produce electric field at the time of their movement and they jump due to the amount of electric potential on the biofilm [6].

3 | ELECTROCHEMICAL COMMUNICATION DURING BIOFILM FORMATION

Bacterial biofilm are prearranged communities comprising billions of densely crowded cells. Such communities can display an interesting macroscopic three-dimensional coordination [32–34]. Usually, biofilm are formed under different environmental stress situations including nutrient limitation [35]. In any group of microorganisms in a biofilm, cells are stuck to each other and often to a surface. A slimy extracellular matrix is composed of extracellular polymeric substances (EPS), in which the adherent cells are embedded. In the biofilm, the cells produce the EPS, which are typically a polymeric cluster of DNA, lipids, extracellular

polysaccharides, and proteins. When bacterial communities grow larger, due to the high growth of the peripheral cells in the biofilm, the nutrient supply of the interior cells becomes inadequate. When there is nutrient deficiency, the interior cells are protected by the peripheral cells, which remain in a critical situation for the survivability due to the presence of different external challenges. In a bacterial community, an important confrontation occurs between the opposing stresses for biofilm growth and upholding the capability of protected (interior) cells. The identification of electrochemical communication mechanisms present in the bacterial biofilm community is responsible for the sustainability of the protected interior cells, which is important to understand biofilm development [36].

However, it is not clear how microscopic bacteria can successfully interconnect in large distances. To examine this question, scientists have studied *B. subtilis* microbial community, revealing that these bacteria show metabolic oscillations activated by nutrient limitation conditions [16]. The oscillatory dynamics results from long-range metabolic co-dependence among the cells in the interior and periphery of the biofilm [16]. Specifically, the interior and peripheral cells of the biofilm share ammonium ions but compete for glutamate. Therefore, biofilm growth stops intermittently due to the increase in nutrient availability for the protection of interior cells. Remarkably, glutamate and ammonium ions are both charged metabolites, which leads to cellular uptake of these compounds, which is recognized by the proton motive force and transmembrane electrical potential. In bacterial motility, membrane potential plays a common role in their communication [37,38]. Consequently, the metabolic coordination in the biofilm community among the interior and peripheral cells might be involved in electrochemical signaling.

For the measure of electrical signaling, scientists used the fluorescent cationic dye thioflavin T to quantify the membrane potential within the bacterial biofilm community. Within the biofilm community, thioflavin T is used for the measurement of global alternations in membrane potential. Thioflavin T is a highly positively charged molecule and it is attracted to cells due to the negative membrane potential of the bacterial cell. The experimental result shows that thioflavin T increases inside the cell when the cell becomes more negative, and thus thioflavin T is inversely related to the membrane potential [18]. These membrane potential oscillations are highly coordinated among the most distant areas of the biofilm. Actually, biofilm community or bacterial cells can transfer charge particles in their membrane, which occurs only for electrochemical signaling communication.

4 | BACTERIAL ION CHANNEL-MEDIATED ELECTRICAL SIGNALING

The ion channels of the bacterial membrane possess different ion-transferring mechanisms by the electrochemical signal. It is evidenced that YugO (K^+ channel) in *B. subtilis* is important for biofilm formation [39]. This potassium flux pump has an intracellular TrkA domain, which is regulated by the metabolic state of the cell [40–42]. For better understanding the hypothesis, wild-type and YugO-deleted mutant strains were used, which revealed that extracellular K^+ increased for the wild-type strain, but not for the mutated strain. Consequently, the metabolic limitation could form the primary trigger for YugO activation. Specifically, the fundamental metabolic oscillations are determined by glutamate limitation [16], which is due to the release of K^+ and the elimination of glutamate. The neighboring cells become depolarized due to the presence of K^+ outside the cells, restraining glutamate uptake, which creates additional nitrogen limitation, and thus metabolic stress is generated. These cyclic consequences occur due to cell–cell transmission of the potassium signal. These findings hypothesized that glutamate limitation can trigger potassium signal via the YugO potassium channel [43].

In *B. subtilis*, YugO also has a role in the active propagation of the potassium signal. Wild-type and YugO mutant strains have transient bursts of external K^+ concentration (300-mM KCl). As can be predicted, K^+ causes short-term membrane potential depolarization in both strains. However, in the wild-type strain, this primary depolarization is naturally monitored by a protracted hyperpolarization phase, which was not observed in the YugO mutant strain. This period of hyperpolarization is complemented by an increase in extracellular K^+ ions. This YugO was triggered by intracellular potassium, because when an equal concentration of sorbitol (an uncharged solute) was used, but it did not stimulate an equal response, producing purely osmotic effects. Therefore, YugO seems to have a role in propagating the extracellular potassium signal within the biofilm [18].

The K^+ channel shows the electrochemical activity and the mechanism is experimentally observed in the form of propagating pulses of electrical activity. A temporary depolarization is monitored by hyperpolarization in reaction to native proliferations in extracellular potassium concentration. Additionally, the model demonstrates that long-range proliferation of these excitations does not show a decrease in the amplitude of membrane potential oscillations. The bacterial cells release intracellular potassium when they are in a metabolically stressed condition, and this extracellular potassium generates more metabolic

stress on neighboring cells. *B. subtilis* cotransported glutamate with two protons by the GltP transporter, and this process is influenced by the proton motive force [37]. Potassium-mediated depolarization of the membrane potential can permanently decrease the electrical module of the proton motive force, [44] and thus lower glutamate acceptance and intracellular ammonium retention [37,38]. Consequently, this potassium-intermediated signaling could proliferate metabolic stress on distant cells. With the increase of cells in glutamine, the response to extracellular potassium can be reduced. Glutamate and ammonium requirement can be compensated by two main factors: an uncharged metabolite and a favored nitrogen source [45]. Hence, potassium-mediated ion channel of bacteria is formed by an electrical signal that controls the metabolic stress. In *Bacillus* sp., the YugO channel transfers the ion and creates an effective electrical communication between distant cells [26].

5 | CROSS-SPECIES COMMUNICATION

Biofilm refer to the compressed relationship of microorganisms and their environment. The chemical signaling mechanism in a bacterial communication network is quorum sensing. Recently, it has been revealed that electrical signaling is mediated through the ion channels of bacterial cells. Long-range behavior of bacteria is also influenced by their signaling mechanism. As a result, in a bacterial community, long-range cross-species communication has been possible. This considerable result has provided a new example to examine the complex coexistence of biofilm societies and distant cells, with a probable scope of application in synthetic biology.

In bacterial motility, membrane potential plays a common role in signal communication [46]. Therefore, a new suggestion is that the process of attraction based on persuading alterations in membrane potential can apply to other bacteria as well. To answer this hypothesis, scientists studied the interaction of *Pseudomonas aeruginosa* cells with the pre-existing *B. subtilis* biofilm and demonstrated that the motile *P. aeruginosa* cells are intermittently attracted to the *B. subtilis* biofilm during electrical oscillations. It has been experientially proved that a difference in the period of electrical signaling within the biofilm is directly coordinated by the period of *P. aeruginosa* magnetism to the biofilm edge. This implies that the mechanism of electrically arbitrated attraction is not restricted to *B. subtilis* cells, therefore allowing cross-species interaction also [43].

Bacterial ion channels generated long-range electrochemical signals; for example, K^+ channel generates a

rapid response in the cell motility, because any biochemical synthesis or any complex signaling networks are not required in this response. This study also proposes a new hypothesis that cross-species signaling occurs in long range and is generic in nature, where no exact receptor or signaling pathways are required. The result of this effort leads to many motivating questions concerning the result of the newly invented signaling procedure over the quorum-sensing bacterium in the multifaceted coexistence of the biofilm communities and neighboring cells [43,46,47].

The bacterial ion channel-mediated signaling mechanism results in a quick response in cell motility of even physically distant cells, due to its individuality on a multifaceted signaling network. Consequently, due to distant species electrochemical signaling, bacteria from diverse species are involved and incorporated in a pre-existing biofilm. Therefore, the complex coexistence of a biofilm with its neighboring cross-species societies has led to an increase in many fascinating features of the signaling mechanism in the secretive microorganism community.

6 | ELECTRICAL COMMUNICATION DURING INTERSPECIES-SPECIFIC CROSSTALK

When an electron is moved between different species of microbes, is known as interspecies electron transfer (IET) mechanism. This IET mechanism has been established on the basis of obliging behaviors and community purposes. IET mechanisms depend on the circulation of redox chemical species or direct interaction in cell aggregates. Following IET, bacteria generate their membrane potential and proton motive force as one of their communicative way among bacterial communities [48].

In growing biofilm, bacteria surrender their freedom and settle into large stationary societies. Suel and colleagues grew a biofilm of *B. subtilis* to understand the communication process within the bacterial cells with the outer cells, when to divide or relax. The biofilm of *B. subtilis* were treated with fluorescent markers that were energized by potassium and sodium ions, and the potassium marker lit up, as ions flowed out of starved cells. The biofilm cells also released K^+ , refreshing the signal, when the ions reached closer to them. The signal flowed outward in this way until it reached the biofilm's edge, and in response to the signal border, cells stopped dividing until the intramural cells received a feed, after which they stopped releasing potassium. Suel's team then created mutant bacteria without potassium channels, and they found that the mutant cells did not grow in the same stop-start manner of wild-type

cells. Like neurons, to communicate electrical signals, bacteria evidently use K^+ [18,43,47].

The significant flow of electrons through a small cable is called an electric current. In bacteria, the pili act as nanowires, which transfer electrons to the surrounding environment. Flagella are the extracellular projection of bacteria, which transfer electrons to electrodes, which are called bacterial nanowires. Bacterial nanowire formation was established by atomic force and transmission electron microscopy and by electrochemical techniques, and its conductive nature was investigated. It can be observed from analyzing marine bacteria that live in the mud at the bottom of the sea that an electric current is propagated through the layers of mud. Cyclic voltammetry (CV) and electrochemical impedance spectroscopy (EIS), nondestructive voltammetry techniques, suggest that bacterial nanowires could be the source of electrons, which may be used in various applications, for example, microbial fuel cells, biosensors, organic solar cells, and bioelectronic devices. Underneath the layer of mud, bacteria generate energy, and the electrons thus released reach the top layer, where they subsequently react with O_2 . These electrons travel a distance of 12 mm, which is 10,000 times of body length of bacteria [16,43,46].

In contrast, *Bacillus* sp. uses a K^+ channel to convert free-swimming cells to their static society. Remarkably, the bacteria attract not only *Bacillus* sp. but also other dissimilar species. Bacteria seem to live in diverse communities, not just in monocultures. These two *Bacillus* species exchange potassium signals, and two *Bacillus* biofilm can “time-share” nutrients also. In an experiment, where two bacterial communities have been employed and allowed to utilize glutamate, the biofilm are allowed to ingest the desired nutrients more professionally. As a result of the sharing of two different bacterial communities, the biofilm grew more rapidly than they could have if the bacteria had consumed the nutrients without the interference of any other bacteria [18]. When the ion channel was modified, they gave weaker signals in the biofilm community and they were not properly able to coordinate their feeding and grew more slowly. Therefore, it is clear that the same species of different bacteria also communicate by generating electrochemical signals [44].

7 | ELECTRICAL COMMUNICATION DURING INTRASPECIES-SPECIFIC CROSSTALK

Bacteria within biofilm communities can organize their behavior through cell-to-cell signaling. However, it remains uncertain if these signals can stimulate the

behavior of distant cells that are not part of the community. In *B. subtilis* biofilm community, there is a K^+ channel-mediated electrical signaling communication between the interior and peripheral cells. An electrochemical potassium signal is generated inside the biofilm, which alters the membrane potential of distant cells, thus leading to their motility [16,18].

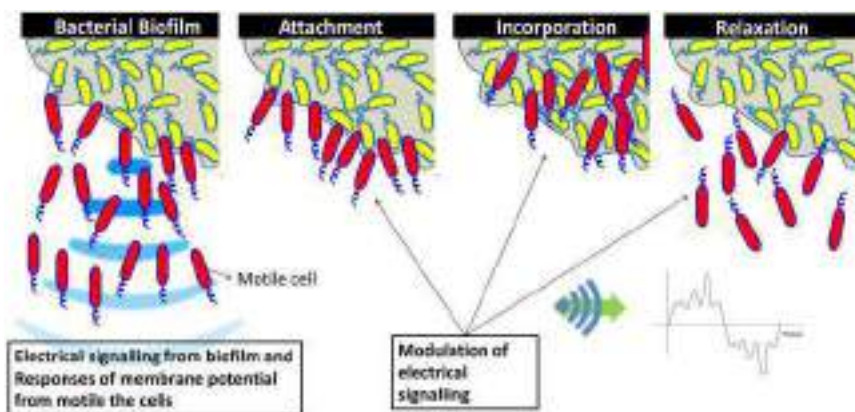
This electrical signal is generated by different organisms, and the attraction seems to be a generic mechanism that allows cross-species interactions. *B. subtilis* biofilm released the electrical signal by its ion channel and *P. aeruginosa* cells became attracted to this electrical signal. Through the long-range electrical signaling, the cells of the bacterial community can coordinate their own behavior and also affect the behavior of different bacteria at a particular distance [43,46].

The communication mechanisms between the biofilm and distant cells occur between the evolutionarily distant bacteria, and are therefore not restricted to cells from a single species. In a biofilm community, the effect of extracellular K^+ on membrane potential is communal among all cells, and therefore communication is physical in nature (Figure 2). The long-range cross-species signaling is generic and it does not require specific receptors or any signaling mechanism. Stimulatingly, due to cross-species attraction, bacteria from a different species can be assimilated into a pre-existing biofilm. In cross-species bacterial community, they have different membrane potential and thus generate electrochemical signal by their membrane ion channels. This electrochemical signal might be their way of communication [16,18,43].

8 | ELECTROCHEMICAL SIGNALING VIA MEMBRANE POTENTIAL AND RESISTANCE DEVELOPMENT

In recent years, bacterial electrophysiology has been demonstrated to have important roles in the various physiological processes like cellular proliferation, electrochemical communication, persister cell formation, and antibiotic resistance [49–52]. Electrochemical signaling via K^+ channels, together with resultant membrane potential, which is specific for different bacterial communities, is a way of electrochemical communication in bacterial biofilm. Biofilm formation is also stimulated by a variety of natural products including surfactin, which induces potassium leakage that triggers multicellularity. Potassium leakage stimulates a membrane protein kinase, KinC, which regulates the genes involved in the biofilm formation [53]. Interestingly, surfactin possesses antimicrobial activities, but it generates the chances for

FIGURE 2 Migration, attachment, incorporation, and relaxation of motile cells in biofilm, depending on the modulation in electrochemical signaling in bacterial biofilm community



resistance development against itself and other antimicrobials by induction of genes involved in biofilm formation via potassium leakage. In addition, potassium leakage results in depolarization of membrane potential that might play role in resistance development against positively charged antimicrobials. Next, bacterial biofilm formation and cell-to-cell communication within biofilm have already been reported for their role in the development of drug resistance [47,54]. Electrochemical signaling in bacterial biofilm has also demonstrated to have a role in cell-to-cell communication via differences in membrane potential [18,43]. However, a direct link between electrochemical signaling in bacterial biofilm and its role in drug resistance development is missing.

During IET in bacterial biofilm, which is important for cell-to-cell communication, a high membrane potential is generated in biofilm, which is key to biofilm matrix production [55]. Furthermore, it has been shown that bacterial membrane potential dynamics in biofilm facilitates electrical signaling in both intra- and intercellular levels. This membrane potential derived from electrical signaling is found to be proportional to cellular proliferation capacity [51]. The increase in membrane potential induces a higher cellular proliferation, which helps in the development of resistance and required antimicrobials that are more potent. In a recent report, it has been confirmed that K^+ transport system of *Staphylococcus aureus* plays an important role in resistance development against aminoglycoside antibiotics and cationic antimicrobial peptides [56]. In conclusion, here we have suggested that disruption of electrochemical signaling by targeting bacterial cell membrane potential could be a promising alternative to confront the rapid emergence of multidrug resistance [57].

9 | CONCLUSION

Electrophysiology is a well-known branch of neurosciences. In the recent past, multiple studies have

shown that bacterial communities like biofilm utilize electrochemical signals for communication, based on the fundamentals of electrophysiology. K^+ channels are the major channels that help in long-distance electrochemical communication in biofilm and in developing a dynamic membrane potential across interior and peripheral cells within the biofilm. This resultant dynamic potential propagated in the form of electrical pulses between the distant cells of biofilm induces biofilm formation. The electrochemical communication within biofilm may also be involved in the measurement of electrical resistance or development within the bacterial communities by membrane depolarization and induction of multicellularity. Therefore, electrochemical control of biofilm may develop as a potential biofilm treatment strategy and confront multidrug-resistant biofilm-forming bacterial pathogens.

CONFLICT OF INTERESTS

The authors declare that there are no conflict of interests.

ORCID

Santi M. Mandal  <http://orcid.org/0000-0002-0119-7138>

REFERENCES

- [1] Mozes N, Rouxhet PG. Microbial hydrophobicity and fermentation technology. In: Doyle RJ, Rosenberg M, editors. Microbial cell surface hydrophobicity. Washington, DC: American Society for Microbiology; 1990. p. 75-105.
- [2] Kureisaite-Ciziene D, Varadajan A, McLaughlin SH, Glas M, Montón Silva A, Luirink R, et al. Structural analysis of the interaction between the bacterial cell division proteins FtsQ and FtsB. *mBio*. 2018;9:01346-18.
- [3] Beveridge TJ, Graham LL. Surface layers of bacteria. *Microbiol Rev*. 1991;55:684-705.
- [4] Wilson WW, Wade MM, Holman SC, Champlin FR. Status of methods for assessing bacterial cell surface charge properties based on zeta potential measurements. *J Microbiol Methods*. 2001;43:153-64.
- [5] Saito T, Takatsuka T, Kato T, Ishihara K, Okuda K. Adherence of oral streptococci to an immobilized agent. *Arch Oral Biol*. 1997;42:539-45.

- [6] Czerwinska-Glowkaa D, Kurkiewicz K. A journey in the complex interactions between electrochemistry and bacteriology: from electroactivity to electromodulation of bacterial biofilms. *Bioelectrochemistry*. 2020;131:10740.
- [7] Howard JJ, Perkins JSB, Pettitt M. The behavior of ions near a charged wall-dependence on ion size, concentration, and surface charge. *J Phys Chem B*. 2010;114:6074-83.
- [8] Brown MA, Bossa GV, May S. Emergence of a Stern layer from the incorporation of hydration interactions into the Gouy-Chapman model of the electrical double layer. *Langmuir*. 2015;42:11477-83.
- [9] Beveridge TJ. The bacterial surfaces: general considerations towards design and function. *Can J Microbiol*. 1988;34:363-72.
- [10] Nikaido H. Molecular basis of bacterial outer membrane permeability revisited. *Microbiol Mol Biol Rev*. 2003;67:593-656.
- [11] Dominique HL, Christopher JJ, Wozniak DJ. Bacterial extracellular polysaccharides in biofilm formation and function. *Microbiol Spectr*. 2015;3:3.
- [12] Sleytr UB, Schuster B, Egelseer E, Pum D. S-layers: principles and applications. *FEMS Microbiol Rev*. 2014;38:823-64.
- [13] Shapiro JA. Thinking about bacterial populations as multicellular organisms. *Ann Rev Microbiol*. 1998;52:81-4.
- [14] Waters CM, Bassler BL. Quorum sensing: cell-to-cell communication in bacteria. *Annu Rev Cell Dev Biol*. 2005;21:319-46.
- [15] Brameyer S, Bode HB, Heermann R. Languages and dialects: bacterial communication beyond homoserine lactones. *Trends Microbiol*. 2015;23:521-3.
- [16] Liu J, Prindle A, Humphries J, Gabalda-Sagarra M, Asally M, Lee DY, et al. Metabolic co-dependence gives rise to collective oscillations within biofilms. *Nature*. 2015;523:550-4.
- [17] Miller MB, Bassler BL. Quorum sensing in bacteria. *Annu Rev Microbiol*. 2001;55:165-99.
- [18] Prindle A, Liu J, Asally M, Ly S, Garcia-Ojalvo J, Suel GM. Ion channels enable electrical communication in bacterial communities. *Nature*. 2015;527:59-63.
- [19] Bradbeer C. The proton motive force drives the outer membrane transport of cobalamin in *Escherichia coli*. *J Bacteriol*. 1993;175:3146-50.
- [20] Rollet C, Gal L, Guzzo J. Biofilm-detached cells, a transition from a sessile to a planktonic phenotype: a comparative study of adhesion and physiological characteristics in *Pseudomonas aeruginosa*. *FEMS Microbiol Lett*. 2009;290:135-42.
- [21] Liu J, Martinez-Corral R, Prindle A, Lee DD, Larkin J, Gabalda-Sagarra M, et al. Coupling between distant biofilms and emergence of nutrient time-sharing. *Science*. 2017;356:638-42.
- [22] Hille B. Ion channels of excitable membranes. Washington, DC: University of Washington, Sinauer Associates, Inc.; 2001.
- [23] MacKinnon R. Potassium channels and the atomic basis of selective ion conduction. *Biosci Rep*. 2004;24:75-100.
- [24] Doyle DA. The structure of the potassium channel: molecular basis of K1 conduction and selectivity. *Science*. 1998;28:69-77.
- [25] Ren D, Navarro B, Xu H, Yue L, Shi Q, Clapham D. A prokaryotic voltage-gated sodium channel. *Science*. 2001;294:2372-5.
- [26] Iyer R, Iverson TM, Accardi A, Miller C. A biological role for prokaryotic ClC chloride channels. *Nature*. 2002;419:715-8.
- [27] Jing X, Yang Y, Ai Z, Chen S, Zhou S. Potassium channel blocker inhibits the formation and electroactivity of *Geobacter* biofilm. *Sci Total Environ*. 2020;705:135796.
- [28] Chen GQ, Cui C, Mayer ML, Gouaux E. Functional characterization of a potassium-selective prokaryotic glutamate receptor. *Nature*. 1999;402:817-21.
- [29] Kuo MMC, Haynes WJ, Loukin SH, Kung C, Saimi Y. Prokaryotic K1 channels: from crystal structures to diversity. *FEMS Microbiol Rev*. 2005;29:961-85.
- [30] Saimi Y, Loukin SH, Zhou XL, Martinac B, Kung C. Ion channels in microbes. *Methods Enzymol*. 1998;294:507-24.
- [31] Martinac B, Buechner M, Delcour AH, Adler J, Kung C. Pressure-sensitive ion channel in *Escherichia coli*. *Proc Natl Acad Sci USA*. 1987;84:2297-301.
- [32] Costerton JW, Stewart PS, Greenberg EP. Bacterial biofilms: a common cause of persistent infections. *Science*. 1999;284:1318-22.
- [33] Wilking JN, Zaboradaev V, Volder MD, Losick R, Brenner MP, Weitz DA. Liquid transport facilitated by channels in *Bacillus subtilis* biofilms. *Proc Natl Acad Sci USA*. 2013;110:848-52.
- [34] Payne S, Li B, Cao Y, Schaeffer D, Ryser MD, You L. Temporal control of self-organized pattern formation without morphogen gradients in bacteria. *Mol Syst Biol*. 2013;9:697.
- [35] Hall-Stoodley L, Costerton JW, Stoodley P. Bacterial biofilms: from the natural environment to infectious diseases. *Nature Rev Microbiol*. 2004;2:95-8.
- [36] Vlamakis H, Aguilar C, Losick R, Kolter R. Control of cell fate by the formation of an architecturally complex bacterial community. *Genes Dev*. 2008;22:945-53.
- [37] Tolner B, Ubbink-Kok T, Poolman B, Konings WN. Characterization of the proton/glutamate symport protein of *Bacillus subtilis* and its functional expression in *Escherichia coli*. *J Bacteriol*. 1995;177:2863-9.
- [38] Boogerd FC, Ma H, Bruggeman FJ, van Heeswijk WC, Garcia-Contreras R, Molenaar D, et al. AmtB-mediated NH₃ transport in prokaryotes must be active and as a consequence regulation of transport by GlnK is mandatory to limit futile cycling of NH₄(+)/NH₃. *FEBS Lett*. 2011;585:23-8.
- [39] Lundberg ME, Becker EC, Choe S. MstX and a putative potassium channel facilitate biofilm formation in *Bacillus subtilis*. *PLOS One*. 2013;8:e60993.
- [40] Cao Y, Pan Y, Huang H, Jin X, Levin EJ, Kloss B, et al. Gating of the TrkH ion channel by its associated RCK protein TrkA. *Nature*. 2013;496:317-22.
- [41] Roosild TP, Miller S, Booth IR, Choe S. A mechanism of regulating transmembrane potassium flux through a ligand-mediated conformational switch. *Cell*. 2002;109:781-91.
- [42] Schlosser A, Hamann A, Bossemeyer D, Schneider E, Bakker EP. NAD1 binding to the *Escherichia coli* K1-uptake protein TrkA and sequence similarity between TrkA and domains of a family of dehydrogenases suggest a role for NAD1 in bacterial transport. *Mol Microbiol*. 1993;9:53343-543.
- [43] Humphries J, Xiong L, Liu J, Prindle A, Yuan F, Arjes HA, et al. Species-independent attraction to biofilms through electrical signaling. *Cell*. 2017;168:200-9.
- [44] Krulwich TA, Sachs G, Padan E. Molecular aspects of bacterial pH sensing and homeostasis. *Nature Rev Microbiol*. 2011;9:330-43.
- [45] Fisher SH. Regulation of nitrogen metabolism in *Bacillus subtilis*: vive la difference. *Mol Microbiol*. 1999;32:223-32.

- [46] Majumdar S, Pal S. Cross-species communication in bacterial world. *J Cell Commun Signal*. 2017;11:187-90.
- [47] Qi L, Li H, Zhang C, Liang B, Li J, Wang L, et al. Relationship between antibiotic resistance, biofilm formation, and biofilm-specific resistance in *Acinetobacter baumannii*. *Front Microbiol*. 2016;7:483.
- [48] Katoa S, Hashimoto K, Watanabea K. Microbial interspecies electron transfer via electric currents through conductive minerals. *Proc Natl Acad Sci USA*. 2012;109:10042-6.
- [49] Verstraeten N, Knapen WJ, Kint CI, Liebens V, van den Bergh B, Dewachter L, et al. O₂ and membrane depolarization are part of a microbial bet-hedging strategy that leads to antibiotic tolerance. *Mol Cell*. 2015;59:9-21.
- [50] Damper PD, Epstein W. Role of the membrane potential in bacterial resistance to aminoglycoside antibiotics. *Antimicrob Agents Chemother*. 1981;20:803-8.
- [51] Stratford JP, Edwards CLA, Ghanshyam MJ, Malyshev D, Delise MA, Hayashi Y, et al. Electrically induced bacterial membrane-potential dynamics correspond to cellular proliferation capacity. *Proc Natl Acad Sci U S A*. 2019;116:9552-7.
- [52] Sultana ST, Call DR, Beyenal H. Eradication of *Pseudomonas aeruginosa* biofilms and persister cells using an electrochemical scaffold and enhanced antibiotic susceptibility. *NPJ Biofilms Microbiomes*. 2016;2:2.
- [53] López D, Fischbach MA, Chu F, Losick R, Kolter R. Structurally diverse natural products that cause potassium leakage trigger multicellularity in *Bacillus subtilis*. *Proc Natl Acad Sci USA*. 2009;106:280-5.
- [54] Hirakawa H, Tomita H. Interference of bacterial cell-to-cell communication: a new concept of antimicrobial chemotherapy breaks antibiotic resistance. *Front Microbiol*. 2013;4:114.
- [55] Qin Y, He Y, She Q, Larese-Casanova P, Li P, Chai Y. Heterogeneity in respiratory electron transfer and adaptive iron utilization in a bacterial biofilm. *Nat Commun*. 2019;10:3702.
- [56] Gries CM, Bose JL, Nuxoll AS, Fey PD, Bayles KW. The Ktr potassium transport system in *Staphylococcus aureus* and its role in cell physiology, antimicrobial resistance and pathogenesis. *Mol Microbiol*. 2013;89:760-73.
- [57] Goldberg K, Sarig H, Zaknoon F, Epanand RF, Epanand RM, Mor A. Sensitization of Gram-negative bacteria by targeting the membrane potential. *FASEB J*. 2013;27:3818-26.

How to cite this article: Manna S, Ghanty C, Baindara P, Barik TK, Mandal SM. Electrochemical communication in biofilm of bacterial community. *J Basic Microbiol*. 2020;60:819–827.
<https://doi.org/10.1002/jobm.202000340>



Prospect of nanotechnology: A brief review

Tarun Kumar Barik^{*a}, Santi M. Mandal^b, Soma Mitra (Banerjee)^c, Gopal Chandra Maity^d,
Gourisankar Roymahapatra^e and Tuhin Shubhra Santra^f

^aDepartment of Physics, Achhruram Memorial College, Jhalda, Purulia-723 202, West Bengal, India

^bCentral Research Facility, Indian Institute of Technology Kharagpur, Kharagpur-721 302, West Bengal, India

^cDepartment of Physics, University of Gour Banga, Malda-732 103, West Bengal, India

^dDepartment of Chemistry, Abhedananda Mahavidyalaya, Sainthia-731 234, Birbhum, West Bengal, India

^eSchool of Applied Science and Humanities, Haldia Institute of Technology, Haldia-721 657, West Bengal, India

^fDepartment of Engineering Design, Indian Institute of Technology Madras, Chennai-600 036, India

E-mail: tarun.barik2003@gmail.com

Manuscript received online 18 November 2020, revised and accepted 30 November 2020

Nanotechnology has offered a great improvement in science, engineering, medicine, biomedical engineering, food technology, packing technologies, clothes, robotics, and computing from the beginning of twenty-first century. As the maximum potential of scientific discovery always contains some good and bad effects in human civilization, nanotechnology is not an exception among them. The major drawbacks consist of economic disruption and possible threats to security, privacy, health, and environmental hazards, etc. The advancements and benefits of nanotechnology are discussed along with different drawbacks in health-related problems due to their extensive application in medicine, food, agriculture, etc., are summarized. Besides, it highlights the social-economic disruption due to rapid use of nanotechnology. The nanopollution, not only affects human beings but also influences the existence of other living beings like microorganisms, animals and plants, which are also briefly reviewed. The safety and security of nanotechnological developments, current policies, regulation status, challenges and future trends using nanomaterials in humans are demonstrated. In conclusion, while nanotechnology offers more efficient power sources, faster and modern kinds of computers and life-saving medical treatments but some negative issues and limitations are prominent due to their toxicity. Finally, rapid research on nanotechnology bounds to think twice before any advanced technological applications on its safety and security aspect will revolutionize the whole world in near future.

Keywords: Progress in nanotechnology, nanotoxicity, nanopollution, human health, safety.

Introduction

Nanoscience are the emerging field in modern technology with numerous applications in biomedical and manufacturing of new smart materials¹. In the last two decades, nanotechnology integrates with the mechanical and electronic engineering to develop micro/nano-electromechanical systems (MEMS/NEMS) devices, which have diverse applications in different fields of science and engineering. These devices are potentially applicable for different sensing, actuating as well as biomedical analysis purposes². Recently quantum dots have acquired much attention in biological fields owing to its unique size, tunable light absorption and

emission properties³. Further, biocompatible nanomaterials have many applications in biomedical purposes such as orthopedic, cardiovascular, contact lenses, catheter, prosthetic replacement, etc.^{4,5}. Past three decades, extensive research has been carried out to develop nanomedicine and nanoscience based biomedical sensor and instruments^{6,7}. Metallic nanoparticles have unique optical, electrical and biological properties, that have attracted significant attention in applications, like catalysis, ultrasensitive chemical and biological sensors, bio-imaging, targeted drug delivery and fabrication⁸⁻¹⁵. It also comprise of large surface area to volume ratio, unique quantum size, having excellent magnetic proper-

ties, heat conductivity additionally to some catalytic and antimicrobial properties¹⁶. Nanoparticles are often synthesized via various chemical and physical routes like chemical reduction^{17–19}, photochemical reduction^{20–24}, electrochemical reduction^{25,26}, heat evaporation^{27,28}, etc. A series of reducing agents like sodium or potassium borohydrate, hydrazine and salts of tartrate, or organic ones like sodium citrate, vitamin-C, or amino acids are used to get oxidized. Several studies have reported shape and size dependency of silver nanoparticles formation on capping agents like dendrimer²⁹, chitosan³⁰, ionic liquid³¹, and poly(vinylpyrrolidone) PVP³². These capping agents control the nanoparticle growth via reaction confinement within the matrix or through preferential adsorption on specific crystal facets. But, these approaches are costly and hazardous, with the involvement of toxic, non-environment-friendly agents. Hence, evaluation of the risk of these nanoparticles to human health becomes critical. Multiple studies have shown the increase of leukocytes number, neutrophils, in the lungs and bronchoalveolar lavages during airway exposure of nanoparticles in *in vivo* models of inflammation. The neutrophil counts act as biomarkers for inflammation. Therefore, selection of a synthesis route that minimizes the toxicity and increases the stability of nanoparticle leads to enhanced biomedical applications of silver and gold nanoparticles. The development of better experimental procedures for the synthesis of nanoparticles employing variety of chemical compositions and controlled polydispersity offers considerable advancement³³. Methods of nanoparticle fabrication through different physical and chemical process as mentioned above have their demerits as they produce enormous environmental contaminations and unsafe byproducts. Thus, there's a necessity for "green chemistry" that ensures clean, non-toxic, and environment-friendly nanoparticles production³⁴. Nowadays nanomaterials are produced by industries for commercial applications with enormous benefits. While there lies an enormous potential of nanomaterials for fulfilling human requirements, likewise it also correspond to potential risks to human health³⁵.

In recent times, eco-friendly approaches have been developed to engineer stable nanoparticles with intelligible morphology and configured constricted sizes³⁶. Additionally, owing to the high demand for precious metals like silver and gold and their oxides is of great significance and interest^{37,38}.

Bio-inspired synthesis of nanoparticles is an advanced, cost-effective, environment-friendly approach over chemical and physical methods, without any inclusion of high pressure, energy, temperature, and toxic chemicals³⁹. For example, plant leaf extract is used for the biosynthesis of silver and gold nanoparticles for pharmaceutical and biomedical applications, without employing any toxic chemicals in the synthesis protocols⁴⁰. Eco-friendly acceptable reducing and capping agents are considered to be an effective one for "green" synthesis nanoparticles⁴¹. The fabrication process also necessitates the use of non-toxic solvents to make eco-friendly. Generally in this technique, microwave retains a constant temperature of the solvent systems. In conventional extraction techniques hexane, ethanol and water are used for the collection of bioactive molecules⁴². But hexane and ethanol are immensely problematic due to their instability as well as environmental and health hazards⁴³. To overcome this problem, researchers developed the supercritical fluid (SCF) extraction technology to avoid toxic organic solvents in green technology. SCF possesses physical properties intermediate between CO₂ gas and a liquid at a temperature and pressure above of its critical point. Supercritical CO₂ is non-polar, non-toxic, non-flammable, and has low critical temperature. In this regard, nanomaterials, including metal nanoparticles, carbon nanotubes, quantum dots, and other active nanomaterials can be used to develop biosensors against a broad spectrum of microorganisms for the formulation of a new generation of antimicrobial agents. Among noble metals, silver (Ag) and gold (Au) nanoparticles synthesis via marine algae are used as a broad-spectrum antimicrobial agent towards a variety of pathogens in the biomedical field⁴⁴. Many microorganisms are used for the synthesis of nanoparticles such as cyanobacteria, eukaryotic algae, and fungi. Biosynthesis of nanoparticles by plant extracts are better source in comparison to the various biological processes often considered as eco-friendly substitutes of chemical and physical methods^{1,5}. Seaweeds with rich in organic and inorganic is used widely in agriculture, pharmaceutical, biomedical, and nutraceutical industries for consisting high amount of vitamins and minerals^{45,46}. Among several genera of microalgae, *Spirulina platensis* is blue-green algae of the cyanobacteria family grown in temperate water in the whole world. A blue-green algae has served as food with high protein content and nutritional value from ancient

times⁴⁷. The algae produce novel and potentially useful bioactive compounds^{48,49}. The bioactive materials have gained significant attention in recent years and have been used considerably in the development of new pharmaceutical products, food products, renewable bio-energy and biomedical applications^{50–52}. However, antibiotic resistance is a global issue that lowers these drugs' effectiveness via genetic mutation or gene acquisition. Therefore, new classes of antibiotics with novel structural diversity are required to battle this trend. Now food preservation is dealing with severe concern of microorganisms mediated spoilage along with fall in quality and nutrition worldwide⁵³. Recently, nanoparticles are used in various industries like electronics, aerospace, cosmetics, textile, and even in food. Consequently, the chance of human exposure to nanoparticles is rising, heading towards the time when nanoparticles will eventually be present in blood circulation interacting with immune blood cells.

Advantages and growth of nanotechnology

Recently, research and development in nanotechnology have seen exponential growth due to advantages in different fields like drug delivery, cell imaging, material improvement, medical devices for diagnosis and treatment. More powerful computers are being designed using nonmaterial having faster in speed and consuming very less power, long-life batteries.

The term nanocomputers framed in several ways, using mechanical, electronic, biochemical, or quantum nanotechnology. Circuits consisting of carbon nanotubes can maintain the computer system more advance. Carbon nanotubes are also commercially used in sports equipment, with light weight and high strength. Nanoparticles in fabrics improve the water-resistance, stain resistance, and flame resistance, without putting on extra weight, stiffness, or thickness of the fabric⁵⁴. Nanoparticles are used in medical products for dermal, oral or inhalation applications. Tiny insize, corresponds to higher surface area of nanomaterials offering greater strength, stability, chemical, physical, and biological activity. The carbon-based nanomaterials (fullerenes and nanotubes) are employed in thin films, coatings, and electronics. The metal-based nanomaterials (nanosilver, nanogold) and metal oxides (titanium dioxide (TiO₂)) are useful for food, cosmetics, and drug-related products. The dendrimers are nano-poly-

mers, an ideal candidate for drug delivery. Composites such as nanoclays are formed with a combination of nanoparticle with other particles. Many beverage bottles are made up of plastics with nanoclays. The nanoclay reinforcement increases penetration resistance to oxygen, carbon dioxide, moisture and thus increases shelf life and thus nanoclays are also being used in packaging. It helps to improve vehicle fuel efficiency and corrosion resistance by using diamond-like-nanocomposite (DLN) materials that are lighter, stronger, and high chemical resistant^{55,56}. The DLN film exhibits biocompatibility in nature, which have potential applications as a coating material for biomedical purpose. Few nanoparticles are also used in water filter technology that can remove heavy metals, kill viruses and bacteria. These cost-effective, portable water-treatment systems are ideal for the improvement of drinking water quality in developing countries. Now a day, most sunscreens also contain nanoparticles for effective absorption of light including the more dangerous ultraviolet range and pass the other wavelengths, which is healthy for skin. Recently, nanosensors are able to detect a toxic chemical at very low levels, for example, single molecule detection, out of billions of molecules^{57,58}. In medical science, the detection of single biomolecules has tremendous applications for DNA/RNA sequencing and disease analysis. The nanobiosensors can be used to precisely identify particular cells or substances in the body for different diagnostics purposes. Current research is focused on preparing the smaller, highly sensitive and cost-efficient biosensors. The new biosensors are updated to even detect odors specific diseases for medical diagnosis, pollutant detection, and gas leaks for environmental protection.

Nanoparticles in pharmaceutical products facilitate improved absorption within the human body along with easy delivery, often in association with medical devices. For example, magnetite, a metal oxide has great potential applications in nanomedicine. Nanoparticles can assist targeted delivery of chemotherapy drugs to specific cells, i.e. cancer cells. Superparamagnetic iron oxide nanoparticles (SPIONs) and ultra-small superparamagnetic iron oxide (USPIO) have also proved its significance for targeted drug delivery⁵⁹. Nanoparticles can improve the water-solubility of weakly soluble drugs. It can increase drug half-life, modify pharmacokinetics, perk up bioavailability, diminish drug metabolism, assist to controlled and targeted drug delivery, and also com-

bined drug delivery^{60–64}. According to the data by the International Agency for Research on Cancer (IARC), estimates nearly 13.1 million deaths due to cancer by 2030. It is obvious that the low survival rate occurs not because of scarcity of potent, natural, or synthetic antitumor agents but owing to inadequate drug delivery systems. This develops the requirement of technology advancement to need to develop carriers and delivery systems, capable of targeted and efficient delivery of the chemotherapeutic agents without unwanted systemic side effects⁶⁵. The solid lipid nanoparticles and nano-emulsions are the most employed lipid-based drug delivery particles. However, nanosilver based commercial products are capturing market.



Fig. 1. Technological tsunami due to nanotechnology.

The newly developed nanomaterials for theranostics are being employed alone or in association with “classical” drugs, e.g. cytostatic drugs, or antibiotics. Theranostics is a combined term for nanomaterials with diagnostic and therapeutic properties⁶⁴. Fig. 1 shows Technological tsunami occurs due to nanotechnology in the fields of energy storage, defense and security, metallurgy and materials, electronics, optical engineering and microelectromechanical systems (MEMS), biomedicine and drug delivery, agriculture, food science, cosmetics and paints, textile, etc.⁶⁶. According to Zion market research analysis in 2017⁶⁷, there is a rapid increase

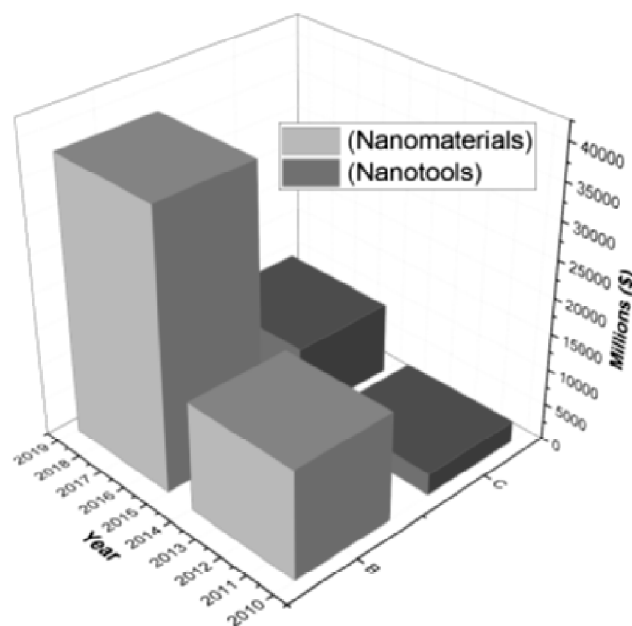


Fig. 2. Global nanotechnology review for nanomaterials, nanotools and nanodevices market from 2011 to 2017 (in Million USD).

of global nanomaterials market volume (in kilo tons) and revenue (in USD Billion), which is estimated from 2014 to 2022, is shown in Fig. 2(a). Other statistical surveys from two different agencies (see Fig. 2(b) and Fig. 2(c) (BCC research)) also confirmed the rapid increase of global nanotechnology market of nanomaterials, nanotools and nanodevices, etc.^{68,69}. Some important key points are summarized below about the advantages and growth of nanotechnology. The key benefits of nanotechnology are:

- (i) Reduction of size of any material, machine or equipment.
- (ii) Reduction of amount of energy and resource.
- (iii) Helps to clean up the existing nano-pollution.
- (iv) Able to secure economy once it can be fully implemented.
- (v) Can alter the basic of technology for human, in its matured phase.
- (vi) Early stage detection of some diseases.
- (vii) Improvement of the drug therapeutic index by increasing efficacy and/or reducing toxicities.
- (viii) Targeted delivery of drugs in tissue-, cell- or organelle-specific manner.

- (ix) Enabling sustained or stimulus-triggered drug release.
- (x) More sensitive cancer diagnosis and imaging.
- (xi) Better pharmaceutical properties like stability, solubility, and half-life of drug molecules.
- (xii) Approaches to develop synthetic vaccines.

Limitations of nanotechnology

Nanomaterials are being employed in different industries and everyday life. Therefore, the interplay of nanomaterials and human surroundings is worth scientific exploration. Nanomaterials with several benefits can be toxic in nature. Various studies also confer with the above-mentioned effects, indicating the potential toxicological effects on human environment⁶⁰. Different toxic and hazardous effects of nanotechnology are briefly discussed below.

Potential routes for nanomaterials to enter into human body:

Nanomaterials can enter into human body in various ways. Potential routes nanomaterials entry into human body are ingestion, inhalation and skin absorption⁷⁰. Many nanomaterials are employed in drug transport or cell imaging via intravenous entry to the human body. In the body, nanomaterials are translocated throughout the body by blood circulation. For the purpose, the nanoparticles must fulfill the requirement of permeability across the barrier of blood vessel wall. Absorption through the skin serves as an alternate route of entry for nanoparticles inside a human body. The skin is the largest organ of the human body, provides a large surface area for interactions with the external environment. TiO₂ nanoparticles can take either route for entry i.e. the lungs or gastrointestinal tract. Nanomaterials can enter into the body through skin due to various reasons, such as use of medicine, cosmetics, ointments and use of clothes containing nanomaterials, occupational contact in industry etc. Soaps, shampoos, toothpaste, hair gels, creams, and some cosmetics containing the nanosilver, which can enter into the body through skin. Cream or solution containing silver nanoparticles is used for treatment of wounds, burns, etc. to prevent infections and damaged skin and the size of nanoparticles drive the penetrating ability in cell. The smaller the nanoparticle, has a greater penetrating ability. The inhaled particulate matter gets accumulate in human respiratory tract, while one major portion of those inhaled particles gets deposited in the lungs. Nanoparticles also have

the potential to travel across the placenta in pregnant women to the fetus along with other organs i.e. brain, liver, spleen and induce lung inflammation and heart disease⁷⁰. The pulmonary inflammation is due to the inhalation of nano-sized urban particulate matter appear due to the oxidative stress, imposed by these particles in the cells^{60,71,72}. The first reported nanoparticle is nano-silver, which can damage DNA molecules. Silver nanoparticles have the most harmful effects on the most sensitive biological groups^{60,73–76}. This nanoparticle can penetrate into blood through the skin. Silver binds with the thiol group of some proteins. If silver complexes with thiol groups are located near-skin region, it gets readily available to get reduced either by visible or UV light into metallic nanosilver particles. This results in immobilization of silver nanoparticles in the skin. Further, the effect of nano copper-induced renal proximal tubule necrosis in kidneys has been reported by Liao and Liu⁷⁷.

Toxicity of nanomaterials:

Greater the human exposure of nanomaterials presents in environment, greater is the harmful effect on human health. The assessment of the cytotoxicity of nanomaterials assists in proper elucidation of their biological activity. Gerloff *et al.*⁷⁸ reported the cytotoxicity of various nanoparticles such as zinc oxide (ZnO), SiO₂, and TiO₂ on human Caco-2 cells. Shen *et al.*⁷⁹ showed the human immune cells are prone to toxicity due to ZnO nanoparticles⁸⁰. The ZnO nanoparticles damage mitochondrial and cell membranes in rat kidney ultimately leading to nephrotoxicity⁸⁰. Generally, nanomaterial toxicity mechanism comprises reactive oxygen species formation and genotoxicity. But as described earlier, toxicity of ZnO nanoparticles particularly affects immune cells. Various nanomaterials with their diverse sizes alter mitochondrial function. For example, ZnO nanoparticles generate Zn²⁺ ions, which disrupts charge balance in electron transport chain in the mitochondria and therefore triggers reactive oxygen species generation. Nanosilver particle has a genotoxic effect. Nanosilver (~20 nm) has a genotoxic effect on human liver HepG2 and colon Caco2 cells. It has also increased mitochondrial injury as well as loss of double-stranded DNA helix in both cell types⁸¹. TiO₂ nanoparticles inhalation, resulted in pulmonary overload in rats and mice with inflammation^{82,83}. The cytotoxic and genotoxic effects of TiO₂ nanoparticles on human lung have been reported by Jugan *et al.*⁸⁴. TiO₂ nanoparticles are genotoxic and it can induce pathological

damage of the liver, kidney, spleen, and brain. Du *et al.* reported cardiovascular toxicity of silica nanoparticles in rats⁸⁵. The surface coating of quantum dots causes toxicity to the skin cells including cytotoxicity and immunotoxicity⁸⁶. Nanosilver is used in wound dressings, affects both keratinocytes and fibroblasts. Fibroblasts show higher sensitivity towards nanosilver than by keratinocytes. Again, iron oxide nanoparticles rapidly get endocytosis on cultured human fibroblasts and interrupt the function. Citrate/gold nanoparticles have shown toxicity on human dermal fibroblasts⁸⁷. Carbon nanotubes have high toxicity and produce harmful effects on human. The nanoparticles can penetrate into the lungs, then reached blood and act as barrier for the circulation of blood into brain. They can also enter inside other organs like bone marrow, lymph nodes, spleen, or heart. Sometimes, nanoparticles can incite inflammation along with oxidant and antioxidant activities, oxidative stress, and change in mitochondrial distribution. These effects depend on the type of nanoparticles and their concentrations⁶⁹. Copper nano particles (diameter 40 nm and 60 nm) have harmful effect on brain cell at low concentration. It activated the proliferation of the endothelial cells in brain capillaries. Ag nanoparticles (25, 40, or 80 nm) influenced the blood-brain barrier, causing a proinflammatory reaction, which might induce a brain inflammation with neurotoxic effect. Smaller Ag nanoparticles (25 nm and 40 nm diameter) can induce cytotoxic effect at a greater rate compared to larger nanoparticles. Nanoparticles also have harmful effects on the brain cell of the mouse and rat. The high concentration of nanoparticles can affect brain blood fluxes, with consequent cerebral edema. Pathogenic effects of Ag-nanoparticles (25, 40, and 80 nm diameter), Cu-nanoparticles (40 and 60 nm) and Au-nanoparticles (3 and 5 nm) on the blood-brain barrier of pig have been reported⁸⁸. Silver nanoparticles (45 nm) influenced the acetylcholine activity via nitric oxide generation; it induces hyperactivity of rat tracheal smooth muscle⁸⁹. It is also reported that Ag-nanoparticles (25 nm) produced an oxidative stress after the injection into the mouse. The nanoparticles were aggregated in the kidneys, lungs, spleen red pulp and in the nasal airway, with no observable morphological changes apart from nasal cavity⁹⁰.

Very few cells do not undergo morphological changes after withstanding the air-liquid interface culture for an extended duration. Au-nanoparticles (5 nm and 15 nm diameter) penetrated into the mouse fibroblasts, where they re-

mained stocked. Only the presence of 5 nm Ag-nanoparticles disrupted cytoskeleton resulting in narrowing and contraction of cells. Many engineered nanomaterials, such as TiO₂, magnetite iron, CeO₂, carbon black, SWCNTs, and MWCNTs, also might cause different levels of inflammatory reactions, including enhanced pro-inflammatory cytokines expression, target inflammation-related genes, and micro-granulomas formation^{91,92}. The intra-tracheal administration of MWCNTs with variable length and iron content in hypertensive rats Led to the lung inflammation with increased blood pressure and lesions in abdominal arteries along with accumulation in multiple organs i.e. liver, kidneys, and spleen post 7 days and 30 days exposure⁹³. Maneewattapaninyo *et al.* studied acute toxicity of colloidal silver nanoparticles administered in laboratory mice and observed neither any mortality any acute toxicity symptoms after a limited dose of 5.000 mg/kg post 14 days of oral administration. No differences could be observed in among groups after hematological and biochemical assessment and the histopathological study. The instillation of silver nanoparticles at the concentration of 5.000 ppm developed a transient eye irritation for 24 h. The application of these nanomaterials on skin did not produce any micro or macroscopic toxicity⁹⁴. The schematic mechanism of silver nanoparticles toxicity in human body is shown in Fig. 3⁹⁵. Liver and spleen are maximum exposed organs to nanomaterials owing to the prevalence of phagocytic cells in the reticuloendothelial system. Also, the organs with high blood flow such as kidneys and lungs can be affected.

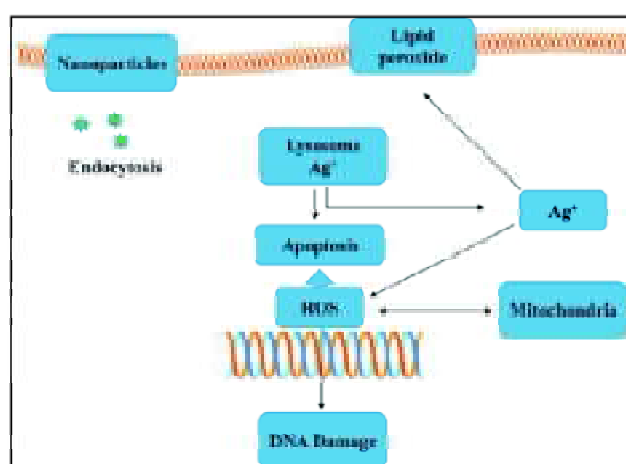


Fig. 3. Mechanism of silver nanoparticles toxicity (Abbreviations: NPs – nanoparticles; ROS – reactive oxygen species; Ag⁺ – silver ions) Redrawn from⁹⁵.

Health hazards in human:

In spite of having many benefits and uses the nanomaterials may cause health hazards to humans owing to very small size. The large absorption surface of lung, the thinner air-blood barrier, and comparatively less inactivation of enzymes leads to faster entry for particles into the systemic blood circulation at higher drug concentrations. Additionally, intentional uptake, exposure of particles carried by the wind from the environment, and nanoparticles released at manufacturing units may also cause health hazards for human. Usually, the biological effects of nanomaterials are based on their size, composition, shape and also on their electronic, magnetic, optical, and mechanical properties. Presently, the influence of nanotechnology on human health and environment is still controlled. Most of the studies assessed the outcomes of unintentional and accidental exposure (inhalation, medical procedures, or accidental ingestion) and focused on local effects only^{66,67}. Though, along with introducing nanomaterial-based biomedical procedures, it is mandatory to analyze their toxicity at a systemic level. Centuries before, Paracelsus said, "everything is a poison, and nothing is a poison, it is only a matter of a dose". For nanomaterials, it is applicable in both the aspects of dose and particle size⁶⁸. There is a huge demand for the use of nanomaterials in various applications, ranging from diagnostic technology, bioimaging, to gene/drug delivery⁹⁶⁻⁹⁸. Therefore, intended or unintended human exposure to nanomaterials is unavoidable and has greater prospects of exposure in the future. Therefore, a branch of science is developing, named "nanotoxicology", the study of toxicity of nanomaterials. Nanotoxicology assess the role and safety of nanomaterials on human health. Several anthropogenic sources like power plants, internal combustion engines and other thermo-degradation reactions also generate nanoparticles and therefore develop the need to assess them as well⁶⁹.

Hazards in nanomedicine:

The nanomaterials represent a variety of biomedical applications, however, there is some potential risks factor related to the toxic issue. For example, cytotoxicity, genotoxicity, oxidative stress and inflammation have been reported on *in vitro* and *in vivo* models for testing nanoparticles. The difference in the size of nanomaterial and bulk comes with the differences in properties and toxicity as well. Nanomaterials are tremendously beneficial yet can be toxic. Ag, ZnO, or

CuO nanoparticles are frequently used as bactericides⁷⁹. But waste disposal in the environment can also negatively affect non-target organisms.

Hazards in medical instrumentation:

Nanomaterials are involved in medical interventions like prevention, diagnosis, and treatment of diseases. With development of science and technology, more accurate and multi functional medical diagnostic equipment are being fabricated for easy and safe operation. The 'lab-on-a-chip' technology facilitates instantaneous point-of-care testing, enhancing the standards of medical care. Nanomaterial based thin films on implant surfaces improve the wear and resist infection. But until now, these medical nanodevices are not 100% hazard free due to manufacturing processes, not following guidelines of nanotoxicity and also operating without the assessment of long term effects of nanotoxicity.

Hazards in food product:

Nanotechnology is used to produce advanced food products and smart packaging technology⁹⁹⁻¹⁰¹. In this way, the possibility of direct exposure of nanomaterials with human beings is enhanced and different types of long-term or short-term toxicity may occur^{102,103}. Nanoparticles and diamond-like nanocomposite (DLN) thin films are used in food packaging to reduce UV exposure and prolonged shelf life. Due to very few articles being reported in this area, further research is needed to fully explore the potential use of these nanoparticles for food products and medical treatments.

Environmental nanopollution and its effect in society:

Environment conservation is a challenging task. Its vastness and complexity make this even more difficult. As the production of nanomaterials is growing multiple issues concerning nanotechnology arise as environmental pollution and industrial exposure. Nanoparticles serve as pollutants in diesel exhaust or welding fumes, presenting new toxicological mechanisms^{104,105}. It also makes us face pollution in macro, micro, and nano-scale. New branches of electronics are also creating new sources of occupational exposure hazard. The circumstances produce new challenges for both classical toxicology and nanotoxicology. Though nanotechnology is improving the living standard, simultaneous increase in water and air pollution has also occurred. As the origin of this pollution lies in nanomaterials hence termed as "nanopollution". Nanopollution is extremely lethal to both

underwater flora and fauna and organisms living on soil. The pollutants can enter in human body in multiple ways. Cellular mechanisms can get affected by nanomaterial toxicity, which mainly comprises reactive oxygen species generation and genotoxicity^{105,106}. The nanoparticle's exposure on humans can occur unintentionally by environmental particles (e.g. air pollution) and deliberately because of a diversity of consumer products, cosmetics, and medical products containing nanoparticles. The release of nanoparticles during the manufacturing process may result in exposure on workers via dermal, oral, and inhalation routes. Exposure to air pollutants, such as ultrafine particles, is known to cause inflammatory air-way diseases and also cardiovascular problems in humans¹⁰⁷. Pope *et al.*¹⁰⁸ stated that even very very low amount of ambient nanoparticle exposure, have a momentous consequence on mortality. To decrease nanopollution, scientists and researchers used nanotechnology to develop nanofilters, which can eliminate almost all airborne particles¹⁰⁹.

Economic and social disruption due to rapid use of nanotechnology:

As the speed of nanotechnology development is growing, as a consequence the job opportunities are decreasing, arising the problem of unemployment in fields like industrial sector, manufacturing, and traditional farming¹¹⁰. Nanotechnology-based devices and machines have replaced humans to furnish the job more rapidly and efficiently, which has pointed out the importance of manpower in the field of practical work. Increasing growth and instant performance of nanotechnology have compromised the worth of commodities like diamond and oil. As an alternative technology i.e. nanotechnology has a detrimental effect on the demand as substitutes have more efficiency and do not need fossil fuels. Diamonds are losing the worth due to greater availability from nanotechnology-based fabrication methods. Currently, manufacturing companies are equipped for the production of the bulk of these products at a molecular scale, followed by disintegration to create new components.

At present, nanotechnology involves high investment technologies; raising the cost daily. The high cost is the resultant of intricate molecular structure and processing charges of the product. The whole process makes it difficult for manufacturers to randomly produce dynamic products using nanotechnology. Currently, it is an unaffordable business

owing to huge pricing of nanotechnology-based machines. Hence, nanotechnology can also bring financial risks as manufacturers have to invest large sum of money for setting up nanotech plants. The manufacturers have to face a huge loss if by any chance the manufactured products fail to satisfy the customers. Alternate options such as recovery of the original product or maintenance of the nanomaterials are also a costly and tedious affair. Further, nanotechnology does not leave any byproducts or residues, generally basis for the small industries, therefore creating huge risk of extinction for small scale industries. As an outcome, the quantity of sub-products of coal and petroleum is deteriorating. Another gigantic threat (like Covid-19 pandemic situation), which is born with the arrival of nanotechnology. It can make the easy accessibility of bio-chemical weapons or nano-bio engineered biological weapons. Nanotechnology is making these weapons more powerful and destructive. Unauthorized criminal bodies or corrupt politicians can steal the formulations and may reach these hazardous weapons easily and they can easily destroy our civilization¹¹¹.

Effect of nanotechnology on microorganisms, animals, and plants:

Some nanomaterials are not only hazardous to human beings but are also harmful to the existence of different microorganisms, animals, and plants. Man-made nanopollution is very much unsafe for living microorganisms, animals, and plants under the water or on the earth. As a result, many microorganism's families have completely disappeared from the world. Recently, due to rapid application of nanotechnology in the agriculture sector without proper nanotoxicological analysis, many plants are directly exposed to nanotoxicity and animals are indirectly exposed. Thus, in last two decades, a vast number of valuable plants and animals are completely disappeared from our world.

Key points about limitations of nanotechnology:

Some key points about limitations of nanotechnology are summarized below:

- (i) Still at its infancy stage.
- (ii) More research and developmental work need to be done.
- (iii) Expensive technology till now.
- (iv) Creates environmental nanopollution.
- (v) Huge initial cost for implementation.

(vi) Resistance from culture perspective, activists, journalists and even within the government.

(vii) Knowledge limitation from many industries and misperception among many fields about its capabilities.

(viii) Nanomaterials are not regulated by the government.

(ix) Requirement of large investment and research but yield is still a limiting factor.

(x) Some nanoparticles may be toxic to humans.

(xi) Nanotechnology made weapons are more powerful and more destructively increasing the explosion potential.

(xii) Lack of employment in the fields of traditional farming, manufacturing, and industrial sector.

Safety and security of nanotechnological developments

Nanotechnology is an extensively expanding field. Researchers, scientists, and engineers are getting high success to produce nano-materials and take the advantages of improved properties, such as higher strength, lighter weight, increased electrical conductivity, and chemical reactivity with respect to their macro equivalents¹¹². Human health concerns are also growing due to nanomaterials. The attempts of technological manipulations raise vocational risk to the workers in case of accidental exposures. Major cases of poisoning occur during coatings on the products. These micro or nano particles penetrate inside the brain, while in contact with humans and to lungs during inhalation. So it is matter of ethical issue. The problem can be addressed by using nanoscale materials to overcome the negative effects of micro or nano particles coatings in industry and health sectors. Academic and industry experts suggest that there exists ambiguity regarding the toxic effects of releasing nanoparticles into the environment. It is also noteworthy that, there is a lack of knowledge of nanoparticles interactions with humans and environment. Similar to most of the emerging technologies nanotechnology and nanochemistry industries have both benefits and challenges. To get maximum benefits the challenges must be overcome, managed and endured. Mesoporous silicates, alone or in combination with other inorganic or organic counterparts have been extensively explored for targeted drug delivery and cancer treatment. Even though the long-term toxicity of the nanoparticles is subjected to controversies and doubts, the use of gold and silver nanoparticles have provided more advantages in comparison to other actual alternatives (cytostatics). Conse-

quently, there is a growing interest in developing *in vitro* assays for nanotoxicology study¹¹³, it is strongly encouraged to use primary human cells as a source for *in vitro* study with nanoparticles since different origins of cancerous cell lines complicate data interpretation for human risk evaluation. Till now, the environmental effects and the toxicity of nanomaterials to organisms are in infancy state. The evaluation methods need to be cost-effective rapid, and quantity efficient.

Current policy and regulation status

The social implications of nanotechnology comprise of many fundamental aspects like ethics, privacy, environment, and security. Occasionally, the negative impacts on environment are too adverse to handle that the people simply give up. However, nanoscience researchers are still optimistic to see light of hope on the other side of the tunnel. Environmental clean-up is possible via design and manipulation of atomic and molecular scale of materials. It would develop cleaner energy production, energy efficiency, water treatment, and environmental remediation. Nanoscale fluid dynamics deciphers flow of nanoparticles in environment as a result of interactions with biological and environmental systems. Researchers are keen to understand the transportation of nanomaterials in association with environmental contaminants through groundwater systems. For food authenticity, safety, and traceability, every food company should need to use smart labels at stronger and innovative functional lightweight packaging. Now, each developed and developing countries have a separate policy and regulation for the use of nanotechnological products and applications. Explicit initiatives on nanotechnology must be needed to pledge that, the prospects provided by nanotechnology are not misused and research does not become bitty. The ambiguity, complication, and diversity of nanotechnology mean that any such initiative should not be a strictly predetermined closed program. Flexibility will be needed to stay side by side of development as they arise.

Challenges and future trends in using nanomaterials in humans

Nanotechnology-based production uses very little manpower, land, maintenance and it is cost-effective, high productivity with modest requirements of materials and energy. The extensively growing field offers scientists and engineers

a great opportunity to manipulate or alter the materials at nanoscale to yield benefit of enhanced material characteristics like enhanced strength, lightweight, higher electrical conductivity, and chemical activity in comparison to their large-scale counterparts. However, for biomedical applications, the toxicity evaluation of nanomaterials should be performed. Broadly, detailed physicochemical characterization of nanomaterial should be performed before and during any toxicity study. Important properties that can control nanomaterial-induced toxicity, including size and shape of the nanomaterials, coating, chemical composition, crystal growth, nanomaterials purity, structure, surface area, surface chemistry, surface charge, agglomeration, and solubility should also be taken care. Measurements should be performed in full stable state of nanomaterials in the most relevant test medium, i.e. aggregation status and ion release from metallic nanomaterials. Various engineered materials should be tested for their multidisciplinary tiered toxicity using diverse models and experiments^{114,115}. Therefore, the first step in the genotoxicity is an assessment of physicochemical properties of nanomaterials. The validation of the proposed tiered approaches is still waiting for future. The researchers are continuously trying to increase the relevant database with an increasing number of publications (papers, reviews, or even patents) every year¹¹⁶, particularly market share of the nanotechnology products is also growing up to thousands of billions of Euros¹¹⁷. Balanced use of the nanotechnologies/nanomaterials must be arranged, to optimize the opportunities/risks factors. Further research related to the size and shape, capping agents, receptors immobilization onto the metal nanoparticles are still a matter of keen interest with high necessity. Surface plasmon resonance can be tuned by varying sizes, shape of the nanomaterials and different surface functionalization of both silver and gold nanoparticles can reduce the toxicity and enhance a variety of biomedical applications in future. For example, CNT toxicity can be reduced via functionalization, surface coating, and stimulation of the autophagic flux. The amino functionalization decreases the CNT toxicity to the cells¹¹⁸, along with albumin coating for SWCNTs¹¹⁹.

Conclusions

Nanoparticles can enter and get distributed around the human body very easily. After entering into human, it moves within the body and creates cellular toxicity. Then it attacks

respiratory system, cardiovascular system, brain, skin, gut, and other organs. Again, some nanomaterials kill harmful bacteria within body and some of them kill good bacteria and live-cell of human body. Nanoparticles with different substances are used in SIM cards of cell phones or sunscreens. When these are used, free nanoparticles get released in the environment (air, water or soil). Engineering fields like civil and electronics also create new occupational health risks; making new potentially toxic nanomaterials. The toxicity of nanoparticles depends on their shape, size, and chemical composition. Centuries before, Paracelsus quoted, "everything is a poison, and nothing is a poison, it is only a matter of a dose". In regards to nanomaterials, the quotes hold value for both dose and particle size. The new interdisciplinary investigations explore the potentially harmful effects of these useful NPs and help in environmental preservation. Owing to smaller size the inhalation of nanomaterials imposes harmful effects on human health. The inhalation causes severe injury to the lungs and can also become fatal. The deterioration of lungs can be observed even after 60 s of nanoparticle inhalation. Therefore, for sustainable nanotechnology development, it is mandatory to evaluate and spread knowledge about the short term and long term exposure benefits and hazards for nanomaterials. To conclude, nanotechnology has the potential to impact society, both positively or negatively. Its consumers, producers and dealers include all the members of the society and all stakeholders; so we should collectively raise the voice in its various growth and commercialization phases. Currently, nanotechnology is in its infancy stage with a significant lack of awareness about its effects on humans and the environment. As civilization moves forward, the vital query is: how should we manage the risks and uncertainties of this emergent technology? Is anyhow COVID-19 pandemic situation manmade? If not, we can face such type of situations due to careless application of nanotechnology in different fields. However, all these limitations can be overcome itself by the rapid research on each such suspected fields of nanotechnology.

References

1. T. S. Santra, F-G. Tseng and T. K. Barik, *J. Nanopharmaceutics Drug Deliv.*, 2014, **2**, 1.
2. A. R. Jha (ed.), "MEMS and nanotechnology-based sensors and devices for communications, medical and aerospace applications", CRC Press, 2008.

3. I. L. Medintz, H. T. Uyeda, E. R. Goldman and H. Mattoussi, *Nat. Mater.*, 2005, **4(6)**, 435.
4. Y. Oshida (ed.), "Bioscience and bioengineering of titanium materials", Elsevier Science, eBookISBN: 9780080467191, 2006.
5. T. S. Santra, F.-G. Tseng and T. K. Barik, *Am. J. Nano Res. Appl.*, 2014, **2**, 5.
6. N. Savithamma, M. L. Rao, S. Ankanna and P. Venkateswarlu, *Int. J. Pharma. Sci. and Res.*, 2012, **3(4)**, 1141. <http://dx.doi.org/10.13040/IJPSR.0975-8232>.
7. P. S. Chikramane, A. K. Suresh, J. R. Bellare and S. G. Kane, *Homeopathy*, 2010, **99**, 231.
8. K. Aslan, Z. Leonenko, J. R. Lakowicz and C. D. Geddes, *J. Phys. Chem. B*, 2005, **109**, 3157.
9. J. J. Diao and Q. Cao, *AIP Adv.*, 2011, **1**, 012115. <https://doi.org/10.1063/1.3568815>.
10. J. K. Lim, K. Imura, T. Nagahara, S. K. Kim and H. Okamoto, *Chem. Phys. Lett.*, 2005, **412**, 41.
11. E. Hutter and D. Maysinger, *Microsc. Res. Tech.*, 2011, **74**, 592.
12. G. Schider, R. Krenn, A. Hohenau, H. Ditlbacher, A. Leitner, R. Aussenegg, L. Schaich, I. Puscasu, B. Monacelli and G. Boreman, *Phys. Rev. B: Condens. Matter Mater. Phys.*, 2003, **68**, 155427.
13. X. Lou, Y. Zhang, J. Qin and Z. Li, *Chem. - A Eur. J.*, 2011, **17**, 9691.
14. J. M. Pingarrón, P. Yáñez-Sedeño and A. González-Cortés, *Electrochim. Acta*, 2008, **53**, 5848.
15. C. D. Geddes, A. Parfenov, I. Gryczynski and J. R. Lakowicz, *Chem. Phys. Lett.*, 2003, **380**, 269.
16. M. Ra, A. Gade, S. Gaikwad, P. D. Marcato and N. Durán, *J. Braz. Chem. Soc.*, 2012, **23**, 14.
17. D. G. Yu, *Colloids Surfaces B: Biointerfaces*, 2007, **59**, 171.
18. Y. Tan, Y. Wang, L. Jiang and D. Zhu, *J. Colloid Interface Sci.*, 2002, **249**, 336.
19. C. Petit, P. Lixon and M. P. Pileni, *J. Phys. Chem.*, 1993, **97**, 12974.
20. S. A. Vorobyova, A. I. Lesnikovich and N. S. Sobal, *Coll. Surf. A*, 1999, **152**, 375.
21. K. Mallick, M. J. Witcomb and M. S. Scurrrell, *Mater. Chem. Phys.*, 2005, **90**, 221.
22. S. Kéki, J. Török, G. Deák, L. Daróczi and M. Zsuga, *J. Colloid Interface Sci.*, 2000, **229**, 550.
23. M. P. Pileni, *Pure Appl. Chem.*, 2000, **72(1-2)**, 53.
24. Y. P. Sun, P. Atorngitjawat and M. J. Mezziani, *Langmuir*, 2001, **17**, 5707.
25. Y. C. Liu and L. H. Lin, *Electrochem. Commun.*, 2004, **6**, 1163.
26. G. Sandmann, H. Dietz and W. Plieth, *J. Electroanal. Chem.*, 2000, **491**, 78.
27. C. H. Bae, S. H. Nam and S. M. Park, *Appl. Surf. Sci.*, 2002, **197-198**, 628.
28. A. B. Smetana, K. J. Klabunde and C. M. Sorensen, *J. Colloid Interface Sci.*, 2005, **284**, 521.
29. K. Esumi, R. Isono and T. Yoshimura, *Langmuir*, 2004, **20**, 237.
30. A. Murugadoss, A. Khan and A. Chattopadhyay, *J. Nanoparticle Res.*, 2010, **12**, 1331.
31. H. Zhang, X. Li and G. Chen, *J. Mater. Chem.*, 2009, **19**, 8223.
32. Y. Sun and Y. Xia, *Science*, 2002, **298**, 2176.
33. R. Bhattacharya and P. Mukherjee, *Adv. Drug Deliv. Rev.*, 2008, **60**, 1289.
34. D. Raghunandan, P. A. Borgaonkar, B. Bendegumble, M. D. Bedre, M. Bhagawanraju, M. S. Yalagatti, D. S. Huh and V. Abbaraju, *Am. J. Anal. Chem.*, 2011, **02**, 475.
35. R. K. Bera, S. M. Mandal and C. R. Raj, *Lett. Appl. Microbiol.*, 2014, **58(6)**, 520.
36. K. Kathiresan, S. Manivannan, M. A. Nabeel and B. Dhivya, *Colloids Surfaces B: Biointerfaces*, 2009, **71**, 133.
37. Y. Konishi, T. Tsukiyama, K. Ohno, N. Saitoh, T. Nomura and S. Nagamine, *Hydrometallurgy*, 2006, **81**, 24.
38. E. Castro-Longoria, A. R. Vilchis-Nestor and M. Avalos-Borja, *Colloids and Surfaces B: Biointerfaces*, 2011, **83(1)**, 42.
39. D. S. Goodsell (ed.), "Bionanotechnology: Lessons from Nature", ISBN: 978-0-471-41719-4, 2004.
40. N. S. Thakur, B. P. Dwivedee, U. C. Banerjee and J. Bhaumik (ed.), "Bioinspired Synthesis of Silver Nanoparticles: Characterisation, Mechanism and Applications", eBook ISBN9781315370569, CRC Press, 2016.
41. J. Xie, J. Y. Lee, D. I. C. Wang and Y. P. Ting, *ACS Nano.*, 2007, **1**, 429.
42. M. Hayes (ed.), "Marine Bioactive Compounds: Sources, Characterization and Applications", DOI: 10.1007/978-1-4614-1247-2_2, Springer Science+Business Media, LLC, 2012
43. G. Wenqiang, L. Shufen, Y. Ruixiang and H. Yanfeng, *Nat. Prod. Res.*, 2006, **20**, 992.
44. D. Fawcett, J. Verduin, M. Shah, S. Sharma and G. E. J. Poinern, *J. Nanoscience*, Article ID 8013850, 2017, DOI: 10.1155/2017/8013850.
45. S. Cox, N. Abu-Ghannam and S. Gupta, *Int. Food Res. J.*, 2010, **17**, 205.
46. M. De Pádua, P. S. G. Fontoura and A. L. Mathias, *Brazilian Arch. Biol. Technol.*, 2004, **47**, 49.
47. P. Kumari, M. Kumar, V. Gupta, C. R. K. Reddy and B. Jha, *Food Chem.*, 2010, **120**, 749.
48. S. Ravikumar, S. Krishnakumar, S. J. Inbaneson and M. Gnanadesigan, *Archives of Applied Science Research*, ISSN 0975-508X, 2010, **2(6)**, 273.

Barik et al.: Prospect of nanotechnology: A brief Review

49. S. Krishnakumar, J. Premkumar, R. Alexis Rajan and S. Ravikumar, *Int. J. Appl. Bioengineering*, 2011, **5(2)**, 12.
50. P. Manivasagan, J. Venkatesan and S.-K. Kim (ed.), "Marine Algae: An Important Source of Bioenergy Production", eBook ISBN9780429076282, CRC Press, 2015.
51. S. Ermakova, M. Kusaykin, A. Trincone and Z. Tatiana, *Front. Chem.*, 2015, **3**, 39.
52. J. Venkatesan, I. Bhatnagar, P. Manivasaga, K. H. Kang and S.-K. Kim, *Int. J. Biol. Macromol.*, 2015, **72**, 269.
53. A. M. Fayaz, K. Balaji, M. Girilal, R. Yadav, P. T. Kalaiichelvan and R. Venketesan, *Nanomedicine*, 2010, **6(1)**, 103.
54. G. Roymahapatra, Towels Made of Nano Cloth - An Alternative Concept, 'Charoibeti', published on the occasion of 14th Years Celebration of Education and Health Day organized by 'Smile', 12th January, 2018
55. T. S. Santra, T. K. Bhattacharyya, F. G. Tseng and T. K. Barik, *AIP Adv.*, 2012, **2**, 022132.
56. T. S. Santra, T. K. Bhattacharyya, P. Patel, F. G. Tseng and T. K. Barik, *Surf. Coatings Technol.*, 2011, **206**, 228.
57. T. S. Santra, C. H. Liu, T. K. Bhattacharyya, P. Patel and T. K. Barik, *J. Appl. Phys.*, 2010, **107**, 124320.
58. T. S. Santra, T. K. Bhattacharyya, P. Mishra, F. G. Tseng and T. K. Barik, *Science of Advanced Materials*, 2012, **4(1)**, 110, doi.org/10.1166/sam.2012.1258.
59. D. De, S. M. Mandal, J. Bhattacharya, S. Ram and S. K. Roy, *Journal of Environmental Science and Health. Part A, Toxic/Hazardous Substances and Environmental Engineering*, 2009, **44(2)**, 155.
60. S. M. Mandal, W. F. Porto, D. De, A. Phule, S. Korpole, A. K. Ghosh, S. K. Roy and O. L. Franco, *The Analyst*, 2014, **139(2)**, 464.
61. R. Singh and J. W. Lillard, *Exp. Mol. Pathol.*, 2009, **86(3)**, 215.
62. A. Z. Wang, R. Langer and O. C. Farokhzad, *Annu. Rev. Med.*, 2012, **63**, 185.
63. T. W. Prow, J. E. Grice, L. L. Lin, R. Faye, M. Butler, W. Becker, E. M. T. Wurm, C. Yoong, T. A. Robertson, H. P. Soyer and M. S. Roberts, *Adv. Drug Deliv. Rev.*, 2011, **63(6)**, 470.
64. J. Xie, S. Lee and X. Chen, *Adv. Drug Deliv. Rev.*, 2010, **62(11)**, 1064.
65. L. Brannon-Peppas and J. O. Blanchette, *Adv. Drug Deliv. Rev.*, 2004, **56**, 1649.
66. <https://www.iberdrola.com/innovation/nanotechnology-applications>.
67. <https://www.zionmarketresearch.com/news/nanomaterials-market>.
68. <https://www.statista.com/statistics/1073886/global-market-value-nanotechnology>.
69. [https://www.bccresearch.com/pressroom/nan/global-nanotechnology-market-to-reach-\\$64.2-billion-in-2019](https://www.bccresearch.com/pressroom/nan/global-nanotechnology-market-to-reach-$64.2-billion-in-2019).
70. A. Elsaesser and C. V. Howard, *Adv. Drug Deliv. Rev.*, 2012, **64(2)**, 129.
71. T. Papp, D. Schiffmann, D. Weiss, V. Castranova, V. Vallyathan and Q. Rahman, *Nanotoxicology*, 2008, **2**, 9.
72. G. Oberdörster, E. Oberdörster and J. Oberdörster, *Environ. Health Perspect.*, 2005, **113**, 823.
73. S. A. Love, M. A. Maurer-Jones, J. W. Thompson, Y.-S. Lin and C. L. Haynes, *Annu. Rev. Anal. Chem.*, 2012, **5**, 181.
74. M. Ahamed, M. S. AlSalhi and M. K. J. Siddiqui, *Clin. Chimica Acta*, 2010, **411**, 1841.
75. A. Manke, L. Wang and Y. Rojanasakul, *Biomed Res. Int.*, 2013, **2013**, 1.
76. C. Beer, R. Foldbjerg, Y. Hayashi, D. S. Sutherland and H. Autrup, *Toxicol. Lett.*, 2012, **208**, 286.
77. M. Y. Liao and H. G. Liu, *Environ. Toxicol. Pharmacol.*, 2012, **34**, 67.
78. K. Gerloff, C. Albrecht, A. W. Boots, I. Frster and R. P. F. Schins, *Nanotoxicology*, 2009, **3**, 355.
79. C. Shen, S. A. James, M. D. De Jonge, T. W. Turney, P. F. A. Wright and B. N. Feltis, *Toxicol. Sci.*, 2013, **136**, 120.
80. G. Yan, Y. Huang, Q. Bu, L. Lv, P. Deng, J. Zhou, Y. Wang, Y. Yang, Q. Liu, X. Cen and Y. Zhao, *J. Environ. Sci. Heal., Part A*, 2012, **47**, 577.
81. S. C. Sahu, J. Zheng, L. Graham, L. Chen, J. Ihrle, J. J. Yourick and R. L. Sprando, *J. Appl. Toxicol.*, 2014, **34**, 1155.
82. M. Semmler, J. Seitz, F. Erbe, P. Mayer, J. Heyder, G. Oberdörster and W. G. Kreyling, *Inhal. Toxicol.*, 2004, **16**, 453.
83. J. Ferin, G. Oberdörster and D. P. Penney, *Am. J. Respir. Cell Mol. Biol.*, 1992, **6**, 535.
84. M. L. Jugan, S. Barillet, A. Simon-Deckers, S. Sauvaigo, T. Douki, N. Herlin and M. Carrière, *J. Biomed. Nanotechnol.*, 2011, **7**, 22.
85. Z. Du, D. Zhao, L. Jing, G. Cui, M. Jin, Y. Li, X. Liu, Y. Liu, H. Du, C. Guo, X. Zhou and Z. Sun, *Cardiovasc. Toxicol.*, 2013, **13**, 194.
86. H. Shi, R. Magaye, V. Castranova and J. Zhao, *Part. Fibre Toxicol.*, 2013, **10**, 1.
87. R. Landsiedel, L. Ma-Hock, T. Hofmann, M. Wiemann, V. Strauss, S. Treumann, W. Wohlleben, S. Gröters, K. Wiench and B. Van Ravenzwaay, *Fibre Toxicol.*, 2014, **11**, 16.
88. W. J. Trickler, S. M. Lantz-Mcpeak, B. L. Robinson, M. G. Paule, W. Slikker, A. S. Biris, J. J. Schlager, S. M. Hussain, J. Kanungo, C. Gonzalez and S. F. Ali, *Drug Metab. Rev.*, 2014, **46**, 224.
89. C. González, S. Salazar-García, G. Palestino, P. P. Martínez-Cuevas, M. A. Ramírez-Lee, B. B. Jurado-Manzano, H. Rosas-Hernández, N. Gaytán-Pacheco, G. Martel, R. Espinosa-Tanguma, A. S. Biris and S. F. Ali, *Toxicol. Lett.*, 2011, **207**, 306.

90. M. B. Genter, N. C. Newman, H. G. Shertzer, S. F. Ali and B. Bolon, *Toxicol. Pathol.*, 2012, **40**, 1004.
91. H. Tsuda, J. Xu, Y. Sakai, M. Futakuchi and K. Fukamachi, *Asian Pac. J. Cancer Prev.*, 2009, **10**, 975.
92. E. J. Park, H. Kim, Y. Kim, J. Yi, K. Choi and K. Park, *Toxicology*, 2010, **275**, 65.
93. R. Chen, L. Zhang, C. Ge, M. T. Tseng, R. Bai, Y. Qu, C. Beer, H. Autrup and C. Chen, *Chem. Res. Toxicol.*, 2015, **28**, 440.
94. P. Maneewattanapinyo, W. Banlunara, C. Thammacharoen, S. Ekgasit and T. Kaewamatawong, *J. Vet. Med. Sci.*, 2011, **73**, 1417.
95. S. Clichici and A. Filip, "in vivo Assessment of Nanomaterials Toxicity", in: *Nanomater. - Toxic. Risk Assess.*, InTech, 2015, 93.
96. P. Shinde, A. Kumar Kavitha, K. Dey, L. Mohan, S. Kar, T. K. Barik, J. Sharifi-Rad, M. Nagai and T. S. Santra, "Physical approaches for drug delivery", in: *Deliv. Drugs*, Elsevier, 2020, 161.
97. T. S. Santra, P. C. Wang, H. Y. Chang and F. G. Tseng, *Appl. Phys. Lett.*, 2013, **103**, 233701.
98. A. K. Narasimhan, S. B. Lakshmi, T. S. Santra, M. S. R. Rao and G. Krishnamurthi, *RSC Adv.*, 2017, **7**, 53822.
99. C. Silvestre, D. Duraccio and S. Cimmino, *Prog. Polym. Sci.*, 2011, **36(12)**, 1766.
100. S. D. F. Mihindukulasuriya and L. T. Lim, *Trends Food Sci. Technol.*, 2014, **40(2)**, 149.
101. B. S. Sekhon, *Nanotechnol. Sci. Appl.*, 2010, **4(3)**, 1.
102. V. K. Bajpai, M. Kamle, S. Shukla, D. K. Mahato, P. Chandra, S. K. Hwang, P. Kumar, Y. S. Huh and Y. K. Han, *J. Food Drug Anal.*, 2018, **26(4)**, 1201.
103. Q. Chaudhry, M. Scotter, J. Blackburn, B. Ross, A. Boxall, L. Castle, R. Aitken and R. Watkins, *Food Addit. Contam. - Part A: Chem. Anal. Control. Expo. Risk Assess.*, 2008, **25(3)**, 241.
104. R. K. Ibrahim M. Hayyan, M. A. Alsaadi, A. Hayyan and S. Ibrahim, *Environ. Sci. Pollut. Res.*, 2016, **23**, 13754.
105. P. Mehndiratta, A. Jain, S. Srivastava and N. Gupta, *Environ. Pollut.*, 2013, **2(2)**, 49.
106. B. Zhang, H. Misak, P. S. Dhanasekaran, D. Kalla and R. Asmatulu, *Am. Soc. Eng. Educ.*, 2011, **1845(1)**, 1.
107. V. C. Van Hee, J. D. Kaufman, G. R. Scott Budinger and G. M. Mutlu, *Am. J. Respir. Crit. Care Med.*, 2010, **181**, 1174.
108. A. C. Pope, R. T. Burnett, D. Krewski, M. Jerrett, Y. Shi, E. E. Calle and M. J. Thun, *Circulation*, 2009, **120**, 941.
109. N. Bernd, *Nanotechnology*, 2005, **39(5)**, 106A.
110. S. Wood, A. Geldart and R. Jones, *TATuP-Zeitschrift Für Tech. Theor. Und Prax.*, 2003, **12**, 7.
111. A. Khan, Ethical and social implications of nanotechnology, *QScience Proc.*, 2015. <https://doi.org/10.5339/qproc.2015.elc2014.57>.
112. Encyclopedia of Nanotechnology, 2012. <https://doi.org/10.1007/978-90-481-9751-4>.
113. S. Arora, J. M. Rajwade and K. M. Paknikar, *Toxicol. Appl. Pharmacol.*, 2012, **258**, 151.
114. K. Savolainen, H. Alenius, H. Norppa, L. Pylkkänen, T. Tuomi and G. Kasper, *Toxicology*, 2010, **269**, 92.
115. A. Kumar and A. Dhawan, *Arch. Toxicol.*, 2013, **87**, 1883.
116. Scopus-Document search Signed in, (n.d.). <https://www.scopus.com/search/form.uri?display=basic> (accessed June 9, 2020).
117. Nanomaterials: Toxicity and Risk Assessment - Google Books, (n.d.). <https://books.google.co.jp/books/> (accessed June 9, 2020).
118. W. Chen, Q. Xiong, Q. X. Ren, Y. K. Guo and G. Li, *Neural Regen. Res.*, 2014, **9**, 285.
119. Y. Liu, L. Ren, D. Yan and W. Zhong, *Part. Part. Syst. Charact.*, 2014, **31**, 1244.

ISSN : 2319-5282

EDU CARE

A Multidisciplinary International
Peer Reviewed/Refereed Journal

Vol. IX, Number - 8

January-December, 2020

Chief Editor

Dr. S. Sabu

Principal, St. Gregorios Teachers' Training College, Meenangadi P.O.,
Wayanad District, Kerala-673591. E-mail: drssbkm@gmail.com

Co-Editor

S. B. Nangia

A.P.H. Publishing Corporation

4435-36/7, Ansari Road, Darya Ganj,

New Delhi-110002

Children Education During COVID-19 Pandemic and Related NSS Activities

Dr. Tarun Kumar Barik*

ABSTRACTS

During the COVID-19 pandemic, we are facing a serious living and learning crisis. Children and youth of primary, secondary and higher secondary school age were out of school. Actually, COVID-19 threatens the education systems in our lifetimes. Different crisis and approach to recover children's education system from this hazardous emergency situation and related NSS activities have been summarized in this article. The schools, colleges and universities need proper master plan to start reopening and stabilizing the education system slowly but more carefully. The present analysis suggests to emphasis on the maintenance of hygiene level, following digital systems and regular basis online counseling of school children are required on priority basis. School authorities are most responsible to upgrade their digital systems timely and make a long-term resilience in our education system. NSS volunteers play a prime role to spread the awareness through online and one to one personal communication about the importance of hand hygiene, respiratory hygiene, social distancing, importance of mask wearing in the public places and also the importance of COVID-19 vaccination.

Keywords: COVID-19; Hygiene, Online Education, NSS

INTRODUCTION

The shocking pandemic outbreak of coronavirus disease -2019 (COVID-19) is a severe threat to our human society. COVID-19 is caused by a new type corona virus, SARS-CoV-2 (Severe acute respiratory syndrome coronavirus 2) and in the case of infection, most of the people fall sick with mild to moderate symptoms. It becomes deadly serious when virus transmitted to lungs and subsequently occurred complications like acute respiratory failure. The virus spread easily among people by person to person contact (within about 6 feet, or nearly 2 meters), by the droplets released from coughing, sneezing or talking of infected person. Till now, COVID-19 patient's complications, risk factors and prevention strategies are announced and well documented. Researchers through worldwide have already discovered COVID-19 vaccines; most of them have completed phase-3 clinical trials successfully. Doctors are trying to manage the symptomatic treatment to increase the recovery rate. However, whole World is following the lockdown based option of prevention strategy by staying home as much as possible to stop the spreading in our community. It is recommended to work from home. This is going for long days that will make an immense problem in our society or nation. This is the era of World Wide Web (www), where maximum work can complete by the help of web based technologies. Therefore, the educational systems have the major role in this period to grow up our nation in a required standard.

The Post-COVID emergence or ongoing the pandemic scenario have multidirectional consequences on various spheres of life apart from deterioration of human health. The economical

cost associated with COVID-19 pandemic is very high as it inferred from high costs of medical care, intensive care, loss of productive working days, major impact on travel and tourism, ban on entry of agricultural product from affected regions, etc. Similarly, if the growths of educational system become weaken that can't be compensated by means of anything else. Students' mental health is also very much important for his learning, appearance and attitude. In this critical situation, the roles of teachers are extraordinarily important to save our student's health and growth out there.

SHARING OF KNOWLEDGE ON HEALTH AND HYGIENE

Hygiene is the attitude, behaviour and practices for the protection of health consequently healthy living. Poor health hygiene practices are the major cause of several communicable diseases in developing countries, the primary causes of morbidity and mortality among young or school children are the acute respiratory and intestinal infections [1]. School is the only place where students acquire not only education but also provoke their attitude, behaviour and environment. The United Nations Children's Fund (UNICEF) confirmed that knowledge, attitudes, and practices (KAP) are the basic principle of hygiene. Simple hygienic process by washing hands with soap is poorly practiced in India and almost no culture in any school, college or university systems. It is necessary to prepare real hand washing facilities including enough knowledge in awareness which may lead to some changes in behaviour and attitude. Lack of resources like soap, sanitizing material, and very poor sanitizing system in educational institutes in India may be the main reasons not to develop their attitude and behavior.

Recent awareness regarding the pandemic outbreak of coronavirus disease (COVID-19) is extremely important due to its pathogenic and contamination nature because it is caused by a virus SARS-CoV-2. Currently, COVID-19 has caused global health concern. Human to human transfer by contact or through the aerosols from sneezing and coughing is widely confirmed. To reduce the transmission of current outbreak, lockdown emergency is going on including banned the international and domestic flights and social distancing etc. World health Organization (WHO) gives a general advice on how to comply with "social distancing" while also fulfilling family and work responsibilities and provides guidance on the hygiene measures to protect someone from infected patients. All the students must have to follow the points in future and make their attitude to continue with these habits:

- Wash hands with soap and water before and after meal for at least 20 seconds.
- Wash hands with soap and water after toilet and urination.
- Maintain good respiratory hygiene (covers mouth and nose when coughing or sneezing and immediately disposes of tissues and wash hands).
- Use alcohol-based (>70%) hand sanitizers when necessary.
- Provide basic knowledge about how sanitizers and soap kills the virus (SARS-CoV-2)
- Avoid touching eyes, nose and mouth.
- Clean and disinfect surfaces you use often such as bench tops, desks and doorknobs
- Increase the amount of fresh air by opening windows or changing air conditioning
- Frequent cleaning of work surfaces and touch points such as door handles etc.
- Use mask when it is necessary to go outside.

The maintenance of personal hygiene is of great importance to decrease the trouble of not only COVID-19 but also from any other infectious diseases.

Emphasis on Home School

Recently, the COVID-19 pandemic has altered the education system all over the world. Globally due to pandemic situation, billions of students are out of their usual classrooms teaching. As a result education has changed noticeably, with the characteristic rise of e-learning, whereby teaching is

Accessed remotely on digital platforms. Recent research suggests that online learning has been shown to increase retention of information, and take less time [2]. While some people believe that unplanned and rapid move to online learning – without proper training, insufficient bandwidth, and little preparation – will result in a poor user experience that is un-conducive to sustain growth. On the other hands, others believe that a new hybrid model of digital education will emerge with significant benefits. According to Wang Tao, Vice President of Tencent Cloud and Vice President of Tencent Education “The integration of information technology in education will be further accelerated and that online education will eventually become an integral component of school education”. Again, according to Dr. Amjad, a professor at the University of Jordan, who has been using Lark to teach his students, says, “It has changed the way of teaching. It enables me to reach out to my students more efficiently and effectively through chat groups, video meetings, voting and also document sharing, especially during this pandemic. My students also find it is easier to communicate on Lark. I will stick to Lark even after coronavirus, I believe traditional offline learning and e-learning can go hand by hand.” [2] There are, however, challenges to overcome online learning. Some students without reliable internet access and/or technology struggle to participate in digital learning; this gap is seen across countries and between income brackets within countries. Hence, schools, college, ministry or government authorities should think about this matter seriously in near future for uniform learning [2]. For those, who do have access to the right technology, there is evidence that learning online can be more effective in a number of ways. Some research shows that on average, students learn 25-60% more material when learning online compared to only 8-10% in a classroom. This is mostly due to the students being able to learn faster online; e-learning requires 40-60% less time to learn than in a traditional classroom setting because students can learn at their own swiftness, going back and re-reading, skipping, or accelerating through concepts as they choose [2]. But the effectiveness of online learning varies amongst age groups. BYJU's Mrinal Mohit says “Over a period, we have observed that clever integration of games has demonstrated higher engagement and increased motivation towards learning especially among younger students, making them truly fall in love with learning”. It is clear that this pandemic has completely disrupted the education system, while some worry that the hasty nature of the transition online may have hindered the goal, others plan to make e-learning part of their 'new normal' after experiencing the benefits first-hand [2]. Like, e-commerce post-SARS, it is yet to see an inflection point for rapid innovation occurs in the case of e-learning post-COVID-19.

The horror of Covid-19 outbreak has shut-down schools, college and universities in India. Preliminary data analysis about online teaching indicates that it is a non-starter for most students and institutions in India. Maximum student of India comes from backward class of rural or urban area, where less possibility of access home internet. Actually, it is easy to connect to one set of students, reaching others through the internet would be tough. The digital divide should be evident in teaching resources but every student must have access to it. Few privileged educational institutions in India have good platform of e-learning because of their maximum students come from a creamy society but other have to struggle with inequality for successful implementation of digital drive of e-learning at home. However, internet access at home is pitifully low in India. This is a combination of low internet coverage in India as well as the fact that many households do not own smart phones that can get them on the internet. As the Covid-19 infections rise in India, and there is justified pressure to keep educational institutions closed, one must be mindful of these numbers when suggesting online teaching. While the long-term strategies may involve increasing internet connectivity, or subsidizing data on mobiles, it would seem that device ownership is a matter of concern, especially for children coming from rural places. If universities remain closed for a long time, it is important for the universities to subsidize cheap smart phones for students

to get on with the business of teaching. This is in addition to any subsidies that need to be paid for bandwidth (assuming that it is a surmountable problem). Without such help, online teaching is a non-starter for most institutes of India. Central- and state-government, different NGOs and every hearty peoples of India should come forward and work together to solve this inequality in the post pandemic situation and should fulfill the dream of digital India.

At the time of nationwide lockdown schools, colleges and universities are depending on the online mode of teaching in order to maintain the continuity of education. Schools are launching apps, conducting classes over Google meet/ Google Hangouts / Zoom / Teams, and sending interactive worksheets and videos for learning in WhatsApp or facebook groups. Even though internet-based teaching is the most appropriate stop-gap arrangement now, it has highlighted the inequalities in the education system in major portion of India. A majority of the student population is being left out in the pursuit of basic education. Many schools, colleges and universities of India are using WhatsApp or facebook groups, to connect to their students or guardians. Teachers have been asked to make WhatsApp group of all parents in their respective classes and send those lessons so that students can learn at home. Teachers are taking help from the central government's digital learning portal DIKSHA, which has lessons in multiple languages for all classes from primary to UG/PG. Some teachers are also making videos on practical concepts and these videos are then shared on the WhatsApp groups to connect to their students. As for example, nearly 50% school students (of class-V to Class-XII) and 75% college or university students of Medinipur municipality, Paschim Medinipur, West Bengal, India are accessing this facility. The students below the class-V of the above locality have accessed e-learning facilities only 20%. On the other hand, the situation of rural students of Paschim Medinipur district is very bad compared to students of urban area [This is the approximate data survey by the author in his district]. Table-I shows the list of e-learning resources, platforms and educational applications to help parents, teachers, school/college/university administrators, and students during the COVID-19 outbreak [3].

Resource Generation by Teachers

School teachers have to be more conscious about their teaching and course work generation. It may not be the same as in practical class teaching. School teachers can sign up to provide their teaching material to enrolled students with full and free access or make web based industry partners. They must be careful about a long-term plan for web based virtual learning classes and accordingly design their course work. Few important points are discussed below to sharing the knowledge and resource management-

- **Design an online course-** Develop online course tutorial for classroom, planning and designing online lessons following modern and advanced educational tools.
- **Be an online tutor-** Self practice necessary training to teaching about online education processes. Follow several online teaching modules like Online Learning Technology Landscape, e-learning management tools, and communication and creation tools.
- **Directory of open educational resources-** There are over 7000 resources on higher education, open schooling, teacher education, and technical and vocational skills development. anyone can take help.
- **Open resources for english language teaching** is intended to support classroom activities for teachers.
- **COL's institutional repository** provides access to a large number of resources on online learning and guides to help teachers plan, design, develop and offer quality online learning
- **Digital/ WhatsApp and Facebook educator Information hub** may consider engaging with your students on WhatsApp and make group. Be part of what's happening around the world in real-time, no matter where you are.

BUILD UP THE LONGER-TERM RESILIENCE OF EDUCATION SYSTEMS

It is commonly accepted that countries demand well-built education systems that advocate knowledge, life skills, and social consistency. However, systems sometimes fail to deliver education services in adverse situation such as natural disaster, political crisis, health epidemic, invasive violence, and armed quarrel etc. Ironically, education can also lend a hand to take the edge off the risks of such hardship and help students to succeed over the situation despite of unremitting challenges. This is one aspect of the kind of pliability of individuals, communities, and the institutions that providing development to convalesce and understanding positive change in the face of hardship. The Education Resilience Approaches (ERA) program applied by World Bank Group (WBG) is an important tool in facing this hardship [5]. This program is designed to provide relative analysis of resilience processes in education system based on local statistics on adversity, school-neighbourhood relations, education policies, and services in adverse situation. Several countries have been using Systems Approach for Better Education Results (SABER) to analyze various aspects of their education systems [6]. WBG launched the 'Education Sector Strategy 2020: Learning for All', in 2011, with the aim to 'Invest early, invest smartly, and invest for all' [7]. The strategy "holds that investments in education should achieve learning for all because growth, development and poverty reduction depend on the knowledge and skills that people acquire, not the number of years that they sit in a classroom." The main theme of SABER is to provide 'Learning for All' by targeting on three main pillars (i) "Public access to systematic, accurate, and comparable data on the quality of countries' education policies and the quality of implementation of those policies", (ii) "Awareness and utilization of these data by countries and development partners in sector analyses, policy dialogue, and planning processes", (iii) "More informed global discussion and debate about strengthening education systems to increase countries' learning for all". These areas are supposed to take part in a big role in education system reforms on both for a country and global level also. There are thirteen domains that are currently evaluated through SABER, and education resilience is a major domain among these. The thirteen areas are- (i) Early Childhood Development (ECD), (ii) Education Management and Information Systems (EMIS), (iii) Education Resilience (ERA), (iv) Engaging the Private Sector (EPS), (v) Equity and Inclusion (E&I), (vi) Information and Communication Technologies (ICT), (vii) School Autonomy and Accountability (SA&A), (viii) School Finance (SF), (ix) School Health and School Feeding (SH&SF), (x) Student Assessment (SA), (xi) Teachers (T), (xii) Tertiary Education (TE), (xiii) Workforce Development (WID). The initial focus of SABER is to evaluate education environments by investigating the existing documented education policies. Then assess the efficacy of these policies and institutions in practice at the classroom level, and to identify policy implementation gaps within and across countries. SABER then propose a new tool to explicate the linkages between these gaps to explore an overall systems approach. Knowledge regarding human development and learning has grown at a rapid pace; the opportunity to shape more effective educational practices has also increased.

Even before the COVID-19 pandemic, the world was living a learning crisis. Before the pandemic, 258 million children from primary and secondary-school age, were out of school education system. Another adverse impact is of low schooling quality which means many students, who were in school learned too little. It can be defined as 'Learning Poverty'. The Learning Poverty rate in low-and middle-income countries was 53 % percent before COVID-19 pandemic, meant that more than half of all 10-year-old children couldn't read and comprehend a simple story. Even worse, the most underprivileged children had the worst access to schooling leads to highest dropout rates, and the largest learning deficits. It proves that, the world was already far behind the target of 'Sustainable Development Goal (SDG)', which include, "all girls and boys complete

free, equitable and quality primary and secondary education." The COVID-19 pandemic added new challenges in this context. The pandemic has created a deep impact on education by closing schools almost everywhere in the world. It has impacted nearly 1.57 billion learners out of school and 191 country-wide school closures, impacting 91.3% of the world's total enrolled learners as per UNESCO estimation up to April 20, 2020. Drop-out rates across the globe are likely to rise as a result of this massive disruption to education access [8, 9]. It has created a severe dent to all education systems in our lifetimes. The damage will become even more rigorous as the COVID-19 pandemic will be translated into global recession. Out of school, children are more likely to be exposed to risks like child labor, family violence, forced marriage, trafficking and exploitation and so many. For the most vulnerable children, education is life saving drug, it also inculcate hope for a brighter future. However, it is possible to counter this damage, and to turn emergency in to opportunity. The first step is to manage effectively with the school closures, by protecting health, safety and doing what they can to prevent students' learning loss using remote learning. Secondly, countries need to start planning for reopening of school with a proper framework. That means preventing dropout, ensuring healthy school conditions, and using new techniques to promote rapid learning recovery, once the students are back in school. Teachers have a major role in framing out the new system, within the school as well as the government systems, and also to implement them effectively at earliest. And during the Lockdown, continuing education through alternative learning pathways must also be a top priority right now, to ensure the interruption to education is as limited as possible. We urgently need to support teachers, parents/caregivers, innovators, communications experts and all those who are positioned to provide education, whether through radio programmes, home-schooling, online learning and other innovative approaches.

REGULAR BASIS ONLINE COUNSELING

The pandemic has radically changed the concept of traditional education in the past few months and virtual learning will be the new future of education. Before the pandemic, technology was just considered as a means of entertainment. Today, keeping teachers and the students engaged in learning process has become the priority during lockdown, and virtual classes have proved to be helpful in these difficult times. This powerful medium has diversified the field of teaching. Earlier, teachers were not so familiar with online teaching at the school level, except for the computer lectures. Now, along with teachers, every profession has chosen the virtual platform, providing precious opportunities to both new learners and experts. There appears to be no deficiency of online resources of academic value. And therefore, online teaching is more an opportunity than a challenge for teachers today. Mental health of students is the topic of major concern during COVID-19 pandemic, especially when school and colleges and other academic institutes are closed due to 'LOCK DOWN'. The overall education is not only dependent on academic curriculum but also on his mental health. Disturbances in the mental health have an extreme negative impact to a student and also on the community. Today's student is the future citizen of the country; contributing to the development of a nation by serving various roles like teacher, engineers, doctors, nurse etc. Hence, the mental health of the students has to be given at most importance. Till date, there is no proven treatment to manage the Novel corona virus disease, though some vaccines are in trial, lockdown is the only option available to slowdown the rate of spreading the infection by restricting community-infection path. In this process, all the education institutes suddenly were declared 'locked down'. The students were in different phases of their academic year. It is well known that the students experience lots of stress especially before and during the examinations [10,11].

Table-1: The list of e-learning resources, platforms and educational applications below to help parents, teachers, school/college/university administrators, and students during the COVID-19 outbreak [3].

System management platforms	Systems built for use on basic mobile phones	External repositories of distance learning solutions	Massive Open Online Course (MOOC) Platforms	Self-directed learning content	Mobile reading applications	Collabora- tion platforms that support live-video communica- tion	Tools for teachers to create of digital learning content
1 Century Tech 2 CusDojo 3 Edmodo 4 Edraak 5 EdStep 6 Google Classroom 7 Moodle 8 Naham 9 Paper Applines 10 Schoology 11 Seesaw 12 Stooler	1. Coll-Ed 2. Eneza Education 3. Funzi 4. KalOS 6. Ubongo 7. Ustad Mobile	1. UNHCR 2. UNEVOC Resources 3. Organisation International de la Francophonie 4. Koulu.me 5. Keep Learning Going 6. Global Business Coalition for Education 7. European Commission Resources 8. EdSurge 9. Education Nation 10. Brookings Common Sense Education Common wealth of Learning	1. Alison 2. Canvas 3. Coursera 4. European Schoolnet Academy 5. EdX 6. iCourse 7. Future 8. Learn 9. icourses 10. TED-Ed Earth School 11. Udemy 12. XuetangX	1 British Council 2 Byju's 3. Code It 4. Code.org 5. Code Week 7. Discovery Education 8. Duolingo 9. Edraak 10. Facebook. Get Digital 11. Feed the Monster 12. Geekie 13. Khan Academy 14. KitKit School 15. Lab X change 16. Minds park 17. Mosoteach 18. Music Crab 19. OneCourse 20. Polyup 21. Quizlet 22. Siyavula 23. Smart 24. History 25. YouTube	1 African Storybook 2. Biblioteca 3 Digital del Institute Latino americano de la Comunicacion Educativa 5 Global Digital Library 6. Interactive 7. Learning Program 8. Reads 9. Room to Read 10. Story Weaver 11. World reader	1 Dingtalk 2 Lark 3 Hangouts Meet 4 Teams 5. Skype 6. eChat Work 7. Whats App 8 Zoom	1 Trello 2. Sound 3. Peer Desk 4. Nearpod 5. Kaltura 6. Ed. Course 7. Ed Puzzle 8. Edmentum 9. Think ink

The students were preparing the examinations especially the entrance examinations for years together. For example, in India, NEET is the common entrance examination to enter into the professional colleges. Students will be preparing for this exam since two years as the scores will decide their admission criteria. Some students might be allotting an extra year to get through the entrance examinations. These students are in high anxiety because their pre-examination

phase will prolong till they complete their examination, further, as there is no proclamation of the date of exam, there is quiet improbability about their future. Parents may add up more anxiety to the system, as they are equally undergoing stress regarding their kid's career in future. Though many of the educational institutes have launched online classes, adaptation of the student to the sudden change from habitual teaching method to a new system is stressful. This is true chiefly in case of the slow learners. The fear of corona pandemic will add up to their stress. There for, the need of psychiatrist, in this circumstance to keep the mental balance of the students is extremely necessary. Every educational institution may think of establishing a mental health cell, or student counseling centre that comprises of psychiatrist(s) or psychologist(s) with a proper management system. Regular online counseling should be planned along with the online teaching classes. Importance should be given to counsel the parents with equal importance along with students. Regular monitoring of the stress levels using different online tools can be done to prevent the student to enter into the state of depression. And teacher who is a pivot of this whole system, simultaneously be counseled in handling the students with the new teaching process. The student should be priory convinced that there will not be any loss of academic year. The entrance examinations may be planned to conduct online as majority of the universities/ institutes throughout the world is already following the same. The counseling cell should also monitor the students even after the lockdown as it takes time for the students to normalize himself after the long, unexpected break of his studies. Continuous monitoring, offering counseling to the needy students will help to keep the students mentally sound and do well in personal and professional life. For example, to uphold student's mental health during the lockdown the Student Counseling Unit (SCU) of Unit-Fort Hare University (UFHU) has moved its services to an online platform [13]. By visiting the SCU facebook page, students are able to engage with qualified Psychologists in a safe and confidential space. The SCU of UFH University is managed by a psychologist on a daily basis. The platform allows psychologists from the unit to participate in live chats and offer one-on-one assistance via private online sessions. Psychological advice on how to manage lockdown related stress and anxiety is also shared on the page. The SCU also suggested their students to stay connected with their peers, share study materials and approaches in order to feel connected with like-minded people. They also suggested some following tips [13] to their students to remove stress during and make one feel goal-directed during lockdown.

- To prepare a special routine during lockdown and maintain it.
- Planning of study sessions and including break time.
- Self-care is an important aspect
- Never stay in empty stomach, intake meal in regular time
- Drink sufficient water time to time
- Listening to good music and engaging in dance once in a while can have a positive impact on mental health
- Not spending too much time on social media, especially at night, as this may lead to sleep problems and fatigue.

In our India, Calcutta University has started free online psychological counseling [14] service for all its students to beat any stress during the COVID-19 lockdown. The university has also issued a circular with the name and number of the faculty members whom the students may call at specified time slots for counselling services. Thirteen teachers - five from the Department of Psychology and eight from the Department of Applied Psychology - is provide counseling session to students of undergraduate and postgraduate courses available for 12 hours daily.

SACHING TO CHILDREN OF MIGRANT LABOUR

Refugees, displaced and migrant children, often fall between the cracks as national policies do not necessarily include these helpless groups. They must be included and provided for in special responses to this crisis. While we are practising social distancing, and trying to practice stay at home, in the hope of a better tomorrow, there is a possibility that a significant number of children would appear as victims of such measures. One impact would be an increase in the number of child workers. Along with the health crisis, the pandemic has generated a huge shock on economic and labour market. And millions of child labour would be in vulnerable condition which needs serious attention. According to ILO (International Labour Office) the Global Estimates of Child Labour: Results and Trends (2012-2016) presented in Geneva in 2017 [16], there were 152 million child labourers worldwide, of which 73 million were in hazardous work. Among these 152 million, 88 million are boys (58%) and 64 million are girls (42%). Among these children, 48% are 5-11 years-olds, 28% are 12-14 years-olds and only 24% are 15-17 years-olds. In another statistics, 70.9% of these children were engaged in Agriculture sector, 11.9% in Industry and 17.2% in Service sector. If we do address this issue with immediate and accelerated efforts, we are going to lose the battle of eliminating all forms of child labour by 2025, a commitment under the SDG. And the bare fact is that a very large number of children in child labour are completely deprived of education.

Children of the age group 5-14 years, there are 36 million are in child labour who are out of school, which is 32 per cent of all those in child labour in this age range. It is one of the most important indicators to address of the impact of child labour on sustainable livelihood prospects. The crisis created by the pandemic of COVID-19, will push millions of vulnerable children into child labour, specially the children of migratory labour. The Government of India has also declared for a countrywide school closure. UNESCO also estimates that around 32 crore learners are had an affected, of which 16.2 crore are boys 15.8 crore are girls. The bulk of these students are enrolled in primary and secondary schools (86%), followed by tertiary (10%) and pre-primary (4%) level of education [8]. Governments have adopted a variety of hi-tech, low-tech and no tech solutions to ensure the continuity of learning during this period. Most of the focus has been on online learning reforms, though nearly half of our country has no internet access. We can't think about internet access of children living in remote village, staying at foot-path or in slams. The MHRD (Ministry of Human Resource Development) of Govt. of India has suggested that all schools should connect their students through digital platforms to compensate for the loss of school hours. But the reality is that, as of now, mostly private schools (Generally CBSE and ICSE affiliated schools) and selected Govt. schools like Kendriya Vidyalaya have started online classrooms. However, most state government schools do not have the technology and equipment to provide online teaching. Moreover, the majority of students do not have access to internet, smart phones or a computer. Therefore, a large number of children studying in public schools remain cut off from online education. This will inexplicably affect children who already experience barriers in accessing education. This includes children with disabilities, students in remote locations, children of migrant workers, and children from the poor family. The millions of children who will be victims of the COVID-19 pandemic need immediate attention from states and communities. The starting point should be the parents: coordinated policy efforts should be taken income support to all informal sector workers, migrant workers to stimulate their family needs. As a direct measure, states should prioritise efforts to ensure education for all children, using all available technology. But school teachers have a vital role to address this issue. Teachers have the direct relation with students in education process. So, they will take initiative to discuss with school authorities and need to ensure that every student will get lunch at home until schools open. Special efforts should be taken to identify children

orphaned due to COVID-19, and arrangements of shelter and foster care for them should be made on a priority basis. Apart from teaching process, teachers have a role to support the Govt. policy adopted during this pandemic period. States are also working on food distribution to all Govt. school children. For example, while Kerala and Delhi government are delivering food packets as a part of mid-day meals for government school children at their develop, West Bengal and Andhra Pradesh are providing dry rations to children. But distribution of foods in terms of food packets or dry rations can be smoothly organized with the help of teachers. Another hard problem for migrant children is to adopt the language of education. As their parents are migrant labour, they have to move around with their parents, thorough the India, which is multilingual country. In COVID-19 pandemic, when most of the migrant labours are coming back to their home state, both students and teacher will face a problem to use the common language for education. Kerala [16] can be a model in this situation. Kerala's economy is dependent on migrants. Kerala sending out large numbers of workers overseas (2.4 million in 2013, based on a May 2013 report by the Centre for Development Studies) it needs migrants from other Indian states for Kerala's economic activities. The exact number of migrants coming to Kerala is unknown. According to 2017 estimations by CMID, (Centre for Migration and Inclusive Development, an Emakulam-based non-profit organization) as much as 11% of the population of Kerala) would be migrant and the figure may turn to 3.5 - 4 million. The Kerala government has been more proactive compared to other states to address situation as their economy is directly relate to it. There are three types of migrant workers at Kerala; those who come for work and sell a calamities. The migrant student drop-out rate depends on the nature of migration. The problem starts with the language barrier first. Keral Govt. through Sarva Shiksha Abhiyan (SSA) has appointed a large number of volunteer to help those students understand Malayalam, which is the medium of education in all Govt. schools. These measures will no doubt respond to the emergency created by COVID-19 directly or indirectly to some extent. However, it is clear that more needs to be done to prevent children from lapsing into child labour and teacher as a main pillar of education system has a major role to address this situation.

ROLE OF NSS VOLUNTEERS IN COVID-19 OUTBREAK

Maximum schools, colleges and universities of India have National Service Scheme (NSS) volunteers since 1969. The number of NSS volunteers was 40,000 in 1969 and 3.8 million in March 2018. A NSS volunteer is a student of school or college or university who has enrolled his/her name in the National service Scheme. The roles of the NSS volunteers are very significant according to the National Service Scheme because they are the main beneficiaries of the programme. It provides the opportunity to the youth students of class-XI and XII in schools and graduate and post graduate students of colleges and university level of India to take part in various community service activities and programmes. The slogan of NSS is NOT ME BUT YOU [4]. The NSS programme aims to encourage social welfare in students, and to provide service to society without bias. NSS volunteers work to ensure that everyone who is needy gets help to enhance their standard of living and lead a life of dignity. In doing so, volunteers learn from people in adopted villages how to lead a good life despite a shortage of resources. The first thing NSS provide is to develop their own thought process by doing community services. Society is a group of persons who may have different ideology. NSS volunteers through their skills and dedication build it a homogenous ideological group. NSS volunteers also provide help in natural and man-made disasters by providing food, clothing and first aid to the disaster victims. NSS volunteers take care of cleanliness, blood donation, health awareness issues, child education, and many other activities. NSS is always trying to bring smiles on innocent faces through empowering the

education. In this way NSS makes its volunteer a good human being. While studying, these volunteers undertake community development activities which help to build their personality and develop the belongingness towards the society. The NSS volunteers are performing the role as a bridge between the education system and the community which is helpful for the nation building. By developing their qualities of leadership, skills to become an organizer, and an administrator to attain the multi-faceted development of their personality as a whole. Whenever there is a need, NSS volunteers appear themselves to serve the nation. NSS volunteers always take up relief and rescue operations on priority whenever a natural disaster occurs in any part of the country. It may be in the form of environment enrichment, malnutrition, immunization, or the issue of natural disaster; NSS volunteers are becoming the saviors for the victims [17].

Recently, Maximum NSS volunteers with their NSS programme officers and coordinators have completed iGOT (Integrated Govt. Online Training) courses about COVID-19 pandemic on DIKSHA platform. There are different iGOT courses about COVID-19 like Basic of COVID-19, Infection Prevention and Control, Clinical Management of COVID-19, ICU Care and Ventilation Management, Infection Prevention through PPE, Management of COVID-19 cases, Quarantine and Isolation, Psychological support of patients with COVID-19 etc. The trained volunteers are also trying to attract the attention of other students of the school, college or university towards these courses about Covid-19 outbreak awareness activity.

National Service Scheme (NSS) volunteers in India have taken up different awareness activities for basic infection, prevention and control of COVID-19 in war-footing basis to the common people during the lockdown period of COVID-19 pandemic. Different NSS units across the India are fully involved in the relief activities to the poor. The NSS volunteers are sanitising the affected area, preparing food packets for the flood victims, running common kitchen and distributing medicines. The NSS volunteers and other functionaries are distributing food packets to the affected people at various places and are also helping in rescue operations with the health workers. They are collecting items like dry ration, drinking water, clothes, soaps, medicines, sanitary napkins, milk powder, washing powders, hand wash, sanitizers etc. These volunteers work tirelessly to mobilise relief materials and work for the smooth distribution of the collected materials in the affected area in close coordination with the district administration. They are also collecting money for the PM Relief Fund of different states of India. As for example, Md. Salauddin Ansari, a NSS volunteer (member) of Achhruram Memorial College, Jhalda, Purulia, West Bengal, India participated in different COVID-19 related activities [see Fig.-1] to aware and help the common people. At present about 20000 NSS volunteers are enrolled in this programme in 426 universities of India covering about 32000 villages. NSS nodal or programme officers circulate and forward materials including Covid-19 awareness guide, packet book and awareness posters etc to all NSS volunteers and then they in-ward these materials through email, whatsapp and other social media platforms to all other NSS volunteers and students of University /Directorate /College /schools /institutions to propagate the right messages on Corona virus and clear all myths, misconceptions, stigma & discrimination about Covid-19. At this critical juncture, NSS play the prime role to spread the awareness through one to one personal communication about the importance of hand hygiene, respiratory protection, minimum 1 meter social distancing in the public places. Students of the National Service Scheme are not discouraged by the lockdown, and are doing their bit by spreading awareness on various posters, videos, quizzes, etc. The NSS coordinators are performing their responsibility by converting old newspapers into little napkins that can be used to open the gate or correct method of using gloves and even ways to handle those under home quarantine. Also some educational institutions have started creating quizzes or webinar about COVID-19.



Fig.1: Some COVID-19 related NSS activities performed by Md. Salauddin Ansari, NSS volunteer (unit-III) of Achhruram Memorial College, Jhalda, Purulia, West Bengal, India.

REFERENCES

- 1 <https://www.sciolsp.org/sciolo.php?lng=en>
- 2 <https://www.weforum.org/agenda/2020/04/coronavirus-education-global-covid-19-online-digital-learning>
- 3 <https://en.unesco.org/covid19/educationresponse/solutions>

1. <https://www.who.int/news-room/feature-stories/2020/04/2020-04-20-covid-19>
2. <https://www.unicef.org/india/stories/2020/04/2020-04-20-covid-19>
3. <https://www.unicef.org/india/stories/2020/04/2020-04-20-covid-19>
4. <https://www.unicef.org/india/stories/2020/04/2020-04-20-covid-19>
5. <https://www.unicef.org/india/stories/2020/04/2020-04-20-covid-19>
6. <https://www.unicef.org/india/stories/2020/04/2020-04-20-covid-19>
7. <https://www.unicef.org/india/stories/2020/04/2020-04-20-covid-19>
8. <https://www.unicef.org/india/stories/2020/04/2020-04-20-covid-19>
9. <https://www.unicef.org/india/stories/2020/04/2020-04-20-covid-19>
10. <https://www.unicef.org/india/stories/2020/04/2020-04-20-covid-19>
11. <https://www.unicef.org/india/stories/2020/04/2020-04-20-covid-19>
12. <https://www.unicef.org/india/stories/2020/04/2020-04-20-covid-19>
13. <https://www.unicef.org/india/stories/2020/04/2020-04-20-covid-19>
14. <https://www.unicef.org/india/stories/2020/04/2020-04-20-covid-19>
15. <https://www.unicef.org/india/stories/2020/04/2020-04-20-covid-19>
16. <https://www.unicef.org/india/stories/2020/04/2020-04-20-covid-19>
17. <https://www.unicef.org/india/stories/2020/04/2020-04-20-covid-19>

Basics of Foam Science – A Brief Review

Article History	
Received:	19. 01.2021
Revision:	31. 01.2021
Accepted:	12.02.2021
Published:	25.02.2021
Author Details	
Tarun Kumar Barik	
Authors Affiliations	
Department of Physics, Achhruram Memorial College, Jhalda, Purulia-723202, West Bengal, India	
Corresponding Author*	
Tarun Kumar Barik	
How to Cite the Article:	
Tarun Kumar Barik (2021). Basics of Foam Science – A Brief Review . <i>IAR J Eng Tech</i> , 2(1), 55 -64.	

Abstract: Wet foam is a very common example of soft matter. In wet foam, molecules are more structured than in liquids but more random than they are in solids. Recently, physics of foam has become a rapidly developing branch in science and engineering. A deeper understanding is crucial for many technological applications of wet foam. Hence, in this article, the basic structure and properties of foam are reviewed based on the literature survey of published research work. Some research works, available in the literature, in which optical probes have been used to study the structure, properties and dynamics of foam. In this article, wet foam is used to study the basic structure and properties of foam for better understanding. Raman Spectroscopy and Diffusing wave Spectroscopy have been used on wet foam to establish its structure and properties are also reported. Finally, in conclusion, recent scientific, technological and commercial applications and future prospects of wet foam are proposed to build impulse on the wet foam science more to enrich our day to day life with the modern concepts of nanofoam technology. Recently, due to rapid increase of nanotechnology, different metallic (Cu, Au, Ni, Pt, Pd etc.) or nonmetallic (C) solvent-assisted nanofoam have modernized the structure, properties of foam science and hence have accelerated its day to day technological applications.

Keywords: Wet foam, Rheology, Coarsening, Liquid drainage, Collapse, Raman Spectroscopy, Diffusing wave spectroscopy, nanofoam.

INTRODUCTION:

Imagine opening a carbonated cold drink bottle or a soda can after shaking it: almost instantaneously, gas bubbles rise and crowd together at the surface of the liquid forming a soft foam. Inside the bottle or can, carbon dioxide is dissolved in liquid at high pressure. Shaking of the container results in the creation of a large number of little bubbles as the agitation unbinds the carbonation from the solution. By opening the container, these gas bubbles rise to the liquid surface to release carbon dioxide into the surrounding air. Similar incident also occurs at the time of washing or shaving with soap. These are the common examples of sort lasting wet foam. The history of foam can be traced from the publication in 1873 titled *Statique Experimentale et Theorique des Liquides soumis aux seules Forces Moleculaires* by the Belgian physicist Joseph Antoine Ferdinand Plateau (Plateau, J.A.F. 1873). This book summarizes the previous history of foam research and also presents author's own work, which laid the foundation for the future studies. Soft foam is a very common example of soft matter (a matter which is neither liquid nor solid, but something in between). In foam, molecules are more structured than in liquids but more random than they are in solids. Foam physics has become a rapidly developing branch in science. This is due to the fact that the physics of foam is, as yet, ill-understood. Further, a deeper understanding is crucial for many technological applications of foam. There are a number of models are available in the literature to simulate the bubble growth in foam in two or three dimensions, its bubble size distribution and most essential properties of foam (Glazier, J. A. Glazier, J. A. *et al.*, 1990; Lim, K. S., & Barigou, M. 2005; Magrabi, S. A. *et al.*, 1999; Monsalve, A., & Schechter, R. S. 1984; Lemlich, R. 1978; Hutzler, S., & Weaire, D. (2000; Ganan-Calvo, A. M *et al.*, 2004; Kabla, A. *et al.*, 2007; Gardiner, B. S. *et al.*, 1999; Gardiner, B. S. *et al.*, 2000; Sun, B. *et al.*, 2015; & Tenneti, S. *et al.*, 2013). There are also a lot of experiments with wet foam in the literature to establish its essential properties (Feitosa, K. *et l* 2006; Saint-Jalmes, A. *et al.*, 2000; Barik, T. K., & Roy, A. 2009; Bandyopadhyay, P. *et al.*, 2008; & Barik, T. K. *et al.*, 2009). Recently, carbon nanofoam is one of the lightest solid materials known today, having a density of ~ 2 mg/cm³. It has an extremely high surface area and is a good electrical insulator. It is fairly transparent, quite brittle and can withstand very high temperature. Highly uniform samples of carbon nanofoam from hydrothermal sucrose carbonization were studied by helium ion microscopy (HIM), X-ray photoelectron spectroscopy (XPS), and Raman spectroscopy (Frese, N. *et al.*, 2016). Facile synthesis of Ni nanofoam using aqueous solutions at room temperature is studied for flexible and low-cost non-enzymatic glucose sensing (Iwu, K. O. *et al.*, 2016). Once more, hierarchical NiCo₂O₄ nanosheets are grown on Ni nanofoam as high-performance electrodes for supercapacitors (GAO, G. *et al.*, 2015). Cu nanofoams are also fabricated using a simple powder-metallurgy method which is useful for potential energy applications (Jo, H. *et al.*, 2014). Bimetallic Pd/Pt nanostructures deposited on Cu nanofoam substrate by galvanic replacement are also fabricated as an effective electrocatalyst for hydrogen evolution reaction (Rezaei, B. *et al.*, 2015). Gold nanofoams were synthesized in the Deep Eutectic Solvent (DES) with no templates, seeds, or additives (Jia, H. *et al.*, 2015). Thus, there are many such foam with different advanced technological applications are reported in recent literature, but this article is focused to study the basic structure and properties of foam.

Basic Structure of foam:

Foam is a two-phase cellular structure either of gas and liquid (liquid foam) or of gas and solid (solid foam). Here, in this article, we shall concentrate only on

liquid foam. Liquid foam consists of a collection of gas bubbles surrounded by thin liquid films. A typical microscope image of wet foam (Gillette shaving foam) is shown in Fig. 1.



Fig. 1: A typical microscope image of Gillette shaving foam.

For better stability, some surface active substances (i.e. surfactants) are used while preparing liquid foam. There are mainly two types of liquid foam depending upon its liquid content (a) *dry foam* has less liquid and consists of thin films between bubbles. These bubbles take the form of polyhedral cells and have a poly-disperse distribution and (b) *wet foam*, which has high liquid content. All bubbles in wet foam are spherical in shape and nearly mono-disperse at the initial state. In a statistical analysis of bubble size distribution using Gillette shaving foam shows coarsening of bubbles and the change in bubble size distribution in wet foam with ageing. It also shows an increase in polydispersity of foam with ageing and the growth of larger bubbles at the cost of the smaller bubbles, during ageing (Barik, T. K., & Roy, A. 2009). In a foamy network, the three liquid films from three nearby bubbles meet to form a scalloped-triangular channel, which is known as Plateau border. Only four Plateau borders meet at a region shared by four neighboring bubbles making equal

angles and this region is known as the vertex. In foam, the Plateau borders and vertices form a continuous network. The law of Plateau defines few rules, which are necessary to obtain an equilibrium configuration of a foamy network. These rules are:

- **Rule 1:** For dry foam, three films of three nearby bubbles intersect at a time with an angle of 120° to each other. In two dimensions, this applies to the lines, which define the cell boundaries.
- **Rule 2:** For dry foam, four bubbles meet and form a symmetric tetrahedral vertex. The angle between the films is called the Maraldi angle.
- **Rule 3:** In wet foam, Plateau border joins the adjacent films by smooth surfaces.
- Typical schematic diagrams of dry and wet foam with the construction of the corresponding Plateau border network are shown in Fig. 2.

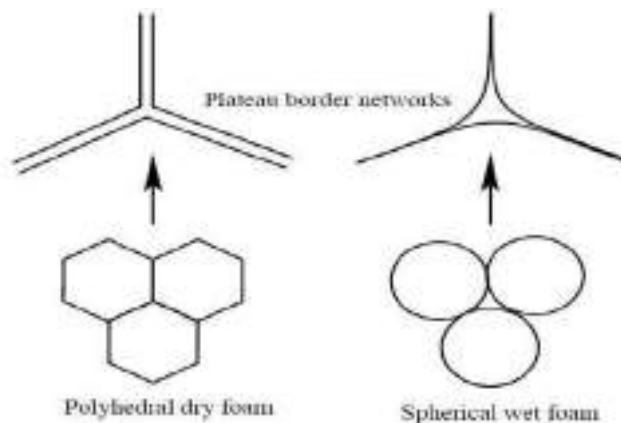


Fig. 2: Schematic representations of dry and wet foam with Plateau border network.

In dry foam, the polyhedral bubbles are with slightly curved edges and faces. Any polyhedron (whose closed surface is topologically equivalent to that of a sphere) in three dimensional space obeys Euler's theorem, $U - E + F = 2$, where, U , E and F are the number of vertices, edges and faces of the polyhedron, respectively. For dry foam bubbles, the polyhedral geometry is further restricted by Plateau's rules. The coordination numbers of Plateau's laws enforce $2E = 3U$ and therefore, $E = 3F - 6$ follows for any foam polyhedron. In other words, for

polyhedra in foam any of the three quantities U , E and F determines the other two. The fascinating properties of foam arise from its topological changes via T1 and T2 processes. While in the T1 process, a fourfold vertex dissociates into a stable threefold vertex (Fig. 3(a)), a three-sided cell may disappear by the T2 process, as shown in Fig. 3(b) [26]. With this introduction to the basic structure of wet foam, its essential properties are discussed in brief below.

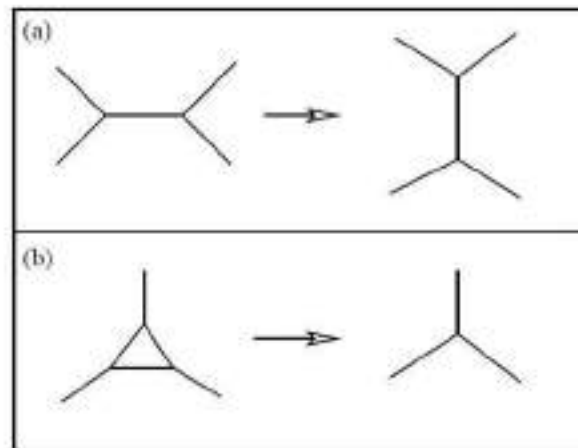


Fig. 3: Schematic representations of topological changes in liquid foam via (a) T1 process and (b) T2 process (Dennin, M., & Knobler, C. M. 1997)

Properties of foam:

To study the properties of foam, we have chosen wet foam for easy understanding. In the following sections of this article, the four most essential properties of foam: (i) Rheology, (ii) Coarsening, (iii) Liquid drainage and (iv) Collapse, are briefly reviewed. A study about the structure and dynamics of wet foam using optical probes are also reported in the following sections.

Rheology:

Foam has unique rheological properties. The mechanical response of liquid foam to an applied force is complex, exhibiting both elastic and viscous character (Kraynik, A. M. 1988). Under low applied shear stress, foam behaves like an elastic solid. However, with an increase in stress it becomes progressively plastic; beyond a certain yield stress, the foam flows along with topological changes. The flow is intermittent and mediated by non-linear rearrangement events in which several neighboring gas bubbles suddenly hop from one tightly packed configuration to another. Such characteristics of foamy structure strongly depend on the bubble size, liquid fraction, viscosity and interfacial tension. The schematic stress-strain relation for the liquid foam is shown in Fig. 4.

Both two and three dimensional foam can be accurately simulated using various models (Weaire, D., & Hutzler, S. 1999). The computer simulation results provide the correlation between the shear modulus and gas/liquid fraction in the tightly packed gas bubbles (Bolton, F., & Weaire, D. 1990; Feng, S. *et al.*, 1985; Hutzler, S. *et al.*, 1995; Princen, H. M., & Kiss, A. D. 1986). For example, the model based on bubble-bubble interaction takes into account the pair-wise quadratic potential energies for connecting bubbles in the low compression limit. The bubble-scale model, proposed by Durian and his co-workers, explains the foam mechanics by solving the equation of motion of the individual disk (two dimensional projection of spheres) and assuming a harmonic potential for interaction between the bubbles (Durian, D. J. 1995; & Durian, D. J. 1997). The effect of liquid flow under low shear has been taken into account by including the viscous term. The model provides a connection between the complex macroscopic rheological behavior of foam and its underlying microscopic structure. Other models are also available in the literature, in which, the various aspects of the stress-strain relation have been dealt with (Glazier, J. A., & Weaire, D. 1992; Weaire, D., & McMurphy, S. 1996; Khan, S. A., & Armstrong, R. C. 1986; Jabarkhyl, S. *et al.*, 2020; Ptaszek, P. 2013).

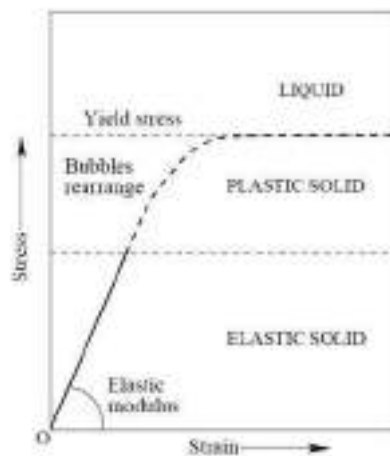


Fig. 4: A schematic diagram of the stress-strain relation for liquid foam.

Coarsening:

Foams are of broad scientific interest for their ability to fill space efficiently with a random packing of bubbles and for the coarsening of this disordered structure with time. Coarsening is the gradual change of

foam structure due to gas diffusion through the films from smaller bubbles to larger bubbles following the well-known Laplace-Young law. This law relates the pressure difference to the mean curvature for a surface in equilibrium. From Laplace-Young law, the

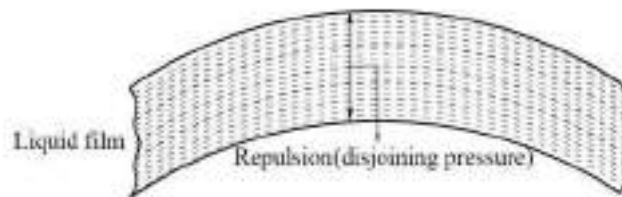


Fig 5: The mutual repulsion (disjoining pressure) between the two surfaces of a thin liquid film.

Balance in pressure difference inside a bubble, ΔP , can be expressed as: $\Delta P = \frac{2\alpha}{r}$; where α is the surface tension of liquid film and r is the mean local radius of curvature of the film surface. r is related to the two principal curvatures r_1 and r_2 as: $\frac{2}{r} = \frac{1}{r_1} + \frac{1}{r_2}$. For wet foam, the bubbles are spherical and hence $r_1 = r_2$. At equilibrium, the Laplace pressure is balanced by the disjoining pressure of the films, which originates from the mutual repulsion between the two surfaces of the thin liquid film (see Fig. 5). In case of wet foam the gas diffusion takes place only through the liquid films not through the Plateau borders (In Ref. [20], see p. 98). The increase in the average bubble size with time can be obtained from the fact that the rate of change of a bubble's volume is proportional to its surface area and to its Laplace pressure difference with respect to a certain mean or critical bubble radius r_c .

Thus,

$$\frac{dr^d}{dt} \propto r^{d-1} \left(\frac{1}{r_c} - \frac{1}{r} \right),$$

for any dimension d . for $d=3$,

$$\frac{dr}{dt} \propto \left(\frac{1}{r_c} - \frac{1}{r} \right).$$

Thus, the large bubbles, $r > r_c$, grow in size, whereas the smaller bubbles $r < r_c$ shrink. If r_a be the average bubble radius, then we have

$$\frac{dr_a}{dt} \propto \frac{1}{r_a},$$

Which implies that $r_a(t) \sim t^{\frac{1}{2}}$. In general, the time-scale of evolution of the average bubble radius can be expressed as:

$$r_a \propto (t - t_0)^{\frac{1}{2}}$$

Where, t_0 is an initial constant. For an infinite foam network the coarsening process has no end. Thus, one can identify the asymptotic scaling behavior of foam with ageing. In 1952, von Neumann demonstrated that the time evolution of bubbles in a two dimensional

foam only depends on the number of its sides, n , rather than on the size or shape of the bubbles (Von Neumann, J. 1952). The rate of change of area, A_n , of the n th bubble is given by the von Neumann's law

$$\frac{dA_n}{dt} = \frac{2\pi}{3} \alpha k(n - 6),$$

where, α and k are the permeability constant and surface tension for the liquid films. The significance of the above equation for $n = 6$, is that the area of the hexagonal bubbles remain constant until they encounter a topological change. A number of models are available

in the literature to simulate the bubble growth in foam in two or three dimensions (Bolton, F., & Weaire, D. 1990; Glazier, J. A., & Weaire, D. 1992; Patzek, T. W. 1993; Avron, J. E., & Levine, D. 1992; & Feitosa, K. *et al.*, 2006).

Liquid drainage:

The liquid between the bubbles can drain out in response to gravity or due to adjacent film rupture to settle into a equilibrium profile. This phenomenon is known as drainage. For fairly dry foams, the liquid is distributed in (a) the flat films that separate two neighboring bubbles, (b) the long Plateau borders and (c) the scalloped-tetrahedral vertices (Bikerman, J. J. 1973; Prud'homme, R. K., & Khan, S. A. 1996; & Weaire, D. *et al.*, 1997). During drainage, the flow of liquid out of foam is assumed to be confined to the network of Plateau borders and/or vertices and it slows down as equilibrium is approached. Due to the density mismatch between gas and liquid, the bubbles rise and collect at the top and the liquid accumulates at the bottom. The liquid also flows because of the capillary effect, which is related to the gradient of liquid fraction in a column of foam. Such a gradient of liquid fraction implies an existence of a pressure gradient in the liquid foam. Thus, a capillary flow is induced by bringing liquid from high liquid fraction regions to regions with low liquid fraction. Liquid drainage in a column of wet foam has been modeled by non-linear partial differential drainage equation, which expresses liquid conservation as it flows in response to gravity, capillarity and viscous forces (Weaire, D. *et al.*, 1997; Bhakta, A., & Ruckenstein, E. 1997; & Koehler, S. A. *et al.*, 1998). However, the analytical solutions of the nonlinear equation can only be obtained by ignoring the capillary term. Durian *et al.*, designed an experiment, minimizing the capillary effect during drainage, to verify the drainage equation (Saint-Jalmes, A. *et al.*, 2000). A generalized drainage equation for arbitrary shape of the container is also available in Ref. (Saint-Jalmes, A. *et al.*, 2000). The complex draining action in a wet foam prompted many experiments in which the drained liquid has been measured as a function of time.

In the experiments based on 'forced drainage', a constant input of external liquid at the top of the foam column maintains a constant flow of liquid throughout the foam. On the other hand, for 'free drainage' experiments, no external liquid is added on the top of foam surface. Free drainage is the unavoidable fate of aqueous foams under earth's gravity (Bikerman, J. J. 1973; & Prud'homme, R. K., & Khan, S. A. 1996). Drainage of liquid in wet foam has been studied using various optical techniques, like absorption or transmission measurements. A detailed review is available in (Saint-Jalmes, A. 2006). Free drainage with slow as well as fast coarsening of gas is a coupled phenomenon in wet foam (Saint-Jalmes, A. 2006; & Patzek, T. W. 1993). In spite of a thorough endeavor to understand the free drainage process in wet foam, the problem is still not well understood (Saint-Jalmes, A. *et al.*, 1999).

Collapse:

Usually, most liquid foams do not last for long, as the bubbles collapse by the rupture of the exposed liquid films. Many factors like liquid drainage, coarsening, evaporation, impurities and additives are responsible for foam collapse. The study of foam collapse has a great practical importance because it deals with the stability of the film. Topological change in foam structure due to the bubble growth by film rupturing is less studied in the literature and remains very poorly understood. A crucial feature of liquid foam is that it irreversibly evolves with time. The spherical bubbles in fresh foam take the form of polyhedra while minimizing the energy of the system. The evolution of the bubbles in foam with time can be described by the above four mutually coupled mechanisms.

Measurement of properties of wet foam with light:

Structure and properties of foam have been probed extensively using various optical techniques. Here we mention some of the earlier works, where light has been used to measure the size, wetness, movement of bubbles and other properties of foam. Diffusing wave spectroscopy (DWS) is the most commonly used optical tool to study the behavior of foam (Miri, M. F., & Stark, H. 2004; Gittings, A. S., & Durian, D. J. 2006; Gopal, A. D., & Durian, D. J. 1999; & Höhler, R. *et al.*, 2003). This technique is an extension of Dynamic light scattering technique for a strongly scattered medium, where the propagation of light is described by the diffusion approximation (Weitz, D. A. *et al.*, 1993). The autocorrelation function of the multiple scattering of light is calculated by dividing the photons into separate diffusive paths. The distribution of these paths and the

probability that the photon will follow a path of a given length is determined through the diffusion equation of light. The total correlation function is then determined by summing the contributions from all possible paths with weighted probabilities, assuming that each path is uncorrelated with the other path. The fluctuations of the transmitted scattered light result from the variation in total optical path length. The decay of the temporal autocorrelation function of the intensity of the scattered light, which reflects the temporal evolution of the path length, provides the dynamics of the medium. DWS has been extensively used to study bubble size and liquid fraction in wet foam. Using this technique the static transmission coefficient (T) of light through foam of a given thickness has been measured. Diffusion of light is characterized by the transport mean free path, l^* , of the transmitted light. It has been shown that

$$T \approx \frac{5l^*}{3L}$$

(considering the large thickness of the foam, L , and no absorption of light by foam). Using this relation, average bubble diameter d_a can be estimated from the relation $l^* = (3.5 \pm 0.5)d_a$ (Saint-Jalmes, A. *et al.*, 1999). The scaling behavior of the bubble growth, discussed in the above section-3, has been verified experimentally with the average bubble diameter growing in time as \bar{r}^z , with $z = 0.45 \pm 0.05$ (Durian, D. J. *et al.*, 1991). It is reported that the changes in the packing conditions during the coarsening process give rise to a dynamical process that also exhibits temporal scaling. In Ref. (Vera, M. U. *et al.*, 2001), Vera *et al.*, used the multiple scattering of light by aqueous foam to study the coupling between drainage and coarsening mechanisms. Other than confirming the fact that the transport mean free path is proportional to the bubble diameter, authors have shown that the liquid fraction in foam is proportional to $\frac{1}{l^*}$. Furthermore, DWS is a potential tool to study the viscoelastic behavior of foam (Mason, T. G. *et al.*, 1997). The technique has also been applied to model foam subjected to shear stress. The observed data reflect the local rearrangement events in the foam (Earnshaw, J. C., & Wilson, M. 1995). Along DWS, various other optical techniques have been used to study the behavior of wet foam. The change in the degree of depolarization of a collimated, polarized incident light on non-absorbing foams has been studied by Wong *et al.*, (2002). It is observed that the denser media (with a large number of bubbles) tend to depolarize the incident beam more. The degree of depolarization can be correlated to the bubble size distribution in wet foam. Durian and his coworkers used the photon channelling experiments to study the absorptivity and liquid fraction in foams (Gittings, A. S. *et al.*, 2004). The authors added a dye to the continuous liquid phase for the absorption of diffuse photons in the

aqueous foams and studied the absorption mechanisms under different experimental conditions.

Study Wet foam by Raman scattering:

In this thesis, we have studied the properties of the soft Gillette shaving foam, using an optical spectroscopic technique, based on Raman scattering. Raman spectroscopy is a powerful noninvasive tool to probe the structure and dynamics of a system at the molecular level. Our aim is to investigate, if this technique can be used to study the effect of ageing on molecular structure and to characterize the stability of wet foam. In addition, Raman scattering is caused by deformation/stretching of different vibrational bonds of molecules. Thus, if macroscopic and microscopic properties in foam are related, one expects that the analysis of Raman line profiles can be used to probe the elastic properties of wet foam, indirectly, by studying its molecular behavior. The main hindrance in using Raman spectroscopy to probe wet foam arises due to multiple scattering of light within the bubbles, which masks the Raman signal from the foamy structure, to a large extent. The signal to noise ratio in the spectrum is always poor in this case. Thus, in the literature, we do not find too many articles on Raman studies of wet foam. The most significant one is by Goutev and Nickolov (1996), where the authors have studied the microstructure of stable three-dimensional foam on the basis of its molecular behavior. Based on Raman measurements of foam, authors have shown that (a) two distinct phases can exist in wet foam|a lamellar phase (with an ordered multilayer structure of surfactant molecules) and an isotropic phase, (b) in fresh foam small bilayer lamellae are dispersed in foam films and with ageing they self-organize around the bubble in large shell-like bilayer structures. It is to be noted that the quantitative estimates of the structure and properties

of liquid foam depend on the liquid fraction and the chemical constituents. However, the generic features are expected to remain same for all. Since, the other groups have worked on various aspects of foam using Gillette shaving foam as their sample (Durian, D. J. *et al.*, 1991a; Durian, D. J. *et al.*, 1991b; Earnshaw, J. C., & Jaafar, A. H. (1994; Goutev, N., & Nickolov, Z. S. 1996), it is preferable to use the same material for further investigation while using a new experimental technique. Therefore, we have chosen the Gillette foam in our work. The basic ingredients of Gillette shaving foam are triethanolamine stearate with small amount (< 1%) of sodium lauryl sulphate, polyethylene glycol lauryl ether and emulsified liquid hydrocarbon gases. These ingredients are kept in an aqueous solution under high pressure. The foam is produced after expansion of the above mixture in air. It is reproducible and stable over the duration required for an optical measurement. For Raman measurements this commercial foam offers an extra advantage|when laser light is incident on foam it undergoes multiple scattering. In order to obtain the optimum Raman signal, the mean free path, l^* , [$\cong 3.5 \times$ average diameter of the bubbles (d_a)] of light within the foam should be comparable with the slit-width of the spectrometer collecting the scattered light (Nieto, M. I. *et al.*, 2014). The mean diameter of bubbles in fresh Gillette shaving foam is close to $30 \mu\text{m}$ and the maximum diameter, which we have studied, is $\approx 350 \mu\text{m}$ |comparable with the slit-width of our spectrometer ($\cong 100 \mu\text{m}$) in order of magnitude. Below we discuss the basic principle of Raman scattering and also the instrument used by us for the Raman measurements. Different recent researches on wet foam have explained the gross properties of wet foam in light of its characteristic molecular structure using Raman spectroscopy. They have related the observed shift in the low frequency Raman peak position of the methylene rocking mode with the variation in internal stress in the system. The analysis of Raman data over the range between 1000 cm^{-1} and 1450 cm^{-1} indicates the gradual structural change of wet foam from all-trans conformation to crystalline structure with ageing (Kraynik, A. M. 1988). Drainage of water from wet foam is discussed and in addition to free water molecules, which drain out with ageing of foam, water clusters of only a few water molecules are also present in foam. It is also shown that the correlation between the internal stress and the characteristics of a vibrational mode in wet foam. Thus the capability of the Raman spectroscopy to reveal the crystallinity in foamy materials is established (Bandyopadhyay, P. *et al.*, 2008; & Barik, T. K. *et al.*, 2009).

In conclusion, the basic structure and properties of wet foam are reviewed in the light of present scientific literature to reveal interesting essential properties of wet foam. The optical probes (specially, Raman spectroscopy and Diffusing wave spectroscopy) used to study the wet foam are also briefly discussed. There are huge applications of solid foam compared to wet foam reported in the literature. Similarly, recent researches suggest that wet foam has also the huge possibilities in different technological applications like fire extinguishing, food processing, commercial chemicals and cosmetics, agricultural fields, biomedical fields, environmental safety and toy-making industries etc. (Nieto, M. I. *et al.*, 2014; Takahashi, M. *et al.*, 2009; & Subagyono, D. J. *et al.*, 2011). Recently, the higher density foams like carbon nanofoam, however, show an advanced graphitization degree and a stronger sp^3 -type electronic contribution, related to the inclusion of sp^3 connections in their surface network (Frese, N. *et al.*, 2016). Again, by employing Ni nanofoam flexible and highly sensitive glucose sensors have been produced on a plastic substrate with excellent performances (Iwu, K. O. *et al.*, 2016). A high-performance electrode for supercapacitors is also designed and synthesized by growing electroactive NiCo_2O_4 nanosheets on conductive Ni nanofoam (Gao, G. *et al.*, 2015). Again, Cu nanofoams are also very much useful for potential energy application (Jo, H. *et al.*, 2014). The gold nanofoams with no capping agents have more catalyst active sites and excellent catalytic efficiency (Jia, H. *et al.*, 2015). The main objective of this article is to review the structure and properties of foam to attract more research attention towards foam technology and develop this field for more scientific, technological and commercial applications for our day to day life. Diffusing wave spectroscopy and Raman spectroscopy are quick and noninvasive tool to measure the strain and hence, the stability of a wet foam (Bandyopadhyay, P. *et al.*, 2018; & Barik, T. K. *et al.*, 2009) and hence, these spectroscopic techniques can act as optical probe to study the properties of foam. Some papers use Gillette shaving foam to study wet foam characteristics. But, the composition of commercial shaving foams (like Gillette foam) is quite complex and its physicochemical properties are ill defined; it is worth to study the wet foam using simple foamy materials with well controlled composition, specially made in a laboratory. Further experiments on known surfactants will also indicate if the observed behavior of the wet foam originates from the characteristics of the surfactant itself or from its foamy structure (Jabarkhyl, S. *et al.*, 2020; de Moraes, E. G., & Colombo, P. 2014; & Zhao, J. *et al.*, 2018). Furthermore, using the experimental method stated in (Bandyopadhyay, P. *et al.*, 2018) at different heights of the column of foam, one can experimentally study the coupling between coarsening and drainage of liquid in wet foam.

CONCLUSION:

Acknowledgement:

The author wishes to acknowledge Prof. Anusree Roy, Department of Physics and Meteorology, Indian Institute of Technology, Kharagpur, India for her helpful discussions and guidance.

REFERENCES:

- Avron, J. E., & Levine, D. (1992). Geometry and foams: 2D dynamics and 3D statics. *Physical review letters*, 69(1), 208.
- Bandyopadhyay, P., Ojha, A. K., Barik, T. K., & Roy, A. (2008). Drainage and water clusters in Gillette foam. *Journal of Raman Spectroscopy: An International Journal for Original Work in all Aspects of Raman Spectroscopy, Including Higher Order Processes, and also Brillouin and Rayleigh Scattering*, 39(7), 827-831.
- Barik, T. K., & Roy, A. (2009). Statistical distribution of bubble size in wet foam. *Chemical engineering science*, 64(9), 2039-2043.
- Barik, T. K., Bandyopadhyay, P., & Roy, A. (2009). Probing Internal Stress and Crystallinity in Wet Foam via Raman Spectroscopy. *International Journal of Modern Physics B*, 23(19), 3913-3924.
- Bhakta, A., & Ruckenstein, E. (1997). Decay of standing foams: drainage, coalescence and collapse. *Advances in Colloid and Interface Science*, 70, 1-124.
- Bikerman, J. J. (1973). *Foams*, (Springer-Verlag, New York, 1973).
- Bolton, F., & Weaire, D. (1990). Rigidity loss transition in a disordered 2D froth. *Physical review letters*, 65(27), 3449.
- de Moraes, E. G., & Colombo, P. (2014). Silicon nitride foams from emulsions. *Materials Letters*, 128, 128-131.
- Dennin, M., & Knobler, C. M. (1997). Experimental studies of bubble dynamics in a slowly driven monolayer foam. *Physical review letters*, 78(12), 2485.
- Durian, D. J. (1995). Foam mechanics at the bubble scale. *Physical review letters*, 75(26), 4780.
- Durian, D. J. (1997). Bubble-scale model of foam mechanics: mMelting, nonlinear behavior, and avalanches. *Physical Review E*, 55(2), 1739.
- Durian, D. J., Weitz, D. A., & Pine, D. J. (1991a). Multiple light-scattering probes of foam structure and dynamics. *Science*, 252(5006), 686-688.
- Durian, D. J., Weitz, D. A., & Pine, D. J. (1991b). Scaling behavior in shaving cream. *Physical Review A*, 44(12), R7902.
- Earnshaw, J. C., & Jaafar, A. H. (1994). Diffusing-wave spectroscopy of a flowing foam. *Physical Review E*, 49(6), 5408.
- Earnshaw, J. C., & Wilson, M. (1995). Strain-induced dynamics of flowing foam: an experimental study. *Journal of Physics: Condensed Matter*, 7(5), L49.
- Feitosa, K., Halt, O. L., Kamien, R. D., & Durian, D. J. (2006). Bubble kinetics in a steady-state column of aqueous foam. *EPL (Europhysics Letters)*, 76(4), 683.
- Feitosa, K., Halt, O. L., Kamien, R. D., & Durian, D. J. (2006). Bubble kinetics in a steady-state column of aqueous foam. *EPL (Europhysics Letters)*, 76(4), 683.
- Feng, S., Thorpe, M. F., & Garboczi, E. (1985). Effective-medium theory of percolation on central-force elastic networks. *Physical Review B*, 31(1), 276.
- Frese, N., Mitchell, S. T., Neumann, C., Bowers, A., Götzhäuser, A., & Sattler, K. (2016). Fundamental properties of high-quality carbon nanofoam: from low to high density. *Beilstein journal of nanotechnology*, 7(1), 2065-2073.
- Ganan-Calvo, A. M., Fernandez, J. M., Marquez Oliver, A., & Marquez, M. (2004). Coarsening of monodisperse wet microfoams. *Applied physics letters*, 84(24), 4989-4991.
- Gao, G., Wu, H. B., Ding, S., Liu, L. M., & Lou, X. W. (2015). Hierarchical NiCo₂O₄ nanosheets grown on Ni nanofoam as high-performance electrodes for supercapacitors. *Small*, 11(7), 804-808.
- Gardiner, B. S., Dlugogorski, B. Z., & Jameson, G. J. (1999). The evolution of defects in a two-dimensional wet foam. *Journal of Physics: Condensed Matter*, 11(28), 5437.
- Gardiner, B. S., Dlugogorski, B. Z., & Jameson, G. J. (2000). The steady shear of three-dimensional wet polydisperse foams. *Journal of non-newtonian fluid mechanics*, 92(2-3), 151-166.
- Gittings, A. S., & Durian, D. J. (2006). Gaussian and non-Gaussian speckle fluctuations in the diffusing-wave spectroscopy signal of a coarsening foam. *Applied optics*, 45(10), 2199-2204.
- Gittings, A. S., Bandyopadhyay, R., & Durian, D. J. (2004). Photon channelling in foams. *EPL (Europhysics Letters)*, 65(3), 414.
- Glazier, J. A., & Weaire, D. (1992). The kinetics of cellular patterns. *Journal of Physics: Condensed Matter*, 4(8), 1867.
- Glazier, J. A., Anderson, M. P., & Grest, G. S. (1990). Coarsening in the two-dimensional soap froth and the large-Q Potts model: a detailed comparison. *Philosophical Magazine B*, 62(6), 615-645.
- Gopal, A. D., & Durian, D. J. (1999). Shear-induced "melting" of an aqueous foam. *Journal of Colloid and Interface Science*, 213(1), 169-178.
- Goutev, N., & Nickolov, Z. S. (1996). Raman studies of three-dimensional foam. *Physical Review E*, 54(2), 1725.

30. Hilgenfeldt, S., Koehler, S. A., & Stone, H. A. (2001). Dynamics of coarsening foams: accelerated and self-limiting drainage. *Physical review letters*, 86(20), 4704.
31. Höhler, R., Labiausse, V., & Cohen-Addad, S. (2003). High-resolution diffusing-wave spectroscopy using optimized heterodyne detection. *JOSA A*, 20(11), 2179-2184.
32. Hutzler, S., & Weaire, D. (2000). Foam coarsening under forced drainage. *Philosophical magazine letters*, 80(6), 419-425.
33. Hutzler, S., Weaire, D., & Bolton, F. (1995). The effects of Plateau borders in the two-dimensional soap froth III. Further results. *Philosophical Magazine B*, 71(3), 277-289.
34. In Ref. [20], see p. 98.
35. Iwu, K. O., Lombardo, A., Sanz, R., Scirè, S., & Mirabella, S. (2016). *Sens Actuators B*. 224, 764–771.
36. Jabarkhyl, S., Barigou, M., Badve, M., & Zhu, S. (2020). Rheological properties of wet foams generated from viscous pseudoplastic fluids. *Innovative Food Science & Emerging Technologies*, 64, 102304.
37. Jia, H., An, J., Guo, X., Su, C., Zhang, L., Zhou, H., & Xie, C. (2015). Deep eutectic solvent-assisted growth of gold nanofoams and their excellent catalytic properties. *Journal of Molecular Liquids*, 212, 763-766.
38. Jo, H., Cho, Y. H., Choi, M., Cho, J., Um, J. H., Sung, Y. E., & Choe, H. (2014). Novel method of powder-based processing of copper nanofoams for their potential use in energy applications. *Materials Chemistry and Physics*, 145(1-2), 6-11.
39. Kabla, A., Scheibert, J., & Debregeas, G. (2007). Quasi-static rheology of foams. part 2. continuous shear flow. *Journal of Fluid Mechanics*, 587, 45-72.
40. Khan, S. A., & Armstrong, R. C. (1986). Rheology of foams: I. Theory for dry foams. *Journal of non-newtonian fluid mechanics*, 22(1), 1-22.
41. Koehler, S. A., Stone, H. A., Brenner, M. P., & Eggers, J. (1998). Dynamics of foam drainage. *Physical Review E*, 58(2), 2097.
42. Kraynik, A. M. (1988). Foam flows. *Annual Review of Fluid Mechanics*, 20(1), 325-357.
43. Lemlich, R. (1978). Prediction of changes in bubble size distribution due to interbubble gas diffusion in foam. *Industrial & Engineering Chemistry Fundamentals*, 17(2), 89-93.
44. Lim, K. S., & Barigou, M. (2005). Pneumatic foam generation in the presence of a high-intensity ultrasound field. *Ultrasonics sonochemistry*, 12(5), 385-393.
45. Magrabi, S. A., Dlugogorski, B. Z., & Jameson, G. J. (1999). Bubble size distribution and coarsening of aqueous foams. *Chemical engineering science*, 54(18), 4007-4022.
46. Mason, T. G., Gang, H., & Weitz, D. A. (1997). Diffusing-wave-spectroscopy measurements of viscoelasticity of complex fluids. *JOSA A*, 14(1), 139-149.
47. McDaniel, J. G., Akhatov, I., & Holt, R. G. (2002). Inviscid dynamics of a wet foam drop with monodisperse bubble size distribution. *Physics of Fluids*, 14(6), 1886-1894.
48. Miri, M. F., & Stark, H. (2004). The role of liquid films for light transport in dry foams. *EPL (Europhysics Letters)*, 65(4), 567.
49. Monsalve, A., & Schechter, R. S. (1984). The stability of foams: Dependence of observation on the bubble size distribution. *Journal of colloid and interface science*, 97(2), 327-335.
50. Nieto, M. I., Santacruz, I., & Moreno, R. (2014). Shaping of dense advanced ceramics and coatings by gelation of polysaccharides. *Advanced Engineering Materials*, 16(6), 637-654.
51. Patzek, T. W. (1993). Self-similar collapse of stationary bulk foams. *AIChE journal*, 39(10), 1697-1707.
52. Plateau, J.A.F. (1873). *Statique Experimentale et Theorique des Liquides soumis aux seules Forces Moleculaires*, (Gauthier-villars, Paris, 1873), 2 vols.
53. Princen, H. M., & Kiss, A. D. (1986). Rheology of foams and highly concentrated emulsions: III. Static shear modulus. *Journal of colloid and interface science*, 112(2), 427-437.
54. Prud'homme, R. K., & Khan, S. A. (1996). *Experimental results on foam rheology* (p. 217). Marcel Dekker, New York.
55. Ptaszek, P. (2013). The non-linear rheological properties of fresh wet foams based on egg white proteins and selected hydrocolloids. *Food research international*, 54(1), 478-486.
56. Rezaei, B., Mokhtarianpour, M., & Ensafi, A. A. (2015). Fabricated of bimetallic Pd/Pt nanostructure deposited on copper nanofoam substrate by galvanic replacement as an effective electrocatalyst for hydrogen evolution reaction. *International Journal of Hydrogen Energy*, 40(21), 6754-6762.
57. Saint-Jalmes, A. (2006). Physical chemistry in foam drainage and coarsening. *Soft Matter*, 2(10), 836-849.
58. Saint-Jalmes, A., Vera, M. U., & Durian, D. J. (1999). Uniform foam production by turbulent mixing: new results on free drainage vs. liquid content. *The European Physical Journal B-Condensed Matter and Complex Systems*, 12(1), 67-73.

59. Saint-Jalmes, A., Vera, M. U., & Durian, D. J. (2000). Free drainage of aqueous foams: container shape effects on capillarity and vertical gradients. *EPL (Europhysics Letters)*, 50(5), 695.
60. Saint-Jalmes, A., Vera, M. U., & Durian, D. J. (2000). Free drainage of aqueous foams: container shape effects on capillarity and vertical gradients. *EPL (Europhysics Letters)*, 50(5), 695.
61. Subagyono, D. J., Liang, Z., Knowles, G. P., Webley, P. A., & Chaffee, A. L. (2011). PEI modified mesocellular siliceous foam: A novel sorbent for CO₂. *Energy Procedia*, 4, 839-843.
62. Sun, B., Tenneti, S., & Subramaniam, S. (2015). Modeling average gas–solid heat transfer using particle-resolved direct numerical simulation. *International Journal of Heat and Mass Transfer*, 86, 898-913.
63. Takahashi, M., Menchavez, R. L., Fuji, M., & Takegami, H. (2009). Opportunities of porous ceramics fabricated by gelcasting in mitigating environmental issues. *Journal of the European Ceramic Society*, 29(5), 823-828.
64. Tenneti, S., Sun, B., Garg, R., & Subramaniam, S. (2013). Role of fluid heating in dense gas–solid flow as revealed by particle-resolved direct numerical simulation. *International Journal of Heat and Mass Transfer*, 58(1-2), 471-479.
65. Vera, M. U., Saint-Jalmes, A., & Durian, D. J. (2001). Scattering optics of foam. *Applied optics*, 40(24), 4210-4214.
66. Von Neumann, J. (1952). *Metal Interfaces*, (Am. Soc. for Metals, Cleveland, 1952), p. 108.
67. Weaire, D., & Hutzler, S. (1999). *The Physics of Foams*, (Oxford University Press, Oxford, 1999), pp. 215-217.
68. Weaire, D., & McMurry, S. (1996). Some fundamentals of grain growth, in *Solid State Physics: Advances in Research and Applications*, H. Ehrenreich and F. Spaepen (Editors) (Academic Press, Boston, 1997), Vol. 50.
69. Weaire, D., Hutzler, S., Verbist, G., & Peters, E. A. J. F. (1997). A review of foam drainage. *Advances in chemical Physics*, 102, 315-374.
70. Weitz, D. A., Zhu, J. X., Durian, D. J., Gang, H., & Pine, D. J. (1993). Diffusing-wave spectroscopy: The technique and some applications. *Physica Scripta*, 1993(T49B), 610.
71. Wong, B. T., & Mengüç, M. P. (2002). Depolarization of radiation by non-absorbing foams. *Journal of Quantitative Spectroscopy and Radiative Transfer*, 73(2-5), 273-284.
72. Zhao, J., Yang, C., Shimai, S., Guan, X., Zhou, G., Zhang, J., ... & Wang, S. (2018). The effect of wet foam stability on the microstructure and strength of porous ceramics. *Ceramics International*, 44(1), 269-274.



Short Communication

Dual macrocyclic chemical input based highly protective molecular keypad lock using fluorescence in solution phase: A new type approach

Monaj Karar^a, Provakar Paul^a, Rajib Mistri^b, Tapas Majumdar^{a,*}, Arabinda Mallick^{c,*}^a Department of Chemistry, University of Kalyani, Nadia, West Bengal 741235, India^b Department of Chemistry, Achharam Memorial College, Purulia, West Bengal 723202, India^c Department of Chemistry, Kazi Nazrul University, Asansol, West Bengal 713340, India

ARTICLE INFO

Article history:

Received 12 January 2021

Received in revised form 11 February 2021

Accepted 13 February 2021

Available online 20 February 2021

Keywords:

Chemical input

Fluorescence

Keypad lock

Opto-chemical password

ABSTRACT

Generally, the non-bonding interactions provide the stability to the host-guest complexes without affecting the molecular identity of macrocyclic host and guest (probe) molecules. As a result, macrocyclic-based systems are far more deserving candidates over the ionic systems, as the chance of chemical bleaching is suitably dodged due to the weaker non-bonding interaction. The present article intends to highlight an unconventional and completely innovative designing strategy to validate the operation of a highly protective opto-chemical keypad lock driven by the macrocyclics. Herein, we have utilized the reversible photoswitching phenomenon between two prototropic forms (cationic and neutral) of Harmine (HM) regulated by the dual macrocyclic components, CTAB and β -CD. Most interestingly, methodology provides the choice of the selection of emission detector one at a time between two available emission channels (416 and 365 nm), which have been considered as the "optical inputs". Substantial emission intensities of the probe at the respective emission channels have been treated as the "optical outputs". On the basis of a cautious literature survey, we anticipate that, this kind of designing for a highly protective opto-chemical security device driven by the macrocyclic "chemical inputs" has never explored yet.

© 2021 Elsevier B.V. All rights reserved.

1. Introduction

As representative of superior alternative of the silicon based modern computing technology, numerous molecular interactions with versatile analytes based smart molecular systems having potential to execute binary logic operations are attracting special attentions in recent times [1–7]. Several researchers developed and utilized various small molecular systems as the multipurpose building blocks for multidimensional digital applications like data storage [8–10] and data processing [11–14], switches [15,16], wires [17,18], and molecular machines [19–22]. One of the premium applications of molecular logic circuits is its implementation for the designing of password protected molecular security devices and specifically molecular keypad locks [23,24].

Information protections at the molecular level assisted by extremely secure keypad locks are capable to create and process strong passwords for separate end-users. Currently used security devices utilize silicon-based electronic circuits that need the input of password 'keys' manually for protection of data against illegal information invasion. Limited numbers of keys/digits reduce the level of security of the current

security gadgets. Compared to current silicon-based password systems that use limited alphabets (A-Z), characters (@,%,# etc.) and numbers (0-9) as input keys, opto-chemical molecular security devices were expected to be more secure as they needed to be operated through optical parameters and chemicals as input keys. These newer opto-chemical security systems are evolving as next-generation security gadgets, as hackers require the exact information of the chemical component (s) used in a particular device along with exact optical parameter(s). Endless optical and chemical options and countless possibilities of their combinations make opto-chemical security systems extremely complex and almost impossible to crack, over the conventional silicon-based password circuitry.

Counteracting the social stipulation, scientists engaged themselves with enormous efforts to design keypad locks at the molecular level based on the photo-physical responses [23–26]. These keypad locks are generally constructed based on different optical responses received from the interactions of probe molecules with ions/molecules. In this context, we note that among large number of available molecular keypad lock reports, the use of macrocyclic component/s in molecular logic arena are feeble [27–31]. To the best of our knowledge concern, only one report [30] of chemical security device based on macrocyclics as the chemical inputs is available till date.

Previously, we have studied and reported the structural switching of the cationic and neutral forms of Harmine, HM (Scheme 1) in presence

* Corresponding authors.

E-mail addresses: tapasmju@gmail.com (T. Majumdar), ampcju@yahoo.co.in (A. Mallick).

of CTAB and β -CD in water medium [32,33]. Our current investigation utilizes the same probe (HM) for the construction of molecular keypad lock by using the fluorescence responses upon interaction between macrocyclic components with HM, individually and sequentially. Forward and reverse structural switching of HM upon sequential interactions with CTAB followed by β -CD (macrocyclic 'inputs') resulted in changes of the associated fluorescence intensities at 365 nm & 416 nm (optical 'outputs'). Among many possibilities, a different set of input-output combinations have compiled to produce different sets of passwords. Interaction of macrocyclics with the probe molecule is assumed non-covalent [34–36]. In comparison to the previously reported macrocyclic based keypad lock [30], we propose our lock system seems to be more superior, appealing, and more realistic since it can generate, process, and authenticate a series of passwords accessible for different end-users.

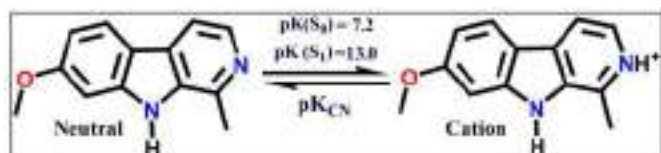
2. Materials and methods

HM and β -CD were procured from Aldrich (Missouri, USA) and used as received. Surfactant, CTAB was procured from Lancaster (England) and used as received. HPLC grade water was used throughout the experiments. Steady-state fluorescence experiments were carried out on Hitachi F-7000 spectrofluorometer (Tokyo, Japan) keeping the slit ratio 1 (Ex. slit = 5 nm, Em. slit = 5 nm) and PMT voltage at 500V. For all fluorescence measurements, a cuvette of 10 mm width was utilised. Concentration of stock HM was 0.335 mM. Pre-weighted β -CDs were gradually added into the cuvette owing to its very low solubility in water, and sonicated for plenty times to obtain thermally equilibrated homogeneous solutions. All other fluorescence measurements were also carried out after proper thermal equilibration of the resultant solution in quartz cuvette through suitably stirred on a magnetic stirrer. Throughout the experiments, temperature was kept constant at 300 K.

3. Results and discussion

It is well established in our previous report that addition of macrocyclic components in a proper chronology leads to switching between the cationic and neutral forms of HM in water medium [33]. In lieu of further detailing, to design the molecular keypad lock, in this present report we have only considered the typical emission spectral changes of HM after the sequential interactions with CTAB and β -CD. In water medium, with λ_{exc} of 300 nm, pure HM exhibited a sharp single emission band at 416 nm, accounted well for its cationic form [37]. With gradual increase of macrocyclic CTAB micelles concentrations, drastic changes in the emission properties of HM were observed. Initial intensity of the existing 416 nm cationic band significantly decreased with simultaneous appearance of a new blue-shifted band close to 365 nm, through a discrete isoemissive point. As per the existing literature, this 365 nm band is well elucidated for the neutral form of HM [36]. Interestingly, with further addition of another macrocyclic component, β -CD within the micelle bound HM, the initial cationic band at 416 nm was almost restored with the outlay of neutral band at 365 nm i.e., almost reverse switching of spectral response was observed (Fig. 1).

In this report, our proposed opto-chemical lock operates through manual entry of a five-digit password and its successive authentication



Scheme 1. Molecular structure of HM with indicated neutral and cationic forms.

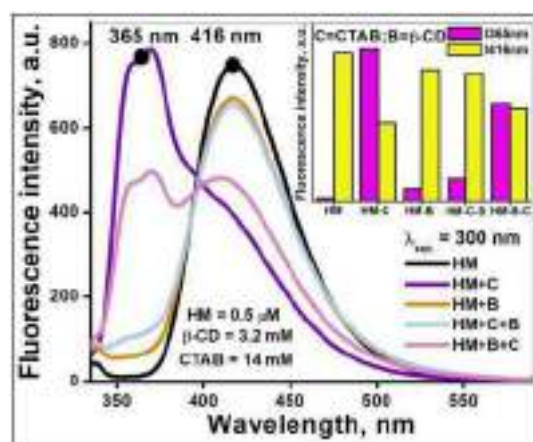


Fig. 1. Fluorescence spectral responses of HM in water upon interactions with CTAB and β -CD sequentially; [HM] = 0.5 μ M; [CTAB] = 14 mM; [β -CD] = 3.2 mM; λ_{exc} = 300 nm; temp. = 300 K.

by the system i.e., the end-user needs to press exactly five input keys in correct sequence for successful password authentication. To construct and track the primary operational trajectory of a functional password, the most important directive is one needs to press 'D4 or D3' key initially, and after each successive entry of chemical inputs, 'C or B', on the system (Fig. 2). Therefore, according to the assigned trajectory of this opto-chemical security device, a general format of the opto-chemical password must follow the sequence as 'D4 or D3' at first, then 'C or B', again 'D4 or D3' key, again 'B or C' and finally 'D4 or D3' again to complete and generate a unique optical pattern as the output response. After each pressing of the optical input key, excitation light (λ_{exc} = 300 nm) must remain "ON" for a pre-fixed time. Within this time-window, corresponding emission must be recorded at the step-correlated detector. Finally, corresponding to that emission intensity, a bar would be generated at the recorder. Ultimately, after completion of a 5-digit password entry, following the proper password trajectory (Fig. 2), a bar pattern would be generated at the recorder.

The back-to-back entry of similar kinds of input keys i.e. optical (D3/D4) or chemical (C/B) during the course of a password entry led to the violation of the preset trajectory pattern embedded within the system. For example, if the end-user does not follow the password format and presses D4/D3 key immediately after entering D3 key or C/B key after entering B key. It would ultimately lead to an erroneous opto-chemical trajectory that will mismatch with the preset password

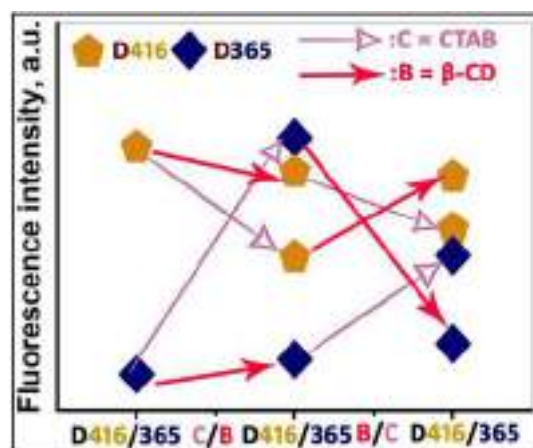


Fig. 2. Password trajectory of the HM system with some specific sequence of password entry. Some typical password recognition patterns have been displayed herein.

trajectory stored within the system. At those situations, the system would display an “error” message, immediately after the wrong entry and alert the administrator for an unauthorized attempt for access. Therefore, it will be an additional advantage of this proposed opto-chemical security device over the conventional chemical password systems [23–25,30,38] that the system could be programmed to alert the administrator for any incorrect key pressing at any step, even before the completion of the password entry, smartly minimizing the chances of password hack through trials.

Ultimately, tracking the above-described guidelines for password compositions, the dual macrocyclics tuned HM system would be able to construct, recognize and authenticate 16 distinct passwords with respective 16 unique emission intensity bar patterns (Fig. 3). These exclusive passwords as the combinations of optical and chemical input keys could be assigned to different end-users for login and other authentication purposes. Any arbitrary entry of opto-chemical input keys beyond the pre-assigned password to a particular end-user must fail to generate an exclusive pattern at the recorder. Only a valid opto-chemical password entry with the correct sequence without any error at any step would successfully operate the lock. Therefore, our proposed system is quite flexible and robust to support and authenticate unique passwords for different end-users on the single chemical platform.

In tune with these advantages, against the illegal invasion this proposed macrocyclics driven opto-chemical security system would perform a dual defence mechanism. At first, during the course of password entry the end-user requires to match/follow the preset password trajectory or exact password sequence of the input keys and secondly it is required to put the exact assigned opto-chemical password, in order to open the lock. If any anomaly found at any step during the course of password entry, the system will alert the administrator. With these

absolute advantages, our proposed macrocyclic component based molecular security device is more promising, versatile, and highly secure compared to so far reported macrocyclics driven lock [30] through supporting a greater number of passwords for multiple users and a step-wise monitoring feature preventing unauthorized access through adopting trials.

In tune with our previous report [37], to illustrate the operational principle of the proposed macrocyclic based molecular keypad lock, let us have a look at the detailed operational mechanism. Suppose an end-user has been assigned with a five-digit password '23452' for login purpose. Now, the end-user needs to press the input keys of that password in the proper sequence. Incipiently, upon pressing the “ON” button the lock starts working. Then the end-user enters the password '23452' on the physical PIN pad of the lock. As the first character of the password '2' is entered, the system is so programmed that it recognizes it as 'D3' input and the detector responsible to measure the emission of HM at 365 nm gets activated. Similarly, the next consecutive four keys, '3', '4', '5' & '2' of the password could be assigned as 'C', 'D4', 'B' & 'D3' input keys, respectively, to the system. As the user enters these password keys in sequence, the system performs next four sequential and independent operations. Complete five-step operations performed by the system could be presented as follows: Step 1) pressing of key '2': system measures the emission intensity of pure HM at 365 nm and at the recorder subsequent bar is generated; Step 2) pressing of key '3': incorporation of CTAB within the HM takes place; Step 3) pressing of key '4': the system monitors the emission of HM-CTAB complex at 416 nm and the corresponding bar is generated at the recorder; Step 4) pressing of key '5': addition of β -CD to the HM-CTAB solution takes place; Step 5) finally, pressing of key '2': the emission intensity of HM-CTAB- β -CD solution is measured at 365 nm and the corresponding

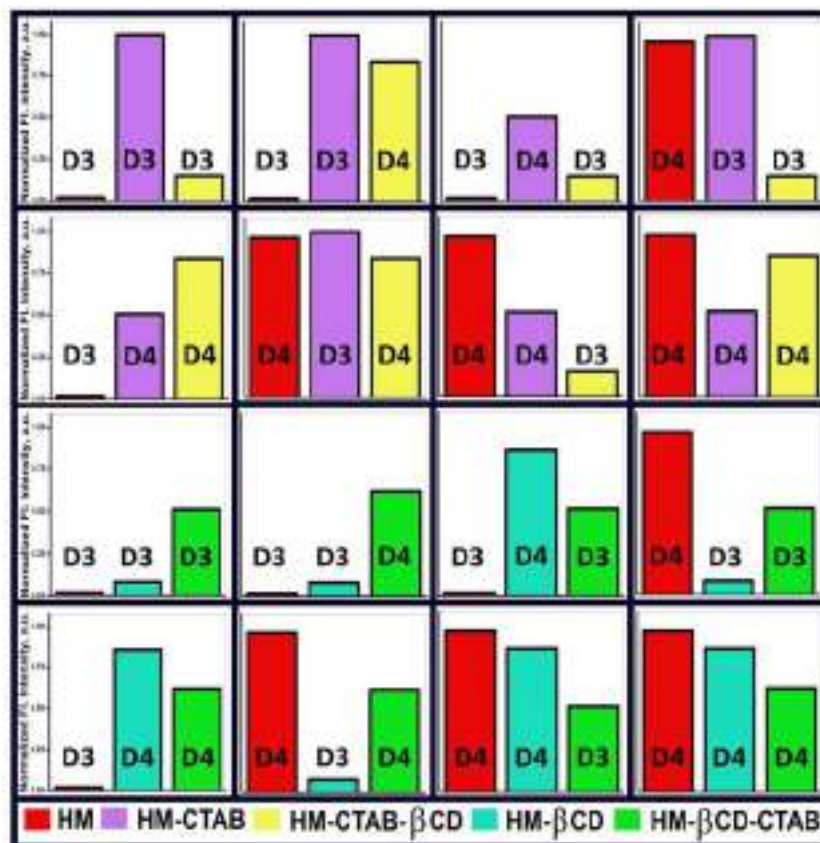


Fig. 3. Derived combinational bar patterns for passwords considering output responses of HM at 365 and 416 nm and altering chemical (CTAB and β -CD) and optical (D4 and D3) inputs; those, in turn, could authenticate the respective opto-chemical passwords.

bar is recorded with the sequence. After successful entry of the complete password, a unique pattern is generated at the recorder with a set of three bars, guided by the stepwise entry of individual and alternate chemical and optical inputs. These unique bar patterns resulting from sequential chemical and optical inputs (Fig. 3) ultimately make different distinct passwords recognized and authenticated by the system to open the lock.

Other arbitrary entry of password keys by unauthorized users would not be validated as the system fails to generate recognizable and authenticated bar patterns at the recorder and ultimately denies the access. Moreover, the lock would not respond if the end-user uses a password less than five digit. Further, if the end-user enters the input keys of the password assigned to him/her in any other arbitrary way (say 24352); the system will immediately alert the administrator as it would fail to meet the stipulated opto-chemical trajectory. A pictorial layout of the above said operational mechanism is given below (Fig. 4).

Virtue of this security device lies in the fact that all possible bar patterns generated following the above-prescribed guidelines are unique and easily distinguishable against each password (Fig. 3). Beyond such 16 possible unique input-output guided bar patterns, the versatility of the keypad lock could be enhanced farther by increasing the number of unique passwords. If we consider the repeated additions of the same substrate at the two addition steps then the allowed and unique passwords should be 32. Further, considering "addition of nothing" at each addition step as a third option, as many as 72 different and unique passwords could be generated. Hitherto, round about all the reported molecular keypad locks were proposed based on the interactions of a particular molecule with a specific set of ions [23–25]. In the ionic environment, it was observed that the structural switching of the main device molecule from one state to another was about irreversible and the molecule more or less lose its originality after only a few cycles of operations. Compared to such ionic components based molecular lock,

the superiority of our proposed macrocyclics driven molecular keypad lock is that the structural switching of our device molecule is completely guided by macrocyclic induced non-ionic chemical environments and the interactions are purely non-covalent rather guided by mildly electrostatic and hydrogen-bonding interactions.

4. Conclusion

A new concept to design molecular keypad lock has been demonstrated on the dynamic switching of HM between cationic and neutral prototropic forms in the presence of macrocyclic chemical inputs, CTAB and β -CD. Since, HM generates dual-band ratiometric emission responses during such differential interactions, the choice of a detector for emission intensity measurement, either at 416 nm or at 365 nm, were considered as optical inputs and designated as D4 or D3, respectively. Finally, different set of emission intensities at the specified wavelengths were considered as optical outputs. Stepwise changes in the intensity values next to the entry of a full-course opto-chemical password were so arranged with step sequencing that specific bar patterns were created against each individual password. Reported macrocyclics based opto-chemical password protection system features formidable security characteristics in terms of non-identifiable chemical and optical elements, error detection during password entry along with reversibility, reusability, energy efficiency, and rapid response. This report might be sighted as a wide-ranging tactic towards the designing of molecular security devices for a category of molecules, specifically, other members of the β -carboline family like, harmine, norharmine, proving similar optical switchability as that of HM, in course of differential interactions with these macrocyclic inputs.

Author contributions

TM and AM conceived the idea and coordinated the project. MK,PP, RM carried out the experiments. TM and MK prepared the graphics. TM and AM co-wrote the manuscript.

Declaration of Competing Interest

"There are no conflicts to declare."

Acknowledgements

Research reported in this paper was supported by Department of Science and Technology, Govt. of India under the award number of DST YSS/2015/000904, dated 17-Nov-2015 sanctioned to Tapas Majumdar. Authors also thank University of Kalyani for funding through DST PURSE and DST-FIST (level-2, SR/FST/CS-II/2019/96, Dt. 07.01.2020) programs. M. K. gratefully acknowledges CSIR, Govt. of India for his senior research fellowship. P. P. sincerely acknowledges CSIR, Govt. of India for his junior research fellowship.

References

- [1] A.P. de Silva, H.Q.N. Gunaratne, C.P. McCoy, A molecular photoionic AND gate based on fluorescent signalling, *Nature* 364 (1993) 42–44.
- [2] L.M. Adleman, Molecular computation of solutions to combinatorial problems, *Science* 266 (1994) 1021–1024.
- [3] V. Balzani, M. Venturi, A. Credi, *Molecular Devices and Machines: A Journey into the Nanoworld*, Wiley-VCH, Weinheim, 2003.
- [4] A.P. de Silva, M.R. James, B.O.F. McKinney, D.A. Pears, S.M. Weir, Molecular computational elements encode large populations of small objects, *Nat. Mater.* 5 (2006) 787–790.
- [5] R. Beckman, E. Johnston-Halperin, Y. Luo, J.E. Green, J.R. Heath, Bridging Dimensions: demultiplexing ultrahigh-density nanowire circuits, *Science* 310 (2005) 465–468.
- [6] J.E. Green, J.W. Choi, A. Boukai, Y. Bunimovich, E. Johnston Halperin, E. Delonno, Y. Luo, B.A. Sheriff, K. Xu, Y.S. Shin, H.R. Tseng, J.F. Stoddart, J.R. Heath, A 160-kilobit molecular electronic memory patterned at 10^{11} bits per square centimeter, *Nature* 445 (2007) 414–417.

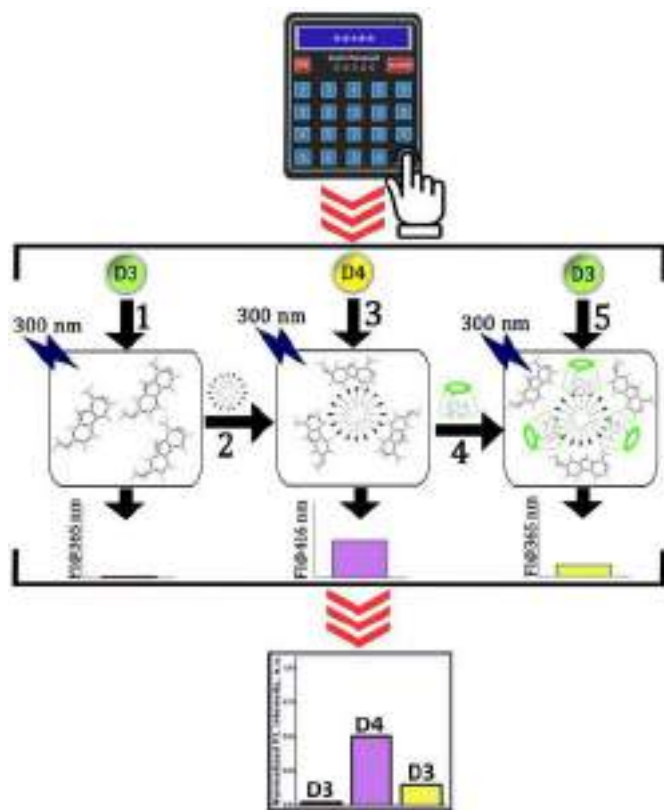


Fig. 4. Operational layouts of the proposed keypad lock considering an authenticated specific five-digit password, '23452', as an example.

- [7] M. Karar, P. Paul, B. Biswas, A. Mallick, T. Majumdar, Excitation wavelength as logic operator, *J. Chem. Phys.* 152 (2020) 075102–075110.
- [8] M. Irie, Diarylethenes for memories and switches, *Chem. Rev.* 100 (2000) 1685–1716.
- [9] J.Y. Jiang, S. Wang, W.F. Yuan, L. Jiang, Y.L. Song, H. Tian, D.B. Zhu, Highly fluorescent contrast for rewritable optical storage based on photochromic bisthiénylene-bridged naphthalimide dimer, *Chem. Mater.* 18 (2006) 235–237.
- [10] S.J. Lim, J. Seo, S.Y. Park, Photochromic switching of excited-state intramolecular proton-transfer (ESIPT) fluorescence: A unique route to high-contrast memory switching and nondestructive readout, *J. Am. Chem. Soc.* 128 (2006) 14542–14547.
- [11] D. Margulies, G. Melman, A. Shanzer, Fluorescein as a model molecular calculator with reset capability, *Nat. Mater.* 4 (2005) 768–771.
- [12] Y.C. Zhou, H. Wu, L. Qu, D.Q. Zhang, D.B. Zhu, A new redox-resettable molecule-based half-adder with tetrathiafulvalene, *J. Phys. Chem. B* 110 (2006) 15676–15679.
- [13] U. Pischel, Chemical approaches to molecular logic elements for addition and subtraction, *Angew. Chem. Int. Ed.* 46 (2007) 4026–4040.
- [14] J. Andreasson, S.D. Straight, S. Bandyopadhyay, R.H. Mitchell, T.A. Moore, A.L. Moore, D. Gust, Molecular 2:1 digital multiplexer, *Angew. Chem. Int. Ed.* 46 (2007) 958–961.
- [15] P.R. Ashton, V. Balzani, J. Becher, A. Credi, M.C.T. Fyfe, G. Matternsteig, S. Menzer, M.B. Nielsen, F.M. Raymo, J.F. Stoddart, M. Venturi, D.J. Williams, A three-pole supramolecular switch, *J. Am. Chem. Soc.* 121 (1999) 3951–3957.
- [16] A.P. de Silva, H.Q.N. Gunaratne, T. Gunnlaugsson, A.J.M. Huxley, C.P. McCoy, J.T. Rademacher, T.E. Rice, Signaling recognition events with fluorescent sensors and switches, *Chem. Rev.* 97 (1997) 1515–1566.
- [17] R. Ziessel, A. Harriman, Building photoactive molecular-scale wires, *Coord. Chem. Rev.* 171 (1998) 331–339.
- [18] A. Harriman, R. Ziessel, Making photoactive molecular-scale wires, *Chem. Commun.* (1996) 1707–1716.
- [19] N. Koumura, R.W.J. Zijlstra, R.A. van Delden, N. Harada, B.L. Feringa, Light-driven unidirectional molecular rotor, *Nature* 401 (1999) 152–155.
- [20] C.D. Mao, W.Q. Sun, Z.Y. Shen, N.C. Seeman, A nanomechanical device based on the B–Z transition of DNA, *Nature* 397 (1999) 144–146.
- [21] C.P. Collier, E.W. Wong, M. Belohradsky, F.M. Raymo, J.F. Stoddart, P.J. Kuekes, R.S. Williams, J.R. Heath, Electronically configurable molecular-based logic gates, *Science* 285 (1999) 391–394.
- [22] M. Asakawa, P.R. Ashton, V. Balzani, A. Credi, G. Matternsteig, O.A. Matthews, M. Montalti, N. Spencer, J.F. Stoddart, M. Venturi, Electrochemically induced molecular motions in pseudorotaxanes: a case of dual-mode (Oxidative and Reductive) dethreading, *Chem. Eur. J.* 3 (1997) 1992–1996.
- [23] D. Margulies, C.E. Felder, G. Melman, A. Shanzer, A molecular keypad lock: A photochemical device capable of authorizing password entries, *J. Am. Chem. Soc.* 129 (2007) 347–354.
- [24] W. Sun, C. Zhou, C.H. Xu, C.J. Fang, C. Zhang, Z.X. Li, C.H. Yan, A fluorescent-switch-based computing Platform in defending information risk, *Chem. Eur. J.* 14 (2008) 6342–6351.
- [25] S. Kumar, V. Luxami, R. Saini, D. Kaur, Superimposed molecular keypad lock and half-subtractor implications in a single fluorophore, *Chem. Commun.* (2009) 3044–3046.
- [26] J. Andre Asson, U. Pischel, Molecules for security measures: from keypad locks to advanced communication protocols, *Chem. Soc. Rev.* 47 (2018) 2266–2279.
- [27] U. Pischel, V.D. Uzunova, P. Remon, W.M. Nau, Supramolecular logic with macrocyclic input and competitive reset, *Chem. Commun.* 46 (2010) 2635–2637.
- [28] M. Karar, P. Paul, S. Paul, B. Haldar, A. Mallick, T. Majumdar, Dual macro-cyclic component based logic diversity, *Dyes Pigments* 174 (2020) 108060–108066.
- [29] A.P. de Silva, I.M. Dixon, H.Q.N. Gunaratne, T. Gunnlaugsson, P.R.S. Maxwell, T.E. Rice, Integration of logic functions and sequential operation of gates at the molecular-scale, *J. Am. Chem. Soc.* 121 (1999) 1393–1394.
- [30] C.P. Carvalho, Z. Dominguez, J.P. Da Silva, U. Pischel, A supramolecular keypad lock, *Chem. Commun.* 51 (2015) 2698–2701.
- [31] B. Daly, T.S. Moody, A.J.M. Huxley, C. Yao, B. Schazmann, A. Alves-Areias, J.F. Malone, H.Q.N. Gunaratne, P. Nockemann, A.P. de Silva, Molecular memory with downstream logic processing exemplified by switchable and self-indicating guest capture and release, *Nat. Commun.* 10 (2019) 49.
- [32] M. Karar, S. Paul, A. Mallick, T. Majumdar, Interaction behavior between active hydrogen bond donor-acceptors as a binding decoration for anion recognition: experimental observation and theoretical validation, *Chemistryselect* 2 (2017) 2815–2821.
- [33] M. Karar, S. Paul, A. Mallick, T. Majumdar, Shipment of a photodynamic therapy agent into model membrane and its controlled release: A photophysical approach, *Chem. Phys. Lipids* 210 (2018) 122–128.
- [34] A. Chakraborty, D. Seth, P. Setua, N. Sarkar, Photoinduced electron transfer reaction in polymer-surfactant aggregates: photoinduced electron transfer between N,N-dimethylaniline and 7-amino coumarin dyes, *J. Chem. Phys.* 128 (2008) 204510.
- [35] P. Das, A. Mallick, A. Chakraborty, B. Haldar, N. Chattopadhyay, Effect of nanocavity confinement on the rotational relaxation dynamics: 3-acetyl-4-oxo-6,7-dihydro-12H indolo-[2,3-a] quinolizine in micelles, *J. Chem. Phys.* 125 (2006). 044516.
- [36] D. Chakraborty, A. Chakraborty, D. Seh, N. Sarkar, Effect of alkyl chain length and size of the headgroups of the surfactant on solvent and rotational relaxation of Coumarin 480 in micelles and mixed micelles, *J. Chem. Phys.* 122 (2005) 184516.
- [37] T. Majumdar, B. Haldar, A. Mallick, A strategic design of an opto-chemical security device with resettable and reconfigurable password based upon dual channel two-in-One chemosensor molecule, *Sci. Rep.* 7 (2017) 42811–42817.
- [38] M. Karar, P. Shit, B. Halder, A. Mallick, T. Majumdar, Multifunctional logic applications of a single molecule: a molecular photo-switch performing as simple and complex gates, memory element, and a molecular keypad lock, *Chemistryselect* 3 (2018) 5277–5282.



REVIEW

Supported Transition Metal Catalysts for Organic Fine Chemical Synthesis: A Review

RAJIB MISTRI*^{ORCID} and BIDYAPATI KUMAR^{ORCID}

Department of Chemistry, Achhruram Memorial College, Jhalda, Purulia-723202, India

*Corresponding author: E-mail: rajibmistri@yahoo.co.in

Received: 9 October 2020;

Accepted: 8 December 2020;

Published online: 16 February 2021;

AJC-20239

Transition metal catalysts play an important role for synthesis of industrially and laboratory important organic fine chemicals to control the selectivity, activity and stability. In this review, we focus on mainly transition metal based supported catalyst, mainly oxide supported catalyst for heterogeneous catalytic hydrogenation and oxidation of some synthetically important organic molecules. First we discuss the industrially important catalytic organic synthetic reactions. This is followed by the role of supported metal catalysts in the heterogeneous synthetic catalytic reactions with specific attention to hydrogenation and oxidation of organic molecules. The role of base metals and noble metals in monometallic and bimetallic catalysts are then discussed. Some synthetic routes for preparation of oxide supported metal catalysts are also discussed. Finally, a general discussion of the metal-support interaction (MSI) in oxide supported metal catalysts is made.

Keywords: Heterogeneous catalyst, Transition metal, Oxidation, Hydrogenation, Important organic molecules.

INTRODUCTION

A chemical industry is in need of technology having maximum activity as well as selectivity towards organic synthetic reactions. Similarly, the requirement is also to adopt “clean” chemical processes having minimum impact on the environment. Hydrogenation and oxidation of organic functional group with high activity and selectivity is one of such requirement. Heterogeneous catalysis plays an important role in wide variety of industrial processes. The most important synthetic use of heterogeneous catalysts are for common synthetic organic transformation. The heterogeneous catalysts can be either oxides [1-6] or metals [7-11]. Most synthetically useful catalytic processes are run over metal catalysts [10-12]. The metal catalyst can be composed of a single metallic component or a mixture of metals [12]. Either of these types can be supported or unsupported. Metal catalysts are used primarily for hydrogenation, hydrolysis, isomerization and oxidation reactions, *etc.* [13-16].

The catalytic activity of dispersed metals on an oxide support is influenced by a number of factors. These include size, shape, extent of dispersion, relative amount of metals present, chemical nature of support and strength of interaction between

the support and metal [17]. A support can alter the behaviour of metal in a number of ways. Several explanations have been given to understand enhanced activity of metal doped oxide supported catalysts [18]. They are easily prepared and can be characterized without too many difficulties. Due to this, metal catalysts are generally preferred for basic research. The active catalytic species is believed to be finely dispersed metal particles of sizes in the nano region. Lots of research works have been done on metal-support interaction in supported metal catalysts. Yet the exact nature of active site and the exact role of the support in terms of metal-support interaction are less understood.

Synthetically important organic reaction: Organic synthesis is a key step for the preparation of fine chemicals, pharmaceuticals, agrochemicals, food additives, dyes and pigments. An important factor in developing synthetic reactions is choosing the reaction route to the final product. Catalytic routes have been proven to be one of the most effective ways in simplifying the reaction routes to these compounds by increasing selectivity and reducing waste and hazardous materials handling [19-21]. Additionally, reactions should proceed under mild conditions to reduce the costs of energy. The ultimate aim is of course to adopt a green synthetic route for organic transformations. In

this context, good catalyst performance can be characterized by: (i) high activity and selectivity; (ii) little or no alteration of activity and selectivity with time; (iii) low sensitivity of activity and selectivity to contaminant in the feedstock; and (iv) favourable separation properties.

Organic synthetic chemists are in search of more active, selective and environmentally benign catalyst for their synthesis applications. Alkylation or arylation of aromatic or aliphatic, dehydrogenation, dehydration, hydrogenation, selective oxidation and isomerization are important organic synthesis reactions. A number of new precious catalysts are used for this type of synthetic reactions [22-24].

The alkylation of aromatic compounds is extensively used in the synthesis of various intermediates, fine chemicals and petrochemicals [25]. The necessary feature of this reaction is the replacement of the hydrogen atom of aromatic compound containing alkyl group derived using an alkylating agent. If acid catalyst is used, a replacement occurs in the aromatic ring and base catalyst replaced at side chain of the ring [26]. The commercial alkylations are acid catalyzed [25,27,28]. These include acidic halides such as AlCl_3 , BF_3 , acidic oxides, HF , H_2SO_4 [27], H_3PO_4 and zeolites [28]. The intramolecular isomerization and the transfer alkyl groups between aromatic molecules are also catalyzed by acid catalysts [29-31].

Dehydrogenation of aromatic hydrocarbons (ethylbenzene, diethylbenzene) and alcohols are also industrially important. The ethylbenzene dehydrogenation (EBDH) products are styrene and H_2 [32,33]. Iron oxide is mainly used as a catalyst for the production of styrene [32]. The incorporation of V, Ce and Mo improved the catalytic properties of iron oxide [34]. Catalytic

dehydrogenation of primary and secondary alcohols gives corresponding aldehydes and ketones [34,35]. A large number of solid metal oxide catalysts have been effectively used for alcohol dehydrogenation [36,37]. Most of the oxide catalysts possess also dehydration activity and in some of them, such as alumina, the dehydration predominates [35]. The ratio of the dehydration and dehydrogenation depends on catalyst preparation and its purity. However, some exhibit only dehydrogenation activity, such as oxides of copper, zinc, chromium, iron, *etc.* [36-40]. Metals are also used as dehydrogenation catalysts. Copper is used most frequently, while silver is applied in the combined dehydrogenation-oxidative dehydrogenation processes for production of formaldehyde from methanol or acetaldehyde from ethanol. Noble metals Pt, Pd, Ru, Ir can also be used as oxidative-dehydrogenation catalysts [41-43].

Hydrogenation is the addition of H_2 molecule to a multiple bond ($\text{C}=\text{C}$, $\text{C}\equiv\text{C}$, $\text{C}=\text{O}$, $\text{C}=\text{N}$, $\text{C}\equiv\text{N}$, $\text{N}=\text{O}$, $\text{N}=\text{N}$, $\text{N}\equiv\text{N}$, *etc.*) to reduce it to a lower bond order (Fig. 1). Catalysts are required for the reaction to be usable as the non-catalytic hydrogenation takes place only at very high temperatures.

Platinum, rhodium, palladium and ruthenium form various highly active catalysts and operate at low hydrogen pressures and low temperatures [44-46]. Moreover, inexpensive metal catalysts, based on nickel (such as Raney nickel [47,48] and Urushibara nickel [49]) are established as economical alternatives for expensive catalysts. However, they often provide slow catalysis or operate at high temperatures. Two broad families of catalysts, homogeneous and heterogeneous, are simultaneously important for catalytic hydrogenation. The rhodium based Wilkinson's catalyst and the iridium based Crabtree's homo-

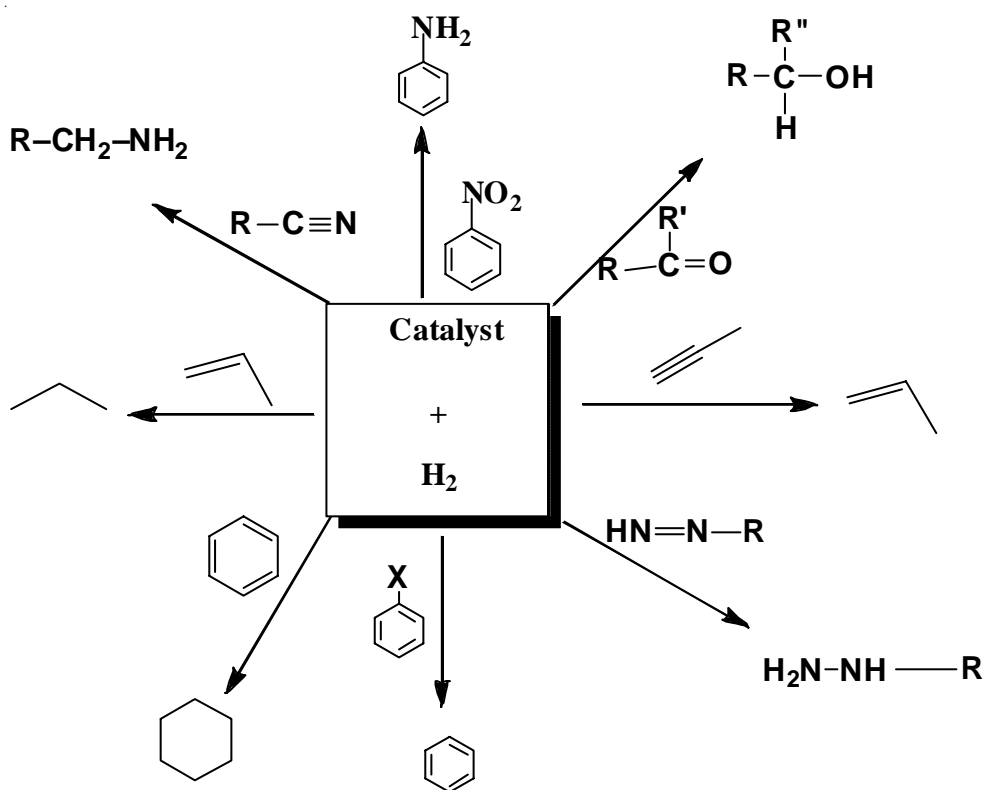


Fig. 1. Common hydrogenation reactions

geneous catalyst are exclusively used as hydrogenation catalyst [50-53].

Heterogeneous catalysts for hydrogenation are more common in industrial synthetic reactions. As in homogeneous catalysts, the activity of the catalyst is adjusted through changes in the environment around the metal, *i.e.* coordination sphere. Different faces of a crystalline heterogeneous catalyst show distinct activities. Similarly, the activity of the heterogeneous catalysts are affected by their supports, *i.e.* the material on which the heterogeneous catalyst is bound [53,54]. A number of new precious catalysts such as Pd/C [55], Pt/C [56] and immobilized Rh [57] catalyst have been successfully commercialized in recent years.

Selective oxidation of functional group is another industrially important catalytic reaction (Fig. 2). Catalytic oxidation in the liquid phase is widely used in bulk chemicals manufacture [58] and become increasingly important in the synthesis of fine chemicals.

A traditional process involving stoichiometric inorganic oxidants is receiving increasing environmental pressure [59]. Generally, in the liquid phase, catalytic oxidation employs soluble complexes or metal salts combined with inexpensive and clean oxidants such as O_2 , H_2O_2 , or RO_2H [20,21].

However, compared with their homogeneous counterparts, heterogeneous catalysts present the advantage of facile recycling and recovering. Large-scale selective oxidation is based on heterogeneous metallic catalysts. Silver is exclusively used as an epoxidation catalyst for the production of ethylene epoxide

from ethylene. Palladium is used as oxidative coupling catalyst for the production of vinyl acetate from ethylene and acetic acid. Cu, V, Mn, Ru, *etc.* are also used as oxidation catalysts for the cycloalkanes, cycloalkenes, benzene and benzyl alcohol [26,60-62].

Common organic hydrogenation reactions: The most common use of catalysts in organic synthesis is the hydrogenation of functional groups. The number of books and reviews published in this area underscores the synthetic importance of these reactions [63-66]. Hydrogenation is commonly a chemical reaction between molecular hydrogen (H_2) and another compound or element, usually in the presence of a catalyst. Hydrogenation of organic functional groups can be categorized into (a) addition of hydrogen across single bonds leading to cleavage of functional groups (hydrogenolysis), (b) addition of hydrogen to unsaturated groups as, for example, in the hydrogenation of ketone to alcohol and (c) removal of oxygen by hydrogen, for example, aromatic nitro to aniline (Fig. 3). Alkenes, alkynes, aromatics, heteroaromatics, ethers, ketones, esters, acids and amides can all be hydrogenated to industrially or synthetically important chemicals.

Catalytic hydrogenation can either be heterogeneous or homogeneous. Metal salts and complexes have provided some homogeneous hydrogenating agents [67-70]. The major disadvantage of the large-scale utilization of metal salts and complexes is their high cost. Due to the inefficient and stoichiometric nature of reactions, for hydrogenation, large quantities of metals or metal salts are required. Furthermore, separating products

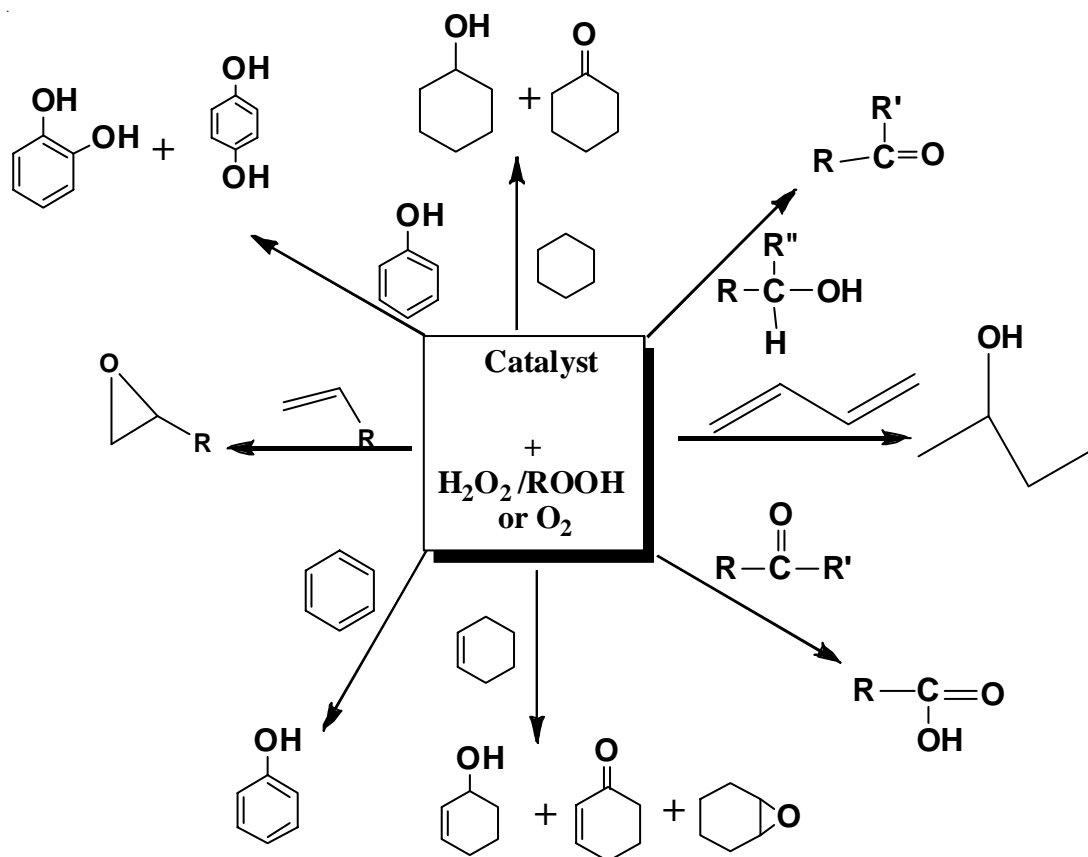


Fig. 2. Common oxidation reactions

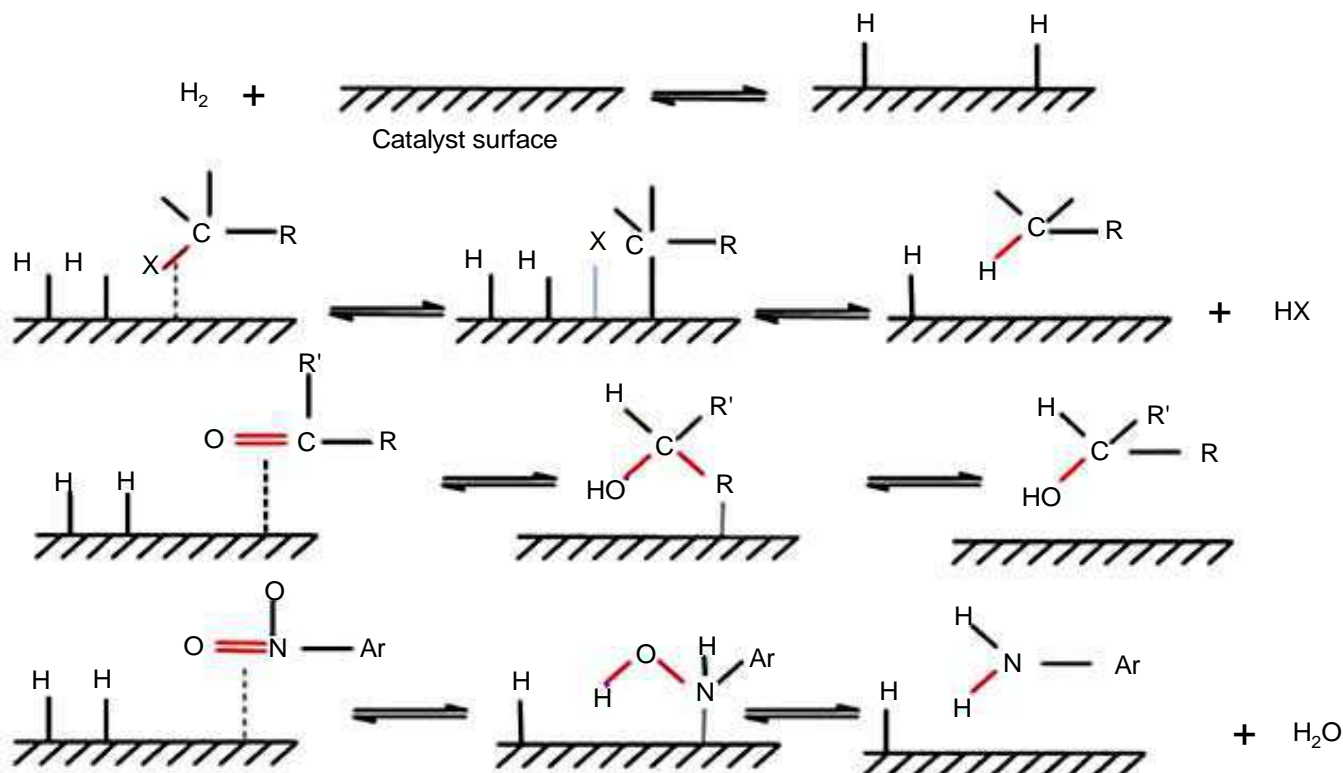


Fig. 3. Catalytic hydrogenation of organic functional groups *via* (a) hydrogenolysis, (b) hydrogen addition and (c) oxygen removal by hydrogen [R, R' = alkyl group; Ar = Aryl group and X = halogen]

from large volumes of metal complex or salt solutions can be inefficient and laborious. These disadvantages can be eliminated by using supported or unsupported heterogeneous metal catalysts, which leads to the easily separation of products and catalysts from reaction mixtures.

Metal-based catalysts are the most active for heterogeneous transfer hydrogenation. Palladium is highly active for the hydrogenation of alkynes or alkenes into alkanes and most commonly used catalyst for hydrogenolyses (benzylic and allylic C=O and C=N bonds, carbon-halogen and het=het, where het = N,O). For the hydrogenation of double bonds (C=N, C=C, and C=O), platinum is highly active [71,72]. When Pt is used, hydrogenolysis does not occur [17]. Under mild conditions, rhodium based catalysts are employed for the hydrogenation of aromatic compounds [73]. By contrast, at high pressures and temperatures, ruthenium usually is employed for the hydrogenation of carbonyl functional groups and aromatic compounds. Nickel, especially Raney nickel, is suitable for the hydrogenation of nitriles to amines and carbonyl groups (ketones and aldehydes) [74]. Under rather harsh conditions, copper-based catalysts are utilized in the hydrogenation of esters into the corresponding alcohols [75].

The catalytic activity of metals depends mainly on three factors (i) catalyst selection, (ii) reaction medium, (ii) reaction condition [76]. The order of the influence of these factors on selectivity is, in general, catalyst > reaction medium > reaction conditions. Catalyst selection depends on metal selection, chemical composition of support, catalyst particle size, particle morphology and oxidation state of metal. The metal influences both the characteristic adsorption/desorption and the surface

reaction. So a right choice of metal is very important for an efficient catalytic reaction. Supports interact with the metal, which influences its structural (morphology and size) and electronic properties, thereby results a lot the catalytic reactions. The rate of the hydrogenation reaction depends on metal particle size and shape or morphology. The smaller the particles, the larger the surface area and thus the activity increase. The catalytic hydrogenation reactions are mainly run in liquid solvent medium. The solvent polarity and hydrogen adsorption capacity and acidity of the medium influence the catalytic reactions. The activity can also depend on the reaction temperature and pressure.

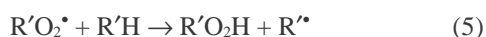
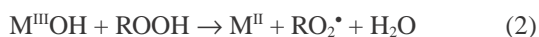
Metal catalysts can be finely divided, pure bulk metal, a skeletal or porous type (Raney Ni), nanoparticles and metals dispersed on different supports or carriers such as inorganic oxides (BaSO_4 , CaCO_3 , SiO_2 and Al_2O_3), carbon (charcoal), polymer, asbestos and zeolites. Some variations found in the metal catalytic activity in supported and free finely divided (blacks) forms results from various ageing treatments and preparation methods. Finely divided metals forms are prone to agglomeration, and in the long run, lose the catalytic activity. This agglomeration can even be accelerated through substrate action or substrate polymerization onto catalysts [77]. Metal precipitation on the support surface is advantageous because it results in a more uniform cluster or particle size of atoms than unsupported metals do and because it provides a large active surface area for the given metal mass (high specific surface density). Metal nanoparticles supported on mesoporous silicas [78,79], hydroxylapatites [80], porous carbons [81,82], zeolite [83], alumina [84] and titanium oxides [85] have been reported

to be highly active for various hydrogenation reactions. The direct synthesis of nanoparticles is limited and preparatory procedures are difficult. So supported metal catalysts are useful for hydrogenation reactions.

Hydrogenation of molecules containing single functional group is a common synthetic transformation. The selective hydrogenation of one functional group in presence of other groups is very important for the synthesis of industrially important chemicals. But if the functional groups have relatively similar or close activities, selectivity can sometimes be achieved by manipulating reaction condition or using proper catalysts. Therefore, recent research effort has been focused strongly on maximizing the catalytic efficiency of the precious metal catalyst by optimizing their physico-chemical properties [86,87], forming alloy structures [72], developing new catalyst supports [88], adding promoters [89,90] and modifying the metal-support interactions [91]. Both heterogeneous [92] and homogeneous metal catalysts [93] have been used in hydrogenation reactions for several decades.

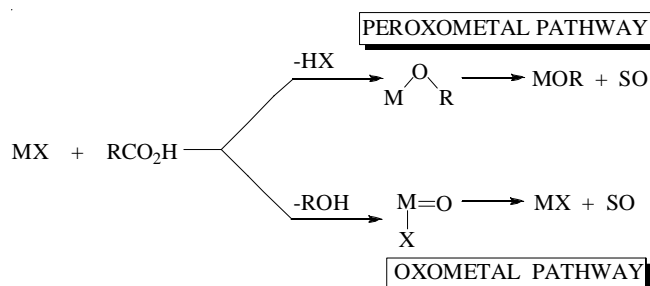
Common organic oxidation reaction: Like hydrogenation, the oxidation of organic functional groups is an important synthetic reaction [58,59]. Most oxidation reactions are run using inorganic oxidants such as permanganate and chromium oxide. The disposal of their reduction products is environmentally unacceptable [20,21]. In the manufacture of bulk chemicals, catalytic oxidation has become very important due to its low impact on the environment. The conversions of alkenes, alkanes, alcohols, ketones, epoxides and aromatic compounds into the more valuable oxygen containing materials are important synthetic reactions in industries [58-62].

Many reactions are run either in vapour phase or in liquid phase and the reaction conditions are usually specific for the production of specific products. Various new catalytic systems have been developed for the oxidation in gas phase and in liquid phase using organic peroxides, H₂O₂ or O₂ as an oxidant [81-83]. The catalytic oxidation reactions are run either by free radical auto-oxidation process or by oxygen transfer process. One-electron oxidants, *e.g.*, Cu(II), Mn(III), Co(III), Ce(IV), Fe(III), *etc.* catalyze free radical auto-oxidation processes by promoting the decomposition of alkyl hydroperoxides into chain initiating alkoxy and alkyl peroxy radicals in one-electron transfer processes (**Scheme-I**, reactions 1 and 2). Strictly speaking the metal ion acts as an initiator of free radical auto-oxidation, which proceeds further *via* reactions 3-5, which does not involve the catalytic species.



Scheme-I: Mechanism of metal catalyzed auto-oxidation

Metal ions which catalyze oxygen transfer reactions with H₂O₂ or RO₂H can be divided into two types based on the active intermediate: a peroxometal or an oxometal complex [92] (**Scheme-II**). Peroxometal pathway is usually favoured over early transition elements with *d*⁰ configuration, *e.g.* Mo(VI), W(VI), V(V) and Ti(IV). On the other hand, over the late or first row transition elements, *e.g.* Cr(VI), V(V), Mn(V), Ru(VI), Ru(VIII) and Os(VIII), the oxometal pathway is usually followed. Some elements, *e.g.* vanadium involve both oxometal and peroxometal pathways depending on the substrate.



Scheme-II: Peroxometal vs. oxometal pathways [92]

Heteroatom oxidations and olefin epoxidation are the reactions involving peroxometal routes. By contrast, oxometal species exhibit the broader range of activities, such as allylic and benzylic oxidations. Peroxometal routes do not involve a change in the metal oxidation state, *i.e.*, activity is not restricted to only variable valence elements and the metal behaves as a Lewis acid. By contrast, the oxometal pathway involves a two-electron redox reaction of metal ions. Furthermore, most metals that catalyse oxygen transfer through oxometal or peroxometal pathways can catalyze one-electron transfer by using peroxides. Consequently, free radical processes frequently compete to a lesser or greater extent with oxygen transfer. When alkyl hydroperoxides are employed as oxidants, heterolytic *versus* homolytic processes are distinguished by using a suitable investigated molecule [93]. The unsupported metals usually form soluble peroxo complexes with H₂O₂ or peroxide so these reactions, in reality, homogeneously catalyzed [94]. Separations of the final products thus become very difficult. Supporting the metals in inorganic oxides (such as SiO₂, Al₂O₃) [95,96] or zeolite [96-98] only served to facilitate the dissolution of the metal species by dispersing the metal over the surface of the support and making it more accessible to the peroxides.

Different types of oxide supported metal catalysts such as Fe/MgO [99], Fe/Al₂O₃ [100], Co/Fe₂O₃ [101], Cu/Al₂O₃ [102], Cu/SiO₂ [103], V/SiO₂ [104] and Mn/Al₂O₃ [105] have been reported to be efficient systems for the production of industrially and chemically important products. These catalysts are usually prone to deactivation before the oxidation is completed. The deactivations are thought to be caused by either oxidation of the metals or blocking the active metal surface by the strong adsorption of the reaction byproducts or decrease of active metal component through metal leaching during oxidation.

A number of procedures have been employed to minimize this deactivation. Most of the early work in this area used large

amount of large sized metal particles [106]. These larger metal particles are more resistant to oxidation than the smaller particles present on the supports [107]. In addition, the large quantity of catalyst ensures that some active species will still be available towards the end of the reactions. The adsorption of byproducts can be eliminated by using more selective catalyst or changing solvent or reaction conditions [108]. Adding another metal particle/s significantly reduce the deactivation [109-112]. The metal leaching can be controlled by using proper support where metal support interaction is strong [113]. The metal leaching is also resisted by adopting specific preparation procedure and incorporating with other metals [114]. Association of two or more active metals can perform well in a reaction system with the enhanced degree of interaction of the components over a support with new redox and acid properties [115].

Selective oxidations *via* heterogeneous catalysis occupy a predominant place in both science of catalysis and synthetic based modern industry. These processes, such as benzene to phenol, benzyl alcohol to benzaldehyde, cyclohexane or cyclohexene to corresponding alcohols and carbonyl compounds have been extensively studied [116-119]. Ru, Pd, Mn, Fe, Co, Ni, V and Cu supported catalysts have been extensively used as catalyst for this type of reaction with H₂O₂ or *tert*-butyl hydrogen peroxide (TBHP) as the oxidant [120-122]. Still there are a large number of opportunities to develop suitable supported metal catalysts for this type of reaction.

Supported metal catalysts in organic synthetic reaction:

Catalytic reaction can be run over supported or unsupported metal catalysts. The active sites on a heterogeneous catalyst are found on its surface. Usually, the efficient catalysts have a large catalytically active surface exposed to the reaction medium. One way to maximizing the active surface of a catalyst is it can be used as a very fine powder as unsupported catalyst. The unsupported metals are found in variety of forms; single crystals, colloids, powders, blacks, skeletal and nanoparticles. Single crystals were used somewhat routinely in the early catalytic research for developing the mechanism in vapour phase reactions [123]. Since most of the synthetic reactions are run in liquid phase these single crystal metal catalysts find little use in the study of synthetic reactions. Black or powder is a metallic powder obtained by the reduction of metal salt or condensation of metal vapour [47]. But they are usually composed of relatively large particles having a low surface area and poor activity [17,48]. Skeletal metals are produced by leaching out one component of an alloy and leaving the active species behind in the form of porous materials having a high surface area [47-49]. However, heating of unsupported catalysts usually results in sintering or agglomeration of the small particles into larger, less efficient entities [124]. The most common way to minimizing metal catalyst sintering is to distribute the active component over a porous, thermostable, inert support. The support may be inorganic oxides, active carbon, polymers and zeolites.

Catalysts with a supported metal comprise 0.1-20 wt.% metal from group 8 or 9, which is dispersed on the support surface, usually a high-surface area oxide [125]. These catalysts are widely used in industries and research laboratories. Because an active metallic phase exists as extremely small particles

with a dispersion degree (*i.e.*, the fraction of atoms exposed to the surface) of 10-100%, these catalysts are effective. These catalysts are widely separated from each other and firmly anchored to supports. Thus, they do not readily sinter or coalesce.

The activity of the dispersed catalyst particles in these supported catalysts is influenced by a number of factors, primarily the relative amount of catalytically active materials present, the surface area of the support, nature of the support and the strength of support-catalyst particles interaction. Metal catalysts with a low metal loading are generally composed of very small crystallites widely scattered over the surface of the support. Such crystallites generally have a high dispersion and the metal is efficiently used as catalyst. As the metal load increases, the crystallites become close to each other and frequently get larger in size. Thus the crystallites are become more resistant to thermal sintering. Obviously, if the catalyst crystallites are come in contact to each other then thermal coalescence can be expected to take place with a resulting loss of active surface area. The low metals loaded highly dispersed catalysts provide a maximum surface area per unit mass of metal. While the catalysts having larger number of catalyst particles spread over the support surface also provide a maximum metal surface area per volume of catalyst.

Generally noble metal catalysts have low metal loads and high metal dispersion, while catalysts containing the less expensive base metals have higher metal loadings. The surface area of a support is directly related to pore size, distribution and volume. The maximum surface area for the support or catalyst is the best possible arrangement. The surface area is not only associated with external surface of the particles but also with the surface of all the pores within the particles. A particle with small diameter pores will have a higher surface area than one with larger diameter pores having both the same total pore volume.

In case of vapour phase reaction involving molecules, catalyst particles having a large number of smaller pores and higher surface areas are preferred. Reactions of larger molecules are usually run in a liquid medium. For such reactions catalysts having smaller pores are inefficient since the diffusion restraints would severely hinder the reaction. Catalysts have larger pores with the catalytically active sites located near the surface of the support particles. So diffusion of the reactants to the active sites will not be a significant factor in the reaction.

Synthetic routes to oxide supported metal catalysts:

The metal components are dispersed over the oxide support by various methods that include impregnation, precipitation and coprecipitation, deposition precipitation, ion-exchange, sol-gel, incipient wetness impregnation, spray drying, freeze drying, *etc.* [126,127]. However, all these processes are involved and sometimes require special equipment and are time consuming. Patil *et al.* [128,129] introduced a novel technique, the single-step solution combustion method, which involved the combustion of the metal salts with organic fuels, for the preparation of different fluorite, perovskite, spinel and mixed oxides [130,131].

Some advantages and disadvantages associated with the conventional methods which are coprecipitation and deposition-

precipitation are beneficial for synthesizing catalysts having high metal loadings (*e.g.* >10 wt.%) and those having low metal loadings of 0.01-5 wt.%, respectively. A limited coprecipitation cannot be applied to SiO₂ but supports Al₂O₃ because these hydroxide precursors or metal oxides cannot be coprecipitated using noble metal hydroxides. The sol-gel method can be used instead of coprecipitation for the SiO₂ support. Deposition-precipitation can be applied to basic metal oxides having the point of zero charge (PZC) of >5 pH. On the surfaces of supports of acidic metal oxide having PZC of < pH 5, noble metal hydroxides cannot be precipitated.

Metal-support interaction in supported metal catalysts:

The concept of a metal-support interaction (MSI) is one of the oldest in heterogeneous catalysis. Initially, it was thought that the support material is inert and serves simply as a vehicle for keeping the catalytically active species separated and thus, minimizes sintering. This is accomplished because catalyst crystallinities are formed some type of chemical bond to the support material by so they are not free to migrate across the surface and agglomerate or coalesce with other crystallinities to form larger particles. Since, the catalyst particles are anchored to the support through some form of bonding the support can, potentially, also influence the activity of the catalyst [132].

This support effect can be assumed as taking place in two distinct ways. First, the support could modify the electronic character of the catalyst particles. This could affect the adsorption and reaction characteristic of the catalytically active sites. Another possibility is that the shape of geometry of the catalyst particles. The electronic effect could change the activity of the sites on the surface while geometric effect would modify the number of active sites present. The first specific suggestion of how the catalytic properties of a metal might be influenced by the support came about 85 years ago by Adadurov (1935). He proposed that metals would be polarized by the surface of oxides containing highly charged cations [133]. The catalytic property of the supported metal catalyst is strongly influenced by the metal support interaction [134-136]. According to Bond's proposition, the metal-support interactions are of three types, namely strong (SMSI), medium (MMSI) and weak (WMSI) [137]. As has been discussed, the SMSI is ascribed to transition metals supported on reducible oxides like CeO₂, TiO₂, BaTiO₃, *etc.* [138-143]. The metal-support interaction is increased with more reducible support. The weak metal-support interaction (WMSI) is generally associated with non-reducible oxides such as SiO₂, Al₂O₃, ZrO₂, *etc.* [144-147]. But the classification is not so straightforward. There are instances of SMSI effect in non-reducible oxide supports [148,149]. The difference between the two categories lies in the facts that MSI is induced under more severe conditions and the property of the catalyst is less pronounced in case of nonreducible oxides.

The catalytic activity of noble metals is decreased significantly as the metal-support interaction increase with reducible support. Several explanations are given for the deactivation behaviour associated with SMSI [150,151]. Four models are proposed for the origin of SMSI, namely, electron transfer, morphological effects, alloying and decoration [152]. Even after extensive studies, a fundamental understanding of the origin

of the SMSI effect remains unclear and it is still a subject of current research [153].

Conclusion

From the foregoing discussion, it is suggested that there is lot of scope towards design of effective catalytic formulations. The preparation of industrially or synthetically important active catalyst for hydrogenation and oxidation reactions has been the constant motivation of researchers in this area of catalysis as outlined above. Inorganic oxide supported noble or base metal catalysts are extensively used as active catalyst for the synthetic organic reactions. It must be kept in mind that the sources of noble metal are limited and also the extraction procedure is costly, which in turn increases the cost of noble metals or its salts. Thus, urge is to reduce the amount of noble metal in the catalyst. But this should not affect the catalyst activity adversely. Conventional dispersion of metal component as zero-valent metal gives rise to finely dispersed nanocrystallinities of size ~3-5 nm on oxide surface. Further reduction of metal crystallinities size to ~1 nm will further increase the dispersion with lower amount of metal doping and hence the rate of reaction will be enhanced. Whatever may be the size of the crystallite, only the metal atoms at the surface of it takes part in chemisorption and catalytic action. The highest possible dispersion with highest activity can be achieved by dispersing each metal atom at the surface, which is not possible by the conventional methods of dispersing metals since due to metal-metal interaction, agglomerated metal crystallites are formed in the end. Thus the catalyst is multiphasic in nature. To make use of each metal atom as the adsorption site, the metal atoms should be placed at particular lattice positions. If the metals are substituted in support lattice in the form of metal-ion by using proper support or proper catalytic preparation methods, then the predominant electronic interaction will be a strong ionic interaction between metal ion and the oxide support. This means that substitution of metal ion in the support lattice is to be achieved forming single phase metal-ion substituted oxide. The metal ions in its positive oxidation state can easily be reduced by other oxidizable substances. Therefore, if the metal is dispersed as ionic form and if one is able to keep the oxidation state in positive state, in principle oxidation can be carried out over such ionically dispersed catalyst. The questions which automatically arise are: (i) How to substitute metal in its ionic form; and (ii) whether the catalytic capability would be the same in its oxidized state and in the zero-valent metallic state? So it is still challenging to prepare an efficient catalyst for synthetically important organic reactions in 21st century.

CONFLICT OF INTEREST

The authors declare that there is no conflict of interests regarding the publication of this article.

REFERENCES

1. T. Curtin, J.B. Mcmonagle, M. Ruwet and B.K. Hodnett, *J. Catal.*, **142**, 172 (1993); <https://doi.org/10.1006/jcat.1993.1199>
2. M. do Ce'v Costa, R. Taveres, W. Motherwell and M.J.M. Curto, *Stud. Surf. Sci. Catal.*, **78**, 639 (1993).

3. A. Servino, J. Vital and L.S. Lobo, *Stud. Surf. Sci. Catal.*, **78**, 685 (1993).
4. L. Posner and R. L. Augustine, *Chem. Ind.*, **62**, 531 (1995).
5. J. Kobayashi, T. Shimizu and K. Inamura, *Chem. Lett.*, **21**, 211 (1992); <https://doi.org/10.1246/cl.1992.211>
6. F. Cavani, G. Centi, F. Parrinello and F. Trifiro, *Stud. Surf. Sci. Catal.*, **31**, 227 (1987).
7. F. Sondheimer and S. Wolfe, *Can. J. Chem.*, **37**, 1870 (1959); <https://doi.org/10.1139/v59-274>
8. A.A. Wismejer, A.P. Kieboom and H. van Bekkum, *Recl. Trav. Chim. Pays Bas*, **105**, 129 (1986); <https://doi.org/10.1002/recl.19861050406>
9. K. Heyns and H. Paulsen, *Newer Methods of Preparative Organic Chemistry*, Interscience: New York, vol. II, p. 303 (1963).
10. R. Egli and C.H. Eugster, *Helv. Chim. Acta*, **58**, 2321 (1975); <https://doi.org/10.1002/hlca.19750580814>
11. R.W. Clayton and S.V. Norval, *Catalysis*, **3**, 70 (1980); <https://doi.org/10.1039/9781847553140-00070>
12. A. Roberti, V. Ponce and W.M.H. Sachtler, *J. Catal.*, **28**, 381 (1973); [https://doi.org/10.1016/0021-9517\(73\)90131-0](https://doi.org/10.1016/0021-9517(73)90131-0)
13. H.A. Smith and R.G. Thompson, *Adv. Catal.*, **9**, 727 (1957); [https://doi.org/10.1016/S0360-0564\(08\)60225-4](https://doi.org/10.1016/S0360-0564(08)60225-4)
14. P.N. Rylander, N. Rakonczka, D. Steele and M. Bollinger, *Engelhard Ind. Tech. Bull.*, **4**, 95 (1963).
15. W. Reeve and J. Christian, *J. Am. Chem. Soc.*, **78**, 860 (1956); <https://doi.org/10.1021/ja01585a042>
16. A.A. Alshaheri, M.I.M. Tahir, M.B.A. Rahman, T.B.S.A. Ravooof and T.A. Saleh, *Chem. Eng. J.*, **327**, 423 (2017); <https://doi.org/10.1016/j.cej.2017.06.116>
17. R.L. Augustine, *Heterogeneous Catalysis for the Synthetic Chemist*, Marcel Dekker: New York, p. 153 (1996).
18. S. Bernal, J.J. Calvino, M.A. Cauqui, J.M. Gatica, C. Larese, J.A. Pérez Omil and J.M. Pintado, *Catal. Today*, **50**, 175 (1999); [https://doi.org/10.1016/S0920-5861\(98\)00503-3](https://doi.org/10.1016/S0920-5861(98)00503-3)
19. S. Bernal, J.J. Calvino, M.A. Cauqui, J.M. Gatica, C. Larese, J.A. Pérez Omil and J.M. Pintado, *Appl. Catal. A Gen.*, **209**, 125 (2001); [https://doi.org/10.1016/S0926-860X\(00\)00750-X](https://doi.org/10.1016/S0926-860X(00)00750-X)
20. E.L. Pires, J.C. Magalhaes and U. Schuchardt, *Appl. Catal. A Gen.*, **203**, 231 (2000); [https://doi.org/10.1016/S0926-860X\(00\)00496-8](https://doi.org/10.1016/S0926-860X(00)00496-8)
21. R.S. da Cruz, J.M. de Souza e Silva, U.I. Arnold and U. Schuchardt, *J. Mol. Catal. Chem.*, **171**, 251 (2001); [https://doi.org/10.1016/S1381-1169\(01\)00111-X](https://doi.org/10.1016/S1381-1169(01)00111-X)
22. Kirk-Othmer, *Encyclopedia of Chemical Technology*, Wiley: New York, edn 4 (1991).
23. H. Pines, *The Chemistry of Catalytic Hydrocarbon Conversions*, Academic Press: New York (1981).
24. N.Y. Chen, W.E. Garwood and R.H. Heck, *Ind. Eng. Chem. Process Des. Dev.*, **26**, 706 (1987); <https://doi.org/10.1021/ie00064a014>
25. F.G. Dwyer and P.J. Lewis, in eds.: J.J. McKetta and W.A. Cunningham, *Encyclopedia of Chemical Processing and Design*, Marcel Dekker: New York, vol. 20, p. 77 (1997).
26. G. Ertl, H. Knozinger and J. Weitkamp, in: *Hand book of Heterogeneous Catalysis*, Marcel Dekker, New York, vol. 5 (1995).
27. G.A. Olah, *Fridel-Crafts Chemistry*, Wiley: New York (1973).
28. W.L. Lenneman, R.D. Hites and V.I. Komarewsky, *J. Org. Chem.*, **19**, 463 (1954); <https://doi.org/10.1021/jo01368a028>
29. M.B. Welch, Zinc Aluminate Double Bond Isomerization Catalyst and Process for its Production, US Patent 4692430 (1986).
30. P. Wimmer, H.-J. Buysch and L. Puppe, Process for the Preparation of Thymol, US Patent 5030770 (1991).
31. S. Velu and S. Sivasanker, *Res. Chem. Intermed.*, **24**, 657 (1998); <https://doi.org/10.1163/156856798X00555>
32. J. Stell, *Oil Gas J.*, **99**, 74 (2001).
33. J. Weitkamp and Y. Traa, in eds.: G. Ertl, H. Knozinger and J. Weitkamp, *Handbook of Heterogeneous Catalysis*, VCH: Weinheim, vol. 4, p. 2039 (1997).
34. K.K. Kearby in eds.: P. Emmett, *Catalysis*, Rheinhold: New York, vol. III, p. 469 (1955).
35. E.H. Lee, *Catal. Rev.*, **8**, 285 (1974); <https://doi.org/10.1080/01614947408071864>
36. R. Connor, K. Folkers and H. Adkins, *J. Am. Chem. Soc.*, **54**, 1138 (1932); <https://doi.org/10.1021/ja01342a042>
37. A.H. Blatt, *Organic Syntheses*, vol. 2, p. 142 (1943).
38. K. Weissermel and H.J. Arpe, *Industrielle Organische Chemie*, VCH, Weinheim, edn 4 (1994).
39. T. Hirano, *Appl. Catal.*, **26**, 81 (1986); [https://doi.org/10.1016/S0166-9834\(00\)82543-9](https://doi.org/10.1016/S0166-9834(00)82543-9)
40. I.E. Wachs and R.J. Madix, *Surf. Sci.*, **76**, 531 (1978); [https://doi.org/10.1016/0039-6028\(78\)90113-9](https://doi.org/10.1016/0039-6028(78)90113-9)
41. M.A. Barteau, M. Bowker and R.J. Madix, *Surf. Sci.*, **94**, 303 (1980); [https://doi.org/10.1016/0039-6028\(80\)90009-6](https://doi.org/10.1016/0039-6028(80)90009-6)
42. T. Mallat, T. Allmendinger and A. Baiker, *Appl. Surf. Sci.*, **52**, 189 (1991); [https://doi.org/10.1016/0169-4332\(91\)90047-N](https://doi.org/10.1016/0169-4332(91)90047-N)
43. T. Mallat, E. Orglmeister and A. Baiker, *Chem. Rev.*, **107**, 4863 (2007); <https://doi.org/10.1021/cr0683663>
44. J. Wang, L. Huang and Q. Li, *Appl. Catal. A Gen.*, **175**, 191 (1998); [https://doi.org/10.1016/S0926-860X\(98\)00216-6](https://doi.org/10.1016/S0926-860X(98)00216-6)
45. B. Cornils and E. Wiebus, *Chemtech*, 33 (1999).
46. V.L. Khilnani and S.B. Chandalia, *Org. Process Res. Dev.*, **5**, 257 (2001); <https://doi.org/10.1021/op9900380>
47. H. Adkins and G. Krsek, *J. Am. Chem. Soc.*, **70**, 412 (1948); <https://doi.org/10.1021/ja01181a501>
48. M. Yadav and R.K. Sharma, *Curr. Opin. Green Sustain. Chem.*, **15**, 47 (2019); <https://doi.org/10.1016/j.cogsc.2018.08.010>
49. Y. Urushibara, *Bull. Chem. Soc. Jpn.*, **26**, 280 (1952); <https://doi.org/10.1246/bcsj.25.280>
50. A.M. Bennett and A.P. Longstaff, *Chem. Ind.*, 846 (1965).
51. A.J. Birch and D.H. Williamson, *Organic Reactions*, 24 (1976).
52. B.R. James, *Homogeneous Hydrogenation*, John Wiley & Sons: New York, (1973).
53. R.H. Crabtree, *Acc. Chem. Res.*, **12**, 331 (1979).
54. J.H. Kang, L.D. Menard, R.G. Nuzzo and A.I. Frenkel, *J. Am. Chem. Soc.*, **128**, 12068 (2006); <https://doi.org/10.1021/ja064207p>
55. P. Ehrburger and P.L. Walker, *J. Catal.*, **55**, 63 (1978); [https://doi.org/10.1016/0021-9517\(78\)90187-2](https://doi.org/10.1016/0021-9517(78)90187-2)
56. W.F. Newhall, *J. Org. Chem.*, **23**, 1274 (1958); <https://doi.org/10.1021/jo01103a009>
57. J.W. Bozzelli, Y.M. Chen and S.C. Chuang, *Chem. Eng. Commun.*, **115**, 1 (1992); <https://doi.org/10.1080/00986449208936024>
58. R.A. Sheldon and J.K. Kochi, *Metal Catalyzed Oxidations of Organic Compounds*, Academic Press: New York (1981).
59. R.A. Sheldon and R.S. Downing, *Appl. Catal. A Gen.*, **189**, 163 (1999); [https://doi.org/10.1016/S0926-860X\(99\)00274-4](https://doi.org/10.1016/S0926-860X(99)00274-4)
60. R.L. Augustine, *Catalytic Hydrogenation, Techniques and Application in Organic Synthesis*, Dekker: New York (1965).
61. S. Parashar and S. Khare, *React. Kinet. Mech. Catal.*, **127**, 469 (2019); <https://doi.org/10.1007/s1144-019-01559-z>
62. R.L. Augustine, *Catal. Rev.*, **13**, 285 (1976); <https://doi.org/10.1080/00087647608069940>
63. P.N. Rylander, in: *Hydrogenation Methods*, Academic Press: New York (1985).
64. M. Freifelder, *Practical Catalytic Hydrogenation*, Wiley-Interscience: New York (1971).
65. A.P.G. Kieboom and F. van Rantwijk, *Hydrogenation and Hydrogenolysis in Synthetic Organic Chemistry*, Delft University Press, Delft (1977).
66. F. Zaera, *ACS Catal.*, **7**, 4947 (2017); <https://doi.org/10.1021/acscatal.7b01368>
67. S.A. Mahood and P.V. Schaffner, in eds.: A. H. Blatt, *Organic Synthesis*, Wiley: New York, vol. 11, p. 160 (1969).
68. O. Kamm, in eds.: A.H. Blatt, *Organic Synthesis*, Wiley: New York, vol. 11, p. 445 (1948).
69. H.E. Bigelow and D.B. Robinson, in eds.: E.C. Horning: *Organic Synthesis*, Chapman and Half Loncn, vol. 111, p. 103 (1955).
70. H.E. Bigelow and A. Palmer, in eds.: A.H. Blatt, *Organic Syntheses*, Wiley: New York, vol. 11, p. 57 (1969).

71. H. Hattori, *Chem. Rev.*, **95**, 537 (1995); <https://doi.org/10.1021/cr00035a005>
72. T. Punniyamurthy, S. Velusamy and J. Iqbal, *Chem. Rev.*, **105**, 2329 (2005); <https://doi.org/10.1021/cr050523v>
73. G. Gilman and G. Cohn, *Adv. Catal.*, **9**, 733 (1957); [https://doi.org/10.1016/S0360-0564\(08\)60226-6](https://doi.org/10.1016/S0360-0564(08)60226-6)
74. H. Hauptmann and W.F. Walter, *Chem. Rev.*, **62**, 347 (1962); <https://doi.org/10.1021/cr60219a001>
75. H. Adkins, *Organic Reaction*, vol. VIII, p. 1 (1994).
76. R.A.W. Johnstone, A.H. Wilby and I.D. Entwistle, *Chem. Rev.*, **85**, 129 (1985); <https://doi.org/10.1021/cr00066a003>
77. J.R. Weir, B.A. Patel and F.R. Heck, *J. Org. Chem.*, **45**, 4926 (1980); <https://doi.org/10.1021/jo01312a021>
78. W. Zhou, J.M. Thomas, D.S. Shephard, B.F.G. Johnson, D. Ozkaya, T. Maschmeyer, R.G. Bell and Q. Ge, *Science*, **280**, 705 (1998); <https://doi.org/10.1126/science.280.5364.705>
79. V. Hulea, D. Brunel, A. Galarneau, K. Philippot, B. Chaudret, P.J. Kooyman and F. Fajula, *Micropor. Mesopor. Mater.*, **79**, 185 (2005); <https://doi.org/10.1016/j.micromeso.2004.10.041>
80. C.M. Ho, W.Y. Yu and C.M. Che, *Angew. Chem. Int. Ed.*, **43**, 3303 (2004); <https://doi.org/10.1002/anie.200453703>
81. L. Fabre, P. Gallezot and A. Perrard, *J. Catal.*, **208**, 247 (2002); <https://doi.org/10.1006/jcat.2002.3567>
82. E. Crezee, B.W. Hoffer, R.J. Berger, M. Makkee, F. Kapteijn, A. Jacob and J.A. Moulijn, *Appl. Catal. A Gen.*, **251**, 1 (2003); [https://doi.org/10.1016/S0926-860X\(03\)00587-8](https://doi.org/10.1016/S0926-860X(03)00587-8)
83. M.L. Kantam, B.P.C. Rao, B.M. Choudary and B. Sreedhar, *Adv. Synth. Catal.*, **348**, 1970 (2006); <https://doi.org/10.1002/adsc.200505497>
84. B. Kusserow, S. Schimpf and P. Claus, *Adv. Synth. Catal.*, **345**, 289 (2003); <https://doi.org/10.1002/adsc.200390024>
85. A.T. Bell, *Science*, **299**, 1688 (2003); <https://doi.org/10.1126/science.1083671>
86. J. Zhang, K. Sasaki, E. Sutter and R.R. Adzic, *Science*, **315**, 220 (2007); <https://doi.org/10.1126/science.1134569>
87. V.R. Stamenkovic, B. Fowler, B.S. Mun, G. Wang, P.N. Ross, C.A. Lucas and N.M. Markovic, *Science*, **315**, 493 (2007); <https://doi.org/10.1126/science.1135941>
88. S.H. Joo, S.J. Choi, I. Oh, J. Kwak, Z. Liu, O. Terasaki and R. Ryoo, *Nature*, **412**, 169 (2001); <https://doi.org/10.1038/35084046>
89. T.W. Hansen, J.B. Wagner, P.L. Hansen, S. Dahl, H. Topsøe and C.J.H. Jacobsen, *Science*, **294**, 1508 (2001); <https://doi.org/10.1126/science.1064399>
90. R. Mistri, J. Llorca, B.C. Ray and A. Gayen, *J. Mol. Catal. Chem.*, **376**, 111 (2013); <https://doi.org/10.1016/j.molcata.2013.04.018>
91. Q. Fu, H. Saltsburg and M. Flytzani-Stephanopoulos, *Science*, **301**, 935 (2003); <https://doi.org/10.1126/science.1085721>
92. J.V. Porcelli, *Catal. Rev.*, **23**, 151 (1981); <https://doi.org/10.1080/03602458108068073>
93. W.M.H. Sachtler, C. Backx and R.A. Van Santen, *Catal. Rev.*, **23**, 127 (1981); <https://doi.org/10.1080/03602458108068072>
94. R.K. Grasselli, *ACS Symp. Ser.*, **222**, 317 (1983); <https://doi.org/10.1021/bk-1983-0222.ch025>
95. M.G. Noppenhuis, A. Baiker, P. Barnickel and A. Wokaun, *Appl. Catal. A Gen.*, **85**, 157 (1992); [https://doi.org/10.1016/0926-860X\(92\)80149-7](https://doi.org/10.1016/0926-860X(92)80149-7)
96. A. Sakthivel and P. Selvam, *J. Catal.*, **211**, 134 (2002); [https://doi.org/10.1016/S0021-9517\(02\)93711-5](https://doi.org/10.1016/S0021-9517(02)93711-5)
97. M.L. Neidig and K.F. Hirsekorn, *Catal. Comm.*, **12**, 480 (2011); <https://doi.org/10.1016/j.catcom.2010.10.024>
98. R.A. Sheldon, *Top. Curr. Chem.*, **164**, 21 (1993); https://doi.org/10.1007/3-540-56252-4_23
99. P.A. MacFaul, I.W.C.E. Arends, K.U. Ingold and D.D.M. Wayner, *J. Chem. Soc., Perkin Trans. II*, 135 (1997); <https://doi.org/10.1039/a606160e>
100. I.W.C.E. Arends, K.U. Ingold and D.D.M. Wayner, *J. Am. Chem. Soc.*, **117**, 4710 (1995); <https://doi.org/10.1021/ja00121a031>
101. R.A. Sheldon, in eds.: R. Ugo, *Aspect of Homogeneous Catalysis*, Reidel, Dordrecht, vol. 4, p. 1 (1981).
102. J. Sobczak and J.J. Ziolkowski, *React. Kinet. Catal. Lett.*, **11**, 359 (1979); <https://doi.org/10.1007/BF02079726>
103. R.A. Sheldon, in eds.: S. Patai, *The Chemistry of Functional Groups-Peroxides*, Wiley: New York, p. 161 (1982).
104. R.A. Sheldon and J. Dakka, *Catal. Today*, **19**, 215 (1994); [https://doi.org/10.1016/0920-5861\(94\)80186-X](https://doi.org/10.1016/0920-5861(94)80186-X)
105. M.G. Clerici, *Stud. Surf. Sci. Catal.*, **78**, 21 (1993); [https://doi.org/10.1016/S0167-2991\(08\)63301-7](https://doi.org/10.1016/S0167-2991(08)63301-7)
106. C. Ferrini and H.W. Kouwenhoven, *Stud. Surf. Sci. Catal.*, **55**, 53 (1990); [https://doi.org/10.1016/S0167-2991\(08\)60133-0](https://doi.org/10.1016/S0167-2991(08)60133-0)
107. N.K. Renuka, *J. Mol. Catal. Chem.*, **316**, 126 (2010); <https://doi.org/10.1016/j.molcata.2009.10.010>
108. H.H. Monfared and Z. Amouei, *J. Mol. Catal. Chem.*, **217**, 161 (2004); <https://doi.org/10.1016/j.molcata.2004.03.020>
109. H. Kanzaki, T. Kitamura, R. Hamada, S. Nishiyama and S. Tsuruya, *J. Mol. Catal. Chem.*, **208**, 203 (2004); [https://doi.org/10.1016/S1381-1169\(03\)00516-8](https://doi.org/10.1016/S1381-1169(03)00516-8)
110. J. Okamura, S. Nishiyama, S. Tsuruya and M. Masai, *J. Mol. Catal. Chem.*, **135**, 133 (1998); [https://doi.org/10.1016/S1381-1169\(97\)00298-7](https://doi.org/10.1016/S1381-1169(97)00298-7)
111. K. Heynes and H. Paulsen, in eds.: W. Forest and F.K. Kirchner, *Newer Methods of Preparative Organic Chemistry*, Academic Press: New York, vol. 2, p. 303 (1963).
112. M. Boudart, A. Aldag, J.E. Benson, N.A. Dougharty and C. Girvin Harkins, *J. Catal.*, **6**, 92 (1966); [https://doi.org/10.1016/0021-9517\(66\)90113-8](https://doi.org/10.1016/0021-9517(66)90113-8)
113. T. Mallat and A. Baiker, *Catal. Today*, **19**, 247 (1994); [https://doi.org/10.1016/0920-5861\(94\)80187-8](https://doi.org/10.1016/0920-5861(94)80187-8)
114. T. Mallat and A. Baiker, *Appl. Catal. A Gen.*, **79**, 41 (1991); [https://doi.org/10.1016/0926-860X\(91\)85005-1](https://doi.org/10.1016/0926-860X(91)85005-1)
115. T. Mallat, A. Baiker and L. Botz, *Appl. Catal. A Gen.*, **86**, 147 (1992); [https://doi.org/10.1016/0926-860X\(92\)85145-2](https://doi.org/10.1016/0926-860X(92)85145-2)
116. T. Miyahara, H. Kanzaki, R. Hamada, S. Kuroiwa, S. Nishiyama and S. Tsuruya, *J. Mol. Catal. Chem.*, **176**, 141 (2001); [https://doi.org/10.1016/S1381-1169\(01\)00242-4](https://doi.org/10.1016/S1381-1169(01)00242-4)
117. I.W.C.E. Arends and R.A. Sheldon, *Appl. Catal. A Gen.*, **212**, 175 (2001); [https://doi.org/10.1016/S0926-860X\(00\)00855-3](https://doi.org/10.1016/S0926-860X(00)00855-3)
118. X. Liu, J. He, L. Yang, Y. Wang, S. Zhang, W. Wang and J. Wang, *Catal. Commun.*, **11**, 710 (2010); <https://doi.org/10.1016/j.catcom.2010.01.026>
119. K.T. Makhmudov, R.A. Alieva, S.R. Gadzhieva and F.M. Chyragov, *J. Anal. Chem.*, **63**, 435 (2008); <https://doi.org/10.1134/S1061934808050055>
120. L. Lin, J. Liuyan and W. Yunyang, *Catal. Commun.*, **9**, 1379 (2008); <https://doi.org/10.1016/j.catcom.2007.11.041>
121. M.R. Morales, B.P. Barbero and L.E. Cadus, *Appl. Catal. B*, **74**, 1 (2007); <https://doi.org/10.1016/j.apcatb.2007.01.008>
122. H. Liu, Z. Fu, D. Yin, D. Yin and H. Liao, *Catal. Commun.*, **6**, 638 (2005); <https://doi.org/10.1016/j.catcom.2005.06.002>
123. S.K. Pardeshi and R.Y. Pawar, *Mater. Res. Bull.*, **45**, 609 (2010); <https://doi.org/10.1016/j.materresbull.2010.01.011>
124. J.W. Geus, *Stud. Surf. Sci. Catal.*, **16**, 1 (1983); [https://doi.org/10.1016/S0167-2991\(09\)60006-9](https://doi.org/10.1016/S0167-2991(09)60006-9)
125. G.C. Bond, *Acc. Chem. Res.*, **26**, 490 (1993); <https://doi.org/10.1021/ar00033a006>
126. F.J. Janssen, in eds.: G. Ertl, H. Knozinger and J. Weitkamp, *Hand Book of Heterogeneous Catalysis*, VCH, Weinheim, vol. 1, p.191 (1997).
127. G. Y. adachi and T. Masui, in eds.: A. Trovarelli, *Catalysis by Ceria and Related Materials*, Imperial College Press: London, p. 52 (2002).
128. M.M.A. Sekar, S.S. Manoharan and K.C. Patil, *J. Mater. Sci. Lett.*, **9**, 1205 (1990); <https://doi.org/10.1007/BF00721893>

129. K.C. Patil, S.T. Aruna and S. Ekambaram, *Curr. Opin. Solid State Mater. Sci.*, **2**, 158 (1997);
[https://doi.org/10.1016/S1359-0286\(97\)80060-5](https://doi.org/10.1016/S1359-0286(97)80060-5)
130. K. Suresh and K.C. Patil, eds.: K.J. Rao, Perspective in Solid State Chemistry, Narosa Publishing House: New Delhi, p. 376 (1995).
131. A. Gayen, K.R. Priolkar, P.R. Sarode, V. Jayaram, M.S. Hegde, G.N. Subbanna and S. Emur, *Chem. Mater.*, **16**, 2317 (2004);
<https://doi.org/10.1021/cm040126l>
132. G.C. Bond and R. Burch, eds.: G.C. Bond and G. Webb, A Specialist Periodical Report: Catalysis, The Royal Society of Chemistry, London, vol. 6, 27 (1983).
133. S.A. Stevenson, G.B. Raupp, J.A. Dumesic, S.J. Tauster and R.T.K. Baker, eds.: S.A. Stevenson, G.B. Raupp, J.A. Dumesic, S.J. Tauster R.T.K. Baker and E. Ruckenstein, Metal-Support Interaction in Catalysis, Sintering and Redispersion, Van Nostrand-Reinhold, New York, p. 3, (1987).
134. J.G. Dickson, L. Katz and R. Ward, *J. Am. Chem. Soc.*, **83**, 3026 (1958);
<https://doi.org/10.1021/ja01475a012>
135. J.H. Sinfelt, *J. Phys. Chem.*, **68**, 344 (1964);
<https://doi.org/10.1021/j100784a023>
136. G.M. Schwab, *Advances Catalysis*, Academic Press: Orlando, FL, vol. 1, (1978).
137. G.C. Bond, *Metal-Support and Metal Additive Effect in Catalysis*, Elsevier Scientific Pub. Co.: Amsterdam, (1982).
138. S.J. Tauster, S.C. Fung and P.L. Garten, *J. Am. Chem. Soc.*, **100**, 170 (1978);
<https://doi.org/10.1021/ja00469a029>
139. L.E. Oi, M.-Y. Choo, H.V. Lee, H.C. Ong, S.B.A. Hamid and J.C. Juan, *RSC Advances*, **6**, 108741 (2016);
<https://doi.org/10.1039/C6RA22894A>
140. A.K. Datye, D. Kalakkad, M.H. Yao and D.J. Smith, *J. Catal.*, **155**, 148 (1995);
<https://doi.org/10.1006/jcat.1995.1196>
141. C. Hardacre, R.M. Ormerod and R.M. Lambert, *J. Phys. Chem.*, **98**, 10901 (1994);
<https://doi.org/10.1021/j100093a036>
142. S. Bernal, G. Blanco, J.M. Gatica, C. Larese and H. Vidal, *J. Catal.*, **200**, 411 (2001);
<https://doi.org/10.1006/jcat.2001.3210>
143. S. Penner, D. Wang, D.S. Su, G. Rupprechter, R. Podloucky, R. Schlögl and K. Hayek, *Surf. Sci.*, **532-535**, 276 (2003);
[https://doi.org/10.1016/S0039-6028\(03\)00198-5](https://doi.org/10.1016/S0039-6028(03)00198-5)
144. N.R. Socolova, *Colloids Surf. A Physicochem. Eng. Asp.*, **239**, 125 (2004);
<https://doi.org/10.1016/j.colsurfa.2003.11.037>
145. K.D. Ghuge and G.P. Babu, *J. Catal.*, **151**, 453 (1995);
<https://doi.org/10.1006/jcat.1995.1047>
146. D.C. Koningsberger and M. Vaarkamp, *Physica B*, **208-209**, 633 (1995);
[https://doi.org/10.1016/0921-4526\(94\)00776-R](https://doi.org/10.1016/0921-4526(94)00776-R)
147. D.E. Ramaker, J. de Graaf, J.A.R. van Veen and D.C. Koningsberger, *J. Catal.*, **203**, 7 (2001);
<https://doi.org/10.1006/jcat.2001.3299>
148. H. Praliaud, *J. Catal.*, **72**, 394 (1981);
[https://doi.org/10.1016/0021-9517\(81\)90028-2](https://doi.org/10.1016/0021-9517(81)90028-2)
149. T. Ren-Yuam, W. Rong-An and L. Li-Wu, *Appl. Catal.*, **10**, 163 (1984);
[https://doi.org/10.1016/0166-9834\(84\)80101-3](https://doi.org/10.1016/0166-9834(84)80101-3)
150. J.P. Belzunegui, J. Sanz and J.M. Rojo, *J. Am. Chem. Soc.*, **112**, 4066 (1990);
<https://doi.org/10.1021/ja00166a069>
151. J.P. Belzunegui, J. Sanz and J.M. Rojo, *J. Am. Chem. Soc.*, **114**, 6749 (1992);
<https://doi.org/10.1021/ja00043a019>
152. S.A. Stevenson, G.B. Raupp, J.A. Dumesic, S.J. Tauster and R.T.K. Baker, eds.: S.A. Stevenson, G.B. Raupp, J.A. Dumesic, S.J. Tauster R.T.K. Baker and E. Ruckenstein, Metal-Support Interaction in Catalysis, Sintering and Redispersion, Van Nostrand-Reinhold: New York, p. 77 (1987).
153. S.J. Tauster, eds.: R.T. Baker, S.J. Tuaster and J.A. Dumesic, Strong Metal-Support Interactions, ACS Symposium, Series No. 298, ACS, Washington DC, p. 1 (1986).

Contents lists available at [ScienceDirect](#)

International Journal of Geoheritage and Parks

journal homepage: <http://www.keaipublishing.com/en/journals/international-journal-of-geoheritage-and-parks/>

Exploring the potential for development of Geotourism in Rarh Bengal, Eastern India using M-GAM

Manoj Kumar Mahato*, Narayan Chandra Jana

Department of Geography, The University of Burdwan, West Bengal, India

ARTICLE INFO

Article history:

Received 28 September 2020

Received in revised form 21 April 2021

Accepted 19 May 2021

Available online xxxxx

Keywords:

Rarh Bengal

Geotourism

Geosites

Potential

Modified Geosite assessment model

ABSTRACT

The Rarh Bengal of India has huge potential for development of geotourism due to its diverse landscape consisting of hills, dome shaped inselbergs, tors, dams, badlands, springs, waterfall, ravines etc. The combination of vast dense forest and diverse flora and fauna with various geomorphic features has created a prosperous and complex geodiversity in the Rarh region. However, the potential of geotourism in the region has not yet fully developed. The main objective of this study is to emphasize the potential for geotourism in the Rarh region of West Bengal and to determine the existing status and geotourism prospective of geosites in this region. In this paper, the authors have proposed an inventory of geosites in the Rarh region and analyzed the vast potential of geotourism among them. A comparative analysis of the selected sites has been carried out by applying the Modified Geosite Assessment Model (M-GAM), which has exposed the most suitable geosites for the development of future geotourism. The M-GAM provided the significant assessment of both Main Values and Additional Values of the sites according to the status of each sub-indicator in the valuation model assumed by tourists. The results of this study reveal information about the major aspects of the development of each geosites and identify which sites need more attention and better management in future, so that the region becomes much attractive to larger number of tourists and becomes a well-known geotourism destination.

© 2021 Beijing Normal University. Publishing services by Elsevier B.V. on behalf of KeAi Communications Co. Ltd. This is an open access article under the CC BY-NC-ND license (<http://creativecommons.org/licenses/by-nc-nd/4.0/>).

1. Introduction

The “geotourism: approach was developed in the late 1980s after the recognition by the geologists of schools, universities and museums in United Kingdom (Hose, Markovi, Komac, & Zorn, 2011). The term “geotourism” has been invented rather recently and was first coined in 1995 by Thomas A Hose, Professor of Earth Science at the University of Bristol in the United Kingdom (Antic & Tomic, 2017; Grover & Mahanta, 2018). According to Thomas A Hose (2005), the definition of geotourism is “to ensure the value and social preservation of geological and geomorphological sites and their materials and to provide interpretative facilities and services for the use of students, tourists and other casual recreationalists” (Hose, 2005, p 27; Hose, 1997, p 2955). This definition clearly represents that the key focus of geotourism is on interpretation, promotion and preservation, which are all significant elements for the development of geotourism. According to Newsome and Dowling (2010), geotourism is an arrangement of natural area tourism that specially focuses on landscape and geology and their interpretation, promotion and conservation with the help

* Corresponding author.

E-mail address: mahatomanojkumar16@gmail.com. (M.K. Mahato).

<https://doi.org/10.1016/j.ijgeop.2021.05.002>

2577-4441/© 2021 Beijing Normal University. Publishing services by Elsevier B.V. on behalf of KeAi Communications Co. Ltd. This is an open access article under the CC BY-NC-ND license (<http://creativecommons.org/licenses/by-nc-nd/4.0/>).

Please cite this article as: M.K. Mahato and N.C. Jana, Exploring the potential for development of Geotourism in Rarh Bengal, Eastern India using M-GAM, International Journal of Geoheritage and Parks, <https://doi.org/10.1016/j.ijgeop.2021.05.002>

of appreciation and education. The definition of geotourism has evolved throughout the years, and Hose and Vasiljevic gave an updated version of definition in 2012 (Jonic, 2018). According to them “geotourism is the providing of informative and service facilities for geosites and geomorphosites and their surrounding topography together through their allied in-situ and ex-situ artifacts, to build of constituency for their conservation by making appreciation, learning and research for current and future generations” (Hose & Vasiljevic, 2012, p 25; Jonic, 2018, p 113). The definition and the approach of geotourism (Hose, 1995) was accepted and endorsed by UNESCO in its preliminary geopark documentation (Hose et al., 2011; Patzack & Eder, 1998).

Geotourism is a nature of tourism that renovates its activities (Pereira, da Cunha, & Nascimento, 2018), involving abiotic ingredients (geology, landscape, geomorphic forms, climate etc.), biotic components (flora & fauna) and culture (Dowling, 2013; Wulung & Rajoendah, 2019). Geotourism is a comparatively new phenomenon based on old ideas about tourism and belongs to a category of special interest tourism (Antic & Tomic, 2017). In the general sense, geotourism signifies the upgrade and protection of geological heritage care of tourism through the education and interpretation (Tomic, 2016). This is a new emerging type of tourism that environmentally innovative (Dowling, 2013). It promotes geosites into a tourist destination and preserves the geodiversity with the understanding of earth science. It has been proposed that greater concentration should be given to environmentally innovative forms of tourism, which encourage both environmental and social obligation (Paskova, 2012). Geotourists travel individually or in groups and they may visit whether these are natural areas or built-up areas, they opt the areas that have geological attraction for tourism.

Rarh Bengal Region is a toponym for an area in the Indian subcontinent (Faridi, 2013), which lies between the Ganges Delta on the east and Chhotanagpur Plateau on the west. The Rarh Bengal Region is very rich in terms of geodiversity existing in numerous forms. This province is very rich with numerous hills, dome-shaped inselbergs, tors, dams, badlands, springs, waterfall and ravines, which is located in a relatively small area. Besides, this territory is well-known lateritic landscape endowed with lots of geoarchaeological sites (Chakrabarty & Mandal, 2019). These sites are outstanding representatives of this area's geodiversity. Geotourism sites usually consist of all geological, geomorphological and pedological values produced through the formation of the Earth's crust (Djurovic & Mijovic, 2006). All of these values are being present in the region of Rarh Bengal in India, which has made this territory extremely promising for the development of geotourism in the future. Therefore, we can say that the Rarh Bengal Region is underdeveloped in agriculture and industry, if geotourism was developed here, the region may be economically dependent on the combined influence of agriculture, industry and geotourism.

The main objective of this study is to explore the potential of geotourism in the Rarh Bengal of eastern India and to identify the most suitable geosites for the development of geotourism. This study is based on the Modified Geosite Assessment Model (M-GAM) provided by Tomic and Bozic (2014). M-GAM is a modified version of GAM (Geosite Assessment Model) by Vujicic et al. (2011), where incorporate the opinions of the visitors or tourists (Pal & Albert, 2018; Tomic & Bozic, 2014). M-GAM has been used to compare the existing status of selected sites and compare their geotourism potential.

This model has been applied to eleven geosites in the Rarh Bengal of eastern India. The results of the analysis provide information on major areas of improvement and identify which areas need more attention and better management in future so that the region can become a recognized geotourism destination, which will be able to mesmerize a large number of tourists in the future years to come. So keeping in view of the above discussion, this paper has given emphasis an enquiry about how the geosites are more potential for geotourism in Rarh Bengal.

2. Materials and methods

2.1. Study area

Rarh Bengal is a major part of the physiographical divisions of West Bengal, which lies between the Chhotanagpur Plateau in the west of India and the Ganges Delta in the east of India. The Rarh Bengal is located in the southwestern part of the Indian state of West Bengal, bounded by latitudes of 21°39'43" N to 24°35'51"N and longitudes of 85°49'27" E to 88°28'43"E (Fig. 1). Purulia, Bankura, Jhargram, Birbhum, Paschim Bardhaman, Purba Bardhaman and Paschim Medinipur are located in Rarh Bengal. In addition, promotion of geotourism can generate employment opportunities for towards pandering rural economy in these districts of Rarh Bengal. Rarh Bengal is diversified with number of hills, dome-shaped inselbergs, tor topography, undulating upland, valleys, erosional plain and ravines; the regions is characterized by lateritic land surface and sub-tropical monsoon type of climate with very high day temperatures during the summer months reaching up to 47 °C (Purulia district in January 2020) (IMD, Kolkata). The region is not favorable for agricultural development and any capital-intensive industry due to the deficit of adequate water. However, the area has great potentially for tourism promotion (Chakrabarty & Mandal, 2018, 2019) because of its richness in terms of geodiversity existing in numerous forms.

The proposed geosites inventory comprises eleven geosites located throughout the Rarh Bengal in India (Fig. 1. & Table 1). In addition to these geosites, many other sites can be included in the geotourism activities. However, priority should be given to the eleven selected geosites at the initial stage of geotourism development in this region, as they already have some infrastructural necessities for tourism development along with their attractiveness and accessibility.

2.2. Methodology

The methodology of this study is based on the Modified Geosite Assessment Model (M-GAM), provided by Tomic and Bozic (2014). The M-GAM method has developed based on previous geosite assessment methods established by different authors

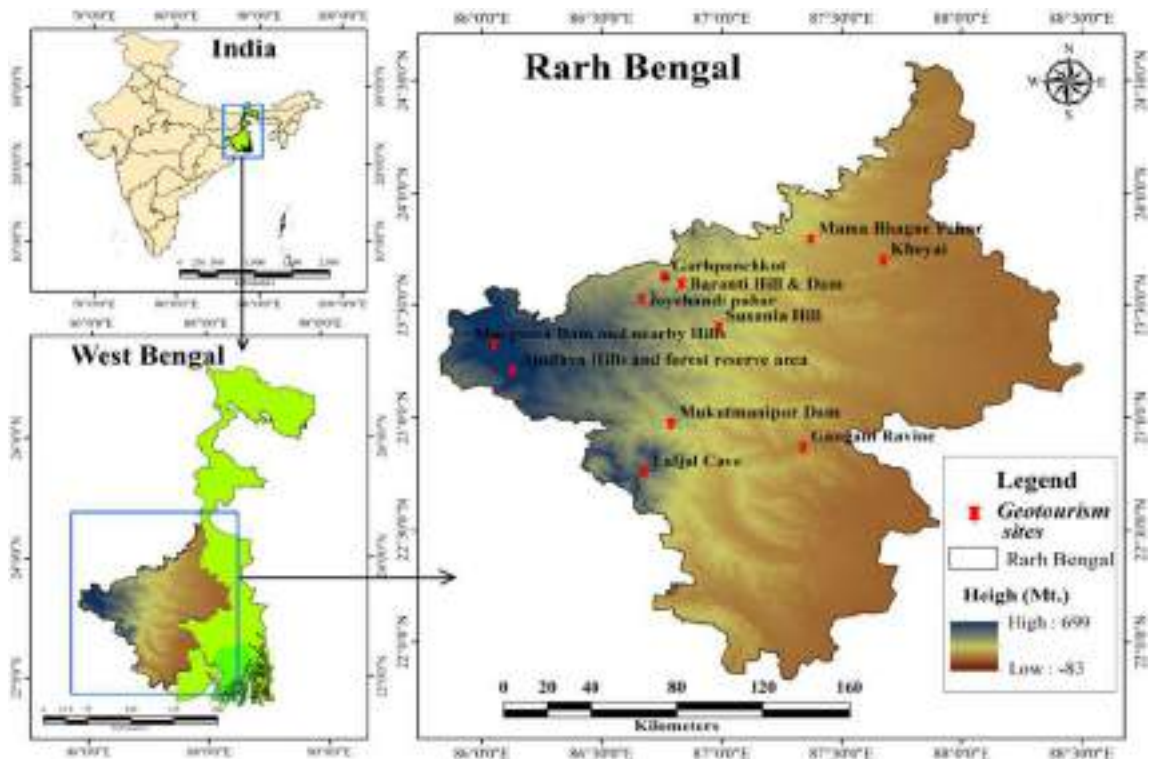


Fig. 1. Location of proposed geotourism sites of the Rarh Bengal.

Table 1

Proposed geosites in the Rarh Bengal of eastern India.

Geosites label	Geosites name	Geographical location
GS ₁	Ajodhya Hills and forest reserve area	23°06'25.53"N to 23°21'30.46"N 85°57'22.53"E to 86°14'08.87"E
GS ₂	Murguma Dam and nearby Hills	23°18'54.29"N to 86°03'01.24"E
GS ₃	Joychandi Pahar	23°31'21.07"N to 86°40'01.08"E
GS ₄	Baranti Hill & Dam	23°35'20.19"N to 86°49'58.16"E
GS ₅	Garhpanchkot	23°37'06.65"N to 86°45'45.60"E
GS ₆	Susunia Hill	23°23'42.51"N to 86°59'14.76"E
GS ₇	Mukutmanipur Dam	22°57'50.07"N to 86°47'20.39"E
GS ₈	Laljal Cave	22°44'55.24"N to 86°40'43.88"E
GS ₉	Gangani Ravine	22°51'28.68"N to 87°20'22.96"E
GS ₁₀	Khoyai	23°41'30.43"N to 87°40'23.32"E
GS ₁₁	Mama Bhagne Pahar	23°47'06.98"N to 87°22'19.50"E

(Bruschi & Cendrero, 2005; Coratza & Giusti, 2005; Erhartic, 2010; Hose, 1997; Jonic, 2018; Pereira, Pereira, & Caetano Alves, 2007; Pralong, 2005; Reynard, 2008; Reynard, Fontana, Kozlik, & Scapozza, 2007; Serrano & Gonzalez-Trueba, 2005; Tomic, 2011; Tomic, Markovic Slobodan, Antic, & Tesic, 2020; Vukovic & Antic, 2019). It combines the views of both side's tourists and experts with equal importance, in such a way, no one is favored in the evaluation process (Tomic et al., 2020; Vukovic & Antic, 2019). The M-GAM has been efficaciously tested and applied several times for the appraisalment of various geosites (Bozic, Tomic, & Pavic, 2014; Boskov et al., 2015; Antic & Tomic, 2017; Ticar et al., 2018; Vukoicic, Milosavljevic, Valjarevic, Nikolic, & Sreckovic-Batocanin, 2018; Antic, Tomic, & Markovic, 2019).

The M-GAM contains two basic indicators: Main Values (MV) and Additional Values (AV), which are furthermore divided into 12 and 15 sub-indicators respectively and each indicator is individually denoted by a value from 0.00 to 1.00. This category is created due to two common types of values: the Main Values - which are mostly generated by the natural properties of the geosite and the Additional Values - these are mostly human-induced and created by modifications in its use by visitors. The Main Values consist of three groups of sub-indicators: (i) scientific/educational values (VSE), (ii) scenic/aesthetic values (VSA) and (iii) protection (VPr). In addition, Additional Values are divided into two groups of sub-indicators: (iv) functional values (VFn) and (v) touristic values (VTr). The structure of indicators and sub-indicators of Main Values and Additional Values are shown in Table 2a and grades values in Table 2b.

Table 2a
The structure of M-GAM.

Indicators/Sub-indicators	Description
Main Values (MV)	
Scientific/Educational value (<i>VSE</i>)	
(1) Rarity	Number of closest identical sites
(2) Representativeness	Didactic and exemplary features of the site due to its own value and general configuration
(3) Knowledge on geoscientific issues	Number of papers written in recognized journals, theses, exhibitions and other publications
(4) Level of interpretation	Levels of explanatory potential on Geological and geomorphological processes, phenomena, shapes and stages of scientific knowledge
Scenic/Aesthetic values (<i>VSA</i>)	
(5) Viewpoints	Number of viewpoints accessible by pedestrian path. Everyone must present a specific perspective and be located less than 1 km from the site.
(6) Surface	Surface means the entire surface of the site. The quantitative relationship of each site with other sites is considered.
(7) Surrounding landscape and nature	The quality of the panoramic view, the presence of water body and natural vegetation, the absence of human-induced degradation, the vicinity of urban areas, etc.
(8) Environmental fitting of sites	The level of contrast with nature, the contrast of color, the presence of size and shapes, and so on.
Protection (<i>VPr</i>)	
(9) Current condition	Current state of geosite
(10) Protection level	State of protection by local groups, state govt., national govt., international organizations, etc.
(11) Vulnerability	Vulnerability level of geosite
(12) Suitable number of visitors	The proposed number of visitors entering the geosite at the same time according to the space, vulnerability and existing status of the geosite.
Additional values (AV)	
Functional values (<i>VFn</i>)	
(13) Accessibility	Opportunities of approaching to the site
(14) Additional natural values	Number of extra natural values in the radius of 5 km (geosites are also included)
(15) Additional anthropogenic values	Number of auxiliary anthropogenic values in the radius of 5 km
(16) Vicinity of emissive centers	Proximity to emissive centers
(17) Vicinity of important road network	Proximity to important road networks within a radius of 20 km
(18) Additional functional values	Parking services and facilities, gas station, mechanical facilities etc.
Touristic values (<i>VTr</i>)	
(19) Promotion	Level and number of promotional agencies and resources
(20) Organised visits	Total number of organised visits to the geosite annually
(21) Vicinity of visitors centers	Proximity to the visitor center on the geosite
(22) Interpretative panels	Interpretative features of text, graphics, size and volume of material, quality and decoration of surroundings etc.
(23) Number of visitors	Number of annual visitors
(24) Tourism infrastructure	Additional infrastructural facilities for tourists (internal pathways, resting spaces, drinking water facilities, garbage cans, toilets etc.)
(25) Tour guide service	If existing, their level of skill, knowledge of local and foreign languages (speaking), explanatory skills etc.
(26) Hostelry service	Hostelry service near to the geosite
(27) Restaurant service	Hotel and restaurant service near to the geosite

The sum of the grades 0.00 to 1.00 of the 12 sub-indicators of Main Values and 15 sub-indicators of Additional Values are defined using the following simple equation (Eq. 1):

$$M - GAM = MV + AV \tag{1}$$

Where, *MV* represents Main Values and *AV* represents Additional Values. Since the Main Values and Additional Values contain 3 and 2 groups of sub-indicators, so the values are determined by these two equation:

$$MV = VSE + VSA + VPr \tag{2}$$

$$AV = VFn + VTr \tag{3}$$

This model is done for each sub-indicator after which the values are added up according to the M-GAM equation but this time due to the adding of the importance factor (*Im*), it indicates a more objective and accurate result finally. Visitors in the same way like the experts, determine a numerical value of this parameter for the Main Values and Additional Values of each of these

Table 2b
Grades values of M-GAM.

Sub-indicators	Grades (0.00–1.00)				
	0.00	0.25	0.50	0.75	1.00
1	Common	Regional	National	International	The only occurrence
2	None	Low	Moderate	High	Utmost
3	None	Local publications	Regional publications	National publications	International publications
4	None	Processes are moderate level, but the detection is difficult to interpret to non-experts	Good examples of processes, but difficult to interpret to non-experts	Processes are moderate level, but easy to interpret to the average visitor	Good examples of processes and easy to interpret to the average visitor
5	None	1	2 to 3	4 to 6	> 6
6	Small	–	Medium	–	Large
7	–	Low	Medium	High	Utmost
8	Unfitting	–	Neutral	–	Fitting
9	Completely damaged (due to the various activities of human)	Extremely damaged (due to the natural processes)	Moderate level of damaged (with necessary geomorphological features are preserved)	Slightly damaged	No damage
10	None	Local	Regional	National	International
11	Irrevocable (with the probability of total loss)	High (can be damaged simply)	Moderate (can be damaged by any of the natural processes or human activity)	Less (can only be harmed by human activity)	None
12	0	1 to 10	11 to 20	21 to 50	> 50
13	Unreachable	Low (walking with special equipment through expert tourist guide)	Moderate (via bicycles and other means of transport that uses muscle power)	High (by car)	Utmost (by bus, train, helicopter, etc.)
14	None	1	2 to 3	4 to 6	> 6
15	None	1	2 to 3	4 to 6	> 6
16	> 100 km	100 to 50 km	50 to 25 km	25 to 5 km	< 5 km
17	None	Local	Regional	National	International
18	None	Low	Medium	High	Utmost
19	None	Local	Regional	National	International
20	None	< 12 per year	12 to 24 per year	24 to 48 per year	> 48 per year
21	> 50 km	50 to 20 km	20 to 5 km	5 to 1 km	< 1 km
22	None	Low quality	Medium quality	High quality	Utmost quality
23	None	Low (< 5000)	Medium (5001 to 10,000)	High (10,001 to 100,000)	Utmost (> 100,000)
24	None	Low	Medium	High	Utmost
25	None	Low	Medium	High	Utmost
26	>50 km	25 to 50 km	10 to 25 km	5 to 10 km	< 5 km
27	>25 km	10 to 25 km	5 to 10 km	1 to 5 km	< 1 km

sub-indicators. These numeric values are marked as 0.00, 0.25, 0.50, 0.75 and 1.00. The importance factor (*Im*) is determined as follows:

$$Im = \frac{\sum_{k=1}^K Iv_k}{K} \tag{4}$$

Where, *Iv_k* is the assessment or score for each sub-indicator given by a visitor, whereas *K* is total number of visitors. Here the value of *Im* can be any value from 0.00 to 1.00.

Finally, the equation of M-GAM is presented as follows:

$$M-GAM = MV + AV$$

Where, $MV = \sum_{i=1}^n Im_i * MV_i$ (5)

$$AV = \sum_{i=1}^n Im_i * AV_i \tag{6}$$

The M-GAM equation shows that the values of the *Im* of each sub-indicator determined individually by the visitors are multiplied by the values of each sub-indicator given by the experts. In this way, the value of each sub-indicator in the model is determined.

Survey was conducted in March 2019 to study various geotourist sites and calculated the importance factor (*Im*) for each sub-indicator in this model. The questionnaire contained 27 sub-indicators or questions and every visitor was questioned to rate the importance of all sub-indicator on a five-point Likert scale (ranging from 0.00 to 1.00), it was done in the same way as the experts did. A total of 164 visitors completed the questionnaire. However, the main fact is that all the geosites of Rarh Bengal have not yet become such a popular tourist destination and the analyzed Baranti hill and dam, Khoyai and Laljal cave are not visited by more than 500 visitors every year. Thus, it can be said that the size of the sample is sufficient for judgment and decision-making.

3. Results and discussion

For this study, previously described eleven geosites of the Rarh Bengal were evaluated by applying the M-GAM method. The final results of this assessment are shown in Tables 3 and 4 as well as in Fig. 2. The comprehensive analysis of the results is comprised the assessment of the Main Values and Additional Values of the geosites. The Main Values contain 12 sub-indicators of geosites associated with scientific/educational values (*VSE*), scenic/aesthetic values (*VSA*) and protection (*VPr*). The Additional Values contain 15 sub-indicators of geosites related to functional values (*VF_n*) and tourist values (*VTr*).

Table 4 and Fig. 2 show that the Main Values of Ajodhya Hills and forest reserve area is highest, which is 9.21, followed by Garhpanchkot is 9.00, Mukutmanipur Dam is 9.00 and Gangani Ravine is 8.65 respectively. All these geosites have extremely high scientific/educational values (*VSE*) and scenic/aesthetic values (*VSA*), especially in case of rarity (*SIMV₁*), representativeness (*SIMV₂*), level of interpretation (*SIMV₄*), viewpoints (*SIMV₅*), surrounding landscape and nature (*SIMV₇*) and environmental fitting of sites (*SIMV₈*); while *SIMV₂* and *SMIV₅* at Mukutmanipur Dam, *SIMV₄* at Garhpanchkot and *SIMV₅* at Gangani Ravine are slightly lower. These four geosites have the highest Main Values due to the high values of the importance factor (*Im*) for these sub-indicators. Although the Susunia Hill has the best in representativeness (*SIMV₂*), environmental fitting of sites (*SIMV₈*), accessibility (*SI_{AV₁}*), annual number of organised visits (*SI_{AV₈}*) and tourism infrastructure (*SI_{AV₁₂}*), it is at a lower end of scale in geotourism development due to its lower Main Values. The main reason for this is the very low scenic/aesthetic values (*VSA*), especially the surface (*SIMV₆*) is very low, the surrounding landscape and nature (*SIMV₇*) is moderate and there are no separate viewpoints except a temple and a spring in the hill. Similarly, the main reason for the lesser Main Values (6.00) in Laljal Cave is resulted from the lower scenic/aesthetic values (*VSA*) (1.31). Khoyai also has very low scenic/aesthetic (*VSA*) (1.73) and protection (*VPr*) (1.60) values, so its Main Value is very low (5.95). Moreover, for Murguma Dam and nearby Hills Joychandi Pahar, Baranti Hill & Dam and Mama Bhagne Pahar, the values of all the main indicators present a consistent level in terms of its different values i.e., scientific/educational values (*VSE*), scenic/aesthetic values (*VSA*) and protection (*VPr*).

The geosites with the lowest Main Values are Susunia Hill (5.67), Khoyai (5.95) and Laljal Cave (6.00). The values of the sub-indicators underlying to Main Values of these geosites, such as surface (*SIMV₆*), knowledge on geo-scientific issues (*SIMV₃*), viewpoints (*SIMV₅*) and surrounding landscape and nature (*SIMV₇*) are very low, although knowledge on geo-scientific issues (*SIMV₃*) is much higher in the Laljal Cave due to its geological significance. The main reason why visitors visit these geosites is that these are located on the way to other important geosites in the area. The sites like Susunia Hill, Joychandi Pahar, Baranti Hill & Dam and Garhpanchkot are located side by side, so tourists visit all the sites together. Tourists visit Khoyai as it is located near important cultural center like the Santiniketan.

In terms of protection values (*VPr*), these four geosites i.e., Ajodhya Hills and forest reserve area, Murguma Dam and nearby Hills, Garhpanchkot and Mukutmanipur Dam have the highest protection values (*VPr*), each of which has the equal value (2.51). These four are followed by Joychandi Pahar (2.36), Gangani Ravine (2.36), Baranti Hill & Dam (2.34), Mama Bhagne Pahar (2.29) and Susunia Hill (2.12) etc. respectively. The four geosites with the highest protection values are protected on a national level, and they are located in rural environment far away from the urban center, so they do not suffer any damage. Khoyai is the site with the lowest protection values (*VPr*), which is 1.60. Even though it is under national level of protection, the values of current condition (*SIMV₉*) and vulnerability (*SIMV₁₁*) are much lower due to the presence of excessive erosion prone lateritic soil.

In terms of Additional Values, the highest value is seen in the Ajodhya Hills and forest reserve area (8.17), which is followed by Joychandi Pahar (7.57), Mukutmanipur Dam (7.02),

Garhpanchkot (6.64), Gangani Ravine (6.22) etc. respectively. Although the functional values (*VF_n*) of these sites are almost the same, the greater disparity in tourist values (*VTr*) has led to diversity among them. In addition, Laljal Cave and Baranti Hill & Dam are located in very remote areas, so the value of their all sub-indicators in the Additional Values (*AV*) is much lower.

In case of functional values (*VF_n*), Garhpanchkot, Khoyai, Ajodhya Hills and forest reserve area, Gangani Ravine, Joychandi Pahar and Mama Bhagne Pahar have highest values, which are 3.35, 3.03, 3.00, 2.94, 2.90 and 2.85 respectively. There are ample facilities to reach these six sites, they are connected to the important road network of national highways and state highways and the location away from the big urban centers has increased their functional values (*VF_n*). Therefore, their values of accessibility (*SI_{AV₁}*), vicinity of important road network (*SI_{AV₅}*) and vicinity of emissive centers (*SI_{AV₄}*) are at the utmost or greatest level on the five-point Likert scale. Moreover, the score of additional functional values (*SI_{AV₆}*) of these sites ranges from high to the utmost. To reach the three sites of Laljal Cave, Baranti Hill & Dam and Murguma Dam and nearby Hills, visitors has to take private car on rural roads, which are inaccessible to big buses; again during the rainy season no visitors can go due to the bad condition of the road, so their functional values is lowest.

Lastly, from the point of view of tourist values (*VTr*), it can be seen that its values is the lowest in Laljal cave (0.58), which is followed by Baranti Hill & Dam (1.83), Khoyai (1.93), Mama Bhagne Pahar (2.08), Susunia Hill (2.45) and Murguma Dam and nearby Hills (2.51) etc. respectively. Although promotion (*SI_{AV₇}*), annual number of organised visits (*SI_{AV₈}*) and annual number of visitors (*SI_{AV₁₁}*) are present in lower range at Laljal cave, but others sub-indicators of tourist values (*VTr*) are completely

Table 3
Sub-indicators values given by experts for each analyzed geosite.

Main indicators/sub-indicators	Values given by experts (0 to 1)											Im	Total value											
	GS ₁	GS ₂	GS ₃	GS ₄	GS ₅	GS ₆	GS ₇	GS ₈	GS ₉	GS ₁₀	GS ₁₁		GS ₁	GS ₂	GS ₃	GS ₄	GS ₅	GS ₆	GS ₇	GS ₈	GS ₉	GS ₁₀	GS ₁₁	
Main values																								
(I) Scientific/Educational values (VSE)																								
1. Rarity (SIMV ₁)	1.00	0.50	1.00	0.75	1.00	0.50	1.00	1.00	1.00	1.00	0.75	1.00	0.95	0.95	0.48	0.95	0.71	0.95	0.48	0.95	0.95	0.95	0.71	0.95
2. Representativeness (SIMV ₂)	1.00	1.00	0.75	1.00	1.00	0.75	1.00	1.00	1.00	1.00	0.50	0.50	0.79	0.79	0.79	0.59	0.79	0.79	0.79	0.59	0.79	0.79	0.40	0.40
3. Knowledge on geo-scientific issues (SIMV ₃)	1.00	0.50	1.00	0.75	1.00	0.50	1.00	0.75	1.00	1.00	0.75	1.00	0.66	0.66	0.33	0.66	0.50	0.66	0.33	0.66	0.50	0.66	0.66	0.33
4. Level of interpretation (SIMV ₄)	1.00	1.00	1.00	0.50	0.75	0.50	1.00	0.50	1.00	1.00	1.00	1.00	0.85	0.85	0.85	0.85	0.43	0.64	0.43	0.85	0.43	0.85	0.85	0.85
(II) Scenic/aesthetic values (VSA)																								
5. Viewpoints (SIMV ₅)	1.00	0.50	0.50	0.50	1.00	0.50	0.75	0.50	0.50	0.25	0.50	0.50	0.83	0.83	0.42	0.42	0.42	0.83	0.42	0.62	0.42	0.42	0.21	0.42
6. Surface (SIMV ₆)	1.00	0.75	0.50	0.50	1.00	0.00	1.00	0.00	1.00	0.50	0.50	0.50	0.84	0.84	0.63	0.42	0.42	0.84	0.00	0.84	0.00	0.84	0.42	0.42
7. Surrounding landscape and nature (SIMV ₇)	1.00	1.00	0.75	1.00	1.00	0.50	1.00	0.50	1.00	0.25	0.50	0.50	0.91	0.91	0.91	0.68	0.91	0.91	0.46	0.91	0.46	0.91	0.23	0.46
8. Environmental fitting of sites (SIMV ₈)	1.00	1.00	1.00	1.00	1.00	1.00	1.00	0.50	1.00	1.00	1.00	1.00	0.87	0.87	0.87	0.87	0.87	0.87	0.87	0.87	0.44	0.87	0.87	0.87
(III) Protection (VPr)																								
9. Current condition (SIMV ₉)	1.00	1.00	1.00	1.00	1.00	0.75	1.00	1.00	1.00	0.50	0.75	0.75	0.89	0.89	0.89	0.89	0.89	0.67	0.89	0.89	0.89	0.45	0.67	
10. Protection level (SIMV ₁₀)	0.75	0.75	0.75	0.75	0.75	0.75	0.75	0.50	0.75	0.75	0.75	0.75	0.67	0.50	0.50	0.50	0.50	0.50	0.50	0.34	0.50	0.50	0.50	0.50
11. Vulnerability (SIMV ₁₁)	0.75	0.75	0.50	0.75	0.75	0.75	0.75	0.50	0.50	0.25	0.75	0.75	0.58	0.44	0.44	0.29	0.44	0.44	0.44	0.44	0.29	0.29	0.15	0.44
12. Suitable number of visitors (SIMV ₁₂)	1.00	1.00	1.00	0.75	1.00	0.75	1.00	0.75	1.00	0.75	1.00	1.00	0.68	0.68	0.68	0.68	0.51	0.68	0.51	0.68	0.51	0.68	0.51	0.68
Additional values																								
(I) Functional values (VFn)																								
13. Accessibility (SIAV ₁)	1.00	0.75	1.00	0.75	1.00	1.00	1.00	0.75	1.00	1.00	1.00	1.00	0.87	0.87	0.65	0.87	0.65	0.87	0.87	0.65	0.87	0.87	0.87	0.87
14. Additional natural values (SIAV ₂)	1.00	0.50	0.50	0.50	1.00	0.50	0.75	0.50	0.75	0.25	0.50	0.50	0.67	0.67	0.34	0.34	0.34	0.67	0.34	0.50	0.34	0.50	0.17	0.34
15. Additional anthropogenic values (SIAV ₃)	1.00	1.00	0.75	0.50	1.00	1.00	0.75	0.25	0.50	1.00	0.50	0.50	0.48	0.48	0.48	0.36	0.24	0.48	0.48	0.36	0.12	0.24	0.48	0.24
16. Vicinity of emissive centers (SIAV ₄)	0.00	0.00	0.50	0.25	0.50	0.25	0.00	0.25	0.50	0.75	0.75	0.75	0.71	0.00	0.00	0.36	0.18	0.36	0.18	0.00	0.18	0.36	0.53	0.53
17. Vicinity of important road network (SIAV ₅)	0.75	0.75	0.75	0.50	0.75	0.50	0.75	0.50	0.75	0.75	0.75	0.75	0.74	0.56	0.56	0.56	0.37	0.56	0.37	0.56	0.37	0.56	0.56	0.56
18. Additional functional values (SIAV ₆)	1.00	0.50	1.00	0.50	1.00	1.00	1.00	0.25	1.00	1.00	0.75	0.75	0.42	0.42	0.21	0.42	0.21	0.42	0.42	0.42	0.11	0.42	0.42	0.32
(II) Tourist values (VTr)																								
19. Promotion (SIAV ₇)	0.75	0.75	1.00	0.50	0.75	0.50	0.75	0.50	1.00	0.75	0.75	0.75	0.56	0.42	0.42	0.56	0.28	0.42	0.28	0.42	0.28	0.56	0.42	0.42
20. Annual number of organised visits (SIAV ₈)	1.00	0.50	1.00	0.25	0.75	1.00	0.75	0.25	1.00	0.50	0.50	0.50	0.62	0.62	0.31	0.62	0.16	0.47	0.62	0.47	0.16	0.62	0.31	0.31
21. Vicinity of visitors centres (SIAV ₉)	1.00	0.50	0.25	0.00	0.25	0.25	0.00	0.00	0.25	0.00	0.00	0.00	0.81	0.81	0.41	0.20	0.00	0.20	0.00	0.00	0.00	0.20	0.00	0.00
22. Interpretive panels (SIAV ₁₀)	1.00	0.00	0.75	0.00	0.50	0.25	1.00	0.00	0.75	0.25	0.50	0.75	0.76	0.76	0.00	0.57	0.00	0.38	0.19	0.76	0.00	0.57	0.19	0.38
23. Annual number of visitors (SIAV ₁₁)	1.00	0.50	0.75	0.25	1.00	0.50	0.75	0.25	0.75	0.50	0.75	0.75	0.58	0.58	0.29	0.44	0.15	0.58	0.29	0.44	0.15	0.44	0.29	0.44
24. Tourism infrastructure (SIAV ₁₂)	0.75	0.00	1.00	0.50	0.75	0.75	1.00	0.00	0.50	0.25	0.75	0.75	0.70	0.53	0.00	0.70	0.35	0.53	0.53	0.70	0.00	0.35	0.18	0.18
25. Tour guide service (SIAV ₁₃)	0.00	0.00	0.50	0.00	0.00	0.25	1.00	0.00	0.00	0.00	0.00	0.00	0.63	0.00	0.00	0.32	0.00	0.00	0.16	0.63	0.00	0.00	0.00	0.00
26. Hostelry service (SIAV ₁₄)	1.00	0.50	1.00	0.25	0.00	0.00	0.25	0.00	0.00	0.00	0.00	0.00	0.73	0.73	0.37	0.73	0.18	0.00	0.00	0.18	0.00	0.00	0.00	0.00
27. Restaurant service (SIAV ₁₅)	1.00	1.00	0.75	1.00	1.00	0.25	1.00	0.00	0.75	0.75	0.50	0.75	0.72	0.72	0.72	0.54	0.72	0.72	0.18	0.72	0.00	0.54	0.54	0.36

GS₁ - Ajothya Hills and forest reserve area, GS₂ - Murguma Dam and nearby Hills, GS₃ - Jyochandi Pahar, GS₄ - Baranti Hill & Dam, GS₅ - Garhpanchkot, GS₆ - Susunia Hill, GS₇ - Mukutmanipur Dam, GS₈ - Laljal Cave, GS₉ - Gangani Ravine, GS₁₀ - Khoyai, GS₁₁ - Mama Bhagne Pahar.

Table 4
Overall position of the analyzed geosites by using M-GAM.

Geosites label	Geosites name	Main Values		Additional Values		Field
		VSE + VSA + VPr	Σ	VFn + VTr	Σ	
GS ₁	Ajodhya Hills and forest reserve area	3.25 + 3.45 + 2.51	9.21	3.00 + 5.17	8.17	Z ₃₂
GS ₂	Murguma Dam and nearby Hills	2.45 + 2.83 + 2.51	7.79	2.23 + 2.51	4.74	Z ₂₁
GS ₃	Joychandi Pahar	3.05 + 2.39 + 2.36	7.80	2.90 + 4.67	7.57	Z ₂₂
GS ₄	Baranti Hill & Dam	2.42 + 2.62 + 2.34	7.38	1.99 + 1.83	3.82	Z ₂₁
GS ₅	Garhpanchkot	3.04 + 3.45 + 2.51	9.00	3.35 + 3.29	6.64	Z ₃₂
GS ₆	Susunia Hill	1.82 + 1.74 + 2.12	5.67	2.65 + 2.45	5.1	Z ₂₂
GS ₇	Mukutmanipur Dam	3.25 + 3.24 + 2.51	9.00	2.71 + 4.31	7.02	Z ₃₂
GS ₈	Laljal Cave	2.66 + 1.31 + 2.03	6.00	1.76 + 0.58	2.34	Z ₂₁
GS ₉	Gangani Ravine	3.25 + 3.04 + 2.36	8.65	2.94 + 3.28	6.22	Z ₃₂
GS ₁₀	Khoyai	2.62 + 1.73 + 1.60	5.95	3.03 + 1.93	4.96	Z ₂₁
GS ₁₁	Mama Bhagne Pahar	2.53 + 2.16 + 2.29	6.98	2.85 + 2.08	4.93	Z ₂₁

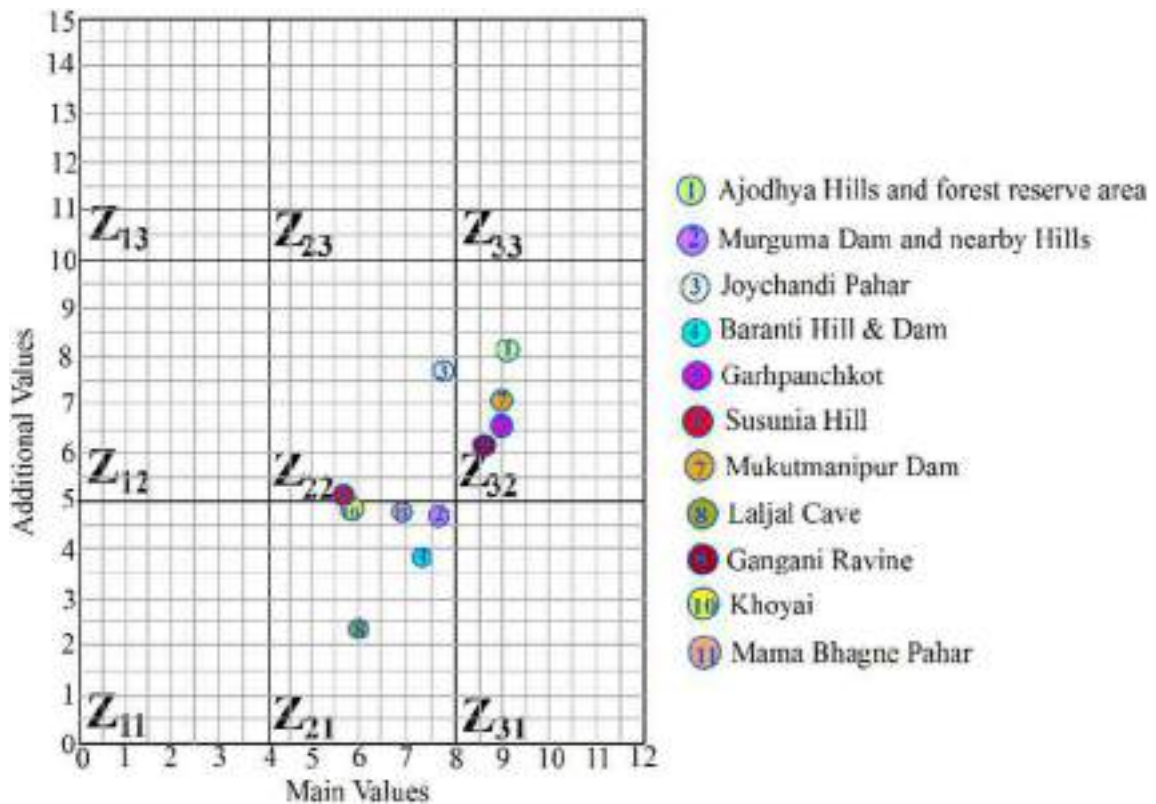


Fig. 2. Position of the analyzed geosites in the M-GAM matrix.

absent. On one hand, there are not any tourist guide, hostelry service, interpretive panels and such tourism infrastructure. On the other hand, the sites with higher tourist values (*VTr*) are Ajodhya Hills and forest reserve area (5.17), Joychandi Pahar (4.67), Mukutmanipur Dam (4.31), Garhpanchkot (3.29) and Gangani Ravine (3.28). These sites attract a large number of tourists and organizations every year in the autumn, winter and spring seasons as they have high quality restaurants service including government youth hostels and also have promotions from national to international level. Tourist guides of different languages are available in Joychandi Pahar and Mukutmanipur Dam, but they are inexperienced in foreign languages.

Based on the Main Values and Additional Values, all the sites of Rarh Bengal have been divided into three groups of sites with the help of M-GAM matrix (Fig. 2). The first group has the highest Main Values and moderate Additional Values, it includes Ajodhya Hills and forest reserve area, Mukutmanipur Dam, Gangani Ravine, and Garhpanchkot, all positioned in the Z₃₂ field of the matrix. The second group comprises sites with moderate Main Values and lowest Additional Values, which is located in the Z₂₁ field of the matrix in Fig.2. These sites are Murguma Dam and nearby Hills, Baranti Hill & Dam, Mama Bhagne Pahar, Khoyai and Laljal Cave. The third group has the moderate Main Values and moderate Additional Values, it includes Joychandi Pahar and Susunia Hill and is located in the Z₂₂ field of the matrix in Fig.2.

The key feature of M-GAM matrix is that sites with higher Main Values and higher Additional Values are suitable sites for the successful development of geotourism. Again, the sites with lower Main Values and lower Additional Values are not suitable sites for the development of geotourism. On the other hand, the sites that have lower Additional Values but the Main Values especially the scientific/educational values (VSE) and scenic/aesthetic values (VSA) of which are higher, can also have the possibility to develop geotourism by improving other necessary sub-indicators through further more investment (Bozic et al., 2014; Bozic & Tomic, 2015; Jonic, 2018; Tomic et al., 2020; Vukovic & Antic, 2019).

Based on the M-GAM matrix, it can be said that the first group sites located in the Z₃₂ fields have great potential for the development of geotourism. It is seen that out of these, the Ajodhya Hills and forest reserve area has highest probability for the development of geotourism, as it has vast area based on hilly and forested environment with more view points, improved transportation and communication facilities, government hostelry service, restaurant service etc. Looking at the overall results, it can be concluded that all the sites located in Z₃₂ can attract a larger number of tourists through the improvement of promotional activities, basic tourism infrastructure, visitor centers and tourist guide services etc. Located under Z₂₂ field but at the edge of Z₃₂ field, the Joychandi Pahar has potentiality of geotourism like the first group sites. In the Z₂₁ field, the Main Values of Murguma Dam and nearby Hills and Baranti Hill & Dam are greater than 7.00, so it is possible for these sites to develop geotourism by improving the values of sub-indicators of these sites.

4. Conclusion

In the view of above discussion, it can be concluded that Rarh Bengal in eastern India has many notable geosites with a lot of potential for the development of geotourism. The sites in this region already have all the natural elements required for the development of geotourism, but most of the sites lack tourist facilities. The M-GAM method evaluates the assessment of both Main Values and Additional Values of each site according to their importance for tourists and the ultimate results has revealed that there is plenty of room for geotourism improvement in these sites, especially in terms of the tourist values. It explicitly refers to the investment for the improvement of tourism infrastructure based on the development of tourism as well as the enhancement of management and planning. In addition, with all those enhancement as well as embodying the promotional activities, these geosites could attract more visitors every year, which can benefit local community by creating new jobs and incomes towards strengthening the local economy. However, the geotourism development at these sites needs to strictly adhere to the principles of sustainable development as they belong to hilly and forested environments.

Credit author statement

Narayan Chandra Jana; Introduction
 Manoj Kumar Mahato; Study Area
 Manoj Kumar Mahato; Methodology
 Manoj Kumar Mahato and Narayan Chandra Jana; Objective of the study
 Manoj Kumar Mahato and Narayan Chandra Jana; Results and discussion
 Manoj Kumar Mahato and Narayan Chandra Jana; Conclusion
 Manoj Kumar Mahato; Computation of Tables and Mapping in softwares
 Manoj Kumar Mahato; Photo-plates

Declaration of Competing Interest

None.

References

- Antic, A., & Tomic, N. (2017). Geoheritage and geotourism potential of the Homolje area (eastern Serbia). *Acta Geoturistica*, 8(2), 67–78.
- Antic, A., Tomic, N., & Markovic, S. B. (2019). Karst geoheritage and geotourism potential in the Pek River lower basin (Eastern Serbia). *Geographica Pannonica*, 23(1), 32–46.
- Boskov, J., Kotrla, S., Jovanovic, M., Tomic, N., Lukic, T., & Rvovic, I. (2015). Application of the preliminary geosite assessment model (GAM): The case of the Bela Crkva municipality (Vojvodina, North Serbia). *Geographica Pannonica*, 19(3), 146–152.
- Bozic, S., & Tomic, N. (2015). Canyons and gorges as potential geotourism destinations in Serbia: Comparative analysis from two perspectives – General geotourists' and pure geotourists'. *Open Geosciences*, 7, 531–546.
- Bozic, S., Tomic, N., & Pavic, D. (2014). Canyons as potential geotourism attractions of Serbia – Comparative analysis of Iazar and Uvac canyons by using M-GAM model. *Acta Geoturistica*, 5(2), 18–30.
- Bruschi, V. M., & Cendrero, A. (2005). Geosite evaluation. Can we measure intangible values? *II Quaternario*, 18(1), 293–306.
- Chakrabarty, P., & Mandal, R. (2019). Geoarchaeosites for geotourism: A spatial analysis for Rarh Bengal in India. *Geo Journal of Tourism and Geosites*, 25(2), 543–554.
- Chakrabarty, P., & Mandal, T. (Eds.). (2018). *Tourism and sustainability: A geographical study in the Rarh Region of West Bengal*. Kolkata: Anjan Publisher.
- Coratza, P., & Giusti, C. (2005). Methodological proposal for the assessment of the scientific quality of geomorphosites. *II Quaternario*, 18(1), 307–313.
- Djurovic, P., & Mijovic, D. (2006). Geoheritage of Serbia-representative of its total geodiversity. *Collection of papers*, 54, 5–18.
- Dowling, R. K. (2013). Global Geotourism – An emerging form of sustainable tourism. *Czech Journal of Tourism*, 2(2), 59–79.
- Erhartic, B. (2010). Geomorphosite assessment. *Acta Geographica Slovenica*, 50(2), 295–319.
- Faridi, R. (2013). Rahr Plains of West Bengal, India. (August 18, 2013), from <https://rashidfaridi.com/2013/08/18/rahr-plains-of-west-bengal-india/>.

- Grover, A. K., & Mahanta, B. N. (2018). Geotourism potential in Arunachal Pradesh – A preliminary appraisal. *Indian Journal of Geosciences*, 72(4), 345–360.
- Hose, T. A. (1995). Selling the story of Britain's stone. *Environmental Interpretation*, 10(2), 16–17.
- Hose, T. A. (1997). Geotourism – Selling the Earth to Europe. In P. G. Marinos, G. C. Koukis, G. C. Tsiambaos, & G. C. Stournaras (Eds.), *Engineering geology and the environment* (pp. 2955–2960). Rotterdam: A. A. Balkema.
- Hose, T. A. (2005). *Geo-Tourism-Appreciating the deep side of landscapes in Novelli. Niche tourism; contemporary issues, trends and cases*. Oxford, UK: Elsevier Science Ltd, 27–37<https://silo.pub/niche-tourism-contemporary-issues-trends-and-cases.html>.
- Hose, T. A., Markovi, S. B., Komac, B., & Zorn, M. (2011). Geotourism - A short introduction. *Acta Geographica Slovenica*, 51(2), 339–342.
- Hose, T. A., & Vasiljevic, D. A. (2012). Defining the nature and purpose of modern geotourism with particular reference to the United Kingdom and South-East Europe. *Geoheritage*, 4, 25–43.
- Jonic, V. (2018). Comparative analysis of Devil's town and Bryce Canyon geosites by applying the modified Geosite assessment model (M-GAM). *Researches Review DGTH*, 47(2), 113–125.
- Newsome, D., & Dowling, R. K. (Eds.). (2010). *Geotourism: The tourism of geology and landscape*. Oxford: Goodfellow Publishers.
- Pal, M., & Albert, G. (2018). Comparison of geotourism assessment models: And experiment in Bakony-Balaton UNSECO global Geopark, Hungary. *Acta Geoturistica*, 9(2), 1–13.
- Paskova, M. (2012). Tourism Environmentalism. *Czech Journal of Tourism*, 1(2), 77–113.
- Patzack, M., & Eder, W. (1998). UNESCO GEOPARK, a new programme – A new UNESCO label. *Geologica Balcania*, 28, 3–4.
- Pereira, L. S., da Cunha, L. S., & Nascimento, M. L. A. (2018). Emergence of geotourism activity at Joao Pessoa municipality and South Coast of Paraiba (Na Brazil). *Sustainable Geoscience and Geotourism*, 1, 1–10.
- Pereira, P., Pereira, D., & Caetano Alves, M. I. (2007). Geomorphosite assessment in Montesinho Natural Park (Portugal). *Geographica Helvetica*, 62, 159–168.
- Pralong, J. P. (2005). A method for assessing the tourist potential and use of geomorphological sites. *Geomorphologie: Relief, Processus, Environnement*, 3, 189–196.
- Reynard, E. (2008). Scientific research and tourist promotion of geomorphological heritage. *Geografia Fisica e Dinamica Quaternaria*, 31, 225–230.
- Reynard, E., Fontana, G., Kozlik, L., & Scapozza, C. (2007). A method for assessing "scientific" and "additional values" of geomorphosites. *Geographica Helvetica*, 62, 148–158.
- Serrano, E., & Gonzalez-Trueba, J. J. (2005). Assessment of geomorphosites in natural protected areas: The Picos de Europa National Park (Spain). *Geomorphologie: Relief, Processus, Environnement*, 3, 197–208.
- Ticar, J., Tomic, N., Breg Valjavec, M., Zorn, M., Markovic, S. B., & Gavrilov, M. B. (2018). Speleotourism in Slovenia: Balancing between mass tourism and geoheritage protection. *Open Geosciences*, 10(1), 344–357.
- Tomic, N. (2011). The potential of lazar canyon (Serbia) as a geotourism destination: Inventory and evaluation. *Geographica Pannonica*, 15(3), 103–112.
- Tomic, N. (2016). *Geoheritage of the middle and lower Danube Region in Serbia: Inventory, geo-conservation and geotourism*. Ph. D. thesis Serbia: University of Novi Sad.
- Tomic, N., & Bozic, S. (2014). A modified geosite assessment model (M-GAM) and its application on the lazar canyon area (Serbia). *International Journal of Environmental Research*, 8(4), 1041–1052.
- Tomic, N., Markovic, S. B., Antic, A., & Tesic, D. (2020). Exploring the potential for geotourism development in the Danube region of Serbia. *International Journal of Geoheritage and Parks*, 8, 123–139.
- Vujcic, M., Vasiljevic, D., Markovic, S., Hose, T. A., Lukic, T., Hadzic, O., & Janicevic, S. (2011). Preliminary geosite assessment model (gam) and its application on Fruska gora mountain, potential geotourism destination of Serbia. *Acta Geographica Slovenica*, 51(2), 361–377.
- Vukoicic, D., Milosavljevic, S., Valjarevic, A., Nikolic, M., & Sreckovic-Batocanin, D. (2018). The evaluation of geosites in the territory of National Park "Kopaonik" (Serbia). *Open Geosciences*, 10, 618–633.
- Vukovic, S., & Antic, A. (2019). Speleological approach for geotourism development in Zlatibor County (West Serbia). *Turizam*, 23(1), 53–68.
- Wulung, S. R. P., & Rajoendah, M. I. K. (2019). Sustainable tourism development through geotourism route planning: A case study of natuna island. *Paper presented at the First Sustainable Tourism National Seminar, STP Mataram*.

'এবং মত্হুয়া' -বিশ্ববিদ্যালয় মঞ্জুরী আয়োগ (U.G.C.-CARE List) অনুমোদিত

তালিকার অন্তর্ভুক্ত। ২০২০ সালে প্রকাশিত ৮৬ পৃ.

তালিকার ৬০ পৃ. এবং ৮৪ পৃ. উল্লেখিত।

এবং মত্হুয়া

(বাংলা ভাষা, সাহিত্য ও গবেষণাধর্মী মাসিক পত্রিকা)

২২ তম বর্ষ, ১২৫ সংখ্যা, অক্টোবর, ২০২০

সম্পাদক

ডা. মদনমোহন বেরা

কে.কে. প্রকাশন

গোবর্দ্ধনচক, মেদিনীপুর, পূ.বঙ্গ।

১২ নারীক : অগণ, জনগণ ও গণসংগণ	
:: পুরুষাচারী শিল্পী	১৪৪
১৩. অভিব্যক্তি : সার্ব ব্যক্তির এক নিম্নতরিত কেন্দ্র	
:: সমস কতি চক্রবর্তী	১০২
১৪ 'কর্প' নাটকে নারীর অর্ধ-স্বাধীন	
:: পৌরস্বয় শ্রমকারিত	১১২
১৫. পুরুষের জেগেছি এগারোজয় : কুর্ভাগ্য, চিকিৎসাবিধি ও মিশনালী	
:: জায়গা মতিগোপ	১২০
১৬. 'অবতর'-এর বিপর্যয় ও মানব প্রতিষ্ঠা : অক্ষয়	
:: কল্যাণী কব	১০২
১৭. উদ্বোধনপাঠি বাঙালি : অষ্টম-উদ্বোধন শতাব্দী	
:: অতিথ্য দে	১৪০
১৮. মূলমন্ত্র জেনের জোকপুত্রের অধিকতর স্বেচ্ছিক গণ	
:: টেকনিক স্বাক্ষর	১৪৮
১৯. পিতৃশ্রম ও শিল্প : সনদাই দুই নারিকার	
:: নিষ্কর্ষ চক্রবর্তী	১৬৩
২০. সংস্কৃত নাট্যচলিত	
:: স্বপ্নবিত্ত অগা	১৭৬
২১. রবীন্দ্রনাথের জনতা : 'স্বাভা ও গাণী' থেকে 'অপলী'	
:: তথ্য নিবন্ধ মহাপাঠ	১৮৪
২২. সিন্ধুকলিন আন্দোলন কবিতা : পঠকের অঙ্গুতর	
:: সেনগুপ্ত দে	১৭২
২৩. পদ, ব্যক্তিগত : বাঙালির কল্যাণ ও বাঙালি সাহিত্য	
:: অধিকতর মুখোপাধ্যায়	২০০
২৪. মনস্বয়গণ ও জগৎকরণের যৌথ অভিব্যক্তি	
:: কনাই বর্মন	২০৭
২৫. কবি কবিত্ত্বজনন ও বৃহত্তর মনস্বয়	
:: ভদ্র চক্রবর্তী	২১৩
২৬. 'কিনোজমা' মনস্বয়-এর উৎসাহে পূর্ণতার বর্ণনা প্রতিষ্ঠান :	
প্রসঙ্গ 'অধীন ও চারকনা'	
:: স্বপ্নবিত্ত বিদ্য	২২৬

২৭. কৃষ্ণকলিন মনস্বয়-এর অধিকতর প্রাথমিক জগৎ ও জগৎকরণ	
:: সনদই কব	২২৪
২৮. 'কলি' কবিতার মর্মে এবং 'কলি' কবিতা : কলি চক্রবর্তীর কবিতার বিচার আলোচনা	
:: বাণী দে	২৩০
২৯. কথন কথন মুখোপাধ্যায়ের গল্প 'মতিগণ পদার্থ' :	
কলি কবিতার আলোচনা মানসিক তেজনা	
:: দেবী গাভ	২৩৫
৩০. সনদই দেবী কৌমারী : উৎসাহিতিক কবিতার বিচার আলোচনার অঙ্গুতর উল্লেখ	
:: চিত্র সেন পরামর্শিক	২৪৫
৩১. 'কলি' মর্মে 'কলি'-এর প্রাথমিক বিচার	
:: বিদ্যাধা মহাশয় (কলি)	২৫৩
৩২. রবীন্দ্রনাথের : বাঙালির থেকে নৈতিক অভিব্যক্তি	
:: সুনন্দ চক্রবর্তী	২৬৭
৩৩. কলিগণী মহাশয়-এর মনস্বয়িক ও মনস্বয়িক কবিতা	
:: কৌমারী	২৭৪
৩৪. 'উদ্বোধন পদ' : এক বিশেষ সময়ের হৃদয়বৃত্তি ও গীতিক	
:: বৈশাখী কু	২৮২
৩৫. রবীন্দ্রনাথের প্রাথমিক নারী	
:: তাহমিনা কলি	২৮৭
৩৬. 'কলি' জেনের মুখে কবিতা 'রবীন্দ্রনাথ	
:: জ. অগণ সনদই	২৯৪
৩৭. কথন মনস্বয় আলোচনার সংকট	
:: জ. শঙ্কর কলি	৩০৩
৩৮. কথন মনস্বয় আলোচনার সংকট	
:: জ. বিদ্যাধা মহাশয়	৩১৪
৩৯. পদার্থস্বয়ক রচনিতা রবীন্দ্রনাথ	
:: জ. অগণ সনদই	৩২৪
৪০. 'কলি' ও 'কলি' মর্মে অধীন মুখোপাধ্যায়ের উৎসাহ	
:: জ. সুনন্দচক্রবর্তী	৩৩৩
৪১. কথন মনস্বয় কবিতা : প্রসঙ্গ 'রবীন্দ্রনাথ কবিতা'র জগৎকরণ	
:: জ. শঙ্কর কলি	৩৪৩

অভিব্যক্তি : রাঢ় বাংলার এক শিল্পচর্চা কেন্দ্র সময় কাটি চক্রবর্তী

বঙ্গের অন্ন কীকৃৎ। জেলের ছোট গ্রাম চন্দ্রধার। লোকসুখে তা বর্তমান স্থাপত্য বা স্থাপত্য। অতেনা অজানা অখ্যাত গ্রামটির সুখ্যাতি আজ বিস্ময়জনক। স্থাপ্যার অল্প জেনার্য ভৌমণিক পত্নী পেরিয়ে শিখিবীর মনটিমে স্থান করে নিয়েছে।

যনে ধন জগতেই পারে কেন ? কী আছে এখানে ? ইত্যাদি ইত্যাদি...। উত্তর কৃকিচ্য আছে লেখ্য কাহিনির অস্তরালে।

স্থাপ্যার জািন, বর্তমানে প্রতি সুস্থতে অতীতকে পিছনে ফেলে অভিব্যক্তের নিকে অস্তের হয়ে চলেছে। অজ্ঞ থেকে তন্ন মনকেয়ও কিছু পূর্বে এমন একজন ব্যক্তি এখানে এসেছিলেন যার তুলনা হয় না। জহুটী তোম্ব তিনি বুঝতে পেরেছিলেন, রাঢ় বাংলার এক ভ্রুপ মাটি জাে একদিন লোলর কলম ফলবে। আর পঁতাভানের যতে সাপাখাটা আটপোঁরে কীকল স্থাপন করলেও তিনি ছিলেন কিছুটা ব্যতিক্রমী। অস্থান উৎসর্গী, অস্ত্রাভ পেরিস্টী, স্বভবকালী, সন্তানস্বামী, সায়কক জাবরণে অস্থানিত, সুন্দরের পুজারী, নির স্বকৃতি মনর দুরদৃষ্ট সম্পন্ন মানুষটি ত্রিভূতিল করে যতে তুলেছিলেন কঁর অম্বর নিরচর্চা কেন্দ্র 'অভিব্যক্তি'।

টৌম্বকবি মেথায়র আশানামকক কহাইত যজ্ঞকটিন অথচ সুন্দর কোমল জুন্দরের নীরর শিল্পী কয়েকটি, সখাসী স্বীকপুত্রখটি অর কেউ নন, তিনি হলেন এই প্রতিষ্ঠানের (অভিব্যক্তি) স্থাপ প্রতিষ্ঠাতা— উৎপল চক্রবর্তী।

রাঢ় বাংলার এক অখ্যাত নন্দন কামনে যে শিল প্রতিষ্ঠানটি পথ হয়েছিল; তার নামকরণ ছিল শ্রী চক্রবর্তীর মন্ডির প্রসূত জাবনা। যার অর্থ যনের তার প্রকাশ কর।

প্রসঙ্গক্রমে বিশাছিনমান প্রাচীন রাঢ়পতি ড. এ. সি. জে. আকুল কালাম্বের পিন্যাত উক্তি অস্থর করে বল যার উৎপলকবু কুনিছে স্বপ্ন লেখেতেন না, বর উঁকে স্থ্যাত নিচ না।

এক সংখ্যা - অক্টোবর, ২০২০ । ১১

২০২

নিখতে লেছেছিলেন।

স্বস্থুই প্রতিষ্ঠায়র উৎপল চক্রবর্তীর কীকল বাংলার প্রতি পঁতা, আটিনে থাকা আনের পথবর্তীর পথের ধীক, উৎসর্গ-উৎসর্গী, অত-অতিথ্যত, স্বপ-সুখ, যদি-কায়, জােগা-স্বপ প্রাণুতি স্বপ্ণায় ষেপলভার নানারঙের স্রাসধু অঁকা-মুককটি পিনতলির কথ, স্মৃতিচারণের মাধ্যমে নানন টুকরো টুকরো ঘটনা নিয়ে একটি কীকল কোলাজ টেরি করার চেষ্টা করেছিলেন।

উৎপল চক্রবর্তীর পিতৃহুনি ছিল বাংলারদেশের বড়জা জেলার কুপুটী গ্রামে। পিতা কৃতি অস্থল চক্রবর্তী ছিলেন সরকারী কর্মচারী। যাতা সবিভা নেই ছিলেন প্রবধ। াঠ আইনবানের মাথে তিনিই জোড়পুত্র। এক শিকিত স্বপ্ন সস্তর পরিবারের সুন্দরন। তিনি ১৩ই জেঠ, ১৩৪৫ বঙ্গাব্দে অবিভক্ত নিরুপপুর জেলার কায়রখটি শহরে (মাহুলালয়) জন্মগ্রহণ করেন। ষেপ, কেশোর ও স্বাস্থীকল লেখ্যসই অতিথ্যহিত হয়। কতোজ পাঠরত অস্থয়র টাঙ্গিও চলিয়েছেন।

যায শনিবারের টিঠ, অচলপর, সুগ্ণের প্রুতি পর-পরিবার নিখতেন, মা জ্যোনা যান জলতেন। লেবন থেকেই উৎপলকবুর লেখ্যকোষি ও সশীভের জেঠগা পান। স্থাপর করে মা জাকতেন কেটৌ ধরন।

মায়রর ধামোদরপুর প্রাথমিক বিদ্যালয়ের শিক্ষকরূপে তিনি কর্মজীবন শুরু করেন। তারপর নদিয়ার মেহেশপুর হাইস্কুল, ২৪ পরপার বিগাটির াগিনা,কোটা বিদ্যালয়। এক বৎসর শিক্ষালয়ের হকীজ হতনামণী বিভাগে কাজ করেন। পরে কলীপুর ২নং শিক্ষক শিক্ষন মহাবিদ্যালয়ের অধ্যাপক ছিলেন। লেখান থেকে ১৯৬৮ যানে কীকৃৎ জেলের স্থাপ্যারে স্থানিরর কৌলিক ট্রেনিং কলেজে অধ্যাপক হিসাবে যোগদান করেন।

কিকৃটিনের অন্য এই জেলার আকড়াকল বেণিক ট্রেনিং সেন্টারের ভারতর অধ্যাপকর পথ অস্থককত করেছিলেন। নুনজার কিত্রে এসে অধ্যাপক পদে যোগদান করতে তাঁর বিয়েকে কাঁধে। পরাধীনতার কাগলাস হুজু জীবনানলের জন্য ১৯৮৬ যানে বেজাবঙ্গর নিলেন। তারপর থেকে অভিব্যক্তিই হয়ে উঠল তাঁর ধ্যান জ্ঞান ও সাধনার কাউর্ষ। শিল্লের লেশর কঁক হয়ে যতে অঠেন সৃষ্টি যুথের উঠলেন।

মাগলায চাকরী করার সময় প্রায়ই টৌজ যোতেন। টৌজই গুড়বন শিল্ল টৌজ এনেটই তাঁর প্রবধ ইচ্ছা। পরে জাবনা পর্সেন্ট হাল কাটীপুর। অস্থশরে তা পূর্কতা লেল কীকৃৎর স্থাপ্যারে।

সময়টা ১৯৭২, উত্তর ২৪ পরপারর কাটীপুরে থাকাকালীন 'সেন্টার ফল কাগজারাজ অরকুনিবেশন' তথা এংলার সারগী শিল্লিকার সম্পাদক শ্রী সঞ্জীব সরকারের আরাধ্যে কোলকাতার সেন্টপলস কাথিফুল চাট প্রাশনে সুব উৎসবে টিঠ প্রকাশির জন্য একটি সংখ্য পঠন করেন, সঙ্গে ছিলেন শিল্পী ও পুরণাবরক শ্রীহর থোর এক সংখ্য কর।

২০৩

১১। এক সংখ্যা - অক্টোবর, ২০২০

২০১৪ সালে বিদ্বানবিশ্বাসের আশ্রিত হয় এবং ২০১৭ সালে আভিযান্ত্রিক গ্রন্থ করে শুরু হয় আভিযান্ত্রিক বিদ্বানবিশ্বাসের অর্থ। উৎসবসমূহের বিদ্বানবিশ্বাসের ইচ্ছা ছিল এখানে একটি আর্ট কলেজ গড়ান। আর সেই অর্থকে আভিযান্ত্রিক করার লক্ষ্যে উপলব্ধি হল। বীকুণ্ডা বিদ্বানবিশ্বাসের ৪র্থ কাঙ্গালন হিসাবে এখানে আভিযান্ত্রিক হয়— ‘আভিযান্ত্রিক শ্রীয়া ইনসিটিউট অফ আর্ট এন্ড ডিজাইন’। ২০১৮ সালের ২০ই মার্চ এটিটা ছিল ‘আভিযান্ত্রিক’ এবং ‘বিদ্বানবিশ্বাসের’ দ্বীপ উদ্দেশ্যে আশ্রিত হয়।¹¹

উৎসব সজবসঁজি করাণের পর বিদ্বানবিশ্বাসে কর্তৃলক্ষ এককল্পে পরিবর্তন ঘটতে গেল। তাই ফুলসমূহ শ্রেষ্ঠ নামে একজন গোত্র আভিযান্ত্রিক জিনি ইনসিটিউট হিসাবে নির্দেশ করেন। ফুলসমূহ আভিযান্ত্রিক প্রাক্তন থেকে নতুনদের সঙ্গে যোগাযোগ করে সনাতন বিশ্বাস ওয়ালন, বৃদ্ধায়েন ও জাণন। জাণনের সীমিত করে বৃদ্ধায়েন প্রতিবেদন আভিযান্ত্রিক অর্থবিশ্বাসের সঙ্গে নির্ভর মতো করে জাণন গড়ান খোলা থেকে উৎসবের মেলা জমা— লোকসভায় বাবু এবং শিষ্টার শ্রেষ্ঠকে আভিযান্ত্রিক, ফুলসমূহ জাণন। তাই সেই সনাতন প্রত্যেক ও সনাতনকারে যুক্ত সনাতনকে মার্গাণ্ড।

নতুন করে সনাতন আভিযান্ত্রিক ২টি বিদ্বানবিশ্বাসের সীমিত রূপ করে রয়েছে। খোকেন যখনই উচ্চ মাধ্যমিক উত্তীর্ণ ১ বছরের আভিযান্ত্রিক শ্রেষ্ঠ করে করার সূচনা খোকেন। বর্তমান বিদ্বানবিশ্বাস Art এবং Samdhi Folk শ্রীয়া ওয়ালন।

সম্প্রতি একত্রিক বিদ্বানবিশ্বাস সূচন আভিযান্ত্রিক থেকে উৎসব খোকেন বীকুণ্ডা বিদ্বানবিশ্বাসের এই প্রতিষ্ঠান। জাণন হল—

- Prof. Jonathan Sweet (University of Deakin)
 Prof. Bill Ashcroft (University of New South Wales)
 Prof. Helen Springale (University of New South Wales)
 Prof. Paul Sharrod (University of Wollongong)
 Prof. Eileen Chanin (Australian National University)
- প্রতিষ্ঠানের শিল্পীর প্রাথমিক প্রদর্শন শুরু, লোকসভায়ের সূচন প্রাথমিক প্রদর্শন, Folk Dance সনাতন উৎসব এবং Instrument সনাতন করে যান্ত্রিক প্রদর্শন প্রদর্শন। আরও ধন শিল্পে আভিযান্ত্রিক সনাতন প্রদর্শন প্রাথমিক প্রাথমিক। এতে মুঠ সনাতন প্রাথমিক প্রাথমিক ও সনাতন প্রদর্শন সনাতন সনাতন করে বিদ্বানবিশ্বাস। এ সনাতন প্রাথমিক বিদ্বানবিশ্বাস। আরও আভিযান্ত্রিক সূচন প্রদর্শন শুরু হয়।
- শিল্পীদের তাই সনাতনই যা সনাতন ‘আভিযান্ত্রিক’ প্রদর্শন সনাতন উৎসব সনাতনই নতুন প্রদর্শন সনাতন প্রাথমিক।

১. APJ Abdul Kalam, SPIRIT OF INDIA, RAMPAL : Delhi, 5th Edition-2014, p. 96
২. ফুলসমূহ শ্রেষ্ঠ, আভিযান্ত্রিক সনাতন, বীকুণ্ডা বিদ্বানবিশ্বাস, ২০১৯, পৃ. ২০।
৩. জাণন, ২০১৯, পৃ. ০৪।
৪. ফুলসমূহ শ্রেষ্ঠ, ২০২০, পৃ. ০৫।
৫. ড. শান্তিনী মাস, বীকুণ্ডার জাণনবিশ্বাস ও শিল্পী সনাতন, প্রথম, ২০১৫, পৃ. ১৯২।
৬. ফুলসমূহ শ্রেষ্ঠ, আভিযান্ত্রিক সনাতন, বীকুণ্ডা বিদ্বানবিশ্বাস, ২০১৯, পৃ. ২০।
৭. ফুলসমূহ শ্রেষ্ঠ, আভিযান্ত্রিক সনাতন, বীকুণ্ডা বিদ্বানবিশ্বাস, ২০২০, পৃ. ৪১।
৮. বীকুণ্ডার সূচনসনাতন, সনাতন নাম বীকুণ্ডা, আরও আভিযান্ত্রিক, ২০১৯, পৃ. ৭৫।
৯. ফুলসমূহ শ্রেষ্ঠ, আভিযান্ত্রিক সনাতন, বীকুণ্ডা বিদ্বানবিশ্বাস, ২০১৯, পৃ. ২৫।
১০. ফুলসমূহ শ্রেষ্ঠ, আভিযান্ত্রিক সনাতন, বীকুণ্ডা বিদ্বানবিশ্বাস, ২০২০, পৃ. ১৮।
১১. কাণন জাণন, সনাতন বীকুণ্ডা, প্রথম প্রাথমিক, ২০১৮, পৃ. ৮৫।
১২. নির্দল প্রাথমিক, শিল্প প্রদর্শন, সনাতনবিশ্বাস, ২০০৯, পৃ. ৯১।
১৩. ফুলসমূহ শ্রেষ্ঠ, আভিযান্ত্রিক সনাতন, বীকুণ্ডা বিদ্বানবিশ্বাস, ২০১৯, পৃ. ২৫।
১৪. ফুলসমূহ শ্রেষ্ঠ, আভিযান্ত্রিক সনাতন, বীকুণ্ডা বিদ্বানবিশ্বাস, ২০২০, পৃ. ২৭।
১৫. ফুলসমূহ শ্রেষ্ঠ, আভিযান্ত্রিক সনাতন, বীকুণ্ডা বিদ্বানবিশ্বাস, ২০২০, পৃ. ২০।

সনাতন :

১. সনাতন (বীকুণ্ডা জাণন সনাতন), তথ্য ও সনাতন সনাতন, সনাতন সনাতন।
২. ফুলসমূহ শ্রেষ্ঠ, ২০১৮, ১৯৮২- তথ্যসনাতন, আভিযান্ত্রিক।
৩. ফুলসমূহ শ্রেষ্ঠ, ০৬, ০২, ১৯৮৯, শিল্পে সনাতনসনাতন, শিল্পের সনাতন সনাতন।
৪. সনাতন সনাতন সনাতন।
৫. সনাতন সনাতন সনাতন।
৬. সনাতন সনাতন সনাতন।
৭. সনাতন সনাতন সনাতন।
৮. সনাতন সনাতন সনাতন।
৯. সনাতন সনাতন সনাতন।
১০. সনাতন সনাতন সনাতন।

সনাতন শীকন :

১. ফুলসমূহ শ্রেষ্ঠ, আভিযান্ত্রিক সনাতন-ইন-সনাতন (বীকুণ্ডা বিদ্বানবিশ্বাস)।
২. সনাতন সনাতন, আভিযান্ত্রিক প্রাথমিক, কাণন, সনাতন ও বীকুণ্ডা।
৩. সনাতন সনাতন, আভিযান্ত্রিক সনাতন।

Spectroscopic investigation of complex nuclear excitations in ^{66}Ga

U. S. Ghosh,¹ S. Rai,^{1,*} B. Mukherjee^{1,†}, A. Biswas,¹ A. K. Mondal,¹ K. Mandal,¹ A. Chakraborty,¹ S. Chakraborty^{1,2,‡},
G. Mukherjee³, A. Sharma⁴, I. Bala,⁵ S. Muralithar^{1,5}, and R. P. Singh^{1,5}

¹Department of Physics, Siksha-Bhavana, Visva-Bharati, Santiniketan, West Bengal 731235, India

²Department of Physics, Institute of Science, Banaras Hindu University, Varanasi 221005, India

³Variable Energy Cyclotron Centre, 1/AF Bidhannagar, Kolkata 700064, India

⁴Department of Physics, Himachal Pradesh University, Shimla 171005, India

⁵Inter University Accelerator Centre (IUAC), Aruna Asaf Ali Marg, New Delhi 110067, India



(Received 23 November 2019; revised 5 July 2020; accepted 29 July 2020; published 24 August 2020)

In-beam spectroscopic technique using the fusion evaporation reaction $^{52}\text{Cr}(^{18}\text{O}, 1p3n)$, at a beam energy of 72.5 MeV, was employed to explore the structural phenomena in ^{66}Ga , mainly at intermediate and high spins. The experimental setup involved an array of 14 Compton suppressed Ge clover detectors, placed around the target position to detect emitted γ rays from excited states. A new level scheme has been proposed, which is enriched with more than 20 new transitions and is extended up to an excitation energy ≈ 12 MeV. A few observed intermediate spin states of ^{66}Ga are discussed in the framework of coupling of single-particle configurations with the vibrational core of ^{64}Zn . Shell model calculations have also been performed with two different interactions, viz., jj44bpn and jun45pn , for the interpretation of the observed level structure in ^{66}Ga .

DOI: [10.1103/PhysRevC.102.024328](https://doi.org/10.1103/PhysRevC.102.024328)

I. INTRODUCTION

Complex excitations, including single-particle and collective ones, have been observed in Zn [1–8], Ga [9–12], and Ge [13,14] isotopes, manifesting various shapes, which are explained by simple theoretical models like the shell model, the interacting Boson model, and cranked Nilsson Strutinsky calculations. Nuclear level structures in $^{65,67}\text{Ga}$ are explained in the framework of the interacting boson-fermion plus broken pair model (IBFBPM), where low and medium spin negative parity yrast states are explained as originating from the coupling of one quasiproton of the negative parity $1f$ or $2p$ orbital with the multiphonon vibrational states of ^{64}Zn and ^{66}Zn , respectively. High spin states in the former two nuclei are mainly of three-quasiparticle nature, originating from coupling of one proton with a broken neutron pair excitations. A similar study on ^{63}Ga and ^{65}Ga by Weiszflog *et al.* [9] revealed rotational-like structures built on $9/2^+$ and $19/2^{(-)}$ states in both nuclei. Angular momenta of the rotational states, built on the $9/2^+$ states, were reported to be generated from the alignment of a neutron pair in the $g_{9/2}$ orbital. As the $g_{9/2}$ orbital is occupied by a single proton, proton crossing is blocked by the Pauli exclusion principle. All the observations in $^{63,65,67}\text{Ga}$ suggest that a large variety of phenomena emerge out of the competition between single-particle and collective excitations, consisting of both

vibrational and rotational degrees of freedom. Interestingly, in ^{68}Ga , high spin states, viz., 9^+ , 11^+ , 13^+ , were compared respectively with $9/2^+$, $13/2^+$, $17/2^+$ energy states of ^{67}Ga by Singh *et al.* [12]. Configurations of these states in ^{67}Ga were stated to be built predominantly from one $\pi g_{9/2}$ quasiproton plus phonon configuration coming from the vibrational core of ^{66}Zn . Alternatively, it can be understood that 11^+ and 13^+ states of ^{68}Ga originate from the couplings of 9^+ ($\pi g_{9/2} \otimes \nu g_{9/2}$) state of ^{68}Ga with multiphonon vibrational states of ^{66}Zn .

In order to understand how this coupling of phonons with single particles qualifies to yield the measured energy values, we have compared some already existing data with the coupling configurations. Intermediate spin states of $^{63,65,67}\text{Ga}$, viz., $13/2^+$, $17/2^+$ and $21/2^+$ [9,11], are compared with $2_1^+ \otimes 9/2^+$, $4_1^+ \otimes 9/2^+$ and $6_1^+ \otimes 9/2^+$ coupled states, respectively, in Fig. 1. As is evident from the figure, observed states $13/2^+$, $17/2^+$, and $21/2^+$ of ^{63}Ga are very close in energy respectively to those states originating from couplings of 2_1^+ , 4_1^+ , and 6_1^+ core states of ^{62}Zn [4] with the $9/2^+$ state of ^{63}Ga . Similarly, in the case of ^{65}Ga and ^{67}Ga , core states are the multiphonon vibrational states of ^{64}Zn [7] and ^{66}Zn [15], respectively. In the case of ^{65}Ga , good agreement is observed for $13/2^+$ and $17/2^+$ states but some discrepancy appears at $21/2^+$, whereas in ^{67}Ga only the $13/2^+$ state is in close proximity to the core-coupled state. This could be due to the significant contribution arising from residual interaction between the core and the particle with increasing spin and mass number.

So, situated in between ^{65}Ga and ^{67}Ga , ^{66}Ga is expected to have a similar kind of systematics and intermediate spin states will have complex structures, with contributions from

*Presently at Department of Physics, Salesian College, Siliguri Campus, Siliguri 734001, India.

†buddhadev.mukherjee@visva-bharati.ac.in

‡Presently at IUAC, New Delhi, India.



FIG. 1. (a) Energy values of the observed $13/2^+$, $17/2^+$ and $21/2^+$ states in ^{63}Ga (data taken from Ref. [9]) are compared with the sum energy values of $9/2^+$ state (of ^{63}Ga) coupled to, respectively, 2_1^+ , 4_1^+ , and 6_1^+ vibrational states of ^{62}Zn [4] forming, respectively, coupled states $13/2^+$, $17/2^+$, and $21/2^+$ in ^{63}Ga . Here, energy values are quoted in keV. (b) Same as panel (a) but for ^{65}Ga , which has core states originating from ^{64}Zn [7] and $9/2^+$, $13/2^+$, $17/2^+$ and $21/2^+$ states from ^{65}Ga [9,11]. (c) Same as panel (a) but for ^{67}Ga , which has core states originating from ^{66}Zn [15] and $9/2^+$, $13/2^+$, $17/2^+$ and $21/2^+$ states of ^{67}Ga [11]. Please see text for details.

both single-particle and collective excitations. This kind of investigation on observed levels in $^{66,68}\text{Ga}$ has been performed and is described later in detail in the discussion section.

Earlier studies on ^{66}Ga were done with modest detector setups using electron-capture decay and reactions like $^{64}\text{Zn}(\alpha, p n \gamma)$, $^{63}\text{Cu}(\alpha, n \gamma)$, $^{64}\text{Zn}(\alpha, d)$, $^{66}\text{Zn}(p, n \gamma)$, $^{66}\text{Zn}(^3\text{He}, t)$, and $^{56}\text{Fe}(^{13}\text{C}, p 2 n \gamma)$, which were used to explore only low and medium spin states [16–23]. The most recent study by Bhattacharjee *et al.*, [10] was performed using 15 Compton suppressed Ge clover detectors; the level scheme was extended up to $21^{(+)}$. Two bandlike structures were observed, with the positive and negative parity bands being described to have originated from $\nu(g_{9/2})^3(f_{5/2})^2 \otimes \pi(g_{9/2})^1(f_{5/2})^2$ and $\nu(g_{9/2})^2(f_{5/2})^1 \otimes \pi(g_{9/2})^1(f_{5/2})^2$ configurations, respectively. As in $^{63,65}\text{Ga}$ and ^{65}Zn , the role of the $g_{9/2}$ neutron pair appears to be very significant in ^{66}Ga , as its alignment along the rotational axis generates the angular momenta of the high spin states in the bands. Here, we report on an experimental investigation on medium and high spin excitations of ^{66}Ga as well as its shell model description mainly at low and intermediate spin values.

II. EXPERIMENTAL DETAILS AND DATA ANALYSIS

In the fusion-evaporation reaction, an ^{18}O beam at 72.5 MeV was obtained from the 15-UD pelletron accelerator [24] at the Inter University Accelerator Centre (IUAC), New Delhi. An isotope of ^{52}Cr of thickness 1 mg/cm² (isotopic abundance $\approx 99\%$), backed by 7 mg/cm² gold, was used as target. The emitted γ rays were detected in coincidence with 14 Compton suppressed high-purity germanium (HPGe) clover detectors of the Indian National Gamma Array (INGA) [25]. Detectors were placed at three different angles, viz., 123° , 148° , and 90° with respect to the beam direction. Time-stamped data were collected in list mode with the help of the computer-aided measurement and control (CAMAC) based data acquisition software CANDLE [26]. Different symmetric and angle dependent E_γ - E_γ matrices from coincidence data were constructed using analysis packages, viz., RADWARE [27] and INGASORT [28]. More details about the target, experimental setup, and data analysis procedure can be found in Refs. [5,29]. Multipolarity of a transition was determined from the DCO ratio (R_{DCO}) [30], which in the present INGA

geometry is defined as

$$R_{DCO} = \frac{I_{\gamma_1} \text{ at } 148^\circ \text{ gated by } \gamma_2 \text{ at } 90^\circ}{I_{\gamma_1} \text{ at } 90^\circ \text{ gated by } \gamma_2 \text{ at } 148^\circ},$$

where I_{γ_1} is the measured intensity of γ_1 when the gating transition is γ_2 . The expected R_{DCO} values for the stretched quadrupole and the dipole transitions are ≈ 1.0 (2.0) and ≈ 0.5 (1.0), for pure quadrupole (dipole) gates respectively. In this work, R_{DCO} values are measured by using stretched $E2$ gates of 1189 ($9_1^+ \rightarrow 7_1^+$), 1268 ($9_2^+ \rightarrow 7_2^+$), 947 ($13_1^+ \rightarrow 11_1^+$), 1058 ($15^+ \rightarrow 13_2^+$), and 1002 keV ($14_1^- \rightarrow 12_3^-$) of ^{66}Ga . Electric or magnetic nature of γ -ray transitions was determined from the polarization measurement [31,32], which was analyzed by constructing two asymmetric matrices, one with perpendicular and the other with parallel scattered events (i.e., the events with γ rays scattered perpendicular or parallel to the emission plane) of 90° detectors in one axis and corresponding γ rays detected at all angles on another axis. The asymmetry parameter was calculated as

$$\Delta_{\text{asym}} = \frac{a(E_\gamma)N_\perp - N_\parallel}{a(E_\gamma)N_\perp + N_\parallel},$$

where $a(E_\gamma)$ represents the experimental asymmetry correction factor for clover detectors at 90° of the present INGA setup and was determined from the ratio of the parallel (N_\parallel) and the perpendicular (N_\perp) scattered events obtained from an unpolarized source. It is defined as

$$a(E_\gamma) = \frac{N_\parallel(\text{unpolarized})}{N_\perp(\text{unpolarized})}.$$

The value of the asymmetry correction factor for the present detector setup is found to be $\approx 1.03(2)$ in the energy range ≈ 0.1 – 1.5 MeV using the standard ^{152}Eu radioactive source. Electric (magnetic) type transitions will have positive (negative) polarization asymmetry (Δ_{asym}) value, while a near zero value of Δ_{asym} indicates that there is a strong admixture. Figures 2 and 3 represent, respectively, the plots of R_{DCO} and polarization asymmetry values for different transitions belonging to ^{66}Ga , which were observed in the measurements.

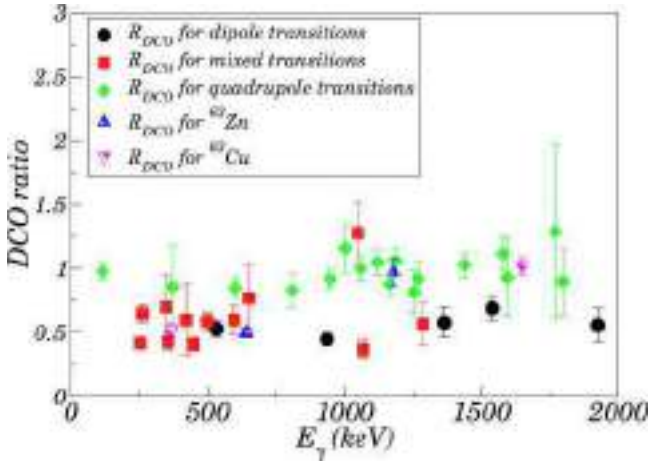


FIG. 2. R_{DCO} values for different transitions of ^{66}Ga (gated by different $E2$ transitions as mentioned in the text and in Table I) along with those of selected transitions having definite multiplicities, viz., of ^{63}Cu ($E_\gamma = 365$ and 1650 keV respectively, for $7/2^- \rightarrow 5/2^-$ and $13/2^+ \rightarrow 9/2^+$ transitions) and ^{63}Zn ($E_\gamma = 640$ and 1179 keV respectively, for $9/2^+ \rightarrow 7/2^-$ and $17/2^+ \rightarrow 13/2^+$ transitions), populated in the fusion evaporation reaction. The latter four transitions are used to fix the reference values in the current analysis and to validate the same. For ^{63}Cu and ^{63}Zn the gating transitions are 342 ($17/2^+ \rightarrow 13/2^+$) and 882 keV ($13/2^+ \rightarrow 9/2^+$) stretched $E2$ type, respectively.

III. RESULTS AND DISCUSSION

A new level scheme of ^{66}Ga (Fig. 4) has been proposed in the present work, which is based on the coincidence relationship, relative intensity balance, angular correlation, and polarization measurements of the emitted γ rays. Almost all the transitions reported previously are observed in this measurement. New transitions are marked with asterisks in the level scheme. A total of 21 new transitions and 20 new

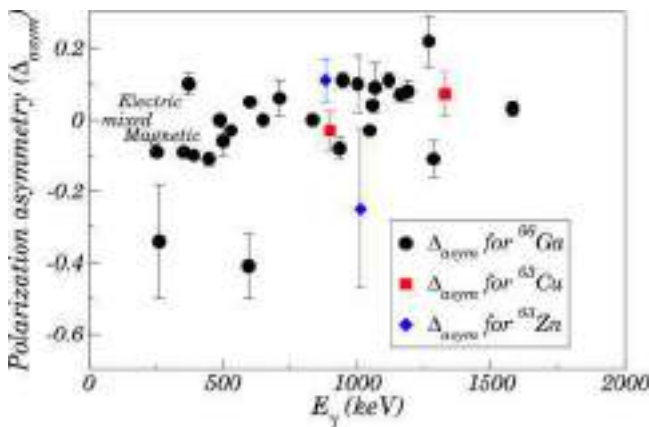


FIG. 3. Polarization asymmetry values (Δ_{asym}) for different transitions in ^{66}Ga , measured in the present experiment. Here, the asymmetry values of 1013 keV ($7/2^- \rightarrow 5/2^-$) and 882 keV ($13/2^+ \rightarrow 9/2^+$) transitions of ^{63}Zn and 899 ($7/2^- \rightarrow 5/2^-$) and 1327 keV ($7/2^- \rightarrow 3/2^-$) transitions of ^{63}Cu are also plotted for the same purpose as in the DCO plot (Fig. 2).

levels have been placed in the level scheme. Transitions which are in coincidence are shown in the typical gated spectra (Fig. 5). Here, the gated spectra are generated through a “logical AND” of the two single gates, which is a feature available in RADWARE.

The 44 ($1^+ \rightarrow 0^+$) and 22 keV ($2^+ \rightarrow 1^+$) γ -ray transitions, which decay respectively from the 44 ($I^\pi = 1^+$) and 66 keV ($I^\pi = 2^+$) states, as were reported previously [16,17], are not observed in the present work as the energies are below the measured energy threshold of the γ -ray spectrometer, we used. So, the ground 0^+ state is not shown in the new level scheme. Najam *et al.* [20] argue, in part, for a spin of 2 for the state at 66 keV based on the absence of feeding from a 0^+ parent in electron-capture decay, as noted by de Boer *et al.* [33]. Morand *et al.* [17] subsequently considered the argument strengthened somewhat based on lifetime measurements made in other works that suggested that the 22 and 44 keV γ rays are $M1$ in nature, and thus that the 2^+ assignment is firm. There is a conflict between those authors and Evaluated Nuclear Structure Data File (ENSDF) evaluators regarding this firm 2^+ spin-parity assignment. However, lifetimes likely do not adequately distinguish between $1^+ \rightarrow 1^+$ and $2^+ \rightarrow 1^+$ $M1$ transitions. So, these are probably considered to be weak arguments by ENSDF evaluators and they also continue to show the state at 66 keV as $(2)^+$. To keep things simple in this work, we have followed the assignment of Refs. [20] and [17], and multiplicities of the higher spin states are determined based on this assignment.

In this work the DCO ratios of many transitions are determined using 1189 keV ($9^+ \rightarrow 7^+$) $E2$ gate. Multipolarity of the 1189 keV γ ray is adopted from the literature [10]. Determination of multipolarity of all the transitions (as given in Table I) was not possible using a single gate, so other transitions, which are stretched quadrupole in the 1189 keV $E2$ gate, are used for this purpose.

Here, the states with energies 863 , 414 , and 162 keV decay in cascade respectively by strong 448 , 253 , and 96 keV γ rays to the 2^+ state at 66 keV. The measured value of the DCO ratio (R_{DCO}) of 96 keV, and also the measured R_{DCO} and polarization asymmetry (Δ_{asym}) of 253 and 448 keV γ rays suggest 3^+ , 4^+ , and 5^+ spin-parity assignments for 162 , 414 , and 863 keV states respectively. Measured R_{DCO} and Δ_{asym} of 834 and 935 keV transitions suggest a 5^+ spin-parity assignment for the 1350 keV state.

Figure 5(a) indicates that the height of the 834 keV peak is about one third of that of 935 keV peak. These transitions decay from the 1350 keV level and have been found to be present in the spectrum gated on 1189 and 1540 keV transitions that feed the 1350 keV level. However, the measured intensity of the 935 keV transition indicates that the size of this transition is significantly larger in the table than is seen in the figure. This anomaly in branching is suggestive of the possible presence of a weak doublet 834 keV transition which could neither be properly identified nor be placed in the level scheme due to the lack of sufficient statistics.

The state at 516 keV is assigned with a spin-parity 4^+ , depending upon the measured R_{DCO} and Δ_{asym} of the depopulating 354 keV γ ray. The state at 1463 keV decays to that at 863 keV (5^+) by a strong 601 keV γ -ray transition. Measured

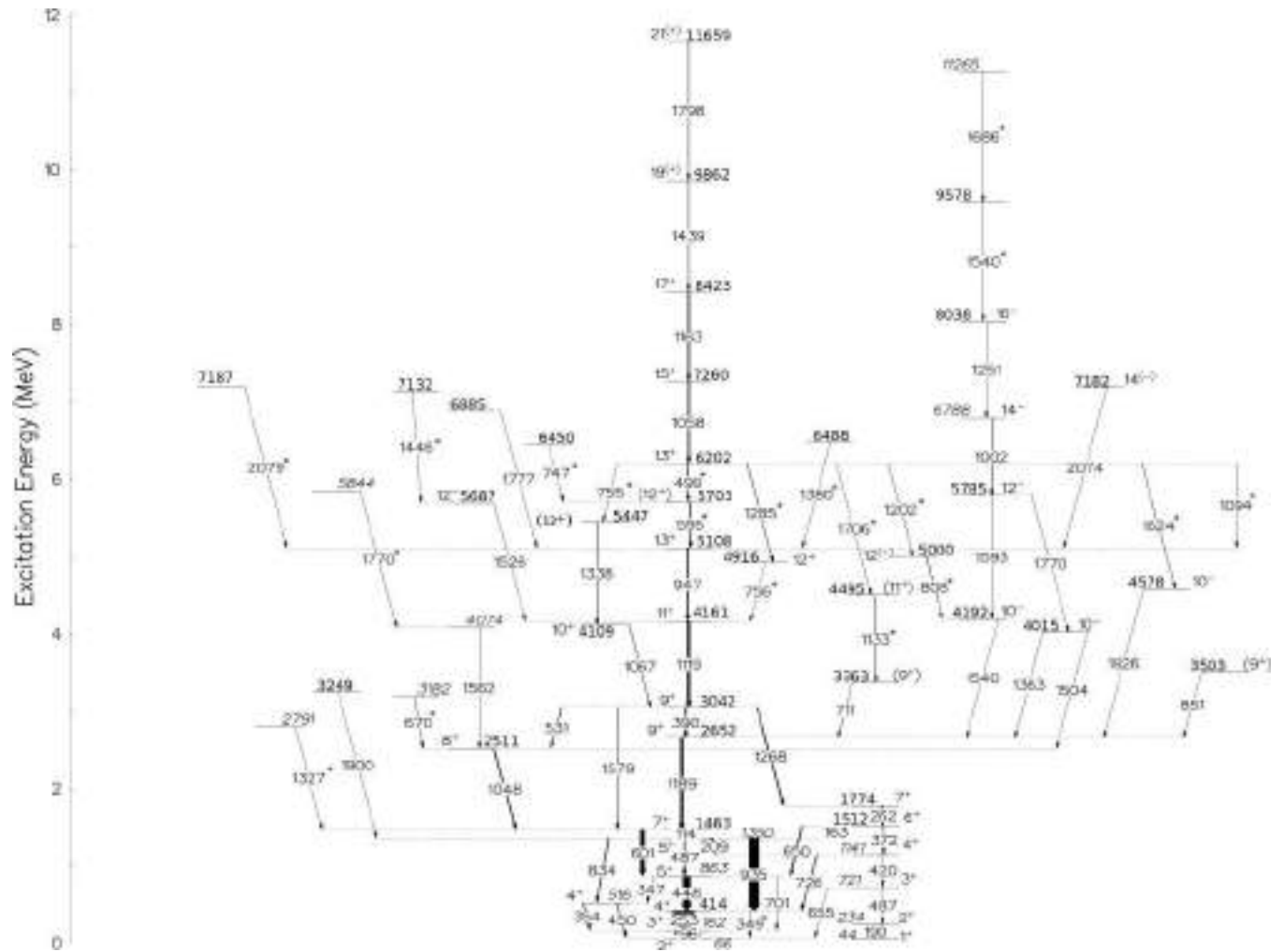


FIG. 4. Proposed level scheme of ⁶⁶Ga. Widths of the arrows are proportional to the relative intensity of the respective transition observed in the present experiment. New transitions are marked with asterisks. The energies in the figure are in keV.

R_{DCO} and Δ_{asym} of the 601 keV transition suggest quadrupole nature of this γ ray, so a spin-parity 7^+ is assigned to the 1463 keV state. This state at 1463 keV is fed by a strong 1189 keV γ -ray transition depopulating the state at 2652 keV. Previous observations predicted $E2$ nature for the 1189 keV transition, so the state at 2652 keV is assigned with a 9^+ spin-parity value. The state at 3042 keV is depopulated by 390, 531, 1268, and 1579 keV γ rays to states at 2652 (9^+), 2511, 1774, and 1463 keV (7^+), respectively. Measured R_{DCO} and Δ_{asym} of the 1048 keV γ ray suggest 8^+ spin-parity for the state at 2511 keV, so measured values of those for 531 and 1579 keV transitions suggest a spin-parity value of 9^+ for the state at 3042 keV. As a result, the 390 keV ($9^+ \rightarrow 9^+$) transition could be assumed to be dipole in nature, though it has $R_{DCO} \approx 1.0$. This is possible, as the $\Delta I = 0$ transition will have the same angular correlation as that of a quadrupole one.

A negative polarization asymmetry value has been obtained for the 390 keV γ ray that decays from the 3042 keV level. Combining the measured values of polarization asymmetry and the corresponding DCO ratio, the $\Delta I = 0$, 390 keV transition can be characterized as a magnetic dipole type with the probable presence of a very small admixture of $E2$

component. Hence, the assignment of $M1(+E2)$ multipolarity has been made for the 390 keV transition. The measured R_{DCO} and Δ_{asym} values of 1268 and 262 keV γ rays suggest 7^+ and 6^+ spin-parities for 1774 and 1512 keV states, respectively.

We would also like to mention here that the peak height of 1268 keV transition as can be seen from Figs. 5(c)–5(e) is not in accordance with that of the 1579 keV γ ray as far as the measured intensities of the two transitions are concerned (see Table I). Both the transitions decay from 3042 keV level and the measured intensities suggest that the height of the 1268 keV peak should be more than that of the 1579 keV peak in the gated spectra of Figs. 5(c)–5(e) obtained with the gating transitions that feed the 3042 keV level. It is worthwhile mentioning that the quoted intensities of Table I for the 1268 and 1579 keV branches have been obtained from the gated spectrum of the 253 keV γ -ray lying below the 3042 keV level. The analysis of the gated spectrum provides clear indication of a larger peak area of the 1268 keV transition in comparison to that of the 1579 keV transition. The anomalies in the peak count for 1268 and 1579 keV transitions between the top gated and bottom gated coincidence spectra may possibly reflect a missing

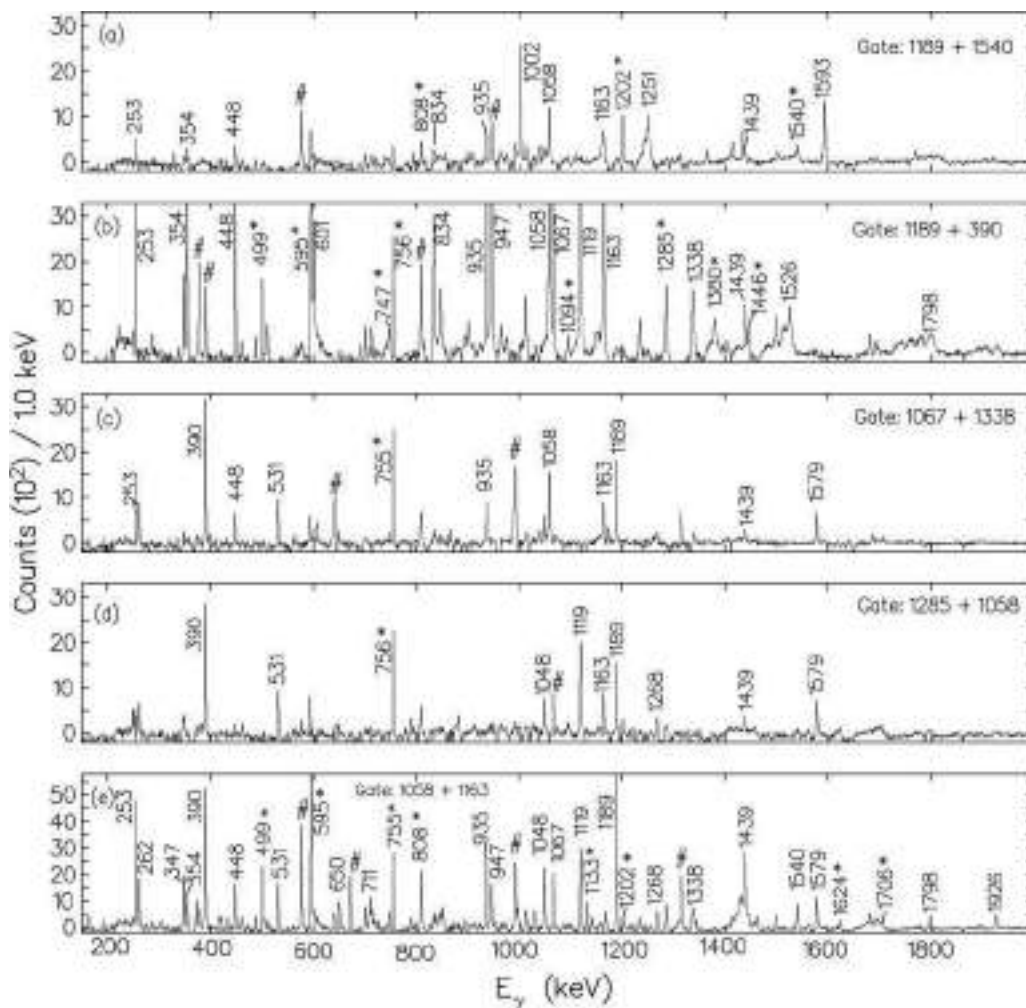


FIG. 5. Background subtracted γ - γ coincidence spectra for ^{66}Ga in the sum gates of (a) 1189 ($9^+ \rightarrow 7^+$) and 1540 keV ($10^- \rightarrow 9^+$), (b) 1189 ($9^+ \rightarrow 7^+$) and 390 keV ($9^+ \rightarrow 9^+$), (c) 1067 ($10^+ \rightarrow 9^+$) and 1338 keV ($12^{(+) } \rightarrow 10^+$), (d) 1285 ($13^+ \rightarrow 12^+$) and 1058 keV ($15^+ \rightarrow 13^+$), and (e) 1058 ($15^+ \rightarrow 13^+$) and 1163 keV ($17^+ \rightarrow 15^+$) γ rays. New transitions are marked by asterisks (*). The inset of (e) contains the portion of 1058 + 1163 keV gated spectrum (from 1600 to 1800 keV in energy in the x axis, and 0 to 800 in counts in the y axis), which is expanded to show the presence of newly observed (weak) 1624 and 1706 keV γ rays. A few strong peaks are marked with “#” symbols indicating contaminant γ rays or ones which could not be placed in the level scheme.

1268 keV doublet transition. This missing weak doublet transition is probably in coincidence with the 253 keV γ ray and not in coincidence with either the cascade transitions of 1285, 1058, and 1163 keV or the cascade transitions of 1067 and 1338 keV. However, the doublet nature of the 1268 keV transition could not be confirmed from the present analysis.

Spin-parities of both 1141 and 721 keV states are assigned to be 4^+ and 3^+ , depending upon the measured R_{DCO} of 372 and 420 keV γ rays. Here, the measured R_{DCO} and Δ_{asym} of 372 keV suggest $E2$ nature for this transition. No information regarding the spin-parity of the 1141 keV state was given by previous work. Also, the state at 721 keV was assigned with a tentative spin 3 but definite positive parity [i.e., $(3)^+$] in Ref. [10], but, as mentioned, we assign definite spin-parity to this state, from the derived multipolarity nature of 372 ($E2$) and 420 keV ($M1/E2$) transitions. The 44 and 234 keV states are reported to be 1^+ and 2^+ by previous observations [10,16,17,20,23]. Due to weak intensities of 190

and 487 keV γ rays, measurement of R_{DCO} and Δ_{asym} of these two transitions, depopulating the 234 and 721 keV states respectively, was not possible.

Measured R_{DCO} and Δ_{asym} of 1363 keV transition predicts its dipole nature to be of electric type, therefore a 10^- spin-parity is assigned to the state at 4015 keV. Following the measured R_{DCO} and Δ_{asym} of the 1540 keV γ ray and a previous assignment [10], a 10^- spin-parity value is confirmed for the state at 4192 keV.

Here, a notable fact is that the 935 keV γ -ray transition depopulating the 1350 keV (5^+) state is visible in the spectrum gated by 1189 and 1540 keV γ rays [panel (a), Fig. 5], while 601 keV γ -ray depopulating the 1463 keV (7^+) state is not. However, this 601 keV transition is also in coincidence with the 1189 and 1540 keV γ rays and has a strong peak area with sufficient statistics. This 7^+ state is an isomeric state with a half-life of 57 ns. If the coincidence time window used during the experiment was small compared to the 57 ns half-life then

TABLE I. Values of the level energy (E_i) in keV, γ -ray energy (E_γ) in keV, initial spin-parity (I_i^π) \rightarrow final (I_f^π), intensity (I_γ), DCO ratio (R_{DCO}), polarization asymmetry (Δ_{asym}) and multipolarity assignment of the γ -ray transitions, as obtained in ^{66}Ga .

Level energy ^a E_i (keV)	Gamma-ray energy E_γ (keV)	Initial \rightarrow final spin-parity $I_i^\pi \rightarrow I_f^\pi$	Relative intensity I_γ	DCO ratio R_{DCO}	Polarization asymmetry Δ_{asym}	Assignment
161.5(4)	95.9(3)	$3^+ \rightarrow (2)^+$	100	0.62(7) ^b		($M1 + E2$)
234.02(23)	190.21(23)	$2^+ \rightarrow 1^+$	0.21(7)			
414.4(4)	252.93(24)	$4^+ \rightarrow 3^+$	87.76(95)	0.42(4) ^b	-0.09(1)	$M1 + E2$
	348.61(23) ^h	$4^+ \rightarrow (2)^+$				
515.5(4)	353.83(18)	$4^+ \rightarrow 3^+$	2.50(27)	0.43(7) ^b	-0.09(1)	$M1 + E2$
	450.36(12)	$4^+ \rightarrow (2)^+$	3.04(29)			
720.8(3)	486.74(20) ^h	$3^+ \rightarrow 2^+$				
	655.37(18)	$3^+ \rightarrow (2)^+$	0.20(4)			
862.6(4)	347.39(28)	$5^+ \rightarrow 4^+$	0.53(19)	0.70(25) ^b		$M1 + E2$
	448.22(19)	$5^+ \rightarrow 4^+$	29.82(53)	0.41(5) ^b	-0.11(2)	$M1 + E2$
	701.1(3)	$5^+ \rightarrow 3^+$	0.68(12)			
1140.8(4)	419.7(4)	$4^+ \rightarrow 3^+$	0.21(7)	0.60(28) ^c		$M1 + E2$
	726.40(19)	$4^+ \rightarrow 4^+$	2.75(22)			
1349.5(4)	208.62(10)	$5^+ \rightarrow 4^+$	0.71(13)			
	486.94(15)	$5^+ \rightarrow 5^+$	3.88(24)	0.96(29) ^b	-0.03(2)	($M1 + E2$)
	834.13(13)	$5^+ \rightarrow 4^+$	3.29(38)	0.52(7) ^b	≈ 0	($M1 + E2$)
	934.89(16)	$5^+ \rightarrow 4^+$	40.96(68)	0.45(5) ^b	-0.08(3)	$M1$
1463.3(4)	113.70(24)	$7^+ \rightarrow 5^+$	12.33(34)	0.98(7) ^b		Q
	600.67(10)	$7^+ \rightarrow 5^+$	18.21(94)	0.85(8) ^b	+0.05(1)	$E2$
1512.2(4)	162.5(3)	$6^+ \rightarrow 5^+$	1.93(27)	0.54(13) ^c		(D)
	371.69(30)	$6^+ \rightarrow 4^+$	1.17(18)	0.86(32) ^c	+0.10(3)	$E2$
	649.52(13)	$6^+ \rightarrow 5^+$	5.02(37)	0.77(27) ^c	≈ 0	$M1 + E2$
1773.9(4)	261.68(16)	$7^+ \rightarrow 6^+$	3.45(22)	0.65(7) ^c	-0.34(16)	$M1 + E2$
2511.3(4)	1047.90(11)	$8^+ \rightarrow 7^+$	4.41(32)	1.28(24) ^d	-0.03(2)	$M1 + E2$
2651.9(4)	1188.64(12)	$9^+ \rightarrow 7^+$	11.83(33)	1.06(10) ^d	+0.08(3)	$E2$
2790.7(5)	1327.36(22)		0.35(10)			
3042.1(4)	390.24(12)	$9^+ \rightarrow 9^+$	6.06(26)	1.08(8) ^b	-0.10(1)	$M1(+E2)$
	530.72(17)	$9^+ \rightarrow 8^+$	2.25(21)	0.53(7) ^d	-0.03(1)	$M1$
	1268.20(16)	$9^+ \rightarrow 7^+$	4.88(25)	0.92(14) ^d	+0.22(7)	$E2$
	1578.87(15)	$9^+ \rightarrow 7^+$	3.26(21)	1.12(13) ^d	+0.03(2)	$E2$
3181.7(5)	670.40(17)		0.90(14)			
3249.1(7)	1899.6(5) ^h					
3362.8(5)	710.92(24)	$(9^+) \rightarrow 9^+$	0.72(16)	1.11(26) ^b	-0.06(5)	($M1 + E2$)
3503.0(6)	851.1(4)	$(9^+) \rightarrow 9^+$	0.31(11)	1.12(44) ^b		($M1 + E2$)
4015.2(4)	1363.41(10)	$10^- \rightarrow 9^+$	0.40(8)	0.54(8) ^b	+0.03(2)	$E1$
	1503.79(18)	$10^- \rightarrow 8^+$	0.23(8)	1.07(60) ^f		(Q)
4073.8(4)	1562.48(13)		0.60(8)			
4109.0(4)	1066.81(14)	$10^+ \rightarrow 9^+$	1.16(14)	0.37(7) ^b	+0.09(7)	$M1 + E2$
4160.7(4)	1118.70(16)	$11^+ \rightarrow 9^+$	10.66(29)	1.05(10) ^b	+0.11(2)	$E2$
4192.0(4)	1540.08(14)	$10^- \rightarrow 9^+$	0.53(8)	0.69(9) ^e	+0.10(2)	$E1^s$
4495.3(5)	1132.5(3)	$(11^+) \rightarrow (9^+)$	0.66(7)	1.07(36) ^b		(Q)
4577.5(5)	1925.58(17)	$10^- \rightarrow 9^+$	0.49(8)	0.56(13) ^b		$E1^s$
4916.2(5)	755.58(12)	$12^+ \rightarrow 11^+$	0.95(10)			
5000.0(5)	808.08(24)	$12^{(-)} \rightarrow 10^-$	0.87(18)	0.83(14) ^b		Q
5107.5(5)	946.75(12)	$13^+ \rightarrow 11^+$	5.90(22)	0.92(8) ^b	+0.11(2)	$E2$
5446.9(5)	1337.75(18)	$(12^+) \rightarrow 10^+$	0.88(12)	0.85(27) ^b		(Q)
5686.5(5)	1525.80(22) ^h	$12^- \rightarrow 11^+$				
5703.0(5)	595.45(13)	$(12^+) \rightarrow 13^+$	3.56(50)	0.60(11) ^d	-0.41(9)	$M1 + E2$
5785.3(4)	1593.28(15)	$12^- \rightarrow 10^-$	0.32(9)	0.93(30) ^b		$E2^s$
	1770.04(12)	$12^- \rightarrow 10^-$	0.87(25)	1.29(68) ^f		$E2$
5844.0(5)	1770.22(25) ^h					
6201.8(4)	498.77(19)	$13^+ \rightarrow (12^+)$	2.17(29)	0.59(7) ^d	-0.06(4)	$M1 + E2$
	754.81(18)	$13^+ \rightarrow 12^{(+)}$	0.57(7)			
	1094.4(4) ^h	$13^+ \rightarrow 13^+$				
	1201.85(17)	$13^+ \rightarrow 12^{(-)}$	0.59(10)	0.57(15) ^b		($D + Q$)

TABLE I. (Continued).

Level energy ^a E_i (keV)	Gamma-ray energy E_γ (keV)	Initial→final spin-parity $I_i^\pi \rightarrow I_f^\pi$	Relative intensity I_γ	DCO ratio R_{DCO}	Polarization asymmetry Δ_{asym}	Assignment
	1285.69(17)	$13^+ \rightarrow 12^+$	1.10(3)	0.57(16) ^b	-0.11(5)	$M1 + E2$
	1624.34(23)	$13^+ \rightarrow 10^-$	0.55(10)			
	1706.5(3)	$13^+ \rightarrow (11^+)$	0.20(7)			
6449.9(5)	746.87(22) ^h					
6487.7(5)	1380.23(23) ^h					
6787.7(5)	1002.41(16)	$14^- \rightarrow 12^-$	1.89(22)	1.16(19) ^b	+0.10(8)	$E2$
6884.9(5)	1777.39(23) ^h					
7132(3)	1445.8(26)		0.35(10)			
7181.5(11)	2074 ^{h,i}	$14^{(-)} \rightarrow 13^+$				
7186.5(11)	2079 ^{h,i}					
7259.7(5)	1057.87(12)	$15^+ \rightarrow 13^+$	5.05(30)	1.00(10) ^b	+0.04(1)	$E2$
8038.4(5)	1250.67(19)	$16^- \rightarrow 14^-$	0.57(14)	0.82(17) ^f		Q
8422.6(6)	1162.9(4)	$17^+ \rightarrow 15^+$	4.05(20)	0.88(9) ^b	+0.07(2)	$E2$
9578.4(11)	1540 ^{h,i}					
9861.6(7)	1438.95(20)	$19^{(+)} \rightarrow 17^+$	0.72(11)	1.03(10) ^e		Q
11264.9(12)	1686.44(11)		0.34(9)			
11659.3(7)	1797.7(3)	$21^{(+)} \rightarrow 19^{(+)}$	0.67(11)	0.90(26) ^e		Q

^aLevel energies are obtained from least-squares fit to the γ energies using the GTOL code [22].

^bGate on $E2$, 1189 keV.

^cGate on $E2$, 1268 keV.

^dGate on $E2$, 947 keV.

^eGate on $E2$, 1058 keV.

^fGate on $E2$, 1002 keV.

^gCorroborated also with Ref. [10].

^hIntensity measurement was not possible due to low statistics.

ⁱ γ -energy error of 1 keV was assumed to get least-squares fit level energy.

some of that coincidence intensity would be lost, but it was ≈ 250 ns. So, coincidence time window is probably not the reason behind this. The reason for the disappearance of the 601 keV transition in the sum gate of 1189 and 1540 keV γ rays is not confirmed in this work.

A positive parity band was observed by the authors of Ref. [10], and was reported to be built on the 11^+ state, consisting of 947, 1058, 1163, 1439, and 1799 keV γ rays depopulating, respectively, states at 5108 (13^+), 6167 (15^+), 7330 (17^+), 8769 ($19^{(+)}$), and 10568 keV ($21^{(+)}$). Now, it is evident in the gated spectra (Fig. 5) that 1058, 1163, and 1439 keV γ rays are in coincidence with 1338 and 1067 keV transitions. So, a new linking transition of 755 keV (6202 \rightarrow 5447 keV) has been placed connecting former transitions with 1338 and 1067 keV transitions depopulating the states at 5447 and 4109 keV, respectively. As a result, the previously reported positive parity yrast band has been modified and the energy values of the states depopulated by 1058, 1163, 1439, and 1798 keV γ rays have been changed to 7260 (15^+), 8423 (17^+), 9862 ($19^{(+)}$), and 11 659 keV ($21^{(+)}$) respectively. The state at 5108 keV decays to the 9^+ (3042 keV) state via two strong 947 and 1119 keV γ rays in cascade. The measured values of R_{DCO} and Δ_{asym} of the former two transitions suggest 13^+ and 11^+ spin-parity values for states at 5108 and 4161 keV, respectively.

The state at 6202 keV, which is newly observed in this work, decays mainly by fragmented γ rays of 755, 499, 1094, 1285, 1202, 1624, and 1706 keV energy to the states at 5447,

5703, 5108, 4916, 5000, 4578, and 4495 keV, respectively. The fragmented decay pattern of the former state suggests that the wave function corresponding to this state is of complex nature. This state decays to that at 5108 keV (13^+) via the cascade of two newly observed 499 and 595 keV γ rays as well as by the direct 1094 keV transition. Measured values of the DCO ratio of newly observed 1202 and 808 keV transitions suggest a spin value of 13 for the state at 6202 keV, while the measured values of DCO ratio and polarization asymmetry of 499 and 595 keV transitions confirm positive parity for this state. The state at 5703 keV is assigned with a tentative spin-parity 12^+ , based on the assigned spin-parities of the states at 6202 and 5108 keV, and further it is confirmed by the measured DCO ratio and polarization asymmetry values of 499 and 595 keV transitions.

Measured values of DCO ratio and polarization asymmetry of 595 keV γ ray do suggest a 14^+ spin-parity value for the state at 5703 keV. But in that case measured values of DCO ratio and polarization asymmetry of 499 keV transition would suggest 15^+ spin-parity for the 6202 keV state. As a result, many of the γ -ray transitions depopulating this 6202 keV state would have ambiguous multiplicities; for example, the 755 keV γ ray would be $M3$ in nature and the 1624 keV one would be $E5$ in nature. So, a tentative 12^+ spin-parity is assigned to the 5703 keV state.

The state at 6202 keV also decays to that at 4161 keV via the cascade of 1285 and 756 keV γ rays, and the measured values of DCO ratio and polarization asymmetry of the

1285 keV γ ray predict a spin-parity of 12^+ for the state at 4916 keV. Interestingly, the state at 6202 keV decays to that at 4578 keV via a 1624 keV $E3$ type γ ray. The $E3$ type transition is observed for the first time in this nucleus in the present work, but, due to very low intensity of this γ ray, measurements of R_{DCO} and Δ_{asym} were not possible.

Here, an important fact is that the 499 and 595 keV transitions should have similar peak areas when gated from above, but the 595 keV γ ray appears with a nearly double peak area compared to the 499 keV γ -ray as is evident from gated spectrum (e) of Fig. 5. This could be due to the presence of a 595 keV doublet or could reflect missing transitions, which is not confirmed by the present observation.

The spin-parities of the states at 8423 and 7260 keV are estimated to be 17^+ and 15^+ , respectively, from the observed stretched electric quadrupole nature of both the depopulating 1163 and 1058 keV γ rays. The measured R_{DCO} value of the 1439 keV γ ray suggests stretched quadrupole nature of this transition but, as polarization measurement was not possible due to low intensity of this transition, a tentative positive parity is assigned to the state at 9862 keV. The state at 11 659 keV is assigned $21^{(+)}$ spin-parity value, based on the measured R_{DCO} value of the 1798 keV transition.

Placement of the state at 5447 keV was tentative in previous work [10], but its presence is confirmed in the present experiment, as we could detect the depopulating 1338 keV γ ray in strong coincidence with the 1067 keV transition and other strong and weak transitions in cascade, as shown in the gated spectra (Fig. 5).

The 5446 keV level decays through a single branch of the 1338 keV transition. The level is found to be populated very weakly in the present experiment. Hence, the extracted DCO value of the 1338 keV transition is associated with a large uncertainty and a tentative (12^+) assignment has been made for the 5446 keV level.

The state at 3363 keV is assigned with a tentative spin-parity of (9^+) based on the measured values of R_{DCO} and Δ_{asym} of the 711 keV transition decaying from the 3363 keV level. Previously, it was assigned as 10^+ [10]. The measured values of R_{DCO} and Δ_{asym} for the 711 keV transition suggest that the state at 3363 keV could perhaps be assigned with a spin-parity value of 11^- , but in that case the 711 keV γ ray would be of $M2$ multipolarity which is supposed to be less probable. Here, the measured uncertainty in R_{DCO} also suggests that the 711 keV transition may have considerable mixing, so a tentative ($M1 + E2$) multipolarity is assigned to this γ ray and the state at 3363 keV is assigned tentatively with (9^+) spin-parity. Following the same assumption, the state at 3503 keV is also assigned tentatively with 9^+ spin-parity, though it is depopulated by the 851 keV γ ray which has $R_{DCO} \approx 1.0$. The state at 3363 keV is connected to that at 6202 keV via two newly observed γ rays in cascade, i.e., 1133 and 1706 keV. The new state at 4495 keV is assigned with a tentative spin-parity 11^+ , on the basis of the measured value of DCO ratio of the 1133 keV γ ray transition. The negative parity state at 8038 keV decays to that at 4192 keV by 1251, 1002, and 1593 keV γ rays in cascade. Measured R_{DCO} and Δ_{asym} predict stretched quadrupole nature of electric type for the 1002 keV γ ray and the measured R_{DCO} for 1251

and 1593 keV transitions suggest quadrupole nature. The negative-parity band has been extended up to an excitation energy ≈ 11 MeV by placing two new transitions, viz., of 1540 and 1686 keV, in cascade above the state at 8038 keV.

The 9^+ state of ^{66}Ga at 2652 keV has a single-particle origin from contributions of both the $1g_{9/2}$ proton and $1g_{9/2}$ neutron. So, the coupling of the 9^+ state with the 2^+ , 3^+ , 4^+ , 6^+ , and 8^+ states of ^{64}Zn , which has one proton and one neutron less than ^{66}Ga , can produce, respectively, 11^+ , 12^+ , 13^+ , 15^+ , and 17^+ states of ^{66}Ga . In order to search for the possibility of such coupling, we have compared (Fig. 6) the observed energy states with 11^+ , 12^+ , 13^+ , 15^+ , and 17^+ spin-parity values of ^{66}Ga with those originating from coupling of 9^+ state (at 2652 keV) of ^{66}Ga with 2^+ , 3^+ , 4^+ , 6^+ , and 8^+ states of ^{64}Zn [7,22]. In Fig. 6, a similar comparison is made in ^{68}Ga , for standardization purpose. In ^{68}Ga , the energies of 9^+ , 11^+ , 13^+ , 15^+ , and 17^+ states are taken from Ref. [12] and the National Nuclear Data Center (NNDC) [34]. In the case of ^{68}Ga , coupled states are coming from the coupling of the 9^+ state of ^{68}Ga at 2894 keV with 2_1^+ , 2_2^+ , 4_1^+ , 6_1^+ , and 8_1^+ states of ^{66}Zn [15]. As is evident from Fig. 6, the observed states are in close proximity in energy with the coupled states in the case of ^{68}Ga , compared to ^{66}Ga . Variation in energy with spin for the observed states follows the same pattern as that of the coupled states, in the case of ^{68}Ga , but does not follow the pattern in the case of ^{66}Ga . The energy states at 12^+ and 17^+ are lower in energy with respect to $9^+ \otimes 3_1^+$ and $9^+ \otimes 8_1^+$ coupled states, respectively, whereas the energy values of yrast 11^+ , 13^+ , and 15^+ states are higher than those of $9^+ \otimes 2_1^+$, $9^+ \otimes 4_1^+$, and $9^+ \otimes 6_1^+$ coupled states, respectively. All the observed states are lower in energy values compared to the coupled states, in the case of ^{68}Ga . The reason behind this behavior could be due to the complex interaction nature between the core and particles in the case of ^{66}Ga compared to ^{68}Ga . As far as the residual interactions between the core and particles are concerned, we may infer from this observation that ^{66}Zn is behaving more as a pure core than ^{64}Zn . This nature of the vibrating core, in the case of ^{68}Ga , gives rise to a platform for more simple kinds of excitations at intermediate and high spins, compared to ^{66}Ga . Therefore, a complex nature of excitations in ^{66}Ga draws special attention to explore the fundamental single-particle configurations related to its structure.

IV. SHELL MODEL CALCULATIONS

In order to understand the observed nuclear structure in ^{66}Ga , shell model calculations have been performed in the present work using two different interactions, viz., jun45pn [35] and jj44bpn [36]. The shell model code NUSHELLX@MSU [37] was used for this purpose. With the ^{56}Ni core, the valence space for the calculation consists of $2p_{3/2}$, $1f_{5/2}$, $2p_{1/2}$, and $1g_{9/2}$ proton and neutron orbitals. The effective Hamiltonian jun45pn [35] has been obtained from a realistic interaction based on the Bonn-C potential, with a total of 133 two-body matrix elements and four single-particle energies modified empirically so as to fit 400 experimental energy values of 69 nuclei with mass numbers $A = 63\text{--}96$. In the derivation of this effective Hamiltonian, experimental

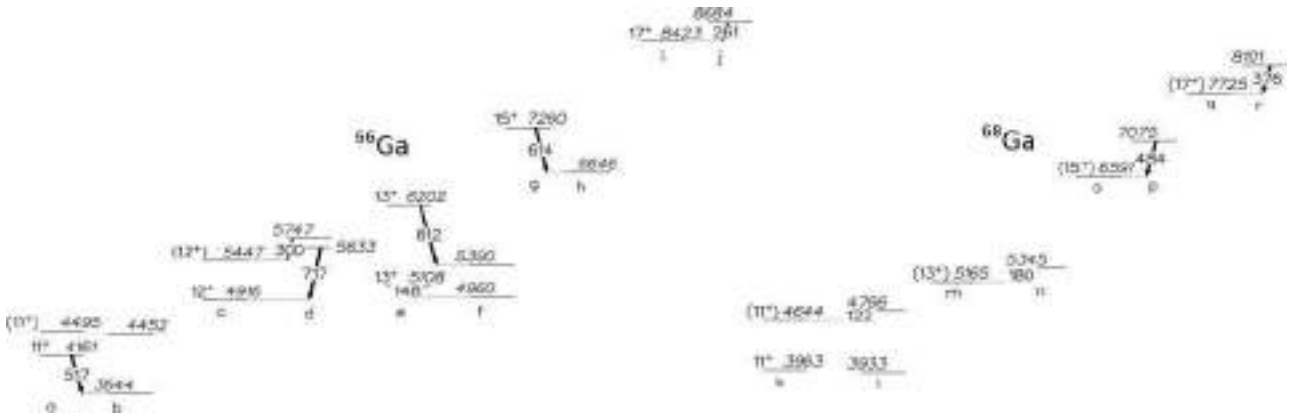


FIG. 6. A comparison of observed states with coupled states in $^{66,68}\text{Ga}$. Panel a: Observed energy states of 11_1^+ and 11_2^+ in ^{66}Ga obtained from the present experiment. Panel b: Calculated sum energy of the 9_1^+ state of ^{66}Ga (2652 keV, observed in the present experiment) plus 2_1^+ , 2_2^+ of ^{64}Zn [7,22], producing coupled states 11_1^+ and 11_2^+ of ^{66}Ga . Similarly, panels (c and d), (e and f), (g and h), and (i and j) for different mentioned states in ^{66}Ga . Here, the observed states compared are 11^+ , 12^+ , 13^+ , 15^+ , and 17^+ of ^{66}Ga . Panel k: Observed energy states of 11_1^+ and 11_2^+ in ^{68}Ga [12]. Panel l: Calculated sum energy of 9^+ state of ^{68}Ga [12] plus 2_1^+ , 2_2^+ of ^{66}Zn [15], producing coupled states 11_1^+ and 11_2^+ of ^{68}Ga . Similarly, panels (m and n), (o and p), and (q and r) for different mentioned states in ^{68}Ga . Here, the observed states compared are 11^+ , 13^+ , 15^+ , and 17^+ of ^{68}Ga . Each arrow represents the energy difference between the observed and coupled states (true for all pairs > 100 keV apart, for visualization purpose). See text for details.

data are not taken from $N = Z$ nuclei, specifically the Ni and Cu isotopes, because the model space may not be sufficient to describe the collectivity expected in these nuclei. The single-particle energies for this Hamiltonian are -9.8280 , -8.7087 , -7.8388 , and -6.261 MeV, respectively for the $2p_{3/2}$, $1f_{5/2}$, $2p_{1/2}$, and $1g_{9/2}$ orbitals. The effective Hamiltonian jj44bnp , due to Brown and Lesitskiy [36], is a realistic interaction based on the Bonn-C potential, which has been obtained by fitting binding energies and excitation energies in the Ni, Cu, and Zn isotopes and nuclei close to $N = 50$. The single-particle energies are taken to be -9.6566 , -9.2859 , -8.2695 , and -5.8944 MeV for the $2p_{3/2}$, $1f_{5/2}$, $2p_{1/2}$, and $1g_{9/2}$ orbitals, respectively. Previous calculations for ^{63}Zn [5], ^{63}Cu [29], and $^{60,62,64,66}\text{Zn}$ [38] with similar interaction and model space have produced very good agreements.

Observed levels in the present experiment, which are assigned with definite or tentative spin-parities, are compared with shell model calculations in Fig. 7. Those observed levels which are not assigned with spin-parities are not compared with calculated levels. The dominant particle configurations, constituting the wave functions of the levels, are represented in Tables II and III.

We have calculated occupation probabilities of protons and neutrons for two different interactions, and the results of these calculations are presented in Figs. 8–13. The wave function of a shell model state is the superposition of different orbitals included in the valence space, and occupation probability corresponding to an orbital indicates the fraction of the total number of valence nucleons (either protons or neutrons) occupying that particular orbital. So, an occupation probability gives the strength of individual contributions of different orbitals ($2p_{3/2}$, $1f_{5/2}$, $2p_{1/2}$, and $1g_{9/2}$ orbitals in the present calculation) of both the protons and neutrons in the total wave function.

Shell model calculations with jj44bnp interaction predict the first 1^+ state at just 27 keV higher in energy value with

respect to the observed value, but it is 142 keV higher in energy value as obtained by using the jun45pn interaction. So, the jj44bnp interaction produces the energy of the 1^+ state better than the jun45pn interaction. The energy of the first excited 3^+ state is better predicted by the jun45pn interaction than by the jj44bnp interaction but both fail to produce the energy value of the second excited 3^+ state, giving a result ≈ 350 keV lower in energy than the experimental value. The configuration of the first excited 3^+ state is predicted to be $[\pi(p_{3/2})^3]_{j_p=3/2} \otimes [v(f_{5/2})^3(p_{3/2})^4]_{j_v=5/2}$ (probability $\approx 13\%$) by jun45pn (Table III). Energies of the first and the second excited 5^+ states are well predicted by the jun45pn interaction, while they are overpredicted by the jj44bnp interaction. The predicted configurations by the jun45pn interaction for these states are $[\pi(f_{5/2})^1(p_{3/2})^2]_{j_p=5/2} \otimes [v(f_{5/2})^3(p_{3/2})^4]_{j_v=5/2}$ (probability $\approx 15\%$) and $[\pi(p_{3/2})^3]_{j_p=3/2} \otimes [v(f_{5/2})^3(p_{3/2})^4]_{j_v=9/2}$ (probability $\approx 11\%$), respectively. Neither interaction could produce the energy values of the first and the second excited 7^+ states, and shell model calculated values are far above the observed values. It is evident from the occupation number plots (Figs. 8 and 9) that significant contributions are coming from the $g_{9/2}$ proton and neutron orbitals in the case of the first 7^+ state, as calculated by the jj44bnp interaction. From the configuration tables of wave functions (Tables II and III), it is clear that the configurations with the highest probability for the first excited 7^+ states are $[\pi(p_{3/2})^1(p_{1/2})^1(g_{9/2})^1]_{j_p=5/2} \otimes [v(f_{5/2})^2(p_{3/2})^4(g_{9/2})^1]_{j_v=9/2}$ (probability $\approx 2\%$) and $[\pi(f_{5/2})^1(p_{3/2})^2]_{j_p=5/2} \otimes [v(f_{5/2})^3(p_{3/2})^4]_{j_v=9/2}$ (probability $\approx 11\%$) as predicted by jj44bnp and jun45pn interactions, respectively. Both interactions predict a full alignment of angular momenta contributed by both types of nucleons, i.e., proton and neutron, in forming the 7_1^+ state. No particular configuration appears to be dominant in forming the wave function for the first 7^+ state; rather, there is large competition between different configurations.

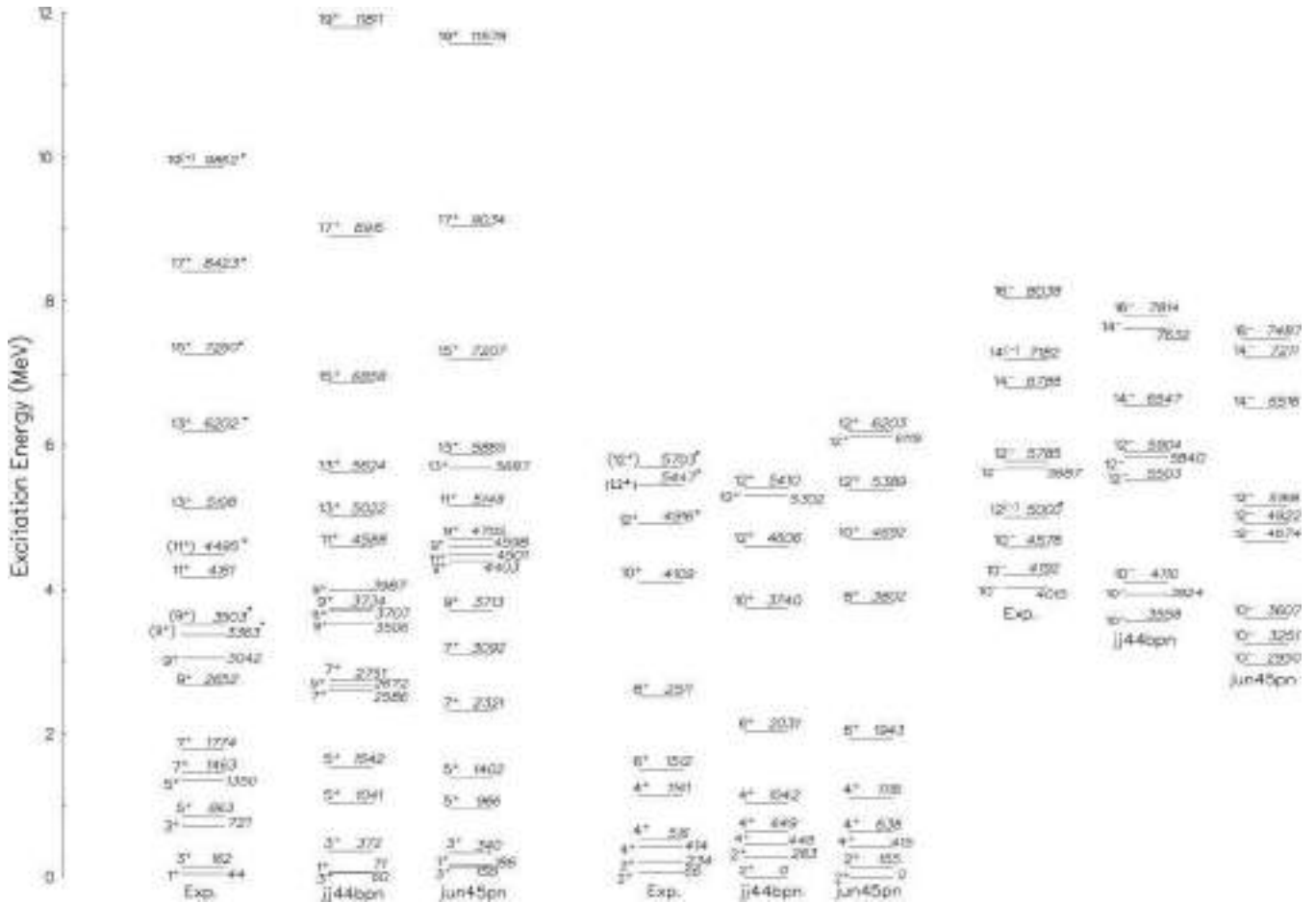


FIG. 7. Comparison of the observed levels of ^{66}Ga with shell model calculations using *jj44bpn* [36] and *jun45pn* [35] interactions. Newly observed levels in this experiment are identified with asterisks (*). The energies in the figure are in keV.

The first 2^+ excited state is predicted by both interactions to be at 0 keV, whereas the experimental energy value is 66 keV. The second excited 2^+ state is overpredicted by the *jj44bpn* interaction and is underpredicted by the *jun45pn* interaction. Energy values of the three 4^+ states, as calculated using the *jj44bpn* interaction, are in moderate

agreement with the observed values, whereas the *jun45pn* interaction predicts the proper value of 415 keV for the first excited 4^+ state, and the second and the third excited 4^+ states are also well predicted by the *jun45pn* interaction in comparison with *jj44bpn*. Configurations corresponding to these 4^+ states, as given by calculations using *jun45pn*

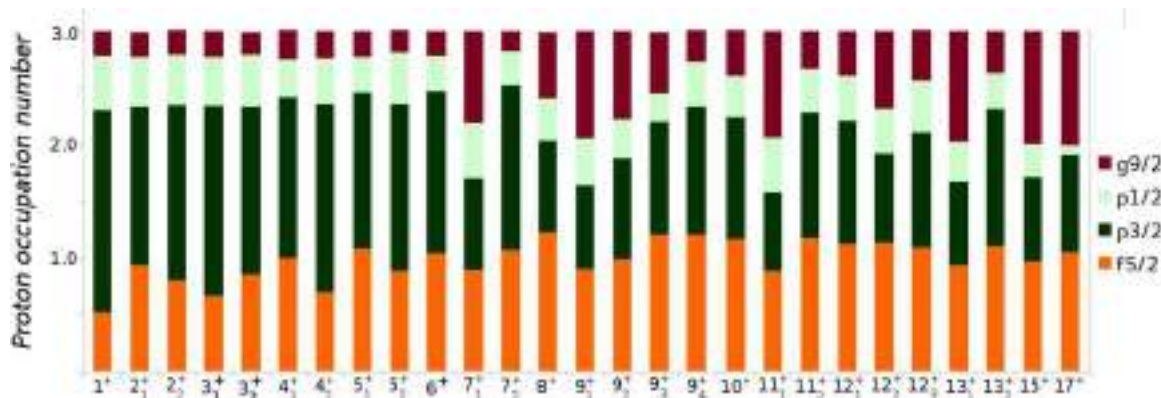


FIG. 8. Calculated occupation probabilities of the $f_{5/2}$, $p_{3/2}$, $p_{1/2}$, and $g_{9/2}$ orbitals for the positive parity states for protons in ^{66}Ga . The occupation probabilities are calculated from the shell model using the *jj44bpn* interaction. Please see text for details.

TABLE II. Configurations with the highest probabilities of different states in ^{66}Ga , calculated by the shell model using $f_{5/2}p_{g_{9/2}}$ model space with jj44bnp interaction.

Spin-parity(j^π)	Configuration	Probability
Positive parity		
1 ⁺	$\pi(f_{5/2})^0(p_{3/2})^3(p_{1/2})^0(g_{9/2})^0 \otimes \nu(f_{5/2})^2(p_{3/2})^4(p_{1/2})^1(g_{9/2})^0$	9.03
2 ⁺	$\pi(f_{5/2})^1(p_{3/2})^2(p_{1/2})^0(g_{9/2})^0 \otimes \nu(f_{5/2})^3(p_{3/2})^4(p_{1/2})^0(g_{9/2})^0$	3.59
3 ₁ ⁺	$\pi(f_{5/2})^0(p_{3/2})^3(p_{1/2})^0(g_{9/2})^0 \otimes \nu(f_{5/2})^2(p_{3/2})^4(p_{1/2})^1(g_{9/2})^0$	3.44
3 ₂ ⁺	$\pi(f_{5/2})^1(p_{3/2})^2(p_{1/2})^0(g_{9/2})^0 \otimes \nu(f_{5/2})^4(p_{3/2})^3(p_{1/2})^0(g_{9/2})^0$	4.23
4 ₁ ⁺	$\pi(f_{5/2})^1(p_{3/2})^2(p_{1/2})^0(g_{9/2})^0 \otimes \nu(f_{5/2})^3(p_{3/2})^4(p_{1/2})^0(g_{9/2})^0$	4.32
4 ₂ ⁺	$\pi(f_{5/2})^0(p_{3/2})^3(p_{1/2})^0(g_{9/2})^0 \otimes \nu(f_{5/2})^3(p_{3/2})^4(p_{1/2})^0(g_{9/2})^0$	5.44
4 ₃ ⁺	$\pi(f_{5/2})^1(p_{3/2})^2(p_{1/2})^0(g_{9/2})^0 \otimes \nu(f_{5/2})^3(p_{3/2})^2(p_{1/2})^0(g_{9/2})^2$	1.56
5 ₁ ⁺	$\pi(f_{5/2})^1(p_{3/2})^2(p_{1/2})^0(g_{9/2})^0 \otimes \nu(f_{5/2})^3(p_{3/2})^4(p_{1/2})^0(g_{9/2})^0$	9.33
5 ₂ ⁺	$\pi(f_{5/2})^0(p_{3/2})^2(p_{1/2})^1(g_{9/2})^0 \otimes \nu(f_{5/2})^3(p_{3/2})^4(p_{1/2})^0(g_{9/2})^0$	4.92
6 ⁺	$\pi(f_{5/2})^1(p_{3/2})^2(p_{1/2})^0(g_{9/2})^0 \otimes \nu(f_{5/2})^4(p_{3/2})^3(p_{1/2})^0(g_{9/2})^0$	5.17
7 ₁ ⁺	$\pi(f_{5/2})^0(p_{3/2})^1(p_{1/2})^1(g_{9/2})^1 \otimes \nu(f_{5/2})^2(p_{3/2})^4(p_{1/2})^0(g_{9/2})^1$	1.93
7 ₂ ⁺	$\pi(f_{5/2})^1(p_{3/2})^2(p_{1/2})^0(g_{9/2})^0 \otimes \nu(f_{5/2})^3(p_{3/2})^4(p_{1/2})^0(g_{9/2})^0$	6.87
8 ⁺	$\pi(f_{5/2})^2(p_{3/2})^1(p_{1/2})^0(g_{9/2})^0 \otimes \nu(f_{5/2})^2(p_{3/2})^3(p_{1/2})^0(g_{9/2})^2$	2.45
9 ₁ ⁺	$\pi(f_{5/2})^0(p_{3/2})^2(p_{1/2})^0(g_{9/2})^1 \otimes \nu(f_{5/2})^2(p_{3/2})^4(p_{1/2})^0(g_{9/2})^1$	4.13
9 ₂ ⁺	$\pi(f_{5/2})^0(p_{3/2})^2(p_{1/2})^0(g_{9/2})^1 \otimes \nu(f_{5/2})^2(p_{3/2})^3(p_{1/2})^1(g_{9/2})^1$	4.24
9 ₃ ⁺	$\pi(f_{5/2})^1(p_{3/2})^2(p_{1/2})^0(g_{9/2})^0 \otimes \nu(f_{5/2})^2(p_{3/2})^3(p_{1/2})^0(g_{9/2})^2$	5.63
9 ₄ ⁺	$\pi(f_{5/2})^1(p_{3/2})^2(p_{1/2})^0(g_{9/2})^0 \otimes \nu(f_{5/2})^2(p_{3/2})^2(p_{1/2})^1(g_{9/2})^2$	2.78
10 ⁺	$\pi(f_{5/2})^1(p_{3/2})^2(p_{1/2})^0(g_{9/2})^0 \otimes \nu(f_{5/2})^3(p_{3/2})^2(p_{1/2})^0(g_{9/2})^2$	4.10
11 ₁ ⁺	$\pi(f_{5/2})^2(p_{3/2})^0(p_{1/2})^0(g_{9/2})^1 \otimes \nu(f_{5/2})^4(p_{3/2})^2(p_{1/2})^0(g_{9/2})^1$	3.15
11 ₂ ⁺	$\pi(f_{5/2})^1(p_{3/2})^2(p_{1/2})^0(g_{9/2})^0 \otimes \nu(f_{5/2})^3(p_{3/2})^2(p_{1/2})^0(g_{9/2})^2$	3.73
12 ₁ ⁺	$\pi(f_{5/2})^1(p_{3/2})^2(p_{1/2})^0(g_{9/2})^0 \otimes \nu(f_{5/2})^3(p_{3/2})^2(p_{1/2})^0(g_{9/2})^2$	8.48
12 ₂ ⁺	$\pi(f_{5/2})^1(p_{3/2})^1(p_{1/2})^0(g_{9/2})^1 \otimes \nu(f_{5/2})^2(p_{3/2})^4(p_{1/2})^0(g_{9/2})^1$	4.88
12 ₃ ⁺	$\pi(f_{5/2})^1(p_{3/2})^1(p_{1/2})^0(g_{9/2})^1 \otimes \nu(f_{5/2})^2(p_{3/2})^4(p_{1/2})^0(g_{9/2})^1$	2.11
13 ₁ ⁺	$\pi(f_{5/2})^1(p_{3/2})^1(p_{1/2})^0(g_{9/2})^1 \otimes \nu(f_{5/2})^2(p_{3/2})^4(p_{1/2})^0(g_{9/2})^1$	5.07
13 ₂ ⁺	$\pi(f_{5/2})^1(p_{3/2})^2(p_{1/2})^0(g_{9/2})^0 \otimes \nu(f_{5/2})^1(p_{3/2})^4(p_{1/2})^0(g_{9/2})^2$	6.29
15 ⁺	$\pi(f_{5/2})^1(p_{3/2})^1(p_{1/2})^0(g_{9/2})^1 \otimes \nu(f_{5/2})^3(p_{3/2})^3(p_{1/2})^0(g_{9/2})^1$	10.58
17 ⁺	$\pi(f_{5/2})^1(p_{3/2})^1(p_{1/2})^0(g_{9/2})^1 \otimes \nu(f_{5/2})^2(p_{3/2})^3(p_{1/2})^1(g_{9/2})^1$	16.62
Negative parity		
10 ₁ ⁻	$\pi(f_{5/2})^1(p_{3/2})^2(p_{1/2})^0(g_{9/2})^0 \otimes \nu(f_{5/2})^3(p_{3/2})^3(p_{1/2})^0(g_{9/2})^1$	2.76
10 ₂ ⁻	$\pi(f_{5/2})^1(p_{3/2})^1(p_{1/2})^1(g_{9/2})^0 \otimes \nu(f_{5/2})^3(p_{3/2})^3(p_{1/2})^0(g_{9/2})^1$	3.61
10 ₃ ⁻	$\pi(f_{5/2})^1(p_{3/2})^2(p_{1/2})^0(g_{9/2})^0 \otimes \nu(f_{5/2})^3(p_{3/2})^3(p_{1/2})^0(g_{9/2})^1$	8.99
12 ₁ ⁻	$\pi(f_{5/2})^1(p_{3/2})^2(p_{1/2})^0(g_{9/2})^0 \otimes \nu(f_{5/2})^2(p_{3/2})^4(p_{1/2})^0(g_{9/2})^1$	5.51
12 ₂ ⁻	$\pi(f_{5/2})^1(p_{3/2})^1(p_{1/2})^1(g_{9/2})^0 \otimes \nu(f_{5/2})^2(p_{3/2})^4(p_{1/2})^0(g_{9/2})^1$	6.43
14 ₁ ⁻	$\pi(f_{5/2})^2(p_{3/2})^0(p_{1/2})^0(g_{9/2})^1 \otimes \nu(f_{5/2})^3(p_{3/2})^2(p_{1/2})^0(g_{9/2})^2$	11.78
14 ₂ ⁻	$\pi(f_{5/2})^1(p_{3/2})^1(p_{1/2})^0(g_{9/2})^1 \otimes \nu(f_{5/2})^2(p_{3/2})^2(p_{1/2})^1(g_{9/2})^2$	12.58
16 ⁻	$\pi(f_{5/2})^1(p_{3/2})^0(p_{1/2})^1(g_{9/2})^1 \otimes \nu(f_{5/2})^3(p_{3/2})^2(p_{1/2})^0(g_{9/2})^2$	9.19

interaction, are $[\pi(p_{3/2})^3]_{j_p=3/2} \otimes [\nu(f_{5/2})^3(p_{3/2})^4]_{j_v=5/2}$ (probability $\approx 20\%$), $[\pi(f_{5/2})^1(p_{3/2})^2]_{j_p=5/2} \otimes [\nu(f_{5/2})^3(p_{3/2})^4]_{j_v=5/2}$ (probability $\approx 13\%$) and $[\pi(p_{3/2})^3]_{j_p=3/2} \otimes [\nu(f_{5/2})^2(p_{3/2})^4(p_{1/2})^1]_{j_v=7/2}$ (probability $\approx 6\%$). It is evident that first excited 4⁺ state originates from the maximum alignment of proton and neutron angular momenta, whereas the other two 4⁺ states arise from the partial alignment. The 6⁺ excited state is overpredicted in energy value by both interactions. Here, both occupation number plots (Figs. 8–11) and configurations of wave

functions (Tables II and III), show that the 6⁺ state arises mainly due to the occupation of protons and neutrons in $f_{5/2}$ and $p_{3/2}$ orbitals.

With ten valence particles and with large model space, many possible configurations arise for a given total angular momentum, as there are many different ways to distribute valence particles among the $f_{5/2}$, $p_{3/2}$, $p_{1/2}$, and $g_{9/2}$ orbitals which add up to the same spin value. So, a large number of configurations to compete with each other for the construction of the wave function for a particular state, and it is evident

TABLE III. Configurations with the highest probabilities of different states in ^{66}Ga , calculated by the shell model using $f_{5/2}p_{g_{9/2}}$ model space with jun45pn interaction.

Spin-parity(j^π)	Configuration	Probability
Positive parity		
1 ⁺	$\pi(f_{5/2})^0(p_{3/2})^3(p_{1/2})^0(g_{9/2})^0 \otimes \nu(f_{5/2})^3(p_{3/2})^4(p_{1/2})^0(g_{9/2})^0$	12.27
2 ⁺	$\pi(f_{5/2})^0(p_{3/2})^3(p_{1/2})^0(g_{9/2})^0 \otimes \nu(f_{5/2})^3(p_{3/2})^4(p_{1/2})^0(g_{9/2})^0$	15.02
3 ₁ ⁺	$\pi(f_{5/2})^0(p_{3/2})^3(p_{1/2})^0(g_{9/2})^0 \otimes \nu(f_{5/2})^3(p_{3/2})^4(p_{1/2})^0(g_{9/2})^0$	12.59
3 ₂ ⁺	$\pi(f_{5/2})^0(p_{3/2})^2(p_{1/2})^1(g_{9/2})^0 \otimes \nu(f_{5/2})^3(p_{3/2})^4(p_{1/2})^0(g_{9/2})^0$	12.91
4 ₁ ⁺	$\pi(f_{5/2})^0(p_{3/2})^3(p_{1/2})^0(g_{9/2})^0 \otimes \nu(f_{5/2})^3(p_{3/2})^4(p_{1/2})^0(g_{9/2})^0$	20.43
4 ₂ ⁺	$\pi(f_{5/2})^1(p_{3/2})^2(p_{1/2})^0(g_{9/2})^0 \otimes \nu(f_{5/2})^3(p_{3/2})^4(p_{1/2})^0(g_{9/2})^0$	12.53
4 ₃ ⁺	$\pi(f_{5/2})^0(p_{3/2})^3(p_{1/2})^0(g_{9/2})^0 \otimes \nu(f_{5/2})^2(p_{3/2})^4(p_{1/2})^1(g_{9/2})^0$	6.32
5 ₁ ⁺	$\pi(f_{5/2})^1(p_{3/2})^2(p_{1/2})^0(g_{9/2})^0 \otimes \nu(f_{5/2})^3(p_{3/2})^4(p_{1/2})^0(g_{9/2})^0$	15.20
5 ₂ ⁺	$\pi(f_{5/2})^0(p_{3/2})^3(p_{1/2})^0(g_{9/2})^0 \otimes \nu(f_{5/2})^3(p_{3/2})^4(p_{1/2})^0(g_{9/2})^0$	10.86
6 ⁺	$\pi(f_{5/2})^1(p_{3/2})^2(p_{1/2})^0(g_{9/2})^0 \otimes \nu(f_{5/2})^2(p_{3/2})^4(p_{1/2})^1(g_{9/2})^0$	9.90
7 ₁ ⁺	$\pi(f_{5/2})^1(p_{3/2})^2(p_{1/2})^0(g_{9/2})^0 \otimes \nu(f_{5/2})^3(p_{3/2})^4(p_{1/2})^0(g_{9/2})^0$	11.22
7 ₂ ⁺	$\pi(f_{5/2})^0(p_{3/2})^3(p_{1/2})^0(g_{9/2})^0 \otimes \nu(f_{5/2})^4(p_{3/2})^3(p_{1/2})^0(g_{9/2})^0$	20.98
8 ⁺	$\pi(f_{5/2})^1(p_{3/2})^2(p_{1/2})^0(g_{9/2})^0 \otimes \nu(f_{5/2})^2(p_{3/2})^4(p_{1/2})^1(g_{9/2})^0$	10.52
9 ₁ ⁺	$\pi(f_{5/2})^0(p_{3/2})^2(p_{1/2})^0(g_{9/2})^1 \otimes \nu(f_{5/2})^4(p_{3/2})^2(p_{1/2})^0(g_{9/2})^1$	8.06
9 ₂ ⁺	$\pi(f_{5/2})^1(p_{3/2})^2(p_{1/2})^0(g_{9/2})^0 \otimes \nu(f_{5/2})^3(p_{3/2})^4(p_{1/2})^0(g_{9/2})^0$	18.88
9 ₃ ⁺	$\pi(f_{5/2})^0(p_{3/2})^2(p_{1/2})^0(g_{9/2})^1 \otimes \nu(f_{5/2})^2(p_{3/2})^3(p_{1/2})^1(g_{9/2})^1$	5.38
9 ₄ ⁺	$\pi(f_{5/2})^1(p_{3/2})^2(p_{1/2})^0(g_{9/2})^0 \otimes \nu(f_{5/2})^3(p_{3/2})^2(p_{1/2})^0(g_{9/2})^2$	2.35
and		
	$\pi(f_{5/2})^1(p_{3/2})^2(p_{1/2})^0(g_{9/2})^0 \otimes \nu(f_{5/2})^2(p_{3/2})^3(p_{1/2})^0(g_{9/2})^2$	2.35
10 ⁺	$\pi(f_{5/2})^1(p_{3/2})^2(p_{1/2})^0(g_{9/2})^0 \otimes \nu(f_{5/2})^2(p_{3/2})^3(p_{1/2})^0(g_{9/2})^2$	6.65
11 ₁ ⁺	$\pi(f_{5/2})^0(p_{3/2})^2(p_{1/2})^0(g_{9/2})^1 \otimes \nu(f_{5/2})^4(p_{3/2})^2(p_{1/2})^0(g_{9/2})^1$	5.05
11 ₂ ⁺	$\pi(f_{5/2})^1(p_{3/2})^2(p_{1/2})^0(g_{9/2})^0 \otimes \nu(f_{5/2})^3(p_{3/2})^2(p_{1/2})^0(g_{9/2})^2$	5.74
12 ₁ ⁺	$\pi(f_{5/2})^1(p_{3/2})^2(p_{1/2})^0(g_{9/2})^0 \otimes \nu(f_{5/2})^3(p_{3/2})^2(p_{1/2})^0(g_{9/2})^2$	12.30
12 ₂ ⁺	$\pi(f_{5/2})^2(p_{3/2})^1(p_{1/2})^0(g_{9/2})^0 \otimes \nu(f_{5/2})^3(p_{3/2})^2(p_{1/2})^0(g_{9/2})^2$	4.12
12 ₃ ⁺	$\pi(f_{5/2})^0(p_{3/2})^2(p_{1/2})^0(g_{9/2})^1 \otimes \nu(f_{5/2})^3(p_{3/2})^3(p_{1/2})^0(g_{9/2})^1$	6.90
13 ₁ ⁺	$\pi(f_{5/2})^1(p_{3/2})^1(p_{1/2})^0(g_{9/2})^1 \otimes \nu(f_{5/2})^4(p_{3/2})^2(p_{1/2})^0(g_{9/2})^1$	5.36
13 ₂ ⁺	$\pi(f_{5/2})^1(p_{3/2})^2(p_{1/2})^0(g_{9/2})^0 \otimes \nu(f_{5/2})^3(p_{3/2})^2(p_{1/2})^0(g_{9/2})^2$	9.39
15 ⁺	$\pi(f_{5/2})^1(p_{3/2})^1(p_{1/2})^0(g_{9/2})^1 \otimes \nu(f_{5/2})^4(p_{3/2})^2(p_{1/2})^0(g_{9/2})^1$	6.19
17 ⁺	$\pi(f_{5/2})^1(p_{3/2})^1(p_{1/2})^0(g_{9/2})^1 \otimes \nu(f_{5/2})^2(p_{3/2})^4(p_{1/2})^0(g_{9/2})^1$	15.28
Negative parity		
10 ₁ ⁻	$\pi(f_{5/2})^1(p_{3/2})^2(p_{1/2})^0(g_{9/2})^0 \otimes \nu(f_{5/2})^3(p_{3/2})^3(p_{1/2})^0(g_{9/2})^1$	9.55
10 ₂ ⁻	$\pi(f_{5/2})^1(p_{3/2})^2(p_{1/2})^0(g_{9/2})^0 \otimes \nu(f_{5/2})^3(p_{3/2})^3(p_{1/2})^0(g_{9/2})^1$	7.72
10 ₃ ⁻	$\pi(f_{5/2})^1(p_{3/2})^2(p_{1/2})^0(g_{9/2})^0 \otimes \nu(f_{5/2})^2(p_{3/2})^3(p_{1/2})^1(g_{9/2})^1$	9.51
12 ₁ ⁻	$\pi(f_{5/2})^1(p_{3/2})^2(p_{1/2})^0(g_{9/2})^0 \otimes \nu(f_{5/2})^2(p_{3/2})^3(p_{1/2})^1(g_{9/2})^1$	14.64
12 ₂ ⁻	$\pi(f_{5/2})^1(p_{3/2})^2(p_{1/2})^0(g_{9/2})^0 \otimes \nu(f_{5/2})^2(p_{3/2})^4(p_{1/2})^0(g_{9/2})^1$	8.40
14 ₁ ⁻	$\pi(f_{5/2})^0(p_{3/2})^2(p_{1/2})^0(g_{9/2})^1 \otimes \nu(f_{5/2})^3(p_{3/2})^2(p_{1/2})^0(g_{9/2})^2$	9.04
14 ₂ ⁻	$\pi(f_{5/2})^1(p_{3/2})^2(p_{1/2})^0(g_{9/2})^0 \otimes \nu(f_{5/2})^3(p_{3/2})^3(p_{1/2})^0(g_{9/2})^1$	12.95
16 ⁻	$\pi(f_{5/2})^1(p_{3/2})^0(p_{1/2})^1(g_{9/2})^1 \otimes \nu(f_{5/2})^3(p_{3/2})^2(p_{1/2})^0(g_{9/2})^2$	8.12

that, for almost all the lower excited states up to 9₃⁺ and 6⁺, as calculated respectively by jun45pn and jj44bpn interactions in ^{66}Ga , the dominant contributions come from the fp shell. It is evident from the wave function tables (Tables II and III) that, up to the 6⁺ spin state, the probability of a particular dominant configuration is significantly larger when calculated using the jun45pn interaction compared to that using jj44bpn.

The energy values of 3₁⁺, 4₁⁺, 4₂⁺, 4₃⁺, 5₁⁺, and 5₂⁺ states, as calculated using the jun45pn interaction, are in better agreement with the experimental values, whereas only that of the 2₂⁺ state calculated using the jj44bpn interaction is in good agreement with the observation. So, as far as the lower excited states are concerned, the jun45pn interaction is more efficient than the jj44bpn interaction in producing the level structure.

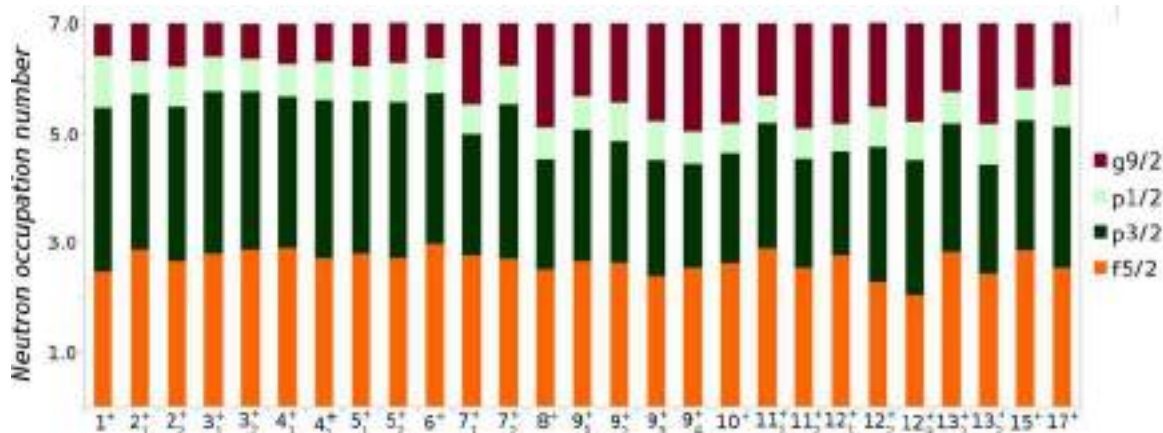


FIG. 9. Calculated occupation probabilities of the $f_{5/2}$, $p_{3/2}$, $p_{1/2}$, and $g_{9/2}$ orbitals for the positive parity states for neutrons in ^{66}Ga . The occupation probabilities are calculated from the shell model using the jj44bnpn interaction. Please see text for details.

The first excited 9^+ state is well reproduced by the jj44bnpn interaction but the other three 9^+ states are overpredicted by the same interaction. Here, all the 9^+ excited states are overpredicted by the jun45pn interaction. Among the different 11^+ , 12^+ , 13^+ , and 15^+ states, the energies of the second 11^+ , second 12^+ , and first 13^+ states, respectively, with configurations $[\pi(f_{5/2})^1(p_{3/2})^2]_{j_p=5/2} \otimes [\nu(f_{5/2})^3(p_{3/2})^2(g_{9/2})^2]_{j_n=17/2}$ (probability $\approx 4\%$), $[\pi(f_{5/2})^1(p_{3/2})^1(g_{9/2})^1]_{j_p=15/2} \otimes [\nu(f_{5/2})^2(p_{3/2})^4(g_{9/2})^1]_{j_n=9/2}$ (probability $\approx 5\%$), and $[\pi(f_{5/2})^1(p_{3/2})^1(g_{9/2})^1]_{j_p=17/2} \otimes [\nu(f_{5/2})^2(p_{3/2})^4(g_{9/2})^1]_{j_n=9/2}$ (probability $\approx 5\%$) are, as predicted by the jj44bnpn interaction, in good agreement with the experimental values, whereas only the energy state of 15^+ with the configuration $[\pi(f_{5/2})^1(p_{3/2})^1(g_{9/2})^1]_{j_p=17/2} \otimes [\nu(f_{5/2})^4(p_{3/2})^2(g_{9/2})^1]_{j_n=13/2}$ (probability $\approx 6\%$) is well reproduced by jun45pn interaction. As far as intermediate and high spin positive parity states are concerned, energy values calculated by both the interactions are in moderate agreement with the observed values but, compared to jun45pn , the jj44bnpn interaction is more able to reproduce the intermediate and high spin structure within the given $f_{5/2}p_{3/2}g_{9/2}$ model space. In all the intermediate and high spin states in ^{66}Ga , contributions to the wave functions are mainly dominated

by the $f_{5/2}$, $p_{3/2}$, and $g_{9/2}$ proton and neutron orbitals, as is obvious from the occupation probability plots and from the tables of configurations.

Higher spin states like 19^+ and above, for which the energy values as calculated by both interactions are greater than 1 MeV compared to the observed values, are not shown in configuration tables or occupation plots. So, it could be argued that a new mode of excitations is appearing at such high spin, which is different from single-particle nature. Large mixing of various orbitals at higher spins, predicted by the shell model calculations, also confirms the nature of a typical onset of collective behavior. A significant contribution, coming from $g_{9/2}$ proton and $g_{9/2}$ neutron orbitals, is very prominent, as reflected in the occupation number plots.

Three 10^- negative parity states are underpredicted in energy by both interactions, and the configurations for these states are mainly contributed from the protons in $f_{5/2}$ and $p_{3/2}$ orbitals and the neutrons in $f_{5/2}$, $p_{3/2}$, and $g_{9/2}$ orbitals. The second and the third 12^- excited states, as calculated by the jj44bnpn interaction, are in good agreement, whereas the first 12^- excited state is overpredicted by the same interaction. Here, all the 12^- states are underpredicted by the jun45pn interaction. The second excited 14^- state is well predicted by the jun45pn

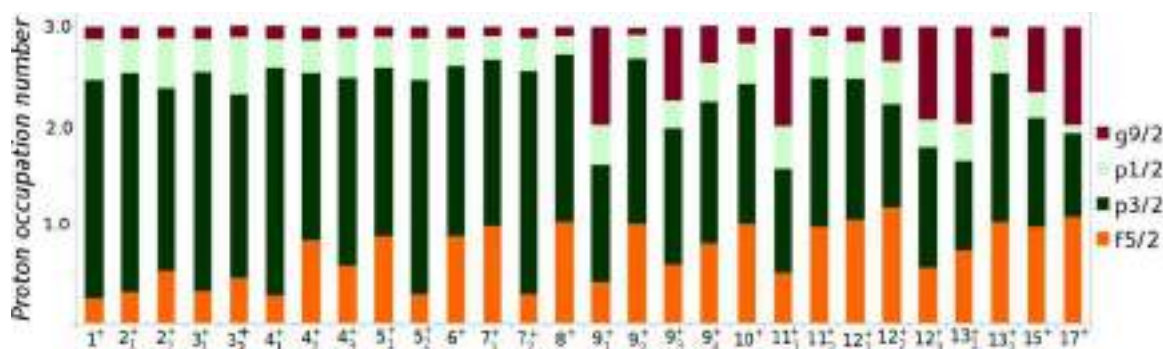


FIG. 10. Calculated occupation probabilities of the $f_{5/2}$, $p_{3/2}$, $p_{1/2}$, and $g_{9/2}$ orbitals for the positive parity states for protons in ^{66}Ga . The occupation probabilities are calculated from the shell model using the jun45pn interaction. Please see text for details.

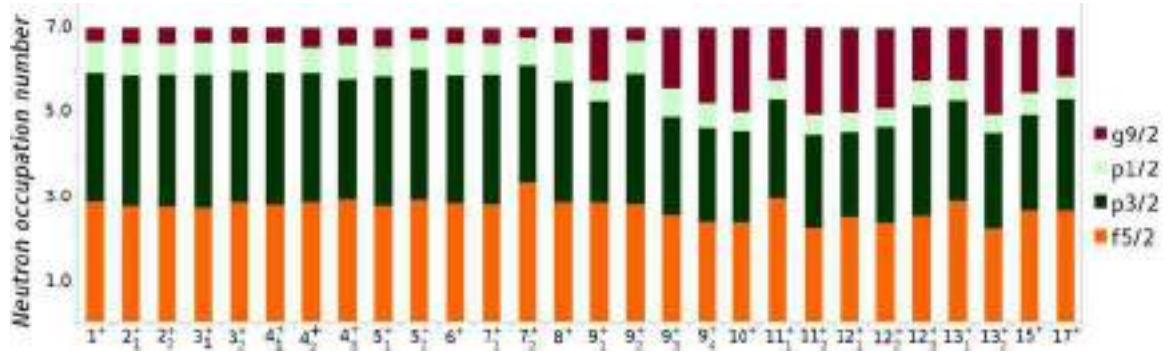


FIG. 11. Calculated occupation probabilities of the $f_{5/2}$, $p_{3/2}$, $p_{1/2}$, and $g_{9/2}$ orbitals for the positive parity states for neutrons in ^{66}Ga . The occupation probabilities are calculated from the shell model using the jun45pn interaction. Please see text for details.

interaction, whereas the first 14^- state is underpredicted by 271 keV in energy. The main configuration of the first excited 14^- state, as predicted by the jun45pn interaction, is $[\pi(p_{3/2})^2(g_{9/2})^1]_{j_p=9/2} \otimes [\nu(f_{5/2})^3(p_{3/2})^2(g_{9/2})^2]_{j_n=19/2}$ and that of second excited 14^- state is $[\pi(f_{5/2})^1(p_{3/2})^2]_{j_p=9/2} \otimes [\nu(f_{5/2})^3(p_{3/2})^3(g_{9/2})^1]_{j_n=19/2}$. So, for the first excited 14^- state, contributions of $g_{9/2}$ orbitals for both protons and neutrons are significantly large with respect to the second 14^- state, and this is also obvious from the occupation number (calculated using the jun45pn interaction) plot (Fig. 13). The energy of the 16^- state is in moderate agreement with the jj44bpn calculation but is well underpredicted by jun45pn. The configuration of this state is mainly originating from protons and neutrons in the $f_{5/2}$, $p_{3/2}$, and $g_{9/2}$ orbitals. The occupation number plots (Figs. 8–13) also suggest that, for both kinds of interaction, the contributions coming from both protons and neutrons in the $g_{9/2}$ orbitals are significantly large for high spin positive and negative parity states. Hence, a variety of structural effects are expected due to the occupancy of the shape driving $g_{9/2}$ orbitals. The low spin positive parity states up to 4^+ are mainly due to the occupation of protons in the $p_{3/2}$ orbital, and those above are due to protons in the $f_{5/2}$ and $p_{3/2}$ orbitals up to spin value $\approx 8\hbar$, as obtained from the calculations using the jun45pn interaction. Significant contributions in wave functions for low spin positive parity states up to 8^+ originate from neutrons occupying the $f_{5/2}$ and $p_{3/2}$ orbitals. For high spin positive (13^+ to 17^+) and negative (14^- and 16^-) parity states, angular momenta are mainly generated by the $(\pi f_{5/2}p_{3/2}g_{9/2})^3 \otimes (\nu f_{5/2}p_{3/2}g_{9/2})^7$ configuration, as predicted by both interactions. It is also

evident from the calculations with both interactions that the participation of the $p_{1/2}$ orbital for the generation of both low and high angular momentum states is insignificant.

V. CONCLUSION

A new level scheme of ^{66}Ga has been proposed in this present work, which is enriched with 21 new transitions and 20 new levels. Some of the previously observed states, without any definite spin-parities, are assigned with definite or tentative values in this work, from the measured values of DCO ratio and polarization asymmetry of depopulating transitions. Multipolarities of many new transitions are determined from the measurements. The level scheme has been extended up to ≈ 11.6 MeV in energy. Some intermediate spin states of ^{66}Ga are explained in the framework of coupling of single-particle configurations with the vibrational core. Shell model calculations have also been performed in $f_{5/2}pg_{9/2}$ model space using two different interactions, viz., jj44bpn and jun45pn. Comparative study shows that the jun45pn interaction is more efficient in explaining the lower excitations than jj44bpn. Both interactions are in moderate agreement in explaining intermediate spin states. With an improved set of the two-body matrix elements and incorporating the full $fpg_{9/2}$ model space, i.e., including the $1f_{7/2}$ orbital for calculations, a more accurate description may be obtained. High spin states above 15^+ are observed to be different from the single-particle nature, and it is probably the collective degrees of freedom that come into play at such high spin. More experimental investigation is required to confirm the nature of the collectivity at such high spin.

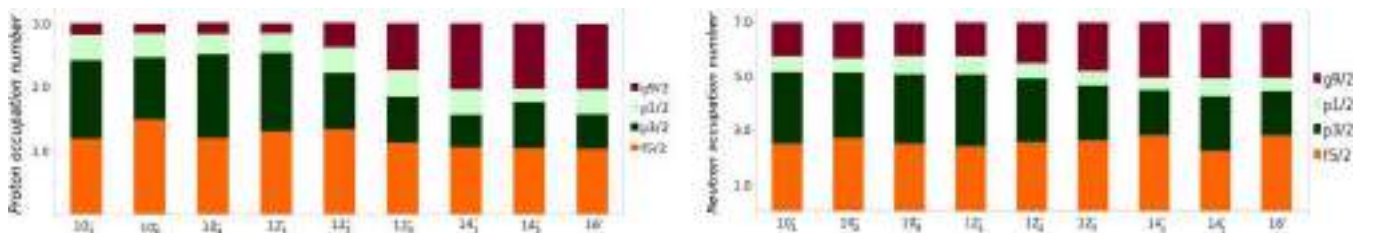


FIG. 12. Calculated occupation probabilities of the $f_{5/2}$, $p_{3/2}$, $p_{1/2}$, and $g_{9/2}$ orbitals for the negative parity states for protons and neutrons in ^{66}Ga . The occupation probabilities are calculated from the shell model using the jj44bpn interaction. Please see text for details.

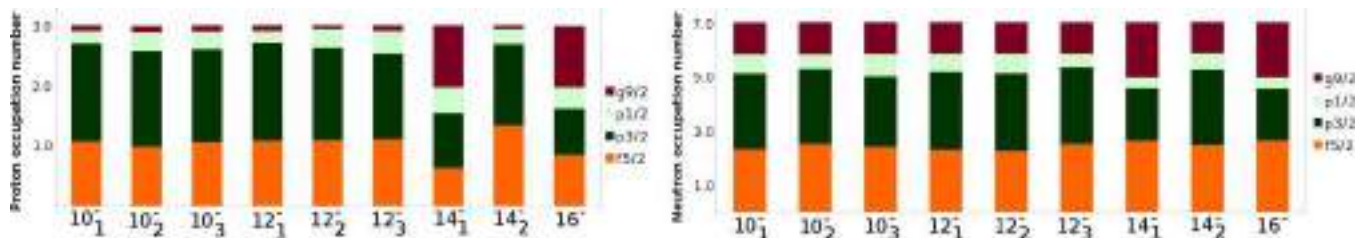


FIG. 13. Calculated occupation probabilities of the $f_{5/2}$, $p_{3/2}$, $p_{1/2}$, and $g_{9/2}$ orbitals for the negative parity states for protons and neutrons in ^{66}Ga . The occupation probabilities are calculated from the shell model using the jun45pn interaction. Please see text for details.

ACKNOWLEDGMENTS

We would like to acknowledge the Pelletron staff of IUAC for providing excellent beams and INGA collaborators for the loan of detectors. Support from the target laboratory and from D. Kanjilal, IUAC is gratefully acknowledged. We would like

to thank S. Nandi (VECC), S. S. Bhattacharjee (TRIUMF, Canada), and R. Garg (IUAC) for their help during the experiment. We would also like to acknowledge financial support from SERB/DST (New Delhi), file No. EMR/2015/000891, IUAC (New Delhi), file No. UFR49318 and DAE-BRNS, Project Sanction No. 37(3)/14/17/2016-BRNS.

- [1] C. E. Svensson *et al.*, *Phys. Rev. Lett.* **82**, 3400 (1999).
 [2] L.-L. Andersson *et al.*, *Phys. Rev. C* **79**, 024312 (2009).
 [3] C. E. Svensson *et al.*, *Phys. Rev. Lett.* **79**, 1233 (1997).
 [4] C. E. Svensson *et al.*, *Phys. Rev. Lett.* **80**, 2558 (1998).
 [5] U. S. Ghosh *et al.*, *Phys. Rev. C* **100**, 034314 (2019).
 [6] A. K. Singh *et al.*, *Phys. Rev. C* **57**, 1617 (1998).
 [7] D. Karlgren *et al.*, *Phys. Rev. C* **69**, 034330 (2004).
 [8] B. Mukherjee, S. Muralithar, R. P. Singh, R. Kumar, K. Rani, R. K. Bhowmik, and S. C. Pancholi, *Phys. Rev. C* **64**, 024304 (2001).
 [9] M. Weiszflog *et al.*, *Eur. Phys. J. A* **11**, 25 (2001).
 [10] S. S. Bhattacharjee *et al.*, *Phys. Rev. C* **95**, 054330 (2017).
 [11] I. Dankó *et al.*, *Phys. Rev. C* **59**, 1956 (1999).
 [12] A. K. Singh *et al.*, *Eur. Phys. J. A* **9**, 197 (2000).
 [13] D. Ward *et al.*, *Phys. Rev. C* **63**, 014301 (2000).
 [14] E. A. Stefanova *et al.*, *Phys. Rev. C* **67**, 054319 (2003).
 [15] L. Cleemann *et al.*, *Nucl. Phys. A* **386**, 367 (1982).
 [16] H. H. Bolotin and D. A. McClure, *Phys. Rev.* **180**, 987 (1969).
 [17] C. Morand, M. Agard, J. F. Bruandet, A. Dauchy, A. Giorni, F. Glasser, and T. U. Chan, *Nucl. Phys. A* **308**, 103 (1978).
 [18] C. C. Lu, M. S. Zisman, and B. G. Harvey, *Phys. Rev.* **186**, 1086 (1969).
 [19] J. Timár, T. X. Quang, T. Fényes, Z. Dombrádi, A. Krasznahorkay, J. Kumpulainen, R. Julin, S. Brant, V. Paar, and L. Šimičič, *Nucl. Phys. A* **573**, 61 (1994).
 [20] M. R. Najam, W. F. Davidson, W. M. Zuk, L. E. Carlson, and M. A. Awal, *Nucl. Phys. A* **173**, 577 (1971).
 [21] R. A. Hinrichs, R. Sherr, G. M. Crawley, and I. Proctor, *Phys. Rev. Lett.* **25**, 829 (1970).
 [22] <http://www.nndc.bnl.gov>.
 [23] A. Filevich, A. Ceballos, M. A. J. Mariscotti, P. Thieberger, and E. D. Mateosian, *Nucl. Phys. A* **295**, 513 (1978).
 [24] G. K. Mehta *et al.*, *Nucl. Instrum. Methods Phys. Res. A* **268**, 334 (1988).
 [25] S. Muralithar *et al.*, *Nucl. Instrum. Methods Phys. Res. A* **622**, 281 (2010).
 [26] B. P. Ajith Kumar *et al.*, in *Proceedings of the 44th DAE-BRNS Symposium on Nuclear Physics* (Department of Atomic Energy, Government of India, Mumbai, 2001), p. 390.
 [27] D. C. Radford, *Nucl. Instrum. Methods Phys. Res., Sect. A* **361**, 297 (1995).
 [28] R. K. Bhowmik *et al.*, in *Proceedings of the 44th DAE-BRNS Symposium on Nuclear Physics* (Department of Atomic Energy, Government of India, Mumbai, 2001), p. 422.
 [29] S. Rai *et al.*, *Eur. Phys. J. A* **54**, 84 (2018).
 [30] K. S. Krane *et al.*, *Nucl. Data Tables* **11**, 351 (1973).
 [31] G. Duchene *et al.*, *Nucl. Instrum. Methods Phys. Res. A* **432**, 90 (1999).
 [32] K. Starosta *et al.*, *Nucl. Instrum. Methods Phys. Res. A* **423**, 16 (1999).
 [33] F. W. N. de Boer *et al.*, *Nucl. Phys. A* **158**, 166 (1970).
 [34] E. A. McCutchan *et al.*, *Nucl. Data Sheets* **113**, 1735 (2012).
 [35] M. Honma, T. Otsuka, T. Mizusaki, and M. Hjorth-Jensen, *Phys. Rev. C* **80**, 064323 (2009).
 [36] A. F. Lisetskiy, B. A. Brown, M. Horoi, and H. Grawe, *Phys. Rev. C* **70**, 044314 (2004).
 [37] A. Brown and W. D. M. Rae, *Nucl. Data Sheets* **120**, 115 (2014).
 [38] S. Rai *et al.*, *Int. J. Mod. Phys. E* **25**, 1650099 (2016).

Evolution of collectivity and shape transition in ^{66}Zn

S. Rai ^{1,*} U. S. Ghosh ¹ B. Mukherjee ^{1,†} A. Biswas,¹ A. K. Mondal,¹ K. Mandal ¹ A. Chakraborty ¹
S. Chakraborty ^{2,‡} G. Mukherjee ³ A. Sharma ⁴ I. Bala,⁵ S. Muralithar,⁵ and R. P. Singh ⁵

¹Department of Physics, Siksha-Bhavana, Visva-Bharati, Santiniketan, West Bengal-731235, India

²Department of Physics, Institute of Science, Banaras Hindu University, Varanasi-221005, India

³Variable Energy Cyclotron Centre (VECC), 1/AF Bidhannagar, Kolkata-700064, India

⁴Department of Physics, Himachal Pradesh University, Shimla-171005, India

⁵Inter University Accelerator Centre (IUAC), Aruna Asaf Ali Marg, New Delhi-110067, India



(Received 22 August 2020; accepted 16 November 2020; published 14 December 2020)

Excited states in ^{66}Zn were investigated through the in-beam γ -ray spectroscopic techniques using the $^{52}\text{Cr}(^{18}\text{O}, 2p2n)$ fusion-evaporation reaction at a beam energy of 72.5 MeV. The γ -rays emitted by the de-exciting nuclei were recorded in coincidence mode using the 14 Compton suppressed Ge clover detectors of the Indian National Gamma Array. With 14 new transitions being identified, the level scheme of ^{66}Zn has been extended up to the excitation energy ≈ 12.3 MeV and spin $\approx 17\hbar$. A rotational band, associated with the two quasineutrons from the $1g_{9/2}$ orbital, has been found to exhibit a band crossing with the ground-state band at a spin of $6\hbar$. The evolution of the collectivity and shape transition in this nucleus have been discussed in the framework of the total Routhian surface calculations and in comparison with the neighboring $^{68,70}\text{Ge}$ nuclei.

DOI: [10.1103/PhysRevC.102.064313](https://doi.org/10.1103/PhysRevC.102.064313)

I. INTRODUCTION

Nuclei in the mass region $A \approx 60$ –70 having its Fermi surfaces lying in between that of the $N = Z = 28$ doubly magic ^{56}Ni and the semi-magic $N = 40$ subshell gap are known to exhibit a complex interplay of the single-particle and the collective modes of excitation. While the single particle excitation involves the valence nucleons outside the ^{56}Ni core, the collective excitation has been attributed to the gaps observed in the Nilsson energy diagram at $N = Z = 34$, 36 for the oblate deformation and $N = Z = 38$ for the prolate deformation. In this mass region, the high- j unique parity $1g_{9/2}$ orbital is found to play a major role in the configuration of high spin states and it has been attributed in producing several exciting high spin phenomena [1–8]. Collective structures arising out of the different quasiparticle configurations based on the $\pi 1g_{9/2}$ and/or $\nu 1g_{9/2}$ orbitals have been found to give rise to the different kinds of shape evolution with the increasing spin. In this mass region, the octupole correlations are also expected due to the presence of orbitals satisfying $\Delta L = \Delta J = 3$ criterion, arising out of the $2p_{3/2}$ ($L = 1$) and the $1g_{9/2}$ ($L = 4$) orbitals around the Fermi surface.

Lying in the transitional region encompassing the doubly magic spherical ^{56}Ni and the strongly deformed Sr, Kr isotopes, ^{66}Zn is an interesting candidate for studying the phenomena of shape transitions from the spectroscopic point of view. In the neighboring nuclei, the alignment of the neutrons and protons in the $1g_{9/2}$ orbitals have been observed

leading to the band crossing between the collective structures of different configurations [9–14]. Several superdeformed and terminating bands have been reported in the lighter Zn and other slightly heavier even-even $^{68,70}\text{Ge}$ isotopes [3,4,9–12]. These observations have motivated us for studying the nuclear structure in ^{66}Zn , the latest studies of which date back to the 1970s. Furthermore, most of the previously reported level-structure investigations were performed using the β -decays [15,16], transfer reactions [17] or light-ion induced reactions [18–22] with modest experimental setups. Moreover, Morand *et al.* [23] have measured the lifetimes of a few yrast states in ^{66}Zn via the Doppler shift attenuation method (DSAM), while Cleemann *et al.* [21] have measured lifetimes of some of the negative parity levels using the recoil Doppler method (RDM).

In this article, we report for the first time on the high spin states in ^{66}Zn populated using a heavy-ion induced reaction. The emitted γ -rays were detected with a high resolution and efficient array of high-purity germanium (HPGe) clover detectors. The level scheme of ^{66}Zn has been revisited using the γ - γ coincidence technique and extended significantly in the present work. A collective band based on two $1g_{9/2}$ quasineutrons has been found to exhibit a band crossing with the ground-state band at a spin of $6\hbar$. The evolution of the collectivity and shape transition in this nucleus have been discussed in the framework of the total Routhian surface (TRS) calculation and compared with the neighboring $^{68,70}\text{Ge}$ nuclei, which have similar kind of collective features.

II. EXPERIMENTAL DETAILS AND DATA ANALYSIS

The fusion evaporation reaction $^{52}\text{Cr}(^{18}\text{O}, 2p2n)$ at a beam energy of $E_{\text{lab}} = 72.5$ MeV was used to populate the high

*Present address: Forensic Science Laboratory, 37/1/2 Belgachia Road, Kolkata-700037, India.

†buddhadev.mukherjee@visva-bharati.ac.in

‡Present address: Inter University Accelerator Centre, New Delhi.

TABLE I. Values of the level energies (E_i) in keV, γ -ray energies (E_γ) in keV, initial (I_i^π) \rightarrow final (I_f^π) spin-parity, relative intensities (I_γ), DCO ratio (R_{DCO}), and polarization asymmetry (Δ_{asym}) of the γ -ray transitions as obtained in this work for ^{66}Zn .

Level energy E_i (keV)	Gamma-ray energy E_γ (keV)	Initial \rightarrow Final spin-parity $I_i^\pi \rightarrow I_f^\pi$	Relative Intensity ^a I_γ	DCO ratio R_{DCO}	Polarization asymmetry Δ_{asym}	Assignment
1039	1038.91(13)	$2^+ \rightarrow 0^+$	100(3)	1.01(9) ^c	0.14(4)	$E2$
1872	833.19(19)	$2^+ \rightarrow 2^+$	25.72(92)	0.88(8) ^b	-0.16(6)	$M1(+E2)$
2450	1411.14(15)	$4^+ \rightarrow 2^+$	$62 < I_\gamma < 69$	1.03(13) ^f	0.12(4)	$E2$
2764	891.91(19)	$4^{(+)} \rightarrow 2^+$	3.77(26)	1.32(27) ^b		($E2$)
2826	1787.32(13) ^d	$3^{(-)} \rightarrow 2^+$	< 3			
3077	627.20(18)	$(4^+) \rightarrow 4^+$	8.00(38)	0.86(26) ^b		($M1$)
	1205.21(14)	$(4^+) \rightarrow 2^+$	2.13(21)	1.01(20) ^b		($E2$)
3746	668.80(21)	$5^- \rightarrow (4^+)$	10.96(47)	0.77(13) ^b		($E1$)
	920.34(17)	$5^- \rightarrow 3^{(-)}$	2.81(23)	1.28(30) ^b		($E2$)
	981.72(15)	$5^- \rightarrow 4^{(+)}$	2.80(23)	0.46(20) ^b		($E1$)
	1296.34(11)	$5^- \rightarrow 4^+$	40.15(140)	0.57(4) ^b	0.12(7)	$E1$
4074	328.40(17)	$6^- \rightarrow 5^-$	24.80(89)	0.70(5) ^b	0.11(9)	$M1 + E2$
4179	1728.67(18)	$6^+ \rightarrow 4^+$	13.57(55)	1.09(13) ^b	0.13(8)	$E2$
4250	176.34(14)	$7^- \rightarrow 6^-$	11.97(50)	0.76(6) ^b		$M1 + E2$
	504.45(15)	$7^- \rightarrow 5^-$	23.38(85)	1.05(9) ^b	0.08(5)	$E2$
4812	738.45(15)	$(7^-) \rightarrow 6^-$	2.33(21)	0.83(27) ^b		($M1 + E2$)
5110	860.13(18) ^e	$8^{(-)} \rightarrow 7^-$	1.30(18)			
	1035.90(17)	$8^{(-)} \rightarrow 6^-$	4.20(27)	1.09(22) ^b		($E2$)
5205	1026.46(18)	$8^+ \rightarrow 6^+$	11.25(48)	1.06(14) ^b	0.04(2)	$E2$
	954.42(21)	$8^+ \rightarrow 7^-$	15.23(60)	0.47(5) ^b		$E1$
5463	1213.22(14)	$9^- \rightarrow 7^-$	17.63(67)	1.13(13) ^b	0.08(1)	$E2$
6075	1262.89(15)	$(9^-) \rightarrow (7^-)$	2.83(14)	1.20(27) ^b		($E2$)
6291	1085.65(10)	$10^+ \rightarrow 8^+$	19.75(74)	1.00(10) ^b	0.06(4)	$E2$
	827.80(13)	$10^+ \rightarrow 9^-$	3.70(26)	0.45(10) ^c		$E1$
6418	1308.15(23)	$\rightarrow 8^{(-)}$	1.03(18)			
6874	1411.11(13)	$11^- \rightarrow 9^-$	< 4	1.10(18) ^c	0.05(1)	$E2$
7517	1225.56(16)	$12^+ \rightarrow 10^+$	13.39(55)	1.06(16) ^b		$E2$
	642.77(16)	$12^+ \rightarrow 11^-$	2.64(22)			
7613	1537.97(19)	$\rightarrow (9^-)$	0.65(11)			
7918	1627.30(24)	$(12^+) \rightarrow 10^+$	2.08(10)	0.78(20) ^f		($E2$)
8675	1800.63(31) ^e	$(13^-) \rightarrow 11^-$	< 1			
8889	1371.75(22) ^e	$\rightarrow 12^+$	< 1			
9304	1787.13(19)	$14^+ \rightarrow 12^+$	< 10	1.15(28) ^c		($E2$)
	1385.58(18)	$14^+ \rightarrow (12^+)$	0.77(17)			
9823	518.74(19)	$(15^+) \rightarrow 14^+$	5.90(32)	0.64(16) ^b		$M1 + E2$
10880	1575.62(30)	$(16^+) \rightarrow 14^+$	1.60(19)	0.83(14) ^c		($E2$)
11187	1364.41(21)	$(17^+) \rightarrow (15^+)$	0.72(17)	1.05(66) ^f		($E2$)
12278	1090.65(18) ^e	$\rightarrow (17^+)$	< 1			
	1398.41(24) ^e	$\rightarrow (16^+)$	< 1			

^aThe quoted error includes the fitting error plus an additional error of 3% taken due to the uncertainties in efficiency, background subtraction, etc.

^bGate on $E2$, 1039 keV.

^cGate on $E2$, 1411 keV.

^dMeasurement of R_{DCO} and Intensity were not possible due to the presence of overlapping γ -energies.

^eMeasurement of R_{DCO} or Intensity were not possible due to the weak statistics.

^fGate on $E2$, 1086 keV.

γ - γ coincidence spectra gated by the 1039, 1411 and 519 keV transitions of ^{66}Zn are shown, respectively, in Figs. 2(a)–2(c), wherein most of the new transitions reported in the present work can be seen.

Apart from the ground-state band structure, the positive parity structures have also been established [19–21], which are weakly populated in the present work. The 1872 keV level

decaying to the yrast 2^+ level by the 833 keV γ -ray transition, has been observed in conformity with the earlier spin-parity assignment 2^+ . This state is fed by a 1205 keV transition and a relatively intense 892 keV transition, both having the quadrupole nature as evident from their DCO ratios. The (4^+) level at 3077 keV is fed by a 669 keV transition of $E1$ nature from the strongly populated 5^- state at 3746 keV. It decays

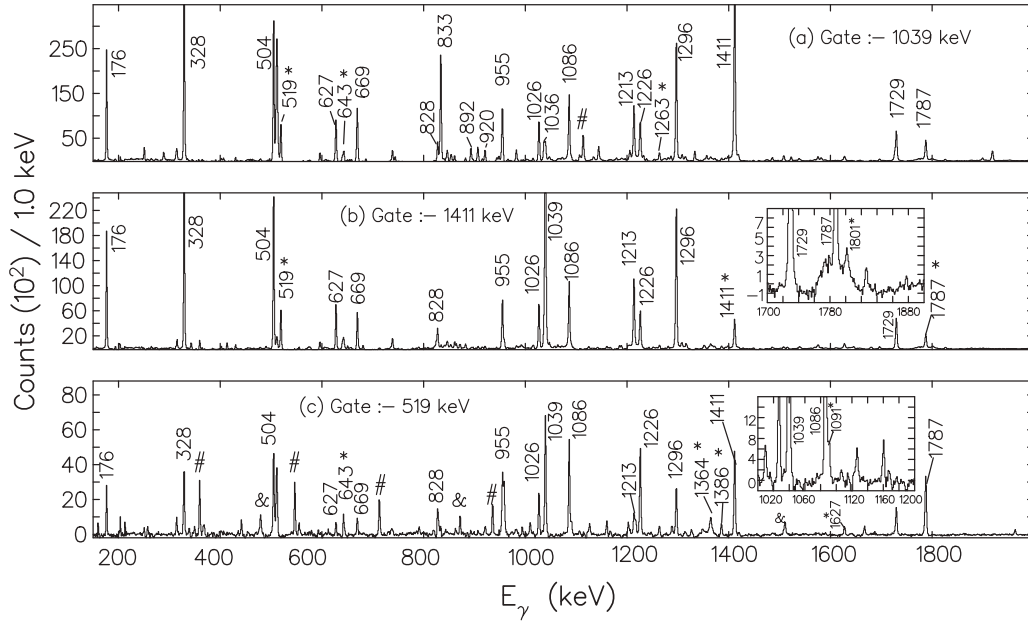


FIG. 2. Background subtracted $\gamma\text{-}\gamma$ coincidence spectra for ^{66}Zn gated on (a) 1039 keV ($2^+ \rightarrow 0^+$), (b) 1411 keV ($4^+ \rightarrow 2^+$), which also contains the contribution from the 1411 keV ($11^- \rightarrow 9^-$) transition. The inset shows the newly identified 1801 keV transition along with the 1729 keV and the 1787 keV transitions, and (c) 519 keV ($15^+ \rightarrow 14^+$) transition. The inset shows the newly identified 1091 keV transition along with the 1089 keV transition. Here, y-axis represents counts per 1.0 keV. New transitions are marked by the asterisks (*). Strong peaks which are marked with the “#” indicate contaminant γ -rays and those marked by the “&” represent transitions which may belong to ^{66}Zn but could not be placed in the level scheme due to the insufficient coincidence statistics. Here, the contaminant γ -rays are appearing from the $^{61,62}\text{Cu}$ and ^{67}Ga nuclei which are also populated in the same fusion evaporation reaction.

via the 627 keV γ -ray transition to the yrast 4^+ level at the 2450 keV and to the 1872 keV level via the 1205 keV γ -ray transition.

The lowest negative parity state at 2826 keV which was previously established as the 3^- from angular correlation of the de-exciting 1787 keV transition [19], is weakly populated in the present reaction. Due to the presence of an overlapping 1787 keV transition, a firm spin-parity assignment to this state could not be done. This state is fed by a weak 920 keV transition from the 3746 keV level. The 3746 keV level is strongly populated which decays dominantly to the 4_1^+ state. The R_{DCO} and the polarization asymmetry values of the 1296 keV transition feeding the 2450 keV level confirm the 5^- spin-parity assignment to 3746 keV state. Above this level, three strongly populated negative parity states, viz, the 6^- at 4074 keV, 7^- at 4250 keV and the 9^- at 5463 keV, which have been previously established, are confirmed as evident from the electromagnetic nature of the 328, 504, and the 1213 keV transitions, respectively. This sequence is extended by two new levels, one at 6874 keV with the spin-parity 11^- and the other at 8675 keV for which no spin-parity could be assigned due to its weak intensity. The three members of the negative parity sequence i.e, the 7^- , 9^- , and 11^- states are found to be connected to the yrast positive parity states, namely 8^+ , 10^+ , and 12^+ , respectively, by the 955, 828, and 643 keV transitions. A negative parity sequence built on the 6^- , 4074 keV state has been extended with the addition of two new levels at 6075 and 7613 keV. Another cascade of the 1036 and 1308 keV transitions feeding the 6^- level is

observed in accordance with the previous work [20], however spin-parity assignment could not be done for the 6418 keV state due to the weak intensity of the transition decaying from the state. A background subtracted $\gamma\text{-}\gamma$ coincidence spectrum gated by the newly identified 519 keV transition of ^{66}Zn is shown in Fig. 2(c), wherein most of the transitions reported in the present work can be observed.

IV. DISCUSSION

^{66}Zn has two protons and eight neutrons outside the doubly magic core, ^{56}Ni . In the valence configurations, the active orbitals are those of the $N = 3$, $2p_{3/2}$, $1f_{5/2}$, and $2p_{1/2}$ subshells and the $N = 4$, $1g_{9/2}$ intruder subshell. ^{66}Zn , being transitional nucleus, displays a complex spectrum and the description of its level structure from the viewpoint of a single model is difficult. Various theoretical approaches such as the spherical shell-model [35], crude shell model [17], deformed configuration mixing shell-model [36], Hartree-Fock-Bogoliubov calculation [37] and the two-proton cluster vibrator model [21,38] calculations have been used earlier to understand the positive parity and the negative parity level structures in ^{66}Zn .

Using the deformed configuration mixing shell model in the $p_{3/2}f_{5/2}p_{1/2}g_{9/2}$ model space, Ahalpara *et al.* have interpreted fairly well the positive parity high spin states in ^{66}Zn in terms of various configurations [36]. The observation of the sudden dip in the $B(E2)$ value of the $8^+ \rightarrow 6^+$ transition has been attributed to the band crossing between

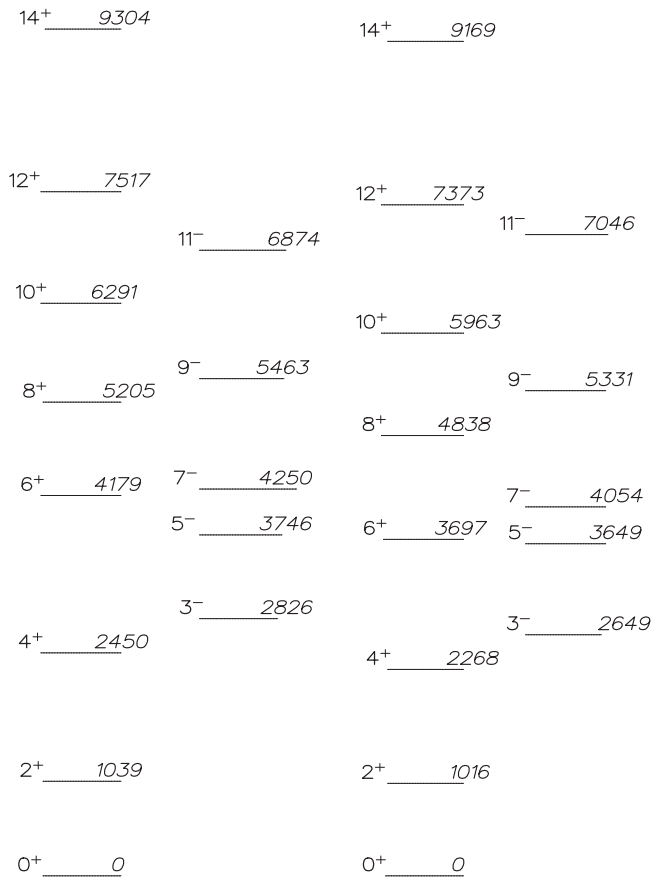


FIG. 3. Comparison of the yrast band and the negative parity level structure of ^{66}Zn (present work) and ^{68}Ge [9]. Numbers along the right side of the levels denote the level energies in keV and that in the left denote the spin(in \hbar)-parity.

the ground-state band and the deformed excited state band arising from the two particle-hole (2p-2h) excitation to the $1g_{9/2}$ orbital [36]. The ground-state band comprising of the $J^\pi = 0^+, 2^+, 4^+, 6^+$ states, has been assigned with the configuration $\pi\nu(p_{3/2}f_{5/2}p_{1/2})^{10}$ and the excited state band comprising of the $8^+, 10^+, 12^+, 14^+$ states to the 2p-2h $(p_{3/2}f_{5/2}p_{1/2})^8(g_{9/2})^2$ configuration. Assuming a configuration of $[\pi(p_{3/2})^2\nu(f_{5/2}p_{1/2})^6]_{6^+} \otimes [\nu(g_{9/2})^2]_{8^+}$, a maximum spin of $14\hbar$ can be obtained and the corresponding (terminating) state has been observed in our work. Beyond this state, a change in the structure or shape transition can be expected which could be predicted by the theoretical calculations. Interestingly, in their calculations, Ahalpara *et al.* predicted the yrast 14^+ level (unobserved experimentally at that time) to lie at ≈ 9.4 MeV, which is very close to the experimentally observed 9.3 MeV level in the present work. In the present investigation, this band is also extended by the placement of the three new connecting γ -ray transitions of 1787, 519 and 1364 keV.

In terms of the level energy, intensity, and decay pattern, a great similarity of the level structure of ^{66}Zn with the neighboring ^{68}Ge isotope is observed. A comparison of the yrast and few negative parity level structure of ^{66}Zn with the isotonic ^{68}Ge is shown in Fig. 3. This kind of

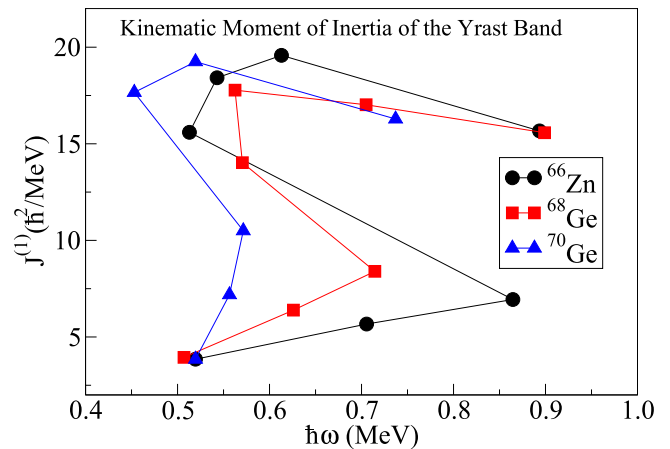


FIG. 4. Variation of the experimentally deduced kinematic moment of inertia as a function of the rotational frequency ($\hbar\omega$) for the yrast positive parity band in ^{66}Zn (present work). The corresponding values of the neighboring $^{68,70}\text{Ge}$ [9–11,14] isotopes are also shown for comparison.

comparison is useful in building the level structure systematics of nuclei in this mass region and in assigning the wave function configurations to the analogous quantum states. In $^{68,70}\text{Ge}$, above the 6^+ state of the ground-state band, two 8^+ states appear leading to the forking of the ground-state band into two quadrupole excited bands [9–11,39]. Theoretical studies [40–42] have suggested this forking phenomena as the band-crossing of the ground-state band with the two excited deformed bands having the two-neutron ($\nu 1g_{9/2}^2$) and the two-proton ($\pi 1g_{9/2}^2$) quasiparticle configurations, respectively. Interestingly in ^{70}Ge , the simultaneous band crossing of the two-neutron aligned configuration and the γ band have been reported leading to the forking of the ground-state band [10].

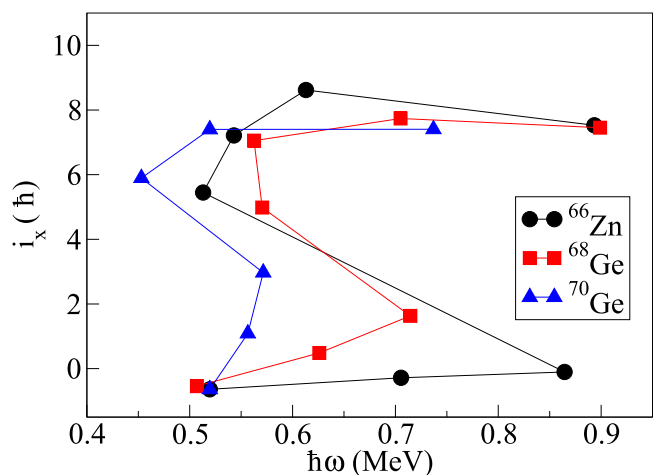


FIG. 5. Experimental alignments of the yrast positive parity band as a function of the rotational frequency for ^{66}Zn (present work) and $^{68,70}\text{Ge}$ [9–11]. The reference rotor, which was subtracted, is based on the Harris parameters, $J_0 = 6.0\hbar^2/\text{MeV}$ and $J_1 = 3.5\hbar^4/\text{MeV}^3$. Please see text for details.

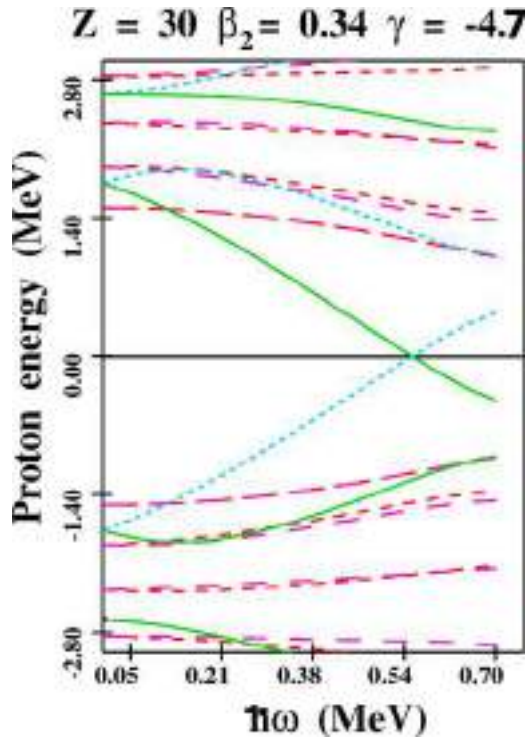


FIG. 6. Calculated quasiparticle Routhians for protons in ^{66}Zn as a function of the rotational frequency $\hbar\omega$ obtained from TRS calculation [44] for $\beta_2 = 0.34$ and $\gamma = -4.7^\circ$. Green and blue lines denote the positive parity, positive signature and positive parity, negative signature, respectively, whereas the red and magenta lines denote the negative parity, positive signature and the negative parity, negative signature respectively. Please see text for more details.

Figures 4 and 5 show the variation of the experimentally deduced kinematic moment of inertia and alignment, respectively, as a function of the rotational energy for ^{66}Zn for the observed yrast positive parity band consisting of 0^+ , 2^+ , 4^+ , 6^+ , 8^+ , 10^+ , 12^+ , and 14^+ states. Here, the kinematic moment of inertia and the alignment are defined, respectively, as $J^{(1)} = i_x/\omega$ and $i = i_x - i_{\text{ref}}$. It is to be noted here, that i_x is the x component (rotational component) of the total angular momentum and i_{ref} corresponds to the value of a reference rotor. The expressions for i_x and i_{ref} are, respectively,

$$i_x = \sqrt{I(I+1) - K^2}$$

and

$$i_{\text{ref}} = (J_0 + \omega^2 J_1)\omega,$$

where K refers to the projection of the total angular momentum on the symmetry axis. J_0 and J_1 represent the Harris parameters. Here, the values of Harris parameters as accepted in this mass region are taken from the Refs. [10,11].

In both figures, the corresponding quantities for the nearby $^{68,70}\text{Ge}$ [9–11] isotopes are also shown for comparison. It is evident that the variation of the kinematic moment of inertia and the alignment as a function of the rotational frequency ($\hbar\omega$) in ^{66}Zn follow the same trend as that in $^{68,70}\text{Ge}$, which in turn indicates a similar intrinsic structure of the observed bands in these three nuclei. The observed backbending in $^{68,70}\text{Ge}$ have been understood to be due to the alignment

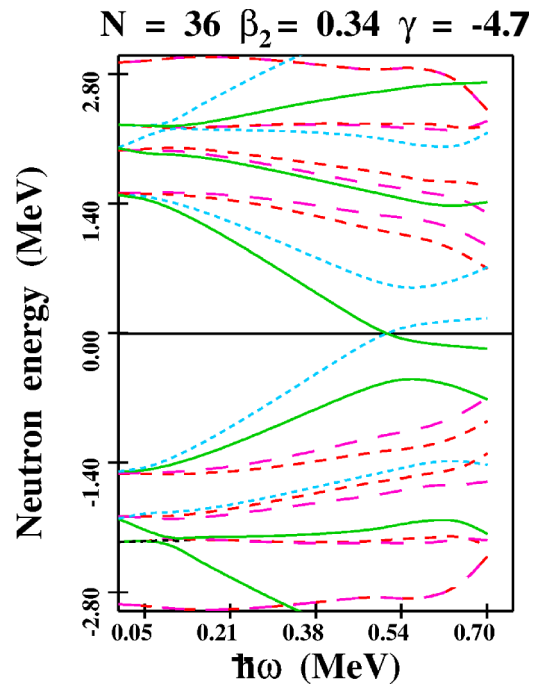


FIG. 7. Same as the Fig. 6 but for the neutrons. Please see text for details.

of a pair of neutrons in the $1g_{9/2}$ orbital [9,10]. As evident from the plots in the Figs. 4 and 5, the first alignment of a pair of neutrons in the $1g_{9/2}$ orbital in $^{68,70}\text{Ge}$ occurs at the frequencies of ≈ 0.60 MeV and ≈ 0.5 MeV, respectively.

The alignment plot for ^{66}Zn indicates that there is a total gain in the alignment of $\approx 8\hbar$ at a frequency of ≈ 0.6 MeV. To understand the observed alignment, quasiparticle Routhians for both the protons and neutrons have been calculated and are plotted, respectively, in the Figs. 6 and 7. The quasi-

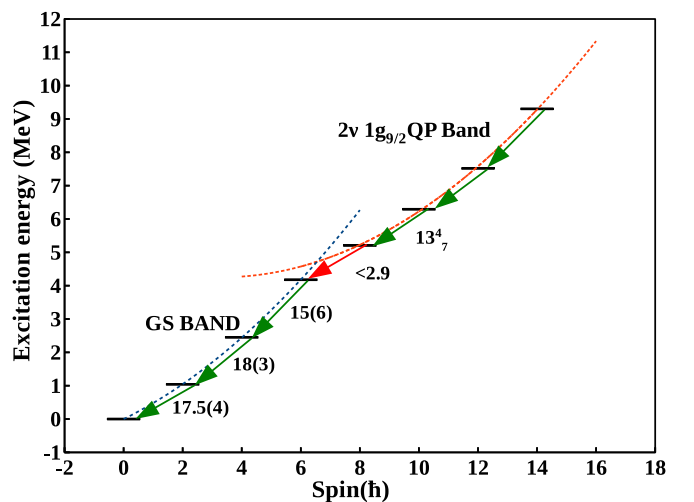


FIG. 8. Excitation energy vs. spin plot for the yrast bands of ^{66}Zn . Reduced transition probabilities $B(E2)$ of the corresponding γ -transitions, which are taken from the literature [43], are also plotted. The dashed lines represent the extrapolation of the bands through the second-order polynomial fitting.

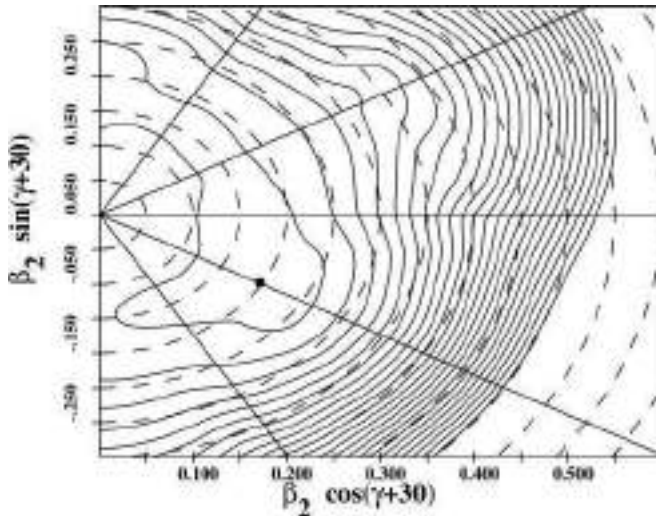


FIG. 9. Contour plots of the TRS calculations in ^{66}Zn for the zero quasiparticle (vacuum) at the rotational frequency ($\hbar\omega$) 0.100 MeV. The energy separation between the two consecutive surface contours is 250 keV.

particle Routhians are calculated using TRS codes based on the Hartree-Fock-Bogoliubov formalism [44], which is discussed later in this manuscript. These plots show that the first crossing of a neutron pair is possible at $\hbar\omega \approx 0.55$ MeV, while that for a pair of protons is feasible at $\hbar\omega > 0.70$ MeV. So, the band built on the 8^+ (5205 keV) state extending to the 14^+ can be understood to be due to the alignment of a pair of neutrons in the $1g_{9/2}$ orbital.

Band crossing has also been reported in the lighter ^{65}Zn isotope, where the two-proton alignment has been found to be responsible for the observed band crossing at a rotational frequency ~ 0.6 MeV [12] with the neutron alignment being blocked. The TRS calculations of ^{65}Zn have predicted that it undergoes a shape transition from a near oblate at lower spin to triaxial at intermediate spin [12]. In ^{66}Zn , the band

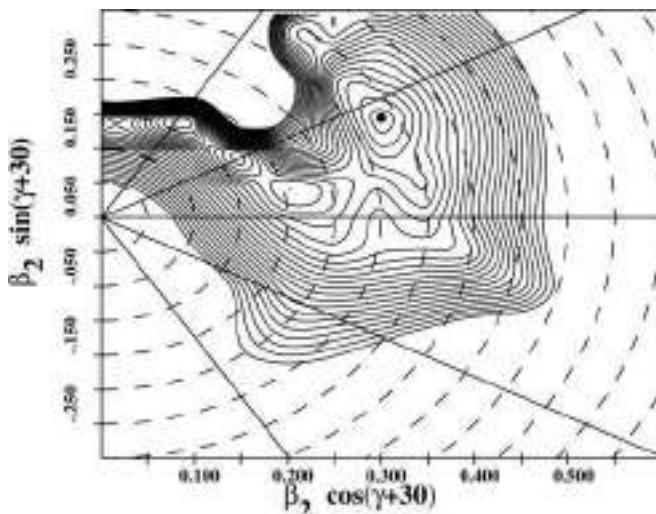


FIG. 10. Same as the Fig. 9 but for the 2ν quasiparticle band (positive parity, positive signature) at $\hbar\omega = 0.5$ MeV in ^{66}Zn .

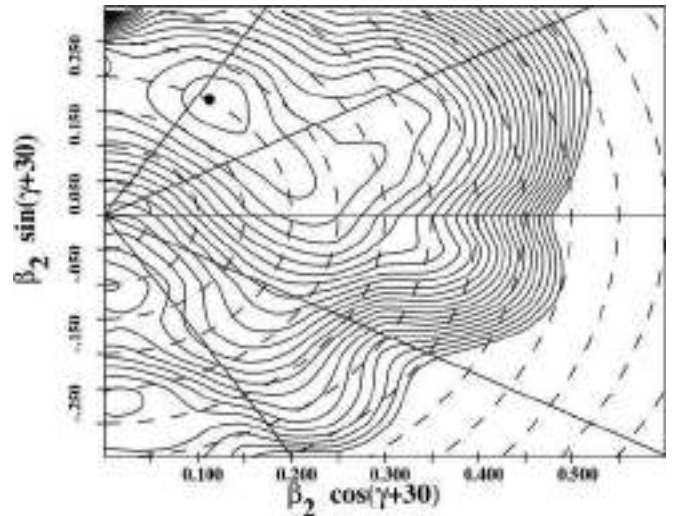


FIG. 11. Contour plots of the TRS calculations for the configuration $\pi(f_{5/2})^2 \otimes \nu(f_{5/2})^3(p_{3/2})^4(g_{9/2})^1$ of the negative parity quadrupole band like structure consisting of the 7^- (4250 keV), 9^- (5463 keV), and 11^- (6874 keV) states in ^{66}Zn at a rotational frequency ($\hbar\omega$) 0.40 MeV. Here, the energy separation between the two consecutive surface contours is 250 keV.

crossing of the ground-state band and the two-quasiparticle band occurs at 6^+ , which is evident from the sudden drop in the $B(E2)$ value (< 2.9 W.u.) for the $8^+ \rightarrow 6^+$, 1026 keV transition [43]. The band crossing is also apparent from the excitation energy vs spin plot for the yrast band illustrated in Fig. 8. The reduced transition probability [$B(E2)$] values for the transitions ($J \rightarrow J-2$) de-exciting along the yrast line, which are taken from the literature [23,43] are also given in the plot. The bands are extrapolated by using a second order polynomial fitting and are given by dashed lines in the plot. The configuration of the two-quasiparticle band is certainly of a two-neutron character, i.e., $(\nu g_{9/2})^2$, as the proton alignment is known to occur at the higher frequencies and one can expect it to undergo a similar shape transition as ^{65}Zn [12] along the positive parity yrast band. However, the two-quasiproton aligned band could not be observed in this nucleus. This may be because of its light nature ($Z = 30, N = 36$), compared to the $^{68,70}\text{Ge}$, leading to the unavailability of the $\pi 1g_{9/2}$ orbital near the proton Fermi surface. The two-neutron quasiparticle structure is well connected to the negative parity states (7^- , 9^- , 11^-), respectively, by the 955, 828, and the 643 keV transitions as seen from the level scheme. This may suggest the fact that these negative parity states also have the similar configurations as the positive parity band.

The TRS calculations for ^{66}Zn have been performed to understand the possible shape evolution using the Woods-Saxon potential. The Hartree-Fock-Bogoliubov code of Nazarewicz *et al.* [44] has been used for the calculations. Equilibrium shapes were calculated in the β_2 - γ plane with the minimization on the β_4 at different values of $\hbar\omega$. Shell corrections have been taken into account and as a residual interaction, the mono pole pairing force has been taken with the strength from Ref. [44]. Figures 9 and 10 show, respectively, the contour plots for the zero quasiparticle and the positive parity, positive

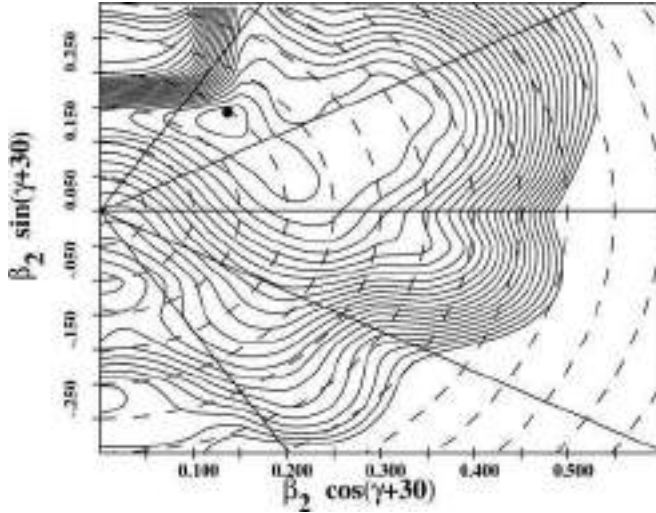


FIG. 12. Same as the Fig. 11 at the rotational frequency ($\hbar\omega$) 0.45 MeV.

signature two neutron quasiparticle sequence in ^{66}Zn . The calculation predicts a collective oblate shape of $\beta_2 \simeq 0.20$ at the lower frequencies up to $\hbar\omega = 0.25$ MeV albeit the flatness of the γ plane indicates a possible triaxial shape as shown in the Fig. 9. With the further increase of the rotational frequency the nucleus becomes more γ soft in nature, which means that the nucleus is triaxial in shape at intermediate spin. At a higher frequency of $\hbar\omega = 0.50$ MeV, it assumes a collective prolate shape having deformation $\beta_2 = 0.34$ ($\gamma \simeq -4^\circ$) as evident from the plot in Fig. 10. These values of $\beta_2 = 0.34$ and $\gamma \simeq -4^\circ$ have been used to calculate the quasiparticle Routhians (Figs. 6 and 7) from which the crossing frequencies are estimated. The TRS calculations thus predict that the alignment of a neutron pair drives the ^{66}Zn nucleus from a collective oblate shape at the ground state via the triaxial shape at the intermediate spin to a collective prolate shape at the high spin.

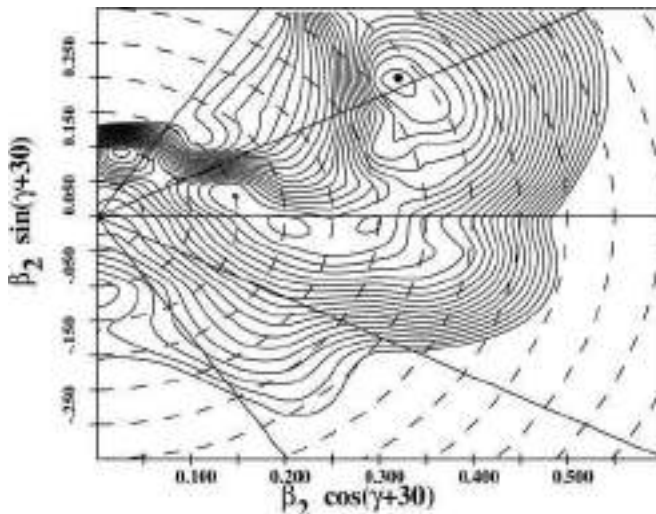


FIG. 13. Same as the Fig. 11 at the rotational frequency ($\hbar\omega$) 0.55 MeV.

The configuration of the negative parity band consisting of the 7^- (4250 keV), 9^- (5463 keV), and 11^- (6874 keV) states is assumed to be of $\pi(f_{5/2})^2 \otimes \nu(f_{5/2})^3(p_{3/2})^4(g_{9/2})^1$. This configuration can generate a maximum angular momentum value of $13\hbar$ which is consistent with the observed highest spin state of the band. Figures 11, 12, and 13 represent the TRS plots for this configuration. As is evident from the plots, the TRS calculations for the negative parity band predict an evolution of shape from a moderately deformed ($\beta_2 \approx 0.20$, $\gamma \approx 23^\circ$) triaxial at $\hbar\omega = 0.40$ MeV to well deformed ($\beta_2 \approx 0.37$, $\gamma \approx 3^\circ$) prolate at $\hbar\omega = 0.55$ MeV.

V. CONCLUSION

Excited states of ^{66}Zn have been studied following their population in a heavy-ion induced fusion-evaporation reaction and using an array of the 14 Compton suppressed clover detectors. Combining the measurement of the energy, angular correlation, linear polarization, intensity and coincidence relationship of the emitted γ -rays, the level scheme of ^{66}Zn has been constructed. With 14 new transitions being identified, the level scheme of this nucleus has been extended up to the excitation energy ≈ 12.3 MeV and a tentative spin of $(17^+)\hbar$. Further, the positive parity $[\pi(p_{3/2})^2\nu(f_{5/2}p_{1/2})^6] \otimes [\nu(g_{9/2})^2]$ yrast band and the negative parity band corresponding to the $\pi(f_{5/2})^2 \otimes \nu(f_{5/2})^3(p_{3/2})^4(g_{9/2})^1$ configuration have been identified up to their terminating states. A qualitative discussion of the observed band crossing phenomenon and the structure of other levels were presented in the light of various quasiparticle configurations which are based on the existing theoretical studies for this nucleus and the other neighboring nuclei (viz. $^{68,70}\text{Ge}$). TRS calculations predict a shape transition of this nucleus from a collective oblate at $\hbar\omega = 0.10$ MeV to a collective prolate at $\hbar\omega = 0.55$ MeV via triaxial shapes at the intermediate spins along the positive parity yrast band. This shape transition has been attributed to the alignment of a pair of neutron in the $1g_{9/2}$ orbital. Similar TRS calculations corresponding to the negative parity quadrupole band predict an evolution of the shape from the triaxial with a moderate deformation to the prolate with a higher deformation value. Thus, the present study points towards the established fact that the unique parity $1g_{9/2}$ orbital unequivocally plays a major role in the underlying structure of this nucleus as is observed in this work.

ACKNOWLEDGMENTS

The authors thank the operating crew of the Pelletron facility and the target laboratory at IUAC, New Delhi for providing excellent support throughout the experiment. We thank S. Nandi (VECC, Kolkata), S.S. Bhattacharjee (IUAC), and R. Garg (IUAC) for their help during the experiment. Constant encouragement from D. Kanjilal (IUAC) is gratefully acknowledged. We acknowledge the financial assistance received from the IUAC (New Delhi) via Project No. UFR-49318, SERB-DST (India) via Project No. EMR/2015/000891, and DAE-BRNS (India), Project No. 37(3)/14/17/2016-BRNS.

- [1] D. Rudolph *et al.*, *Phys. Rev. L* **80**, 3018 (1998).
[2] C. E. Svensson *et al.*, *Phys. Rev. L* **82**, 3400 (1999).
[3] A. Galindo-Uribarria *et al.*, *Phys. Lett. B* **422**, 45 (1998).
[4] D. Karlgren *et al.*, *Phys. Rev. C* **69**, 034330 (2004).
[5] J. Gellanki *et al.*, *Phys. Rev. C* **86**, 034304 (2012).
[6] M. Albers *et al.*, *Phys. Rev. C* **94**, 034301 (2016).
[7] M. Devlin *et al.*, *Phys. Rev. L* **82**, 5217 (1999).
[8] U. S. Ghosh *et al.*, *Phys. Rev. C* **102**, 024328 (2020).
[9] D. Ward *et al.*, *Phys. Rev. C* **63**, 014301 (2000).
[10] M. Kumar Raju *et al.*, *Phys. Rev. C* **93**, 034317 (2016).
[11] B. Mukherjee *et al.*, *Act. Phys. Hung.: HIP* **13**, 253 (2001).
[12] B. Mukherjee, S. Muralithar, R. P. Singh, R. Kumar, K. Rani, R. K. Bhowmik, S. C. Pancholi, *Phys. Rev. C* **64**, 024304 (2001).
[13] E. A. Stefanova *et al.*, *Phys. Rev. C* **67**, 054319 (2003).
[14] R. A. Haring-Kaye, S. I. Morrow, J. Döring, S. L. Tabor, K. Q. Le, P. R. P. Allegro, P. C. Bender, R. M. Elder, N. H. Medina, J. R. B. Oliveira, and V. Tripathi, *Phys. Rev. C* **97**, 024308 (2018).
[15] A. Gade, H. Klein, N. Pietralla, P. von Brentano, *Phys. Rev. C* **65**, 054311 (2002).
[16] P. M. Endt *et al.*, *Nucl. Phys. A* **575**, 297 (1994).
[17] A. Boucenna, L. Kraus, I. Linck, T. U. Chan, *Phys. Rev. C* **42**, 1297 (1990).
[18] G. P. Couchell *et al.*, *Phys. Rev.* **161**, 1147 (1967).
[19] J. F. Braundet *et al.*, *Phys. Rev. C* **12**, 1739 (1975).
[20] G. F. Neal *et al.*, *Nucl. Phys. A* **280**, 161 (1977).
[21] L. Cleemann *et al.*, *Nucl. Phys. A* **386**, 367 (1982).
[22] B. Erlandsson *et al.*, *Phys. Scr.* **22**, 432 (1980).
[23] C. Morand *et al.*, *J. Phys. Fr.* **38**, 1319 (1977).
[24] D. Kanjilal *et al.*, *Nucl. Instrum. Methods Phys. Res. Sect., A* **328**, 97 (1993).
[25] S. Muralithar *et al.*, *Nucl. Instrum. Methods Phys. Res. Sect., A* **622**, 281 (2010).
[26] B. P. Ajith Kumar *et al.*, in *Proceedings of the 44th DAE-BRNS Symposium on Nuclear Physics* (Department of Atomic Energy, Government of India, Mumbai, 2001), p. 390.
[27] R. K. Bhowmik *et al.*, in *Proceedings of the 44th DAE-BRNS Symposium on Nuclear Physics* (Department of Atomic Energy, Government of India, Mumbai, 2001), p. 422.
[28] D. C. Radford, *Nucl. Instrum. Methods Phys. Res., Sect. A* **361**, 290 (1995).
[29] K. S. Krane *et al.*, *Nucl. Data Tables* **11**, 351 (1973).
[30] K. Starosta *et al.*, *Nucl. Instrum. Methods Phys. Res., Sect. A* **423**, 16 (1999).
[31] R. Palit *et al.*, *Pramana J. Phys.* **54**, 347 (2000).
[32] S. Rai *et al.*, *Eur. Phys. J. A* **54**, 84 (2018).
[33] U. S. Ghosh *et al.*, *Phys. Rev. C* **100**, 034314 (2019).
[34] S. Rai, Ph.D. thesis, Visva-Bharati University (2019).
[35] J. F. A. Van Heinen *et al.*, *Nucl. Phys. A* **269**, 159 (1976).
[36] D. P. Ahalpara *et al.*, *Nucl. Phys. A* **371**, 210 (1981).
[37] S. K. Sharma, *Phys. Rev. C* **22**, 2612 (1990).
[38] V. Lopac and V. Paar, *Nucl. Phys. A* **297**, 471 (1978).
[39] U. Hermkens *et al.*, *Z. Phys. A* **343**, 371 (1992).
[40] A. P. de Lima *et al.*, *Phys. Rev. C* **23**, 213 (1981).
[41] P. A. Dar, R. Devi, S. K. Khosa, J. A. Sheikh, *Phys. Rev. C* **75**, 054315 (2007).
[42] M. Hasegawa, K. Kaneko, T. Mizusaki, *Phys. Rev. C* **70**, 031301(R) (2004).
[43] ENSDF Database, <https://www.nndc.bnl.gov/ensdf>.
[44] W. Nazarewicz *et al.*, *Nucl. Phys. A* **512**, 61 (1990).



A New Look at Stoic Ethical Precept for Sustainability

Dr. Arup Kanti Konar
Principal & Associate Professor of Economics
Achhruram Memorial College
Jhalda, Purulia, West Bengal, India

ABSTRACT

This paper seeks to run back over the Stoic Seneca's ethical precept: "live or life according to Nature" once again for the realization or restoration of sustainability. Though ancient Greek Stoicism is no longer existent, yet Stoic Seneca's ethical precept has not been forgotten. Like tradition, the Nature embedded ethical precept of Stoicism should or can be defended, but not in the traditional way, since tradition defended in traditional way implies fundamentalism.

Key Words: Stoicism, Nature, Conservation, Fundamentalism, Precept

1. Introduction

In the age of sustainability revolution, which has started its effective life since the 1970s, various preconditions, precautions, principles and/or policies are being adopted for the conservation of Nature. But, without clear-cut understanding of Nature, and the way of its conservation, how is it possible to conserve Nature? Should we not decide today what nature is and how we should reorganize our way of living in relation to it before taking conservation action? Though ancient Greek Stoicism is no longer existent, yet Stoic Seneca's ethical precept: "live or life according to Nature" has not been forgotten. Like tradition, the Nature embedded ethical precept of Stoicism should or can be defended, but not in the traditional way, since tradition defended in traditional way implies fundamentalism. Today's humanized or socialized Nature and ecology should or can be conserved or restored, but not in the traditional way. Nature, ecology and tradition are equivalent in the sense that these are erroneously treated as pre-given and independent of "humanization or socialization" (Konar, 2013). Their restoration should never deliberately be backed up by fundamentalism. This paper seeks to run back over the Stoic Seneca's ethical precept once again for the realization or restoration of sustainability (Konar & Chakraborty, 2011).

2. Conflicting Perspectives of Nature

Humans are advised by the Stoic ethical precept to “live according to Nature”. But, if conflicting perspectives of Nature are existent in the interdisciplinary literature, then Stoic ethical precept must involve conflicting pathways. Then, comes the problem of choice from the multitude of pathways. Now, our discussion will be concentrated on the conflicting perspectives of Nature on which the Stoic ethical precept is based. The perspective of Nature is shaped by social as well as ecological frameworks, since humans are impacted by both the social and ecological factors, given the natural instability indicated by natural catastrophes and natural stability indicated by the equilibrium of various natural life support systems. Further, the perspective of Nature is determined by the following two factors:

(i) The ways of human interaction with the Nature determine the ways of human perception and interpretation of Nature

(ii) The ways of human perception and interpretation of nature determine how humans interact with the Nature.

In this context Milton’s (1997) remark is noteworthy. He says that “cultural perspectives thus guide human activity. This activity, in turn, yields experiences and perceptions, which shape people’s understanding of the world. The process is not unidirectional, but dialectical”.

Moreover, how the perspective of Nature is embedded in the minds of the people should be looked at from two sets of peoples such as:

(i) Peoples who act as analysts, scholars, researchers, authors or scientists (observers)

(ii) Peoples who are studied by the former (observed).

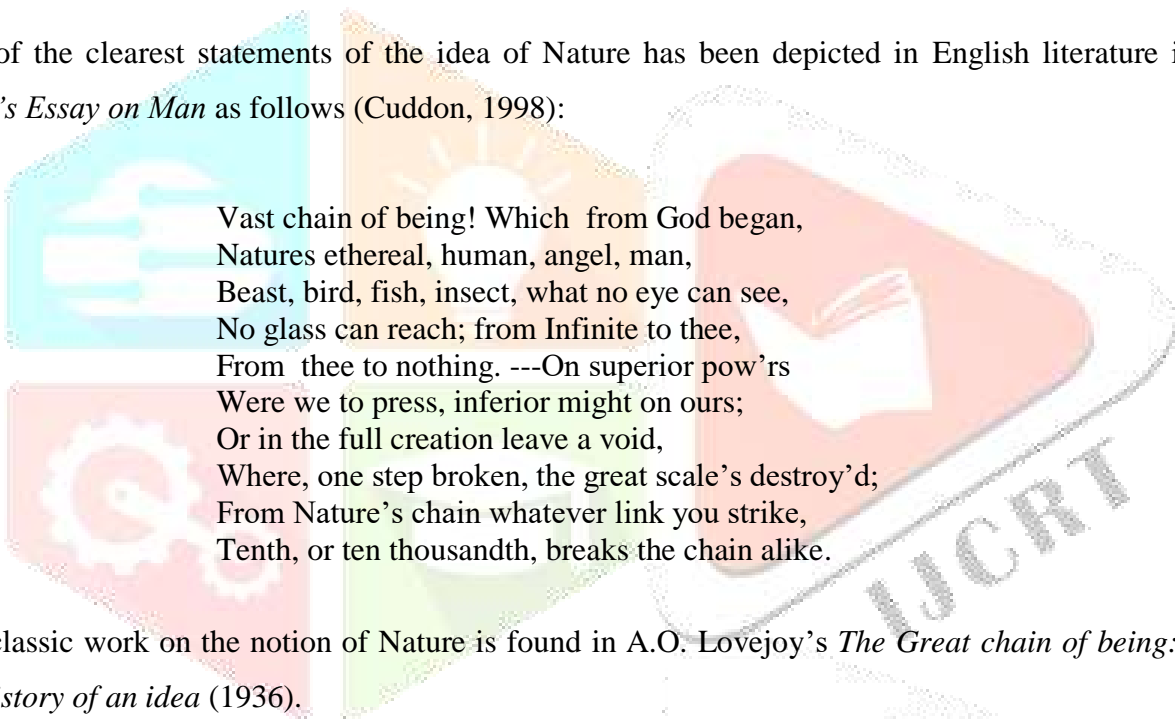
In this connection, the comment of Dawkins (1995) should be recalled: “we are just brought up in a culture that sees the world in a scientific way. They (tribe, who believe that the moon is an old calabash tossed into the sky, hanging only just out of reach above the treetops) are brought up to see the world in another way. Neither way is more true than the other”. In a similar vein, Dwyer (1996) has argued that the capacity of a particular society to develop a concept of Nature depends on whether they view their environment as an integrated whole or divide it into familiar and unfamiliar spaces, and this, in turn, depends on how they live in and their environment. He suggests that, in the fully integrated world of the Kubo, there is no sphere sufficiently distinct from the human world to merit the label Nature, while the Siane environment contains unused and familiar spaces, which might be so labeled. Further, Ingold (1996) says that hunter-gatherer communities do not have a concept of Nature because the world can only be Nature for a being that does not belong there. Similarly, Howell (1996) points out that the jungle in its totality as a material and spiritual world iscultural space, not natural. They (Chewong of Malay rainforest) move around in it with confidence derived from understanding and knowledge. In this case, the label is applied by the analyst, there is no suggestion that the people themselves would describe their environment in this way.

Various perspectives of Nature are existent in the interdisciplinary literature. However, Beck's (1994) notion of Nature should be prioritized first as follows:

Nature is not nature, but rather a concept, norm, memory, utopia, counter-image. Today more than ever, now that it no longer exists, nature is being rediscovered, pampered. The ecology movement has fallen prey to a naturalistic misapprehension of itself.... 'nature' is a kind of anchor by whose means the ship of civilization, sailing over the open seas, conjures up, cultivates, its contrary: dry land, the harbour, the approaching reef.

Beck's remark cannot cease us from searching for the definitions of Nature. For evidences show that A.D. Lovejoy was capable of counting over sixty different shades of meaning of Nature. The preferred notions of Nature are given below:

One of the clearest statements of the idea of Nature has been depicted in English literature in terms of *Pope's Essay on Man* as follows (Cuddon, 1998):



Vast chain of being! Which from God began,
Natures ethereal, human, angel, man,
Beast, bird, fish, insect, what no eye can see,
No glass can reach; from Infinite to thee,
From thee to nothing. ---On superior pow'rs
Were we to press, inferior might on ours;
Or in the full creation leave a void,
Where, one step broken, the great scale's destroy'd;
From Nature's chain whatever link you strike,
Tenth, or ten thousandth, breaks the chain alike.

The classic work on the notion of Nature is found in A.O. Lovejoy's *The Great chain of being: A study of the history of an idea* (1936).

A considerable emphasis on imitating the law of Nature is seen in pope's *An Essay on Criticism* (1711) [Cuddon, 1998] as follows:

First follow Nature, and your judgement frame
By her just standard, which is still the same;
Unerring NATURE, still divinely bright,
One clear, unchang'd and universal light.

According to Whitehead (1953), "The whole life of Nature is dominated by the existence of periodic events, that is, by the existence of successive events so analogous to each other that, without any straining of language, they may be termed recurrences of the same event,"

Ellen (1996) has identified three distinct senses in which Nature is understood in Western society:

- (i) As space which is not human

(ii) As a category of things

(iii) As inner essence, where Nature seen as (ii) and (iii) includes both human and non-human beings.

Escobar (1997) views that Nature can no longer be seen as an essential principle and foundational category, an independent domain of intrinsic value and truth but as the object of constant reinventions, especially by unprecedented forms of technoscience.

In the eyes of Sheldrake (1991), Nature is alive, which oppose mechanistic approach to Nature in which Nature is treated as an inanimate sources of natural resources. Sheldrake (1991) says that such a view is implicitly feminine, for the words Nature and natural have their origins in the mothering process. How Nature is seen through the eyes of the famous poet Hopkins [Dyson, 1995] will be obvious from the following lines of his poem *Brothers*:

Ah Nature, framed in fault,
There's comfort then, there's salt;
Nature, bad, base, and blind,
Dearly thou canst be kind;
There dearly then, dearly
I'll cry thou canst be kind.

Giddens's (1994) conceivability of Nature is as follows:

The paradox is that nature has been embraced only at the point of its disappearance. We live today in a remoulded nature devoid of nature... nature can not any longer be defended in the natural way...socialized nature is by definition no longer natural. The longing for a return to nature.... is a healthy nostalgia... Nature has come to an end in a parallel way to tradition...Instead of being concerned above all with what nature could do to us, we have now to worry about what we have done to nature.

According to Vernadsky (1965), "The biosphere is the environment in which we live, it is the 'nature' that surrounds us and to which we refer in common parlance". Lotka (1925) says that "The picture (of Nature) we must keep before us, then, is that of great world engine or energy transformer composed of a multitude of subsidiary units, each separately and all together as a whole, working in a cycle".

"There is no state of nature, such as posited by Rousseau" (Giddens, 1994).

According to *Pope's Essay on Man* (Copleston, 1962):

All are but parts of one stupendous whole,
Whose body Nature is and God the soul.

According to T. S. Eliot, "The external Nature is always an accomplice of the illusory reality" (Sen, 1967). But, William Wordsworth proves that Nature is always interesting because of its inherent truth and simple beauty (Sen, 1967). In *The Creative Experiment*, Bowra says that "The whole order of Nature seems to be breaking, and strange sounds and sights testify to the general decomposition" (Rosset, 1948). Stephen

Spender (1950) wanted to substitute the modern civilization with his desired nature of Nature and that is why he said:

Unless, governor, teacher, inspector, visitor,
This map becomes their window and these windows
That shut upon their lives like catacombs,
Break O break open till they break the town
And show the children to green fields, and make their world
Run azure on gold sands, to let their tongues
Run naked into books, the white and green leaves open
History theirs whose language is the sun

What Nature teaches us and what ways of life we should follow will be amply clear from the remark of Kropotkin (1925):

“Don’t compete! ---- competition is always injurious to the species, and you have plenty of reasons to avoid it!”. That is the tendency of Nature, not always realized in full, but always present. That is the watchword which comes to us from the bush, the forest, the river, the ocean. “Therefore combine --- practice mutual aid! That is the surest means for giving to each and all the greatest safety, the best guarantee of existence and progress, bodily, intellectual, and moral”. That is what Nature teaches us; and that is what all those animals which have attained the highest position in their respective classes have done. That is also what man--- the most primitive man -- has been doing; and that is why man has reached the position upon which we stand now....

The Greek sophist Anaxagoras (Stace, 1972) argues that an antithesis is existent between Nature and man. Another Greek sophist Alcidamas of Elaea (Nersesyants, 1986) remarks that “God has set all men free; Nature has made no man a slave”. Regarding the relationship between the humans and Nature, the Greek philosopher Aristotle (384-322 BC) says that:

If Nature is to be understood, we must keep in mind certain general points of view....Nature seeks everywhere to attain the best possible....But if nothing in Nature is aimless or useless, this is not to be interpreted in a narrow anthropocentric spirit. It does not mean that everything exists for the use of man....It is true that, in a certain sense, everything else sublunary is for man. For man is the highest in the scale of beings in this terrestrial sphere....But this does not exclude the fact that lower beings have each its end. They exist for themselves and not for us” (Stace, 1972). He also adds that humanness can not exist apart from human beings, any more than heaviness apart from the heavy object.

Nature can be conceived broadly from three perspectives such as (i) Traditional perspective, (ii) Modern perspective and (iii) New perspective.

2.1. Traditional Perspective of Nature

If human “figure” and its “nose” (recall Gogol’s story, called, *The Nose*), which is an inseparable part of the “figure”, are respectively likened to the “Nature” and the “human”, then traditional perspective shows that “nose” has an independent existence, which means that “nose exists without an owner” and by analogy, it can be said that human society exists without Nature. Traditional perspective is determined by the nature of tradition, traditionalism and traditionalists. Tradition refers to the customs, beliefs, practices, ceremonials, rituals, etc. by which the past can be substituted for the present. Tradition is something, which is given, fixed, or constant, not variable; exogenous, not endogenous; autonomous, not induced; static, not dynamic, and unchallengeable. Tradition is assumed to influence human social life, which can not influence tradition. Human social life is exceptionally dynamic, while tradition is exceptionally static, though it is humanly constructed. Recently tradition is being detraditionalized and reconstructed or reinvented deliberately. The most important characteristic of traditional tradition is that tradition should or can be defended in the traditional way. Like rail lines tradition and Nature go in parallel way. They have vast similarities. The salient features of traditional perspective of Nature are as follows:

If Earth is likened to a model, and if society is treated as endogenous variable (obviously dynamic), then Nature is looked upon as an exogenously and permanently fixed landscape. Symbolically, if Y stands for “index of Nature or Naturalness” measured along the vertical axis and X stands for “index of humanization or socialization” measured along the horizontal axis, then in the two-dimensional diagram, the mathematical function $Y = F(X)$ can be represented by a straight line which is parallel to the X-axis. Nature refers to environment and events which is pre-given independently of human social actions. Nature is devoid of human social spheres. Nature is an autonomously given physical environment that persists only for absorbing social and ecological shocks. It is an external framework for human activity. It is looked at in an instrumental way. It is an external platform of social life and is pre-given and largely unchallengeable. It can or should be returned to its original state by human efforts. The metaphor of Nature as Mother Nature is seriously taken as valid. It is regarded as an object of beauty, separated from human social life. Nature should and can be defended in the natural way as it is “larger than human beings” (Goodin, 1992). It is a non-humanized physical objects or processes (or environment) given independently of human intervention. A return to an independent Nature is advocated by traditionalists. “How shall we live in a world of socialized or lapsed Nature?” is the moral question of traditionalists. Naturalness of Nature can be restored in the natural way. Socialization or humanization of Nature is the only cause of ecological crisis leading to the emerging threat of unsustainability. All humans should become conservative in the conservative way. For the return to natural Nature, traditionalists suggest to follow primitive civilizations and to abandon modern civilizations. As Naess (1972) says that “..... people will be able to live as ‘future primitives’, recovering ecological diversity as ‘dwellers in’ the land”. Similarly Goldsmith (1988) suggests that it is to

the traditional societies of the past that we must turn for inspiration. Nature should be defended against the inroads of economic expansionism, which threatened its inner harmonies as well as its beauties. The deep ecologists Porritt and Winner seeks to call for a non-violent revolution to overthrow our whole polluting, plundering and materialistic industrial society and, in its place, to create a new economic and social order which will allow human beings to live in harmony with the planet (Dobson, 1990). According to traditionalists, living “close to Nature” implies more harmony with it than living in modern society. Hence primitive ethnoecologies and tribal communities comprising of hunter- gatherers, horticulturists, pastoralists, marginal peasants and the like are placed for admiration. Socialization or humanization of Nature leads to destruction of Nature. Urbanization and globalization backed up by scientific and technological revolution are discouraged. Defending of Nature in the natural way should be paralleled by the defending of tradition in the traditional way. The emphasis on a return to Nature also includes the revival of traditional medicine, substitution of herbs for modern drugs with the exclusion of modern medical methodology. Traditional perspective of Nature has its origin in Cartesian philosophy which indicates the dualistic view of a mind-body actor whose mind chooses between options available to the body in its lived-in situation by a reasoning which transcends the situation, and which then makes the body execute its choice (Bird-David, 1997). Cartesian view also suggests the principles that (a) Everything is revisable, (b) We cannot be sure even about our most cherished ideas and (c) Science is supposed to produce certainties for us. Mastery over Nature means destruction of it, since humanized or socialized Nature is no longer natural by traditional definition. Local, small, diversified and primitive communities are adaptable more gracefully to Nature. So decentralization of cities and reconstruction of ethnoecologies are blissfully encouraged. Conservation of tradition should be coupled with conservation of Nature. So constructions of historical and aesthetical importance should be conserved in the conservative way in the name of conservation of Nature, since these are “larger than humans”. Conservation decisions and planning should be undertaken by reference to natural Nature, not humanized or socialized Nature. Scientific and technological civilization should be banned. Nature, ecology and environment are often confused. Villages are more natural than cities.

There are authors who have spoken of the relation between human and Nature, but they have not clarified what Nature and Natural are. For example, according to Smith (1997) for sustainability we require living in peace and comfort within natural limits and preservation of the natural environment in its unaltered state. Living in harmony with natural environment has been suggested by Heang (1997). For sustainability, Posey (1992) has suggested to use the techniques for living in harmony with nature, obtaining favourable results without degrading or exhausting the environment. Living in harmony with surrounding is also the view of Lewis (1992). Man must bring himself into conformity with nature if he wants to exist as part of nature’s unity, and must fit his demands to nature’s availabilities (Reichel-Dolmatoff, 1976). Living in relative

harmony with nature, and living within the limit fixed as a challenge by nature ensures sustainability (Cavalcanti, 1997).

Traditional perspective of nature is based on the following frameworks, paradigm, doctrines and/or isms:

- (a) Possibilism, which means that nature is seen as setting the limits on cultural development, as dictating what is possible (Kroeber, 1939; Stenning, 1957)
- (b) Cultural core or cultural ecology of Steward (1955)
- (c) Substantivism, which concerns itself with the economy as an instituted process (Sahlins, 1972; Polanyi et al., 1957; Halperin, 1988) neglecting the individual.
- (d) Formalism, which concerns with the rational individual and the economy at large, as the aggregate of such individuals (Halperin, 1988).
- (e) Symbolism or economic symbolism (Sahlins, 1976; Mintz, 1985)
- (f) Instrumental rationality.
- (g) Old environmental determinism or anthropogeography (Geertz, 1963; Mason, 1896; Huntington, 1924).
- (h) Cultural materialism of Harris (1968).
- (i) Cultural relativism of Holy and Stuchlik (1981).
- (j) Social constructivism of Ingold (1992).
- (k) French structuralism of Levi-Strauss (1963).
- (l) Cultural economics of Gudeman (1986).
- (m) Ecosystem or ecological system (Rapport, 1971).
- (n) Cognitive anthropology (Tyler, 1969).
- (o) Ethnoecology (Hunn, 1985).

2.2. Modern Perspective of Nature

Giddens (1994) is eulogized for his significant contribution to the modern perspective of Nature. We are living today in a world in which the Nature is being humanized, socialized, remoulded, managed or denatured at an increasing rate. The naturalness of Nature is being faded out and instead, denaturing is taking its place. The humanized or socialized Nature is being substituted for Natural Nature. That is why today's Nature should be designated as humanized, socialized, remoulded or managed Nature. By any criterion, Nature must be conserved, defended or safeguarded. But the way of conservation should be changed. Nature should and can not be defended in the natural way. Conservation of Nature should come from non-natural way. Both the Nature and tradition are alike in the sense that they need defending, since both are disappearing and as tradition should and cannot be defended in traditional way, similarly Nature should and cannot be defended in the natural way. Tradition defended in traditional way means "fundamentalism" which, is dangerous to the society and can arise in all the dimensions of human life.

Nature is going to an end in a parallel way to tradition. Conservation of tradition should effectively be separated from the conservation of Nature. Tradition should be preserved, but the ways of life with which they were associated should and cannot be preserved. For example, we might wish to preserve the local gibbet on account of its history, but not the practice of publicly hanging petty criminals on it (Giddens, 1994). Return to Nature does not necessarily mean the return of the present scientific and technological civilization to the early rude, crude or primitive society, as claimed by traditionalists. Modernists do not believe that communities comprising of hunter-gatherers, horticulturalists, pastoralists, peasants etc. are more natural than modern scientific and technological communities, for their living close to Nature. Because all are human productions and humans are part of Nature. Traditionalist Goodin (1992) argues that “natural products or processes are larger than ourselves or humans”. But the modernist Giddens’s (1994) counter-argument is that that we need something larger or more enduring than ourselves to give our lives purpose and meaning may be true, but this is plainly not equivalent to a definition of the natural. Mastery over Nature does not mean destroying it. Rather mastery can quite often mean caring for Nature as much as treating it in a purely instrumental or indifferent fashion. Conservation decision and planning should not be undertaken by reference to natural or original Nature, but to humanized or socialized Nature. We have to decide today what nature is and how we should organize our lives in relation to it. The longing for a return to original Nature is a healthy nostalgia, since Nature can never be returned in the natural way. Instead of being concerned above all with what Nature could do to us, we have now to worry about what we have done to Nature. Human constructions such as old buildings, churches, palaces, temples and similar things should be preserved only for their historical importance, not for the fact that they are “larger than ourselves” (Goodin, 1992) and not in the traditional way. We should all become conservative now, but not in the conservative way. Decision about what to conserve or to strive to recover should be determined by reference to denaturing of Nature and detraditionalization of tradition. We should seek to remoralize our lives in a situation where Nature and tradition can be reconstructed in deliberately conscious way. “How shall we live? in a world of lost tradition and socialized Nature” should not be treated as moral despair. We should not start to mistrust science and technology for the lost natural harmonies. Environment, ecology and Nature should not be confused. We can not go back to tradition which is ingrained the community, where tradition is defended in the traditional way. History does not express the will of God but is the result of the active struggles, and creativity, of human beings themselves. The human authorship of history has been hidden by religious dogma and by the dead hand of tradition. The task ahead for humanity is to take hold of its own social development and direct it in a conscious way. We are or can become the masters of our own destiny (Giddens, 1994).

2.3. New Perspective of Nature

The relationship between the Nature and the human society can be likened to the relationship between the Nation State and its government. Government is the subset of the Nation State in the sense that wherever government exists, there is also Nation State, but the converse is not true. Similarly, human society is the subset of Nature, which means that wherever human society exists, Nature follows suit, but wherever Nature exists human society does not exist. Nature should be divided into three zones such as (i) “free-entry zone”, (ii) “quasi-entry zone” and (iii) “no-entry zone”. So, Nature should be confined not only to the Earth, but a part of the outer space of the universe into which human intrusions are still going on and the rest part of the outer space, which is left untouched till now, should also be included in Nature. Because a part of the outer space of the universe is recently being humanized or socialized in terms of launching of variously artificial satellites and diverse explorations of space to satisfy the human common purposes. Besides, several natural satellites have already been humanized or socialized and many other natural satellites have remained under the queue of humanization or socialization for the common good or bad of the society. Thus, socialized as well as non-socialized parts of the universe should also be included into the new conception of Nature.

Socialization of Nature is a matter of degree, like privatization of national economy, and mathematization of various disciplines or sciences. Though socialization of Nature is going up at an increasing rate, yet full-fledged socialization of Nature is neither physically possible, nor socially desirable. So the moral despair that Nature has fully been denatured or exhausted, or in other words, Nature has ceased to exist, is a sophisticated nostalgia. Unless government ceases to exist how is it possible to realize full-fledged privatization of a national society? Should the national society not decide the degree of privatization consciously for the benefit or desirability of the society? Likewise, while mathematics itself is non-mathematical, since literary or verbal reasoning is still existent in mathematics, is it possible to attain full-fledged mathematization of any science or discipline such as physics, chemistry or the like? If full-fledged socialization of Nature is possible by any means or criterion, then what name should be substituted for remaining non-socialized part of the infinite universe and will diverse non-anthropogenic natural instabilities cease from recurring? And by what name will non-anthropogenic natural instabilities be called? No scientist can predict the upper and lower limits of socialized Nature in the universe despite unprecedented boon of scientific and technological revolution.

Socialization of Nature does not necessary lead to destruction of Nature or natural disequilibrium. All kinds of destructions of nature may be brought about by socialization of Nature, but the converse cannot be true, that is, all kinds of socialization of nature can never be directed to the destruction of Nature. Since human society is a subset of Nature so any kind of socialization of Nature means deliberate intrusion of human intervention into the non-socialized part of the universe. Such human intervention may involve two types of

socialization such as positive and negative. Both the deforestation and reforestation of Nature are the examples of socialization of Nature. But while the former should be called negative socialization, the latter the positive socialization of Nature. If the warfare and the age-old conflicts among diverse fundamentalisms can be ruled out by the conscious and morally optimistic efforts and if at least a few of the lost non-human species can be revived or reinvented by the newly invented technology or methodology, then should these kinds of socialization of Nature be labeled as destruction to Nature? Again the same kind of socialization of Nature may bring about either beneficial or destructive outcome depending upon the politics of the nation state or the scope of socialization. For example, the artificial communication satellite may be used to satisfy socially desirable purpose, say, needs of the scholars and the scientists for internet searching or socially undesirable purpose, say, bringing about future warfare. Since humans rank highest in the scale of species, so they should continue the process of socialization of Nature resorting rationality, morality and consciousness so long as the social instability and ecological instability cannot be wiped out and thereby the newly emerging harmony of socialized Nature can be reestablished, since according to Wilkie (1993) “Human beings retain a moral value, which is irreducible.”

The traditionalist insistence that living “close to Nature” (e.g. subsistence living of primitive and tribal communities comprising of hunter-gatherers, horticulturalists, pastoralists, small peasants etc.) is more natural than the living remotely from Nature (e.g. modern scientifically and technologically developed cities). But the question is: which is more natural, the primitive and tribal communities facing large scale poverty, hunger, malnutrition, illiteracy accompanied by high birth and death rates, or the modern developed communities devoid of some of the foregoing social instabilities? In truth, the degree of naturalness of any event or process should not be judged by reference to the natural or crude Nature, rather it should be judged by reference to socialized Nature. Which is more natural, a community “where there is no doctor” (Werner, 1977), or a community where doctor is available for safeguarding the community’s health status?

Preservation or conservation of tradition should not be confused with that of Nature. In the socialized Nature, there must be an effective separation between the two. For this confusion may lead to unexpectedly adverse outcomes.

The socialization of Nature is also a natural process, since humans are embedded in the Nature. Through the universal process of evolution, which has not stopped yet, rather is continuing, it has become obvious to the humans that “Man is the highest phenomenon of Nature”, according to Greek Stoicism (Copleston, 1962). Owing to humans’ supremacy over the Earth, socialization of Nature has become naturally congealed in human nature. By the kind Nature’s gentlest boon, humans have been gifted with such qualities as consciousness, morality, rationality etc. by which they can socialize the Nature in the positive direction to bring about a transition to the dynamically social stability and ecological stability, given the constant threat

of exogenously determined non-anthropogenic natural instability. The Greek philosopher Heraclitus (535-475 BC) said that “Everything in the universe has in it its own opposite” (Stace, 1972). Further according to the principle of antinomy of terminology, concepts arise in science in pairs---every phenomenon must have a corresponding anti-phenomenon and every process must have a process with its opposite polarity. Thus, we cannot speak of the Nature or Natural without denoting its opposite---- anti-Nature or anti-Natural. Traditionalists backed up by fundamentalism insist that the opposite of Nature, Natural, Naturing or Naturalization is society (humanity), social (human), socializing (humanizing) or socialization (humanization). But they can be reminded that the latter is embedded in the concept of the former.

3. Interpretation of Stoic Ethical Precept

According to Stoics, the end of life is to attain happiness, which is possible in the Natural life or life according to Nature, which means the agreement of human action with the law of Nature. For man to conform himself to the laws of universe in the wider sense, and for man to conform his conduct to his own essential nature, that is, reason, is the same thing, since universe is governed by the law of Nature. While earlier stoics such as Zeno, Cleanthes, Chrysippus, et al. thought of Nature which man should follow, rather as the Nature of the universe, later Stoics such as Seneca, Epictetus, Aurelius, et al. tended to conceive Nature from a more anthropological point of view. The conflicting senses of the Stoic ethical maxim “live or life according to Nature” are as follows:

By Nature, Cynics mean rather the primitive and instinctive, and so life according to Nature implies a deliberate flouting of the conventions and traditions of civilized society, a flouting that externalizes itself in conduct that is eccentric and not infrequently indecent.

According to Stoics, life according to Nature indicates life according to the principle that is active in Nature. The ethical end of life lies in submission to the order and arrangement of the universe. Man is endowed with reason, the faculty which gives him his superiority over the brute and so for man life according to Nature is rightly understood to mean life according to reason. The end of life is a life which follows Nature, whereby is meant not only our own nature, but the Nature of the universe, a life wherein we do nothing that is forbidden by the universe i.e. by right reason. The ethical teaching of the Stoics thus declares that happiness is a life according to Nature, while a life according to Nature is a life according to right reason.

By “live or life according to Nature”, the traditional perspective indicates that humans should live in accordance with the non-socialized, crude or natural Nature as primitive and tribal communities do, for maintaining globally ecological equilibrium or sustainability, irrespective of social sustainability or unsustainability.

But modern perspective expresses just opposite view, which means that humans as the part of Nature must live in accordance with the humanized or socialized Nature and socialization of Nature can not be stopped so long as humans survive in the Earth as the highest creature.

Stoic Seneca's ethical precept "live or life according to Nature" has been renamed by the new paradigm as "sustainability" provided that the negative autonomous socialization of Nature can be at least compensated (or overcompensated, not undercompensated) by the positive autonomous socialization backed up by human trinity "rationality, consciousness and morality", treating such socialization as a sustained and dynamic process. This means that positive accommodating socialization of Nature must reproduce "socialized sustainability" (obviously renewed) on the assumption that society itself has been "optimally socialized" without any kind of fundamentalism.

4. Should Society Sustain Stoic Ethical Precept?

The Northern scholar Smith (1997) claims that "the notion of environmentally sustainable development was promoted in the 1970s most prominently by Herman Daly (1972) and 'sustainable development' as a concept is a product of the North". But, retrospective evidences reveal that 1970s-Northern concept of "sustainability" is congealed in the ancient Greek Stoic ethical precept "live or life according to Nature". So Greek Stoicism should be admired for the invention of the present day concept of sustainability. Regarding the foregoing question indicated by this section my suggestion is that the world in which today we live should be labeled as a "runaway world" (Giddens, 1994), which should be characterized by "global unsustainability syndrome" caused by increasing socialization of Nature, in which "negative socialization" is partly offset by the "positive socialization" (Konar, 2013) of Nature. In such a situation, we should stoop to the Stoic ethical precept under the following preconditions:

- (i) The first precondition to be remembered is that our Nature is the humanized or socialized Nature.
- (ii) Socialization of Nature can never be stopped. Its sustenance and dynamism are consistent with the sustained process of universally natural evolution and humanly induced various revolutions.
- (iii) Along with rationality, consciousness and intelligence, humans are also endowed with moral values by which they should be directed along such a pathway of continuous socialization of Nature so that the "negative socialization" (Konar, 2013) can be overcompensated by the "positive socialization" (Konar, 2013) of Nature.

5. Concluding Comments

Following Maxim Gorky (Borisov, 1986) who in praise of human reason, science and technology wrote: “In nature there is nothing more miraculous than the human brain, more amazing than the process of thinking, more precious than the fruits of scientific research”, it may be concluded that Stoic ethical dictum “ Live or life according to Nature” should be sustained for the potential transition to the world of secularly renewed sustainability indicated by ecological (stability) sustainability coupled with social (stability) sustainability, given the exogenously determined non-anthropogenic Natural instability, through the socialization of Nature only in rational, conscious and moral pathway, though the uncertainty expressed by Georgescu- Roegen (1971) that “no social scientist can possibly predict what kinds of social organization mankind will pass in its future” may be unavoidable and unchallengeable.

6. References

- Beck, U.(1994). *Ecological politics in an age of risk* .Cambridge: Polity Press.
- Bird-David, N. (1997). Economies: A cultural-economic perspective. *International Social Science Journal*, December, 463-475.
- Borisov, V. (1986). *Militarism and science*. Moscow: Progress Publishers.
- Cavalcanti, C. (1997). Patterns of sustainability in the Americas: The U.S. and Amerindian lifestyles. In: F .Smith (Ed.), *Environmental sustainability*, pp. 27-45 .Florida: St. Lucie Press.
- Copleston, S. J. F. (1962) *A history of philosophy*. (Vol-1).New York: Image Books.
- Cuddon, J. A. (1998). *The Penguin dictionary of literary terms*. London: Penguin Books.
- Dawkins, R. (1995). *River out of Eden*. London: Weidenfeld and Nicholson.
- Dobson, A. (1990). *Green political thought*. London: Unwin Hyman.
- Dwyer, P. D.(1996). The invention of nature. In: R.F. Ellen & K. Fukui (Eds.), *Redefining nature: Ecology, culture and domestication*. Oxford: Berg.
- Dyson, A. E. (Ed.)(1975). *Gerard Manley Hopkins: Poems*. London: Macmillan Press.
- Ellen, R. F. (1996).The cognitive geometry of nature: A contextual approach. In: G. Palsson & P. Descola (Eds.), *Nature and society: Anthropological perspectives*. London: Routledge.
- Escobar, A. (1997). Anthropology and development. *International Social Science Journal*, December, 497-515.
- Geertz, C. (1963). *Agricultural involution: The process of ecological change in Indonesia*. Berkeley and Los Angles: California University Press.

- Georgescu- Roegen, N.(1971). *The entropy law and the economic process*. Cambridge: Harvard University Press.
- Giddens, A. (1994). *Beyond left and right*. Cambridge: Polity Press.
- Goldsmith, E. (1988). *The great –U turn*. Hartland: Green Books.
- Goodin, R.E. (1992). *Green political theory* .Cambridge: Polity Press.
- Gudeman, S. (1986). *Economics as cultures: Models and metaphors of livelihood*. London: Routledge & Kegan Paul.
- Halperin, R. H. (1988). *Economies across cultures: Towards a comparative science of the economy*. New York: St. Martin Press.
- Harris, M. (1968). *The rise of anthropological theory: A history of theories of culture*. London: Routledge & Kegan Paul.
- Heang, K.B. (1997). Sustainable development: A Southeast Asian perspective. In F .Smith (Ed.) *Environmental Sustainability* (pp. 67-83). Florida: St. Lucie Press.
- Holy,L. & Stuchlik, M.(1981). *The structure of folk models* .London: Academic Press.
- Howell, S. (1996). Nature in culture and culture in nature. In G. Palsson & P. Descola (Eds.) *Nature and society: Anthropological perspectives*. London: Routledge.
- Hunn, R. (1985). The utilitarian factor in folk biological classification. In J.W.D. Dougherty (Ed.), *Directions in Cognitive anthropology*. Urbana, Illinois: Illinois University Press.
- Huntington, E. (1924). *Civilisation and culture*. New Haven: Yale University Press.
- Ingold, T. (1992). Culture and the perception of the environment. In: E. Croll & D. Parkin (Eds.), *Bush, Base: Forest Farm*. London: Routledge.
- Ingold, T. (1996). Hunting and gathering as ways of perceiving the environment. In: R.F. Ellen & K. Fukui (Eds.), *Redefining nature: Ecology, culture and domestication*. Oxford: Berg.
- Konar, A. K. & Chakraborty, J. (2011). Substantive signification of sustainability. *Mother Pelican: A Journal of Sustainable Human Development*, 7(8/August). Retrieved from <http://www.pelicanweb.com>.
- Konar, A. K. (2013). (Un)Sustainability by Socialization. *Mother Pelican: A Journal of Sustainable Human Development*, 9 (1). Retrieved from <http://www.pelicanweb.org>.
- Kroeber, A. L.(1939). *Cultural and natural areas of native North America*. Berkeley: California University Press.
- Kropotkin, Peter.(1925). *Mutual Aid: A Factor of Evolution*. New York: Alfred A. Knopf, Inc.
- Levi- Strauss, C. (1963). *Structural anthropology*. New York: Basic Books.
- Lewis, M.W. (1992). *Green Delusions: An environmentalist critique of radical environmentalism*. Durham: Duke University Press.

- Lotka, A. J. (1925). *Elements of physical biology*. Baltimore: Williams and Wilkins.
- Mason, O.T. (1896). Influence of environment upon human industries or arts, Annual Report of the Smithsonian Institution for 1895, Washington,(pp. 639-665).
- Milton, K. (1997). Ecologies: Anthropology, culture and the environment, *International Social Science Journal*, December, 477-495.
- Mintz, S.W. (1985). *Sweetness and power: the place of sugar in modern history*. New York: Viking.
- Naess, A. (1972). The shallow and the deep, long range ecology movement: a summary, *Inquiry*, 16, 95-100.
- Nersesyants, V. S. (1986). *Political thought of ancient Greece*. Moscow: Progress Publishers.
- Polyani, K.et al. (Eds.)(1957). *Trade and market in the early empires*. Glencoe: Free Press.
- Posey, D.A. (1992). Introduction to the relevance of indigenous knowledge. In: A. Engracia de Oliveira & D. Hamu (Eds.), *Kayapo science: Alternatives to destruction* pp.15-18. Belem, Brazil: Museu Goeldi.
- Rapport, R. (1971). Nature, culture and ecological anthropology. In: H. L. Shapiro (Ed.) *Man, culture and society*. Oxford: Oxford University Press.
- Reichel- Dolmatoff, G. (1976). Cosmology as ecological analysis: A view from the rain forest, *Man*, 2, 307-318.
- Rossett, Barney. (1948). *The Creative Experiment*. New York: Grove Press (Evergreen edition).
- Sahlins, M.D. (1972). *Stone Age Economics*. Chicago: Aldine.
- Sahlins, M. D.(1976). *Culture and practical reason*. Chicago: Chicago University Press.
- Sen, M. K. (1967). *Inter-war-English Poetry*. Burdwan (West Bengal, India): University of Burdwan.
- Sheldrake, R. (1991). *The rebirth of nature*. London: Rider.
- Smith, F. (1997). Preface & A synthetic framework and a heuristic for integrating multiple perspectives on sustainability. In: F .Smith (Ed.), *Environmental Sustainability* pp. xi-xiv, &1-24. Florida: St. Lucie Press.
- Spender, S. (1950). *Collected poems 1928-1953*. London: Faber.
- Stace, W.T. (1972). *A critical history of Greek philosophy*. London: Macmillan Press.
- Stenning, D.J. (1957). Transhumance, migratory drift, migration. *Journal of the Royal Anthropological Institute*, 87, 57-73.
- Steward, J.(1955). *Theory of cultural change*. Urbana, Illinois: Illinois University Press.
- Tyler, S.(1969). *Cognitive anthropology* .New York: Holt, Rinehart and Winston.

Vernadsky, V. I.(1965). *The chemical structure of the earth biosphere and its environment*. Moscow: Moscow Publishers.

Werner, D.(1977). *Where there is no doctor*. Palo Alto: Hesperian Foundation.

Whitehead, A.N. (1953). Periodicity in nature. In: *An Introduction to Mathematics*. Oxford: Oxford University Press, Home University Library No. 18, 12/ i.

Wilkie T. 1993. *Perilous Knowledge*. London: Faber.



ISSN 2278 - 1811

₹ 500/-

ARTHSHAstra INDIAN JOURNAL OF ECONOMICS & RESEARCH

VOLUME : 11

ISSUE NUMBER : 2
(QUARTERLY)

APRIL - JUNE 2022

In This Issue

**Effects of Tax Revenue and Capital
Expenditure on Economic Growth :
A Case Study of the Union
Territory of Puducherry, India**

Joel Basumatary

**Steering Future Research in Microfinance :
Standing Atop Existing Literature**

N. V. Vijaykumar

**Pradhan Mantri Jan Dhan Yojana (PMJDY) :
Analyzing Performance Using
Financial Inclusion Indicators**

Shalvi Thakur

**The Embeddedness of Depression in
the Simple Keynesian Model**

Arup Kanti Konar

The Embeddedness of Depression in the Simple Keynesian Model

Arup Kanti Konar¹

Abstract

The sole objective of this very short paper was to disclose that depression is ingrained in the simple Keynesian model of hydraulic Keynesianism. Depression occurs in the Simple Keynesian Model because of the fact that the rate of change (growth) of saving is greater than the rate of change (growth) of investment. Depression can be cured, or prosperity can be realized if the rate of change (growth) of saving is equal to or less than the rate of change (growth) of investment.

Keywords: Keynesianism, consumption, saving, investment, stability

JEL Classification Codes: E12, E21, E32, E53

Paper Submission Date: April 18, 2022 ; **Paper sent back for Revision:** April 20, 2022 ; **Paper Acceptance Date:** April 30, 2022

The sole objective of this very short paper is to disclose that depression is ingrained in the simple Keynesian model of hydraulic Keynesianism, coined by Alan Coddington (1976, 1983). It is noteworthy that the other two types of Keynesianism are (a) fundamentalist Keynesianism and (b) disequilibrium Keynesianism or reconstituted reductionism. Further, it can be pointed out that the other three variants of hydraulic Keynesianism are: (a) special Keynesian model, (b) IS-LM Keynesian model or more general Keynesian model, and (c) generalized or complete Keynesian model.

Hydraulic Keynesianism was devised by Hicks (1937), Meade (1937), Samuelson (1939a, 1939b, 1946, 1947, 1948), Harrod (1937), Hansen (1936a, 1936b, 1938, 1941, 1947, 1951, 1953), Smith (1956), and so forth.

The simple Keynesian model is based on the following three equations, which have been translated into Figure 1.

(1) $S = S_0 + S(Y)$ such that $S_0 < 0$ and $1 > S'(Y) = MPS > 0$

(2) $I = I_0 + I(Y)$ such that $I_0 > 0$ and $0 < I'(Y) = MPI < S'(Y) = MPS$

where,

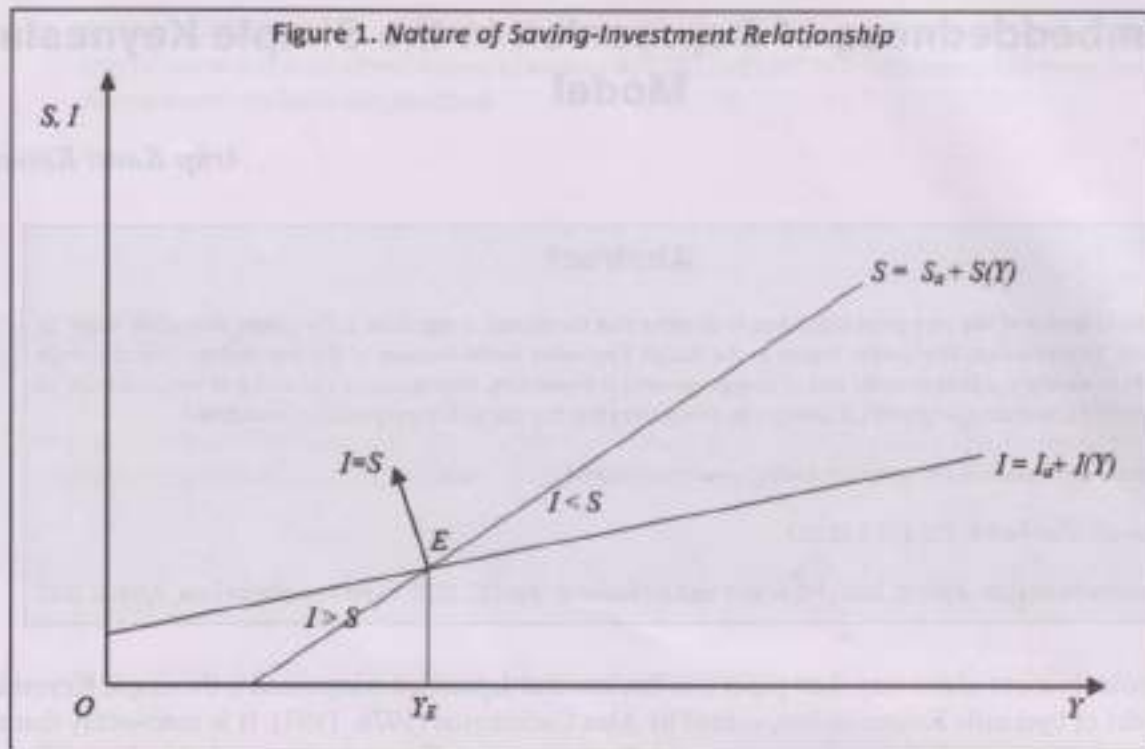
MPS = marginal propensity to save (slope of saving function) and MPI = marginal propensity to invest (slope of investment function).

(3) $S = I$ (equilibrium condition of commodity market)

The point elasticity of S with respect to Y of the S function = $E_{S,Y} = (dS/S)/(dY/Y) = (dS/dY)/(S/Y) = S'(Y)/(S/Y) = MPS/APS > 1$, since $MPS > APS$, where $APS = S/Y$. So, $E_{S,Y} > 1$, which means that $dS/S > dY/Y$. This implies that the rate of change (growth) of saving is greater than the rate of change (growth) of income.

¹ Principal & Associate Professor of Economics, Achhruram Memorial College, Jhalda, Purulia - 723 302, West Bengal. (Email: akkonar@gmail.com)

Figure 1. Nature of Saving-Investment Relationship



On the other hand, the point elasticity of I with respect to Y of the I function $= E_{IY} = (dI/I)/(dY/Y) = (dI/dY)/(I/Y) = I'(Y)/(I/Y) = MPI/API < 1$, since $MPI < API$, where $API = I/Y$. So, $E_{IY} < 1$, which means that $dI/I < dY/Y$. This implies that the rate of change (growth) of investment is less than the rate of change (growth) of income.

Thus, at the point of equilibrium denoted by E in Figure 1, though $S = I$ and $MPS > MPI$, yet we have: $E_s > E_{IY}$, which means $dS/S > dI/I$, that is, the rate of change (growth) of saving is greater than the rate of change (growth) of investment, which is the vital condition of depression. Hence, in the developed capitalist economy, depression is inevitable owing to the fact that $MPS > MPI$ and $dS/S > dI/I$. Depression can be cured, or prosperity can be realized if $dS/S = dI/I$, which is the condition of stability, and it implies that the rate of change (growth) of saving is equal to the rate of change (growth) of investment or, $dS/S < dI/I$, which is the condition of prosperity and it implies that the rate of change (growth) of saving is less than the rate of change (growth) of investment.

References

- Coddington, A. (1976). Keynesian economics: The search for first principles. *Journal of Economic Literature*, 14(4), 1258–1273. <https://www.jstor.org/stable/2722548>
- Coddington, A. (1983). *Keynesian economics: The search for first principles*. George Allen & Unwin.
- Hansen, A. H. (1936a). Mr. Keynes on underemployment equilibrium. *Journal of Political Economy*, 44(5), 667–686.
- Hansen, A. H. (1936b). Underemployment equilibrium. *Yale Review*, 25(Summer), 828–830.

- Hansen, A. H. (1938). Keynes on underemployment equilibrium. In A. H. Hansen, *Full recovery or stagnation*. A & C Black.
- Hansen, A. H. (1941). *Fiscal policy and business cycles*. Norton.
- Hansen, A. H. (1947). *Economic policy and full employment*. McGraw-Hill.
- Hansen, A. H. (1951). *Business cycles and national income*. Norton.
- Hansen, A. H. (1953). *A guide to Keynes*. McGraw-Hill.
- Harrod, R. F. (1937). Mr. Keynes and traditional theory. *Econometrica*, 5(1), 74 – 86. [https://doi.org/0012-9682\(193701\)5:1<74:MKATT>2.0.CO;2-U](https://doi.org/0012-9682(193701)5:1<74:MKATT>2.0.CO;2-U)
- Hicks, J. R. (1937). Mr. Keynes and the "classics": A suggested interpretation. *Econometrica*, 5(2), 147 – 159.
- Meade, J. E. (1937). A simplified model of Mr. Keynes' system. *The Review of Economic Studies*, 4(2), 98 – 107. <https://doi.org/10.2307/2967607>
- Samuelson, P. A. (1939a). Interactions between the multiplier analysis and the principle of acceleration. *The Review of Economics and Statistics*, 21(2), 75–78.
- Samuelson, P. A. (1939b). A synthesis of the principle of acceleration and the multiplier. *Journal of Political Economy*, 47(6), 786–797.
- Samuelson, P. A. (1946). Lord Keynes and the general theory. *Econometrica*, 14(3), 187–200. <https://doi.org/10.2307/1905770>
- Samuelson, P. A. (1947). *Foundations of economic analysis*. Harvard University Press.
- Samuelson, P. A. (1948a). *Economics: An introductory analysis*. McGraw-Hill.
- Samuelson, P. A. (1948/1965). *The simple mathematics of income determination*. In M. G. Mueller (ed.), *Readings in macroeconomics*. Surjeet Publications.
- Smith, W. L. (1956). A graphical exposition of the complete Keynesian system. *Southern Economic Journal*, 23(October), 115 – 125.

About the Author

Dr. Arup Kantil Konar has acquired his Ph.D degree from IGNOU, New Delhi. His research interests and publications are not confined to the economics discipline only. He is the Principal and Associate Professor of Economics of Achhruram Memorial College, Jhalda, Purulia, West Bengal. He is a member of the editorial board of more than seven national and international journals.

Published on the 5th and 6th Day of Every Three Months
Registered with the Registrar of Newspapers under Regd. No. DELENG/2012/43957

Printed and Published by Satya Gilani on behalf of Associated Management Consultants (P) Ltd. Y-21, Hauz Khas, New Delhi-110016 and Printed at M. S. Printers, C-108/1 Back side, Naraina Industrial Area, Phase - 1, New Delhi - 110028 and Published at Y-21, Hauz Khas, New Delhi-110016. Editor: Satya Gilani.



<https://doi.org/10.11646/phytotaxa.522.3.1>

Aerofilum fasciculatum gen. nov., sp. nov. (Oculatellaceae) and *Euryhalinema pallustris* sp. nov. (Prochlorotrichaceae) isolated from an Indian mangrove forest

SANDEEP CHAKRABORTY^{1,2,6}, VEERABADHRAN MARUTHANAYAGAM^{3,7}, ANUSHREE ACHARI^{4,8}, ARNAB PRAMANIK^{5,9}, PARASURAMAN JAISANKAR^{4,10} & JOYDEEP MUKHERJEE^{1,11*}

¹School of Environmental Studies, Jadavpur University, Kolkata 700 032, India

²Department of Botany, Achhruram Memorial College, Jhalda, Purulia 723 202, India

³Hunan Provincial Key Laboratory of Clinical Epidemiology, Xiangya School of Public Health, Central South University, 110 Xiangya Road, Changsha, Hunan, 410078, China

⁴Indian Institute of Chemical Biology, Jadavpur, Kolkata 700 032, India

⁵Department of Biochemistry, University of Calcutta, 35, Ballygunge Circular Road, Kolkata 700 019, India

⁶✉ sandeep061192@gmail.com; <https://orcid.org/0000-0001-5393-0998>

⁷✉ vmaruth@gmail.com; <https://orcid.org/0000-0002-5378-6567>

⁸✉ achari.anushree@gmail.com; <https://orcid.org/0000-0001-8544-605X>

⁹✉ arnab.ju9@gmail.com; <https://orcid.org/0000-0002-7675-7339>

¹⁰✉ drpjaisankar@gmail.com; <https://orcid.org/0000-0003-0583-4920>

¹¹✉ joydeep.mukherjee@jadavpuruniversity.in; <https://orcid.org/0000-0001-5068-8112>

* Corresponding author

Tel. 0091 33 2414 6147

Fax 0091 33 2414 6414

✉ joydeep.mukherjee@jadavpuruniversity.in

Abstract

Two novel cyanobacteria (AP3 and AP3b) with thin cells and simple morphology were isolated from two islands of the Indian Sundarbans. The 16S rRNA phylogeny data revealed the distinct lineage of AP3b which was nearest to the clade incorporating the genus *Oculatella* and *Tildeniella*. Strain AP3 shared a common ancestor with the species *Euryhalinema mangrovii*. Additionally, the novel 16S rRNA gene sequences of strains AP3 and AP3b showed similarities about 98% and 93% respectively compared to those of established genera or species to which they were phylogenetically related. Furthermore, the folding patterns of semi-conservative structures like D1-D1', Box-B and V2 helices of 16S-23S ITS region for both strains AP3 and AP3b displayed significant variations and uniqueness when compared with their respective reference strains (*Euryhalinema mangrovii* for AP3 and all the genera of Oculatellaceae for AP3b). Strain AP3 shared similar morphological features with its reference strain which confirmed its inter-species relationship. The diagnostic features of AP3b including the presence of necridic cells, aerotopes and a cluster-like growth pattern were found to be very contrasting. Altogether, these results substantiated the establishment of strain AP3b as a novel mono-specific genus named *Aerofilum fasciculatum* and strain AP3 as the second novel species under the genus *Euryhalinema*, referred to as *Euryhalinema pallustris*.

Keywords: *Aerofilum*, *Euryhalinema*, cyanobacteria, 16S-23S ITS, 16S rRNA, Sundarbans

Introduction

Cyanobacteria are well diversified group of organisms and undergo speciation. One of the main governing factors in their evolution is horizontal gene transfer which takes place among related cyanobacterial populations (Tooming-Klunderud *et al.* (2013). This evolution is further indicated by substantial variations in the morphology and ecophysiological characters (Komarek & Anagnostidis 2005). The speciation event promoted by the phenomenon of horizontal gene transfer depends on the environment of the organism and the degree of shared genes among the inhabiting species increases with increase in the extremities of the environment (Fuchsman *et al.* 2017). The intertidal regions of the world's largest mangrove forest, the *Sundarbans* are characterized by periodic changes in the physical parameters like water salinity, temperature, pH, carbon dioxide levels that can vary widely (Neogi *et al.* 2016). The biofilm

forming cyanobacteria residing in this intertidal zone are adapted to this variable poikilotrophic environment, leading to alterations in their genomes which culminate into eventual diversification as novel organisms (Debnath *et al.* 2017). Recent investigations on the cyanobacterial diversity of the Indian *Sundarbans* has resulted in the description of novel genera and species like *Leptolyngbya indica* (Debnath *et al.* 2017:105), *Oxynema aestuarii* (Chakraborty *et al.* 2018:37), *Euryhalinema mangrovii* (Chakraborty *et al.* 2019:70) and *Leptoelongatus litoralis* (Chakraborty *et al.* 2019:70). These findings suggest that biofilm-forming cyanobacteria of the intertidal regions of the Indian Sundarbans hold the potential for further discovery of novel cyanophyta.

Cyanobacterial systematics is currently founded on the polyphasic approach to taxonomy where the primary systematic position is determined on the basis of phylogeny established by the genetic markers, mainly 16S rRNA gene, located in the DNA sequence, supported by ecological variations and specific shared and derived morphological as well as ultrastructural features (Komarek *et al.* 2014). Contemporary literature demonstrates that growth of phylogenetic trees representing the evolutionary relationships among the members of cyanobacteria is occurring continuously as evidenced by descriptions of many new genera and species. Out of eight orders described by Komarek *et al.* (2014), Synechococcales is challenging because this order consists of members which are phylogenetically intermixed. Leptolyngbyaceae and Prochlorotrichaceae are believed to be the most polyphyletic families in this order. Sequences of many strains submitted in the National Center for Biotechnology Information (NCBI, <http://www.ncbi.nlm.nih.gov/genbank/>) database were named as “*Leptolyngbya* species” or “Leptolyngbyaceae”, although they were evolutionarily distinct from the *Leptolyngbya* generitype (Becerra-Absalon *et al.* 2018, Mai *et al.* 2018). These inappropriate names resulted in a polyphyly within the *Leptolyngbya* genus. Although Leptolyngbyaceae and Prochlorotrichaceae families were subjected to many taxonomic revisions, further taxonomic reconsiderations following the polyphasic approach is required for many of these misnamed strains. Over the last ten years, many new generic entities were separated from the polyphyletic genus *Leptolyngbya*. These novel genera include *Phormidesmis* (Komarek *et al.* 2009: 53, Turichhia *et al.* 2009: 179), *Nodosilinea* (Perkerson *et al.* 2011: 1404), *Haloleptolyngbya* sp. (Dadheech *et al.* 2012: 272), *Chroakolemma* sp. (Becerra-Absalon *et al.* 2018: 204) and *Albertania* sp. (Zammit, 2018: 483). Furthermore, Mai *et al.* (2018) proposed a family-level taxonomic reorganization on the basis of the polyphasic approach which eventuated into the division of family Leptolyngbyaceae into four monophyletic families comprising of two novel families Oculatellaceae and Trichocoleaceae and two previously-described families Leptolyngbyaceae and Prochlorotrichaceae. Mai *et al.* (2018) proposed six new genera under the novel family Oculatellaceae containing 14 new species which established the family Leptolyngbyaceae as a well-defined and monophyletic clade. Moreover, the family Prochlorotrichaceae was redefined by Mai *et al.* (2018) containing the genera *Prochlorothrix*, *Nodosilinea*, *Halomicronema* and some members without any specific generic identity. Chakraborty *et al.* (2019) described two novel monospecific genera *Euryhalinema mangrovii* and *Leptoelongatus litoralis* which shared well-supported molecular phylogenetic relationships with the other genera of Prochlorotrichaceae. Family-level taxonomic analyses based on phylogenetic relationship among the families under the Synechococcales order had established a monophyletic trend. Nevertheless, further revision for the establishment of monophyletic affiliation at the inter-generic level is essential owing to the presence of several unidentified generic entities. Most of the filamentous taxa in the Synechococcalean order have a simple morphology but they are genetically very divergent. Becerra-Absalon *et al.* (2018) specified the requirement of more in-depth taxonomical evaluation for the description of new genera and naming a genus is consequently followed by description of new species under it. For instance, many genera like *Oculatella*, *Oxynema*, *Nodosilinea* were regularly revised and new species were subsequently added thus increasing the resolution of the phylogenetic clade. In this context, all the strains with ambiguous identity and nomenclature like “*Leptolyngbya* species” (excluding the clade of *Leptolyngbya sensu stricto*) and “*Calothrix* sp. 96/26 LPP3” which are till date incompletely studied, requires to be examined thoroughly. This could be a resourceful approach for the establishment of complete monophyletic groups of genera under a family (Becerra-Absalon *et al.* 2018, Chakraborty *et al.* 2019).

This article contributes to the alpha-level taxonomy of the family Oculatellaceae and Prochlorotrichaceae. The present study aimed to investigate two strains, AP3 and AP3b isolated from the mangrove forest of the Indian Sundarbans by applying the polyphasic approach to taxonomy. Through a combination of morphological, ultrastructural and molecular data as well as ecological considerations we propose that strain AP3 should be recognized as the second novel species of the newly established genus *Euryhalinema* (Chakraborty *et al.* 2019) as *Euryhalinema pallustris* sp. nov. while strain AP3b should be accepted as a monospecific novel genus *Aerofilum fasciculatum* gen. nov.

Materials and methods

2.1 Study site, collection and maintenance of strains Strains AP3 and AP3b were obtained from the biofilms present on the soil surface of the Sagar and Lothian islands of the Indian Sundarbans respectively (Fig. 1). The physical characteristics of the collection site were detailed by Pramanik *et al.* (2011). The isolated cyanobacteria were purified and propagated in the laboratory and were checked in every stages of their growth period for the stability of their phenotypic characteristics at monthly intervals. No changes were observed during the successive sub-cultures. The pure cultures of the cyanobacteria were maintained in ASN III liquid medium (Rippka *et al.* 1979) as well as in solid medium. The cyanobacteria were cultivated in a controlled environment having fluorescent irradiance ($50 \mu\text{mol photons m}^{-2} \text{s}^{-1}$) with 12 : 12 hrs light : dark photoperiod at $25 \pm 1 \text{ }^\circ\text{C}$ (Chakraborty *et al.* 2018, Chakraborty *et al.* 2019). Isolate AP3 having accession number MCC 3172 and AP3b bearing accession number MCC 3478 were deposited in the Microbial Culture Collection (MCC), India where they are being cryopreserved.



FIGURE 1. Map showing the location of sample collection sites of the Sundarbans forest located in the state of West Bengal, India. Samples were collected from the Sagar and the Lothian island of Indian Sundarbans. Blue pin = Sagar island; Red pin = Lothian island

2.2 Light microscopy Morphological examination was carried out using a light microscope (Model DM750; Leica Microsystems, Buffalo Grove, USA) under 1000X magnification. Photomicrographs of the filaments from the exponential as well as stationary phases of the life cycle of AP3 and AP3b were acquired by a camera (ICC50 HD) attached to the microscope (Chakraborty *et al.* 2018, Chakraborty *et al.* 2019). Cellular dimensions were recorded by the aid of auxiliary software (LAS-EZ, Leica Microsystems) available with the microscope.

2.3 Scanning electron microscopy One milliliter suspension of fresh filaments of test strains (AP3 and AP3b) were concentrated by centrifugation at 8000 rpm (Eppendorf 5810R, rotor F-34-6-38, Hamburg, Germany). The cells were fixed in 3% glutaraldehyde for 2 hrs and successively washed in distilled water. Cells were dehydrated applying enhancing concentrations of ethanol from 30% for 15 min to 100% for 60 min. The samples were ultimately dried at the critical point and the grids were examined under a scanning electron microscope (Jeol JSM-6700F, Jeol, Tokyo, Japan) following Chakraborty *et al.* (2018) and Chakraborty *et al.* (2019).

2.4 Transmission electron microscopy About 1 ml suspension of fresh cyanobacterial cells from 8-10 days old cultures of the strains under examination were centrifuged at 8000 rpm (Eppendorf 5810R, rotor F-34-6-38, Hamburg, Germany). The pellet was washed carefully in distilled water and successively pre-fixed in 2.5% glutaraldehyde and 2% paraformaldehyde in 0.1 M phosphate buffer (pH 7.8) for 5-6 hrs at 4 °C. The samples were rinsed in 0.1 M phosphate buffer and the surplus fixative was washed off with the buffer. Post fixation of the cells with osmium tetroxide (1% solution) was carried out for 60 minutes. Subsequently, cells were dehydrated by passing through enhancing concentrations of ethanol. Afterwards, samples were infiltrated and embedded in Araldite CY 212 (Agar Scientific, Stansted, UK) for incising of sections. The resin blocks were polymerized by heat treatment at 50 °C overnight and then subjected to a second treatment at 60 °C for 2 days. An ultramicrotome was applied to cut thin sections of the samples. Sections were contrasted with uranyl acetate and lead citrate and examined under a TECNAI G20 transmission electron microscope (FEI, Eindhoven, Netherlands) as described in Chakraborty *et al.* (2018) and Chakraborty *et al.* (2019).

2.5 DNA extraction, PCR amplification and sequencing DNA was extracted from the exponential phase of growth of the axenic cultures of the test strains (AP3 and AP3b) using Gene JET™ Genomic DNA Purification Kit (Cat. No. K0721, Thermo Scientific, Waltham, USA) following the manufacturer's instructions. The DNA extracts were stored at -20 °C. Polymerase Chain Reaction (PCR) was applied to amplify the partial 16S rRNA region and the associated 16S-23S ITS region as described in Chakraborty *et al.* (2018) and Chakraborty *et al.* (2019). Briefly, we employed cyanobacterial specific forward primer CYA106F (5'-CGGACGGGTGAGTAACGCGTGA-3') (Nubel *et al.* 1997) and universal reverse primer 1492R (5'-ACCTTGTTACGACTT-3') (Lane 1991) for the amplification of 16S rRNA gene. Forward primer 16SF (5'-TGTACACACCGGCCCGTC-3') and reverse primer 23SR (5'-CTCTGTGCCTAGGTATCC-3') as designed by Iteaman *et al.* (2000) were applied for the amplification of the 16S-23S ITS region. The program used for the PCR reaction using primers CYA106F and 1492R was: 94 °C for 5 minute, 94 °C for 1 minute, 72 °C for 2 minutes (30 cycles), followed by a 10 minute extension at 72 °C (Chakraborty *et al.* 2018, Chakraborty *et al.* 2019). Amplified PCR products were stored at 4°C. The PCR program for amplification of the 16S-23S ITS regions were: initial denaturation at 95 °C for 5 min thereafter 30 cycles at 95 °C for 30 sec; 58 °C for 15 sec; 72 °C for 40 sec and ultimate elongation step at 72 °C for 5 min (Chakraborty *et al.* 2018, Chakraborty *et al.* 2019). Reactions were carried out using Mastercycler Nexus Gradient PCR machine (Eppendorf, Hamburg, Germany). PCR products were detected by standard agarose gel electrophoresis with ethidium bromide staining. The PCR products obtained for 16S rRNA and ITS regions were cloned into plasmids containing the sites for their respective primers on either side of the insert site using InstAclone™ PCR cloning kit (Cat. no. K1213, K1214, Thermo Scientific, Waltham, USA). The commercial vector used for insertion of the sequence was pCR 2.1 (Life Technologies, Invitrogen, USA). Competent *E. coli* DH5α cells were used for the transformation. Colonies were selected by blue-white screening method and the plasmid DNA was purified and obtained from the resultant clones using Thermo Scientific GeneJET Plasmid Miniprep Kit (Cat. no. K0502, K0503, Waltham, USA). Clones containing PCR products were digested with EcoRI and Hind III enzyme and run on an electrophoresis gel to estimate the size of the inserts. Four clones for strain AP3b and three for strain AP3 were selected for sequencing. Finally, sequencing was performed using an automated DNA sequencer (Genetic Analyzer 3500xL, Applied Biosystems, Waltham, USA) as described in Chakraborty *et al.* (2018) and Chakraborty *et al.* (2019). The sequences of 16S rRNA and 16S-23S ITS regions of all the clones of the isolates AP3 and AP3b obtained were checked for its authenticity and reliability by determining the quality control values and any chimeric sequence, if present, using online software tool DECIPHER (<http://www2.decipher.codes>). Sequences were subsequently submitted to GenBank and their accession numbers are presented in Table 1.

TABLE 1. Gene sequences of the cyanobacterial test strains submitted in the NCBI database with their accession numbers.

Strain Id	NCBI Accession numbers	
	16S rRNA	16S-23S ITS
<i>Euryhalinema pallustris</i> AP3 clone 1	MT310717.2	MT310719.2
<i>Euryhalinema pallustris</i> AP3 clone 2	MT947790	MT943581
<i>Euryhalinema pallustris</i> AP3 clone 3	MT947791	MT943582
<i>Aerofilum fasciculatum</i> AP3b clone 1	MT310718.3	MT310720.2
<i>Aerofilum fasciculatum</i> AP3b clone 2	MT947792	MT943583
<i>Aerofilum fasciculatum</i> AP3b clone 3	MT947793	MT943584
<i>Aerofilum fasciculatum</i> AP3b clone 4	MT947794	NA

2.6 Examination of the 16S rRNA gene sequence and phylogenetic analysis The gene sequences of all the clones of the isolates under investigation (AP3 and AP3b) were examined by using Basic Local Alignment Search Tool (BLAST) and compared with the other sequences available in the robust database of the National Center for Biotechnology Information (NCBI, <http://www.ncbi.nlm.nih.gov/genbank/>). Additional sequences were also obtained based on the classification criteria involving the sequences of many recently described genera of the family Oculatellaceae as well as Prochlorotrichaceae within the order Synechococcales. A consensus phylogenetic tree was constructed on the basis of the similarity values obtained in the BLAST hits and the sequences selected based on the classification criteria. The taxa used in the construction of phylogenetic tree included in total 115 OTUs and *Gloeobacter violaceus* was selected as the outgroup. The multiple sequence alignment of these OTUs was performed in the Clustal W program (Larkin *et al.* 2007). Bayesian Inference (BI), and Maximum Likelihood (ML) analyses were performed using 16S rRNA gene sequences of the 116 OTUs with maximum of 1778 characters containing nucleotides and indels. Maximum Likelihood (ML) tree was reconstructed using MEGA program package version 6.0 (Tamura *et al.* 2013) employing Kimura's two parameter model of sequence evolution with gamma distributed evolutionary rates and an estimated proportion of invariable sites. Bootstrap values to test the robustness of the phylogenetic tree for ML analysis were set to 1000 replications. Bayesian Inference analysis was executed by submitting the alignment to MrBayes (Ronquist *et al.* 2012) on XSEDE (3.2.6) available on CIPRES Science Gateway v.3.3 (Miller *et al.* 2010) applying a GTR+G+I model of nucleotide substitutions. Two independent runs with four chains were executed and each of the two runs was simultaneously conducted for 30 million Markov Chain Monte Carlo (MCMC) generations. Temperature was empirically set to 0.2 and permitted the sampling of trees after every 500 generations. The Estimated Sample Size (ESS) of this analysis exceeded 300 for all parameters which are usually considered acceptable by all phylogeneticists (Drummond *et al.* 2006). The final average standard deviation of split frequencies was lower than 0.008. The Potential Scale Reduction Factor (PSRF) value for all the parameters was 1.00 signifying the statistical attainment of the convergence of MCMC chains (Gelman & Rubin 1992). The first 500 trees were rejected as burn-in phase and a 50% majority rule consensus tree was evaluated comprising posterior probabilities. The resultant tree was visualized in the FigTree 1.3.1 (<http://tree.bio.ed.ac.uk/software/figtree>) software. An array of 16S rRNA and ITS divergence rates among the sequences was studied by the computation of uncorrected p-distance for 16S rRNA and ITS regions in MEGA 6.0 and the output was used to calculate similarity matrix (as percentage) [$100 \times (1-p)$] for 16S rRNA data and a dissimilarity matrix (as percentage) ($100 \times p$ -distance) for the ITS data. 16S rRNA sequences for both the studied strains were also utilized for examining the conserved regions and the secondary structures of its various helices following Rehakova *et al.* (2014) and to verify the quality of sequences for our strains by aligning them with other reference strains identified by Rehakova *et al.* (2014). Sequences of the conserved regions were folded in M-fold web server (Zuker 2003).

2.7 Analysis of 16S - 23S ITS secondary structures The sequences of 16S - 23S ITS regions were also utilized for the taxonomic resolution of the strains under investigation, AP3b and AP3 at the genus and species levels respectively. The complete ITS sequences for both strains were aligned with their respective reference strains (AP3 with its reference strain *Euryhalinema mangrovii* and AP3b with the other related genera belonging to the family Oculatellaceae) and all the variable as well as conserved regions were identified. The complete ITS sequences of the reference strains were obtained from the NCBI. The constituent ITS regions like D1-D1' helix, Box- B, V2 and V3 helices were folded for AP3b and D1-D1' helix, Box- B and V2 helices for AP3 by operating the M-fold web server, version 2.3 (Zuker 2003) and redrawn employing Adobe Illustrator 2020. The secondary structures were created applying ideal conditions with the temperature fixed at default value 37 °C and the structure assigned as untangle loop fix. Additionally, the sequence length of the various constituent regions of the ITS were determined and compared with their respective reference strains following Johansen *et al.* (2011). The sequence lengths of the various constituent regions of ITS of the reference strains were obtained from Chakraborty *et al.* (2019) and Mai *et al.* (2018).

Results

3.1 Morphological characterization When provided with the ASN III medium, strains under investigation (AP3 and AP3b) displayed moderate growth in the Erlenmeyer flasks. Strain AP3 formed a uniform, thin mat-like greenish biofilm attached to the surface of the flask. Strain AP3b grew in clusters, appearing as fascicles (Komarek & Anagnostidis 2005) rather than forming a consistent biofilm attached to the surface. Strains under investigation (AP3 and AP3b) were characterized by light microscopy (Fig. 2). Trichomes of AP3b appeared in clusters. Individual

filaments consisted of a facultative sheath. Trichomes were isopolar, uniseriate, unbranched, thin having cells slightly longer than their width, cell length ranged from 1.4 - 2.1 μm and width 0.9 - 1.1 μm . Cells showed fine constrictions at their cross walls (Fig. 2c & 2d). Trichomes were cylindrical, immotile, did not contain any heterocyte or akinete. Small disintegrated filaments were found as hormogonia which help in propagation of the cyanobacterial cells. Cells of strain AP3 possessed dimensions 1.1 - 1.6 μm (length) and 0.4 - 0.5 μm (width) (Fig. 2a & 2b). Cells of the filaments were much longer than their width. General features were alike strain AP3b except that isolate AP3 was not covered by any mucilage sheath. Scanning electron microscopy (Fig. 3) also demonstrated features that were similar to that revealed by light microscopy. Presence of a facultative mucilaginous sheath covering the trichome of strain AP3b was confirmed by the scanning electron microscopy (Fig. 3e) while Fig. 3b shows the presence of a necridic cell (sacrificing cell) (Komarek & Anagnostidis 2005) separating from the terminal part of the parent trichome to form hormogonia.

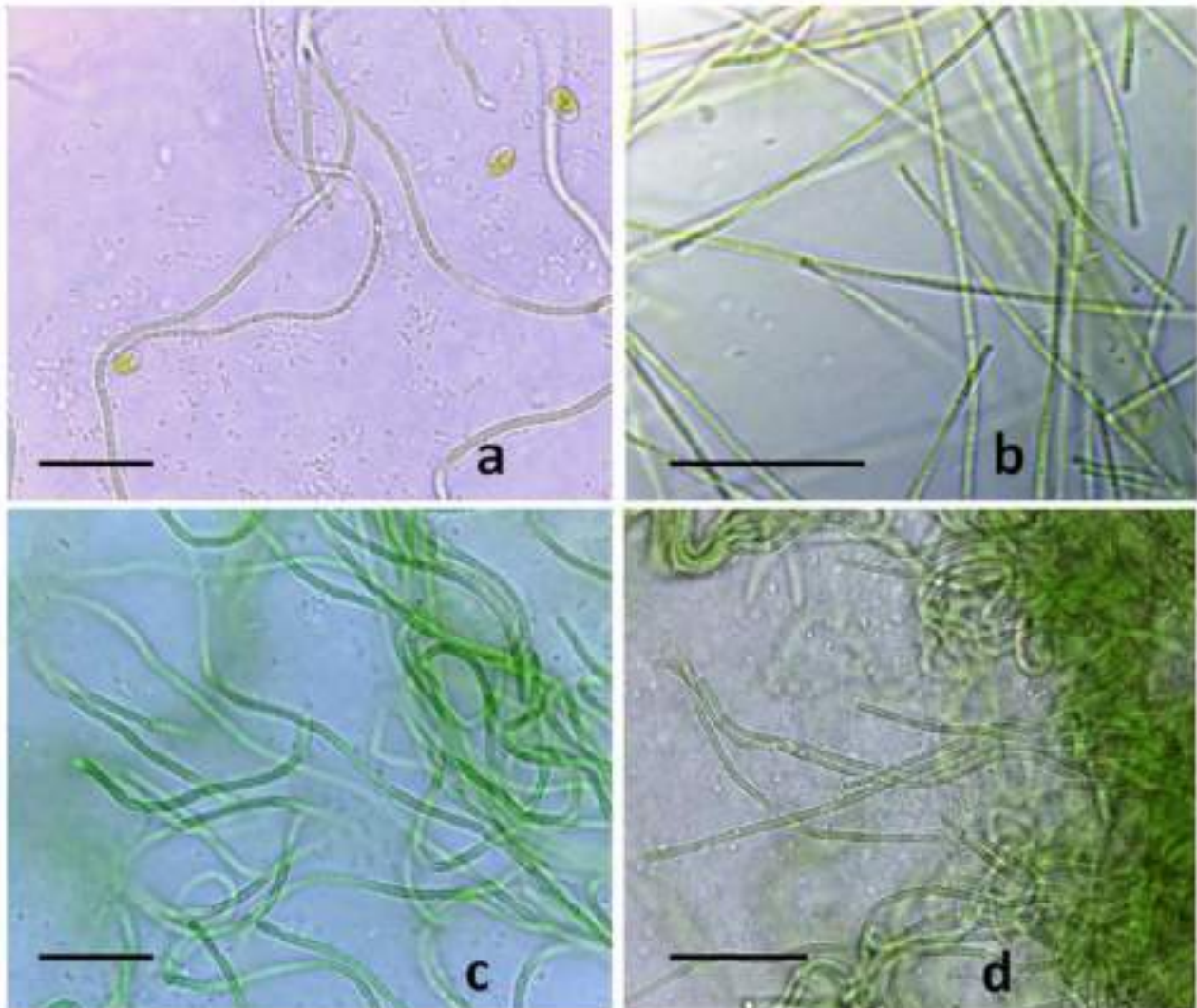


FIGURE 2. Light microscopy of strain AP3 and AP3b (non-axenic cultures). **a** and **b**. Microphotographs showing the filaments of strain AP3. **c** and **d**. Microphotographs showing the filaments of strain AP3b. Filaments observed in **a** & **c** were from exponential phase and in **b** & **d** were from stationary phase of the growth period for the respective strains. Scale = 10 μm

The closest species to be compared with AP3 on the basis of phylogenetic data as well as morphometric analysis was the mono-specific genus *Euryhalinema mangrovii* under the family Leptolyngbyaceae recently described by us (Chakraborty *et al.* 2019). The studied isolate AP3 showed high affinity with this genus in the morphological characters. Similarly, strain AP3b was found to be most closely related to *Oculatella atacamensis* as well as *Tildeniella torsiva* belonging to a recently described family Oculatellaceae (Mai *et al.* 2018). Therefore, a morphometric comparison amongst AP3 and *Euryhalinema mangrovii* (Table 2) and a comparative account of morphological features of AP3b in contrast with the phylogenetically closest relative *Oculatella atacamensis* as well as other related genera of

family Oculatellaceae are presented (Table 3). Table 2 depicts that the strain AP3 showed most of the morphological features similar to its reference *Euryhalinema mangrovii* except their collection site which was two separate islands, geographically 10 kms apart. Table 3 showed diagnostic morphological features of strain AP3b which were distinct from the other genera compared like the presence of aerotopes and fascicular growth pattern while some features like cellular dimensions, cellular constrictions, cell shapes and apical cell morphology in AP3b were shared with the other genera of the family Oculatellaceae.

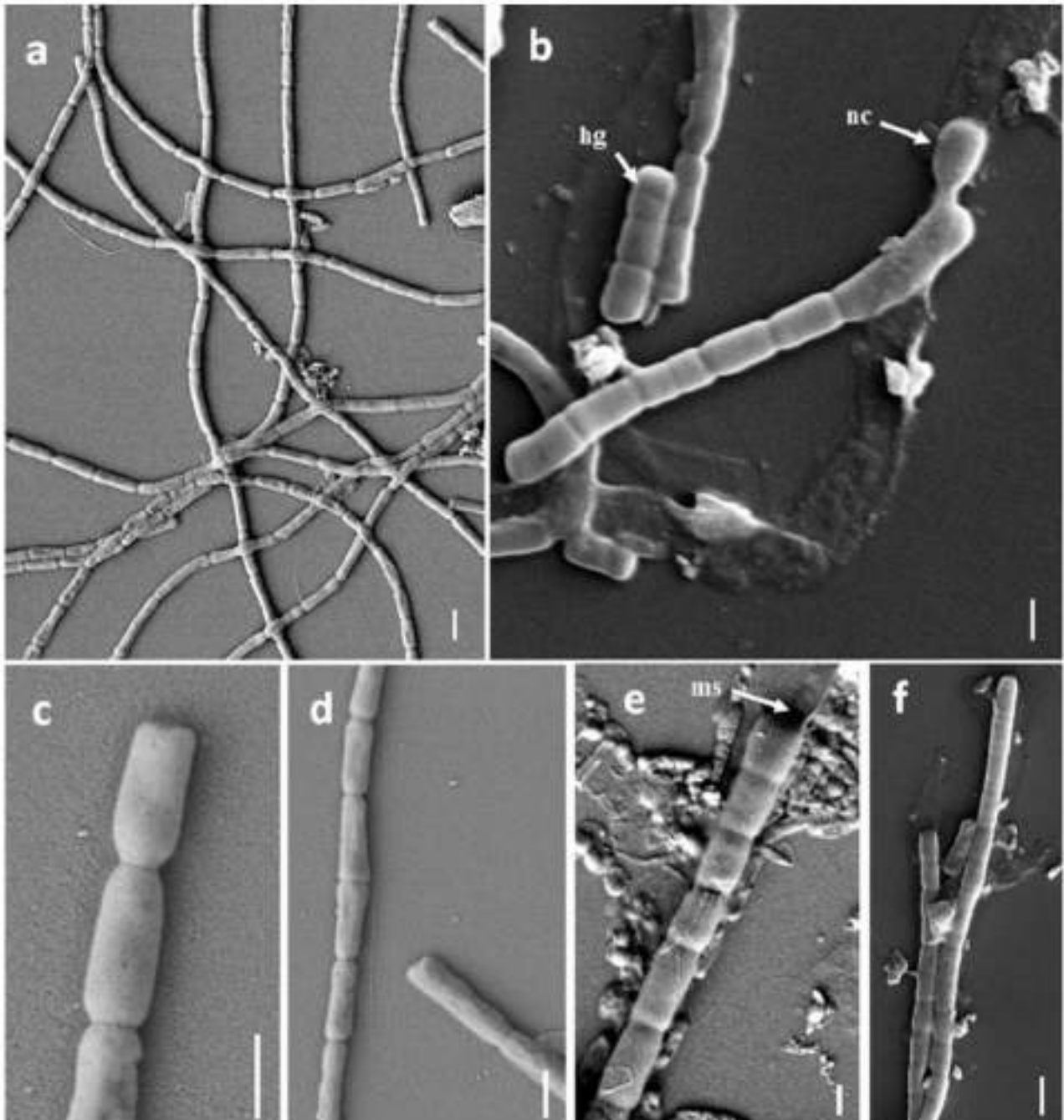


FIGURE 3. Scanning electron microscopy of strains AP3 and AP3b. **a, c and d.** Filaments of strain AP3. **b.** Filaments of strain AP3b (non-axenic) showing a hormogonium and a necridic cell. **e and f.** Filaments of strain AP3b showing presence of a facultative mucilaginous sheath. hg = hormogonium; nc = necridic cell; ms = mucilaginous sheath

TABLE 2. Comparative analysis of the morphological features of test strain *Euryhalinema pallustris* AP3 and reference strain *Euryhalinema mangrovii*. Characteristics of previously described genus *Euryhalinema mangrovii* AP9F was obtained from Chakraborty *et al.* (2019).

Feature	<i>Euryhalinema pallustris</i> AP3	<i>Euryhalinema mangrovii</i> AP9F
Thallus	Thin biofilm of light greenish color	Pale bluish-green color mats
Filaments	Thin, long, unbranched, isopolar, straight	Thin, long, unbranched, straight, isopolar
Mucilage sheath	Absent	Absent
Cell length (µm)	1.1 – 1.6	1.25 – 2.6
Cell width (µm)	0.4 – 0.5	0.4 – 0.6
False branching	Absent	Absent
Cell form	Distinctly much longer than wide	Distinctly much longer than wide
Cross walls	Constricted	Constricted
Trichome apex	Rounded, not attenuated	Rounded not attenuated
Habitat	Sub-aerophytic, in the soils of intertidal area of estuary with salinity ranging from 1.7-1.8 ‰	Sub-aerophytic, in the soils of intertidal area of estuary with salinity ranging from 1.7-1.8 ‰

TABLE 3. Comparison of the features of *Aerofilum fasciculatum* AP3b along with other related genera of the family Oculatellaceae. Features of previously described genera were extracted from Osorio-Santos *et al.* (2014) (for *Oculatella atacamensis*) and Mai *et al.* (2018) (for other published genera of Oculatellaceae).

	<i>Aerofilum fasciculatum</i>	<i>Oculatella atacamensis</i>	<i>Pegethrix convoluta</i>	<i>Drouetiella hepatica</i>	<i>Timaviella radians</i>	<i>Tildeniella torsiva</i>
Thallus	Blue-green, trichomes appears in clusters like 'fascicles'	Thin mat, growing diffusely from the centre	Bright blue-green, radially spreading in the agar	Brownish or purplish-brown floating mucilaginous mats	Thallus leathery, dark olive-brown to olive-green colour	Bright blue-green colour colony spreading irregularly, fasciculated
Filaments	Filaments long, straight, isopolar	Filaments flexuous, long, straight	Filaments long, fasciculated, sometimes form nodules, straight or bent	Filaments long, straight	Filaments relatively short, wide, forming radial colonies	Filaments flexuous or spirally coiled
Cell length (µm)	1.4 - 2.1	1.5 - 7.4	1.0 - 2.5	3.1 - 4.5	1.2 - 2.2	1.5 - 2.7
Cell width (µm)	0.9 - 1.1	1.5 - 2.3	1.3 - 2.5	2.8 - 3.7	1.8 - 3.7	1.7 - 2.5
Cell form	Cells slightly longer than wide to isodiametric	Cells mostly longer than wide	Cells shorter than wide but after division longer than wide	Cells mostly longer than wide to elongated with a central at centre	Cells shorter than their width	Mostly longer than wide, rarely isodiametric
Cross walls	Distinctly constricted	Slightly constricted with oblique wall formation	Slightly constricted	Slightly constricted	Distinctly constricted	Slightly constricted
Sheath	A thin facultative sheath present	Distinct sheath present	Distinct sheath present	Distinct, firm sheath present	Sheath diffluent, rarely distinct	Distinct, firm, thin sheath
False branching	Absent	Rarely present	Infrequently present	Occasionally present	Present	Rarely present
Apical cell	Rounded end apical cell with homogeneous contents	Bluntly-rounded end apical cell with reddish-orange spot in the apex	Rounded apical cell	End cells with cylindrical-rounded end	Round to conical round-ended apical cell	Rounded end apical cells
Aerotopes	Present	Absent	Absent	Absent	Absent	Absent
Necridic cells	Present	Absent	Present	Present	Absent	Absent
Habitat	Sub-aerophytic soil biofilm from intertidal estuarine region	Rock-soil interface in Atacama Desert	Soil microbial layer from a seep wall in USENEM, USA	Sub-aerophytic, found in limestone, Slovakia	Mats in the waterfall, Navajo Sandstone, USA	Sub-aerophytic mats on the limestone wall, Slovakia

3.2 Ultrastructural studies Transmission electron microscopic studies on the two strains under investigation were conducted. The microphotographs of the sections of strains AP3 and AP3b revealed the pattern of thylakoidal arrangement as well as the granulation which were in agreement with the archetype of the thylakoids of the family Leptolyngbyaceae (Komarek & Anagnostidis 2005) as well as with the family Oculatellaceae (Mai *et al.* 2018). The thylakoidal arrangement of strain AP3b was peripheral. The presence of facultative sheath in the cross section was also confirmed by transmission electron microscopy (Fig. 4d). The cross section of the cell also disclosed the presence of aerotopes which were colorless, nearly circular in shape, irregularly distributed throughout the cell and were of various sizes, 4-7 in numbers per cell (Fig. 4c). Strain AP3 showed the presence of various granulations like carboxysomes and polyphosphate bodies (Fig. 4b) in the cross section of its cells.

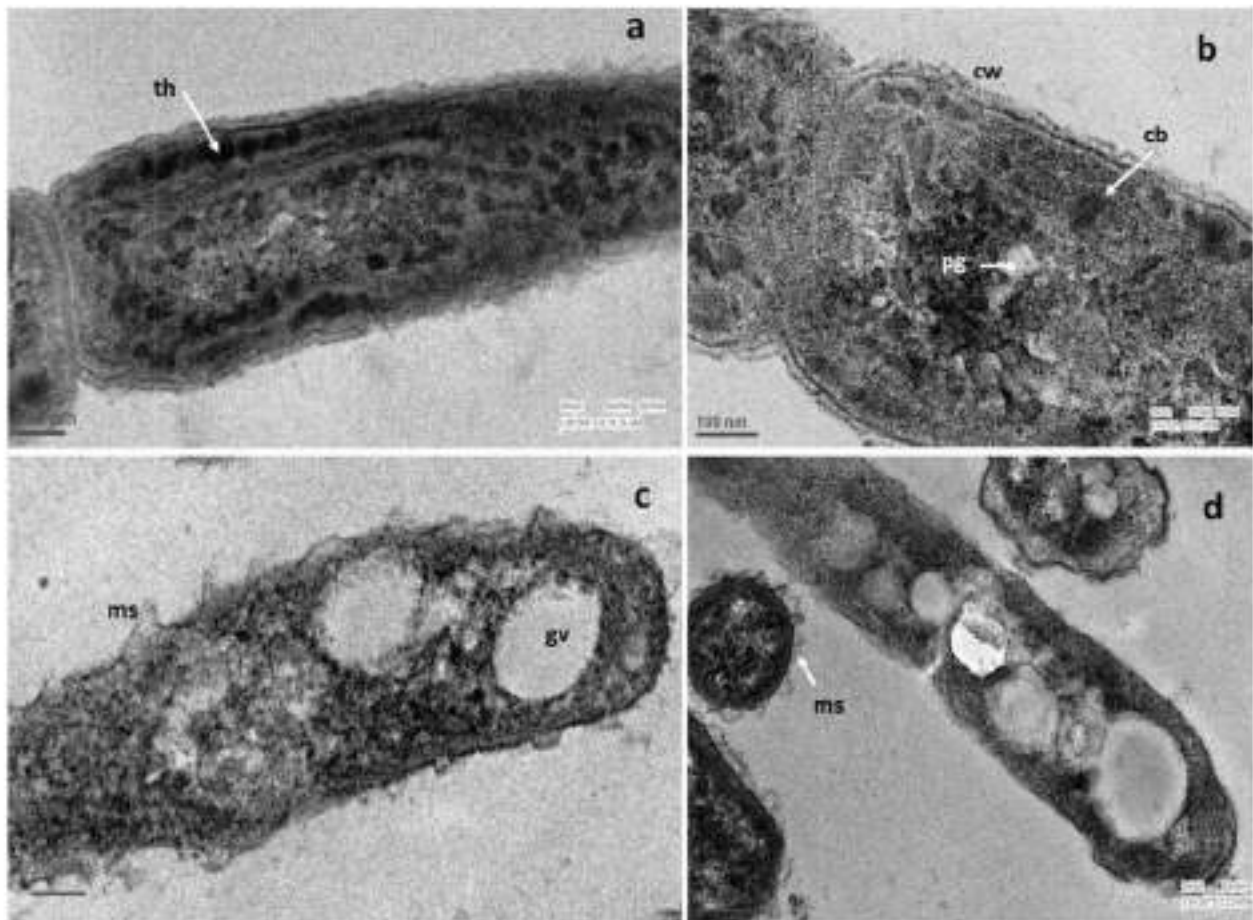


FIGURE 4. Transmission electron microscopy of strain AP3 and AP3b. **a** and **b**. Cross-section of a part of filament of strain AP3 showing thylakoidal arrangement and granulations. **c** and **d**. Cross-sectional view of cell of strain AP3b showing aerotopes distributed throughout the cell. th = thylakoids; pg = polyphosphate granules; cb = carboxysomes; cw = cell wall; ms = mucilaginous sheath; gv = gas vesicles.

3.3 Alignment of the 16S rRNA gene sequence and phylogenetic analysis A partial sequence of the 16S rRNA gene of AP3 (1282 nucleotides) and AP3b (1126 nucleotides) was obtained by the PCR as described in section 2.5. The sequences obtained for both the strains were checked and authenticated with appropriate quality control values as well as verified to be pure without any chimera. The two sequences were compared with the other sequences available in GenBank. The nearest hit showing highest similarity (about 98.2%) with strain AP3 was *Euryhalinema mangrovii* strain AP9F (Accession number MK402979) which was recently published as a monospecific genus by us (Chakraborty *et al.* 2019). The second hit was with the cyanobacterium named ‘*Calothrix* sp. 96/26 LPP3’ (Accession number KM019977) having similarity around 97%. This strain was incorrectly named and submitted in the GenBank and should be revised for a proper taxonomic affiliation (Chakraborty *et al.* 2019). Barring these two cyanobacteria, others strains in the NCBI hits were found to be significantly distant from our isolate AP3 having similarities less than 94%. Hence, it was decided to select *Euryhalinema mangrovii* as the reference strain for the test strain AP3 for further phylogenetic analysis and eventual proposal as a novel species under the genus *Euryhalinema* in this present communication. Furthermore, the strain AP3 established itself as a sister taxon with the genus *Euryhalinema* and

along with ‘*Calothrix* sp. 96/26 LPP3’ formed a well-supported clade sister to the clade of genus *Leptoelongatus litoralis*. *L. litoralis* was concomitantly a novel genus described by us (Chakraborty *et al.* 2019) from the same field area of the Indian Sundarbans. The phylogenetic tree consisted of the members of Synechococcalean order including some of the genera of family Leptolyngbyaceae, almost all the genera of family Oculatellaceae (Mai *et al.* 2018) and key genera from the family Prochlorotrichaceae as proposed by Becerra-Absalon *et al.* (2018).

The closest relative of strain AP3b in the NCBI was a strain named *Oculatella atacamensis* (Accession number KF761587) which demonstrated about 93.82% genetic similarity. The second top hit with proper designation mainly included the species of genus *Tildeniella* (KY498228) of the family Oculatellaceae with a similarity about 92.77%. Other hits also included genera of Oculatellacean members like *Timaviella radians* (KY078774) and *Drouetiella hepatica* (HM018689), displaying a range of 92-90% genetic similarity with the test strain AP3b. This similarity (as percentage) was definitely justified in context to the threshold likeliness in between two genera, which should be less than 94.7% (Yarza *et al.* 2014). Therefore, the morphological likeliness as well as the molecular similarity leads to the proposal that strain AP3b must belong to the family Oculatellaceae. Species of the genus *Oculatella*, i.e., *Oculatella subterranea* (Zammit *et al.* 2012) and *O. atacamensis* (Osorio-Santos *et al.* 2014) along with other genera of family Oculatellaceae were selected as the reference strains solely on the basis of the genetic similarity of 16S rRNA gene sequence for further phylogenetic studies. Subsequently, a consensus phylogenetic tree was constructed including all the clones of the strains under investigation (AP3 and AP3b) along with their closest relatives and other members of the family Oculatellaceae and Prochlorotrichaceae to justify the evolutionary relationship. The outcome of the tree demonstrated that the clones of strain AP3b were clustered together in a well-supported clade under the family clade of Oculatellaceae and separated from its nearest relative *Oculatella* genus and other genus clades and formed a novel distant phylogenetic lineage according to BI and ML analyses supported by high posterior probability and bootstrap values (Fig. 5). As the resulting trees from the ML and BI method provided closely matching topologies, only the ML tree is presented in Fig. 5 with the bootstrap values for node support along with the Bayesian posterior probabilities (Chakraborty *et al.* 2018, Chakraborty *et al.* 2019). The expanded version of the phylogenetic tree can be viewed in Supplementary Figure S1.

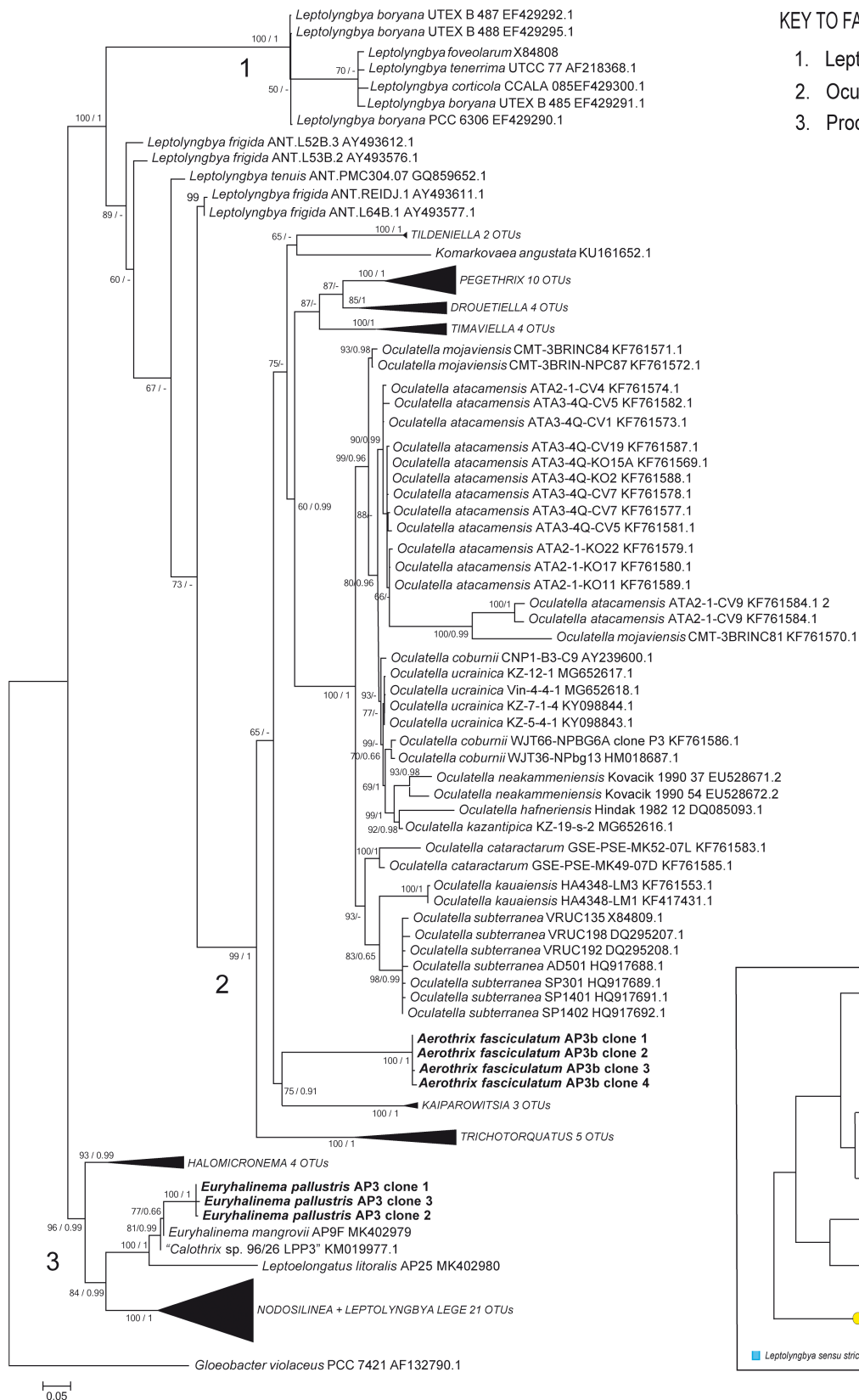
The analysis of p-distance for establishing an inter-species relationship between AP3 and *Euryhalinema mangrovii* AP9F showed 98.3% similarity for 16S rRNA data (Table 4) and a dissimilarity of their ITS regions about 10.6% among both the strains (Table 5). The p-distance analysis for the sequences compared for AP3b revealed that the similarity (as percentage) varied in the range 89% to 93% similarity (Table 6) among the members of family Oculatellaceae including strain AP3b while the dissimilarity percentage for their ITS sequences displayed a range from 15.9% to 30.7% (Table 7). The various conserved helices of 16S rRNA were identified and folded for both the strains under investigation. The folded conserved structures for the strains were represented in Supplementary Figure S2. The aligned sequences of the conserved helices of 16S rRNA were also displayed as Supplementary Table S3.

TABLE 4. Similarity (as percentage) of strain AP3 along with *Euryhalinema mangrovii* AP9F based on p-distance analysis of 16S rRNA gene sequence data. Isolate studied in this investigation indicated in bold font.

	1	2	3
1 <i>Euryhalinema pallustris</i> AP3 clone 1			
2 <i>Euryhalinema pallustris</i> AP3 clone 2	99.9		
3 <i>Euryhalinema pallustris</i> AP3 clone 3	100	99.9	
4 <i>Euryhalinema mangrovii</i> AP9F	98.3	98.3	98.3

TABLE 5. Dissimilarity (as percentage) of strain AP3 and *Euryhalinema mangrovii* based on p-distance analysis of 16S-23S ITS gene sequence data. Isolate investigated in this manuscript indicated in bold font. Only the operon with both tRNA genes were considered for each strain under comparison.

	1	2	3
1 <i>Euryhalinema pallustris</i> AP3 clone 1			
2 <i>Euryhalinema pallustris</i> AP3 clone 2	0.00		
3 <i>Euryhalinema pallustris</i> AP3 clone 3	0.20	0.20	
4 <i>Euryhalinema mangrovii</i> AP9F	10.6	10.6	10.8



KEY TO FAMILY-LEVEL CLADES

1. Leptolyngbyaceae
2. Oculatellaceae
3. Prochlorotrichaceae

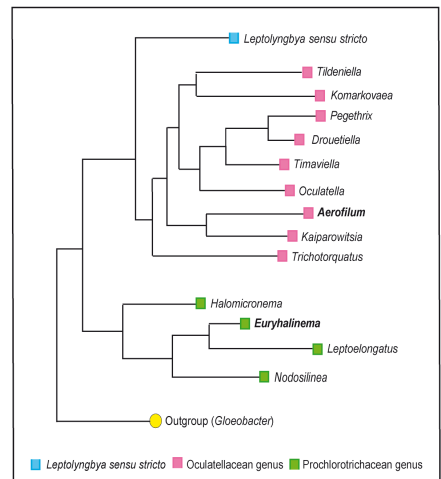


FIGURE 5. Phylogenetic tree based on 16S rRNA gene sequences of total 115 OTUs belonging to 3 families of Synechococcalean order and *Gloeobacter violaceus* as outgroup. Bootstrapping with 1000 resamplings was performed. Support values are ML bootstrap/ BI posterior probability. Scores denoted by ‘-’ for any node showed no support in that analysis. The investigated strains with clones (AP3 and AP3b) are shown in bold. Taxon name in quotation mark, e.g. “*Calothrix*” in our opinion represents an incorrectly submitted sequence and requires revision. Collapsed clades can be viewed expanded in Fig. S1. Designation of families according to Mai *et al.* (2018).

TABLE 6. Similarity (as percentage) of strain AP3b and some strains of family Oculatellaceae based on p-distance analysis of 16S rRNA gene sequence data. Isolate studied in this investigation indicated in bold font.

	1	2	3	4	5	6
1 <i>Aerofilum fasciculatum</i> AP3b						
2 <i>Oculatella subterranea</i> VRUC192	92.8					
3 <i>Oculatella atacamensis</i> ATA2-1-CV24	92.9	97.2				
4 <i>Pegethrix convoluta</i> GSE-PSE-MK38-07D	89.0	92.7	92.1			
5 <i>Drouetiella hepatica</i> UHER 2000/2453	89.5	92.9	93.2	93.6		
6 <i>Timaviella radians</i> GSE-TBD6-7R	90.3	93.1	93.1	91.3	92.7	
7 <i>Tildeniella torsiva</i> Lubos34 UHER 1998/13d	92.5	92.7	93.1	91.4	92.1	93.6

TABLE 7. Dissimilarity (as percentage) of strain AP3b and some strains of family Oculatellaceae based on p-distance analysis of 16S-23S ITS gene sequence data. Isolate studied in this investigation indicated in bold font. Only the operon with both tRNA genes were considered for each strain under comparison.

	1	2	3	4	5
1 <i>Aerofilum fasciculatum</i> AP3b					
2 <i>Oculatella atacamensis</i> ATA2-1-CV24	15.9				
3 <i>Pegethrix convoluta</i> GSE-PSE-MK38-07D	22.1	18.4			
4 <i>Drouetiella hepatica</i> UHER 2000/2453	24.2	18.2	19.9		
5 <i>Timaviella radians</i> GSE-TBD6-7R	30.7	22.0	21.2	20.6	
6 <i>Tildeniella torsiva</i> Lubos34 UHER 1998/13d	23.4	17.9	21.8	22.8	23.8

3.4 Analysis of 16S-23S ITS secondary structures The 16S-23S ITS sequence of strain AP3 (475 bp) showed 87.92% similarity with its closest species, *Euryhalinema mangrovii* while the sequence of the strain AP3b (562 bp) showed 83.91% similarity with the nearest relative *Oculatella atacamensis* (KF761575). The complete ITS region of the strains under investigation (AP3 and AP3b) consisting of distinct variable and conserved domains were compared with their respective reference strains to find out the molecular unlikeliness as well as resemblances. This comparison is presented in Table 8. Additionally, the structures of D1-D1' helix, Box-B helix, V2 helix and the V3 region were folded and characterized for the strain AP3b and D1-D1' helix, Box-B helix and V2 helix for AP3. The examined strains possessed two definite operons, one having both the genes for tRNA^{ile} and tRNA^{ala} while the other operon lacked both the genes.

TABLE 8. Comparison of the nucleotide lengths of the ITS regions of *Euryhalinema pallustris* AP3 with *Euryhalinema mangrovii* and *Aerofilum fasciculatum* AP3b with other related genera of family Oculatellaceae. Only operons containing both tRNA genes are reported in this table for each strain. Data of reference strains *Euryhalinema mangrovii* and Oculatellacean genera were obtained from Chakraborty *et al.* (2019), Osorio-Santos *et al.* (2014) and Mai *et al.* (2018).

Strain ID	Leader	D1-D1' helix	Spacer + D2 + spacer	D3 + spacer	tRNA ^{ile} gene	V2 spacer	tRNA ^{ala} gene	Pre-Box B spacer	Box B	Post Box B spacer	Box A	D4	V3	D5
<i>Euryhalinema pallustris</i> AP3	8	63	39	9	74	15	73	37	32	24	11	11	24	18
<i>Euryhalinema mangrovii</i> AP9F	8	63	36	12	74	7	73	34	32	19	11	7	20	16
<i>Aerofilum fasciculatum</i> AP3b	7	73	41	13	74	12	73	56	38	15	11	22	49	17
<i>Oculatella atacamensis</i> ATA2-1-CV24	7	62	37	11	74	8	73	33	33	15	11	23	52	14
<i>Pegethrix convoluta</i> GSE-PSE-MK38-07D	7	91	12	33	74	14	73	64	36	19	11	16	110	23
<i>Drouetiella hepatica</i> UHER 2000/2452	7	64	35	12	74	42	73	39	34	19	11	14	52	51
<i>Timaviella radians</i> GSE-TBD6-7R	8	81	42	22	74	14	73	41	33	18	11	14	59	34
<i>Tildeniella torsiva</i> UHER 1998/13D	7	66	33	14	74	11	73	35	49	18	11	15	92	16

The conserved basal sequences of strain AP3 were identified as carried out for *Euryhalinema mangrovii* (Chakraborty *et al.* 2019). The D1-D1' helix of strain AP3 (65 nt) was characterized by the presence of one short terminal loop (5 nt) followed by a large single bilateral bulge and two small bilateral loops. A unilateral bulge (7 nt) near the basal stem region was present which was a conserved structure of the D1-D1' helix in most of the Synechococcalean members; however, the sequences varied from species to species. On the contrary, the D1-D1' helix of the reference strain

Euryhalinema mangrovii consisted of 63 nucleotides and the structure depicted the overall pattern to be similar to the D1-D1' helix of AP3 but there existed variations in sequences due to substitution of nucleotides (Fig. 6). On the other hand, the complete structure of Box B helix for both AP3 and *Euryhalinema mangrovii* AP9F were almost similar with a length of 32 nt consisting of a terminal loop (6 nt) and a single nucleotide bulge near stem region. Nucleotide substitution occurred in strain AP3 in two consecutive bases in the terminal loop and a non-canonical base pairing 5'-G::U-3' substituted a canonical base pairing 5'-A::U-3'. The secondary structure of the V2 helix in case of strain AP3 contained 15 nucleotides with a 5 nt terminal loop and a basal stem. This structure differed from the V2 region of *Euryhalinema mangrovii* having a very small helix of length 7 nt.

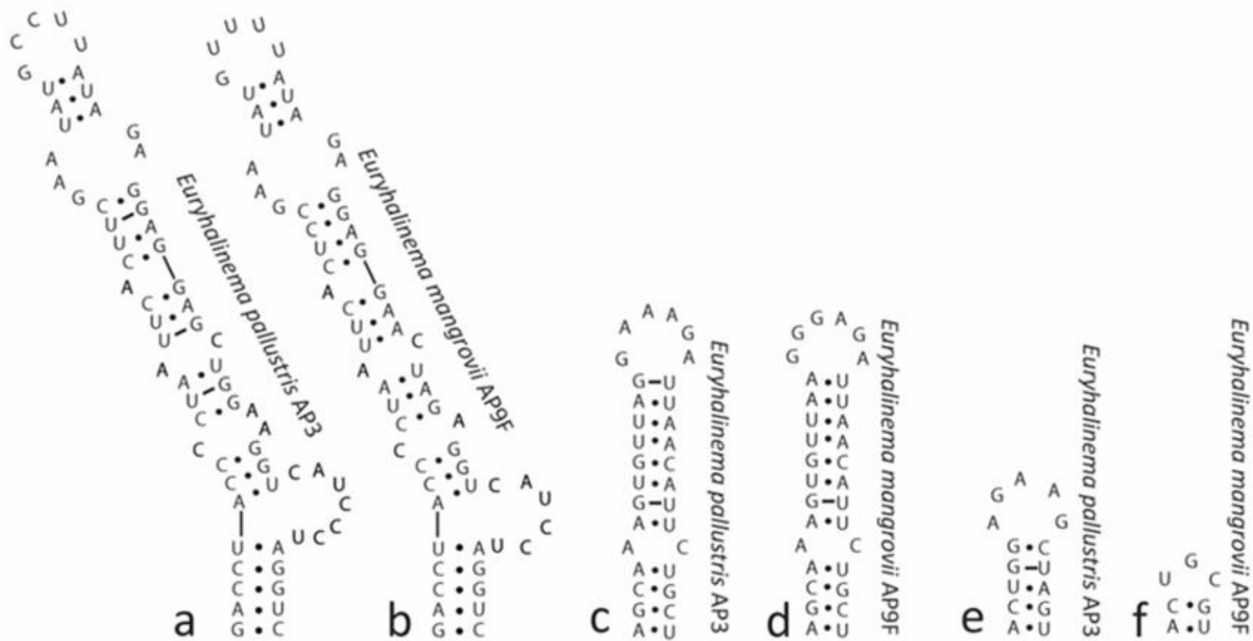


FIGURE 6. Comparative analysis of D1-D1' helix, Box-B and V2 helix of 16S-23S ITS region of test strain AP3 (*Euryhalinema pallustris*) and reference strain *Euryhalinema mangrovii*. **a-b.** D1-D1' helix. **c-d.** Box-B helix. **e-f.** V2 helix

Analysis of the ITS folded secondary structures of strain AP3b in comparison to other strains of family Oculatellaceae revealed that strain AP3b contained unique genus-specific features in the ITS structures. The D1-D1' helix for strain AP3b was 73 nt long, constituting of a small terminal loop (5 nt) followed by a large bilateral bulge and a small, 2 nt bulge in the middle of the helix. A unilateral bulge near the basal stem existed which possessed a unique sequence of nucleotides which differed from the other genera under comparison (Fig. 7). All the strains possessed the same basal sequence 5'GACC::CUGG3' in the D1-D1' helix. Box-B helix domain of the ITS secondary structure of strain AP3b was 38 nucleotides long, with two small sized bilateral bulges and a terminal loop (5 nt) while the corresponding Box-B structure for other genera under comparison varied in length and differed in the structural features (Fig. 7). The comparison of V2 and V3 helices of AP3b along with other Oculatellacean members (Fig. 8) displayed many variations among them. V2 helix and V3 helix of strain AP3b were 12 nt and 49 nt long respectively. V2 helix possessed a terminal loop (4 nt) and a small basal stem. V3 helix of AP3b showed a terminal loop (4 nt), two large bilateral bulges in the middle of the helix and a small, 2 nt unilateral bulge in the lower portion of the helix. Fig. 8 depicts an overall comparison of V2 and V3 helices of AP3b with other Oculatellacean members disclosing that these helices varied in length as well as sequence when compared among each other.

Discussion

This article describes the study and taxonomic characterization of two cyanobacterial strains using the polyphasic approach to taxonomy. This study is a sequel to the investigation of Pramanik *et al.* (2011) who isolated eight cyanobacterial strains from the Sagar and Lothian islands of Indian Sundarbans and primarily assigned them to the LPP (*Lyngbya-Phormidium-Plectonema*) Group B and Oscillatoriales groups. Further analysis on four of the eight

cyanobacteria performed by Chakraborty *et al.* (2018) and Chakraborty *et al.* (2019) following the polyphasic approach to taxonomic analyses established *Oxynema aestuarii* *sp. nov.* (Microcoleaceae) as a novel species and *Euryhalinema mangrovii* *gen. nov., sp. nov.* as well as *Leptoelongatus litoralis* *gen. nov., sp. nov.* (Leptolyngbyaceae) as novel genera. These two novel genera were described by Chakraborty *et al.* (2019) under the family Leptolyngbyaceae by following Komarek *et al.* (2014) although Becerra-Absalon *et al.* (2018) defined the same family clade as Prochlorotrichaceae. Two other strains (namely AP3 and AP3b) from the collection of Pramanik *et al.* (2011) were compared with close members of the *Euryhalinema* and Oculatellacean genera on the basis of the polyphasic approach to taxonomic analyses incorporating molecular phylogenetic relationships. Many phenotypic features overlapped between the investigated strains and the reference strains due to their simple morphology. However, molecular phylogenetic analyses along with ecological considerations and some distinct cellular features (presence of aerotopes, fascicular growth pattern in case of AP3b) advocated that the strains AP3 and AP3b should be designated as novel species and genus respectively. The discussion of this work has been suitably divided into two sections, each of which includes the justification of the proposed taxonomic assignment of the two isolates investigated in this study, namely AP3 and AP3b.

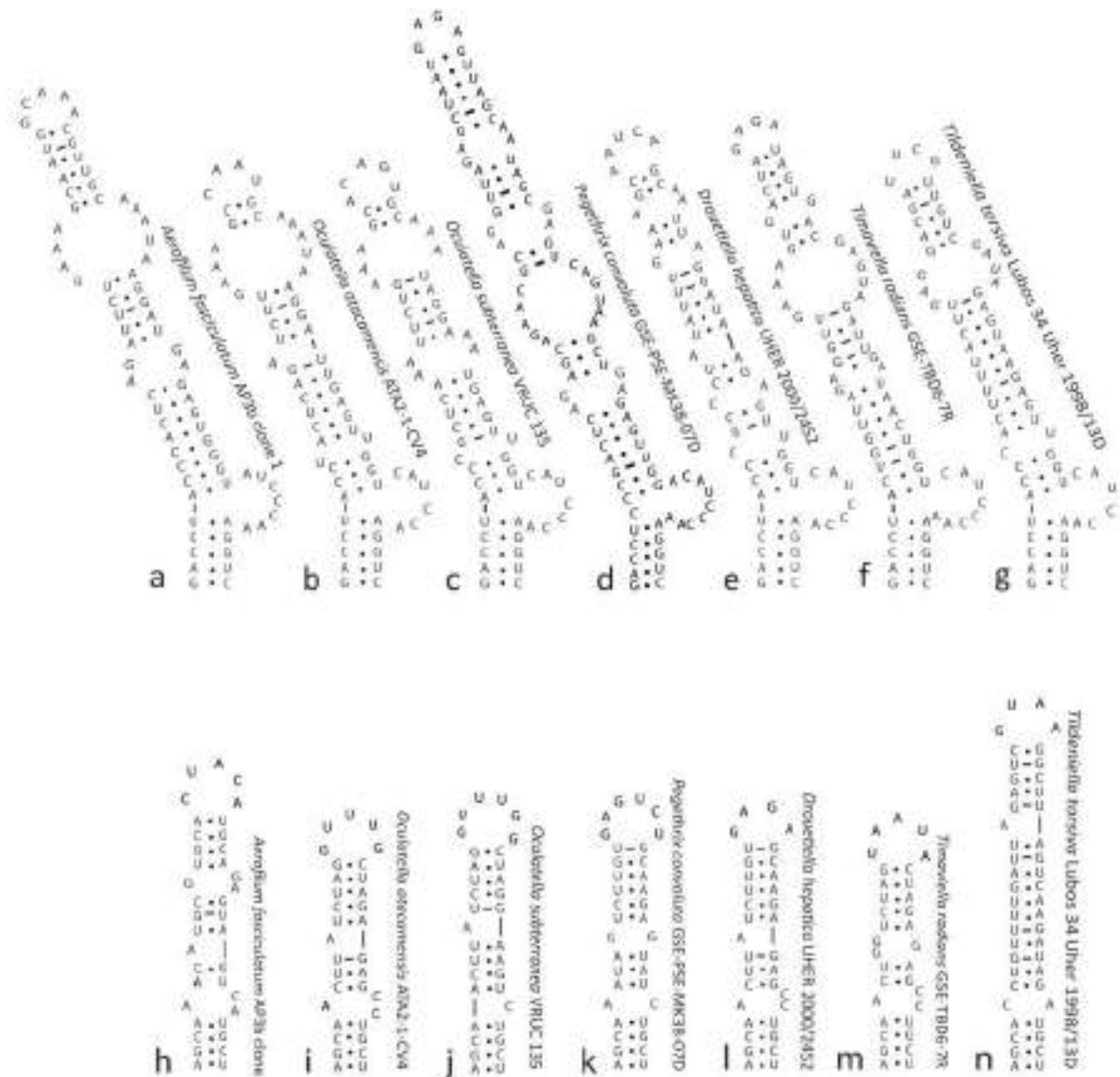


FIGURE 7. Comparative analysis of D1-D1' helix and Box-B helix of 16S-23S ITS region of test strain AP3b (*Aerofilum fasciculatum*) with the genera of Oculatellaceae family. **a-g.** D1-D1' helix. **h-n.** Box-B helix.

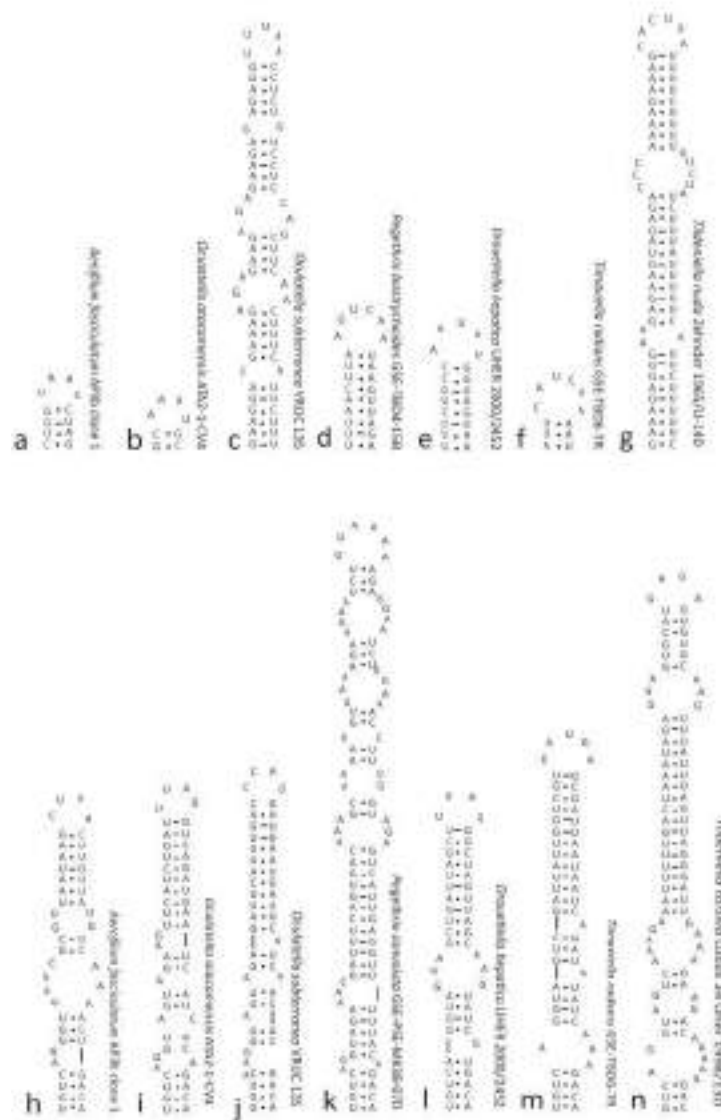


FIGURE 8. Comparative analysis of V2 and V3 helix of 16S-23S ITS region of test strain AP3b (*Aerofilum fasciculatum*) with the genera of Oculatellaceae family. **a-g.** V2 helix. **h-n.** V3 helix.

We provided evidences based on the polyphasic approach to taxonomy to claim that isolate AP3 should be considered as a novel species under the genus *Euryhalinema*. Following the cladistical information provided by Mai *et al.* (2018), the strain AP3 along with its proposed sister species AP9F (Chakraborty *et al.* 2019) fits well in the family Prochlorotrichaceae. This was also supported by the analysis of the conserved helices of 16S rRNA performed in this article (Supplementary Table. S3). Comparison of helix 23 and 27 of AP3 with the sequences for different within Synecococcales also showed affinity of AP3 with Prochlorotrichaceae. This analysis was an important observation for family affiliation (Mai *et al.* 2018). In general, morphological data were corroborative with the phylogenetic studies (Chakraborty *et al.* 2019). The comparison of strain AP3 with its reference strains was primarily focused on the molecular data. The sequence similarity of the 16S rRNA gene sequence was found to be around 98.2% which was comparable to the recommended value to ascertain inter-specific differentiation (Yarza *et al.* 2014). In a recent work reported by Jung *et al.* (2020), delineation of a novel species, *Oculatella crustae-formantes* from *O. ucrainica* was based on 98.8% genetic similarity of 16S rRNA sequence. Similarly, other reports primarily, (Osorio-Santos *et al.* 2014, Vinogradova *et al.* 2017, Mai *et al.* 2018) also followed the same threshold of less than 98.7% genetic similarity set by Yarza *et al.* (2014) for species delineation. Hence, in this present study delineation of two species under a single genus (*Euryhalinema*) was primarily well supported by molecular evidence also combined with morphological

and ecological confirmations. Phylogenetic tree (Fig. 5) also demonstrated well-supported clade to validate strain AP3 as the second and a novel species under the genus *Euryhalinema*. The inclusion of a wrongly named strain “*Calothrix* sp. 96/26 LPP3” into the tree also indicated that it can further be established as a novel species under this clade following the polyphasic approach to taxonomic analysis (Chakraborty *et al.* 2019). Molecular analysis for the delineation of species also involved the study of 16S-23S ITS secondary structures which was considered to be an essential evaluation criterion for the alpha-level taxonomy (Boyer *et al.* 2001, Johansen *et al.* 2011, Chakraborty *et al.* 2018). The output of the folded structures of D1-D1’ region, Box-B helix and V2 helix region revealed that the overall structure of Box-B helix was slightly different in the investigated strain AP3 when compared with *Euryhalinema mangrovii*; however the structure of D1-D1’ and V2 helices differed among the test and reference strains (Fig. 6). The D1-D1’ helix comparison revealed nucleotide substitutions in five different positions in the strain AP3, while the basic conserved motifs remained alike. These motifs were always conserved for the post-transcriptional processing of the ribosomal operon (Johansen *et al.* 2011). The unilateral bulge near the basal stem showed a mutation which resulted in a different sequence in AP3 (5’-CAUCCCU-3’) in comparison to the *Euryhalinema mangrovii* (5’-CAUCCU-3’). The terminal loop also contains a 2-nucleotide substitution as in AP3 (5’-GCC-3’) which differed from the reference (5’-GUU-3’). The stem region also contained minor substitutions which implied the sequential insertion-deletion events articulating the evolutionary changes during speciation (Johansen *et al.* 2011). V2 region of AP3 was significantly longer than the V2 region in *Euryhalinema mangrovii* (Fig.6) with varying terminal loops among them. However, only the structure of Box-B showed differences among their terminal loops with a substitution of 5’-GAA-3’ in AP3 to 5’-GGG-3’ in the reference strain. According to Johansen *et al.* (2011), the conserved and variable regions of the ITS sequences were not flexible like any morphological features. Moreover, due to strong selection pressure the changes of the ITS regions were much more stable and hence reliable for species identity. The separation of a novel species *Leptolyngbya corticola* from another species of the *Leptolyngbya* genus on the basis of the ITS folding patterns was described by Johansen *et al.* (2011). Recent works in the taxonomical revisions of cyanobacteria also included the comparative analysis of dissimilarity (as percentage) of the ITS regions based on the p-distance analysis, especially to establish an inter-species relationship (Erwin and Thacker 2008, Osorio-Santos *et al.* 2014, Pietrasiak *et al.* 2014, Johansen *et al.* 2017, Shalygin *et al.* 2017, Gonzalez-Resendiz *et al.* 2018a,b, Mai *et al.* 2018, Vazquez-Martinez *et al.* 2018) with a threshold value of >7% dissimilarity to be considered as separate species (Gonzalez-Resendiz *et al.* 2019). The dissimilarity (as percentage) of ITS for AP3 and *Euryhalinema mangrovii* was observed to be 10.6% (Table 5) which reflected their status to be two different species under the genus *Euryhalinema*. Gonzalez-Resendiz *et al.* (2019) showed that although the ITS secondary structures among the species do not show significant differences, still the separation of *Desertifilum fontinale* from the other species, *D. tharense*, *D. dzianense* and *D. salkalinema* was reported mainly on the basis of >3% dissimilarity in ITS regions by p-distance analysis.

Morphological features of AP3 like absence of sheath, type of constriction in the cross walls and apical cell morphology were considered as synapomorphies that were in common with the species *Euryhalinema mangrovii* which further corroborated its assignment as a novel species under the same genus (*Euryhalinema*). Only the cell size differed between AP3 and the reference strain which could be attributed to the variation in their habitats. The morphological changes due to long-term culturing was not detectable, and therefore the difference in the cellular length could be considered as a diagnosable feature in this case. This evidence was supported by the findings of Zhou *et al.* (2018), who described two novel genera based on the differences in cellular length which was considered as an autapomorphic feature. Besides the genetic isolation, the ecological origin of both AP3 and *Euryhalinema mangrovii* also suggested that the two isolates must have evolved as two different species under the genus *Euryhalinema* because the two species were collected from two different islands of the Indian *Sundarbans* separated by 24 kms (Fig. 1). Thus, AP3 and *Euryhalinema mangrovii* are two ecotypes isolated geographically.

The second strain investigated in this study was AP3b which was very interestingly proposed to be a new genus under the recently described novel family Oculatellaceae (Mai *et al.* 2018). The affiliation to family Oculatellaceae of the strain AP3b was primarily supported by 100% similarity of helix 23 and 27 with family Oculatellaceae (Supplementary Table S3). This claim is very well supported by various morphological, ultrastructural and molecular data examined in the present work. Strain AP3b was found to be more than 6.2% variable (in terms of genetic variability compared with other genera) based on the 16S rRNA sequence data (Table 6) with the genus *Oculatella atacamensis*, *Tildeniella torsiva* and other Oculatellacean members. All the clones of strain AP3b clustered together and were well separated as a lineage from the *Oculatella* and the *Tildeniella* genus clade. Becerra-Absalon *et al.* (2018) had separated the novel genus *Chroakolemma* sp. from its closest relative *Scytolyngbya timoleontis* placed as the nearest clade in the phylogenetic tree on the basis of more than 5% genetic variability. Additionally, Mai *et al.* (2018) described six new genera containing 14 new species under the novel family Oculatellaceae where genetic variation among the genera

belonging to same families was on average 6.7 – 8.5%. Our strain AP3b also belonged to the clade next to the genus-level clade of *Kaiparowitsia* and *Oculatella*, well-fitted phylogenetically under the family Oculatellaceae along with the other Oculatellalean genera. Based on this evolutionary relationship of the strain AP3b with other genera in the phylogenetic tree, we considered all the genera of the family Oculatellaceae to be satisfactory representatives for inter-generic comparative analysis with our strain AP3b. Mai *et al.* (2018) further explained that the genera under the family Oculatellaceae revealed many autapomorphic specificities based on the study of the secondary structures of the ITS region. The folded secondary structures of ITS region of strain AP3b also disclosed a substantial degree of dissimilarity in comparison to the other members of Oculatellaceae not only in its conformation but also in its sequence length. The lengths of various regions of ITS of strain AP3b compared in Table 8 revealed that the conserved and variable regions of the members of Oculatellaceae possessed high variation where the length of various regions of ITS of each genus was specific. The D1-D1' helix which was considered to be highly conserved differed significantly between strain AP3b and the reference strains. The basal sequence of the helix (5'GACC-GGUC 3') was common to strain AP3b and all other compared genera (Fig. 7) which appeared to be a confirmed feature of the family Oculatellaceae (Mai *et al.* 2018). The unilateral bulge near the basal stem of D1-D1' helix for all of the strains in comparison was found to be varying in 1-2 nucleotides among the genera. Similarly, in case of AP3b, a unique sequence 5'-AUCCCAA-3' was observed (Fig. 7) which was dissimilar compared to any other genera of the Oculatellaceae family. Moreover, only genus *Pegethrix* (Mai *et al.* 2018) possessed very large structure of the D1-D1' helix (91 nt) and the corresponding structure of AP3b was found to be significantly longer than any other genera except *Pegethrix*. The terminal loop also differed in size as well sequence when compared with the references (Fig. 7). Box-B helix of strain AP3b was also noticed to be considerably longer than the Box-B helix of its closest related member genus *Oculatella*. Besides the sequence variation of the terminal loop, AP3b also differed in possessing an extra small bilateral bulge in comparison to the genus *Oculatella* (*O. atacamensis* and *O. subterranea*). Box-B helix length in the genus *Tildeniella* is very long and rest of the genera possesses comparably similar length of Box B. So, in the complete Box-B helix comparison with other genera (Fig. 7), it is clear that the length of the Box-B helix in AP3b is unique, being of intermediate length. During the comparison of V2 and V3 helices among strain AP3b and other genera (Fig. 8), these highly variable helical regions of the ITS showed a genus-specific conformation where the length of both helices (V2 and V3) for each genus were unique. Moreover, as the homology in the sequences of V2 and V3 compared among the genera was very low, the patterns and number of bilateral bulges as well as the sequences of the stem regions showed significant variations. Considering the ITS region to be a genus-specific trait in family Oculatellaceae, the D1-D1' helix, Box-B, V2 and V3 region represented in Fig. 7 and Fig. 8 presented significant divergences from strain *Oculatella atacamensis* as well as other Oculatellacean genera. Alike the present investigation, comparison of ITS secondary structures of *Oculatella subterranea* with the type species of *Leptolyngbya* supported the separation of *Oculatella subterranea* as a monospecific genus from the *Leptolyngbya* genus (Zammit *et al.* 2012). According to Mai *et al.* (2018) Oculatellaceae and Prochlorotrichaceae genera had very divergent characters and distinct autapomorphies which were genus specific. This observation was corroborative with our taxonomic assignment of strain AP3b. There were more than one stable and contrasting features identified in the strain AP3b which can undoubtedly be considered as diacritical markers at the genus level. These features included presence of aerotopes in the cross section of the cell causing buoyancy to float which was substantiated by the unique growth pattern of this strain appearing as a fascicle instead of forming mat-like biofilm. Necridic cells were detected by scanning electron microscopy which were contrastingly absent in the reference strain. The related genus *Oculatella* which was regarded as one of the reference strains for AP3b was characterized by the presence of an orange colored spot in its apical cell which was the most striking and genus-specific feature for genus *Oculatella* (Zammit *et al.* 2018). This feature was completely absent in the strain under investigation (AP3b). Moreover, the cellular features of AP3b like nearly isodiametric shape along with the presence of necridia, aerotopes and distinctly constricted cross walls and the given discontinuity of these features in *Tildeniella* and *Oculatella* were the morphological differences supported by the substantial genetic variability in 16S rRNA sequences. Overall study of strain AP3b demonstrated that this strain consisted of a set of comparable morphological characteristics with respect to the genus-specific characters of the reference genera of Oculatellaceae which was justified by the position of strain AP3b under the family Oculatellaceae. Genus can be defined as a group of one or more species bearing at least some morphological characters which distinguishes them from the species of other genera and must constitute a well-defined monophyletic clade (Mai *et al.* 2018). Although, the simple morphology of strain AP3b was similar to the related genus *Oculatella*, however the studied characters like presence of aerotopes aiding to the fascicular growth pattern, presence of necridia, significant differences in the cell forms (cellular length to width ratio) and absence of any orange-colored spot in the apical cell in any phase of its growth period were substantial and stable features to be considered as autapomorphic characters differentiating a species from another species of different genus. Justifying the definition of

genus (Mai *et al.* 2018), and on the basis of the above-mentioned contrasting morphological features substantiated by the molecular data of unlikelihood with the closest member (sister clade), we propose the novel monospecific genus, *Aerofilum fasciculatum* under the family Oculatellaceae.

Conclusion

In this article AP3 was described as a novel species *Euryhalinema pallustris sp. nov.* (Prochlorotrichaceae) and AP3b as a novel genera *Aerofilum fasciculatum gen. nov., sp. nov.* (Oculatellaceae) based on the polyphasic approach to taxonomy. This work is important as it corroborated the creation of well-supported monophyletic groups in their respective families. This investigation also brings the world's largest tidal mangrove forest, the Sundarbans to the forefront as a repository of novel cyanobacteria. This intertidal region warrants further exploration for the discovery of new cyanophytes because fossil records indicate intertidal regions were locations of cyanobacterial diversification globally (Demoulin *et al.* 2019).

Description

Order: Synechococcales

Family: Oculatellaceae

Aerofilum Chakraborty et Mukherjee, *gen. nov.*

Thallus blue-green, growth like fascicles or bundles. Filaments isopolar, uniseriate, unbranched, cells slightly longer than their width, cell length ranged from 1.4 - 2.1 μm and width 0.9 - 1.1 μm . Cross walls have distinct constrictions.

Type species (designated here): *Aerofilum fasciculatum* Chakraborty et Mukherjee

Etymology: The generic epithet “*Aerofilum*” is derived from *Aero* Greek for ‘air’ as the strain possesses gas vesicles (aerotopes) and *filum* Greek for ‘filament’.

Aerofilum fasciculatum sp. nov. Chakraborty et Mukherjee

Description Thallus blue-green, growth pattern appears like fascicles or bundles rather than forming a mat-like biofilm. Filaments isopolar, uniseriate, unbranched, cells slightly longer than their width, cell length ranged from 1.4 - 2.1 μm and width 0.9 - 1.1 μm . Cross walls have distinct constrictions. Trichomes were cylindrical, immotile, no heterocyte or akinete. Small sized filaments known as hormogonia helps in propagation. Necridic cells present. Ultrastructure includes parietal thylakoids, aerotopes present.

Holotype (designated here): Holotype (AP3b) deposited and cryopreserved in the Microbial Culture Collection (MCC), India having accession number MCC 3478.

Type locality: Lothian island (21.39.1N 88.19.37E) of the Indian Sundarbans, India.

Etymology: The specific epithet ‘*fasciculatum*’ reflects the growth pattern of the strain appearing to grow as a cluster or fascicles instead of forming a mat-like biofilm.

Order: Synechococcales

Family: Prochlorotrichaceae

Genus: *Euryhalinema*

Euryhalinema pallustris Chakraborty & Mukherjee *sp. nov.*

Description Thallus greenish in color, forming a mat-like biofilm. Filaments typically unbranched, straight, isopolar, attached to the soil surface (mainly sub-aerophytic) growing as an extensive mat-like biofilm. Cells of the intermediate trichome were larger in size than the cells towards apex, cells much longer than wide, cellular dimensions 1.1 - 1.6

µm (length) and 0.4 - 0.5 µm (width), mucilaginous sheath absent, cell contents homogeneous, green without any granulated appearance, aerotopes absent. No heterocytes and akinetes. Cell division takes place by asymmetrical binary fission. Reproductive propagation by the help of hormogonia.

Holotype: Holotype (AP3) deposited and cryopreserved in Microbial Culture Collection (MCC), India bearing an accession number MCC3172.

Type locality: Sagar island (21.44.7N 88.7.2E) of the Indian Sundarbans, India.

Etymology: The specific epithet '*pallustris*' represents the swampy habitat of the strain from where it was collected.

Acknowledgements

Authors thank Ministry of Earth Sciences, Government of India for financial assistance through the sub-project "Identification of eight obligately halophilic cyanobacteria of the Sundarbans and molecular characterization of antimicrobial compounds therefrom" (File No. MoES/09- DS/10/2013 PC-IV) of the project "Drugs from Sea" and the Department of Science and Technology, Government of India for financial support through the DST PURSE Phase II project awarded to Jadavpur University.

References

- Becerra-Absalón, I., Johansen, J.R., Muñoz-Martín, M.A. & Montejano, G. (2018) *Chroakolemma* gen. nov. (Leptolyngbyaceae, Cyanobacteria) from soil biocrusts in the semi-desert Central Region of Mexico. *Phytotaxa* 367: 201–218.
<https://doi.org/10.11646/phytotaxa.367.3.1>
- Boyer, S.L., Flechtner, V.R. & Johansen, J.R. (2001) Is the 16S–23S rRNA Internal Transcribed Spacer region a good tool for use in molecular systematics and population genetics? A case study in cyanobacteria. *Molecular Biology and Evolution* 18: 1057–1069.
<https://doi.org/10.1093/oxfordjournals.molbev.a003877>
- Chakraborty, S., Maruthanayagam, V., Achari, A., Mahansaria, R., Pramanik, A., Jaisankar, P. & Mukherjee, J. (2018) *Oxynema aestuarii* sp. nov. (Microcoleaceae) isolated from an Indian mangrove forest. *Phytotaxa* 374: 24–40.
<https://doi.org/10.11646/phytotaxa.374.1.2>
- Chakraborty, S., Maruthanayagam, V., Achari, A., Pramanik, A., Jaisankar, P. & Mukherjee, J. (2019) *Euryhalinema mangrovii* gen. nov., sp. nov. and *Leptoelongatus litoralis* gen. nov., sp. nov. (Leptolyngbyaceae) isolated from an Indian mangrove forest. *Phytotaxa* 422: 58–74.
<https://doi.org/10.11646/phytotaxa.422.1.4>
- Dadheech, P.K., Mahmoud, H., Kotut, K. & Krienitz, L. (2012) *Halolectolyngbya alcalis* gen. et sp. nov., a new filamentous cyanobacterium from the soda lake Nakuru, Kenya. *Hydrobiologia* 691: 269–283.
<https://doi.org/10.1007/s10750-012-1080-6>
- Debnath, M., Singh, T. & Bhadury, P. (2017) New records of Cyanobacterial morphotypes with *Leptolyngbya indica* sp. nov. from terrestrial biofilms of the Lower Gangetic Plain, India. *Phytotaxa* 316: 101–120.
<https://doi.org/10.11646/phytotaxa.316.2.1>
- Demoulin, C.F., Lara, Y.J., Cornet, L., Francois, C., Baurain, D., Wilmette, A. & Javaux, E.J. (2019) Cyanobacteria evolution: Insight from the fossil record. *Free Radical Biology and Medicine* 140: 206–223.
<https://doi.org/10.1016/j.freeradbiomed.2019.05.007>
- Drummond, A.J., Ho, S.Y.W., Phillips, M.J. & Rambaut, A. (2006) Relaxed phylogenetics and dating with confidence. *PLoS Biology* 4: e88.
<https://doi.org/10.1371/journal.pbio.0040088>
- Erwin, P.M. & Thacker, R.W. (2008) Cryptic diversity of the symbiotic cyanobacterium *Synechococcus spongiorum* among sponge host. *Molecular Ecology* 17: 2937–2947.
<https://doi.org/10.1111/j.1365-294X.2008.03808.x>
- Fiore, M.F., Sant'Anna, C.L., Azevedo, M.T.D., Komarek, J., Kastovsky, J., Sulek, J. & Lorenzi, A.S. (2007) The cyanobacterial genus *Brasilonema*, gen. nov., a molecular and phenotypic evaluation. *Journal of Phycology* 43: 789–798.
<https://doi.org/10.1111/j.1529-8817.2007.00376.x>
- Fuchsman, C.A., Collins, R.E., Rocap, G. & Brazelton, W.J. (2017) Effect of the environment on horizontal gene transfer between bacteria

- and archaea. *PeerJ* 5: e3865.
<https://doi.org/10.7717/peerj.3865>
- Gelman, A. & Rubin, D.B. (1992) Inference from iterative simulation using multiple sequences. *Statistical Science* 7: 457–472.
<https://doi.org/10.1214/ss/1177011136>
- Gonzalez-Resendiz, L., Johansen, J.R., Escobar-Sanchez, V., Segal-Kischinevzky, C., Jimenez-Garcia, L.F. & Leon-Tejera, H. (2018a) Two new species of *Phyllonema* (Rivulariaceae, Cyanobacteria) with an emendation of the genus. *Journal of Phycology* 54: 638–652.
<https://doi.org/10.1111/jpy.12769>
- Gonzalez-Resendiz, L., Johansen, J.R., Alba-Lois, L., Segal-Kischinevzky, C., Escobar-Sanchez, V., Jimenez Garcia, L.F., Hauer, T. & Leon-Tejera, H. (2018b) *Nunduva*, a new marine genus of Rivulariaceae (Nostocales, Cyanobacteria) from marine rocky shores. *Fottea* 18: 86–105.
<https://doi.org/10.5507/fot.2017.018>
- Gonzalez-Resendiz, L., Johansen, J.R., Leon-Tejera, H., Sanchez, L., Segal-Kischinevzky, C., Escobar-Sanchez, V. & Morales, M. (2019) A bridge too far in naming species: A total evidence approach does not support recognition of four species in *Desertifilum* (Cyanobacteria). *Journal of Phycology* 55: 898–911.
<https://doi.org/10.1111/jpy.12867>
- Iteman, I., Rippka, R., de Marsac, N.T. & Herdman, M. (2000) Comparison of conserved structural and regulatory domains within divergent 16S rRNA–23S rRNA spacer sequences of cyanobacteria. *Microbiology* 146: 1275–1286.
<https://doi.org/10.1099/00221287-146-6-1275>
- Johansen, J.R., Kovacik, L., Casamatta, D.A., Fučíková, K. & Kaštovský, J. (2011) Utility of 16S-23S ITS sequence and secondary structure for recognition of intrageneric and intergeneric limits within cyanobacterial taxa: *Leptolyngbya corticola* sp. nov. (Pseudanabaenaceae, Cyanobacteria). *Nova Hedwigia* 92: 283–302.
<https://doi.org/10.1127/0029-5035/2011/0092-0283>
- Johansen, J.R., Mares, J., Pietrasiak, N., Bohunicka, M., Zima, J. Jr, Stenclova, L. & Hauer, T. (2017) Highly divergent 16S rRNA sequences in ribosomal operons of *Scytonema hyalinum* (Cyanobacteria). *PLoS ONE* 12: e0186393
<https://doi.org/10.1371/journal.pone.0186393>
- Jung, P., Mikhailiuk, T., Emrich, D., Baumann, K., Dultz, S. & Budel, B. (2020) Shifting boundaries: Ecological and Geographical range extension based on three new species in the cyanobacterial genera *Cyanocohniella*, *Oculatella* and *Aliterella*. *Journal of Phycology* 56 (5): 1216–1231. [Early view]
<https://doi.org/10.1111/jpy.13025>
- Komarek, J. & Anagnostidis, K. (2005) *Cyanoprokaryota. 2. Teil: Oscillatoriales*. In: Büdel, B., Gärdner, G., Krienitz, L. & Schagerl, M. (Eds.) *Süßwasserflora von Mitteleuropa*. Elsevier, München, 759 pp.
- Komarek, J., Kaštovský, J., Ventura, S., Turicchia, S. & Šmarda, J. (2009) The cyanobacterial genus *Phormidesmis*. *Algological Studies* 129: 41–59.
<https://doi.org/10.1127/1864-1318/2009/0129-0041>
- Komarek, J., Kastovsky, J., Mares, J. & Johansen, J.R. (2014) Taxonomic classification of cyanoprokaryotes (cyanobacterial genera) using a polyphasic approach. *Preslia* 86: 295–335.
- Lane, D.J. (1991) 16S/23S rRNA sequencing. In: Stackebrandt, E. & Goodfellow, M. (Eds.) *Nucleic acid techniques in bacterial systematics*. Chichester, United Kingdom: John Wiley and Sons, pp. 115–175.
- Larkin, M.A., Blackshields, G., Brown, N.P., Chenna, R., McGettigan, P.A., McWilliam, H., Valentin, F., Wallace, I.M., Wilm, A., Lopez, R., Thompson, J.D., Gibson, T.J. & Higgins, D.G. (2007) Clustal W and Clustal X version 2.0. *Bioinformatics* 23: 2947–2948.
<https://doi.org/10.1093/bioinformatics/btm404>
- Mai, T., Johansen, J.R., Pietrasiak, N., Bohunicka, M. & Martin, M.P. (2018) Revision of the *Synechococcales* (Cyanobacteria) through recognition of four families including *Oculatellaceae* fam. nov. and *Trichocoleaceae* fam. nov. and six new genera containing 14 species. *Phytotaxa* 365: 1–59.
<https://doi.org/10.11646/phytotaxa.365.1.1>
- Miller, M.A., Pfeiffer, W. & Schwartz, T. (2010) Creating the CIPRES Science Gateway for inference of large phylogenetic trees. *Proceedings of the Gateway Computing Environments Workshop (GCE)* 2010: 1–8.
<https://doi.org/10.1109/GCE.2010.5676129>
- Neogi, S.B., Dey, M., Kabir, S.M.L., Masum, S.J.H., Kopprio, G., Yamasaki, S. & Lara, R. (2016) Sundarban mangroves: diversity, ecosystem services and climate change impacts. *Asian Journal of Medical and Biological Research* 2: 488–507.
<https://doi.org/10.3329/ajmbr.v2i4.30988>
- Nübel, U., Garcia-Pichel, F. & Muyzer, G. (1997) PCR primers to amplify 16S rRNA genes from cyanobacteria. *Applied Environmental Microbiology* 63: 3327–3332.

- Osorio-Santos, K., Pietrasiak, N., Bohunická, M., Miscoe, L.H., Kovacik, L., Martin, M.P. & Johansen, J.R. (2014) Seven new species of *Oculatella* (Pseudanabaenales, Cyanobacteria) *European Journal of Phycology* 49: 450–470.
<https://doi.org/10.1080/09670262.2014.976843>
- Perkerson III, R.B., Johansen, J.R., Kovacik, L., Brand, J., Kastovsky, J. & Casamatta, D.A. (2011) A unique Pseudanabaenalean (cyanobacteria) genus *Nodosilinea* gen. nov. based on morphological and molecular data. *Journal of Phycology* 47: 1397–1412.
<https://doi.org/10.1111/j.1529-8817.2011.01077.x>
- Pietrasiak, N., Muhlsteinova, R., Siegesmund, M.A. & Johansen, J.R. (2014) Phylogenetic placement of *Symplocastrum* (Phormidiaceae) with a new combination *S. californicum* and two new species: *S. flechtnerae* and *S. torsivum*. *Phycologia* 53: 529–541.
<https://doi.org/10.2216/14-029.1>
- Pramanik, A., Sundararaman, M., Das, S., Ghosh, U. & Mukherjee, J. (2011) Isolation and characterization of cyanobacteria possessing antimicrobial activity from the Sundarbans, the world's largest tidal mangrove forest. *Journal of Phycology* 47: 731–743.
<https://doi.org/10.1111/j.1529-8817.2011.01017.x>
- Řeháková, K., Johansen, J.R., Bowen, M.B., Martin, M.P. & Sheil, C.A. (2014) Variation in secondary structure of the 16S rRNA molecule in cyanobacteria with implications for phylogenetic analysis. *Fottea* 14: 161–178.
<https://doi.org/10.5507/fot.2014.013>
- Rippka, R., Deruelles, J., Waterbury, J.B., Herdman, M. & Stanier, R.Y. (1979) Generic assignments, strain histories and properties of pure cultures of cyanobacteria. *Journal of General Microbiology* 111: 1–61.
<https://doi.org/10.1099/00221287-111-1-1>
- Ronquist, F., Teslenko, M., van der Mark, P., Ayres, D., Darling, A., Höhna, S., Larget, B., Liu, L., Suchard, M.A. & Huelsenbeck, J.P. (2012) MrBayes 3.2: efficient Bayesian phylogenetic inference and model choice across a large model space. *Systematic Biology* 61: 539–542.
<https://doi.org/10.1093/sysbio/sys029>
- Shalygin, S., Shalygina, R., Johansen, J.R., Pietrasiak, N., Berrendero Gomez, E., Bohunicka, M., Mares, J. & Sheil, C.A. (2017) *Cyanomargarita* gen. nov. (Nostocales, Cyanobacteria): convergent evolution resulting in a cryptic genus. *Journal of Phycology* 53: 762–777.
<https://doi.org/10.1111/jpy.12542>
- Tamura, K., Stecher, G., Peterson, D., Filipski, A. & Kumar, S. (2013) MEGA 6: Molecular Evolutionary Genetic Analysis Version 6.0. *Molecular Biology and Evolution* 30: 2725–2729.
<https://doi.org/10.1093/molbev/mst197>
- Tooming-Klunderud, A., Sogge, H., Rounge, T.B., Nederbragt, A.J., Lagesen, K., Glockner, G., Hayes, P.K., Rohrlack, T. & Jakobsen, K.J. (2013) From Green to Red: Horizontal Gene Transfer of the Phycoerythrin Gene cluster between *Planktothrix* strains. *Applied and Environmental Microbiology* 79: 6803–6812.
<https://doi.org/10.1128/AEM.01455-13>
- Turicchia, S., Ventura, S., Komárková, J. & Komárek, J. (2009) Taxonomic evaluation of cyanobacterial microflora from alkaline marshes of northern Belize: 2. Diversity of oscillatorialean genera. *Nova Hedwigia* 89: 65–200.
<https://doi.org/10.1127/0029-5035/2009/0089-0165>
- Vazquez-Martinez, J., Gutierrez-Villagomez, J.M., Fonesca-Garcia, C., Ramirez-Chavez, E., Mondragon-Sanchez, M.L., Partida-Martinez, L., Johansen, J.R. & Molina-Torres, J. (2018) *Nodosilinea chupicuarensis* sp. nov. (Leptolyngbyaceae, Synechococcales) a subaerial cyanobacterium isolated from a stone monument in central Mexico. *Phytotaxa* 334: 167–182.
<https://doi.org/10.11646/phytotaxa.334.2.6>
- Vinogradova, O., Mikhailyuk, T., Glaser, K., Holzinger, A. & Karsten, U. (2017) New species of *Oculatella* (Synechococcales, Cyanobacteria) from terrestrial habitats of Ukraine. *Ukrainian Botanical Journal* 74: 509–520.
<https://doi.org/10.15407/ukrbotj74.06.509>
- Yarza, P., Yilmaz, P., Pruesse, E., Glöckner, F.O., Ludwig, W., Schleifer, K.H., Witman, W.B., Euzéby, J., Amann, R. & Rosselló-Móra, R. (2014) Uniting the classification of cultured and uncultured bacteria and archaea using 16S rRNA gene sequences. *Nature Reviews Microbiology* 12: 635–645.
<https://doi.org/10.1038/nrmicro3330>
- Zammit, G. (2018) Systematics and biogeography of sciophilous cyanobacteria; an ecological and molecular description of *Albertania skiophila* (Leptolyngbyaceae) gen. & sp. nov. *Phycologia* 57: 481–491.
<https://doi.org/10.2216/17-125.1>
- Zammit, G., Billi, D. & Albertano, P. (2012) The subaerophytic cyanobacterium *Oculatella subterranea* (Oscillatoriales, Cyanophyceae) gen. et sp. nov.: a cytological and molecular description. *European Journal of Phycology* 47: 341–354.
<https://doi.org/10.1080/09670262.2012.717106>
- Zhou, W., Ding, D., Yang, Q., Ahmad, M., Zhang, Y., Lin, X., Zhang, Y., Ling, J. & Dong, J. (2018) *Marileptolyngbya sina* gen. nov., sp.

nov. and *Salileptolyngbya diazotrophicum gen. nov., sp. nov.* (Synechococcales, Cyanobacteria), species of cyanobacteria isolated from a marine ecosystem. *Phytotaxa* 383: 75–92.

<https://doi.org/10.11646/phytotaxa.383.1.4>

Zuker, M. (2003) Mfold web server for nucleic acid folding and hybridization prediction. *Nucleic Acids Research* 31: 3406–3415.

<https://doi.org/10.1093/nar/gkg595>



Review

Mushroom-derived polysaccharides as antitumor and anticancer agent: A concise review

Md Salman Hyder^a, Sayan Deb Dutta^{b,*},¹^a Department of Botany, Achhruram Memorial College, Jhalda, Purulia, 723202, West Bengal, India^b Mycology and Plant Pathology Research Laboratory, Department of Botany, University of Kalyani, India

ARTICLE INFO

Keywords:

Mushroom
Antimicrobial
Immunomodulatory
 β -glucan
Functional food

ABSTRACT

Nowadays, mushrooms with enhanced medicinal properties are being focused on finding such compounds that could modulate the immune systems of the human body. Mushrooms are extensively known for their antimicrobial, antidiabetic, antiviral, hepatoprotective, antitumor, and immunomodulatory properties owing to the presence of various bioactive components. However, a few of them are characterized and reported so far. Various polysaccharides, including β -glucans, are the principal constituent of the mushroom cell wall and play a significant role in their biological activity. This review aimed to focus on a concise report on the extraction process of the active ingredients from a mushroom with some therapeutic applications. Here, we have briefly described the medicinal properties of some commonly used mushroom extracts or their derivatives. It is interesting to note that mushroom is a potential source of many bioactive products that boost immunity. Thus, the development of functional medicinal food is essential for human welfare.

1. Introduction

Mushrooms are widely cultivated worldwide due to their excellent medicinal properties. The mushrooms can be defined as aerial umbrella-shaped macrofungi, commonly found on the forest floor. However, most of the drugs synthesized nowadays are based on chemical functionalization; some have deleterious effects on living systems. The concept of producing herbal drugs from natural sources is very primitive, authentic, and immensely important. Examples of such herbal drugs derived from natural resources may include digitoxin, morphine, progesterone, vinblastine, vincristine, taxol, etc. Unlike plant products, mushroom-derived bioactive components were also reported with enhanced bioactivity. Mushroom belongs to a large group of macrofungi, commonly known as *Basidiomycetes*, and a few from *Ascomycetes* (Moradali et al., 2007; Ferreira et al., 2010). Various bioactive compounds were extracted from mushrooms as a source of an immunomodulatory agent. *Agaricus* spp. (button mushroom), *Pleurotus* spp. (Oyster mushroom), *Lentinus* spp. (shiitake mushroom) are commonly eaten in Asian countries, such as China, Japan, and India. Most well-known species with potential medicinal properties may include

Ganoderma (Lingzhi), *Lentinus* (shiitake), *Auricularia*, *Flammulina*, *Gri-fola* (Maitake), *Trametes* and *Tremella*, *Pleurotus*, *Agaricus*, *Clitocybe*, *Antrodia*, *Trametes*, *Cordyceps*, *Xerocomus*, *Calvatia*, *Schizophyllum*, *Flammulina*, *Suillus*, *Inonotus*, *Inocybe*, *Funlia*, *Lactarius*, *Albatrellus*, *Russula*, and *Fomes* spp (Acharya et al., 2018). Fig. 1 depicts some of the essential medicinal mushrooms that have been used as antitumor and anticancer agents.

Most of the bioactive components extracted from mushrooms are the product of secondary metabolism. These metabolites are of low molecular weight substances, principally produced in response to extracellular stress (Chaturvedi et al., 2018). It was reported earlier that mushroom-derived polysaccharides could inhibit cancer progression and therefore be recognized as an anticancer or antitumor agent. Cancer is considering the cause of second-most death worldwide after cardiovascular diseases (CVD) (Ayeka, 2018). It is estimated that death caused by cancer will be about thirteen million by 2030 (Ferlay et al., 2008; Torre et al., 2012). Cancer is a result of uncontrolled cell division and mainly spread into surrounding tissues. Such forms of cancer may result in visible growths, known as tumors, such as teratoma, leukemia, and others (Borchers et al., 2004; Zaidman et al., 2005; Ruddon, 2007).

* Corresponding author.

E-mail address: duttasayan@kangwon.ac.kr (S.D. Dutta).¹ Present Address: Department of Biosystems Engineering, College of Agriculture and Life Sciences, Kangwon National University, Chuncheon-24341, Republic of Korea.



Fig. 1. Some of the well-known mushrooms with enhanced anticancer and antitumor properties.

Several factors, including genetic, biophysical, and biochemical processes, may induce cancer progression and metastasis. The conventional treatment strategies for cancer include the application of various chemotherapeutic drugs. However, the available procedures negatively affect patients' health; therefore, an alternative way to treat the disease is of great concern.

According to some pharmacological studies polysaccharides has found as a primary bioactive compound of mushroom (Zhang et al., 2007). Polysaccharides are bio-macromolecules forms by monosaccharide units linked together with glycosidic bonds, which may sometimes give a more complex structure (Daba and Ezeronye, 2003). The monosaccharide composition, their sugar sequence, linkage pattern, length, and nature of side-chain determine the polysaccharide structures (Tang et al., 2020a). Due to its high potential of structural variability, polysaccharides can carry the highest biological information (Wasser, 2002). The most known polysaccharides of mushrooms belong to the 1, 3- β -glucans family (Chaturvedi et al., 2018). The beta-glucan polymers often form a chain with β -(1 \rightarrow 3) linkages with some occasional β -(1 \rightarrow 6) linkages. Isolated naturally occurring polysaccharides of mushrooms are both neutral and acidic (Zhang et al., 2007). Some polysaccharides consist of simple chains linked by glycosidic bonds, while in more complicated forms, it binds with protein and peptide ones.

Besides the primary structure, a more complex chain structure also has important antitumor properties (Wasser, 2002). Although there is a predominantly occurrence of glucan that has been found, heteroglucan has also discovered. Glucans consist exclusively of D-glucose subunits, whereas heteroglucans consist of the side chain of monosaccharides (Zhang et al., 2007). Some most essential polysaccharides used in the field of medicine are lentinan extracted from *Lentinan edodes*, krestin from fruiting bodies of *T. Versicolor*, Schizophyllan from *S. Commune*, PSP from *Tricholoma loboyense*, polysaccharides from the fruiting body of *H. Erinaceus*, and Pleuran from *P. Ostreatus* (Zhu et al., 2015). In comparison to the total content of β -glucan highest percentage of 1, 3- β -D-glucan and 1, 6- β -D-glucan detected as follows: *G. cyanescens* (54%), *S. granulatus* (49.8%), *A. auricula-judae* (47.9%), and *S. Variegates* (40.6%). A human cannot digest the most common polysaccharides from mushrooms, such as glycan, due to its beta bond, which cannot be broken down inside the body. Nevertheless, these molecules potentially trigger the immune system to be absorbed by the gastrointestinal tract. The antitumor activity of these polysaccharides is due to their potential to stimulate immune responses via macrophage or lymphocyte. β -glucan raised the secretion of various pro-inflammatory and anti-inflammatory cytokines, NK cells, T cells, macrophages, which interact with the tumor

cells. Therefore, this review briefly discusses some commonly used mushroom-derived polysaccharides and their anticancer/antitumor properties. Moreover, a detail of extraction, purification, and potential application is also well-described in this article.

2. Bioactive polysaccharides from mushrooms

Various bioactive polysaccharides isolated from mushrooms are shown in Fig. 2. Glucan is the principal constituent of mushroom polysaccharides. Two glucose monomers bind together by the α - or β -glycosidic bond in C1–C3, C1–C4, or C1–C6 manner to produce glucan chain (Pandya et al., 2018). Heteroglycans may also produce by binding arabinose, fructose, mannose, xylose, etc. Polysaccharides sometimes bind with protein or peptide and form complexes (Cui and Chisti, 2003). Most of the essential polysaccharides are products of the C1–C3 bonding of glucans. 1–6 β -D glucans. Other polysaccharides, such as lentinan isolated from *Lentinus edodes*, krestin or (polysaccharide K, PSK) derived from *T. versicolor*, polysaccharide-protein complex (PSPC) from *Tricholoma loboyense*, Pleuran from *P. ostreatus*, also polysaccharides from fruiting bodies and mycelium of *H. Erinaceus* (Zhu et al., 2015). Lentinan derived from *L. edodes* is (1 \rightarrow 3)- β -glucan containing five (1 \rightarrow 3)- β -glucose residues arranged in linear linkage along with two (1 \rightarrow 6)- β -glucopyranoside branches inside chains gives its structure (Pandya et al., 2018). Lentinan is chiefly composed of beta-glucan, which shows potential antitumor activity. The molecular weight of lentinan is about 400–800 kDa. Lentinan shows antitumor properties by enhancing cytokine secretion. Schizophyllan, another important mushroom-derived polysaccharide is having (1 \rightarrow 3)- β -glucan. It contains a β -glucopyranosyl group joined by a β -(1 \rightarrow 6) linkage to every third or fourth residue of the main chain. The molecular weight of Schizophyllan is about 450 kDa (Zhang et al., 2014). The polysaccharide krestin derived from *T. versicolor* (Zhu et al., 2015) has a molecular weight of 94 kDa and is a beta-glucan-protein complex. It contains acidic amino acids like aspartate, glutamate, essential amino acids like lysine arginine, and neutral amino acids like valine and leucine. For every fourth glucose unit, there are (1 \rightarrow 6)- β -glucopyranosidic side chains in (1 \rightarrow 4)- β -glucan (Maehara et al., 2012). Maitake D-fraction obtain from *Grifola frondosa* contains β -D-glucan with β -(1 \rightarrow 6) leading chains with β -(1 \rightarrow 4) branches, it also contains more β -(1 \rightarrow 3) leading chains and β -(1 \rightarrow 6) branches (Matsui et al., 2001a,b).

Usually, polysaccharides remain embedded with proteins forming polysaccharides protein complex, also known as PSPC. For example, *T. loboyense* consists of 54.3% polysaccharides and 35.9 % proteins. These polysaccharides are composed of galactose, glucose, arabinose, xylose, rhamnose, fucose, and mannose with corresponding proteins, such as aspartic acid, glutamic acid, serine, glycine, lysine, and threonine (Liu et al., 1995). The molecular weight is 154 kDa. GLPP was obtained from *Ganoderma lucidum*, which is reported as a polysaccharide-peptide. Ganderon that contains D-rhamnose, D-xylose, D-fructose, D-galactose, and D-glucose. GLPP stimulates interferon- γ (IFN- γ) and interferon-inducible protein-10 (IP-10). Ganoderon is another important polysaccharide derived from *G. lucidum*, having a molecular weight of 20 kDa. Similarly, *G. applanatum* contains several kinds of glucans with an average molecular weight of 300–1000 kDa (Xu et al., 2011). *G. tsugae* contains seven potential antitumor polysaccharides–protein complexes, out of which 2 are glucogalactans with similar protein content to mannose or fucose, and 5 are protein-containing (1 \rightarrow 3)- β -glucan (Pandya et al., 2018).

3. Extraction and purification of polysaccharides

The extraction of polysaccharides is a crucial step for obtaining bioactive material with good quality and amount (Chen et al., 2018). There are several specialized methods for the extraction of polysaccharides (Pan et al., 2013) The selection method and purification procedure depend on the cell wall type (Mizuno, 1996). Hot water

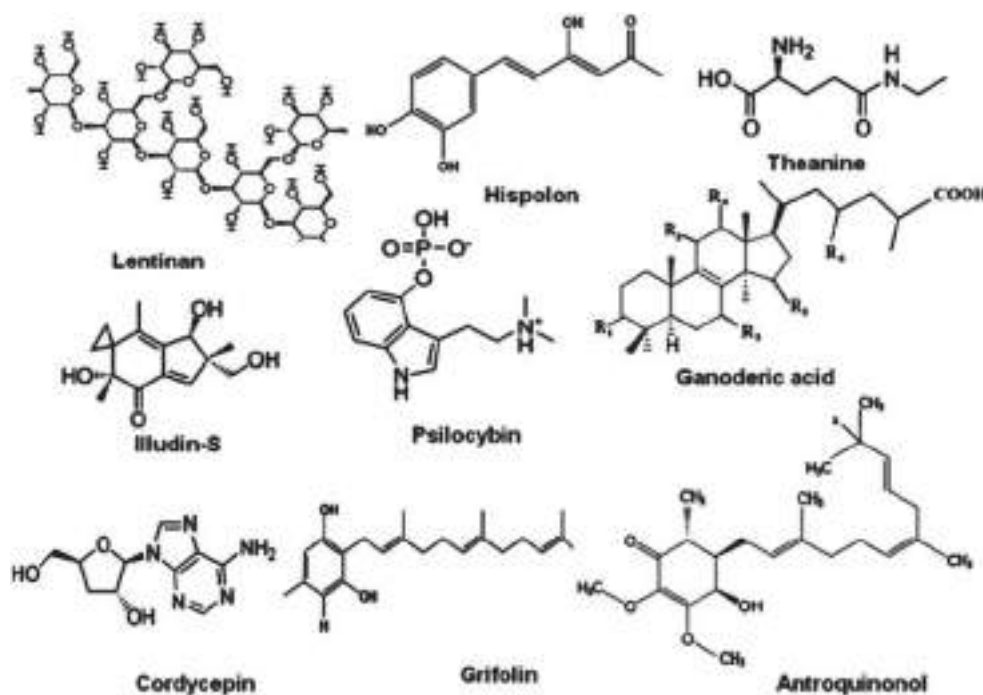


Fig. 2. Examples of some mushroom derived active components.

extraction is a very popular, easy, and standard process for extraction. According to Yan et al. (2018), fruiting bodies are mixed with 95% ethanol (w/v, 1:10) to remove fat. The residues were now extracted with distilled water (w/v, 1:20) three times at 100 for 4hrs. Extracts now precipitated using 95% ethanol (4 vol) at 4 for 12h followed by concentrated under vacuum at 60. Now centrifugation at 4000 rpm done for 15min. After collecting the precipitate, it is re-dissolved in water (Yan et al., 2018). Three successive extractions can also extract polysaccharides with water (100 for 3h), 2% ammonium oxalate (100 for 6h), 5% sodium hydroxide (80 for 6h). The extraction with hot water gives water-soluble polysaccharides, and that of alkali gives water-insoluble ones. The mixture of extracted polysaccharides can be separated with a sequential extraction method (Tang et al., 2020c). Polysaccharides with different properties can be separated by cold and hot water, ammonium oxalate, HCl, Na₂CO₃, NaOH (2M and 4M concentration) sequentially (Colodel et al., 2018). Isolation of isolated pectin and hemicelluloses by cold water, boiling water, 1% ammonium oxalate solution, and 10% sodium hydroxide solution, successively was done by Jackson).

For retaining the acetyl group, DMSO can be used before alkali treatment during the extraction of hemicelluloses. Extraction with the only alkali may remove the acetyl group. Water at room temperature or in boiling state or followed by alkaline solutions can easily extract D-glucans (Ruthes et al., 2015). In some studies, the optimum condition for alkaline extraction was found using NaOH (0.5 mol/L) at 60°C for 2 h (Li et al., 2015 ; Jia et al., 2019). Several impurities like pigments, starch, and several small molecules may be associated with extracted polysaccharides. The impurities must be removed. Impurities like small molecules can be removed by dialysis (Du et al., 2018), ethanol precipitation (Ruthes et al., 2015; Smiderle et al., 2006), or ultrafiltration. Starch can be removed by α -amylase through the enzyme hydrolysis method (Chen et al., 2018b; Yi et al., 2019). Chloroform and n-butanol can be used to precipitate the protein molecules from polysaccharides. Although it has been reported that enzyme hydrolysis in mild doses is more effective for removing impurities (Zhang et al., 2014).

Nowadays, some modified and new techniques have arrived for the separation of proteins. Freeze-thaw techniques target the changing of buffer environment to precipitate protein (Xiong et al., 2017). Pigments

can be removed from polysaccharides by various methods like anion-exchange macroporous resin (Cao et al., 2019; Wang et al., 2018a), organic solvents successive rinse and activated carbon adsorption (Chai and Zhao, 2016), hydrogen, using of peroxide (H₂O₂) (Chen et al., 2019; Kasipandi et al., 2019). Polysaccharides now finally fractionate and purified by various methods like gradient ethanol precipitation method (Hu and Goff, 2018), salt gradient fractionate method (Guan et al., 2015), using cetyltrimethylammonium bromide (CTAB) (Phélippé et al., 2019; Lei, 2016), ultrafiltration (Delcroix et al., 2015; Emami et al., 2018; Liu et al., 2018), ion-exchange column chromatography (Henke et al., 2019; Chen et al., 2018c), gel-column chromatography (Chen et al., 2018c; Han, 2018; Ghosh et al., 2019), affinity chromatography (Magdeldin, 2012), etc. Table 1 depicts some of the standard extraction techniques and their potential advantages and disadvantages.

4. Antitumor and anticancer properties

The β -glucans is the main compound which makes mushroom therapeutically important (Baldassanom et al., 2017; Chen et al., 2014). *Trametes robiniophila*, *Murill* spp., *Coriolus versicolor*, *Grifola frondosa*, *Flammulina velutipes*, and many others show potential antitumor, anticancer properties (Ayeka, 2018). Instead of directly arresting cancer cells, polysaccharides enhance the immunomodulatory effect of the host (Xu et al., 2015). In addition to chemotherapy, surgery the effects of beta-glucan can be used in immune-stimulatory and antitumor effects (Twardowski et al., 2015). β -glucan shows a direct inhibition effect on tumor metastasis and prevents oncogenesis, (Neergheen et al., 2020) and by inducing an immune response in the host, it shows its antitumor activity (Table 2) (Pandya et al., 2018a,b,c; Wang et al., 2017a; Hapuarachchi et al., 2017). Mushroom-derived polysaccharides and their protein complexes are significant sources of antitumor and immunomodulatory agents (Sarangi et al., 2006; Hong et al., 2004; Mizuno, 2002). The first report of the use of polysaccharides in anti-cancer and antitumor therapy was reported by Nauts et al., in 1946, and the use of mushroom-derived polysaccharides was reported by Chihara. The first reported mushroom-derived polysaccharide was lentinan, which was effective against both mice and human cancer cells. Fig. 3

Table 1

List of some potential antitumor and anticancer polysaccharides extracted from mushroom (Tang et al. SP 2020).

Source mushroom	Name of the polysaccharides	References
<i>Agaricus subrufescens</i>	glucans	Oshiman et al. (2002)
<i>Armillaria tabescens</i>	α -(1 \rightarrow 6)-D-glucan	Luo et al. (2008)
<i>Auricularia polytricha</i>	(1 \rightarrow 3)-linked- β -D glucopyranosyl	Song and Du (2010)
<i>Cordyceps sinensis</i>	Polysaccharides	Sheng et al. (2011)
<i>Ganoderma lipsiense</i>	exopolysaccharides, glucans	Lee et al. (2007a)
<i>Grifola frondosa</i>	Maitake D-Fraction	Matsui et al. (2001)
<i>Hericium erinaceus</i>	xylan, glucoxytan, β -glucans	Kim et al. (2011)
<i>Lentinula edodes</i>	Lentinan Zhang et al., 2011 β -(1 \rightarrow 3; 1 \rightarrow 6)-glucan Chain of (1 \rightarrow 4), (1 \rightarrow 3) glucanose residues with side chains of (1 \rightarrow 4) glucanose	Zhang et al. (2011) Yu et al. (2010)
<i>Lentinus polychrous</i>	Polysaccharides	Thetsrimuang et al. (2011)
<i>Lentinus strigellus</i>	Polysaccharides	Lin et al. (2004)
<i>Phellinus igniarius</i>	Endo-polysaccharide	Yang et al. (2009) Chen et al. (2011)
<i>Pleurotus citrinopileatus</i>	PCP-3A (Nonlectin glycoprotein) immunomodulatory protein	Chen et al. (2010a)
<i>Sparassis crispa</i>	β -(1 \rightarrow 3)-D-glucan	Ohno et al. (2003)
<i>Schizophyllum commune</i>	Schizophyllan	Hobbs (2005)
<i>Taiwanofungus camphorates</i>	Polysaccharides	Chen et al. (2010b)
<i>Trametes versicolor</i>	Polysaccharide peptide Protein bound β -(1 \rightarrow 3; 1 \rightarrow 6)-glucan Polysaccharide-Kureha or polysaccharide-K, krestin	Ooi and Liu (2000)
<i>Tremella fuciformis</i>	β -(1 \rightarrow 3)-D-glucans, heteroglycans with α -(1 \rightarrow 3)-mannan backbone & xylose- and glucuronic acid side chain	Bin (2010)
<i>Tremella mesenterica</i>	GXM (glucuronoxylomannan α -(1 \rightarrow 3)-mannan)	Vinogradov et al. (2004) Wu et al., 2018
<i>Inonotus obliquus</i>	α -linked fucoglucomannan	Mizuno et al. (1999)

demonstrates some of the mushroom-derived anticancer polysaccharides and their applications. Udchumpisai and Bangyeekhun show that polysaccharides isolated from *Lentinus velutinus* show cytotoxic effects against cancer cells. The polysaccharides show an effective anticancer property on human HeLa and HepG2 cell lines in a time and concentration-dependent manner. The underlying mechanism of β -glucan in triggering immune response is probably through the

Table 2

Advantages and disadvantages of some common extraction procedures of polysaccharides (Tang et al., 2020a,b,c).

Purification methods	Applicable polysaccharide fractions	Advantages	Disadvantages
Gradient ethanol precipitation	Fractions with large difference on <i>Mw</i> distribution	Simple, inexpensive	Low efficiency, unhomogeneous polysaccharides after purification
Salt fractionation	Fractions with large difference on <i>Mw</i> distribution	Simple, inexpensive	Low efficiency; easy co-precipitation
CTAB method	Fractions embracing neutral and acid polysaccharides	Good selectivity for acid polysaccharide	Low efficiency, requirement of desalting
Ultrafiltration	Fractions with large difference on <i>Mw</i> distribution	Easy scale-up, high efficiency	Low yield, time-consuming
Ion-exchange column chromatography	Fractions bearing different charge strength	High purity of eluate, easy operation	Time-consuming, expensive, sometimes the height of column bed may change when buffer pH changes
Gel column chromatography	Fractions with difference on <i>Mw</i> distribution	Good separation effect, mild condition	Expensive, inefficient, hard for scale-up
Affinity column chromatography	Fractions having matched ligand	High purity, few steps	Difficult to find a proper ligand for a given polysaccharide

activation of complement-component receptor-3 (CR3) that systematically induce the neutrophil or NK cells response. The CR3 is primarily expressed by myeloid cells and NK cells which induce the production of various cytotoxic granules or enzymes (Hong et al., 2004). Recently, it was reported that the β -glucan-mediated antitumor effect is mainly due to the activation of C-type lectin receptor Declin-1 (CLR1), activation of several APCs, and pro-inflammatory macrophages (M1 type), respectively (Alexander et al., 2018) (see Table 3).

Yukawa shows that the polysaccharides extracted from *L. edodes* have a cytotoxic effect on HepG2 cells. In this case, Polysaccharides treated cancer cells detached from the surface and became shrunken and rounded. According to Li et al. (2015), the viability of HeLa and A549 cancer cells was 0%–67.9% when treated with 600 mg/mL of polysaccharide mushrooms extracts for 48h. B. Chen (2010) shows that polysaccharides extracted from *Tremella fuciformis* show a practical inhibitory effect on HepG2 cells, and at 50 mg/mL concentration, it shows 92% antitumor property. The proliferation of CD4⁺ T cells in scald mice infected by *Pseudomonas aeruginosa* can be changed by the polysaccharides extracted from *T. fuciformis*, resulting in a decline in IL-10 level (Shi et al., 2014). Chen et al. (2007) show that the skin pulp of two Bufo species showed potential antitumor property when it was treated with polysaccharides extracts from mushrooms like *Polyporus umbellatus*, *Poria cocos*. Both in vitro and in vivo experiments were performed by Weng and Yen) using *G. lucidum*, which shows anticancer property by modulation of kinase signaling. The apoptotic property of polysaccharide extract of *G. lucidum* on human gastric carcinoma cells was shown by Jang et al. (2010). Ishii et al. (2011) reported that α -(1 \rightarrow 4)-Glucan- β -(1 \rightarrow 6)-glucan protein complex of *A. Subrufescens* shows a potential antitumor property. Water-soluble polysaccharides extracted from king oyster mushrooms were done by Liu et al. (2015a,b). The polysaccharide shows an inhibitory effect on tumor cells and serum cytokine IL-2, TNF- α , thymus and spleen indices, and LPS- or ConA-induced lymphocytes proliferation. The potent antitumor activity in A549 cells of water extracted polysaccharides from *Fomes fomentarius* was shown by Kim et al. (2015). Polysaccharides extracted from the *Pleurotus ostreatus* mycelia component show a significant inhibitory effect on the BGC-823 human gastric cancer cell line in vitro (Cao et al., 2015). In another experiment, a water-soluble extract containing polysaccharide extracted from *P. Ostreatus* inhibits the invasion of Caco-2 cells, that is, the colon cancer cells, through the basement membrane (Cojocar et al., 2013). Polysaccharides polysaccharide POPS-1 from *P. Ostreatus* show potential antitumor activity against HeLa cells (Tong et al., 2009). Moharib et al. (2014) show that clinically induced colon cancer in HCT-116 cells shows anti-proliferative nature after treatment with *Pleurotus Sajor-caju*. Fan et al. (2011) show that crude extract of *Agaricus brasiliensis* has an apoptosis effect on CAL-27 (human oral cancer cell). An investigation on Maitake D-fraction by Alonso et al. (2017) and Alonso et al. (2018) showed the apoptotic effect on

Table 3

An overview of some commonly used mushrooms as immunomodulatory agents with detailed emphasis.

Name of the mushroom	Bioactive compound	Source	Antitumor and anticancer activity	Reference
<i>Agaricus bisporus</i>	α -glucans and β -glucans	fruiting body	Has potent Immunomodulation properties	Kozarski et al. (2011)
<i>Boletus edulis</i>	Heteropolysaccharide with a Heterogeneous main chain	fruiting body	Potent immunomodulatory effect	Wang et al. (2014)
<i>Dictyophora indusiata</i>	Heteroglycan, mannan, glucan from.	fruiting body	Antitumor activity	Liao et al. (2015) Thekkuttuparambill et al., 2007
<i>Pleurotus ostreatus</i>	polysaccharides 2 (POMP2), polysaccharides -1(POPS-1).	mycelium	Anticancer activity	
<i>Cordyceps militaris</i>	β -glucan.		Inhibition of IL-1 β , TNF- α , and COX-2 expression	Smiderle et al. (2014)
<i>Pleurotus tuber-regium</i>	β -D-glucan	Sclerotium, mycelium	anti-breast cancer activity	Zhang et al. (2006)
<i>Inonotus obliquus</i>	Glucan	Fruiting body, mycelium	Antitumor, immunomodulation	Kim et al. (2005)
<i>Pleurotus citrinopileatus</i>	Galactomannan	Fruiting body	Antitumor	Wang et al. (2005)
<i>Phellinus linteus</i>	Glucan	Fruiting body	Antitumor	Kim et al. (2004)
<i>Polyporus umbellatus</i>	Glucan	Mycelium	Antitumor, immunomodulation	Yang et al. (2005)
<i>Agaricus blazei</i>	Fruiting body; Mycelium	Glucan, heteroglycan, glucan protein, glucomannan-protein complex	Antitumor activity	Mizuno (1995)
<i>Agaricus bisporus</i>	Fruiting body	α -glucans and β -glucans.	Immunomodulation and antioxidative activities	Kozarski et al. (2011)
<i>Auricularia auricula-judae</i>	(1 \rightarrow 4)-linked D-glucopyranosyl main chain with (1 \rightarrow 6)-linked D-glucopyranosyl branch at O-6	Fruiting body.	Antitumor activity	Xu et al. (2012)
<i>Boletus edulis</i>	Heteropolysaccharide with a heterogeneous main chain (GlcP, GalP and RhaP)	Fruiting body.	Immunomodulatory activity	Wang et al. (2014)
<i>Calocybe indica</i>	Heteropolysaccharide with a heterogeneous main chain (GalP and GlcP)	Fruiting body	Immunomodulatory and cytotoxic activities	Mandal et al. (2011)
<i>Dictyophora indusiata</i>	Heteroglycan, mannan, glucan	Fruiting body	Antitumor and hyperlipidemia activity	Liao et al. (2015)
<i>Ganoderma applanatum</i>	Glucan	Fruiting body	Antitumor activity	Nakashima et al. (2013)
<i>Ganoderma lucidum</i>	hetero- β -D-glycans (glucurono- β -D-glucan, arabinoxylo- β -D-glucan, xylo- β -D-glucan, manno- β -D-glucan and xylomanno- β -D-glucan)	Fruiting body	Induced cell-cycle arrest and apoptosis	Zhang et al. (2010)
<i>G. frondosa</i>	β -glucan		stimulates differentiation of haematopoietic progenitor cells, production of granulocyte colony-stimulating factor, and the recovery of peripheral blood leukocytes	Wesa et al. (2015)
<i>Coriolus versicolor</i>	glucan	fruiting bodies	novel antitumor	Awadasseid et al. (2017)
<i>Pleurotus pulmonarius</i>	Beta-glucan		Inhibit the leukocyte migration to injured tissues. Mice previously treated with beta-glucan showed a reduction of writhes	
<i>Trametes versicolor</i>	glucan		improved survival and immune function in human randomized, controlled trials in cancer patients	
<i>Coriolus versicolor</i>	polysaccharide K (PSK)		increased the survival of patients after curative gastric cancer resection over chemotherapy alone	Oba et al. (2007)
<i>Amauroderma rude</i>	polysaccharide		inhibited tumour growth in mice via regulation of the immune system at the molecular and cellular levels	Chang et al. (2015)
<i>Hericium erinaceus</i>	Polysaccharide		prevented migration of cancer cells of implanted colon tumors in mice to the lung	Li et al. (2015)
<i>Coriolus versicolor</i>	polysaccharides		Shows anticancer property and shows anti-metastasis effects on mouse mammary 4T1 carcinoma	Zhu et al. (2014)
<i>Phellinus linteus</i>	Hispolon Water-soluble polysaccharide (POPS-1)		Induced apoptosis of breast- and bladder-cancer cell) Exhibited significantly lower cytotoxicity to human embryo kidney 293T cells than HeLa tumour cells compared with anticancer drug 5-fluorouracil	Lu et al. (2009)
<i>Cordyceps taiti</i>	Chlorophorm extract		has potent in vivo antitumor and antimetastatic activities	Liu et al. (2015)
<i>Ganoderma formosanum</i>	PS-F2, a polysaccharide fraction		Worked as stimulant for tumour-specific cellular and humoral immune responses	Wang et al. (2014), Baldassanom et al. (2017)

(continued on next page)

Table 3 (continued)

Name of the mushroom	Bioactive compound	Source	Antitumor and anticancer activity	Reference
<i>Ganoderma lucidum</i>	GP-1 and GP-2 types of polysaccharides		Increased the proliferation and pinocytic activity of macrophage significantly and inhibited effect on the cancer cell	Zhao et al. (2010)
<i>Sarcodon aspratus</i>	Two polysaccharide fractions (PSAN and PSAA)		At a concentration of 400 mg/L and an exposure time of 24 h, the inhibition rates for PSAN and PSAA were 65 and 80%, respectively	Chen et al. (2013)

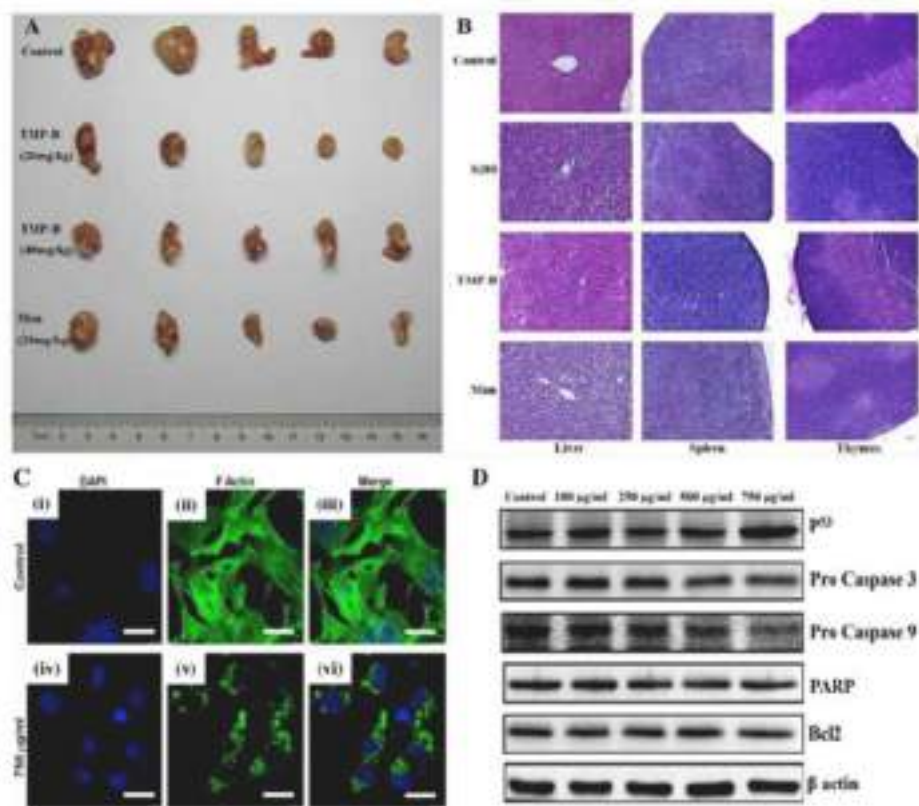


Fig. 3. *In vitro* and *in vivo* antitumor activity of mushroom-derived polysaccharides. (A) Effect of *Tricholoma matsutake*-derived polysaccharides (TMP-B) on relative tumour volume of Kunming male mice after 4 weeks' post-administration. (B) Haematoxylin & Eosin (H&E) staining indicating the tissue sections of liver, spleen, and thymus after administration of TMP-B as compared to the control group (Sanyal and Ghosh, 2019). (C) Confocal laser scanning microscopy (CLSM) images of *HeLa* cells after treatment with *Lenzites betulina* extracts at indicated concentrations resulting in the change of cell morphology (Sanyal and Ghosh, 2019). (D) Western blotting of major apoptosis related proteins expressed in *L. betulina* treated *HeLa* cells (Sanyal and Ghosh 2012).

MDA-MB-231 cells, which in turn effective against breast cancer. Da Silva et al., 2012 showed that the isolated polysaccharide from *Macrocybe titans* showed the anticancer property *in vitro* in murine melanoma cells B16-F10. Migration of cancer cells stopped by the effect of polysaccharides. Polysaccharides extracted from *Collybia radicata* also show potential immunomodulatory effects (Wang et al., 2018). Under both *in vitro* and *in vivo* conditions, the polysaccharide extracted from *Pleurotus pulmonarius* suppresses PI3K/AKT signaling pathway activates Myr-AKT, which shows anti-proliferations in hepatocellular carcinoma (S. Xu et al., 2012). polysaccharide from *Grifola frondosa* when taken orally, the immune system of breast cancer patients stimulated (Fortes et al., 2008). Beta-glucan lentinan increases the survivability of patients with prolonged gastric cancer (Deng et al., 2009). Polysaccharides (GTM1 to GTM6) isolated from *Ganoderma* by Peng et al. exhibited superior antitumor property by increasing activity of NK cells and cytotoxic T-lymphocytes. Polysaccharide extract from mycelium biomass of *Pleurotus ostreatus* shows inhibitory effect on Ehrlich Tumor (ET) and Sarcoma 180 (S180) cells (Pauliuc et al., 2013). Cao et al. demonstrated that *Ganoderma lucidum* polysaccharides-peptide (GLPP) shows an anti-angiogenic effect. The GLPP stimulates interferon- γ , interferon-inducible protein 10, and interleukin-12 level.

5. Mode of action

Previous studies indicate that β -glucans themselves have no significant cytotoxicity in the human body. However, it stimulates monocyte recruitment and acts as an immunomodulant. In addition, β -glucan and ganoderic acid extracted from *G. lucidum* showed direct anticancer effects via activating the host-specific tumor immune responses through activation of pro-inflammatory macrophages (M1 type) and subsequently killing of HepG2 cells. Many mushroom-derived active compounds act through binding with pattern recognition receptors (PRRs) to stimulate immune responses, such as α -glucan, β -glucan, β -fructan, mannan, and chitosan (Jin et al., 2018). Fig. 4 briefly illustrates an overview of the possible mechanism of host-induced tumor immune responses. An ideal immunomodulator with enhanced anticancer property mainly stimulated by complement receptor-3 (CR-3) or macrophage-1, which trigger dectin-1-My-D88 mediated cytokine secretion and targeted killing of cancer cells. Mushroom-derived β -glucan also acts through the CR3 mediated My-D88 pathway. Therefore, mushrooms act as a natural antibody against certain malignant tumors by initiating tumor-specific host immune responses (Jin et al., 2018). Table 4 represents some of the examples of β -glucan that act as adjuvants in anticancer therapy.

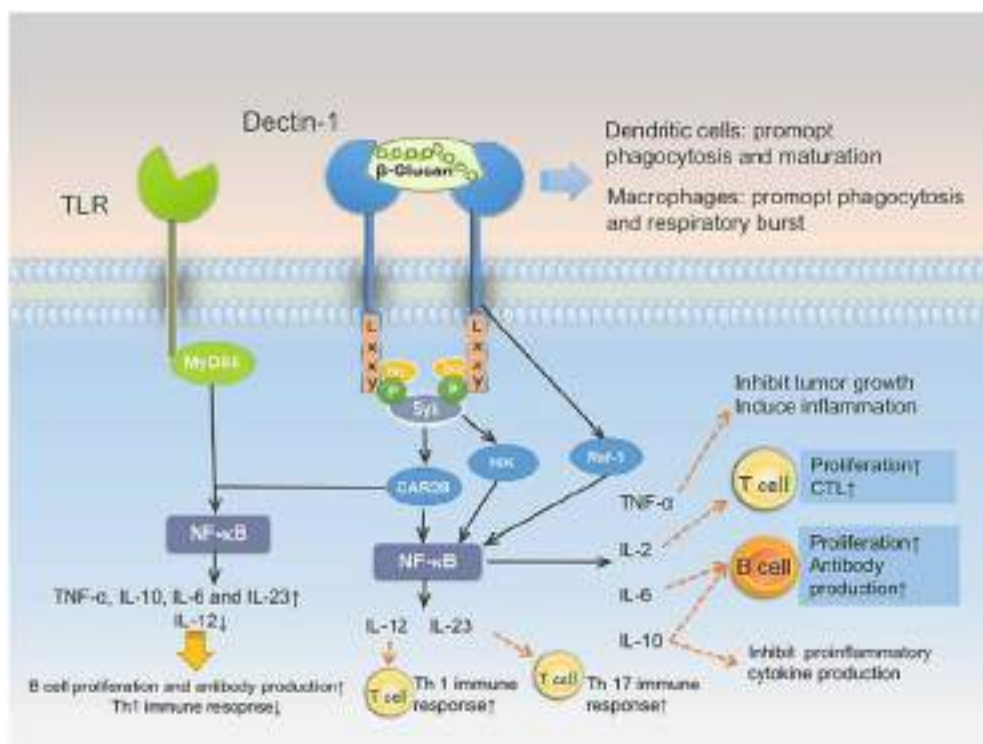


Fig. 4. Signal pathway of β -glucan binding to dectin-1 initiates the activation of various factors during immunomodulation. After binding of β -glucan with dectin-1, it activates spleen associated tyrosine kinase (Syk) which trigger the nuclear factor kappa-beta (NF- κ B) transcription factor through caspase recruitment domain family proteins (CARD9) or mitogen-activated protein kinases (NIK) to produce IL-10, IL-2, IL-23, IL-6, and TNF. The activation of these cytokines induce the proliferation of T and B cells along with DCs. Interestingly, when dectin-1 and MyD88 are activated, a series of other signaling pathways were triggered. As a result of that various cytotoxic factors secreted from the T, B, and DCs, which initiate the host-specific tumor immune responses (Jin et al., 2018).

Table 4
An overview of β -glucan action as adjuvants in anti-cancer therapy (Jin et al., 2018).

Subjects	β -glucan origin	Administration route	mAb/vaccine	Administration route of mAb or vaccine	Tumor cells	Inoculation route of tumor cells	Effects
BALB/c and C57Bl/6 mice	Yeast	Orally	Anti-GD2 mAb or anti-MUC1 mAb	Intravenously	RMA-S-MUC1 cells	Mammary fat pad (subcutaneously)	Tumor regression in all models, tumor-free survival occurred in models of stable expression of target antigen
C57Bl/6 mice	Yeast	Intravenously	Anti-GD2 mAb	Intravenously	RMA-S-MUC1 cells	Mammary fat pad (subcutaneously)	Tumor regression and survival
Several combined immunodeficiency mice	Yeast	Intravenously	Bevacizumab	Intravenously	SKOV-3 cells	Mammary fat pad (subcutaneously)	The therapeutic efficacy mediated by bevacizumab
Human	Yeast	Orally	Bivalent gangliosides vaccine	Subcutaneously	Neuroblastoma	N/A	Antibody responses against GD2 and/or GD3 in 12 of 15 patients; Assessment of minimal residual disease are disappeared in 6 of 15 patients
BALB/c mice	Yeast	Orally	Survivin peptide vaccine	Subcutaneously	A20 cells	Left flank (intradermally)	The number of macrophages, DC and IFN- γ -secreting CD8 ⁺ T cells increased; tumor size decreased
BALB/c mice	Maitake mushroom	Intraperitoneally	DC vaccine	Intraperitoneally (stimulated with β -glucan)	Colon-26 sarcoma cells	N/A	Expression of maturation markers on DC gradually increased; DC ability to induce antigen-specific T cell responses; Antitumor efficacy of DC vaccines enhanced
BALB/c mice	Yeast	Orally	N/A	N/A	Ehrlich ascites tumor cells	N/A	Resistance to tumour-induced immune suppression via enhancing secretion of colony-stimulating factors, IL-1 α , IL-6 and IFN- γ
BALB/c mice	Yeast	Orally	N/A	N/A	Ptas-64 cells	Mammary fat pad (subcutaneously)	Conversion of non-protective Th2 response to protective Th1
C57Bl/6 mice	Yeast	Orally	N/A	N/A	RMA-S-MUC1 cells	N/A	Tumor size decreased

6. Conclusion

Mushrooms have been considered a significant amount of interest from the scientific community due to their high nutritional and medicinal values. It is frequently used as a food supplement that induced the immunity of individuals through their different bio-active components. Notably, the decrease of *M. tuberculosis* bacteria in the presence of mushrooms extract enables a new possibility to treat TB disease in place of commercially available medicines that have some cytotoxic issues. In addition, a significant decrease in cell viability of tumor cells has occurred in the presence of mushroom-derived polysaccharides indicated their antitumor activity. Therefore, mushroom extracts have the potential to use as biomaterials for therapeutic applications.

Declaration of competing interest

The authors declare no competing financial interests.

Acknowledgments:

This work was supported by the funds received from the Department of Botany, Achhruram Memorial College, West Bengal. All the authors read and approved the final draft of the manuscript.

References

- Acharya, K., Ghosh, S., Dutta, A.K., 2018. Pharmacognostic standardization based on physicochemical and molecular parameters of a medicinal mushroom *Schizophyllum commune*. *Orient. Pharm. Exp. Med.* 16 (4), 259–266. <https://doi.org/10.1007/s13596-016-0241-y>.
- Alonso, E.N., et al., 2017. Antitumoral effects of D-fraction from *Grifola frondosa* (maitake) mushroom in breast cancer. *Nutr. Canc.* 69, 29–43. <https://doi.org/10.1080/01635581.2017.1247891>.
- Alexander, M.P., fiering, S.N., Ostroff, G.R., Cramer, R.A., Mullins, 2018. Beta-glucan-induced inflammatory monocytes mediate antitumor efficacy in the murine lung. *Canc. Immunol. Immunother.* 67, 1731–1742. <https://doi.org/10.1007/s00262-018-2234-9>.
- Alonso, E.N., Ferronato, M.J., Fermento, M.E., et al., 2018. Antitumoral and antimetastatic activity of Maitake D-Fraction in triple-negative breast cancer cells. *Oncotarget* 9 (34), 23396–23412. <https://doi.org/10.18632/oncotarget.25174>.
- Awadasseid, A., Hou, J., Gamallat, Y., et al., 2017. Purification, characterization, and antitumor activity of a novel glucan from the fruiting bodies of *Coriolus versicolor*. *PLoS One* 12 (2), e0171270. <https://doi.org/10.1371/journal.pone.0171270>.
- Ayeka, A., 2018. Potential of mushroom compounds as immunomodulators in cancer immunotherapy: a review. *Hindawi Evidence-Based Complementary and Alternative Medicine* 2018. <https://doi.org/10.1155/2018/7271509>. Article ID 7271509, 9 pages.
- Baldassanom, S., Accardi, G., Vasto, S., 2017. Beta-glucans and cancer: the influence of inflammation and gut peptide. *Eur. J. Med. Chem.* 142, 486–492. <https://doi.org/10.1016/j.ejmech.2017.09.013>, 2017.
- Bin, C., 2010. Optimization of extraction of *Tremella fuciformis* polysaccharides and its antioxidant and antitumor activities in vitro. *Carbohydr Polym* 81, 420–424. <https://doi.org/10.1016/j.carbpol.2010.02.039>.
- Borchers, A.T., Keen, C.L., Gershwin, M.E., 2004. Mushrooms, tumors, and immunity: an update. *Exp Biol Med* (Maywood) 229, 393–406. <https://doi.org/10.1177/153537020422900507>.
- Cao, J., Lv, Q., Zhang, B., Chen, H., 2019. Structural characterization and hepatoprotective activities of polysaccharides from the leaves of *Toona sinensis* (A. Juss). *Roem. Carbohydr. Polym.* 212, 89–101. <https://doi.org/10.1016/j.carbpol.2019.02.031>.
- Cao, X.Y., Liu, J.L., Yang, W., Hou, X., Li, Q.J., 2015. Antitumor activity of polysaccharide extracted from *Pleurotus ostreatus* mycelia against gastric cancer in vitro and in vivo. *Mol. Med. Rep.* 12, 2383–2389. <https://doi.org/10.3892/mmr.2015.3648>.
- Chai, Y., Zhao, M., 2016. Purification, characterization and anti-proliferation activities of polysaccharides extracted from *Viscum coloratum* (Kom. Nakai). *Carbohydrate Polymers* 149, 121–130. <https://doi.org/10.1016/j.carbpol.2016.04.090>.
- Chang, J.S., Kuo, H.P., Chang, K.L., Kong, Z.L., 2015. Apoptosis of hepatocellular carcinoma cells induced by nano encapsulated polysaccharides extracted from *Antrodia camphorata*. *PLoS One* 10, e0136782. <https://doi.org/10.1371/journal.pone.0136782>, 2015.
- Chaturvedi, V.K., Agarwal, S., Gupta, K.K., Ramteke, P.W., Singh, M.P., 2018. Medicinal mushroom: boon for therapeutic applications. *Biotech* 8, 334. <https://doi.org/10.1007/s13205-018-1358-0>.
- Chen, B., 2010. Optimization of extraction of *Tremella fuciformis* polysaccharides and its antioxidant and anti-tumor activities in vitro. *Carbohydr. Polym.* 81 (2), 420–424. <https://doi.org/10.1016/j.carbpol.2010.02.039>.
- Chen, G., Chen, K., Zhang, R., Chen, X., Hu, P., Kan, J., 2018. Polysaccharides from bamboo shoots processing by-products: new insight into extraction and characterization. *Food Chem.* 245, 1113–1123. <https://doi.org/10.1016/j.foodchem.2017.11.059>.
- Chen, J.N., Yu, M.C., Tsai, P.F., Wang, Y.T., Wu, J.S., 2010a. In Vitro antitumor and immunomodulatory effects of the protein PCP-3A from mushroom *Pleurotus citrinopileatus*. *J. Agric. Food Chem.* 58, 12117–12122. <https://doi.org/10.1016/j.intjmedmushrooms.2019031857>.
- Chen, L., Pan, J., Li, X., Zhou, Y., Meng, Q., Wang, Q., 2011. Endopolysaccharide of *Phellinus igniarius* exhibited anti-tumor effect through enhancement of cell mediated immunity. *Int Immunopharmacol* 11, 255–259. <https://doi.org/10.1016/j.intimp.2010.11.033>.
- Chen, Q., Li, K., Chen, J., Chen, R., Chen, Z., Zhao, J., Wang, L., Su, X., Zheng, S., Wang, Y., 2007. Pharmaceutical and Health Food Tablets Containing Enzymolysis Products of Bufo and Polyporus and Poria for the Prevention of Radiation Damages. *China patent application CN1994335A*. 2007.07.11.
- Chen, S., Shang, H., Yang, J., Li, R., Wu, H., 2018b. Effects of different extraction techniques on physicochemical properties and activities of polysaccharides from comfrey (*Symphytum officinale*) root. *Ind Crops Prod* 121, 18–25. <https://doi.org/10.1016/j.indcrop.2018.04.063>.
- Chen, S.N., Chang, C.S., Hung, M.H., et al., 2014. The effect of mushroom beta-glucans from solid culture of *Ganoderma lucidum* on inhibition of the primary tumor metastasis. *Evid. Based Complementary Altern.* 2014 <https://doi.org/10.1155/2014/252171>. Article ID 252171, 2014.
- Chen, X., Han, Y., Meng, H., Li, W., Li, Q., Luo, Y., et al., 2019. Characteristics of the emulsion stabilized by polysaccharide conjugates alkali-extracted from green tea residue and its protective effect on catechins. *Ind Crops Prod* 140, 111611. <https://doi.org/10.1016/j.indcrop.2019.111611>.
- Chen, Y., Hu, M., Wang, C., Yang, Y., Chen, J., Ding, J., Guo, W., 2013. Characterization and *in vitro* antitumor activity of polysaccharides from the mycelium of *Sarcodon aspratus*. *Int J Biol Macro* 52, 52–58. <https://doi.org/10.1016/j.jbiomac.2012.09.005>.
- Chen, Y., Jiang, X., Xie, H., Li, X., Shi, L., 2018c. Structural characterization and antitumor activity of a polysaccharide from *Ramulus mori*. *Carbohydr. Polym.* 190, 232–239. <https://doi.org/10.1016/j.carbpol.2018.02.036>.
- Chen, Y.C., Ho, H.O., Su, C.H., Sheu, M.T., 2010b. Anticancer effects of Taiwano fungus camphoratus extracts, isolated compounds and its combinational use. *J. Exp. Clin. Med.* 2 (6), 274–281. <https://doi.org/10.1016/j.jecm.2010.08.003>.
- Cojocaru, S., Radu, M., Bodea, L.G., Cimpeanu, M.M., Gheorghita, G., Stoian, G., Dinischioti, A., 2013. Water soluble *Pleurotus ostreatus* polysaccharide down-regulates the expression of MMP-2 and MMP-9 in caco-2 cells. *Not Bot Horti Agrobo* 41, 553–559. <https://doi.org/10.15835/nbha4129305>.
- Colodel, C., Vriesmann, L.C., Oliveira, D., Petkowicz, C.L., 2018. Cell wall polysaccharides from *Ponkan Mandarin* (*Citrus reticulata* Blanco cv. Ponkan) peel. *Carbohydr. Polym.* 195, 120–127. <https://doi.org/10.1016/j.carbpol.2018.04.066>.
- Cui, J., Chisti, Y., 2003. Polysaccharopeptides of *Coriolus versicolor*: physiological activity, uses, and production. *Biotechnol. Adv.* 21, 109–122. [https://doi.org/10.1016/S0734-9750\(03\)00002-8](https://doi.org/10.1016/S0734-9750(03)00002-8).
- Daba, A.S., Ezeronye, O.U., 2003. Anti-cancer effect of polysaccharides isolated from higher basidiomycetes mushrooms. *Afr. J. Biotechnol.* 2, 672–678. <https://doi.org/10.5897/AJB2003.000-1123>.
- Delcroix, C., Bonnet, J., Etienne, M., Moulin, P., 2015. Influence of ionic strength on membrane selectivity during the ultrafiltration of sulphated pentasaccharides. *Carbohydr. Polym.* 116, 243–248. <https://doi.org/10.1016/j.carbpol.2014.07.013>.
- Deng, G., Lin, H., Seidman, A., Fournier, M., D'Andrea, G., Wesa, K., Yeung, S., Cunningham-Rundles, S., Vickers, A.J., Cassileth, B.A., 2009. Phase I/II trial of a polysaccharide extract from *Grifola frondosa* (Maitake mushroom) in breast cancer patients: immunological effects. *J. Canc. Res. Clin. Oncol.* 135, 1215–1221. <https://doi.org/10.1007/s00432-009-0562-z>.
- Du, J., Li, J., Zhu, J., Huang, C., Bi, S., Song, L., et al., 2018. Structural characterization and immune modulatory activity of a novel polysaccharide from *Ficus carica*. *Food & Function* 9, 3930–3943. <https://doi.org/10.1016/j.cfb.2018.05.024>.
- Emami, P., Motevalian, S.P., Pepin, E., Zydney, A.L., 2018. Impact of module geometry on the ultrafiltration behavior of capsular polysaccharides for vaccines. *J. Membr. Sci.* 561, 19–25. <https://doi.org/10.1016/j.memsci.2018.05.024>.
- Fan, M.J., Lin, Y.C., Shih, H.D., Yan, J.S., Liu, K.C., Yang, S.T., Lin, C.Y., Wu, R.S.C., Yu, C.S., Ko, Y.C., Chung, J.G., 2011. Crude extracts of *Agaricus brasiliensis* induce apoptosis in human oral cancer CAL cells through a mitochondria-dependent pathway. *In Vivo* 25, 355–366. ISSN No. 0258-851X/2011.
- Ferlay, J., Shin, H.R., Bray, F., Forman, D., Mathers, C., Parkin, D.M., 2008. Estimates of worldwide burden of cancer in 2008: GLOBOCAN 2008. *Int. J. Canc.* 127 (12), 2893–2917. <https://doi.org/10.1002/ijc.25516>, 2010.
- Ferreira, I.C.F.R., Vaz, J.A., Vasconcelos, M.H., Martins, A., 2010. Compounds from wild mushrooms with antitumor potential. *Anticancer Agents Med Chem* 10, 424–436. <https://doi.org/10.2174/1871520611009050424>.
- Fortes, R.C., Recóva, V.L., Melo, A.L., Novaes, M.R.C.G., 2008. Effects of dietary supplementation with medicinal fungus in fasting glycemia levels of patients with colorectal cancer: a randomized, double-blind, placebo-controlled clinical study. *Nutr. Hosp.* 23, 591–598. ISSN No. 0212-1611.
- Ghosh, R., Smith, S.A., Nwangwa, E.E., Arivett, B.A., Bryant, D.L., Fuller, M.L., et al., 2019. *Panax quinquefolius* (North American ginseng) cell suspension culture as a source of bioactive polysaccharides: immuno stimulatory activity and characterization of a neutral polysaccharide AGC1. *Int. J. Biol. Macromol.* 139, 221–232. <https://doi.org/10.1016/j.jbiomac.2019.07.215>.

- Guan, Y., Zhang, B., Qi, X., Peng, F., Yao, C., Sun, R., 2015. Fractionation of bamboo hemicelluloses by graded saturated ammonium sulphate. *Carbohydr. Polym.* 129, 201–207. <https://doi.org/10.1016/j.carbpol.2015.04.042>.
- Han, Q., 2018. Critical problems stalling progress in natural bioactive polysaccharide research and development. *J. Agric. Food Chem.* 66, 4581–4583. <https://doi.org/10.1021/acs.jafc.8b00493>.
- Hapuarachchi, K.K., Cheng, C.R., Wen, T.C., et al., 2017. Mycosphere essays 20: therapeutic potential of *Ganoderma* species: insights into its use as traditional medicine. *Mycosphere* 8 (10), 1653–1694. <https://doi.org/10.5943/mycosphere/8/10/5>.
- Henke, S., Hinkova, A., Gillarova, S., 2019. Colour removal from sugar syrups. In: *Applications of Ion Exchange Materials in Biomedical Industries*. Springer Cham, pp. 189–225. https://doi.org/10.1007/978-3-030-06082-4_10.
- Hobbs, C.R., 2005. The chemistry, nutritional value, immune pharmacology, and safety of the traditional food of medicinal split-gill fungus *Schizophyllum commune* Fr.:Fr. (Aphyllorphomycetidae). A literature review. *Int. J. Med. Mushrooms* 7, 127–140. <https://doi.org/10.1615/IntJMedMushr.v7.i12.130>.
- Hong, F., Yan, J., Baran, J.T., et al., 2004. Mechanism by which orally administered β -1,3-glucans enhance the tumoricidal activity of antitumor monoclonal antibodies in murine tumor models. *J. Immunol.* 173 (2), 797–806. <https://doi.org/10.4049/jimmunol.173.2.797>.
- Hu, X., Goff, H.D., 2018. Fractionation of polysaccharides by gradient non-solvent precipitation: a review. *Trends Food Sci. Technol.* 81, 108–115. <https://doi.org/10.1016/j.tifs.2018.09.011>.
- Ishii, P.L., Prado, C.K., Mauro, M.O., Carreira, C.M., Mantovani, M.S., Ribeiro, L.R., Dich, J.B., Oliveira, R.J., 2011. Evaluation of *Agaricus blazei* in vivo for antigenotoxic, anticarcinogenic, phagocytic and immunomodulatory activities. *Regul. Toxicol. Pharmacol.* 59, 412–422. <https://doi.org/10.1016/j.yrtph.2011.01.004>.
- Jang, K.J., Han, M.H., Lee, B.H., Kim, B.W., Kim, C.H., Yoon, H.M., Choi, Y.H., 2010. Induction of apoptosis by ethanol extracts of *Ganoderma lucidum* in human gastric carcinoma cells. *J. Acup Mer* 3, 24–31. [https://doi.org/10.1016/S2005-2901\(10\)60004-0](https://doi.org/10.1016/S2005-2901(10)60004-0).
- Jia, Li, et al., 2019. Alkaline extraction, structural characterization, and bioactivities of (1 → 3)- β -D-Glucan from *Lentinus edodes*. *Molecules* 24 (8), 1610. <https://doi.org/10.3390/molecules24081610>.
- Jin, Y., Li, P., Wang, F., 2018. β -glucan as potential immunoadjuvants: a review on the adjuvency, structure-activity relationship and receptor recognition properties. *Vaccine* 36 (35), 5235–5244. <https://doi.org/10.1016/j.vaccine.2018.07.038>.
- Kasipandi, M., Vrindarani, A.S., Sreeja, P.S., Thamburaj, S., Saikumar, S., Dhivya, S., et al., 2019. Effect of *in vitro* simulated digestion on sugar content and biological activities of *Zehneriamaysorensis* (Wight & Arn.) Arn. Leaf polysaccharides. *J. Food Measur* 13, 1765–1772. <https://doi.org/10.1007/s11694-019-00094-8>.
- Kim, G., Choi, G., Lee, S., Park, Y., 2004. Acidic polysaccharide isolated from *Phellinus linteus* enhances through the up-regulation of nitric oxide and tumor necrosis factor- α from peritoneal macrophages. *J. Ethnopharmacol.* 95, 69e76. <https://doi.org/10.1016/j.jep.2004.06.024>.
- Kim, S.H., Jakhar, R., Kang, S.C., 2015. Apoptotic properties of polysaccharides isolated from fruiting bodies of medicinal mushroom *Fomes fomentarius* in human lung carcinoma cell line. *Soudi J Biol Sci* 22 (4), 484–490. <https://doi.org/10.1016/j.sjbs.2014.11.022>.
- Kim, S.P., Kang, M.Y., Kim, J.H., Nam, S.H., Friedman, M., 2011. Composition and mechanism of antitumor effects of *Hericitum erinaceus* mushroom extracts in tumor-bearing mice. *J. Agric. Food Chem.* 59 (18), 9861–9869. <https://doi.org/10.1021/jf201944n>.
- Kim, Y., Han, L., Lee, H., Ahn, H., Yoon, Y., Jung, J., et al., 2005. Immuno-stimulating effect of the endo-polysaccharide produced by submerged culture of *Inonotus obliquus*. *Life Sci.* 77, 2438e2456. <https://doi.org/10.1016/j.lfs.2005.02.023>.
- Kozarski, M., Klaus, A., Niksic, M., Jakovljevic, D., Jpfg, H., Ljld, V.G., 2011. Antioxidative and immunomodulating activities of polysaccharide extracts of the medicinal mushrooms *Agaricus bisporus*. *Food Chem.* 129 (4), 1667–1675. <https://doi.org/10.1016/j.foodchem.2011.06.029>.
- Lee, W.Y., Park, Y., Ahn, J.K., Ka, K.H., Park, S.Y., 2007. Factors influencing the production of endopolysaccharide and exopolysaccharide from *Ganoderma applanatum*. *Enzym. Microb. Technol.* 40, 249–254. <https://doi.org/10.1016/j.enzmictec.2006.04.009>.
- Lei, S., 2016. Bioactivities, isolation and purification methods of polysaccharides from natural products: a review. *Int. J. Biol. Macromol.* 92, 37–48. <https://doi.org/10.1016/j.ijbiomac.2016.06.100>.
- Li, Y.H., Niu, Y.B., Sun, Y., Zhang, F., Liu, C.X., Fan, L., Mei, Q.B., 2015. Role of phytochemicals in colorectal cancer prevention. *World J. Gastroenterol.* 21, 9262–9272. <https://doi.org/10.3748/wjg.v21.i31.9262>.
- Liao, W., Yu, Z., Lin, Z., Lei, Z., Ning, Z., Regenstein, J.M., Yang, J., Ren, J., 2015. Biofunctionalization of selenium nanoparticle with *Dictyophora indusiata* polysaccharide and its antiproliferative activity through death-receptor and mitochondria-mediated apoptotic pathways. *Sci. Rep.* 5, 18629. <https://doi.org/10.1038/srep18629>.
- Lin, Y., Lai, P., Huang, Y., Xie, H., 2004. Immune-competent polysaccharides from the submerged cultured mycelium of culinary-medicinal mushroom *Lentinus strigellus* Berk. & Curt. (Agaricomycetidae). *Int. J. Med. Mushrooms* 6, 49–55. <https://doi.org/10.1615/IntJMedMushr.v6.i1.50>.
- Liu, F., Ooi, V.E.C., Chang, S.T., 1995. Anti-tumor components of the culture filtrate from *Tricholoma* sp. *World J. Microbiol. Biotechnol.* 11, 486–490. <https://doi.org/10.1007/BF00286357>.
- Liu, J., Zhao, Y., Wu, Q., John, A., Jiang, Y., Yang, J., et al., 2018. Structure characterisation of polysaccharides in vegetable “okra” and evaluation of hypoglycemic activity. *Food Chem.* 242, 211–216. <https://doi.org/10.1016/j.foodchem.2017.09.051>.
- Liu, X., Wang, L., Zhang, C., Wang, H., Zhang, H., Li, Y., 2015a. Structure characterization and anti-tumor activity of a polysaccharide from the alkaline extract of king oyster mushroom. *Carbohydr. Polym.* 15 (118), 101–106. <https://doi.org/10.1016/j.carbpol.2014.10.058>.
- Liu, X., Wang, L., Zhang, C., Wang, H., Zhang, H., Li, Y., 2015b. Structure characterization and anti-tumor activity of a polysaccharides from the alkaline extract of king oyster mushroom. *Carbohydr. Polym.* 118, 101–106.
- Lu, T.L., Huang, G.J., Lu, T.J., Wu, J.B., Wu, C.H., Yang, T.C., Iizuka, A., Chen, Y.F., 2009. Hispolon from *Phellinus linteus* has antiproliferative effects via MDM2-recruited ERK1/2 activity in breast and bladder cancer cells. *Food Chem. Toxicol.* 47. <https://doi.org/10.1016/j.fct.2009.05.023>, 2013–2021.
- Luo, X., Xu, X., Yu, M., Yang, Z., Zheng, L., 2008. Characterisation and immunostimulatory activity of an α -(1→6)-D-glucan from the cultured *Armillaria tabescens* mycelia. *Food Chem.* 111, 357–363. <https://doi.org/10.1016/j.foodchem.2008.03.076>.
- Maehara, Y., Tsujitani, S., Saeki, H., Oki, E., Yoshinaga, K., Emi, Y., Morita, M., Kohnoe, S., Kakeji, Y., Yano, T., Baba, H., 2012. Biological mechanism and clinical effect of protein-bound polysaccharide K (KRESTIN): review of development and future perspectives. *Surg. Today* 42, 8. <https://doi.org/10.1007/s00595-011-0075-7>.
- Magdeldin, S., 2012. *Affinity Chromatography*. INTECH, Croatia, ISBN 978-953-51-0325-7.
- Mandal, E.K., Maity, K., Maity, S., Gantait, S.K., Maiti, S., Maiti, T.K., Sikdar, S.R., Islam, S.S., 2011. Structural characterization of an immune enhancing cytotoxic heteroglycan isolated from an edible mushroom *Calocybe indicava*. *APK2*. *Carbohydr Res.* 346 (14), 2237–2243. <https://doi.org/10.1016/j.carres.2011.07.009>.
- Matsui, K., Kodama, N., Nanba, H., 2001a. Effects of Maitake (*Grifola frondosa*) D-fraction on the carcinoma angiogenesis. *Canc. Lett.* 172, 193–198. [https://doi.org/10.1016/S0304-3835\(01\)00652-8](https://doi.org/10.1016/S0304-3835(01)00652-8).
- Matsui, K., Kodama, N., Nanba, H., 2001b. Effects of Maitake (*Grifola frondosa*) D-fraction on the carcinoma angiogenesis. *Canc. Lett.* 172, 193–198. [https://doi.org/10.1016/S0304-3835\(01\)00652-8](https://doi.org/10.1016/S0304-3835(01)00652-8).
- Mizuno, T., 1995. *Yamabu shitake*: bioactive substances and medicinal utilization. *Food Rev. Int.* 11 (1), 173–178. <https://doi.org/10.1080/87559129509541027>.
- Mizuno, T., 1996. Development of antitumor polysaccharides from mushroom fungi. *Food and Food Ingredient Japanese Journal* 167, 69e87.
- Mizuno, T., 2002. Medicinal properties and clinical effects of culinary-medicinal mushroom *Agaricus blazei* murrill (agaricomycetidae) (review). *Int. J. Med. Mushrooms* 4 (4), 14. <https://doi.org/10.1615/IntJMedMushr.v4.i4.30>.
- Mizuno, T., Zhuang, A.K., Okamoto, H., Kihou, T., Ukai, S., Leclerc, S., Meijer, L., 1999. Antitumor and hypoglycemic activities of polysaccharides from the sclerotia and mycelia of *Inonotus obliquus* (Pers.: Fr.) Pil. (Aphyllorphomycetidae). *Int. J. Med. Mushrooms* 1, 301–316. <https://doi.org/10.1615/IntJMedMushr.v1.i4.20>.
- Moharib, M.A., Maksud, N.A.E., Ragab, H.M., Shehata, M.M., 2014. Anticancer activities of *Sarosia* polysaccharides on chemically induced colorectal cancer in rats. *J. Appl. Pharmaceut. Sci.* 4. <https://doi.org/10.7324/JAPS.2014.4.0710>, 054–063.
- Moradali, M.F., Mostafavi, H., Ghods, S., Hedjaroude, G.A., 2007. Immunomodulating and anticancer agents in the realm of macrofungi (macrofungi). *Int. Immunopharmacol.* 7, 701–724. <https://doi.org/10.1016/j.intimp.2007.01.008>.
- Nakashima, S., Umeda, Y., Kanada, T., 2013. Effect of polysaccharides from *ganoderma applanatum* on immune responses. i. enhancing effect on the induction of delayed hypersensitivity in mice. *Microbiol. Immunol.* 23 (6), 501–513.
- Neergheen, V.S., Hip Kam, A., Pem, Y., Ramsaha, S., Bahorun, T., 2020. Regulation of cancer cell signalling pathways as key events for therapeutic relevance of edible and medicinal mushrooms. *Seminars in Cancer Biology*. <https://doi.org/10.1016/j.semcancer.2020.03.004>.
- Oba, K., Teramukai, S., Kobayashi, M., Matsui, T., Koderu, Y., Sakamoto, J., 2007. Efficacy of adjuvant immune chemotherapy with polysaccharide K for patients with curative resections of gastric cancer. *Cancer Immunol. Immunother.* 56, 905–911. <https://doi.org/10.1007/s00262-006-0248-1>.
- Ohno, N., Nameda, S., Harada, T., et al., 2003. Immunomodulating activity of a S-glucan preparation, SCG, extracted from a culinary medicinal mushroom, *Sparassis crispa* Wulf.: Fr. (Aphyllorphomycetidae), and application to cancer patients. *Int. J. Med. Mushrooms* 5, 359–368. <https://doi.org/10.1615/InterJMedMush.v5.i4.30>.
- Ooi, V.E., Liu, F., 2000. Immunomodulation and anti-cancer activity of polysaccharide-protein complexes. *Curr. Med. Chem.* 7, 715. <https://doi.org/10.2174/0929867003374705>.
- Oshiman, K., Fujimiyama, Y., Ebina, T., Suzuki, I., Noji, M., 2002. Orally administered β -1,6-D-polyglucose extracted from *Agaricus blazei* results in tumor regression in tumor-bearing mice. *Planta Med.* 68, 610–614. <https://doi.org/10.1055/s-2002-32904>.
- Pan, K., Jiang, Q., Liu, G., Miao, X., Zhong, D., 2013. Optimization extraction of *Ganoderma lucidum* polysaccharides and its immunity and antioxidant activities. *Int. J. Biol. Macromol.* 55, 301–306. <https://doi.org/10.1016/j.ijbiomac.2013.01.022>.
- Pandya, U., Dhuldhaj, U., Nirmal, S.S., 2018a. Bioactive mushroom polysaccharides as antitumor: an overview, *Natural Product Research*. <https://doi.org/10.1080/14786419.2018.1466129>.
- Pandya, U., Dhuldhaj, U., Sahay, N.S., 2018b. Bioactive mushroom polysaccharides as antitumor: an overview. *Nat. Prod. Res.* 4, 1–13. <https://doi.org/10.1080/14786419.2018.1466129>.
- Pandya, U., Dhuldhaj, U., Sahay, N.S., 2018c. Bioactive mushroom polysaccharides as antitumor: an overview. *Nat. Prod. Res.* <https://doi.org/10.1080/14786419.2018.1466129>.

- Pauliuc, I., Cimporescu, A., Daliborca, C.V., Popescu, R., Botau, D., Dumitrascu, V., 2013. Antitumor activity of *Pleurotus ostreatus* gemmotherapeutic extract. *Annals of RSCB* 18, 178–181.
- Phélippé, M., Gonçalves, O., Thouand, G., Cogne, G., Laroche, C., 2019. Characterization of the polysaccharides chemical diversity of the cyanobacteria *Arthrospira platensis*. *Algal Research* 38, 101426. <https://doi.org/10.1016/j.algal.2019.101426>.
- Ruddon, R.W., 2007. *Cancer Biology*, fourth ed. Oxford University Press, USA.
- Ruthes, A.C., Smiderle, F.R., Iacomini, M., 2015. d-Glucans from edible mushrooms: a review on the extraction, purification and chemical characterization approaches. *Carbohydr. Polym.* 117, 753–761. <https://doi.org/10.1016/j.carbpol.2014.10.051>.
- Sanyal, T., Ghosh, S.K., 2019. Anti-cancer property of Lenzites betulina (L) Fr. on cervical cancer cell lines and its anti-tumor effect on HeLa-implanted mice. *BioRxiv* 540567. <https://doi.org/10.1101/540567>, 2019.
- Sarang, I., Ghosh, D., Bhutia, S.K., Mallick, S.K., Maiti, T.K., 2006. Anti-tumor and immunomodulating effects of *Pleurotus ostreatus* mycelia-derived proteoglycans. *Int. Immunopharm.* 6 (8), 1287–1297. <https://doi.org/10.1016/j.intimp.2006.04.002>.
- Sheng, L., Chen, J., Li, J., Zhang, W., 2011. An exopolysaccharide from cultivated *Cordyceps sinensis* and its effects on cytokine expressions of immunocytes. *Appl. Biochem. Biotechnol.* 163, 669–678. <https://doi.org/10.1007/s12010-010-9072-3>.
- Shi, Z.W., Liu, Y., Xu, Y., Hong, Y.R., Liu, Q., Li, X.L., Wang, Z.G., 2014. *Tremella* polysaccharides attenuated sepsis through inhibiting abnormal CD4(+)CD25(high) regulatory T cells in mice. *Cell. Immunol.* 288 (1–2), 60–65. <https://doi.org/10.1016/j.cellimm.2014.02.002>.
- Silva, D.D., Rapior, S., Fons, F., Ali, H., et al., 2012. Medicinal mushrooms in supportive cancer therapies: an approach to anti-cancer effects and putative mechanisms of action. *Fungal Divers.* 55, 1–35. <https://doi.org/10.1007/s13225-012-0151-3>. <https://doi.org/10.1007/s13225-012-0151-3>.
- Smiderle, F.R., Baggio, C.H., Borato, D.G., Santanafilho, A.P., Sasaki, G.L., Iacomini, M., 2014. Anti-inflammatory properties of the medicinal mushroom *Cordyceps militaris* might be related to its linear (1→3)-β-D-glucan. *PLoS One* 9 (10), e110266. <https://doi.org/10.1371/journal.pone.0110266>.
- Smiderle, F.R., Carbonero, E.R., Mellinger, C.G., Sasaki, G.L., Gorin, P.A.J., Iacomini, M., 2006. Structural characterization of a polysaccharide and a β-glucan isolated from the edible mushroom *Flammulina velutipes*. *Phytochemistry* 67, 2189–2196. <https://doi.org/10.1016/j.phytochem.2006.06.022>.
- Song, G., Du, Q., 2010. Isolation of a polysaccharide with anticancer activity from *Auricularia polytricha* using high-speed countercurrent chromatography with an aqueous two-phase system. *J. Chromatogr. A* 1217, 5930–5934. <https://doi.org/10.1016/j.chroma.2010.07.036>.
- Tang, W., Liu, D., Yin, J.Y., Nie, S.P., 2020a. Consecutive and progressive purification of food-derived natural polysaccharide: based on material, extraction process and crude polysaccharide. *Trends Food Sci. Technol.* <https://doi.org/10.1016/j.tifs.2020.02.015>.
- Tang, W., Liu, D., Yin, J.Y., Nie, S.P., 2020b. Consecutive and progressive purification of food-derived natural polysaccharide: based on material, extraction process and crude polysaccharide. *Trends Food Sci. Technol.* <https://doi.org/10.1016/j.tifs.2020.02.015>.
- Tang, W., Liu, D., Yin, J.Y., Nie, S.P., 2020c. Consecutive and progressive purification of food-derived natural polysaccharide: based on material, extraction process and crude polysaccharide. *Trends Food Sci. Technol.* 99, 76–87. <https://doi.org/10.1016/j.tifs.2020.02.015>.
- Thekkuttuparambill, A., Ajith, Kainoor, K.J., 2007. Indian Medicinal Mushrooms as a source of antioxidant and antitumor agents. *J. Clin. Biochem. Nutr.* 40, 157–162. <https://doi.org/10.3164/jcbs.40.157>.
- Thetsrimuang, C., Khamuang, S., Chiablaem, K., Srisomsap, C., Sarnthira, R., 2011. Antioxidant properties and cytotoxicity of crude polysaccharides from *Lenzites polychrous* Lév. *Food Chem.* 128, 634–639. <https://doi.org/10.1016/j.foodchem.2011.03.077>.
- Tong, H., Xia, F., Feng, K., Sun, G., Gao, X., Sun, L., Gao, X., Sun, L., Jiang, R., Tian, D., Sun, X., 2009. Structural characterization and in vitro antitumor activity of a novel polysaccharide isolated from the fruiting bodies of *Pleurotus ostreatus*. *Bioresour. Technol.* 100, 1682–1686. <https://doi.org/10.1016/j.biortech.2008.09.004>.
- Torre, L.A., Bray, F., Siegel, R.L., Ferlay, J., Lortet-Tieulent, J., 2012. “Global cancer statistics, 2012.” *CA: A Cancer Journal for Clinicians* 65 (2), 87–108. <https://doi.org/10.3322/caac.21262>, 2015.
- Twardowski, P., Kanaya, N., Frankel, P., et al., 2015. A phase 1 trial of mushroom powder in patients with biochemically recurrent prostate cancer: roles of cytokines and myeloid-derived suppressor cells for *Agaricus bisporus*-induced prostate-specific antigen responses. *Cancer* 121, 2949–2950. <https://doi.org/10.1002/cncr.29421>.
- Vinogradov, E., Petersen, B.O., Duusb, J.O., Wasserc, S., 2004. The structure of the glucuronoxylmannan produced by culinary medicinal yellow brain mushroom (*Tremella mesenterica* Ritz.:Fr., Heterobasidiomycetes) grown as one cell biomass in submerged culture. *Carbohydr. Res.* 339, 1483–1489. <https://doi.org/10.1016/j.carres.2004.04.001>.
- Wang, C.L., Lu, C.Y., Hsueh, Y.C., Liu, W.H., Chen, C.J., 2014. Activation of antitumor immune responses by *Ganoderma formosanum* polysaccharides in tumor-bearing mice. *Appl. Microbiol. Biotechnol.* 98, 9389–9398. <https://doi.org/10.1007/s00253-014-6027-6>.
- Wang, J., Hu, S., Liang, Z., Yeh, C., 2005. Optimization for the production of water-soluble polysaccharide from *Pleurotus citrinopileatus* in submerged culture and its antitumor effect. *Applied Microbiology and Biotechnology* 67, 759e766. <https://doi.org/10.1007/s00253-004-1833-x>.
- Wang, X.L., Ding, Z.Y., Zhao, Y., et al., 2017. Efficient accumulation and in vitro antitumor activities of triterpene acids from submerged batch-cultured Lingzhi or Reishi medicinal mushroom, *Ganoderma lucidum* (Agaricomycetes). *Int. J. Med. Mushrooms* 19 (5), 419–431. <https://doi.org/10.1615/IntJMedMushrooms.v19.i5.40>.
- Wang, Y., Tian, Y., Shao, J., et al., 2018. Macrophage immunomodulatory activity of the polysaccharide isolated from *Collybia radicata* mushroom. *Int. J. Biol. Macromol.* 108, 300–306. <https://doi.org/10.1016/j.ijbiomac.2017.12.025>.
- Wang, Z., Zhang, H., Shen, Y., Zhao, X., Wang, X., Wang, J., et al., 2018a. Characterization of a novel polysaccharide from *Ganoderma lucidum* and its absorption mechanism in Caco-2 cells and mice model. *Int. J. Biol. Macromol.* 118, 320–326. <https://doi.org/10.1016/j.ijbiomac.2018.06.078>.
- Wasser, S.P., 2002. Medicinal mushrooms as a source of antitumor and immunomodulating polysaccharides. *Appl. Microbiol. Biotechnol.* 60, 258–274. <https://doi.org/10.1007/s00253-002-1076-7>.
- Wesa, K.M., Cunningham-Rundles, S., Klimek, V.M., et al., 2015. Maitake mushroom extract in myelodysplastic syndromes (MDS): a phase II study. *Cancer Immunol. Immunother.* 64 (2), 237–247. <https://doi.org/10.1007/s00262-014-1628-6>.
- Wu, Y., Wei, Z., Zhang, F., Robert, J., Linhardt, A., Sun, P., Zhang, A., 2018. Structure, bioactivities and applications of the polysaccharides from *Tremella fuciformis* mushroom: a review. *Bio. Biotechnol.* <https://doi.org/10.1016/j.jbiomac.2018.10.117>.
- Xiong, Q., Huang, S., Chen, J., Wang, B., He, L., Zhang, L., et al., 2017. A novel green method for deproteinization of polysaccharide from *Cipangopaludinachinensis* by freeze-thaw treatment. *J. Clean. Prod.* 142, 3409–3418. <https://doi.org/10.1016/j.jclepro.2016.10.125>.
- Xu, S., Xu, X., Zhang, L., 2012. Branching structure and chain conformation of water-soluble glucan extracted from *Auricularia auricula-judae*. *J. Agric. Food Chem.* 60 (13), 3498–3506. <https://doi.org/10.1021/jf300423z>.
- Xu, X., Yang, J., Ning, Z., Zhang, X., 2015. *Lenzites edodes*-derived polysaccharide rejuvenates mice in terms of immune responses and gut microbiota. *Food Funct* 6 (8), 2653–2663. <https://doi.org/10.1039/C5FO00689A>.
- Xu, Z., Chen, X., Zhong, Z., Chen, L., Wang, Y., 2011. *Ganoderma lucidum* polysaccharides: immunomodulation and potential anti-tumor activities. *Am. J. Chin. Med.* 39 (1), 15–27. <https://doi.org/10.1039/C5FO00689A>.
- Yan, J., Zhu, L., Qu, Y., Qu, X., Mu, M., Zhang, M., Muneer, G., Zhou, Y., Sun, L., 2018. Analyses of active antioxidant polysaccharides from four edible mushrooms. *Bio. Biotechnol.* <https://doi.org/10.1016/j.jbiomac.2018.11.079>.
- Yang, D.H., Bae, A.H., Koumoto, K., Lee, S.W., Sakurai, K., Shinkai, S., 2005. In situ monitoring of polysaccharide polynucleotide interaction using a schizophyllan-immobilized QCM device. *Sensor. Actuator. B Chem.* 105, 490e494. <https://doi.org/10.1016/j.snb.2004.07.008>.
- Yang, Y., Ye, L., Zhang, J.S., Liu, Y.F., Tang, Q.L., 2009. Structural analysis of a bioactive polysaccharide, PISPI, from the medicinal mushroom *Phellinus igniarius*. *Biosci. Biotechnol. Biochem.* 73, 134–139. <https://doi.org/10.1271/bbb.80546>.
- Yi, Y., Huang, X.Y., Zhong, Z.T., Huang, F., Li, S.Y., Wang, L.M., et al., 2019. Structural and biological properties of polysaccharides from lotus root. *Int. J. Biol. Macromol.* 130, 454–461. <https://doi.org/10.1016/j.ijbiomac.2019.02.146>.
- Yu, Z., Ming, G., Kaiping, W., Zhixiang, C., Lijuan, D., Jingyu, L., Fang, Z., 2010. Structure, chain conformation and antitumor activity of a novel polysaccharide from *Lenzites edodes*. *Fitoterapia* 81, 1163–1170. <https://doi.org/10.1016/j.fitote.2010.07.019>.
- Zaidman, B.Z., Yassin, M., Mahajna, J., Wasser, S.P., 2005. Medicinal mushroom modulators of molecular targets as cancer therapeutics. *Appl. Microbiol. Biotechnol.* 67, 453–468. <https://doi.org/10.1007/s00253-004-1787-z>.
- Zhang, H.L., Cui, S.H., Zha, X.Q., Bansal, V., Xue, L., Li, X.L., et al., 2014. Jellyfish skin polysaccharides: extraction and inhibitory activity on macrophage-derived foam cell formation. *Carbohydr. Polym.* 106, 393–402. <https://doi.org/10.1016/j.carbpol.2014.01.041>.
- Zhang, J., Tang, Q., Zhou, C., Jia, W., Da Silva, L., Nguyen, L.D., Reutter, W., Fan, H., 2010. GLIS, a bioactive proteoglycan fraction from *Ganoderma lucidum*, displays antitumor activity by increasing both humoral and cellular immune response. *Life Sci.* 87 (19–22), 628–637. <https://doi.org/10.1016/j.lfs.2010.09.026>.
- Zhang, M., Chiu, L.C.M., Cheung, P.C.K., Ooi, V.E.C., 2006. Growth-inhibitory effects of a β-glucan from the mycelium of *Poria cocos* on human breast carcinoma MCF-7 cells: cell cycle arrest and apoptosis induction. *Oncol. Rep.* 15, 637e643. <https://doi.org/10.3892/or.15.3.637>.
- Zhang, M., Cui, S.W., Cheung, P.C.K., Wang, Q., 2007. Anti-tumor polysaccharides from mushroom: a review on their isolation process, structural characteristics and antitumor activity. *Trends Food Sci. Technol.* 18 (1), 4–19. <https://doi.org/10.1016/j.tifs.2006.07.013>.
- Zhang, Y., Li, S., Wang, X., Zhang, L., Cheung, P.C.K., 2011. Advances in lentinan: isolation, structure, chain conformation and bioactivities. *Food Hydrocolloids* 25, 196–206. <https://doi.org/10.1016/j.foodhyd.2010.02.001>.
- Zhao, L., Dong, Y., Chen, G., Hu, H., 2010. Extraction, purification, characterization and antitumor activity of polysaccharides from *Ganoderma lucidum*. *Carbohydr. Polym.* 80 (3), 783–789. <https://doi.org/10.1016/j.carbpol.2009.12.029>.
- Zhu, F., Dua, B., Bian, Z., et al., 2015. Beta-glucans from edible and medicinal mushrooms: characteristics, physicochemical and biological activities. *J. Food Compos. Anal.* 41, 165–173. <https://doi.org/10.1016/j.jfca.2015.01.019>.
- Zhu, Y., Li, Q., Mao, G., Zou, Y., Feng, W., Zheng, D., Wang, W., Zhou, L., Zhang, T., Yang, J., et al., 2014. Optimization of enzyme-assisted extraction and characterization of polysaccharides from *Hericium erinaceus*. *Carbohydr. Polym.* 101, 606–613. <https://doi.org/10.1016/j.carbpol.2013.09.099>.

'এবং মত্য়' -বিশ্ববিদ্যালয় মঞ্জুরী আয়োগ(UGC-CARE list-I 2021)
অনুমোদিত তালিকার অন্তর্ভুক্ত ।
২০২১সালে প্রকাশিত ১৬পৃ.তালিকার(৩১৯টির মধ্যে) ৩ পৃ.৬০নং উল্লেখিত ।

এবং মত্য়

(বাংলা ভাষা, সাহিত্য ও গবেষণামূলক মাসিক পত্রিকা)

২৩তম বর্ষ, ১৩৮ সংখ্যা
সেপ্টেম্বর, ২০২১

সম্পাদক

ড. মদনমোহন বেরা

সহসম্পাদক

পায়েল দাস বেরা

মৌমিতা দত্ত বেরা

যোগাযোগ :

ড. মদনমোহন বেরা, সম্পাদক ।

গোলকুঁয়াচক, পোষ্ট-মেদিনীপুর, ৭২১১০১, জেলা-প.মেদিনীপুর, প.বঙ্গ ।

মো.-৯১৫৩১৭৭৬৫৩

কে.কে. প্রকাশন

গোলকুঁয়াচক, মেদিনীপুর, পশ্চিমবঙ্গ ।

৫৪.বিজন ভট্টাচার্যের নাটকে লোকায়ত জীবন: প্রসঙ্গ 'নবায়'	
:: ড. মিঠু দেব.....	৪১৪
৫৫.নারীর কলমে বাংলা উপন্যাসের বিবর্তন : সূচনা থেকে	
প্রাক-স্বাধীনতা :: ড. শান্তনু ভট্টাচার্য.....	৪২২
৫৬..বাউল গানের চর্চায় লালন ও কাঙাল ফিকিরচাঁদ ফকির	
:: ড. বিপ্লব সরকার.....	৪২৮
৫৭..ঝাপান মল্লভূমের অঙ্গনে :: ড. চৈতালী মান্ডি.....	৪৩৯
৫৮..শক্তিপদ ব্রহ্মচারীর 'অন্নদাস' কবিতা : অসমবদ্ধতা,	
শৃঙ্খলা ও সত্যের সন্ধান :: ড. কালীপদ দাস.....	৪৪৪
৫৯..রবীন্দ্রনাথের 'ঘরে বাইরে' উপন্যাসে দাম্পত্যের নানা মাত্রা	
:: ড. কৃষ্ণকান্ত রায়.....	৪৫১
৬০.প্রেম : এক মহামারি ও তার মহানায়কগণ	
:: ড. রাজ নারায়ণ পাল.....	৪৫৭
৬১.ভারতীয় অর্থনীতিতে শিল্পক্ষেত্রের স্থিতাবস্থা - একটি	
সংক্ষিপ্ত বিশ্লেষণ :: ড. শুভব্রত চক্রবর্তী.....	৪৬৫
৬২.মহাশ্বেতা দেবীর 'ব্যাধখণ্ড' : প্রতিনির্মাণে অভয়ামঙ্গল	
:: ড. ঋষিপ্রতিম ঘোষ.....	৪৭৩
৬৩.রবীন্দ্রানুসারী কবি ভূজঙ্গধর রায়চৌধুরীর কাব্য-সাধনায়	
গীতার প্রভাব :: ড. সৌমিত্র মুখোপাধ্যায়.....	৪৭৭
৬৪.'নীলদর্পণ' : ঔপনিবেশিক শক্তির প্রকৃত দর্পণ	
:: ড. প্রকাশ বিশ্বাস.....	৪৯০
৬৫..ঝাড়খণ্ডী বাংলা উপভাষার লোকসঙ্গীত	
:: ড.যশোদা বেরা.....	৪৯৬
৬৬..অপ্রতিম নাটককার তারাশঙ্কর	
:: ড. নন্দকুমার বেরা.....	৫০০
৬৭..আধুনিকের মধ্যযুগ চর্চা : একটি সমীক্ষা	
:: ড. আশিস অধিকারী.....	৫০৬
০০লেখক পরিচিতি.....	৫১৩
০০০UGC-CARE list.....	৫১৭

নারীর কলমে বাংলা উপন্যাসের বিবর্তন : সূচনা থেকে প্রাক্-স্বাধীনতা

ড. শান্তনু ভট্টাচার্য

‘আমি নারী, আমি মহীয়সী
আমারে স্মরি সুর বেঁধেছে
জ্যোৎস্না-তারায় নিদ্রাবিহীন শশী।
আমি নইলে মিথ্যা হত সূর্য চন্দ্র ওঠা,
মিথ্যা হত কাননে ফুল ফোটা।’

— রবীন্দ্রনাথ ঠাকুর

নারী এবং পুরুষের যৌথ জীবন যাত্রায় নারীর কাছে শিক্ষার আলো অনেক পরে পৌঁছেছে। পুরুষ প্রথম থেকেই যে সুযোগ সুবিধা পেয়ে এসেছে নারী তা পায়নি। শিক্ষার আলোয় আলোকিত হচ্ছে যখন পুরুষ, নারী তখন পারিবারিক গার্হস্থ্য কর্তব্য পালনেই সীমাবদ্ধ থাকে। পরবর্তীকালে সময়ের সঙ্গে সঙ্গেই পরিস্থিতিও বদলেছে। উনিশ শতকের নবজাগরণের আলোকে উদ্ভাসিত হয়েছে নারী এবং পুরুষ উভয়েই। তবে পুরুষের ক্ষেত্রে সবকিছু যতটা সহজ ছিল, নারীদের ক্ষেত্রে তা ছিল না। সাহিত্য ক্ষেত্রেও প্রথমদিকে অনুরূপভাবেই পুরুষের তুলনায় নারীর পদচারণা ছিল অনেক কম। প্রাক্-আধুনিক বাংলা সাহিত্যে হাতে গোনা কয়েকজন নারী সাহিত্যিককে পাওয়া যায়। আধুনিক যুগের সূচনা পর্বেও নারী সাহিত্যিকের সংখ্যা পুরুষের তুলনায় অপেক্ষাকৃত কম। বর্তমানে অবশ্য সেই ব্যবধান অনেক কমেছে এবং প্রায় নেই বললেই চলে।

আমার আলোচ্য বিষয় নারীর কলমে লেখা বাংলা উপন্যাস, প্রথম থেকে প্রাক্-স্বাধীনতা কালপর্ব পর্যন্ত। এই সময় পর্বে বেশকিছু মহিলা ঔপন্যাসিক বাংলা উপন্যাস লিখেছেন। যাদের লেখার মূলত দুটি দিক ধরা পড়ছে। পারিবারিক গার্হস্থ্য জীবনচিত্র, যা মূলত পারিবারিক দাম্পত্য সমস্যা এবং তার সমাধান কেন্দ্রিক এবং আধুনিক শিক্ষার শিক্ষিত মধ্যবিত্ত নারী সমাজের জীবন সংগ্রামের কথা-যাদের পারিবারিক জীবন এবং বাইরের জীবনের সঙ্গে সামঞ্জস্য রক্ষা করতে হয় প্রতিনিয়ত। পরিবারের মধ্যেই যেহেতু বেশিরভাগ সময় নারীরা আবদ্ধ থাকেন তাই পারিবারিক জীবনের খুঁটিনাটি সূক্ষ্মতিসূক্ষ্ম বিষয়ের বর্ণনা, চাওয়া-না-পাওয়া কিংবা বঞ্চনার বিষয়গুলি বারবার ঘুরে ফিরে আসে মহিলা ঔপন্যাসিকদের লেখনিতে। উনিশ শতকের শিক্ষার আলোয় আলোকিত হয়ে নারীমন সমকক্ষতা চায় পুরুষের। পায়ের নীচে নয় পাশে অবস্থান চায়। সমস্ত কাজে

'এবং মহুয়া'-বিশ্ববিদ্যালয় মঞ্জুরী আয়োগ(UGC-CARE list-I 2021)
অনুমোদিত তালিকার অন্তর্ভুক্ত।

২০২১সালে প্রকাশিত ১৬পৃ.তালিকার(৩১৯টির মধ্যে) ৩ পৃ.৬০নং উল্লেখিত।

এবং মহুয়া

(বাংলা ভাষা, সাহিত্য ও গবেষণাধর্মী মাসিক পত্রিকা)

২৩তম বর্ষ, ১৩৭ সংখ্যা

আগস্ট, ২০২১

সম্পাদক

ড. মদনমোহন বেরা

সহসম্পাদক

পায়েল দাস বেরা

মৌমিতা দত্ত বেরা

যোগাযোগ :

ড. মদনমোহন বেরা, সম্পাদক।

গোলকুয়াচক, পোষ্ট-মেদিনীপুর, ৭২১১০১, জেলা-প.মেদিনীপুর, প.বঙ্গ।

মো.-৯১৫৩১৭৭৬৫৩

কে.কে. প্রকাশন

গোলকুয়াচক, মেদিনীপুর, পশ্চিমবঙ্গ।

U.G.C.- CARE List-I 2021 approved journal, Indian
Language-Arts and Humanities Group, out of 16 pages
placed in Page 3 & No.60 out of 319

EBONG MOHUA

Bengali Language, Literature, Research and Referred with
Peer-Review Journal

23th Year, 137 Volume

Aug, 2021

Published By

K. K. Prakashan

Golekuachawk, P.O.-Midnapur,721101.W.B.

DTP and Printed By

K.K.Prakashan

Cover Designed By

Kohinoorkanti Bera

Special Editorial Co-ordinator

Amit Kumar Maity

Communication :

Dr. Madanmohan Bera, Editor.

Golekuachawk, P.O.-Midnapur, 721101. W.B.

Mob.-9153177653

Email- madanmohanbera51@gmail.com /

kohinoor bera @ gmail.com

Rs 500

৩৫. ভারতের জাতি-ভিত্তিক রাজনীতিতে মতুয়া আন্দোলন	
:: স্বপন সরকার.....	২৬৬
৩৬. বাঙালির খাদ্যাভ্যাসের ইতিবৃত্ত :: তারক হালদার.....	২৮০
৩৭. স্বাধীনতা আন্দোলনে নদীয়া জেলার ভূমিকা	
:: সুমিত ঘোষ.....	২৮৪
৩৮. সংবাদপত্র থেকে ডিজিটাল মিডিয়া : একটি পর্যালোচনা	
:: মুক্ত সেনগুপ্ত.....	২৯৯
৩৯. কথক নৃত্যের প্রচার ও প্রসারে লক্ষ্মী দরবার	
:: মানব পাড়ই.....	৩০৭
৪০. আদি-মধ্যযুগের মধ্য ভারতের ইতিহাসের বৈশিষ্ট্য অনুসন্ধান	
:: মল্লিকা ঘোষ.....	৩১১
৪১. ব্রিটিশ শাসনে মালদায় মৎস্যজীবীদের জীবিকার সংকোচন	
:: গৌরব দাশগুপ্ত.....	৩১৭
৪২. রবীন্দ্র ছোটগল্প : নিবাচিত নারী চরিত্রের পর্যালোচনা	
:: দীপিকা দাস.....	৩২৩
৪৩. বাংলা বিকল্প নাটক : বাদল সরকার ও প্রবীর গুহ	
:: মোহন চন্দ্র ঘোষ.....	৩২৯
৪৪. নিপীড়িত মানুষের কণ্ঠে সৈয়দ বদরুদ্দোজা	
:: সুমিত দাস.....	৩৩৯
৪৫. বাণী বসুর উপন্যাস : রাজনৈতিক পরিসরের আবর্তে	
:: তানিয়া রায়.....	৩৪৮
৪৬. 'সন্দেশ' এর বিবর্তন পর্ব-একটি বিশ্লেষণাত্মক অধ্যয়ন	
:: ড. অনুপম সরকার.....	৩৫৫
৪৭. সংস্কারক বিদ্যাসাগর : আজও প্রাসঙ্গিক	
:: ড. মনমোহন গুরু.....	৩৬৪
৪৮. বাংলা উপন্যাসে তিন বিধবা চরিত্র : উত্তরণ ও সংকট	
:: ড. সুজিত কুমার বিশ্বাস.....	৩৭০
৪৯. বৈষ্ণব পদকর্তা ও পদ সংকলক রবীন্দ্রনাথ	
:: ড. প্রকাশচন্দ্র সরদার.....	৩৭৯
৫০. রবীন্দ্র-দৃষ্টিতে রবীন্দ্র-কাব্য :: ড. অরুণাভ মুখার্জী.....	৩৯২
৫১. নৈতিকতার আলোয় যৌনতা প্রসঙ্গে বট্টাভ রাসেল :	
একটি দার্শনিক অনুসন্ধান :: ড. ডরত মালাকার.....	৩৯৯
৫২. শ্রমী বিবেকানন্দের সমাজতান্ত্রিক ভাবনা: একটি মূল্যায়নের সন্ধানে	
:: ড. বিদ্যা রতন টিকাদার.....	৪০৬

রবীন্দ্র-দৃষ্টিতে রবীন্দ্র-কাব্য

ড. অরুণাভ মুখার্জী

সারসংক্ষেপ :

কবিগুরু রবীন্দ্রনাথ তাঁর প্রতিভার ঐশ্বর্যে প্রত্যক্ষ বা পরোক্ষভাবে সর্বদিকে বিরাজিত— 'সবার হৃদয়ে রবীন্দ্রনাথ'। তাই নানান জনের দৃষ্টিতে অনন্য রবীন্দ্রনাথ নানানভাবে বিশ্লেষিত হয়েছেন এবং হচ্ছেনও। কিন্তু কবি নিজেকে, নিজের সত্তাকে, নিজের কাব্যকে অর্থাৎ নিজের সৃষ্টিচক্রকে কীরূপে দেখেছেন, কালাশ্রয়ী অন্তর্জীবনের বিবর্তনের ক্রমিক রূপান্তর ও বিকাশের মধ্যে দৃশ্যমান জগতে রূপ এবং সীমাতে আবদ্ধ না থেকে তাকে ছাড়িয়ে যাওয়ার এক মহৎ আবেদন রবীন্দ্রদর্শনে নিজেকে কীভাবে ব্যক্ত হয়েছে, তাঁর কাব্যসমগ্র বিশ্লেষণে সে বিষয়েই পক্ষাবলোকন করার প্রয়াস নেওয়া হয়েছে আলোচ্য রচনায়।

সূচক শব্দ :

আপনার অভিজ্ঞান, চক্রপথ প্রদক্ষিণ, আমি কবি মাত্র, সৌন্দর্যানুভূতি, ঐকান্তিক অন্তর্মুখীন, কল্পনির্মাণক্ষমপ্রজ্ঞা, সমগ্রতা, গঙ্গাজলে গঙ্গাপূজা, কপিবুকের কবিতা, হৃদয় অরণ্য, স্বকীয় ভাব, জীবনদেবতা, আন্তিক্যবাদী।

প্রতিপাদ্য বিষয় :

রবীন্দ্রজীবন চক্রের বিচিত্র অভিজ্ঞতা নানা কর্মের উপলক্ষে নানা জনের নিকট নানাভাবে আলোচিত হয়েছে। কিন্তু তাতে যে রবীন্দ্র পরিচয়ের সমগ্রতা নেই, তা রবীন্দ্রনাথ নিজেরই উপলব্ধি করতে পেরেছিলেন। আর তাই তিনি নিজেকে ব্যক্ত করতে নিজের সম্পর্কে জানিয়েছেন— "নিজের সত্য পরিচয় পাওয়া সহজ নয়। জীবনের বিচিত্র অভিজ্ঞতার মূল ঐক্যসূত্রটি ধরা পড়তে চায় না। ... নানাখানা করে নিজেকে দেখেছি, নানা কাজে প্রবর্তিত করেছি, ক্ষণে ক্ষণে তাতে আপনার অভিজ্ঞান আপনার কাছে বিক্ষিপ্ত হয়েছে। জীবনের সেই দীর্ঘ চক্রপথ প্রদক্ষিণ করতে করতে বিদায়কালে আজ সেই চক্রকে সমগ্ররূপে বসন দেখতে পেলাম তখন একটা কথা বুঝতে পেরেছি যে, একটা মাত্র পরিচয় আমার আছে, সে আর কিছুই নয়, আমি কবি মাত্র"। সুতরাং রবীন্দ্র অনুভবে রবীন্দ্রনাথ ঠাকুরের প্রথম এবং প্রধান পরিচয় তিনি কবি - সৌন্দর্যানুভূতির কবি। ধর্মও ছিল তাঁর কবির ধর্ম। জীবনের বারো বছর বয়স থেকে শুরু করে মৃত্যুর পূর্ব সময় অর্থাৎ একশি

এবং প্রান্তিক

An International Peer-Reviewed Multi-Disciplinary Journal

SJIF Approved Impact Factor : 7.16

Vol. 8th Issue 18th, Sept., 2021

সম্পাদক

আশিস রায়



এবং প্রান্তিক

চণ্ডিবেড়িয়া, সারদাপল্লী, পোঃ - কেটপুৰ, কলকাতা - ৭০০১০২

Ebong Prantik

An International Peer-Reviewed Multi-Disciplinary Journal

SJIF Approved Impact Factor : 7.16

[ISSN : 2582-3841(O), 2348-487X(P)].

*Published & Edited by Dr. Ashis Roy, Chandiberiya, Saradapalli,
Kestopur, Kolkata - 700102, and*

Printed by Ananya, Burobattala, Sonarpur, Kolkata - 150,

Vol. 8th Issue 18th, Sept. 2021, Rs. 650/-

E-mail : ebongprantik@gmail.com

Website : www.ebongprantik.in

প্রকাশ

৮ম বর্ষ ও ১৮ তম সংখ্যা

২০ সেপ্টেম্বর, ২০২১

ISSN : 2582-3841 (Online)

2348-487X (Print)

DOI : 10.5281/zenodo.5517966

কপিরাইট

সম্পাদক, এবং প্রান্তিক

প্রকাশক

এবং প্রান্তিক

আশিস রায়

রেজিস্টার্ড অফিস

চণ্ডিবেড়িয়া, সারদাপল্লী, পোঃ - কেটপুৰ, কলকাতা - ৭০০ ১০২

ফোন - ৯৮০৪৯২৩১৮২

সার্বিক সহায়তা - সৌরভ বর্মন

ফোন - ৮২৫০৫৯৫৬৪৭

মুদ্রণ

অনন্যা

বুড়ো বটতলা, সোনারপুর, কলকাতা - ৭০০ ১৫০

ফোন - ৯১৬৩৯৩১৪৬৫

মূল্য : ৬৫০ টাকা

আনিসুজ্ঞামানের জীবনী: একটি সংক্ষিপ্ত পাঠ	
আসরাফুন্নেনসা বেগম	২৩৪
হাস্যরসিক স্বিজেন্দ্রলাল ও তাঁর অর্চিত হাসির কাব্য	
সুদীপ্ত সাধুর্থা	২৪৪
সৈকত রক্ষিতের উপন্যাস 'স্তিমিত রণতূর্ষ'; শাঁখচির বা শাঁখারি	
জনগোষ্ঠীর 'অস্তিত্ব' বিপন্নতার আখ্যান	
উৎপল ডেম	২৫০
নজরুল কাব্যে পুরাণ ভাবনা	
অরুনাভ মুখার্জী	২৬১
তারানাথ তর্কবাচস্পতি ও ঔপনিবেশিক বাংলায় সংস্কৃতচর্চাঃ	
একটি স্বল্পচর্চিত অধ্যায়	
শ্রীতম গোস্বামী	২৭০
রহস্যময় গল্পলোক : নারায়ণ গঙ্গোপাধ্যায়	
জ্যোৎস্না দত্ত	২৮৭
নারায়ণ গঙ্গোপাধ্যায়ের 'রামমোহন' নাটক : একটি পর্যালোচনা	
অভিজিৎকুমার ঘোষ	২৯৪
সুন্দরবনে চিৎড়িচাম্ব, সমাজ-অর্থনীতি ও পরিবেশ প্রসঙ্গ	
উজ্জ্বল বিশ্বাস	৩০৩
চৈতন্যসমকালীন বৈষ্ণব মহিলা পদকর্ত্রী মাধবী দাস ও তাঁর পদাবলী	
মনীষা পাল	৩১৩
অর্চিত চারপ কবি বৈদ্যনাথ বন্দ্যোপাধ্যায়ের কবিতায় প্রেম ও প্রতিবাদ	
সুমন্ত মণ্ডল	৩২৩
মহাত্মারত ও সংস্কৃত সাহিত্যে অস্ত্রাজ	
দেবজ্যোতি শীট	৩৩৪

নজরুল কাব্যে পুরাণ ভাবনা

অরুনাভ মুখার্জী

সহকারী অধ্যাপক, বাংলা বিভাগ

অজুরাম মেমোরিয়াল কলেজ, ঝালদা, পুরুলিয়া

সারসংক্ষেপ : 'নিখিল বাংলার চরণকবি' কাজী নজরুল ইসলামের চিন্তা-চেতনাতে পুরাণ ভাবনার স্বরলিপি সুর হয়ে প্রতিধ্বনিত হয়েছে বারে বারে। বিংশ শতাব্দীর এক জসসভাবের সম্ভাবনার যুগে পরাধীনতার অন্তর্জ্বালা বুকে নিয়ে 'একহাতে বাঁকা বাঁশের কাঁপুড়ী, আর হাতে রণতুর্য' এর মধ্যদিয়ে নজরুলের আবির্ভাব। বিদ্রোহ, প্রেম, মানবতা, উন্মাদ, আবেগ-উন্মাদনা প্রকাশের অকুণ্ঠ প্রয়াসে তিনি এত সাবলীল ভাবে পৌরাণিক মিথকে ব্যবহার করেছেন, যা বহুল পরিমাণে আমাদের কাছে 'অ-চর্চিত'ই থেকে গেছে। আর বাংলা সাহিত্যের ইতিহাসে এক বিরল প্রতিভার অধিকারী কাজী নজরুল ইসলাম তাঁর জীবনে ও সাহিত্যে পুরাণের প্রত্যক্ষ ও পরোক্ষ প্রভাবকে কীরূপ আত্মীকরণ করেছিলেন, সেই আপাত 'অ-চর্চিত' বিষয়কে 'চর্চার' আলোকে উদ্ভাষিত করতেই আলোচ্য রচনায় অবতারণা।

মূলশব্দ : সামূহিক চেতন্য, উপনিবেশ-শৃঙ্খলিত, বৈশ্বিক প্রতিক্রিয়া, শিবতত্ত্ব, ভূমিলীন মানবমহিমা, জীবনাদর্শ, সামন্ততান্ত্রিক সমাজ, সমবায়ী ঐতিহ্য, জীবনবেদ।

মূল বিষয় :

বর্তমান শতাব্দীর ছিন্নমূল, অস্তিত্বচেতন, দ্বন্দ্বজর্জর এবং সংগ্রাম-মুখর সময় প্রেক্ষিতে পুরাণ বা মিথ ভাবনা একটি গুরুত্বপূর্ণ প্রাসঙ্গিক বিষয় সন্দেহ নেই। কারণ ব্যক্তি প্রতিভা অন্তর্গত সত্তায় ও অন্ধকার আবর্তনে শুধু নিজস্ব অভিজ্ঞতা ও অভিজ্ঞান-ই বহন করে না, সৃষ্টি মুহূর্তে তাঁর হৃদয় হয়ে ওঠে সামূহিক চেতন্যের আধার। পুরাণ এই সামূহিক চেতন্যেরই অংশ - "একটি চেতনা, যা মানুষের কল্পনা এবং অভিব্যক্তি প্রকাশের সঙ্গে জড়িত। এতে অতীতের স্মৃতি, বর্তমানের অভিজ্ঞতা ও ভবিষ্যতের আদর্শ সব মিলিয়ে এমন একটি প্যাটার্ন সৃষ্টি হয়েছে, কল্পনা যেখানে বস্তুভিত্তিক এবং প্রত্যয়গ্ৰাস্য হতে পারে"²।

সাহিত্য রচনায় মিথ চেতনা তথা পৌরাণিক ভাবনার প্রয়োগ একটি বিদগ্ধ রীতি বলেই সর্বদেশে ও সর্বকালে স্বীকৃত। সমকালীন জীবন ও বাস্তব পরিপ্রেক্ষিতের মধ্যে সাহিত্য-প্রতিভা যখন তার অন্তর্গত অভীলার রূপায়ণ অসম্ভব বলে মনে করেন, তখন

मासिक

RNI No. MPHIN/2004/14249

अक्षर वार्ता

वर्ष-18 अंक-1 (नवंबर-2021)
Vol - XVIII Issue No - 1
(November - 2021)

मूल्य 100/- रुपये

Indexed In International, Impact Factor Services (IIFS) Database and Indexed with IJIF
Indexed In the international, Institute of Organized Research, (I2OR) Database
Monthly International, Refereed Journal & Peer Reviewed



ISSN 2349 - 7521 , IMPACT FACTOR - 5.125

कला-मानविकी समाजविज्ञान जनसंचार-याण्ड्य-विज्ञान-वैचारिकी की अंतरराष्ट्रीय रेफर्ड त्रिय पत्रिका

aksharwarta@gmail.com www.facebook.com/aksharwartawebpage +918989547437

AKSHARWARTA IS registered MSME with Ministry of MSME, Government of India
MSME Reg. No. UDYAM-MP-49-0005021

हिस्सा काटकर मात्र सत्रह रुपये पुलिस हरनाम सिंह को शिकायत करते हुए धमाका वापस चला जाता है। हसनदीन द्वारा हरनाम सिंह से सत्रह रुपये भीगे जन्म पर उसे हरनाम सिंह खन्ना लाहब के शिकायत के आधार पर पीटकर खने के करावास में डाल देता है और सत्रह में से आठ रुपये उपर के अफसर को पहुँचाकर शेष सात रुपये अपने सहयोगी के साथ मिलकर दबा लेता है। ईपू और ममदु इस घोर अमानवीय-गैरकानूनी कृत्य को चुपचाप खड़े होकर देखते रह जाते हैं और जब सूचना पाकर चासमन हसनदीन की फन्नी) खाना पहुँचती है तो उससे हसनदीन को छुड़ाने के लिए हरनाम सिंह द्वारा पचास रुपये माँगा जाता है। इसी कशमकश वाली स्थिति में कबा का समापन हो जाता है। कथनक का सबसे महत्वपूर्ण हिस्सा इसका अंतिम पड़ाव है, जहाँ कथाकार ने तात्कालीन भ्रष्ट व व्यर्थ सत्ता के कारण घोर गरीबी में जी रहे हसनदीन के परिवार को घोर अमानवीय कतना के सम्मुख होना पड़ता है। अमूमन किसी भी मानव समुदाय के लिए शोषण की यह अंतिम सीमा होती है। इसके बाद व्यवस्था के प्रति उनमें विद्रोह की भावना का पनपना स्वाभाविक बात है। यही कारण है कि प्रस्तुत पुस्तक के पलेप पर लिखित इस कथन में थोड़ी सी भी अतिशयोक्ति का भाव नहीं दिखता- 'अरक ने इस उपन्यास को ऐसे स्वैह हाथों और मर्मिकता के साथ रचा है कि उस सारे शोषण के प्रति, जो गरीब कश्मीरियों को सहना पड़ता है, पाठक के मन में क्रोध और बगावत की एक तेज लपट भड़क उठती है।' इसके साथ ही साथ यह भी कहा जा सकता है कि इस स्थिति में यदि वह समुदाय किसी कुशल नेतृत्व के अभाव में विद्रोह का रास्ता अख्तियार करने का सहस न भी दिखा पाये तो कम से कम उनका बालाक व बहकाउ नेतृत्व के बहकावे में आ जाना लाजिमी हो है। जिस पर यदि बहकावे के भीतर सांप्रदायिकता का इधन मौजूद हो तो मानवीयता का घोर रूप में शर्मसार होना तय ही होता है और कश्मीर में ऐसा ही हुआ भी।

हम इस बात को झूटला नहीं सकते कि एक तरफ धर्म ने मानव को मानव बने रहने का पाठ पढ़ाया है तो दूसरी ओर इसके ठेकेदारों ने अपनी स्वयंपूर्ति के बरवस मानव समुदाय को बौटने और उन्हें आपस में लड़ने जैसे घोर अमानवीय कार्य को भी बड़ी आसानी से अंजाम दिया है। इस तरह के कार्य को अंजाम देने में उन्होंने सांप्रदायिकता का इस्तेमाल सबसे बड़े हथियार के रूप में किया है। जब बात सांप्रदायिकता की ही है तो सबसे पहले रुककर उससे जुड़े विभिन्न पहलुओं पर विचार कर लेना जरूरी है। राम पुनियाजी व शरद शर्मा के शब्दों में - 'सांप्रदायिकता एक ऐसा विश्वास या विचारधारा है जिसके अनुसार एक धर्म से तालुक रखनेवाले सभी लोगों के सामान्य आर्थिक, राजनीतिक और सामाजिक हित समान होते हैं और ये हित दूसरे धर्म से जुड़े लोगों के हितों से अलग होते हैं।' पृथक सामुदायिक हितों के आधार पर एक समुदाय का दूसरे समुदाय से अलग होने व समझने के कारण उनमें संपर्क वाली स्थिति का आना या उत्पन्न किये जाने की संभावना हमेशा ही बनी रहती है और भारत जैसा बहुधर्मीय देश तो लंबे समय से इसका दृष्टांत ही बना हुआ है। यही कारण है कि भारत के सदर्थ से जोड़ते हुए विभिन्न चंद्र सांप्रदायिकता को इस प्रकार परिभ्रमित करते हैं- 'सांप्रदायिकता एक ऐसी विचारधारा है जो इस विश्वास पर आधारित है कि भारतीय समाज ऐसे धार्मिक समुदायों में बँटा हुआ है जिसके आर्थिक, राजनीतिक, सामाजिक और सांस्कृतिक हित अलग-अलग हैं और यहाँ तक कि अपने धार्मिक अंतरों के कारण एक दूसरे के शत्रु हैं।' बावजूद इसके आजादी के बाद धर्मनिरपेक्ष संविधान के निरवकों को मानकर चली आ रही भारत देश में इस शत्रुता को

प्रत्यक्ष रूप में प्रकट होने का मौका वदा-कदा ही मिल पाया है। पर इसका मतलब यह कदाई नहीं है कि सांप्रदायिकता की भावना खत्म हो गई है क्योंकि विचारधारा के रूप में इसे सभी समुदाय के तथाकथित ठेकेदारों ने हमेशा प्रचारित-प्रसारित करने का काम किया है और वे अपने इस मकसद में बहुत हद तक सफल भी हुए हैं। अमूमन हम इस विचारधारा की मिनाखा तब तक नहीं कर पाते हैं जब तक कि यह उग्र रूप धारण कर सांप्रदायिक दंगों के रूप में परिवर्तित न हो जाए जबकि दंगों से पहले यह विचारधारा प्रभाव रूप में परिवर्तित व परिवर्तित-प्रसारित होती रहती है। यही कारण है कि सांप्रदायिक दंगों के उभरने के साथ प्रक्षेत्र रूप में चलनेवाली सांप्रदायिक विचारधारा के बीच के संबंध पर प्रकटा डालते हुए विभिन्न चंद्र कहते हैं- 'सांप्रदायिक हिंसा आम तौर पर उस समय उभरती है जब पहले से चली आ रही सांप्रदायिक चिंतन की तीव्रता एक खास स्तर तक पहुँच जाती है और सांप्रदायिक भय, संदेह और तकरत में वृद्धि के कारण बालाकरण दृष्टि हो जाता है। इसलिए सांप्रदायिक विचारधारा बिना हिंसा के भी बनी रह सकती है परंतु सांप्रदायिक हिंसा बिना सांप्रदायिक विचारधारा के अस्तित्व में नहीं रह सकती। दूसरे शब्दों में, सांप्रदायिक विचारधारा राजनीति रोग है, सांप्रदायिक हिंसा मात्र बाहरी लक्षण है। दुर्भाग्यवश, सांप्रदायिक हिंसा की प्रस्तावना और पूर्वाभास के रूप में सांप्रदायिक विचारधारा की मौजूदगी को आमतौर पर नजरअंदाज किया जाता है, सांप्रदायिकता का बोध सिर्फ उसी समय दर्ज किया जाता है जब हिंसा भड़क उठती है।'।

यह बात भी गौरतलब है कि प्रक्षेत्र रूप से चलती रहनेवाली सांप्रदायिक विचारधारा को पुट करने में कतिपय कारकों का योगदान रहता है। इन कारकों में राजनीति और धर्म का घालमेल एक महत्वपूर्ण कारक है। आजादी के पहले से ही भारतीय राजनीति ने इस चरित्र को अपना लिया था या यूँ कहें कि कुछ राजनेताओं ने अपनी कुटील स्वार्थपूर्ति हेतु भारतीय राजनीति को इस चरित्र में डालने में बहुत हद तक सफलता पा लिया था जिसके परिणामस्वरूप आजादी के बाद देश को विभ्रान्त की त्रासदी के सम्मुख होना पड़ा था। पर वास्तव में देखा जाये तो धर्म और राजनीति दो पृथक संकल्पनाएँ हैं। राजनीति को धर्म से पृथक कर उसकी वास्तविक प्रकृति को स्पष्ट- जानने के लिए अस्गर अली इजीनियर के इस कथन को देखा जा सकता है कि 'धर्म की ऐसी कोई भी व्याख्या, जो असहिष्णुता और हिंसा को बढ़ावा देती हो, कभी भी स्वीकार्य और सही नहीं हो सकती। सत्य, न्याय, प्रेम और सहृदयता के अतिरिक्त धर्म और किसी चीज को बढ़ावा नहीं देता। इन मूल्यों के बिना धर्म राजनीतिक विचारधारा तो हो सकता है परन्तु धर्म नहीं कहला सकता।' कहने का मूल तात्पर्य है कि धर्म कभी भी हिंसा का समर्थन नहीं करता। प्रस्तुत उपन्यास में धर्म की इस प्रवृत्ति (कश्मीरियत) का चित्रण मिलता है, जहाँ हसनदीन अपने सैलानियों को लेकर बापम ऋषि के दरबार में पहुँचते हैं। उसकी मनोदशा का चित्रण करते हुए अरक जी कहते हैं - 'मन उसका उत्पुल था। बाबा ऋषि के लिए एक असीम भ्रष्टा से भरा हुआ था। खुदा और बाबा ऋषि में यह कोई अन्तर न देख पाता था। बाबा ऋषि पहुँचे हुए फकीर थे और जन-साधारण की भाषा में पहुँचे हुए का मतलब खुदा को पहुँचे हुए से है और इसलिए हसनदीन की दृष्टि में बाबा पामदीन और खुदा कोई दो नहीं थे।' साथ ही उग्र सांप्रदायिकता और सत्त्वा राजा रणजीत सिंह का शासनकाल) की प्रताड़ना के बरवस कश्मीर के मुस्लिम समुदाय के मन में सिवलों के प्रति मौजूद टीस का भी चित्रण मिलता है। उपन्यास के एक स्थल पर खन्ना साहब जब हसनदीन को अलग से बाय पीने के पैसे देने के

बजाय एक सिवख दुकानदार के वहाँ उसे धाय पीने के लिए कहा तो वह बात उसे बहुत दुरा लगा और उसे (हसनदीन को) पूरे दिन में पहली बार लगा कि उसका सैलानी केवल अपने स्वार्थ में विश्व रखनेवाला इंसान है। उसे दूसरी की भावना का कष्ट करना नहीं आता, जो इस्लामियत के नाले बहुत गलत प्रवृत्ति है। इस स्थिति को उपन्यासकार इस तरह बयां करते हैं - "उसका माया पहली बार उनका और उसे लगा कि नबारीयों को समझने में उससे भारी गलती हो गयी है। अच्छे खानदानी विजिटर अपने साईसों को ऐसे मजबूर नहीं करते। बनी हुई बात थी, सब जानते थे कि खश्मीर के मुसलमान सिवखों के हाथ का नहीं खाते। बात केवल हलात-इन्तके की थी या उसकी जड़ें उस गहरी, तीव्र घृणा में जमी थी, जो राजा रणजीत सिंह के सिवख सुबेदारों के अत्याचारों का कुछ ही वर्ष पहले के सांप्रदायिक दंगों ने मुस्लिम कश्मीरी जनता के दिलों में कर दी थी, कारण कुछ भी हो, हसनदीन बचपन से यह देखता आया था कि अच्छे विजिटर, हिंदू हो, अंग्रेज हों या सिवख, उलकी इस भावना का मान रखते थे।"

सांप्रदायिक विचारधारा को पुष्ट करनेवाला दूसरा महत्वपूर्ण कारण है - सत्ता की व्यर्थता के कारण लम्बे अरसे तक एक बहुसंख्यक समुदाय का घोर गरीबी में जीने को मजबूर होना। वर्तमान भारत में सांप्रदायिकता की जमीन का हमेशा तैयार रहने के संदर्भ में विधि-निराका कहना है - "दरअसल पूँजीवादी विकास ने स्पष्ट और तीव्र असमानताओं को जन्म दिया है एवं इस संदर्भ में पिछले वर्षों के दौरान परिस्थिति बदतर ही हुई है। हालाँकि मोटे तौर पर आर्थिक अघसर जनता को पहले से कहीं ज्यादा उपलब्ध है परंतु जहाँ तक उन अवसरों तक पहुँच का सवाल है अब कहीं अधिक असमानता मौजूद है। लोगों की आकांक्षा जितनी तेजी से बढ़ रही है उतनी रफ्तार से उन्हें पूरा होना संभव ही नहीं है। इसलिए सांप्रदायिकता के विकास के लिए जमीन तैयार करने में आर्थिक असमानता की स्थिति का भी महत्वपूर्ण योगदान रहता है। जिस पर बात जब आजादी के बाद से लेकर कश्मीरी पंडितों के विस्थापन तक के काल खंड में कश्मीर घाटी की आर्थिक असमानता और प्रशासनिक विफलता की ही तो उसकी बराबरी कोई नहीं कर पायेगा। खासकर अधिसंख्यक आम जनता की आर्थिक विपन्नता बेहद चिंताजनक दिखती है। प्रस्तुत उपन्यास की पृष्ठभूमि कश्मीर के दूसरे प्रधानमंत्री बख्शी गुलाम मुहम्मद का शासनकाल है, जो आर्थिक, शैक्षिक व सांस्कृतिक दृष्टि से तब तक का स्वर्णिम काल था। इसके बावजूद उपन्यास के एक स्थल पर अशक ने घाटी की घोर गरीबी को हसनदीन के फिरन से जुड़े संदर्भ के स्वाल्प के मार्फत बयां करते हैं - "कश्मीर के लोग इसके (फिरन के) बिना कैसे जिंदा रहते? मीठी हो या किसान, गुजर हो या पण्डित, यहाँ पर तो प्रायः सभी घोर गरीबी में दिन गुजारते हैं। बरसों में एक बार ईद या नौराते पर फिरन सिलवा पाते हैं, सोते-जागते उसे पहने रहते हैं। सदी-गर्मी उसी में गुजार देते हैं।"

उक्त परिस्थितियों की मौजूदगी ने कश्मीरी पंडितों के विस्थापन (1990) में महत्वपूर्ण योगदान तो दिया ही पर साथ ही साथ विस्थापन के दशक की राजनैतिक अपरिपक्वता एवं गलतियों ने इस नारकीय घटना को अंजाम दिया। इस दशक का इतिहास केन्द्र सरकार की राजनीतिक गलतियों एवं फातक अब्दुल्ला की अपरिपक्वता का इतिहास है। इस दौर के इतिहास पर टिप्पणी करते हुए अशोक कुमार पांडेय का कहना है - "इस दौरान कश्मीर समस्या को सुलझाने के लिए वहीं लोकतांत्रिक स्पेस का

सृजन करने की जगह उन्नी नींदियों की और कड़ाई से लागू किया गया जिन्होंने वहाँ यह भाव बनाया था कि कश्मीरी जनमत का दिल्ली की नजर में कोई सम्मान नहीं। नतीजा यह हुआ कि समस्या सुलझाने की जगह और उलझती चली गई। कश्मीर में अलग-अलग स्तरों पर असंतोष लगातार बढ़ता गया जिससे अन्ततः पाकिस्तान-परस्त सांप्रदायिक ताकतों को अपने एजेंडे के विस्तार में मदद मिली। और जैसा कि खान बताते हैं, बंदूक के असर और बंदूक के भय से जिहाद की एक ऐसी परिभाषा लगातार फैलाई और आम कश्मीरी के जेहन में पैबस्त की गई जो सतही, विकृत और भ्रामक थी; जिसमें लोगों को भरसा दिलाया गया कि वे ब्राह्मण कालीवाद और हिंदू साम्राज्यवाद के शिकार हैं और जिहाद 'निजाम-ए-मुस्तफा' बनकर इससे मुक्ति दिलाएगा।" इसी विकृत और भ्रामक भावना ने घाटी से कश्मीरी पंडितों के विस्थापन को अंजाम दिया।

निष्कर्षतः यह कहा जा सकता है कि अशक ने इस उपन्यास में हसनदीन जैसे छोड़वानों के कारुणिक जीवन के चित्रण के माध्यम से उन तमाम कारणों की पड़ताल करने की कोशिश की है जिसने कश्मीर को बदलने में महत्वपूर्ण भूमिका निभाई थी। जिसके कारण ये घोर गरीबी से युक्त अभिशप्त जीवन जीने के लिए बाध्य थे। इस पड़ताल की सबसे बड़ी खासियत यह है कि इसमें तब के कश्मीरी वादियों में निहित उस आसन्न औंधी की झलक भी मिलती है, जो आगे चलकर विध्वंसक रूप धारण किया था। अतः यह कहना अत्युक्ति नहीं होगी - "उपेन्द्रनाथ अशक कृत 'पत्थर अल पत्थर' उपन्यास अपने छंदों से कलेवर में कश्मीरी गरीबों के शोषण और उत्पीड़न की महामुग्धा है। कश्मीर की पृष्ठभूमि पर लिखा गया यह पहला उपन्यास है, जिसमें एक गरीब कश्मीरी छोड़वान हसनदीन की जिंदगी के माध्यम से शुरू होता है, लेकिन पाठक इसकी पंक्तियों के बीच से उस आसन्न औंधी की झलक पा जाते हैं जिसने आज समूचे कश्मीर को अपनी गिरफ्त में ले रखा है।" संदर्भ सूची :-

1. शुभल, रजनीश कुमार (संरक्षक), बहुवचन, प्रक- 64-65-66, महात्मा गांधी अंतरराष्ट्रीय हिंदी विश्वविद्यालय, वाराणसी, पृ. - 17।
2. पांडेय, अशोक कुमार, कश्मीर और कश्मीरी पंडित, राजकमल पेंथरबैक, दरियागाज, नई दिल्ली, तीसरा संस्करण : 2020, पृ. - 233।
3. अशक, उपेन्द्रनाथ, पत्थर अल पत्थर, हार्पर हिन्दी, नौरात, संस्करण : 2011, पृ. 1।
4. पुनिया, रम्य, एव शर्मा, शब्द, सांप्रदायिकता व पाकिस्तान एकाउंट, कर्लंड कमिश्न इंडिया एव वाणी प्रकाशन, प्रथम संस्करण : 2011, पृ.-73
5. चन्द, विधि, आजादी के बाद का भारत, हिंदी माध्यम कार्यन्वय निदेशालय, दिल्ली विश्वविद्यालय, संस्करण 2017, पृ.-610।
6. वही, पृ. : 611।
7. इंगोनिगर, असमर अली, धर्म और सांप्रदायिकता, वाणी प्रकाशन, नयी दिल्ली, प्रथम संस्करण : 2012, पृ. : 175।
8. आशक, उपेन्द्रनाथ, पत्थर अल पत्थर, हार्पर हिन्दी, नौरात, संस्करण : 2011, पृ.- 57।
9. वही, पृ. 3 79।
10. चन्द, विधि, आजादी के बाद का भारत, हिंदी माध्यम कार्यन्वय निदेशालय, दिल्ली विश्वविद्यालय, संस्करण : 2017, पृ.-613।
11. आशक, उपेन्द्रनाथ, पत्थर अल पत्थर, हार्पर हिन्दी, नौरात, संस्करण : 2011, पृ. : 7।
12. पांडेय, अशोक कुमार, कश्मीर और कश्मीरी पंडित, राजकमल पेंथरबैक, दरियागाज, नई दिल्ली, तीसरा संस्करण : 2020, पृ. : 268।
13. आशक, उपेन्द्रनाथ, पत्थर अल पत्थर, हार्पर हिन्दी, नौरात, संस्करण : 2011, पृ. 1।



Emergence, entry and guarding behaviour at the nest-opening site of the yellow crazy ant *Anoplolepis gracilipes* (Jerdon)

K Naskar^{1*}, SK Raut²

¹ Department of Zoology, Achhruram Memorial College, Jhalda, Purulia, West Bengal, India

² Ecology and Ethology Laboratory, Department of Zoology, University of Calcutta, Kolkata, West Bengal, India

Abstract

The yellow crazy ant *Anoplolepis gracilipes* is a notorious invasive animal species causing serious problems in the areas where it has been introduced so far. Accordingly various attempts have been made to collect biological information to manage the said ant species. Recently, we had the opportunity to study the behavioural events in respect to emergence from the nest, entering the nest as well as guarding the nest –hole in *A. gracilipes* occurring in the Achhruram Memorial College campus, Purulia, West Bengal, India. It is revealed that these ants are habituated to go out of the nest on average 13.92 ± 1.12 SE, entering the nest 10.9 ± 0.75 SE and guarding the nest –hole 12.73 ± 1.16 SE (N=85) per minute during day hours. While such numbers differed significantly ($p < 0.05$) with respect to behavioural events considered for studies, no significant difference could be established in respect to seasons ($p < 0.06$). Thus the present findings suggest that, being invasive species *A. gracilipes* have developed various devices to protect them from the attack of endemic species on way of exploiting the endemic species.

Keywords: *Anoplolepis gracilipes* ants, emergence, entry, nest guarding

Introduction

The yellow crazy ant *Anoplolepis gracilipes* is one of the notable invasive animal species as could be revealed from the listed one hundred species presented by Lowe *et al* (2004) [10]. The said ant species is a native of the moist tropical lowlands of Southeast Asia and adjacent islands of the Indian and Pacific oceans (Guénard, 2019) [4]. However, nowadays, these ants are creating problems as invasive agents in certain parts of Australia, New Zealand, Chile, Durban, South Africa, Zayul, Tibet, Mexico, as well as in the Caribbean, Central and South America (Küchler, 1964, Lester and Tavite, 2004, Wettre, 2005) [7, 9]. Almost in all regions *A. gracilipes* are causing serious problems on way of threatening the endemic species of the introduced localities and they are very much involved in biodiversity degradation. (O' Dowd *et al.* 2003, Lester and Tavite, 2004, Drescher *et al.* 2007, Plentovich *et al.* 2018) [14, 9, 3, 15].

Following invasion and with the development of subsequent environmental hazards various workers have paid due attention to note the biology and inter-specific interactions of *A. gracilipes* in respect to the ecosystem where these ants became serious nuisance (Lester and Tavite, 2004, Abbott, 2005, Drescher *et al.* 2007, Kaiser - Bunbury *et al.* 2014, Lee *et al.* 2017, Plentovich *et al.* 2018) [9, 1, 3, 5, 8, 15]. However, still to date no attention has been paid by any worker to note the behaviour of these ants in respect to emergence from the nest, entry into the nest from the outside and guarding strategy encircling the opening of the nest. Thus, in course of our studies on the bioecology of ants occurring in and around Jhalda (Achhruram Memorial College premises), Purulia, West Bengal, India we took the liberty to note these behavioural events during the period of day hours at an interval of 1 hour, and the findings are worth reporting.

Materials and Methods

The nest we considered for our studies was located on the ground but very close to a big *Albizia lebbbeck* tree. The ants were seen to come out of the nest through a hole as well as entering into the nest through the said hole of and on, while certain individuals were seen to roam encircling the nest hole all along. We spent 1 minute in each occasion during any time in an hour between 06.00 h and 18.00 h at random during the period of September 6, 2008 and December 23, 2014. The data collected during an hour period were considered to calculate the mean and standard error values. Also two-way ANOVA was applied to justify the effect of the hours of the day in respect to the strategies developed by the ants regarding the frequency of emergence from the nest and entry into the nest keeping the number of ant individuals engaged in guarding the nest-hole in view.

Results

During the period of six years, we recorded data on 85 days, irrespective of seasons, at random, on the frequency of emergence from the nest, entry into the nest as well as the numbers of *A. gracilipes* were guarding the nest-hole. The behavioural variations in respect to these events have been shown in Figs. 1-12. Irrespective of study hours 1-64 (12.73 ± 1.16 SE) ant individuals kept them engaged in nest guarding, 0-33 (10.9 ± 0.75 SE) were entering the nest, and 1-59 (13.92 ± 1.12 SE) were emerging out of the nest. Results of ANOVA tests clearly indicate that the number of ant individuals took part in executing the behavioural events like emergence from the nest, entering the nest and guarding the nest –hole differed significantly ($p < 0.05$) throughout while such numbers irrespective of seasons did not differ significantly ($p < 0.06$).

Explanation of Figures

Figs. 1-12 represent the mean (+/- SE) number of ants noted guarding the nest-hole (S), entering the nest (I) and

emerging out of the nest (O) during one minute time period between 06:00 h and 07:00 h

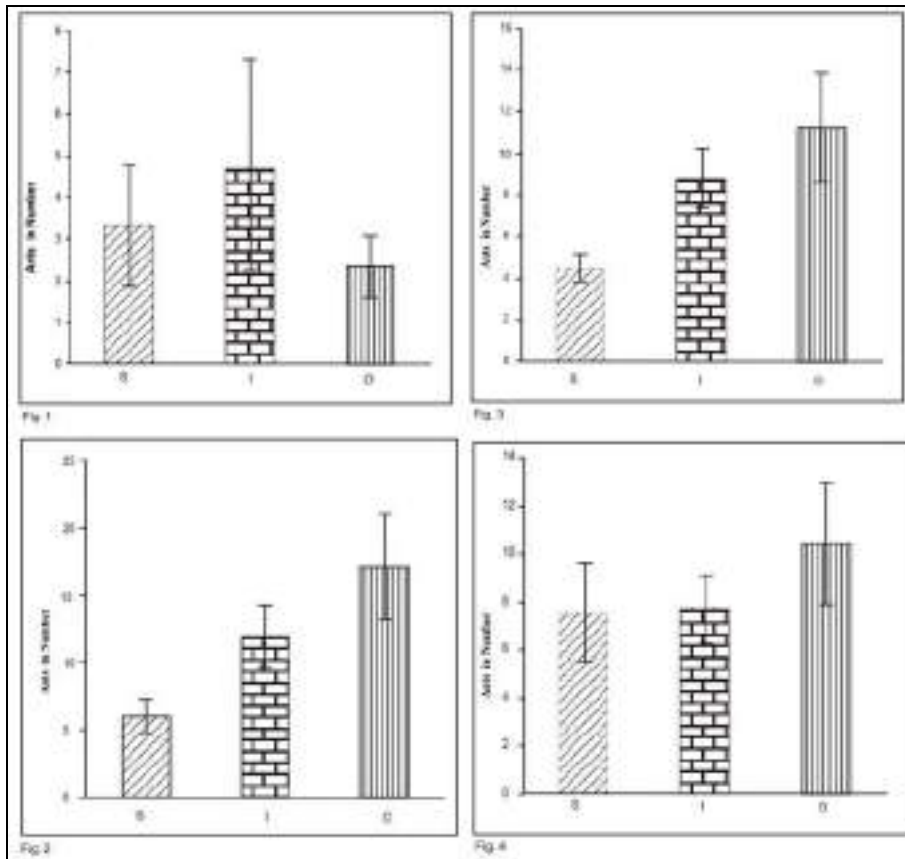


Fig 1: 07:00 h and 08:00 h (Fig.2), 08:00 h and 09:00 h (Fig.3), 09:00 h and 10:00 h (Fig.4), 10:00 h and 11:00 h

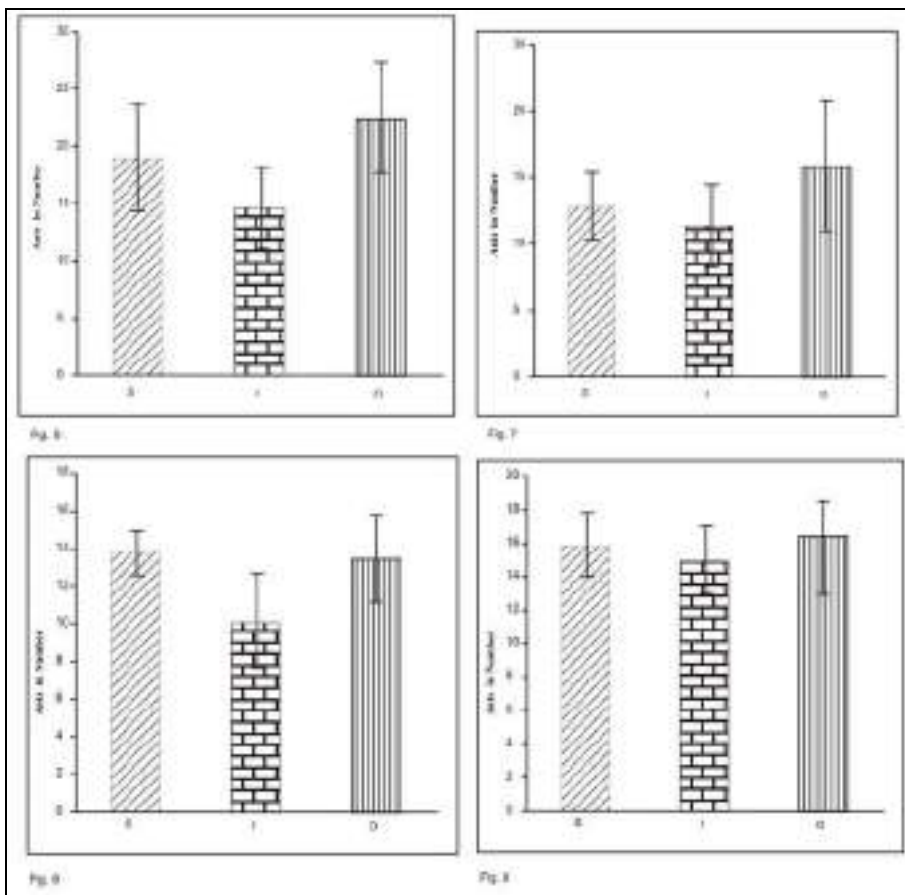


Fig 5: 11:00 h and 12:00 h (Fig.6), 12:00 h and 13:00 h (Fig.7), 13:00 h and 14:00 h (Fig.8), 14:00 h and 15:00 h

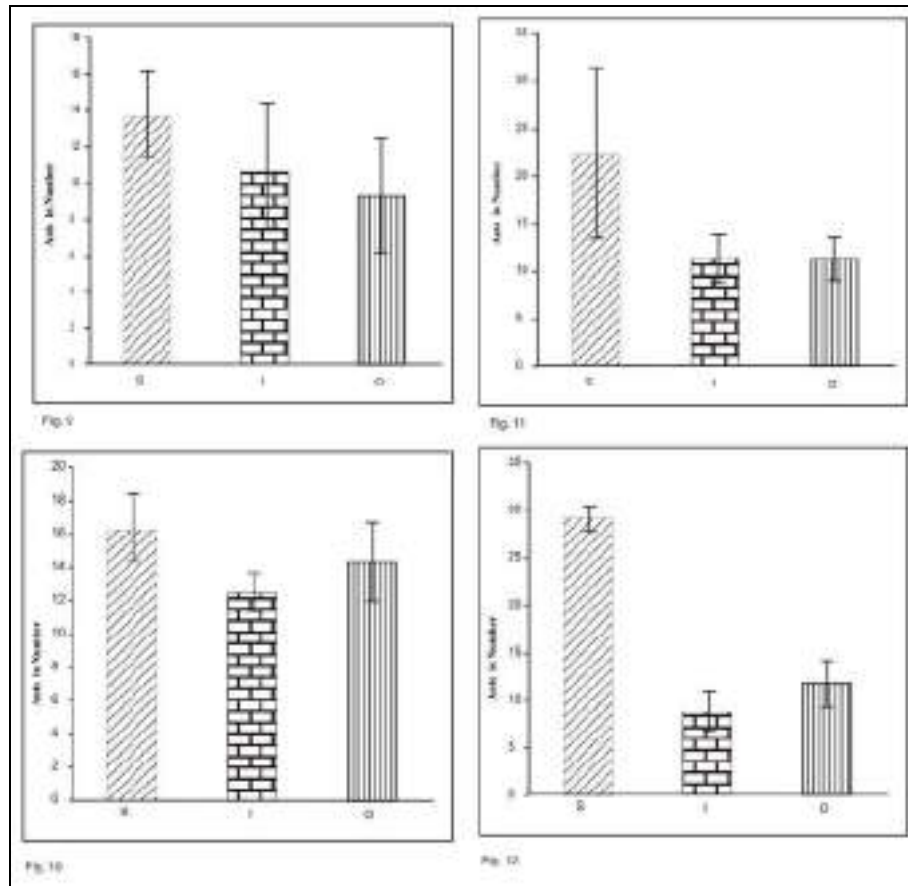


Fig 9: (Fig.9), 15:00 h and 16:00 h (Fig. 10), 16:00 h and 17:00 h (Fig. 11), 17:00 h and 18:00 h (Fig.12).

Discussion

From the results it is clear that the yellow crazy ants *A. gracilipes* are habituated to maintain a strategy for effective foraging efforts at least in respect to the hours of the day time. Though it is customary that the foragers go out of the nest from time to time and also entry of the individuals is continued simultaneously the occurrence of certain number of individuals encircling the opening of the nest is undoubtedly, a matter of interest. *A. gracilipes* ants have been listed as one of the world's most invasive alien species (Lowe. *et al.* 2004) [10]. It is reported that *A. gracilipes* are apt to establish them in a new geographical area because of traits such as aggression toward other ant species, little aggression toward members of their own species (Kirschenbaum and Grace 2008) [6]. These ants get much of their food requirements from scale insects, aphids and other Sternorrhyncha. Also, they get their carbohydrates from plant nectar. Since report on the food storage of these ants is not on record, it is, at this moment very difficult to explain why certain members remain engaged at the nest-door as guards. It may assume that, there exists possibility of robbing food from the nest by other ant species or by the members of the same species belong to the other nest-colony.

Food-snatching, robbing of the food materials from the nest as well as cleptobiosis habits have been observed in the ants *Pheidole roberti*, *Paratrechina longicornis*, *Oecophylla smaragdina*, *Tetraponera rufonigra*, *Messor aciculatus*, *Prenolepis imparis*, *Ectatomma recidumand*, and *Messor capitatus* (Lynch *et al.*, 1980, Yamaguchi, 1995, Breed *et al.*, 2012, Naskar and Raut 2019) [11, 17, 2, 12]. Also, in respect to such behavioural events fighting between the owner and snatcher ants have been noted in some ant species (Naskar

and Raut 2020) [13]. Thus, it is most likely that, *A. gracilipes*, being an invasive species creates different kinds of conflicts at least with endemic ones to establish their aggressive and dominant habit so as to keep the victimized ant species under fear psychosis. This sort of behaviour may force the endemic species for retaliation, if possible unitedly. Perhaps, anticipating such an attack *A. gracilipes* left no effective strategy to protect them and to establish them in a new area successfully.

References

1. Abbott KL. Supercolonies of the invasive yellow crazy ant, *Anoplolepis gracilipes*, on an oceanic island: forager activity patterns, density and biomass. *Insectes Sociaux*,2005:52(3):266-273.
2. Breed MD, Cook C, Krasnec MO. Cleptobiosis in social insects. *Psyche*,2012:7(2). DOI - 10.1155/2012/484765
3. Drescher J, Blüthgen N, Feldhaar H. Population structure and intraspecific aggression in the invasive ant species *Anoplolepis gracilipes* in Malaysian Borneo. *Molecular Ecology*,2007:16(7):1453-1465.
4. Guénard B. *Anoplolepis gracilipes*: The global ant biodiversity informatics (GABI) database. 2019: Retriever, 2019.
5. Kaiser-Bunbury C, Cuthbert H, Fox R, Birch D, Bunbury, N. Invasion of yellow crazy ant *Anoplolepis gracilipes* in a Seychelles UNESCO palm forest. *NeoBiota*,2014:22:43-57.
6. Kirschenbaum R, Grace JK. Agonistic interactions among invasive ant species (Hymenoptera: Formicidae) from two habitats on Oahu, Hawaii. *Sociobiology*,2008:51(3):543-554.

7. Kuchler AW. Natural vegetation (maps), 1964. 16, 17, 97, 141, 161, & 162. Ed. By E. B. Espenshade Jr. Goode's World Atlas, 12th edn. Rand McNally. Chicago.
8. Lee CC, Nakao H, Tseng SP, Hsu HW, Lin GL, Tay JW *et al.* Worker reproduction of the invasive yellow crazy ant *Anoplolepis gracilipes*. *Frontiers in zoology*,2017;14(1):1-12.
9. Lester PJ, Tavite A. Long-legged ants, *Anoplolepis gracilipes* (Hymenoptera: Formicidae), have invaded Tokelau, changing composition and dynamics of ant and invertebrate communities. *Pacific Science*, 2004;58(3):391-401.
10. Lowe S, Browne M, Boudjelas S, De Poorter M. *100 of the world's worst invasive alien species: a selection from the global invasive species database* (Vol. 12). Auckland: Invasive Species Specialist Group, IUCN, Switzerland, 2004, (12).
11. Lynch JF, Balinsky EC, Vail SG. Foraging patterns in three sympatric forest ant species, *Prenolepis imparis*, *Paratrechina melanderi* and *Aphaenogaster rudis* (Hymenoptera: Formicidae). *Ecol. Ento*,1980;5:353-361
12. Naskar K, Raut SK. Ant's necrophagy on ants. *Global Journal of Bio-Science and Biotechnology*, 2019;8(4):335-339.
13. Naskar K, Raut SK. Food-snatching behaviour in ants. *Proceedings of Zoological Society India*,2020;19(2):7-15.
14. O'Dowd DJ, Green PT, Lake PS. Invasional 'meltdown' on an oceanic island. *Ecology letters*,2003;6(9):812-817.
15. Plentovich S, Russell T, Fejeran CC. Yellow crazy ants (*Anoplolepis gracilipes*) reduce numbers and impede development of a burrow-nesting seabird. *Biological invasions*,2018;20(1):77-86.
16. Wetterer JK. Worldwide distribution and potential spread of the long-legged ant, *Anoplolepis gracilipes* (Hymenoptera: Formicidae). *Sociobiology*, 2005;45(1):77-97.
17. Yamaguchi T. Interspecific competition through food robbing in the harvester ant, *Messor aciculatus* (Fr. Smith), and its consequences on colony survival. *Insectes Sociaux*,1995;42:89-101.

Author's copy

provided for non-commercial and educational use only



No material published in Journal of Insects as Food and Feed may be reproduced without first obtaining written permission from the publisher.

The author may send or transmit individual copies of this PDF of the article, to colleagues upon their specific request provided no fee is charged, and further-provided that there is no systematic distribution of the manuscript, e.g. posting on a listserv, website or automated delivery. However posting the article on a secure network, not accessible to the public, is permitted.

For other purposes, e.g. publication on his/her own website, the author must use an author-created version of his/her article, provided acknowledgement is given to the original source of publication and a link is inserted to the published article on the Journal of Insects as Food and Feed website by referring to the DOI of the article.

For additional information
please visit
www.wageningenacademic.com/jiff.

■ Editor-in-chief:

Prof. Arnold van Huis, Wageningen University, the Netherlands

■ Associate editors:

Prof. Eraldo M. Costa-Neto, Universidade Estadual de Feira de Santana, Brazil; **Dr Arnout Fischer**, Wageningen University, the Netherlands; **Dr Laura Gasco**, University of Turin, Italy; **Dr John N. Kinyuru**, Jomo Kenyatta University of Agriculture & Technology, Kenya; **Dr Cecilia Lalander**, Swedish University of Agricultural Sciences, Sweden; **Dr Dennis G.A.B. Oonincx**, Wageningen University, the Netherlands; **Prof. Santos Rojo**, University of Alicante, Spain; **Dr Nanna Roos**, University of Copenhagen, Denmark; **Dr Birgit Rumpold**, Technische Universität Berlin, Germany; **Prof. Jeffery K. Tomberlin**, Texas A&M University, USA; **Prof. Leen Van Campenhout**, KU Leuven, Belgium

■ Editorial board:

Prof. Jérôme Casas, University of Tours, France; **Dr Adrian Charlton**, FERA, United Kingdom; **Dr Florence Dunkel**, Montana State University, USA; **Patrick Durst**, Forestry and natural resources consultancy, Thailand; **Prof. Jørgen Eilenberg**, University of Copenhagen, Denmark; **Dr Sunday Ekesi**, *icipe*, Kenya; **Prof. Kokoete Ekpo**, Federal University Otuoke, Nigeria; **Prof. Ying Feng**, Research Institute of Resources Insects, China; **Dr Mark Finke**, Mark Finke LLC, USA; **Prof. Lynn Frewer**, Newcastle University, United Kingdom; **Prof. Richou Han**, Guangdong Academy of Sciences, China; **Dr Yupa Hanboonsong**, Khon Kaen University, Thailand; **Dr Marc Kenis**, CABI, Switzerland; **Dr Catriona Lakemond**, Wageningen University, the Netherlands; **Prof. Harinder Makkar**, University of Hohenheim, Germany; **Dr José Manuel Pino Moreno**, Universidad Nacional Autónoma de México, Mexico; **Prof. Benno Meyer-Rochow**, Oulu University, Finland; Andong University, South Korea; **Prof. Kenichi Nonaka**, Rikkyo University, Japan; **Dr Søren Bøye Olsen**, University of Copenhagen, Denmark; **Prof. Maurizio G. Paoletti**, University of Padova, Italy; **Prof. John Schneider**, Mississippi State University, USA; **Dr Oliver Schlüter**, Leibniz Institute for Agricultural Engineering Potsdam-Bornim, Germany; **Prof. Joop van Loon**, Wageningen University, the Netherlands; **Dr Teun Veldkamp**, EAAP Commission on Insects / Wageningen Livestock Research, the Netherlands; **Prof. Wim Verbeke**, Ghent University, Belgium; **Dr Jintana Yhoung-Aree**, Institute of Nutrition, Mahidol University, Thailand; **Prof. Jibin Zhang**, Huazhong Agricultural University, China; **Prof. Jose Jacobo Zubcoff Vallejo**, University of Alicante, Spain

■ Publication information

Journal of Insects as Food and Feed
ISSN 2352-4588 (online edition)

Subscription to 'Journal of Insects as Food and Feed' (4 issues a year) is either on institutional (campus) basis or on personal basis. Subscriptions can be online only. Prices are available upon request from the publisher or from the journal's website (www.wageningenacademic.com/jiff). Subscriptions are accepted on a prepaid basis only and are entered on a calendar year basis. Subscriptions will be renewed automatically unless a notification of cancellation has been received before the 1st of December before the start of the new subscription year.

Further information about the journal is available through the website www.wageningenacademic.com/jiff.

■ Paper submission

Manuscripts should be submitted via our online manuscript submission site, www.editorialmanager.com/jiff. Full instructions for electronic submission, as well as the guideline for authors are directly available from this site or from www.wageningenacademic.com/jiff.

■ Internet access

The online edition is available at www.wageningenacademic.com/jiff with free abstracts and keywords. A RIS alert for new online content is available as well.

■ Editorial office

jiff@wageningenacademic.com

■ Orders and claims

P.O. Box 220, 6700 AE Wageningen
The Netherlands
jiff_cr@wageningenacademic.com
Tel: +31 317 476516



**Wageningen Academic
Publishers**

Taxonomic analysis of some forest insects used in the diets in Mexican rural areas: evaluation and perspectives

J.M. Pino Moreno^{1*}, A. Ganguly² and H. Reyes-Prado³

¹Institute of Biology, National Autonomous University of Mexico, Department of Zoology, Entomology Laboratory, Ap. Postal 70-153, 04510 Mexico City, México; ²Department of Zoology, Achhruram Memorial College, Jhalda 723202 Dist. Purulia, India; ³Chemical Ecology Laboratory, ESS Jicarero – Universidad Autónoma del Estado de Morelos. Carretera Galeana-Tequesquitengo s/n, C.P. 62909, Jojutla de Juárez, Morelos, México; jpino@ib.unam.mx

Received: 13 August 2020 / Accepted: 12 January 2021

© 2021 Wageningen Academic Publishers

RESEARCH ARTICLE

Abstract

In the present work a taxonomic analysis of Mexican edible forest insects along with their host plants have been reviewed. We have recorded 73 insect species under 26 families and 6 orders, namely: Orthoptera, Hemiptera-Heteroptera, Lepidoptera, Coleoptera, Diptera and Hymenoptera, with the highest number of species belonging to Coleoptera (19) followed by Hymenoptera (18). Additionally a total of 51 host plant species under 17 families, and their distribution among the different vegetation types also have been presented. The importance of insects in the diet of rural communities has been discussed in the light of different socioeconomic and biological factors. These issues must be addressed and resolved, to carry out the coherent management of edible insects, considering the traditional knowledge that the rural inhabitants possess.

Keywords: aboriginal, entomophagy, Mexico

1. Introduction

Human societies have consumed insects for thousands of years as emergency foodstuff, staple foodstuff or delicacy. At a global level, in total 1,900 edible insect species have been registered until today (Van Huis *et al.*, 2013). This proves entomophagy (the habit of consuming insects by man) has persisted for centuries, being insects a highly nutritious food resource (Ramos-Elorduy, 2004). Unfortunately, serious scientific works have started at a comprehensive level only in the last decade (Dossey *et al.*, 2016; Halloran *et al.*, 2018; Schowalter, 2013; Van Huis and Tomberlin, 2017).

In relation to their abundance, even though insects represent the largest quantity of biomass in forests, they have been little studied in these ecosystems. In addition, these animals have an enormous economic value due to the environmental services they render. They are main pollinators, they carry out diverse cleansing activities that include manure elimination, carcass decay and organic matter decomposition and recycling, they are soil producers

and conditioners, and a great food resource for wildlife (invertebrates, amphibia, reptiles, birds, fish and mammals) (Govorushko, 2018). In spite of all this, almost all the forest insects are considered as pests by the forest engineers (Cibrian *et al.*, 1995). In Mexico, indigenous people have vast entomophagic traditional knowledge on various forest insects, and hence the great diversity of forest habitats and the variety of edible insects represent a range of opportunities for its management and exploitation.

Studies on forest insect collection and management are limited in Mexico. However, there are successful examples in other parts of the world that illustrate the potential of forest insects as foodstuffs for man, as in case of the larvae of the weevil *Rhynchophorus ferrugineus papuanus* (Coleoptera: Curculionidae), called sagu parasites or sagu worms of the palm *Metroxylon sagu* (Family: Areaceae); in Papua New Guinea they are an important nutritious food resource (Onyeike *et al.*, 2005). This is also the case of the palm weevil *Rhynchophorus phoenicis* in Cameroon (Fogot *et al.*, 2015). The rustic exploitation of the edible

caterpillars *Gynanisa maya* and *Gonimbrasia zambesina* (Lepidoptera: Saturniidae) is made by the natives in the north of Zambia and the Democratic Republic of Congo, as they frequently bring young larvae from the forest and put them on acacias (Family: Fabaceae) near their homes and rear them until they are ready to be eaten. Finally, in the tropical areas of America toasted larvae and adults of the palm weevil *Rhynchophorus* spp., are harvested from different palm species and are consumed as delicacies.

Insects are highly nutritious in terms of protein and amino acids (Ramos-Elorduy *et al.*, 1997) and in the Mexican Republic they are traditional foodstuffs in the rural areas, they are used by diverse cultural groups such as: *chol*, *huasteco*, *lacandón*, *maya*, *mazateco*, *mazahua*, *mixteco*, *nahuatl*, *otomí*, *otopame*, *popolaca*, *tarahumara*, *tarasco*, *tlapaneco*, *tojolabal*, *tononaco*, *tzeltal*, *tzotzil*, *zapoteco*, *zoque* and *mestizos*; as hundreds of species have been consumed since pre-Hispanic times (Ramos-Elorduy, 2004; Ramos-Elorduy and Pino, 1989, 2002; Ramos-Elorduy *et al.*, 1985, 1998b, 2002a), more in depth studies on forest insects are of great importance. On the other hand, the Mexican flora is one of the most diverse on a worldwide level. In Mexico the concept of forest vegetation is defined as the group of plants and fungi that grow and develop naturally, forming forests, rainforests, arid and semiarid zones and other ecosystems, giving place to the development and well-balanced coexistence of other natural resources and processes.

The vegetation types most widely distributed in the country are the following ones:

- Coniferous forest: vegetation dominated by evergreen trees of the conifer group among them pines (*Pinus*) and firs (*Abies*) are the dominant ones. They are generally found in the temperate and cold climates of the upper zones of mountain ranges that exist almost in the entire country.
- Oak forests: are a plant community made up of different oak species of the genus *Quercus* that grow in diverse ecological conditions, ranging from sea level to almost 3,000 m altitude. The distribution of oak forests is similar to the coniferous forests.
- Mountain cloud forest: in terms of physiognomy it is a dense type of vegetation, typical of mountainsides that are protected from strong winds and excessive sunshine. They develop at an altitude where fog banks appear and where mist forms throughout the year. This is an exuberant forest, rich in ferns and lianas, as well as epiphytes that grow on the trees. An important portion of the flora is endemic. These forests are found along the Sierra Madre Oriental where they extend along certain portions of several states, usually on mountainsides facing the Gulf of Mexico.
- Evergreen rainforest: the vegetation is dominated by several tree species, it is one of the most diverse

biological communities in the world, it is found in warm and rainy climates. The crown of the trees can be higher than 40 m and conserves an important part of its foliage throughout the year. It is found in San Luis Potosí, Veracruz, and certain regions of Hidalgo, Puebla, Oaxaca, Chiapas Tabasco, Campeche, Quintana Roo, Yucatán, Nayarit and Guerrero.

- Deciduous and sub-deciduous rainforests: the vegetation is dominated by different tree species whose leaves are deciduous. They develop in warm environments with summer rains, they are divided in medium and low according to the height of the dominant arboreal vegetation. The canopy rarely surpasses 15 m in height, even though in some cases it can reach up to 30 m. Among the characteristic genera are *Bursera* sp. (Family: Burseraceae) and *Ceiba* sp. (Family: Malvaceae) and several species of columnar cacti. It exists, for example, in a discontinuous form, from the centre of Sinaloa to the coastal zone of Chiapas, Yucatán and Veracruz.
- Thorn forest: it is a community dominated by thorny trees such as ebony, *cascalote*, *brasil* and *mezquite*. It covers a great extension in the north-western coastal plains, from Sonora to Sinaloa, the Balsas Depression and the Isthmus of Tehuantepec. Along the Gulf of Mexico coast it covers a big area in Tamaulipas, Campeche, Quintana Roo, Chiapas and Yucatán.
- Cactus scrub desert: vegetation dominated by shrubs, typical of arid and semiarid zones, this type is the most widespread in Mexico. It covers the greater part of the territory of the Baja California peninsula, as well as great extensions of the coastal plain and the low mountains of Sonora. It is typical of great areas in the Central Basin from Chihuahua and Coahuila to San Luis Potosí, Guanajuato, Hidalgo, Estado de México, Puebla, Oaxaca, Coahuila and Tamaulipas.
- Natural grasslands: it is a community dominated by grass species, occasionally accompanied by herbaceous species and shrubs of different families. It is found in Sonora and even though it exists in almost all the states of the country, it is most widely distributed in Chihuahua, Jalisco and Guanajuato.
- Mezquite forest: the plant community is dominated mainly by *mezquites* (*Prosopis* spp.) that develop as shrubs. It is common to find this community in a mixed state, for example, with the *huizaches* (*Acacia* spp.), both from the Family Fabaceae. It is distributed mainly in the central plateau, Baja California Sur, Sonora, Tamaulipas and Jalisco.

The forest vegetation of arid zones is the plant community that develops in a spontaneous way, in the regions with arid or semiarid climates, forming masses greater than 1,500 square meters (CONAFOR, 2012).

Considering the aforementioned entomological and botanical aspects and in face of the lack of entomophagic

information about forested areas, we have carried out this research with the objective of gaining knowledge about the edible forest insects of Mexico, as well as of their hosts, and thus analysing and discussing the perspectives for their tangible exploitation.

2. Materials and methods

The Institute of Biology of the National Autonomous University of Mexico (UNAM) is carrying out research in the field of 'insects as future protein sources' since 1976 (Ramos-Elorduy, 1982). Studies have been conducted in several places of the Mexican Republic like the Milpa Alta municipality of Mexico City (Ramos-Elorduy *et al.*, 1992), and in the states of Chiapas (Ramos-Elorduy and Pino, 2002), Guerrero (Ramos-Elorduy *et al.*, 1985), Hidalgo (Ramos-Elorduy and Pino, 2001a), Estado de México (Ramos-Elorduy *et al.*, 1998a), Oaxaca (Ramos-Elorduy *et al.*, 1997), Puebla (Ramos-Elorduy *et al.*, 1988a) during last 4-5 decades by means of a series of research projects that comprised field work, data collection through questionnaires, and collection of both insects and of their host plants, many of which were still unknown. The insects that were collected in diverse plant communities were placed in jars with 70% alcohol and the plants were preserved in a botanical press; in both cases we have recorded the collection data that include date, locality, collector's name, common name, native linguistic name, vegetation type and edible stage of development. The collected specimens were taken to the Institute of Biology at UNAM to be mounted, labelled, catalogued and preserved for future use. For the taxonomic work we have collaborated with several botanists and especially entomologists, as the identification of immature stages such as larvae, pupae and nymphs of different insect orders is extremely difficult. The identified insects are kept in the National Collection of Edible Insects which is housed in the Department of Zoology, UNAM.

We have also carried out a retrospective bibliographical review that consisted of diverse sources such as thesis, research papers and books on entomology where edible forest insects have been reported; in this regard the works of Durst and Shono (2012), Johnson (2012), Martínez (2016), SEMARNAT (2010) and Rzedowski (2006) were found to be extremely useful.

3. Results

The edible insects collected in the forest vegetation of Mexico are depicted in Supplementary Table S1, that includes order, family, scientific name, common name, edible stage of development, consumption site and the related references. To date, we have registered 73 species of edible forest insects under the orders Orthoptera (11 species, i.e. 15.06%), Hemiptera-Heteroptera (10 species, i.e.

13.69%), Coleoptera (19 species, i.e. 26.02%), Lepidoptera (12 species, i.e. 16.93%), Diptera (3 species, i.e. 4.10%) and Hymenoptera (18 species, i.e. 24.65%). The most represented orders are Coleoptera (genus *Mallodon* being the dominant one with 4 species that are commonly known as 'stick worms'), and Hymenoptera that includes social insects, that is, bees, wasps and ants. The most demanded and commercialised insects are grasshoppers, maguey red and white worm, *escamoles*, *jumiles*, a type of ants known as *chicatanas* and the cochineal grana; the latter has multiple applications in pharmaceutical, food, cosmetic and wine industries. We therefore appreciate that the great diversity of forest habitats harbouring edible insects presents an array of opportunities for innovative management of edible insects so as to simultaneously contribute to maintaining habitat diversity for other life forms (Defoliart, 1997). Nevertheless it is necessary to assess the link between insect gathering and the forest ecosystem, wildlife conservation and bushmeat consumption patterns (Vantomme *et al.*, 2004).

Some examples of case studies are:

Cuetla (Arsenura armida) – jonote (Heliocarpus sp., Family: Tiliaceae): in a study carried out in the Sierra de Zongolica, Veracruz, the Sierra Negra of Puebla and the Sierra Norte of Chiapas (Gomez, 2009), 63 individuals were interviewed, 84% (53.7 persons) of which are collectors that have learned the activity throughout generations for more than 30 years, while the rest (9.3) are collector-vendors of these larvae. Collection season begins in June and is over by November, and it is closely related to the rainy season, it is carried out in the woods where there are approximately 15 *jonote* trees per hectare, 8 of which are covered with worms each season. Collection is carried out only one day and in only three trees as a conservation strategy, and it is done when the worms form groups in the trunk and branches, and only the most 'fat' are collected. For collection a container is used (plastic bags, buckets, satchels), and they are fetched using poles or people climb the trees to collect them by hand. Per tree and per day a mean of 17.2 kg is collected, 76% of which is for self-consumption, 16.5% is given as a present to relatives and 7.2% is sold. A management practice can also be understood as an incipient breeding technique or 'protoculture' and it consists on moving *cuetlas* of 5 or 6 cm in length that are on trees far from the homes to *jonotes* that are nearer, so that their development can be monitored until they are 'fat' enough, thus guaranteeing their production and consumption; this practice is implemented to obtain a higher production in less time, thus rendering benefits for the local population just as, for example, the 'farm' culture carried out in Cameroon for the larvae of the weevil *Rhynchophorus phoenicis* (Fogot *et al.*, 2015), that are considered a veritable delicacy (Dounias, 2010). Of the interviewed persons, 98.8% like to eat worms, they say they taste like *chicharrón*, pork meat or fish, pumpkin seeds or

sheep barbecue; 92.0 % of the families consume a mean of 8.2 kg per season, 62.15% of the interviewed persons point out that consumption has been steady and is on the rise. For their culinary preparation they are cleaned (the intestinal tract is taken out) and then they are washed, boiled and drained, and there are recipes to prepare them fried, in broths, toasted or roasted, with scrambled eggs, as pie filling, in stews, etc. People prefer them fried as they say they are easy to prepare and are an excellent appetiser. Of the interviewees, 95.4% say they are innocuous, and there are different forms in which they can be preserved such as sun dried, toasted, refrigerated in a plastic bag or refrigerated after being boiled, and so they can last for a whole year. Their commercialisation is not a priority as only 6.6 % of the interviewees, that is 4.1 persons, carry out this activity; nevertheless they point out that it is an important source of economic income during the season in which they are abundant and that they have been selling the product for 17.4 years. For their commercialisation they are boiled with salt and chili, they are cleaned and washed, and they are sold directly in the markets to retailers or to customers on demand. In the markets they are sold in 1 kg bags and in 200 g bags, in a small plate used as a measure for 100 g or boiled and wrapped in a *tamal* leaf, also in this case approximately 100 g (Gómez, 2009).

The *chichas* (*Mallodon dasystomus* (Say) and *Mallodon molarius* Bates 1879) – walnut tree (*Carya illinoensis*, Family: Juglandaceae). Their collection takes place between January and April in the localities of Tlaxepex, Pedregal de Zaragoza and San Cristóbal in the region of Metztitlán, Hidalgo, mainly in fallen trunks of walnut trees (*Carya illinoensis*) in different states of decay. For larvae collection wood is removed by means of an electric saw, a hatchet, wedges and entomological pliers so as to render its removal easy (Acosta *et al.*, 2019). Due to their saproxilophagous habit this larvae have diverse secondary hosts such as *Acer* sp. (Aceraceae), *Bursera simaruba* (Burseraceae), *Cordia inermis* (Boraginaceae), *Quercus* sp. (Fagaceae), *Inga* sp. (Mimosaceae), *Ficus* sp. (Moraceae), *Salix* sp. (Salicaceae) and *Celtis* sp. (Ulmaceae) (Maes *et al.*, 2010). In respect to their management, the larvae thus collected are placed in plastic boxes that contain the host's wood and sawdust at room temperature and their development is monitored daily till they reach the adequate size for their consumption and/or to obtain new adults so as to start over their biological cycle. For their preparation the biggest *chichas* are placed for 24 hours at room temperature in a plastic tray so that they pass excreta and then they are washed to eliminate organic detritus that sticks to their bodies. Afterwards they are prepared according to the consumers taste, specifically fried, toasted, covered in ground bread or as appetisers or garnish that are eaten accompanied by *tortillas* and sauce (Acosta *et al.*, 2019). The diverse larval phases are considered a complementary foodstuff in terms of diet and nutrition for the population of Metztitlán, as the majority

of the inhabitants recognise their nutritive value in terms of proteins and minerals (Ramos-Elorduy, 1998b; Ramos-Elorduy and Pino, 1990) and above all because obtaining larvae does not have an economic cost. Collection is mainly for family self consumption, people consume them because they like them, because it is a tradition and because they are abundant, and they also say they are clean and tasty. In this case it is convenient to point out that insects play an important role in the functioning of the ecosystems they inhabit by means of a group of processes that can be classified as ecosystem services, for example in the regulation of nutrient recycling when they contribute to the decay of wood. Therefore, in the broadest sense, insects have enormous economic value in terms of the ecological services they provide (Johnson, 2012). The relevance of dead wood has even been recognised, for example, for the biodiversity of forest systems as an important habitat for wildlife (Merganičová *et al.*, 2012) and as an indicator and key component of the forest structural diversity and functioning, carbon sources and fuel loads (Vandekerckhove *et al.*, 2009; Woodall and Williams, 2005) and is becoming an integral part of forest management as it performs a function very important for purposes of conservation and biodiversity management (Marage and Lemperiere, 2005). These insects are currently threatened by the expansion of agriculture, since in these localities the following are cultivated: corn, bean, lettuce, walnut, tomato and cauliflower.

Chicatanas (*Atta* spp.) – black zapote (*Dyospyros digyna*). The ants of the genus *Atta* have been used since pre-hispanic times as food and it is part of traditional nutritional habits because of their agreeable taste and its high protein content (Sahagún, 1975). In Huatusco, Veracruz, *Atta cephalotes* is the most common species and, as we have said, they are known as *chicatanas*, a term that applies to the reproductive caste especially in the localities of El Coyolito and Palmillas in the aforementioned municipality of Huatusco, Veracruz, where their nests are abundant (Landerio *et al.*, 2005). Their collection is done in May and June (the highest biomass is present in June), when the ants defoliate two or three plants and place the leaves over the nest; this is a peculiar habit of the species that enables their capture by hand when they exit the nest for their nuptial flight. They can also be collected by placing a broom made out of dry sticks over the nest, then by awaiting for the ants to climb it and then shaking it over a bucket full of hot water so as to prevent their flight. In these localities two questionnaires were applied, the first to 100 persons of the municipality head of Huatusco, in the market and surrounding area, the sample consisting of 60 adults between 20 and 65 years and 40 children between 8 and 10 years. The second was applied to 50 adults between 20 and 65 years and 20 children between 8 and 10 in the village of El Coyolito, with a similar sample for Palmillas (Landerio *et al.*, 2005). According to the replies of the adults of rural zones, 100% knows them, 100% consumes

them, 90% prefers them toasted, 10% prefers them in a sauce made of *pajarito chili* or they eat them raw and only 30% knows their price in the market which varies because when populations are high they are quite cheap but become expensive when populations are low. In relation to their consumption, of the children of rural areas interviewed, 100% knows them and consumes them toasted, of the adults of urban zones 90% knows them and 80% consumes them toasted and 20% in sauces, and 85% knows their price in the market. Of the children in urban zones 60% knows them and of them 100% consumes them, 50% toasted and 50% in the form of soft toffee. And as in rural zones only 30% knows their price, which means people collect them for self consumption, that is, they are not commercialised, some persons even freeze them to consume them along the year. According to the questionnaires their consumption is higher in rural zones where it contributes significantly to the diet's nutritional content; this is different from what happens in urban areas where alimentary biodiversity is higher as well as purchasing power, and so we can say this knowledge is being lost in a day to day basis, especially in the children that live in cities because of the introduction of junk food and the emigration of people from rural areas due to the lack of employment sources (Landeró *et al.*, 2005). Nevertheless, presently there is a growing interest among entrepreneurs for manufacturing products based on *chicatanas* (Avendaño, 2002). In the same manner there are reports of great business opportunities when these insects are classified as 'exotic foods' and their culinary preparation becomes gourmet by the addition of diverse dressings that render them more attractive, palatable and colourful. For example, they are prepared in sauces known as 'saucettes', soft toffees, salts and bars known as *Nukuquetas* whose flavour is similar to that of nuts. All this is a sign of their gastronomic versatility and its potential in the national market; they are even asked for by many restaurant owners particularly in the USA and in some European cities such as London, Berlin, Barcelona, etc., where they are canned or covered in chocolate and included in cakes and cookies that are successfully sold in gourmet outlets.

In Supplementary Table S2, we summarise the taxonomical list of the host plants of the edible forest insect; it includes vegetation type, scientific names and the related references. We have documented a total of 52 forest host plants under 18 families. The ones that harbour the maximum number of edible hosts insects are Fagaceae (13 species), followed by Poaceae (11), Asparagaceae (8) and Pinaceae (7). The families we report and the genera they encompass are the following: Altingiaceae: *Liquidambar*, Arecaceae: *Cocos*, Asparagaceae: *Agave*, Asteraceae: *Thitonia*, Betulaceae: *Alnus*, Cactaceae: *Opuntia*, Cupressaceae: *Juniperus*, Ebenaceae: *Dyospyrus*, Ericaceae: *Arbutus*, Fabaceae: *Prosopis*, *Acacia* Fagaceae: *Quercus*, Juglandaceae: *Carya*, Poaceae: *Bromus*, *Chloris*, *Bouteloua*, *Hilaria*, *Cynodon*,

Echinochloa, *Andropogon*, *Paspalum*, *Panicum*, Solanaceae: *Solanum* and Tilliaceae: *Heliocarpus*.

We have documented a total of 6 types of vegetation and the number of edible insect species pertaining to each one are: (a) savannah (12); (b) pine-oak forest (12), oak forest (7), pine forest (8); (c) rain forest (8); (d) tropical deciduous forest (8); (e) cloud forest (4); and (f) cactus scrub desert (16). In the vegetation types known as pine-oak forest (oak forest and pine forest), cactus scrub desert and savannah, we registered the highest number of edible insect species, being 27, 16 and 12 (Figure 1 and Table 1) (SEMARNAT, 2010). In the case of the pine-oak forest, this result is due to the high number of genera and species that make it up and for the case of cactus scrub desert the explanation may lie in the fact that it is the most prevalent vegetation type in Mexico.

It is important to point out that in Supplementary Table S2 we only include the hosts of the localities where the insects reported in Supplementary Table S1 were collected; because of this, the number of host species may vary in a significant manner. For example, if we consider the ecologic and geographic assets of the *escamoles* (*Liometopum apiculatum*), we can see they are found in all ecosystems, ranging from deserts to forests (Hernández *et al.*, 2017) while the *cuetla* (*Arsenura armida armida*) has been registered for the states of Chiapas, Colima, Estado de México, Nuevo León, Oaxaca, Puebla, Quintana Roo, San Luis Potosí, Tabasco, and Veracruz (Beutelspacher and Balcazar, 1994) and therefore in different vegetation types (Gómez, 2009). Finally, some localities like Milpa Alta are characterised by presenting diverse vegetation types like cactus scrub desert, pine forest and fir forest. We must also say that in Mexico there exist diverse approximate equivalences in the nomenclature of vegetation types and that in this case we use as reference the book by Rzedowski (2006).

In Supplementary Table S3, where we show the nutritional value of some forest insects, the grasshoppers present the highest protein values that range between 56.19 and 77.13 g/100 g; nevertheless, *Mischocyttarus* sp. (74.51 g/100 g) and *Proarna* sp. (72.02 g/100 g), are also rich in this parameter. In fat content the insects with the highest quantities are *Phassus triangularis* (77.17 g/100 g) and *R. palmarum* (66.54 g/100 g); *Copestylum haggi* and *Copestylum anna* (8.30 g/100 g) are rich in ash content while *Arsenura armida armida* has 8.23 g/100 g. In the case of raw fibre the most significant results are those of *Callipogon barbatus* (22.71 g/100 g) and *Aplagiognathus* sp. (22.04 g/100 g), and in carbohydrates the larvae of *Hylesia frigida* and the larvae and pupae of *Apis mellifera* have the highest quantities, being respectively 29.53 and 29.46 g/100 g.

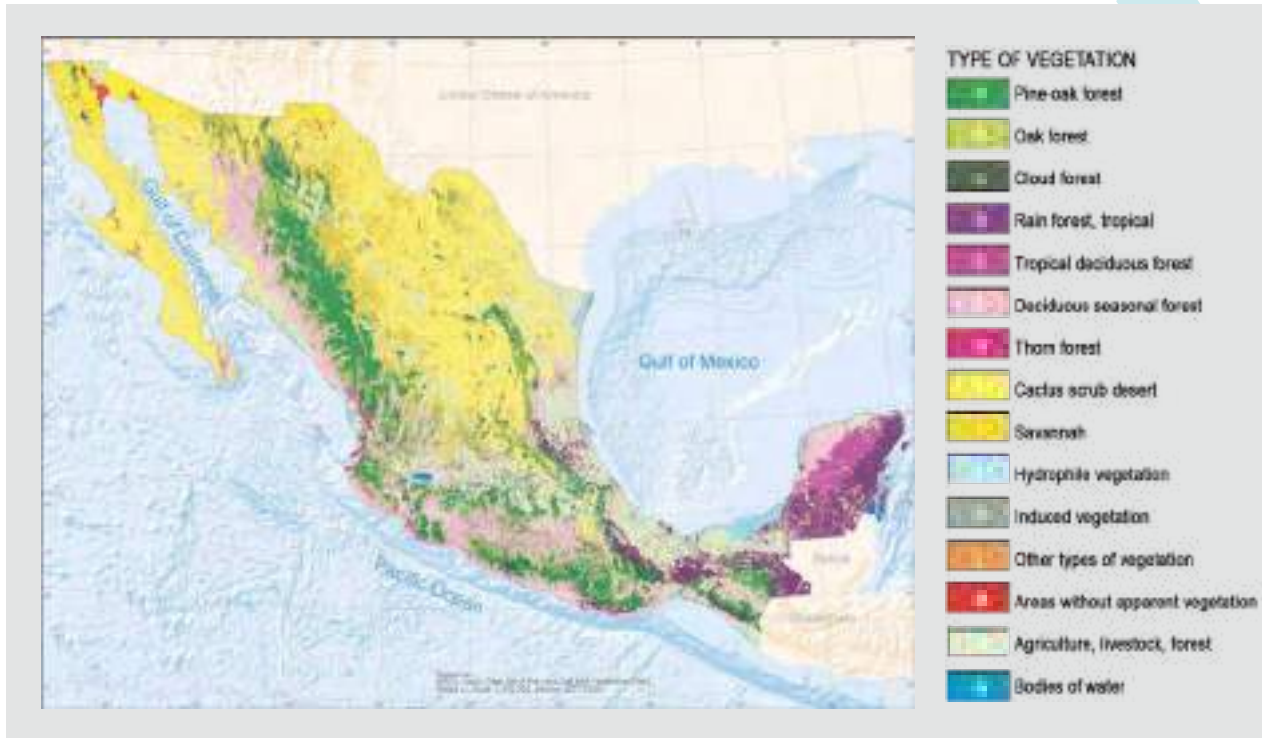


Figure 1. Types of vegetation in Mexico (SEMARNAT, 2010).

Table 1. Distribution of some edible forest insects in Mexico, by type of vegetation (modified from SEMARNAT, 2010).¹

Type of vegetation	Scientific name
A: pine-oak-forest	<i>Aplognathus spinosus</i> , <i>Malodon dasystemus</i> , <i>Malodon molarius</i> , <i>Malodonopsis mexicanus</i> , <i>Derobracus procerus</i> , <i>Derobracus</i> sp., <i>Callipogon barbatus</i> , <i>Leptinotarsa decemlineata</i> , <i>Oileus rimator</i> , <i>Brachygastra lecheguana</i> , <i>Polybia occidentalis bohemani</i> , <i>Polybia parvulina</i>
-A- in Figure 1	Oak forest: <i>Euschistus taxcoensis</i> , <i>Euschistus strenuus</i> (<i>Euschistus zopilotensis</i>), <i>Euschistus</i> sp., <i>Edessa mexicana</i> , <i>Stenodontes cer. maxillosus</i> , <i>Polybia occidentalis nigratella</i> , <i>Brachygastra mellific</i>
-B- in Figure 1	Pine forest: <i>Hoplophorion monograma</i> , <i>Catasticta teutila</i> , <i>Eucheira socialis</i> , <i>Phassus triangularis</i> , <i>Synopsisia mexicanaria</i> , <i>Arhopalus rusticus</i> , <i>Trichoderes pini</i> , <i>Apis mellifera</i>
C: cloud forest (-C- in Figure 1)	<i>Cerambix</i> sp., <i>Atta cephalotes</i> , <i>Atta mexicana</i> , <i>Atta texana</i>
D: rain forest, tropical evergreen forest (-D- in Figure 1)	<i>Malodon</i> sp., <i>Phassus</i> sp., <i>Arsenura armida armida</i> , <i>Trigona</i> sp., <i>Melipona</i> spp., <i>Brachygastra azteca</i>
E: tropical deciduous forest (-E- in Figure 1)	<i>Hylesia frigida</i> , <i>Ascalapha odorata</i> , Cicadidae, <i>Rhynchophorus palmarum</i> , <i>Passalus punctiger</i> , <i>Lestrimelitta limao</i> , <i>Parachartegus apicalis</i> , <i>Mischocyttarus</i> sp.
H: cactus scrub desert (-H- in Figure 1)	<i>Strategus aloeus</i> , <i>Metamasius spinolae</i> , <i>Scyphophorus acupunctatus</i> , <i>Copestylum haggi</i> , <i>Copestylum anna</i> , <i>Campylostoma</i> sp., <i>Liometopum apiculatum</i> , <i>Liometopum occidentale</i> var. <i>luctuosum</i> , <i>Camponotus</i> sp. <i>Thasus gigas</i> , <i>Proarna</i> sp., <i>Dactylopius coccus</i> , <i>Castnia chelone</i> , <i>Laniifera cyclades</i> , <i>Aegiale hesperiaris</i> , <i>Comadia redtenbacheri</i>
I: savannah (-I- in Figure 1)	<i>Sphenarium histrio</i> , <i>Sphenarium purpurascens</i> , <i>Sphenarium magnum</i> , <i>Taeniopoda</i> sp., <i>Ochrotettix salinus</i> , <i>Tropinotus mexicanus</i> , <i>Osmilia flavolineata</i> , <i>Schistocerca paranensis</i> , <i>Schistocerca</i> sp., <i>Trimerotropis pallidipennis</i> , <i>Melannoplus</i> sp., <i>Euschistus egglestoni</i>

¹ In these types of vegetation we have no records of edible insects: F = deciduous seasonal forest, G = thorn forest, J = hydrophile vegetation, K = induced vegetation, L = other types of vegetation, M = areas without apparent vegetation, N = agricultural, livestock, forest, Ñ = bodies of water.

4. Discussion

If we intend to preserve, disseminate and rationally exploit insects as a renewable natural resource, it is necessary to consider their ecological interaction with their respective environments; therefore, taxonomical, biological, ecological (population dynamics), genetic and environmental impact studies must be carried out in order to assess the current situation of their populations and the genetic diversity of the species. It must also be considered that environmentally there is the problem of agrochemicals polluting insects, so that consumers must be aware of their places of origin, as in the case of the grasshoppers. Besides, in Mexico, the current vegetation reflects the great changes it has suffered due to human activities like agriculture, fires, livestock production and deforestation, that cause desertification and the loss of biodiversity in certain regions (SEMARNAT, 2010). For example, logging disrupts insect biology and continuous use of insecticides can cause a decrease in their populations, and in an extreme case, favour their extinction. For example, in the state of Hidalgo, overexploitation of edible insects for socio-economic purposes (commercialisation) is a danger in some areas, as this aspect has gradually reduced the populations of the most sought and commercialised insect species, so that they are now in an endangered status and potentially at risk of extinction. Nevertheless, as has been pointed out by Ramos-Elorduy *et al.* (2006), the main problem is that there is no regulation for their collection, preparation, distribution and commercialisation, as they are equally sold in markets or *tianguis* as well as in five-star restaurants without sanitary control. In this case some researchers believe that creating a wider market for edible insects could provide an economic incentive for the conservation of insect habitats in the forest.

In addition, in Mexico there is almost no information related to the management of edible insects in forest vegetation, so in this case it should be necessary to enhance the forest environments in Mexico and gradually reduce pesticide use and thus reduce pollution. The majority of the edible insects reported in the present study were harvested in small quantities from the forests, in most cases, minimal management of forest vegetation has been practiced in association with the exploitation of forest insects, and actual domestication of insects thus far has been limited to only a few species such as silkworms and bees (Johnson, 2012), even though they represent a significant amount of food for people living near forest vegetation.

Consequently, for the rational exploitation of insects it is convenient to become acquainted with edible forest insect biology, their cultivation and/or breeding, as well as practicing and exploring opportunities for the domestication of forest insects using host plants for feeding them (Balinga *et al.*, 2004; Illgner and Nel, 2000). It has even been pointed out that raising edible insects does not require

complex infrastructure, they feed by themselves, plant debris or animal organic matters can be used as manure and their maintenance is easy, they require little space and cause little pollution (Ramos-Elorduy *et al.*, 1988b, 2002b). Therefore, insect breeding offers opportunities that are compatible with forest management. It is important to quantify the impact that insect overexploitation could have on the ecosystems and assess the management of vegetation forest experiences and the insect harvesting practices with the aim of maintaining and maximising the populations. It is also important to gain knowledge about the ecological status of the insect species involved; additionally, the traditional knowledge of the forest inhabitants that still include insects in their diets must be rescued.

Notwithstanding these problems, in Mexico the capture, processing, transportation and commercialisation of edible insects in general, are income-generating activities that potentially improve the life quality of the local inhabitants. In short, there exists an established market and the significant potential of increasing the commercialisation of edible insects. This involves the promotion and adoption of modern standards of alimentary technology so that they can be sold in several innocuous preparations. Some researchers even consider that creating a bigger insect market could provide an economic incentive for the preservation of their habitat, that is, the commercial potential of forest insects must be determined.

Equally important is highlighting once again the advantages that edible insects possess as an alternative to solve the world's alimentary problem (Van Huis *et al.*, 2013) and their management in laboratory conditions may help reduce the environmental impacts that have their origin on stockbreeding. In addition, the nutritional value of various edible species from Mexico has been reported in terms of their contents of protein (essential and non-essential amino acids), fats (saturated and unsaturated fatty acids), vitamins (A, C, riboflavin, niacin) and minerals (Na, K, Ca, P) (Pino and Ganguly, 2016; Ramos-Elorduy and Pino, 1990, 2001a,b; Ramos-Elorduy *et al.*, 1992, 1997, 1998a,b, 2002a,b, 2012).

Consequently, in depth studies will help revitalise the traditional knowledge of several cultural groups, favouring a sense of connection with nature as well as the development of recommendations and strategies for the promotion of forest insects, enabling a rational and sustainable management on a wider scale (Aldasoro, 2000; Durst and Shono, 2012).

Finally, edible forest insects offer a variety of research, conservation and commercialisation opportunities, like contributing to biodiversity maintenance (DeFoliart, 1997); it has been demonstrated that insects contribute significantly to the diets, as in the case of the Yukpa Indians of Colombia (Ruddle, 1973). Even the Food and Agriculture

Organisation (FAO) has pointed out that the exploitation of forests and the associated insects is a very important factor in the fight against hunger, and therefore must be integrated into food security policies, since they contribute to the livelihood of more than a billion people, including most of the world's disadvantaged groups. As an example, insects are the main source of easily accessible protein and honey to the forest dwelling people (FAO, 2013).

5. Conclusions

A wide variety of different insect species are part of the diet of many cultures in Mexico. The use of some edible forest insects by diverse indigenous and *mestizo* groups of rural areas represents rich sources of protein for the improvement of human diet, especially for individuals suffering poor nutrition due to protein deficit; gram per gram, insects often contain more proteins and minerals than meat (Johnson, 2012). These insects, in a smaller scale, are commercialised in the times of highest abundance; their collection is characterised by low production and thus has a minimal impact upon the forest vegetation. But the demand of this product has grown and it has generated new commercialisation opportunities as well as local jobs, so it is important to promote and preserve anthropoentomophagic activity, aiming at the rescue, conservation, application and promotion of the traditional knowledge so that the management of the insect and plant resources may be exploited viably. For example, we recommend the design of new breeding methods, a 'farm system' or 'mini-husbandry', so as to ensure continuous production and enhance the lifestyle of the local communities.

Supplementary material

Supplementary material can be found online at <https://doi.org/10.3920/JIFF2020.0099>.

Table S1. Taxonomic list of some edible insects registered in the forest vegetation of Mexico.

Table S2. Taxonomic analysis of host plants.

Table S3. Nutritive value of some forest insects of Mexico (dry basis g/100 g).

Acknowledgements

The authors thank M. en C. Enrique Mariño P. (Order Orthoptera), M. en C. Cristina Mayorga M., Dr Harry U. Brailovsky A. (Order Hemiptera-Heteroptera), Mr Adolfo Ibarra V. (Order Lepidoptera), M. en C. Enrique Ramírez G. (Order Diptera), Dr Santiago Zaragoza C. (Order Coleoptera), Dr Ricardo Barajas A. (Order Hymenoptera), for their taxonomic support regarding the identification of insects, Dr Oscar F. Francke B. for proofreading, and

the graphic designer N. Malerva P. for his aid in the modification of Table 1.

Conflict of interest

The authors declare no conflict of interest.

References

- Acosta, M.M., Martínez, I.S., Rodríguez, A.O., San Juan, J.L., Ventura, A.M. and Joshua, U.S., 2019. La chicha como insecto comestible (Coleoptera: Cerambycidae) en la región de la vega de Metztlitlán, Hidalgo. *Entomología Mexicana* 6: 82-88.
- Aldasoro, M.E.M., 2000. Etnoentomología de la comunidad Hñahñu El Dexthi San Juanico Hidalgo. BSc-thesis, Facultad de Estudios Superiores Iztacala, National Autonomous University of Mexico, Mexico, 125 pp.
- Avendaño, R.J.A., 2002. Concurso Local de Emprendedores. Aprovechamiento de las propiedades nutritivas de *Atta* sp. Procomex. S. A. de C. V. Instituto Tecnológico de Orizaba Veracruz – México. Colonia Emiliano Zapata No. 852. Orizaba Veracruz México, pp. 10-15.
- Balinga, M.P., Mapunzu, P.M., Moussa, J.B. and N'Gasse, G., 2004. Contribution des insectes la forêt à la sécurité alimentaire: L'exemple des chenilles d'Afrique Centrale. Programme des Produits Forestiers non Ligneux. FAO, Rome, Italy.
- Beutelspacher, B.C. and Balcazar, M.L., 1994. Catálogo de la familia Saturniidae de México. *Tropical Lepidoptera* 5: 1.
- Cano, V.N. and Hernández, J.A., 1998. Monografía de Huatusco. Publisher Ayuntamiento de Huatusco, Veracruz, México.
- Cibrian, T.D., Méndez, T.J.M., Campos, R.B. and Flores, J.L., 1995. Insectos Forestales de México. Universidad Autónoma Chapingo, México, 453 pp.
- CONAFOR, 2012. Inventario Nacional Forestal y de Suelos. Comisión Nacional Forestal. Secretaria de Medio Ambiente y Recursos Naturales, Informe 2004-2009. Coordinación General de Planeación e Información-Gerencia de Inventario Forestal y Geomática. Zapopan Jalisco, México.
- Defoliart, G.R., 1997. An overview of the role of edible insects in preserving biodiversity. *Ecology Food Nutrition* 36: 109-132.
- Dossey, T.A., Morales-Ramos, J.A. and Rojas, M.G., 2016. Insects as sustainable food ingredients (production, processing and food applications). Elsevier, New York, NY, USA, 402 pp.
- Dounias, E., 2010. Edible weevil larvae: a pest for palm trees but a delicacy for city-dwellers. Exploring alternative foods for world hunger (the potential of edible insects). International Conference, Alabama, USA, pp. 10-12.
- Durst, B. and Shono, K., 2012. Insectos forestales comestibles: explorando nuevos horizontes y prácticas tradicionales. In: Durst, B.P., Johnson, D.V., Leslie, R.N. and Shono K. (eds.) *Forest insects as food: humans bite back*. FAO, Rome, Italy, pp. 1-4.
- Escamilla, F.E., 2008. 'Chicatana' (*Atta mexicana* Smith, *A. cephalotes* Latreille y *A. texana* Buckley) insectos comestible en los cafetales de tres comunidades del municipio de Huatusco, Veracruz. Un estudio etnoentomológico. PhD-thesis, Universidad Autónoma Chapingo, Mexico, 104 pp.

- Espina, P.D. and Ordetx, G.S., 1984. Apicultura tropical. Tecnológica de Costa Rica, Cartago, Costa Rica, 506 pp.
- Fogot, M.J., Ayemele, G.A., Le Gall, P. and Levang, P., 2015. Exploitation, trade and farming of palm weevil grubs in Cameroon. Working Paper No. 178. Center for International Forestry Research, Bogor, Indonesia, 32 pp.
- Food and Agriculture Organisation (FAO), 2013. Los productos forestales son esenciales en la lucha contra el hambre, insectos incluidos. Organización de las Naciones Unidas para la Alimentación y la Agricultura. FAO, Rome, Italy. Available at <http://www.fao.org/news/story/es/item/175974/icode/>
- Gómez, U.J.M., 2009. Estudio etnoentomológico del 'gusano del jonote' (*Arsenura armida armida* Cramer, 1779), en tres regiones cafetaleras de México. BSc-thesis, Universidad Autónoma Chapingo, Huatusco Veracruz, Mexico, 95 pp.
- Govorushko, S., 2018. Human-insect interactions. CRC Press, New York, NY, USA, 428 pp.
- Halloran, A., Flore, R., Vantomme, P. and Roos, N., 2018. Edible insects in sustainable food systems. Springer, Dordrecht, the Netherlands, 479 pp.
- Hernández, R.E., Tarango, L.A.A., Ugalde, S.L., Hernández, A.J., Cortéz, C.R. and Morales, F.J.F., 2017. Hábitat y densidad de nidos de la hormiga escamolera (*Liometopum apiculatum* Mayr) en una UMA de Zacatecas, México. Agroproductividad 10: 3-9.
- Illgner, P. and Nel, E., 2000. The geography of edible insects in sub-Saharan Africa: a study of the mopane caterpillar. The Geographical Journal 366: 336-351.
- Johnson, V.D., 2012. The contribution of edible forest insects to human nutrition and to forest management: current status and future potential. In: Durst, B.P., Johnson, D.V., Leslie, R.N. and Shono, K. (eds.) Forest insects as food: humans bite back. FAO, Rome, Italy, pp. 5-25.
- Landero, T.I., Murguía, G. and Ramos-Elorduy, J., 2005. Estudio etnográfico sobre el consumo de las 'chicatanas' (hymenoptera: formicidae) en Huatusco, Veracruz, México. Folia Entomologica Mexicana 44: 109-113.
- Landero, T.I., Oliva, H.R., Galindo, M.E.T., Balcazar, M.A.L., Murguía, J.G. and Ramos-Elorduy, J., 2012. Uso de la larva de *Arsenura armida armida* (Cramer, 1779) (Lepidoptera: Saturniidae), 'cuecla' en Ixcuhuapa, Veracruz, México. Cuadernos de Biodiversidad 38: 4-8.
- López, H.A., 2014. Extracción, identificación y cuantificación de ácidos grasos presentes en las larvas y pupas del insecto comestible denominado 'ticoco'. BSc-thesis, Universidad Tecnológica de la Mixteca, Huajuapán Oaxaca, México, 71 pp.
- Maes, J.M., Van der Berghe, E., Dauber, D., Audureau, A., Nears, E., Skilman, F., Heffern, D. and Monné, M., 2010. Catálogo ilustrado de los Cerambycidae de Nicaragua-Parte I-Lamiinae. Revista Nicaraguense de Entomología 70: 1-102.
- Marage, D. and Lemperiere, G., 2005. The management of snags: a comparison in managed and unmanaged ancient forests of the Southern French Alps. Annals of Forest Science 62: 135-142.
- Martínez, H.J., 2016. Cosmovisión del consumo de insectos y uso medicinal en dos comunidades: Mirador Saltillo y Ocozotepec, Municipio Soteapan Veracruz. BSc-thesis, Universidad Veracruzana, Mecayapan Veracruz, México, 92 pp.
- Martínez, M., 1979. Catálogo de nombres vulgares y científicos de plantas mexicanas. Fondo de Cultura Económica, México, 1220 pp.
- Merganičová, K., Merganic, J. and Hasenauer, H., 2012. Assessing the carbon flux dynamics within virgin forests: the case study 'Babia Hora' in Slovakia. Austrian Journal of Forest Science 1: 1-2.
- Onyeike, E.N., Ayalogu, E.O. and Okaraonye, C.C., 2005. Nutritive value of the larvae of raphiapalm beetle (*Oryctes rhinoceros*) and weevil (*Rhynchophorus phoenicis*). Journal Science Food Agricultural 85: 1822-1828.
- Pino Moreno, J.M. and Ganguly, A., 2016. Determination of fatty acid contents in some edible insects of Mexico. Journal Insects as Food Feed 2: 37-42.
- Ramos-Elorduy J., Pino Moreno, J.M. and Conconi, M., 2006. Ausencia de una reglamentación y normalización de la explotación y comercialización de insectos comestibles en México. Folia Entomologica Mexicana 45: 291-318.
- Ramos-Elorduy, J. and Pino Moreno, J.M., 1989. Los insectos comestibles en el México antiguo (estudio etnoentomológico). A.G.T., México, 139 pp.
- Ramos-Elorduy, J. and Pino Moreno, J.M., 1990. Contenido calórico de algunos insectos comestibles de México. Revista de la Sociedad Química de México 34: 56-68.
- Ramos-Elorduy, J. and Pino Moreno, J.M., 2001a. Insectos comestibles del Estado de Hidalgo. Anales del Instituto de Biología, Universidad Nacional Autónoma de México, Serie Zoología 72: 43-84.
- Ramos-Elorduy, J. and Pino Moreno, J.M., 2001b. Contenido de vitaminas en algunos insectos comestibles de México. Revista Sociedad Química de México 45: 66-76.
- Ramos-Elorduy, J. and Pino Moreno, J.M., 2002. Edible insects of Chiapas, Mexico. Ecology of Food and Nutrition 41: 271-299.
- Ramos-Elorduy, J., 1982. Los insectos como una fuente de proteínas en el futuro. Limusa, México, 144 pp.
- Ramos-Elorduy, J., 2004. La etnoentomología en la alimentación, la medicina y el reciclaje. In: Llorente, J.E.B., Morrone, J.J., Yañez, O.O. and Vargas, I.F. (eds.) Biodiversidad, taxonomía y biogeografía de artrópodos de México hacia una síntesis de su conocimiento. Vol. IV. Universidad Nacional Autónoma de México, Facultad de Ciencias, México City, Mexico, pp. 329-413.
- Ramos-Elorduy, J., Ávila, E.G., Rocha, A.H. and Pino Moreno, J.M., 2002b. Use of *Tenebrio molitor* L. (Coleoptera-Tenebrionidae) to recycle organic wastes and as feed for broiler chickens. Journal of Economic Entomology 95: 214-220.
- Ramos-Elorduy, J., Flores, R.A., Sandoval, C.E., Pino Moreno, J.M. and Bourges, R.H., 1992. Composición química de insectos comestibles de la delegación Milpa Alta, D.F. Tecnología de Alimentos (México) 27: 23-33.
- Ramos-Elorduy, J., Muñoz, J.L. and Pino Moreno, J.M., 1998b. Determinación de minerales de algunos insectos comestibles de México. Revista de la Sociedad Química de México 42: 18-33
- Ramos-Elorduy, J., Pino Moreno, J.M. and Cuevas, S.C., 1998a. Insectos comestibles del Estado de México y determinación de su valor nutritivo. Anales del Instituto de Biología, Universidad Nacional Autónoma de México, Serie Zoología 69: 65-104.
- Ramos-Elorduy, J., Pino Moreno, J.M. and Martínez, C.V.H., 2008. Base de datos de la colección nacional de insectos comestibles de México. UNIBIO-IBUNAM, Mexico City, Mexico.

- Ramos-Elorduy, J., Pino Moreno, J.M. and Martínez, C.V.H., 2012. Could grasshopper be a nutritive meal. *Food and Nutrition Sciences* 3: 164-175.
- Ramos-Elorduy, J., Pino Moreno, J.M. and Morales, J.L., 2002a. Análisis químico proximal, vitaminas y nutrimentos inorgánicos de insectos consumidos en el estado de Hidalgo, México. *Folia Entomológica Mexicana* 41: 15-29.
- Ramos-Elorduy, J., Pino Moreno, J.M. and Romero, L.A.S., 1988a. Determinación del valor nutritivo de algunas especies de Insectos comestibles del Estado de Puebla. *Anales del Instituto de Biología, Universidad Nacional Autónoma de México, Serie Zoología* 58: 335-372.
- Ramos-Elorduy, J., Pino Moreno, J.M. and Villegas, J., 1988b. The efficiency of the insect *Musca domestica* in recycling organic wastes as a source of proteins. *Biodeterioration* 8: 805-810.
- Ramos-Elorduy, J., Pino Moreno, J.M., Corona, R.C. and Medina, V.D., 1985. Estudio de los insectos comestibles de Guerrero y su valor nutritivo. *Memorias del 8° Congreso Nacional de Zoología, Parte II. Sociedad Mexicana de Zoología, México*, pp. 1107-1126.
- Ramos-Elorduy, J., Pino Moreno, J.M., Escamilla, E.P., Pérez, M.A., Lagunez, J.O. and De Guevara, O.L., 1997. Nutritional value of edible insects from the state of Oaxaca, México. *Journal of Food Composition and Analysis* 10: 142-157.
- Rivera, G.E., 1989. Utilización de recursos alimenticios por acrididos en pastizales áridos del Bolson de Mapimi, Durango. MSc-thesis, Colegio de Postgraduados, Montecillo, México, 75 pp.
- Ruddle, K.A., 1973. The human use of insects: examples from the Yukpa. *Biotropica* 5: 94-101.
- Rzedowski, J., 2006. Vegetación de México. Comisión Nacional para el Conocimiento y Uso de la Biodiversidad, México, 417 pp.
- Sahagún, F.B., 1975. Códice Florentino. Archivo General de la Nación, Libro XI, pp. 221-261.
- Salazar, A.R.N., 2019. Servicios ecosistémicos de las 'chizas' (Coleoptera-Cerambycidae) en el municipio de Isidro Fabela, Estado de México, México. BSc-thesis, Faculty of Sciences, National Autonomous University of Mexico, Mexico, 56 pp.
- Schowalter, D.T., 2013. Insects and sustainability of ecosystems services. CRC Press, New York, NY, USA, 396 pp.
- Secretaría del Medio Ambiente y Recursos Naturales (SEMARNAT), 2010. Atlas Geográfico del Medio Ambiente y Recursos Naturales. Secretaria del Medio Ambiente y Recursos Naturales. SEMARNAT, México, Mexico, 105 pp.
- Van Huis, A. and Tomberlin, J.K., 2017. Insects as food and feed: from production to consumption. Wageningen Academic Publishers, Wageningen, the Netherlands, 447 pp.
- Van Huis, A., Itterbeeck, J.V., Klunder, H.H., Mertens, E., Halloran, A., Muir, G. and Vantomme, P., 2013. Edible insects: future prospects for food and feed security. Food and Agriculture Organization of Unites Nations, Rome, Italy, 201 pp. Available at: <http://www.fao.org/docrep/018/i3253e/i3253e.pdf>.
- Vandekerkhove, K., De Keersmaecker, L., Menke, N., Meyer, P. and Verschelde, P., 2009. When nature takes over from man: deadwood accumulation in previously managed oak and beech woodlands in Northwestern and Central Europe. *Forest Ecology and Management* 258: 425-435.
- Vantomme, P., Göhler, D. and N'Deckere-Ziangba, F., 2004. Contribution of forest insects to food security and forest conservation. the example of caterpillars in Central Africa. *Wildlife Policy Briefing* 3: 1-4.
- Vázquez, M.A., 2005. El chapulin, (Orthoptera: Acridoidea), un recurso alimenticio de las poblaciones circunvecinas a la Facultad de Estudios Superiores Cuautitlan UNAM, municipios de Cuautitlan, Cuautitlan Izcalli y Tepotzotlan, Edo. de Mexico. Tesis de Maestría en Ciencias Biológicas, Facultad de Ciencias UNAM (Biología), Mexico, 126 pp.
- Woodall, C. and Williams, M.S., 2005. Sampling protocol, estimation and analysis procedures for the down woody materials indicator of the FIA program. General Technical Report. US Department of Agriculture, Forest Service, Northern Research Station, 68 pp. <https://doi.org/10.2737/NRS-GTR-22>

ISSN 2319 – 8389, Vol : 44, Issue : 44

KHOAI
UGC Care Listed Journal
Art and Humanities
Tri - Annual Journal

KHOAI

A Collector on Literature and Culture

Chief Editor
Kishore Bhattacharya

VOLUME 44
8 August, 2021

SANTINIKETAN, BIRBHUM, PIN- 731235, W.B. INDIA

Aesthetics of Raga- লোকবিশ্বাস ও লোকসংস্কার : মহাশক্তি দেবীর একটি উপন্যাস- নেল নভিসেস এর শিক্ষাভাবনা- উনবিংশ শতাব্দীর দ্বিতীয়ার্ধে উত্তরবঙ্গের নগরায়ন ও নাগরিক পরিবেশ : প্রসঙ্গ মালদহ জেলা- ডিজিটাল ও অনলাইন দুনিয়ায় রবীন্দ্রগানের প্রচার ও প্রসার এবং করোনা আবহে তার ইতিবাচক ও নেতিবাচক প্রভাব - একটি সমীক্ষা ভিত্তিক মূল্যায়ন-	Shyamal Makhai শিবির সিং মন্দিরা সিংহ	২০৭ ২১৭ ২১৬
Unselfishness is the essence of Morality according to Swami Vivekananda- রবীন্দ্রসঙ্গীতে ভারতীয় সংস্কৃতির নবজাগরণ- The Effectiveness of Virtual Field Trip on Academic Achievement of Students in Inclusive Classroom with respect to Teaching Forest Resources at Higher Secondary Level- 'ধুম্রিলালের দুই সঙ্গী' গল্পে সাম্প্রদায়িক দাঙ্গা ও সংকট উত্তরণের ছবি- ঔপনিবেশিক আমলে মালদা-র সীওতাল সমাজ- চৈতন্য সংস্কৃতি ও বর্তমান সময়ে তার প্রাসঙ্গিকতা- 'ইতিহাস ও ঐতিহ্যের সংস্কৃতি পৌষ সংক্রান্তি'- Teaching-Learning Strategies for Children with Disabilities in Inclusive Classrooms- রবীন্দ্রনাথের 'সক্কাসংগীত' কাব্যে নদীর স্থান- 'নতুন ইহুদি' : দেশভাগের জীবন্ত দলিল- ✓পারিবারিক সম্পর্কের আলোকে 'চোখের বালি'- Population Education & Geography of Surul village: a Study- 'দেশ' পত্রিকার ছেটিগল্পে গ্রামবালোর লোকসংস্কার- মহামারি করোনার করাল ছায়ায় : প্রসঙ্গ সাহিত্য প্রেম- বাংলা মঙ্গলকাব্যের পাঠক রবীন্দ্রনাথ- বিংশ শতাব্দীর ক্রিবেদগ্ৰী মহিলা সংগীতশিল্পী বেগম আখতার- Leadership Needs a Strategic Change to Prevent Child Labour : A Stage of Covid-19 Epidemic- Impact of Family Environment and Mobile Phone Addiction on the Academic Achievement of Undergraduate Students- Dhrupad Tradition of Vishnupur Gharana in West Bengal- উনবিংশ শতকের পটভূমিকায় বিশ্ববোধের উন্মেষ : বিশ্বশান্তির বাণী প্রচারে রামমোহন থেকে রবীন্দ্রনাথ- Evolution and Growth of Market System, Economy in Kolkata- Genesis and Development of Drainage and Sewerage System during Colonial period in Calcutta -1800-1948 A Historical Analysis of Ayacut settlement in Travancore in Southern India from 1883-1911- ভগবত গীতার আয়ত্ত্বঃ অদ্বৈত ও দ্বৈতবাদের আলোকে পুনঃমূল্যায়ন- বাংলার নবজাগরণ ও জোড়াসাঁকো ঠাকুরবাড়ীর সঙ্গীত শিক্ষা- অর্থনৈতিক সংকটের প্রেক্ষাপটে দীপেন্দ্রনাথ বন্দ্যোপাধ্যায়ের জটামু : পুরাণের নবনির্মাণ- EARLY PANDYA INVASIONS IN SOUTH T	শ্রী কৌশল কামিকার Sabyasachi Mondal অনিবার্ণ সাহু Sanjoy Dutta & Dr. Mousumi Boral মুদুল ঘোষ রাঞ্জন হেমরম প্রবীর কুমার পাল অঞ্জন কর Dr.Gopal Singh Dr.Sharmila Yadav শুভাশিষ গোস্বামী শিবীণ মুস্তাফি অসীম কুমার মুখার্জী স্ক Rashidul Haque রূপশ্রী ঘোষ সমীর প্রসাদ মুনময় কুমার মাহাত ড. চন্দ্রানী দাস Pritam Pyne & Dr. Umakant Prasad Dr. Prarthita Biwas & Dr. Shyamsundar Bairagya Ashok Barman DR. CHITRALEKHA MAITI & DR. ATREYA PAUL Dr. Atreya Paul DR . SURESH .J দীনাকী ভট্টাচার্য্য সোমা দাস মণ্ডল অর্পিতা দাস Sajeew Singh. M. K	২১০ ২১১ ২১২ ২১৩ ২১৪ ২১৫ ২১৬ ২১৭ ২১৮ ২১৯ ২২০ ২২১ ২২২ ২২৩ ২২৪ ২২৫ ২২৬ ২২৭ ২২৮ ২২৯ ২৩০ ২৩১ ২৩২ ২৩৩ ২৩৪ ২৩৫ ২৩৬ ২৩৭ ২৩৮ ২৩৯ ২৪০ ২৪১ ২৪২ ২৪৩ ২৪৪ ২৪৫ ২৪৬ ২৪৭ ২৪৮ ২৪৯ ২৫০

পারিবারিক সম্পর্কের আলোকে 'চোখের বালি'

অসীম কুমার মুখার্জী

কৃত্রিম : সিক্ত ও সছাত্ত মনোভীর নগরিক জীবনচর্চাই রবীন্দ্র উপন্যাসের বিবরণী। নবম শতাব্দীর বঙ্গের
পিতামহে প্রেরিত সিক্ত মনোভীর জীবন ধারণ উৎস সন্ধান নিবৃত্ত ছিলেন বহিঃ। নবকালীন জীবন প্রসঙ্গে
উপন্যাসে স্পষ্ট হয়নি। বঙ্গ পেশাবৃত্ত বিশেষ লক্ষ্য ছাড়াই মনোভীরের মনসজীবন ব্যাপ্তি একটি অনির্দিষ্ট
ভাষ্যেই সীমিত উপন্যাসের প্রধান উদ্দেশ্য। বালিই এই কাহিনীর একমাত্র নিয়ন্ত্রণ। ব্যক্তিবর্গের বিচিন্তন
কিন্তু বঙ্গের বঙ্গীয় উপন্যাসে প্রচলিত অঙ্গের হতে সোচ্চারিত। জীবনচিত্রে যৌক্তিকতা এসেছে, তার নিয়ম
বালিবর্গেরই পরম্পরিক সত্যতা। কখন আত্মতত্ত্বই বিচিত্র তাঁনে অনিবার্য হতে উঠেছে সমস্যা।

এই চিত্রের পর বঙ্গ উপন্যাসকে চিত্রিত্বিত্তি বহন করাই রবীন্দ্রনাথের বিশিষ্ট অবদান। বহিঃ
সংগঠন মনসজীবন করেছিলেন, আজ তারই কলে আদর্শ প্রাচীর মতো পাওয়া গিয়েছে তাঁরই কবিতা। এই
চিত্রিত্তি রচনারই ছিল উপন্যাসের শক্তিবিদ্যার প্রথম ধাপ। চিত্রিত্তি যিক এর পত্রের প্রত্যেক। রবীন্দ্র
মনোভীরের সত্যই অবলম্বন করে ব্যক্তি অস্তর রাজ্যকে উন্মোচিত করেছেন। উপন্যাসের বিবৃতি ও কলে
প্রথম কেন্দ্রবিন্দু হতে তাঁনে চিত্রিত্তি অর্থাৎ ব্যক্তি। সূত্রের ব্যক্তির অবিদ্যমান ঘটনা কুশলার্থেই প্রতিশ্রুতি সূত্র
রবীন্দ্র উপন্যাসে এই নবা গতি প্রকৃতি সোচ্চারিত। ব্যক্তির আত্মনির্ভর অধিকাংশের আনন্দপ্রতি সোচ্চারিত
উপন্যাসে উপস্থিত। স্বর্ষ, সত্যতা, স্বাভাবিকতা, প্রেম, পরিবার-সংগঠন ইত্যাদিকে বিধে ব্যক্তির বিচিত্র ধর্ম ও
ব্যক্তিবর্গের সোচ্চারিত রবীন্দ্র রচনার প্রবর্তিত। 'চোখের বালি'র পারিবারিক কাহিনী ও সম্পর্কের কলে
প্রথম নিদর্শন।

মহাপুত্র : রাজলক্ষী ও মহেন্দ্র

'চোখের বালি' পারিবারিক উপন্যাস : তার নবম শতাব্দীর পারিবারিক গন্ধের মধ্যে সীমাবদ্ধ। পরিবার
চলনধারার কলে যে বহুস্তর সমাজ 'চোখের বালি' উপন্যাসে আপাতদৃষ্টিতে তার স্বাভাবিক লক্ষ্য কলে যে
একটিমাত্র পরিবারের কেন্দ্র করে কাহিনীর সূত্রপাত — অঙ্গগতি ও কলে পরিণতি। এই পরিবারের সত্য সত্য
মাত্র চলে কলে রাজলক্ষী-মহেন্দ্র-আশা-ও অঙ্গপূর্ণ। এই চতুর্ভুজের মধ্যেই কাহিনী কিন্ত হতেছে। মনে রাজলক্ষী
একমাত্র পুত্র মহেন্দ্র পিতৃহীন মাত্রের স্নেহ ছাড়াই বেড়ে ওঠে। অন্দের আকর্ষণ যাই হোক সখী মাকে নিয়ে নিজে
কলে সখী হরিমতের কলে বিনোদিনীর সন্ত রাজলক্ষী পুত্রের বিবাহ নিতে চাইলে মহেন্দ্র তাতে অসম্মত হলে
এসে অতি মাকে ছাড়িয়ে উঠে এই মাত্র মহেন্দ্র অন্দের দিন বিবাহ করলে না। "ম-সম্বন্ধে তাহার বাক্যের সত্যতা
লোকের মতে ছিল না। বয়স প্রায় বইশ হইল। এমএ পাশ করিয়া তাজলি পড়িতে আরম্ভ করিয়াছে শুধু মাকে
শরীরে তাহার প্রতিদিন মন-অভিমান, অন্দের-অবলাবে অস্ত ছিল না। কায়দার শাওরের মতে মাতৃগর্ভ হইতে
হইয়াও মাত্রের বর্ধিত্বের বিলিতির মধ্যে অবৃত থাকায় তাহার অভ্যাস হইয়া গিয়াছিল। মাত্র সত্যতা যাত্রের কলে

Contents lists available at [ScienceDirect](https://www.sciencedirect.com)

Current Research in Green and Sustainable Chemistry

journal homepage: www.elsevier.com/journals/current-research-in-green-and-sustainable-chemistry/2666-0865



Green microalgae derived organic nanodots used as food preservative

Smritikana Pyne^{a,b}, Kishalay Paria^{c,*}, Santi Mohan Mandal^d, Prem Prakash Srivastav^b, Paramita Bhattacharjee^a, Tarun Kumar Barik^e



^a Department of Food Technology and Biochemical Engineering, Jadavpur University, Kolkata, 700032, West Bengal, India

^b Agricultural and Food Engineering Department, Indian Institute of Technology, Kharagpur, 721302, West Bengal, India

^c Department of Biotechnology, Oriental Institute of Science and Technology, Vidyasagar University, Midnapore, West Bengal, India

^d Central Research Facility, Indian Institute of Technology Kharagpur, Kharagpur, 721302, India

^e Department of Physics, Achchuram Memorial College, Jhalda, Purulia, 723202, India

ARTICLE INFO

Keywords:

Spirulina platensis
Supercritical carbon dioxide extraction
Organic nanodot
Antimicrobial effect
Food preservative

ABSTRACT

Spirulina platensis derived organic nanodots (ND) may be used as an alternative of chemical food preservative that can increase shelf life of food and beverages. Microalgal nanodots were isolated by the supercritical carbon dioxide extraction (SCE) method. Then SCE extract was subjected to thin-layer chromatography (TLC) and fractions were screened by a well diffusion method to identify the active compound with strong antibacterial ability. A characteristic of ND is the emitting of red colour upon the absorbance of ultra-violet (UV) light. The isolated ND is active against both Gram-positive and Gram-negative bacteria that significantly avoid their auto-aggregation. The nanodots were characterized by using TEM, UV-VIS, FTIR and NMR spectroscopy. FTIR and NMR analysis revealed the presence of hydrogen-bonded hydroxyl and amide groups. In addition, ND is applied in litchi juice as a preservative to extend the shelf life. In general, our results revealed that the sensory quality i.e. colour, aroma and overall appearance were significantly affected by duration of storage. It proves that *Spirulina platensis* derived organic nanodots act as a strong food and beverage preservative.

1. Introduction

Few of traditional chemical preservatives act as chemical contaminant of food, during adverse effect in human health. Because of our society can find out an alternative way for bypass of chemical pollutants of food. As of now, food preservatives are important to reduce food spoilage caused by microorganisms preventing loss of its quality and nutritive value. Recently, it has created a major global concern due to the excessive and indiscriminate use of antimicrobial compounds; resulting pathogens have developed resistance via genetic mutation or gene acquisition. Therefore, new types of safe antimicrobials urgently require combating this trend. Nevertheless, nano particles have various exceptional properties, viz. large unique nano size, surface area/volume ratio and antimicrobial properties. Efforts are given for the biogenic and rational design of metal or peptide based nanoparticles for their use as antimicrobial agents [1–3]. In this time, novel nanodots (ND) have increased great interest in biological fields owing to the unique size-tunable light absorption and emission properties. The light emission ability of ND can be adjusted through their size and shape with extraordinary biochemical

properties. The ND is also highly photo stable than synthetic organic fluorescent dyes. It has a profound wide range of applications in biological sciences with remarkable healthcare systems due to their unique optical and electronic properties [4]. During the past century, exhaustive research has accounted for countless benefits on nanomaterials. Nanomaterials are used in several sectors, among them the food industry is one of the prime industries. Even though, the need of nanotechnology in the food industry has prominently increased day by day. Nanotechnology assures various benefits like safety, security, quality and shelf life of the food products in food processing industries. The application of nanomaterials in food technology is based on the characteristics of the nanoparticles. On the other hand nano-food processing is accomplished in three main aspects i.e. production (conversion of edible food materials from raw food), processing (enhance of taste, shelf life and safeguard from contaminants) and maintenance of proper nutritional standards. It also plays an efficient role in food preservation and packaging i.e., use in sweets, chewing gums and candies preparation. As of now, the production of nanoparticles has been reported by many photoautotrophic microorganisms such as cyanobacteria, eukaryotic algae, and fungi [5].

* Corresponding author. Department of Biotechnology, Oriental Institute of Science and Technology, Vidyasagar University, Midnapore, West Bengal, 721102, India.
E-mail address: kishalayparia@gmail.com (K. Paria).

<https://doi.org/10.1016/j.crgsc.2022.100276>

Received 5 December 2021; Received in revised form 12 January 2022; Accepted 15 January 2022

Available online 20 January 2022

2666-0865/© 2022 The Authors. Published by Elsevier B.V. This is an open access article under the CC BY-NC-ND license (<http://creativecommons.org/licenses/by-nc-nd/4.0/>).

Several scientific evidences proved that the biogenic nanoparticles production via micro algae is considered to be a harmless and eco-friendly green chemistry technique with the potential variety of compositions and physicochemical properties [6]. It is widely documented that green seaweed is used in agriculture, pharmaceutical, biomedical and nutraceutical industries for its presence of high amount of vitamins and minerals. Among several genera of microalgae *Spirulina platensis*, blue green microalgae of cyanobacteria family has grown in temperate waters around the world. A few cross-sectional investigations support that blue green microalgae has been used as a source of food supplement for its high protein content and nutritional value from ancient times [7]. The microalgae produce novel and potentially useful bioactive compounds. Recently the presence of the bioactive compounds has concerned significant interest resulting in the synthesis of new pharmaceutical products, food products, biomedical applications and renewable bioenergy [8]. There are various conventional extraction techniques using hexane, ethanol and water for the collection of bioactive molecules. But they are very problematic due to instability as well as environmental and health hazards. At this time to overwhelm this problem the researchers developed a new approach i.e. supercritical fluid (SCF) extraction technology for avoiding toxic organic solvents in green technology [9]. SCF possesses physical properties intermediate between CO₂ gas and a liquid at a temperature and pressure above its critical point. Besides that, addition of a small amount of co-solvents can cause swelling of algal cells, facilitating the rapid mass transfer of analytes from the matrix [10].

In this research study, we have developed a new way to isolate the organic nanodots from edible freshwater blue green microalgae, *Spirulina platensis*. This is the first report for the production of organic ND from *S. platensis* and their application as food preservative.

2. Materials and methods

2.1. Collection of sample

During this research study *Spirulina platensis* var. lonor was collected from Antenna Green Trust, Madurai, Tamil Nadu, and India. Samples were stored under dry and dark conditions in the sealed container for further analysis.

2.2. Cultivation of bacteria

In laboratory cultures conditions both Gram-positive and Gram-negative food poisoning bacteria i.e. *E. coli*, *B. subtilis*, *S. aureus* and *V. cholerae* were selected for anti-bacterial experiment [11]. The appreciable amounts of autoclaved Muller Hinton Agar (Hi-Media) media was dispensed into sterile plates and allowed to solidify under aseptic conditions. Both types of bacterial strains were spreaded on agar containing sterilized plates. Then the plates were incubated at 37 °C for 24 h. After that the developed bacterial colonies were transferred to nutrient broth medium (Hi-Media) and incubated in a shaking incubator at 37 °C for 24 h.

2.3. Bioactive molecule extracted by supercritical carbon dioxide extraction method

The supercritical carbon dioxide extraction of *Spirulina* microalgae was done by means of a Speed_SFE System of Applied Separations, USA extraction unit. The system comprises a pump fitted with a refrigerated cooling bath to chill the pump head at -4 °C. In case of long run, 50 g (50 g) of freeze dried *Spirulina* powder was weighed accurately in a weight balance. Then it was packed into a 100 ml stainless steel vessel. The glass wool was to be put at both ends of the extraction vessel to avoid the leakage from the vessel. After that the compressed CO₂ was passed from the bottom most of the vessel at a flow rate of 300 ml/min using micro-metering valves. A co-solvent pump of 100% ethanol was added in the extraction vessel at a flow rate of 1 ml/min. The extraction pressure and

temperature were set at 200 bar and 35 °C respectively. According to the experimental set up the total time was fixed as 120 min according to static (60 min) and dynamic extraction time (60 min). After dynamic extraction time microalgae extract was collected in a SFE glass vial. During all extractions conditions the outlet valve temperature of SFE system was regulated greater than the oven temperature to avoid the break of glass vials owing to the increase of ethanol vapours and compressed CO₂ [12].

2.4. Isolation and purification of bio-active compound from microalgae extract

The extract was subjected to thin layer chromatography (TLC) plate to fractionate and isolate the active compound from microalgae that has shown antibacterial activity. A running solvent (acetic acid: butanol: water = 1.5:6:2.5) was used for the separation of an active compound from microalgae. An aliquot of SFE microalgae extract was dotted on the TLC plate using a micro needle. The spots were allowed for dryness. Then the plate was positioned in a TLC chamber containing the running solvent. After that when the solvent was touched approximately 1 cm from the top, TLC plate was removed from the solvent and dried at 45 °C. Pictures of the developing red colour spots in TLC plate were taken. These colour spots were scraped and dissolved in ethyl acetate to isolate the compound from the *Spirulina* biomass extract [13].

2.5. Isolated compounds characterization

2.5.1. Functional group detection by fourier transforms infrared spectrometer (FT-IR) study

According to the method of Jagmohan, 2005 the FT-IR studies have been performed. The potassium bromide (KBr) pellet was added to the sample [14]. Then the sample was placed in a transparent disc of thickness 1 mm and diameter 13 mm and subjected to about 5 × 10⁶ Pa pressure in an evacuated die. IR spectra region of 4000–500 cm⁻¹ were recorded on a FT-IR Nexus TM 870 spectrophotometer (PerkinElmer) [15].

2.5.2. Structural analysis by transmission electron microscope (TEM)

The microalgal sample with concentration of 1 mg/ml was drop casted on a Cu-grid. After drying at room temperature, the samples were directly viewed under TEM following the guidelines as described earlier by Mahata et al., 2017 [16]. The HR-TEM (JEOL JEM 2100 instrument) was used to analyze the samples and capture the images.

2.5.3. Structural analysis through nuclear magnetic resonance (NMR) spectroscopy

¹H NMR can be used to study the presence of hydroperoxy groups as well as of hydrogen, carbonyl and carbon atoms associated in conjugated-dienoic systems. Data was recorded on a DPX200 Bruker (200 MHz for ¹H and 500 MHz for ¹³C) in D₂O with tetramethylsilane (TMS) as an internal standard. Every signal was compared within ±0.1 ppm to standard solution [13].

2.5.4. Antimicrobial activity assessment of bio-active nanodots

The Luria broth (LB) agar plate was prepared with 30 µl inoculums and different doses of active fractions from 1 to 250 µg/ml. Then the agar plates were incubated for 24 h at 37 °C for bacterial growth. Negative controls were prepared adding 30 µl of 50% ethanol in 20 ml LB medium as the solvent used to prepare the ND. The minimum inhibitory concentration (MIC) values were recorded where no visible growth was observed [16]. The plates without compound were treated as positive control for each bacterial inoculums.

2.5.5. Determination of auto-aggregation ability of selected bacteria

Auto-aggregation experiment of bacteria was conducted by use of nutrient broth medium. Selected strains of bacteria, *Vibrio cholerae* were

cultured in nutrient broth in 30 °C at 120 rpm in a shaker incubator. The proper growth of bacteria was checked by measurement of the optical density at 600 nm (OD₆₀₀) through using a spectrophotometer (VARIAN, INC. Carry^R 50 Bio). Without centrifugation an aliquot of cell suspensions of 1.5 ml were taken for measuring the OD at 600 nm, other 1.5 ml aliquots were separated and centrifuged at 650×g for 5 min. After that supernatant was collected and measured the OD at 600 nm. The OD at 600 nm of the samples was recorded three times. The bacterial aggregation index was then calculated with average value as [17]:

$$\text{Aggregation index} = \text{OD}_{(\text{Total})} - \text{OD}_{(\text{Supernatant})} / \text{OD}_{(\text{Total})}$$

2.6. Shelf life estimation of litchi beverage preserved with purified compound

From the local market ripe litchi were collected. During proper grinding and filtration by muslin cloth litchi juice was extracted. Before heating on low flame, 2% sugar was added with prepared juice. Then ND was added as preservative in litchi juice. The treated juice was filled in a glass bottle under sterilized conditions. The glass bottles were shielded immediately using a hand shielding machine. Finally, a total two sets of studies were conducted by varying storage temperature viz. refrigerated (4 ± 2 °C) and ambient storage (room temperature) at specific time interval (0, 7, 15, 30, 45, 60 days) [6].

2.6.1. Physico-chemical analysis of litchi beverage

The litchi juice samples were taken from bottles at specific time intervals and were analysed for total bacterial counts, total fungal count, total soluble/suspended solid, pH, acidity. The pH of the litchi juice was determined with the help of a digital pH meter (Systronics, Model 361). According to the method of Sivakumar and Korsten, titratable acidity was estimated [18]. At first 5 ml of litchi juice was taken and diluted to 50 ml using milli Q water. 100 ml of 0.1% phenolphthalein was then added to 10 ml of diluted juice. 0.1 N NaOH was used to titrate juice containing solution. After a certain period the pink coloration appeared. The volume of used 0.1 N NaOH in titration was noted as the titre value. The titratable acidity of juice was calculated as citric acid percentage. Total soluble solids (TSS) was determined using hand held refractometer (ERMA, Japan; 0–32) at room temperature [19].

2.6.2. Estimation of total bacterial and fungal count of storage litchi beverage

Total plate counts (TPC) were estimated on nutrient agar media (Hi media). The serial dilution of the sample was made sequentially and plated on LB agar plate. After incubation at 37 °C for 24 h colony forming units (CFU) were counted. Fungal counts were estimated on potato dextrose agar (Hi media) after serial dilution of sample. After incubation at 28 °C for 72 h CFU were counted [20].

2.6.3. Sensory evaluation of storage litchi beverage

The litchi juice was selected by sensory evaluation on 9 point Hedonic Scale for different sensory attributes like colour, flavour, appearance and overall acceptability by a panel of 10 non-smoker judges having prior experience of sensory evaluation of fruits and vegetable products. A scale from 1 to 9, where 1 represented extremely disliked and 9 represent extremely liked [21].

3. Results and discussion

The following results of the assessment of organic nanodot as food preservative from *Spirulina platensis* are presented and discussed. This assessment is built upon several sections to analyze and inform.

3.1. Isolation and purification of bio-active compound

The supercritical fluid extract of *Spirulina platensis* biomass (Fig. 1a and b) was fractionated by TLC analysis (Fig. 1c). The active fractionate was then separated from the silica plate and dissolved in ethyl acetate. The solution was further centrifuged at 8000 rpm to separate the active purified compound (Fig. 1d) and lyophilized for further analysis. TEM analysis revealed the average size of the ND is 40–45 nm.

3.2. Spectral characterization of the purified bio-active compound

Ultra violet-visible (UV-VIS) spectroscopy usually provides the characterization of nanodot molecules. When white light is passed through a coloured substance, a distinctive portion of the mixed wavelengths is absorbed. The residual light then will assume the complementary colour to the wavelength (s) absorbed. The ultra-violet spectral absorbance of purified compound was found to be λ_{max} at 400 nm which is corresponding to the presence of olefinic chromophore (conjugated) (Fig. 2a). Bio-material planes can be observed as a variety of functional groups that are responsible for association of metal ions, with hydroxide (–OH), amide (–NH₂), thiols (–SH), carboxylate (–COO–), and phosphate (PO₄^{3–}) [22]. The IR spectrum at 3307 cm^{–1} signifies the ranging vibration of hydroxyl groups. The C–H stretching of vibration indicated at 2986 cm^{–1}. The spectra at 1751 cm^{–1} and 1638 cm^{–1} were recognized to the stretching of C=O vibrations (Fig. 2b). The compound has a signal for C–H aliphatic protons that involved with O- atom at 3.31 ppm. The aliphatic protons signals were further shown at 2.17–0.85 ppm region. The ¹H NMR spectrum also indicated the absence of aromatic proton signals (Fig. 2c). The ¹³C NMR was consistent with the skeletal structure (Fig. 2d).

3.3. Assay of antimicrobial activity of purified compound

Antimicrobial activity of the nanodot was tested against four bacterial pathogens such as *E. coli*, *B. subtilis*, *S. aureus* and *V. cholerae* (Fig. S1) following agar well diffusion assay. The result revealed that 250 mg/l concentration of nanodot exhibits a small clear zone around the well. Minimum inhibitory concentration (MIC) was determined following serial dilution assay and was observed 1 mg/ml for *E. coli*, *V. Cholerae* and 500 mg/l for *S. aureus* and *B. Subtilis* [13].

3.4. Assessments of auto-aggregation ability of compound

Communication among same bacterial species is very much necessary for initial colonization and subsequent their biofilm formation [23]. Therefore, auto-aggregation is the initial step of planktonic cells to develop biofilm over there. Control of auto-aggregation is the easiest way and first step to control the biofilm inhibition. In auto-aggregation, bacteria of the same type form clumps to multicellular structures that ultimately settle down at the bottom of culture tubes. The auto-aggregation is generally done by self-interaction of cell surface molecules, such as proteins and exopolysaccharides [24]. The auto-aggregation ability of targeted nanodots was assessed at different time periods throughout the growth phase. Bacterial auto-aggregation ability was determined by a specific aggregation index. For auto-aggregation study, a food borne pathogen, *V. cholerae* was selected. Here, the obtained result revealed that auto-aggregation was increased in the control group (without ND) in comparison to the treated sample (ND at 250 mg/l) (Fig. 3). Lower auto-aggregation means to inhibit the bio-film formation.

3.5. Changes in quality of litchi beverage

The different physico-chemical and biological quality parameters of litchi beverage using preservative (ND) under refrigerated and ambient temperature were studied. The good quality of food product was first

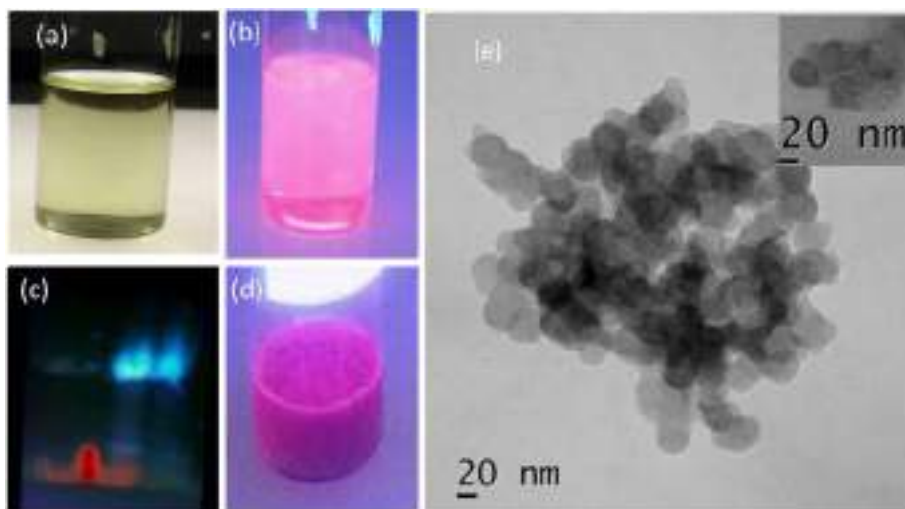


Fig. 1. Separation of active compound. Supercritical fluid extract of *Spirulina platensis* in visible light (a), under UV light (b), The selected area of TLC plate (c), The selected area was collected and concentrated for structural characterization (d), TEM analysis of ND (e).

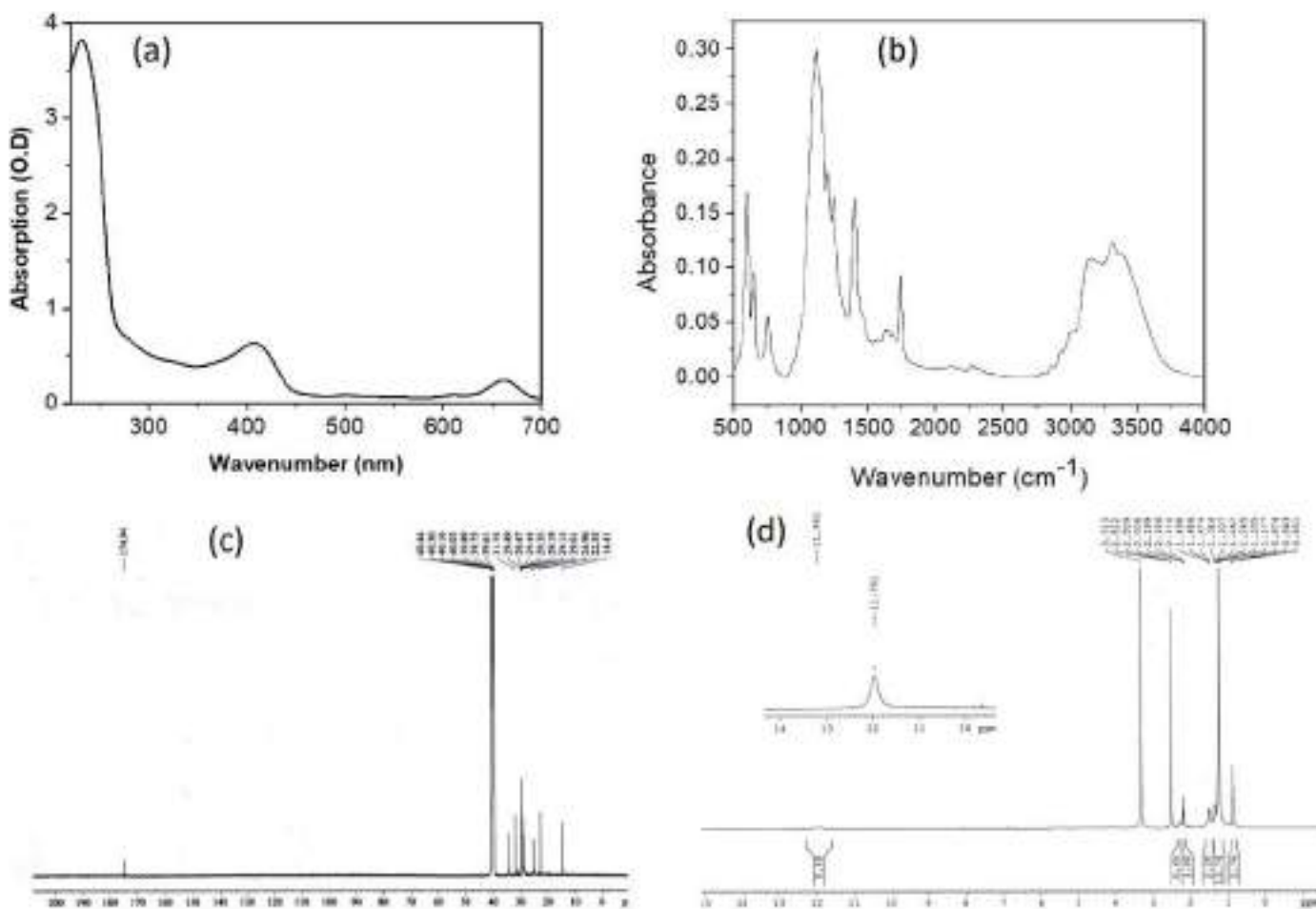


Fig. 2. Spectral characterization of the synthesized NDs. UV-Visible spectrum (a), FT-IR spectrum (b); ^1H NMR spectrum (c) and ^{13}C NMR spectrum of purified ND (d).

determined by pH. The Fig. S2 showed the changes of pH values in the litchi juice samples during storage. It was observed that with the increase of storage period and temperature, pH decreased whereas the acidity and TSS were increased. Data revealed that at refrigerated storage on day

30th, pH decreased for ND sample. TSS of the juice was observed to be higher in ambient storage, being 16.8° Brix as compared to 11.8° Brix at refrigerated storage. On day 30th acidity of juice increased at refrigerated storage.

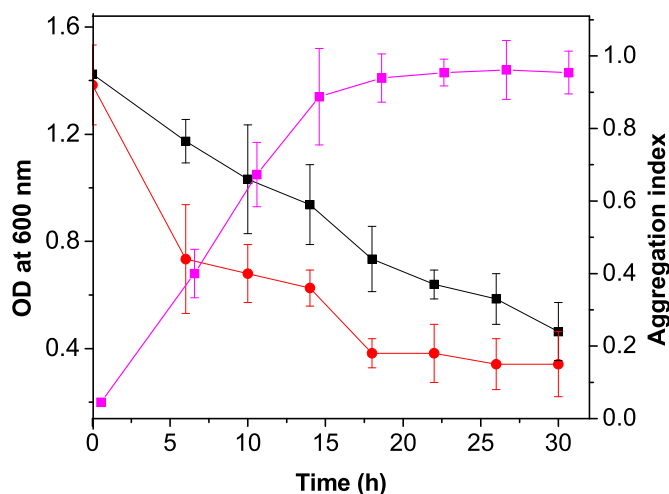


Fig. 3. Determination of auto-aggregation index in the presence and absence of compound NDs. Growth curve of bacteria *V. cholerae* represented the lines with pink colour, auto-aggregation index without NDs (black line) and auto-aggregation index with NDs (red line). Data are the mean of triplicates \pm S.E. (For interpretation of the references to colour in this figure legend, the reader is referred to the Web version of this article.)

3.5.1. Microbial count

At ambient storage more microbial growth was observed as compared to storage at refrigerated condition. It was found that total bacterial and fungal counts are less in ND treated sample than untreated ones (Table S1 and Table S2).

3.5.2. Shelf life analysis of litchi beverage

The suitability of food products during refrigerated storage is related with the variations in their sensory properties. As assessed by the sensory panel, the scores for colour, appearance, taste, odor and overall acceptability of the litchi beverage decreased significantly during the storage

period. The results presented that the beverage fortified with organic ND significantly have better sensory scores. The storage time of the treated and untreated juice was judged on the basis of sensory quality. The sensory score of 6 and above on 9 point Hedonic scale rating was used as a threshold for estimating of shelf life for beverage preservation [25]. The analysis of the data showed that storage condition and treatment had a significant effect on overall acceptability of litchi juice. The sensory quality i.e. colour, aroma, and overall appearance were significantly affected by duration of storage. The overall quality changes of the juice with various storage times at refrigerated and ambient conditions were presented in Fig. S3.

4. Practical application of this research study

For instance, nanotechnology has been used for food quality improvement, shelf-life extension, cost reduction, and nutrition enhancement. Exploration of naturally occurring nanostructures in food is one of the hottest topics in the scientific community.

Although orally administered nonmaterial get absorbed and move across the gastrointestinal tract and distributed in the body parts like kidney, liver, spleen, brain. But *Spirulina platensis* derived organic nanodot is easily digested in our gastrointestinal tract during variation of pH and ultimately undigested molecules are released through defecation (Fig. 4). Generally nanomaterials having size around 5 nm and present in blood circulation undergo renal clearance. Those having 10–20 nm are separated by liver; 200 nm sized NPs get picked up by Kupffer's cells and sinusoidal spleen. Higher concentrations of nanomaterials were excreted via kidney, hepatobiliary pathway. Prior research proved that nano products of ZnO and Ag significantly increase the shelf-life of orange juice and beer through preventing contamination of food and beverages because of their antimicrobial nature against *E. coli*, *Pseudomonas aeruginosa* and *Aspergillus niger* [26].

Since gut bacteria play a critical role in maintaining human health, nanoparticles in food could result in adverse health effects through changes in the gut microbiota. To the best of our knowledge, there are no reports on the impact of ND on gut bacteria. In contrast, the antibacterial abilities of



Fig. 4. Organic nanodot synthesized from *Spirulina platensis* used as a preservative.

ND have been demonstrated. The antimicrobial ability was affected by surface groups, charge, shape, and size of ND [27]. Our knowledge about the bio-effects of food borne organic ND is still in its infancy. *Spirulina platensis* derived ND being an organic molecule has a large surface area but very small in size (about 40–45 nm), that can easily penetrate into microbial cell [28]. Thereafter this is important to meet the criteria of food preservative. In view of all these considerations, longer experimental studies are needed to test the durability of the ND with proper efficacies for their reuse as preservative. However, compared to commercial preservatives, ND is considered a low-cost technological approach which can also become cost-effective and beneficial from the commercial perspectives. Food preservation has emerged as an efficient option for food storage but many challenges and constraints with regard to its practical applications on a large commercial scale still prevail. The following points are needed to be addressed to get the adequate benefit of the preservation methods for practical applications in food and beverages storage.

1. Food borne disease and toxicity of chemical preservatives in food are serious threats to human civilization. The feasibility of food preservation by cost-effective and efficient technique should be explored.
2. The mechanism of antimicrobial activities of *Spirulina platensis* derived nanodots are still not fully clear which are required to be understood with more transparency in the perspective of food preservation.
3. The culture of *Spirulina* is an economically viable approach for food preparation and thereby, their use under strict monitoring can be recommended for agricultural applications parallel with bioremediation of wastewater [29].
4. Bio-energy (hydrogen) production from *Spirulina* alongside undertaking food preparation can become a unique approach that will not only generate food but also lead to the generation of eco-friendly fuels. This technology must be further explored with the aim at achieving possible commercialization [30].
5. The use of algal derived nano based bio-composites may become an effective tool for the adsorption of toxic metal [31].

5. Future prospect

In the face of a significantly growing human population and with the scarcity of healthy food, the world has been facing the challenge of safeguarding human health. Future research studies about the development of *Spirulina* derived nanodots should be focused on food preservation, which demonstrate much better efficacy than traditional ones. In addition, different scientific facts generated from the present research study have touched upon and established the forthcoming multidimensional application of *Spirulina* derived organic nanodots for preservation of food and beverages and thereby further investigations are required to find out the proper mechanism in food preservation, mainly for the under mentioned reasons:

1. The existing output of this research holds greater promise in predicting the antimicrobial potential of *Spirulina* derived nanodots and their practical applicability in food and beverage preservation.
2. Based on earlier information alongside the current research findings, it can be concluded that the nanodots of *Spirulina* can increase shelf life of food and beverages during potential antibacterial as well as anti-fungal activities.
3. Nonetheless, there is a need to undertake more in depth studies with proper chemical analyses that are proposed to constitute the foundation of future research ventures.
4. Organic nanodots will alternatively be used as chemotherapeutics when human pathogens are resistant to antibiotics.

Even though, the traditional chemical food preservatives are also available in the market to increase the shelf life of beverages. Sodium benzoate (SB) can inhibit the growth of spoilage microbes in beverages

i.e. *Saccharomyces cerevisiae*, *Lactobacillus plantarum*. It has been also reported that SB is more effective against yeasts during the 1st day of storage (2–2.5 log CFU reduction) and the microbial growth reduction rates were highest up to 15th day [32]. But those have different side effects including allergy, hypersensitivity, and neurological disorder [33]. Parabens, benzoic acid (BA) and sorbic acid (SA) are commonly used chemical preservatives that are used in beverages. It is reported that among them parabens are esters of the p-hydroxybenzoic acid that have endocrine and reproductive toxicity [34]. Due to such side effects the chemical preservatives are not too recommendable in so many cases whereas organic nanodots have achieved popularity for its no side effects. It was found that total bacterial and fungal counts are less in ND treated sample than untreated sample on 30 days of storage time during refrigerated condition and 15 days during ambient storage. Given such a proposition, it can be concluded that *Spirulina* derived organic nanodots, may also be recommended for the ideal food and beverage preservative. We trust that this research article will pave the way for developing better economically viable as well as significantly acceptable techniques with the focus on food preservation.

6. Conclusion

The present study has established the roles of organic nanodots from microalgae; *Spirulina platensis* holds great promise having numerous potential applications in food industries. This research has opened up new vistas by identifying and establishing the potential efficiency *Spirulina platensis* derived organic nanodot as the food preservative that reaches in several bioactive phytochemicals. Thus this research work is essential to endure the ND research more precisely to progress their surface functionalization and conjugation with bio-molecules. It can also be summarised under four major facts: 1) SFE extract of *Spirulina platensis* was found to produce organic nanodot; 2) nanodot molecule significantly inhibit both Gram positive (*B. subtilis* and *S. aureus*) and Gram negative bacteria (*E. coli*, and *V. cholerae*) as well as fungal contaminants; 3) the organic nanodot able to prevent bacterial biofilm formation; 4) nanodot showing a significantly better sensory quality and enhance shelf life of litchi beverage.

Declaration of competing interest

Authors have no conflict of interest. There is no financial involvement in this work.

Acknowledgement

Authors are acknowledged to the University Grants Commission, India.

Appendix A. Supplementary data

Supplementary data to this article can be found online at <https://doi.org/10.1016/j.crgsc.2022.100276>.

References

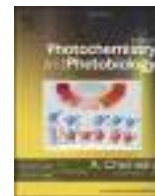
- [1] R. De Vries, C.A. Andrade, A.F. Bakuzis, S.M. Mandal, O.L. Franco, Next-generation nanoantibacterial tools developed from peptides, *Nanomedicine* 10 (2015) 1643–1661, <https://doi.org/10.2217/nmm.15.9>.
- [2] M. Das, K. Senapati, S.S. Panda, P. Bhattacharya, S. Jana, S.M. Mandal, A. Basak, π -Stacking assisted redox active peptide-gallol conjugate: synthesis of a new generation of low toxicity antimicrobial silver nanoparticles, *RSC Adv.* 6 (2016) 85254–85260, <https://doi.org/10.1039/C6RA13075E>.
- [3] A. Roy, S.L. Shrivastava, S. Saha, S. Khamrai, M. Jana, S.M. Mandal, Crede's method in eye water finds a nanomedicine base: a potential candidate to control ophthalmia neonatorum, *Eur. J. Nanomed.* 8 (2016) 233–237.
- [4] M.H. Chan, R.S. Liu, M. Hsiao, Graphitic carbon nitride-based nanocomposites and their biological applications: a review, *Nanoscale* 11 (32) (2019) 14993–15003, <https://doi.org/10.1039/C9NR04568F>.

- [5] S.S. Salem, A. Fouda, Green synthesis of metallic nanoparticles and their prospective biotechnological applications: an overview, *Biol. Trace Elem. Res.* 199 (1) (2021) 344–370, <https://doi.org/10.1007/s12011-020-02138-3>.
- [6] D. Sharma, S. Kanchi, K. Bisetty, Biogenic synthesis of nanoparticles: a review, *Ara. j. chem.* 12 (2019) 3576–3600.
- [7] W.M. Qazi, S. Ballance, A.K. Uhlen, K. Kousoulaki, J.E. Haugen, A. Rieder, Protein enrichment of wheat bread with the marine green microalgae *Tetraselmis chuii*—Impact on dough rheology and bread quality, *Lebensm. Wiss. Technol.* 143 (2021) 111115, <https://doi.org/10.1016/j.lwt.2021.111115>.
- [8] A. Kartik, D. Akhil, D. Lakshmi, K.P. Gopinath, J. Arun, R. Sivaramakrishnan, A. Pugazhendhi, A critical review on production of biopolymers from algae biomass and their applications, *Bioresour. Technol.* (2021) 124868, <https://doi.org/10.1016/j.biortech.2021.124868>.
- [9] K.I.B. Moro, A.B.B. Bender, L.P. da Silva, N.G. Penna, Green extraction methods and microencapsulation technologies of phenolic compounds from grape pomace: a review, *Food Bioprocess Technol.* (2021) 1–25, <https://doi.org/10.1007/s11947-021-02665-4>.
- [10] K.C. Badgajar, R. Dange, B.M. Bhanage, Recent advances of use of the supercritical carbon dioxide for the biomass pre-treatment and extraction: a mini-review, *J. Indian Chem. Soc.* (2021) 100018, <https://doi.org/10.1016/j.jics.2021.100018>.
- [11] S. Manna, M. Ghosh, R. Chakraborty, S. Ghosh, S.M. Mandal, A review on quantum dots: synthesis to In-silico analysis as next generation antibacterial agents, *Curr. Drug Targets* 20 (2019) 255–262.
- [12] C. Crampon, O. Boutin, E. Badens, Supercritical carbon dioxide extraction of molecules of interest from microalgae and seaweeds, *Ind. Eng. Chem. Res.* 50 (15) (2011) 8941–8953, <https://doi.org/10.1021/ie102297d>.
- [13] S.M. Mandal, S. Chakraborty, S. Sahoo, S.K. Pyne, S. Ghosh, R. Chakraborty, Novel compound from flowers of moringa oleifera active against multi-drug resistant gram-negative Bacilli, *Infect. Disord. - Drug Targets* 20 (1) (2020) 69–75.
- [14] J. Mohan, *Organic Spectroscopy Principles and Applications*, second ed., Narosa publishing House, Daryagan, Delhi, 2005. ISBN 13: 9780849310072.
- [15] K. Paria, S.K. Chakraborty, Eco-potential of *Aspergillus penicillioides* (F12): bioremediation and antibacterial activity, *SN Appl. Sci.* 1 (2019) 1545–1546, <https://doi.org/10.1007/s42452-019-1545-6>.
- [16] D. Mahata, M. Jana, A. Jana, A. Mukherjee, N. Mondal, T. Saha, S.M. Mandal, Lignin-graft-polyoxazoline conjugated triazole a novel anti-infective ointment to control persistent inflammation, *Sci. Rep.* 7 (2017) 46412.
- [17] E. Vlkova, V. Rada, Smehilova, M.J. Killer, Auto-aggregation and co-aggregation ability in bifidobacteria and clostridia, *Folia Microbiol.* 53 (3) (2008) 263–269.
- [18] D. Sivakumar, L. Korsten, Influence of modified atmosphere packaging and postharvest treatments on quality retention of litchi cv. Mauritius, *Postharvest Biol. Technol.* 41 (2006) 135–142, <https://doi.org/10.1016/j.postharvbio.2006.03.007>.
- [19] S. Teerachaichayut, H.T. Ho, Non-destructive prediction of total soluble solids, titratable acidity and maturity index of limes by near infrared hyperspectral imaging, *Postharvest Biol. Technol.* 133 (2017) 20–25, <https://doi.org/10.1016/j.postharvbio.2017.07.005>.
- [20] R. Bhat, N.S.B.C. Kamaruddin, L. Min-Tze, A.A. Karim, Sonication improves kasturi lime (*Citrus microcarpa*) juice quality, *Ultrason. Sonochem.* 18 (6) (2011) 1295–1300.
- [21] M. Ayub, J. Ullah, A. Muhammad, A. Zeb, Evaluation of strawberry juice preserved with chemical preservatives at refrigeration temperature, *Int. J. Nutr. Metabol.* 2 (2010), <https://doi.org/10.5897/IJNAM.9000015>, 027-032.
- [22] K. Paria, S.M. Mandal, S.K. Chakraborty, Simultaneous removal of Cd (II) and Pb (II) using a fungal isolate, *Aspergillus penicillioides* (F12) from Subarnarekha Estuary, *Int. J. Environ. Res.* 12 (2018) 77–86, <https://doi.org/10.1007/s41742-018-0070-6>.
- [23] I. Dige, M.K. Raarup, J.R. Nyengaard, M. Kilian, B. Nyvad, *Actinomyces naeslundii* in initial dental biofilm formation, *Microbio* 155 (2009) 2116–2126, <https://doi.org/10.1099/mic.0.027706-0>.
- [24] T. Trunk, H.S. Khalil, J.C. Leo, Bacterial auto aggregation, *AIMS microbio.* 4 (1) (2018) 140, <https://doi.org/10.3934/microbiol.2018.1.140>.
- [25] A. Martínez-Sánchez, A. Allende, R.N. Bennett, F. Ferreres, M.I. Gil, Microbial, nutritional and sensory quality of rocket leaves as affected by different sanitizers, *Postharvest Biol. Technol.* 42 (2006) 86–97.
- [26] T. Sun, Y. Kang, J. Liu, Y. Zhang, L. Ou, X. Liu, L. Shao, Nanomaterials and hepatic disease: toxicokinetics, disease types, intrinsic mechanisms, liver susceptibility, and influencing factors, *J. Nanobiotechnol.* 19 (1) (2021) 1–23, <https://doi.org/10.1186/s12951-021-00843-2>.
- [27] R. Sharma, S.M. Jafari, S. Sharma, Antimicrobial bio-nanocomposites and their potential applications in food packaging, *Food Control* 112 (2020) 107086, <https://doi.org/10.1016/j.foodcont.2020.107086>.
- [28] J.M.V. Makabenta, A. Nabawy, C.H. Li, S. Schmidt-Malan, R. Patel, V.M. Rotello, Nanomaterial-based therapeutics for antibiotic-resistant bacterial infections, *Nature reviews Microbio* 19 (1) (2021) 23–36.
- [29] N. Geetha, G. Bhavya, P. Abhijith, R. Shekhar, K. Dayananda, S. Jogaiah, Insights into nanomycoremediation: secretomics and mycogenic biopolymer nanocomposites for heavy metal detoxification, *J. Hazard Mater.* 409 (2021) 124541, <https://doi.org/10.1016/j.jhazmat.2020.124541>.
- [30] F.F. de Araújo, D. de Paulo Farias, I.A. Neri-Numa, G.M. Pastore, Polyphenols and their applications: an approach in food chemistry and innovation potential, *Food Chem.* 338 (2021) 127535, <https://doi.org/10.1016/j.foodchem.2020.127535>.
- [31] T.A. Ngo, M.S. Kim, S.J. Sim, High-yield biohydrogen production from biodiesel manufacturing waste by *Thermotoga neapolitana*, *Int. J. Hydrogen Energy* 36 (10) (2011) 5836–5842.
- [32] A. Panitsa, T. Petsi, P. Kandyliis, M. Kanellaki, A.A. Koutinas, Tubular cellulose from orange juice by-products as carrier of chemical preservatives; delivery kinetics and microbial stability of orange juice, *Foods* 10 (8) (2021) 1882, <https://doi.org/10.3390/foods10081882>.
- [33] F.C. Martins, M.A. Sentanin, D. De Souza, Analytical methods in food additives determination: compounds with functional applications, *Food Chem.* 272 (2019) 732–750.
- [34] Y. Bian, Y. Wang, J. Yu, S. Zheng, F. Qin, L. Zhao, Analysis of six preservatives in beverages using hydrophilic deep eutectic solvent as disperser in dispersive liquid-liquid microextraction based on the solidification of floating organic droplet, *J. Pharmaceut. Biomed. Anal.* 195 (2021) 113889.



Contents lists available at ScienceDirect

Journal of Photochemistry & Photobiology, A: Chemistry

journal homepage: www.elsevier.com/locate/jphotochem

Ammonium phosphomolybdate $[(\text{NH}_4)_3\text{PMo}_{12}\text{O}_{40}]$ an inorganic ion exchanger for environmental application for purification of dye contaminant wastewater

Arun Kumar Sinha^a, Anup Kumar Sasmal^b, Anjali Pal^c, Debasish Pal^c, Tarasankar Pal^{d,*}

^a Department of Chemistry, Achhruram Memorial College, Jhalda 723202, Purulia, India

^b Department of Chemistry and Department of Civil Engineering, Indian Institute of Technology, Kharagpur 721302, India

^c Department of Civil Engineering, Indian Institute of Technology, Kharagpur 721302, India

^d Department of Chemical Sciences, Auckland Park Kingsway Campus, University of Johannesburg, South Africa

ARTICLE INFO

Keywords:

Yellow ammonium phosphomolybdate
UV light
Green ammonium phosphomolybdate
Wastewater
Dye removal

ABSTRACT

Yellow ammonium phosphomolybdate (YAPM), a waste product of all under graduate (UG) chemistry laboratory classes, has been proved to be an efficient adsorbent for environmental application as a cationic ion exchanger. The water insoluble YAPM selectively removes cationic dye molecules from dye contaminated wastewater. Consequently, dye infested YAPM solid is produced with fascinating color but bears altered band gap energy. Dye contaminated yellow APM is regenerated in air oven from the dye infested YAPM solid powder by heat treatment at $\sim 300^\circ\text{C}$ and reused with full potential. So it becomes a solid phase extractant. Robust yellow APM turns to green APM (GAPM) upon UV light exposure because of the hoarded electrons in the basket like Keggin structure of phosphomolybdate ($\text{PMo}_{12}\text{O}_{40}^{3-}$) moiety, and thereby the dye exchange capability is improved, admirably. Thus, the remediation of dye contaminated wastewater by YAPM has been found to be fruitful by YAPM and more potential dye remediation by GAPM.

1. Introduction

Polyoxometalates (POMs) are extremely large group of anionic clusters with frameworks built from transition metal oxo anions linking shared oxide ions [1]. Most of the elements in the periodic table can be incorporated as cations into the structural framework of these robust compounds. Yellow ammonium phosphomolybdate (YAPM), $[(\text{NH}_4)_3\text{PMo}_{12}\text{O}_{40}]$ is a low cost polyoxometalate compound, and a waste product of the undergraduate (UG) laboratory. We have shown useful application of YAPM vis-à-vis UV exposed YAPM i.e., GAPM for purification of dye contaminant wastewater through ion exchange method. Here inorganic ammonium phosphomolybdate acts as an ion exchanger.

Dye contaminated wastewater effluents comes from different industries and that causes a global problem. Particularly cloth-dyeing industries discharge a huge amount of waste organic dye molecules into rivers without any scientific treatment. Public news media reported serious water pollution caused by organic dye molecules in different rivers of many countries. China [2], India [3] and Bangladesh [4] suffer

from this problem. Thus many rivers flows with different organic chemicals, and as a result flora and fauna are affected. In future, it will be a serious problem for aquatic environment as well as human life. To save the clean environment, proper treatment of wastewater is a challenging task to the environmental scientists. There are so many well-known processes for removal of dye molecules from the water bodies. Photocatalysis [5], adsorption [6] and ion exchange process [7] are widely used methodologies. In general, metal oxides [8], sulphides [9] are used as photocatalyst and ion exchangers [10] for demineralization of water. Photocatalytic reaction for purification of dye contaminant wastewater requires visible or UV light for photo-assisted mineralization reaction to proceed. A proper light source (visible light [11] or UV light [12]) is required depending on the nature of dye and band gap of photocatalyst. But in the dark, an adsorbent becomes appropriate than a photocatalyst for dye removal from wastewater. The traditional adsorbents are activated carbon material [13], oxides [14] and sulfides [10] which are used for purification of water bodies. Recently, researchers have exploited CNT [15], graphene oxide [16], reduced graphene oxide [17], organic gel [18] and inorganic gel [19] materials for dye removal

* Corresponding author.

E-mail address: tpal@chem.iitkgp.ac.in (T. Pal).

<https://doi.org/10.1016/j.jphotochem.2021.113427>

Received 27 February 2021; Received in revised form 29 May 2021; Accepted 21 June 2021

Available online 4 July 2021

1010-6030/© 2021 Elsevier B.V. All rights reserved.

by adsorption of dye molecules since these materials often bear large surface area. Generally, forces, operate between the adsorbent and adsorbate dyes may be hydrophobic interaction, [20] hydrogen bonding attraction [21] and electrostatic force [22] in ion exchange processes. The adsorbent with ion exchange property is a better option than adsorbent with non-ion exchange capability as in the latter case there happens stronger electrostatic attraction, selective binding minimization of leaching of adsorbate happen from the adsorbent.

Junbai Li et al. reported that MnO_2 hollow sphere can separate Congo red effectively from dye contaminated wastewater [14]. Purely inorganic material, indium selenide $(\text{NH}_4)_4\text{In}_{12}\text{Se}_{20}$, has cation ion exchange property which can remove different toxic metal ions such as Cs^+ , Rb^+ , Hg^{2+} and Pb^{2+} etc. via electrostatic interaction [23]. So they are used to purify these heavy metal ions from water bodies. An important layered sulfide material $\text{K}_{2x}\text{Mn}_x\text{Sn}_{3-x}\text{S}_6$ ($x = 0.5-0.95$) which bears highly mobile or exchangeable K^+ ions in their interlayer spaces. So, K^+ is easily exchanged with other toxic metal ions such as Sr^{2+} ion [24], UO_2^{2+} ion [10], Hg^{2+} ion [25], Cs^{+1} ion [26] etc. via electrostatic force that helps purification of contaminated water reserves.

In this article, we have reported a unique method for removal of cationic dye molecules using water suspension of low cost and readily available yellow ammonium phosphomolybdate $[(\text{NH}_4)_3\text{PMo}_{12}\text{O}_{40}]$ (YAPM) and also UV exposed green ammonium phosphomolybdate (GAPM) which is proved to be a more efficient inorganic ion exchanger [27,28]. After dye exchange reaction, the dye infested YAPM upon heat treatment at $\sim 300^\circ\text{C}$ regenerates the parent adsorbent, YAPM with the retention of original chemical stability and recyclability. The electrostatically bound dyes are not at all leached out from the adsorbent, YAPM. The most interesting phenomenon is that the yellow APM is photoreduced to green ammonium phosphomolybdate (GAPM) upon UV ($\sim 360\text{ nm}$) light irradiation. As a noticeable result, GAPM acquires more effective dye removal capacity again through ion exchange reaction step. It is observed that the dye exchange capacities of YAPM and GAPM have higher values than common polystyrene based cation exchange resins. However, the dye removal capacity varies from dye to dye. In the present investigation, different types of dye molecules (such as cationic, anionic and neutral dye) are used for exchange reaction with APM materials. Among them methylene blue (MB), malachite green (MG) and rhodamine B (RhB) have experienced exchange reaction with $[(\text{NH}_4)_3\text{PMo}_{12}\text{O}_{40}]$ material as all these dye molecules are cationic in nature. Ammonium ion (NH_4^+) in APM becomes exchangeable with only the cationic dye molecule. So the yellow ammonium phosphomolybdate $[(\text{NH}_4)_3\text{PMo}_{12}\text{O}_{40}]$ (YAPM) and UV exposed GAPM find novel environmental application as inorganic ion exchanger for cationic dye removal from water bodies. Dye infested APM molecules are readily recovered by heat treatment. Thus the method proclaims a unique 'zero waste' strategy for dye removal from wastewater with 100% APM recovery by heat treatment.

2. Experiment and Methods:

2.1. Materials and instruments

The material and instruments are given in the [supporting information SI 1](#).

2.2. Preparation of yellow APM and green APM

In a typical preparation, $(\text{NH}_4)_6\text{Mo}_7\text{O}_{24}\cdot 4\text{H}_2\text{O}$ (4.50 g) and $\text{NaH}_2\text{PO}_4\cdot\text{H}_2\text{O}$ (0.50 g) were added into 200 mL distilled water and warmed on a water bath at $\sim 80^\circ\text{C}$ to obtain a clear solution. Then the warm solution on the water bath was acidified with conc. HNO_3 (3 mL). The solution was stirred by a glass rod for 1–2 min and kept for the next 30 min at the same temperature. The canary yellow material was precipitated and washed several times with distilled water until its pH value lowers down to ~ 6.8 (pH of distilled water) and dried in an air oven at 100°C .

Due to the high water solubility of the parent salts, solid and crystalline form of the synthesized material was washed several times with water. So impurity contamination in the synthesized material becomes redundant. The yellow product is ammonium phosphomolybdate, $[(\text{NH}_4)_3\text{PMo}_{12}\text{O}_{40}]$. The yellow APM material was exposed to UV light ($\sim 365\text{ nm}$ with spectral distribution of 350–400 nm) of power 15 W for 30 days in Air in UV-light. About 1 gm APM was spread as a thin layer on large size petri dish and placed in the UV-light chamber for long time (30 days). Every day, the material was respreads and exposed to UV light and continued for 30 days to ensure the complete surface reduction of yellow APM.

The whole material (YAPM) changed to deep green APM (GAPM) by solid state photochemical reaction. The green APM i.e., GAPM [27,28] was stored in the dark under inert condition (N_2 or argon gas). Upon storing the GAPM sample in an open place at room temperature condition, the material gradually slowly reverts back to YAPM. The green and yellow materials (YAPM and GAPM) were employed as inorganic exchangers for dye removal from wastewater through ion exchange reaction.

2.3. Kinetic studies of dye exchange reaction

The organic dye molecule bearing positively charged structure was used for ion exchange experiment with YAPM. The yellow matrix electrostatically exchanges its NH_4^+ ion with the incoming cationic dye molecules. We have employed four dyes [methylene blue (MB), malachite green (MG), rhodamine B (RhB) and methyl violet (MV)] for the ion exchange reactions to study the efficacy of APM towards the dyes. The progress of dye exchange reaction was monitored by a UV-Visible spectrophotometer at various time intervals.

For each experiment, a total of 100–200 mg of YAPM was weighted in a 250 mL glass beaker. Methylene blue solution (100 mL of $3 \times 10^{-5}\text{ M}$) was added into beaker, and the solution was kept under magnetic stirring condition. The suspension from the reaction mixture was centrifuged at 7000 rpm and the resulted clear solutions were analyzed using UV-Visible spectrophotometer. We have performed similar studies using other dyes (other cationic, anionic and neutral dyes). In case of anionic or neutral dyes, there occurs almost no exchange reaction. APM moiety captures only cationic dyes selectivity.

2.4. Regeneration

Dye-APM colored composite materials were subjected to heat treatment for 12 h at 300°C in an air oven. After the heat treatment, the samples become yellow i.e., YAPM. Thus the original material (yellow APM) was regenerated. DRS spectrum of this sample (after heating) was found to be similar to that of parent APM. This material was reused several times for dye removal through the same ion exchange reaction. We have tested the material for consecutive three cycles. After three cycles, the material was treated with conc. HNO_3 acid and its original activity has been observed to be restored, gratifyingly again it showed the retention of original band gap position.

3. Result and discussion

Solid APM is a well-known intricate polyoxometalate having giant molecular structure. We have presented the cation exchange property of APM and this property has been exploited for the removal of toxic dye molecules from wastewater for environmental abatement. Generally, transition metal oxides and sulfide were used as adsorbents or catalysts to remove organic waste from water by adsorption followed by combustion at relatively low temperature, photocatalytic reactions, etc. In this article, the removal of dyes through ion exchange property of YAPM as well as GAPM are discussed.

YAPM is a compound with UV light absorption capacity. Upon absorption of UV light ($\sim 365\text{ nm}$) over a long time (3 days), the yellow

material is photoreduced to deep green compound in solid state [27] which is named as GAPM. The optical property of both the materials are investigated by DRS spectroscopy (Fig. 1). Broad absorption spectra were observed in both the cases. The peaks at 418 nm and 288 nm are found for the YAPM. Green APM (GAPM) exhibits peaks at 288 nm, 402 nm and with one extra band at 805 nm (Fig. 1a). In accordance with the UV-Visible spectral measurement, inter-band or excitonic transitions in YAPM and GAPM have also been observed. Theoretical expression for the determination of band gap of a semiconductor material is given by the following equation:

$$\alpha E_p = K (E_p - E_g)^{1/2}$$

where α is the absorption coefficient, K is a constant, E_p is the discrete photoenergy, and E_g is the band gap energy. A classical Tauc approach [29] is used to estimate the E_g of the material. The plot of $(\alpha E_p)^2$ versus E_p based on the direct transition and extrapolation of E_p at $\alpha = 0$ gives absorption edge energy which is band gap of the materials (Fig. 1b). From the plots, it is observed that the yellow material (YAPM) has band gap of 2.5 eV.

Remarkably, upon UV light exposure hoarding of electrons in the basket like structure of the yellow materials is readily observed as indicated by the position of band gap change (shown in Fig. 1b). Interestingly this observation complies with our reported EPR results [27] and also with an earlier report [30]. Conversely, this photochemical changeover was not detectable from common physical measurements like FTIR and powder XRD analysis (shown in Fig. S2 in Supporting Information). The dye exchange reaction does not affect the phase purity or crystal bond vibration as dyes remain bound onto the surface electrostatically of the robust anionic $[\text{PMo}_{12}\text{O}_{40}]^-$ moiety. Thus it may be said that the changeover took place only on the upper surface of the material by ion exchange. Presumably rigid skeletal dye moiety cannot invade into the phosphomolybdate skeleton reasonably. Photochemical color change from yellow YAPM to GAPM happens and this change is reversible under the UV light and or dark/ambient material storage conditions (Fig. 2).

This reversible color change is identified by UV-visible study in transmittance mode with time (shown in Fig. S3 in Supporting

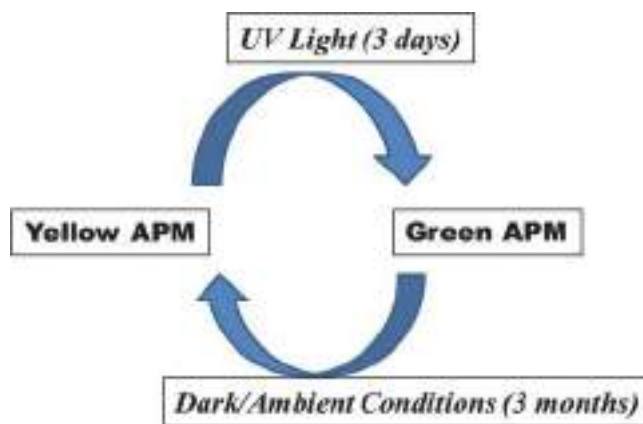


Fig. 2. Reversible conversion of yellow APM and green APM (GAPM).

Information). Actually, the color change from green APM to yellow APM (reaction in the dark takes about 3 months) is extremely slow. That is why, we have shown the time course of UV-vis spectrum for the color change from yellow to green only.

After solid state photochemical reaction, there happens no change or distortion in morphology of APM i.e., anionic $[\text{PMo}_{12}\text{O}_{40}]^-$ moiety (investigated even by FESEM analysis) i.e. the yellow and green APM materials contain same shape and size which is shown in Fig. 3. This type of reversible photochromatic behavior between yellow APM and green APM (GAPM) is unusual and has been found with Ag-TiO₂ [31].

In aqueous solution of dye, solid APM was added and allowed for facile exchange reaction to happen by stirring using a magnetic stirrer. The dye-APM composite material settled down after waiting for 1 h or by centrifugation gives clear supernatant aqueous solution which is readily used for UV-visible studies.

We have monitored the exchange reaction by UV-visible spectroscopy at the band position of 662 nm of methylene blue (Fig. 4). With the progress of the reaction, the absorption value at 662 nm gradually decreases. We have performed the exchange reaction with different amount of yellow APM (0.1–0.2 g) and the spectral profiles as well as

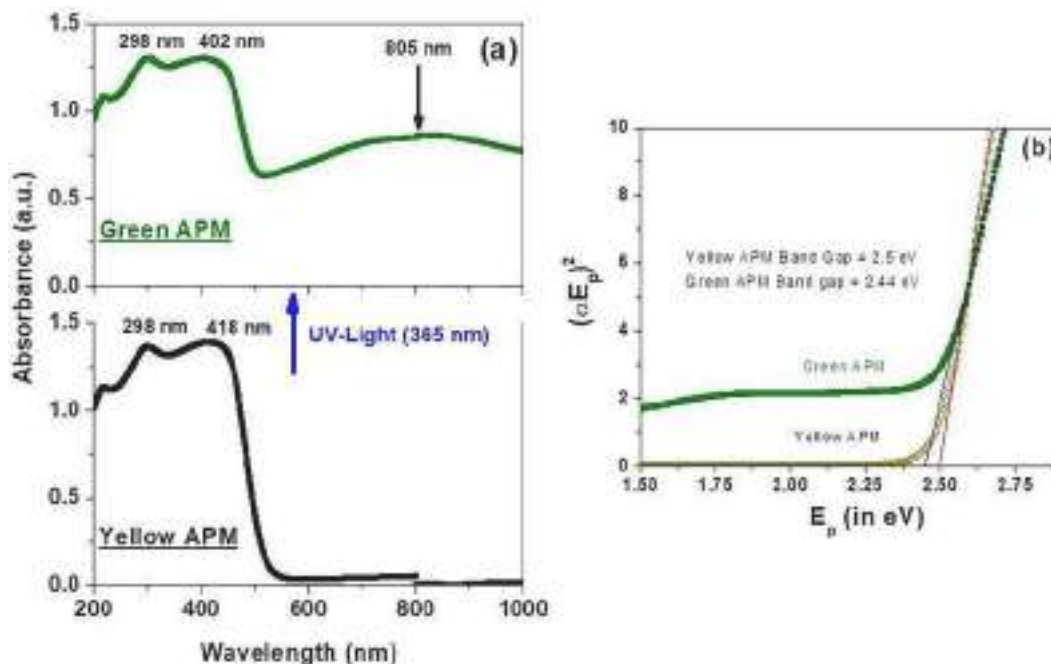


Fig. 1. DRS spectra for the formation of green APM from yellow APM under UV light exposure at 365 nm (a) and indication of the change in band gap while yellow APM changes to green APM (b).

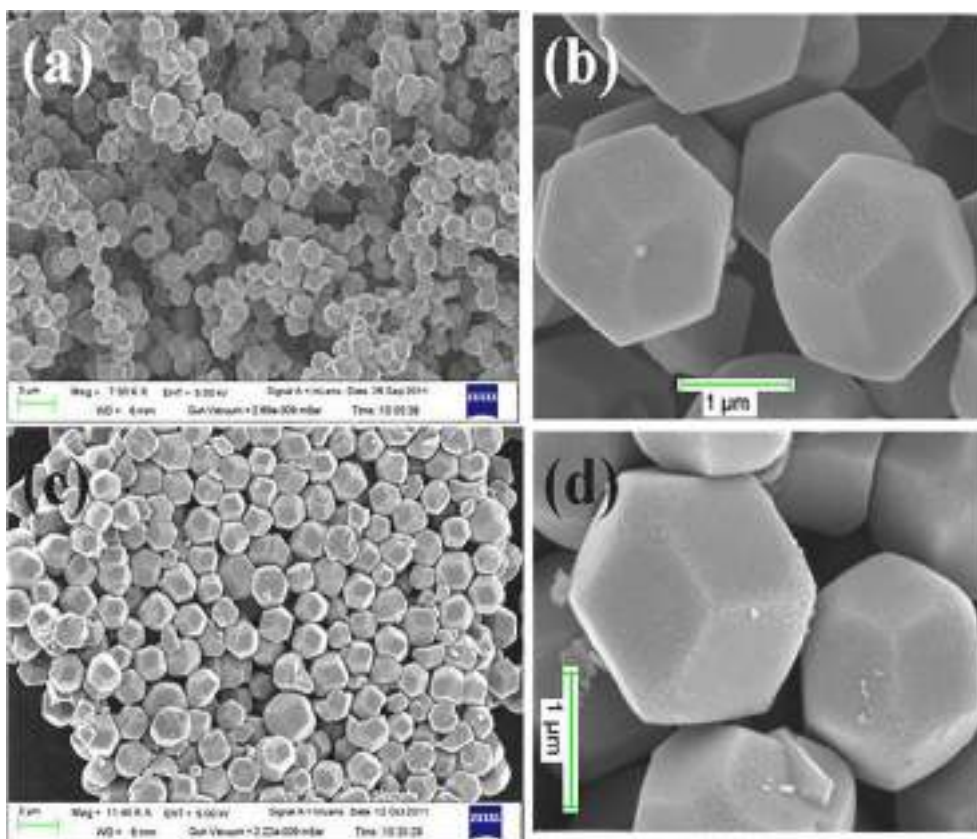


Fig. 3. FESEM image of Yellow APM (a and b) and UV light treated green APM (c and d).

time dependent color change are shown Fig. 4. A higher dose of yellow APM provides larger surface area, so the time of exchange reaction becomes shorter, and conversely, a lower amount of yellow APM sample takes longer time to complete the exchange reaction.

In similar way, other cationic dye molecules (such as rhodamine B, malachite green) are also separated from aqueous solutions and the corresponding dye exchange reactions have also been monitored again by UV–Visible study which is shown in Supporting Information (Fig. S4). After dye exchange reaction on APM, the color of the dye-APM composite changes to the corresponding color of dye which is shown in Fig. 5 by digital images.

Then the dye-APM composite material is heated at $\sim 300\text{ }^{\circ}\text{C}$ for 12 h. Hence, the bound dye molecule in APM matrix is completely decomposed. The decomposition process of organic dye is shown in Fig. 6b by TG analysis. From the TG analysis, at high temperature range ($400\text{--}500\text{ }^{\circ}\text{C}$), it is observed that the host APM material undergoes partial decomposition like other molybdenum compounds [32]. That is way, we select $300\text{ }^{\circ}\text{C}$ for our thermal reaction. The TG profile (at $400\text{--}500\text{ }^{\circ}\text{C}$ range) is little bit different for the above material due to the temperature dependent variation in composition (APM a pure inorganic material and Dye-APM an organic–inorganic hybrid composite material) of the material. The colorful dye-APM composite material regains the original yellow APM color and gets ready for reuse for at least 3 cycles (shown in Fig. 6a).

During heating at temperature $\sim 300\text{ }^{\circ}\text{C}$, the colored Dye-APM composite breaks down to gaseous molecules and leaves yellow APM as the decomposition product. We have used different cationic dye molecules as a model contaminant in water which contain alkyl amine as a functional group. It is expected that Dye-APM change to $(\text{NH}_4)_3\text{PMo}_{12}\text{O}_{40}$ at this elevated temperature and NH_4^+ ions are regenerated or come from nitrogenous part of the dye molecules. This was presumed from the dye adsorption studies with the decomposition product.

After repetitive use, the material loses its original adsorption activity. Consequently, the ion exchange time increases (shown in Fig. S5a–c of Supporting Information). Organic dye molecules upon heat treatment presumably generates small carbon nanoparticles which presumably get deposited on the active surfaces of YAPM. These carbon particles from the active sites of YAPM is easily removed by concentrated HNO_3 acid treatment which removes the carbon NPs from the APM surface. Carbon particles are oxidized by HNO_3 and thus the original activity of yellow APM is restored (shown in Fig. S5d of Supporting Information).

The exchange capacities of yellow and green APM materials were compared with other materials such as oxide matrix and commercial cation exchange resin (information is summarized in Table 1 of Supporting Information). The best result comes out from yellow and green APM compounds. One gram of yellow APM uptakes MB dye molecules from 70 mL of 10^{-3} M and the deep blue color of aqueous solution of methylene blue becomes colorless.

The dye exchange reaction of APM matrix with methylene blue was performed also in presence of different cations such as Na^+ , Ca^{2+} , Mg^{2+} etc. These ions are present in sea water, lake water, pond water and tap water. An aliquot of MB solution was mixed with sea water, lake water, pond water and tap water separately, and the solutions were used for same exchange reaction by YAPM. The UV–Visible study for MB separation from different water system is shown in Fig. S6 Supporting Information. It is evident that when high concentration of alkali metal ions presents in the water sample, the duration of dye exchange reaction increases to a large extent. Precisely, the existing ions in water bodies become the inhibitor for the cationic dye adsorption and slow down the ion exchange reaction.

Dye exchange reaction has been studied using cationic, anionic and neutral dyes, and the mechanism of exchange reaction is shown in Scheme 1. The anionic and neutral dye molecules are not exchanged with the APM, and the corresponding step wise UV–visible study is shown in Fig. S7 of Supporting Information. APM can uptake selectively

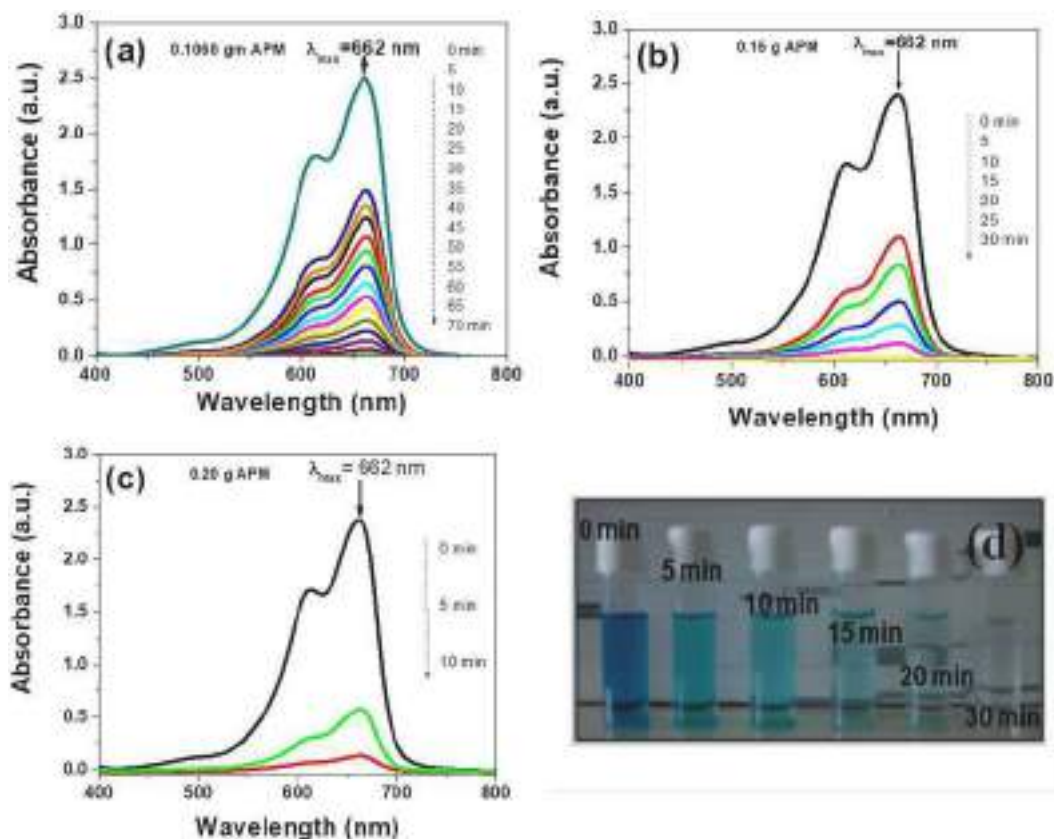


Fig. 4. UV-Visible study of methylene blue dye (5×10^{-5} M) exchange reaction at different time interval with (a) 0.10 g, (b) 0.15 g and (c) 0.2 g of yellow APM and a representative digital images showing methylene blue exchange reaction at different time interval.

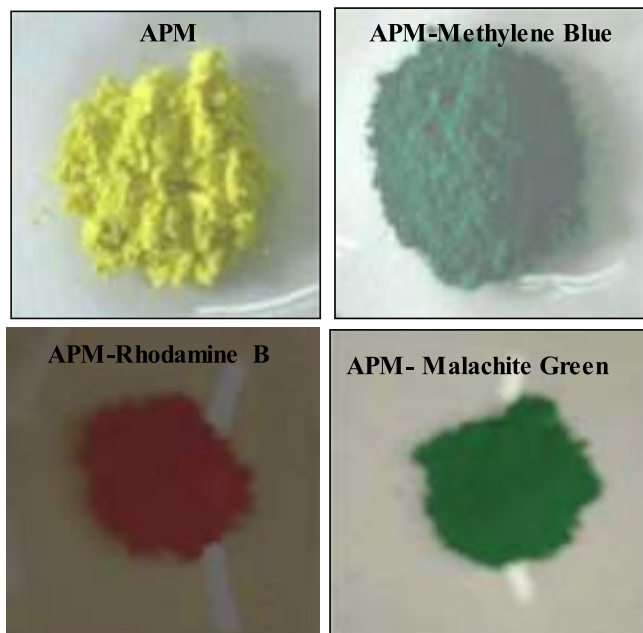


Fig. 5. Digital images of APM after dye exchange reaction: APM-methylene blue, APM-rhodamine B and APM-malachite green.

cationic dye molecules such as methylene blue, malachite green, rhodamine B, methyl violet (all are cationic dyes) effectively under ambient condition with different exchange/separation time. This relates to the skeletal size and electronic properties of the cationic dye molecules with amine functionality. The dye molecules bearing rigid larger

skeletal structure are slowly exchanged with smaller ammonium ion of APM. Anionic and neutral dyes after waiting a longer time, there occurs no exchange and slight decrease in absorbance values occur due to physisorption of dye molecule on APM moiety (Fig. S7 in Supporting Information). On the other hand, cationic dyes require much less time to complete the exchange reaction in comparison to anionic or neutral dyes. Thus physisorption is easily understandable due to the absence of electrostatic attraction. Additionally, the charge of the counter ion i.e. NH_4^+ in $[(\text{NH}_4)_3\text{PMo}_{12}\text{O}_{40}]$ plays an important role in the dye exchange reaction. The cationic dye molecules (dye^+) replace ammonium ion (NH_4^+) and form $[(\text{NH}_4)_m(\text{dye})_n\text{PMo}_{12}\text{O}_{40}]$ ($n + m = 3$). The dye exchange reaction happened only on the outer surface not inside the APM microcrystal because of steric crowding and rigid dye skeleton. The interaction between cationic dye and APM is investigated by solid DRS analysis. The band position of cationic dye molecule is blue shifted in Dye-APM composite material. The DRS spectra of dye-APM composite materials are shown in Fig. S8 Supporting Information. This DRS analysis indicates that there exists an electrostatic interaction between the individual dye molecule and yellow APM matrix furnishing λ_{max} shifting of the dye molecule from the original value. In case of MB-APM composite, the band position of MB is shifted from 662 nm to 628 nm this hypsochromic shift indicates that there is significant electrostatic interaction between APM and MB. The electrostatic interaction is the main cause for the shifting of band position of MB. The exchange capacity values of a particular adsorbent vary from dye to dye depending on the size and electronic property of the dye skeleton as it is understandable. Upon UV light irradiation for a long time, the YAPM material changes to deep green APM (GAPM). The Keggin structure $[(\text{NH}_4)_3\text{PMo}_{12}\text{O}_{40}]$ inherits a special ability to accept one or several electrons, which remain delocalized within the Keggin basket without causing any structural deformation resembling a basket stored with electrons.

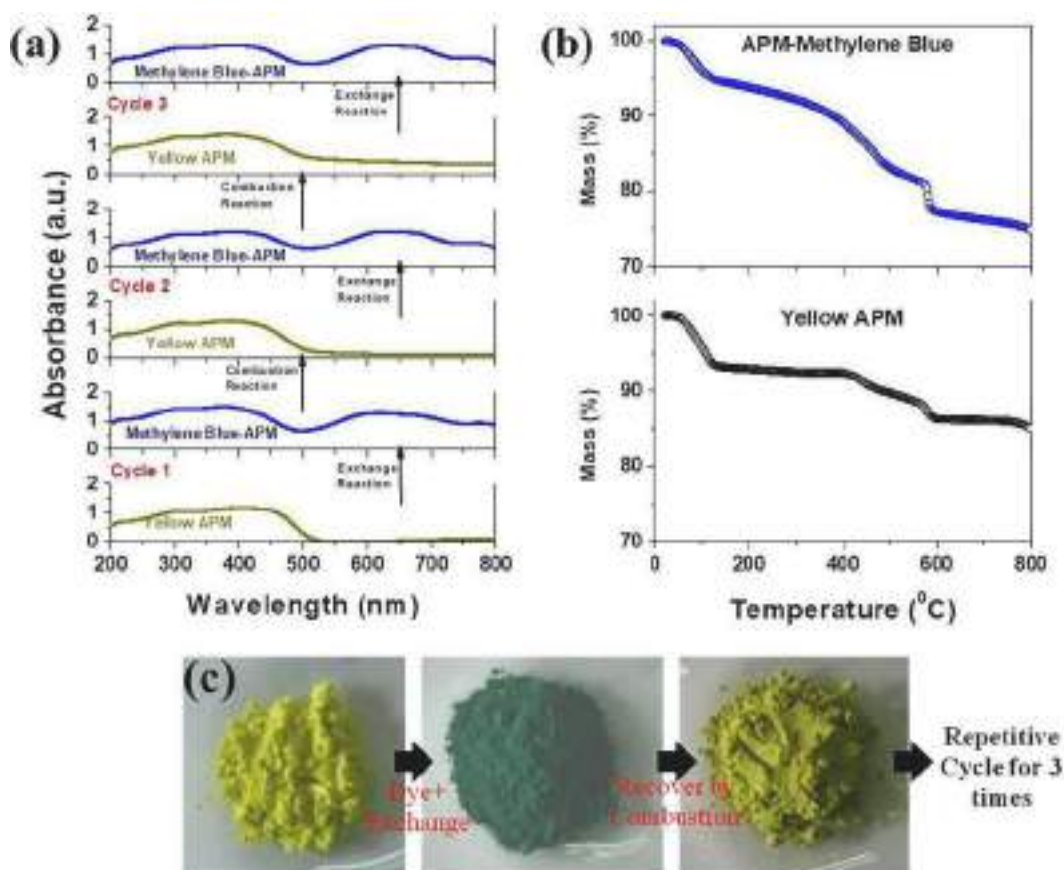
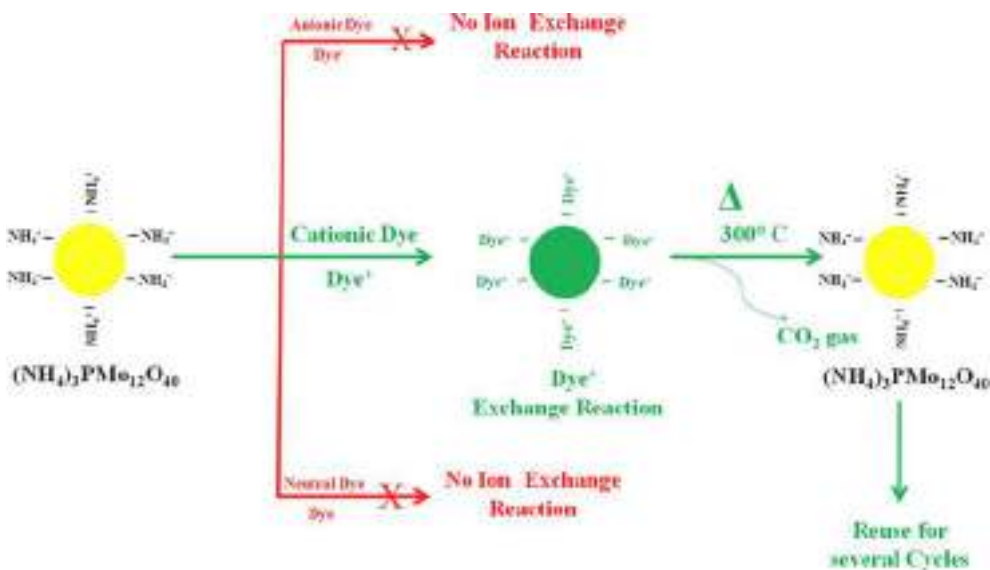


Fig. 6. Reusable of yellow APM (methylene blue dye exchange reaction) in three different cycles (a) and thermogravimetric analysis of methylene blue-APM and yellow APM (b) digital images of before and after methylene blue exchange on yellow APM and recovery of yellow APM by combustion method (c).



Scheme 1. Ion exchange mechanism and removal of dye molecules by yellow ammonium phosphomolybdate (APM) and regeneration of yellow APM.

The photoreduction happens only for the surface molecules of the solid ammonium phosphomolybdate. So it is expected that the ratio $\text{Mo}^{5+}/\text{Mo}^{6+}$ will reach constancy at the surface. The lower oxidation state of Mo^{5+} is stabilized by H^+ ion. Our proposed mechanism has been shown in Fig. 7 where H_2O molecules are dissociated as H^+ and OH^- radical by UV light [33]. The H^+ takes part in the reaction that reduces Mo^{6+} of $(\text{NH}_4)_3\text{PMo}_{12}\text{O}_{40}$ to Mo^{5+} which is stabilized by H^+ , a new

exchangeable site for cationic dye molecules to interact.

The photochemical change i.e. YAPM to GAPM was monitored by UV visible spectroscopy in the transmittance mode (shown in Fig. S3 Supporting Information) through the accumulation of electrons.

The similar phenomenon, the UV light induced heterolysis of water (photo reduction), occur in the following semiconductor surfaces such as TiO_2 [34], ZnO [35], WO_3 [36], V_2O_5 [37] etc. and the materials change

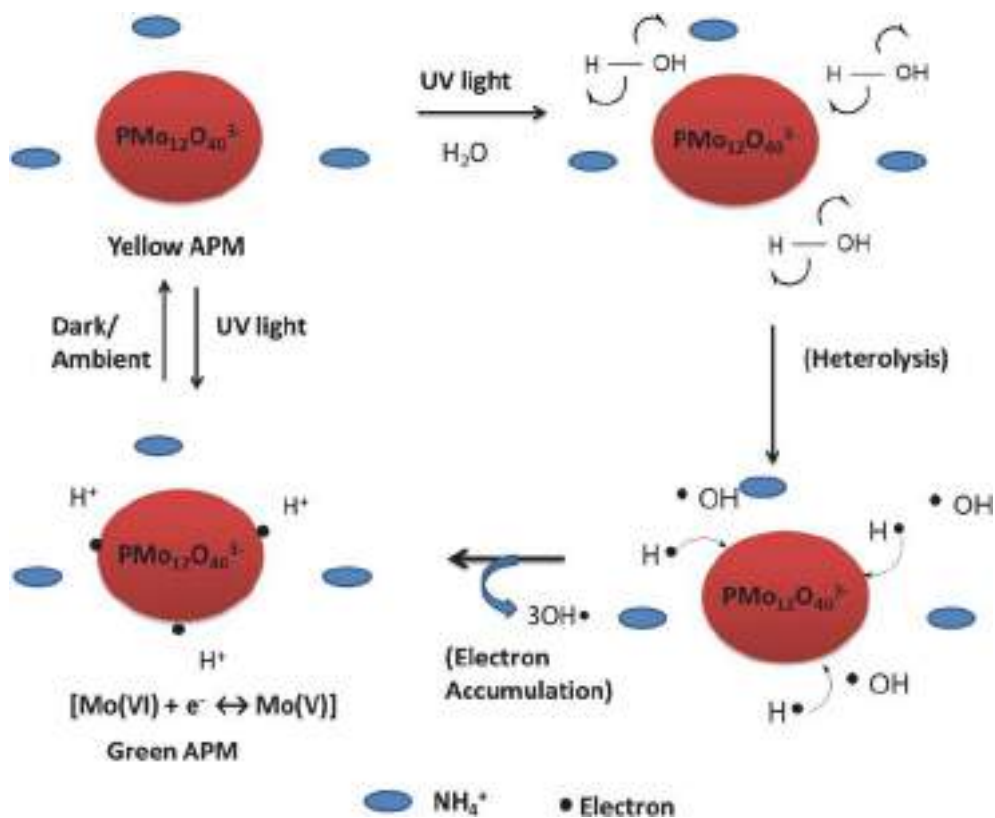


Fig. 7. Reversible pathways between yellow APM and green APM.

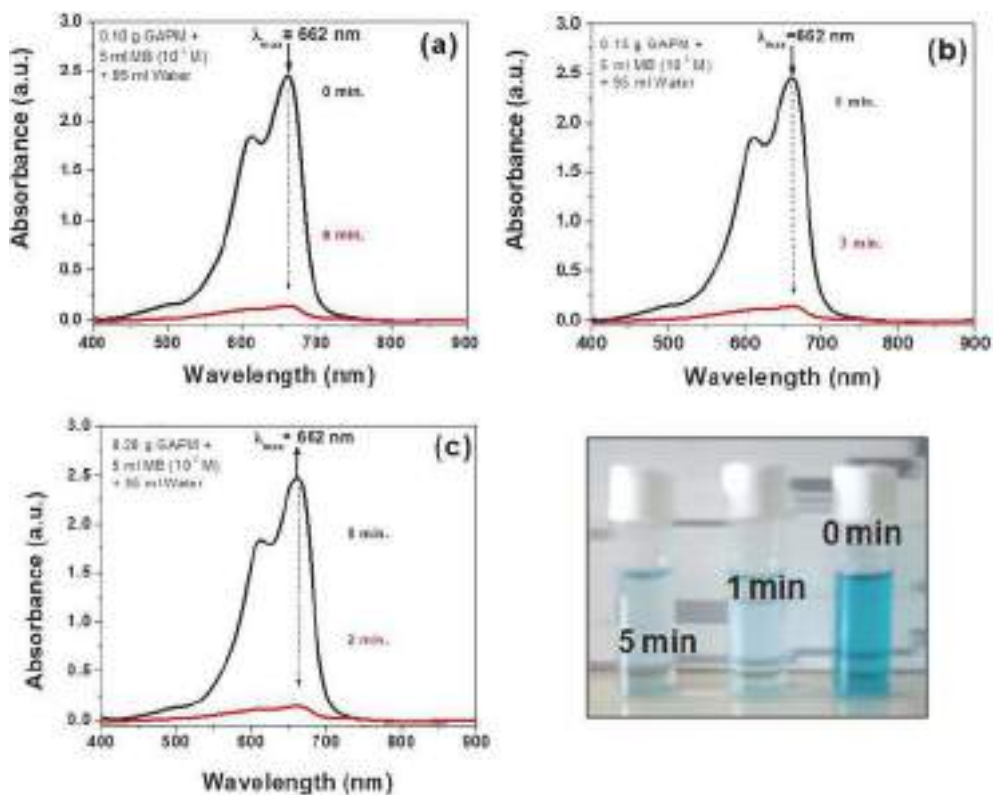


Fig. 8. UV-Visible study of methylene blue dye exchange reaction in different time gap with (a) 0.10 g, (b) 0.15 g and (c) 0.2 g green APM and digital image of methylene blue solution at different time of exchange reaction.

from hydrophobic materials to hydrophilic materials. In our experiment, we propose that yellow APM turns to green APM through capture of electrons from water molecules triggered by UV radiation [27,33]. The Keggin structure has strong ability to capture electron from hydrogen radical [33]. Generated hydroxyl radicals can react easily with water molecules or other species in the atmosphere.

As a result, after electron trapping by the Keggin ion GAPM is obtained reproducibly and the product can act as a better cationic dye scavenger. Within few minutes, the adsorbate dye is exchanged by GAPM through a stronger electrostatic force leaving aside a clear transparent water body at faster rate than yellow APM does. Influence of mass loading have been investigated which shows that dye exchange reaction becomes faster on enhancement of mass loading (Fig. 8a–c).

The dye exchange reaction with green APM (GAPM) is shown in Fig. 8. Thus the GAPM having hoarded electron shows better performances for the dye exchange reaction.

The dye exchange reaction by APM is studied at neutral pH condition and there occurs no deformation of the APM morphology after the cationic dye exchange reaction. It is worth mentioning that strong acidic waste water caused no hindrance for adsorption studies. Yellow ammonium phosphomolybdate (APM) material removes toxic cationic dye molecules from the wastewater of different sources (sea water, lake water, pond water and tap water) quantitatively and leaves no trace of adsorbate.

4. Conclusion

Ammonium phosphomolybdate (APM) collects electrons from photoactivation and becomes green APM. The green ammonium phosphomolybdate inherits basket full of electrons engendering increased cation affinity rendering better cation dye removal efficacy. Thus it becomes the novelty of UV activation process. Experiencing the promising applications of dye infested APM composite to bind simple molecules [34] and dielectric crossover and resistive switching performances of the pure material [35] from XRD, FTIR, Raman [36] and EPR [27] studies it is expected to have other future applications even for dye sensitized solar cell.

CRediT authorship contribution statement

Arun Kumar Sinha: Methodology, Writing - original draft, Investigation. **Anup Kumar Sasmal:** Writing - review & editing. **Anjali Pal:** Writing - review & editing. **Debasish Pal:** Writing - review & editing. **Tarasankar Pal:** Supervision, Writing - review & editing.

Declaration of Competing Interest

The authors declare that they have no known competing financial interests or personal relationships that could have appeared to influence the work reported in this paper.

Acknowledgment

The authors are thankful to the CSIR New Delhi, DST New Delhi, and IIT Kharagpur for financial support.

Appendix A. Supplementary data

Supplementary data to this article can be found online at <https://doi.org/10.1016/j.jphotochem.2021.113427>.

References

[1] D.-L. Long, R. Tsunashima, L. Cronin, Polyoxometalates: building blocks for functional nanoscale systems, *Angew. Chem. Int. Ed.* 49 (10) (2010) 1736–1758, <https://doi.org/10.1002/anie.v49:1010.1002/anie.200902483>.

[2] P. Gleick, China and water. The world's water 2008–2009: the biennial report on freshwater resources, Island Press, Washington, DC, 2008, p. 402.

[3] V.V. Sethuraman, B.C. Raymahashay, Color removal by clays kinetic study of adsorption of cationic and anionic dyes, *Environ. Sci. Technol.* 9 (13) (1975) 1139–1140.

[4] M.M. Islam, K. Mahmud, O. Faruk, M.S. Billah, Textile dyeing industries in Bangladesh for sustainable development, *Int. J. Environ. Sci. Dev.* 2 (6) (2011) 428–436.

[5] Akira Fujishima, Kenichi Honda, Electrochemical photolysis of water at a semiconductor electrode, *Nature* 238 (5358) (1972) 37–38.

[6] Q.H. Hu, S.Z. Qiao, F. Haghseresh, M.A. Wilson, G.Q. Lu, Adsorption study for removal of basic red dye using bentonite, *Ind. Eng. Chem. Res.* 45 (2) (2006) 733–738.

[7] D. Karadag, E. Akgul, S. Tok, F. Erturk, M.A. Kaya, M. Turan, Basic and reactive dye removal using natural and modified zeolites, *J. Chem. Eng. Data* 52 (6) (2007) 2436–2441.

[8] A.K. Sinha, M. Pradhan, S. Sarkar, T. Pal, Large-scale solid-state synthesis of Sn–SnO₂ nanoparticles from layered SnO by sunlight: a material for dye degradation in water by photocatalytic reaction, *Environ. Sci. Technol.* 47 (5) (2013) 2339–2345.

[9] M. Basu, A.K. Sinha, M. Pradhan, S. Sarkar, Y. Negishi, T. Pal, Evolution of hierarchical hexagonal stacked plates of CuS from liquid–liquid interface and its photocatalytic application for oxidative degradation of different dyes under indoor lighting, *Environ. Sci. Technol.* 44 (16) (2010) 6313–6318.

[10] M.J. Manos, M.G. Kanatzidis, Layered metal sulfides capture uranium from seawater, *J. Am. Chem. Soc.* 134 (39) (2012) 16441–16446.

[11] L. Kuai, B. Geng, X. Chen, Y. Zhao, Y. Luo, Facile subsequently light-induced route to highly efficient and stable sunlight-driven ag-agbr plasmonic photocatalyst, *Langmuir* 26 (24) (2010) 18723–18727.

[12] A. Sinha, M. Basu, M. Pradhan, S. Sarkar, T. Pal, Fabrication of large-scale hierarchical ZnO hollow spheroids for hydrophobicity and photocatalysis, *Chem. Eur. J.* 16 (26) (2010) 7865–7874.

[13] S.H. Lin, Adsorption of disperse dye by powdered activated carbon, *J. Chem. Technol. Biotechnol.* 57 (4) (1993) 387–391.

[14] J.B. Fei, Y. Cui, X.H. Yan, W. Qi, Y. Yang, K.W. Wang, Q. He, J.B. Li, Controlled preparation of MnO₂ hierarchical hollow nanostructures and their application in water treatment, *Adv. Mater.* 20 (3) (2008) 452–456.

[15] S. Wang, C.W. Ng, W. Wang, Q. Li, L. Li, A Comparative study on the adsorption of acid and reactive dyes on multiwall carbon nanotubes in single and binary dye systems, *J. Chem. Eng. Data* 57 (5) (2012) 1563–1569.

[16] F. Liu, S. Chung, G. Oh, T.S. Seo, Three-dimensional graphene oxide nanostructure for fast and efficient water-soluble dye removal, *ACS Appl. Mater. Interfaces* 4 (2) (2012) 922–927.

[17] J. Xu, L.i. Wang, Y. Zhu, Decontamination of bisphenol a from aqueous solution by graphene adsorption, *Langmuir* 28 (22) (2012) 8418–8425.

[18] S. Samai, K. Biradha, Chemical and mechano responsive metal organic gels of bis (benzimidazole) based ligands with Cd(II) and Cu(II) halide salts: self sustainability, gas and dye sorptions, *Chem. Mater.* 24 (6) (2012) 1165–1173.

[19] C. Mondal, M. Ganguly, J. Pal, R. Sahoo, A.K. Sinha, T. Pal, Pure inorganic gel: a new host with tremendous sorption capability, *Chem. Commun.* 49 (82) (2013) 9428–9430.

[20] B.o. Pan, B. Xing, Adsorption mechanisms of organic chemicals on carbon nanotubes, *Environ. Sci. Technol.* 42 (24) (2008) 9005–9013.

[21] R.S. Blackburn, Natural polysaccharides and their interactions with dye molecules: applications in effluent treatment, *Environ. Sci. Technol.* 38 (18) (2004) 4905–4909.

[22] B. Gu, Y.-K. Ku, P.M. Jardine, Sorption and binary exchange of nitrate, sulfate, and uranium on an anion-exchange resin, *Environ. Sci. Technol.* 38 (11) (2004) 3184–3188.

[23] M.J. Manos, C.D. Malliakas, M.G. Kanatzidis, Heavy-metal-ion capture, ion-exchange, and exceptional acid stability of the open-framework chalcogenide (NH₄)₄In₁₂Se₂₀, *Chem. Eur. J.* 13 (1) (2007) 51–58.

[24] M.J. Manos, N. Ding, M.G. Kanatzidis, Layered metal sulfides: Exceptionally selective agents for radioactive strontium removal, *Proc. Natl. Acad. Sci. U. S. A.* 105 (10) (2008) 3696–3699.

[25] M.J. Manos, V.G. Petkov, M.G. Kanatzidis, H_{2x}Mn_xSn_{3-x}S₆ (X = 0.11–0.25): a novel reusable sorbent for highly specific mercury capture under extreme pH conditions, *Adv. Funct. Mater.* 19 (7) (2009) 1087–1092.

[26] M.J. Manos, M.G. Kanatzidis, Highly efficient and rapid Cs⁺ uptake by the layered metal sulfide K_{2x}Mn_xSn_{3-x}S₆ (KMS-1), *J. Am. Chem. Soc.* 131 (18) (2009) 6599–6607.

[27] S.K. Ghosh, V.K. Perla, K. Mallick, T. Pal, Ammonium phosphomolybdate: a material for dielectric crossover and resistive switching performances, *Nanoscale Adv.* 2 (11) (2020) 5343–5351.

[28] A.K. Sasmal, A.K. Sinha, K. Mallick, T. Pal, Chromism of phosphomolybdate-dye moiety: a material for molecular nitrogen and oxygen binding, *Catal. Today* 348 (2020) 230–235.

[29] S. Tsunekawa, T. Fukuda, A. Kasuya, Blue shift in ultraviolet absorption spectra of monodisperse CeO_{2-x} nanoparticles, *J. Appl. Phys.* 87 (3) (2000) 1318–1321.

[30] T. Yamase, T. Kurozumi, Photoreduction of polymolybdates(v1) in aqueous solutions containing acetic acid, *J. Chem. Soc., Dalton Trans.* 2205 (1983).

[31] K. Naoi, Y. Ohko, T. Tatsuma, TiO₂ films loaded with silver nanoparticles: control of multicolor photochromic behavior, *J. Am. Chem. Soc.* 126 (11) (2004) 3664–3668.

[32] F. A. Cotton, G. Wilkinson, C. A. Murillo, Adv. Inorg. Chem. (6th Eds.) John Wiley & Sons, Inc.1999, p 923.

- [33] M. Basu, S. Sarkar, S. Pande, S. Jana, A.K. Sinha, S. Sarkar, M. Pradhan, A. Pal, T. Pal, Hydroxylation of benzophenone with ammonium phosphomolybdate in the solid state via UV photoactivation, *Chem. Commun.* 46 (2009) 7191–7193.
- [34] X. Feng, J. Zhai, L. Jiang, The fabrication and switchable superhydrophobicity of TiO₂ nanorod films, *Angew. Chem. Int. Ed.* 44 (32) (2005) 5115–5118.
- [35] X. Feng, L. Feng, M. Jin, J. Zhai, L. Jiang, D. Zhu, Reversible super-hydrophobicity to super-hydrophilicity transition of aligned ZnO nanorod films, *J. Am. Chem. Soc.* 126 (1) (2004) 62–63.
- [36] S. Wang, X. Feng, J. Yao, L. Jiang, Controlling wettability and photochromism in a dual-responsive tungsten oxide film, *Angew. Chem. Int. Ed.* 45 (8) (2006) 1264–1267.
- [37] H.S. Lim, D. Kwak, D.Y. Lee, S.G. Lee, K. Cho, UV-driven reversible switching of a rose-like vanadium oxide film between superhydrophobicity and superhydrophilicity, *J. Am. Chem. Soc.* 129 (14) (2007) 4128–4129.

Oxidation of cyclohexene with hydrogen peroxide over nano-crystalline $Mn_xCe_{1-x}O_{2-\delta}$ catalyst

Rajib Mistri*, Bidyapati Kumar

Department of Chemistry, Achhruram Memorial College, Jhalda, Purulia

Received: 04.10.2021; accepted: 22.11.2021; published online: 30.12.2021

The liquid-phase catalytic oxidation of cyclohexene to produce cyclohexenol and cyclohexenone directly was attempted using Mn ion substituted in ceria in acetonitrile solvent with 30% H_2O_2 as oxidant under atmospheric pressure. Structural studies by XRD show indication of ionically dispersed metal over ceria. Among all the catalysts studied, the $Mn_{0.05}Ce_{0.95}O_{2-\delta}$ catalyst prepared by the solution combustion method has shown more activity (95.3% conversion with 98.7% selectivity) than others. The influences of the amount of Mn loading, temperature, time, the concentration of H_2O_2 and solvent have also been investigated. The enhancement of activity in Mn^{2+} ion substituted ceria as compared to other catalysts has been attributed to Mn–O–Ce ionic interaction in the combustion synthesized catalyst. Ionic substitution also helps to get an active stable catalyst with lower risk of Mn-leaching compared to the impregnated catalyst.

Key words: Oxidation, Cyclohexene, $Mn_{0.05}Ce_{0.95}O_{2-\delta}$ catalyst, Ionic interaction

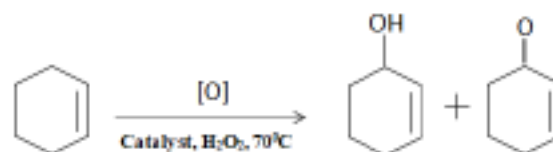
1. Introduction

One of the most important current topics of catalysis research has been to find an efficient catalyst for the selective oxidation of cyclohexene [1–6]. Oxidation of cyclohexene generally yields various products such as cyclohexenol, cyclohexenone, cyclohexene oxide and cyclohexene peroxide etc. [7]. Allylic oxidation of cyclohexene gives the products such as cyclohexenol and cyclohexenone as major products along with cyclohexene oxide as the minor product, indicating the involvement of Fenton-type oxidation reactions [8]. But when the oxidation occurred on the double bond, it gives cyclohexene oxide or epoxide as major products along with cyclohexene diols as minor product [4]. Major formation of the allylic oxidation products show the preferential attack of the activated C–H bond over the C=C bond [9]. However, the selectivity towards these products depends on various parameters like reaction conditions, central metal ion, solvent, oxidizing agent, nature of the catalyst etc. [10–14]. Previously oxidation of cyclohexene oxidation was carried out by using inorganic oxidants such as permanganate and chromium oxide [15]. Among the oxidizing agents hydrogen peroxide was chosen as a clean oxidizing agent, since it is inexpensive, environmentally friendly and generates water as byproduct [16].

Various new efficient catalytic systems have been designed and developed for the oxidation of cy-

clohexene with hydrogen peroxide as an oxidant. Among the catalytic studies, transition metal complexes are used as very effective homogeneous catalysts for this oxidation reaction [17–20]. But decomposition or degradation is one of the major problems in the application of homogeneous transition metal complexes [21, 22]. On the other hand separation of the products from the reaction mixture is also a major problem in case of homogeneous catalysts. Decrease of degradation of homogeneous catalysts have been achieved by the methods such as covalent anchorage on polymers [23], using inorganic oxide as supports [24–26] and also entrapped inside a porous oxide framework [27]. However, deactivation of the metal based catalysts due to leaching of active metal from the catalyst is still challenging [28]. This can be controlled by adopting specific preparation procedure and incorporating with other supports [29].

Here we show that $Mn_{0.05}Ce_{0.95}O_{2-\delta}$ prepared by a single step solution combustion method has a much higher selective oxidation activity towards cyclohexene to cyclohexenol and cyclohexenone than other catalysts at 70 °C in acetonitrile solvent and atmospheric pressure (Scheme 1).



Scheme 1. Catalytic oxidation of Cyclohexene

*Email ID: rajibmistri@yahoo.co.in

2. Materials and Methods

2.1 Preparation of catalyst

We have synthesized the catalysts by single step solution combustion method in an open muffle furnace kept in a fume hood with exhaust by the combustion of the corresponding metal nitrate salts with oxalyl dihydrazide [$C_2H_6N_4O_2(ODH)$] as the fuel. Oxalyl dihydrazide was prepared by the dropwise addition of diethyl oxalate ($C_2H_6N_4O_2$, Sisco Research Laboratories Pvt. Ltd., 99%) to ice-cooled aqueous solution of hydrazine hydrate ($N_2H_4 \cdot 2H_2O$, Qualizens Fine Chemicals, 99%) as reported in [30]. Solution combustion synthesis (SCS) for the preparation of $Mn_{0.05}Ce_{0.95}O_{2-\delta}$ involves combustion of the metal salts ($(NH_4)_2Ce(NO_3)_6$, $Mn(NO_3)_2 \cdot 3H_2O$ with ODH, taken in a molar ratio 0.90 : 0.10 : 2.26, at the temperature of ignition of the redox mixture ($\sim 350^\circ C$). In a typical preparation, 5 g of $(NH_4)_2Ce(NO_3)_6$ (Loba Chemie, 99%), 1.145 mL 10% $Mn(NO_3)_2 \cdot 3H_2O$ (Merck India, 99%) solution and 2.5122 g of ODH are dissolved in 30 mL of double distilled water in a borosilicate dish. The solution is then transferred to the preheated muffle furnace maintained at $\sim 350^\circ C$. Initially the solution boils with frothing and foaming followed by complete dehydration when the surface gets ignited and burns with a flame yielding a voluminous solid product within a minute. We have also prepared $Mn_xCe_{1-x}O_{2-\delta}$ ($x = 0.03, 0.07, 0.10$ and 0.15) catalysts in a similar manner.

In order for comparison, we have also prepared $Mn_{0.05}Ce_{0.95}O_{2-\delta}$ by the incipient wetness impregnation (IWI) methods. For the preparation of the impregnated catalyst, the support (combustion made CeO_2) was first dried and then impregnated with an appropriate volume of the aqueous solution of manganese nitrate, corresponding to the support pore volume. The sample was then dried overnight at $100^\circ C$, crushed and calcined at $500^\circ C$ for 3 h in air to get the catalyst.

2.2 Characterization of catalysts

The synthesized materials have been characterized by XRD. X-ray powder diffraction patterns were collected in a Rigaku diffractometer fitted with a horizontal goniometer mounted on a rotating anode. These data were recorded at 4 kW (40 kV, 100 mA) at 1°min^{-1} with a step size of 0.02° in the range 20 to 80 degrees. The rotating anode has Cu anode with effective wavelength of 1.5418 \AA . There is a diffracted beam monochromator (Graphite crystal) which takes care of K_β lines and fluorescence.

2.3 Catalytic test

The oxidation of cyclohexene by H_2O_2 was carried out in the temperature range $RT-80^\circ C$ at atmospheric pressure. In a typical experiment, 50 mg of catalyst was added to a liquid mixture containing 10 mL of acetonitrile, 2.45 mL of 30 wt% H_2O_2 (24 mmol) and 0.865 mL of cyclohexene (8 mmol) in a 250 mL two-necked round bottomed flask. For uniform mixing, the contents were stirred continuously during the course of reaction by a magnetic stirrer. The reaction system consisted of two liquid phases—an organic phase containing cyclohexene and acetonitrile, and an aqueous phase containing acetonitrile and 30% H_2O_2 .

The reaction compositions were analyzed using a gas chromatograph (Nucon 5765, New Delhi) using a fused silica capillary column (EC5) of $30 \text{ m} \times 0.25 \text{ mm} \times 0.25 \mu\text{m}$ film thickness from Alltech and equipped with a FID detector. The injector and detector temperatures were $220^\circ C$ and $240^\circ C$. The initial and final column temperatures were $110^\circ C$ and $150^\circ C$, respectively with a temperature programmed rate of $80^\circ C \text{ min}^{-1}$. The quantitative analysis was done by standard sample injection.

Catalyst recycling was carried over the most active SCS and its corresponding IWI catalysts only. After each experiment, the reaction mixture was allowed to settle. Then the solution was filtered and the solid residue was washed thoroughly with the solvent. After washing, the solid residue was dried at $100^\circ C$ for overnight. This was used as catalyst for the next cycles to check the recycling ability of the catalysts.

3. Results and Discussion

3.1 XRD studies

Powder XRD patterns of SCS made $Mn_xCe_{1-x}O_{2-\delta}$ catalysts as well as the IWI catalyst are shown in Figure 1. All the diffraction lines can be indexed to the fluorite structure of Ceria (Fm3m) only [31] [JCPDS card no. 34-0394]. Thus other than the solid solutions phase no other peak(s) due to manganese oxide or metal are detected in XRD. This again points to Mn^{2+} ion substitution for Ce^{4+} in CeO_2 matrix. The corresponding IWI catalyst in which MnO is dispersed over ceria also shows no peak due to this phase in the XRD pattern. Thus, MnO crystallites in the IWI catalyst are so finely distributed over ceria that they escape XRD analysis. A much slower scan might have shed more light on the evolution of different Mn-phase(s).

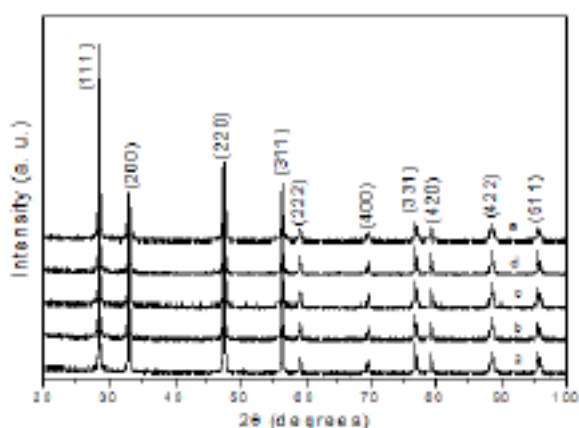


Figure 1. XRD patterns of (a) $Mn_{0.05}Ce_{0.95}O_{2-\delta}$, (b) $Mn_{0.07}Ce_{0.93}O_{2-\delta}$, (c) $Mn_{0.10}Ce_{0.90}O_{2-\delta}$, (d) $Mn_{0.05}Ce_{0.95}O_{2-\delta}$ aged and (e) $Mn_{0.05}Ce_{0.95}O_{2-\delta}$ IWI

4. Activity studies

4.1 Screening of catalysts

Table 1 lists cyclohexene oxidation activities of all the catalysts investigated here. The $Mn_{0.05}Ce_{0.95}O_{2-\delta}$ catalyst shows much higher reactivity ($\sim 95\%$ conversion) and selectivity (99%) to cyclohexenol and cyclohexenone than the other catalysts after 3 h. The effect of varying catalyst loading of on the reaction is also investigated (Table 1). The enhanced oxidation activity over $Mn_{0.05}Ce_{0.95}O_{2-\delta}$ catalyst indicates promoting effect of ceria in the combustion synthesized catalyst.

Table 1: Cyclohexene oxidation activities of different catalyst.

Catalyst	Amt. of cat. (mg)	Conv. (%)	Products (%)			Sel. (%)
			Cyclohexenol	Cyclohexenone	By-product*	
$Mn_{0.03}Ce_{0.97}O_{2-\delta}$	50	86.4	26.6	53.9	5.9	93.2
$Mn_{0.05}Ce_{0.95}O_{2-\delta}$	50	95.3	26.8	67.3	1.2	98.7
$Mn_{0.07}Ce_{0.93}O_{2-\delta}$	50	95.6	25.9	65.2	4.5	95.3
$Mn_{0.10}Ce_{0.90}O_{2-\delta}$	50	88.3	23.7	59.1	5.5	93.8
$Mn_{0.15}Ce_{0.98}O_{2-\delta}$	50	86.4	21.5	53.5	13.3	86.8
$Mn_{0.05}Ce_{0.95}O_{2-\delta}$	30	92.3	26.1	63.8	2.4	97.4
$Mn_{0.05}Ce_{0.95}O_{2-\delta}$	70	93.2	25.5	63.6	4.1	95.6

Reaction condition: 0.865 mL cyclohexene + 10 mL MeCN + 2.450 mL H_2O_2 + 70 °C + 3 h;

*byproducts are mainly cyclohexene oxide and a little bit of cyclohexenediols.

The $Mn_{0.03}Ce_{0.97}O_{2-\delta}$ sample and 30 mg $Mn_{0.05}Ce_{0.95}O_{2-\delta}$ catalyst are also found to be already very active. But a conversion of 95.3% with 98.7% selectivity was observed for 50 mg $Mn_{0.05}Ce_{0.95}O_{2-\delta}$ catalyst which is

higher than other catalysts. Although the 7 atom% metal loaded catalyst ($Mn_{0.07}Ce_{0.93}O_{2-\delta}$) showed slightly higher conversion than the $Mn_{0.05}Ce_{0.95}O_{2-\delta}$ catalyst, the latter showed higher selectivity than the former. Any further increase in manganese content and amount of catalyst caused a decrease in the cyclohexenol and cyclohexenone formation. The lower activity of higher loaded (> 5 atom%) catalysts indicate that as manganese loading increased, percentage of MnO phase increased and manganese dispersion decreased resulting in reduced activity and selectivity. Hence we chose $Mn_{0.05}Ce_{0.95}O_{2-\delta}$ as the best formulation for further investigation.

4.2 Temperature effect

The effect of temperature on the oxidation of cyclohexene was studied by varying the temperature from 35 °C to 80 °C over the catalyst (50 mg) with other parameters kept constant and the results are shown in Figure 2. Selection of this particular temperature range is due to the fact that at higher temperatures the decomposition of H_2O_2 predominates [32]. At room temperature (35 °C)

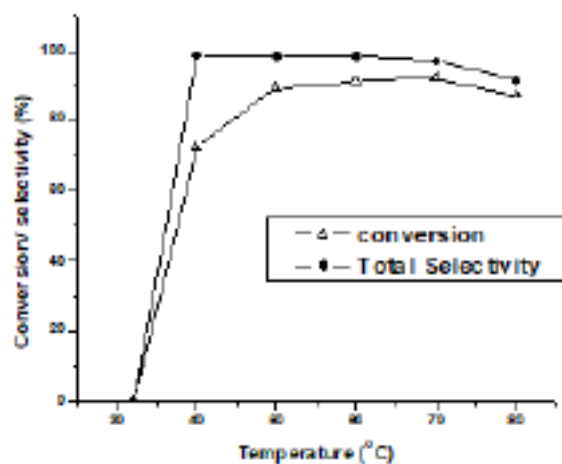


Figure 2. Conversion of cyclohexene/selectivity of cyclohexenol and cyclohexenone as a function of temperature over $Mn_{0.05}Ce_{0.95}O_{2-\delta}$ catalyst. Reaction condition: 50 mg catalyst + 0.865 mL cyclohexene + 10 mL MeCN + 2.450 mL H_2O_2 + 3 h.

cyclohexene was not oxidized, showing no reactivity of the catalyst. But an increase of the reaction temperature by just 5 °C leads to a conversion of $\sim 31\%$ with total selectivity of $\sim 90\%$ to cyclohexenol and cyclohexenone. Further 10 °C raise in temperature increases the conversion ($\sim 80\%$) and selectivity remains similar. The conversion is maximum (95%) between 60–70 °C with $\sim 99\%$

selectivity. It decreases marginally to $\sim 88\%$ when reaction temperature was increased to $80\text{ }^\circ\text{C}$. The above data indicates that the competition between the products and byproduct occurs above $70\text{ }^\circ\text{C}$. Hence, the reaction temperature higher than this optimum temperature is in favour of byproduct formation in addition to the self-decomposition of hydrogen peroxide resulting to a relatively lower conversion. Thus $70\text{ }^\circ\text{C}$ has been chosen as the most suitable temperature for the selective oxidation of cyclohexene under our reaction conditions.

4.3 Effect of reaction time

The cyclohexene conversion over $\text{Mn}_{0.05}\text{Ce}_{0.95}\text{O}_{2-\delta}$ as a function of reaction time at $70\text{ }^\circ\text{C}$ is presented in Figure 3. The oxidation starts at ~ 30 min over the catalyst, progresses linearly to $\sim 80\%$ upto 120 min and maximum activity ($\sim 95\%$ conversion) and selectivity (99%) is reached beyond ~ 180 min. This is why we chose 3 h as reaction time in our studies.

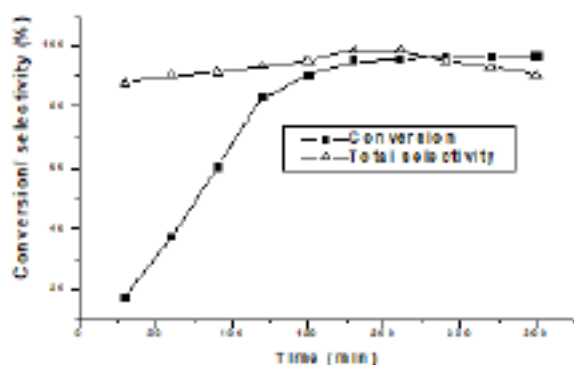


Figure 3. Conversion of cyclohexene/selectivity of cyclohexenol and cyclohexenone as a function of time over $\text{Mn}_{0.05}\text{Ce}_{0.95}\text{O}_{2-\delta}$ catalyst. Reaction condition: 50 mg catalyst + 0.865 mL cyclohexene + 10 mL MeCN + 2.450 mL H_2O_2 + $70\text{ }^\circ\text{C}$.

4.4 Influence of H_2O_2 concentration

Cyclohexene oxidation was carried out by adding H_2O_2 to the reaction mixture in one lot at the reaction temperature. To study the effect of varying the amount of H_2O_2 , the reaction was carried out with 50 mg of catalyst and the amounts of H_2O_2 from 8 mmol to 40 mmol while keeping other conditions unchanged. The results are shown in Figure 4. In absence of H_2O_2 , cyclohexene was not oxidized which indicates that the catalyst cannot oxidize cyclohexene in presence of air (O_2) only. Percentage conversion and total selectivity for cyclohexene oxidation reaches a maximum value with 24 mmol of H_2O_2 and then these

starts decreasing. The distribution of allylic oxidation products shows the same trend but the cyclohexene oxide percentage shows a gradual increase [4]. Even though the theoretical molar ratio of cyclohexene to H_2O_2 for the oxidation reaction is 1 : 1 and concentration of H_2O_2 was 8 mmol, here the results show that H_2O_2 needed was triple its stoichiometry. This can result from the fact that not all the H_2O_2 can take part in the oxidation due to its unavoidable self-decomposition under the reaction conditions [33].

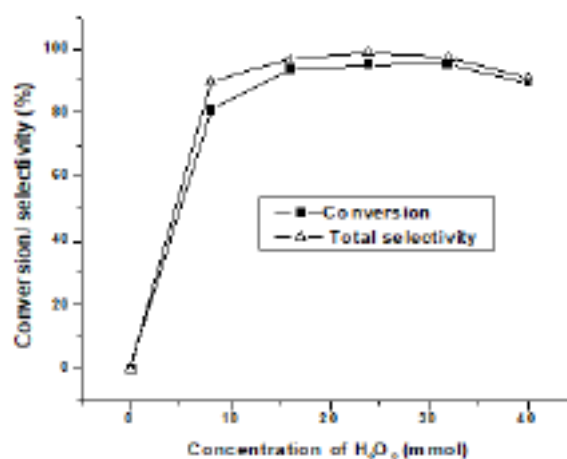


Figure 4. Conversion of cyclohexene/selectivity of cyclohexenol and cyclohexenone as a function of H_2O_2 concentration over $\text{Mn}_{0.05}\text{Ce}_{0.95}\text{O}_{2-\delta}$ catalyst. Reaction condition: 50 mg catalyst + 0.865 mL cyclohexene + 10 mL MeCN + $70\text{ }^\circ\text{C}$ + 3 h.

4.5 Effect of solvent

The cyclohexene oxidation was carried out using various solvents such as acetonitrile, methanol, ethanol and toluene over $\text{Mn}_{0.05}\text{Ce}_{0.95}\text{O}_{2-\delta}$ catalyst and the results are presented in Figure 5. Acetonitrile is found to be the best solvent for cyclohexene oxidation with highest conversion of 95.3% and selectivity of 98.7%. Toluene showed lowest cyclohexene conversion (70%) but the selectivity (93%) was very high. Using ethanol or methanol as a solvent, comparatively lower conversion is observed.

In this study, it is believed that the solvent acetonitrile acted as a 'media' serving homogeneity for the liquid phase(s). Cyclohexene and hydrogen peroxide are both soluble in acetonitrile and the reaction products; viz., cyclohexenol and cyclohexenone are not only soluble in the reaction mixture but also can be displaced from the surface of catalyst as they are formed. Acetonitrile, an aprotic solvent, can also activate H_2O_2 .

The $Mn_{0.05}Ce_{0.95}O_{2-\delta}$ prepared by IWI method ($Mn_{0.05}Ce_{0.95}O_{2-\delta}$ IWI) gives a conversion of $\sim 81\%$ with $\sim 92\%$ selectivity than the same catalyst prepared by SCS method. These values are quite lower compared to those of the SCS catalyst.

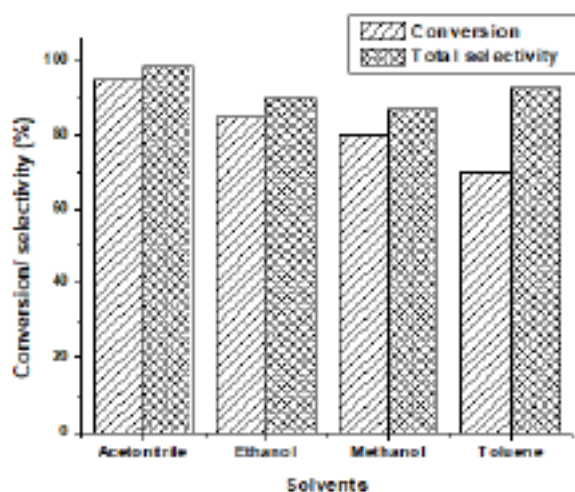


Figure 5. Solvent effects on cyclohexene oxidation activities over $Mn_{0.05}Ce_{0.95}O_{2-\delta}$. Reaction condition: 50 mg catalyst + 0.865 mL cyclohexene + 2.450 mL H_2O_2 + 70 °C + 3 h.

To check the stability and recycling ability of the SCS catalyst, the used catalyst was separated from the reaction mixture and dried in air at 110 °C, and then oxidation experiments were performed under the typical reaction conditions used here. The results show that the $Mn_{0.05}Ce_{0.95}O_{2-\delta}$ catalyst maintains its activity after three consecutive cycles without any appreciable loss of conversion and selectivity.

The result of ageing experiments over both SCS and IWI catalysts show a decreasing trend for the IWI catalyst, whereas the SCS catalyst more or less maintains its activity (Figure 6). The loss of activity of the IWI catalyst during ageing is likely due to leaching of MnO from the catalyst.

The different catalytic activity of SCS and IWI catalysts is related to phase composition of the support oxide. In case of $Mn_{0.05}Ce_{0.95}O_{2-\delta}$ made via combustion route, there is no MnO phase (as revealed from XRD study) and it shows better catalytic behavior than the corresponding IWI catalyst that contains very finely distributed MnO over ceria. Thus, Mn^{2+} in the ceria lattice sites (as in $Mn_{0.05}Ce_{0.95}O_{2-\delta}$ catalyst) is more active than MnO (as in $Mn_{0.05}Ce_{0.95}O_{2-\delta}$ IWI catalyst) towards cyclohexene oxidation. This higher activity of combustion synthesized catalyst compared to

the impregnated catalyst can then be attributed to Mn–O–Ce ionic interaction in the $Mn_xCe_{1-x}O_{2-\delta}$ catalyst. The loss of activity of IWI catalyst during ageing is most likely due to leaching of MnO from the catalyst. The SCS catalyst contains Mn^{2+} ion sites in the ceria lattice which is difficult to be leached out from the catalyst surface and hence its activity remains unaltered during ageing in the reaction atmosphere.

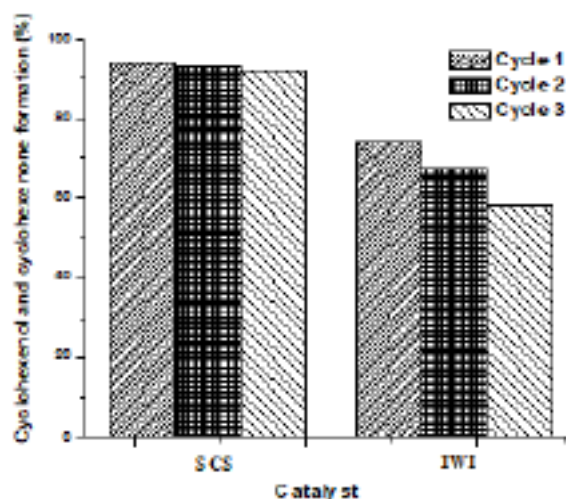


Figure 6. Effect of cycling on cyclohexene oxidation activities of $Mn_{0.05}Ce_{0.95}O_{2-\delta}$ catalyst prepared via (a) solution combustion (SCS), (b) impregnation (IWI). Reaction condition: 50 mg catalyst + 0.865 mL cyclohexene + 2.450 mL H_2O_2 + 10 mL MeCN + 70 °C + 3 h.

Cyclohexene oxidation generally proceeds through a radical pathway in presence of a peroxide oxidant, in which the homolytic cleavage of the oxidant is involved [8,34]. To examine the mechanism involved in the present case, we performed the oxidation in presence of a radical scavenger (quinone). The radical scavenger was added to the reaction mixture after 1 h of reaction and the progress of reaction was monitored. Cyclohexene oxidation was found to be totally stopped after addition of the scavenger. Therefore, we believe that cyclohexene oxidation over the reported catalysts in this study proceeds via a radical mechanism [35]. Hydroxide radical is first produced that subsequently abstracts hydrogen from the reactant to produce cyclohexenyl free radical. This radical is then trapped by O_2 and/or combine with hydroperoxide radical to form cyclohexenyl peroxide intermediate which eventually leads to the formation of cyclohexenol and cyclohexenone.

5. Conclusions

In this study, solution combustion synthesized single phase $\text{Mn}_{0.05}\text{Ce}_{0.95}\text{O}_{2-\delta}$ is shown to be a highly efficient catalyst for the oxidation of cyclohexene in acetonitrile solvent at 70 °C than the other catalysts investigated. The conversion of cyclohexene achieved over this catalyst is ~ 95% and the selectivity of cyclohexenol and cyclohexenone was almost ~ 99%. XRD study indicates ionic substitution of manganese in ceria. The high activity can thus be attributed to active Mn^{2+} ion sites and Mn–O–Ce ionic interaction in the $\text{Mn}_x\text{Ce}_{1-x}\text{O}_{2-\delta}$ catalyst. Since Mn is incorporated as Mn^{2+} ion in the structure of ceria, the possibility of its leaching is diminished. The ageing and recycling experiments confirm this since there was no loss of activity of the SCS catalyst due to these treatments. On the other hand, the activity of the IWI catalyst is lower due to presence of MnO crystallites over the ceria support where leaching of the active phase is easier as observed in the ageing experiment where a decreasing activity trend is observed.

Acknowledgements

Author thanks to Department of Chemistry, Jadavpur University, especially Dr. Arup Gayen for Instrumental analysis.

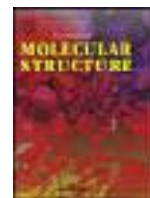
Conflict of interest

The authors have no affiliations with or involvement in any organization or entity with any financial interest or non-financial interest in the subject matter or materials discussed in this manuscript.

References

- [1] K. Sato, M. Aoki and R. Noyori, A green route to adipic acid: Direct oxidation of cyclohexenes with 30 per cent hydrogen peroxide, *Science*, **281**, 1646, (1998).
- [2] R. Noyori, M. Aoki and K. Sato, Green oxidation with aqueous hydrogen peroxide, *Chem. Comm.*, **16**, 1977, (2003).
- [3] A. Abdolmaleki, S.R Adariani, Copper-cationic salen catalysts for the oxidation of cyclohexene by oxygen, *Catal. Comm.*, **59**, 97, (2015).
- [4] K. A. Jorgensen, Transition metal catalyzed epoxidations, *Chem. Rev.*, **9**, 431, (1989).
- [5] O. A. Kholdeeva, T. A. Trubitssina, M. N. Timofeeva, G. M. Maksimov, R. I. Maksimovskaya and V. A. Rogov, The role of protons in cyclohexene oxidation with H_2O_2 catalyzed by Ti(IV)-monosubstituted Keggin polyoxometalate, *J. Mol. Catal. A: Chem.*, **232**, 173, (2005).
- [6] T. Liu, H. Cheng, W. Lin, C. Zhang, Y. Yu and F. Zhao, Aerobic Catalytic Oxidation of Cyclohexene over TiZrCo Catalysts, *Catalysts*, **6**, 24, (2016).
- [7] S. M. Mahajani, M. M. Sharma and T. Sridhar, Uncatalysed oxidation of cyclohexene, *Chem. Eng. Sci.*, **54**, 3967, (1999).
- [8] R. A. Sheldon and J. K. Kochi, *Metal catalyzed oxidations of organic compounds*, Academic Press, New York, (1981).
- [9] M. Salavati-Niasari, P. Salemi and F. Davar, Oxidation of cyclohexene with tert-butylhydroperoxide and hydrogen peroxide catalyzed by Cu(II), Ni(II), Co(II) and Mn(II) complexes of N,N'-bis-(α -methylsalicylidene)-2,2-dimethylpropane-1,3-diamine, supported on alumina, *J. Mol. Catal. A: Chem.*, **238**, 215, (2005).
- [10] R. A. W. Johnstone and A. H. Wilby, Heterogeneous catalytic transfer hydrogenation and its relation to other methods for reduction of organic compounds, *Chem. Rev.*, **85**, 129, (1985).
- [11] F. Pianna, Supported metal catalysts preparation, *Catal. Today*, **41**, 129, (1998).
- [12] Z. Y. Zhong, J. Y. Lin, S.P. Teh, J. Teo and F. M. Dautzenberg, A Rapid and Efficient Method to Deposit Gold Particles onto Catalyst Supports and Its Application for CO Oxidation at Low Temperatures, *Adv. Funct. Mater.*, **17**, 1402, (2007).
- [13] G. Colon, M. Maicu, M. C. Hidalgo, J. A. Navio, A. Kubacka and M. Fernández-García, Gas phase photocatalytic oxidation of toluene using highly active Pt doped TiO_2 , *J. Mol. Catal. A: Chem.*, **320**, 14, (2010).
- [14] G. C. Bond and R. Burch, Specialist Periodically Reports: *Catalysis (The Royal society of London)*, **6**, 27, (1983).
- [15] R. A. Sheldon and R. S. Downing, Heterogeneous catalytic transformations for environmentally friendly production, *Appl. Catal. A: Gen.*, **189**, 163 (1999).
- [16] E. L. Pires, J. C. Magalhaes and U. Schuchardt, Effects of oxidant and solvent on the liquid-phase cyclohexane oxidation catalyzed by Ce-exchanged zeolite Y, *Appl. Catal. A: Gen.*, **203**, 231, (2000).
- [17] R. H. Holm, Metal-centered oxygen atom transfer reactions, *Chem. Rev.*, **87**, 1401, (1987).
- [18] M. Salavati-Niasari, F. Farzaneh and M. Ghandi, Oxidation of cyclohexene with tert-butylhydroperoxide and hydrogen peroxide catalyzed by alumina-supported manganese(II) complexes, *J. Mol. Catal. A: Chem.*, **186**, 101, (2002).
- [19] J. P. Collman, L. S. Hegeudus, J. R. Norton and R. G. Finke (Eds.), *Principles and Applications*

- of *Organotransition Metal Chemistry*, University Science Books, Mill Valley (1987).
- [20] F. Farzaneh, S. Sadeghi, L. Turian and M. Ghandi, The oxidation of alkenes in the presence of some transition metal elements exchanged with zeolites, *J. Mol. Catal. A: Chem.*, **132**, 255, (1998).
- [21] R. Belal and B. Meunier, Iron-Phthalocyanine Catalyzed Epoxidation of Olefins by $KHSO_5$, *J. Mol. Catal.*, **44**, 187, (1988).
- [22] J. V. Porcelli, Ethylene Oxidation—Exploratory Research, *Catal. Rev.*, **23**, 151, (1981).
- [23] M. M. Miller and D. C. Scherrington, Alkene Epoxidations Catalyzed by Mo(VI) Supported on Imidazole-Containing Polymers: I. Synthesis, Characterization, and Activity of Catalysts in the Epoxidation of Cyclohexene, *J. Catal.*, **152**, 368, (1995).
- [24] K. W. Jun, E. K. Shim, S. B. Kim and K. W. Lee, Polymer Supported iron catalysts for the oxidation of cyclohexane, *Stud. Surf. Sci. Catal.*, **82**, 659, (1994).
- [25] R. L. Augustine, *Organic Functional Group Hydrogenation*, *Catal. Revs.*, **13**, 285, (1976).
- [26] P. Battioni, J. P. Lallier, L. Barloy and D. Mansuy, Mono-oxygenase-like oxidation of hydrocarbons using supported manganese-porphyrin catalysts: beneficial effects of a silica support for alkane hydroxylation, *J. Chem. Soc. Chem. Commun.*, 1149, (1989).
- [27] A. Corma, V. Fornes, F. Rey, A. Cervilla, E. Liopis and A. Ribera, Catalytic Air Oxidation of Thiols Mediated at a Mo(VI)O₂ Complex Center Intercalated in a Zn(II)-Al(III) Layered Double Hydroxide Host, *J. Catal.*, **152**, 237, (1995).
- [28] U. Schuchardt, D. Cardoso, R. Sercheli, R. Pereira, M. C. Guerreiro, D. Mandellif, E. V. Spinacé and E. L. Pires, Cyclohexane oxidation continues to be a challenge, *Appl. Catal. A: Gen.*, **211**, 1, (2001).
- [29] T. Miyahara, H. Kanzaki, R. Hamada, S. Kuroiwa, S. Nishiyama and S. Tsuruya, Liquid-phase oxidation of benzene to phenol by CuO–Al₂O₃ catalysts prepared by co-precipitation method, *J. Mol. Catal. A: Chem.*, **176**, 141, (2001).
- [30] G. Gran, The use of oxalyldihydrazide in a new reaction for the spectrophotometric microdetermination of copper, *Anal. Chim. Acta.*, **14**, 150, (1956).
- [31] B. Murugan, A.V. Ramaswam, D. Srinivas, C.S. Gopinath, Veda Ramaswamy, Effect of fuel and its concentration on the nature of Mn in Mn/CeO₂ solid solutions prepared by solution combustion synthesis, *Acta Materialia*, **56**, 1461 (2008).
- [32] G. J. Pereria, R. H. Castra, D. Z. deFlorio, E. N. S. Muccillo and D. Gouvea, Densification and electrical conductivity of fast fired manganese-doped ceria ceramics, *Mat. Lett.*, **59**, 1195, (2005).
- [33] K. M. Parida and D. Rath, Structural properties and catalytic oxidation of benzene to phenol over CuO-impregnated mesoporous silica, *Appl. Catal. A: Gen.*, **321**, 101, (2007).
- [34] C. Yin, Z. Yang, B. Li, F. Zhang, J. Wang and E. Ou, Allylic Oxidation of Cyclohexene with Molecular Oxygen Using Cobalt Resinate as Catalyst, *Catal. Lett.*, **131**, 440, (2009).
- [35] Selective cyclohexene oxidation to allylic compounds over a Cu-triazole framework via homolytic activation of hydrogen peroxide, P. Panchai, K. Adpakpang and S. Bureekaew, *Dalton Trans.*, **50**, 7917, (2021).



Synthesis, characterization of one Cr (III) complex: An efficient chemosensor for Cr (III) ions and designing of a molecular logic gate



Abhishikta Chatterjee^a, Priyanka Chakraborty^a, Bidyapati Kumar^a, Corrado Rizzoli^b, Pinaki Mandal^c, Subrata K. Dey^{a,*}

^a Department of Chemistry, Sidho-Kanho-Birsha University, Purulia, West Bengal 723104, India

^b Dipartimento S.C.V.S.A., Università di Parma, Parco Area delle Scienze 17/A, Parma I-43124, Italy

^c Department of Chemistry, Bankura Sammilani College, Bankura, West Bengal 722102, India

ARTICLE INFO

Article history:

Received 28 September 2021

Revised 23 January 2022

Accepted 24 January 2022

Available online 2 February 2022

Keywords:

Chemosensor

Cr-APC complex

Spectroscopic studies

Structural analysis

Cr (III) and Cr (VI) detection

Molecular logic gate

ABSTRACT

A simple spectrophotometric based method for the detection of both the trivalent and hexa valent forms of chromium using 3-amino-2-pyrazine carboxylic acid (APC) is reported. Using APC as a ligand with Cr(NO₃)₃·6H₂O a new mononuclear complex has also been synthesized and systematically characterized by elemental analysis and IR studies. Single crystal X-ray diffraction analysis reveals octahedral-type geometry with N₃O₃ coordination environments from the ligand. The optical sensing properties of APC for metal ions were enlightened by UV-Vis study. This sensor displays high selectivity and sensitivity towards Cr³⁺ in methanol. Interestingly the ligand displayed enhancement due to chelation with Cr³⁺ and quenching while interacting with Cr⁶⁺ ions. Complete opposite spectroscopic behavior helps us to identify the oxidation state of chromium. The logical response of the molecular AND gate is realized and as the APC can efficiently sense Cr³⁺ in solitary as well as crowded conditions, presence of Mⁿ⁺ ions would not have any effect to the logic functioning of the molecular AND gate.

© 2022 Elsevier B.V. All rights reserved.

1. Introduction

Molecular logic gate is one of the research interests in chemistry for efficient use in information technology, a significant development in the molecular sensing investigations to proposed molecular logic devices, such as logic gates [1–3], molecular keypad locks [4], information storage devices [5] and so on. These logic instruments are supposed to transfer the molecular level information to the obtained optical signals [6]. The first AND logic gate was developed using optical signals by de Silva et al. [7]. Since then, different chemical systems have been developed for various logic functions such as OR, AND, NOT [8]. Designing of molecular logic devices has earned an enormous attention from different research groups across the globe [9–11]. Besides just Boolean functioning, molecular logic gates have shown their potential applicability in diverse fields including ion sensing, [12] neuronal imaging [13] etc.

On the other hand, the carcinogenicity of chromate dust has been documented since the late 19th century. Chromium and its high valent oxoanions result from extensive anthropogenic uses such as leather tanning, electroplating, catalyst for halogenations, alkylation, catalytic cracking of hydrocarbons, in steel in-

dustry, printing, cement, mortar, wood preservative etc [14,15]. Compared to other oxo-species pollutants, hexavalent oxoanions, namely chromate (CrO₄²⁻) and dichromate (Cr₂O₇²⁻), are highly soluble in water and therefore can contaminate into water easily [16]. Water pollution is becoming a major concern to occupational and environmental health and needs to be addressed in recent times. These species may also come into drinking water supply systems from the corrosion inhibitors used in water pipelines [17]. The World Health Organization recommends a maximum allowable concentration of 0.05 mg/L of Cr(VI) in drinking water. Because of its comparatively smaller size, Cr(VI) is genotoxic, hemotoxic and carcinogenic and its high oxidation potential makes it capable to enter through the biological cell membranes easily. On the other hand, Cr(III) is less toxic and less mobile and it is an essential trace mineral for the biological systems. Nonetheless, it can oxidize to carcinogenic Cr(VI) easily by manganese present in the soil and Cr(III) will also show the detrimental health effects if exposed to it for a long time [18]. Cr(VI) is reduced to Cr(III) by various intracellular reducing agents and then Cr(III) binds to DNA through guanine N7 and the adjacent phosphate backbone [19]. Hence, discriminative detection and segregation of the targeted trace level toxic ions from drinking water, physiological or environmental sources is a subject of great importance as potential biomarkers in contemporary environmental research [20]. Al-

* Corresponding author.

E-mail address: skdchem@skbu.ac.in (S.K. Dey).

though there are many conventional instrument-assisted approach like AAS, ICP-AES/MS, HPLC, CPEs etc. but there are several important disadvantages such as high cost, high time consumption and necessity of sophisticated instrumentations [21]. These can be avoided by the use of much simpler methods with rapid response time, high sensitivity and operational simplicity such as spectrophotometric approach. So, there is a growing demand to develop reusable, eco-friendly probes for easy capture of Cr(VI) oxoanions from waste materials selectively and accurately. In the last few years research activities concerning to the organic moiety and MOF [22–24] as luminescent probes have rapidly developed but only a few reports have showed estimation of Cr-species without pre-separation of other individuals by fluorescence quenching techniques and differentiation between two oxidation states of chromium by using one simple organic moiety are still rare in the toxicological studies.

Small molecules are easier to determine as well as manipulate their properties like geometry, coordination or donor strength etc. than surface-graphed or polymer materials. Thus, small molecules are chosen in order to explore underlying efficient sensing phenomena [25]. Addressing these ideas here we report the use of 3-amino-2-pyrazine carboxylic acid (APC) as an efficient spectrophotometric probe that can selectively differentiate between two oxidation states of chromium. APC was chosen as this has the effective binding sites with nitrogen of amine group and oxygen atom at ortho position, which enhances the coordination ability toward different metal ions along with its ability to promote intramolecular charge transfer (ICT). The selected ligand has interesting binding components, may form interesting supramolecular architecture, so can act as a sensor to the metal ions (Scheme 1), causing a change that can be detected by the UV-vis spectroscopy.

As we are interested to find low cost and easy method to sense chromium ion selectively, so this probe may fulfill the requirements and offers a rapid sensitivity for the separation of chromium ion in presence of the other metal ions. This determination is based on the ion-association complex between the organic moiety and Cr(III) ions. The binding of the probe with Cr(III) is firmly established by the SCXRD technique and supported by UV-Vis spectroscopy. Here, two-input-single-output AND and PASS 0 gates are designed considering the opto-chemical responses generated from the ligand (APC) on interaction with different metal ions. Further, the different logic responses are exploited for the selective and efficient sensing of Cr(III) ions in a smart manner utilizing the ligand, APC.

2. Materials and methods

2.1. Materials

All required chemicals and solvents used for the synthesis were of analytical grade and purchased from Sigma-Aldrich.

2.2. Synthesis of $[(C_5H_4N_3O_2)_3Cr]$

10 mL methanolic solution of 3-amino-2-pyrazine carboxylic acid (0.13 g) was added to a 15 mL methanolic solution of $Cr(NO_3)_3 \cdot 6H_2O$ (0.040 g) with continuous stirring. The resulting red colored solution was heated to 120 °C for 6 h in a Teflon flask. The flask was cooled at room temperature. After 3 days orange colored hexagonal crystals suitable for X-ray analysis were collected by filtration and washed with methanol. Yield: 70%. Anal. Calcd (%) for $[C_{15}H_{12}CrN_9O_6]$: C, 38.62; H, 2.59; N, 27.04. Found (%): C, 38.68; H, 2.61; N, 26.97; IR (KBr, cm^{-1}): ν O-H 3338 cm^{-1} ; ν N-H 3456 cm^{-1} ; ν C-N 1317 cm^{-1} ; UV-vis, λ_{max} (nm, CH_3OH): 244 ($\pi-\pi^*$); 341 ($n-\pi^*$).

Table 1
Crystal data and refinement parameters of complex $[(C_5H_4N_3O_2)_3Cr]$.

	Complex
Empirical formula	$C_{15}H_{12}CrN_9O_6$
Formula weight	466.34
Temperature/K	294
Crystal system	Monoclinic
Space group	C 2/c
a/Å	29.937(3)
b/Å	8.2626(9)
c/Å	14.4417(15)
$\alpha/^\circ$	90
$\beta/^\circ$	93.196(4)
$\gamma/^\circ$	90
Volume/Å ³	3566.8(7)
Z	8
$\rho_{calc}/g/cm^3$	1.737
μ/mm^{-1}	0.702
F(000)	1896
Crystal size/mm ³	0.11 × 0.09 × 0.03
Radiation	MoK α ($\lambda = 0.71073$)
Θ range for data collection/ $^\circ$	2.56–25.5
Index ranges	$-36 \leq h \leq 36, -10 \leq k \leq 10, -17 \leq l \leq 17$
Reflections collected	35,241
Independent reflections	3309
Data/restraints/parameters	3309/0/304
Goodness-of-fit on F^2	1.059
Final R indexes [$I > 2\sigma(I)$]	$R_1 = 0.0349$ $wR_2 = 0.0907$

$$w = 1/[\sigma^2(F_o^2) + (0.0331P)^2 + 2.2179P] \text{ where } P = (F_o^2 + 2F_c^2)/3.$$

2.2. Physical measurements

FT-IR spectra were collected by using a Perkin-Elmer FT-IR spectrophotometer in KBr pellets (4000–400 cm^{-1}). Absorption spectra were recorded on Perkin-Elmer Lambda-35 spectrophotometer using a 1.0 cm quartz cell.

2.3. X-ray crystallography

2.3.1. X-ray diffraction data of $[(C_5H_4N_3O_2)_3Cr]$

Diffraction data were collected at 294 K on a Bruker D8 VENTURE CCD diffractometer using graphite monochromated MoK α radiation ($\lambda = 0.71073$ Å). APEX3 and SAINT programs of the Bruker 2016 package [26] were used for data collection, data reduction and cell refinement. The structure was solved by SHELXT [27] and refined by full-matrix least squares based on F^2 with SHELXL-2018/3 [28]. All non-hydrogen atoms were refined anisotropically. The amine H atoms were located in a difference Fourier map and refined freely. All other H atoms were placed geometrically and refined using a riding atom approximation, with $C-H = 0.93$ Å, and with $U_{iso}(H) = 1.2U_{eq}(C)$.

Crystallographic data are summarized in Table 1. Selected bond lengths and angles are given in Table 2. The molecular graphics and crystallographic illustrations were produced using the Ortep-3 [29] and SCHAKAL-99 [30] programs.

3. Results and discussion

3.1. Description of the crystal structure for complex $[(C_5H_4N_3O_2)_3Cr]$ (1)

The asymmetric unit of **1** contains a mononuclear complex molecule including three 3-amino-2-pyrazinecarboxylato anions and one Cr^{3+} cation (Fig. 1). Each anion acts as a bidentate ligand coordinating through a carboxylic O atom and a pyrazine N atom to give a *mer*- CrN_3O_3 octahedral configuration. The coordination geometry around the metal deviates slightly from ideal octahedral as evidenced by the *trans*-oriented coordination angles varying from 169.83(9) to 173.14(8) (Table 2). The *cis*-oriented

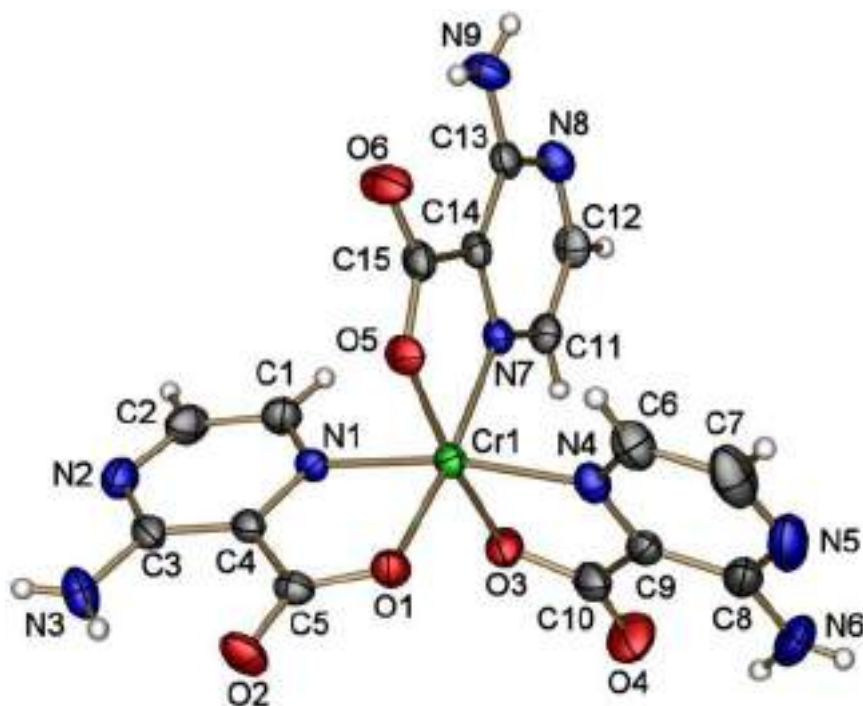


Fig. 1. The molecular structure of complex **1** with displacement ellipsoids drawn at the 50% probability level.

Table 2

Selected (a) Bond lengths (Å) and (b) angles (°) for $[(C_5H_4N_3O_2)_3Cr]$.

Cr1-O1	1.9335(19)	O1-Cr1- O3	94.35(8)
Cr1-O3	1.9378(17)	O1-Cr1- O5	91.93(8)
Cr1-O5	1.9562(17)	O3-Cr1- O5	173.14(8)
Cr1-N1	2.043(2)	O1-Cr1- N1	80.73(8)
Cr1-N4	2.057(2)	O3-Cr1- N1	92.74(8)
Cr1-N7	2.058(2)	O5-Cr1- N1	90.97(8)
		O1-Cr1- N4	91.88(8)
		O3-Cr1- N4	80.78(8)
		O5-Cr1- N4	96.29(8)
		N1-Cr1- N4	169.83(9)
		O1-Cr1- N7	171.94(8)
		O3-Cr1- N7	93.35(8)
		O5-Cr1- N7	80.49(8)
		N1-Cr1- N7	96.54(8)
		N4-Cr1- N7	91.69(8)

angles are in the range 80.49(8)–96.54(8)°. The best equatorial plane is provided by the O1/O3/N7/O5 set of atoms (r.m.s. deviation = 0.0469 Å), with the metal displaced by 0.0059(5) Å toward N1. The Cr–O distances (mean value 2.04(16) Å) are not significantly shorter than the Cr–N bond distances (mean value 2.053(5) Å). The five-membered chelation rings are almost planar (maximum r.m.s. deviation = 0.0468 Å for Cr1/N1/C4/C5/O1). In general, bite distances and angles for five membered chelate rings are approximately 2.6 – 2.7 Å and 84–88°, respectively [31]. In complex **1** the O...O bite distances (2.577(3), 2.591(3) and 2.595(3) Å) and the O–Cr–N bite angles (80.74(8), 80.50(8) and 80.79(8)°) are slightly shorter/narrower because of ligand field strength and distorted octahedral environment around the metal center.

The addition on the pyrazine ring of an electron donating or electron withdrawing functional group, like –COOR, –NH₂, –CONH₂ etc., provides opportunities for more interactions suitable for the development of supramolecular architectures [32]. Due to strength and directionality of O–H...O, O–H...N and N–H...O hydrogen bonds, these interactions play a great role in the develop-

ment of coordination polymers, weak interactions like C–H...O and C–H...N hydrogen bonds can also be considered as supramolecular synthons. In **1**, one amine H atom of each 3-amino-2-pyrazine carboxylate anion is engaged in an intramolecular N–H...O hydrogen bond (Table 3) forming rings of S(6) motif, whereas molecules are linked into 1-D zig-zag chain parallel to the *b* axis (Fig. 2) by the N–H...O involving the second amine H atom of only one anion (O1/O2/N1–N3/C1–C5). The chains are further connected into a three-dimensional network by C–H...O hydrogen bonds (Table 3).

3.2. Infrared spectra and X-ray powder diffraction

The vibrational spectrum of the complex is consistent with the structural data is shown in ESI 1. Peaks between 933 and 1217 cm^{−1} are assigned to the pyrazine moiety [33]. Symmetric and asymmetric N–H stretching frequencies of the amine group appear in the 3338–3456 cm^{−1} region. The broad and strong absorption band at 3338 cm^{−1} is due to the presence of O–H...X hydrogen bonding interactions. Peaks at 1317–1358 cm^{−1} are attributable to C–N stretch of aromatic amine [34]. The appearance of peaks at 474 cm^{−1} indicates the presence of Cr–O bond. The X-ray powder diffraction patterns of the complex are shown in ESI2. The diffraction spectra was recorded in the range of $2\theta = 5\text{--}50^\circ$. The sharp peaks indicate the crystalline nature of the synthesized powder complex. The X-ray diffraction peaks of the bulk powder sample of Cr(III) and the stimulated X-ray diffraction peaks are matched exactly, by which we compare the purity of the bulk complex to the diffraction pattern obtained from single crystal X-ray diffraction pattern.

3.3. UV-Vis absorption study

The UV–vis absorption is measured with 1×10^{-5} mol L^{−1} methanolic solution of the ligand and the metal complex (at different concentrations) are presented in Fig. 3. From the absorption

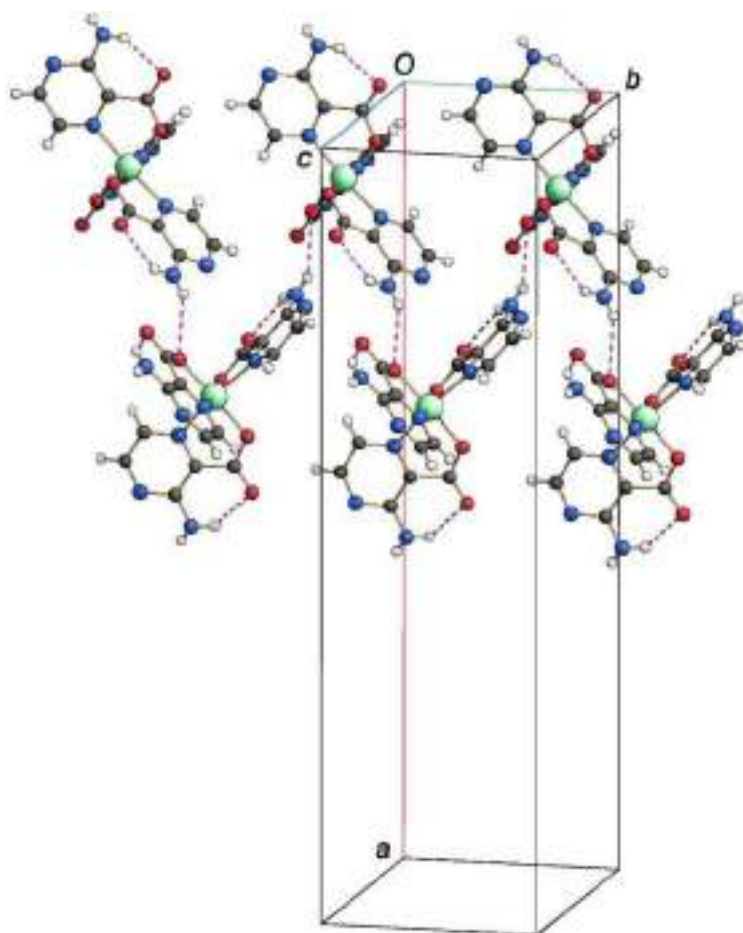


Fig. 2. Partial crystal packing of **1** showing the formation of a zig-zag molecular chain parallel to the *b* axis by N–H...O hydrogen bonds. Intra- and intermolecular hydrogen bonds are shown as dashed lines.

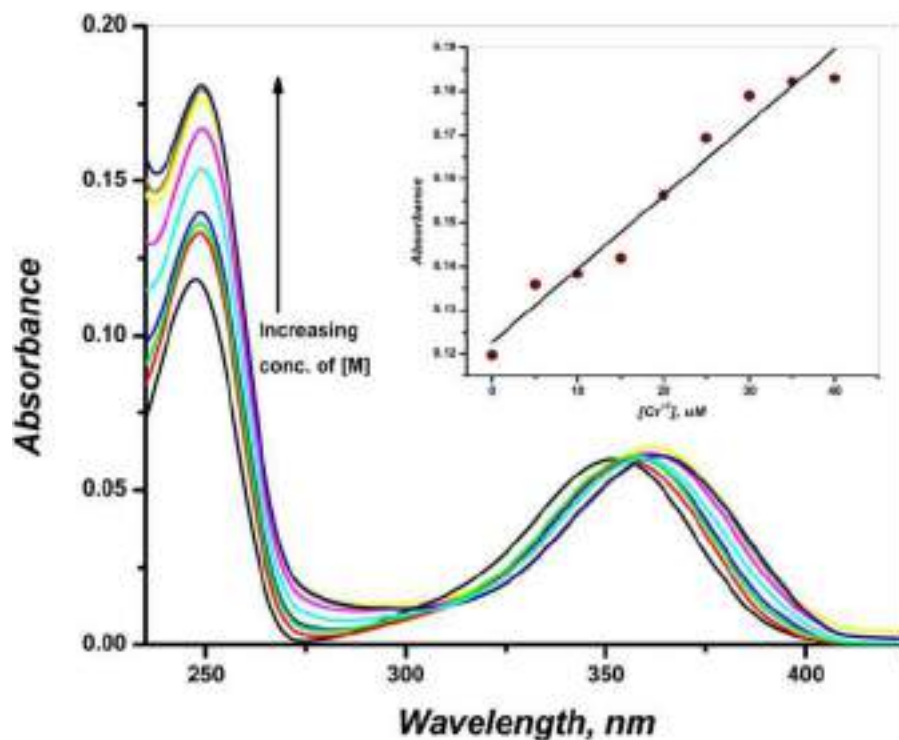
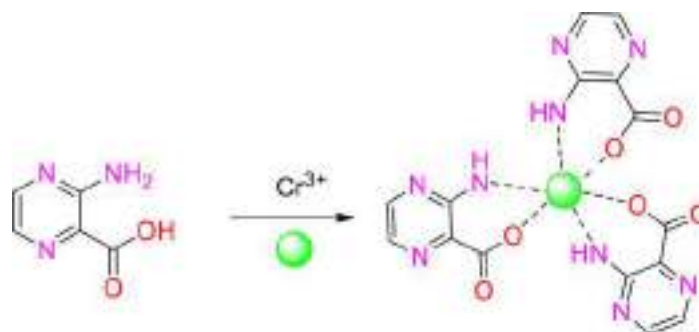


Fig. 3. Absorption spectral change of APC (1×10^{-5} mol L⁻¹) upon addition of Cr(III) in methanol. The arrows showed the increase of Cr(III) ion concentration. The concentration of Cr(III) ion was 0.0, 5.0, 10.0, 15.0, 20.0, 25.0, 30.0, 35.0, 40.0 μ M respectively. (Inset of Fig. 3: Calibration curve at 250 nm).

Table 3
Hydrogen bonds (Å and °) for [(C₅H₄N₃O₂)₃Cr].

D-H...A	D-H/(Å)	H...A/(Å)	D...A/(Å)	<D-H...A/(°)	Symmetry
N3-H1N...O2	0.89(3)	2.10(3)	2.776(4)	131(3)	x, y, z
N3-H2N...O5	0.80(4)	2.48(4)	3.187(3)	148(3)	-x + 1/2, y + 1/2, -z + 1/2
N6-H4N...O4	0.87(4)	2.07(4)	2.737(6)	133(4)	x, y, z
N9-H6N...O6	0.84(4)	2.08(4)	2.768(3)	139(4)	x, y, z
C1-H1...O2	0.93	2.33	3.145(4)	147	-x, 2-y, -1/2 + z
C2-H2...O6	0.93	2.54	3.338(4)	144	x, 1 + y, z
C11-H11...O4	0.93	2.36	3.060(3)	132	-x, 2-y, -z



Scheme 1. Schematic illustration of the sensing mechanism.

maxima profile of the ligand, the higher energy band at 250 nm attributed to π - π^* transitions and lower energy band at 310 to 380 nm could be assigned to n - π^* transitions. The absorption wavelength of ligand APC (350 nm) was slightly red shifted upon addition of gradual addition of 5 μ M Cr³⁺ ions. The change in absorption spectra of ligand is due to the coordination of Cr metal ions by the ligand's N and O binding sites, leads to the formation of new complex (Scheme 1). This bathochromic shift observed after addition of Cr³⁺ metal ion. Thus, the formation of a new complex leads to the relative stabilization of ground state energy alteration which correlates the bathochromic shift.

The increased in absorption intensity may be attributed to the formation of five membered chelate ring through one nitrogen and one oxygen atoms from 3-amino 2-pyrazine carboxylate moiety which enlarges the conjugated systems and reduces the energy difference between n and π^* orbital. Upon increasing the Cr³⁺ ion concentration, the band at 250 nm displays a concomitant increase in optical density. The plot of the absorbance (Fig. 3) at 250 nm generates a calibration curve [(inset of Fig. 3)] keeping the sensor concentration fixed and allows one to detect and estimate the concentration of Cr³⁺ ions present. Detection limit has calculated and the value of LOD is 0.77×10^{-6} M, by using the formula of detection limit $3\sigma/k$: Where σ is the standard deviation, k is the slope between the absorption intensity versus Cr³⁺ concentration [35]. This chemosensory response compares favourably to most of the known Cr³⁺ sensors. Comparative literature studies of chemosensors with present reported Cr³⁺ complexis given in Table S1 [21c,36–40]. From this comparison it can be inferred that our probe makes the current work more attractive and could be the simplest method as it involves a facile one step reaction with readily available chemical.

3.4. Sensing capability in presence of interfering cations

The sensing mechanism is proposed to proceed through the metal–ligand interaction principle. Here coordination of Cr³⁺ ions with the electron rich nitrogen atom of amine moiety and oxygen atom of carboxylic acid moiety leads to the formation of five mem-

bered chelate ring formations. To examine the potentiality of this probe in presence of interfering cations we have added 10 μ M Cr (III) in the mixture of other competitive cations such as Al³⁺, Mn²⁺, Cu²⁺, Ni²⁺, Fe³⁺, Cd²⁺ and Zn²⁺ ions. Concentration of the probe was 1×10^{-5} M in methanol. From Fig. 4 (inset) it is observed that UV-Vis spectral response of the ligand is quite efficient to demonstrate its efficiency to distinguish trivalent chromium in the mixture of interfering cations.

Further to investigate sensor selectivity, we took different metals ions (like Al³⁺, Mn²⁺, Cu²⁺, Ni²⁺, Fe³⁺, Cd²⁺, Zn²⁺) having concentration 10 μ M each in methanol towards the probe concentration 1×10^{-5} mol L⁻¹. From the responses shown in ESI 3, it is observed that the intensity of the probe slightly increases upon addition Al³⁺, Fe³⁺, Cu²⁺, Mn²⁺, Cd²⁺, Ni²⁺, Zn²⁺. But the receptor is highly selective towards Cr³⁺ ions. Selectivity of the probe towards Cr³⁺ only, may be due to the preferential metal bonding over the other metal ions and the generation of three dimensional zig-zag molecular chain parallel to the b axis by N-H...O hydrogen bonds (both inter and intramolecular). Probe performance towards Cr³⁺ in presence of common anions like F⁻, Cl⁻, NO₃⁻ given in ESI 4 and the results for oxoanions (like SO₄²⁻, CrO₄²⁻, Cr₂O₇²⁻) are presented in ESI 6. The figures suggest that the probe can only effectively act as a sensor for Cr³⁺ metal ion in presence of different anions and oxo anions. From literature it is observed that compounds containing amine, thiol, hydroxyl, carboxyl groups have high affinity and coordination capability to the metal ions [41].

To study the practical applicability, the effects of pH on the probe to Cr³⁺ ions are also investigated. The experimental results (ESI 5) clearly demonstrate that the chemosensor is suitable for determining Cr³⁺ in neutral pH range (6.0–8.0), which is favorable for its application in some environmental and physiological conditions. The spectra of only ligand has been checked and provided in inset of ESI 5. The effect of neutral pH on only ligand and in presence of Cr³⁺ has also checked and given in ESI 5. Although use of methanol is restricted in some cases, the comparison of the probe with some other Cr³⁺ sensitive probes (Table S2) [35,42–45] clearly shows the superiority of this method.

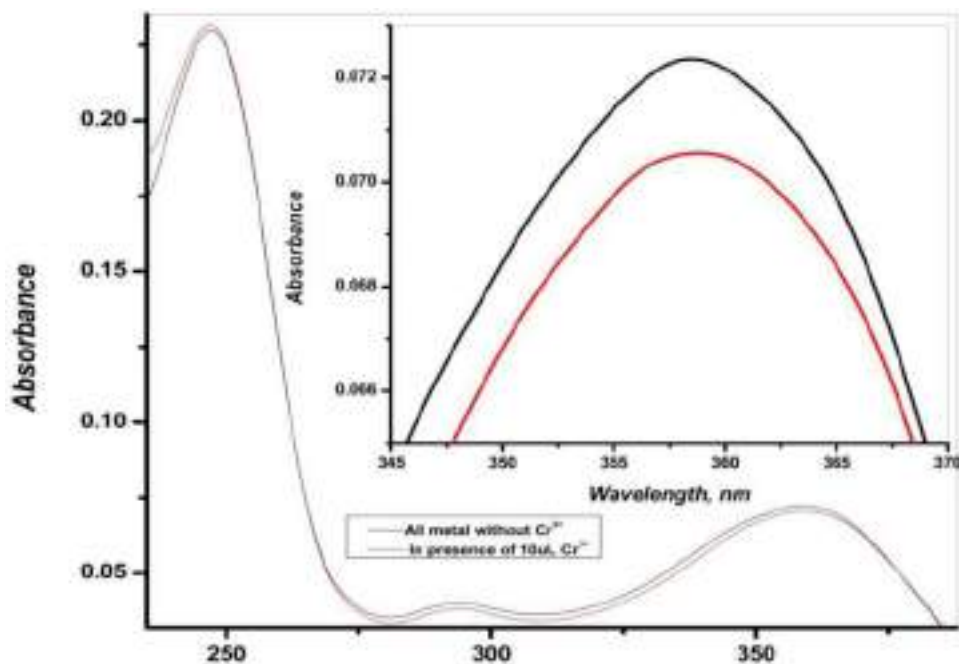


Fig. 4. Sensing capability of probe (1×10^{-5} mol L^{-1}) in the mixture of interfering cations ($10 \mu M$ each) [Inset of Fig. 4. zoom view at 350 nm].

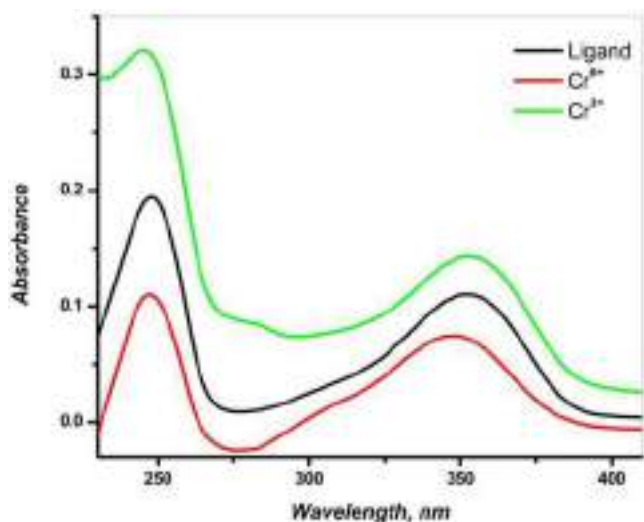


Fig. 5. Differentiation between Cr(III) and Cr(VI) with the ligand (1×10^{-5} mol L^{-1}) in absorption spectrum.

3.5. Interesting opposite spectroscopic behavior

The analysis of the UV-Vis spectra also revealed an interesting feature in presence of different oxidation states of Cr in the same solvent. From Fig. 5 it is clear that the ligand shows increase in intensity for Cr(III) whereas decrease in intensity for Cr(VI) ion with respect to the probe. This type of different spectroscopic behavior for Cr(III) and Cr(VI) is due to the level of different interactions. The extent hyperchromic effect may be due to external electrostatic contacts of the formed complexes. This result clearly implies that the binding of probe with the electron rich nitrogen atom of amine moiety and oxygen atom of carboxylic acid moiety leads to the formation of supramolecular architecture, which enhanced the absorbance intensity for Cr(III) ions. Fate of the probe when both the Cr(III) and Cr(VI) present in a solution is given in ESI 7, in-

dicates the presence of both but detecting specifically Cr(III) ion, based on the λ_{max} .

3.6. Designing of molecular logic gates and smart sensing of Cr^{+3}

The spectroscopic responses that generated from the ligand (APC) on interaction with Cr^{+3} and other metal ions ($M^{+n} = Al^{3+}$, Fe^{+3} , Ni^{+2} , Mn^{+2} , Cu^{+2} , Zn^{+2} , Cd^{+2}) are further exploited to design molecular logic gates. For this purpose, the ligand (APC), Cr^{+3} , and M^{+n} ions are treated as the “chemical inputs”, the absorption intensity at 350 nm (I_{350}) is considered as the “optical output” and pure MeOH is considered as the initial state. A fixed threshold was considered to the 350 nm emission channel to convert the analog spectroscopic data into binary digits. The excitation intensity below and above the threshold is counted as the ‘LOW’ and ‘HIGH’ responses, respectively, and designated as binary digits ‘0’ and ‘1’, respectively. Now, considering APC and Cr^{+3} as the two chemical inputs, MeOH as initial state, and I_{350} as the single optical output, the two-input-single-output AND logic gate is designed [7]. The co-presence of APC and Cr^{+3} , for the input situation (1,1), is the only case where ‘HIGH’ (1) output response is found at I_{350} . The other three input combinations, i.e. (0,0), (1,0), and (0,1), generate ‘LOW’ (0) output response. Thus, the logical response of the molecular AND gate is realized (Fig. 6a1, a2, a3). Notably, as APC can efficiently sense Cr^{+3} in solitary as well as crowded conditions, the presence of M^{+n} ions would not have any effect to the logic functioning of the molecular AND gate. Interestingly, the same molecular AND gate can be modulated to perform the logic action of two-input-single-output PASS 0 gate through simple alteration of the ‘chemical input’ Cr^{+3} to M^{+n} , considering all the other chemical and optical parameters intact. Thus, considering APC and M^{+n} as the two chemical inputs, MeOH as preliminary state and I_{350} as optical output, the PASS 0 gate is realized (Fig. 6b1,b2) [46]. The absorption intensity at 350 nm for all the four input situations, (0,0), (1,0), (0,1), and (1,1), are found to be well below to the applied threshold, ultimately generating ‘LOW’ (0) output response. Thus, in absence of Cr^{+3} , we would observe the PASS 0 logic response. Hence, we would expect the logic responses of the AND or PASS 0 gates based on the presence or absence of Cr^{+3} , respectively. Ulti-

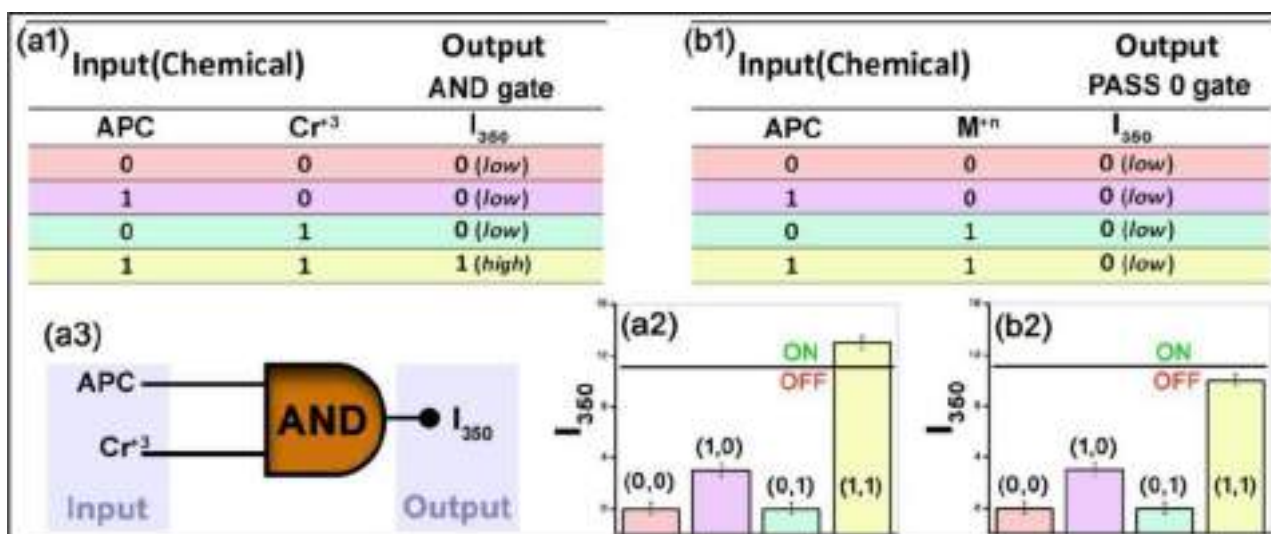


Fig. 6. (a1) Truth table, (a2) bar diagram and (a3) logic gate representation of molecular AND gate; (b1) Truth table and (b2) bar diagram of molecular PASS 0 gate.

mately, all these observations could be taken into account for the smart-sensing of Cr³⁺ via differential logic actions by utilizing the ligand, APC.

4. Conclusion

Chemosensing property of 3-amino-2-pyrazine carboxylic acid (APC) is explored by using UV-Vis spectroscopy, and employed as a selective optical chemo sensor for chromium (III) ions. The binding of the probe with Cr(III) is firmly established by the SCXRD technique that was isolated from APC under solvo-thermal conditions. Structural analysis revealed that the mononuclear Cr(III) complex forms 3-D network by C–H...O hydrogen bonds. Selective sensor property was observed for Cr(III) in presence of interfering ions. The experiments were repeated for three times keeping the concentration same. Another interesting property is that it exhibits opposite spectroscopic behavior for two different oxidation states of Cr. Thus the ligand can differentiate Cr(III) and Cr(VI) with the help of a simple spectrophotometric technique. The developed method is very simple, offers high sensitivity and has the advantage of low cost and does not need any extra fluorophores for the sensitive detection of both the forms of chromium. The spectroscopic responses generated from the ligand (APC) on interaction with Cr³⁺ and other metal ions (Mⁿ⁺ = Al³⁺, Fe³⁺, Ni²⁺, Mn²⁺, Cu²⁺, Zn²⁺, Cd²⁺) are used to design molecular logic gates.

Authorship statement

All persons who meet authorship criteria are listed as authors, and all authors certify that they have participated sufficiently in the work to take public responsibility for the content, including participation in the concept, design, analysis, writing, or revision of the manuscript. Furthermore, each author certifies that this material or similar material has not been and will not be submitted to or published in any other publication before its appearance in the Journal of Molecular Science.

Supplementary materials

For the structural analysis crystallographic data have been deposited with the Cambridge Crystallographic data center, CCDC No. 2108329. Copy of this information may be obtained free of charge from The Director, 12 Union Road, Cambridge, CB2 1EZ, UK (fax:

+44-1223-336033; e-mail: deposit@ccdc.cam.ac.uk or www: <http://www.ccdc.cam.ac.uk>).

Declaration of Competing Interest

The authors declare that they have no known competing financial interests or personal relationships that could have appeared to influence the work reported in this paper.

CRediT authorship contribution statement

Abhishikta Chatterjee: Funding acquisition, Data curation, Formal analysis, Writing – original draft, Writing – review & editing. **Priyanka Chakraborty:** Data curation, Formal analysis. **Bidyapati Kumar:** Data curation, Formal analysis. **Corrado Rizzoli:** Funding acquisition, Data curation, Formal analysis. **Pinaki Mandal:** Writing – review & editing. **Subrata K. Dey:** Conceptualization, Visualization, Writing – original draft, Writing – review & editing.

Acknowledgement

We acknowledge WB-DST for the financial support (Project Memo No 746(Sanc)/ST/P.S&T/15G dt. 22.11.2016.) of this work and the INSPIER fellowship to A.C. (Ref. No. DST/INSPIRE Fellowship/2017/IF170767 dt. 04.05.2018) was funded by DST, New Delhi. Sincere thanks to Dr. Niranjana Koley, Retd. Assoc. Professor in Chemistry of Raghunathpur College, WB and Dr. Arabinda Mallick of Dept. of Chemistry, Kazi Nazrul University, WB for their valuable advices.

Supplementary materials

Supplementary material associated with this article can be found, in the online version, at doi:10.1016/j.molstruc.2022.132486.

References

- [1] N. Kaur, N. Singh, B. McCaughan, J.F. Callan, AND molecular logic using semiconductor quantum dots, *Sens. Actuators B Chem.* 144 (2010) 88–91.
- [2] (a) B.M. Frezza, S.L. Cockcroft, M.R. Ghadiri, Modular Multi-Level Circuits from Immobilized DNA-Based Logic Gates, *J. Am. Chem. Soc.* 129 (2007) 14875–14879; (b) P. Paul, M. Karar, A. Mallick, T. Majumdar, A photonic multi-functional molecular logic powered by two-step energy transfer, *J. Mater. Chem. C* 9 (2021) 11229–11241; (c) M. Karar, S. Paul, B. Biswas, T. Majumdar, A. Mallick, A newly developed highly selective Zn²⁺-AcO⁻ ion-pair sensor through partner preference: equal efficiency under solitary and colonial situation, *Dalton Trans.* 47 (2018) 7059–7069.

- [3] (a) J. Wang, C.S. Ha, Fluorescent logic operations based on azobenzene-containing compounds, *Sens. Actuators B Chem.* 146 (2010) 373–380; (b) G. Sivaraman, M. Iniya, T. Anand, N.G. Kotla, O. Sunnapu, S. Singaravelu, A. Gulyani, D. Chellappa, Chemically diverse small molecule fluorescent chemosensors for copper ion, *Coord. Chem. Rev.* 357 (2018) 50–104.
- [4] P. Singh, J. Kaur, W. Holzer, Acridone based Cu^{2+} -F⁻/F⁻- Cu^{2+} responsive ON/OFF key pad, *Sens. Actuators B Chem.* 150 (2010) 50–56.
- [5] G. Periyasamy, J.P. Collin, J.P. Sauvage, R.D. Levine, F. Remacle, Electrochemically Driven Sequential Machines: An Implementation of Copper Rotaxanes, *Chem. Eur. J.* 15 (2009) 1310–1313.
- [6] A. Credi, V. Balzani, S.J. Langford, J.F. Stoddart, Logic Operations at the Molecular Level. An XOR Gate Based on a Molecular Machine, *J. Am. Chem. Soc.* 119 (1997) 2679–2681.
- [7] A.P. de Silva, N.H.Q. Gunaratne, C.P. McCoy, A molecular photoionic AND gate based on fluorescent signaling, *Nature* 364 (1993) 42–44.
- [8] K. Szacilowski, Digital Information Processing in Molecular Systems, *Chem. Rev.* 108 (2008) 3481–3548.
- [9] S. Erbas-Cakmak, S. Kolemen, A.C. Sedgwick, T. Gunnlaugsson, T.D. James, J. Yoon, E.U. Akkaya, Molecular logic gates: the past, present and future, *Chem. Soc. Rev.* 47 (2018) 2228–2248.
- [10] A.P. de Silva, Molecular Logic Gate Arrays, *Chem. Asian J.* 6 (2011) 750–766.
- [11] (a) M. Karar, P. Paul, B. Biswas, A. Mallick, T. Majumdar, Excitation wavelength as logic operator, *J. Chem. Phys.* 152 (2020) 075102–075106; (b) M. Karar, P. Paul, S. Paul, B. Haldar, A. Mallick, T. Majumdar, Dual macro-cyclic component-based logic diversity, *Dyes and Pigments* 174 (2020) 108060–108064.
- [12] B. Naskar, R. Modak, Y. Sikdar, D.K. Maiti, A. Banik, T.K. Dangar, S. Mukhopadhyay, D. Mandal, S. Goswami, A simple Schiff base molecular logic gate for detection of Zn^{2+} in water and its bio-imaging application in plant system, *J. Photochem. Photobiol. A* 321 (2016) 99–109.
- [13] K.S. Hettie, J.L. Klockow, T.E. Glass, Three-Input Logic Gates with Potential Applications for Neuronal Imaging, *J. Am. Chem. Soc.* 136 (2014) 4877–4880.
- [14] B. Dhal, H.N. Thatoi, N.N. Das, B.D. Pandey, Chemical and microbial remediation of hexavalent chromium from contaminated soil and mining/metallurgical solid waste: A review, *J. Hazard. Mater.* 250–251 (2013) 272–291.
- [15] D. Bagchi, S.J. Stohs, B.W. Downs, M. Bagchi, H.G. Preuss, Cytotoxicity and oxidative mechanisms of different forms of chromium, *Toxicology* 180 (2002) 5–22.
- [16] S. Mukherjee, S. Ganguly, D. Samanta, D. Das, Sustainable Green Route to Synthesize Functional Nano-MOFs as Selective Sensing Probes for Cr^{VI} Oxoanions and as Specific Sequestering Agents for $\text{Cr}_2\text{O}_7^{2-}$, *ACS Sustain. Chem. Eng.* 8 (2020) 1195–1206.
- [17] (a) R. von Burg, D. Liu, Chromium and hexavalent chromium, *J. Appl. Toxicol.* 13 (1993) 225–230; (b) S.R.J. Oliver, Cationic inorganic materials for anionic pollutant trapping and catalysis, *Chem. Soc. Rev.* 38 (2009) 1868–1881.
- [18] J.G. Kim, J.B. Dixon, C.C. Chusuei, Y. Deng, Oxidation of Chromium(III) to (VI) by Manganese Oxides, *Soil Sci. Soc. Am. J.* 66 (2002) 306–315.
- [19] A.K. Bhanja, S. Mishra, K. Naskar, S. Maity, K. Das Saha, C. Sinha, Specific recognition of Cr^{3+} under physiological conditions by allyl substituted appendagerhodamine and its cell-imaging studies, *Dalton Trans* 46 (2017) 16516–16524.
- [20] (a) R. Das, S. Bej, D. Ghosh, N.C. Murmu, H. Hirani, P. Banerjee, Stimuli-responsive discriminative detection of Cu^{2+} and Hg^{2+} with concurrent sensing of S^{2-} from aqueous medium and bio-fluids by C–N fused azophenine functionalized “smart” hydrogel assay @A potential biomarker sensor for Wilson’s disease, *Sens. Actuators B Chem.* 341 (2021) 129925; (b) S. Bej, R. Das, H. Hirani, S. Ghosh, P. Banerjee, Naked-eye detection of CN⁻ from aqueous phase and other extracellular matrices: an experimental and theoretical approach mimicking the logic gate concept, *New J. Chem.* 43 (2019) 18098–18109.
- [21] (a) L. de Oliveira, A.M. Antunes, M.I.M.S. Bueno, Direct chromium speciation using X-ray spectrometry and chemometrics, *X-Ray Spectrom* 39 (4) (2010) 279–284; (b) G.B. Chalmardi, M. Tajbakhsh, A. Bekhradnia, R. Hosseinzadeh, A highly sensitive and selective novel fluorescent chemosensor for detection of Cr^{3+} based on a Schiff base, *Inorg. Chim. Acta* 462 (2017) 241–248; (c) M. Ghaedi, A. Shokrollahi, A.R. Salimibeni, S. Noshadi, S. Joybar, Preparation of a new chromium(III) selective electrode based on 1-[(2-hydroxy ethyl) amino]-4-methyl-9H-thioxanthene-9-one as a neutral carrier, *J. Hazard. Mater.* 178 (2010) 157–163.
- [22] L.E. Kreno, K. Leong, O.K. Farha, M. Allendorf, R.P. Van Duyne, J.T. Hupp, Metal–Organic Framework Materials as Chemical Sensors, *Chem. Rev.* 112 (2012) 1105–1125.
- [23] (a) O. Basu, S. Das, Supramolecular inorganic chemistry leading to functional materials, *J. Chem. Sci.* 132 (2020) 46; (b) D. Liu, K. Lu, C. Poon, W. Lin, Metal–organic framework materials as chemical sensors, *Inorg. Chem.* 53 (4) (2013) 1916–1924.
- [24] (a) Z. Tang, H. Chen, Y. Zhang, B. Zheng, S. Zhang, P. Cheng, Functional two-dimensional coordination polymer exhibiting luminescence detection of nitroaromatics, *Cryst. Growth Des.* 19 (2019) 1172–1182; (b) K.H. Nguyen, Y. Hao, K. Zeng, X. Wei, S. Yuan, F. Li, S. Fan, M. Xu, Y.-N. Liu, A reaction-based long-wavelength fluorescent probe for Cu^{2+} detection and imaging in living cells, *J. Photochem. Photobiol. A: Chem.* 358 (2018) 201–206.
- [25] A.O. Eseola, H. Görls, M. Bangesh, W. Plass, ESIPT-capable 2,6-di(1H-imidazol-2-yl)phenols with very strong fluorescent sensing 1 signals towards Cr(III), Zn(II) and Cd(II): molecular variation effects on turn-on efficiency, *New J. Chem.* 42 (2018) 7884–7900.
- [26] APEX3 Package APEX3, SAINT and SADABS, AXS Bruker, Bruker AXS Inc, Madison, Wisconsin, USA, 2016.
- [27] G.M. Sheldrick, Integrated space-group and crystal structure determination, *Acta Cryst. A71* (2015) 3–8.
- [28] G.M. Sheldrick, Crystal structure refinement with SHELXL, *Acta Cryst. C71* (2015) 3–8.
- [29] L.J. Farrugia, WinGX and ORTEP for Windows: an update, *J. Appl. Cryst.* 45 (2012) 849–854.
- [30] E. Keller, SCHAKAL, University of Freiburg, Germany, 1999.
- [31] M.P. Suh, Macrocyclic Chemistry of Nickel, *Adv. Inorg. Chem.* 44 (1997) 93–146.
- [32] S. Shit, S.K. Dey, C. Rizzoli, E. Zangrando, G. Pilet, C.J. Gómez-García, S. Mitra, The key role of hydrogen bonding in the nuclearity of three copper(II) complexes with hydrazone-derived ligands and nitrogen donor heterocycles, *Inorg. Chim. Acta* 370 (2011) 18–26.
- [33] (a) C.R. Choudhury, S.K. Dey, S. Sen, B. Bag, S. Mitra, V. Gramlich, A Pyrazine-Bridged Ni(II) Coordination Polymer, *Z. Naturforsch. B* 57 (11) (2002) 1191–1194; (b) S.K. Dey, M. Hazra, L.K. Thompson, A. Patra, Manganese(II) coordination polymer having pyrazine and μ -phenolato bridging: Structure, magnetism and biological studies, *Inorg. Chim. Acta* 443 (2016) 224–229.
- [34] (a) K. Nakamoto, Infrared spectra of inorganic and coordination compounds, John Wiley & Sons, New York, NY, 1970; (b) S.K. Dey, B. Bag, Z. Zhou, A.S.C. Chan, S. Mitra, Synthesis, characterization and crystal structure of a monomeric and a macrocyclic copper (II) complex with a large cavity using benzylacetylacetonone ligand, 2004 *Inorg. Chim. Acta*, 357 1991–1996.
- [35] (a) A. Zhu, J. Pan, Y. Liu, F. Chen, X. Ban, S. Qiu, Y. Luo, Q. Zhu, J. Yu, W. Liu, A novel dibenzimidazole-based fluorescent organic molecule as a turn-off fluorescent probe for Cr^{3+} ion with high sensitivity and quick response, *J. Mol. Struct.* 1206 (2020) 127696–12702; (b) R. Das, S. Bej, H. Hirani, P. Banerjee, Trace-Level Humidity Sensing from Commercial Organic Solvents and Food Products by an AIE/ESIPT-Triggered Piezochromic Luminogen and ppb-Level “OFF–ON–OFF” Sensing of Cu^{2+} : A Combined Experimental and Theoretical Outcome, *ACS Omega* 6 (2021) 14104–14121.
- [36] D. Erdener F. Kolcu, İ. Kaya, A Schiff base based on triphenylamine and thiophene moieties as a fluorescent sensor for Cr (III) ions: Synthesis, characterization and fluorescent applications, *Inorganica Chim. Acta* 509 (2020) 119676–119683.
- [37] D. Li, C.Y. Li, H.R. Qi, K.Y. Tan, Y.F. Li, Rhodamine-based chemosensor for fluorescence determination of trivalent chromium ion in living cells, *Sens. Actuators B Chem.* 223 (2016) 705–712.
- [38] L. Rasheed, M. Yousuf, S. Youn, T. Yoon, K.Y. Kim, Y.K. Seo, G. Shi, M. Saleh, J.H. Hur, K.S. Kim, Turn-On Ratiometric Fluorescent Probe for Selective Discrimination of Cr^{3+} from Fe^{3+} in Aqueous Media for Living Cell Imaging, *Chem. Eur. J.* 21 (2015) 16285–16695.
- [39] Y. Yang, H. Xue, L. Chen, R. Sheng, X. Li, K. Li, Colorimetric and Highly Selective Fluorescence “Turn-on” Detection of Cr^{3+} by Using a Simple Schiff Base Sensor, *Chin. J. Chem.* 31 (2013) 377–380.
- [40] D. Karak, A. Banerjee, A. Sahana, S. Guha, S. Lohar, S.S. Adhikari, D. Das, 9-Acridone-4-carboxylic acid as an efficient Cr(III) fluorescent sensor: Trace level detection, estimation and speciation studies, *J. Hazard. Mater.* 188 (2011) 274–280.
- [41] A.Q. Alorabi, M. Abdelbaset, S.A. Zabin, Colorimetric Detection of Multiple Metal Ions Using Schiff Base 1-(2-Thiophenylimino)-4-(N-dimethyl) benzene, *Chemosensors* 8 (2020) 1.
- [42] A. Roy, S. Das, S. Sacher, S.K. Mandal, P. Roy, A rhodamine based biocompatible chemosensor for Al^{3+} , Cr^{3+} and Fe^{3+} ions: extraordinary fluorescence enhancement and a precursor for future chemosensors, *Dalton Trans* 48 (2019) 17594–17604.
- [43] S. Das, A. Sahana, A. Banerjee, S. Lohar, S. Guha, J.S. Matalobos, D. Das, Thiophene anchored naphthalene derivative: Cr^{3+} selective turn-on fluorescent probe for living cell imaging, *Anal. Methods* 4 (2012) 2254–2258.
- [44] J. Zhang, L. Zhang, Y. Wei, J. Chao, S. Wang, S. Shuang, Z. Caia, C. Dong, A selective carbazole-based fluorescent probe for chromium(III), *Anal. Methods* 5 (2013) 5549–5554.
- [45] X. Baoa, Q. Caoa, X. Niec, Y. Zhouc, R. Yec, B. Zhouc, J. Zhuc, Design and synthesis of a novel chromium(III) selective fluorescent chemosensor bearing a thiodiacetamide moiety and two rhodamine B fluorophores, *Sens. Actuators B Chem.* 221 (2015) 930–939.
- [46] J.C. Spiteri, S.A. Denisov, G. Jonusauskas, S. Klejna, K. Szacilowski, N.D. McCleaghnan, David C. Magri, Molecular engineering of logic gate types by module rearrangement in ‘Pourbaix Sensors’: the effect of excited-state electric fields, *Org. Biomol. Chem.* 16 (2018) 6195–6201.

‘এবং মল্লয়া’-নির্ধাবিদ্যালয় মঞ্জুরী আয়োগ (UGC-CARE List-I 2021) অনুমোদিত তালিকার
অন্তর্ভুক্ত। ২০২১সালে প্রকাশিত ১৬পৃ. তালিকার (৩১৯টির মধ্যে) ৩ পৃ. ৬০নং উল্লেখিত।

এবং মল্লয়া

(বাংলা ভাষা, সাহিত্য ও গবেষণাধর্মী মাসিক পত্রিকা)

২৩ তম বর্ষ, ১৪৩ সংখ্যা, ডিসেম্বর, ২০২১

সম্পাদক

ডা. মদনমোহন বেরা

কে.কে. প্রকাশন

গোলকুঁয়াচক, মেদিনীপুর, প.বঙ্গ।

১৭. আত্মতার স্বাক্ষরে পূর্ব প্রেমিকপুত্রের পুঙ্খনামঃ

১৮. কবিত্ব গানঃ..... ১৪০

১৮. অধ্যাত্মীয় বাণীর জাতি-বর্ণ পয়াজে লায়শুর্ড ও লৌক্য
 কাহ্যসূত্রের অবধান : : স্থপন স্তরকার..... ১৪৬

১৯. ইংগা পোষ (মহুমানার) : : অস্কার অধম মতিলা ইঞ্জিনিয়ার
 : : চৌচিন পোষ..... ১৪০

২০. সুকাসর বসুত আত্মকথা : : কবিজীবনের অস্বাভাবি
 : : অতিভীমা খানখানী..... ১৪৮

২১. ডগাই ও হুয়ামের অস্বাভাবী স্নানজ : : সখীকা ও বিবেক
 : : পুতিনা রায়..... ১৬৭

২২. বেলিনীপুত্রের ইতিহাসে ১৯৩০ এর মনক ও কবিজীবনটি
 আত্মস্বপ্নের উদ্ভব - একটি আত্মতত্ত্ব : : শক্তিচন্দন দে..... ১৭০

২৩. বীজালা কাব' : : অরমত বিবেকসুন্দর আত্মোক্ত
 : : বিকশ মণ্ডল..... ১৮০

২৪. শিলালয়, কামালেশ্বর এবং ভক্তসেখ তে রাম এবং কামালায় চর্চা :
 প্রাস উত্তর ভারত, কল এবং আশায় : : প্রমতি চৌধুর বসী..... ১৯১

২৫. মনোজ হিয়ার দিব্যচিত্র নাটকের বিধর বৈচিত্র
 : : মজল নি..... ১৯৭

২৬. সত্যজিত সংকটি : : উপনিবেশবাস বিহারী বসীজনাথ
 : : অরম চক্রবর্তী..... ২০৭

২৭. সারু ঋগ্নের বৈষ্ণব আদেশ : : শ্রীনাথ বায়লাসজা
 : : অরম পোষ..... ২১৪

২৮. 'নাথের নবীর পথ : : কৃতিকর স্বাস্থিক মতবান
 : : বর্ষা মজল..... ২১৯

২৯. 'কারণ ও কারণ-সামাজিক পুষ্টিভবি পোকে একটি উপস্থাপনা
 : : বসুন্ধর গাঙ্গুলী..... ২২৮

৩০. মাহাবতর মাহাই দেবত : : রবীন্দ্র পুস্তিতে পয়াজোনামা
 : : বরবু ছৌচেন..... ২৩২

৩১. কালক্রীড়া কুলবরনের বিচিত্র স্তম্ভিকদের অর্থ-সামাজিক অর্থের
 চৌম্বিক বিবেক : : বিদ্যমান হুয়ার সঙ্গার..... ২৩৮

৩২. 'কটি পুঙ্খের প্রাক-বৈষ্ণব তত্ত্ব : : হুচেন মজল..... ২৪২

৩৩. রবীন্দ্রনাথ ঠাকুরের প্রাথমিক জীবন ও প্রাথমিক অর্থ-সামাজিক
 'প্রাথমিক পুঙ্খচিত্র' : : একটি পয়াজোনামা : : হেমাচন্দ্র ছৌচেন..... ২৪৯

৩৪. ইন্দ্রিয় শতকের নবী শিক্ষা ও প্রমিতিত কলবিদী গাঙ্গুলি
 : : কেশবচন্দ্র পোষ..... ২৫৯

৩৫. পুঙ্খচিত্র আত্মস্বপ্নের প্রাথমিকত : : একটি
 প্রাথমিক বিবেক : : কৃষা বর্ষা..... ২৭৪

৩৬. ভারতের স্বাধীনতা আন্দোলনে শান্তিনগর অঞ্চল
 : : সুকুমার মজল..... ২৮৭

৩৭. লোকতত্ত্ব ও বাণীর শিবলীল উৎস্বপ্নের ইতিহাস
 : : উৎকলিকা সার..... ২৯০

৩৮. সার্বিক লোকসংস্কৃতির জৈবিত আত্মতত্ত্ব ও পয়াজোনামা
 ঠাকুরবীরের শান্তিনগর ও প্রাথমিক চর্চা : : মাহাী সার..... ২৯৭

৩৯. ইন্দ্রিয় শতকের বাণীর মতিলা কবিতা : : ও অসুতা চক্রবর্তী..... ৩০৬

৪০. সাক্ষর বসু : : মনো অধুপে
 : : ও. অরম ফায়াজ দে মতিলা..... ৩১০

৪১. রবীন্দ্রনাথ ও পুঙ্খচিত্র বিপুল্যে বাণীর
 : : ও. চৌচরী মতি..... ৩১৯

৪২. 'সামান্য কবিতার পুঙ্খচিত্র' নামে পুঙ্খচিত্রের 'অস্বাভাবী'
 : : ও. শিবক দেম..... ৩২০

৪৩. শিবস্বপ্নবিহার অধুপেচন্দ্র ও অস্বাভাবী শিবস্বপ্ন
 : : ও. কৃষ্ণ শিবর..... ৩২৭

৪৪. মনোভাষায় পুঙ্খচিত্রের পুঙ্খচিত্র
 : : ও. কৃষ্ণকান্ত রায়..... ৩৩২

৪৫. পুঙ্খচিত্র কবিতা বিচারে পুঙ্খচিত্র অস্বাভাবী কবিতা পুঙ্খচিত্র
 একটি পুঙ্খচিত্র : : ও. মাহাভারম চৌচেন..... ৩৪০

৪৬. উদ্ভবিত পুঙ্খচিত্রে বাণীর পুঙ্খচিত্রের অর্থ সামাজিক
 প্রাথমিক ও উচ্চতর : : একটি মতিলা. তে মতবান শান্তিনগর
 ৪৭. 'পুঙ্খচিত্রের মতিলা' (১৯৩৯) উপনামে শিবলীল শিবস্বপ্ন
 : : ও. শান্তিনগর..... ৩৪৫

৪৮. 'শিবস্বপ্নের 'পুঙ্খচিত্র' : : শিবলীলস্বপ্নের 'পুঙ্খচিত্র'
 : : ও. মাহাভারম..... ৩৫৬

৪৯. অস্বাভাবী কবিতার বাণীর পুঙ্খচিত্র : : ও. পুঙ্খচিত্রের অর্থ
 ৫০. পুঙ্খচিত্রের চৌ-শিল্পী পুঙ্খচিত্র : : শিব ও কবিতা..... ৩৭৬

৫১. 'পুঙ্খচিত্রের মতিলা' : : ও. পুঙ্খচিত্রের অর্থস্বপ্ন
 ৫২. 'পুঙ্খচিত্রের মতিলা' : : ও. শিবলীলস্বপ্নের..... ৩৮০

মুতিটি! যদিও ফলকের লেখাটি জ্বলজ্বল করছে। পরিশেষে এই কথা বলা যায় যে, দারিদ্রতা যতই থাকুক না কেন, প্রতিভা ও সত্যের কাছে সবই জ্ঞান হয়ে যায়। গভীর সিং মুড়া তারই জ্বলন্ত উদাহরণ। তাঁর চরিত্রবল ছিল, তাঁর বড় সম্পদ। তাই ইতিহাসের নিয়মেই তিনি নিজেকে বিশ্ব-পাদ প্রদীপের সামনে উপস্থাপন করেছিলেন। পুরুলিয়া জেলায় যতদিন ছৌ নৃত্য থাকবে লোক সংস্কৃতির ইতিহাসের পাতায় বিশ্ববরেণ্য গভীর সিং মুড়ার নাম ততদিন স্বর্ণাক্ষরে লেখা থাকবে।

তথ্যসূত্র :

১. আশুতোষ ভট্টাচার্য, 'বাংলার লোক সংস্কৃতি', ন্যাশনাল বুক ট্রাস্ট, ইন্ডিয়া, নয়াদিল্লী, ১৯৮২, পৃ. ১১২ - ১১৪।
২. ড. মহীতোষ গায়ের, ড. সমর কান্তি চক্রবর্তী ও কৌশিক দত্ত (সম্পাদিত), 'বাংলার সমাজ ও সংস্কৃতি', রূপালি পাবলিকেশন, কলকাতা, ২০২০, পৃ. ৪৭।
৩. বিনয় ঘোষ, 'পশ্চিম বঙ্গের সংস্কৃতি' (১ম খন্ড), দীপ প্রকাশন, কলকাতা, ২০০৭, পৃ. ৫৩।
৪. দিলীপ কুমার গোস্বামী, 'মানভূম-পুরুলিয়া', বুজভূমি প্রকাশন, ২০০৭, পৃ. ১৬৮-৬৯।
৫. ছৌ-নাচের ইতিকথা, বর্তমান পত্রিকা, (মুখায় চন্দের বিশেষ প্রবন্ধ), ৪ ঠা অক্টোবর ২০২০।
৬. দিলীপ কুমার গোস্বামী, পূর্বোক্ত, পৃ. ১৬৮-১৭০।
৭. স্বপন কুমার কর্মকার বিশেষ সাক্ষাৎকার, গভীর সিংমুড়ার নিজ বাসভবনে, চড়িদা, বাঘমুন্ডি, পুরুলিয়া, ১৯৯০।
৮. স্বপন কুমার কর্মকার, গভীর সিংমুড়ার সঙ্গে সাক্ষাৎকার, এটি প্রকাশিত হয় 'বাংলার আভাষ' পত্রিকায়, ১৯৯১।
৯. গভীর সিংমুড়ার বিদেশে ছৌ-নৃত্য প্রদর্শনের স্থান ও সালের নাম তারই মর্মর মূর্তির প্রস্তর ফলকে খোদাই করা আছে।
১০. স্বপন কুমার কর্মকার, গভীর সিংমুড়ার সঙ্গে সাক্ষাৎকার, ১৯৯৫ (International Famous Adibasi Chhow Dance Party, Prop. Padmshree Gambhir Sing Mura. এই প্যাডটি আমাকে (স্বপন কর্মকার) তাঁর পুত্র শ্রীযুক্ত কার্তিক মুড়া তাঁর পিতার সম্পর্কে বিশেষ গুরুত্বপূর্ণ তথ্য লিখতে অনুরোধ করেন। আমি তা সংক্ষেপে লিপিবদ্ধ করি।
১১. তরুণ দেব ভট্টাচার্য, 'পুরুলিয়া', সেকাল-একাল, ফার্মা কে.এল.এম. প্রা লি, কলকাতা, ১৯৮৬, পৃ. ৩০৯।
১২. স্বপন কুমার কর্মকার, পূর্বোক্ত, 'বাংলার আভাষ' পত্রিকায়, ১৯৯১।

**U.G.C. - CARE List-I 2021 Approved Journal, Indian
Language-Arts and Humanities Group, out of 16 pages
placed in Page 3 & No. 60 out of 319**

EBONG MOHUA

**Bengali Language, Literature, Research and
Refereed with Peer-Review Journal**

23 rd Year, 143 Volume

December, 2021

**Edited, Printed and Published by
Dr. Madanmohan Bera, Editor.
Golekuachawk, P.O.-Midnapur, 721101.W.B.**

Mob.-9153177653

madanmohanbera51@gmail.com

kohinoor.bera @ gmail.com

Rs. 550



Mother Pelican

A Journal of Solidarity and Sustainability

Vol. 18, No. 7, July 2022
Luis T. Gutiérrez, Editor

[Home Page](#)
[Front Page](#)



Social Unsustainability: The Case of Slum Societies

Arup Kanti Konar

July 2022

Abstract: Unsustainability is two dimensional: it encompasses both ecological unsustainability and social unsustainability. Some authors have added one more dimension of unsustainability such as economic unsustainability. But this is incorrect, because economic dimension is included in the social dimension. Unsustainability is a matter of degree, and social unsustainability indicates the quality of the societies. The theoretical and practical concept of social unsustainability has been ignored. Social unsustainability is being aggravated due to the exponential growth of the informal sector in the developing countries. But, first of all, we should know what social unsustainability is and how it is manifested in urban slum societies.

Key Words: Society, Ecology, Nature, Culture, Sustainability, Unsustainability, Stability, Instability

Unsustainability entails ecologically unsustainable social instability, which, in other words, implies the coexistence of persistent social instability and emerging ecological instability *ceteris paribus*. Since every word has its opposite polarity, so sustainability means ecologically sustainable social stability, which, in other words, implies the coexistence of social stability and ecological stability *ceteris paribus*.

Social means what is not natural. It has become both adjective and noun. Further, it is being used in normative (e.g. what we ought to do) and positive sense (e.g. what we do). It consists of various "sub-socials" such as political, economic, psychological, religious, cultural, ethical, spiritual, moral, familial, sexual, gender, scientific, technological, legal, demographic, democratic, marital, etc.

Ecological instability is indicated by depreciation, depletion, degradation, and/or destruction of ecological/natural resources, assets or capital. Social instability consists of various sub-social instabilities such as political instability, economic instability, psychological instability, religious instability, cultural instability, ethical instability, spiritual instability, moral instability, familial instability, sexual instability, gender instability, scientific instability, technological instability, legal instability, demographic instability, democratic instability, marital instability, etc. Social instability is indicated by poverty, unemployment, starvation, malnutrition, inequality (of income, wealth and rights), illiteracy, insecurity, lack of basic needs (food, housing and clothing), injustice, inequity, corruption, killing, lynching, assassination, torture, oppression, subjugation, violence (against women), rape, molestation, tyranny, child-labour, prostitution, trafficking, kidnapping, suicide, witch-hunting, conflict, crime, militarization, war, fundamentalism (religious, cultural, etc) and so forth.

Many authors have written about social sustainability. Alphabetically, the examples of such authors are as follows: Agyeman and Evans (2004); Casula Vifell and Soneryd (2012); Cuthill (2009); Davidson (2009); Dempsey, Bramley, Power and Brown (2011); Dillard, Dujon and King, (2009); Fotzpatrick (2011); Larsen (2009); Lehtonen (2004); Littig and Griessler (2005); Magis and Shinn (2009); Nordstrom Kallstrom and Ljung (2005); Omann and Spangenberg (2002); Pawlowski (2007); Seghezze (2009); Thin, Lockhart and Yaron (2002); Turkington and Sangster (2006). Further, the Special Issue of the journal: *Sustainability: Science, Practice & Policy* (Volume 8, Issue 12, Winter 2012) is devoted to the discussion of "A Missing Pillar? Challenges in Theorizing and Practicing Social Sustainability", in which there are ten articles.

But, there is hardly any author who has written about social unsustainability. Perhaps, he/she

has not seen or observed with his/her own eyes how social unsustainability is. Fortunately, I have discovered an article on social unsustainability by Sultan Qaboos University Professor, Arif Saeed Malik (2018).

If any author wants to know about social unsustainability, he/she should see with his/her own "eyes and heart" the life and living condition of urban slum societies in developing countries. In some developing countries, as much as 90% of the urban population live in slum society. One in three urban residents lives in slum society in developing countries. One in seven people on the planet currently lives in slum society. The slum population of India exceeds the total population of UK. World's largest slum societies, for example, are Khayelitsha in Cape Town (South Africa), Kibera in Nairobi (Kenya), Dharavi in Mumbai (India), Orangi Town in Karachi (Pakistan). The intensity of social unsustainability of the slum society is unprecedented due to lack of basic needs of their day to day life. They are socially deprived and the poorest of the poor section of urban society.

Social unsustainability can be reduced or ruled out by the following ways:

1. Provision of basic needs (food, housing, clothing, etc).
2. Equitable distribution of income and wealth.
3. Arrangement for intra-generational and inter-generational justice among gender, race, class, etc.
4. Equality of rights, including human rights, land users' rights, tenants' rights, indigenous people's rights, etc.
5. Establishment or promotion of democracy.
6. Establishment of peace.
7. Eradication of poverty.
8. Provision of people's meaningful participation in all aspects of state governance.
9. Elimination of corruption in politics at all levels.
10. Implementation of effective measures for addressing the impact of climate change and reducing greenhouse gas emissions.
11. Arrangement for adequate investment in research and development in order to promote sustainable development based on the needs and priorities.
12. Engagement of local people in planning, implementation and monitoring for the management of natural resources.
13. Investment in alternative energy sources.
14. Development of civil society and social capital.
15. Promotion of quality of life, happiness and well-being.

Social unsustainability and ecological unsustainability are not independent, rather, they are interdependent. If we know the way of reducing or ruling out the unprecedented unsustainability of the slum society, then we will be able to reduce or rule out the global social unsustainability.

The terms like welfare, wellbeing, development, prosperity, happiness, quality of life, standard of living, etc. are pointless to the slum society, because the people of slum society do not even know what the standard of life is. The deplorable and pathetic condition of the slum society is the best example of global social unsustainability.

References

- Agyeman, J. & Evans, B. (2004). Just sustainability: The emerging discourse of environmental justice in Britain? *Geographical Journal*, 170(2), 155-164. <https://www.jstor.org/stable/3451592>
- Casula Vifell, A. & Soneryd, L. (2012). Organizing matters: How the "social dimension" gets lost in sustainability projects. *Sustainable Development*, 20(1), 18-27. <https://doi.org/10.1002/sd.461>
- Cuthill, M. (2009). Strengthening the "social" in sustainable development: Developing a conceptual framework for social sustainability in a rapid urban growth region in Australia. *Sustainable Development*, 18(6), 362-373. <http://doi.org/10.1002/sd.397>
- Davidson, M. (2009). Social sustainability: A potential for politics? *Local Environment*, 14(7), 607-619. <https://doi.org/10.1080/13549830903089291>
- Dempsey, N., Bramley, G., Power, S. & Brown, C. (2011). The social dimension of sustainable development: Defining urban social sustainability. *Sustainable Development*, 19(5), 289-300. <https://doi.org/10.1002/sd.417>

Dillard, J., Dujon, V. & King, M. (Eds.)(2009). *Understanding the social dimension of sustainability*. New York: Routledge. <https://www.routledge.com>

Fotzpatrick, T. (Ed.)(2011). *Understanding the environment and social policy*. Bristol: Policy Press. <https://policy.bristoluniversitypress.co.uk>

Larsen, L. (2009). An inquiry into the theoretical basis sustainability: Ten propositions. In J. Dillard, V. Dujon & M. King(Eds.), *Understanding the social dimension of sustainability*, pp. 45-82. New York: Routledge. <https://www.routledge.com/Understanding-the-Social-Dimension-Of-Sustainability/Dillard-Dujon-King/p/book/9780415536677>

Lehtonen, M. (2004). The environmental-social interface of sustainable development: Capabilities, social capital, institutions. *Ecological Economics*, 49(2), 199-214. <https://www.sciencedirect.com/science/article/abs/pii/S092180090400076X>

Littig, B. & Griessler, E. (2005). Social sustainability: A catchword between political pragmatism and social theory. *International Journal of Sustainable Development*, 8(1-2), 65-79. <https://www.inderscienceonline.com/doi/abs/10.1504/IJSD.2005.007375>

Magis, K. & Shinn, C. (2009). Emergent principles of social sustainability. In J. Dillard, V. Dujon & M. King(Eds.), *Understanding the social dimension of sustainability*, pp. 15-44. New York: Routledge. <https://www.routledge.com/Understanding-the-Social-Dimension-Of-Sustainability/Dillard-Dujon-King/p/book/9780415536677>

Malik, A. (2018). The main driver of social unsustainability and its remedy. *International Journal of Social Economics*, 45(6), 973-988. <https://www.emerald.com/insight/content/doi/10.1108/IJSE-01-2017-0005/full/html>

Nordstrom Kallstrom, H. & Ljung, M. (2005). Social sustainability and collaborative learning. *Ambio*, 34(4-5), 376-382. [https://bioone.org/journals/ambio-a-journal-of-the-human-environment/volume-34/issue-4/0044-7447_2005_034_0376_SSACL_2.0.CO_2/Social-Sustainability-and-Collaborative-Learning/10.1579/0044-7447\(2005\)034\[0376:SSACL\]2.0.CO;2.short](https://bioone.org/journals/ambio-a-journal-of-the-human-environment/volume-34/issue-4/0044-7447_2005_034_0376_SSACL_2.0.CO_2/Social-Sustainability-and-Collaborative-Learning/10.1579/0044-7447(2005)034[0376:SSACL]2.0.CO;2.short)

Omann, I. & Spangenberg, J. (2002). Assessing social sustainability: The social dimension of sustainability in a socio-economic scenario. Seventh Biennial Conference of the International Society for Ecological Economics. March 6-9, Sousse, Tunisia. <https://citeseerx.ist.psu.edu/viewdoc/download?doi=10.1.1.201.987&rep=rep1&type=pdf>

Pawlowski, A. (2007). How many dimensions does sustainable development have? *Sustainable Development*, 16(2), 81-90. <https://onlinelibrary.wiley.com/doi/10.1002/sd.339>

Seghezzi, L. (2009). The five dimensions of sustainability. *Environmental Politics*, 18(4), 539-556. <https://www.tandfonline.com/doi/full/10.1080/09644010903063669>

Thin, N. Lockhart, C. & Yaron, G. (2002). *Conceptualizing socially sustainable development*. London: Department for International Development and World Bank. (Link is unavailable)

Turkington, R. & Sangster, K. (2006). From housing to social mix: Housing's contribution to social sustainability. *Town and Country Planning*, 75(6), 184-185. (Link is unavailable)

ABOUT THE AUTHOR

Arup Kanti Konar, PhD, is Principal & Associate Professor of Economics, Achhruram Memorial College, Sidho-Kanho-Birsha University, Jhalda, Purulia West Bengal, India.

[| Back to Title |](#)

[LINK TO THE CURRENT ISSUE](#)

[LINK TO THE HOME PAGE](#)

"A mind at peace does not engender wars."

Sophocles (497-406 BCE)

FREE SUBSCRIPTION








GROUP COMMANDS AND WEBSITES

Write to the [Editor](#)
Send email to [Subscribe](#)
Send email to [Unsubscribe](#)
Link to the [Group Website](#)
Link to the [Home Page](#)



Subscribe to the
Mother Pelican Journal
via the Solidarity-Sustainability Group
[Enter your email address:](#)

Inverse exchange bias effects and magnetoelectric coupling of the half-doped perovskite-type chromites $\text{Gd}_{0.5}\text{Sr}_{0.5}\text{CrO}_3$ and $\text{Gd}_{0.5}\text{Ca}_{0.5}\text{CrO}_3$

Biswajit Dalal ^{1,*} Xun Kang,^{1,2} Yoshitaka Matsushita ³ Alexei A. Belik ¹
Yoshihiro Tsujimoto ^{1,2} and Kazunari Yamaura ^{1,2,†}

¹International Center for Materials Nanoarchitectonics (WPI-MANA), National Institute for Materials Science, Namiki 1-1, Tsukuba, Ibaraki 305-0044, Japan

²Graduate School of Chemical Sciences and Engineering, Hokkaido University, North 10 West 8, Kita-ku, Sapporo, Hokkaido 060-0810, Japan

³Materials Analysis Station, National Institute for Materials Science, 1-2-1 Sengen, Tsukuba, Ibaraki 305-0047, Japan



(Received 28 May 2022; revised 31 July 2022; accepted 9 September 2022; published 21 September 2022)

The Cr^{4+} oxidation state with two electrons in the Cr $3d$ shell is not often observed in perovskite-type oxides, as high pressures and temperatures are generally required to stabilize the octahedral coordination. Herein, we present a comparative study of the half-doped perovskite-type chromites $\text{Gd}_{0.5}\text{Sr}_{0.5}\text{CrO}_3$ (GSCO) and $\text{Gd}_{0.5}\text{Ca}_{0.5}\text{CrO}_3$ (GCCO). Fifty percent of the Cr occurs in the Cr^{4+} oxidation state after high-pressure synthesis at 6 GPa and 1200 °C. The materials were investigated using synchrotron x-ray diffraction, magnetization, heat capacity, and dielectric measurements. The diffraction patterns show that GSCO and GCCO crystallize in orthorhombic ($Pnma$) structures with different degrees of local lattice distortion. GSCO exhibits a long-range magnetic order at temperatures of < 98 K, accompanied by magnetization reversal, suggesting that the magnetic ground state is ferrimagnetic. In contrast, GCCO displays antiferromagnetic characters at temperatures $< \sim 100$ K. In addition, GSCO exhibits a crossover between conventional and inverse exchange bias effects at low temperatures (< 50 K). This is likely caused by asymmetric exchange Dzyaloshinskii-Moriya interactions between the Cr ions of different valences ($+3$ and $+4$). Furthermore, significant magnetoelectric coupling at the onset of the magnetic order is supported by temperature-dependent dielectric measurements.

DOI: [10.1103/PhysRevB.106.104425](https://doi.org/10.1103/PhysRevB.106.104425)

I. INTRODUCTION

Perovskite-type orthochromite $R\text{CrO}_3$, where R is a rare-earth element, receives considerable attention owing to its potential applications and unique physical properties, such as negative magnetization, temperature- and field-induced fast spin switching, spin reorientation, field-induced switchable polarization, magnetoelectric effects, spin-driven ferroelectricity, magnetoelastic coupling, and exchange bias (EB) and giant magnetocaloric effects [1–14]. Most orthochromites crystallize in perovskite-type orthorhombic structures (space groups of $Pnma$ or $Pbnm$) and exhibit canted antiferromagnetic (AFM) orders. An antisymmetric exchange Dzyaloshinskii-Moriya (DM) interaction causes a weak ferromagnetic (FM) component between the Cr^{3+} spins to manifest at temperatures below the AFM transition (Néel) temperature (T_N) [15,16]. Superexchange interactions through the $\text{Cr}^{3+}\text{--O--Cr}^{3+}$ bond likely cause the AFM order, and complex, anisotropic interactions between R^{3+} and Cr^{3+} may cause unusual physical phenomena, e.g., the polar order of $R\text{CrO}_3$ may be primarily caused by $R\text{--Cr}$ exchange striction (i.e., an exchange field between the R ion and Cr sublattice) [6].

Furthermore, the onset temperatures of spin-driven ferroelectricity and long-range AFM order of all $R\text{CrO}_3$ remain within the range 110–290 K, regardless of the ionic radius of R^{3+} [7,12].

GdCrO_3 undergoes a canted AFM transition at a T_N of 167 K, with negative magnetization, spin reorientation, and field-induced polar order. These complex features are likely caused by interactions between two magnetic elements, Gd^{3+} ($4f^7$) and Cr^{3+} ($3d^3$) [2,5,6]. In addition, spontaneous spin reorientation of the ordered Cr sublattice occurs at 7 K [2,5]. The DM interactions and strong AFM coupling between Gd moments and Cr sublattices may lead to negative magnetization at a specific compensation temperature (T_{comp}). Recently, an unusual EB effect and fast spin switching were observed in single-crystal GdCrO_3 [17], which exhibited a giant magnetocaloric effect and temperature-induced magnetization jump [18,19]. Owing to these multiple anomalies, additional studies of GdCrO_3 are required to clarify its fundamental nature.

Half-doped perovskite-type transition metal oxides, such as manganite and cobaltite, were extensively investigated over recent decades owing to their strong intercorrelations among various characteristics—spin, charge, orbital, and lattice [20–24]. Studies of half-doped manganite ($\text{La}_{0.5}\text{Ca}_{0.5}\text{MnO}_3$) were conducted by Wollan and Koehler [25] and Goodenough [26]. The charge-exchanged AFM ground state was associated with the spatial order of the $\text{Mn}^{3+}/\text{Mn}^{4+}$ ions localized

*b.dalal.iitd@gmail.com

†YAMAURA.kazunari@nims.go.jp

in alternate planes. The most notable discovery to date is the colossal magnetoresistance of mixed-valence manganite $\text{Pr}_{0.5}\text{Sr}_{0.5}\text{MnO}_3$ [27], with significant competition between the FM metal and AFM insulator states [28]. Notably, however, there are contradictory reports regarding the origin of the colossal magnetoresistance [29–33].

In addition, half-doped manganites exhibit various phenomena, including double-exchange ferromagnetism, metal-insulator transitions, Griffiths phases, charge-order-driven ferroelectricity, strong magnetoelectric coupling, magnetodielectric and EB effects, and magnetoelectric phase separation [34–44]. Conversely, half-doped cobaltites exhibit unconventional phase transitions and unexpected properties, such as spin-state transitions, spin reorientations, valence-state and photoinduced metal-insulator transitions, and charge transfer [45–52].

The syntheses of half-doped manganites and cobaltites with perovskite structures and Mn^{4+} and Co^{4+} in octahedral coordination yield compounds with unprecedented physical properties. However, the synthesis of half-doped chromite receives less attention, likely because high pressures and temperatures are required to stabilize Cr^{4+} in octahedral coordination within the perovskite-type structure. We thus investigated $\text{Gd}_{0.5}\text{A}_{0.5}\text{CrO}_3$, where $A = \text{Sr}$ or Ca , using a high-pressure and high-temperature method, as half-doped alkaline-earth metal ions could cause distinct electrical transport and magnetic phenomena, such as, semiconducting and ferrimagnetic (FiM) ground state, magnetic frustration associated with competing AFM and FiM/FM interactions, magnetostriction, inverse EB effect, and magnetoelectric coupling accompanying with the ferroelectric relaxorlike state.

In this paper, we reveal the magnetic and electric properties of two half-doped chromites, $\text{Gd}_{0.5}\text{Sr}_{0.5}\text{CrO}_3$ (GSCO) and $\text{Gd}_{0.5}\text{Ca}_{0.5}\text{CrO}_3$ (GCCO), which were synthesized at 6 GPa and 1200 °C. GSCO exhibited a FiM ground state, whereas GCCO exhibited an AFM ground state. In addition, GSCO exhibited magnetization reversal, non-Griffith-like clustered FM features at temperatures of $> T_{\text{FiM}}$ (FiM transition temperature), and inverse EB effects. Furthermore, temperature-dependent permittivity studies revealed magnetoelectric coupling in GSCO and GCCO.

II. EXPERIMENTAL DETAILS

Polycrystalline GSCO and GCCO were synthesized via a solid-state reaction using powders of Gd_2O_3 , SrO (prepared using SrCO_3 by heating at 1300 °C in oxygen), CaO (prepared using CaCO_3 by heating at 1300 °C in oxygen), Cr_2O_3 , and CrO_2 . The powders were thoroughly mixed in an agate mortar in a stoichiometric ratio in an Ar-filled glovebox. Each mixture was sealed in a Pt capsule and loaded into a multi-anvil press (CTF-MA1500P, C&T Factory, Tokyo, Japan), and the capsule was compressed statically and isotropically at a pressure of 6 GPa at 1200 °C for 1 h (temperature ramping required 12 min). After heating, the capsule was quenched to a temperature of < 100 °C within 1 min, and the pressure was gradually released over several hours. The resulting material was a dense, polycrystalline, black pellet. A sample was finely ground for use in phase identification using a MiniFlex600

x-ray diffractometer (Rigaku, Tokyo, Japan) with $\text{Cu K}\alpha$ radiation.

Finely ground powders were used in synchrotron x-ray diffraction (XRD) at temperatures between 120 and 750 K using a large Debye-Scherrer camera at the BL15XU beamline at SPring-8, Sayo, Japan [53,54]. The wavelength of the synchrotron XRD was 0.65297 Å, calibrated using a standard material CeO_2 . Synchrotron XRD data were analyzed via the Rietveld method [55] using RIETAN-FP [56] and MAUD software [57]. Crystal structure was drawn using VESTA software [58].

The direct current (dc) magnetic susceptibilities (χ) of the materials were measured using a superconducting quantum interference device magnetometer (MPMS, Quantum Design, San Diego, CA, USA). To correct for the stray magnetic field of the superconducting magnet, the magnet was degaussed before each measurement. Measurements were conducted in the temperature range 2–350 K at various applied magnetic fields (H) under zero-field-cooled (ZFC) and field-cooled (FC) conditions. Isothermal magnetization loops were collected at various temperatures in the magnetic field range ± 70 kOe. The alternating current (ac) χ of GSCO was measured at 5–350 K using the same instrument. The reproducibility of GSCO and GCCO magnetic data was verified using a set of materials prepared in different high-pressure runs.

The electrical resistivity (ρ) of a polycrystalline material was measured as a function of temperature via a 4-probe method using a physical property measurement system (PPMS, Quantum Design). The electrical contacts on the bar-shaped material comprised Au wires and Ag epoxy. The temperature-dependent specific heat capacity (C_{total}) was measured using a thermal relaxation method under a zero field or an applied field of 90 kOe in the PPMS at temperatures of 2–300 K. We used an Apiezon-N grease to thermally connect the material to the holder stage.

The dielectric properties were measured at temperatures of 5–300 K using an Alpha-A high-performance frequency analyzer (Novocontrol Technologies, Montabaur, Germany) in the frequency range 100 Hz–2 MHz at $H = 0$ or 90 kOe in the PPMS. During the measurement of GSCO, an extrinsic contribution to the dielectric constant was observed between 220 and 270 K, which was likely due to ice. However, the extrinsic contribution was no longer observed under a much higher vacuum [59]. The deviation between the material and system temperatures under a high vacuum became significant at < 50 K. Therefore, we combined the data measured under normal and high-vacuum conditions to confirm the dielectric behavior of the material.

III. RESULTS AND DISCUSSION

A. Crystal structure

The crystal structures of GSCO and GCCO at room temperature (~ 297 K) were investigated via synchrotron XRD and data analysis using the Rietveld method, as shown in Figs. 1(a) and 1(b), respectively. Based on the structure of RCrO_3 at room temperature, we initially refined the crystal structure of GSCO using a distorted orthorhombic model ($Pbnm$ or its axial transformed standard setting $Pnma$, No.

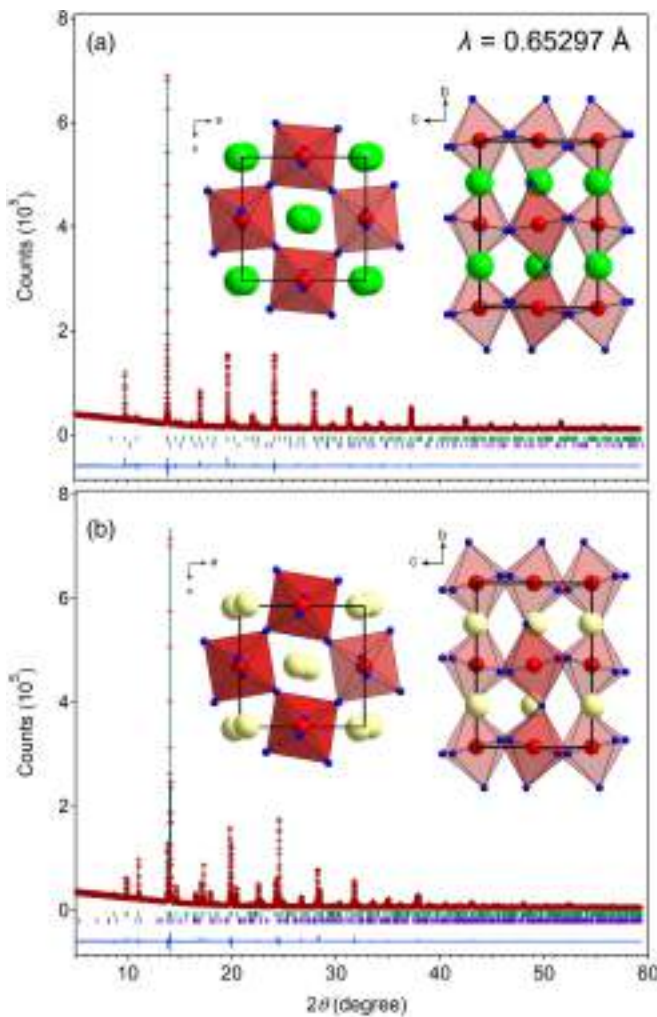


FIG. 1. Rietveld refinement of the synchrotron x-ray diffraction (XRD) patterns of (a) GSCO and (b) GCCO collected at room temperature. The crosses and solid red lines represent the observed and calculated patterns, respectively, with the differences (solid blue lines) shown at the bottom. The vertical ticks indicate the positions of the allowed Bragg reflections. The upper (olive) and bottom (magenta) rows indicate the reflections of the main and secondary phases, respectively. The lattice parameters are $a = 5.41289(2)$ Å, $b = 7.63652(2)$ Å, and $c = 5.39966(2)$ Å for GSCO ($Pnma$), and $a = 5.42543(1)$ Å, $b = 7.54252(1)$ Å, and $c = 5.31059(1)$ Å for GCCO ($Pnma$). The secondary phase is Cr_2O_3 (1.7 wt. %) for GSCO and CaCr_2O_4 (2.5 wt. %) for GCCO. The unit cell of each material is shown as an inset. Green, yellow, blue, and red balls denote Gd/Sr, Gd/Ca, O, and Cr, respectively.

62) and a cubic $Pm\bar{3}m$ model (No. 221). Additionally, we tested a monoclinic $P2_1/c$ model (No. 14) because $P2_1/c$ is in a lower-symmetry subgroup of $Pnma$ and is often observed in double-perovskite materials. As shown in Fig. 1(a), the analysis is successful, indicating that the $Pnma$ model better describes the crystal structure of GSCO. The refined lattice parameters are $a = 5.41289(2)$ Å, $b = 7.63652(2)$ Å, and $c = 5.39966(2)$ Å. The atomic coordinates and isotropic thermal displacement parameters are shown in Table S1 in the Supplemental Material [60]. The inset of Fig. 1(a) shows a structural image of GSCO.

Considering the observed refined tendencies, when we refined the occupation factors for oxygen, the values were slightly > 1 ; the oxygen site is likely occupied fully. Thus, it was reasonable to fix the value to be 1 in the final step. Although the observed pattern was refined to a certain extent using the $P2_1/c$ model, the analysis was unsatisfactory. Detailed inspection, particularly temperature dependence, the standard errors for β angle, and volume increased significantly with temperature. This indicated that GSCO did not crystallize in a monoclinic double-perovskite-based structure with a rock salt-type order.

Meanwhile, GCCO is analyzed well using the orthorhombic $Pnma$ model, which is common in most RCrO_3 materials. Notably, refining the pattern of GCCO using the monoclinic model ($P2_1/c$) failed. Because the end members GdCrO_3 [6] and CaCrO_3 [61] crystallize in the orthorhombic structure ($Pbnm$), GCCO may be regarded as a solid solution. In addition, several small peaks in the synchrotron XRD pattern indicate the presence of 2.5 wt. % orthorhombic CaCr_2O_4 [62]. Rietveld analysis refines the lattice parameters of GCCO and the overall scale factor simultaneously, but the structural parameters of the minor phase remain constant. The final analyzed synchrotron XRD pattern of GCCO is shown in Fig. 1(b), and detailed crystallographic data is shown in Table S2 in the Supplemental Material [60]. The refined lattice parameters are $a = 5.42543(1)$ Å, $b = 7.54252(1)$ Å, and $c = 5.31059(1)$ Å. For comparison, the inset of Fig. 1(b) shows a structural image of GCCO. The overall structure is similar for GSCO and GCCO at this image scale, but the structure has different degrees of local lattice distortion. For example, the Cr–O lengths of the CrO_6 octahedron differ by 0.25% in GSCO and 1.7% in GCCO.

Furthermore, synchrotron XRD patterns were collected at various temperatures from 120 to 750 K to investigate the temperature dependences of the structural properties of GSCO and GCCO. However, neither a change in symmetry nor any additional features were observed. The changes in the lattice parameters of GSCO and GCCO with temperature are shown in Figs. S1(a)–(b) and S1(c)–(d) in the Supplemental Material [60], respectively. All GSCO lattice parameters increase with increasing temperature, exhibiting the expected thermal behavior. The lattice parameters a and c almost converge at ~ 750 K (Fig. S1(a) in the Supplemental Material [60]), indicating that GSCO may approach a structural transition or thermal decomposition. In contrast, the GCCO lattice parameter a decreases with increasing temperature (Fig. S1(c) in the Supplemental Material [60]), although the cause remains unknown. This issue should be investigated in future research.

B. Magnetization

The temperature-dependent dc- χ of GSCO under an applied field of 0.1 kOe, as shown in Fig. 2(a), displays a clear anomaly in the FC curve at ~ 98 K [first derivative spectrum in the inset of Fig. 2(a)], revealing the onset of magnetic order. Below this temperature, the FC curve exhibits a small hump that intersects the zero line at $T_{\text{comp}} = 48$ K. With further cooling, χ decreases until the technical limit (2 K), which is commonly known as magnetization reversal. Conversely, the ZFC curve shows a very weak response at 98 K. Notably,

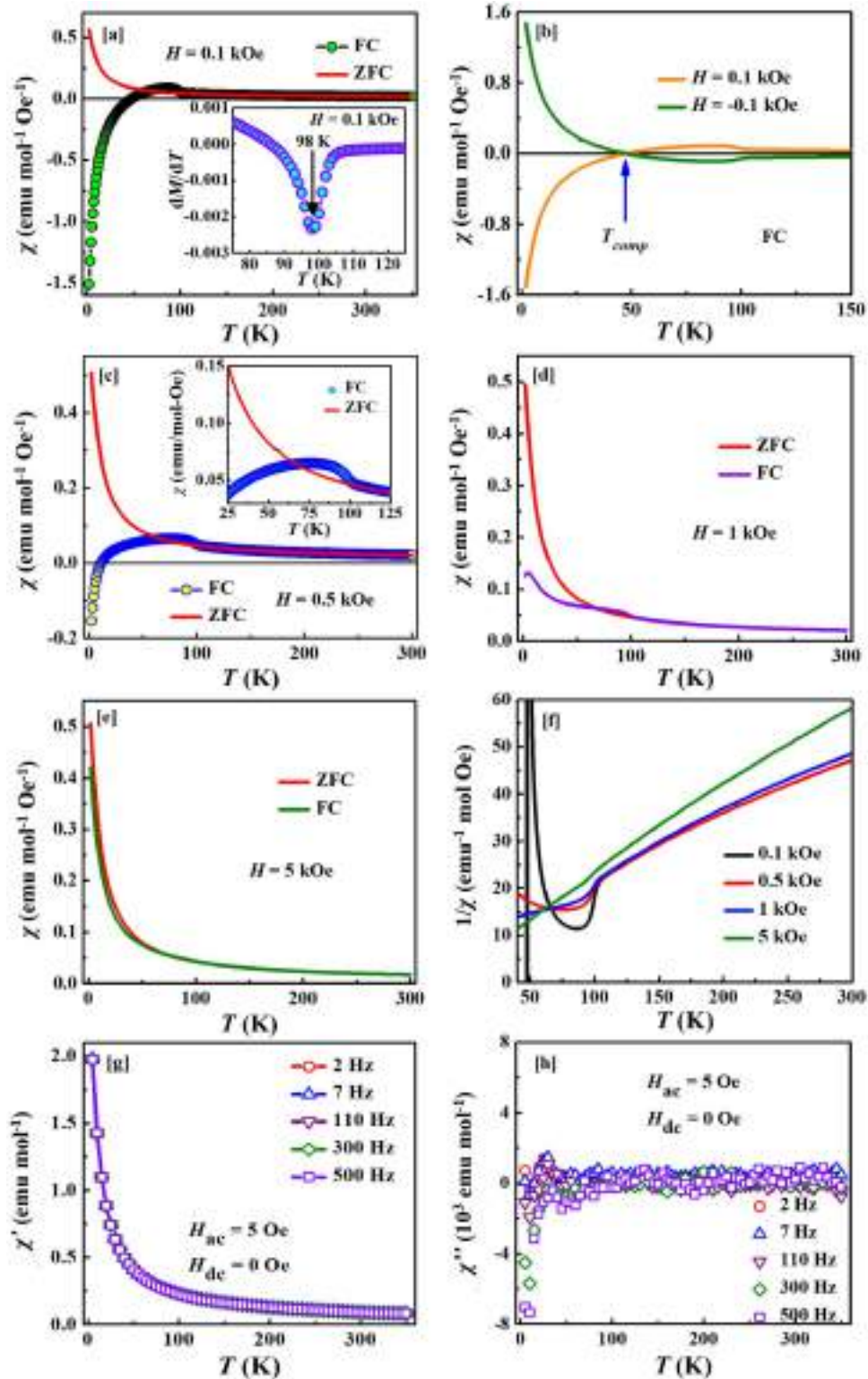


FIG. 2. (a) Zero-field-cooled (ZFC)- and field-cooled (FC)- $\chi(T)$ curves of GSCO measured in a magnetic field of $H = 0.1$ kOe. The inset shows the derivative curve of the FC curve. (b) FC- $\chi(T)$ curves of GSCO measured at $H = 0.1$ and -0.1 kOe. (c)–(e) ZFC- and FC- $\chi(T)$ curves measured at $H = 0.5, 1,$ or 5 kOe, respectively. The inset of (c) displays an enlarged view of the ZFC- and FC- $\chi(T)$ curves at $H = 0.5$ kOe. (f) Inverse χ ($1/\chi$) as a function of temperature and applied field. (g) In-phase (χ') and (h) out-of-phase (χ'') parts of ac- $\chi(T)$ of GSCO measured in an ac magnetic field of 5 Oe at various frequencies.

the FC and post-FC (when heated) curves follow the same trend, unlike those observed for GdCrO_3 . Furthermore, GSCO exhibits no features related to the spin reorientation that occurs in GdCrO_3 [2,5].

As suggested by the GSCO structural analysis, Cr ions with different valences are likely connected by AFM exchange interactions and may induce long-range magnetic order at 98 K. Early studies report a similar magnetic behavior, i.e., by the canted FiM order of the double perovskite $\text{La}_2\text{Ni}_{1.19}\text{Os}_{0.81}\text{O}_6$ [63]. Thus, the developed magnetic order of GSCO is likely a canted FiM order, with a transition temperature $T_{\text{FiM}} = 98$ K. Moreover, the negative internal field on the Gd^{3+} moments produced by the weak FM component of canted $\text{Cr}^{3+}/\text{Cr}^{4+}$ moments are responsible for the observed compensated magnetization and the magnetization reversal phenomenon below T_{comp} . The net moment from the two canted $\text{Cr}^{3+}/\text{Cr}^{4+}$ moments and the Gd^{3+} moments have antiparallel coupling, thus exhibiting FiM ground state in GSCO. Nevertheless, in some ordered double perovskites ($R_2\text{BB}'\text{O}_6$, monoclinic structure with space group $P2_1/n$), the neutron powder diffraction studies confirmed that the FiM ground state is only identified by the coupling between rare-earth moments and FM component of B/B' sublattices and not from the ordered B/B' sublattice magnetization [64–66]. More importantly, the compensated magnetization and/or magnetization reversal phenomenon gives an exceptional indication about the FiM ground state in these kinds of materials, as well as in GSCO.

Under the ZFC condition, when a magnetic field is applied at the lowest temperature, the easy axes of the randomly oriented Gd moments are aligned along the magnetic field direction, and GSCO displays a positive χ . When heated from 2 K, the Gd moments are thermally disturbed and χ decreases. As the magnetizations of the sublattices (Gd and Cr) are unequal, there is no compensation phenomenon.

The FC- χ curve at $H = -0.1$ kOe was also recorded to analyze whether the stray magnetic field plays a role in the observed magnetization reversal. The FC- χ curves measured at $H = 0.1$ and -0.1 kOe are plotted in Fig. 2(b). While measuring the FC- χ curve in the negative field, χ remains negative at $> T_{\text{comp}}$ and becomes positive at $< T_{\text{comp}}$, resembling the inverse behavior of that under the positive field. Because the curves exhibit mirror symmetry in terms of sign reversal, the stray magnetic field exerts little effect on the magnetization reversal.

Figures 2(c)–2(e) show the ZFC- and FC- χ curves measured in different fields ($H = 0.5, 1, \text{ or } 5$ kOe). The magnetization reversal observed at $H = 0.1$ kOe gradually disappears as H increases, and at $H \geq 1$ kOe, the magnetization reversal is challenging to observe. Notably, T_{comp} decreases with increasing H ($T_{\text{comp}} = 11$ K at $H = 0.5$ kOe), indicating the presence of a weaker negative internal field on the Gd moments (produced by weak FM components of the canted Cr moments in opposition to H).

The inverse susceptibility plots ($1/\chi$ vs T) shown in Fig. 2(f) reveal two main features: (i) a sharp decrease in $1/\chi$ at the onset temperature of the long-range magnetic order, which is reminiscent of the canted FiM order. (ii) True paramagnetic behavior is observed at temperatures of

$\gg T_{\text{FiM}} (> \sim 200$ K), suggesting a short-range magnetic correlation between T_{FiM} and ~ 200 K.

The sharp decrease in the $1/\chi$ curve softens with an increasing field, possibly due to the formation of short-range FM clusters. To confirm this, we analyzed the $1/\chi$ vs T curves at 105 K $< T < 200$ K using the power law expression of the Griffith singularity effect.

$$\frac{1}{\chi(T)} = A(T - T_C^R)^{1-\lambda},$$

where A is a constant, T_C^R is the critical temperature below which χ diverges, and λ is an exponent [32,67]. Here, $1/\chi$ does not follow the power law expression well, signifying that the possible magnetic cluster behavior is non-Griffith-like. Similar non-Griffith-like behavior is observed in the half-doped cobaltite $\text{La}_{0.5}\text{Sr}_{0.5}\text{CoO}_3$, wherein AFM clusters are formed in the paramagnetic matrix [68].

Because we observe increasing magnetization of the pure paramagnetic phase by extrapolating the high-temperature Curie-Weiss (CW) line, short-range FM clusters, not AFM clusters, cause the observed non-Griffith-like behavior. Furthermore, T_C^R is much lower than T_{FiM} , which is inconsistent with the anticipated behavior of a Griffiths phase (i.e., $T_C^R > T_{\text{FiM}}$). However, the short-range FM clusters are assumed to originate from the $\text{Cr}^{3+}\text{-O-Cr}^{4+}$ exchange interactions.

The ac- χ ($= \chi' + i\chi''$) of GSCO was measured in an ac magnetic field of 5 Oe at frequencies in the range 2–500 Hz. The in-phase (χ') and out-of-phase (χ'') parts of the zero-field ac- χ as functions of T are shown in Figs. 2(g) and 2(h), respectively. No sharp peak is observed at T_{FiM} , which is consistent with the weak responses of the dc ZFC- χ curves. No additional anomalies or magnetically glassy features are detected. Note that, if a cluster glasslike state is present in the material, a frequency range of up to 500 Hz is usually sufficient to detect it through ac- χ measurements [69–72].

In contrast, GCCO exhibits a completely different magnetic behavior. Figures 3(a)–3(c) show the dc ZFC- and FC- χ curves measured under various magnetic fields ($H = 0.05, 0.1, \text{ or } 0.5$ kOe). The ZFC- and FC- χ curves are identical, increasing continuously as the temperature decreases. No onset of magnetic order is observed, as shown in the inset of Fig. 3(b). However, there is a clear difference between the ZFC and FC curves at < 100 K, as indicated by the arrows shown in Fig. 3(d). The divergence is much more pronounced in the first derivative, as shown in the inset of Fig. 3(d). The random substitution of Ca with Gd may lead to competition between the $\text{Cr}^{3+}\text{-O-Cr}^{3+}$ AFM superexchange and the $\text{Cr}^{3+}\text{-O-Cr}^{4+}$ FM double-exchange interactions, causing a magnetically disordered state. However, the divergence between the ZFC and FC curves may indicate that AFM interactions are slightly dominant. Thus, we specified the point of divergence as T_N of GCCO. Since the local lattice distortion of GCCO is different from that of GSCO, its impact on the magnetic exchange interactions differs reasonably. Thus, the possible magnetic ground states of GSCO and GCCO are different owing to the strong dependence on the local structural properties. Notably, $\beta\text{-CaCr}_2\text{O}_4$ undergoes a magnetic transition characterized by the propagation vector

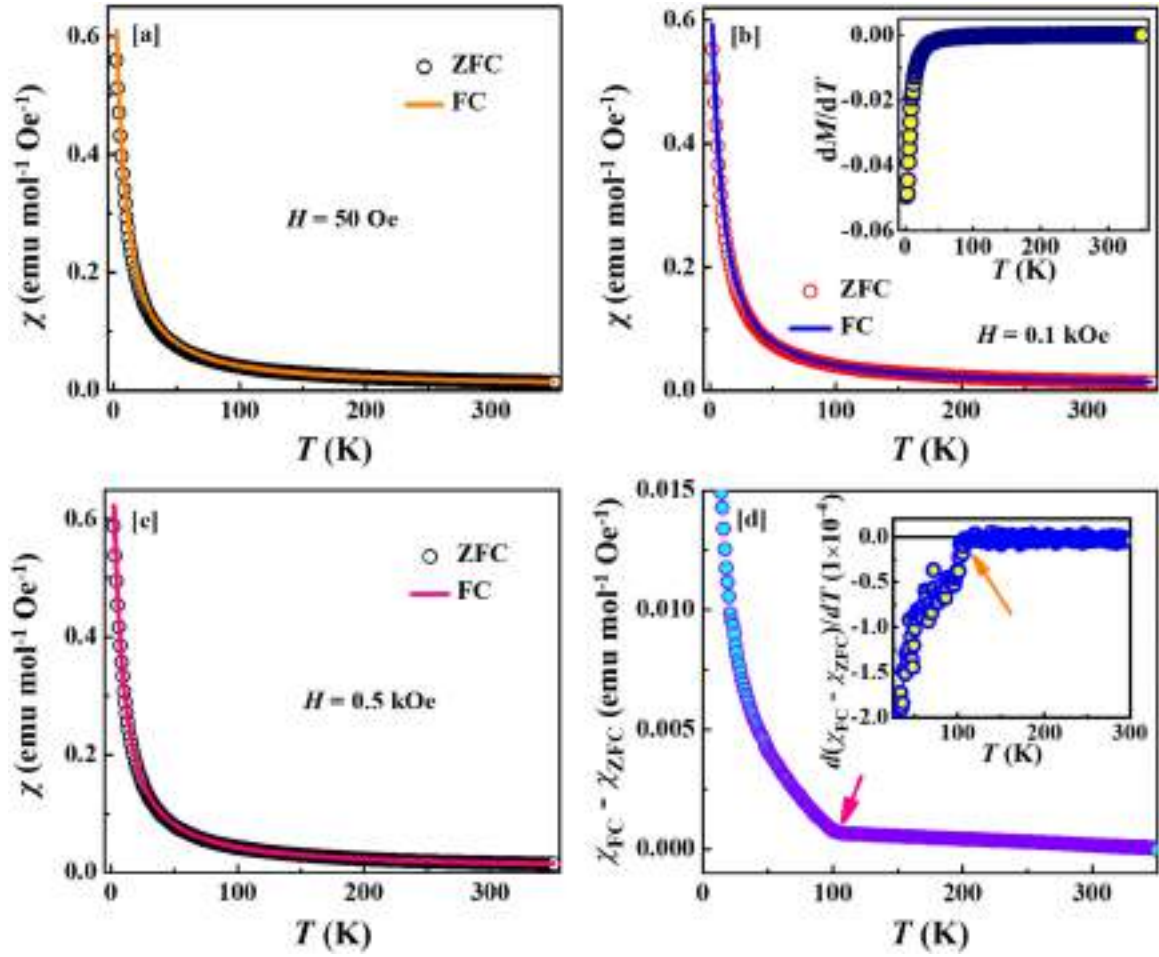


FIG. 3. (a)–(c) Zero-field-cooled (ZFC)- and field-cooled (FC)- $\chi(T)$ curves of GCCO measured at $H = 50$ Oe or 0.1 or 0.5 kOe, respectively. The inset of (b) shows the derivative curve at $H = 0.1$ kOe. (d) Difference between the ZFC- and FC- $\chi(T)$ curves at $H = 0.1$ kOe. Inset of (d) shows the derivative curve of $(\chi_{FC} - \chi_{ZFC})$.

$\mathbf{k} = (0, 0, \sim 0.477)$ at $T_N = 21$ K [62]. Although a small amount of β - CaCr_2O_4 (2.5 wt. %) is detected in GCCO, no corresponding feature is observed in the χ vs T or dM_{FC}/dT vs T plots.

The thermal remanent magnetizations (M_{TRM}) of both materials were measured to further elucidate the onsets of the long-range magnetic order and short-range magnetic correlation. During measurement, the magnetic field was set to zero at 2 K immediately after cooling the sample from the paramagnetic state (350 K) in the presence of $H (= 0.5$ kOe), and the sample was then heated to measure the magnetization. Similar protocols are often used to study the spin dynamics of glassy magnetic materials. In addition, M_{TRM} exhibits clear anomalies at the onset of the magnetic order [73,74]. Here, M_{TRM} of GSCO and GCCO as functions of T are shown in Figs. 4(a) and 4(b), respectively. The magnetization reversal of GSCO is again confirmed by the M_{TRM} measurement. However, the thermal variation of M_{TRM} differs slightly from that observed in the dc FC- χ measurement. In addition to the sharp increase in magnetization at the onset of long-range magnetic order at T_{FIM} , a clear anomaly is detected at ~ 150 K for GSCO [inset of Fig. 4(a)]. This indicates that a significant contribution from the short-range magnetic correlation begins at 150 K, which is $\gg T_{FIM}$. Conversely, GCCO exhibits an

increase in magnetization at ~ 100 K [Fig. 4(b)], which highlights the presence of the magnetic anomaly.

Figures 5(a) and 5(b) show the temperature-dependent $1/\chi$ values of GSCO ($H = 5$ kOe) and GCCO ($H = 0.1$ kOe), respectively. A moderately high magnetic field was used for GSCO to avoid other dilute magnetic interactions. The solid straight lines (red) shown in both plots are guidelines to aid in identifying deviations from CW behavior. The $1/\chi$ curves of GSCO and GCCO deviate from CW behavior at $< \sim 160$ and $< \sim 105$ K, respectively.

To obtain the CW parameters, we fitted the high-temperature $1/\chi$ curves to the CW equation $1/\chi = (T - \Theta)/C$, where $C = N_A \mu_{\text{eff}}^2 / 3k_B$ is the Curie constant, N_A is Avogadro's number, μ_{eff} is the effective magnetic moment, k_B is the Boltzmann constant, and Θ is the Weiss temperature. The fitted curves of GSCO and GCCO are displayed in the insets of Figs. 5(a) and 5(b), respectively, and the respective μ_{eff} values of GSCO and GCCO are 7.04 and 6.75 $\mu_B/\text{f.u.}$. Because half of the Cr^{3+} ions transform to Cr^{4+} ions upon half-doping of Sr^{2+} (Ca^{2+}) at the Gd site of GdCrO_3 , the theoretical moments should be $\mu_{\text{eff}} = 6.53 \mu_B/\text{f.u.}$, based on the equation:

$$\mu_{\text{eff}} = \sqrt{0.5\mu_{\text{Gd}}^2 + 0.5\mu_{\text{Cr}^{3+}}^2 + 0.5\mu_{\text{Cr}^{4+}}^2},$$

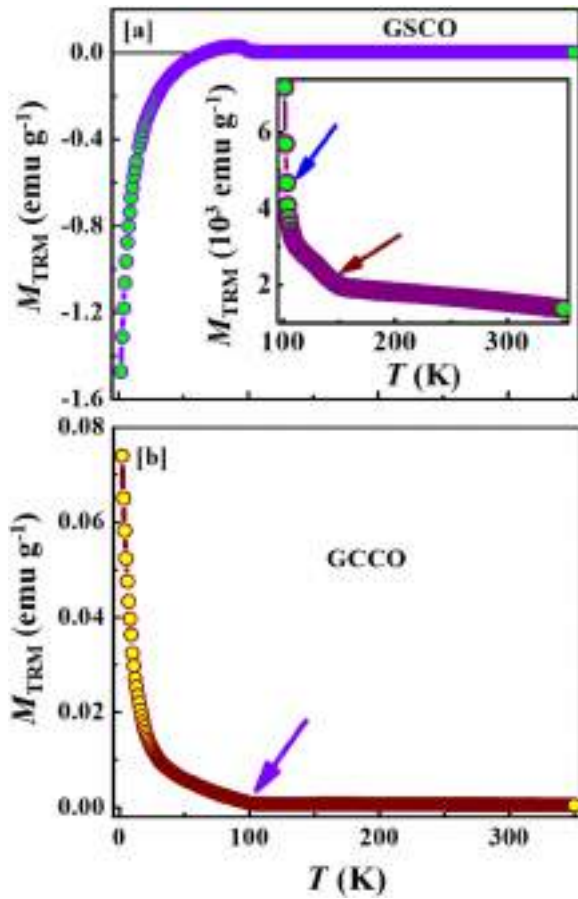


FIG. 4. Thermal remanent magnetizations (M_{TRM}) of (a) GSCO and (b) GCCO, which indicate the onset of magnetic ordering (arrows). The inset shows an enlarged view.

where $\mu_{\text{Gd}} = 7.90 \mu_{\text{B}}$, $\mu_{\text{Cr}^{3+}} = 3.87 \mu_{\text{B}}$ (spin-only due to the quenched $3d$ orbital), and $\mu_{\text{Cr}^{4+}} = 2.82 \mu_{\text{B}}$ (spin-only). This value is close to the experimentally observed values of GCCO and GSCO. In addition, the Θ values of GSCO and GCCO are -63 and -52 K, respectively, with the negative values indicating that AFM interactions are dominant in both materials.

To further elucidate the contrasting magnetic behaviors of these two materials, we recorded isothermal field-dependent magnetization (M vs H) curves under ZFC conditions. Before the measurement of each M - H curve, the material was cooled from well above the onset temperature of magnetic order to the targeted temperature under a zero magnetic field. Figure 6(a) shows the M - H curves of GSCO at temperatures of 2, 10, 40, 60, and 85 K (all less than T_{FiM}). At $T = 40$, 60, or 85 K, linear changes in M vs H are observed in the high-field regions, but weak hystereses are observed in the low-field regions. Much wider hysteresis loops are observed at $T = 2$ or 10 K, indicating the presence of FM and AFM correlations below T_{FiM} .

Regarding the hysteresis loops, we plotted the values of the coercive field (H_{C}) based on the M - H curves at different temperatures in Fig. 6(b). The decrease in H_{C} at < 85 K may be related to the opposite orientation of the Gd sublattice owing to the negative internal field (i.e., the compensation

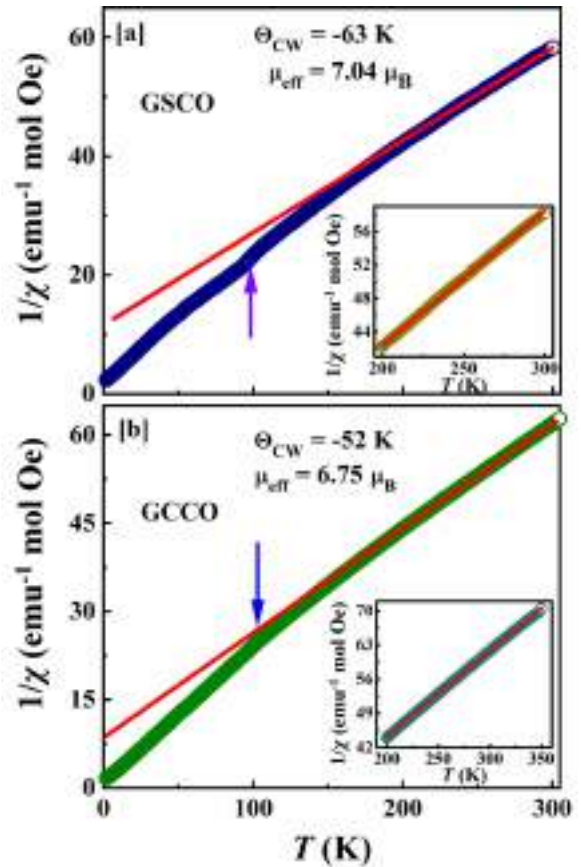


FIG. 5. Inverse magnetic susceptibilities ($1/\chi$) of (a) GSCO (at $H = 5$ kOe) and (b) GCCO (at $H = 0.1$ kOe) as functions of temperature. The solid red lines are guidelines for linear behavior, and the insets show the Curie-Weiss fittings of the high-temperature regions.

phenomenon) with respect to the applied field. An enlarged view of the isotherm at $T = 2$ K is shown in the inset of Fig. 6(b), which indicates that the M - H loop closes within the range ± 20 kOe.

Figure 6(c) shows the M - H isotherms of GCCO at $T = 2, 10, 40, 60,$ and 85 K. Here, H_{C} is 40 Oe at 2 K, which is likely related to the AFM spin correlation. Moreover, even at 70 kOe, the M - H curves are unsaturated, which is typical for materials with AFM-exchange interactions. Nevertheless, the significant S-shapes of the M - H loops of GSCO and GCCO at $T = 2$ or 10 K may be due to the contributions from the much larger Gd³⁺ moments.

To compare the magnetic properties of these two materials, we plotted the isothermal M - H curves measured at $T = 2$ K, as shown in Fig. 6(d), with the inset showing an enlarged view. Notably, there is a small difference in the saturation magnetizations of these compounds at 70 kOe (3.05 and $3.17 \mu_{\text{B}}/\text{f.u.}$ for GSCO and GCCO, respectively), possibly due to the impurities in GCCO. Notably, the H_{C} of GSCO ($= 1089$ Oe) is 27-fold larger than that of GCCO, which demonstrates its different magnetic nature. Generally, materials with canted FiM structures exhibit higher H_{C} values than those of regular AFM materials. Current observations are in line with the general view.

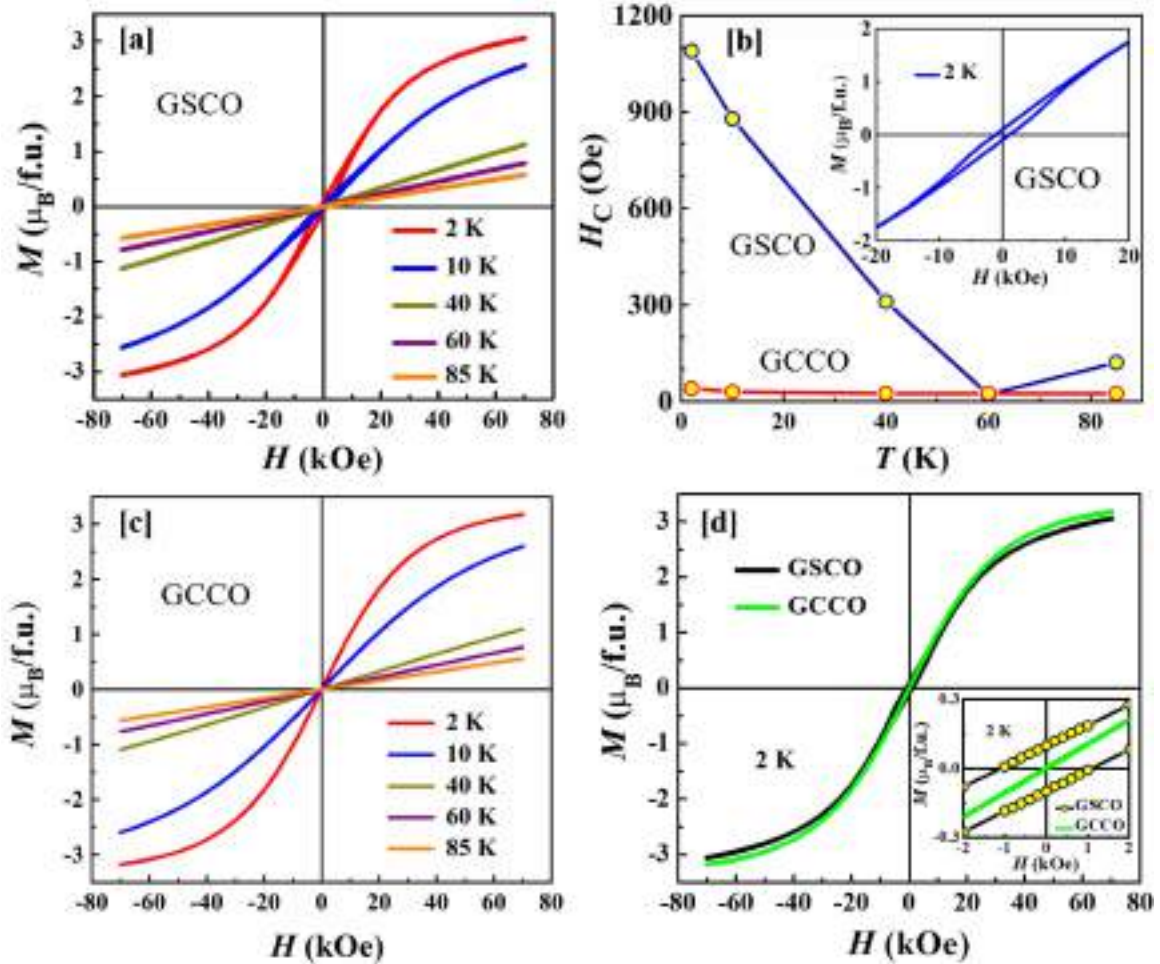


FIG. 6. (a) Isothermal magnetization (M) of GSCO as a function of magnetic field (H) measured under the zero-field-cooled (ZFC) condition at several temperatures ($T = 2, 10, 40, 60,$ and 85 K). (b) Thermal variation of the coercive field (H_C), and the inset shows a magnified view of the ZFC M - H loop at $T = 2$ K. (c) ZFC M - H loops of GCCO measured at temperatures of 2, 10, 40, 60, and 85 K. (d) Comparison of the ZFC M - H loops of GSCO and GCCO at 2 K. The inset shows an enlarged view.

In general, a heterogeneous material with two different magnetic states, such as FM and AFM states [75,76], an FM state and a spin glass [51,52], and FM and FiM states [77], sometimes results in the EB effect. This phenomenon, which is related to the shift of the M - H loop along the magnetic field axis, has considerable applications in spintronic devices. Recently, the EB effect was also observed in a magnetically homogeneous material, i.e., FiM [14]. Because non-Griffith-like FM clusters and canted FiM states coexist in GSCO, we investigated the EB effects by measuring the FC M - H loop at several temperatures. If the cooling field (H_{cool}) is positive, the FC M - H loop shifts toward the negative field axis, which is widely recognized as the conventional EB effect. The EB field (H_{EB}) is a measure of EB anisotropy and defined as $H_{\text{EB}} = (H_1 + H_2)/2$, where H_1 and H_2 are the first (negative) and second (positive) coercive fields at the first and second magnetization reversals, respectively [51]. Notably, H_{EB} should be negative in the conventional EB effect [76].

Figure 7(a) shows the FC M - H loops of GSCO at $H_{\text{cool}} = 20$ kOe at various temperatures ($T = 2, 10, 15,$ or 20 K) below T_{FiM} . Notably, the FC loops were measured within a maximum field (H_{max}) of ± 20 kOe. Contrary to the symmetric

nature of a regular M - H loop at the origin (absence of EB), the FC loop shifts slightly along the field direction from the origin, suggesting that EB anisotropy is induced upon field cooling. The FC loops at $T = 2$ K measured in different directions of $H_{\text{cool}} = 20$ and -20 kOe are shown in Fig. 7(b). The magnitude of the shift may be small, but the loop shifts in the opposite direction.

The enlarged views (within ± 3 kOe) of the FC loops collected in the different directions of H_{cool} at $T = 10, 15, 20, 30,$ or 50 K are shown in Figs. 7(c)–7(g), respectively. Each loop shifts alternatively, i.e., the EB anisotropy undergoes sign reversal when H_{cool} changes direction. Remarkably, the FC loop shifts toward the positive field axis when the material is cooled in the positive field, which contradicts the expectation of the conventional EB effect. This is known as the inverse EB (IEB) effect [78], and the FC loop exhibits the IEB effect at $T \leq 50$ K, whereas the conventional EB effect is observed at $T \geq 70$ K, e.g., an enlarged view of the FC loop within ± 1 kOe at $T = 90$ K [Fig. 7(h)] reveals the conventional EB effect.

Figure 8 shows the temperature dependences of H_1 , H_2 , H_C , and H_{EB} measured at a positive H_{cool} . Here, H_1 and H_2 are

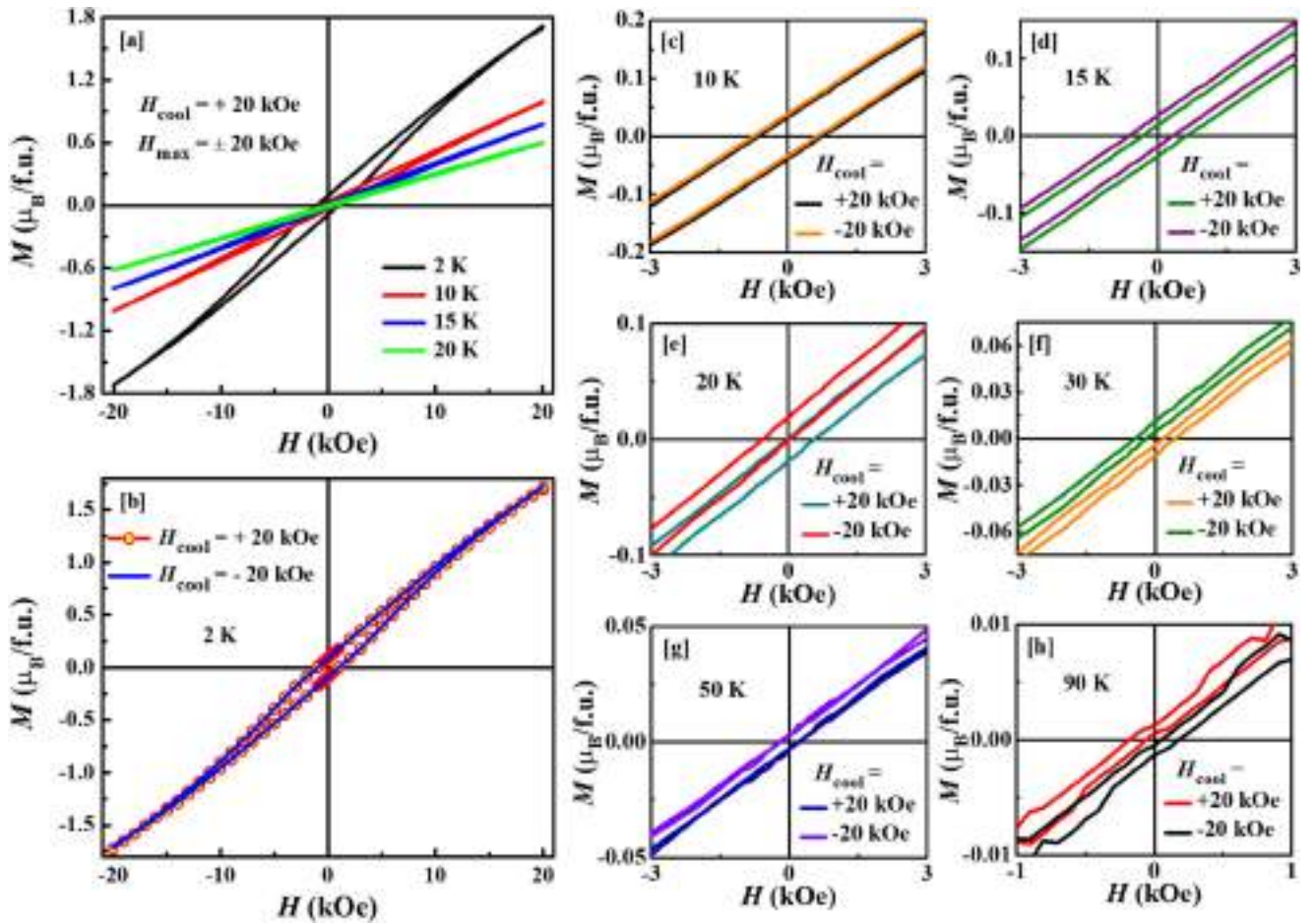


FIG. 7. (a) M - H loops of GSCO measured at $H_{\text{cool}} = 20$ kOe. The maximum field is ± 20 kOe, and the temperatures are $< T_{\text{FiM}}$. (b) Hysteresis loops measured at $T = 2$ K and $H_{\text{cool}} = 20$ or -20 kOe. (c)–(h) Magnified views of the field-cooled (FC) M - H loops measured at $H_{\text{cool}} = \pm 20$ kOe and $T = 10, 15, 20, 30, 50$, or 90 K, respectively.

negative between 70 and 100 K but positive at < 70 K. Also, H_2 remains positive at ≥ 2 K, and H_1 becomes negative again at < 20 K. Clearly, the H_1 and H_2 curves are not monotonous, and thus, a crossover from conventional EB to IEB effects (i.e., negative-to-positive sign inversion of H_{EB}) is observed in GSCO, which may be related to the observed magnetization reversal. Here, H_{EB} approaches zero at < 10 K, confirming the absence of any EB effect. Apart from the small peak at $< T_{\text{FiM}}$, H_C changes monotonically with temperature.

In general, in a strongly anisotropic system, where M does not saturate at the highest H , the minor hysteresis loops hinder us from accurately estimating the EB parameters, which may ultimately lead to erroneous results. Therefore, to detect the true EB effect in such a system, considering an effectively saturated hysteresis loop is recommended [79]. When the loop is closed, M is likely effectively saturated [51]. In this scenario, the FC and ZFC M - H loops are fully closed at 2 K within $H_{\text{max}} = \pm 20$ kOe, as shown in Fig. 7(a) and the inset of Fig. 6(b), respectively. Therefore, the FM component may be saturated, and the minor hysteresis loops may exhibit little effect on the current analysis.

To study the effect of H_{max} on the observed EB phenomenon, we investigated the FC loops at different H_{max} values. FC loops measured at $T = 15$ K

(randomly selected) at a constant $H_{\text{cool}} (= 20$ kOe) and different $H_{\text{max}} (= \pm 20, \pm 25, \pm 30, \text{ or } \pm 70$ kOe) are shown in Fig. 9(a), and an enlarged view of the origin is shown in Fig. 9(b). The magnitude of H_1 increases with increasing H_{max} , and that of H_2 does not change, and thus, the EB effect is reduced by increasing H_{max} . Here, H_C and H_{EB} are plotted as functions of H_{max} at $T = 15$ K in Fig. 9(c), with H_C increasing rapidly up to $H_{\text{max}} = 35$ kOe, beyond which it increases only slightly. Conversely, H_{EB} decreases sharply as H_{max} increases from 20 to 30 kOe and is almost zero at > 30 kOe. In addition, the almost complete suppression of H_{EB} at higher H_{max} values may be associated with suppressed FM contributions from $\text{Cr}^{3+}/\text{Cr}^{4+}$ ions in the FiM structure. At $H_{\text{max}} \geq 30$ kOe, a large paramagnetic Gd^{3+} moment dominates the entire magnetism, which inevitably reduces the exchange anisotropy between the FM clusters and FiM state.

Visualizing the origin of the EB effect, particularly the IEB effect, is rather complex, particularly in single-phase polycrystalline materials with invisible physical boundaries between the two different magnetic phases. Owing to the presence of FM clusters at high-temperatures, complex interfacial magnetic interactions between these clusters and the FiM state may induce EB anisotropy, causing the conventional EB effect in GSCO. Nevertheless, the presence of FM and

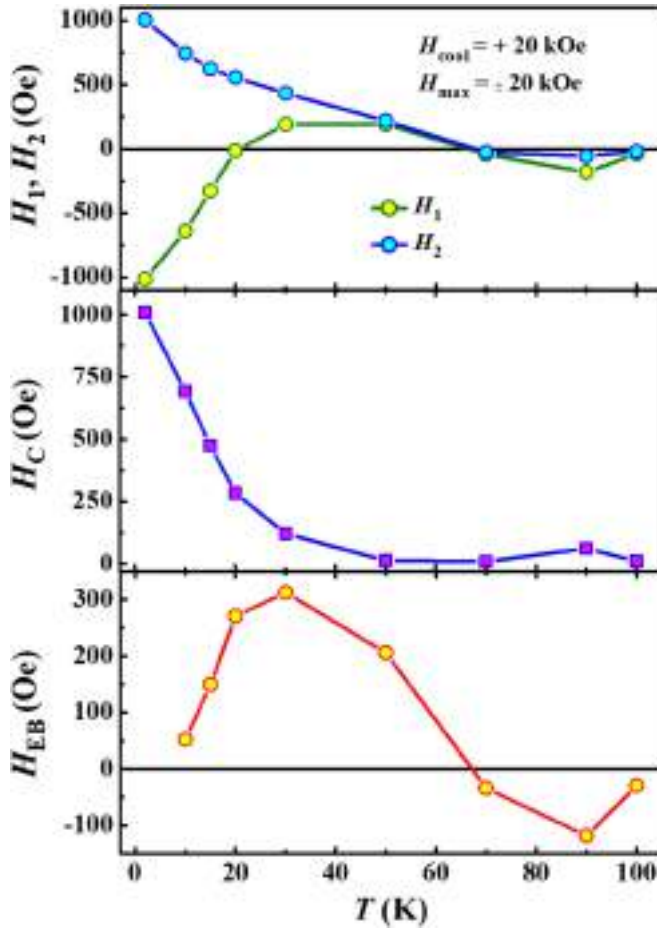


FIG. 8. Thermal profiles of H_1 , H_2 , H_C , and H_{EB} obtained from the field-cooled (FC) M - H loops of GSCO at $H_{cool} = 20$ kOe and $H_{max} = \pm 20$ kOe. Notably, the sign reversal of H_{EB} from negative to positive occurs upon cooling.

AFM components specific to the FiM state may be the real cause of the observed conventional EB behavior.

To gain deeper insight into the IEB phenomenon, we analyzed possible mechanisms to elucidate its origin. In most earlier investigations [80–83], the phenomena of IEB manifest with increasing strength of H_{cool} , in addition to the conventional EB effect at lower H_{cool} values. The sign reversal of H_{EB} is successfully explained for a system wherein FM nanodroplets are embedded in a charge-ordered AFM host using the following equation:

$$-H_{EB} \propto J^2 A L(\mu, H_{cool}, T_f) + J H_{cool},$$

where J is the surface exchange constant, A is a constant (multiplication factor), and L is the Langevin function of the magnetic moment μ of the FM nanodroplets H_{cool} and freezing temperature T_f of the interfacial spin [82]. Clearly, the competition between the surface exchange interaction and H_{cool} may induce the sign reversal of H_{EB} . This equation shows that, for a lower H_{cool} , the first term dominates, and H_{EB} becomes negative, as J^2 is always positive. For a higher H_{cool} , the second term may be significant, and in the case of AFM interfacial coupling, i.e., $J < 0$, sign reversal of H_{EB} may be anticipated.

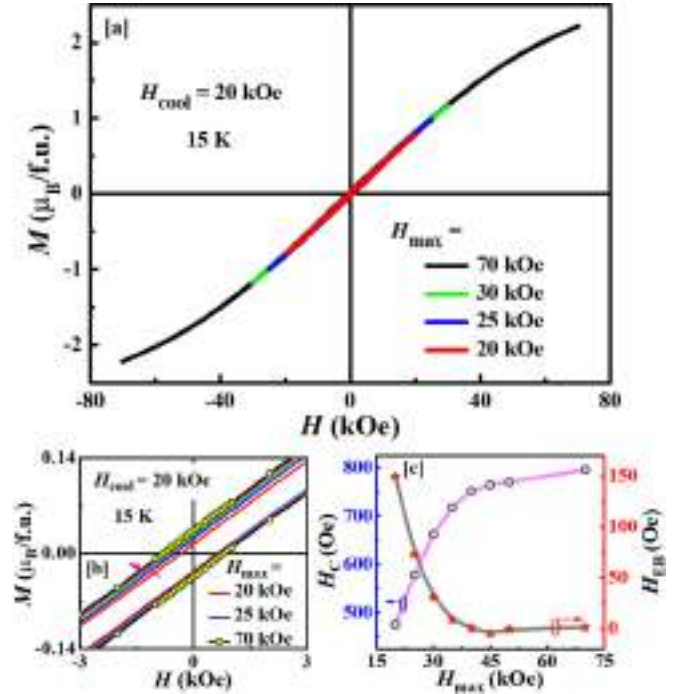


FIG. 9. (a) Field-cooled (FC) M - H loops of GSCO measured at $T = 15$ K at $H_{cool} = 20$ kOe and $H_{max} = \pm 20, \pm 25, \pm 30$, or ± 70 kOe. (b) Enlarged view of the loops. (c) H_C and H_{EB} as functions of H_{max} ($H_{cool} = 20$ kOe) at $T = 15$ K.

In contrast, in this investigation, when T is varied at a fixed H_{cool} and the sign of H_{cool} is changed at a fixed T , sign inversion of H_{EB} is observed. Because the H_{EB} equation does not contain T -dependent terms, the above prediction is unlikely. Another possibility in achieving the IEB effect is a magnetization reversal in the FiM state at $< T_{comp}$, which causes the IEB effect of $\text{LuFe}_{0.5}\text{Cr}_{0.5}\text{O}_3$ [78]. Because sign inversion of H_{EB} is also detected at $< T_{comp}$ of the canted FiM GSCO, these two materials should share a basic physical mechanism. In addition, the various possible pathways of the DM interaction between two Cr ions (with different oxidation states) may lead to a reversal of the magnetic moment, thereby producing the IEB effect. Furthermore, the rough interface between the magnetic layers yields spatially varying mixed AFM and FM couplings, which may generate the IEB effect, even at a lower H_{cool} [81]. In this paper, definitively identifying the origin of the IEB behavior of GSCO is challenging.

C. Heat capacity

To better understand the magnetic properties, the specific heat capacities (C_{total}) of GSCO and GCCO were measured at $H = 0$ and 90 kOe. Figure 10(a) shows the zero-field ($H = 0$ kOe) $C_{total}(T)$ curve of GSCO, which exhibits no λ -like anomaly, which is a common feature of AFM transitions. Instead, a clear anomaly is observed close to $T_{FiM} = 98$ K [Fig. 2(a)]. To estimate the change in magnetic entropy (S_m) by subtracting the lattice contribution ($C_{lattice}$) from C_{total} , combinations of the Debye and Einstein [84] or the two Debye functions [85] were used to fit the high-temperature region of

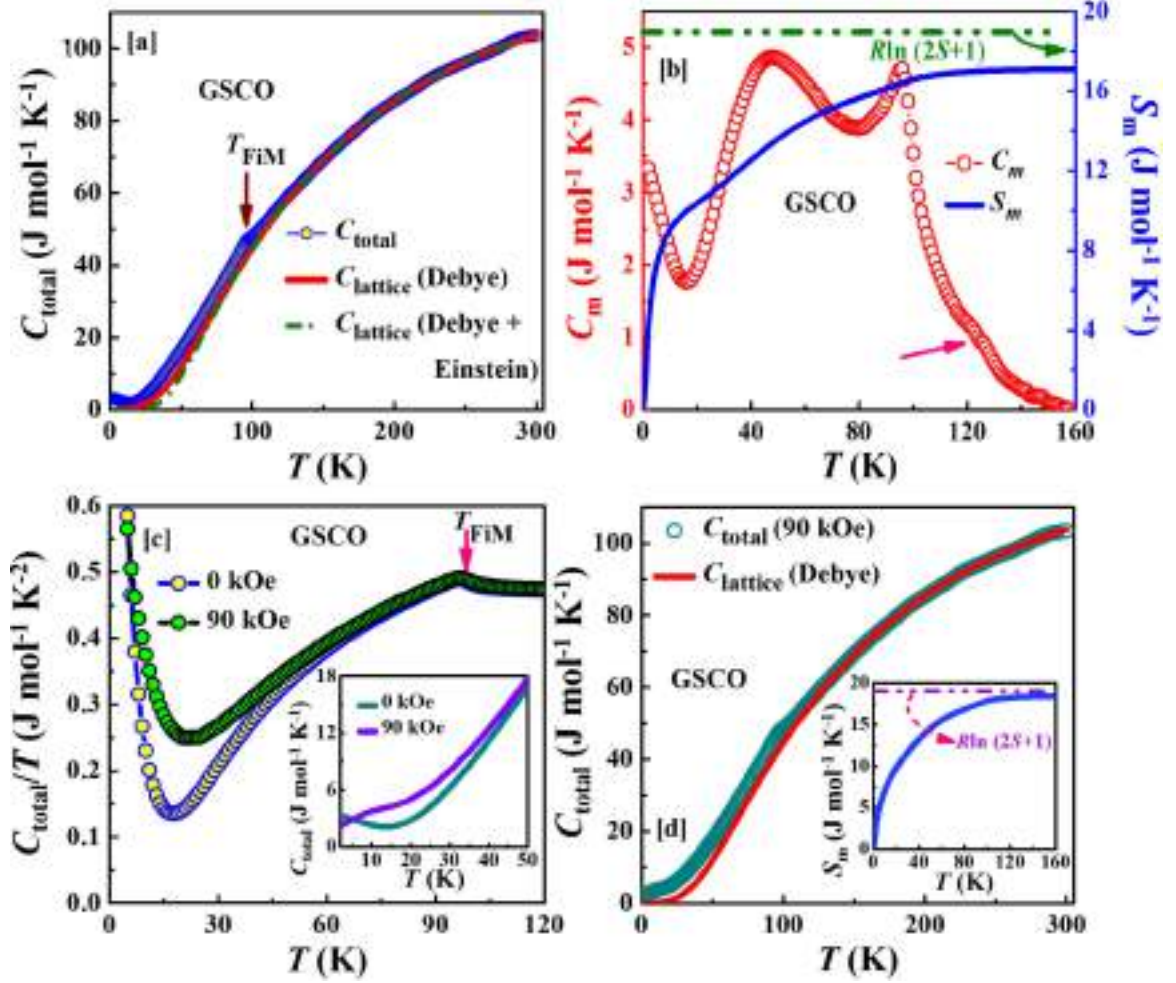


FIG. 10. (a) Temperature dependence of the specific heat capacity (C_{total}) of GSCO under a zero field. The solid and dashed curves show the lattice heat capacities (C_{lattice}) obtained by fitting to the high-temperature region with combinations of two Debye functions or Debye and Einstein functions, respectively. (b) Temperature dependences of the magnetic heat capacity (C_m), which is obtained by subtracting C_{lattice} from C_{total} , and the magnetic entropy (S_m). The dash-dotted straight line represents the theoretical S_m . (c) C_{total}/T vs T plots of GSCO at $H = 0$ and 90 kOe. The inset shows the C_{total} vs T plots. (d) C_{total} of GSCO at $H = 90$ kOe. The solid red curve represents C_{lattice} obtained by fitting to the high-temperature region with a combination of two Debye functions. The inset displays the S_m vs T curve.

$C_{\text{total}} (\gg T_{\text{FIM}})$. In the first case, the formula used is as follows:

$$C_{\text{total}}(T) = n_D \mathcal{D}(T, \Theta_D) + n_E \mathcal{E}(T, \Theta_E),$$

where \mathcal{D} and \mathcal{E} are the Debye and Einstein functions, respectively. Here, Θ_D and Θ_E are the respective Debye and Einstein temperatures, and the scale factors n_D and n_E correspond to the numbers of vibrational modes per formula unit in the Debye and Einstein models, respectively. In the latter case, the heat capacity is approximated by

$$C_{\text{total}}(T) = m_1 \mathcal{D}(T, \Theta_{D1}) + m_2 \mathcal{D}(T, \Theta_{D2}),$$

where m_1 and m_2 are the coefficients related to the vibrational modes per formula unit and Θ_{D1} and Θ_{D2} are the characteristic Debye temperatures. In both cases, proper fitting is observed with the parameters $n_D = 2.34$, $\Theta_D = 859$ K, $n_E = 2.73$, $\Theta_E = 273$ K, $m_1 = 2.09$, $m_2 = 2.99$, $\Theta_{D1} = 888$ K, and $\Theta_{D2} = 385$ K. The total number of vibrational modes in both cases is ~ 5 (i.e., $n_D + n_E \approx 5$ and $m_1 + m_2 \approx 5$), which validates the presence of five atoms per formula unit of GSCO.

Here, C_{lattice} dominates C_{total} at temperatures of $\gg T_{\text{FIM}}$, and thus, the fitted parameters enable the extrapolation of C_{lattice} to the low-temperature limit, as shown by the solid and dotted lines [for C_{lattice} (Debye) and C_{lattice} (Debye + Einstein), respectively] displayed in Fig. 10(a). Because the observed C_{total} and Debye (only) models are very similar, we adopted C_{lattice} (Debye) as a reference to examine the lattice contribution for further analysis. Notably, there is no similar nonmagnetic material that may be used as a reference to properly estimate C_{lattice} of GSCO.

The magnetic contribution to the heat capacity (C_m) is estimated by subtracting C_{lattice} from C_{total} , i.e., $C_m(T) = C_{\text{total}}(T) - C_{\text{lattice}}(T)$. Figure 10(b) shows C_m as a function of T , revealing a sharp peak close to $T_{\text{FIM}} = 98$ K. Additionally, the data show a broad peak at ~ 45 K, with another increase at < 15 K. The broad peak at < 45 K is unusual and is likely due to magnetization reversal, and the increase at < 15 K may be due to the short-range AFM ordering of the Gd moments. Similar increases in C_{total} are also reported in single-crystal and polycrystalline $\text{Gd}_2\text{CoMnO}_6$ [86,87] and single-crystal

Tb₂CoMnO₆ [88]. In addition, an extended plateau of the peak at $\sim T_{\text{FIM}}$ is observed in the high-temperature region of C_m , which suggests the possible presence of short-range magnetic correlations at $> T_{\text{FIM}}$. Moreover, the $C_m(T)$ curve displays several remarkable features but is too complicated to understand clearly.

Finally, S_m is estimated by integrating $C_m(T)/T$ over the studied temperature range [Fig. 10(b)]. Here, S_m increases rapidly with increasing temperature at ≤ 10 K, then gradually increases with increasing temperature, and plateaus at $17 \text{ J mol}^{-1} \text{ K}^{-1}$ at > 130 K. However, the saturation value of S_m is slightly smaller than the expected Boltzmann entropy [$S_m = R \ln(2S + 1) \approx 19 \text{ J mol}^{-1} \text{ K}^{-1}$] based on the mean-field theory for localized Cr^{3+} ($S = \frac{3}{2}$), Cr^{4+} ($S = 1$), and Gd^{3+} ($S = \frac{7}{2}$, $L = 0$). The dashed line in Fig. 10(b) represents the Boltzmann entropy. Several factors may cause the slight discrepancy between the observed and expected S_m , one of which is the short-range AFM ordering of Gd^{3+} moments. In addition, the inadequate estimation of C_m at very low temperatures by extrapolating the high-temperature C_{lattice} may be another cause of the discrepancy. Furthermore, increasing C_{total} at the lowest temperature [2 K, inset in Fig. 10(c)] hinders the proper estimation of C_m .

The C_{total}/T vs T curves of GSCO at $H = 0$ or 90 kOe are plotted in Fig. 10(c). Even at $H = 90$ kOe, no noticeable suppression at $\sim T_{\text{FIM}}$ is observed. Instead, the valleylike features centered at ~ 15 K are moderately suppressed. As shown in the inset of Fig. 10(c), C_{total} at $H = 90$ kOe does not increase as it does under the zero-field but decreases toward zero at < 5 K. Additionally, the short-range ordering of Gd^{3+} moments are significantly disturbed by the application of the 90 kOe field (due to the increased Gd^{3+} polarization). We attempted to estimate the saturation value of S_m again by determining C_{lattice} by fitting the high-temperature region of the C_{total} (90 kOe) curve using the combination of the two Debye functions and extrapolating to $T = 0$ K [Fig. 10(d)]. Remarkably, the temperature dependence of S_m [inset in Fig. 10(d)] shows that S_m generally saturates at a value much closer to the Boltzmann entropy than that at $H = 0$ kOe. Thus, the discrepancy between the observed ($H = 0$ kOe) and expected S_m is likely caused by short-range AFM ordering of Gd^{3+} moments.

To facilitate further comparative studies, we performed a detailed analysis of C_{total} of GCCO. Remarkably, the temperature dependences of the zero-field $C_{\text{total}}(T)$ of both materials are very similar [Figs. 10(a) and 11(a) show those of GSCO and GCCO, respectively], but a clear anomaly is observed at ~ 100 K in the $C_{\text{total}}(T)$ curve of GCCO. The observed anomalies and magnetization data indicate that GCCO undergoes AFM ordering at ~ 100 K. The solid red line shown in Fig. 11(a) represents the GCCO C_{lattice} estimated by combining the two Debye functions. Anomalies are detected at ~ 100 K, but no sharp peaks are observed in the $C_m(T)$ plot close to this temperature (not shown). Instead, a broad peak and an upturn at ~ 75 and < 15 K are observed, respectively.

As shown in the inset of Fig. 11(a), when the temperature is > 130 K, S_m saturates at $17.5 \text{ J mol}^{-1} \text{ K}^{-1}$, which is slightly smaller than the expected Boltzmann entropy. At $H = 90$ kOe, $C_{\text{total}}(T)$ displays no significant change in the

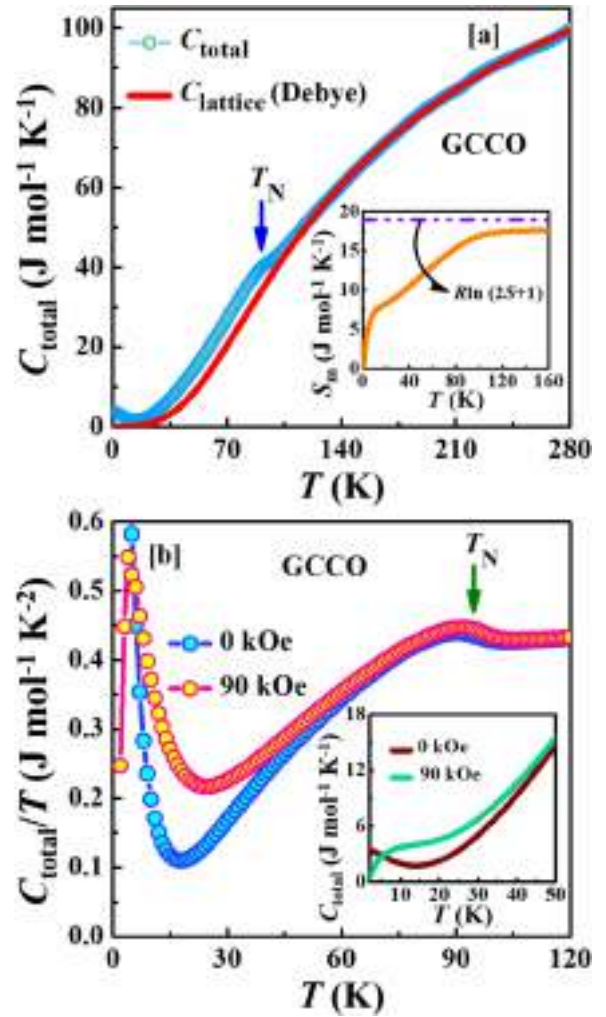


FIG. 11. (a) Specific heat capacity of GCCO as a function of temperature. The red solid curve shows a fitting to a combination of Debye functions, and the inset shows the thermal profile of S_m of GCCO and the theoretical value. (b) C/T vs T plots of GCCO at $H = 0$ or 90 kOe. The inset shows the C_{total} vs T plots.

magnetic transition at 100 K [C/T vs T plot in Fig. 11(b)]. Conversely, valleylike features at 15 K, such as those observed for GSCO, are strongly influenced by the application of H . The inset in Fig. 11(b) shows an enlarged view of the $C_{\text{total}}(T)$ curves at $H = 0$ or 90 kOe, revealing that they intersect at $T = 5$ K.

D. Resistivity

Figure 12(a) shows the temperature-dependent resistivities $\rho(T)$ of GSCO and GCCO. The increase in resistivity with decreasing temperature should yield semiconductorlike behavior. In this context, measuring $\rho(T)$ at temperatures of < 70 K was impossible because of the high resistance which was above the instrumental limit. At room temperature, ρ of GSCO is almost 14-fold higher than that of GCCO ($\rho_{300 \text{ K}} = 57.01$ and $4.19 \text{ } \Omega\text{-cm}$ for GSCO and GCCO, respectively). No metallic behavior is observed within the investigated temperature range, and these features contrast with the electrical

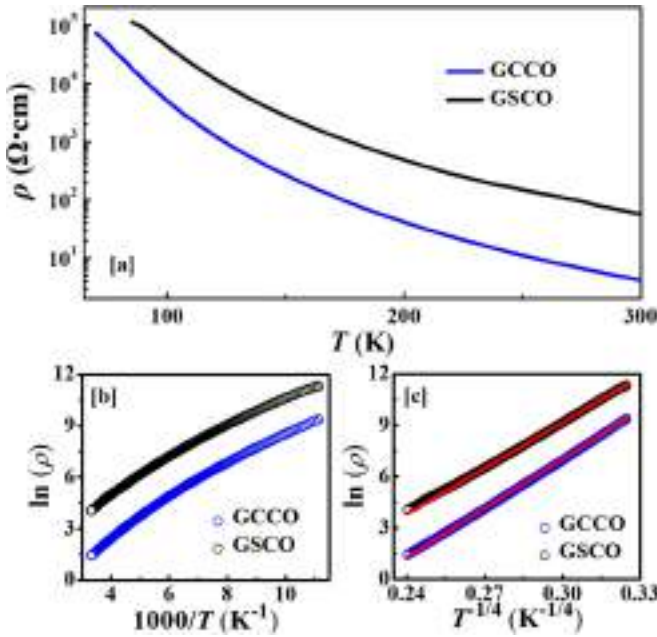


FIG. 12. (a) Temperature dependences of ρ of GSCO and GCCO. (b) Alternative plot of the data. (c) Variable-range-hopping plot of the data. The red solid lines are guidelines.

behaviors of half-doped manganites and cobaltites [36,50]. The resistivity data were analyzed using the Arrhenius model, $\ln\rho$ vs $1000/T$, to investigate the possible conduction mechanisms, as shown in Fig. 12(b). Owing to the nonlinear behaviors of the curves, the $\rho(T)$ curves of both materials are not well modeled by the Arrhenius model. Instead, the linear behavior of the $\ln\rho$ vs $T^{-1/4}$ plot [Fig. 12(c)] shows that variable-range hopping better explains the observed electronic behaviors of GSCO and GCCO.

E. Dielectric behavior

Several $RCrO_3$ materials (excluding $R = \text{Sc-Pr, Pm, Eu, Dy, Yb}$) should exhibit significant magnetoelectric coupling at temperatures of $< T_N$, and thus, they are potential multiferroic materials. Temperature-dependent relative permittivity (ϵ_r) measurements of GSCO and GCCO were performed at various frequencies to investigate possible magnetoelectric coupling. The thermal changes in ϵ_r and its loss factor ($\tan\delta$) are shown in Figs. 13(a)–13(d). The $\epsilon_r(T)$ curves of both materials display three main characteristics: (i) low- T plateaus at ϵ_r of ~ 60 ; (ii) sharply increasing ϵ_r close to $T = 30$ K (at 100 Hz), which is strongly frequency-dependent; and (iii) significant anomalies at $T \approx 100$ K (magnetic transition temperatures of GSCO and GCCO). These are also strongly frequency dependent and shift toward a higher T as the frequency increases [Figs. 13(a) and 13(b)].

In addition, the dielectric anomalies observed at T_{FiM} (for GSCO) and T_N (for GCCO) confirm the presence of significant magnetoelectric coupling in both materials. The frequency dependence of the dielectric anomaly ($\sim T_{\text{FiM}}$ and $\sim T_N$) is characteristic of a ferroelectric relaxorlike state, e.g., spontaneous electrical polarization associated with the anomaly is observed in $RCrO_3$ [12] and the stepwise

increase in ϵ_r at ~ 30 K may be associated with a large frequency-dependent Maxwell-Wagner relaxation [89]. This usually manifests itself as a depletion layer contribution at the interface between the sample and the electrodes or at some grain boundaries. Most importantly, it is not an inherent property of the material but an extrinsic issue. Conversely, the derivative spectra of $\epsilon_r(T)$ exhibit two peaks at $T \approx 100$ K (T_{FiM} and T_N), and the stepped increase in ϵ_r at this temperature indicates the presence of magnetic coupling. For clarity, the derivative spectra of the data measured at 2.71 kHz are shown as examples [insets in Figs. 13(a) and 13(b)].

Strong dielectric losses are observed at this temperature, with stepwise increases in ϵ_r observed [Figs. 13(c) and 13(d)]. The dielectric loss peaks depend on the frequency for both materials. No additional anomalies are observed in these spectra at the magnetic transition temperature, but the derivatives of the loss spectra reveal sharp increases at $\sim T_{\text{FiM}}$ and $\sim T_N$ [as indicated by the arrows and insets in Figs. 13(c) and 13(d)]. Therefore, the dielectric loss spectra reveal the magnetoelectric coupling of both materials. In addition, the application of a magnetic field of 90 kOe results in no significant changes in the $\epsilon_r(T)$ curves and dielectric loss spectra (not shown).

IV. SUMMARY AND CONCLUSIONS

We successfully synthesized the half-doped perovskite-type chromites GSCO and GCCO. These polycrystalline materials were obtained via solid-state reactions at a high pressure and temperature (6 GPa and 1200 °C). Synchrotron XRD at room temperature revealed that GSCO and GCCO crystallized in orthorhombic structures (space group: $Pnma$) with different degrees of local lattice distortion.

We observed magnetization reversal in GSCO, but GCCO displayed a little anomaly. The magnetic ground state of GSCO is FiM, while it is AFM for GCCO. Therefore, the magnetic ground state of half-doped $GdCrO_3$ could be tuned via substitution with various alkaline-earth ions. Moreover, the different magnetic ground states of GSCO and GCCO possibly originate from the different degrees of local lattice distortions, as evident from the structural analysis. In addition, thermal residual magnetization studies confirmed the presence of short-range magnetic correlations within GSCO at temperatures of $> T_{\text{FiM}}$. This was further supported by the heat capacity measurements.

Remarkably, GSCO displayed a crossover from the conventional EB effect to the IEB effect upon cooling. Such a crossover could be caused by the reversal of the magnetic moment due to various competing DM interactions. In general, the key factors of producing DM interaction between two atomic spins are the structural inversion symmetry breaking and the strong spin-orbit coupling (SOC) with magnetic exchange energy. In most cases, the strong SOC is provided by the neighboring atoms in the structure. However, in this paper, since $L = 0$ (for Gd^{3+}), the orbital contribution from the neighboring Gd^{3+} cannot be expected. Therefore, the crystal structure itself may stabilize spin canting by minimizing some free energy [71,90,91]. Moreover, the complex interfacial magnetic interactions between the high-temperature FM clusters and the FiM state is the plausible origin of the

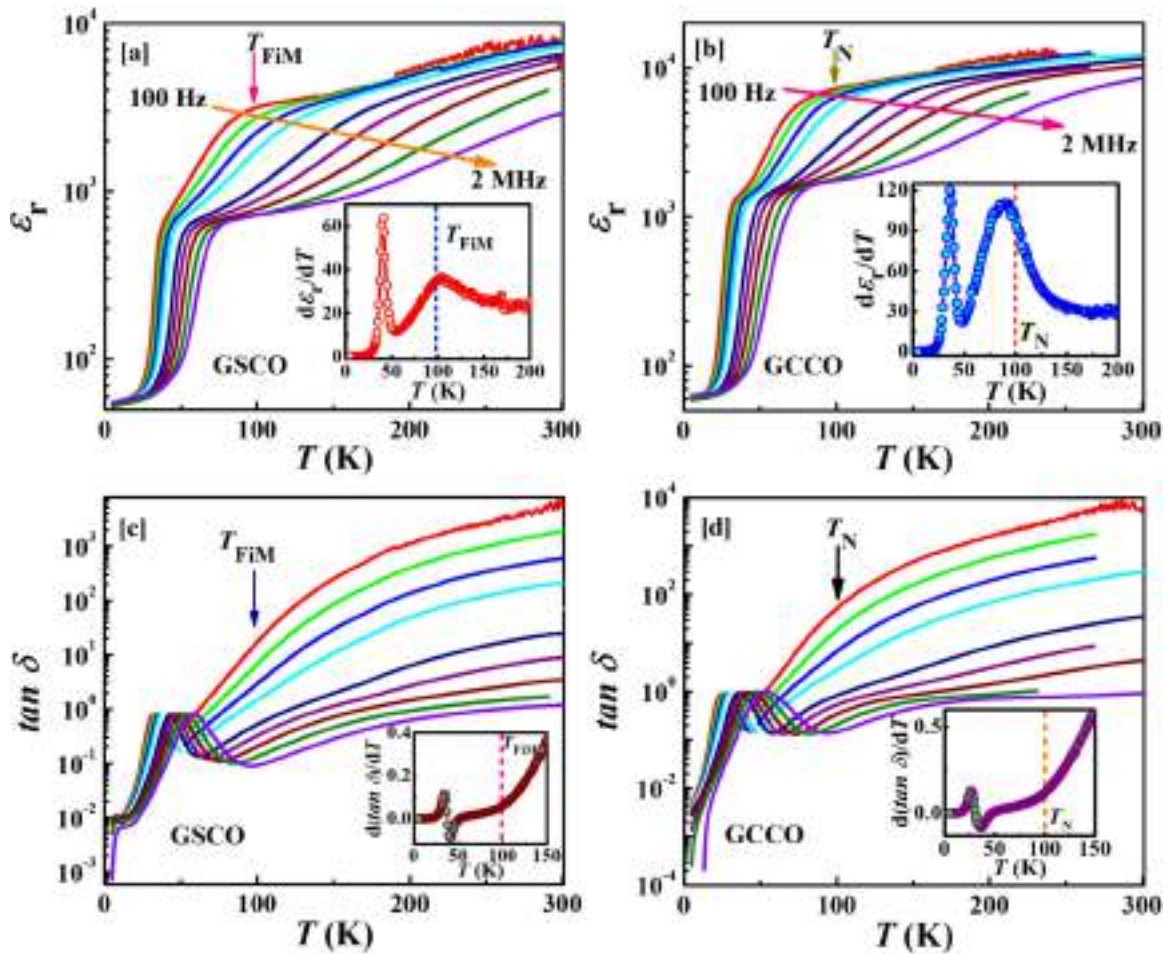


FIG. 13. (a)–(b) Temperature dependences of the dielectric constants (ϵ_r) of GSCO and GCCO, respectively, as recorded at several frequencies in the range 100 Hz–2 MHz ($f = 100$ Hz, 300 Hz, 903 Hz, 2.71 kHz, 8.15 kHz, 24.51 kHz, 73.68 kHz, 221.43 kHz, 665.48 kHz, and 2 MHz). The insets show representative differential curves (at 2.71 kHz). The blue and red dashed lines in the insets indicate the temperature corresponding to the onset of magnetic order of each material. (c)–(d) Temperature-dependent dielectric losses ($\tan \delta$) of GSCO and GCCO, respectively. The insets show representative differential curves (at 2.71 kHz).

conventional EB behavior in GSCO. Although several mechanisms including the competition between interfacial exchange coupling and H_{cool} , the reversal of magnetic moments below T_{comp} , and the spatially varying mixed AFM and FM couplings at the rough interface have been discussed to understand the origin of IEB, we can predict that the IEB effect in GSCO arises due to the magnetization reversal phenomenon. In addition, significant magnetoelectric coupling with ferroelectric relaxorlike states was identified at the onsets of magnetic order of both materials. The presence of the EB effect, particularly the IEB effect, and magnetoelectric coupling yields considerable prospects for application in magnetic memory and spintronic devices.

We interpreted the possible magnetic ground states of both materials as much as possible based on the experimental data, but the exact magnetic structures remain unclear because conducting neutron diffraction studies of highly

neutron-absorbing materials is technically challenging. Further combined studies, such as x-ray magnetic circular dichroism and density functional theory calculations, should contribute to a comprehensive understanding of the magnetic and electronic properties of these half-doped perovskite-type chromites.

ACKNOWLEDGMENTS

Synchrotron radiation was performed at the beamlines for powder diffraction (BL15XU and BL02B2) at SPring-8 with the approval of the Japan Synchrotron Radiation Research Institute (Proposals No. 2020A4501 and No. 2021A1169). This paper was partially supported by Japan Society for the Promotion of Science KAKENHI Grants No. JP20H05276 and No. JP22H04601.

[1] L. Holmes, M. Eibschitz, and L. G. Van Uitert, *J. Appl. Phys.* **41**, 1184 (1970).

[2] A. H. Cooke, D. M. Martin, and M. R. Wells, *J. Phys. C: Solid State Phys.* **7**, 3133 (1974).

- [3] T. Morishita, K. Aoyagi, K. Tsushima, and T. Kigawa, *Solid State Commun.* **20**, 123 (1976).
- [4] K. Toyokawa, S. Kurita, and K. Tsushima, *Phys. Rev. B* **19**, 274 (1979).
- [5] K. Yoshii, *J. Solid State Chem.* **159**, 204 (2001).
- [6] B. Rajeswaran, D. I. Khomskii, A. K. Zvezdin, C. N. R. Rao, and A. Sundaresan, *Phys. Rev. B* **86**, 214409 (2012).
- [7] S. Lei, L. Liu, C. Wang, C. Wang, D. Guo, S. Zeng, B. Cheng, Y. Xiao, and L. Zhou, *J. Mater. Chem. A* **1**, 11982 (2013).
- [8] K. R. S. Preethi Meher, A. Wahl, A. Maignan, C. Martin, and O. I. Lebedev, *Phys. Rev. B* **89**, 144401 (2014).
- [9] A. McDannald, C. R. delaCruz, M. S. Seehra, and M. Jain, *Phys. Rev. B* **93**, 184430 (2016).
- [10] B. Dalal, B. Sarkar, V. D. Ashok, and S. K. De, *J. Phys.: Condens. Matter* **28**, 426001 (2016).
- [11] M. Taheri, F. S. Razavi, Z. Yamani, R. Flacau, P. G. Reuvekamp, A. Schulz, and R. K. Kremer, *Phys. Rev. B* **93**, 104414 (2016).
- [12] A. Indra, K. Dey, A. Midya, P. Mandal, O. Gutowski, U. Rütt, S. Majumdar, and S. Giri, *J. Phys.: Condens. Matter* **28**, 166005 (2016).
- [13] M. Tripathi, R. J. Choudhary, D. M. Phase, T. Chatterji, and H. E. Fischer, *Phys. Rev. B* **96**, 174421 (2017).
- [14] B. Dalal, B. Sarkar, S. Rayaprol, M. Das, V. Siruguri, P. Mandal, and S. K. De, *Phys. Rev. B* **101**, 144418 (2020).
- [15] I. Dzyaloshinsky, *J. Phys. Chem. Solids* **4**, 241 (1958).
- [16] T. Moriya, *Phys. Rev.* **120**, 91 (1960).
- [17] I. Fita, R. Puzniak, A. Wisniewski, and V. Markovich, *Phys. Rev. B* **100**, 144426 (2019).
- [18] L. H. Yin, J. Yang, X. C. Kan, W. H. Song, J. M. Dai, and Y. P. Sun, *J. Appl. Phys.* **117**, 133901 (2015).
- [19] Y. Zhu, P. Zhou, T. Li, J. Xia, S. Wu, Y. Fu, K. Sun, Q. Zhao, Z. Li, Z. Tang *et al.*, *Phys. Rev. B* **102**, 144425 (2020).
- [20] J. van den Brink, G. Khaliullin, and D. I. Khomskii, *Phys. Rev. Lett.* **83**, 5118 (1999).
- [21] F. Damay, C. Martin, A. Maignan, M. Hervieu, B. Raveau, Z. Jirak, G. André, and F. Bourée, *Chem. Mater.* **11**, 536 (1999).
- [22] R. J. Goff and J. P. Attfield, *Phys. Rev. B* **70**, 140404(R) (2004).
- [23] J. Padilla-Pantoja, J. Herrero-Martín, P. Gargiani, S. M. Valvidares, V. Cuartero, K. Kummer, O. Watson, N. B. Brookes, and J. L. García-Muñoz, *Inorg. Chem.* **53**, 8854 (2014).
- [24] J. Padilla-Pantoja, J. Herrero-Martín, E. Pellegrin, P. Gargiani, S. M. Valvidares, A. Barla, and J. L. García-Muñoz, *Phys. Rev. B* **92**, 245136 (2015).
- [25] E. O. Wollan and W. C. Koehler, *Phys. Rev.* **100**, 545 (1955).
- [26] J. B. Goodenough, *Phys. Rev.* **100**, 564 (1955).
- [27] Y. Tomioka, A. Asamitsu, Y. Moritomo, H. Kuwahara, and Y. Tokura, *Phys. Rev. Lett.* **74**, 5108 (1995).
- [28] Y. Tokura, *Rep. Prog. Phys.* **69**, 797 (2006).
- [29] E. Dagotto, *New J. Phys.* **7**, 67 (2005).
- [30] E. Dagotto, *Science* **309**, 257 (2005).
- [31] J. A. Souza, J. J. Neumeier, and Y. -K. Yu, *Phys. Rev. B* **78**, 014436 (2008).
- [32] M. B. Salamon, P. Lin, and S. H. Chun, *Phys. Rev. Lett.* **88**, 197203 (2002).
- [33] J. Fan, L. Pi, Y. He, L. Ling, J. Dai, and Y. Zhang, *J. Appl. Phys.* **101**, 123910 (2007).
- [34] C. Autret, C. Martin, M. Hervieu, A. Maignan, B. Raveau, G. André, F. Bourée, and Z. Jirak, *J. Magn. Magn. Mater.* **270**, 194 (2004).
- [35] K. Tobe, T. Kimura, and Y. Tokura, *Phys. Rev. B* **69**, 014407 (2004).
- [36] H. Kawano, R. Kajimoto, H. Yoshizawa, Y. Tomioka, H. Kuwahara, and Y. Tokura, *Phys. Rev. Lett.* **78**, 4253 (1997).
- [37] V. K. Shukla and S. Mukhopadhyay, *Phys. Rev. B* **97**, 054421 (2018).
- [38] C. R. Serrao, A. Sundaresan, and C. N. R. Rao, *J. Phys.: Condens. Matter* **19**, 496217 (2007).
- [39] T. Zou, F. Wang, Y. Liu, L.-Q. Yan, and Y. Sun, *Appl. Phys. Lett.* **97**, 092501 (2010).
- [40] S. Dash, A. Banerjee, and P. Chaddah, *J. Appl. Phys.* **113**, 17D912 (2013).
- [41] S. M. Zhou, L. Shi, H. P. Yang, Y. Wang, L. F. He, and J. Y. Zhao, *Appl. Phys. Lett.* **93**, 182509 (2008).
- [42] E. Dagotto, *Nanoscale Phase Separation and Colossal Magnetoresistance: The Physics of Manganites and Related Compounds* (Springer-Verlag, Berlin, Heidelberg, 2003).
- [43] A. I. Kurbakov, V. A. Ryzhov, V. V. Runov, E. O. Bykov, I. I. Larionov, V. V. Deriglazov, C. Martin, and A. Maignan, *Phys. Rev. B* **100**, 184424 (2019).
- [44] H. Zhou, Q. Feng, Y. Hou, M. Nakamura, Y. Tokura M. Kawasaki, Z. Sheng, and Q. Lu, *npj Quantum Mater.* **6**, 56 (2021).
- [45] I. O. Troyanchuk, N. V. Kasper, D. D. Khalyavin, H. Szymczak, R. Szymczak, and M. Baran, *Phys. Rev. Lett.* **80**, 3380 (1998).
- [46] J. L. Garcia-Munoz, J. Padilla-Pantoja, X. Torrelles, J. Blasco, J. Herrero-Martín, B. Bozzo, and J. A. Rodríguez-Velamazán, *Phys. Rev. B* **94**, 014411 (2016).
- [47] M. Kriener, C. Zobel, A. Reichl, J. Baier, M. Cwik, K. Berggold, H. Kierspel, O. Zabara, A. Freimuth, and T. Lorenz, *Phys. Rev. B* **69**, 094417 (2004).
- [48] Y. Okimoto, X. Peng, M. Tamura, T. Morita, K. Onda, T. Ishikawa, S. Koshihara, N. Todoroki, T. Kyomen, and M. Itoh, *Phys. Rev. Lett.* **103**, 027402 (2009).
- [49] J. L. Garcia-Munoz, C. Frontera, A. J. Barón-González, S. Valencia, J. Blasco, R. Feyerherm, E. Dudzik, R. Abrudan, and F. Radu, *Phys. Rev. B* **84**, 045104 (2011).
- [50] K. H. Kim, T. Qian, and Bog G. Kim, *J. Appl. Phys.* **102**, 033910 (2007).
- [51] I. Fita, I. O. Troyanchuk, T. Zajarniuk, P. Iwanowski, A. Wisniewski, and R. Puzniak, *Phys. Rev. B* **98**, 214445 (2018).
- [52] I. Fita, I. O. Troyanchuk, T. Zajarniuk, A. Wisniewski, and R. Puzniak, *Phys. Rev. B* **101**, 224433 (2020).
- [53] M. Tanaka, Y. Katsuya, and A. Yamamoto, *Rev. Sci. Instrum.* **79**, 075106 (2008).
- [54] M. Tanaka, Y. Katsuya, Y. Matsushita, and O. Sakata, *J. Ceram. Soc. Jpn.* **121**, 287 (2013).
- [55] H. M. Rietveld, *J. Appl. Cryst.* **2**, 65 (1969).
- [56] F. Izumi and T. Ikeda, *Mater. Sci. Forum* **321–324**, 198 (2000).
- [57] L. Lutterotti, *Nuclear Inst. Methods Phys. Res. B* **268**, 334 (2010).
- [58] K. Momma and F. Izumi, *J. Appl. Crystallogr.* **44**, 1272 (2011).
- [59] R. Liu, R. Scatena, D. D. Khalyavin, R. D. Johnson, Y. Inaguma, M. Tanaka, Y. Matsushita, K. Yamaura, and A. A. Belik, *Inorg. Chem.* **59**, 9065 (2020).
- [60] See Supplemental Material at <http://link.aps.org/supplemental/10.1103/PhysRevB.106.104425> for the atomic positions, occupancies, and thermal displacement parameters of the structures

- of GSCO and GCCO obtained using synchrotron XRD, temperature dependence of the lattice parameters, and volume of the orthorhombic unit cells of GSCO and GCCO.
- [61] A. C. Komarek, T. Möller, M. Isobe, Y. Drees, H. Ulbrich, M. Azuma, M. T. Fernández-Díaz, A. Senyshyn, M. Hoelzel, G. André *et al.*, *Phys. Rev. B* **84**, 125114 (2011).
- [62] F. Damay, C. Martin, V. Hardy, A. Maignan, G. André, K. Knight, S. R. Giblin, and L. C. Chapon, *Phys. Rev. B* **81**, 214405 (2010).
- [63] H. L. Feng, M. Reehuis, P. Adler, Z. Hu, M. Nicklas, A. Hoser, S.-C. Weng, C. Felser, and M. Jansen, *Phys. Rev. B* **97**, 184407 (2018).
- [64] A. B. Antunes, O. Peña, C. Moure, V. Gil, and G. André, *J. Magn. Magn. Mater.* **316**, e652 (2007).
- [65] J. Blasco, J. L. García-Muñoz, J. García, G. Subías, J. Stankiewicz, J. A. Rodríguez-Velamazán, and C. Ritter, *Phys. Rev. B* **96**, 024409 (2017).
- [66] M. K. Kim, J. Y. Moon, S. H. Oh, D. G. Oh, Y. J. Choi, and N. Lee, *Sci Rep.* **9**, 5456 (2019).
- [67] R. B. Griffiths, *Phys. Rev. Lett.* **23**, 17 (1969).
- [68] C. He, M. A. Torija, J. Wu, J. W. Lynn, H. Zheng, J. F. Mitchell, and C. Leighton, *Phys. Rev. B* **76**, 014401 (2007).
- [69] A. Haldar, K. G. Suresh, and A. K. Nigam, *Europhys. Lett.* **91**, 67006 (2010).
- [70] M. Balanda, *Acta Phys. Pol. A* **124**, 964 (2013).
- [71] K. Manna, A. K. Bera, M. Jain, S. Elizabeth, S. M. Yusuf, and P. S. Anil Kumar, *Phys. Rev. B* **91**, 224420 (2015).
- [72] R. Kumar, P. Yanda, and A. Sundaresan, *Phys. Rev. B* **103**, 214427 (2021).
- [73] R. Mathieu, P. Jönsson, D. N. H. Nam, and P. Nordblad, *Phys. Rev. B* **63**, 092401 (2001).
- [74] B. Mali, H. S. Nair, T. W. Heitmann, H. Nhalil, D. Antonio, K. Gofryk, S. R. Bhandari, M. P. Ghimire, and S. Elizabeth, *Phys. Rev. B* **102**, 014418 (2020).
- [75] A. E. Berkowitz and K. Takano, *J. Magn. Magn. Mater.* **200**, 552 (1999).
- [76] J. Nogués, J. Sort, V. Langlais, V. Skumryev, S. Suriñach, J. S. Muñoz, and M. D. Baró, *Phys. Rep.* **422**, 65 (2005).
- [77] M. Patra, M. Thakur, S. Majumdar, and S. Giri, *J. Phys.: Condens. Matter* **21**, 236004 (2009).
- [78] I. Fita, V. Markovich, A. S. Moskvin, A. Wisniewski, R. Puzniak, P. Iwanowski, C. Martin, A. Maignan, R. E. Carbonio, M. U. Gutowska *et al.*, *Phys. Rev. B* **97**, 104416 (2018).
- [79] J. Geshev, *J. Appl. Phys.* **105**, 066108 (2009).
- [80] J. Nogués, D. Lederman, T. J. Moran, and I. K. Schuller, *Phys. Rev. Lett.* **76**, 4624 (1996).
- [81] J. Nogués, C. Leighton, and I. K. Schuller, *Phys. Rev. B* **61**, 1315 (2000).
- [82] D. Niebieskikwiat and M. B. Salamon, *Phys. Rev. B* **72**, 174422 (2005).
- [83] J. Krishna Murthy and P. S. Anil Kumar, *Sci. Rep.* **7**, 6919 (2017).
- [84] Y. Y. Jiao, Q. Cui, P. Shahi, N. N. Wang, N. Su, B. S. Wang, M. T. Fernández-Díaz, J. A. Alonso, and J. -G. Cheng, *Phys. Rev. B* **97**, 014426 (2018).
- [85] D. A. Salamatin, N. Martin, V. A. Sidorov, N. M. Chtchelkatchev, M. V. Magnitskaya, A. E. Petrova, I. P. Zibrov, L. N. Fomicheva, J. Guo, C. Huang *et al.*, *Phys. Rev. B* **101**, 100406(R) (2020).
- [86] J. Y. Moon, M. K. Kim, Y. J. Choi, and N. Lee, *Sci. Rep.* **7**, 16099 (2017).
- [87] M. Das, P. Sarkar, and P. Mandal, *Phys. Rev. B* **101**, 144433 (2020).
- [88] J. Y. Moon, M. K. Kim, D. G. Oh, J. H. Kim, H. J. Shin, Y. J. Choi, and N. Lee, *Phys. Rev. B* **98**, 174424 (2018).
- [89] P. Mandal, V. S. Bhadram, Y. Sundarayya, C. Narayana, A. Sundaresan, and C. N. R. Rao, *Phys. Rev. Lett.* **107**, 137202 (2011).
- [90] A. Shaw, A. Mitra, S. D. Kaushik, V. Siruguri, and P. K. Chakrabarti, *J. Magn. Magn. Mater.* **488**, 165338 (2019).
- [91] M. Goto, T. Oguchi, and Y. Shimakawa, *J. Am. Chem. Soc.* **143**, 19207 (2021).



Spectroscopic and magnetic investigations of the dilute magnetically doped semiconductors $\text{BaSn}_{1-x}\text{Mn}_x\text{O}_3$ ($0.02 \leq x \leq 0.1$)

Ankita Sarkar^{a,1}, Biswajit Dalal^{b,*}, Subodh Kumar De^{a,**}

^a School of Materials Sciences, Indian Association for the Cultivation of Science, 2A & 2B Raja S. C. Mullick Road, Jadavpur, Kolkata, 700032, India

^b Department of Physics, Achhruram Memorial College, Jhalda, Purulia, West Bengal, 723202, India

ARTICLE INFO

Keywords:

Perovskite oxide
Dilute magnetic semiconductor
Antiferromagnetic interaction
Electron paramagnetic resonance
Singly ionized oxygen vacancy

ABSTRACT

Dilute magnetically doped semiconductors (DMSs) are key to fabricating novel spintronic devices with high functionalities, which could be utilized for the next-generation technological development. BaSnO_3 is a transparent wide band gap (~ 3.1 eV) semiconductor, in which magnetism can be induced through a subtle amount of magnetic impurity doping without deterring its optical transparency. In this work, we report an experimental investigation on the optical spectroscopic and magnetic properties of the DMSs $\text{BaSn}_{1-x}\text{Mn}_x\text{O}_3$ ($0 \leq x \leq 0.1$), synthesized using standard solid-state-reaction method at high-temperature and ambient pressure, through various spectroscopic, electron paramagnetic resonance (EPR) and temperature- and field-dependent magnetization measurements. All samples are found to be crystallize in the cubic structure with space group $Pm\bar{3}m$, in which Mn ions are stabilized in the $4+$ valence state. We find that the optical band gap monotonically decreases (from 3.1 eV to 2.08 eV) with increase in Mn doping concentration, which in turn leads to an increase in absorption efficiency in the visible region. An enhanced $sp-d$ hybridization between localized d electrons of Mn ions and band electrons is likely the main reason for such band gap reduction. Interestingly, theoretical simulation of EPR spectra suggests that the signal is primarily arising from a combination of two spin systems, i.e., Mn^{4+} ions and singly ionized oxygen vacancies. The strength of magnetic interaction between Mn^{4+} ions is also increased for higher doped samples. Moreover, the nature of magnetic interaction is predominantly antiferromagnetic in higher doped samples, as corroborated by the negative value of Curie-Weiss temperature from the inverse susceptibility fitting.

1. Introduction

The discovery of ferromagnetism above room-temperature in dilute magnetically doped semiconductors (DMSs), first theoretically predicted by Dietl et al. [1] and later confirmed by numerous experimental results [2–7], has opened up a new window for the development of the spintronics devices, which can simultaneously make use of both the spin and charge degrees of freedom in a materials system. In particular, the wide band gap semiconductors, such as ZnO, SnO_2 , TiO_2 , and In_2O_3 , were extensively investigated through transition-metal (especially Mn and Co) ion doping over the past few decades to achieve the room-temperature ferromagnetism (RTFM) in DMSs [2–11]. Till date, several binary oxides have been widely studied in the progress of the research on DMSs; but they have few limitations, such as, the lack of

high operation speed and good oxygen stability.

Oxide materials with the perovskite structure are known to have extremely good oxygen stability, and have shown a plethora of excellent electronic, optical and magnetic properties, such as, ferroelectricity, multiferroicity, superconductivity, high mobility and transparency, which could introduce new functionalities to spintronic devices [12–14]. In view of this, more comprehensive research effort has been given to obtain new DMSs with high functionalities using such diverse physical properties of perovskite-structured oxides. Till now, several transition-metal doping studies, for example, Co-doped BaTiO_3 and $\text{Ba}_{0.5}\text{Sr}_{0.5}\text{TiO}_3$, and Co- or Fe-doped SrTiO_3 [15–19], have been performed for realizing the RTFM in nonmagnetic perovskite oxides. Moreover, they belong to a class of materials having wide band gap, which could also facilitate them to become a potential candidate for

* Corresponding author.

** Corresponding author.

E-mail addresses: b.dalal.iitd@gmail.com (B. Dalal), msskd@iacs.res.in (S.K. De).

¹ AS and BD contributed equally to this work.

transparent conducting oxides.

In the perovskite family of oxides, the alkaline-earth stannates with the general chemical formula ASnO_3 ($A = \text{Ba, Ca or Sr}$) have attracted much greater attention from researchers due to their interesting physical properties and potential applications, such as photovoltaic and/or photoelectrochemical energy conversions, stable capacitors, humidity sensors, and gas sensors, in semiconductor industry [20–22]. Among ASnO_3 compounds, BaSnO_3 (BSO) usually crystallizes in an ideal cubic structure, and has emerged as a transparent wide band gap semiconductor with an optical band gap of ~ 3.1 eV [23]. Recently, several dopants have been chosen to substitute both the Ba and Sn sites of BSO in order to enhance the electrical conductivity and induce the magnetism. For example, the high electrical conductivity and mobility at room-temperature was found in the transparent perovskite oxides (Ba, La) SnO_3 and $\text{Ba}(\text{Sn,Sb})\text{O}_3$ [14,24]. Nevertheless, the RTFM has been reported for Mn and Fe-doped BSO compounds [25–27], and the origin of such ferromagnetism has been explained on the basis of either the F-center exchange mechanism (for bulk powder samples) or the coalescence of the magnetic polarons (for thin films). However, more comprehensive research using various experimental tools is necessary in order to unveil the change in the structural, optical and magnetic properties of such semiconductor systems due to magnetic ion doping.

In this article, we report the optical spectroscopic and magnetic properties of the polycrystalline $\text{BaSn}_{1-x}\text{Mn}_x\text{O}_3$ ($0 \leq x \leq 0.1$) samples, which typically form an ideal cubic perovskite structure with space group $Pm\bar{3}m$ and contain only Mn^{4+} ions. The vibrational spectroscopy study confirms the successful incorporation of Mn ions into the host lattice and the presence of oxygen vacancy in the doped samples. Optical absorption spectra reveals that the band gap reduces drastically from 3.1 eV for $x = 0$ to 2.08 eV for $x = 0.1$ due to the enhanced $sp-d$ hybridization between localized d electrons of Mn ions and band electrons. Moreover, precise analyses of the EPR and magnetization data suggested that the observed behavior of both these data can only be analyzed by considering the contributions from both Mn^{4+} ions and singly ionized oxygen vacancies. More importantly, the higher doped samples (for example, $x = 0.1$) showed predominant antiferromagnetic interaction, instead of ferromagnetic behavior.

2. Experimental details

High quality single-phase polycrystalline samples with compositions $\text{BaSn}_{1-x}\text{Mn}_x\text{O}_3$ ($0 \leq x \leq 0.1$) were prepared by the standard solid-state-reaction method at high-temperature and ambient pressure. Stoichiometric quantities of high purity oxides BaCO_3 (Sigma Aldrich; 99.999%), SnO_2 (Sigma Aldrich; 99.9%) and MnO_2 (Sigma Aldrich; 99%) were mixed thoroughly in an agate mortar for 1 h and calcined at 1200 °C for 6 h in air. After furnace cooled, these samples were reground thoroughly for better homogeneity and pressed into a cylindrical pellet using uniaxial hydraulic press. The pellets were then sintered twice in air at 1300 °C for 12 h with intermediate grinding to obtain better crystalline phases.

The phase purity of the as-synthesized samples was checked by x-ray powder diffraction (XRD) measurements using X-Pert Pro, PANalytical diffractometer (equipped with $\text{CuK}\alpha$ radiation, $\lambda = 1.5418$ Å) in the 2θ range 10° – 90° . In order to get more information about the crystal structures of the samples, XRD patterns were analyzed by the Rietveld refinement method [28] using the software MAUD [29]. Raman spectra were collected at room-temperature by an He–Ne laser of $\lambda = 632$ nm using a J-Y Horiba (model T64000) Raman spectrophotometer. Fourier transform infrared (FTIR) spectra of the samples were taken using a PerkinElmer Spectrochem 100 FTIR spectrometer. To analyze the chemical states of the constituent atoms, room-temperature core-level x-ray photoelectron spectroscopy (XPS) measurements were carried out with an SSX-100 ESCA spectrometer (Omicron, model: 1712-62-11) using Al $K\alpha$ radiation, 1486.6 eV line, and a spot size of 800 nm.

Room-temperature optical reflectance data of the samples was recorded by a Varian Cary 5000 ultraviolet (UV)-vis-near-infrared (NIR) spectrophotometer. Electron paramagnetic resonance (EPR) measurements at room-temperature were performed at X-band (9.5 GHz) using JEOL spectrometer. The dc magnetization (M) measurements were carried out in a Quantum Design's MPMS 3 superconducting quantum interference device-vibrating sample magnetometer within the temperature (T) interval 2–300 K and a magnetic field (H) up to ± 50 kOe.

3. Results and discussion

3.1. Crystal structure

The XRD patterns of undoped and Mn-doped BSO samples are shown in Fig. 1(a). Pure BSO usually crystallizes in a perfectly cubic structure with space group $Pm\bar{3}m$ (No. 221) at ambient condition [23]. The presence of diffraction peaks (110), (111), (200), (211), (220), (310), (222) and (321) related to the cubic $Pm\bar{3}m$ phase clearly suggests the single-phase nature of the pure BSO. Further, all of the diffraction peaks of Mn-doped BSO samples can be well indexed with the cubic structure (space group: $Pm\bar{3}m$) of pure BSO. No impurity peaks owing to the evolution of any secondary phases are found in the XRD patterns of $x = 0$ – 0.1 samples. However, an attempt to synthesize the higher doped samples (such as, $x > 0.1$) dictates that the single-phase remains intact only up to $x = 0.1$ doping limit in the present synthesis condition.

To identify the subtle structural changes with doping, Rietveld analyses were carried out by refining the structural and microstructural parameters. The Rietveld-fitted XRD patterns along with the difference between the observed and calculated spectra for $x = 0$ and 0.1 are shown in Fig. 1(b) and (c), respectively. No such anomalous changes, which can be attributed to the structural phase changes, with doping is observed from the Rietveld refinements. It is seen that the lattice parameter (a) monotonously decreases with the increases in the Mn-doping level at the Sn-site of pure BSO [see Fig. 1(d)]. The contraction in the lattice parameter is due to the lower effective ionic radius of the six-coordinated (octahedrally) Mn^{4+} ion (0.53 Å) than that of the six-coordinated Sn^{4+} ion (0.69 Å) [30]. This clearly ratifies the successful incorporation of Mn ions into the lattice of BSO.

3.2. X-ray photoelectron spectroscopy

To investigate the chemical valence state of dopant Mn ions, and to probe the existence of surface adsorptive oxygen in the sample, the core-level XPS spectra of Mn and O have been analyzed using XPSPEAK 4.1 software. The Mn $2p$ core-level XPS spectra for $x = 0.06$ is shown in Fig. 2(a). It is seen that the Mn $2p$ spectrum consists of two high intense peaks centered at 639.8 eV and 651.5 eV, and a shoulder peak centered at 643.7 eV. These two high intense peaks mainly correspond to $2p_{3/2}$ and $2p_{1/2}$ spin-orbit (SO) doublets. Thus, the Mn $2p$ SO doublet is separated by about 11.7 eV. It is worthwhile to mention that the energy separation of the SO doublet depends on the strength of SO coupling, and thus on the valence state of the particular ion [31]. An energetic separation of the SO doublets about 11.7 eV confirms that $x = 0.06$ sample contains only Mn^{4+} ions, which is consistent with the earlier reports [32,33]. A small shoulder peak at 643.7 eV can be attributed to Mn^{4+} satellite [32]. Moreover, the satellite to Mn $2p_{3/2}$ peak is reported to be observed on the higher binding energy side, while maintaining the separation energy nearly equal to 12 eV between two satellite peaks [32].

The O $1s$ spectra for $x = 0.06$ is shown in Fig. 2(b). Due to the asymmetric and broad nature of the O $1s$ spectra, deconvolution of the peak profile was done using a Gaussian-Lorentzian distribution function. The O $1s$ peak was fitted considering two peaks, and the obtained peaks are centered at 528.59 eV and 529.77 eV for $x = 0.06$. The peak at lower binding energy is normally associated with the lattice oxygen in

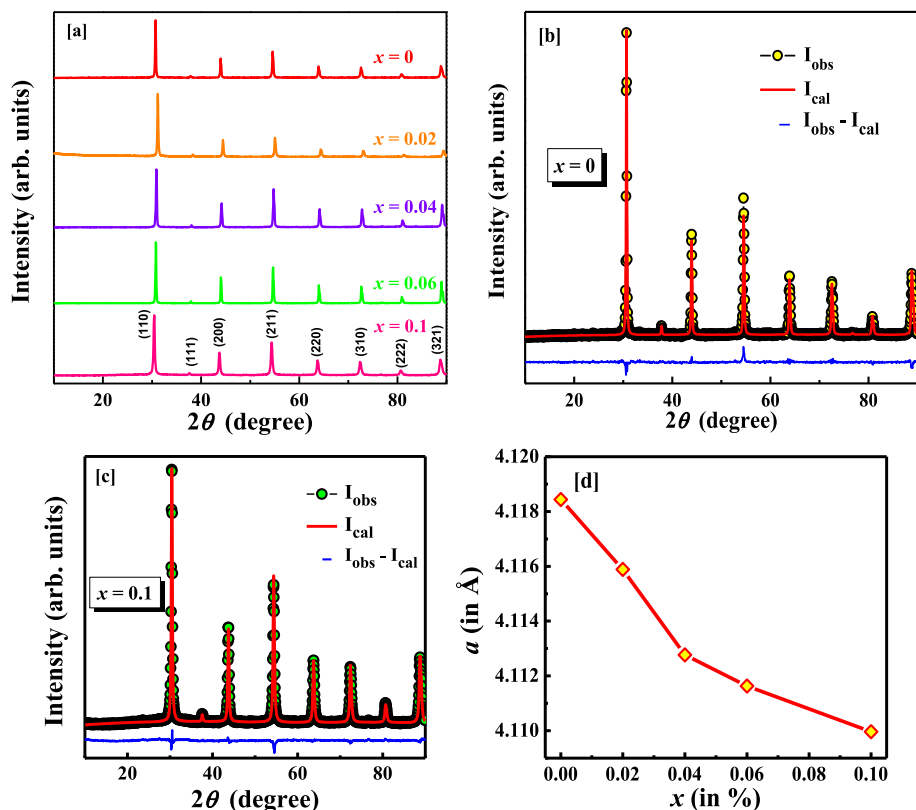


Fig. 1. (a) Room-temperature powder XRD pattern $\text{BaSn}_{1-x}\text{Mn}_x\text{O}_3$ ($0 \leq x \leq 0.1$) samples. Rietveld refinement of powder XRD pattern for (b) $x = 0$ and (c) $x = 0.1$ samples at room-temperature. The black filled circles and solid red line represents the observed and calculated XRD patterns, respectively. The blue line represents the difference between the observed and calculated patterns. (d) The variation of lattice parameter (a) with compositions.

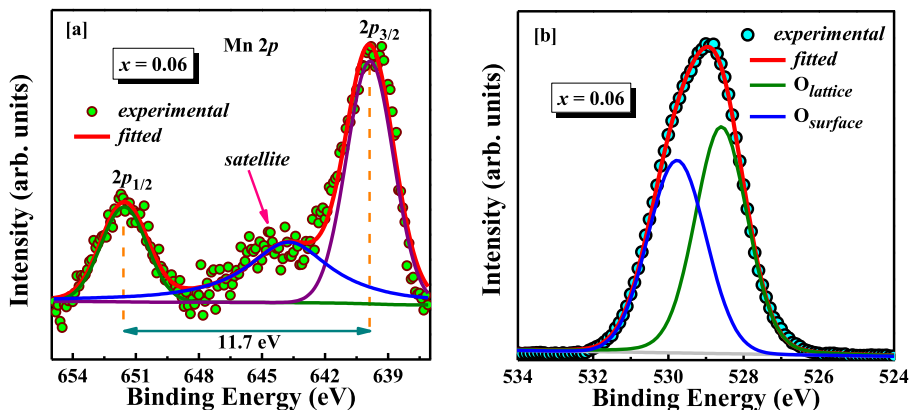


Fig. 2. (a) Core-level XPS spectra of Mn $2p$ level for $x = 0.06$ sample in $\text{BaSn}_{1-x}\text{Mn}_x\text{O}_3$ series at room temperature. (b) The O $1s$ spectra for $x = 0.06$, which shows the presence of surface adsorbed oxygen in the sample.

perovskite oxides. However, according to earlier report [34], the peak at higher binding energy is mainly related to the surface adsorptive oxygen, which has close resemblance to the oxygen vacancy, which has close resemblance to the oxygen vacancy. Note that synthesis procedure can play a crucial role for the creation of oxygen vacancy in the BSO lattice. As the sintering process occurs in air, oxygen is exchanged with the surrounding medium [35].

3.3. Raman spectra

Raman spectroscopy is indeed a powerful experimental technique to probe the dopant incorporation and lattice defects, and to detect the evolution of new phases in the host lattice. Despite the fact that no first-

order Raman-active modes seem to be appeared in the ideal cubic perovskite structure, such as, in highly symmetric cubic BSO with space group $Pm\bar{3}m$, the Raman spectrum for $x = 0$ in Fig. 3 shows some prominent peaks [36,37]. Since the dopant atoms and/or, oxygen vacancies truly affect the translational periodicity of the lattice, the observation of these Raman modes can be ascribed to the local loss of symmetry. Moreover, the most intense Raman bands at 135 cm^{-1} and 154 cm^{-1} for $x = 0$ are quite common in the rhombohedrally distorted perovskite structures [38]. Besides, the lattice-dynamical calculations have predicted that the Raman lines at 135 and 154 cm^{-1} can be assigned to A_{1g} and A_{2g} symmetries, respectively; while, the peak at 570 cm^{-1} is appeared due to Sn-O vibrational mode [37]. So, it can be

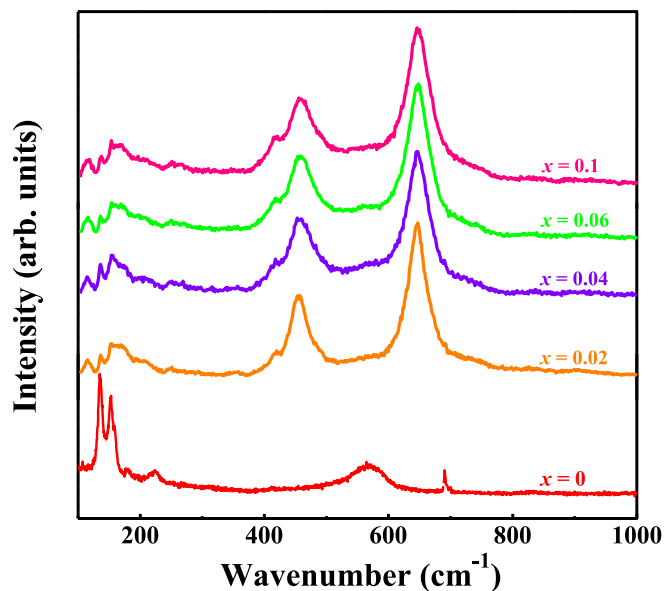


Fig. 3. Raman spectra for $\text{BaSn}_{1-x}\text{Mn}_x\text{O}_3$ ($0 \leq x \leq 0.1$) samples in the wavenumber region $100\text{--}1000\text{ cm}^{-1}$.

concluded that the oxygen vacancies presumably have an important role for the observation of Raman-active modes in $x = 0$.

Furthermore, the breaking of the translational symmetry by virtue of the substitution of Mn^{4+} ion at the Sn-site, in addition to the oxygen vacancy, plays a significant role for the appearance of Raman-active modes in the doped samples [see Fig. 3] [39]. The peak at 570 cm^{-1} for $x = 0$ is completely disappeared with Mn doping; whereas, three new Raman lines centered at 116 , 454 and 648 cm^{-1} appear in the doped samples. The intensity of the Raman lines at 135 and 154 cm^{-1} also reduces with Mn doping, and the Raman modes at 454 cm^{-1} and 648 cm^{-1} become the most intense peaks in doped samples. From our XPS analysis of O 1s spectra, it is evident that the doped samples contain surface adsorptive oxygen and/or, oxygen vacancy, and the percentage of which increases with the increase of doping concentration. The new mode centered at 454 cm^{-1} mainly involved with the oxygen motion, which means the formation of specific defects in host lattice i.e., oxygen vacancies [40,41]. The mode at 648 cm^{-1} is likely to be associated with the Mn–O stretching vibration [42]. Thus, the appearance of a number of Raman-active modes unequivocally fortifies the local lattice distortion induced by oxygen vacancies and dopants in the cubic phase of undoped and doped BSO samples.

3.4. Fourier transform infrared (FTIR) spectra

The FTIR spectra for $x = 0\text{--}0.1$ samples are shown in Fig. 4. A strong minimum in the transmittance data for pure BSO is appeared at 635 cm^{-1} , which can be attributed to the asymmetric stretching vibrational mode of Sn–O bond [43]. It is to be noted that the characteristic vibration of Mn–O and O–Mn–O bonds in the Mn-based oxides usually arise at 522 and 1407 cm^{-1} , respectively [44,45]. Thus, the band centered at 635 cm^{-1} broadens with Mn doping due to the overlap between the Sn–O bond and Mn–O bond. In addition, the vibration of Sn–OH group is most likely to be responsible for the band observed at 1422 cm^{-1} for $x = 0$ [46]. However, the overlapping of O–Mn–O bond and Sn–OH bond causes the band broadening, and as a result, we observe a broader band at 1422 cm^{-1} for the Mn-doped samples. Another broad band centered around 1630 cm^{-1} is seen in the FTIR spectra of $x > 0$, which can be assigned to the stretching mode of OH^- bond [46]. A sharp dip at 860 cm^{-1} for $x > 0$ mainly corresponds to the C–O stretching modes of the CO_3^{2-} ions, signifying that CO_2 is absorbed

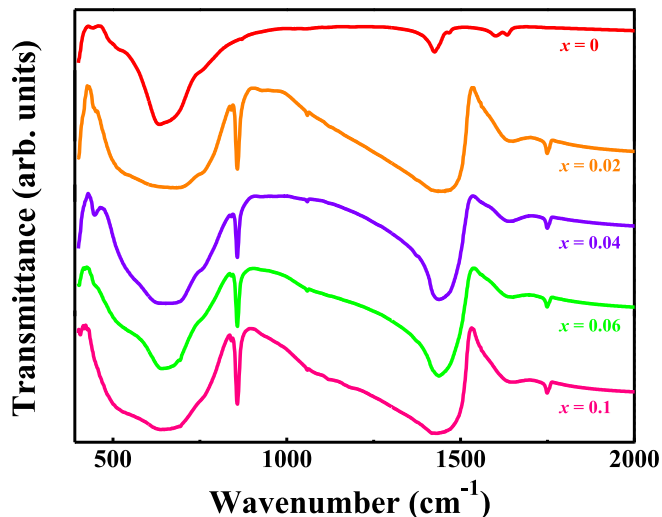


Fig. 4. FTIR spectra for $\text{BaSn}_{1-x}\text{Mn}_x\text{O}_3$ ($0 \leq x \leq 0.1$) samples in the wavenumber region $390\text{--}2000\text{ cm}^{-1}$.

by the samples during the measurement [47].

3.5. Optical absorption spectra

The diffuse reflectance spectra for $x = 0\text{--}0.1$ are displayed in Fig. 5 (a). However, using Kubelka-Munk transformation, we can determine the optical absorbance coefficient (α) for all the samples. The Kubelka-Munk function $F(R)$, which approximately gives us the absorbance, can be defined as [48,49]:

$$F(R) = \frac{(1 - R)^2}{2R} \quad (1)$$

where R is the reflectance. Here, the function $F(R)$ is proportional to optical absorption coefficient (α). The absorption spectra for all the samples are shown in Fig. 5(b). Further, the optical band gap (E_g) can be estimated from the calculated absorption coefficient using the following relation:

$$\alpha h\nu = C(h\nu - E_g)^n \quad (2)$$

where h is the Planck's constant, ν is the incident light frequency, C is the absorption constant, $n = 1/2$ for a direct allowed transition and $n = 2$ for an indirect allowed transition. In this study, the direct band gap for $x = 0\text{--}0.1$ samples has been calculated by extrapolating a straight line towards the $h\nu$ -axis of the Tauc plot [$(\alpha h\nu)^2$ vs $h\nu$], as shown in Fig. 5(c).

The band gap of pure BSO is usually defined as the energy difference between the conduction band minima of Sn 5s bands which are completely vacant for Sn^{4+} ($4d^{10}5s^05p^0$) and the valence band maxima of O 2p bands. From the Tauc plot, the direct band gap of pure BSO is found to be 3.1 eV , which is consistent with the direct band gap value predicted in earlier studies [23]. The hybridization between O 2p orbitals and Sn 5s orbitals results in a clear optical absorption edge at 400 nm [see Fig. 5(b)], thus also confirming the band gap of 3.1 eV for $x = 0$. It is seen that the band gap reduces drastically from 3.1 eV for $x = 0$ to 2.08 eV for $x = 0.1$. Incorporation of Mn^{4+} ions into the lattice of BSO unequivocally enhances the $sp-d$ hybridization between localized d electrons of Mn ions and band electrons, and as a result, the band gap decreases monotonously with increasing doping concentration. In addition, the doped samples appear as darker in color due to the enhanced absorption of light, and thus, increase the absorption efficiency in visible region.

The charge-transfer excitation between O 2p and Mn 3d is considered to be an important precursor for the observed band gap absorption in the

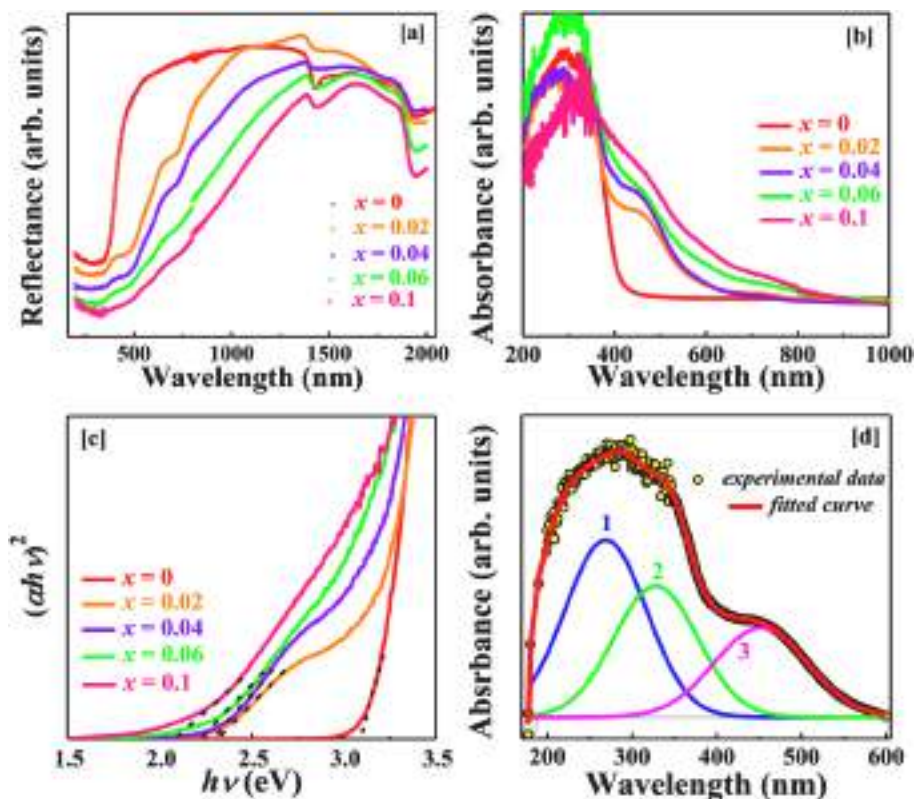


Fig. 5. (a) Optical reflectance spectra for $\text{BaSn}_{1-x}\text{Mn}_x\text{O}_3$ ($0 \leq x \leq 0.1$) samples. (b) UV-vis-NIR optical absorption spectra for $\text{BaSn}_{1-x}\text{Mn}_x\text{O}_3$ ($0 \leq x \leq 0.1$) samples. (c) Tauc plot of $\text{BaSn}_{1-x}\text{Mn}_x\text{O}_3$ ($0 \leq x \leq 0.1$) samples in UV-vis-NIR region for the determination of optical band gap. (d) The deconvoluted optical absorption spectra for $x = 0.02$. The peak 1 corresponds to the charge-transfer excitation band; while, peaks 2 and 3 correspond to the spin-allowed transition bands.

doped samples. To further analyze the origin of broad absorption spectrum, we have deconvoluted the spectrum for $x = 0.02$ with multiple peaks [see Fig. 5(d)]. The absorption band centered at ~ 270 nm (in UV region) mainly appears due to $\text{Mn}^{4+}-\text{O}^{2-}$ charge-transfer transition [50–52]. Besides, the absorption band located at ~ 450 nm can be assigned to the spin-allowed transition of Mn^{4+} : ${}^4\text{A}_{2g} \rightarrow {}^4\text{T}_{2g}$ [51]. Another spin-allowed transition of Mn^{4+} : ${}^4\text{A}_{2g} \rightarrow {}^4\text{T}_{1g}$ results in an absorption band at ~ 320 nm. The overlapping of the charge-transfer band at 270 nm and the spin-allowed transition band at 320 nm leads to a broad absorption band centered at 300 nm in the Mn-doped samples.

3.6. Electron paramagnetic resonance (EPR)

EPR has tuned into an important tool in order to investigate the spin dynamics of the dilute magnetically doped semiconductors (DMSs) having wide band gap. In particular, EPR spectrum provides the information about the nature of spin-spin interactions and the distribution of internal molecular magnetic field, which give us the accessibility to realize the various magnetic phases (such as, paramagnetic, antiferromagnetic cluster, spin-glass) that the materials possess. The EPR spectra at room-temperature for $x = 0.02$ – 0.1 are shown in Fig. 6. The EPR spectra showed a predominant sextet hyperfine structure, arising from the nuclear spin $I = 5/2$ of the isotope Mn^{55} . In this context, it is worthwhile to mention that pure BSO normally shows EPR signal due to the singly ionized oxygen vacancies ($\text{V}_\text{o}^\bullet$) [34].

In order to get a comprehensive idea about the nature of magnetism, the EPR spectrum for each sample was simulated using the *Easyspin* package based on MATLAB [53]. Each spectrum has been simulated by considering a combination of two spin systems (here, *System 1* and *System 2*). *System 1* has spin value $S = 3/2$ with g value centered on 1.958 in rhombic symmetry corresponding to the Mn^{4+} ions, and *System 2* has isotropic g value originating from V_o centers. For d^3 electronic system (S

$= 3/2$), the EPR spectra generally exhibits orthorhombicity [54], which is observed for the doped samples. The ground state of d^3 system ($S = 3/2$) in an octahedral field is ${}^4\text{A}_2$, which interact with excited T_{2g} state by spin-orbit coupling. In an external magnetic field, the degeneracy of the ground state is lifted, and the ground state splits into two Kramer's doublets separated by $2D$ where D is the zero-field splitting parameter. The g value shifts due to the mixing of the ground state and the excited ${}^4\text{T}_2$ state, which splits into an orbital singlet and orbital doublet states. Thus, the mixing with ${}^4\text{T}_2$ state, interaction with other levels and the spin-orbit coupling collectively lead to the zero-field splitting. The spin-Hamiltonian for d^3 electron system ($I = 5/2, S = 3/2$) in octahedral environment is

$$H = \beta B g \cdot S + D \left[S_z^2 - \frac{S(S+1)}{3} \right] + I A \cdot S \quad (3)$$

where the first term is Zeeman interaction, the second term is zero-field splitting, and the third term is hyperfine interaction between electron and nuclear spins.

The value of g , line width (lw) of each component, hyperfine splitting constants, and zero-field splitting parameters have been estimated based on the simulation of experimental data for $x = 0.02$ – 0.1 , as shown in Table 1. Thus, each spectrum consists of a hyperfine split sextet line with splitting constant (A) 78 Oe and a broad signal coming from oxygen vacancy [see Fig. 6(a)–(d)]. This hyperfine structure centered on the parameter $g = 1.958$ and having a hyperfine splitting constant A nearly equal to 78 G (220 MHz) can be attributed to the Mn^{4+} ($3d^3, S = 3/2$) ion [55,56]. It is to be noted that the line width (lw) and the hyperfine splitting constant (A) have one-to-one correspondence between them. Moreover, the combined values of these two parameters result in a measurement of overall width of the sextet. From the obtained simulation results, it is found that the combined value of lw and A for *System 1* increases with increasing Mn doping concentration, suggesting an

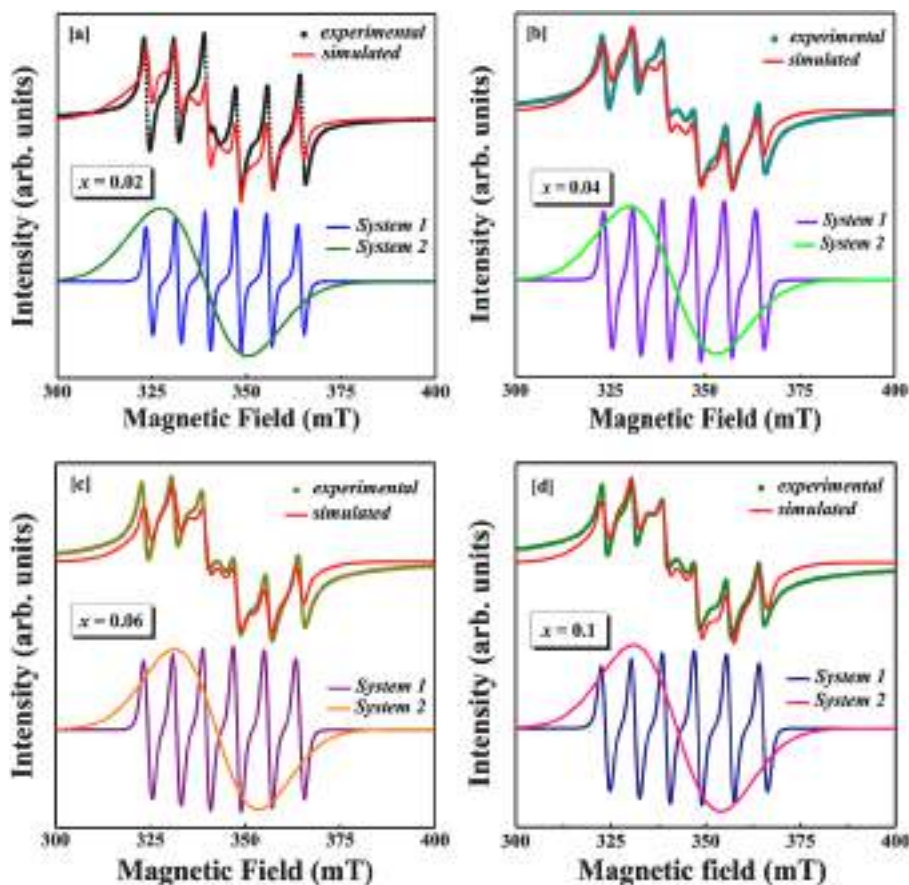


Fig. 6. Experimental (symbols) and simulated (red line) EPR spectra for (a) $x = 0.02$, (b) $x = 0.04$, (c) $x = 0.06$, and (d) $x = 0.1$ at room-temperature. System 1 and System 2 correspond to the contributions from Mn^{4+} ions and V_0 centers, respectively.

Table 1
Simulated parameters of EPR data for different samples at room-temperature.

Doping Concentration (x)	System 1 ($S = 3/2$)					System 2 ($S = 1/2$)	
	g_x	g_y	g_z	A (MHz)	lw (mT)	g	lw (mT)
0.02	1.954	1.958	1.960	220	1.5	1.990	27
0.04	1.954	1.958	1.960	220	2.2	1.975	27
0.06	1.954	1.958	1.960	222	2.2	1.971	27
0.1	1.954	1.958	1.960	228	2.2	1.970	27

increased magnetic interaction between Mn^{4+} ions in the higher doped samples. This also indicates that dipole-dipole interaction is acting among all the paramagnetic centers simultaneously [25]. In contrast, the g value for System 2 slightly decreases with increasing Mn concentration, indicating an enhanced effective molecular magnetic field. However, these g -values for the singly ionized oxygen vacancy lie in the range ~ 1.970 – 1.990 , which is very close to the reported g -value range ~ 1.963 – 1.9920 of singly ionized oxygen vacancy [57].

3.7. Magnetization

The temperature (T) dependence of the zero-field-cooled (ZFC) and field-cooled (FC) magnetic susceptibilities (χ) measured under an applied magnetic field (H) of 500 Oe for $x = 0.06$ and 0.1 are displayed in Fig. 7(a) and (b), respectively. On heating from extreme low temperature (here 2 K), both ZFC and FC susceptibilities for $x = 0.06$ and 0.1 show a decrease in the value with increasing temperature. However, no evidence of long-range magnetic ordering and significant divergence

between ZFC and FC susceptibilities are found for both samples within the investigated temperature range 2–300 K. Although, the samples seem to be paramagnetic (PM) from χ vs. T plots, the inverse susceptibility (χ^{-1}) data do not follow the Curie-Weiss behavior (see the inset in Fig. 7(b)). The observed behavior of $\chi^{-1}(T)$ is quite uncommon in DMSs, and we argue that it may be arising from a combination of two magnetic phases and/or, elements.

As evident from our EPR analysis, both $x = 0.06$ and 0.1 samples contain $3d \text{Mn}^{4+}$ ions and singly ionized oxygen vacancies. Considering that the unusual behavior of $\chi^{-1}(T)$ is arising from a combination of Mn^{4+} ions and singly ionized oxygen vacancies, the $\chi^{-1}(T)$ data is fitted to the equation

$$\chi = \left[(1-y) \frac{C}{T-\theta} + \chi_0 \right] + y \frac{0.363}{T} \quad (4)$$

where y indicates the amount of singly ionized oxygen vacancy, χ_0 is a temperature-independent contribution to the magnetic susceptibility, and C and θ are Curie constant and Curie-Weiss temperature, respectively. The well-fitting to the inverse susceptibility data using above equation for $x = 0.1$ is displayed in Fig. 7(c), which confirms the contributions from both Mn^{4+} ion and singly ionized oxygen vacancy towards the magnetism. The obtained values of y , C , θ and χ_0 are 0.128, 0.0388 (emu-K)/(mol-Oe), -16 K and 6.89×10^{-4} emu mol $^{-1}$ Oe $^{-1}$, respectively. The negative value of θ suggests that the antiferromagnetic (AFM) interaction is dominant in $x = 0.1$ sample, arising from Mn^{4+} -O-Mn $^{4+}$ superexchange interaction. In case of lower doped samples, the non-interacting distant Mn^{4+} ions at the randomly substituted matrix of BSO perhaps induces the paramagnetic nature. Due to the availability of decent Mn^{4+} ions, the AFM coupling becomes stronger in the higher doped sample (e.g., $x = 0.1$).

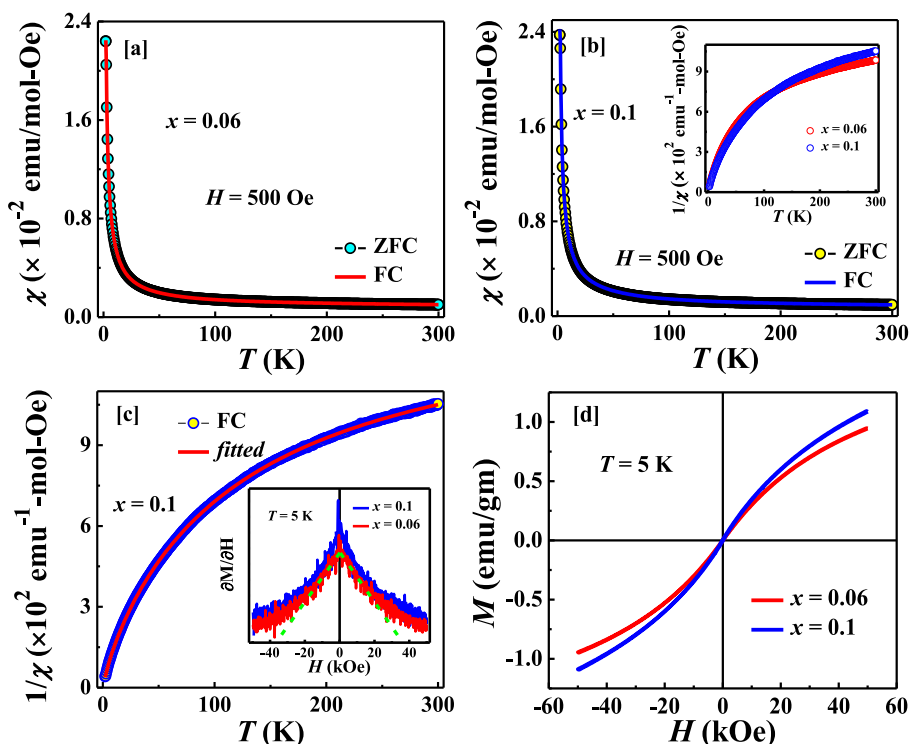


Fig. 7. Temperature dependence of the ZFC (symbols) and FC (lines) magnetic susceptibilities for (a) $x = 0.06$ and (b) $x = 0.1$, measured with an applied magnetic field H of 500 Oe in the temperature range of 2–300 K. Inset in (b) shows the temperature dependence of the inverse susceptibilities for $x = 0.06$ and 0.1, using FC data. The red line in (c) depicts the fit to the inverse susceptibility data using equation (4) for $x = 0.1$. (d) Isothermal magnetic field-dependent magnetization (M – H) curves at $T = 5$ K for $x = 0.06$ and 0.1. Inset in (c) displays the first derivative of magnetization with respect to magnetic field $\partial M/\partial H$ as a function of H for $x = 0.06$ and 0.1.

Isothermal magnetization curves (M versus H) at $T = 5$ K for $x = 0.06$ and 0.1 are shown in Fig. 7(d). The observed M – H curves having negligible coercive field are akin to that of previously reported Mn-based DMS systems [58]. The magnetization does not saturate in both the cases for fields as large as 50 kOe, clearly indicating the PM/AFM nature of the samples. However, a closer inspection of the first derivative of magnetization $\partial M/\partial H$ (see the inset in Fig. 7(c)) reveals a much more complex phenomenon of magnetic interactions, other than simple PM phase. It should be noted that one would expect the constant value of $\partial M/\partial H$ for linear response of magnetization with field in case of an ideal paramagnet.

4. Conclusions

In conclusion, we have successfully synthesized the polycrystalline samples of DMSs $\text{BaSn}_{1-x}\text{Mn}_x\text{O}_3$ ($0 \leq x \leq 0.1$) by standard solid-state-reaction method, and investigated the structural, optical spectroscopic and magnetic properties. Precise analysis of the XRD data reveals that all samples crystallize in the cubic structure with space group $Pm\bar{3}m$, and the lattice parameter monotonously decreases owing to the incorporation of smaller ionic radii Mn^{4+} ions into the lattice of BSO. The optical band gap decreases with increase of Mn dopants concentration due to the enhanced sp – d hybridization between localized d electrons of Mn ions and band electrons. An in-depth analysis of both EPR and magnetization data confirms that Mn^{4+} ions and singly ionized oxygen vacancies are collectively responsible for the observed magnetization behavior in the doped samples, and the nature of magnetic interaction is especially antiferromagnetic in the higher doped samples. We hope the present study provides a deeper understanding of the nature of magnetic interaction in DMSs $\text{BaSn}_{1-x}\text{Mn}_x\text{O}_3$, which allows researchers to design DMSs having unique physical properties based on BaSnO_3 perovskite oxides for potential technological applications.

Declaration of competing interest

The authors declare that they have no known competing financial

interests or personal relationships that could have appeared to influence the work reported in this paper.

Data availability

No data was used for the research described in the article.

Acknowledgments

Ankita Sarkar (IF150001) would like to thank the Department of Science and Technology (DST), Government of India for providing a DST-INSPIRE Fellowship during the tenure of work.

References

- [1] T. Dietl, H. Ohno, F. Matsukura, J. Cibert, D. Ferrand, *Science* 287 (2000) 1019.
- [2] Y. Matsumoto, M. Murakami, T. Shono, T. Hasegawa, T. Fukumura, M. Kawasaki, P. Ahmet, T. Chikyow, S.-Y. Koshihara, H. Koinuma, *Science* 291 (2001) 854.
- [3] K. Ueda, H. Tabata, T. Kawai, *Appl. Phys. Lett.* 79 (2001) 988.
- [4] J.H. Kim, H. Kim, D. Kim, Y.E. Ihm, W.K. Choo, *J. Appl. Phys.* 92 (2002) 6066.
- [5] P.A. Stamps, R.J. Kennedy, Y. Xin, J.S. Parker, *J. Appl. Phys.* 93 (2003) 7864.
- [6] P. Sharma, A. Gupta, K.V. Rao, F.J. Owens, R. Sharma, R. Ahuja, J.M.O. Guillen, B. Johansson, G.A. Gehring, *Nat. Mater.* 2 (2003) 673.
- [7] S.S. Farvid, L. Ju, M. Worden, P.V. Radovanovic, *J. Phys. Chem. C* 112 (2008), 17755.
- [8] J.L. MacManus-Driscoll, N. Khare, Y. Liu, M.E. Vickers, *Adv. Mater.* 19 (2007) 2925.
- [9] S.Y. Park, P.J. Kim, Y.P. Lee, S.W. Shin, T.H. Kim, J.-H. Kang, J.Y. Rhee, *Adv. Mater.* 19 (2007) 3496.
- [10] H.-S. Kim, L. Bi, G.F. Dionne, C.A. Ross, H.-J. Paik, *Phys. Rev. B* 77 (2008), 214436.
- [11] K.G. Roberts, M. Varela, S. Rashkeev, S.T. Pantelides, S.J. Pennycook, K. M. Krishnan, *Phys. Rev. B* 78 (2008), 014409.
- [12] T. Kimura, T. Goto, H. Shintani, K. Ishizaka, T. Arima, Y. Tokura, *Nature (London)* 426 (2003) 55.
- [13] R.J. Cava, B. Batlogg, J.J. Krajewski, R. Farrow, L.W. Rupp Jr., A.E. White, K. Short, W.F. Peck, T. Komietani, *Nature (London)* 332 (1988) 814.
- [14] H.J. Kim, U. Kim, T.H. Kim, J. Kim, H.M. Kim, B.-G. Jeon, W.-J. Lee, H.S. Sik Mun, K.T. Hong, J. Yu, K. Char, K.H. Kim, *Phys. Rev. B* 86 (2012), 165205.
- [15] Y.-H. Lin, S. Zhang, C. Deng, Y. Zhang, X. Wang, C.-W. Nan, *Appl. Phys. Lett.* 92 (2008), 112501.
- [16] L.B. Luo, Y.G. Zhao, H.F. Tian, J.J. Yang, H.Y. Zhang, J.Q. Li, J.J. Ding, B. He, S. Q. Wei, C. Gao, *Appl. Phys. Lett.* 92 (2008), 232507.

- [17] A.B. Posadas, C. Mitra, C. Lin, A. Dhamdhere, D.J. Smith, M. Tsoi, A.A. Demkov, *Phys. Rev. B* 87 (2013), 144422.
- [18] H.-S. Kim, L. Bi, G.F. Dionne, C.A. Ross, *Appl. Phys. Lett.* 93 (2008), 092506.
- [19] H.-S. Kim, L. Bi, D.H. Kim, D.-J. Yang, Y.J. Choi, J.W. Lee, J.K. Kang, Y.C. Park, G. F. Dionne, C.A. Ross, *J. Mater. Chem.* 21 (2011), 10364.
- [20] B. Hadjarab, A. Bouguelia, M. Trari, *J. Phys. Chem. Solid.* 68 (2007) 1491.
- [21] P. Singh, D. Kumar, O. Parkash, *J. Appl. Phys.* 97 (2005), 074103.
- [22] U. Lampe, J. Gerblinger, H. Meixner, *Sens. Actuators, B* 24–25 (1995) 657.
- [23] H. Mizoguchi, H.W. Eng, P.M. Woodward, *Inorg. Chem.* 43 (2004) 1667.
- [24] H.J. Kim, J. Kim, T.H. Kim, W.-J. Lee, B.-G. Jeon, J.-Y. Park, W.S. Choi, D. W. Jeong, S.H. Lee, J. Yu, T.W. Noh, K.H. Kim, *Phys. Rev. B* 88 (2013), 125204.
- [25] K. Balamurugan, N. Harish Kumar, B. Ramachandran, M.S. Ramachandra Rao, J. Arout Chelvane, P.N. Santhosh, *Solid State Commun.* 149 (2009) 884.
- [26] K. Balamurugan, N. Harish Kumar, J. Arout Chelvane, P.N. Santhosh, *J. Alloys Compd.* 472 (2009) 9.
- [27] Q. Liu, Y. He, H. Li, B. Li, G. Gao, L. Fan, J. Dai, *APEX* 7 (2014), 033006.
- [28] H.M. Rietveld, *J. Appl. Crystallogr.* 2 (1969) 65.
- [29] M. Ferrari, L. Lutterotti, *J. Appl. Phys.* 76 (1994) 7246.
- [30] R.D. Shannon, *Acta Crystallogr. A* 32 (1976) 751.
- [31] B. Dalal, B. Sarkar, S.K. De, *J. Phys. Condens. Matter* 29 (2017), 495803.
- [32] S. Li, S. Wang, Y. Lu, C. Zhang, X. Yang, J. Gao, D. Li, Y. Zhu, W. Liu, *AIP Adv.* 8 (2018), 015009.
- [33] Y.-K. Hsu, Y.-C. Chen, Y.-G. Lin, L.-C. Chen, K.-H. Chen, *J. Mater. Chem.* 22 (2012) 2733.
- [34] A. Sarkar, S.K. De, *Semicond. Sci. Technol.* 33 (2018), 035018.
- [35] I.A. Alagdal, A.R. West, *J. Mater. Chem. C* 4 (2016) 4770.
- [36] T.C. Damen, S.P.S. Porto, B. Tell, *Phys. Rev.* 142 (1966) 570.
- [37] C. Bundesmann, N. Ashkenov, M. Schubert, D. Spemann, T. Butz, E.M. Kaidashev, M. Lorenz, M. Grundmann, *Appl. Phys. Lett.* 83 (2003) 1974.
- [38] M.V. Abrashev, A.P. Litvinchuk, M.N. Iliev, R.L. Meng, V.N. Popov, V.G. Ivanov, R. A. Chakalov, C. Thomsen, *Phys. Rev. B* 59 (1999) 4146.
- [39] B. Cheng, Y. Xiao, G. Wu, L. Zhang, *Appl. Phys. Lett.* 84 (2004) 416.
- [40] J.B. Wang, G.J. Huang, X.L. Zhong, L.Z. Sun, Y.C. Zhou, *Appl. Phys. Lett.* 88 (2006), 252502.
- [41] Y. Sun, X. Zhang, N. Li, X. Xing, H. Yang, F. Zhang, J. Cheng, Z. Zhang, Z. Hao, *Appl. Catal., B* 251 (2019) 295.
- [42] J. Xu, J.H. Park, H.M. Jang, *Phys. Rev. B* 75 (2007), 012409.
- [43] C. Shan, T. Huang, J. Zhang, M. Han, Y. Li, Z. Hu, J. Chu, *J. Phys. Chem. C* 118 (2014) 6994.
- [44] S. Maiti, A. Pramanik, S. Mahanty, *ACS Appl. Mater. Interfaces* 6 (2014), 10754.
- [45] D. Ghosh, S. Bhandari, D. Khastgir, *Phys. Chem. Chem. Phys.* 18 (2016), 32876.
- [46] C. Huang, X. Wang, Q. Shi, X. Liu, Y. Zhang, F. Huang, T. Zhang, *Inorg. Chem.* 54 (8) (2015) 4002.
- [47] W. Lu, H. Schmidt, *Ceram. Int.* 34 (3) (2008) 645.
- [48] R.A. Zargar, M. Arora, R.A. Bhat, *Appl. Phys.* 124 (2018) 36.
- [49] R.A. Zargar, *Sci. Rep.* 12 (2022), 10096.
- [50] C. Tian, H. Lin, D. Zhang, P. Zhang, R. Hong, Z. Han, X. Qian, J. Zou, *Opt Express* 27 (22) (2019), 32666.
- [51] R. Cao, F. Zhang, C. Cao, X. Yu, A. Liang, S. Guo, H. Xue, *Opt. Mater.* 38 (2014) 53.
- [52] K. Drdlikova, D. Drdlik, H. Hadraba, R. Klement, K. Maca, *J. Eur. Ceram. Soc.* 40 (14) (2020) 4894.
- [53] S. Stoll, A. Schweiger, *J. Magn. Reson.* 178 (1) (2006) 42.
- [54] A. Zorko, M. Pregelj, H. Luetkens, A.-K. Axelsson, M. Valant, *Phys. Rev. B* 89 (2014), 094418.
- [55] K. Alexander Müller, *Phys. Rev. Lett.* 2 (8) (1959) 341.
- [56] J.M. Peloquin, K.A. Campbell, D.W. Randall, M.A. Evanchik, V.L. Pecoraro, W. H. Armstrong, R. David Britt, *J. Am. Chem. Soc.* 122 (44) (2000), 10926.
- [57] R.A. Zargar, K. Kumar, M. Arora, M. Shkir, H.H. Smaili, H. Algarni, S. AlFaify, *J. Lumin.* 245 (2022), 118769.
- [58] S. Paul, B. Dalal, M. Das, P. Mandal, S.K. De, *Chem. Mater.* 31 (2019) 8191.



REVIEW

Catalytic Organic Reactions in Liquid Phase by Perovskite Oxides: A Review

RAJIB MISTRI

Department of Chemistry, Achhruram Memorial College, Jhalda, Purulia-723202, India

Corresponding author: E-mail: rajibmistri@yahoo.co.in

Received: 20 June 2022;

Accepted: 22 July 2022;

Published online: 19 September 2022;

AJC-20949

The structural flexibility and controllable physico-chemical characters of perovskite oxides have drawn major attention of researchers for catalytic reactions. Perovskite oxide are mainly used as catalysts for electrochemical, high temperature gas-phase and photocatalytic reactions but their uses for catalytic organic reactions in liquid phase are limited. Various porous and nano-perovskite oxides have been prepared by different methods are effectively used as catalyst for different types of organic reactions in liquid phase. The liquid-phase catalytic organic reactions over perovskite oxides have been classified mainly into three groups: (i) acid/base catalyzed, (ii) selective oxidation and (iii) cross-coupling reactions. This review article mainly emphasizes on different examples of perovskite oxides catalyzed organic reactions in liquid phase along with the relationships among the unique catalytic performance with the structural and the physico-chemical properties of perovskites.

Keywords: Organic reactions, Liquid-phase, catalyst, Perovskite oxides, Structures.

INTRODUCTION

Modern day's chemical industry is in need of technology for generation of sustainable as well as environmentally-safe chemical processes [1-12]. In state of conventional technologies, catalytic processes can apply for the production of various industrially important chemicals due to its economic and environmental benefits. Numerous homogeneous catalysts have been industrially applied for catalytic organic reactions in liquid phase through green synthetic route. These catalysts are highly active as well as selective due to their structure and precisely controllable reactivity [13]. However, the major disadvantages of homogeneous catalysts for large scale application in industrial processes are catalyst separation and various problems in reuse of these costly catalysts [14-16]. These disadvantages can be circumvented through the use of easily recyclable heterogeneous catalysts for the environmental friendly synthesis of expensive important chemicals. Several metal hydroxides or oxides [17-20], polyoxometalates [21,22], zeolites [23,24], metal nanoparticles [25,26], metal-organic frameworks [27,28], polymers [29,30], dendrimers [31] and carbon-based materials [32,33] have been efficiently applied as heterogeneous catalysts for organic reactions in liquid-phase.

Recently, perovskite oxides (with common formula ABO_3) have drawn much attention due to their versatile applications likes magnetic, multi-ferroelectric, piezoelectric, superconducting and also heterogeneous catalytic properties [34-51]. Different perovskite oxides were studied as catalyst for electrochemical reactions [34-38], high temperature gas-phase reactions [39-49] and photocatalytic [47-51] due to their structural stability, flexibility, diversity and controllable physico-chemical properties. Though industrially important perovskite catalyzed organic reactions in liquid-phase have been limited reports [52-88]. Recently several researchers reported porous nano perovskite oxide synthesized by different methods could be used as heterogeneous catalyst for organic reactions in liquid-phase such as acid/base-catalyzed organic reactions [52-57], selective oxidations [58-76], cross-coupling reactions [77-81] and some other hydrogenation/oxidation reactions [82-88]. Table-1 listed various examples of perovskite oxide-based materials as heterogeneous catalyst for organic reactions in liquid phase.

Numerous examples of perovskite oxide catalyzed organic reactions in liquid-phase are highlighted in this review. In addition, their synthesis, structures, physico-chemical properties and environmental-friendly catalytic applications are also summarized.

TABLE-1
 VARIOUS HETEROGENEOUS PEROVSKITE OXIDE CATALYSTS FOR ORGANIC REACTIONS IN LIQUID PHASE

Catalyst/additive	Reaction	Yield	Time (h)	Ref.
Acid/base-catalyzed reaction				
BaZrO ₃		53	1.5	[52]
HTiNbO ₅ nanosheets		17	6	[53]
SmFeO ₃		98	1	[54]
Mesoporous ZnTiO ₃		90-94	14-24	[55]
Mesoporous ZnTiO ₃		73-92	15-18	[55]
ZnTiO ₃ /CTAB		71-94	8	[56]
BiFeO ₃		63-88	-	[57]
Selective oxidation				
Cu/LaFeO ₃		99	3	[58]
LaCrO ₃		84-97	7-8.5	[60]
KNbO ₃		30, 70	1	[61]
Y ₂ BaCuO _{3-x}		18, 14, <1	0.5	[62,63]
CuZrO ₃		69	2	[64]
AuPd/LaMnO ₃ NaOH		70, 17	6	[65]

$\text{Pd}_{0.002}\text{K}_{0.17}\text{Ti}_{1.86}\text{Sr}_{0.20}\text{O}_4$ $\text{Pd}_{0.03}\text{K}_{0.03}\text{Ti}_{1.47}\text{Sr}_{1.02}\text{O}_4$		30-99	24	[66]
La_2CuO_4		70-90	–	[67]
SrMnO_3		81-99	1-10	[68]
SrMnO_3		81-94	8-24	[70]
$\text{BaFeO}_{3.6}$		14-59	72-96	[71]
BaRuO_3		50-90	12-60	[72]
$(\text{La,Sr})_{0.5}(\text{Co,Mn})_{0.5}\text{O}_{3.8}/\text{NHPI}$		99	99	[73]
KTaO_3		58	4	[74]
$\text{BaFeO}_{3.6}$		75	30	[76]
Coupling Reaction				
$\text{LaFe}_{0.57}\text{Co}_{0.38}\text{Pd}_{0.05}\text{O}_3$ /base-TBABr		26-95	0.5-18	[77,78]
$\text{La}_{0.9}\text{Ce}_{0.1}\text{Co}_{0.6}\text{Cu}_{0.4}\text{O}_3$ /base-EtOAc		46-90	48	[79]
$\text{La}_{0.9}\text{Ce}_{0.1}\text{Co}_{0.6}\text{Cu}_{0.4}\text{O}_3$ /base		47-96	6-24	[80]
$\text{Bi}_{1.97}\text{Eu}_{0.03}\text{MoO}_6$		90-97	0.5-1	[81]

Other Reaction				
LaFeO ₃ /KOH		78-98	2-6	[82]
LaCo _{0.8} Fe _{0.2} O ₃		89	6	[84]
Pt/YCo _{0.3} Fe _{0.7} O ₃		95	0.5	[85]
LaMnO ₃		99	24	[86]
LaMnO ₃		66	24	[86]
LaMo _{0.1} Fe _{0.9} O ₃		92	0.3	[87]
LaMnO ₃		95	3	[88]

Synthesis and structure of perovskite catalysts: A number of combination of A- and B-site is possible to procedure ABO₃ structure of perovskite oxide [46,89,90]. Partial substitution of either or both sites (A and B) by other metals can control metal cation's oxidation states and oxygen stoichiometry in multi-component perovskite compositions. Therefore, the adjustable composition of perovskites could lead to structure flexibility with useful physico-chemical characters. Many wonderful books and articles presented the synthesis, structures, characteristic features and uses of perovskite oxides in detail [34-51].

Synthesis of perovskite catalysts: The purity, surface area, particles size or shape and pores size/amounts of perovskite oxides are strongly depending on their synthesis methods [34,89,90]. Ultrapure perovskites can be prepared from pure metal component by the solid-state synthesis method but these synthesized perovskites are mainly use for electrical and electronic applications. But the enormously low surface area (~ 1 m² g⁻¹) of these perovskite limits their overall performance as effective bulk catalyst [4]. Liquid-phase organic reactions are

mainly performed under mild reaction conditions; therefore, relatively high surface area of perovskite catalysts is one of most important factor for a highly efficient catalytic system. Generally, perovskite oxide catalysts are prepared by co-precipitation [65,67-69], solgel [61,64,65,69-73], solution combustion [57,58] and hard-soft templating [82] methods. In co-precipitation, a suitable precipitant (NaOH, ammonia, amines) is slowly mixed to an aqueous two or more metal salts solution generally as metal nitrate and gives a homogeneous mixture. The resultant precipitates wash with pure solvents then calcine at a proper temperature. Different perovskites, ABO₃ (A = La, Sm, Pr and B = Fe, Cr, Mn, Ni, Co), are synthesized by co-precipitation method using *n*-butyl amine as a precipitant [68]. A super-critical anti-solvent precipitation method is also used for the synthesis of LaBO₃ (B = Fe, Cr, Co, Ni, Mn) with high surface areas (22-52 m² g⁻¹) [65]. In co-precipitation method, soluble metal complexes are produced in precipitation step and particular cations are also loss in washing step. Thus controlling the composition of perovskites is difficult in this method.

Perovskites with controlled chemical composition as well as relatively high surface areas are prepared by simple and useful sol-gel method. Malic acid and citric acid most frequently used in sol-gel method for synthesis of perovskites [91,92]. $\text{La}_{0.8}\text{Sr}_{0.2}\text{MO}_3$ ($M = \text{Co}$ and Mn with surface area $20 \text{ m}^2 \text{ g}^{-1}$ and $37 \text{ m}^2 \text{ g}^{-1}$, respectively) with high surface-area have synthesized from aqueous metal salts solution and malic acid at pH 3-4 [92]. The polymerized complex method and the Pechini method have also been well-studied for perovskites synthesis [93,94]. Hexagonal SrMnO_3 (surface area $25 \text{ m}^2 \text{ g}^{-1}$) have synthesized by polymerized complex method [69]. SrMnO_3 with appreciable large surface area ($\leq 47 \text{ m}^2 \text{ g}^{-1}$) also fruitfully synthesized without pH adjustment by using metal acetates and aspartic acid rather than metal nitrates [70] and other hexagonal perovskite materials was also synthesized by this method [71,72].

The single step solution combustion method is also use for synthesis of perovskite nanoparticles, which involves the combustion of corresponding metal salts (mostly nitrates and chlorides in some cases) with appropriate organic fuels (citric acid, urea, glycine, glycerol, *etc.*). The reaction itself supplied the required heat for phase formation. Therefore, heating temperature is lower than the conventional paths and calcination step is not required. The copper substituted LaMO_3 ($M = \text{Fe}$, Mn , Co) catalysts with surface area $10\text{-}27 \text{ m}^2 \text{ g}^{-1}$ was synthesis by single-step solution combustion method [58]. This synthesis method has also been useful for rapid synthesis of different multicomponent perovskites. But, it is difficult to control parameters of the process and maintains the quality of final product by using this preparation method.

Soft and hard templating methods most comprehensively studied for the preparation of porous perovskite materials by using porous silicates and polymeric materials [48]. The perovskite nanoparticles have no pores and the reaction happens only on the surface of the catalyst, which restrict the overall catalytic performance [68]. The ZnTiO_3 , mesoporous perovskite, with $136 \text{ m}^2 \text{ g}^{-1}$ surface area and 5.1 nm averaged pore dimension was synthesized by using a nonionic surfactant template (Pluronic P123) in a new evaporation-induced self-assembly method [61]. Hence, the soft and hard templating methods provide large surface areas ($> 100 \text{ m}^2 \text{ g}^{-1}$) with orderly pore structures but the method complicity, requirement of costly templates and also difficulty in their successive removal makes the applicability of this method is limited.

Although, nanosized and porous suitable perovskite oxides prepared by the aforesaid methods are mainly applied as efficient catalysts. The typically inactive perovskite oxides may be used as supports for different supported metal catalysts and a synergistic effect of perovskite oxide and metal nanoparticles has been suggested for some reactions [65,73,85]. The details applications of all these perovskite oxides for catalytic organic reactions in liquid-phase are described as follows:

Structure of perovskite catalysts: The perovskite oxides are ideally cubic in crystal structure, where large cations (A) have twelve-fold and smaller cations (B) have six-fold coordination with BO_6 octahedra corner-sharing [4]. The tolerance factor (t) is used for indexing the deviation from this ideal structure and is estimated from eqn. 1 (r_A = cationic radius of

A, r_B = cationic radius of B and r_O = anionic radius of O^{2-}) [89,90].

$$t = \frac{(r_A + r_B)}{\sqrt{2(r_B + r_O)}} \quad (1)$$

The ideal cubic perovskite has t value 1. When the t value is lower than 1 (0.75 to 1), the perovskite gives tetragonal, rhombohedral, or lower symmetric structure [89]. The greater t values (> 1) are obtained when we use large alkaline-earth metal cations (A^{2+}) or small B cations and showing hexagonal crystal structure with BO_6 octahedra face-sharing [70,71]. Two-dimensional perovskite with inter leaved cations are showing layered structures is also reported [89].

Different perovskite oxides are design for catalytic organic reactions in liquid-phase. The crystalline structure, formation of oxygen vacancy and the oxidation state of B can be changed by controlling the chemical composition of perovskite oxides. When an A^{3+} ion is replaced by an A^{2+} cation from $\text{A}^{3+} \text{B}^{3+} \text{O}_3$ then increased the oxidation state of B or formed oxygen vacancy [4]. The details applications of all these perovskite oxides as catalyst for organic reaction in liquid-phase along with the relationships between the unique catalytic properties and the structural, the physico-chemical properties are also discussed.

Catalytic applications of perovskite oxide for organic reactions in liquid-phase: The catalytic activity of perovskite oxides strongly depends on their physico-chemical properties. It has been reported that crystalline structure [69,70], formation energy for oxygen vacancy [71], oxygen adsorption capacity [65], surface oxygen vacancy [64,73] and oxidation state of B cation [72] play significant roles for the perovskite oxide catalyzed organic reactions in liquid phase. Several absorptions, spectroscopic and computational methods have been used for characterization of the redox and acidic-basic properties of perovskite oxides [21-23,25,26,29]. The oxygen mobility and reducibility are usually analyzed by hydrogen temperature programmed reduction (TPR), isotopic exchange experiments and temperature programmed desorption (TPD) for the characterization of redox properties. Adsorption micro-calorimetry, site titration using Hammett indicators, TPD and spectroscopy are exclusively used for the analysis of surface acidity/basicity of perovskites. The bulk and surface structures are characterized by infrared spectroscopy (IR), X-ray diffraction (XRD), extended X-ray absorption fine structure (EXAFS), X-ray photoelectron spectroscopy (XPS), Raman spectroscopy and high resolution transmission electron microscope (HRTEM) measurements. However, most publications mainly focus on development of perovskite oxide-catalyzed organic reactions in liquid-phase. Hence, such characterizations in most systems are incomplete and lack of comprehensive mechanistic studies. In this review, the important catalytic property of perovskite oxides in liquid phase is comprehensively summarized and some of the reaction mechanism along with the characterization results is also discussed.

Acid/base-catalyzed reactions: The petroleum refining and petrochemical industry have been utilized solid acid-bases as catalysts for lots of important processes [95-100]. Zeolites,

clays, resins, hetero polyacids, mono or mixed metal oxides and a catalyst with surface modification have been extensively examined as acid-base catalyst. However, the performance of perovskite oxides as acid-base catalyst are still under explored. In recent times, a review article systematically summarized catalytic performance of perovskites as acid-base catalyst [42]. The effects of density, strength, surface modification, exposed faces and type of acid-base sites of perovskite oxides to their performance as catalyst have been studied for the conversion of 2-propanol [53]. In contrast, acid-base catalysis in liquid-phase and comprehensive reaction mechanisms studies are still limited.

$\text{HSr}_2\text{Nb}_3\text{O}_{10}$ and HTiNbO_5 nanosheets with modified surface area were reported as acid catalysts for acetic acid esterification, cumene cracking and 2-propanol dehydration [53]. Cyano-silylation with trimethylsilyl cyanide (TMSCN) of carbonyl compounds to corresponding cyanohydrins trimethylsilyl ethers is a key reaction for production of α -hydroxy aldehydes or acids and β -amino alcohols. SmFeO_3 showed significant activity towards the catalytic cyano-silylation of benzaldehyde by trimethylsilyl cyanide in comparison to other catalysts used for this reaction [54]. But, it is proposed that the active sites of SmFeO_3 was the Brønsted acid sites but results were lack of detail characterization. A new mesoporous ZnTiO_3 perovskite was developed as an efficient catalyst for Friedel-Crafts alkylation by benzyl chloride along with the esterification of C_{12} - C_{18} carboxylic acids [55,56]. A probable mechanism was suggested for the ZnTiO_3 -catalyzed esterification that carboxylic acid was activated through coordination with the Lewis acid site. The same group also stated that reusable nano ZnTiO_3 base catalyst with cubic structure prepared *via* sol-gel method for 1,6-naphthyridine synthesis in water [56]. The cooperative action of Ti^{4+} as Lewis acid site and O^{2-} as base site for the probable reaction mechanism is also proposed.

Preparation of hydroxypivaldehyde is a key reaction, since the product gives neopentyl glycol on successive hydrogenation and it is an intermediate of plasticizers, polyesters, lubricants and synthetic paints. SrZrO_3 and BaZrO_3 exhibited good catalytic activity towards this base-catalyzed aldol condensation reaction of isobutyl aldehyde by formaldehyde with 53% yield along with 91% conversion [52].

Different dihydro-2-oxypyrrroles was synthesized by one-pot synthesis from dimethyl acetylene dicarboxylate, formaldehyde and anilines in methanol over BiFeO_3 catalyst at room temperature [57]. An external magnet could easily recover the used catalyst from the reaction medium and the recovered catalyst was efficiently reused. The authors proposed that an imine intermediate was activated through Lewis acid sites of BiFeO_3 helps a Mannich type reactions by successive cyclization reactions, even though there was no physico-chemical evidence regarding this acid sites.

Selective catalytic oxidation: Selective catalytic oxidation of petroleum-based feed stocks into suitable compounds is a significant reaction since the products are extensively applied for synthesis of valuable products and important chemicals [101-108]. The CO oxidation and total oxidation of different hydrocarbons are extensively reported over perovskite oxide

catalysts [39-43,84]. Several efficient perovskite oxides catalysts are used for selective oxidation reactions in liquid phase by using molecular oxygen (O_2), hydrogen peroxide (H_2O_2) and *tert*-butyl hydroperoxide (TBHP) as oxidant [58-76]. The kinds of catalyst and oxidant played important role for the catalytic efficiency as well as for the reaction mechanism. Preparation of particular widely used important carbonyl compounds from corresponding alcohols *via* selective oxidation due to production of fine chemicals and pharmaceuticals products. Copper-substituted $\text{LaFeO}_3(\text{Cu}/\text{LaFeO}_3)$ perovskite developed as a reusable catalyst for selective oxidation of benzyl alcohol with TBHP [58]. The combustion synthesized catalyst showed higher activity due to the presence of a peculiar poorly-defined amorphous CuO along with substitutional Cu^{2+} phase on the top of LaFeO_3 particle. Cerium doped rhombohedral $\text{La}_{1-x}\text{Ce}_x\text{CoO}_3$ nano perovskite was also act as an effective catalyst for the same reaction in liquid medium under atmospheric pressure using highly pure oxygen as oxidant. Under optimum reaction conditions, among the prepared catalysts $\text{La}_{0.95}\text{Co}_{0.05}\text{O}_3$ catalyst showed higher catalytic activity (> 35%) with ~ 100% selectivity upto four cycles [59]. Reusable LaCrO_3 catalyst also reported for the oxidation of alkyl arenes using TBHP under solvent-free condition [60]. However, H_2O_2 and O_2 have received much consideration than organic hydroperoxides due to their environmental-friendly nature (gives water only as byproduct) and also content high active oxygen species. Titanium loaded potassium niobates ($\text{KTi}_{0.2}\text{Nb}_{0.8}\text{O}_3$ and $\text{KTi}_{0.1}\text{Nb}_{0.9}\text{O}_3$) perovskite developed for the selective catalytic oxidation of 2-(methyl-thio)benzothiazole with excess H_2O_2 to the analogous sulfone and sulfoxide [61]. The electronic and structural defects were due to incorporation of titanium ions into the perovskite lattice for the higher activity of titanium substituted catalyst than the pure potassium niobates (KNbO_3). The $\text{Y}_2\text{BaCuO}_{5\pm x}$ perovskite was also reported as recyclable efficient catalyst for the selective catalytic oxidation of phenol to hydroquinone and catechol using H_2O_2 [62,63]. A radical substitution mechanism is proposed but the complete mechanism was still uncertain for the oxidation reactions with H_2O_2 .

Catalytic oxidative promoting reactions of biomass-derived substance into valuable chemicals with O_2 are an important matter to make a sustainable society due to the replacement of non-renewable fossil resources [7-12,109]. However, still now the selective liquid-phase heterogeneous catalytic oxidation under mild conditions with O_2 are limited [101-108,110]. The CuO and CuZrO_3 mixture was developed as heterogeneous catalytic oxidation of vanillyl alcohol (a model compound representing lignin) [64]. The redox properties of the catalyst improved due to the presence of Cu-O-Zr linkages in high concentration as active phase. The perovskite-catalyzed aerobic oxidation of common organic substances was also examined by various researchers. The effect of perovskites supports on glycerol aerobic oxidation was exclusively studied over AuPt nanoparticles supported on lanthanum based oxides LaMO_3 ($\text{M} = \text{Fe}, \text{Cr}, \text{Mn}, \text{Ni}, \text{Co}$) [65]. This oxidation gives different products and the selectivity of the products was depending on the perovskite supports. From mechanistic studies, it was suggested that the oxygen adsorption capacity supports strongly

influence selectivity of the product and LaMnO_3 support inhibits the lactic acid production due to high oxygen capacity. The Pd-containing perovskite oxide ($\text{Pd}/\text{K}_{0.6}\text{Ti}_{1.85}\text{O}_4$) was reported as a highly stable and reusable catalyst for allylic and benzylic alcohols oxidation by using oxygen [66]. Various substituted benzaldehyde with electron-withdrawing and electron-donating groups were selectively oxidized to the desired products over La_2CuO_4 catalyst [67].

The catalytic oxidation over various types of pure rhombohedral and hexagonal perovskite oxides ($\text{BaFeO}_{3-\delta}$, BaRuO_3 and SrMnO_3) with relatively high surface areas are also reported as efficient catalyst for oxidative dehydrogenation of alcohols and other difficult aerobic oxidation of alkanes and sulfides [69-72]. These hexagonal perovskites also selectively catalyzed alcohols, alkanes, alkyl arenes and sulfides in presence of O_2 . Many allylic, aromatic and heteroatom-incorporated primary or secondary alcohols were selectively transformed to the desired carbonyl compounds over hexagonal SrMnO_3 [69]. But the catalyst showed low catalytic activity towards aliphatic alcohols oxidation. The kinetics measurement showed non-dissociative alcohol and oxygen adsorption and Langmuir-Hinshelwood mechanism was proposed for this catalyzed oxidation reaction. The C-H bond breaking was suggested for the rate determination step from kinetic isotope effect. This type of O_2 -activation was also used for oxidative homocoupling reactions of phenols and amines and the selective oxidation of alkyl arenes to corresponding oxygenated/dehydrogenated products. This is the first example of reductive O_2 activation for selective catalytic oxidation over SrMnO_3 in liquid-phase. The kinetic measurement showed that an oxygen species generated from the solid compare to SrMnO_3 is responsible for this oxidation process and Mars-van Krevelen mechanism was proposed for this reaction [111]. Various aromatic and aliphatic sulfides could also efficiently catalyze to the corresponding sulfones and sulfoxides by using O_2 over recyclable rhombohedral BaRuO_3 [71]. The oxygen transfer reactivity of ruthenium based oxides was significantly affected by the crystal structure of oxides. Thus, the oxygen easily transferred to a sulfide from BaRuO_3 and oxygen also re-oxidized the partially reduced BaRuO_{3-x} than other Ru-based perovskites. The aliphatic C-H bond oxidation of alkanes produces industrially important chemicals and it is still challenging in the chemical industries [72]. There are few Ru- and V-based perovskites used as recoverable as well as a reusable heterogeneous catalyst for aerobic oxidation of adamantane [112,113]. Hexagonal, recyclable $6\text{H-BaFeO}_{3-\delta}$ ($\delta = 0.1$) was efficiently catalyzed this oxidation as well as other various hydrocarbons in presence of oxygen [72]. The author proposed that the adamantane oxidation gates through a radical-mediated pathway and abstraction of hydrogen by $\text{BaFeO}_{3-\delta}$ suggested for the rate determining step. The oxygen-deficient, orthorhombic, recyclable $(\text{La,Sr})_{0.5}(\text{Co,Mn})_{0.5}\text{O}_{3-\delta}$ perovskite was basically applied for the selective oxidation of ethylbenzene and toluene to acetophenone and benzoic acid, respectively with *N*-hydroxyphthalimide (NHPI) [73]. It has been proposed that the large oxygen vacancies of this perovskite could activated NHPI to produce phthalimide *N*-oxyl radical (PINO) and the radical promoting the formation of an alkyl radical through hydrogen

abstraction from hydrocarbons. However, mechanistic detail is still required.

A sets of alkaline tantalates (NaTaO_3 , LiTaO_3 , KTaO_3) also selectively catalyzed styrene to form benzaldehyde. The highest conversion ($\sim 58\%$) with 77% selectivity was achieved for KTaO_3 upto six catalytic cycles. It is suggested that the increasing catalytic performance was attributed to crystalline structure of perovskites, the atomic radius of the alkaline-metals and the presence of segregated phases in the component [74]. Sol-gel methods synthesized, pure and Co loaded nano-lanthanum ferrite ($\text{LaFe}_{1-x}\text{Co}_x\text{O}_3$; $x = 0$ to 1) were also examined for selective catalytic oxidation of styrene to benzaldehyde using H_2O_2 as oxidant [75]. The catalyst showed the higher activity at lowest substitution than other higher cobalt loaded ferrite and also than for pure LaFeO_3 .

$\text{BaFeO}_{3-\delta}$ perovskite may well affectively catalyzed oxidative C=C bond cleavage of numerous aromatic alkenes to preferred carbonyl compounds ($\sim 75\%$ yield) under the additive free condition with O_2 as oxidant [76].

Cross-coupling reactions: Several significant organic chemicals (drugs, materials, optical devices, *etc.*) are manufactured by using cross-coupling reactions over transition metal catalyst [114-118]. Palladium(II) complexes are generally used as homogeneous catalyst in case of cross-coupling reactions in environment friendly mild conditions. Thus development of Pd-based easily recoverable and recyclable heterogeneous catalysts are predominantly required for industrial applications. Along with other approaches impregnation and encapsulation have been tried for the immobilization of Pd particles [78]. But Pd leaching is a big problem for this types of catalysts. Thus, the improvement of Pd-based catalysts as actually heterogeneous remains an interesting tusk for researchers.

Furthermore, palladium containing perovskite oxides also developed as efficient popular automotive three-way catalyst with expressively developed stability due to the self-reformative role of Pd [119,120]. Against such a background, Pd-loading $\text{LaFe}_{0.57}\text{Co}_{0.38}\text{Pd}_{0.05}\text{O}_3$ perovskite is developed for the Suzuki reactions of aryl halides with boronic acids [77]. A number of aryl halides and boronic acids combinations were affectively transformed to the analogous bi-aryls and the catalytic efficiency enhanced with tetra-*n*-butyl ammonium bromide (TBABr) addition in several difficult transformations. The reaction between 4-bromoanisole and phenyl boronic acid over $\text{LaFe}_{0.57}\text{Co}_{0.38}\text{Pd}_{0.05}\text{O}_3$ was taken as a model reaction for this coupling reaction and the reaction mechanism was investigated by using kinetics, microscopy, catalyst poisoning and three-phase tests [78]. On the basis of these results, it was proposed that the Pd particles first reduced to Pd^0 by aqueous alcohol solvents and trapped to a solid surface. The soluble Pd species produces by oxidative-addition of aryl halides helped the Suzuki coupling reaction in a usual way. Transmission electron microscopy (TEM) studies showed that there is no Pd black generated. Thus, low amount (2 ppm) of leached Pd particles (confirm from hot filtration test) after reaction indicated that bulk inorganic phase was recaptured the Pd^0 particles.

Furthermore, Ullmann-type condensation of different aryl halides using thiols and phenols to the analogous sulfides and

biaryl ethers could efficiently catalyze by $\text{La}_{0.9}\text{Ce}_{0.1}\text{Co}_{0.6}\text{Cu}_{0.4}\text{O}_3$ perovskite catalyst [79]. Several phenolic compound could effectively couple with an aryl halide in presence of ethyl acetate and Cs_2CO_3 additives. Three Pd-loaded $\text{Na}_{2.04}\text{Cu}_{0.95}\text{Pd}_{0.05}\text{O}_4$, $\text{LaFe}_{0.57}\text{Cu}_{0.38}\text{Pd}_{0.05}\text{O}_3$ and $\text{LaFe}_{0.57}\text{Co}_{0.38}\text{Pd}_{0.05}\text{O}_3$ perovskites developed for Sonogashira coupling of aryl halides with alkynes is also reported [79]. $\text{LaFe}_{0.95}\text{Pd}_{0.05}\text{O}_3$ perovskite deposited CeO_2 was also reported as efficient catalyst for Sonogashira and Heck cross-coupling reactions by flow chemistry technology [80]. But the reaction time profile is very slow and controlling the byproducts formation should be enhanced catalytic efficiency.

The $\text{Bi}_{1.97}\text{Eu}_{0.03}\text{MoO}_6$ double perovskite catalyst was also reported as an effective catalyst for the formation of substituted quinolones from different aliphatic ketones and 2-amino aryl ketones at ambient temperature in water [81].

Other reactions: LaMO_3 ($M = \text{Mn, Fe, Co, Cr, Al}$) catalyst applied for the hydrogenation of substituted and unsubstituted nitrobenzene to synthesize corresponding aniline in presence of KOH promoter in 2-propanol medium [82,83]. Among the catalysts, LaFeO_3 showed highest catalytic activity for this hydrogenation reaction. The same group also examined the strontium loading effect in the $\text{La}_{1-x}\text{Sr}_x\text{FeO}_3$ for nitrobenzene hydrogenation and found $\text{La}_{0.8}\text{Sr}_{0.2}\text{FeO}_3$ as the best active as well as recyclable catalysts [82,83].

Spray-flame synthesized $\text{LaCo}_{0.8}\text{Fe}_{0.2}\text{O}_3$ perovskite nanoparticles catalyst used for the oxidation of cinnamyl alcohol to cinnamaldehyde in liquid phase with TBHP under mild conditions. Waffel *et al.* [84] suggested a synergistic effect of Co and Fe for the best catalytic activity. Platinum nanoparticles supported on modified solgel method synthesized $\text{YCo}_{0.3}\text{Fe}_{0.7}\text{O}_3$ catalyst selectively hydrogenated cinnamaldehyde to cinnamyl alcohol with ~95% selectivity and 100% conversion [85].

Metal-free LaMnO_3 perovskite was reported as an exceptionally effective oxidation catalyst for the conversion of alkyl arenes to corresponding ketones and also for the preparation of 1,1-binaphthyl-2,2-diol (BINOL) through oxidative dimerization of 2-naphthol in presence of molecular oxygen [86]. Citric acid based sol-gel route prepared crumpled nanosheets of molybdenum-doped LaFeO_3 ($\text{LaMo}_{0.1}\text{Fe}_{0.9}\text{O}_3$) were used for the green synthesis of naphthopyrimidines from solvent-free one-pot reaction of different substituted aromatic aldehydes, 2-naphthol and barbituric acid or its derivatives [87]. The oxygen vacancy-rich mesoporous LaMnO_3 prepared through a modified molecular-assembly method, act as a significantly active as well as stable hydrogenation catalyst for synthesis of furfuryl alcohol from furfural with ~100% conversion and 96% selectivity. The author proposed from density functional theory calculation that the interaction of catalyst surface with catalytic substrate facilitated by the expose oxygen deficiency sites of porous LaMnO_3 , which lead to a lower energy barrier for this hydrogenation process [88].

Conclusion

Inspite of low surface areas, structurally modified perovskite oxides show a unique catalytic efficiency for various organic reactions in liquid phase. Various porous and nano

perovskite oxides prepared by different conventional methods as well as modified methods can used as catalyst for the preparation of value-added chemicals. Perovskite oxides can efficiently use as acid-base catalysts for aldol condensation, esterification, Friedel-Crafts alkylation, cyanosilylation and one-pot synthesis. However, the connection of the catalytic efficiency with acid/base properties is still not properly discussed. Alkanes, alcohols, arenes, sulfides, *etc.* can selectively oxidized to the corresponding products over precious metal-supported, oxygen deficient, hexagonal and layered perovskite oxides catalyst with O_2 , H_2O_2 and *tert*-butyl hydroperoxide (TBHP) oxidants. Palladium and copper loaded multi-component perovskite oxides can also effectively catalyze Suzuki, Ullmann and Sonogashira type cross-coupling reactions. Several reactions are employed to increase the surface areas of perovskites, which subsequently increases the catalytic activities. However, the procedures complexity and inapplicability to versatile chemical compositions is the fundamental disadvantages of present synthesis methods. Thus a simple, efficient synthesis methods are still required for synthesis of various perovskite oxides with enhanced surface areas ($\geq 100 \text{ m}^2 \text{ g}^{-1}$) at mild condition. Furthermore, elucidation of proper reaction mechanisms along with the connection of catalytic efficiency of perovskite oxides with the substrate activation modes have to be properly clarified. Therefore, appropriate explanation of the mechanistic data can lead to develop efficient perovskite oxide catalysts with proper composition for different organic reactions in the liquid phase under mild reaction conditions.

CONFLICT OF INTEREST

The authors declare that there is no conflict of interests regarding the publication of this article.

REFERENCES

1. C.-J. Li and B.M. Trost, *PNAS*, **105**, 13197 (2008) <https://doi.org/10.1073/pnas.0804348105>
2. R.A. Sheldon, *Chem. Soc. Rev.*, **41**, 1437 (2012); <https://doi.org/10.1039/C1CS15219J>
3. C.J. Clarke, W.-C. Tu, O. Levers, A. Bröhl and J.P. Hallett, *Chem. Rev.*, **118**, 747 (2018); <https://doi.org/10.1021/acs.chemrev.7b00571>
4. K. Kamata, *Bull. Chem. Soc. Jpn.*, **92**, 133 (2019); <https://doi.org/10.1246/bcsj.20180260>
5. V.L. Sushkevich, D. Palagin, M. Ranocchiarri and J.A. van Bokhoven, *Science*, **356**, 523 (2017); <https://doi.org/10.1126/science.aam9035>
6. S.H. Morejudo, R. Zanón, S. Escolástico, I. Yuste-Tirados, H. Malerød-Fjeld, P.K. Vestre, W.G. Coors, A. Martínez, T. Norby, J.M. Serra and C. Kjøseth, *Science*, **353**, 563 (2016); <https://doi.org/10.1126/science.aag0274>
7. T. Komanoya, T. Kinemura, Y. Kita, K. Kamata and M. Hara, *J. Am. Chem. Soc.*, **139**, 11493 (2017); <https://doi.org/10.1021/jacs.7b04481>
8. S. Kanai, I. Nagahara, Y. Kita, K. Kamata and M. Hara, *Chem. Sci.*, **8**, 3146 (2017); <https://doi.org/10.1039/C6SC05642C>
9. M.J. C liment, A. Corma and S. Iborra, *Green Chem.*, **16**, 516 (2014); <https://doi.org/10.1039/C3GC41492B>
10. M. Hara, K. Nakajima and K. Kamata, *Sci. Technol. Adv. Mater.*, **16**, 034903 (2015); <https://doi.org/10.1088/1468-6996/16/3/034903>

11. D.M. Alonso, S.G. Wettstein and J.A. Dumesic, *Chem. Soc. Rev.*, **41**, 8075 (2012); <https://doi.org/10.1039/c2cs35188a>
12. M. Besson, P. Gallezot and C. Pinel, *Chem. Rev.*, **114**, 1827 (2014); <https://doi.org/10.1021/cr4002269>
13. B. Cornils, W.A. Herrmann, M. Beller and R. Paciello, *Applied Homogeneous Catalysis with Organometallic Compounds: A Comprehensive Handbook in Four Volumes, Ed.: 3*, Wiley-VCH: Weinheim (2017).
14. J. Hagen, *Industrial Catalysis: A Practical Approach*, Wiley-VCH: Weinheim (1999).
15. G. Ertl, H. Knözinger and J. Weitkamp, *Handbook of Heterogeneous Catalysis, Ed. 2*, Wiley-VCH: Weinheim (2008).
16. N. Mizuno, *Modern Heterogeneous Oxidation Catalysis*, Wiley-VCH: Weinheim (2009).
17. K. Yamaguchi and N. Mizuno, *Syn. Lett.*, 2365 (2010); <https://doi.org/10.1055/s-0030-1258565>
18. A. Takagaki, C. Tagusagawa, S. Hayashi, M. Hara and K. Domen, *Energy Environ. Sci.*, **3**, 82 (2010); <https://doi.org/10.1039/B918563A>
19. M. Hechelski, A. Ghinet, B. Louvel, P. Dufrenoy, B. Rigo, A. Daich and C. Waterlot, *ChemSusChem*, **11**, 1249 (2018); <https://doi.org/10.1002/cssc.201702435>
20. S. Ishikawa, Z. Zhang and W. Ueda, *ACS Catal.*, **8**, 2935 (2018); <https://doi.org/10.1021/acscatal.7b02244>
21. N. Mizuno, K. Yamaguchi and K. Kamata, *Catal. Surv. Asia*, **15**, 68 (2011); <https://doi.org/10.1007/s10563-011-9111-2>
22. A. Enferadi-Kerenkan, T.-O. Do and S. Kaliaguine, *Catal. Sci. Technol.*, **8**, 2257 (2018); <https://doi.org/10.1039/C8CY00281A>
23. C. Martínez and A. Corma, *Coord. Chem. Rev.*, **255**, 1558 (2011); <https://doi.org/10.1016/j.ccr.2011.03.014>
24. J. Liang, Z. Liang, R. Zou and Y. Zhao, *Adv. Mater.*, **29**, 1701139 (2017); <https://doi.org/10.1002/adma.201701139>
25. K. Kaneda and T. Mizugaki, *ACS Catal.*, **7**, 920 (2017); <https://doi.org/10.1021/acscatal.6b02585>
26. D. Astruc, F. Lu and J.R. Aranzaes, *Angew. Chem. Int. Ed. Engl.*, **44**, 7852 (2005); <https://doi.org/10.1002/anie.200500766>
27. A. Dhakshinamoorthy, M. Alvaro and H. Garcia, *Chem. Commun.*, **48**, 11275 (2012); <https://doi.org/10.1039/c2cc34329k>
28. J. Liu, L. Chen, H. Cui, J. Zhang, L. Zhang and C.-Y. Su, *Chem. Soc. Rev.*, **43**, 6011 (2014); <https://doi.org/10.1039/C4CS00094C>
29. R. Akiyama and S. Kobayashi, *Chem. Rev.*, **109**, 594 (2009); <https://doi.org/10.1021/cr800529d>
30. Q. Sun, Z. Dai, X. Meng and F.-S. Xiao, *Chem. Soc. Rev.*, **44**, 6018 (2015); <https://doi.org/10.1039/C5CS00198F>
31. D. Wang and D. Astruc, *Coord. Chem. Rev.*, **257**, 2317 (2013); <https://doi.org/10.1016/j.ccr.2013.03.032>
32. K. Nakajima and M. Hara, *ACS Catal.*, **2**, 1296 (2012); <https://doi.org/10.1021/cs300103k>
33. Y. Wang, X. Wang and M. Antonietti, *Angew. Chem. Int. Ed.*, **51**, 68 (2012); <https://doi.org/10.1002/anie.201101182>
34. D. Chen, C. Chen, Z.M. Baiyee, Z. Shao and F. Ciucci, *Chem. Rev.*, **115**, 9869 (2015); <https://doi.org/10.1021/acs.chemrev.5b00073>
35. F. Cheng and J. Chen, *Chem. Soc. Rev.*, **41**, 2172 (2012); <https://doi.org/10.1039/c1cs15228a>
36. D.U. Lee, P. Xu, Z.P. Cano, A.G. Kashkooli, M.G. Park and Z. Chen, *J. Mater. Chem. A Mater. Energy Sustain.*, **4**, 7107 (2016); <https://doi.org/10.1039/C6TA00173D>
37. X. Ge, A. Sumboja, D. Wu, T. An, B. Li, F.W.T. Goh, T.S.A. Hor, Y. Zong and Z. Liu, *ACS Catal.*, **5**, 4643 (2015); <https://doi.org/10.1021/acscatal.5b00524>
38. P. Tan, M. Liu, Z. Shao and M. Ni, *Adv. Energy Mater.*, **7**, 1602674 (2017); <https://doi.org/10.1002/aenm.201602674>
39. S. Royer, D. Duprez, F. Can, X. Courtois, C. Batiot-Dupeyrat, S. Laassiri and H. Alamdari, *Chem. Rev.*, **114**, 10292 (2014); <https://doi.org/10.1021/cr500032a>
40. N. Labhasetwar, G. Saravanan, S.K. Megarajan, N. Manwar, R. Khobragade, P. Daggali and F. Grasset, *Sci. Technol. Adv. Mater.*, **16**, 036002 (2015); <https://doi.org/10.1088/1468-6996/16/3/036002>
41. J. Zhu, H. Li, L. Zhong, P. Xiao, X. Xu, X. Yang, Z. Zhao and J. Li, *ACS Catal.*, **4**, 2917 (2014); <https://doi.org/10.1021/cs500606g>
42. F. Polo-Garzon and Z. Wu, *J. Mater. Chem. A Mater. Energy Sustain.*, **6**, 2877 (2018); <https://doi.org/10.1039/C7TA10591F>
43. H. Zhu, P. Zhang and S. Dai, *ACS Catal.*, **5**, 6370 (2015); <https://doi.org/10.1021/acscatal.5b01667>
44. M. Konsolakis, *ACS Catal.*, **5**, 6397 (2015); <https://doi.org/10.1021/acscatal.5b01605>
45. E.A.R. Assirey, *Saudi Pharm. J.*, **27**, 817 (2019); <https://doi.org/10.1016/j.jsps.2019.05.003>
46. P. Yadav, S. Yadav and R. Tomar, *ChemistrySelect*, **6**, 12947 (2021); <https://doi.org/10.1002/slct.202102292>
47. E. Grabowska, *Appl. Catal. B*, **186**, 97 (2016); <https://doi.org/10.1016/j.apcatb.2015.12.035>
48. W. Wang, M.O. Tadé and Z. Shao, *Chem. Soc. Rev.*, **44**, 5371 (2015); <https://doi.org/10.1039/C5CS00113G>
49. M. Kubicek, A.H. Bork and J.L.M. Rupp, *J. Mater. Chem. A Mater. Energy Sustain.*, **5**, 11983 (2017); <https://doi.org/10.1039/C7TA00987A>
50. P. Chandra, *ChemistrySelect*, **6**, 7557 (2021); <https://doi.org/10.1002/slct.202101434>
51. G.F. Teixeira, E. Silva Junior, R. Vilela, M.A. Zaghete and F. Colmati, *Catalysts*, **9**, 721 (2019); <https://doi.org/10.3390/catal9090721>
52. H. Kleineberg, M. Eisenacher, H. Lange, H. Strutz and R. Palkovits, *Catal. Sci. Technol.*, **6**, 6057 (2016); <https://doi.org/10.1039/C5CY01479D>
53. A. Takagaki, M. Sugisawa, D. Lu, J.N. Kondo, M. Hara, K. Domen and S. Hayashi, *J. Am. Chem. Soc.*, **125**, 5479 (2003); <https://doi.org/10.1021/ja034085q>
54. S. Yamaguchi, T. Okuwa, H. Wada, H. Yamaura and H. Yahiro, *Res. Chem. Intermed.*, **41**, 9551 (2015); <https://doi.org/10.1007/s11164-015-1980-y>
55. N. Pal, M. Paul and A. Bhaumik, *Appl. Catal. A*, **393**, 153 (2011); <https://doi.org/10.1016/j.apcata.2010.11.037>
56. S. Ray, P. Das, B. Banerjee, A. Bhaumik and C. Mukhopadhyay, *ChemPlusChem*, **80**, 731 (2015); <https://doi.org/10.1002/cplu.201402405>
57. H. Singh and J.K. Rajput, *J. Mater. Sci.*, **53**, 3163 (2018); <https://doi.org/10.1007/s10853-017-1790-2>
58. R. Mistri, D. Das, J. Llorca, M. Dominguez, T.K. Mandal, P. Mohanty, B.C. Ray and A. Gayen, *RSC Adv.*, **6**, 4469 (2016); <https://doi.org/10.1039/C5RA22592B>
59. A.A. Ansari, S.F. Adil, M. Alam, N. Ahmad, M.E. Assal, J.P. Labis and A. Alwarthan, *Sci. Rep.*, **10**, 15012 (2020); <https://doi.org/10.1038/s41598-020-71869-z>
60. S.J. Singh and R.V. Jayaram, *Catal. Commun.*, **10**, 2004 (2009); <https://doi.org/10.1016/j.catcom.2009.07.018>
61. C. Saux, C. Leal Marchena, R. Dinamarca, G. Pecchi and L. Pierella, *Catal. Commun.*, **76**, 58 (2016); <https://doi.org/10.1016/j.catcom.2015.12.023>
62. C. Liu, Z. Zhao, X. Yang, X. Ye and Y. Wu, *Chin. J. Chem.*, **14**, 516 (1996).
63. C. Liu, Z. Zhao, X. Yang, X. Ye and Y. Wu, *Chem. Commun.*, 1019 (1996); <https://doi.org/10.1039/CC9960001019>
64. S. Saha and S.B. Abd Hamid, *RSC Adv.*, **7**, 9914 (2017); <https://doi.org/10.1039/C6RA26370D>
65. C.D. Evans, S.A. Kondrat, P.J. Smith, T.D. Manning, P.J. Miedziank, G.L. Brett, R.D. Armstrong, J.K. Bartley, S.H. Taylor, M.J. Rosseinsky and G.J. Hutchings, *Faraday Discuss.*, **188**, 427 (2016); <https://doi.org/10.1039/C5FD00187K>
66. I.B. Adilina, T. Hara, N. Ichikuni, N. Kumada and S. Shimazu, *Bull. Chem. Soc. Jpn.*, **86**, 146 (2013); <https://doi.org/10.1246/bcsj.20120215>
67. A. Rahmani and J. Saari, *J. Nanostruct.*, **6**, 301 (2016); <https://doi.org/10.22052/JNS.2016.34270>

68. S. Sugunan and V. Meera, *Indian J. Chem.*, **34A**, 984 (1995).
69. S. Kawasaki, K. Kamata and M. Hara, *ChemCatChem*, **8**, 3247 (2016); <https://doi.org/10.1002/cctc.201600613>
70. K. Sugahara, K. Kamata, S. Muratsugu and M. Hara, *ACS Omega*, **2**, 1608 (2017); <https://doi.org/10.1021/acsomega.7b00146>
71. K. Kamata, K. Sugahara, Y. Kato, S. Muratsugu, Y. Kumagai, F. Oba and M. Hara, *ACS Appl. Mater. Interfaces*, **10**, 23792 (2018); <https://doi.org/10.1021/acsomega.8b05343>
72. S. Shibata, K. Sugahara, K. Kamata and M. Hara, *Chem. Commun.*, **54**, 6772 (2018); <https://doi.org/10.1039/C8CC02185F>
73. A. Aguadero, H. Falcon, J.M. Campos-Martin, S.M. Al-Zahrani, J.L.G. Fierro and J.A. Alonso, *Angew. Chem. Int. Ed. Engl.*, **50**, 6557 (2011); <https://doi.org/10.1002/anie.201007941>
74. C. Leal Marchena, G.A. Pecchi and L.B. Pierella, *Catal. Commun.*, **119**, 28 (2019); <https://doi.org/10.1016/j.catcom.2018.10.016>
75. I. Jaouali, N. Moussa, M.F. Nsib and M.A. Centeno, Proceedings of 2nd Euro-Mediterranean Conference for Environmental Integration (EMCEI-2), p. 429 (2019).
76. S. Shibata, K. Kamata and M. Hara, *Catal. Sci. Technol.*, **11**, 2369 (2021); <https://doi.org/10.1039/D1CY00245G>
77. M.D. Smith, A.F. Stepan, C. Ramarao, P.E. Brennan and S.V. Ley, *Chem. Commun.*, 2652 (2003); <https://doi.org/10.1039/b308465e>
78. S.P. Andrews, A.F. Stepan, H. Tanaka, S.V. Ley and M.D. Smith, *Adv. Synth. Catal.*, **347**, 647 (2005); <https://doi.org/10.1002/adsc.200404331>
79. S. Lohmann, S.P. Andrews, B.J. Burke, M.D. Smith, J.P. Atteld, H. Tanaka, K. Kaneko and S.V. Ley, *Synlett*, 1291 (2005); <https://doi.org/10.1055/s-2005-865233>
80. C. Battilocchio, B.N. Bhawal, R. Chorghade, B.J. Deadman, J.M. Hawkins and S.V. Ley, *Isr. J. Chem.*, **54**, 371 (2014); <https://doi.org/10.1002/ijch.201300049>
81. T. Dharmana and B.N. Naidu, *Asian J. Chem.*, **34**, 437 (2022); <https://doi.org/10.14233/ajchem.2022.23428>
82. A.S. Kulkarni and R.V. Jayaram, *Appl. Catal.*, **A**, **252**, 225 (2003); [https://doi.org/10.1016/S0926-860X\(03\)00417-4](https://doi.org/10.1016/S0926-860X(03)00417-4)
83. A.S. Kulkarni and R.V. Jayaram, *J. Mol. Catal. Chem.*, **223**, 107 (2004); <https://doi.org/10.1016/j.molcata.2003.12.042>
84. D. Waffel, B. Alkan, Q. Fu, Y.T. Chen, S. Schmidt, C. Schulz, H. Wiggers, M. Muhler and B. Peng, *ChemPlusChem*, **84**, 1155 (2019); <https://doi.org/10.1002/cplu.201900429>
85. Y. Xue, H. Xin, W. Xie, P. Wu and X. Li, *Chem. Commun.*, **55**, 3363 (2019); <https://doi.org/10.1039/C9CC00318E>
86. Y. Sahin, A.T. Sika-Nartey, K.E. Ercan, Y. Kocak, S. Senol, E. Ozensoy and Y.E. Turkmen, *ACS Appl. Mater. Interfaces*, **13**, 5099 (2021); <https://doi.org/10.1021/acsomega.1c02049>
87. S. Rahmatinejad and H. Naeimi, *Polyhedron*, **177**, 114318 (2020); <https://doi.org/10.1016/j.poly.2019.114318>
88. Y. Zheng, R. Zhang, L. Zhang, Q. Gu and Z.A. Qiao, *Angew. Chem. Int.*, **60**, 4774 (2021); <https://doi.org/10.1002/anie.202012416>
89. P. Granger, V.I. Parvulescu, V.I. Parvulescu and W. Prellier, *Perovskites and Related Mixed Oxides*, Wiley-VCH: Weinheim (2016).
90. Y. Wang, H. Arandiyani, J. Scott, A. Bagheri, H. Dai and R. Amal, *J. Mater. Chem. A Mater. Energy Sustain.*, **5**, 8825 (2017); <https://doi.org/10.1039/C6TA10896B>
91. C. Marcilly, P. Courty and B. Delmon, *J. Am. Ceram. Soc.*, **53**, 56 (1970); <https://doi.org/10.1111/j.1151-2916.1970.tb12003.x>
92. Y. Teraoka, H. Kakebayashi, I. Moriguchi and S. Kagawa, *Chem. Lett.*, **20**, 673 (1991); <https://doi.org/10.1246/cl.1991.673>
93. M.P. Pechini, Method of Preparing Lead and Alkaline Earth Titanates and Niobates and Coating Method Using the Same to Form a Capacitor, US Patent, US3330697 (1967).
94. M. Kakihana, *J. Sol-Gel Sci. Technol.*, **6**, 7 (1996); <https://doi.org/10.1007/BF00402588>
95. H. Hattori and Y. Ono, *Solid Acid Catalysis: From Fundamentals to Applications*, CRC Press: Boca Raton (2015).
96. Y. Ono and H. Hattori, *Solid Base Catalysis*, Springer: Berlin/Heidelberg (2011).
97. G. Busca, *Chem. Rev.*, **107**, 5366 (2007); <https://doi.org/10.1021/cr068042e>
98. T. Okuhara, N. Mizuno and M. Misono, *Adv. Catal.*, **41**, 113 (1996); [https://doi.org/10.1016/S0360-0564\(08\)60041-3](https://doi.org/10.1016/S0360-0564(08)60041-3)
99. K. Kamata and K. Sugahara, *Catalysts*, **7**, 345 (2017); <https://doi.org/10.3390/catal7110345>
100. A. Corma and H. Garcia, *Chem. Rev.*, **103**, 4307 (2003); <https://doi.org/10.1021/cr030680z>
101. T. Punniyamurthy, S. Velusamy and J. Iqbal, *Chem. Rev.*, **105**, 2329 (2005); <https://doi.org/10.1021/cr050523v>
102. F. Cavani and J.H. Teles, *ChemSusChem*, **2**, 508 (2009); <https://doi.org/10.1002/cssc.200900020>
103. K. Kamata, *Bull. Chem. Soc. Jpn.*, **88**, 1017 (2015); <https://doi.org/10.1246/bcsj.20150154>
104. N. Mizuno and K. Kamata, *Coord. Chem. Rev.*, **255**, 2358 (2011); <https://doi.org/10.1016/j.ccr.2011.01.041>
105. X. Engelmann, I. Monte-Pérez and K. Ray, *Angew. Chem. Int. Ed.*, **55**, 7632 (2016); <https://doi.org/10.1002/anie.201600507>
106. S.S. Stahl, *Angew. Chem. Int. Ed.*, **43**, 3400 (2004); <https://doi.org/10.1002/anie.200300630>
107. I.A. Weinstock, R.E. Schreiber and R. Neumann, *Chem. Rev.*, **118**, 2680 (2018); <https://doi.org/10.1021/acs.chemrev.7b00444>
108. S. Ishikawa and W. Ueda, *Catal. Sci. Technol.*, **6**, 617 (2016); <https://doi.org/10.1039/C5CY01435B>
109. E. Hayashi, T. Komanoya, K. Kamata and M. Hara, *ChemSusChem*, **10**, 654 (2017); <https://doi.org/10.1002/cssc.201601443>
110. Q. Gao, C. Giordano and M. Antonietti, *Angew. Chem. Int. Ed.*, **51**, 11740 (2012); <https://doi.org/10.1002/anie.201206542>
111. M.A. Vannice, *Catal. Today*, **123**, 18 (2007); <https://doi.org/10.1016/j.cattod.2007.02.002>
112. K. Yamaguchi and N. Mizuno, *New J. Chem.*, **26**, 972 (2002); <https://doi.org/10.1039/b203262g>
113. T. Mitsudome, N. Nosaka, K. Mori, T. Mizugaki, K. Ebitani and K. Kaneda, *Chem. Lett.*, **34**, 1626 (2005); <https://doi.org/10.1246/cl.2005.1626>
114. J.P. Corbet and G. Mignani, *Chem. Rev.*, **106**, 2651 (2006); <https://doi.org/10.1021/cr0505268>
115. S.R. Chemler, D. Trauner and S.J. Danishefsky, *Angew. Chem. Int. Ed.*, **40**, 4544 (2001); [https://doi.org/10.1002/1521-3773\(20011217\)40:24<4544::AID-ANIE4544>3.0.CO;2-N](https://doi.org/10.1002/1521-3773(20011217)40:24<4544::AID-ANIE4544>3.0.CO;2-N)
116. N. Miyaura and A. Suzuki, *Chem. Rev.*, **95**, 2457 (1995); <https://doi.org/10.1021/cr00039a007>
117. F. Bellina, A. Carpita and R. Rossi, *Synthesis*, 2419 (2004); <https://doi.org/10.1055/s-2004-831223>
118. N. Miyaura, T. Yanagi and A. Suzuki, *Synth. Commun.*, **11**, 513 (1981); <https://doi.org/10.1080/00397918108063618>
119. Y. Nishihata, J. Mizuki, T. Akao, H. Tanaka, M. Uenishi, M. Kimura, T. Okamoto and N. Hamada, *Nature*, **418**, 164 (2002); <https://doi.org/10.1038/nature00893>
120. I. Jarrige, K. Ishii, D. Matsumura, Y. Nishihata, M. Yoshida, H. Kishi, M. Taniguchi, M. Uenishi, H. Tanaka, H. Kasai and J. Mizuki, *ACS Catal.*, **5**, 1112 (2015); <https://doi.org/10.1021/cs501608k>

Rajib Mistri*

Selective oxidation of benzene to phenol in the liquid phase over copper-substituted LaFeO₃ perovskite oxide as catalyst

<https://doi.org/10.1515/znb-2023-0016>

Received March 16, 2023; accepted June 10, 2023;

published online June 27, 2023

Abstract: Selective oxidation of benzene to phenol is done in the liquid phase over copper-substituted LaFeO₃ perovskite oxides as catalyst using H₂O₂ as oxidant under mild reaction conditions. Among the different copper-substituted perovskite catalysts synthesized by a novel solution combustion method, the LaFe_{0.90}Cu_{0.10}O₃ catalyst showed highest activity (~56 % with 100 % selectivity of phenol) and also gives better activity than the corresponding catalyst made via incipient wetness impregnation of 10 at % Cu over combustion-synthesized LaFeO₃. XRD analysis revealed formation of the perovskite phase as the predominant one. The greater activity of the combustion-made catalyst has been attributed to the occurrence of a peculiar poorly-defined structure having substitutional copper ion sites on top of the LaFeO₃ particle as observed in HRTEM analysis. Much less occurrence of this phase in the impregnated catalyst, where copper is primarily present as dispersed CuO crystallites, explains its comparatively lower activity in the oxidation reaction. The effect of catalyst recycling shows negligible change of activity for the combustion-made catalyst whereas the analogous impregnated catalyst shows considerable decrease in activity in recycling. This explained to be due to the essentially intact poorly-defined structure in the former and leaching of the finely dispersed CuO crystallites from the latter catalyst during cycling.

Keywords: benzene oxidation; Cu²⁺ ion sites in LaFeO₃; Cu-substituted LaFeO₃ perovskite; reduced copper leaching; solution combustion

1 Introduction

Phenol is a significant chemical compound for preparation of industrially important materials and useful compounds

[1–5]. At present, worldwide almost 95 % of phenol is industrially manufactured through the multi-step “cumene process” from benzene [6]. However, the energy consumption is high due to the requirement of high pressure and high temperature for this process [7]. Additionally, highly explosive cumene hydroperoxide is produced in the “cumene process” as an intermediate [8, 9] and overall yield in this multistage process is low (less than 5 %) [7, 9]. To overcome these disadvantages, the development of more efficient and environmental friendly alternatives for the synthesis of phenol is highly desirable. Hence, great interest is keen to a one-step catalytic oxidation process for phenol production from benzene. Theoretically, the benzene to phenol conversion is well possible by oxidation, but experimentally this goal is difficult [10]. N₂O [11], H₂O₂ [12, 13], O₂ [14] and a mixture of O₂ and H₂ [15] are mostly investigated as oxidant for the direct hydroxylation of benzene to form phenol. Particularly, N₂O allows high selectivity but the limited N₂O sources and requirement of high reaction temperatures are the main drawback for this oxidant. Among the oxidants, H₂O₂ is a particularly useful oxidant due to the formation of only water as by-product. In addition, the procedure is environment-friendly, simple as well as economic [16]. Many homogeneous catalysts have been tested for this oxidation reaction [17–31], such as Cu complexes [22–25], Ni complexes [21], Co complexes [19], iron complexes [26–28] and Os complexes [29]. Polyoxometalate (POM) and phosphovanadomolybdate (V-POM) ionic composites have also been reported as homogeneous catalyst for the benzene to phenol transformation with O₂ as oxidant at room temperature [30, 31].

Different supported transition metal oxides (Fe, Co, Ti, Mo, V, Cr, Mn and others, supported on Al₂O₃, SiO₂ and TiO₂) were exclusively studied as heterogeneous catalysts for the benzene oxidation to form phenol. Among them vanadium-based catalysts showed better activity for the benzene hydroxylation [32–34]. Molecular sieves with incorporated transition metals (like NaY, SBA15, MCM-41, SBA16) also showed excellent catalytic activity for this oxidation due to the presence of isolated, highly dispersed active sites in the silica framework of the molecular sieves [35–37]. Recently, metal-doped carbon nitride [38] has also been reported as active catalyst for benzene hydroxylation using H₂O₂, but

*Corresponding author: Rajib Mistri, Department of Chemistry, Achhruram Memorial College, Jhalda, Purulia 723202, West Bengal, India, E-mail: rajibmistri@yahoo.co.in

further oxidation and the formation of by-products made this process unsatisfactory [16]. Although significant progress has been achieved in the last few years, the reported catalytic systems often showed only limited efficiency due to inherent drawbacks. As an example, the hydrophilic surface of a reported catalyst that adsorbed polar phenol molecules over non-polar benzene, which made benzene conversion lower, and consequently phenol selectivity became poorer [12]. In addition, active species leaching is mainly responsible for the deactivation of the catalysts in some cases [39].

Perovskite oxides (ABO_3) have attracted much attention recently for their useful application as piezoelectric, ferroelectric, magnetic, superconducting and also heterogeneous catalytic properties [40–47]. Various perovskites have been reported as catalyst for industrially important selective oxidation reactions of organic substrates in the liquid phase [48–59]. But the weaker sulphur poisoning resistance and low specific surface area of perovskites as compared to noble metals have restricted their industrial applications [60]. Recently new approaches such as substitutions of the cationic sites (rare earth metals for A and transition metals for B) and using new synthesis methods are applied for the structural modification and enhancement of the catalytic activity [61–66]. Pt-, Pd-, and Rh-substituted $LaMnO_3$ perovskites synthesized by the citrate method have been reported as efficient catalysts for total methane oxidation [66, 67]. Pd-substituted $LaMO_3$ ($M = Fe, Co$) [64, 66], $LaMn_{0.976}Rh_{0.224}O_{3.15}$ [68] and $(La_{0.6}Sr_{0.4})(Co_{0.94}Pt_{0.03}Ru_{0.03})O_3$ [69] were also reported as effective three-way catalysts.

In this study, we report the preparation, characterization and catalytic efficiency of copper-substituted $LaFeO_3$ perovskite oxides for benzene oxidation. Among the prepared perovskite compositions, $LaFe_{0.90}Cu_{0.10}O_3$ has shown the highest activity and selectivity in the formation of phenol by oxidation of benzene in acetonitrile using H_2O_2 under mild reaction conditions.

2 Experimental

2.1 Synthesis of catalysts

Pure $LaFeO_3$ and various copper-substituted $LaFeO_3$ perovskites ($LaFe_{1-x}Cu_xO_3$) ($x = 0.05–0.20$), were synthesized by the solution combustion method (SCS) using oxalyl dihydrazide (ODH; $C_2H_6N_4O_2$) as fuel. In particular, $LaFe_{0.90}Cu_{0.10}O_3$ was prepared by combustion of the metal salts $La(NO_3)_3 \cdot 9H_2O$ (Loba Chem, 99%), $Fe(NO_3)_3 \cdot 9H_2O$ (Merck India, 98%) and $Cu(NO_3)_2 \cdot 3H_2O$ (Merck India, 99%) with oxalyl dihydrazide in molar ratios of 1:0.90:0.10:2.26 at an ignition temperature of $T = \sim 350$ °C. In a specific synthesis, 2 g of $La(NO_3)_3 \cdot 9H_2O$, 1.6794 g of $Fe(NO_3)_3 \cdot 9H_2O$, 1.12 mL of a 10% aqueous $Cu(NO_3)_2 \cdot 3H_2O$ solution and 1.6108 g of ODH

were dissolved in 30 mL of water in a borosilicate dish and then introduced for combustion in a preheated muffle furnace. The surface of the redox mixture got ignited at complete dehydration and gave the perovskite within a minute.

In order for comparison, we prepared $LaFe_{0.90}Cu_{0.10}O_3$ through incipient wetness impregnation (IWI) method. The impregnated catalyst was prepared by impregnation of a proper volume of copper nitrate aqueous solution analogous to the support's pore volume into the combustion-made dried $LaFeO_3$ support. Subsequently it was dried at 100 °C overnight, crushed and calcined at 400 °C in air for 3 h to obtain the $LaFe_{0.90}Cu_{0.10}O_3$ -IWI catalyst.

2.2 Characterization of the catalysts

XRD, BET and HRTEM have been used for characterization of the synthesized materials. Powder X-ray diffraction (PXRD) patterns were collected with a Bruker D8 Advance diffractometer (40 kV, 40 mA) equipped with a Lynxeye detector and using $CuK\alpha$ radiation ($\lambda = 1.5418$ Å). The data was recorded in the 2θ range of 10–100° with 1 s step⁻¹ scanning time and 0.02° step size.

The BET surface areas were estimated with an Autosorb iQ-MP (Quantachrome Instruments, USA) at $T = -196$ °C. The samples were degassed at 300 °C for 7 h before each measurement. The BET equation

$$S_{BET} = V_m \times N_A \times s / V \times a$$

(with S_{BET} = specific surface area, V_m = monolayer adsorbed gas volume, N_A = Avogadro's no., s = cross-section area of adsorbed gas molecule, V = molar volume of adsorbed gas, a = mass of sample) is used for specific surface areas calculation over 0.3 to 0.08 P/P_0 pressure range.

High Resolution Transmission Electron Microscopy (HRTEM) was used for the microstructural characterization with a JEOL 2010F instrument at 200 kV accelerating voltage. The Si standard was used for calibration of the magnification. On prolonged electron beam exposure, no induced damage was observed for the studied samples and all images are raw data only.

2.3 Test of oxidation activity

The benzene oxidation with hydrogen peroxide was performed in the temperature range between room temperature (RT) and 100 °C under atmospheric pressure. In a typical reaction, 0.5 g of the catalyst was added to a liquid mixture containing 5 mL of benzene (56.3 mmol), 10 mL of 30 wt% H_2O_2 (97.9 mmol) and 20 mL of acetonitrile in a 250 mL two-necked round bottom flask under continuous stirring. The reaction system in the beginning consisted of two liquid phases, a benzene- and acetonitrile-containing organic phase and an aqueous phase containing acetonitrile and 30% H_2O_2 . After the start of the reaction the liquid mixture turned into homogeneous.

The homogeneous reaction mixture was analyzed by gas chromatography (Nucon 5765, New Delhi) equipped with a FID detector with a fused silica 30 m × 0.25 mm × 0.25 μm capillary column (EC5) at 220 °C injector and 240 °C detector temperature. The initial and final column temperatures were fixed at 110 and 150 °C respectively, with a temperature rate of 80 K min⁻¹. The standard sample injection method was used for the quantitative analysis.

Recycling tests were carried out for the best active combustion-synthesized $LaFe_{0.90}Cu_{0.10}O_3$ and its analogous impregnated ($LaFe_{0.90}Cu_{0.10}O_3$ -IWI) catalysts only. The solution after each experiment was

filtered and the residue was washed with the solvent. Then the residue was dried at 110 °C overnight and used in the next cycles as catalyst to examine the recycling ability.

Conventional iodometric titration was used for measuring the concentration of consumed H_2O_2 during the oxidation process from which we can calculate the H_2O_2 conversion in mol% (Conv.) and H_2O_2 selectivity in mol% (SE) by using the formulae: Conv. (in mol%) = total H_2O_2 consumption (including self-decomposition)/initial amount of H_2O_2 and SE (in mol%) = consumption of H_2O_2 for phenol formation/total H_2O_2 consumption.

3 Results and discussion

3.1 Screening of catalysts

The catalytic activities of several copper-substituted LaFeO_3 perovskite oxide catalysts for the oxidation of benzene at 70 °C at atmospheric pressure are combined in Table 1. Pure LaFeO_3 is totally inactive for this oxidation. It is clearly marked that the combustion-synthesized $\text{LaFe}_{0.90}\text{Cu}_{0.10}\text{O}_3$ shows much better activity (~56 % conversion with 100 % phenol selectivity) than the other catalysts studied here and any further increase in copper content also decreased the activity as well as selectivity of the catalysts. Thus, the catalyst with the formula $\text{LaFe}_{0.90}\text{Cu}_{0.10}\text{O}_3$ was selected for subsequent studies. Phenol was produced as the predominant oxidation product and hydroquinone (maximum ~8 %) was observed as the byproduct. The analogous IWI catalyst showed much lower conversions (~30 %) with only 95 % selectivity as compared to the combustion-synthesized catalyst (see Table 1).

The catalytic activities of $\text{LaFe}_{0.90}\text{Cu}_{0.10}\text{O}_3$ for the benzene to phenol oxidation in the temperature range 32 °C–80 °C is presented in Figure 1(a). At room temperature (32 °C) benzene was only faintly oxidized, showing more or less no reaction.

Table 1: Benzene oxidation activities of different copper-substituted perovskite catalysts.^a

Catalyst composition	Benzene conversion (%)	Phenol formation (%)	Phenol selectivity (%)
LaFeO_3	–	–	–
$\text{LaFe}_{0.95}\text{Cu}_{0.05}\text{O}_3$	32.6	31.9	97.8
$\text{LaFe}_{0.93}\text{Cu}_{0.07}\text{O}_3$	38.5	37.1	96.4
$\text{LaFe}_{0.90}\text{Cu}_{0.10}\text{O}_3$	56	100	100
$\text{LaFe}_{0.85}\text{Cu}_{0.15}\text{O}_3$	47.9	42.6	88.9
$\text{LaFe}_{0.80}\text{Cu}_{0.20}\text{O}_3$	45.3	38.6	85.2
$\text{LaFe}_{0.90}\text{Cu}_{0.10}$ -IWI	30.4	28.9	95.1

^aReaction conditions: 5 mL benzene + 10 mL H_2O_2 + 0.5 g catalyst + 20 mL MeCN; 6 h at $T = 70$ °C.

After rising the temperature to 40 °C, the oxidation activity increases sharply (around 32 % conversion with 100 % selectivity of phenol). Further increase by 10 K gives rise to an about 12 % increase of benzene conversion and remains almost constant (54–56 %) from 60 °C to 70 °C. However, a decrease of the activity (~47 %) and phenol selectivity (~92 %) was observed at 80 °C due to further oxidation of phenol to 1,4-benzoquinone and hydroquinone at higher temperatures. Benzene vaporization can further lead to decreased activity at this temperature [70].

Figure 1(b) shows the phenol formation percentage as a function of time over $\text{LaFe}_{0.90}\text{Cu}_{0.10}\text{O}_3$ at 70 °C. The catalytic oxidation reaction starts at around 30 min and reaches a maximum (~56 % conversion) beyond 6 h over the catalyst with 100 % selectivity.

3.2 Effect of H_2O_2 concentration on the oxidation of benzene over $\text{LaFe}_{0.90}\text{Cu}_{0.10}\text{O}_3$

The H_2O_2 concentration has a clear impact on the oxidation of benzene. The effect of H_2O_2 concentration was measured by retaining the amount of benzene constant (5 mL or 56.3 mmol) in acetonitrile at $T = 70$ °C (see Figure 2). No oxidation products were observed in the absence of H_2O_2 . 50 mmol H_2O_2 gives ~43 % conversion which reaches the maximum ~56 % at a concentration of 97.9 mmol H_2O_2 . Further increase of H_2O_2 to 195.8 mmol (or a molar ratio of 1:4 after 1:2) did not show any noticeable change in conversion. However, catalytic activity and selectivity decreased from 195.8 mmol H_2O_2 onwards. This can be due to increased water formation at higher concentrations of H_2O_2 which lowers the solubility of phenol. In addition, the formation of byproducts increases due to over oxidation of phenol [71]. Although a theoretical ratio of 1:1 or 56.3 mmol H_2O_2 is needed for this oxidation reaction, in our experiments an optimum ratio of 1:2 (97.9 mmol of H_2O_2) was found. This can be explained by the fact that not all of the H_2O_2 participates actually in the oxidation reaction due to self-decomposition of H_2O_2 , which cannot be avoided under the reaction conditions [72]. Mainly phenol along with small amounts of 1,4-benzoquinone and hydroquinone were identified as products but other oxidized products like catechol were not detected in our study. This may be due to the fact that at low concentrations of H_2O_2 the perovskite-based catalysts mostly form peroxide radicals which subsequently lead to the formation of hydroquinone instead of catechol during the catalytic oxidation [70].

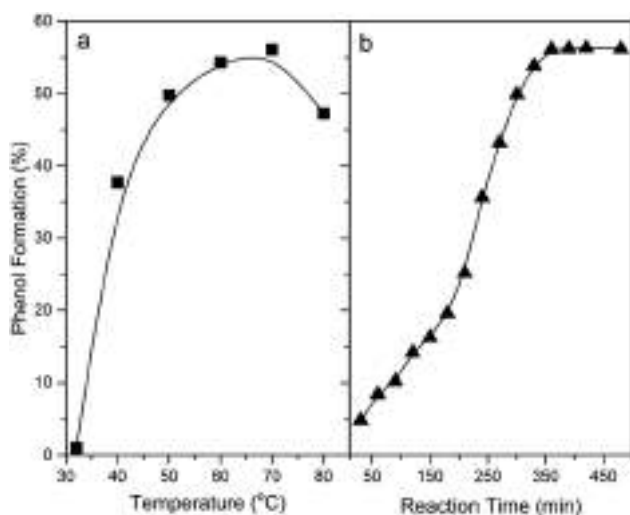


Figure 1: Temperature and time effect on the benzene oxidation. (a) Temperature effect (6 h reaction time) and (b) time effect ($T = 70\text{ }^{\circ}\text{C}$) on the oxidation of benzene over $\text{LaFe}_{0.90}\text{Cu}_{0.10}\text{O}_3$ as catalyst. Reaction conditions: 5 mL benzene + 10 mL H_2O_2 + 0.5 g catalyst + 20 mL MeCN.

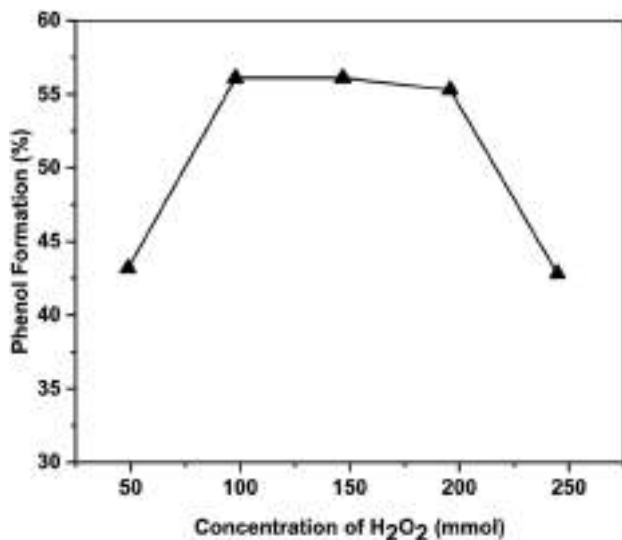


Figure 2: Phenol formation as a function of H_2O_2 concentration over $\text{LaFe}_{0.90}\text{Cu}_{0.10}\text{O}_3$ as catalyst. Reaction conditions: 5 mL benzene + 0.5 g catalyst + 20 mL MeCN; 6 h at $T = 70\text{ }^{\circ}\text{C}$.

3.3 Effect of solvent on the oxidation of benzene over $\text{LaFe}_{0.90}\text{Cu}_{0.10}\text{O}_3$ as catalyst

Different solvents were used for the oxidation of benzene and it was found that the activity decreases in the order acetonitrile > acetic acid > ethanol > water ~ methanol (Figure 3). The highest phenol formation (56 %) with 100 % selectivity was observed in acetonitrile. Although we get high benzene conversion (~30 %) in water, the phenol

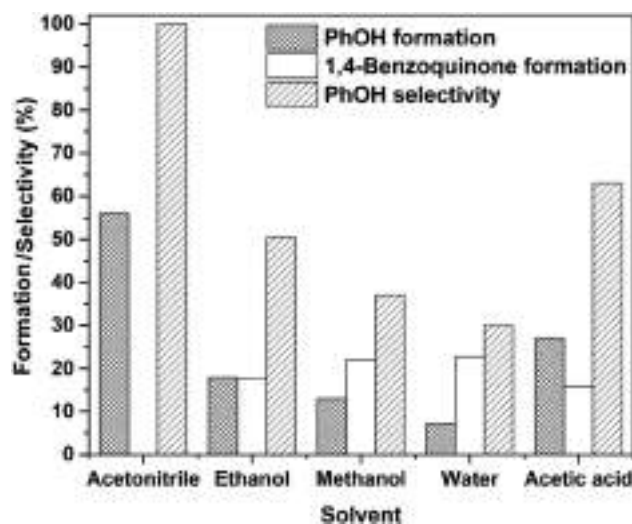


Figure 3: Benzene oxidation activities of $\text{LaFe}_{0.90}\text{Cu}_{0.10}\text{O}_3$ as catalyst in different solvents. Reaction conditions: 5 mL benzene + 0.5 g catalyst + 10 mL H_2O_2 + 20 mL solvent; 6 h at $T = 70\text{ }^{\circ}\text{C}$.

selectivity was very low (~24 %) due to the formation of 1,4-benzoquinone (selectivity ~76 %) mainly by further oxidation. Methanol gave less phenol formation (~13 %) and selectivity (~37 %) mostly due to the lower boiling point (65 °C) of this solvent. On the other hand, ethanol is a higher-boiling solvent than methanol and consequently showed a better phenol formation activity (18 %) as well as selectivity (50 %) which, however, is lower than acetic acid or acetonitrile. Acetic acid as solvent gave higher phenol formation (~27 %) but the phenol selectivity (~63 %) is less than acetonitrile.

Acetonitrile is an aprotic solvent and can easily activate H_2O_2 by formation of a good oxygen transfer intermediate, the perhydroxyl anion, which initiates the oxidation [73]. In addition, the H_2O_2 consumption and its self-decomposition can affect the oxidation activity in various solvents. The effective utilization of H_2O_2 for the oxidation reaction increases when the self-decomposition rate of H_2O_2 is low. Interestingly, the desired product can be obtained by using the appropriate solvent for the oxidation reaction, i.e., water for the formation of 1,4-benzoquinone or acetonitrile for phenol [73, 74].

3.4 Effect of solvent variations on the decomposition of H_2O_2 over $\text{LaFe}_{0.90}\text{Cu}_{0.10}\text{O}_3$

The catalytic activity and selectivity largely depend on the selective H_2O_2 decomposition. The following definitions are used. Decomposition of H_2O_2 means total H_2O_2 consumed

during the entire reaction. H_2O_2 decomposing to water and oxygen is referred to as self-decomposition. H_2O_2 utilized for formation of phenol is referred to as selective decomposition. H_2O_2 utilized for the formation of other by products including self-decomposition is referred as non-selective decomposition.

Thus we estimated the H_2O_2 consumption percentage and its selective decomposition for benzene oxidation over $\text{LaFe}_{0.90}\text{Cu}_{0.10}\text{O}_3$ as catalyst in different solvents by iodometric titration (see Section 2.3, Table 2). The benzene conversion will be higher when the decomposition of H_2O_2 in the overall oxidation process is higher but a high initial decomposition of H_2O_2 will result in nonselective H_2O_2 decomposition and the formation of by-products increases. A high total decomposition of H_2O_2 with minimum initial decomposition (i.e., high selective decomposition of H_2O_2) enhances the effective H_2O_2 utilization and as a result the phenol formation increases. The solvent dependence of the selective conversion of H_2O_2 is following the order: acetonitrile (~56 %) > acetic acid (~29 %) > ethanol (~22 %) > methanol (~14 %) > water (~6 %). The activity of benzene oxidation over $\text{LaFe}_{0.90}\text{Cu}_{0.10}\text{O}_3$ catalyst also follows the same order in different solvents (see Figure 3). In this study, acetonitrile showed the highest conversion with 100 % selectivity under the selected conditions. The poorer selective conversion of peroxide can be made responsible for the lower phenol formation in ethanol, methanol and water. The peroxide radical, which is generated in the oxidation process, acquires additional stability in these polar protic solvents due to the formation of hydrogen bonds. Thus the H_2O_2 decomposition equilibrium is shifted to the right and the self-decomposition rate increases [20].

On the other hand, the peroxide radical does not acquire extra stability in acetonitrile due to the polar aprotic nature of the solvent. In acetic acid, peroxyacetic acid is formed which makes H_2O_2 even more stable and reduces the self-decomposition of H_2O_2 . Thus, the loss of H_2O_2 is lower in these two solvents than in the other polar protic solvents used here and the formation of phenol increases. Interestingly, after 3 h a small decline of peroxide selectivity is observed in acetonitrile and acetic acid. The H_2O_2 self-decomposition is still present up to 3 h of reaction time and some by-products are also formed after this time.

3.5 Test of heterogeneity and recycling ability

In order to see whether the catalytic benzene oxidation was truly heterogeneous or not and also to examine for probable metal leaching, the traditional Sheldon hot-filtration test was performed by using both combustion-made $\text{LaFe}_{0.90}\text{Cu}_{0.10}\text{O}_3$ and incipient wetness-made $\text{LaFe}_{0.90}\text{Cu}_{0.10}\text{O}_3$ -IWI catalysts. For this purpose, after 2 h of catalytic reaction, the catalyst was instantaneously filtered off from the reaction mixture by using a Gooch crucible with a G4 sintered disk to avoid re-adsorption of leached metals onto the catalyst surface. The filtrate was collected in a different preheated round-bottom flask at the same temperature and the reaction was carried on for further 4 h. Gas-chromatographic analysis showed no change in conversion after 2 h up to 6 h (14 %) for the combustion-made $\text{LaFe}_{0.90}\text{Cu}_{0.10}\text{O}_3$ catalyst (see Figure 4). However, a little but definite increase in conversion (from 8 to 15 %) was observed for the $\text{LaFe}_{0.90}\text{Cu}_{0.10}\text{O}_3$ -IWI catalyst in hot-filtration test (see Figure 4). Thus, the nature of this oxidation reaction is purely heterogeneous for combustion-made $\text{LaFe}_{0.90}\text{Cu}_{0.10}\text{O}_3$ catalyst and the possibility of metal leaching or active material decomposition can be excluded.

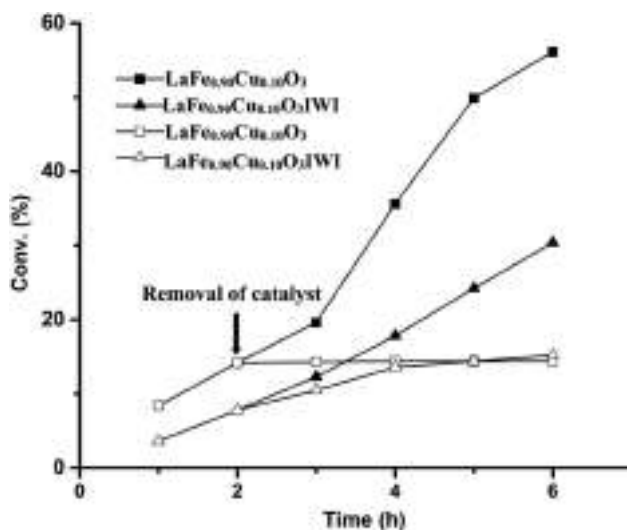


Figure 4: Sheldon hot-filtration test.

Table 2: H_2O_2 conversion (Conv.) and selectivity (SE) in different solvents over $\text{LaFe}_{0.90}\text{Cu}_{0.10}\text{O}_3$ at different time intervals^a.

Time (h)	Acetonitrile		Ethanol		Methanol		Water		Acetic acid	
	Conv.	SE	Conv.	SE	Conv.	SE	Conv.	SE	Conv.	SE
1	30.2	34.6	36.9	12.5	40.2	8.3	47.8	3.2	31.3	17.9
3	62.0	29.8	53.2	14.1	56.3	11.5	67.3	5.6	56.3	15.3
6	99.1	56.1	82.1	22.3	87.6	14.5	95.2	6.4	92.1	29.2

^aReaction conditions: 5 mL benzene + 0.5 g catalyst + 10 mL H_2O_2 + 20 mL solvent; $T = 70^\circ\text{C}$.

The certain enhancement of conversion in the absence of catalyst for $\text{LaFe}_{0.90}\text{Cu}_{0.10}\text{O}_3$ -IWI proves that the nature of catalytic oxidation is not truly heterogeneous in case of this catalyst and a certain amount of active metal is leaching out from this catalyst to the reaction mixture during the oxidation reaction (Figure 5).

The leaching of active metals has been reported to be controlled by using strong metal-supported interactions in $\text{Fe}^{3+}/\text{MgO}$ catalysts and the catalyst is also maintaining the same activity after the first cycle (36 % conversion) [75]. Cu-NaY zeolites were also reported as efficient catalysts with limited metal leaching after the first cycle and the leaching of the metal after the second cycle has almost stopped [76]. The metal leaching problem was controlled in 4 wt% Cu-MCM-41 and the phenol formation was lowered by 5 % only after the third cycle [70]. Bimetallic Co-V-MCM-41 shows reduced metal leaching in the benzene oxidation in acetonitrile with H_2O_2 at 70 °C for 24 h (conversion 48 % and 81 % selectivity of phenol) [77]. The metal leaching was also limited for the $\text{FeVCu}/\text{TiO}_2$ -catalyzed benzene oxidation in ascorbic acid [78]. Thus, the leaching of active metals is an important non-negligible aspect for these catalytic reactions in the literature. In our metal ion-substituted catalyst, where the active metals are incorporated into the perovskite structure, the probability of active metal leaching is expected to be lower. The recycling test of the combustion-made $\text{LaFe}_{0.90}\text{Cu}_{0.10}\text{O}_3$ catalyst retains its activity as well as selectivity in the successive cycles (up to the third cycle) but the conversion as well as the selectivity for the impregnated catalyst ($\text{Cu}_{0.10}\text{LaFe}_{0.90}\text{O}_3$ -IWI) decrease in successive cycles (conversion decreases from ~30 % to 24 % in the second cycle and

to 21 % in the third cycle). Thus, the reduced conversion in the recycling test of the IWI catalyst is accompanied by considerable copper leaching.

3.6 BET studies of the catalysts

The BET surface areas of the catalysts LaFeO_3 , $\text{LaFe}_{0.95}\text{Cu}_{0.05}\text{O}_3$, $\text{LaCu}_{0.10}\text{Fe}_{0.90}\text{O}_3$, the used $\text{LaFe}_{0.90}\text{Cu}_{0.10}\text{O}_3$ -cy2 (after 2nd cycle) and $\text{LaFe}_{0.90}\text{Cu}_{0.10}\text{O}_3$ -IWI are 12.6, 14.6, 26.6, 21.6 and $9.9 \text{ m}^2 \text{ g}^{-1}$ respectively. Among these catalysts, $\text{La}_{0.90}\text{Cu}_{0.10}\text{FeO}_3$ shows the highest surface area along with highest pore volume of $0.260 \text{ cm}^3 \text{ g}^{-1}$. The pore volume varies from 0.019 to $0.260 \text{ cm}^3 \text{ g}^{-1}$ for the other samples. The LaFeO_3 has very small pores of 1.8 nm width but all other catalysts have pore size distributions between 14.6 and 15.3 nm.

3.7 XRD studies

The powder XRD patterns of different perovskite (pure and Cu-substituted) samples show that the major phase formed in the combustion-synthesized and IWI catalysts is orthorhombic perovskite LaFeO_3 (Figure 6). All the diffraction lines could be indexed to the orthorhombic structure of LaFeO_3 (space group $Pnma$; JCPDS 37-1493). Some additional reflections are also present in our study which clearly

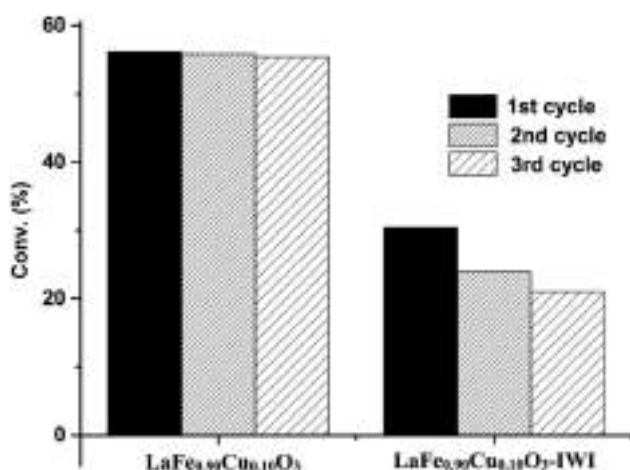


Figure 5: Recycling effect of the catalyst $\text{LaFe}_{0.90}\text{Cu}_{0.10}\text{O}_3$ prepared via (a) solution combustion (SCS), (b) impregnation (IWI) methods on benzene oxidation. Reaction conditions: 0.50 g catalyst + 5 mL benzene + 10 mL H_2O_2 + 20 mL MeCN; 6 h at $T = 70 \text{ }^\circ\text{C}$.

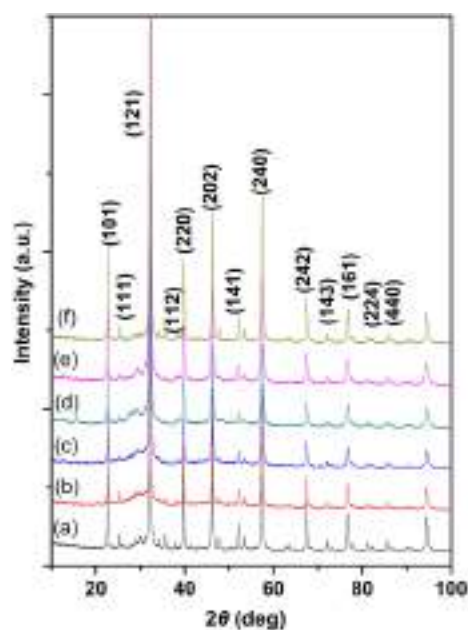


Figure 6: XRD patterns of (a) LaFeO_3 , (b) $\text{LaFe}_{0.95}\text{Cu}_{0.05}\text{O}_3$, (c) $\text{LaFe}_{0.93}\text{Cu}_{0.07}\text{O}_3$, (d) $\text{LaFe}_{0.90}\text{Cu}_{0.10}\text{O}_3$, (e) $\text{LaFe}_{0.85}\text{Cu}_{0.15}\text{O}_3$ and (f) $\text{LaFe}_{0.90}\text{Cu}_{0.10}\text{O}$ -IWI.

indicate the presence of very minor amounts of La_2O_3 and Fe_3O_4 as impurities. However, the parent LaFeO_3 contains more impurity phases which reduces as the Cu content increases. In case of the IWI sample, the peak around 35.6° is broadened and a new peak appears at 38.7° which indicates the formation of an additional phase and the presence of CuO oxide.

3.8 Microstructural studies

The low-magnification TEM image of the as-prepared $\text{LaFe}_{0.90}\text{Cu}_{0.10}\text{O}_{3-\delta}$ sample shows a holey structure with an unusual morphology (Figure 7(a)). The comprehensive HRTEM image of the as-prepared $\text{LaFe}_{0.90}\text{Cu}_{0.10}\text{O}_3$ shows the lattice fringes analogous to the LaFeO_3 phase from Fourier Transform (FT) measurement (Figure 7(b)). Spots at 2.37 and 2.78 Å match exactly the (112) and (121) crystallographic planes of LaFeO_3 , respectively. A poorly-defined structure is also identified over most of the LaFeO_3 crystals by HRTEM. The widening of the area labeled “a” in Figure 7(b) shows the poorly defined structure which comprises 2–4 atomic layers in most cases and an atomic mismatch is also observed among the surface of pure LaFeO_3 crystals with this poorly defined structure.

The $\text{LaFe}_{0.90}\text{Cu}_{0.10}\text{O}_3$ sample after the second cycle ($\text{LaFe}_{0.90}\text{Cu}_{0.10}\text{O}_3\text{-cy2}$) is almost similar to the fresh one and the holey structure is identical as in the as-prepared

sample (Figure 7(c)). Lattice fringes at 2.78 Å are also clearly observable in the areas labeled “a” and “b”, which again corresponds perfectly to the (121) crystallographic planes of LaFeO_3 , but in the enlarged images the existence of the poorly defined phase is marked by arrows (Figure 7(d)).

The general appearance of the sample synthesized by the IWI method ($\text{LaFe}_{0.90}\text{Cu}_{0.10}\text{O}_3\text{-IWI}$) is similar to those defined above for the samples prepared by the SCS method and low magnification image of the sample $\text{LaFe}_{0.90}\text{Cu}_{0.10}\text{O}_3\text{-IWI}$ also shows the characteristic holey structure (Figure 7(e)). However, HRTEM images show well-faceted LaFeO_3 planes and the poorly defined phase is not as common as in the samples prepared by combustion (Figure 7(f)).

Therefore, it can be concluded from HRTEM that the sample is comprised by holey LaFeO_3 crystals and a poorly defined structure located on top of the LaFeO_3 crystals. Cu is likely present as Cu^{2+} ions in the poorly defined areas rather forming a solid solution and an atomic mismatch between the poorly defined structure and the LaFeO_3 crystal surface is also observed. Such poorly defined areas are much more abundant in the sample prepared by combustion with respect to the sample prepared by IWI. In the SCS sample, almost all the LaFeO_3 crystals are covered by the poorly defined phase, whereas in the IWI samples there are abundant clean edges of LaFeO_3 crystals. This suggests that the SCS sample performs better as catalyst due to the existence of the poorly defined phase. Finally, the combustion-made catalyst exhibits a structure after the second cycle similar to

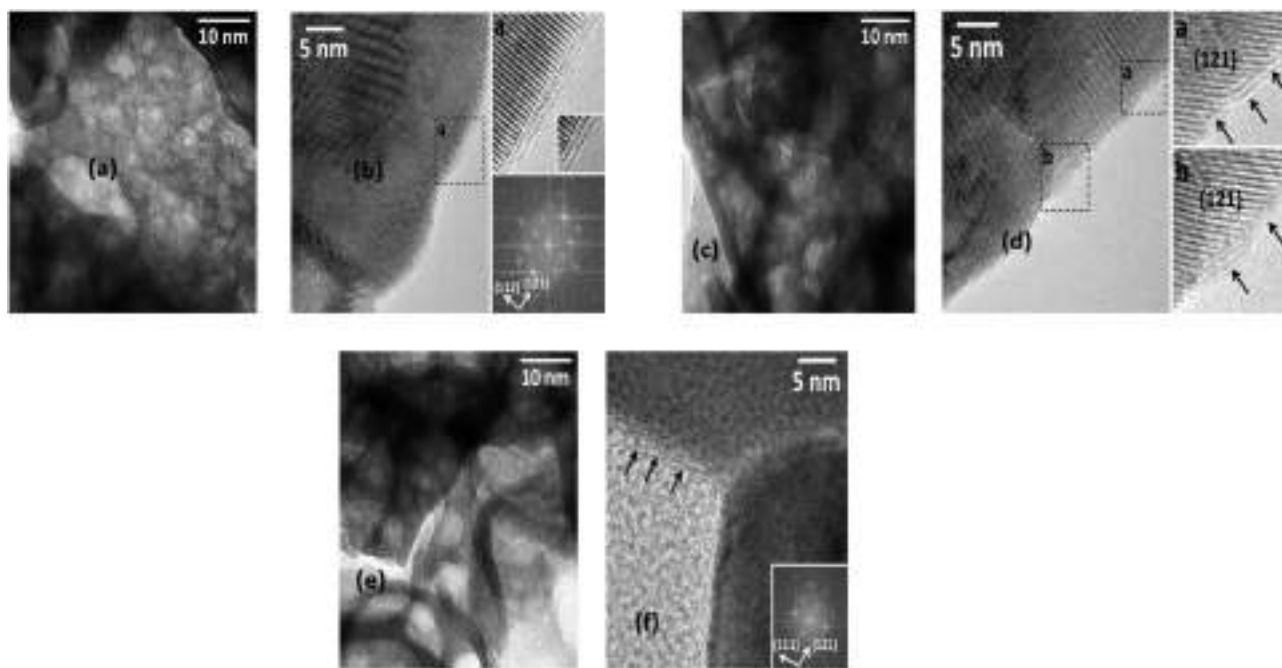


Figure 7: TEM images of (a, b) $\text{LaFe}_{0.90}\text{Cu}_{0.10}\text{O}_3$, (c, d) $\text{LaFe}_{0.90}\text{Cu}_{0.10}\text{O}_3\text{-cy2}$ and (e, f) $\text{Cu}_{0.10}\text{LaFe}_{0.90}\text{O}_3\text{-IWI}$.

the fresh sample at the atomic level, that is, with abundant poorly defined phase over the LaFeO_3 phase. This suggests that the poorly defined phase is not removed in the catalyst recycling.

3.9 General discussion of copper ion-substituted perovskite catalysts for benzene oxidation

Generally, copper in the oxidation state 2+ is believed to act as active site for the catalytic oxidation reaction of benzene to phenol [79–81]. In our study, the combustion-derived $\text{LaFe}_{0.90}\text{Cu}_{0.10}\text{O}_3$ catalyst is surrounded by an unusual surface structure on the surface-subsurface area of perovskite and copper is present as Cu^{2+} atom within the perovskite structure rather than as solid CuO . This unusual structure of $\text{LaFe}_{0.90}\text{Cu}_{0.10}\text{O}_3$ is playing the vital role in the much better oxidation activities of the combustion-synthesized catalyst rather than the corresponding catalyst prepared by incipient wetness impregnation ($\text{LaFe}_{0.90}\text{Cu}_{0.10}\text{O}_3\text{-IWI}$) where finely dispersed CuO is mainly present in the catalyst.

This phenomenon also supports the observation of the best activity of $\text{LaFe}_{0.90}\text{Cu}_{0.10}\text{O}_3$ catalyst among all examined catalysts (Table 1). We surprisingly note that the phenol selectivity increases with longer reaction times (in some cases reaching ~100 %). The decreased decomposition rate of H_2O_2 during reaction progress is primarily responsible for the overall increase of phenol selectivity at longer reaction times (6 h). The H_2O_2 decomposition progressively increases the quantity of water in the reaction mixture and as a result the concentration of oxidant as well as concentration of feebly water-soluble byproducts are decreasing in the presence of water.

Catalytic benzene oxidation in the presence of peroxide is usually following peroxy-metal pathways, similar to Fenton chemistry and the hydroxyl radicals activate the highly stable benzene molecule towards phenol formation [82]. The oxidation of benzene by peroxide over one-electron oxidants like copper is commonly believed to take place through a radical pathway [81, 83]. In the present study, we believe that a similar redox mechanism operates with H_2O_2 in our copper ion-substituted perovskite catalyst. In order to investigate the oxidation mechanism, we have performed the oxidation reaction in the presence of quinone, a radical scavenger. After 2 h of oxidation, the scavenger was added to the reaction mixture and the reaction progression was monitored. The analysis of the reaction aliquot clearly shows that the benzene oxidation is completely paused after the scavenger addition (Figure 8). Thus, we conclude that the

oxidation process over the perovskite catalyst reported in this study proceeds through a radical mechanism similar to previous literature reports [77, 83, 84]. In more detail, the metal ion (here copper) acts as a radical initiator for the auto-oxidation processes by promoting the decomposition of H_2O_2 to radicals mediated by the $\text{Cu}^{2+}/\text{Cu}^+$ redox couple (one-electron transfer process promoted by LaFeO_3 perovskite). Eventually benzyl free radicals are produced by abstraction of hydrogen by homolytic cleavage from benzene. This radical reacts further with the peroxy radical to form phenol and water.

The excellent activity (~56 % conversion with 100 % selectivity) of our $\text{LaFe}_{0.90}\text{Cu}_{0.10}\text{O}_3$ perovskite catalyst becomes even more evident when this system is compared with other catalysts reported previously. Bimetallic Cu-Ce-doped rice husk silica was reported as highly efficient catalyst with a high benzene conversion (84 %) as well as phenol selectivity (96 %) under atmospheric pressure at 70 °C in acetonitrile after 4 h. However, in this study a significant decline in conversion during successive cycles was reported due to active metal leaching [81]. Highly dispersed vanadium oxide on ceria-promoted rice husk silica also acts as a highly selective catalyst for phenol formation from benzene oxidation with H_2O_2 in acetonitrile at 60 °C, but the conversion was much lower (~21 %) [84]. Although our combustion-made catalyst provides lower surface areas than the commonly used supports such as zeolites [74, 77, 85–88], alumina [79], titania [89], magnesia [75] and rice husk silica [81, 83] it still shows significant activity as compared to many other reported catalysts. The peculiar structure of our combustion-made catalyst seems to be an important factor for the significant catalytic activity.

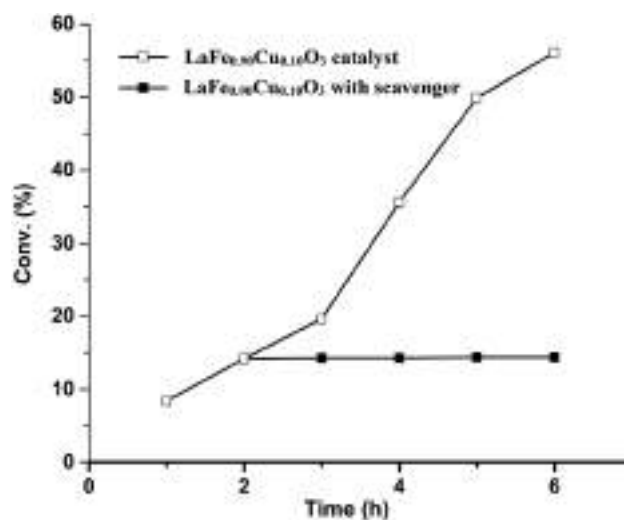


Figure 8: Effect of radical scavenger.

4 Conclusions

Copper-substituted $\text{LaFe}_{1-x}\text{Cu}_x\text{O}_3$ perovskite oxides have been prepared by a simple novel solution combustion method. Combustion-made $\text{LaFe}_{0.90}\text{Cu}_{0.10}\text{O}_3$ is shown to be a very efficient catalyst for the benzene oxidation in acetonitrile at 70 °C (56.1% conversion with 100% phenol selectivity). The effects of different parameters such as copper loading, time, temperature, oxidant concentration and solvent were studied and it was found that acetonitrile is the best solvent at 70 °C with a 1:2 molar ratio of benzene to H_2O_2 . A peculiar poorly defined structure on top of the LaFeO_3 particles in the combustion-made catalyst is characterized by microstructural studies and is probably due to incorporation of copper ion into the perovskite. The probability of active metal leaching is reduced for the combustion-made catalyst as compared to the analogous catalyst made by the incipient wetness impregnation (IWI) method. The recycling experiments also support this phenomenon where the combustion-made catalyst shows almost the same activity up to three cycles whereas the equivalent IWI catalyst shows noticeable loss of activity and selectivity in the successive cycles.

Author contributions: The author has accepted responsibility for the entire content of this submitted manuscript and approved submission.

Research funding: None declared.

Conflict of interest statement: The author declares no conflicts of interest regarding this article.

References

- Schmidt R. J. *Appl. Catal.*, A 2005, 280, 89–103.
- Solyman W. S., Nagiub H. M., Alian N. A., Shaker N. O., Kandil U. F. *J. Radiat. Res. Appl. Sci.* 2017, 10, 72–79.
- Pryde C., Hellman M. J. *Appl. Polym. Sci.* 1980, 25, 2573–2587.
- Takeichi T., Furukawa N. Epoxy resins and phenol-formaldehyde resins. In *Polymer Science: A Comprehensive Reference*. Elsevier BV: Amsterdam, 2021; pp. 723–751.
- Brydson J. A. *Plastics Materials*; Elsevier: Amsterdam, 1999.
- Zakoshansky V. *Pet. Chem.* 2007, 47, 273–284.
- Park H., Choi W. *Catal. Today* 2005, 101, 291–297.
- Fortuin J., Waterman H. *Chem. Eng. Sci.* 1953, 2, 182–192.
- Molinari R., Poerio T. *Asia-Pac. J. Chem. Eng.* 2010, 5, 191–206.
- Mancuso A., Sacco O., Sannino D., Venditto V., Vaiano V. *Catalysts* 2020, 10, 1424–1445.
- Yuranov I., Bulushev D. A., Renken A., Kiwi-Minsker L. *Appl. Catal.*, A 2007, 319, 128–136.
- Hu L., Wang C., Ye L., Wu Y., Yue B., Chen X., He H. *Appl. Catal.*, A 2015, 504, 440–447.
- Jiang T., Wang W., Han B. *New J. Chem.* 2013, 37, 1654–1664.
- Guo H., Chen Z., Mei F., Zhu D., Xiong H., Yin G. *Chem. Asian J.* 2013, 8, 888–891.
- Niwa S., Eswaremoorthy M., Nair J., Raj A., Itoh N., Shoji H., Namba T., Mizukami F. *Science* 2002, 295, 105–107.
- Parida K., Rath D. *Appl. Catal.*, A 2007, 321, 101–108.
- Peng J., Shi F., Gu Y., Deng Y. *Green Chem.* 2003, 5, 224–226.
- Nomiya K., Yagishita K., Nemoto Y., Kamataki T. *J. Mol. Catal. A: Chem.* 1997, 126, 43–53.
- Anandababu K., Muthuramalingam S., Velusamy M., Mayilmurugan R. *Catal. Sci. Technol.* 2020, 10, 2540–2548.
- Mistri R., Rahamana M., Llorca J., Priolkar K. R., Colussi S., Ray B. C., Gayen A. J. *Mol. Catal. A: Chem.* 2014, 390, 187–197.
- Muthuramalingam S., Anandababu K., Velusamy M., Mayilmurugan R. *Catal. Sci. Technol.* 2019, 9, 5991–6001.
- You X., Wei Z., Wang H., Li D., Liu J., Xu B., Liu X. *RSC Adv.* 2014, 4, 61790–61798.
- Tsuji T., Zaoputra A. A., Hitomi Y., Mieda K., Ogura T., Shiota Y., Yoshizawa K., Sato H., Kodera M. *Angew. Chem. Int. Ed.* 2017, 56, 7779–7782.
- Conde A., Diaz-Requejo M. M., Pérez P. J. *Chem. Commun.* 2011, 47, 8154–8156.
- Kumari S., Muthuramalingam S., Dhara A. K., Singh U., Mayilmurugan R., Ghosh K. *Dalton Trans.* 2020, 49, 13829–13839.
- Ramu R., Wanna W. H., Janmanchi D., Tsai Y. F., Liu C. C., Mou C. Y., Yu S. S. F. *Mol. Catal.* 2017, 441, 114–121.
- Yalymov A. I., Bilyachenko A. N., Levitsky M. M., Korlyukov A. A., Khrustalev V. N., Shul'pina L. S., Dorovatovskii P. V., Es'kova M. A., Lamaty F., Bantreil X., Villemejeanne B., Martinez J., Shubina E., Kozlov Y., Shul'pin G. *Catalysts* 2017, 7, 101–119.
- Carneiro L., Silva A. R. *Catal. Sci. Technol.* 2016, 6, 8166–8176.
- Vinogradov M. M., Kozlov Y. N., Nesterov D. S., Shul'pina L. S., Pombeiro A. J., Shul'pin G. B. *Catal. Sci. Technol.* 2014, 4, 3214–3226.
- Sarma B. B., Carmieli R., Collauto A., Efremenko I., Martin J. M., Neumann R. *ACS Catal.* 2016, 6, 6403–6407.
- Li X., Xue H., Lin Q., Yu A. *Appl. Organomet. Chem.* 2020, 34, 5606–5616.
- Dong Y., Niu X., Song W., Wang D., Chen L., Yuan F., Zhu Y. *Catalysts* 2016, 6, 74–90.
- Shijina A. V., Renuka N. K. *React. Kinet. Catal. Lett.* 2009, 98, 139–147.
- Peng G., Fu Z., Yin D., Zhong S., Yang Y., Yu N., Yin D. A. *Catal. Lett.* 2007, 118, 270–274.
- Tanarungsun G., Kiatkittipong W., Praserttham P., Yamada H., Tagawa T., Assabumrungrat S. *Catal. Commun.* 2008, 9, 1886–1890.
- Gu Y. Y., Zhao X. H., Zhang G. R., Ding H. M., Shan Y. K. *Appl. Catal.*, A 2007, 328, 150–155.
- Jourshabani M., Badiei A., Shariatinia Z., Lashgari N., Ziarani G. M. *Ind. Eng. Chem. Res.* 2016, 55, 3900–3908.
- Zhang T., Zhang D., Han X., Dong T., Guo X., Song C., Si R., Liu W., Liu Y., Zhao Z. *J. Am. Chem. Soc.* 2018, 140, 16936–16940.
- Ito S., Mitarai A., Hikino K., Hiramata M., Sasaki K. *J. Org. Chem.* 1992, 57, 6937–6941.
- Chen D., Chen C., Baiyee Z. M., Shao Z., Ciucci F. *Chem. Rev.* 2015, 115, 9869–9921.
- Cheng F., Chen J. *Chem. Soc. Rev.* 2012, 41, 2172–2192.
- Ge X., Sumboja A., Wu D., An T., Li B., Goh F. W. T., Hor T. S. A., Zong Y., Liu Z. *ACS Catal.* 2015, 5, 4643–4667.
- Zhu J., Li H., Zhong L., Xiao P., Xu X., Yang X., Zhao Z., Li J. *ACS Catal.* 2014, 4, 2917–2940.
- Zhu H., Zhang P., Dai S. *ACS Catal.* 2015, 5, 6370–6385.
- Wang W., Tadé M. O., Shao Z. *Chem. Soc. Rev.* 2015, 44, 5371–5408.
- Chandra P. *ChemistrySelect* 2021, 6, 7557–7597.

47. Teixeira G. F., Junior E. S., Vilela R., Zaghe M. A., Colmati F. *Catalysts* 2019, 9, 721–726.
48. Kleineberg H., Eisenacher M., Lange H., Strutz H., Palkovits R. *Catal. Sci. Technol.* 2016, 6, 6057–6065.
49. Yamaguchi S., Okuwa T., Wada H., Yamaura H., Yahiro H. *Res. Chem. Intermed.* 2015, 41, 9551–9561.
50. Singh H., Rajput J. K. *J. Mater. Sci.* 2018, 53, 3163–3188.
51. Mistri R. *Asian J. Chem.* 2022, 34, 2489–2498.
52. Kawasaki S., Kamata K., Hara M. *Chem. Cat. Chem.* 2016, 8, 3247–3253.
53. Shibata S., Sugahara K., Kamata K., Hara M. *Chem. Commun.* 2018, 54, 6772–6775.
54. Marchena C. L., Pecchi G. A., Pierella L. B. *Catal. Commun.* 2019, 119, 28–32.
55. Shibata S., Kamata K., Hara M. *Catal. Sci. Technol.* 2021, 11, 2369–2373.
56. Dharmana T., Naidu B. N. *Asian J. Chem.* 2022, 34, 437–442.
57. Xue Y., Xin H., Xie W., Wu P., Li X. *Chem. Commun.* 2019, 55, 3363–3366.
58. Zheng Y., Zhang R., Zhang L., Gu Q., Qiao Z. A. *Angew. Chem. Int. Ed.* 2021, 60, 4774–4781.
59. Mistri R., Das D., Llorca J., Dominguez M., Mandal T. K., Mohanty P., Ray B. C., Gayen A. *RSC Adv.* 2016, 6, 4469–4477.
60. Sushkevich V. L., Palagin D., Ranocchiaro M., van Bokhoven J. A. *Science* 2017, 356, 523–527.
61. Anastas P., Warner J. *Green Chemistry: Theory and Practice*; Oxford University Press: New York, 1998.
62. Morejudo S. H., Zanón R., Escolástico S., Tirados I. Y., Fjeld H. M., Vestre P. K., Coors W. G., Martínez A., Norby T., Serra J. M., Kjølseth C. *Science* 2016, 353, 563–566.
63. Komanoya T., Kinemura T., Kita Y., Kamata K., Hara M. *J. Am. Chem. Soc.* 2017, 139, 11493–11499.
64. Kanai S., Nagahara I., Kita Y., Kamata K., Hara M. *Chem. Sci.* 2017, 8, 3146–3153.
65. Climent M. J., Corma A., Iborra S. *Green Chem.* 2014, 16, 516–547.
66. Hara M., Nakajima K., Kamata K. *Sci. Technol. Adv. Mater.* 2015, 16, 034903–034925.
67. Alonso D. M., Wettstein S. G., Dumesic J. A. *Chem. Soc. Rev.* 2012, 41, 8075–8098.
68. Cornils B., Herrmann W. A., Beller M., Paciello R. *Applied Homogeneous Catalysis with Organometallic Compounds: A Comprehensive Handbook in Four Volumes*, 3rd ed.; Wiley-VCH: Weinheim, 2017.
69. Besson M., Gallezot P., Pinel C. *Chem. Rev.* 2014, 114, 1827–1870.
70. Chandran R. S., Ford W. T. *J. Chem. Soc., Chem. Commun.* 1988, 46, 104–105.
71. Guilhaume N., Primet M. *J. Catal.* 1997, 165, 197–204.
72. Berger D., Matei C., Papa F., Voicu G., Fruth V. *Prog. Solid State Chem.* 2007, 35, 183–191.
73. Stuchinskaya T. L., Kozhevnikov I. V. *Catal. Commun.* 2003, 4, 417–422.
74. Ferguson G., Ajjou A. N. *Tetrahedron Lett.* 2003, 44, 9139–9142.
75. Kockritz A., Sebek M., Dittmar A., Radnik J., Bruckner A., Bentrup U., Hugl H., Magerlein W. *J. Mol. Catal. A: Chem.* 2006, 246, 85–99.
76. Peyrovi M. H., Mahdavi V., Salehi M. A., Mahmoodian R. *Catal. Commun.* 2005, 6, 476–479.
77. Choudhary V. R., Dumbre D. K. *Appl. Catal., A* 2010, 375, 252–257.
78. Sheldon R. A., Arends I. W. C. E., Dijkman A. *Catal. Today* 2000, 57, 157–166.
79. Shiono M., Kobayashia K., Nguyen T. L., Hosoda K., Kato T., Ota K., Dokiya M. *Solid State Ionics* 2004, 170, 1–7.
80. Giebel L., Kiebling D., Wendt G. *Chem. Eng. Technol.* 2007, 30, 889–894.
81. Sorenson S. C., Wronkiewicz J. A., Sis L. B., Wirtz G. P. *Am. Ceram. Soc. Bull.* 1974, 53, 446–449.
82. Behera G. C., Parida K. M. *Appl. Catal., A* 2012, 413, 245–253.
83. Brunel D., Fajula F., Nagy J. B., Deroide B., Verhoef M. J., Veum L., Peters J. A., van Bekkum H. *Appl. Catal., A* 2001, 213, 73–82.
84. Choudhary V. R., Dumbre D. K., Uphade B. S., Narkhede V. S. *J. Mol. Catal. A: Chem.* 2004, 215, 129–135.
85. Merino N. A., Barbero B. P., Grange P., Cadús L. E. *J. Catal.* 2005, 231, 232–244.
86. Pena M. A., Fierro J. L. G. *Chem. Rev.* 2001, 101, 1981–2018.
87. Royer S., Berube F., Kaliaguine S. *Appl. Catal., A* 2005, 282, 273–284.
88. Koponen M. J., Suvanto M., Pakkanen T. A., Kallinen K., Kinnunen T. J. J., Haörkönen M. *Solid State Sci.* 2005, 7, 7–12.
89. Tanarungsun G., Kiatkittipong W., Praserttham P., Yamada H., Tagawa T., Assabumrungrat S. *J. Ind. Eng. Chem.* 2008, 14, 596–601.



Cite this: DOI: 10.1039/d2ee04211h

Scalable production of an intermetallic Pt–Co electrocatalyst for high-power proton-exchange-membrane fuel cells†

Tae Yong Yoo,^{‡,ab} Jongmin Lee,^{‡,ab} Sungjun Kim,^{‡,ab} Min Her,^{ab} Shin-Yeong Kim,^{‡,ab} Young-Hoon Lee,^{ab} Heejong Shin,^{ab} Hyunsun Jeong,^{ab} Arun Kumar Sinha,^{ab} Sung-Pyo Cho,^c Yung-Eun Sung^{‡,*ab} and Taeghwan Hyeon^{‡,*ab}

Power performance is the primary bottleneck to the industrial application of proton-exchange-membrane fuel cells, which hinges on catalytic activity, oxygen mass transfer, and proton conduction at the cathode catalyst layer. Tackling all these critical factors requires a holistic design of catalyst, embodied by an elaborate synthesis. Here we present a straightforward synthetic approach to address these practical issues. A bimetallic compound, formulated as $[\text{Co}(2,2'\text{-bipyridine})_3][\text{PtCl}_6]$, thermally decomposes and produces carbon-protected sub-5 nm-sized intermetallic Pt–Co nanoparticles, on which compressively-strained and rigid Pt-skin can be formed. In addition to the high intrinsic activity, we achieved the combined features of high electrochemical surface area, N-doping on the mesoporous carbon support, and highly stabilized Co that could promote oxygen mass transfer and proton conduction. In the single cell configuration, the catalyst achieved unprecedented rated power densities of 1.18 W cm^{-2} and $5.9 \text{ W mg}_{\text{Pt}}^{-1}$ at 0.67 V (with a cathode loading of $0.1 \text{ mg}_{\text{Pt}} \text{ cm}^{-2}$), while experiencing voltage loss of only 29 mV (at 0.8 A cm^{-2}) at the end of the test.

Received 31st December 2022,
Accepted 30th January 2023

DOI: 10.1039/d2ee04211h

rsc.li/ees

Broader context

Hydrogen is a promising alternative to fossil fuels that can be produced in sustainable ways and effectively converted into electricity through fuel cell systems. The economic viability of the fuel cell system is a key factor that determines the transition towards a hydrogen economy. However, despite the huge previous efforts on proton-exchange-membrane fuel cells, we are still facing limited performance, mainly regarding the power density, long-term durability, and cost of platinum catalysts. Therefore, a novel production method for platinum-based electrocatalysts is in urgent need, which requires a precise design of the synthesis to overcome the multiple challenging issues. In this study, we present a straightforward and scalable synthetic platform based on thermal annealing for the practical production of a platinum-based fuel cell catalyst with unprecedented power performance. The overall structure of the catalyst, including the rigid platinum-skin surface, stable intermetallic core, sufficient ECSA, and highly porous and nitrogen-doped carbon support, not only gives high intrinsic activity but also promotes the oxygen mass transfer and proton conduction. We believe that the proposed thermal synthetic method will stimulate the practical production of commercially viable electrocatalysts for the fuel cell industry.

Introduction

Proton-exchange-membrane fuel cells (PEMFCs) are a representative system for the widespread use of hydrogen as a clean

energy carrier.^{1,2} Several critical challenges, including improving the power density, reducing the cost of platinum (Pt)-based catalysts and increasing the durability, need to be overcome for the large-scale commercialization of PEMFCs.^{3–5} The energy efficiency of PEMFCs heavily relies on the cathode catalyst layer (CCL) where sluggish kinetics of the oxygen reduction reaction (ORR) greatly reduces the cell voltage, whilst poor oxygen mass transfer and low proton conduction limit the overall power efficiency.^{3,4} Thanks to the intensive efforts to improve the intrinsic catalytic activity through novel nanomaterials,^{5–14} several reports have surpassed the 2025 target of the U.S. Department of Energy (DOE) for the mass activity at 0.9 V ($0.44 \text{ A mg}_{\text{Pt}}^{-1}$).^{5–11} However, their power performance at 0.67 V is still far below the practical level (1 W cm^{-2} and $8 \text{ W mg}_{\text{Pt}}^{-1}$).¹⁵

^a Center for Nanoparticle Research, Institute for Basic Science (IBS), Seoul 08826, Republic of Korea

^b School of Chemical and Biological Engineering, and Institute of Chemical Processes, Seoul National University, Seoul 08826, Republic of Korea.
E-mail: ysung@snu.ac.kr, thyeon@snu.ac.kr

^c National Center for Inter-University Research Facilities, Seoul National University, Seoul 08826, Republic of Korea

† Electronic supplementary information (ESI) available. See DOI: <https://doi.org/10.1039/d2ee04211h>

‡ These authors contributed equally to this work.

Thus, it is now imperative to seek a high-power and durable PEMFC operation based on a practical and scalable synthetic process of catalysts.^{16–18}

Practical design of catalysts for high-power PEMFCs requires a holistic consideration of multiple factors that affect performance at high current density (HCD, $>0.8 \text{ A cm}^{-2}$).¹⁹ Oxygen mass transfer is mainly responsible for the cell voltage reduction at HCD, and various strategies, which include high electrochemical surface area (ECSA) of Pt-based nanoparticles (close to $50 \text{ m}^2 \text{ g}_{\text{Pt}}^{-1}$ for low Pt loadings),^{4,20,21} high mesoporosity of CCL,^{22,23} and heteroatom doping on carbon supports for uniform distribution of ionomers on the catalyst,^{24,25} have been explored to address this key issue. Poor proton conduction is another dominant issue at HCD, which is affected by the presence of dissolved metal ions and the quality of the ionomer.^{26–28} Recently, various highly-ordered Pt-based intermetallic nanomaterials have been extensively investigated to enhance the catalytic activity and stability, even with a significantly decreased amount of Pt.^{5,8–11} In particular, protection of intermetallic crystal cores, such as $\text{L1}_0\text{-PtCo}$ and $\text{L1}_2\text{-Pt}_3\text{Co}$, with a Pt-skin surface not only allows high intrinsic activity but also provides excellent electrochemical stability by preventing the cobalt dissolution that blocks proton conduction, thereby minimizing Fenton reaction that damages the ionomer and membrane.^{8,29,30}

However, for industrial-scale applications, it is challenging to simplify the current complicated synthetic procedures required to get an ideal form of PEMFC catalyst. Synthesis of intermetallic nanoparticles generally requires a high-temperature annealing to get ordered intermetallic structures, which often results in the severe aggregation of the nanoparticles.³¹ Two representative strategies, including physical protection^{32–34} and strong anchoring^{35,36} of nanoparticles on the support, effectively prevent aggregation, but both methods still require huge efforts to create and remove protective shells or anchoring sites, precluding large-scale production. Furthermore, achieving all the desired structural factors of supported nanoparticles without using toxic organic surfactants and solvents remains elusive, which could cause safety issues in the manufacturing process.³¹

Herein we present a practical and facile synthetic approach that addresses all the aforementioned issues and demonstrate an excellent PEMFC power performance. The electrostatic attraction between two oppositely charged metal complexes enables the facile preparation of a bimetallic compound, which provides a unique carbon-confined environment to produce highly dispersed intermetallic alloy nanoparticles on a commercial mesoporous carbon support *via* a simple thermal annealing process.³⁷ Ketjenblack EC-600JD (KB) is chosen as the support for the uniform formation of alloy nanoparticles due to its mesoporosity and high surface area, enabling an effective decomposition and dispersion of the bimetallic compound upon annealing. The overall structure of the prepared electrocatalyst simultaneously tackled the critical issues in PEMFCs, including ORR kinetics (by the strained Pt-skin surface on the intermetallic Pt–Co core), oxygen mass transfer (by the high ECSA and mesoporous N-doped carbon support), and proton conduction (by stabilized Co species in the intermetallic core and Pt-skin) with desirable durability.

Results and discussion

Synthesis of supported intermetallic Pt–Co nanoparticles

The bimetallic $[\text{Co}(\text{bpy})_3][\text{PtCl}_6]$ compound (Co–Pt compound, bpy = 2,2'-bipyridine) was prepared simply by adding $[\text{PtCl}_6]^{2-}$ solution into $[\text{Co}(\text{bpy})_3]^{2+}$ solution (Fig. 1(a)). We confirmed the morphology of the Co–Pt compound and its high crystallinity by transmission electron microscopy (TEM) and X-ray diffraction (XRD) analyses (Fig. S1, ESI†). Energy-dispersive X-ray spectroscopy (EDS) elemental mapping indicates the homogeneous distribution of Co and Pt in the compound with 1:1 atomic composition (Fig. 1(b) and Table S1, ESI†). The bipyridine ligand plays a central role (Fig. S2, ESI†) not only in the formation of Co–Pt compound (Fig. S3, ESI†) but also in the *in situ* formation of the N-doped carbon shell that protects the nanoparticles from aggregation in the subsequent annealing process.³⁷ The attachment of Co–Pt compound on KB was readily done by either grinding them together or ball milling. Scanning electron microscopy (SEM), TEM, and scanning transmission electron microscopy (STEM) images clearly show both the Co–Pt compound and KB in the composite (Fig. 1(c) and Fig. S4, ESI†). Although every grain of the Co–Pt compound was not completely separated and ideally dispersed on KB during this grinding step, the subsequent thermal annealing could induce an effective decomposition of this compound to uniformly cover all the surface of KB, producing alloy nanoparticles. Brunauer–Emmett–Teller (BET) analysis indicated the retention of the pore structure of KB after grinding with the Co–Pt compound (Fig. S5, ESI†).

We induced a thermal decomposition of the Co–Pt compound on KB by annealing the composite at $900 \text{ }^\circ\text{C}$ (Fig. 1(a)). SEM and TEM analyses indicate that KB retains its mesoporous morphology (Fig. 1(d) and Fig. S6, ESI†), while the XRD pattern of the annealed composite reveals the formation of an intermetallic $\text{L1}_0\text{-CoPt}$ (i-CoPt) phase (Fig. S7, ESI†). The annealed sample (denoted as i-CoPt/KB) accommodates i-CoPt nanoparticles of uniform sizes between 3–4 nm due to the presence of an *in situ*-formed N-doped carbon shell as a physical barrier against aggregation (Fig. 1(e), (f) and Fig. S6, ESI†).³⁸ We performed STEM-EDS mapping to characterize the homogeneous distribution of Co, Pt, and N elements in the entire surface of i-CoPt/KB (Fig. S8, ESI†). The high-angle annular dark-field STEM (HAADF-STEM) image in Fig. 1(g) clearly shows the characteristic inter-atomic arrangement in a single i-CoPt nanoparticle.^{36,37} The presence of an N-doped carbon shell was identified by high-resolution TEM imaging, as shown in Fig. S9 (ESI†). It is noteworthy that the use of bipyridine offers a unique route to produce size-confined intermetallic nanoparticles on an irregular porous carbon support without any use of elaborate colloidal synthesis or anti-aggregation treatment. The high surface area of KB played an essential role in the homogeneous decomposition and dispersion of the Co–Pt compound in the annealing conditions.

We further investigated the specific formation mechanism of compound-derived i-CoPt nanoparticles on KB using *ex situ* XRD measurement. The characteristic peaks of the Co–Pt compound completely disappear at $300 \text{ }^\circ\text{C}$ with no sign of metallic phase (Fig. 2(a)). As the temperature increases, both

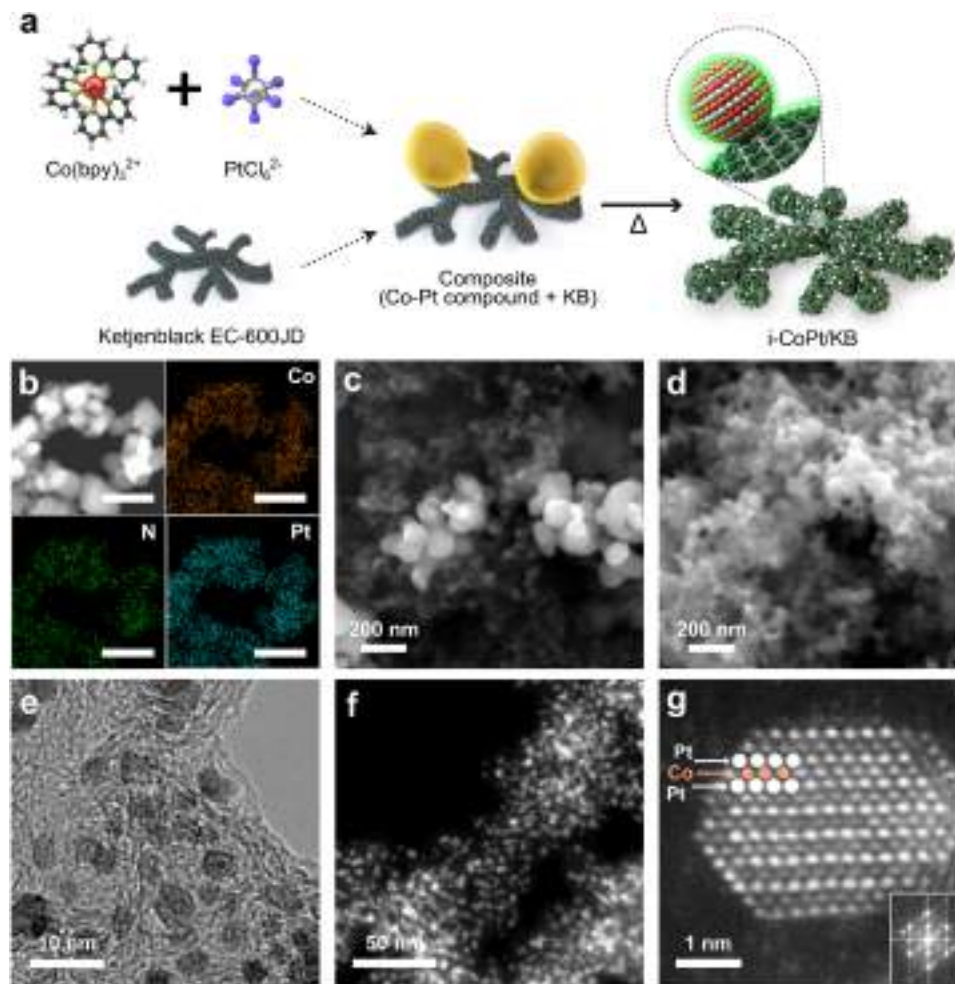


Fig. 1 (a) Schematic illustration of the synthesis of supported Pt–Co nanoparticles. (b) STEM-EDS mapping of the Co–Pt compound. The scale bar is 250 nm. SEM images of the (c) composite, and (d) i-CoPt/KB. (e) TEM, and (f) STEM images of i-CoPt/KB. (g) HAADF-STEM image and its FFT pattern (inset) of i-CoPt/KB. The atomic arrangement of Co and Pt is marked by orange and white colors, respectively.

the Pt-rich Co_xPt_y phase and Co phase evolve at 500 °C, after which the Co phase gradually decreases and finally disappears at 800 °C. The intensity of the main peak at around 41.2 degree continuously increases from 500 to 900 °C, which indicates the growth of CoPt nanoparticles. The clear signs of the intermetallic phase, the (110) peak at around 33.1 degree and two superlattice peaks between 50–65 degree, appear after 2 hours at 900 °C, and become even sharper afterwards. TEM, STEM (Fig. S10, ESI[†]), and X-ray photoelectron spectroscopy (XPS) (Fig. S11, ESI[†]) analyses strongly support the growth mechanism inferred from the XRD data. Based on the above information, we derived four representative stages of nanoparticle formation, as illustrated in Fig. 2(b). Pt and Co ions in carbon (at 300 °C) bond together to form Pt-rich alloys and Co clusters (at 500 °C), which subsequently evolve into CoPt random alloy nanoparticles (at 800 °C) and finally convert into i-CoPt nanoparticles (at 900 °C after 6 hours).

Catalyst activation and structural analysis

We then applied an exquisite thermal activation process to obtain an activated electrocatalyst, denoted as i-CoPt@Pt/KB

(see ESI[†]).³⁹ Air-etching was used to remove the N-doped carbon shell on the surface of the i-CoPt nanoparticles, and the subsequent H_2 -annealing could induce re-alloying of some oxidized Co with CoPt alloy nanoparticles together with the formation of the Pt-skin surface. It is worth noting that the overall thermal process in this study allows consecutive formation and activation of supported i-CoPt nanoparticles in a single furnace, making the entire production simple but highly reproducible. After the activation, 2–3 layers of Pt-skin surface with interior i-CoPt core were obtained without aggregation, which was clearly identified by TEM and HAADF-STEM imaging (Fig. 3(a), (b) and Fig. S12, ESI[†]). The XRD pattern clearly reveals the well-preserved ordered structure of the i-CoPt core after the activation (Fig. S13, ESI[†]). The development of the i-CoPt core and Pt-skin structure was also characterized by X-ray absorption near edge structure (XANES), extended X-ray absorption fine structure (EXAFS), and XPS analyses (Fig. S14 and S15, ESI[†]). The increased white line intensity of i-CoPt@Pt/KB in the Pt L_3 -edge XANES spectrum indicates that the N-doped carbon shell is effectively etched and the Pt-skin is fully exposed to the

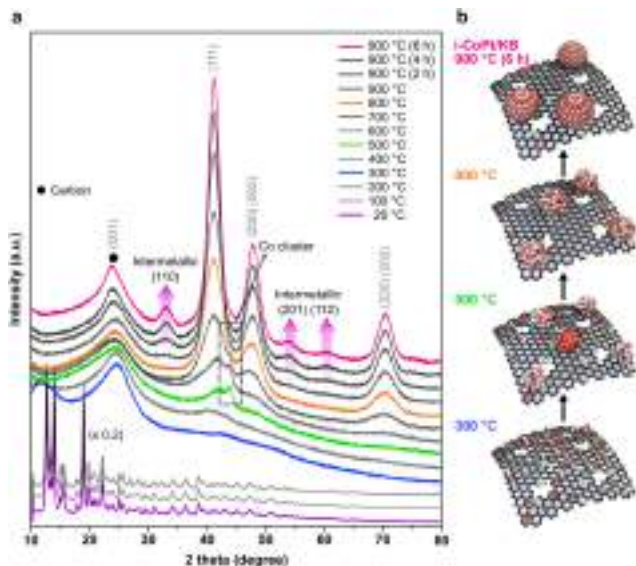


Fig. 2 (a) *Ex situ* XRD patterns at different annealing temperatures from 100 to 900 °C. The intensities of the 20, 100, and 200 °C curves are multiplied by 0.2. (b) Schematic illustration of the formation mechanism of i-CoPt nanoparticles on KB. Each Pt, Co, N, and C atom is colored in gray, red, green, and black, respectively.

air (Fig. 3(c)).⁴⁰ Furthermore, the lattice contraction of Pt in both the i-CoPt core and the Pt-skin was confirmed by Pt EXAFS (Fig. 3(d) and Fig. S16, ESI[†]), and the compressive strain of -4.24% at the outermost surface was observed by HAADF-STEM imaging (Fig. S17, ESI[†]). This compressive strain is

known to tailor the electronic state of the Pt surface by downshift of the d-band center, which is translated to an enhanced ORR activity by weaker binding energy of reaction intermediates compared to pure Pt.^{41–43} Co K-edge XANES and EXAFS spectra demonstrate negligible change after the activation, mainly due to the intact Co species in the i-CoPt core of i-CoPt@Pt nanoparticles (Fig. 3(e) and (f)). XPS analysis on Co further supports this result by the presence of a weak signal of Co⁰ after the activation because of rigid protection by the outermost Pt-skin layer (Fig. S15b, ESI[†]). We confirmed the increment of the Co composition from the surface to the core by controlling the incident photon energy in XPS analysis (Fig. S18, ESI[†]).^{44,45} The exact Pt mass loadings of i-CoPt/KB and i-CoPt@Pt/KB were obtained by inductively coupled plasma atomic emission spectroscopy (ICP-AES), which showed high Co content of 28.4 atom% and Pt mass loading higher than 40 wt% after the activation (Table S2, ESI[†]). This high Pt loading is beneficial for the preparation of a thin CCL that shortens the oxygen transfer pathway (Fig. S19 and S20, ESI[†]). We further confirmed the scalability of the overall synthetic process by gram-scale synthesis of i-CoPt/KB and its activation without compromising the quality of both i-CoPt/KB and i-CoPt@Pt/KB (Fig. S21, ESI[†]).

Electrochemical half-cell performance of i-CoPt@Pt/KB

The electrocatalytic properties of the prepared catalysts were first studied using the rotating-disk electrode (RDE) technique with commercial Pt/C as a benchmark catalyst. We observed a significant difference between the as-prepared i-CoPt/KB and the activated i-CoPt@Pt/KB in their cyclic voltammogram (CV)

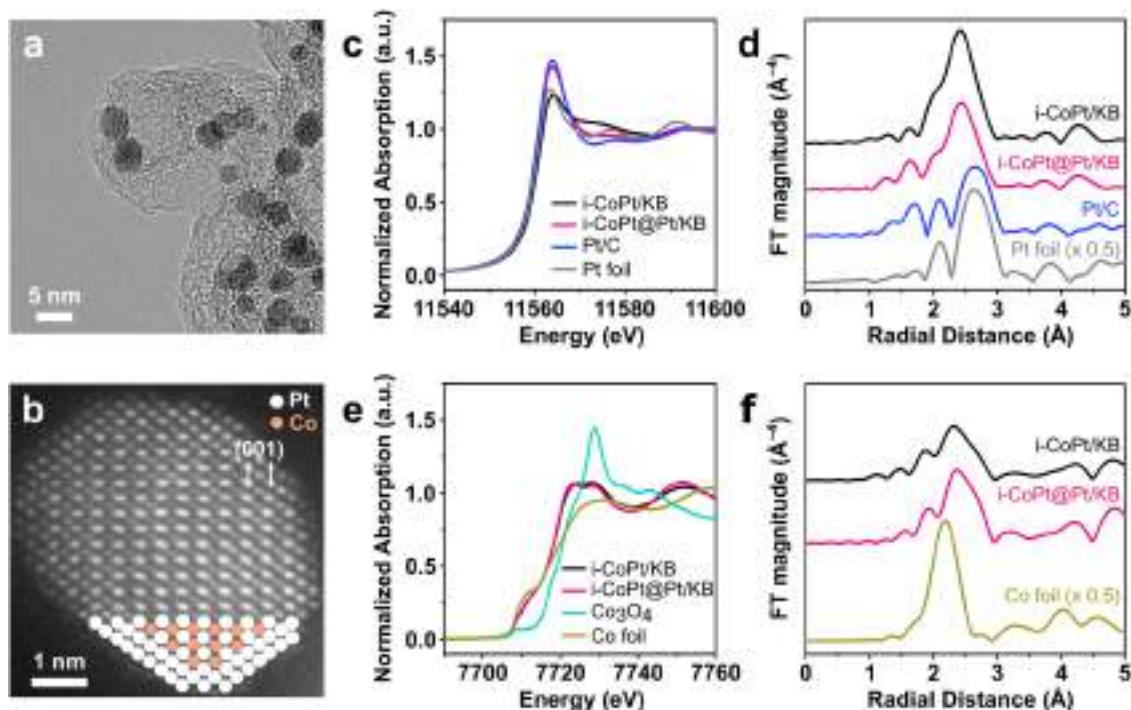


Fig. 3 (a) TEM image of i-CoPt@Pt/KB. (b) HAADF-STEM image of i-CoPt@Pt/KB. The Pt-skin layers and the internal atomic arrangement of Co and Pt are marked by orange and white colors, respectively. (c) Pt L₃-edge XANES, and (d) Pt EXAFS data of i-CoPt@Pt/KB with i-CoPt/KB, commercial Pt/C, and Pt foil. (e) Co K-edge XANES, and (f) Co EXAFS data of i-CoPt@Pt/KB with i-CoPt/KB, Co₃O₄, and Co foil.

curves (Fig. 4(a)). i-CoPt@Pt/KB exhibits only the feature of a double layer capacitance due to the complete coverage of i-CoPt nanoparticles with N-doped carbon shell. The facile air etching at 200 °C effectively exposed the Pt surface with no sign of nanoparticle aggregation or loss of KB. The fully exposed Pt-skin surface in i-CoPt@Pt/KB exhibited high ECSA of 58.2 m² g_{Pt}⁻¹ as measured by a CO stripping experiment (Fig. 4(b) and Fig. S22, ESI[†]) due to the uniform particle sizes of 3 to 4.5 nm (Fig. S12, ESI[†]). As expected, i-CoPt@Pt/KB showed superior ORR activities (mass activity of 2.07 A mg_{Pt}⁻¹ and specific activity of 3.95 mA cm_{Pt}⁻²) compared to those of Pt/C due to the compressive strain on Pt-skin exerted by the i-CoPt core (Fig. 4(c) and Fig. S23, ESI[†]).^{46–50} We confirmed the electron transfer number of i-CoPt@Pt/KB by rotating ring-disk electrode (RRDE) measurement, which demonstrated an excellent 4-electron reaction pathway at all potential ranges along with the commercial Pt/C (Fig. S24, ESI[†]). Owing to the rigid Pt-skin structure, i-CoPt@Pt/KB showed excellent durability after an accelerated durability test (ADT) for 30 000 cycles with barely changed ECSA (Fig. S25 and S26, ESI[†]) and half-wave potential (Fig. S27, ESI[†]),^{51,52} while commercial Pt/C was severely damaged. We also confirmed that the electrocatalytic properties were not affected even in gram-scale synthesis, which sheds light on the mass production of i-CoPt@Pt/KB for its practical application (Fig. S28, ESI[†]).

Practical fuel cell performance

To demonstrate the practical application of i-CoPt@Pt/KB in PEMFCs, the membrane electrode assembly (MEA) using

i-CoPt@Pt/KB was fabricated, and its performance and durability were evaluated under practical operating conditions. For a benchmark, the MEA with commercial Pt/C (HiSPEC 4000, Johnson Matthey Co.) was prepared and tested under the same conditions. Because all the components used in the tested MEAs were identical except for the cathode catalysts, the MEAs were labeled by the name of the cathode catalysts used. For all MEAs, the Pt loading of the cathode was fixed to 0.1 mg_{Pt} cm⁻² to secure reasonable power densities and durability, and the ionomer to carbon weight ratios were optimized to be 0.8 for the i-CoPt@Pt/KB and 0.5 for the Pt/C cathode, respectively (Fig. S29, ESI[†]). SEM images of both catalyst-coated membranes (CCMs) clearly show similar thicknesses and secondary pore geometries of CCLs (Fig. S30, ESI[†]). i-CoPt@Pt/KB exhibited high ECSA of 53.3 m² g_{Pt}⁻¹ (roughness factor of 53.3 cm_{Pt}² cm_{MEA}⁻²) which is close to the value measured in the RDE test (Fig. 4(b) and Fig. S31, ESI[†]). On the contrary, the higher ECSA of the benchmark Pt/C catalyst in RDE (due to the smaller particle size of 3 nm) was not translated to the MEA configuration due to the well-known poisoning of the Pt surface by selective adsorption of the ionomer.¹⁵ Although SEM-EDS mapping data shows comparable distribution of F element for both cathodes (Fig. S32, ESI[†]), this different loss of ECSAs between the two catalysts is mainly attributed to the N-doping in i-CoPt@Pt/KB (Fig. S33, ESI[†]), which enhances the ionomer distribution on the carbon support and contributes to an effective formation of triple phase boundaries (Fig. S34, ESI[†]).²⁴

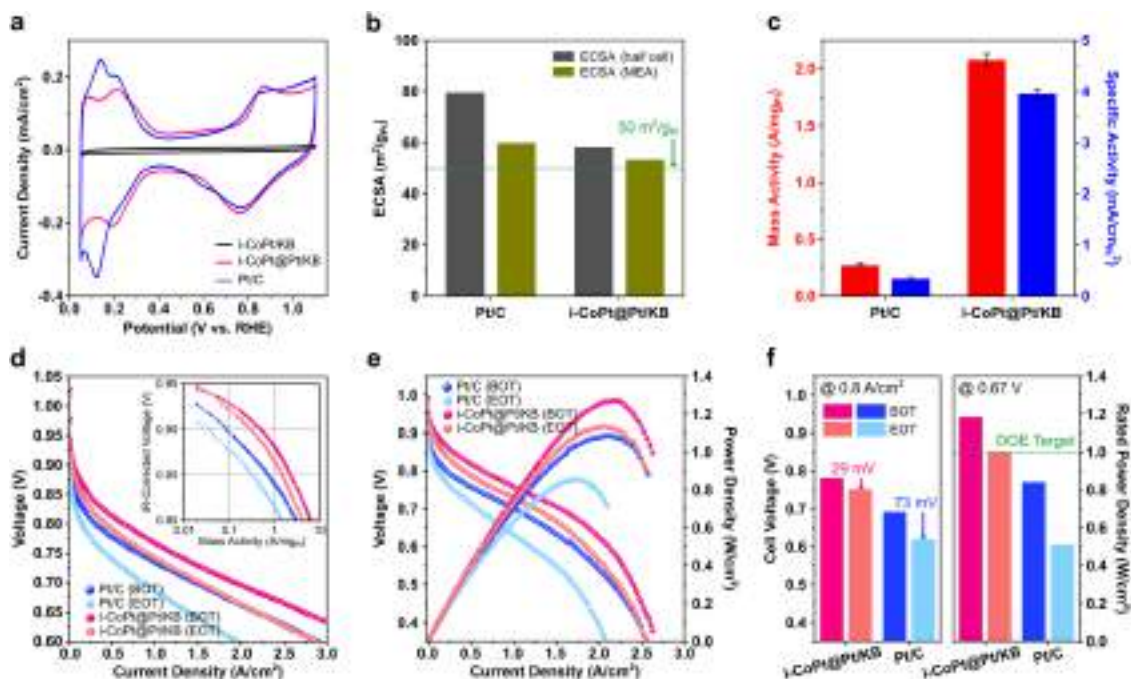


Fig. 4 (a) CV curves of i-CoPt@Pt/KB with i-CoPt/KB, and commercial Pt/C. (b) ECSA of Pt/C and i-CoPt@Pt/KB measured in a half-cell and MEA. (c) Mass and specific activities of i-CoPt@Pt/KB at 0.9 V (versus RHE) compared to commercial Pt/C. (d) H₂-O₂ fuel cell polarization curves and the derived Tafel plots (inset) before and after ADT cycling. H₂ flow rate = 0.2 L min⁻¹, O₂ flow rate = 0.2 L min⁻¹. (e) H₂-air fuel cell polarization and power density curves of i-CoPt@Pt/KB and Pt/C before and after ADT cycling. Anode loading (Pt/C): 0.1 mg_{Pt} cm⁻², cathode loading (i-CoPt@Pt/KB or Pt/C): 0.1 mg_{Pt} cm⁻². Test conditions: 80 °C, 100% relative humidity, 250 kPa_{abs}, H₂ flow rate = 0.2 L min⁻¹, air flow rate = 0.8 L min⁻¹. (f) Cell voltage at 0.8 A cm⁻² (left) and rated power density at 0.67 V (right) of i-CoPt@Pt/KB and Pt/C before and after ADT cycling.

Fig. 4(d) shows the single cell polarization curve of the tested MEAs under H_2 - O_2 conditions, indicating that i-CoPt@Pt/KB outperforms Pt/C throughout the entire voltage region. The internal resistance (iR)-corrected Tafel plots (inset in Fig. 4(d)) and electrochemical impedance spectra (EIS) at 0.05 A cm^{-2} (Fig. S35, ESI[†]) demonstrated that i-CoPt@Pt/KB exhibits superior activity compared to Pt/C in the single cell configuration. In particular, at 0.9 V (iR-corrected), i-CoPt@Pt/KB exhibited 4.4 times higher mass activity ($0.53\text{ A mg}_{Pt}^{-1}$) compared to that of the benchmark catalyst ($0.12\text{ A mg}_{Pt}^{-1}$), which exceeds the 2025 DOE activity target for PEMFCs ($0.44\text{ A mg}_{Pt}^{-1}$) (Fig. S36, ESI[†]). Likewise, we confirmed the superior performance of i-CoPt@Pt/KB under practical H_2 -air operating conditions (Fig. 4(e) and Fig. S37, ESI[†]). At the kinetic dominant region of 0.8 V, i-CoPt@Pt/KB exhibited much higher current density of 0.64 A cm^{-2} than Pt/C (0.20 A cm^{-2}) (Fig. S38, ESI[†]), far surpassing the 2025 DOE target (0.3 A cm^{-2} at 0.8 V). Moreover, at a practical working voltage of 0.67 V for high power output, i-CoPt@Pt/KB reached a current density of 1.76 A cm^{-2} , corresponding to a power density of 1.18 W cm^{-2} (above the DOE target of 1.0 W cm^{-2} for $\leq 0.1\text{ mg}_{Pt}\text{ cm}^{-2}$ in cathode) (Fig. 4(f)). To comprehensively understand the high HCD performance of i-CoPt@Pt/KB, we conducted EIS analysis under H_2 -air conditions (Fig. S39, ESI[†]). Compared to the benchmark Pt/C catalyst, i-CoPt@Pt/KB exhibited a slightly smaller low frequency arc at the current densities above 0.8 A cm^{-2} , which is related to the mass transport resistance in the electrode. Considering that conventional porous carbon-based catalysts have generally shown lower HCD performance due to higher transport resistance than solid carbon-based catalysts (Fig. S40, ESI[†]), it is noteworthy that the porous carbon-based i-CoPt@Pt/KB catalyst showed somewhat lower transport resistance than the benchmark Pt/C catalyst based on solid carbon. Compared to the commercial PtCo/C (Fig. S41, ESI[†]), and the state-of-the-art Pt-based catalysts tested under similar operating conditions (Fig. 5 and Table S3, ESI[†]), i-CoPt@Pt/KB exhibited not only the highest rated power performance but also a notable specific rated power (normalized with the total Pt loading in single cell) in MEA.^{6–11} These results demonstrate that i-CoPt@Pt/KB is a promising ORR catalyst for a

practical PEMFC cathode, as the rated power performance at the critical voltage (0.67 V) is one of the key figures to evaluate the practical applicability of a PEMFC system.^{4,26} This unprecedented power performance originates not only from the intrinsic activity of the strained Pt surface but also from the combination of desirable structural factors that includes sufficient roughness factor ($\text{cm}_{Pt}^2\text{ cm}_{MEA}^{-2}$) higher than 50, mesoporous carbon structure, and nitrogen doping on the support. The major role of Pt roughness factor in low-Pt PEMFC power has been systematically analyzed in a previous study,⁴ which emphasized the rapid voltage loss at HCD (due to high non-Fickian oxygen transport resistance) if the roughness factor falls down to lower than $40\text{ cm}_{Pt}^2\text{ cm}_{MEA}^{-2}$ despite a reasonably high mass activity. The mesoporous carbon support with N-doping reduces the local oxygen transport resistance by providing a pore network and enabling homogeneous distribution of the ionomer in CCL.^{15,24}

The durability of i-CoPt@Pt/KB was evaluated after ADT of square-wave potential cycling between 0.60 V (3 s) and 0.95 V (3 s), which is much harsher than the triangle-wave protocol between 0.6 and 1.0 V.⁵³ After ADT for 30 000 cycles, i-CoPt@Pt/KB preserved 81.2% of its beginning of test (BOT) ECSA while that of Pt/C largely decreased by 62.9% (Fig. S31, ESI[†]). It is important to note that the optimum size of i-CoPt@Pt nanoparticles (3–4.5 nm) contributed both to the balance of a sufficient initial ECSA and to its high retention after ADT.⁵⁴ i-CoPt@Pt/KB retained 64.5% of its BOT mass activity, meeting the durability target (<40%) for mass activity set by the DOE (Fig. S36, ESI[†]). Notably, in the H_2 -air test, the voltage loss for i-CoPt@Pt/KB at HCD of 0.8 A cm^{-2} was 29 mV, which meets the DOE target (<30 mV) (Fig. 4(f)). The rated power performance of the i-CoPt@Pt/KB MEA decreased by only 15.4% while that of Pt/C decreased by 39.4%. The i-CoPt@Pt/KB MEA still exhibited high H_2 -air performance (0.42 A cm^{-2} at 0.8 V, and 1.0 W cm^{-2} at 0.67 V) that meets the BOT performance targets set by the DOE (0.3 A cm^{-2} at 0.8 V, and 1.0 W cm^{-2} at 0.67 V) (Fig. 4(f) and Fig. S38, ESI[†]). TEM analysis on i-CoPt@Pt/KB at the end of the test (EOT) confirmed that the overall sizes of the i-CoPt@Pt nanoparticles remained close to 5 nm even after the harsh ADT cycling (Fig. S42, ESI[†]). We speculate that the better retention of particle size and ECSA in i-CoPt@Pt/KB compared

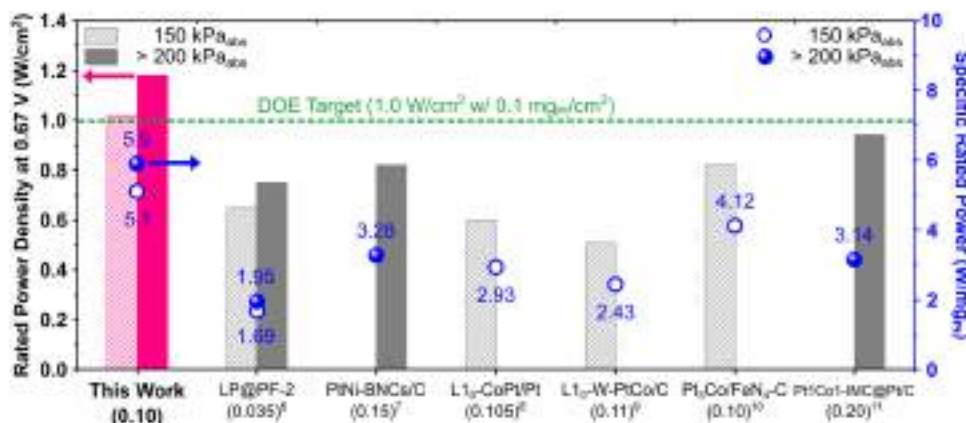


Fig. 5 Comparison of the rated power density and specific rated power at 0.67 V of i-CoPt@Pt/KB and the state-of-the-art Pt-based catalysts in the literature.^{6–11} Cathode Pt loadings ($\text{mg}_{Pt}\text{ cm}^{-2}$) are written in parentheses.

to Pt/C comes from the superior stabilization of i-CoPt nanoparticles by the high temperature annealing on the high surface area carbon. STEM-EDS detected the remaining Co and Pt elements in i-CoPt@Pt/KB at the EOT (Fig. S43, ESI†), indicating more than twice higher Co/Pt ratio (0.23 for i-CoPt@Pt/KB) compared to the commercial Pt₃Co/C catalysts with random alloy nanoparticles (~0.23 after conditioning, and ~0.098 at the EOT) reported in the previous works.^{55,56} This enhanced durability can be attributed to the intermetallic core and Pt-skin surface, which were also confirmed at the EOT (Fig. S44, ESI†).

Conclusion

We presented a straightforward and delicate synthetic platform based on thermal annealing to get a practical ORR catalyst that satisfies comprehensive requirements for both high intrinsic activity and high rated power performance in a PEMFC system. The crystalline ionic compound, composed of [Co(bpy)₃]²⁺ and [PtCl₆]²⁻, enabled a carbon-confined growth of intermetallic nanoparticles with N-doping on the entire mesoporous carbon support. The active Pt-skin with intermetallic L₁₀-CoPt core catalyzed the ORR in efficient ways both in a half-cell and MEA. More importantly, we attained the highest PEMFC rated power per active area (1.18 W cm⁻²) and total platinum loading (5.9 W mg_{Pt}⁻¹) under a practical H₂-air condition owing to the high ECSA, mesoporosity, and N-doping on the carbon support that collectively enhanced oxygen mass transfer. The catalyst endured a harsh durability test with the final rated power density of 1.0 W cm⁻², due to the effective protection of Co dissolution induced by the rigid Pt-skin structure that maintained proton conduction. Overall, this study highlights the importance of meeting all the critical parameters to achieve much higher PEMFC power performance through the development of a facile and scalable production method of the catalyst. Further modifications from this approach, such as doping, tuning the compositions, and using novel metal complexes or carbon supports, could provide enhanced and desirable power performance suited to large-scale industrial applications of PEMFCs.

Data and materials availability

All data that support the findings of this study are available from the corresponding authors upon reasonable request.

Author contributions

T. Y. Y., J. L., S. K., Y.-E. S., and T. H. conceived the ideas, designed the experiments, and wrote the manuscript. T. Y. Y., J. L., S. K., M. H., S.-Y. K., Y.-H. L., H. S., H. J., A. K. S., S.-P. C., Y.-E. S., and T. H. performed the experiments and analysis.

Conflicts of interest

There are no conflicts to declare.

Acknowledgements

This research was supported by the Institute for Basic Science (IBS-R006-D1 and IBS-R006-A2).

References

- 1 K. Jiao, J. Xuan, Q. Du, Z. Bao, B. Xie, B. Wang, Y. Zhao, L. Fan, H. Wang, Z. Hou, S. Huo, N. P. Brandon, Y. Yin and M. D. Guiver, Designing the next generation of proton-exchange membrane fuel cells, *Nature*, 2021, **595**, 361–369.
- 2 O. Z. Sharaf and M. F. Orhan, An overview of fuel cell technology: Fundamentals and applications, *Renewable Sustainable Energy Rev.*, 2014, **32**, 810–853.
- 3 J. Fan, M. Chen, Z. Zhao, Z. Zhang, S. Ye, S. Xu, H. Wang and H. Li, Bridging the gap between highly active oxygen reduction reaction catalysts and effective catalyst layers for proton exchange membrane fuel cells, *Nat. Energy*, 2021, **6**, 475–486.
- 4 A. Kongkanand and M. F. Mathias, The Priority and Challenge of High-Power Performance of Low-Platinum Proton-Exchange Membrane Fuel Cells, *J. Phys. Chem. Lett.*, 2016, **7**, 1127–1137.
- 5 X. X. Wang, M. T. Swihart and G. Wu, Achievements, challenges and perspectives on cathode catalysts in proton exchange membrane fuel cells for transportation, *Nat. Catal.*, 2019, **2**, 578–589.
- 6 L. Chong, J. Wen, J. Kubal, F. G. Sen, J. Zou, J. Greeley, M. Chan, H. Barkholtz, W. Ding and D.-J. Liu, Ultralow-loading platinum-cobalt fuel cell catalysts derived from imidazolate frameworks, *Science*, 2018, **362**, 1276–1281.
- 7 X. Tian, X. Zhao, Y.-Q. Su, L. Wang, H. Wang, D. Dang, B. Chi, H. Liu, E. J. M. Hensen, X. W. Lou and B. Y. Xia, Engineering bunched Pt-Ni alloy nanocages for efficient oxygen reduction in practical fuel cells, *Science*, 2019, **366**, 850–856.
- 8 J. Li, S. Sharma, X. Liu, Y.-T. Pan, J. S. Spendelow, M. Chi, Y. Jia, P. Zhang, D. A. Cullen, Z. Xi, H. Lin, Z. Yin, B. Shen, M. Muzzio, C. Yu, Y. S. Kim, A. A. Peterson, K. L. More, H. Zhu and S. Sun, Hard-Magnet L₁₀-CoPt Nanoparticles Advance Fuel Cell Catalysis, *Joule*, 2019, **3**, 124–135.
- 9 J. Liang, N. Li, Z. Zhao, L. Ma, X. Wang, S. Li, X. Liu, T. Wang, Y. Du, G. Lu, J. Han, Y. Huang, D. Su and Q. Li, Tungsten-Doped L₁₀-PtCo Ultrasmall Nanoparticles as a High-Performance Fuel Cell Cathode, *Angew. Chem., Int. Ed.*, 2019, **58**, 15471–15477.
- 10 Z. Qiao, C. Wang, C. Li, Y. Zeng, S. Hwang, B. Li, S. Karakalos, J. Park, A. J. Kropf, E. C. Wegener, Q. Gong, H. Xu, G. Wang, D. J. Myers, J. Xie, J. S. Spendelow and G. Wu, Atomically dispersed single iron sites for promoting Pt and Pt₃Co fuel cell catalysts: performance and durability improvements, *Energy Environ. Sci.*, 2021, **14**, 4948–4960.
- 11 Q. Cheng, S. Yang, C. Fu, L. Zou, Z. Zou, Z. Jiang, J. Zhang and H. Yang, High-loaded sub-6 nm Pt₁Co₁ intermetallic compounds with highly efficient performance expression in PEMFCs, *Energy Environ. Sci.*, 2022, **15**, 278–286.

- 12 Z. Peng and H. Yang, Designer platinum nanoparticles: Control of shape, composition in alloy, nanostructure and electrocatalytic property, *Nano Today*, 2009, **4**, 143–164.
- 13 H. You, S. Yang, B. Ding and H. Yang, Synthesis of colloidal metal and metal alloy nanoparticles for electrochemical energy applications, *Chem. Soc. Rev.*, 2013, **42**, 2880–2904.
- 14 L. Zhang, K. Doyle-Davis and X. Sun, Pt-Based electrocatalysts with high atom utilization efficiency: from nanostructures to single atoms, *Energy Environ. Sci.*, 2019, **12**, 492–517.
- 15 T. A. M. Suter, K. Smith, J. Hack, L. Rasha, Z. Rana, G. M. A. Angel, P. R. Shearing, T. S. Miller and D. J. L. Brett, Engineering Catalyst Layers for Next-Generation Polymer Electrolyte Fuel Cells: A Review of Design, Materials, and Methods, *Adv. Energy Mater.*, 2021, **11**, 2101025.
- 16 K. Kodama, T. Nagai, A. Kuwaki, R. Jinnouchi and Y. Morimoto, Challenges in applying highly active Pt-based nanostructured catalysts for oxygen reduction reactions to fuel cell vehicles, *Nat. Nanotechnol.*, 2021, **16**, 140–147.
- 17 M. K. Debe, Electrocatalyst approaches and challenges for automotive fuel cells, *Nature*, 2012, **486**, 43–51.
- 18 X. Tian, X. F. Lu, B. Y. Xia and X. W. Lou, Advanced Electrocatalysts for the Oxygen Reduction Reaction in Energy Conversion Technologies, *Joule*, 2020, **4**, 45–69.
- 19 V. R. Stamenkovic, D. Strmcnik, P. P. Lopes and N. M. Markovic, Energy and fuels from electrochemical interfaces, *Nat. Mater.*, 2017, **16**, 57–69.
- 20 M. Shao, A. Peles and K. Shoemaker, Electrocatalysis on Platinum Nanoparticles: Particle Size Effect on Oxygen Reduction Reaction Activity, *Nano Lett.*, 2011, **11**, 3714–3719.
- 21 G. W. Sievers, A. W. Jensen, J. Quinson, A. Zana, F. Bizzotto, M. Oezaslan, A. Dworzak, J. J. K. Kirkensgaard, T. E. L. Smitshuysen, S. Kadkhodazadeh, M. Juelsholt, K. M. Ø. Jensen, K. Anklam, H. Wan, J. Schäfer, K. Čépe, M. Escudero-Escribano, J. Rossmeisl, A. Quade, V. Brüser and M. Arenz, Self-supported Pt–CoO networks combining high specific activity with high surface area for oxygen reduction, *Nat. Mater.*, 2021, **20**, 208–213.
- 22 N. Ramaswamy, W. Gu, J. M. Ziegelbauer and S. Kumaraguru, Carbon Support Microstructure Impact on High Current Density Transport Resistances in PEMFC Cathode, *J. Electrochem. Soc.*, 2020, **167**, 064515.
- 23 H. Adabi, A. Shakouri, N. U. Hassan, J. R. Varcoe, B. Zulevi, A. Serov, J. R. Regalbuto and W. E. Mustain, High-performing commercial Fe–N–C cathode electrocatalyst for anion-exchange membrane fuel cells, *Nat. Energy*, 2021, **6**, 834–843.
- 24 S. Ott, A. Orfanidi, H. Schmies, B. Anke, H. N. Nong, J. Hübner, U. Gernert, M. Glied, M. Lerch and P. Strasser, Ionomer distribution control in porous carbon-supported catalyst layers for high-power and low Pt-loaded proton exchange membrane fuel cells, *Nat. Mater.*, 2020, **19**, 77–85.
- 25 J. Chang, G. Wang, M. Wang, Q. Wang, B. Li, H. Zhou, Y. Zhu, W. Zhang, M. Omer, N. Orlovskaya, Q. Ma, M. Gu, Z. Feng, G. Wang and Y. Yang, Improving Pd–N–C fuel cell electrocatalysts through fluorination-driven rearrangements of local coordination environment, *Nat. Energy*, 2021, **6**, 1144–1153.
- 26 C.-Y. Ahn, J. E. Park, S. Kim, O.-H. Kim, W. Hwang, M. Her, S. Y. Kang, S. Park, O. J. Kwon, H. S. Park, Y.-H. Cho and Y.-E. Sung, Differences in the Electrochemical Performance of Pt-Based Catalysts Used for Polymer Electrolyte Membrane Fuel Cells in Liquid Half- and Full-Cells, *Chem. Rev.*, 2021, **121**, 15075–15140.
- 27 C. Cui, L. Gan, M. Heggen, S. Rudi and P. Strasser, Compositional segregation in shaped Pt alloy nanoparticles and their structural behaviour during electrocatalysis, *Nat. Mater.*, 2013, **12**, 765–771.
- 28 P. P. Lopes, D. Li, H. Lv, C. Wang, D. Tripkovic, Y. Zhu, R. Schimmenti, H. Daimon, Y. Kang, J. Snyder, N. Becknell, K. L. More, D. Strmcnik, N. M. Markovic, M. Mavrikakis and V. R. Stamenkovic, Eliminating dissolution of platinum-based electrocatalysts at the atomic scale, *Nat. Mater.*, 2020, **19**, 1207–1214.
- 29 V. R. Stamenkovic, B. S. Mun, K. J. J. Mayrhofer, P. N. Ross and N. M. Markovic, Effect of Surface Composition on Electronic Structure, Stability, and Electrocatalytic Properties of Pt-Transition Metal Alloys: Pt-Skin versus Pt-Skeleton Surfaces, *J. Am. Chem. Soc.*, 2006, **128**, 8813–8819.
- 30 F. Xiao, Q. Wang, G.-L. Xu, X. Qin, I. Hwang, C.-J. Sun, M. Liu, W. Hua, H.-W. Wu, S. Zhu, J.-C. Li, J.-G. Wang, Y. Zhu, D. Wu, Z. Wei, M. Gu, K. Amine and M. Shao, Atomically dispersed Pt and Fe sites and Pt–Fe nanoparticles for durable proton exchange membrane fuel cells, *Nat. Catal.*, 2022, **5**, 503–512.
- 31 H. Kim, T. Y. Yoo, M. S. Bootharaju, J. H. Kim, D. Y. Chung and T. Hyeon, Noble Metal-Based Multimetallic Nanoparticles for Electrocatalytic Applications, *Adv. Sci.*, 2022, **9**, 2104054.
- 32 J. Kim, C. Rong, J. P. Liu and S. Sun, Dispersible Ferromagnetic FePt Nanoparticles, *Adv. Mater.*, 2009, **21**, 906–909.
- 33 D. Y. Chung, S. W. Jun, G. Yoon, S. G. Kwon, D. Y. Shin, P. Seo, J. M. Yoo, H. Shin, Y.-H. Chung, H. Kim, B. S. Mun, K.-S. Lee, N.-S. Lee, S. J. Yoo, D.-H. Lim, K. Kang, Y.-E. Sung and T. Hyeon, Highly Durable and Active PtFe Nanocatalyst for Electrochemical Oxygen Reduction Reaction, *J. Am. Chem. Soc.*, 2015, **137**, 15478–15485.
- 34 H. Y. Kim, T. Kwon, Y. Ha, M. Jun, H. Baik, H. Y. Jeong, H. Kim, K. Lee and S. H. Joo, Intermetallic PtCu Nanoframes as Efficient Oxygen Reduction Electrocatalysts, *Nano Lett.*, 2020, **20**, 7413–7421.
- 35 R. Ryoo, J. Kim, C. Jo, S. W. Han, J.-C. Kim, H. Park, J. Han, H. S. Shin and J. W. Shin, Rare-earth–platinum alloy nanoparticles in mesoporous zeolite for catalysis, *Nature*, 2020, **585**, 221–224.
- 36 C.-L. Yang, L.-N. Wang, P. Yin, J. Liu, M.-X. Chen, Q.-Q. Yan, Z.-S. Wang, S.-L. Xu, S.-Q. Chu, C. Cui, H. Ju, J. Zhu, Y. Lin, J. Shui and H.-W. Liang, Sulfur-anchoring synthesis of platinum intermetallic nanoparticle catalysts for fuel cells, *Science*, 2021, **374**, 459–464.
- 37 T. Y. Yoo, J. M. Yoo, A. K. Sinha, M. S. Bootharaju, E. Jung, H. S. Lee, B.-H. Lee, J. Kim, W. H. Antink, Y. M. Kim, J. Lee, E. Lee, D. W. Lee, S.-P. Cho, S. J. Yoo, Y.-E. Sung and T. Hyeon, Direct Synthesis of Intermetallic Platinum–Alloy

- Nanoparticles Highly Loaded on Carbon Supports for Efficient Electrocatalysis, *J. Am. Chem. Soc.*, 2020, **142**, 14190–14200.
- 38 M. Karuppanan, Y. Kim, S. Gok, E. Lee, J. Y. Hwang, J.-H. Jang, Y.-H. Cho, T. Lim, Y.-E. Sung and O. J. Kwon, A highly durable carbon-nanofiber-supported Pt–C core-shell cathode catalyst for ultra-low Pt loading proton exchange membrane fuel cells: facile carbon encapsulation, *Energy Environ. Sci.*, 2019, **12**, 2820–2829.
- 39 D. Li, C. Wang, D. Tripkovic, S. Sun, N. M. Markovic and V. R. Stamenkovic, Surfactant Removal for Colloidal Nanoparticles from Solution Synthesis: The Effect on Catalytic Performance, *ACS Catal.*, 2012, **2**, 1358–1362.
- 40 C. Wang, M. Chi, D. Li, D. Strmcnik, D. V. D. Vliet, G. Wang, V. Komanicky, K.-C. Chang, A. P. Paulikas, D. Tripkovic, J. Pearson, K. L. More, N. M. Markovic and V. R. Stamenkovic, Design and Synthesis of Bimetallic Electrocatalyst with Multilayered Pt-Skin Surfaces, *J. Am. Chem. Soc.*, 2011, **133**, 14396–14403.
- 41 Y. Xu, A. V. Ruban and M. Mavrikakis, Adsorption and Dissociation of O₂ on Pt–Co and Pt–Fe Alloys, *J. Am. Chem. Soc.*, 2004, **126**, 4717–4725.
- 42 P. Strasser, S. Koh, T. Anniyev, J. Greeley, K. More, C. Yu, Z. Liu, S. Kaya, D. Nordlund, H. Ogasawara, M. F. Toney and A. Nilsson, Lattice-strain control of the activity in dealloyed core-shell fuel cell catalysts, *Nat. Chem.*, 2010, **2**, 454–460.
- 43 M. Luo and S. Guo, Strain-controlled electrocatalysis on multimetallic nanomaterials, *Nat. Rev. Mater.*, 2017, **2**, 17059.
- 44 D. Choi, J. Y. Jung, M. J. Lee, S.-H. Kim, S. Lee, D. W. Lee, D.-G. Kim, N. D. Kim, K.-S. Lee, P. Kim and S. J. Yoo, Atomic Rearrangement in Core-Shell Catalysts Induced by Electrochemical Activation for Favorable Oxygen Reduction in Acid Electrolytes, *ACS Catal.*, 2021, **11**, 15098–15109.
- 45 D. Y. Chung, S. Park, H. Lee, H. Kim, Y.-H. Chung, J. M. Yoo, D. Ahn, S.-H. Yu, K.-S. Lee, M. Ahmadi, H. Ju, H. D. Abruña, S. J. Yoo, B. S. Mun and Y.-E. Sung, Activity-Stability Relationship in Au@Pt Nanoparticles for Electrocatalysis, *ACS Energy Lett.*, 2020, **5**, 2827–2834.
- 46 D. Wang, H. L. Xin, R. Hovden, H. Wang, Y. Yu, D. A. Muller, F. J. DiSalvo and H. D. Abruña, Structurally ordered intermetallic platinum-cobalt core-shell nanoparticles with enhanced activity and stability as oxygen reduction electrocatalysts, *Nat. Mater.*, 2013, **12**, 81–87.
- 47 P. Hernandez-Fernandez, F. Masini, D. N. McCarthy, C. E. Strebel, D. Friebe, D. Deiana, P. Malacrida, A. Nierhoff, A. Bodin, A. M. Wise, J. H. Nielsen, T. W. Hansen, A. Nilsson, I. E. L. Stephens and I. Chorkendorff, Mass-selected nanoparticles of Pt_xY as model catalysts for oxygen electroreduction, *Nat. Chem.*, 2014, **6**, 732–738.
- 48 M. Escudero-Escribano, P. Malacrida, M. H. Hansen, U. G. Vej-Hansen, A. Velázquez-Palenzuela, V. Tripkovic, J. Schiøtz, J. Rossmeisl, I. E. L. Stephens and I. Chorkendorff, Tuning the activity of Pt alloy electrocatalysts by means of the lanthanide contraction, *Science*, 2016, **352**, 73–76.
- 49 S. Maiti, K. Maiti, M. T. Curnan, K. Kim, K.-J. Noh and J. W. Han, Engineering electrocatalyst nanosurfaces to enrich the activity by inducing lattice strain, *Energy Environ. Sci.*, 2021, **14**, 3717–3756.
- 50 W. Wang, B. Lei and S. Guo, Engineering Multimetallic Nanocrystals for Highly Efficient Oxygen Reduction Catalysts, *Adv. Energy Mater.*, 2016, **6**, 1600236.
- 51 S. Lee, J.-H. Jang, I. Jang, D. Choi, K.-S. Lee, D. Ahn, Y. S. Kang, H.-Y. Park and S. Y. Yoo, Development of robust Pt shell through organic hydride donor in PtCo@Pt core-shell electrocatalysts for highly stable proton exchange membrane fuel cells, *J. Catal.*, 2019, **379**, 112–120.
- 52 M. Luo, Y. Sun, X. Zhang, Y. Qin, M. Li, Y. Li, C. Li, Y. Yang, L. Wang, P. Gao, G. Lu and S. Guo, Stable High-Index Faceted Pt Skin on Zigzag-Like PtFe Nanowires Enhances Oxygen Reduction Catalysis, *Adv. Mater.*, 2018, **30**, 1705515.
- 53 S. Stariha, N. Macauley, B. T. Sneed, D. Langlois, K. L. More, R. Mukundan and R. L. Borup, Recent Advances in Catalyst Accelerated Stress Tests for Polymer Electrolyte Membrane Fuel Cells, *J. Electrochem. Soc.*, 2018, **165**, F492–F501.
- 54 Z. Yang, S. Ball, D. Condit and M. Gummalla, Systematic Study on the Impact of Pt Particle Size and Operating Conditions on PEMFC Cathode Catalyst Durability, *J. Electrochem. Soc.*, 2011, **158**, B1439.
- 55 N. Ramaswamy, S. Kumaraguru, W. Gu, R. S. Kukreja, K. Yu, D. Groom and P. Ferreira, High-Current Density Durability of Pt/C and PtCo/C Catalysts at Similar Particle Sizes in PEMFCs, *J. Electrochem. Soc.*, 2021, **168**, 024519.
- 56 X. Wang, S. DeCrane, T. Nowicki, N. N. Kariuki, S. C. Ball and D. J. Myers, Effect of Particle Size on the Dissolution of Pt₃Co/C and Pt/C PEMFC Electrocatalysts, *J. Electrochem. Soc.*, 2021, **168**, 054516.

সাহিত্য অঙ্গন

(সাহিত্য অঙ্গন // Sahitya Angan)

ISSN : 2394 4889 Vol : VIII, Issue : XVII 4th March 2023

Website : www.sahityaangan.com

মুখ্য সম্পাদক

ড. জয়গোপাল মণ্ডল

কার্যকরী সম্পাদক

ড. প্রণবকুমার মাহাতো

ড. সৌম্যব্রত বন্দ্যোপাধ্যায়

উজ্জ্বল প্রামাণিক



ড. জয়গোপাল মণ্ডল

অভিনেতা টাওয়ার, ৪র্থ তল, ফ্ল্যাট নং-২

কলাকুশমা, ডাক-কে. জি. আশ্রম, ধানবাদ-৩২৮১০৯

SAHITYA ANGAN
An Exclusive Interdisciplinary & Literary Tri-lingual
Peer-reviewed Journal
ISSN : 2394 4889 Vol : VIII, Issue : XVII 4th March 2023

Chief Editor :
Dr. Jaygopal Mandal

Working Editor :
Dr. Pranab Kumar Mahato
Dr. Soumyabrata Bandyopadhyay
Ujjwal Pramanik

© Publisher

Cover Drawing : Sidhartha Bose

Type Setting & Cover Setting :
Manik Sahu
Mob : 9830950380

Printing and Binding :
B.C.D Offset (Dey's House)

Price : 550.00

Published By :
Dr. Jaygopal Mandal
Abhishek Tower, Block-A.
4th Floor, Flat-2, Kalakushma
P. S. Saraidhela, Dhanbad-828109
Phone : 09830633202 / 7003488354
E-mail : joygopalvbu@gmail.com,
sahityaangan@gmail.com
Website : www.sahityaangan.com

সূচি

প্রবন্ধ

গল্প-কথা—গণেশ বসু	১
উত্তরায়ণের দিন—অমর মিত্র	১২
নারী স্বাধীনতার মৃদুস্বর : অবতরণিকা—পিউ মণ্ডল	২৩
অচিরতর্ক কামনার লেলিহান আগ্রাসন এবং 'সোনালি মোরগের গল্প'—ড. পৌলোমী রায়	২৯
সৈয়দ মুস্তাফা সিরাজের নির্বাচিত ছোটগল্পে সমাজ বাস্তবতা—মোহ : নূরুল আমিন	৩৮
সমবেশ বসুর ছোটগল্প : এক জীবনবাদী প্রত্যয়ের সুর—দিলরুবা খাতুন	৪২
ভাষা বৈচিত্র্যে সমবেশের ছোটগল্প—চন্দ্রিমা মৈত্র দুবে	৪৮
মধ্যবিত্তের রুচির বিপরীতে : আখতারুজ্জামান ইলিয়াসের কথাসাহিত্য—ড. মাধুরী বিশ্বাস	৫৭
আখতারুজ্জামান ইলিয়াসের ছোটগল্পে মধ্যবিত্ত বাঙালি সমাজের যত্ন ও প্রত্যয়ের সংকট—অসীম মুখার্জি	৬৪
জোমের চিত্তা : নিম্নবর্গের অস্তিত্ববাদী চেতনার আখ্যান—মধুসূদন সাহা	৭০
নারীমুক্তির প্রেক্ষিতে আশাপূর্ণার সুবর্ণলতা : মাতৃত্বের ভিন্ন স্বর—অভিজিৎ শীট	৭৭
গরম ভাত অথবা নিছক ভূতের গল্প : কুসংস্কারমুক্ত সমাজ ভাবনা কিংবা ক্ষুধা ও দারিদ্র্য—অনিন্দিতা দাস	৮৪
গল্পকার ভগীরথ মিশ্রের গল্পে প্রতিফলিত লৌকিক সংস্কৃতির রূপরেখা—মানস ঘোষ	৯১
আবুল বাশারের গল্প রস্কু দেওয়ান : এক রূপাজীবীর আলোকোজ্জ্বল পরণকথা—রফিয়া সুলতানা মোল্লা	১০০
উদ্বাস্ত নারীদের জীবনযুদ্ধ : নির্বাচিত উপন্যাসে—গৌতম অধিকারী	১০৬
দুই পৃথিবীর সংঘাত: প্রসঙ্গ রমানাথ রায়ের 'ক্ষত ও অন্যান্য গল্প'—মানসী কুইরী	১১২
সুকাণ্ঠি দত্তের 'মহেন-জো-দারোর নগ্নিকা' : মধ্যবিত্ত যৌনজীবন-চেতনার আধুনিক ভাষা—শ্রেয়া ভদ্র	১২০
অভিজিৎ সেনের নির্বাচিত ছোটগল্প : উত্তরবঙ্গের প্রান্তিক মানুষের অনালোকিত যাপনকথা—কৌশিক পাণ্ডে	১২৬
নলিনী বেরার গল্পে মানবজীবন: 'তরঙ্গহীন ভীষণ মৌন'—উজ্জ্বল প্রামাণিক	১৩৮
বাংলা ছোটগল্পে ছেচল্লিশের দাপ্তর প্রতিফলন—বিজেন্দ্র দালাল	১৪৩
শান্ত্রিবিরোধী আন্দোলন : বাংলা ছোটগল্পের ভিন্নতর ধারা—বিশ্বজিৎ বিশ্বাস	১৫০
প্রচৈত গুপ্তের উপন্যাস 'ধুলোবালির জীবন' : যৌনতা, প্রেম এবং দাম্পত্য—সম্পদ দে	১৫৯
নজরুল দৃষ্টিতে ও সৃষ্টিতে রবীন্দ্রনাথ—ড. অরুণাভ মুখার্জী	১৬২
প্রবহমান বাংলা কবিতা : অপ্রতিরোধ্য সুভাষ মুখোপাধ্যায়—ড. মহাশ্বেতা চ্যাটার্জি	১৭২

নজরুল দৃষ্টিতে ও সৃষ্টিতে রবীন্দ্রনাথ

ড. অরুণাভ মুখার্জী

বাংলা কাব্যাকাশের দুই উজ্জ্বল জ্যোতিষ্ক রবীন্দ্রনাথ ও নজরুল। একজন সূর্য, অপরজন চন্দ্র। রবিজ্যোতি ও নজরুল-চন্দ্রিমার সমন্বিত কিরণে বাংলা সাহিত্যবিশ্ব আলোকদীপ্ত ও মহৎ মহিমায় আকীর্ণ। উদ্বেলিত যৌবনোচ্ছ্বাসে আত্মহারা কবি কাজী নজরুল ইসলাম পরাধীন জাতির বৃকে মুক্তির আকাঙ্ক্ষা জাগিয়ে তোলার স্বপ্নে বিভোর হয়ে নিজ প্রতিভার স্বতন্ত্র দীপখানি জ্বালালেও রবি-জ্যোতির আলোকে তাঁর হৃদয় হয়েছে মুগ্ধ বিভোর ও তন্দ্রাতুর। আর সেই মুগ্ধতার প্রকাশ বর্তিকা 'নজরুল দৃষ্টিতে ও সৃষ্টিতে রবীন্দ্রনাথ' এই শিরোনামে আলোচ্য রচনায় ফুটিয়ে তোলার প্রয়াস নেওয়া হয়েছে।

'রবীন্দ্র-যুগ' বলতে আমরা ১৮৬১ সাল থেকে ১৯৪১ সাল পর্যন্ত সময়সীমাকে ধরে থাকি। এই সময় আমরা দেখতে পাই, রবীন্দ্র-নক্ষত্র নিয়ন্ত্রিত নিয়তির মতো বাঙালির শিল্প-সাহিত্য-সংস্কৃতি পরিচালিত হয়েছে। শরৎচন্দ্র লিখেছেন — "কবিগুরু তোমার প্রতি চাহিয়া আমাদের বিশ্বয়ের সীমা নাই"। আর এই সময় পবেই বস্তুত ১৯১৯-'২০ সাল থেকে ১৯৩০-'৩১ সাল পর্যন্ত নজরুলের সাহিত্য সাধনার উৎকৃষ্ট সময়। রবীন্দ্রনাথকে অবলম্বন করে নজরুল কেবলমাত্র কয়েকখানি কবিতাই শুধু রচনা করেন নি, রবীন্দ্রনাথ ছিলেন তাঁর ভাবের গুরু, তাঁর আদর্শের গুরু। রবীন্দ্র প্রসঙ্গ, রবীন্দ্র ভাব-ভাবনা তাঁকে আজীবন যেমন অনুপ্রাণিত করেছে, তেমনি, নজরুলের দৃষ্টিতে রবীন্দ্রনাথ শুধু মাত্র কবি বা ঋষি ছিলেন না, নজরুলের কাছে রবীন্দ্রনাথ ছিলেন 'প্রিয় পরমসুন্দর'—

"বন্ধে তব চির-রূপ-রসবিলাসীয়ে!
হারায়ে ফেলেছি সেথা সত্তা আপনার
কাঁদিয়াছি রূপমুগ্ধা রাধিকার মতো।
হে কবি, আজিও শুনি সে চির-কিশোর
তোমার বেণুতে গাহে যৌবনের গান।
সেথা তুমি কবি নও, ঋষি নহ তুমি,
সেথা তুমি মোর প্রিয় পরম সুন্দর!"

(‘অশ্রু-পুষ্পাঞ্জলি’, ‘নতুন চাঁদ’)

আসলে নজরুল ছিলেন 'রবীন্দ্র-বহিলোকে ঝড়ের পাখি'। কবিতার ক্ষেত্র ছাড়াও নজরুলের গান-গল্প-উপন্যাস-নাটক-চিঠিপত্র-অভিভাষণ—সর্বত্রই একটা রবীন্দ্রভাব-পরিমণ্ডল আমরা লক্ষ করি। রবীন্দ্রনাথ সম্পর্কে নজরুলের অকপট স্বীকারোক্তি — "বিশ্বকবিতে আমি শুধু শ্রদ্ধা নয়, পূজা করে এসেছি সকল হৃদয় মন দিয়ে, ছেলেবেলা থেকে তাঁর ছবি সামনে রেখে গন্ধমুগ্ধ ফুল চন্দন দিয়ে সকাল সন্ধ্যা বন্দনা করেছি"^১।

www.abdpindia.net

ISSN 0974-8849

UGC Care Listed Journal : Group-I, Sl. No.-4

दार्शनिक त्रैमासिक

वर्ष-68

अंक-4

अक्टूबर-दिसम्बर, 2022



अखिल भारतीय दर्शन-परिषद्

1. ऋग्वेद 1.187.1, 20.21.3, 10.92.2, 1.22.18, 5.28.6, 7.43.24, 9.64.1
2. अथर्ववेद 9.9.17
3. श्रीमद्भगवद्गीता 18.46
4. श्रीमद्भगवद्गीता 10.10
5. श्रीमद्भगवद्गीता 12.6-7
6. श्रीमद्भागवत 6.3.22
7. श्रीमद्भागवत 1.2.6
8. मनुस्मृति 2.6.12
9. याज्ञवल्क्यस्मृति 1.7
10. मनुस्मृति 6.92, याज्ञवल्क्यस्मृति 1.122, विष्णुस्मृति 2.8-9, बृहद्गीता
स्मृति 12.2-3
11. याज्ञवल्क्यस्मृति 1.8
12. श्रीमद्भागवत 12.11.31
13. मंत्रायुधुपनिषद् 8, 38
14. बृहदारण्यकोपनिषद् 2.4, 5
15. डॉ पी.वी. क्राफे, धर्मशास्त्र का इतिहास भाग 1, पृ. 4
16. डॉ राजबाली पाण्डेय, हिन्दू धर्म कोश, पृ. 339
17. कल्याण- धर्मशास्त्र अंक, गीताप्रेस, गोरखपुर, 1996, पृ. 87-99

□

अस्तित्व के अद्वैत वेदान्त दर्शन और आस्तिक अस्तित्ववादी दर्शन

डॉ. प्रसिद्ध रंजन घोष *

अद्वैत वेदान्त सबसे अधिक तत्वमीमांसा की पूर्ण वास्तविकता और ब्रह्म के पूर्ण ज्ञान का वर्णन करता है। ब्रह्म शुद्ध चैतन्य है। इस संदर्भ में आस्तिक अस्तित्ववाद एक व्यक्ति की आत्म-चेतना के बारे में केवल अस्तित्व के रूप में अध्ययन करता है। तो, दोनों दर्शन उनके ज्ञानमीमांसा और तत्वमीमांसा के साथ चेतना के साथ-साथ आत्म चेतना के बारे में बर्बाब करते हैं। यह धोकर दिखाना है कि इसका तुलनात्मक अध्ययन गंभीर रूप से है।

1

अस्तित्ववाद के संस्थापक कीर्त्तगार्ड ने व्यक्तिपरक सत्य को ही स्वीकार किया। इतना ही नहीं यह हेगल के वस्तुनिष्ठ सत्य का विशेष करता है और उसने अपने अनुभव में धार्मिक विश्वासों के महत्त्व से अनुभव को काय में ईश्वर के अस्तित्व को स्वीकार किया। उन्होंने परिभाषित किया कि सत्य व्यक्तिपरक सत्य है। इसलिए उन्होंने हेगल के वस्तुनिष्ठ सत्य को अस्वीकार कर दिया जो उनके दर्शन का आधार है। उन्होंने महसूस किया कि ईश्वर विषय है, रांकर के अद्वैत दर्शन ने दिखाया कि एक व्यक्ति स्वयं का विषय है। व्यक्ति की स्वयं चेतना भी आत्म चेतना के रूप में है।

रांकर का अद्वैत दर्शन आत्म-चेतना सहित चेतना से संचालित है। उन्होंने सूत्रबद्ध किया कि जीव = चेतना = ब्रह्म = परम वास्तविकता = परम

* एंथॉसिस्ट्रीट प्रोफेसर एच.ओ.डी और दर्शनशास्त्र विभाग, अणुवृत्तय मेमोरियल कॉलेज, आलवा, पुदुचेरिया, पश्चिम बंगाल

अस्तित्व। तो शंकर के अद्वैत दर्शन और अस्तित्वाद ने पाया कि अस्तित्व स्वयं चेतना है जो प्रकृति में चेतना है। मुख्य शब्द : चेतना, आत्म-चेतना, इत्यादि, विषयपरकता, स्वतंत्रता, परसंद, अस्तित्व, स्वयं व्यक्तिगत में।¹

इस पत्र में शंकर के अद्वैत वेदांत और अस्तिक अस्तित्वावाद के बीच एक तुलनात्मक अध्ययन पर चर्चा की गई है कि चेतना शंकर के अद्वैत वेदांत और ईश्वरवादी अस्तित्वावाद दोनों के दर्शन का प्रमुख विषय है। वर्तमान में चेतना महत्त्वपूर्ण अंतःविषय है।

2

ऋग्वेद में ऐतरेय उपनिषद् का महापाठ्य 'प्रज्ञानं ब्रह्म' है। यह सभी के पूर्ण विवरण के रूप में सार्वभौमिक दर्शन है। यह कहा जा सकता है कि हर चीज का नियम ब्रह्म है। हम प्रज्ञानम को पूर्ण ज्ञान के रूप में नहीं सोच सकते हैं जो कि दिना है एक व्यक्तिगत निज का अस्तित्व। और यह स्पष्ट है कि एक व्यक्ति स्वयं एक व्यक्तिगत व्यक्ति का तात्पर्य है। तो प्रज्ञानं ब्रह्म के महापाठ्य से एक समीकरण इस प्रकार बनाया जा सकता है।

प्रज्ञा पूर्ण चेतना = एक व्यक्ति जीव = एक व्यक्तिगत रस = एक व्यक्तिगत व्यक्ति। पूर्ण चेतन्य से विशेष चेतन्य अथवा व्यक्ति चेतन्य निःसृत होता है शंकर का प्रज्ञा से अस्तित्वादी तथा दूसरे तल का कर्मोपेक्षाओं का दान्यसेन-देन्डाल इगो सभी चेतना निःसृत होता है।

तो एक व्यक्ति का वर्णन, एक व्यक्ति स्वयं अनिवार्य रूप से ब्रह्म है। ब्रह्म वेद ब्रह्म नवति (मुंडक उपनिषद्: 3/2/9)। जब एक व्यक्ति के रूप में एक आकांक्षी, जो ब्रह्म विकार द्वारा वेदांत के श्रावण, मनन और निदिध्यापस के माध्यम से ब्रह्म विद्या का अभ्यास करने का परसुकता से इरादा रखता है और अंत में एक व्यक्ति ब्रह्म बन जाता है, जो एक व्यक्ति की पूर्ण अभिव्यक्ति है। सर्वज्ञ या ब्रह्म के रूप में मनुष्य हमेशा के लिए ऐतिहासिक खोज है। अद्वैत वेदांत में जीव, एक व्यक्तिगत विशेष चेतना रूप का आत्मा और ब्रह्म पूर्ण वास्तव या निरपेक्ष होने के रूप में।

जीव = एक व्यक्तिगत आत्म = ब्रह्म = पूर्ण वास्तविकता = अखंडन (अनंत)।

शंकर के अनुसार, एक व्यक्ति स्वयं और ब्रह्म समान है। ब्रह्म सच्चिदानन्दन है जो सत् (पूर्ण अस्तित्व) के समान शब्द है चित् (पूर्ण चेतना) और आनन्द (पूर्ण शांति)। तो, हम वेदांत से हर चीज का एक कानून बनाते हैं जो इस प्रकार है।

सत् = चित् = आनन्द = सच्चिदानन्द = पूर्ण अस्तित्व = निरपेक्ष धैर्य
= परम शांति।

उपर्युक्त नियम जो वेदांत करता है वह सब कुछ का छाया है, सभी भावों का कुल विवरण।

तो, यह स्पष्ट है कि वेदांत सभी का पूर्ण विवरण घोषित करता है। सब कुछ अनिवार्य रूप से चेतना है। तो, ब्रह्मांड में केवल और एक चीज स्थिर है यह है शुद्ध चेतना।

शंकर ने कहा कि सभी वेदों, उपनिषदों, गीता को केवल अद्वैत वेदांत के सार के रूप में उन्होंने आठ श्लोक (आठ वाक्य) में ही व्यक्त किया। यह इस प्रकार है :

"ब्रह्म सत्यं, जगत् मिथ्या, जिवा ब्रह्मैव नपरा"। ब्रह्म सत्यं जगत् (ब्रह्मांड) झुठा है और जीव और ब्रह्मा (व्यक्तिगत मनुष्य और पूर्ण चेतना है सत्य)।

3

इसका अर्थ है कि ब्रह्म (पूर्ण चेतना) सत्य है। सत्य शाश्वत अस्तित्व है। जगत् (ब्रह्मांड) झुठा है। असत्य वह अर्थ है जो क्षणिक (अनिश्चय) है और शुद्ध चेतना या पूर्ण ब्रह्म और जीव (व्यक्तिगत स्व) के रूप में निम्न नहीं है। सत्य शाश्वत सत्ता है। अपरिवर्तित युनिवर्सल बीजग हमेशा के लिए। शार्दभौमिक सत्ता परम वास्तविकता है, शुद्ध चेतना है। सभी नाम और रूप विषय के रूप में ब्रह्मांड हैं। सभी परिवर्तन नाम और रूपों में भी शामिल हैं।

सभी परिवर्तन = सभी रूप = संपूर्ण ब्रह्मांड = जगत् = असत्य। लेकिन सभी का सार या शाश्वत के लिए सभी चीजों का मूल आधार अपरिवर्तित शाश्वत पूर्ण चेतना या ब्रह्म है।

प्रज्ञा पूर्ण ज्ञान है जो ब्रह्म के लिए स्रष्टा है। यहाँ ज्ञानीमासा और तत्त्वमीमासा एक दूसरे समान है। ज्ञान चेतना है। अनुभव चेतना का एक रूप है। वेदांत में यह अनुदा वर्णन और कानून है जो पूरे ब्रह्मांड का स्पष्ट रूप से वर्णन करता है। पूरे ब्रह्मांड की हर चीज का वर्णन और परिभाषित किया गया है केवल और एक शाश्वत चीज चेतना, ब्रह्म।

यहाँ यह भी निष्कर्ष निकाला गया है कि ब्रह्मांड में केवल एक चीज है जो चेतना के रूप में पूर्ण मुक्त है। तो, स्वतंत्रता चेतना, केवल ब्रह्म, शुद्ध

चेतना ही ब्रह्मांड का नियंत्रक है। चेतना या ब्रह्म सब कुछ नियंत्रित करता है।

एकमान और अद्वितीय सिद्धांत बिल्कुल स्वतंत्र है और यह अनिर्णय रूप से केवल चेतना है। अद्वैत वेदांत ने इसे दुनिया में खोजा। ब्रह्म साक्षात्दानंद या अस्तित्व चेतना और साथ ही पूर्ण शांति है। तो, स्वतंत्रता चेतना के समान है। ब्रह्म या चेतना के रूप में अस्तित्व मुक्त है। ब्रह्म के रूप में अस्तित्व मुक्त है। ब्रह्म हमेशा के लिए स्वतंत्र रूप से मौजूद है। वेदांत घोषणा करता है कि अस्तित्व चेतना है। अस्तित्व मुक्त है। अद्वैत वेदांत के अनुसार अस्तित्व या चेतना या पूर्ण शांति या ब्रह्म स्वतंत्र है जो सभी को नियंत्रित करता है।

अस्तित्ववाद में, अस्तित्व एक शार उभरी मुख्य बर्षा है। वे चेतना, स्वतंत्रता, व्यक्तिगत व्यक्ति, स्वनिर्णयन के बारे में बर्षा करते हैं। वास्तव में अस्तित्ववाद की वे शर्तें कोई नई अवधारणा नहीं है। यह स्पष्ट है, कि आत्म-विरोध वास्तव में हमेशा के लिए झूठ है।¹ अद्वैत वेदांत से पता चलता है कि ब्रह्म अस्तित्व या चेतना या शांति के रूप में आत्म-विरोधभासी वे पूरी तरह मुक्त है। तो, स्पष्ट है कि अस्तित्व सार से पहले होता है स्वयं विरोधाभासी अस्तित्ववाद है। वेदांत से पता चलता है कि, अस्तित्व = चेतना = ब्रह्म = सार।

तो, चेतना से पहले अस्तित्व आत्म-विरोधभासी था। यही अस्तित्व नहीं केना है, अस्तित्ववाद है। लेकिन अद्वैत वेदांत में, अस्तित्व चेतना है। सार = चित = आनंद = साक्षात्दानंद ब्रह्म।

तो, अस्तित्व और चेतना समान है। वे बिल्कुल अलग नहीं है लेकिन एक ही चीज है। मनुष्य चेतना है। उसका लक्ष्य ब्रह्म बनना है। सभी व्यक्ति चेतना या आत्म चेतना के रूप में (क्योंकि आत्म चेतना शुद्ध चेतना का एक रूप है) ब्रह्म बन रहे हैं। यह वास्तव में मनुष्य बनने की प्रक्रिया है जिसे अद्वैत वेदांत को ब्रह्म को प्राप्त करने की प्रक्रिया के रूप में कहा जा सकता है (ब्रह्म वेद ब्रह्मव भावती)।

पूर्व-चित्तनशील चेतना और चित्तनशील चेतना प्रकृति में चेतना है। वे समान और अद्वैत हैं। यह कहना स्पष्ट है कि चेतना ही अस्तित्व है और सभी से पहले है। इसलिए सारा शुद्ध चेतना है। शुद्ध चेतना सभी से मुक्त है। तो,

चेतना और स्वतंत्रता एक ही है। स्वतंत्रता का अर्थ है चेतना या आत्म-चेतना। यह निष्कर्ष निकाला जा सकता है कि चेतना पूर्ण अस्तित्व = स्वतंत्रता = अद्वैत = अखंडन या अनंत चेतना है। तर्क यह है कि अद्वैत के रूप में केवल परम वस्तु। शाश्वत अस्तित्व वाले सभी में व्याप्त चेतना है। तो, चेतना सभी चीजों को नियंत्रित करती है, जिसमें सभी व्यक्ति भी शामिल है। केवल एक चीज मौजूद है क्योंकि चेतना सभी बहुलताएं और अंतर है।

सन्दर्भ—सूची

1. स्वामी विरेश्वरानंद, ब्रह्म सूत्र, अद्वैत आश्रम, पृ. 78
2. संकराचार्य पथिकरणम्, उद्देश्यम्, कलकत्ता, पृ. 15
3. श्री श्री सदानंद योगेंद्र, वेदांतसर, बी. के. पाल संस्कृत पुस्तक भंडार, कोलकाता-4, ऐतरयो उपनिषद्।
4. ऐतरयो उपनिषद्।
5. ए. क्रिटिकल स्टडी ऑफ साट्टेस ऑन्टोलीची ऑफ कॉन्शियसनेस, वर्धमान युनिवर्सिटी, वर्धमान, 1978, पृ. 71
6. शोरेन कीर्कगार्ड, अलैजाजिक पोस्ट्रिक्ट का स्थापन, ट्रान्, की स्वेन्सन, प्रिंसटन युनिवर्सिटी प्रेस, 1981, पृ. 251
7. जीन-पॉल सार्त्र, शीडिंग एंड नाथिगलेस, टी. आर. हेजलर्ड, ब्लूम्स पृ. 161

□



Printed by : Sanyam Publication, Delhi & Patna, (91)011-2656031

ISSN 2278 - 0688

Volume - XXII

ऋतायनी

A REFEREED RESEARCH JOURNAL OF SANSKRIT

ऋतायनी

VOLUME-XXII

ISSN 2278 - 0688

December 2022

Purulia , West Bengal

December 2022

RITAAAYANI

Vol. - XXII

ISSN 2278 - 0688

Volume -XXII

December 2022

ऋतायनी

RITAAAYANI

A REFEREED RESEARCH JOURNAL OF SANSKRIT

(U.G.C. Approved Journal No. 40947)

Chief Editor

Dr. Chandrakanta Panda

Editor

Dr. Jagamohan Acharya

Associate Editors

Dr. Buddheswar Sarangi

Dr. Jogeswar Mahanta

Sushant Pradhan

Purulia, West Bengal

भक्तिप्रस्थानस्य परिचयः महत्त्वम् अवदानं च

Somen Dutta

भक्तेः स्वरूपम्

भज् इति धातोः भक्तिशब्दस्य निष्पन्नः भवति । हिन्दुधर्मे भक्तिः आराधना तथा उपासनायाः एक-विशेषः रीतिः इति मन्यते । पूजितदेवे व्यक्तित्वं प्रति वा विशेषः स्नेहः प्रेमः वा भक्तिः इति कथ्यते । ईश्वरसमर्पणं पूर्णतया भक्तिः इति पण्डिताः उच्यन्ते । भक्तिमार्गे यः जनः ईश्वरं भजति सः व्यक्तिः भक्तः नाम अभिधीयते । भक्तिदर्शनं भक्तिमार्गः इति उच्यते । भक्तिवादः हिन्दुधर्मस्य अनेकसंप्रदायानाम् आधारः अस्ति । भिन्न-भिन्न-सम्प्रदायाः भक्तिवादस्य भिन्न-भिन्न-प्रकारेण व्याख्यां कुर्वन्ति । भक्तिवादः रीतिनां संस्काराणां च उपरि ईश्वरप्रेमं स्थापयति । प्रमि, मित्रम्, माता-पिता-सन्ततिः, गुरु-शिष्यः इव ईश्वर-मनुष्ययोः मानवीयसम्बन्धः भक्तिवादस्य मुख्यस्तम्भः अस्ति । ईश्वरस्य विशिष्टरूपस्य, ईश्वरस्य निराकाररूपस्य वा गुरुं प्रति विशेष-भक्तिः भक्तिवादस्य प्रधान-अङ्गः । हिन्दुधर्मे भिन्नसंप्रदायेषु भक्तिवादस्य विशिष्टरूपाः प्रचलिताः सन्ति । यथा— शैवाः शिवस्य तथा शिवसम्बद्धदेवतानां भक्ताः, वैष्णवः विष्णुः तथा तस्य अवताराणां भक्ताः, शाक्ताः च महाशक्तेः विभिन्नरूपस्य भक्ताः सन्ति ।

वैदिकसाहित्ये देवानां भक्तिसाहचर्यं लक्षते । श्रुत्विकसमर्पितस्य हविर्भार्गस्य सेवार्थं ते देवाः संहतिं सम्पतिञ्च दर्शयन्ति । यथा—

आस्य जानन्तो नाम धिद्विवक्तन

महस्ते विष्णो सुमतिं भजामहे ॥

भज् सेवयाम् इति धात्वर्थबलेन देवनिष्ठप्रौढ्यनुकूलव्यापारो भजेरर्थः ।

यथा गरुडपुराणे उक्तम्—

भज इत्येष वै धातुः सेवायां परिकीर्तितः ।

तस्मात् सेवा बुधैः प्रोक्ता भक्तिः साधनभूयसी ॥

अर्थात् सेव्य-सेवकसम्बन्धमूलतया सेव्य इष्टदेव सेवकश्च जीवो भवति । भक्तेः क्रमविकासे साध्यरूपायाः साधनरूपायाश्च भक्तेः भर्षणं प्रायशो दृश्यते ।

स्मरन्तः स्मारयन्तश्च मिथोपौषहरं हरिम् ।

भक्त्या सञ्जातया भक्त्या बिभ्रत्युत्पुलकां तनुम् ॥

श्रीमद्भागवते नवधाभक्तेः पुंस्वानुपुंस्वविवरणमुदाहरणञ्च दृश्यते । तथैव नारदभक्तिसुत्रे अपि भक्तेः स्वरूपस्य विषयो वर्णितः । इश्वरे परमप्रेमारुपा एव भक्तिः सा च अमृतारुपा

अस्ति । अर्थात् यथा वृक्षस्य पूर्णत्वं गौरवं च फले प्राप्तं भवति तथैव भक्तेः स्वरूपं गौरवं च भवति परमप्रेमलक्षणे एव अस्ति । शाण्डिल्येन अपि स्वभक्तिमुने परमतत्त्वं प्रति परानुरक्तिरेव भक्तिः इति उक्तम् । तथैवाध्यात्मरामायणे अपि अमस्त्येन-भक्तिरुपामृतं विना स्वप्ने अपि मोक्षः न भवेत् इति कथितम् । नारदचरित्रे अपि देह-मनो-बुद्ध्यहंकारैः रहित ज्ञानयोगावरणात् मुक्तः शुद्धभावेन सर्वैरिन्द्रियैः इन्द्रियाधिपतेः श्रीहृषीकेशस्य पदानुशीलनं नतेव भक्तिरिति उच्यते । बृहदारण्यकश्रुतौ उक्तम्-तमेव धीरो विज्ञानमेव भक्तिरुच्यते । भक्तवदग्दीतायां भगवता कृष्णेन सर्वेषु भूतेषु समः ब्रह्मभुतः भाव एव भक्तिरिति कथितम् । भक्तिरसामृतसिन्धौ प्रेमरूप सूर्यकिरणवत् स्वकीयकान्तिद्वारा चिन्तमध्ये द्वीभाबोत्पन्नमः शुद्धसत्त्वब्रह्मरूपभाव एव भक्तिरिति श्रीरूपनोस्वामिना उक्तम् । छान्दोग्योपनिषदि श्यामाच्छक्तं प्रपद्य । शवलाच्छ्यामं प्रपद्ये इतीयं प्रपत्तिः शारणागतिर्वा भक्तिरिति कथितम् । भागवते श्रीकपिलेन-यद्गुणश्रुतिमात्रेण मयि सर्व-गुहाशये । मनोगतिरविच्छन्ना यथा गंगान्धसो अम्बुधौ । इति भक्तेः निर्गणस्वरूपमुत्कृतम् । श्री सुतेन इयम् अहेतुकी भक्तिः जीवस्य श्रेष्ठधर्मरूपेण प्रतिपादिता । यथा—

स वै पुंसां परो धर्मो यतो भक्तिरधोक्षणे ।

अहेतुव्यप्रतिहता यथात्मा सम्प्रसीदति ॥

अर्थात्, येनेन्द्रियज्ञानातीतं श्रीकृष्णं प्रति अवणादिलक्षणा फलाभिसंधान-रहिता ऐकान्तिकी निरपेक्षा भक्तिर्नयते सैव पुंसां परोधर्मः भवति तथा भक्त्या आत्मा प्रसीदति ।

एवं भक्तेः सामान्यस्वरूपं वेदोपनिषत्त्रयदभक्तिसुत्र-शाण्डिल्य भक्तिसुत्र-भागवताध्यात्मरामाणादिषु आर्षग्रन्थेषु समुपलभ्यते ।

वैदिकसाहित्ये भक्तिः

भक्तिः वैदिकसाहित्ये मानवजीवनस्य लक्ष्यरूपेण स्वीक्रियते । वैदिकमंत्रेषु अपि भक्तिधारायाः संकेतः प्राप्तुं शक्यते । श्रवण-कीर्तन-स्मरण-पादसेवनार्चनबन्धन-दास्य सख्यात्मनिवेदनदि रूपेण भक्तेः नवधा वर्णनमुपलभ्यते । तत्र परमात्मनः श्रीविष्णोः यशःकथायाः पुनः पुनः श्रवणाय ऋग्वेदस्य मंत्रे प्रमाणं प्राप्यते । यथा—सेतु श्रवोभिर्यज्यं चिदभ्यसत् । कीर्तनभक्तेः सूचना अपि प्राप्यते तत्र विष्णोर्नु कं वीर्याणि प्रयोचम् अर्थात् श्रीविष्णोः लीलापराक्रमादितत्त्वं वर्णयामि इति परमात्मनः लीला-गुणानुकीर्तनस्य सूचना मंत्रे अस्मिन् प्राप्यते ।

प्रविष्णवे शुभमेतु मन्त्र विरिञ्चित उरुगायाय वृष्णे ।

अत्र उरुगाये भगवति मम स्मरणं सुदुर्लभं भवत्विति मंत्रे अस्मिन् पादसेवनभक्तेः विषये सूचना प्राप्यते यथा—

यस्य त्री पूर्णा मधुना पदान्यक्षीयमाणा-स्वधवा मवन्ति ।

भगवतः विष्णोः माधुर्यमण्डिताक्षयपादत्रयस्य सेवनेन आनन्दः प्राप्यते इति अस्मिन् मंत्रे कथितम् ।

अर्चनभक्तिविषये कथ्यते यथा— प्र वः पान्तमन्त्रो धियायते महे शुराय विष्णवे चार्चत अत्र महत्पराक्रमस्य विष्णोः भगवतः अर्चना सूचिता ।

वन्दनभक्तिविषये कथ्यते यथा— नमोरुचाय ब्राह्मणे अस्मिन् मंत्रे ब्रह्म-विश्वस्य नमस्कारः निर्देश्यते ।

दास्यभक्तिविषये कथ्यते-ते विष्णो सुमतिं भजामहे अत्र भगवतः विष्णोः सेवां कर्तुं सूचना प्राप्यते । सख्यभक्तिविषये कथ्यते-उरुक्रमस्य स हि बन्धु रित्था विष्णोः अत्र भगवतः उरुक्रमस्य विष्णोः सख्यरूपेण सेवां कर्तुं सूचना प्राप्यते ।

आत्मनिवेदनात्मकभक्तिविषये कथ्यते—

यः पूर्याय वेधसे नवीयसे सुमज्जानये विष्णवे ददाशति ।

अत्र जगत्-स्रष्टारं, नित्यनवीनं भगवन्तं प्रति आत्मसमर्पणं कर्तुं कामना क्रियते ।

एवं वैदिकसाहित्ये भक्तोः नवसाधनै यथा— श्रवण-कीर्तन-स्मरण-पादसेवनार्चन-वन्दन-दास्य-सख्यात्मनिर्वदनभक्तिभिः प्रभावः परवर्तेश्रीमद्भगवतगीता पुराण सूत्रालंकारसाहित्येषु परिलक्ष्यते ।

वैदिकसाहित्ये देवस्तुनिपरका मन्त्राः भक्तितत्त्वस्य बीजं वहन्ति । तत्रापि लोभत्यागपूर्वकात्मसमर्पणस्य तथा आत्मनः तुच्छभावस्य निवेदनेन सह स्वस्वेष्टदेवकृपाकटाक्षलाभाय ये प्रत्यक्ष-परोक्षाध्यात्मिकमन्त्राः परिगीताः तत्र भक्तोः गन्धः अनन्तरवर्तितसाहित्यं सुवासयति, इति अत्र नास्ति संशितिलेशः ।

श्रीमद्भगवद्गीतायां भक्तिः

यथा वैदिकसाहित्येषु नवधाभक्तोः सूचना प्राप्यते तथैव सर्वेपनिपदा स्वरस्वतरुपायां श्रीमद्भगवद्गीतायामपि नवधाभक्तोः प्रमाणमुपलभ्यते । श्रवणभक्तिविषये भगवता कृष्णेन अर्जुनं प्रति उपदिश्यते । यथा—

श्रद्धावानसूयञ्च शृणुयादपि यो नरः ।

सोपि मुक्तः शुभान् लोकान् प्राप्नुयात् पुण्यकर्मणाम् ।।

अस्मिन् श्लोके श्रद्धावान् अनसुयो गीताश्रवणात् एव मुक्तिं प्राप्नोति इति उक्तम् । कीर्तन-स्मरणभक्तिविषये तत्र सूचना उपलभ्यते । यथा—

मच्चित्ता मद्गतप्राणा बोधयन्तः परस्परम् ।

कथयन्तश्च मां नित्यं तुष्यन्ति च रमन्ति च ।।

अत्र नित्यं परस्मैर् बोधयन्त इति पदेन सर्वदा भगवतः कीर्तनं कर्तुं संकेतः लभ्यते । पुनश्च मच्चित्ता मद्गतप्राणा इति पदेन भगवतः स्मरणं ततः पादसेवनभक्तिविषये वर्णयते यथा—

अभ्यासेष्वसमर्थोऽसि मन्तर्मपरमो भव ।

मदर्थमपि कर्माणि कुर्वन् सिद्धिमवापस्यसि ॥

अत्र अभ्यासेवोये असमर्थोऽपि भगवतकर्मपरायणो भूत्वा तस्य कथाश्रवण-कीर्तन-वंदनार्चन-तन्मन्दिरमार्जन-पुष्पचयन-ततपरिचर्यादि कर्तुं सूचना प्राप्यते । पुनश्च दास्यभक्तिविषये तत्र प्रमाणं प्राप्यते ।

मन्मना भव मद्भक्तो मद्याजी मां नमस्कुरु ।

माभेवैष्यसि युक्तत्वैवमात्मानं मत्परायणः ।

अत्र मद्भक्ताशब्देन भगवान् एव एकमात्रपरमगतिः भर्ता-स्वामी इति मत्त्वा तत्राम-रुप-गुण-प्रभाव-लौलादी श्रवण-कीर्तन-स्मरणेषु तस्मै सर्वसमर्पणभाव एव दास्यभक्तोः सूचना लभ्यते । ततः सख्यभक्तिविषये प्रमाणं प्राप्यते यथा—

गतिर्भर्ता प्रभुः साक्षी निवासः शरणं सुहृत् ।

प्रभवः प्रलयः स्थानं निधानं बीजमव्ययम् ॥

अत्र गतिः भर्ता-प्रभुः साक्षी सुहृत् इति मत्त्वा तस्मिन् शरणापन्नभाव एव सख्यभक्तिरिति कथ्यते इति सूचना प्राप्यते । ततः आत्मनिर्वदन-भक्तिविषये सूचना प्राप्यते यथा—

सर्वधर्मान् परित्यज्य मामेकं शरणं ब्रज ।

अहं त्वां सर्वपापेभ्यो मोक्षयिष्यामि मा शुचः ।

अत्र मामेकं शरणं ब्रज इति वाक्येन चिन्ता-सेवा-पूजा-प्रणति पूर्वकं सर्वधर्मपरित्यागेन केवलं भगवतः शरणागतिः एव आत्मनिर्वेदनात्मिका भक्तिरिति कथ्यते ।

भगवद्गीतायां ज्ञानयोगः कर्मयोगः भक्तियोगः इति योगसमुच्चये भक्तियोगस्य विवेचनं कृतम् । तत्र सम्प्रदायभेदेन ज्ञानस्य कर्मणो भक्तेः वा प्रधानाप्रधानताविमर्शः । अन्ततो गत्वा त्रयाणां योगानां समुच्चयविषयः सकलतत्त्वमौलिभूतः प्रतिपादितः । तथापि तत्र उपास्योपासक-सम्बन्धरूपाया भक्तेरपि च पत्रपुष्पफलतोयोत्सर्गपूर्वकं भगवत्प्राप्तिरूपायाः भक्तेः अनन्यता संसाधिता ।

वैदिकसाहित्यात् श्रीमद्गीतायां च परं पुराणसाहित्ये भक्तितत्त्वस्य पुंखानुपुंखं वर्णनं दृश्यते । उक्तितत्त्वस्य विवेचनं प्रायतः अष्टादशपुराणेषु उपलभ्यते । यद्यपि सर्वेषु पुराणेषु भक्तेः स्वरूपाणां यत्र तत्र वर्णनं दृश्यते तथापि ब्रह्म-पदम-विष्णु-भागवतादि भक्तिप्रधानपुराणेषु भक्तितत्त्वस्य सर्वाधिकं वर्णनमुपलभ्यते ।

ऋग्वेदपुराणे श्रीकृष्णभक्तितत्त्वस्य विस्तारेण सह वर्णनानन्तरं तत्सम्बन्धि ज्ञानमिश्रितभक्तितत्त्वं वर्णितम् । यथा—

अप्यन्यचित्तोऽशुद्धो वा यः सदा कीर्तयेद्हरिम् ।

सोऽपि दोषक्षयान् मुक्तिं लभेच्चैदिपतिर्यथा ॥

अत्र भगवतः नामकीर्तनेन द्रव्यभक्तापि मुक्तिः प्राप्ता इति कथितम् ।

पद्मपुराणे भक्तेः प्रमुखाङ्गरूपेण ख्याताया कीर्तनभक्तेः महत्त्वं वर्णितम् । एवं तत्र भगवतः कीर्तनमण्डलीनां नामोल्लेखोऽपि विद्यते । यथा—

अप्यन्यचित्तोऽशुद्धो वा यः सदा कीर्तयेद्हरिम् ।

सोऽपि दोषक्षयान् मुक्तिं लभेच्चैदिपतिर्यथा ॥

अत्र भगवतः नामकीर्तनेन द्रव्यभक्तापि मुक्तिः प्राप्ता इति कथितम् ।

पद्मपुराणे भक्तेः प्रमुखाङ्गरूपेण ख्याताया कीर्तनभक्तेः महत्त्वं वर्णितम् । एवं तत्र भगवतः कीर्तनमण्डलीनां नामोल्लेखोऽपि विद्यते । यथा—

प्रहादस्तालधारी तरलगीततया चोद्धवः कांस्यधारी

वीणाधारी सुरर्षिः स्वरकुशलतया रागकर्तार्जुनोभूत् ।

इन्द्रोवादीन्मृदङ्गं जयजयसुकराः कीर्तने ते कुमारा-

सत्राग्रे भाववक्ता सरसरचनया व्यासपुत्रो बभूव ॥

अत्र प्रहादोद्धव-नारदाजुनिन्द्र-सनात्कुमारा इत्यादयः परमभागवताः स्व स्व वाद्ययंत्रैः सह भगवतः नामकीर्तनं कृतवन्त इति सूचना प्राप्यते ।

ततः विष्णुपुराणे पञ्चमांशे अष्टाध्याये केवलायाः भक्तेः स्वरूप-वर्णनमुपलभ्यते । भक्तेः प्रमुखसाधनरूपस्मरणभक्तिप्रसङ्गे इत्थं वर्णितम्—

स्मृते सकलकल्याणभाजनं यत्र जायते ।

पुरुषस्तमजं नित्यं व्रजामि शरणं हरिम् ॥

अत्र भगवतः स्मरणमात्रेणैव सर्वकल्याणं भजते पुरुषः इति कथितम् । पुनश्च तत्र अङ्कुरेण श्रीकृष्णस्य ब्रह्मस्वरूपमनुभूय तस्मिन् भक्तिः कृता दृश्यते ।

तस्मादहं भक्तिविनम्रचेता, व्रजामि सर्वेश्वरमीश्वराणाम् ।

अंशावतारं पुरुषोत्तमस्य हृनादिमद्भान्तमजस्य विष्णोः ॥

ततः भक्तिप्रधानपुराणेषु भागवतस्य स्थानमन्यतमम् । अस्मिन् पुराणे भक्तेः स्वरूपस्य सभेत्तं सतत्त्वं वर्णनमुपलभ्यते । अत्र भक्तेः द्विविधः मार्गो वर्णितः । तयोः साध्यसाधनयोः साधनमार्गः भक्तिसाधनस्य सुगमोपाय इति वर्णितम् । यथा—

न साधयति मां योगो न सांख्यं धर्म उद्धव ।

न स्वाध्यायस्तपस्त्रागो यथा भक्तिर्ममोर्जिता ॥

अत्र योग-सांख्य-स्वाध्याय-तपस्त्रागादि विना भगवति भक्तिः सञ्जाता इति सूचना प्राप्यते ।
पुनश्च सप्तमाध्याये परमभक्तप्रह्लादोपि भक्तेः उपादेयतायाः प्रसङ्गे कथितवान्—

प्रीणनाथ मुकुन्दस्य न वृत्तं न बहुज्ञता

न दानं न तपो नेज्या न शौचं न व्रतानि च ।

प्रीयनेमलया भक्त्या हरिरन्यद् विडम्बनम् ॥

अत्र भगवतः भक्तिं विना भक्तास्य अन्यसाधनं यथा— दान-तपो-यज्ञ-व्रतादि उपहस्यमेव प्राप्नोति किन्तु अमलया भक्त्या एव भगवान् प्रीयते इति सूचना प्राप्यते । तत्र पुनश्च भक्तिरेव वैराग्यसाधिका तथा कर्मणः उपयोगः वैराग्यस्य हेतोः उच्यते । यावत् वैराग्यस्योत्पत्तिः न भवेत् तावत् वर्ज्यमविहिताचाराः सदा पालनीयाः । तथा च उक्तम्—

तावत् कर्माणि कुर्वीत न निर्विद्येत यावत्त ।

मक्तथाश्रवणाद्यै वा श्रद्धा यावत् जायते ॥

पुनश्च कथ्यते तत्र—श्रेयसः मूलस्रोतोरुपिणीं भाक्तिं परिहृत्य बोध्यते प्राप्यते उद्योगशीलानां मानवानां प्रयत्नः नथैव निष्कलः तथा कलेशोत्पादकश्च भवति यथा स्थूलतुषावर्धतिनाम् ।

श्रेयः श्रुतिं भक्तिमुदस्य ते विभो

क्लिशयन्ति ये केवलबोधलब्धये ।

तेषामसौ क्लेशाल एव शिष्यते

नान्यद् यथा स्थूलतुषावर्धतिनाम् ॥

पुनश्च तत्र ज्ञानपेक्षया भक्तेः उपादेयता प्रतिपादिता । साधनभक्तिः नक्था भवति । पुराणसाहित्ये विशेषतः भागवते सत्संगतेः महिमगानं सर्वत्र दृश्यते । साध्यरूपा अथवा फलरूपा भक्तिः प्रेमलक्षणा इति गृह्यते । प्रेमलक्षणा युक्तभक्ताः बाह्येन्द्रचक्रवर्तिनां पदं तथा योगस्य श्रेष्ठसिद्धानामपि मोक्षपदं नेच्छन्ति । भगवता सार्धं नित्यवृन्दावने ललितविह्वरार्थमावेशितधीः भगवच्चञ्चरीकः भक्तः शुष्कां रसशुन्यां मुक्तिमपि तिरस्कारोति । यथा—

न पारमेष्ठ्यं न महेन्द्रधिष्यं

न सार्वभौमं न रसाधिपत्यं ।

न योगसिद्धीरपुनर्भवं वा

मर्यापितात्मेच्छति मद् विनान्यत् ॥

पुनश्च तत्र भगवतः दर्शनिच्छुभवतानां स्वभाव-विषये वर्णितम् । यथा—

अजातपक्षा इव मातरं खगाः
स्तन्यं यथा वत्सतराः क्षुधार्ताः ।
प्रियं प्रियेव व्युषिनं विषण्णा
मनोरविन्द्राक्ष दिदृशते त्वाम् ॥

उपसंहारः

अयं भक्तिरसः प्रत्यक्षभक्तिरसः परोक्षभक्तिरसः इति द्विविधा विभज्यते । पुनश्च प्रत्यक्षभक्तिरसः शान्त-दास्य-सख्य-वात्सल्य-माधुर्यादिरूपेण पञ्चधा विभज्यते । पुनश्च परोक्षभक्तिरसः ह्रस्य-करुण-क्रोध-शौर्य-भय-विस्मय-बीभत्सादिरूपेण सप्तधा विभज्यते । द्वादश-रसानुसारं-कपिल-माधव-उपेन्द्र-नृसिंह-नन्द-नन्दन-वलराम-कूर्म-कल्की-राघव-वराह-मत्स्यादिद्वादशानाम् अवताराणां कल्पना क्रियते ।

सन्दर्भग्रन्थसूची—

1. Ujjvalanīlāma.Ei of RUpagoswami, Edited by Tukaram JA'vajl', Mumbai, 1835.
2. History of Sanskrit Poetics by S.K. De, Calcutta Oriental Press, Calcutta, 1925.
3. Rasadī'ghikā' of Vidyā'rA'ma, Edited by Gopal Narayan BahuDa, Rajasthan Oriental Research Institute, Jodhpur, 1956.
4. The Number of Rasas by V. Raghvan, The Theosophical Publishing House, Adyar, Madrass, 1975.
5. Bhaktiramā'sasindhu of RUpagoswA'mi, Edited by I'rī' Bhakti VedA'ntaSwA'mi, BhaktivedA'nta Book Trust, Mumbai, 1980.
6. 16. EkA'vall' of Vidyadhara, with the Commentary of Tarala by MallinA'tha, Osmania University, Hyderabad, 1981.
7. षड्विंशतिरसः, षड्विंशतिरसः, Odisha Sahitya Academy, Bhubaneswar, 1981.

Research Scholar
S.K.B. University,
Purulia, West Bengal
Mob : 7384860243



ISSN : 2347-7180

(A Bilingual Research Journal, Indexed in UGC-Care list)

DOGO RANGSANG

Research Journal, Vol-13, Issue. 3, No.3, March 2023

दगो बांछां

CHIEF EDITOR (HON.)
EDITORS (HON.)

मुख्य सम्पादक (अबैतनिक)
सम्पादकद्वय (अबैतनिक)

: Dr. Upen Rabha Hakacham
: Dr. Lalit Chandra Rabha
: Dr. Dhaneswar Kavitha
: ड॰ उपेन बाबा हाकाचाम
: ड॰ ललित चन्द्र बाबा
: ड॰ धनेश्वर कलिता

A Peer Reviewed Bilingual Research Journal
(Indexed in UGC-CARE List)

ISSN 2347-7180

DOGO RANGSANG RESEARCH JOURNAL

দগো বাংছাং গবেষণা পত্রিকা

Chief Editor (Hon.) : Dr. Upen Rabha Hakacham
Editors (Hon.) : Dr. Lalit Chandra Rabha
Dr. Dhaneswar Kalita

মুখ্য সম্পাদক (অবৈতনিক) : ড° উপেন বাছা হাকচাম
সম্পাদকসমূহ (অবৈতনিক) : ড° ললিত চন্দ্র বাছা
ড° ধনেশ্বর কলিতা



Dogo Rangsang Research Society
Reg. No. KAM-M/263/L/ 595 of 2015-16
দগো বাংছাং গবেষণা সমিতি

HYDRAULIC STRUCTURES IN ANCIENT INDIA: PEOPLE'S WISDOM

Dr. Samar Kanti Chakrabarty, Head, Department of History, Achhruram Memorial College,
Jhalda, Purulia (Affiliated to Sidho-Kanho-Birsha University, Purulia, West Bengal, India)

Abstract

Water is the name of life. The dry climate and water scarcity are not phenomena of recent times. They existed in the past just as they do now. In ancient India, different water harvesting practices developed along with high levels of hydraulic structures. This article reviews studies of traditional water collection mechanisms, with two themes. It provides brief descriptions of unique water harvesting systems and the most critical debates on the issue of ancient India. The essay argues that interest in the subject must now attempt to chase great questions as well. Towards the end, it is argued that much insight and theoretical traction may be gained from the 'well water harvesting structures'. This work also explains how ecology-based societies were developed, and how they encountered social threats to maintaining the balance between men and the environment for the future generation.

Key Words: Agricultural Development, Indigenous people, rain-water, Hydraulic structure, Practices

Introduction

The civilizations of ancient India flourished on the banks of rivers and seas over the ages. The importance of water resources is highlighted in the hymns of the Vedas, the Puranas, the Upanishads, the epics, and other classical literature of ancient India. These records show the birth of hydraulic structures and water management systems and the awareness of ancient people prevalent in the country. The people of the Indus-Valley Civilization, Vedic Civilization, and those belonging to Maurya, the Guptas, the Cholas, the Pallavas, and other periods had achieved a high level of excellence in the use and management of water resources. The prime objective of the water management system in early India was to enhance the irrigation system in a decentralized manner. Perhaps this water management system was first implemented across the banks of the rivers in the study area to serve the interests of the local communities. Agriculture was the primary source of livelihood for people in the past. Even today, it is the principal source of income for millions of people worldwide.

Statement of the Problem

Traditional water collection systems can determine if it is possible to mitigate the enormous water crisis at present. Ancient hydraulic structures were formed and functioned well thanks to the comprehensive cooperation, supervision, maintenance, and topographical knowledge of the ancestors. In the early days, long-standing wars and conflicts created a chaotic environment that disrupted the smooth flow of water through the channels. Even minor irrigation systems were not regularly cleaned, and maintainers failed to repair the hydraulic structures owing to the age of decline of the particular kingdom. It is experienced that traditional knowledge-based water management was only appropriate for minor cultivation. In addition, due to the shifting of livelihood patterns of the communities' neglected the local irrigation systems. Irrigation projects, on the other hand, fail due to the patronage of village chiefs and local kings. Traditional knowledge deteriorated massively when extensive cultivation started without regard for the laws of nature. Moreover, natural disasters also hampered the proper functioning of water structures and management in early days. For example, in the Mayura era, Sudarshana Lake was one of the finest examples of this.

Objectives of the study

- Explain topography characteristics based on traditional knowledge.
- Identify the collective cooperation and wisdom of your forefathers.
- Explain how important the laws of nature are.

- > Depicting wars and conflicts hinders the socio-economic structures of communities.

Review of Literature

Anupam Mishra's pioneering work (2013) '*Aaj Bhi Khare Hain Talab*' gives a detailed description about the hydraulic structures and its multiple uses and impact on the communities. A *Nagajasthi* or wooden pillar was set up in the middle of the *talab* by the local experts through the ceremony to measure water level of the pond/talab periodically. John M Fritz & George Michell (2017) has highlighted its geographical location, indigenous water harvesting practices, (aqueduct, stone-well, dug well, stepped well), royal's water tapping mechanism from the Tungabhadra rivers and surrounding hills in Vijayanagara. The 'city of victory' Vijayanagara is the growth of meeting not only for its historical importance; its remarkable landscape, the innovative agricultural method in the foothills of the empire, religious association, archaeological evidence, etc had made it an outstanding destination of international significance. Arjun Appadurai's pioneer work (1986) expressed the reality that nature may exist outside society, but natural resources are social phenomena treated by human beings to their benefit. Debasish Sengupta, Paramesh Goswami and Kalyan Rudra (2013) noted that ancient India artificially preserved rainwater by applying traditional knowledge and wisdom.

Research Methodology

Methods have been used to write this article that includes both requisite historical method as well as the basic primary sources. Apart from secondary sources like books, articles, relevant images and archeological sources have been used to find out the hydraulic structure of ancient India's past, and their resource evaluation management in the drought landscapes has been explained in a scientific manner. This study has used four methods: theoretical, observational, experimental and empirical.

Results and Discussion

There are four stages in the result analysis. There are three factors; topographical location, past and present performance analysis, and the number of beneficiaries. This study has investigated the water harvesting practices of some states like West Bengal, Bihar, Assam, and Meghalaya. Traditional water management practices are moribund in West Bengal, whereas Purulia is maintaining the traditional practice perfectly. On the other hand, North Bihar has also been following the same practices from time immemorial. Indigenous communities of south India and the north-western part of the country are trying to revive traditional practices on the basis of the topographical features of the study area, and some conservationists like Rajender Singh, Anna Hazare, and many more are raising their voices to retrieve dying practices on the basis of wisdom.

Table No. 1: Topographical location and Performance of the water Harvesting Management

Names	Location in Foothills	Status of the Past	Status of the Present	Beneficiaries Communities
Ponds, hapa, Johad, well, Step-farming	West Bengal	Fostered well	Almost dried up except Purulia	Santal, mundia, Mahato, Kumar & Kurnia
Ging	Jammu & Kashmir	Maintained well	maintaining	Balti, Boda, Bor, Beta
Kul	Himachal Pradesh & Uttarakhand	Maintained well	maintaining	Kinnar, Jhal, Pangi
Step farming	Arunachalpradesh, Nagaland	maintained well	maintaining	Aptani tribe
Rainbow Strip	Meghalaya, West Bengal and other North-eastern states	maintained well	maintaining	Modo, Mech, Naga, Lepcha etc
Khadir	Rajasthan	maintained well	Medium	Maldhari, Rabari
Kanali, Johar, jumar Keri	Rajasthan & Maharashtra	maintained well	Medium	Maldhari, Rabari, Koriau tribe
Vardha & Rawali	Gujarat & Rajasthan	maintained well	In moribund condition	Maldhari, Rabari, Dhot, Dhelo Bhol
Fat & Kanath	Madhya Pradesh	maintained well	In moribund condition	Agariya, Anbh, Baiga, Bhaim.

En	Tamil Nadu	maintained well	Medium	Aravadi, Erodatan, Irar
Katte & Kere	Karnataka	maintained well	Medium	Adiyar, Barda, Bevachia, Bamscha, Bholi, Bholi, Gamsia, Dholi, Dholi
Johad	West Bengal	maintained well	Maintaining well in Purulia and Some part of Bankura, Birbham, Jhurgram	Santal, Jhanda, Kumar, Karama
Ahar-pyne	Bihar and West Bengal	maintained well	Limited in North Bihar and Purulia in West Bengal	Santal, Jhanda, Kumar, Karama, Mahata

The above table shows the names of the water collection practices, the topographic location of the States, past performance vis-à-vis the several services of the traditional knowledge, the current scenarios, and the status of the water managers. This study looked at almost many traditional water collection structures in West Bengal, Bihar, Jharkhand, Meghalaya, Assam, etc. to collect authentic information on traditional water harvesting systems. In addition, it also examines many water management structures at the beginning of India.

Discourse on Hydraulic Structures

Ancient India had several types of water management systems like *johad*, *ahar-pyne*, *kund*, *hapa* (*hapa* means small pond and digs up in corner of field for soil moisture.), pond, *anicut*, *dam*, *bundh*, *mulha*, *bawli*, *eri*, *pat*, *rapot*, *jalhara* etc.¹ Their techniques and structures were different due to the different configurations of the lands. These bear ample testimony to the technologies and their mosaic past based on the topographical features and climate of the region. The 'Arthashastra' refers to the method of lifting water from artificial water bodies like lakes, tanks, and wells.² It refers to making tiny heaps of sand before the end of the monsoon. Such rain gauges were used for farming and cultivation in Kerala. During monsoon season, the rainwater was trapped in the heaps to recharge groundwater levels. This practice became popular among the farmers to avoid the evils of the water crisis in drought-prone areas. This practice was also used to remove weeds and loosen up the soil to make it suitable for agriculture. Some water-harvesting management is mentioned below to clarify the theme of the work.

Halagatti is an ancient water-tapping practice. Embankments were constructed at different levels to retain rain-water that runs down the slopes. The aim, however, was not to stop all the water. The remaining water was released into the following field when the field was adequately wet. This method of outflowing water was called halagatti. The size and height of the mouth of the halagatti (wasteway) practice were determined based on the rain and the slope. This is generally constructed at a slightly higher level than the field. Stones are laid on the side of the outlet as well as its base.³ These measures are followed for the conservation of topsoil and drought relief.⁴ The Arthashastra also mentions the different water harvesting systems prevalent in ancient India. In Sringerapur, near Allahabad (in the state of Uttar Pradesh), there existed a sophisticated water harvesting system that stored the flood water of the river Ganges on the natural slope of the land. Karikala Chola (c. 120 CE), the greatest among the early Chola Kings of the Sangam Age in South India, built the Grand Anicut or Kallanai (Dam) across the river Kaveri to divert water for irrigation and cultivation.⁵

Jhalara is an age-old water conservation method practiced in Rajasthan to cope with scanty rainfall. *Jhalaras* are typically rectangular-shaped step wells with multi-layer steps on three or four sides. These step-wells collect the subterranean water of an upstream reservoir. *Jhalaras* were built to ensure an easy and regular water supply for religious rites, royal ceremonies, and the daily chores of the local communities. The oldest step wells may date back to 550 AD. However, the most illustrious step wells were constructed in the medieval period. It is roughly estimated that more than 3000 step wells were constructed in two central northern states of India.⁶ The city of Jodhpur has eight such *jhalaras*, the oldest of which is the Mahamandir *Jhalara*, which dates back to 1660 AD. A large number of reservoir wells were constructed in the tract between the Sutlej and the Ravi rivers in the Montgomery district

of Pakistan. These would be filled during a flood and be transformed into lakes. When the rivers remained dry in summer, the water of the lakes was used for irrigation using jhalara.⁷

The Ahar Pyne system is an indigenous irrigation technology that continues to irrigate areas of south Bihar in India. Nirmal Sengupta, in his article, 'Indigenous Irrigation Organization in South Bihar', has stated that it was introduced around 3000 years ago for tapping rain-water. Ahars (channels) are reservoirs with embankments on three sides and are built at the ends of drainage lines such as rivulets or artificial works like pynes.⁸ Pynes are diversion channels led off from the river for irrigation purposes and impounding water in the ahars. It is mostly to the credit of these that paddy cultivation has been possible in this region owing to the preservation of rain-water by ahar-pyne water management. The system attained its highest development in the district of Gaya. This article provides an account of the ahar-pyne systems in South Bihar and the need to build organizational and institutional capacities of civil society and government agencies to undertake ahar-pyne renovation and management. Nowadays, the ahar-pyne system has witnessed a tendency toward sharp decline, yet even today, it constitutes nearly three-fourths of the total irrigation facilities in South Bihar. More than sixty percent of these are defunct now, and the rest are poorly managed. Nirmal Sengupta has attributed factors to the decline of Ahar-pyne practice in South Bihar, such as the loss of interest among the zamindars (landlords) in maintaining the system and the introduction of a new system by the irrigation department of South Bihar in the 1960s.⁹

Johad, one of the oldest systems of conserving groundwater, has existed since ancient times in the Alwar district of Rajasthan. They are small earthen check dams that capture and store rain-water. Johad, popularly known as a small dam, was dug up to meet the water needs in the non-rainy season. It is a community-owned traditional rain-water principally used for agriculture.¹⁰ Nowadays, such water harvesting management is used for irrigation in several states like Haryana, Punjab, Rajasthan, and Gujarat. Generally, johads are built along the foothills and river basins. Sluice gates were built in every johads on the earthen-*bundhi* to discharge water from the water body. Thus, the water-saturated land is then used for crop production. Archaeologists like Sunila Narin and Sunita Narin have dated that this crescent-shaped system of effective water management was introduced by the Paliwal Brahmins of Jaisalmer, Rajasthan, in the 15th century.¹¹

The following picture deals with the structural management of johad which managed the water-related needs in the states of Haryana, Uttar Pradesh, and Rajasthan many years ago. The covered area of johad varies from 2 hectares to 100 hectares in the Alwar district.¹² Essentially, the johad captures runoff water from monsoon floods and allows it to percolate down to lower fields during the dry months.¹³

Panam Kenies were used to store rain-water by the *Kuruma tribe* in Rajasthan. This water management system was also developed many years ago. Wooden cylinders are made by soaking the stems of today's palms in water for a long time so that the core rots away until only the hard outer layer remains. This system is used only for drinking water in the different parts of Rajasthan and Gujarat.¹⁴

In northeastern Meghalaya, a 200-year-old system of tapping stream and spring water using **bamboo pipes** is prevalent. The primitive tribes had developed this simple and effective method of water preservation for irrigation and drinking. Generally, water is collected using different sizes of bamboo pipes from the perennial springs of the hills,¹⁵ fewer watering crops are grown under this water management system. Drops of water are directly put into the roots of the plants. Nowadays, this age-old practice is followed by the farmers of the Khasi and Jaintia hills to cultivate nut orchards and black peppers.

The **Ramtek model** has been named after the water harvesting structures in the town of Ramtek in Maharashtra. It is a series of ponds designed to harvest the seasonal rain-water available in the ponds and lakes of the region. Ramtek management preserves runoff water and recharges the ground or earth during the monsoon. It has been maintained mainly by the *malguzari* (landowners) of the region.¹⁷ Nowadays, about 41000 hectares of agricultural land are being irrigated by this practice.

The **Pat system** had been built in the undulating terrain to divert water from hills-streams to irrigation channels. Such a practice was formed at the Bhitada village in the Jhabua district of Madhya Pradesh.

Diversion *bunds* are made across a stream by the people surrounding the *bunds*. The Pat channel passes through deep ditches, and then water is brought into the rice field through the stone aqueducts.¹⁸

The *Eri* (tank) is one of the oldest water management systems in Tamil Nadu. In most cases, an *Eri* or tank is excavated in the foothills. It is fed by the channels of the diverted river's water. The local people used it for multi- purposes, such as controlling the flood of the area, recharging groundwater, preventing soil erosion, and stopping the wastage of runoff water during the heavy monsoon. Even today, it is widely used for the same purposes.¹⁹ Tanks can supply water to the remotest villages for irrigation and other daily chores. Presently, this water tapping system is prevalent in many districts (Ramanathapuram, Tanjabbhur, and Pudukottai) of Tamilnadu.

The *Kund* is an old water-tapping practice. A plastered *kund* is so foolproof that not a single drop of water ever leaks or gets spoiled, and the water remains clean for the entire year.²⁰ The purpose of it is to harvest rain-water for drinking. *Kunds* dot the sandier tracts of western Rajasthan and Gujarat.²¹ According to Raja Sur Singh, the earliest evidence of this date was discovered in the village of Vadi Ka Milan in the year 1607 AD. Anil Agarwal and Sunita Narain, in their edited book, '*Dying Wisdom: Rise, Fall and Potential of India's Traditional Water Harvesting Systems* (1997) have described in detail the '*community kundis*' that had been built by collective initiative.²²

The excavation of ponds or *tababs* for tapping rainwater is one of the oldest practices in our country, initiated in very early ages. Anupam Mishra's pioneering work, '*Aaj Bhi Khare Hain Talab*' gives a detailed description of its multiple uses and its impact on the lives of the communities. Of course, individual homes in the drought-prone regions of the country have their smaller *talabs* or ponds for bathing, clothing, fishing, and other daily chores.²³ Besides, this practice was/is found around villages, homes, temples, mosques, and forts. A *Nagejasthi*, or wooden pillar, in the middle of the *talab* was set up by the local people during the ceremony to measure the water level of the pond periodically.²⁴

The traditional eco-friendly systems are viable and cost-effective alternatives to rejuvenate India's depleted water resources.²⁵ These structures, along with modern rainwater-saving techniques, such as percolation tanks, injection wells, and subsurface barriers, can be the answer to India's water scarcity. The indigenous people of ancient India had exercised the traditional water practices, and such old systems formed and operated on the basis of 'laws of nature'.²⁶ Arjun Appadurai's pioneer work (1986) expressed the reality that nature may exist outside society, but natural resources are social phenomena treated by human beings to their benefit.²⁷

Conclusion

This paper attempts to unravel the awareness of indigenous people related to various forms of water preservation systems prevalent in ancient India. Many societies flourished on the banks of rivers and other water bodies in the past, and their fate was essentially linked with effective water hydraulic engineering. Historically, many communities such as Maldhari, Rabari, Gond, and others relied heavily on the various services provided by water bodies. Many kingdoms in ancient India had developed various water management practices in the past and had maintained them well in a decentralized manner to meet local needs without compromising the availability of water resources for future generations. Currently, traditional water harvesting systems (*Viridha*, *Kanath*, and *Johad*) are on the verge of extinction, and many old hydraulic structures have been depleted. The British government implemented an extra tax on water bodies, and it caused a disruption in traditional water conservation systems. During British rule, a whole water-network system developed against individual water harvesting practices. This change not only destroyed ancient hydraulic structures but also made them difficult to retrieve. By demonstrating the ancient water conservation systems, the common people took on the responsibility of public welfare.

Acknowledgement

I am extremely thankful to Professor (Dr.) Pradip Chattopadhyay, Dean of Arts of the University of Burdwan and express my deep respect to Dr. Ranjan Chakrabarti, former Vice-Chancellor, The University of Vidyasagar for facilitating this study. I am also grateful to the editors of DRSR for giving me an opportunity.

References

1. Sengupta, D., Goswami, D. & Rudra, R. (2014), "Water", Arenal Publication: Burdwan, 2014, PP. 211-22 (see detail in A. Agarwal and S. Narain, S. (ed.), (1997), *Dying Wisdom: Rise, Fall and Potential of India's Traditional Water Harvesting Systems*, Center for Science and Environment, New Delhi, PP.73-115.
2. Shah, J. "The Kautilya's Arthashastra", (2014), Jaico Publishing House: Mumbai, P.85
3. Krishna, N. and Sing, A. (2014) (ed.), *Ecological Tradition of India*, C.P.R. Environmental Education Center of Excellence of the Ministry of Environment and Forests, Government of India, P.9.
4. Sengupta, N. "The Indigenous irrigation Organization in South Bihar", (1980) Indian Economic and Social History Review, Vol-XVII, NO. 2, PP. 157-189
5. Iyengar, V. "Waternama, A Collection of Traditional Practices for Water Conservation and Management in Karnataka", (2007), Communication for Development and Learning: Karnataka, P. 26.
6. Fisher, M.H. "An Environmental History of India: From Earliest Times to the Twenty-First Century" (2018), Cambridge University Press: UK, First Published P, 36
7. Agarwal, A and Narain, S (ed.), (1997), "Dying Wisdom: Rise, Fall and Potential of India's Traditional Water Harvesting Systems", Center for Science and Environment, New Delhi, 1997, p. 229.
8. Rangarajan, M.& Sivaramakrishnan,K. (eds.), (2012), "Indian Environmental History: From Ancient Times to Colonial Period", Vol. I, Permanent Black: New Delhi, P. 41.
9. Sengupta, N. op.cit., PP. 161-175.
10. Gupta, S. (2011), "Demystifying Tradition: The Politics of Rainwater Harvesting in Rural Rajasthan", India, Vol.4, Issue-3, PP. 347-364.
11. Kashwan, P. (2006), "Traditional Water Harvesting Structure: Community behind Community", Economic and Political Weekly, Vol. 41, No. 7, PP. 596-598.
12. Agarwal, A. and Narain, S. (1997), "Dying Wisdom: Rise and Fall of India's Traditional Water Harvesting System", Center for Science and Environment: New Delhi, P, 129.
13. Sengupta, N.op.cit., P.182.
14. Gupta, S. op.cit., P. 359.
15. Kashwan, P. op.cit., PP. 599-601.
16. Fritz, J.M & Michell, M. (2017), "Hampi Vijayanagara", Jaico Publishing House: Mumbai 2017, PP. 29-33.
17. Agarwal, A. and Narine, S.op.cit., PP. 177-180.
18. Pant, N. (1998) "Indigenous Irrigation in South Bihar: A Case of Congruence of Boundaries", Economic and Political Weekly, Vol. 33, No. 49 (Dec. 5-11), PP. 3136-3137.
19. Jain, S. K., Agarwal, P. K., and Singh, V. P. (2007), "Hydrology and Water Resources of India", Springer Science & Business Media, Dordrecht, P. 45
20. Sengupta, D., Goswami, D. & Rudra, R. (2014), "Water", PP. 211-22.
21. Gupta, S.op.cit., P. 26.
22. Agarwal, A. and Narain, S. op.cit., P.13.
23. Mishra, A. (2013), "Aaj Bhi Khare Hain Talab", (Hindi), Rajasthani Granthahar: Jodhpur, Third revised edition, PP. 38-43.
24. Ibid. PP. 76
25. Trivedi, A. (2006), "Management of Environment Through Ages. (History of Ecology and Environment: India), International Book Distribution Company: Lucknow, PP. 22-24
26. Nirarjan Pant & R.K. Verma, (eds.), *Tanks In Eastern India : A Study in Exploration*, IWMI, Tata Policy Research Programme & Center For Development Studies, 2010, PP. 20-30.
27. Appadurai, A. (1986), *The Social Life of Things: Commodities in Cultural Perspectives*, CUP, P.1



ISSN 2347-7180

Published by Dr. Angshuman Das, Secretary,
Dogo Rangsang Research Society, Guwahati &
Printed at Dream Graphics, Naokata, Tamulpur (BTR), Assam



Cover Designed at Dream Graphics by Kamal K Sarmah



ISSN : 2347-7180

(A Bilingual Research Journal, Indexed in UGC-Care list)

DOGO RANGSANG

Research Journal, Vol-13, Issue-6, No. 09, June 2023

দগো বাংছাং

CHIEF EDITOR (HON.)
EDITORS (HON.)

মুখ্য সম্পাদক (অবৈতনিক)
সম্পাদকদ্বয় (অবৈতনিক)

: Dr. Upen Rabha Hakacham
: Dr. Lalit Chandra Rabha
: Dr. Dhaneswar Kavitha
: ড° উপেন বাভা হাকাচাম
: ড° ললিত চন্দ্র বাভা
: ড° ধনেশ্বর কলিতা

A Peer Reviewed Bilingual Research Journal
(Indexed in UGC-CARE List)

ISSN 2347-7180

DOGO RANGSANG RESEARCH JOURNAL

দগো বাংছাং গবেষণা পত্রিকা

Chief Editor (Hon.) : Dr. Upen Rabha Hakacham
Editors (Hon.) : Dr. Lalit Chandra Rabha
Dr. Dhaneswar Kalita

মুখ্য সম্পাদক (অবৈতনিক) : ডা' উপেন বাজা হাকচাম
সম্পাদকদ্বয় (অবৈতনিক) : ডা' ললিত চন্দ্র বাজা
ডা' ধনেশ্বর কলিতা



Dogo Rangsang Research Society
Reg. No. KAM-M/263/L/ 595 of 2015-16
দগো বাংছাং গবেষণা সমিতি

SORROW OF SANDBARS: UNDERSTANDING THE HUMAN ROLE IN CHANGING ENVIRONMENT OF DAMODAR RIVER, INDIA

Samar Kantti Chakrabartty Head, Department of History, Achhruram Memorial College, Affiliated to Sidho-Kanho-Birsha University, Purulia, West Bengal, India samarkantichakrabartty@gmail.com

Abstract

Sandbars are narrow ridges of sand formed by the river system in the Bengal delta in eastern India. Some sandbars are often found in the middle of the Damodar River, and they can serve as an essential habitat for some people and animals. Since the beginning of time, the Damodar River has been known for its slanders (Sorrow of Bengal). 'Sandbars' have been colonized in various stages after the partition of India in 1947. Prior to partition, they were wide fields covered with grass and wild bushes. This essay demonstrates how marginalized Bangladeshis have been living on sandbars while dealing with a variety of problems, including storms, floods, soil erosion, and a lack of access to basic amenities like water, electricity, medical care, as well as connectivity with the outside world. Moreover, sandbars are often isolated from the mainland, making it harder for people to access necessary services such as education and employment. Despite these challenges, many refugees have learned how to adapt to living on passing sandbars. It also explains how they often develop unique techniques and methodologies for mitigating the effects of natural disasters. Overall this research demonstrates that assessments of vulnerability and insecurity are arbitrary and insignificant, however immediate survival is very crucial.

Keywords: Migration, Environmental-crisis, Sandbar, problem, Land-accretion, Refugees

Introduction

EKISTICS first provides background information on the region, the scope of the authority of Damodar Valley, the study's findings and recommendations, and finally the case for a rehabilitation programme for people from submerged lands. The source of the Damodar River is situated around 200 miles west of Calcutta and flows through the Indian states of Bihar and West Bengal. Despite its tiny size (9400 square miles), the Damodar Valley is abundant in natural resources. Nature has provided the valley with the land, water, minerals, and labour it needs to be prosperous. But much of the land particularly in the upper valley is deteriorating rapidly unless it is reconditioned erosion will spread to its lower reaches ultimately the whole valley will be destined to become desert. ¹ Due to this, numerous sand bars appeared on the Lower Damodar river's edges as well as in the middle, and the same process is still occurring today. After two steps partition of India in 1947, these alluvial river beds were acquired by empty-handed refugees, and they played a crucial role in converting the remote land accumulations into productive and livable landscapes for their immediate survival. But there are numerous problems, including safety concerns during storms, a lack of access to basic amenities such as water, electricity, and medical facilities, and challenges in transportation. Sandbars are prone to flooding, and people living in these areas have to frequently evacuate their homes during natural disasters. Migration communities from Bihar and Bangladesh settle on the sandbar despite the environmental dangers because the soils are productive and because untitled land is less expensive than the main land.

However, these sandbars are curved or patchy landscapes. Sand bars fluctuate frequently, forcing vulnerable people to move 2-4 times in 15-16 years due to their fluctuating nature. ² Their destiny is their present and future gift; they have no voice or option. The inhabitants of the sandbars are stateless and unable to integrate into "main land society" because to their acute destitution. ³ Refugees from Bangladesh had a steady existence and were considered as full citizens of Eastern Pakistan before to division. At the same time, indigenous populations in West Bengal used the alluvial land accretions of the Lower Damodar River as pasture fields. In these sand bars, immigrants are dealing with severe environmental problems and socioeconomic hardship as a result of the pain of partition. ⁴ This article describes the environmental difficulties that refugees and native submerged settlers deal with on a daily basis on the erratic terrain of Lower Damodar. Still, refugees and local outcasts must

choose the running land accretions as a point of entrance where there are ongoing threats of storms, floods, and land erosion as well as a lack of connectivity, access to healthcare, education, and other essentials.⁵ The capacity of those residing on the sandbars to adapt to what is typically perceived as an unstable environment is a problem that merits more investigation. The investigation detailed in this paper started with a series of queries about potential residents' perceptions of the sandbars as a safe location to live. Why, given the extreme insecurity, do individuals choose to live in the remote environment of sand bars? How many options do they have when choosing a home? Do the residents of sandbars consider them to be permanent homes or do they utilize them as a launching pad to travel to other locations?

Statement of the Problem

In late colonial West Bengal, this approach explains the paradoxical relationship between partition and environment. This study investigates why local outcasts and refugees must choose the unstable land accretions (sandbars) as a point of entrance into a region that is continuously threatened by storms, floods, and land erosion as well as by a lack of connectivity, access to basic services like healthcare and education, and other necessities. Despite these difficulties, many Bangladeshi refugees choose to settle on the perilous sandbars, where they develop their ability to adapt to a changing environment. They frequently create original methods and tools for reducing the consequences of natural calamities while preserving their way of life and dwellings. This work needs more research is how well those living on the sandbars can adjust to what is often seen as an unstable environment. This paper's inquiry began with a series of questions on how prospective residents felt about the sandbars as a safe place to live. Why do people decide to live in the isolated sand bar area considering the great insecurity? This study shows that judgements of security and vulnerability are arbitrary and unimportant, but that immediate survival is essential.

Objectives of the Study

- To clarify the paradoxical connection between changing fluvial environment and partition.
- It explains why refugees choose to reside on the perilous sandbars.
- Determine the causes of their physical and social isolation.
- Examine their various viewpoints, resource management strategies, and survival tactics.

Review of Literature

According to Haroun er Rashid (*Geography of Bangladesh*, Dhaka, 1991, p. 18), "Char fields are perilous territory all year long, but especially during the rainy season. These 'chars' are the emblem of uncertainty, poverty, vulnerability, border disputes between states and countries, and a lack of governance leading to the exercise of different forms of crime and criminality." In her article, (*No Voice No Choice*) Gineya Mukherjee makes a very apparent discovery. She writes that due to the continuous emergence, submergence, re-emergence, and re-submergence of the 'chars', we find that the people living in the 'chars' (the erosion victims) suffer from the "settlement>displacement>re-settlement>re-displacement" ('SDRR') syndrome, where hazards (mainly in the form of river-bank erosion and inundation) easily transform them elsewhere.

Morisawa (*Rivers: Form and Process*, London: Longman, 1985) demonstrates how sandbars are referred to technically as "bars," "river islands," and "sloughs." Additionally, he has discussed the various characteristics of the residents of the sandbars. Sandbars and other associated wetland ecosystems are used by people in different ways in different countries. In the modern world, river islands are good candidates for environmental protection since they contain areas with uncommon and unusual plants and animals. Public leisure activities including boating, fishing, and hunting for game are frequently conducted in these regions. In this regard, M. Chowdhury (*Women's Technological Innovations and Adaptations for Disaster Mitigation: A Case Study of Charlands in Bangladesh*, 2001) stated that "lost people"—stranded Afghan refugees of various ethnic backgrounds who were "rediscovered" by the larger humanitarian and media worlds—find refuge on the sandbars in the Pjang River on the border between Afghanistan and Tajikistan. In this context, M. Chowdhury, (*Women's Technological Innovations and Adaptations for Disaster Mitigation: A Case Study of Charlands in Bangladesh*, 2001), said "lost people"—stranded Afghan refugees of various

ethnic backgrounds who were "rediscovered" by the larger humanitarian and media worlds—find refuge on the sandbars in the Pjang River on the border between Afghanistan and Tajikistan. Samar Kanti Chakrabarty, (*A History of Receding Wetlands in West Bengal: Ecology, society and Environment (1947-2000)*), Unpublished Ph.D Thesis, The University of Burdwan, 2021) himself has investigated the misery of the people of the sandbars. Kumkum Bhattachayya, (*The Lower Damodar River, Understanding the Human Role in Fluvial Environment*), Springer, 2011) has pointed out many aspects of changing fluvial environment of Lower Damodar basin in West Bengal.

This work explains that nowadays, the most susceptible refugees are facing the same plight, and they have no direct road communication. They have to cover a distance of 1-2 miles on a sandy-path every day to communicate with the nearest towns.³³ Moreover, they cannot avail of government facilities like medical assistance, education, the transport system, ration facilities, etc. They suffer a lot from environmental calamities and identity crises. Generally, they are poverty-stricken people, and the number of dropout students, child labour, and illiteracy is very high and increasing at an alarming rate. Their existence is always fraught with uncertainty and insecurity. From dawn to dusk, they have to work hard in the agricultural field, fishing, selling vegetables, as labourers, and so on. Very often, they become victims of sexual harassment.

Research Methodology

The present study's foundation is made up of four sets of data that have been gathered. It has been extensively utilized to follow the shifting course of the Lower Damodar and its flood history to use archived data from historical maps, official reports, legal deeds of refugees and *pattas*, and other necessary records. To trace the history of embankments, the original control structures, archival data has once again been utilized. The Damodar Valley Corporation (DVC), the Irrigation and Waterways Department (I&WD), and other departments have all provided quantified information on stream flow, sedimentation, rainfall, and cross sections.

In the current study, there are no specific models that can be replicated. Although the benefits of the DVC have been highlighted in several official papers and publications, no attempt has been made to evaluate the project's other facets. Numerous studies on flow regimes, riparian ecosystems, and sedimentation patterns below key control points have been conducted and published in numerous nations. None of these, however, highlight the dangerous sandbars that are still cut off from the mainland or discuss the social significance of local control structures in the riverbed. There is no a priori model for the current study because the emphasis is on socio-economic difficulties that arise from control structures. This study has placed a strong emphasis on field methods for a number of reasons. First off, because these micro landforms are so dynamic, multiple field trips are necessary. Second, field survey techniques were essential for the gathering of active data from repeated trips because air pictures and Land sat imagery were unavailable for all sections of the river or were inaccessible due to these issues. Third, government organizations do not have access to ongoing data on land usage in the riverbed. Due to the importance of this topic in this study, data on land use and river bed landscape characteristics were gathered through several field visits.

Results and Discussion

According to the results of the current study, the Damodar River's flood characteristics are quite unusual and determine the safety and unpredictability of life on the sandbars. Additionally, it learns that poor settlers and Bangladeshi refugees relocate to alluvial plains to meet their socioeconomic requirements rather than seeing them as permanent or transient. In other words, by describing how people, from refugees to local settlers, driven by a variety of cultural, economic, religious, and political forces, have changed the fluvial landscape and are living with hazards, this research reviews the impacts of control structures in the downstream environment and also attempts to understand anthropogenic changes to the river regime.

The results of the current study demonstrate that colonial and postcolonial artificial control techniques have both been useless and successful in accomplishing the desired socioeconomic goals, as demonstrated by the history of continuous flooding. (ii) In reality, sandbars are portions of the

that have been used carelessly and without regard for the surrounding ecosystem. (iii) This research reveals that the rapid anthropogenic stabilization of the river bottoms is to blame for the eroding sandbars and escalating channel degradation. It demonstrates how the fluvial ecology has been impacted by partition and how various steps have been made to regulate the river's mood. Last but not least, arbitrary changes to the river's path are enhancing the Damodar River's peculiar character.

Why Refugee Settled on Sandbars

After Partition, Bangali Hindus from Bangladesh (Formerly Eastern Pakistan) started migrating to this part of India in quest of a quick source of income and social security. The governments labeled all the sandbars as *bhaslands* (government property). The newly relocated immigrants and other local residents, on the other hand, believed they have no legal rights and that these isolate landscapes are appropriate for their relocation.⁶ A few rehabilitated individuals displayed their *patta*, or legal documents, during the field survey. The migration into southern West Bengal over the Bangladesh border greatly increased after the Liberation Movement of 1971. Migration on sandbars accelerated as a result of the movement.⁷ However, in the vast Lower Damodar Basin (LDB), refugees have experienced knowledge on ecological management to prevent the occurrence of catastrophic disasters. The list of explanations for why refugees are relocating to the unstable sandy areas includes their practical solutions and resources based knowledge management :- (i) Grasses and soil-binding shrubs are allowed to grow to protect land erosion. (ii) Jute is grown alongside the banks that are prone to erosion. (iii) They cultivate different types of crops throughout the year on higher land above the inundation level. (iv) On the unauthorized (newly established) sandbar plots, more crops are cultivated. The local government is more accommodating to refugees. The cost of land is lower than on the mainland, making it simple for local settlers and refugees to buy land property for farming without encountering any administrative obstacles. They therefore give immediate security top priority before considering the study area's lack of protection. Thus, they are enabled them in the vulnerable parts of the changing fluvial environment of the Damodar river. In order to appropriately address them, the notion of refuge must be defined in this context.

The concept of a refugee is a legal, political, cultural, and sociological category). The technical meaning of the term "refugee" was developed between the two world wars.⁸ The 1951, "UN Convention Relating to the Status of Refugees", emerged due to the European experience of the Second World War. The Government of India's notes also refer to them as 'refugees'. A refugee is defined in Article 1 of the 1951 UN Convention as amended by the 1967 Protocol as: "A person who, owing to a well-founded fear of being persecuted for reasons of race, religion, nationality, membership in a particular social group, or political opinion, is outside the country of his nationality and is unable or, owing to such fear, is unwilling to avail himself of the protection of that country."⁹

The partition of India in 1947 gave birth to the refugee problem in West Bengal. The first phase of the refugee influx perhaps began after the *Noakhali* riots in 1946 and continued until March 1977.¹⁰ The Hindus who had crossed over to India from East Pakistan were issued a receipt for their entry into the country. These people are considered legal refugees. Between 1947 and 1952, millions of refugees migrated from erstwhile East Pakistan (present-day Bangladesh) to West Bengal. In 1947, the census found that 26.6 percent of what had become East Pakistan was Hindus. It was officially reported that 41.17 lakh refugees escaped to India differently between October 1946 and March 1958. Nearly 31.32 lakh of them are estimated to have remained in West Bengal, while the rest dispersed throughout India. From 1964 to 1970, 18.14 lakh refugees were displaced from Eastern Pakistan, and they chose to stay in West Bengal.¹¹ During the Liberation Movement of Bangladesh, West Bengal received 95 lakh people. Of course, a hefty proportion was settled in the Calcutta Metropolitan District; the third most significant concentration, after 24 Parganas and Nadia. But there were fewer opportunities for farming and fishing in the camps in urban and semi-urban areas for the Dalit Hindu refugees. Hence, a sizable number of refugees rejected this dole-sustained existence under the government's camps, and they searched *chars* lands/sand bars in the lower Damodar basin, which are fit for cultivation, animal husbandry, fishing, etc for immediate survival.¹²

The silty and sandy sandbars are physically on the border between the realms of land and water; they are the 'edges' where the cultures and ecologies of the two spheres collide and are separated from human habitation.¹³ The relationship between "partition" and "environment" has received the least attention in debates despite the fact that human use of these borderlands raises a wealth of metaphors and unique concerns of environmental dynamics and management. This essay is especially interested in investigating how well the disadvantaged can adapt to fluvial environments. In addition, the overall setting for this study is one of poverty and a lack of options.

Partly Water and Partly Land: Sandbars

"Ecologically, the "sand bars" of the Lower Damodar Basin in the Burdwan and Bankura districts of eastern India, are a singular illustration of the river's inner-delta development process. During the monsoon, the waves of rivers regularly create and erode sandbars. A significant area of sandbar is said to have been examined and inhabited in 1842, a few miles upstream of Burdwan (Ricketts, 1853).¹⁴ Captain C.H. Dicknes (1853) examined these grounds in 1854 and produced a map of them. These lands were likely developed as a result of the disastrous flood of 1840. Large floods have been demonstrated to alter the location and large floods have been proven to alter the size and placement of the sand bars along this section of river. There were more than 38 flowing sandbars between 1929 and 1943 that were all covered with a variety of bushes and grasses. According to the mouza maps surveyed between 1954 and 1957, some of the sand bars have developed a distinct shape. The government had resettled some refugees on the sand bars, which have been impacted by human involvement to the present day.¹⁵ Before the partition, such isolated landscapes had been a suitable abode for wild animals, birds, rare species of plants, and shrubs, including invisible creatures.

The Ganges, Brahmaputra, and Meghna rivers work together to form the biggest delta on earth in the eastern India, and their integrated river system is a crucial element of the Bengal Delta's scenery. The amount of silt carried by these rivers, which make up roughly 25% of the global total, and wind through the delta in countless branches before emptying into the Bay of Bengal, is the highest of any river system in the world. On its way to the Bay of Bengal, silt is thought to settle on the deltaic plain at a rate of about 40 billion cubic feet per year, forming the vast *chars* and *diaras* that make up the deltaic plain.¹⁶

Technical terms for sandbars include "bars," "river islands," and "sloughs." People's utilization of sandbars and other related wetland environments differs greatly from nation to nation. In the modern world, river islands are good candidates for environmental protection since they contain areas with uncommon and unusual plants and animals. Public leisure activities including boating, fishing, and hunting for game are frequently conducted in these regions.¹⁷ In this context, the "lost people"—stranded Afghan refugees of various ethnic backgrounds who were "rediscovered" by the larger humanitarian and media worlds—find refuge on the sandbars in the Pjäng River on the border between Afghanistan and Tajikistan.¹⁸ Few people are aware that there exist river islands and sandbars where people live, despite the fact that millions of people in low-lying regions of developing countries, such those in the Bengal delta, do.

The Bengal delta in South Asia is perhaps the best-known example of sandbars since it was formed by river-borne sediment from the Himalayas. Kunkum Bhattacharyya's 2010 study (The Lower Damodar) demonstrates how, recently, less flooding has caused the Lower Damodar River, one of the several important streams that feed the delta, to become increasingly "colonized" with sandbars.

¹⁹ Due to the significance of riparian zones to the lives and economics of the nation, the sandbars of Bangladesh further east have been the focus of resource management and policy discussions. According to Baqee, the pioneer of research into the human occupancy of Bangladeshi chars, they house "some of the most desperate people in the country," who, through their risk-taking behaviour, have established a unique subculture separate from the ways of the majority of the population.²⁰

The shifting sandbars and their people are mostly invisible to the larger economy and society in the Lower Damodar Valley, an area with high levels of urbanization and very prosperous agriculture.²¹

The locals exclusively utilized sandbars for pasture and regarded those uncultivated fields. In most cases, refugees occupied these areas and turned them into "green landscapes." The Bhasapur Sand bar and adjacent sand bars are some of the best examples of dangerous terrain where people are

learning using knowledge of resource management and sustainable development. For the sake of this study, some special featured sand bars like Bhasapur, Bara Mana, Shikarpur, Rangamati-Kenety of the Lower Damodar Basin (LDB) in Bengal delta of eastern India have been chosen as case studies.

Study Area: Human's Perceptions and Management

The term "perception" refers to both the way in which the senses react to outside stimuli and the deliberate effort of registering and filtering out specific occurrences. Culture, sex, education, upbringing, familial standing, neighbourhood standing, length of stay, and environmental attitudes are just a few of the variables that influence perception. There is a discernible difference between new explorers, colonists, and locals with different backgrounds and experiences evaluate the same landscape.²² Although Brookfield included perception in the approach of cultural and historical geography, the idea of perception may be applied to a number of different branches of geography, including human geography and geomorphology. He makes the distinction between "environmental perception" and the "perceived environment." The entire "monistic surface" on which judgments are made, encompassing natural and non-natural, visible and non-visible, geographical, political, economic, and sociological components, is referred to as the perceived environment.²³

Bhasapur Sand Bar

This sandbar is located under the jurisdiction of Golshi block in Burdwan district. It came into prominence after independence. Almost all Bengali Hindus of Eastern Pakistan and other local settlers of West Bengal (99%) have been living on the sand bar. There are several refugee colonies established on the sand bars of Lower Damodar Basin (LDB). On the right side of the river are seen several sand bars such as *Ranghamati, Nityanandapur, Chhoto Mana, Bara Mana, Patashpur, Gindali Char, Gobindapur, Chair-Gaitampur, Panchpara, Salkhara* etc., are situated on the right bank of the river. Whereas *Telenda Mana, Ramakrishna Palli, Pallishri and Sitarampur Mana, Lalohampur, South Bhasapur, Satyanandapur-Kalimohampur, Gaitampur and Fakirpur sand bar* etc., are located on the left bank of the Lower Damodar river. On these sandbars, more than 150,000 people have been residing. In addition to these, seven sand bars are also located in the centre of the river. Their livelihood patterns and ecological management are different than other marginal people of the river. Every day life on these seven sandbars is very difficult for the residents. Such as susceptible people have to cross half km every on sand road to communicate local towns.²⁴ Within 20 km, there are no primary medical health centres or educational facilities. Patients die while travelling. The percentage of students that drop out is dramatically rising. There are no fundamental means of support. Because of this, there is a significant rate of labour migration, and child labour is always growing. These *sand bars* depicts in the following map to show its geographical location where refugee colonies were established after two-steps-partition.



Fig. 1 Location of sand bars where refugees are predominant population

The sand bar's evolving biological configuration since 1930 is depicted on the lower map of the Baramana sand bar, which is under the control of the Bankura district. Here, we can observe how the cultivated area, human habitation, and roadways on the sand bar have occasionally changed sites. This occurs frequently in nature because of all the sand bars. Ecologically, the sand bar was joined to Sri Rampur's mainland in the 1960s under the Durgapur subdivision of Burdwan district in West Bengal. But the disastrous flood of 1978 cut it off from the mainland. In more recent times, it has reunited with the mainland once more. After 10 to 15 years, this type of ecological change has taken place in all of the Damodar basin's designated sandbars. Although the size of these sand bars varies, their landscape features are often the same.

It is a sand bar or land accumulation that is dominated by refugees. Due to issues with water and soil erosion, the area on this sand bar was unsuitable for agriculture until 1970. It was then a desolate land. When the refugees arrived, they started establishing bushes that would hold the soil together and plant trees on the edge of sandbars to stop land erosion. The silt deposited during the flood each year makes the entire land accretion fruitful. Around here, people grow a variety of crops all year round.²⁵ In the 1970s, farmers would only plant jute because there was no irrigation infrastructure and the sand bar was unsuitable for growing vegetables and legumes. They have been able to grow a variety of crops year-round since the 1980s because to the growth of the irrigation infrastructure, and the area along riverbeds is now suited for high-value crops owing to silt disposition every year. Today, every square inch of the land is used for agriculture, producing a variety of crops, including traditional ones as well as pulses, oil seeds, and vegetables.²⁶ In the vast Lower Damodar Basin (LDB), Bangladeshi refugees have experienced some ecological management to prevent the occurrence of catastrophic disasters. Their pragmatic measures and sensible actions include: (i) Grasses and soil-binding shrubs are allowed to grow on the erosion-prone banks. (ii) Jute is grown along banks that are prone to erosion (iii) They cultivate different types of crops throughout the year on higher land above the inundation level. (iv) On the unauthorized (newly established) sandbar plots, more crops are cultivated. However, the sand bar's land is ephemeral and vulnerable. High-yielding rice varieties (HYV) are grown here as silt de-poisoning progresses. In order to prevent crop loss, less important crops and vegetables are typically produced in the flood-free perimeter zone. An additional common employment among the locals is raising cattle. Schools and concrete homes are situated in elevated regions where they are hardly ever affected by flooding. In 1956, refugees started inhabiting the Telenda char/colony under the Mejia block of Bankura district. A short canal divides this sandbar into two halves. 28 households made up the *char*/sand bar's entire population of roughly 225. Previously, vegetation and wild grasses covered practically the whole sandbar.²⁷

The refugees arrived here and made the bushes bearable by cutting them back. For the purpose of reducing soil erosion, particularly during floods, they planted trees next to the chars. Here, during the rainy season, floods are a frequent occurrence. They plant crops that will be ready for harvest before the flood's onslaught. They grow a variety of vegetables (spinach, beans, tomatoes, carrots, potatoes, cabbage, cauliflower, etc.), fruits like cucumbers and watermelons, as well as rice and jute in the flood-free areas.

Shikarpur Sand Bar

Ecologically, the Shikarpur sand bar was the main course of the river Damodar until 2000. Recently, a group of small *chars*/sandbars has emerged just below the *Bhasapur sand bar* and together they are called *Shikarpur* land accretion. So, formation of inner-delta is a special character of the river and it continues since the dawn of civilization. Nowadays this land has been illegally occupied by the new infiltrators from Bangladesh and local settlers of West Bengal in India. The Bhashapur sand bar's eastern edge is still prone to erosion, and in order to survive, the refugees must adjust to the shifting fluvial environment. The only option left to them is to make an effort to survive.

Rangumati-Kenety Sand Bar

Rangumati-Kenety (RK) Char is under the jurisdiction of the Sonamukhi Block of Bankura district. Its width is about 2.5 km and its length is 3.5 km. This sand bar lies in the dam area of Rondiha Weir. In 1920, there were only fragmentary transit sandbars.²⁸ By 1957, land was added to the existing bars despite shape distortion and size reduction in some portions of the bars. Some new bars also appeared towards the left bank.²⁹ The 1978 floods caused extensive damage to these bars, and they were reduced in size. The thalweg has changed positions several times between 1921 and 2003 but has retained its braided channel pattern.³⁰ The households in R.K sandbar are about 800, and there have been about 15,000 people. Earlier, jute was a major cash crop when the water crisis was massive. Then, rice was the main crop in RK before the 1990s.³¹ Nowadays, potato cultivation has become more popular than the other crops in the winter season. Almost all types of vegetables are grown here because there are ready markets for them at Sonamukhi, Panagarh, Bankura, and Durgapur. Recently, marigold flower cultivation has become very popular in RkK sandbar. For more clarification, flower cultivation is now a common cash crop on all the sandbars in the Lower Damodar Basin. Generally, sandy soil is very suitable for marigold cultivation. Such flowers are grown at a low cost and in a short period.

Char lands are risky territory throughout the year, especially during the rainy season. These "chars" are the emblem of uncertainty, poverty, vulnerability, border disputes between states and countries, and a lack of governance leading to the exercise of different forms of crime and criminality. Due to the continuous emergence, submergence, re-emergence, and re-submergence of the 'chars', we find that the people living in the 'chars' (the erosion victims) suffer from the "settlement>displacement>re-settlement>re-displacement" ('SDRR') syndrome, where hazards (mainly in the form of river-bank erosion and inundation) easily transform them elsewhere.³²

Nowadays, the most susceptible refugees are facing the same plight, and they have no direct road communication. They have to cover a distance of 1-2 miles on a sandy-path every day to communicate with the nearest towns. Moreover, they cannot avail of government facilities like medical assistance, education, the transport system, ration facilities, etc. They suffer a lot from environmental calamities and identity crises. Generally, they are poverty-stricken people, and the number of dropout students, child labour, and illiteracy is very high and increasing at an alarming rate. Their existence is always fraught with uncertainty and insecurity. From dawn to dusk, they have to work hard in the agricultural field, fishing, selling vegetables, as labourers, and so on. Very often, they become victims of sexual harassment.

A Lesson of Survival Strategies

Analyses of human perceptions and behaviours in many environmental contexts, particularly those involving the natural world, have been comprehensive. Our understanding is that flood occurrences and the ensuing bank erosion are directly related to perceptions of security in the sand bars. However, the majority of the residents of Damodar have also dealt with social unrest brought on by political unrest, religious persecution, and cross-border migration. Ironically, because of the susceptibility brought on by these socioeconomic variables, people are now more accepting of natural disasters.

It has been said previously, refugees from Bangladesh are entering India through West Bengal and establishing colonies on the sandbars. The sandbars' ecological system has been compromised as a result. For those who live on the sandbars, it has exacerbated socioeconomic issues.

As a result of their ancestry in agriculture and fishing, they are accustomed to cultivating, farming, and fishing in flood-prone areas and are still honing their coping mechanisms for the natural disasters of the perilous char regions or sand bars depicted in the figures. -1 and 2. In the enormous Lower Damodar Basin (LDB), Bangladeshi refugees have implemented some practical methods to prevent the incidence of natural disasters. These survival strategies are: (i) Grasses and soil-binding shrubs are allowed to grow on the erosion-prone banks. (ii) Jute is cultivated by erosion-prone banks. (iii) They cultivate different types of crops throughout the year on higher land above the inundation level. (iv) Additional crops are grown on the unauthorized (newly formed) plots of the chars. (v) Linear

cottages and houses are found on the higher ground in flood-free areas. (vi) Nowadays floriculture is flourishing in the higher parts of the chars. (vii) A cooperative society, club, playground, and school are established in the flood-free zone. (viii) The people whose houses and lands have been engulfed by the river during the flood make huts in the unauthorized land of the char. (ix) Generally they built low-cost houses with jute sticks and bamboo and avoid clay houses. (x) Almost every house has an upper shelf to keep their valuables and take shelter during the flood. xi. Almost all the families have boats and most can drive them.³³



Despite that, still today, they have to dance to the moods of the river. They are the poorest, the most industrious masses in the uncertain fluvial environment. Indeed, they are the people with no voice, hence no choice. Let's now take a closer look at the different perceptions and protection challenges that the individuals we spoke here with Bhashapur sand bar identified as crucial. Case studies finds out those same occurrences are happened in the all selected sand bars.

People Survives with Security and Insecurity

Physical Isolation

Individuals and populations frequently react to environments differently. Some people thrive in their environments more, while others do not. Some people can cope with adverse environmental conditions without problem, while others can only do so by changing their perceptions. Varied responses could result from varied environmental sensitivities or perceptions, or they might be the result of different environmental abilities.

The Bangladeshi immigrants who settle in the Damodar charlands frequently lack valid entrance documents. However, this is not a significant barrier to resettlement on its own. Relatives provide housing for the new immigrants so they can live without worrying about the authorities spying on them all the time or unpleasant neighbours. And over time, a loose network of local political figures, panchayat members, and community development block administrators helps people acquire legal documents like ration cards or voter identification cards. Therefore, vulnerability can be viewed as transitory or ephemeral phenomena since they serve as an entry point to mainland society and economy.

According to the settler, Swapan Sarkar:

We don't intend to stay here for an extended period of time, We are very aware of how fragile these sandbars are. Each year, due to bank erosion during the wet season, I have witnessed acres of land disappear into the river. The river might erode my house at any time during the upcoming flood, I've lived here for four years, and my wife and I both have citizenship papers, I'm still here since I still need to get my two sons' citizenship papers.

Swapan Sarkar and other residents of sandbars are vulnerable to flooding and river erosion as a result of their illegal immigration to India, which has complicated and interconnected effects on their poverty and vulnerability. Not all sandbar residents, however, are watching for a chance to flee. Regardless of whether they get citizenship credentials, some inhabitants choose to dwell in the sandbars because they view it as a safe neighbourhood. In this scenario, isolation, which is typically

to be avoided when choosing a place to live, is frequently a strong suggestion. A 35-year-old lady named Rani Sarkar described her life on a sandbar as follows:

We have improved a lot since we left Bangladesh. We never have hunger pains here. More or less all year round, we can find work as agricultural labourers. My spouse and I will go fishing in the river even if we ever lose our jobs. In order to catch fish every day, we must work hard. The fish can be sold to the neighbours. We have set up the union of our eldest daughter with a man who also resides on the sandbar. We used our own labour to construct them a home. We don't lack for food here, and we are content to stay put since we lack any legal documents to leave.

Social Isolation

Strangely, one of the reasons individuals choose to live in the country occasionally is the lack of proximity to their social networks of family and friends. In several cases, whether in Bangladesh or elsewhere in West Bengal, people expressed satisfaction at how little about them was known outside of their previous existences.

Flood of River Controls the Lives

Our understanding of environmental uncertainty, susceptibility, and livelihood is lighted by an awareness of the circumstances in which people live in a setting that is perceived by the majority as marginal and unsafe. Our work has shown that people's feelings of security, insecurity, and vulnerability are all subjective and can vary greatly among various social groups—even locally. While some people obviously feel safer living in sandbars than they do in neighbourhoods with unfriendly neighbours, others see these locations as immediate life-supportive land without touch of local administration to dwell temporarily, while still others think the sandbars are completely unsuitable for occupancy. Others who live on sandbars are more aware of the defenselessness of the sandbars and only utilize them as a transitory haven while some strive to build permanent structures and make plans for a long-term settle.

Since the Damodar Valley Corporation (DVC, established-1948) dams were built, we have observed a decrease in the frequency and severity of floods in the Damodar sand bars. The residents of sand bars have felt more secure as a result of the flow and frequency of catastrophic floods, which has led to a greater use of the local resources at the same time. More intensive farming methods have, however, been implemented as a result of the growing competition for limited land. This raises the question of whether or not vulnerability has increased or lessened as a result of the constant influx of people into this vulnerable environment and the more intensive use of the sand bars.

Under the British government, the value of land ownership increased, and the agricultural department saw significant change. This reinforced the idea that land is more important than water and that perspective of rivers was altered. Rivers were re-conceived as disruptive factors that needed to be tamed in order to serve the land-based economy, in addition to changing agricultural practices, which earlier were frequently in harmony with this hybrid ecosystem.

Conclusion

This study investigates why Bangladeshi refugees decided to establish second houses in riverbeds. After India's independence in 1947, river resources were required to solve socioeconomic issues. There is no a priori model for the relationships between people and the environment, which further illustrates that decisions on specific land uses and assessments of the advantages of water from a DVC reservoir are based on personal experience. Environmentalists haven't paid much attention to the paradoxical relationship between "environment" and "partition" or its negative effects. Therefore, this study suggests some cutting-edge theories, discussions, and various points of view for the future of environmental history.

Acknowledgement

The University of Burdwan's Dean of Arts, Professor (Dr.) Pradip Chattopadhyay, and previous Vice-Chancellor Dr. Ranjan Chakrabarti, who helped make this study possible, have my sincere gratitude and respect. I also want to thank Sri Bidyapati Kumar and Principal Dr. Arup Kanti Konar.

References

1. A Case Study of the Damodar Valley Corporation and Its Projects, (1952), United Nations Economic Commission, *Ekistics*, Vol. 13, No. 77, 145-151, <https://www.jstor.org/stable/43615970>. Accessed, 17th February 2021
2. Mukherjee, G. (2011), *No voice, no Choice: Riverine Changes and Human Vulnerability in the 'chars' of Malda and Murshidabad*, Institute of Development of Studies, Calcutta, 13-16.
3. Chakrabarty, S.K. (2011) *A History Receding Wetlands in West Bengal (1947-2000): Society, Ecology and Environment*, The University of Burdwan, Burdwan, 195-96.
4. Basu, M. (1998) *'Marginalization and flood: A case of east Bengalee migrants in the Ajoy valley in Burdwan Distriet'*, University of Monitoba, Canada, 26-7.
5. Bhattacharyya, K.(1960) *'A Case Study of Damodar Valley Corporation and Its Project, Flood Control Series No. 16*, Bangkok, United Nation; Economic Commission for Asia and Far East, 9-33.
6. Lahiri-Dutt, K. (2000) *'Imagining Rivers'*, in *Economic and Political Weekly*, Vol.35, no.27, 395-400
7. Lahiri-Dutt, K. (2003) *'People, Power and Rivers: Experiences from the Damodar River, India'*, in *Water Nepal*, Vols.9/10, nos.1 & 2, 251-67
8. Kuper & J.Kuper, (1987), *'The Social Science Encyclopedia'*, 1st edn. . Route ledge, New York, P.726.
9. Chakraborty, P. (1990), *The Marginal Man: The Refugee and Left Political Syndrome*, Lumiere books, Calcutta, 80-85
10. Chowdhuri, S. (1995), ed., *The Calcutta: The past and the Present*, Oxford / publications, New Delhi, 72-73.
11. Bhattacharyya, K. (1999), *Floods, Flood Hazards and Hazards Reduction Measures: A Model – The Case in the Lower Damodar Basin*, *Indian Journal of Landscape System and Ecological Studies*, Vol-I, No-II, Calcutta
12. Ghosh, S., Ghosh, S., (2014), eds., *Refugee Problem in Undivided Bengal*, Reader Publications, Calcutta, 72.
13. McCay, B. 'Edges, (2000), *Fields and Regions'*, in *The Common Property Digest*, Vol.54, ,6-8.
14. D.Charles, (1854) *'Memorandum on the Survey of the Damodar and Question of the Abandonment of Bunds on Right Bank to Accompany*, the map received with superintending engineer South-eastern Province 's letters no. 1473, Bengal Government, Selection no. 15. Calcutta Bengal Military Orphan Press, Calcutta, 86-125
15. H. Rickets, (1853) *'Notes on the Management of the Embankment'*, Bengal Govt., selection No., 12, Calcutta, Bengal Military Orphan Press, Calcutta, 1-12
16. I. Iftekhar , (2010), *The Bengal Delta - Ecology, State and Social Change: 1840-1943*, Palgrave Macmillan, P. 15.
17. M. Morisawa, *Rivers: Form and Process* (London:Longman, 1985); and R.J. Chorley, S.A. Schumm and D.E. Sugden, *Geomorphology* (London:Methuen, 1984).
18. See <http://www.eurasianet.org/departments/rights/articles/eay100101.shtml>
19. Chowdhury, M. (2001), *'Women's Technological Innovations and Adaptations for Disaster Mitigation: A Case Study of Charlands in Bangladesh'*, Expert Group Meeting on Environmental Management and the Mitigation of Natural Disasters: A Gender Perspective, Ankara, 6- 9 November 2001.
20. Bagee, A. (1098), *Peopling in the Land of Allah Jaane: Power, Peopling and Environment, the Case of Charlands of Bangladesh* (Dhaka: The University Press Limited, 1.
21. Zaman, M.Q. (1989) *'The Social and Political Context of Adjustment to Riverbank Erosion Hazard and Population Resettlement in Bangladesh'*, in *Human Organization*, Vol.48, no.3 197.

22. Burton I, Kates RW, (1964), The perception of natural hazards in resource management. 3:412-421
23. Brookfield HC, (1969), On the environment as perceived. In: Board C, Chorley RJ, Haggett P, Stoddart DR (eds) Progress in geography, vol 1. Edward Arnold, London, 53-80
24. Chakrabarty, S.K. (2016), 'The Marginal Men in the 'Charlands' of Lower Gangetic Basin and Lower Damodar Basin' Journal of People's History and Culture Volume 2, 20210510044102.pdf, 25-27.
25. Bhattacharyya, K. (2011), *The Lower Damodar River: India, Advances in Asian Human - Environmental Research*, P.151.
26. Saha, M. (2010), *Duranta Damodar*, Lesser Art Publication, Hooghly, 165.
27. Bergkenp, G. McCartney, M., Dugan, P., Mc Neely, J., Acreman, M., (2000), ' *World commission on Dams Thematic Review, Dams , Ecosystem, Functions and Environmental Restoration*, (Environmental Issue-II. 1, Cape Town, South Africa, 55.
28. Samanta, G. & Lahiri Dutta, K., (2017), 'Like the Drifting Grains of Sand: Vulnerability, Security and Adjustment by communities in the Char-lands of the Damodar Rivers', India, Journal of South Asian Studies, 342-45.
29. DVC (Damodar Valley Corporation), (1975a). 'Report of Lower Damodar Investigation Committee', DVC, Calcutta-I.
30. DVC (Damodar Valley Corporation), (1975b). 'Report of Lower Damodar Investigation Committee', DVC, Calcutta-II.
31. WL. Vooduin, (2007), *Preliminary Memorandum on the Unified Development of the Damodar*, 1945, Central Technical Power Board, on behalf Government of India Press, Calcutta, P.156. (See, Original document from the University of Wisconsin, Digitized on 2007).
32. Samanta, G. & Lahiri Dutta, K. (2014), Dancing with the River: People and Life on the Chars of South Asia, Martin Luther University Halle-Wittenberg, 32-34.
33. S.K. Chakrabarty, 'Human Vulnerability in the Chars of Malda and Murshidabad and Lower Damodar Basin', in 'Modern Trends in Social and Basic Sciences', eds., Sailen Debnath, Bhaskar Bagchi and Subhra Mishra, (Reader Service, Calcutta, 2015), 667-670.



ISSN 2347-7180



Published by Dr. Angshuman Das, Secretary,
Dogo Rangsang Research Society, Guwahati &
Printed at Dream Graphics, Naokata, Tamulpur (BTR), Assam

Cover Designed at Dream Graphics by Kamal K Sarmah



ISSN : 2347-7180

(A Bilingual Research Journal, Indexed in UGC-Care list)

DOGO RANGSANG

Research Journal, Vol-13, Issue-6, No. 15, June 2023

দগো ঝাংছাং

CHIEF EDITOR (HON.)
EDITORS (HON.)

মুখ্য সম্পাদক (অবৈতনিক)
সম্পাদকদ্বয় (অবৈতনিক)

: Dr. Upen Rabha Hakacham
: Dr. Lalit Chandra Rabha
: Dr. Dhaneswar Kavitha
: ড° উপেন ঝাভা হাকাচাম
: ড° ললিত চন্দ্র ঝাভা
: ড° ধনেশ্বর কলিতা

A Peer Reviewed Bilingual Research Journal
(Indexed in UGC-CARE List)

ISSN 2347-7180

DOGO RANGSANG RESEARCH JOURNAL
দগো বাংছাং গবেষণা পত্রিকা

Chief Editor (Hon.) : Dr. Upen Rabha Hakacham
Editors (Hon.) : Dr. Lalit Chandra Rabha
Dr. Dhaneswar Kalita

মুখ্য সম্পাদক (অবৈতনিক) : ড° উপেন বাভা হাকচাম
সম্পাদকস্বয়ং (অবৈতনিক) : ড° ললিত চন্দ্র বাভা
ড° ধনেশ্বর কলিতা



Dogo Rangsang Research Society
Reg. No. KAM-M/263/L/ 595 of 2015-16
দগো বাংছাং গবেষণা সমিতি

PEOPLE'S WATER HARVESTING MANAGEMENT OF PURULIA DISTRICT (1947-2000): A GEO-HISTORICAL STUDY

Dr. Samar Kanti Chakrabartty Head Department of History Achhruram Memorial College, Sidho-Kanho-Birsha University Jhalda, Purulia, Pin-723202, W.B., India. Email id: samarkantichakrabartty@gmail.com

Abstract

It analyses how the native population of the Purulia district improved water harvesting management, which has sped up agricultural development and allowed them to live in and around artificial water bodies since the dawn of time. Particularly, our investigation has highlighted a number of services provided by various water body groupings in drought-prone areas between 1947 and 2000. It also looks at the socioeconomic advantages of water-taping techniques in the relevant research area, as well as how they affected the lives and means of subsistence of the oppressed people in the late 1980s and early 1990s. The majority of research on this area in West Bengal focuses on issues like migration, politics, cultural change, etc. The locals' concerns for the environment and a recent pattern of human involvement with water bodies, however, have received the least attention.

Key Words:

Agriculture, Migration, Culture, Sustainable Environment, Sustainable Environment

Introduction

The Purulia district is a peculiar location distinguished by enormous regions of plateaus, hills, woods, rivers, large deep tanks, and jor-bundh (medium-sized reservoirs), which are situated between the Chhotanagpur and the Ajodhya plateaus. With the ongoing threat of drought, a drinking problem, and storm surge, and several cultures can be witnessed. In a few West Bengal districts, including Bankura, Birbhum, West Midnapur, and Jhargram, especially Purulia district, which is distinct from the rest of the state, landscape and indigenous water-taping practices, are being successfully implemented. From prehistoric times to the twenty-first century, the westernmost areas of the state, including the study area, have been seriously threatened by dry temperatures and a lack of water. The district's ground water is insufficient because it is located on a rock-lying substrate. As a result, the district's water supply is derived from the storage of rainfall during wet monsoons. Because of this, the indigenous people of the area developed some unusual methods of collecting water, including: (i) ponds; (ii) bundh (big, deep tanks); (iii) jor-bundh (medium-sized reservoirs); (iv) hapa (extremely small size with an l-shaped deep water body); and (v) dug wells. Due to a wider use of local water-harvesting knowledge, the residents of the district conserve more water than the residents of the other districts in the state. According to the edited book *Water* by Debasish Sengupta, Paramesh Goswami, and Kalyan Rudra, this drought-prone region saves 21% of its water each year during the monsoon. Since the dawn of the Christian period, indigenous people have benefited from a number of these historical hydraulic engineering skills. However, since the 1980s and 1990s, the population's way of life and means of support have substantially improved because to the construction and maintenance of traditional water tapping practices. Despite the enormous threat posed by environmental crises and social pressures, they continue to persist and have been successfully cultivating these practices.

Statement of the Problem

In order to improve socioeconomic conditions, it intends to demonstrate how indigenous people have spread the Jor-bundh practise or new water-storing management in the drought-prone district. The farmers were able to establish themselves in and around the water bodies thanks to this creative, sustainable development. The work aims to promote flexibility in the drought-prone terrain and decrease socio-economic risks. The long-standing modes of subsistence of the indigenous people of

The district of South-West Bengal, India, have been impacted by both sustainable development and the growth of traditional water collecting.

Objective of the Study

- > Describe how the Jor-Bundh hydraulic system was found and developed by native people.
- > Determine the wisdom and collaboration of the entire community for holistic development.
- > Learn how crucial a single drop of water is in a drought area.

Review Literature

The relationship between water and society is integral to the larger interaction between man and nature. Social and political organisations of civilizations have been directly influenced in all ages by the ecology of water flows. Mahasweta Devi, has pointed out in her book entitled '*Purulia Jol-Chitror Manashjhon*' (2013) that Purulia and other western regions of West Bengal need many *jor-bandhs*, ponds, and brick-made dug wells for the development of irrigation, fish cultivation, and meeting daily chores. Rainwater harvesting in *jor-bandhs*, or ponds, is important for maintaining a sound ecological balance. People of the Rarh region believed that water bodies were not only a manifestation of nature but also revered sectors of social customs observed by primitive communities since ancient times, some of which are still practiced today. Debasish Sengupta, Paramesh Goswami, and Kalyan Rudra's pioneering work '*Water*' (2013), has notably mentioned that each and every drought-prone district of North and South-West Bengal preserves rainwater artificially or naturally, but Purulia collects the maximum (21% of the total) of water through the application of traditional water management practice in West Bengal. Kalyan Rudra's recent work, '*Paschim Banger Jolasampad Sankater Utsasandhane*' (2015), has highlighted the issues and factors relating to water scarcity faced by the people of West Bengal. Among various factors, failure of monsoon rain, deforestation, soil erosion, water waste, the extension of the process of urbanization, and global warming have been held responsible for water inadequacy in West Bengal. They have argued that there are basic similarities of thought between the 'environmental laws of *Arthashastra*' and the principles of the '*Stockholm Conference*' in 1972. '*Banglar Dighi o Jolashoy*' (2003) has narrated various issues related to the water bodies of the state. It deals with history, mythology, etc., and also discusses its ecology and management.

Research Methodology

This article was written using a combination of historical research techniques and primary source analysis. For producing an environmental history of water resources, information has also been gathered through field surveys in addition to secondary sources like books and journals. However, with the use of an interview schedule, they have been personally interviewed to better understand the various socio-economic patterns and stages of life of the indigenous people. Consequently, a field survey was carried out for this.

Results and Discussion

There are three factors: topographical location, present performance analysis, and the number of beneficiaries. This district having four water collection practices vis-à-vis the several services of the traditional knowledge, the current scenarios, and the status of the water managers. This study looked at almost many traditional water collection structures in West Bengal to collect authentic information on traditional water harvesting systems.

The discussion on water harvesting practices perhaps seems incomplete without a reference to the perceived threat of water-scarcity confronted now by all the nations of the world. Water, as one of the gifts of nature, is no longer considered inexhaustible, and with the passage of time and as a consequence of rising global warming, the water resource is also showing signs of depletion. In the closing decade of the 20th century, it has been calculated by geographers that approximately 110 corer people all over the world are still living in arid zones, and many of them have to undertake a journey

of more than five kilometers every day to fetch drinking water.¹ The severe water crisis in some parts of this planet has had an adverse impact on human societies. It is a problem on more or less all the continents, like India, Africa, Europe, Southeast Asia, etc. Even some highly developed countries like the USA, France, Britain, and Russia are also facing water-related problems today.²

Every person needs some water to meet his daily chores. It is reported that a person living in Phoenix, Arizona, in the state of Arizona, USA, needs 1000 litres of water every day, whereas a person living in an African city like Mozambique gets only 10 litres, and an Indian gets 139 litres of water per day.³ The two most important organizations—the WHO and the United Nations Children's Fund—both have suggested that every person should have 50 litres of water a day for drinking and other purposes in order to maintain good health. But the fact is that only 20 percent of the world's population can enjoy this minimum amount of water, and the rest have to remain satisfied with whatever little quantity of water is available.

Water deficiency is a global problem. In countries like India, Bangladesh, and China, the problem has become acute due to the tremendous growth in population. It is quite clear (*from the data of the West Bengal Pollution Corporation Board / Poribesh Bhavan, 2009*) that the demand for water in West Bengal was 121 cubic-kilometres per year up to 2011, and it seems to increase up to 143 cubic-kilometres per year by 2021. But, unfortunately, the state's present water resource can meet the demand of only 129 cubic-kilometer.⁴ This problem is very severe in the districts of Purulia, Bankura, Birbhum, West Burdwan, and Jhargram, and therefore these districts have been declared arid zones (Rarh). Drought in 1982 had affected the socio-economic life of the people of the region. In the 1970s and 1980s, the State Ground Water Board has reported that the ground water of many districts of West Bengal like Malda, North and North-South Dinajpur, Murshidabad, Midnapur, North 24 Parganas have diminished due to the massive extraction of ground water that has affected the surface water resources and its surrounding ecological set up.⁵ In the states like Chhattrishgrah, Madhya Pradesh, Rajasthan and some parts of Maharashtra, Gujarat, Andhra Pradesh, Karnataka and Jharkhand the crisis is even more acute and more than 45 per cent area of these states is under massive water crisis. For example, the villagers of Vadhavan village in Vadodara district of Gujarat have to get-down to about 24 meters deep well to collect muddy-water.⁶ According to NITI (National Institution for Transforming India, formed via a resolution of the Union Cabinet on 1 January 2015) Aayog report (on 18 June, 2018) of Central Government of India has rightly revealed that 600 million people have been facing high extreme water stress in the country, and 2, 00,000 people died every year due to inadequate water. About three-fourths of the households in the country do not have drinking water in their premises. With nearly 70% of water being contaminated, India is placed at 120th among 122 countries in the water quality index.⁷ According to the Niti Aayog's *Composite Water Management Index (CWMI)* of India has said and proved that twenty-one cities including Bangalore, Chennai, Delhi and Hyderabad will run out of ground water by 2020.⁸ Therefore, the government has launched a new department as "*Jal Shakti Ministry*" to mitigate drinking water crisis of the country.⁸

Due to insufficient rainfall, the Purulia district had severe droughts in 1953, 1966, 1972, and 1976, which had a negative impact on the region after partition (1947). As a result, there was a severe food crisis in several areas of the district. In response to this appalling condition, the district's political leaders in the 1980s spoke out in favour of rainwater conservation.⁹ They sought an increasing number of *bundhs* and *jor-bundhs* (big ponds and tiny dams) in order to prevent the district's ongoing water issue. For the purpose of presenting their demand for water preservation to the State Ministry of Irrigation, a sizable contingent of district residents marched (*poda yatra*) from Purulia to Kolkata. In order to get people's attention, they also brought up this important subject in the State Assembly and Parliament.

New Water Management: Jor-bundh

The Rarh region's Jor-bundhs are also significant bodies of water. Both the socioeconomic and ecological balance of the area are greatly impacted by them. They are typically U-shaped, and a shallow

It is installed on the Jor-bundh side to allow water to exit. In the vicinity's foothills, it excavates. There must be springs or streams at the top of the hills in order to build the Jor-bundh. Farmers in the area discovered a natural way to conserve water for farming. Such a Kuki Jor-bundh was built in Jhalda Block I at the base of the Parundih-Khamar Gramme Panchayat. In order to maintain the natural balance of the dam, the rainforest surrounding the jore-bundh is kept in this mountainous, jungle-covered area.. This is a jungle covered hilly area and the jungle around the jore-bundh is preserved for the ecological balance of the dam under the Bagmundi Forest Range. The most important dam in the district is Kumari dam that has been constructed down the two springs at Ghalbere village under the Niyodhya hills of Balarampur block. Hanumata is a drought-stricken area of Tamarsol Gram Panchayat and Terlo Gram Panchayat under the same block. A spring of Dumri hills is the main source of water of the dam. Karior dam is located at Baro Gata village under the Karior G.P of Jhalda block I. Some Jor-bundhs like Golamator and Dimu have been constructed at the basin of its catchment area. Such Jor-bundhs are exceptional dams which are built without the water from the hills or streams. Earlier the surrounding arealay barren for want of water. And after the construction of the dam the area has become a highly cultivated zone. Bagmundi is the ending point of Purulia district where the dam Ukadha was constructed to preserve water of the Ukhada hill for the development of irrigation and cultivation. A list of major dams and their associated details of the district are given below.

Table-1. Jor-Bundhs in Purulia District

Sl. No.	Year of Completion	River & Dam	Height above lowest Foundation Level/ Mt	Volume Content of dam /h	Gross Storage capacity,	Effective storage capacity	Purpose	Desi gned spill way capacity	Year of Commen cement	Len gth of dam / mt.	Reser voir Area/ ha.
1	1984	Kumari	9.6	233	7521.5	4320	irriga tion	765.14	1970-71	976.8	2348
2	1982	Saharjore	22.9	1110	8384.7	7406	irriga tion	4.8.07	1976-77	2195	1721
3	1988	Rupai/ Kuki	12.07	110	1617.1	1559	irriga tion	362.73	1970-71	2615	761
4	1982	Kestobazar	7.2	158	796.5	707.2	irriga tion	119.02	1969-70	954.12	176
5	1989	Karior	11.5	125	389.6	388.5	irriga tion	117.6	1979-80	904.57	232.8
6	1982	Parga	15.76	163	2219.4	1580	irriga tion	129.96	1976-77	721.34	526.3
7	1984	Khairabera	21	184	2347.7	5195	irriga tion	119.87	1980-81	371.95	404.8
8	2004	Patloi	13.5	141	5548.7	4212	irriga tion	265.82	1976-77	952.74	1822
9	1984	Goalma rajore	13	196	24.4.40	1712	irriga tion	137.44	1976-77	1073.17	951.4
10	1989	Demu	12	157	926	677.6	irriga tion	48.97	1979-80	827.74	340
11	1982	Buridumur	6.93	54	191.1	117.2	irriga tion	22.84	1976-77	533.53	64.7

1 2	1982	Sankha	6.7	13	641.9 2	395.6	irriga tion	382.5 7	1974-75	67	217.6
1 3	1984	Turga	20.73	320	1372. 8	4213	irriga tion	96.86	1948- 1949	360. 36	323.9
1 4	1975	Nimgiri						26.5	1948- 1949	99.3 9	1619

Source: This source has been collected by me from the irrigation the District Purulia, Submitted to the Director, Dam Safety Organization, I & W Director, Jalasampad Bhawan Salt Lake City, 13.03.08, Memo No. 476/S-140, (Third Minor Irrigation Census (2000-2001) in West Bengal Water Investigation and Development Department, GOWB, December 2003, PP.171-77)¹¹

UPPER-DAM AND LOWER-DAM IN AJODHYA

The Ajodhya pump storage hydroelectricity project was constructed on a 373.20-hectare area of dense rainforest between 1994 and 2002. Under the Baghmundi block, it is Asia's largest pump storage and power generation facility. Here, two reservoirs that go by the names of higher dam and lower dam have been built. The Kestobazar River existed before the dams were built. The dams' combined water storage capacity is currently at around 6.5 million cubic metres.¹²

The dense jungle around the Upper-Dam and the Lower-Dam on the Ajodhya hills destructed little during the construction of the two dams. Huge number of trees like eucalyptus, *sal*, and *mehagiri* were planted as the substitute to restore ecological balance of the region. Despite construction of dams the natural vegetation has not changed much in the entire region. The bio-physical zone around the reservoirs is highly rich. Four types of plant species namely - dry peninsular *sal*, dry mixed deciduous plants, deciduous scrub and *butea* plants; mammal species like elephant, bat, wild bear, deer, leopard and birds' species etc., are found surrounding the dams.¹³ In addition to these, in each and every part of the district has numerous micro/major *jor-bundhs* namely *Shyam bundh*, *Cheliyamabundh*, *Baro-bundh* at Manbazar block, *Shuribundh* at Hura, and *Jhalda* block has more 150 big *bundhs*.



Ecological Set Up Around the *Jor-Bundhs*

Dams / *jor-bundhs* are thought to make good habitats for a variety of biological systems. Due to the abundance of natural foods around the *bundhs*, a variety of bird species can be found in the area around the *jor-bundh*. The aforementioned *jor-bundhs* offer the wild kingdom different types of food, refuge, breeding grounds, or other essentials. In most cases, the *jor-bundhs* had dug in the isolated parts of the districts. The *jor-bundhs*' surroundings provide a specific haven for wildlife, particularly elephants, deer, wild pigs, foxes, jackals, and bears. Prior to the 1980s, the region surrounding the *jor-bundhs* was mostly made up of open fields. Following construction, the *jor-bundhs*' surrounding vegetation, streams, and climatic conditions have improved and are now more favourable for wildlife.¹⁴

Different Water Harvesting Systems and Roles

Long-standing irrigation practises and accompanying water-tapping traditions have a significant impact on irrigation systems in the Rarh region. Water scarcity is a major obstacle to the region's plan

to increase irrigation. However, in the latter half of the 20th century, it was controlled and developed through the use of water conservation techniques, which decreased the farmers' socioeconomic susceptibility. The irrigation system in the area is built on three main principles: 1) rainwater conservation in the jor-bundhs and bundhs, 2) storing precipitation in dug-out wells, and 3) utilising rivers to raise irrigation water.

Role of Jor-Bundh Practiccin Irrigation

By building jor-bundhs, the artificial irrigation system was expanded to dry terrain in the 1950s and 1980s. As a result, the installation of jor-bundhs brought 5–10% of the land in the Bankura and Purulia districts under a minor irrigation system.

The Purulia district has the best tradition of *jor-bundh* water management. Several *jor-bundhs* are contributing a lot to the advancement of irrigation in the district. About 42,953 thousand hectares' land came under irrigation systems after the 1980s. Consequently, many unproductive lands and one-crop lands have been transformed into multi-crop lands due to the availability of irrigation facilities, which have increased agricultural production in the entire district.¹⁶ The production of vegetables has also increased remarkably. The construction of *Khairabera-jor-bundh* was completed in 1982 in the Ayodhya Hills of Purulia district, which can irrigate about 1.5-thousand hectares of land in the rainy season. The villages around the dams, namely *Bhukadi, Burda, Mankidi, Koreng, Gurshu, Rotung, Kushadih, Pogradih, Sarjumata, and Bankadih* under *Bagmundi* block, have reaped agricultural benefits from the irrigation system facilitated by the dam. Paddy and other crops, including vegetables, are grown enormously here with the irrigation water. Thus, the single crop or barren lands have altered into multi-crop lands.

The *Khairabera-jor-bundh* is another important tank for irrigation under the *Bagmundi* block. The villages under the *Burdha Gram Panchayat* of *Jhalda Subdivision* are the main beneficiaries of the *jor-bundh*. These two pictures of the dam are portrayed below to show its irrigation potential.



Khairabera jor-bundh and its water channel enters into the agricultural field

Murguma Jor-Bundh

Saharjor jor or *Murguma bundh* is considered as the lifeline of the poor people of several mouzas under *Begunkodar Gram Panchayat*. It was built mainly for supply of drinking water and irrigation. The *Jhalda* municipality is fully dependent for its supply of drinking water that has minimized water crisis in the area. The water of the *jor-bundh* is also being used for irrigation purpose. The total irrigation area of the dam is about 5,095 thousand hectares.¹⁷ The main beneficiary villages are *Murguma, Laxmipur, Chatombhari, Bagandih, Keta, Gugui, Batoliya, Raghunathpur, Rampur, Harbaha, Jhari and Baram* under the *Jhalda-II* block. This zone is very famous as 'basket of rice and vegetables'. *Kuki jor* is another important *jor-bundh* of the district. It was established for the expansion of irrigation in the fallow land. The irrigation potential area of the dam is about 1088.50 hectare.¹⁵ More than 80% vegetables of the area are grown here with the help of irrigation water. Earlier most of the villages are mono-cropped but after the construction of the *bundh* these villages have become multi-cropped area. The following beneficiary villages of the dam are mentioned in the table.

Table -2. Kuki Dam and Its Benefitted Mouzas

Name of Jore-Bundh	Gram Panchayat and Block	Benefitted Villages
Kuki/ Rupai	Ichag under Jhalda -I	Mahaldih ,Sajumetspilai, Kuki,Palashdih, Bhutidih, Maisha, Jamlohar, Harahara, Birudih, Magha, Dharpa, Dibirtika, Jargo, Mathai, Ilu, Mahadih, Chandai, Nowadih, Rotiadih

Source: Field Survey

Kumari Jor-Bundh

The farmers are also receiving the same service from the Kumari Jor-bundh. Almost 3642 thousand hectares have the capacity to be irrigated as a result of the jor-bundh's construction. Following settlements are benefiting from the water preservation strategy of the dam since 1982 in terms of agriculture. The villages that received benefits are:

Table -3, Kumari Dam and Its Benefitted Mouzas

Name of Dam	G.P & Block	Benefitted Mouzas
Kumari Dam	Baro Urma under Balarampur Block	Baradiya, Taltar, Valaidih, Bhagabundh, Chandanpur, Rawtara, Kharipari, Chipingdih, Kharipari, Dhatkidih, Nadiya, Bamandih, Manpur, Rangagara, Murgabere Bastebpur, Arabundha, Turku, Raghinathpur, Tetlo Tosho and Shukuruta

Hanumata Jor-Bundh

Similar picture is found in the Hanumata-jor under the Choto Urma mouza of Balarampur block. It provides the same irrigation facility in the advancement of agriculture in the region. The following table shows the benefitted villages under the Balarampur block.

Table -4

Name of Dam	G.P & Block	Benefitted Mouzas
Hanumata Dam	Tetlo & Balarampur Block	Chhogadha, Chholagara, sabardih, Bonbadha, Hansapur, Muradih, Lakhmapur, Pursha, Amagara, Gosaidih, Tuimabaradih, Baistandih and Tumarsol

To address the serious groundwater and surface water crises in the state of West Bengal, the 'Jal Dharo and Jal Bharo' Scheme was created a programme designed to capture valuable rainfall during wet monsoons, was introduced in 2011-2012. The Water Resources Investigation & Development Department, GOWB, has taken on the significant role of large-scale rainwater collection as well as detention of surface runoff for enhancement and availability of priceless water resources through the erection and management of Minor Irrigation Constructions. This is necessary for the program's successful implementation.¹⁸

The aim of the project "Jal Dharo-Jal Bharo" programme is to detain rainwater in all kinds of water bodies, viz. *hapa*, (I shaped deep pond) tanks, ponds, reservoirs, canals, and underground artificial recharge through rooftop rainwater harvesting. For conservation and storage, rainwater and surface run-off is arrested in derelict or silted tanks after proper de-siltation, mainly for irrigation in the drought prone areas of West Bengal.¹⁹ Since December 2014, around 817 ponds and 7,319 water reservoirs have been excavated and renovated by the government, and approximately 3,000 ponds have been

further excavated under the scheme of "Jol Dahro and Jol Bhoro" of the state Government in the year 2015-16. The Jal Tirtha Scheme under the West Bengal Accelerated Development of Minor Irrigation Project (WBADMIP) has spent Rs 1380 crore to make an additional 1.39 lakh hectares of land irrigable in the districts of Purulia, Birbhum, Bankura, and West Medinipur. About 15,000 hectares of land have been made crop-worthy through micro-irrigation techniques.²⁰ This irrigation scheme has stressed water bodies across the state, which has enhanced job opportunities among the rural Bengalis through fish farming and cultivation. **Dug-Well Practice**
Dug wells in the Purulia district are the basic source of irrigation system throughout the year.



Nowadays around 31,370 hectares' lands are under the irrigation system owing to the contribution of 13,135 dug wells across the district.²¹ Needless to say that it has facilitated agricultural production in the region. In the past three decades to four decades, the irrigation through dug wells in Birbhum and Bankura has been hit hard with the construction of barrages. But nowadays the excellence of wells based agriculture is particularly appreciated in Purulia district.¹⁷ The farmers of the district are fully dependent on rain-fed wells cultivation owing to the capricious nature of monsoon and lack of whole water- net-work project. In order to these, configuration of land of the district is curse but dug well based cultivation has enhanced the settlement in study area. Whatever, the exact figures in terms of number are not available but many tones vegetables are being produced in the entire district through this practice. Presently the food-stricken district Purulia exports tons of vegetables in the neighbouring states Bihar and Jharkhand owing to these practices. Water harvesting scenario through the dug-well of the district is highlighted below.

Table-5. Source of Irrigation and Irrigated areas in Purulia: 1998-1999

Sl. NO.	Name of the Block	Canal Area	Wells Based Irrigation		River Lifting Irrigation	
			No	Area ha	No	Area ha
1	2	3	4	5	6	7
1	Arsha	3100	822	1442	7	190
2	Bagmundi	2830	1001	1480	6	170
4	Bandowan	880	304	3437	8	580
5	Barabazar	1931	600	1477	12	1005
6	Hura	635	524	2460	4	155
7	Jaipur	535	1523	1510	3	150
8	Jhlada	3717	330	740	13	315
9	Jhalda II	2825	339	1660	3	182
10	Manbazar	860	536	1821	10	384
11	Manbazar I	740	450	1470	5	180
12	Puncha	635	300	2240	9	151
13	Purulia	1885	1252	955	7	315
16	Neturia	725	237	802	4	66
17	Para	1096	1309	1155	6	190
18	R.N.Pur I	420	370	1818	4	167

19	R.N.Pur II	1115	211	1650	4	120
20	Santuri	1005	1034	694	4	85
	Total	28639	13135	31370	135	5285

Source: District Statistic Hand book, Purulia, Bureau of Applied Economics&Statistics, 1999 – 2000, P. 50²²

Rain-Fed Irrigation

Besides these, another rain-fed irrigation is being followed by the marginal farmers of the Purulia district. A high mound embankment is built around agricultural field to tap rain water. Each and every field has its own earthen-embankment to preserve water from top to bottom of the area. This picture shows an innovative rain-fed irrigation from top to bottom of the field.

After the 1980s, the gross production of Purulia district increased greatly due to well-maintained hydraulic structures and a huge amount of vegetables were exported to neighbouring states of the district like Bihar and Jharkhand. The number of hats and bazaars (*Puncha hat, Rakhbar hat, Taltaol hat, Cheliyama hat, Adra, Borabazar hat, Kotshila hat, (Monday), Jhalda, Balarampur Ludhurka hat (Tuesday), Hura, Bandwan, Pundag, Bagmundi, Arsha, and Tulin hat (Thursday)* of Purulia district has developed owing to the extension of age-old water harvesting practices after partition of India.²³

Hapa Practice

For a very long time, this district has enjoyed the best hapa tradition. As a result of the expansion of minor irrigation and fishing, it has recently grown to be quite well known in the Kotshila and Arsh blocks of the district. Typically, a "hapa" is excavated in a field corner to collect rainwater during the wet monsoon. The command irrigation area now includes about 20–25 bigha unfarmed fields in these two blocks, which have more than 50–60 hapas combined. Additionally, it is crucial to cultivate a variety of veggies in the summer.

Impact on Labour Migration

The long-standing practice of labour migration in the district, as well as the newly developed jor-bundh practice has altered the rural economy of the study area and its surrounding regions. In the past, a sizable portion of the district's population had to leave in pursuit of work. Ben Rogal has demonstrated that seasonal migration in West Bengal is not just a necessary component of the debt cycle. Seasonal agricultural labourers from border regions like Bihar and West Bengal as well as other parts of West Bengal have a long history of working in the state's south central region.²⁵ With increase in rice production in west Bengal in the 1980s and early 1990s employment opportunities were created for seasonal migrants in transplanting and harvesting in a season which would be continuous rather than sporadic. Around 65,190 workers left Purulia for other locations in 1900. Nearly 30,777 labourers left the country in 1901. The rate of labour migration has definitely decreased. Only 15,492 labourers from the Purulia region moved to West Bengal, Assam, and Bihar in 1909. In 1911, H. Coupland recorded and published this official data in the Bengal District Gazetteer: Manbhum, statistics.²⁶ Even after India gained its independence, the trend of worker migration from the colonies has persisted. However, census statistics reveal the character and patterns of the migration process. 16.4% of the people in Purulia moved to other West Bengal districts, and 33.03% left the city for other states, per the census of 1961. Most of the modest emigration from Purulia (47, 101) took place in the Bankura and Burdwan (13,984). The district's agricultural labour facilities expanded after the 1980s and 1990s. They therefore have the opportunity to work in their home districts. Due to the greater growth of old water management systems; such labour migration has decreased in the present

Conclusion

Locals here actually believe that a body of water on the surface of the ground is not a hole or puddle. Instead, their cultures and beliefs are influenced by these water bodies either directly or indirectly.

Actually, they treat the water bodies they foster on a regular basis as their sons, and the water bodies offer everything they have to the area's poor. The societies of the district have enabled commercial growth through a considerable expansion of the district's historic infrastructure for water tapping. In order to survive and maintain ecological equilibrium, they are currently protecting themselves from environmental threats and conserving water gathering practices.

Acknowledgement

For helping to make this study possible, I sincerely thank Vice-Chancellor Dr. Ranjan Chakrabarti of the University of Vidyasagar and Professor (Dr.) Pradip Chattopadhyay of the University of Burdwan. I also want to thank Sri Bidyapati Kumar and Principal Dr. Arup Kanti Konar.

REFERENCES:

1. Debasish, S., Paromesh, G., & Kalyan, K. eds., (2014) *Water*, Avenal Publication: Memari, Burdwan, pp. 15-16.
2. S. Seth M, *Let There Be Water: Israel's Solution for A Water-Starved World*, 2015, Thomas Dunne Books, St. Martin's Press: New York, p. 4.
3. Debasish, S., Paromesh, G., & Kalyan, K. op.cit., 19.
4. Debasish, S., Paromesh, G., & Kalyan, K., op.cit., P. 39.
5. *Semi-Detail Ground Water Survey in Purulia District*, (1977), Government of West Bengal, Rural Development Centre, Indian Institute of Technology, Kharagpur, pp.1-2.
6. *Ananda Bazar Patrika*, (written by an eminent journalist Jaya Mitra, *Ei Sujala Sufala Desher Emon Abostha Halo Ki Kore*, 21st July, 2019, Section - II, p. 8.
7. *Report of the NITI Aayog*, "Government of India", (12th June 2018), (Dahlberg Development Advisors Pvt. Ltd: New Delhi), pp.17-19.
8. *Semi-Detail Ground Water Survey in Malda & West Dinajpur District*, Government of West Bengal, Rural Development Centre, Indian Institute of Technology, Kharagpur, 1976, pp. 1-2.
9. *Ananda Bazar Patrika*, (2011), Jaya Mitra, *Ei Sujala Sufala Desher Emon Abostha Halo Ki Kore*, *Report of the NITI Aayog*, "Government of India", New Delhi, 12th June 2018, pp.17-19.
10. This source has been collected by me from the Department of Irrigation, Purulia District in West Bengal, India. Submitted to the Director, Dam Safety Organization, Director of Irrigation & Water, Jalasampad Bhawan, Salt Lake City, 13.03. 08, Memo No. 476/S-140, (Third Minor Irrigation Census (2000-2001) in West Bengal Water Investigation and Development Department, GOWB, December 2003, pp.171-77
11. Chowdhur, M., *Sanskriti Purulia*, (2012,),Raghnath Publishers, Ketaki, Purulia, West Bengal,p.71.
12. Biswas,A., '*Puruliar Jela Sankhya*', Information of Cultural Affairs, (, March 22, 2007) , Government of West Bengal, India, pp.63-65 .
13. Ray,S., *Puruliar Jela Sankhya*, Information of Cultural Affairs, (2008), Government of West Bengal, India, February 17, pp. 67-74.
14. Devi.M. *Puruliar Jol-Chitror Mamushjhon*, (2003) (in Bengali) in the edited book, *Banglar Nadi Nadi O Jalashoy*, Pronab Saekar, Sarkar, p. Lok Patrika, Kolkata . p.76.
15. R.Kalyan, *Paschim Banger Jalasampad Sankater Utsasandhane*, (2015), Ppublisher - Sahitya Samsad, Kolkata, p.19.
16. Basu.K.*Jol Sankot*, (in Bengali), '*Bartaman Patrika*', July7, 2019
17. Water Resource Development Directorate,(2010-11) , "Government of West Bengal", p.21.
18. Hand Book of Fisheries Statistics. (2000) , Government of West Bengal, India, p.26.
19. Sarkar.K.*Banglar Dighi o Jolashoy*, 2004, (in Bengali),(Lokpatrika, Sonarpur, Kolkata) , pp. 393-396.
20. *Bureau of Applied Economics & Statistics*, (1999 - 2000), District Statistic Hand book, Purulia, "Government of West Bengal", "India", p.49.

- 21 Bureau of Applied Economics & Statistics, (1995 - 1996), District Statistic Hand book, Purulia, West Bengal, India, p.50.
22. Chakrabarty.S.K, *A History of Receding Wetlands (1947-2000): Ecology, Society and Environment*, Unpublished Thesis, The University of Burdwan, 2021, Burdwan, West Bengal, India, p. 45
23. Ben, R. *Workers on the Move: Seasonal Migration and Changing Social Relations in Rural India*, 1998, Gender and Development, Vol. 6, No. 1, (Mar.), p. 22.
24. Ibid, p. 24
25. West Bengal District Gazetteers of :Purulia,(1972), p.164.
26. R . Ben, (ed.) *Seasonal Migration, Social Change and Migrants' Rights: Lessons from West Bengal*, Economic and Political Weekly, Vol. 36, No. 49 (Dec. 8-14), pp.4551.



ISSN 2347-7180

Published by Dr. Angshuman Das, Secretary,
Deoga Rangsang Research Society, Guwahati &
Printed at Dream Graphics, Naokata, Tamulpur (BTR), Assam



Cover Designed at Dream Graphics by Kamal K Sarma

Role of Youth in India's National Integration

Jayanta Pandey

Assistant Professor, Department of History
Achhruram Memorial College, Jhalda

Abstract: It is apodictic to assert that there is a close connection between youth and national integration. India is a land of unity in diversity. The future of this country lies in the hands of the young generation. They are considered to be the voice of the nation. They can make a huge difference. Youths can be involved actively in bringing up several changes - development, prosperity, and respect for our nation. This article first touches on India's vulnerability as a nation at the time of independence. It tries to identify various internal challenges relevant to India's national unity. Furthermore, it discusses elaborately how can our youth contribute through different ways to the national integration of India and concludes with a note that they would eradicate all internal threats and make our country stronger than ever before.

Keywords: Youth, National Integration, Communalism, Terrorism, Demographic dividend, Nation building.

Introduction:

On 15 August 1947, a hard earned, prized independence was won by the people of India after long, glorious years of struggle against the Britishers. India's freedom represents for its people the beginning of a long march to overcome the colonial legacy of economic underdevelopment, gross poverty, near total illiteracy, the wide prevalence of diseases, stark social inequality, and lack of political unity. Since the beginning, many critics have expressed doubts about India's ability to sustain its national integration and continue to progress as a nation. There have been vocal prophets of doom and gloom who predicted that neither freedom nor democracy would survive in India for long, that the Indian political system would collapse sooner or later, that the Indian Union would not survive and the nation-state would disintegrate into linguistic and ethnic fragments. They have repeatedly argued that India's numerous religious, caste, linguistic, and tribal

Conclusion:

Historian Ramchandra Guha said, "The forces that divide India are many...But there are also forces that have kept India together, that have helped transcend or contain the cleavages of class and culture, that - so far, at least - have nullified those many predictions that India would not stay united and not stay democratic."⁸ At the same time, we shouldn't take independence for granted. As mentioned earlier, India is enjoying a demographic dividend. India can reap the economic benefits of it as well as strengthen national unity by mobilising its huge young population. The role of the Youth is very important in nation building. They can easily influence society and can also solve problems by introducing innovative and impactful ideas that will only help in the betterment of the country. They have the ability to create an identity for themselves, which will help in creating an impact. All the youth need is the support of their family and friends, and they can make our country great. So our youth can play a vital role in promoting national integration.

References:

1. Chandra, Bipan, and others, India Since Independence, Penguin Books, New Delhi, 1999, p. 5.
2. Harrison, S. S., India-The Most Dangerous Decades, Princeton University Press, Princeton, 1960, p.338.
3. Upadhyay, S. P. and R. Robinson, Revisiting Communalism and Fundamentalism in India, EPW, Vol. 47, No. 36, Sep. 2012, pp. 40-41.
4. Deaton, Angus, and Jean Dreze, Poverty and Inequality in India: A Re-Examination, EPW, Vol. 37, No. 36, 2002, pp. 3729-48.
5. Bose, Nirmal, National Integration, The Indian Journal of Political Science, Vol. 52, No. 1, 1991, p. 2.
6. Mukherjee, Rohan, and David M. Malone, Indian Foreign Policy and Contemporary Security Challenges, International Affairs, Vol. 87, No. 1, 2011, p. 99.
7. Sharma, M. D., Paramilitary Forces of India, Kalpaz Publication, New Delhi, 2008, p. 305.
8. Guha, Ramchandra, India After Gandhi, Picador India, New Delhi, 2007, p. xxix.